Gustavo S. Oderich
Editor

Endovascular Aortic Repair



Current Techniques with Fenestrated, Branched and Parallel Stent-Grafts

Illustrated by David Factor

Springer

Endovascular Aortic Repair

Gustavo S. Oderich
Editor

Endovascular Aortic Repair

Current Techniques with Fenestrated, Branched and Parallel Stent-Grafts

Illustrated by David Factor

Springer

Editor
Gustavo S. Oderich
Division of Vascular and Endovascular Surgery,
Department of Surgery
Mayo Clinic
Rochester, MN, USA

ISBN 978-3-319-15191-5 ISBN 978-3-319-15192-2 (eBook)
DOI 10.1007/978-3-319-15192-2

Library of Congress Control Number: 2016961221

© Mayo Foundation for Medical Education and Research 2017
This work is subject to copyright. All rights are reserved by the Publisher, whether the whole or part of the material is concerned, specifically the rights of translation, reprinting, reuse of illustrations, recitation, broadcasting, reproduction on microfilms or in any other physical way, and transmission or information storage and retrieval, electronic adaptation, computer software, or by similar or dissimilar methodology now known or hereafter developed.
The use of general descriptive names, registered names, trademarks, service marks, etc. in this publication does not imply, even in the absence of a specific statement, that such names are exempt from the relevant protective laws and regulations and therefore free for general use.
The publisher, the authors and the editors are safe to assume that the advice and information in this book are believed to be true and accurate at the date of publication. Neither the publisher nor the authors or the editors give a warranty, express or implied, with respect to the material contained herein or for any errors or omissions that may have been made. The publisher remains neutral with regard to jurisdictional claims in published maps and institutional affiliations.

Printed on acid-free paper

This Springer imprint is published by Springer Nature
The registered company is Springer International Publishing AG
The registered company address is: Gewerbestrasse 11, 6330 Cham, Switzerland

To my wife, Thanila, and my children, Gabriel and Victoria,
without whom I would have plenty of time with no inspiration or purpose.

and to my parents, Ernesto and Maria Helena, who instilled me with their passion, integrity, dedication and altruism.

Foreword

The introduction of endovascular stent-grafts dramatically improved treatment for many abdominal and thoracic aortic aneurysms. More recently the development of endovascular methods to treat complex aortic aneurysm disease that involved vital branch arteries has been an equally dramatic sea change in the way aortic pathology can be effectively managed. Many ingenious methods have been advocated to revascularize these involved branches. These include a variety of fenestrated, branched, and parallel endografts. All can work effectively, but all can be associated with problems if performed imperfectly.

This treasure trove of a text has been edited and largely written by a master in the field of complex aortic aneurysm repairs. Clearly described chapters on all sorts and combinations of fenestrated and branched endografts for various aortic pathologies are included. Some other chapters have been written by other experts who are the key leaders, innovators, or advocates of a specific technique or most experienced in a given anatomical area. Many of the chapters include technical tips on how these techniques are best performed and how to avoid pitfalls and treat complications. Most chapters are richly and beautifully illustrated by a single talented artist to explain clearly these complex procedures and how they should be performed.

Other chapters deal with all possible related issues, including variations in normal aortic anatomy, mechanisms and natural history of aortic disease, analysis of imaging techniques, how to prevent and manage complications, how to manage an endovascular inventory, how to build an endovascular aortic program, preoperative planning and postoperative follow-up, regulatory and off-label issues, and an analysis of all the global industry and physician-modified devices for treating lesions in various parts of the aorta. In addition, there is an extensive case study atlas which provides examples of preparation and implantation of custom-made, off-the-shelf-manufactured, physician-modified, off-label, and parallel aortic stent grafts.

Thus, this jewel of a text is an encyclopedia of everything one needs to know about the endovascular treatment of complex aortic pathology. It covers the field in a most thorough, up-to-date and unbiased way. This volume is a must have for those who will make the treatment of complex aortic pathology a major part of their practice. It will also be an often-used reference source for students and trainees interested in these exciting new treatments. And even though most vascular surgeons may not have the expertise of the editor and authors of these outstanding chapters, they will find this book a great way to plan, prepare, and execute their treatment of common juxtarenal and pararenal aortic aneurysms and those with extensive common iliac involvement requiring hypogastric artery revascularization.

This volume will deservedly become a classic text in vascular surgery and of great value to all other specialists interested in complex aortic disease.

New York, NY, USA — Frank J. Veith

Preface



Open surgical repair has remained the gold standard for treatment of complex aortic aneurysms for over 6 decades. This has been recently challenged by novel endovascular techniques that use fenestrations, branches, and parallel stent grafts to incorporate side branches of the aorta. The indications and applications of stent grafts were broadened to include patients with complex aortic aneurysms, including those considered good candidates for open surgical repair. Although there are many reasons for the successful dissemination of endovascular aortic repair, including many advances and refinements in vascular imaging, catheter skills, and endovascular technology, none is more important than the passion of vascular surgeons to challenge the status quo and come up with better alternatives to treat complex aortic aneurysms.

Endovascular Aortic Repair: Current Techniques with Fenestrated, Branched, and Parallel Stent Graft has one purpose, which is to fill the gap between clinical knowledge and the technical expertise needed to master novel endovascular approaches to treat a complex aortic disease. The book is organized in a logical fashion to address every step in the care of the patient with aortic aneurysms and dissections. The book is divided into eight sections that address basic

concepts and imaging methods, how to build complex aortic programs, and the technical aspects of managing aneurysms that involve the visceral, arch, and iliac vessels. A special section is devoted to physician-modified grafts and one to complications of endovascular techniques.

The techniques of fenestrated, branched, and parallel stent grafts are described in detail in three main areas: arch, visceral, and iliac. Because these techniques and the technology itself are rapidly evolving, we felt it was important to summarize the evolution of approaches over the last decades using as many illustrations as possible in a didactic manner. The editor worked closely with Mr. David Factor, who has illustrated our work at the Mayo Clinic for many years. The collaboration between the editor and Mr. Factor took over 2 years and over 1000 h, which are reflected in over 600 illustrations (Fig. P.1) that depict every important technical aspect of these procedures. Although these illustrations accurately reflect the editor or authors' preferences, one must recognize that these are subject to rapid change.

It is the editor's hope that this collection of 49 chapters and over 600 special illustrations provided by an international panel of faculty experts will help enhance the diagnosis and treatment of complex aortic diseases using fenestrated, branched, and parallel stent grafts and, most importantly, will benefit patients in need with complex aortic aneurysms and dissections.

Rochester, MN, USA Gustavo S. Oderich

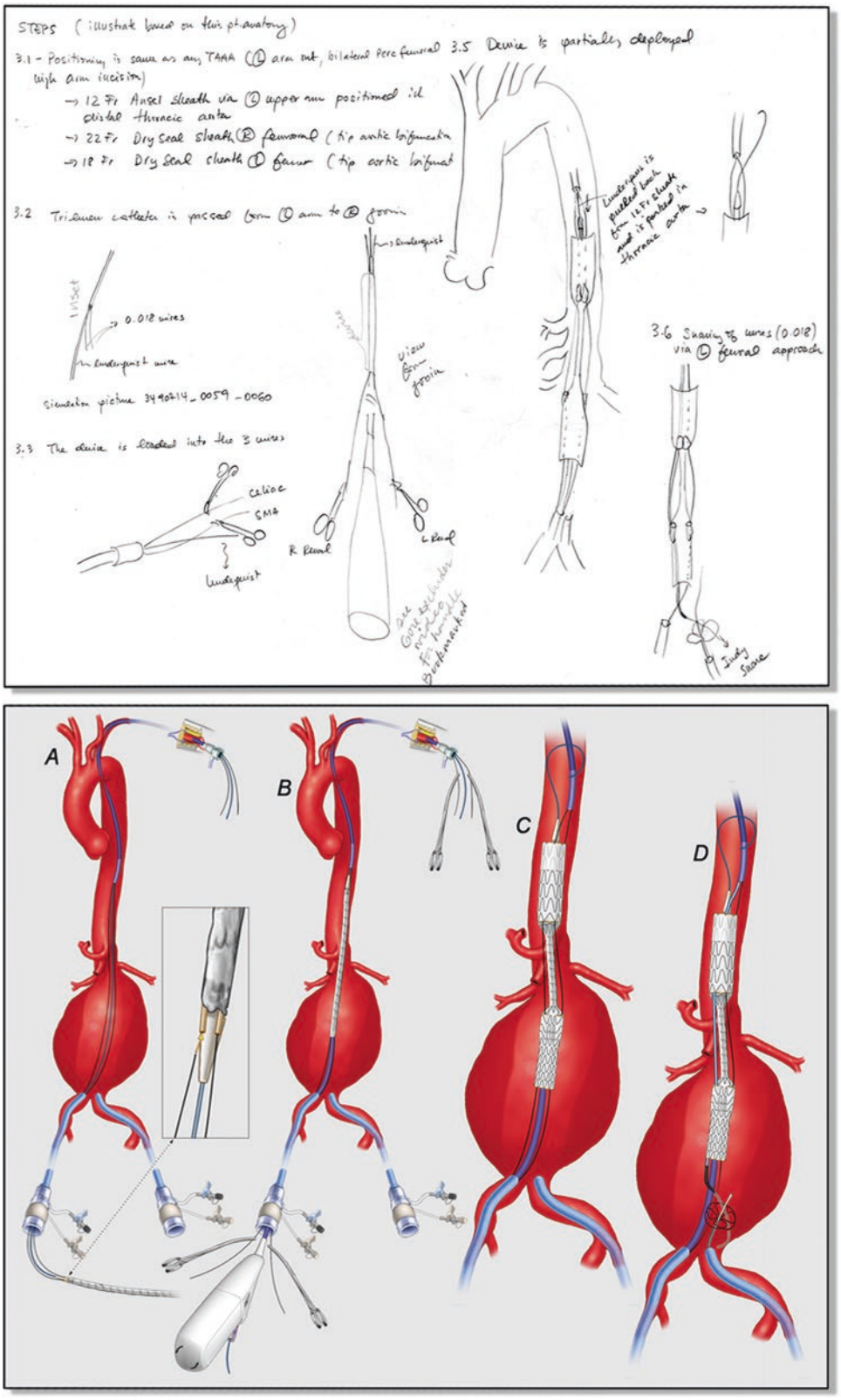


Fig. P.1 The editor and illustrator collaborated during 2 years to help create over 600 figures to depict techniques of fenestrated, branched, and parallel stent grafts. Note that the many sketches by the editor (*left panel*) are translated into expert illustrations (*right panel*)

About the Illustrator



David Factor

This book would not be possible without Mr. Factor and his 40 years of experience as a world-class medical illustrator. David obtained his bachelor's degree in fine arts in 1973 and Master of Science in Medical and Biological Illustration in 1975, both at the University of Michigan. Subsequently, he worked as medical illustrator at the University of California San Francisco (1976–1979), SUNY Upstate Medical Center (1979–1982), and as a freelance medical illustrator in Syracuse, NY (1982–1989). He joined the Mayo Clinic in 1989, contributing during the last 27 years with more than 10,000 illustrations appearing worldwide in textbooks, atlases, book chapters, scientific journals, and presentations.

Mr. Factor developed incredible acumen for endovascular procedures and its nuances in techniques and evolving technology. During the last decade, we had the chance to work on numerous projects, which have greatly enhanced the ability to describe and educate our colleagues, residents, and patients. For this book, we had countless meetings where I would share

sketches that would be translated into magnificent masterpieces displaying the art and science of complex endovascular procedures. His immense expertise and pursuit of perfection led to the creation of well over 2,000 illustrations compiled in 600 figures. As I tell my friends and colleagues, the top three things that kept me at the Mayo Clinic, for all these years was certainly not the weather, but Mr. Factor, my team, and my partners. It has been a privilege and an honor to work tirelessly with Mr. Factor on the creation of this magnificent book.

Gustavo S. Oderich
Editor

Acknowledgements

The editor would like to express great and humble appreciation to all the individuals who made this book possible. First, to my inspiring mentors who passed on to me their passion for complex aortic diseases and taught me the skills needed to treat these patients by open or endovascular approaches—in particular, Dr. Thomas Bower, Peter Gloviczki, and the late Dr. Roy Greenberg, master surgeons, friends, teachers, and role models, who never compromised the highest standards of ethics, science, technique, and patient care. To Mr. David Factor, our tireless illustrator, for his clinical acumen, eye for detail, and perfection, and Mr. James Rownd, who faithfully created the faces of key leaders in the field. To the section coordinators, authors, their secretaries, members of the Mayo Clinic Division of Scientific Publications, the staff from Springer, and especially our families, who supported us during this effort. I am especially appreciative of our publisher, Springer, and grateful to my development editor, Mrs. Diane Lamsback, for her wonderful and tireless job putting this book together.

Contents

Part I Basic Concepts, Mechanisms of Disease and Pre-operative Planning
Tiziano Tallarita and Gustavo S. Oderich

1 Historical Aspects and Evolution of Fenestrated and Branched Technology 3
Blayne Roeder, David Hartley, and Michael Lawrence-Brown

2 Mechanisms of Disease and Natural History 19
Bulat A. Ziganshin and John A. Elefteriades

3 Genetic Considerations in Patients with Aortic Disease 45
Sherene Shalhub

4 Normal Aortic Anatomy and Variations of Its Branches 63
Randall R. DeMartino

5 Classification Systems Relevant to Complex Endovascular Aortic Repair 73
Gustavo S. Oderich and Tiziano Tallarita

6 Intravascular Ultrasound to Guide Complex Endovascular Aortic Repair 95
David E. Timaran, Martyn Knowles, and Carlos H. Timaran

7 The Spinal Cord Collateral Network: Implications for Endovascular Aortic Repair 105
Sarah Geisbüsch, Gabriele Di Luozzo, Eva Botstein Griepp, and Randall B. Griepp

8 Role of Fusion Cone-Beam Computed Tomography Imaging During Complex Aortic Procedures 113
Timothy A. Resch, Per Törnqvist, and Nuno V. Dias

9 3D Printing to Create Templates for Patient-Specific Fenestrated Stent Grafts 125
Benjamin W. Starnes and Daniel F. Leotta

10 Preoperative Evaluation and Clinical Risk Assessment 131
Ying Huang and Gustavo S. Oderich

11 Computed Tomography/Computed Tomography Angiography for Evaluation, Planning, and Surveillance of Complex Endovascular Repair 149
Terri J. Vrtiska, Thanila A. Macedo, and Gustavo S. Oderich

12 Duplex Ultrasound for Evaluation and Surveillance of Fenestrated, Branched, and Parallel Stent-Grafts 189
Thanila A. Macedo and Gustavo S. Oderich

13 Magnetic Resonance Angiography for the Initial Assessment and Follow-Up of Acute Aortic Syndromes 201
Eric Y. Yang, Adeline Schwein, Dipan Shah, and Jean Bismuth

Part II Building Advanced Endovascular Aortic Programs
Jesse M. Manunga and Gustavo S. Oderich

14 Managing Endovascular Inventory 215
Jesse M. Manunga, Gustavo S. Oderich, Karl E. Bjellum, and Karen M. Bjellum

15 Integration of Clinical Practice, Research, Innovation, and Education 233
Gustavo S. Oderich and Jesse M. Manunga

16 Endovascular Training and Learning Curve for Complex Endovascular Procedures 245
Jesse M. Manunga and Gustavo S. Oderich

17 Regulatory Pathway for Physician-Sponsored Studies Evaluating Endovascular Aortic Repair 259
Dorothy Abel, Karen Ulisney, Fabienne J. Santel, and Jose Pablo Morales

18 Developing Physician-Sponsored Investigational Device Exemption Protocols 271
Benjamin W. Starnes

Part III Techniques of Implantation and Adjunctive Procedures to Minimize Complications
Aaron C. Baker and Gustavo S. Oderich

19 Principles of Side Branch Incorporation and "Bail Out" Maneuvers 277
Aaron C. Baker and Gustavo S. Oderich

20 Strategies to Minimize Risk of Spinal Cord Injury During Complex Endovascular Aortic Repair 295
Gustavo S. Oderich, Aaron C. Baker, and Peter Banga

21 Strategies to Minimize Risk of Acute Kidney Injury During Complex Endovascular Aortic Repair 313
Mark A. Farber and Raghuveer Vallabhaneni

22 Anesthetic Considerations for Complex Endovascular Aortic Repair 323
Juan N. Pulido, Erica D. Wittwer, Aaron C. Baker, and Gustavo S. Oderich

23 Techniques of Iliofemoral Conduit for Endovascular Repair 337
Aaron C. Baker and Gustavo S. Oderich

Part IV Visceral Artery Incorporation
Bernardo Mendes and Gustavo S. Oderich

24 Current Device Designs to Incorporate Visceral Arteries 349
Bernardo C. Mendes and Gustavo S. Oderich

25 Selection of Optimal Bridging Stents for Fenestrations and Branches 359
Bernardo C. Mendes and Gustavo S. Oderich

26 Sizing and Planning Fenestrated and Multibranched Endovascular Repair 375
Gustavo S. Oderich and Bernardo C. Mendes

27 Limitations for Branch Incorporation and Implications on Off-the-Shelf Designs 395
Bernardo C. Mendes, Mauricio S. Ribeiro, and Gustavo S. Oderich

28 Techniques of Implantation of Fenestrated and Multibranched Stent Grafts for Visceral Artery Incorporation 413
Gustavo S. Oderich and Bernardo C. Mendes

29 Results of Fenestrated, Branched, and Parallel Stent Grafts for Pararenal and Thoracoabdominal Aortic Aneurysms 449
Gustavo S. Oderich and Bernardo C. Mendes

30 Parallel Graft Techniques to Treat Complex Aortic Aneurysms Involving the Renal and Mesenteric Arteries 463
Jason T. Lee

31 Hybrid Repair Using Visceral Debranching and Aortic Stent Grafts to Treat Complex Aortic Aneurysms 483
Gustavo S. Oderich, Guillermo A. Escobar, Peter Gloviczki, Thomas C. Bower, and Bernardo C. Mendes

Part V Arch Branch Incorporation
Mohammad Ali Rana and Gustavo S. Oderich

32 Current Device Designs to Incorporate Supra-aortic Arch Trunks for Endovascular Repair 501
Muhammad Ali Rana and Gustavo S. Oderich

33 Technical Aspects and Results of Branched Endografts for Repair of Aortic Arch Aneurysms 507
Charles P.E. Milne, Stéphan Haulon, and Gustavo S. Oderich

34 Techniques and Results of Endovascular In Situ Arch Fenestrations 531
Joseph C. Wuamett, S. Sadie Ahanchi, and Jean M. Panneton

35 Parallel Stent Graft Techniques to Facilitate Endovascular Repair in the Aortic Arch 543
Frank J. Criado

36 Techniques and Results of Aortic Arch Hybrid Repair 555
Muhammad Ali Rana, Gustavo S. Oderich, and Alberto Pochettino

37 Techniques and Results of Hybrid Arch Replacement with Elephant Trunk 567
Ourania Preventza and Joseph S. Coselli

Part VI Internal Iliac Artery Branch Stent-Grafts
Javariah Fatima and Gustavo S. Oderich

38 Iliac Branch Device Designs 579
Javariah Fatima and Gustavo S. Oderich

39 Preoperative Planning and Sizing for Iliac Branch Devices 583
Javariah Fatima and Gustavo S. Oderich

40 Techniques of Endovascular Repair of Aorto-Iliac Aneurysms Using Iliac Branch Devices 595
Gustavo S. Oderich and Javariah Fatima

41 Results of Iliac Branch Stent-Grafts 623
Fabio Verzini, Gianbattista Parlani, Paola De Rango, Luca Farchioni, Gioele Simonte, and Piergiorgio Cao

42 Technical Aspects and Results of Hybrid Iliac Revascularization 641
Javairiah Fatima and Gustavo S. Oderich

43 Off-Label Use of Aortic Devices and Parallel Stent Grafts for Iliac Revascularization 651
David J. Minion

Part VII Physician-Modified Endovascular Stent-Grafts
Mauricio S. Ribeiro and Gustavo S. Oderich

44 Clinical Applications and Regulatory Issues for Physician-Modified Endovascular Grafts (PMEGs) 665
Jessica P. Simons and Andres Schanzer

45 Techniques of Physician-Modified Endovascular Grafts (PMEGs) for Incorporation of Renal Mesenteric Arteries 671
Gustavo S. Oderich and Mauricio S. Ribeiro

Part VIII Complications of Complex Endovascular Aortic Repair
Leonardo Reis de Souza and Gustavo S. Oderich

46 Thromboembolic Complications During Endovascular Repair of Complex Aortic Aneurysms 691
Mauricio S. Ribeiro, Leonardo Reis de Souza, and Gustavo S. Oderich

47 Spinal Cord Injury Prevention and Management 709
Matthew J. Eagleton

48 Renal Function Deterioration in Complex Aortic Repair 721
Leonardo Reis de Souza and Gustavo S. Oderich

49 Late Branch-Related Complications and Management 733
Meryl Davis, Jason Constantinou, and Tara Marie Mastracci

Index 745

Abbreviations

AAA	Abdominal aortic aneurysm
ACC/AHA	American College of Cardiology/American Heart Association
ACEI	Angiotensin-converting enzyme inhibitor
ACS	American College of Surgeons
AEC	Automatic exposure control
AKIN	Acute Kidney Injury Network
AOS	Aneurysms–osteoarthritis syndrome
ARB	Angiotensin II receptor blockers
ARMA	Anterior radicular–medullary arteries
ASA	American Society of Anesthesiology
ASA	Anterior spinal artery
bEVAR	Branched endovascular aortic repair
CAD	Coronary artery disease
ch-EVAR	"Chimney" techniques
CIN	Contrast-induced nephropathy
CLF	Centerline of flow
CNP	Collateral network pressure
COPD	Chronic obstructive pulmonary disease
CSF	Cerebrospinal fluid drainage
CT	Computed tomography
CTA	Computed tomography angiography
CTD	Connective tissue disease
CUSUM	Cumulative sum failure method
DTA	Descending thoracic aorta aneurysm
ePTFE	Expanded polytetrafluoroethylene
ESC/ESA	European Society of Cardiology/European Society of Anesthesiology
ET	Elephant trunk repair
EVAR	Endovascular abdominal aortic aneurysm repair
F-BEVAR	Fenestrated and branched EVAR
FEP	Fluorinated ethylene propylene
FEVAR	Fenestrated endovascular aortic aneurysm repair
GOLD	Global Initiative for Chronic Obstructive Lung Disease
HU	Hounsfield unit
IBE	Iliac branch endoprosthesis
IDE	Investigational device exemption
IVUS	Intravascular ultrasound
JAA	Juxtarenal aortic aneurysm
LDS	Loeys–Dietz syndrome
LSA	Left subclavian artery
MACE	Major adverse cardiac events
MAP	Mean arterial pressure
MFS	Marfan syndrome

MICA	Myocardial infarction cardiac arrest calculator
MIP	Maximum intensity projections
MLA	Measure minimum luminal area
MPR	Multiplanar reconstructions
MRI	Magnetic resonance imaging
NSQIP	National Surgical Quality Improvement Program
PAD	Peripheral arterial disease
PAU	Penetrating ulcers
PMEGs	Physician-modified endovascular grafts
PTFE	Polytetrafluoroethylene
RCRI	Revised cardiac risk index
SA	Segmental artery (intercostal or lumbar artery)
SCBF	Spinal cord blood flow
SCI	Spinal cord ischemia
SCPP	Spinal cord perfusion pressure
SFP	Spinal fluid pressure
TAAA	Thoracoabdominal aortic aneurysm
TAAD	Thoracic aorta leading to acute aortic dissections
TAASA	Thoracoabdominal segmental artery
TASP	Temporary aneurysm sac perfusion
TEE	Transesophageal echocardiography
TEVAR	Thoracic endovascular aortic repair
TIMP	Tissue inhibitor of metalloproteinase
TIVA	Total intravenous anesthesia
VEDS	Vascular Ehlers–Danlos syndrome
ZCLE	Zenith crimped limb extension

Contributors

Dorothy Abel Division of Cardiovascular Devices, Center for Devices and Radiological Health, United States Food and Drug Administration, Silver Spring, MD, USA

S. Sadie Ahanchi Division of Vascular Surgery, Eastern Virginia Medical School, Sentara Healthcare, Sentara Medical Group, Sentara Heart Hospital, Norfolk, VA, USA

Aaron C. Baker Division of Vascular and Endovascular Surgery, Department of Surgery, Mayo Clinic, Rochester, MN, USA

Peter Banga Department of Vascular Surgery, Cardiovascular Center, Semmelweis University, Budapest, Hungary

Jean Bismuth Department of Vascular Surgery, DeBakey Heart and Vascular Center, Houston Methodist Hospital, Houston, TX, USA

Karl E. Bjellum Division of Vascular and Endovascular Surgery and Division of Thoracic Surgery, Mayo Clinic, Rochester, MN, USA

Karen M. Bjellum Division of Vascular and Endovascular Surgery, Mayo Clinic, Rochester, MN, USA

Thomas C. Bower Division of Vascular and Endovascular Surgery, Mayo Clinic, Rochester, MN, USA

Piergiorgio Cao Gruppo Villa Maria GVM, Rome, Italy

Jason Constantinou Department of Vascular Surgery, Royal Free London NHS Foundation Trust, London, UK

Joseph S. Coselli Department of Surgery, CHI St Luke's Health-Baylor St. Luke's Medical Center, Texas Heart Institute, Houston, TX, USA

Division of Cardiothoracic Surgery, Department of Surgery, Baylor College of Medicine, Texas Heart Institute, Houston, TX, USA

Frank J. Criado Department of Vascular Surgery, MedStar Union Memorial Hospital, Baltimore, MD, USA

Meryl Davis Department of Vascular Surgery, Royal Free London NHS Foundation Trust, London, UK

Randall R. DeMartino Division of Vascular and Endovascular Surgery, Department of Surgery, Mayo Clinic, Rochester, MN, USA

Nuno V. Dias Vascular Center, Skane University Hospital, Malmö, Sweden

Matthew J. Eagleton Department of Vascular Surgery, Cleveland Clinic Lerner College of Medicine-CWRU, Cleveland, OH, USA

John A. Elefteriades Yale University School of Medicine, Aortic Institute at Yale-New Haven Hospital, New Haven, CT, USA

Guillermo A. Escobar Department of Vascular and Endovascular Surgery, University of Arkansas for Medical Sciences, Little Rock, AR, USA

Mark A. Farber Department of Surgery and Radiology, UNC Aortic Center, University of North Carolina, Chapel Hill, NC, USA

Luca Farchioni Unit of Vascular Surgery, Santa Maria della Misericordia, University of Perugia, Perugia, Italy

Javariah Fatima Division of Vascular and Endovascular Surgery, University of Florida, Gainesville, FL, USA

Sarah Geisbüsch Department of Vascular and Endovascular Surgery, Klinikum rechts der Isar der Technischen Universität München, Munich, Germany

Peter Gloviczki Division of Vascular and Endovascular Surgery, Mayo Clinic, Rochester, MN, USA

Eva Botstein Griepp Department of Cardiothoracic Surgery, The Mount Sinai School of Medicine, New York, NY, USA

Randall B. Griepp Department of Cardiothoracic Surgery, The Mount Sinai School of Medicine, New York, NY, USA

David Hartley Radiology Department, Royal Perth Hospital, Wannanup, WA, Australia

Stéphan Haulon Aortic Centre, Hôpital Cardiologique, Centre Hospitalier Régional Universitaire de Lille (CHRU), Lille, France

Ying Huang Division of Vascular and Endovascular Surgery, Mayo Clinic, Rochester, MN, USA

Martyn Knowles Department of Surgery, University of North Carolina Rex Hospital, Raleigh, NC, USA

Michael Lawrence-Brown Faculty of Health Sciences, Curtin University of Technology, Perth, WA, Australia

Jason T. Lee Division of Vascular Surgery, Stanford University Medical Center, Stanford, CA, USA

Daniel F. Leotta Applied Physics Laboratory, University of Washington, Seattle, WA, USA

Gabriele Di Luozzo Department of Cardiac Surgery, Hackensack University Medical Center, Hackensack, NY, USA

Thanila A. Macedo Department of Diagnostic Radiology, Mayo Clinic, Rochester, MN, USA

Jesse M. Manunga University of Minnesota, Minneapolis, MN, USA

Department of Vascular and Endovascular Surgery, Abbott Northwestern Hospital/Minneapolis Heart Institute, Minneapolis, MN, USA

Tara Marie Mastracci Department of Aortic Surgery, Royal Free London NHS Foundation Trust, London, UK

Bernardo C. Mendes Division of Vascular and Endovascular Surgery, Mayo Clinic, Rochester, MN, USA

Charles P.E. Milne Department of Surgery, The Alfred Hospital, Monash University, Melbourne, VIC, Australia

Aortic Centre, Hôpital Cardiologique, Centre Hospitalier Régional Universitaire de Lille (CHRU), Lille, France

David J. Minion Division of Vascular Surgery, University of Kentucky Medical Center, Lexington, KY, USA

Jose Pablo Morales Division of Cardiovascular Devices, Center for Devices and Radiological Health, United States Food and Drug Administration, Silver Spring, MD, USA

Gustavo S. Oderich Division of Vascular and Endovascular Surgery, Department of Surgery, Mayo Clinic, Rochester, MN, USA

Jean M. Panneton Division of Vascular Surgery, Eastern Virginia Medical School, Sentara Healthcare, Sentara Medical Group, Sentara Heart Hospital, Norfolk, VA, USA

Gianbattista Parlani Unit of Vascular Surgery, Santa Maria della Misericordia, University of Perugia, Perugia, Italy

Alberto Pochettino Department of Cardiovascular Surgery, Mayo Clinic Hospital, Rochester, MN, USA

Ourania Preventza Division of Cardiothoracic Surgery, Micheal E. DeBakey Department of Surgery, Baylor College of Medicine, Texas Heart Institute, Houston, TX, USA

Department of Surgery, CHI St Luke's Health-Baylor St. Luke's Medical Center, Texas Heart Institute, Houston, TX, USA

Juan N. Pulido Divisions of Cardiovascular Anesthesiology and Critical Care Medicine, Department of Anesthesiology, Mayo Clinic, Rochester, MN, USA

Muhammad Ali Rana Division of Vascular Surgery, University of New Mexico, Albuquerque, NM, USA

Timothy A. Resch Vascular Center, Skane University Hospital, Malmö, Sweden

Mauricio S. Ribeiro Department of Surgery and Anatomy, Ribeirão Preto Clinical Hospital, Ribeirão Preto Medical School, University of São Paulo, São Paulo, Brazil

Blayne Roeder Aortic Intervention, Cook Medical, Bloomington, IN, USA

Fabienne J. Santel Center for Devices and Radiological Health, United States Food and Drug Administration, Silver Spring, MD, USA

Andres Schanzer Division of Vascular and Endovascular Surgery, University of Massachusetts Medical School, Worcester, MA, USA

Adeline Schwein Department of Vascular Surgery, DeBakey Heart and Vascular Center, Houston Methodist Hospital, Houston, TX, USA

Dipan Shah Cardiovascular MRI Laboratory, DeBakey Heart and Vascular Center, Houston Methodist Hospital, Houston, TX, USA

Sherene Shalhub Department of Surgery, Division of Vascular Surgery, University of Washington Medical Center, Seattle, WA, USA

Jessica P. Simons Division of Vascular and Endovascular Surgery, University of Massachusetts Medical School, Worcester, MA, USA

Gioele Simonte Unit of Vascular Surgery, Santa Maria della Misericordia, University of Perugia, Perugia, Italy

Leonardo Reis de Souza Postgraduate Program in Surgery, School of Medicine, Universidade Federal do Rio Grande do Sul, Porto Alegre, Brazil

Benjamin W. Starnes Division of Vascular Surgery, Department of Surgery, University of Washington, Seattle, WA, USA

Tiziano Tallarita Division of Vascular and Endovascular Surgery, Mayo Clinic, Rochester, MN, USA

David E. Timaran Department of Surgery, University of Texas Southwestern Medical Center, Dallas, TX, USA

Carlos H. Timaran Division of Vascular and Endovascular Surgery, Department of Surgery, University of Texas Southwestern Medical Center, Dallas, TX, USA

Per Törnqvist Vascular Center, Skane University Hospital, Malmö, Sweden

Karen Ulisney Clinical Trials Program, Office of Device Evaluation, Center for Devices and Radiological Health, United States Food and Drug Administration, Silver Spring, MD, USA

Raghuveer Vallabhaneni Division of Vascular Surgery, Department of Surgery, University of North Carolina-Chapel Hill, Chapel Hill, NC, USA

Fabio Verzini Unit of Vascular Surgery, Santa Maria della Misericordia, University of Perugia, Perugia, Italy

Terri J. Vrtiska Section of Vascular CT, Department of Diagnostic Radiology, Mayo Clinic, Rochester, MN, USA

Erica D. Wittwer Department of Anesthesiology, Mayo Clinic, Rochester, MN, USA

Joseph C. Wuamett Division of Vascular Surgery, Eastern Virginia Medical School, Sentara Healthcare, Sentara Medical Group, Sentara Heart Hospital, Norfolk, VA, USA

Eric Y. Yang Baylor College of Medicine, Houston, TX, USA

Department of Medicine, Houston Methodist Hospital, Houston, TX, USA

Department of Cardiovascular Imaging, DeBakey Heart and Vascular Center, Houston Methodist Hospital, Houston, TX, USA

Bulat A. Ziganshin Yale University School of Medicine, Aortic Institute at Yale-New Haven Hospital, New Haven, CT, USA

Department of Surgical Diseases, Kazan State Medical University, Kazan, Russia

Part I

Basic Concepts, Mechanisms of Disease and Pre-operative Planning

1 Historical Aspects and Evolution of Fenestrated and Branched Technology

Blayne Roeder, David Hartley,
and Michael Lawrence-Brown

Introduction

Endovascular repair of aortic aneurysms (EVAR) has been disseminated worldwide since the first report by Juan Parodi in 1991 (Fig. 1.1). Since this initial disclosure, several innovators have worked on broadening the indications of EVAR to treat patients with complex anatomy. The Zenith AAA Endovascular Graft resulted from the collaboration of a global team of innovators. This team shared a common philosophy that the endovascular repair must seal in healthy aorta to provide a durable repair over the life of the patient. As a result of this philosophy, the Zenith was the first endovascular graft to incorporate proximal fixation and a modular three-piece system in combination with a delivery system that allowed for precise deployment. This enables the physician to place the graft in a position that takes advantage of all the available healthy aortic seal zone possible, while active fixation acts to maintain the seal over a prolonged period, ultimately resulting in a durable endovascular repair. Subsequently, nearly every commercially available endovascular graft for abdominal aortic aneurysm (AAA) repair has evolved to incorporate proximal fixation, modularity, and delivery systems offering more control of graft placement.

As experience grew in the early days of endovascular stent graft repair, it was quickly realized that not all patients were suitable candidates for standard infrarenal or thoracic endovascular grafts. These grafts were limited to the repair of lesions between the renal arteries and internal iliacs, or between the left subclavian and the celiac artery, where a suitable proximal and distal sealing zone remained without coverage of any major aortic branches. As disease encroached towards these branches, the options were to either compromise on the quality of the seal zones or incorporate the branches in order to have seal zones in healthy aorta. Driven by the aforementioned philosophy that the endovascular repair must land in a healthy segment of aorta to provide a durable repair, the group embarked upon developing the ability to incorporate critical branches into the seal zone. Ultimately these developments resulted in the possibility of treating patients with branches in the seal zones and branches arising from the aneurysm itself, making repair of complex thoracoabdominal (TAAA) and arch pathologies possible.

This chapter details the development of fenestrated and branched endografts from the first prototypes and clinical cases with simple fenestrated grafts in the late 1990s to the most recent developments where patients can be offered the possibility of endovascular treatment of the entire aorta from the sino-tubular junction to the internal and external iliacs.

Development of the Zenith Fenestrated Graft

The simplest structure that can be added to an endovascular graft to allow blood flow to a branch vessel is a fenestration (or hole) through the graft material. Challenges arise from the need to align the fenestration with the branch vessel during deployment, and in maintaining alignment with the vessel during the life of the endovascular repair, to ensure long-term branch patency. The need for three-dimensional precise alignment is the primary challenge in fenestrated endovascular repair when compared to infrarenal AAA repair. The Zenith AAA Endovascular Graft has a delivery system that allows for precise placement and proximal fixation to reduce migration and provide an ideal basis for incorporation of fenestrations.

B. Roeder (✉)
Aortic Intervention, Cook Medical,
750 Daniels Way, P.O. Box 489, Bloomington, IN 47402-0489,
USA
e-mail: Blayne.Roeder@CookMedical.com

D. Hartley
Radiology Department, Royal Perth Hospital,
73 Sandpiper Island, Wannanup, WA 6210, Australia
e-mail: david.hartley@cookmedical.com

M. Lawrence-Brown
Faculty of Health Sciences, Curtin University of Technology,
Bentley Campus, Perth, WA 6845, Australia
e-mail: mlabrown@iinet.net.au

© Mayo Foundation for Medical Education and Research 2017

G.S. Oderich (ed.), *Endovascular Aortic Repair*, DOI 10.1007/978-3-319-15192-2_1



Fig. 1.1 Parodi, Palmaz, and Barone from Argentina reported in 1991 (Ann Vasc Surg 1991(6): 491–499) their initial animal experiments and clinical experience with endovascular aortic aneurysm repair. By permission of Mayo Foundation for Medical Education and Research. All rights reserved

The first fenestrated repair was reported by Park in 1996 using a device modification to incorporate an accessory renal artery in a patient with infrarenal aneurysm. In 1997, Dr. Tom Browne (Fig. 1.2) with the research team in Perth led by Michael Lawrence-Brown and David Hartley demonstrated deployment of an endovascular graft in an animal model in which a fenestration was aligned both longitudinally and rotationally to perfuse an aortic branch, which would otherwise have been covered [1]. This was achieved by deploying the fenestration over a balloon placed in the orifice of the target vessel. The first successful clinical fenestrated endovascular aneurysm repair (Fig. 1.3) was completed the next year by Dr. John Anderson in Adelaide, Australia. The first case was not aligned by stent in the fenestration. Later, John Anderson and the Perth team ensured long-term alignment by placing a balloon-expanded stent to hold tight the fenestration and target orifice. The technique was quickly disseminated through workshops run in Perth to the rest of Australasia, Europe, and Southeast Asia. Wolf Stelter (1998) in Germany suggested a composite body to the stent graft with a tubular upper module and a separate distal bifurcated component (Fig. 1.4). The upper tubular module was adapted for the fenestrations in Australia and in the USA Roy Greenberg (2001) energetically took up the technology and, by the force of large numbers of cases, excellent data, and concise presentations, demonstrated to the world that it was a viable method of treatment. Michael Denton performed the first thoracoabdominal repair using the fenestrated endograft to incorporate the celiac axis and superior mesenteric artery (Fig. 1.5). In the initial version of the device, two wires were used to constrain, and reduce the diameter of the device in its posterior wall. Today, fenestrated grafts with up to five fenestrations and scallops are routinely placed to treat short-neck AAA, juxtarenal AAA, pararenal AAA, and type IV TAAAs.

The simple hole in the graft material evolved to include nitinol rings on the margins of the fenestration to make a more durable connection with the stent (Fig. 1.6a), and covered balloon-expandable stents replaced bare stents (Fig. 1.6b) as they proved a more durable repair [2]. The use of covered stents also facilitated bridging small gaps between the endograft and aortic wall without the endoleak that would otherwise occur through the bare stent and into the aneurysm.

As the technique developed, there were several deployment-related improvements that enhanced the Zenith system to better facilitate fenestrated endovascular repair. Gold radiopaque markers were added to demonstrate the margins of the fenestration under fluoroscopy and facilitate location and alignment of the fenestrations with their respective target arteries (see Fig. 1.6a). Diameter-reducing ties were added to partially constrain the graft following release of the graft from the delivery sheath (Fig. 1.6c). In this way, some repositioning of the endovascular graft to perfectly align the fenestrations was possible. Further, the "composite" design wherein the body of the graft was manufactured in two parts, the proximal fenestrated component being a tube, and a separate distal component being bifurcated, simplifies the procedure by allowing alignment of the fenestrations during deployment of the proximal fenestrated component independent of the positional requirements of the bifurcation. It is also perceived that the sliding connection between the proximal and distal components reduces displacement forces applied to the fenestrations and connecting stents in the event of movement of the bifurcated component.

These developments above are all features of the commercially available Zenith Fenestrated AAA Endovascular, which was CE marked in 2005 and following a prospective trial of 67 patients at 14 centers in the USA was approved by FDA in 2012. The trial reported 100 % technical success, and no aneurysm ruptures or conversions during a mean follow-up of 37 ± 17 months (range, 3–65 months), and patient survival was 91 ± 4 % at 5 years [3]. Patient follow-up will continue through 5 years.

Regardless of the clinical success of the fenestrated platform, the need to cannulate branch vessels through fenestrations in the graft and placement of stents through these

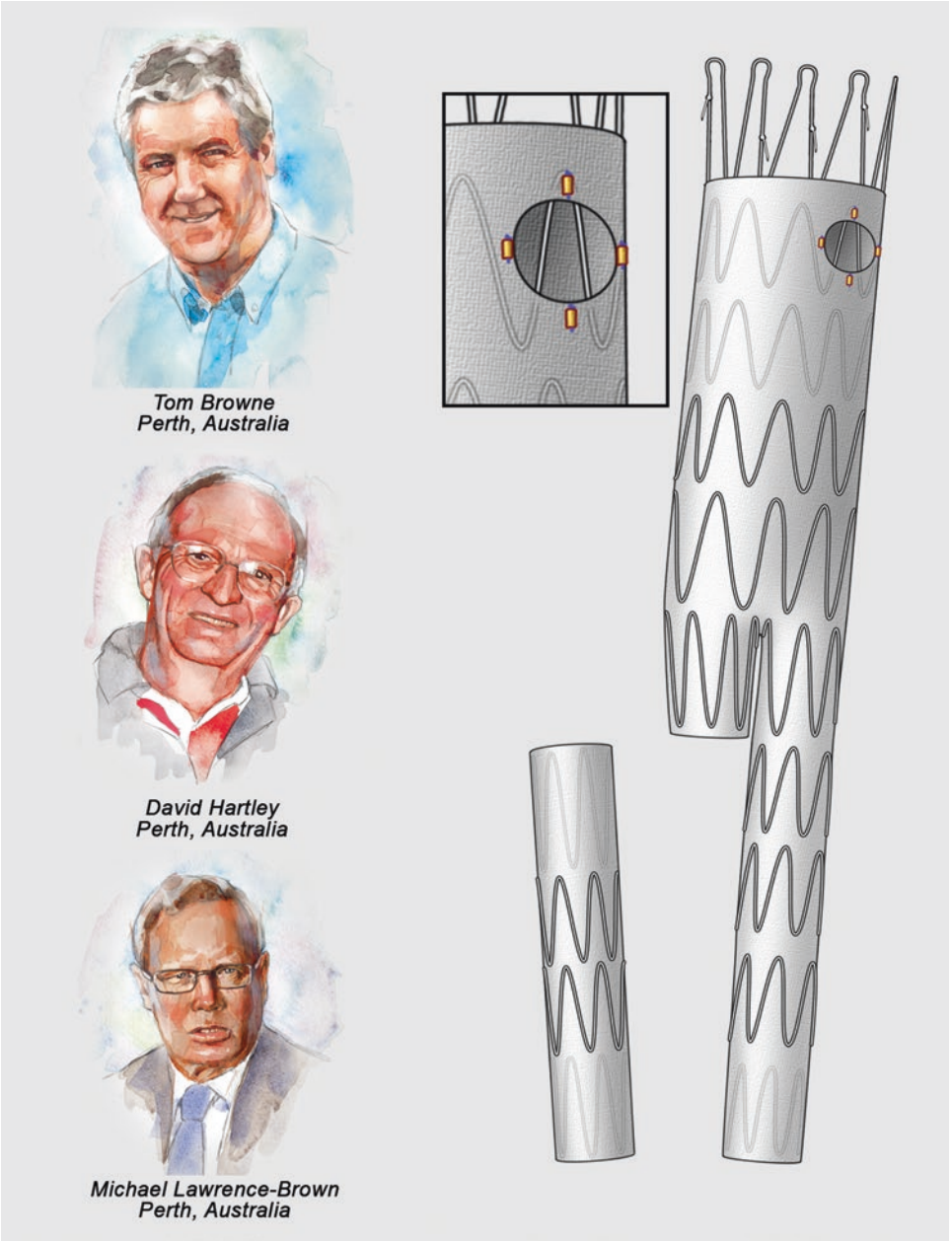


Fig. 1.2 The Perth research team of Tom Browne, David Hartley, and, led by, Michael Lawrence-Brown were instrumental in the initial animal experiments. The initial graft design was based on the Zenith Bifurcated Stent with suprarenal fixation. The fenestration was not reinforced and had radiopaque markers. Stent struts are noted across the fenestration, which at the time was not intended to be stented. The detailed designs and prototypes for the majority of the subsequent Cook production fenestrated and branched devices evolved out of the Perth R&D facility. By permission of Mayo Foundation for Medical Education and Research. All rights reserved

fenestrations from a contralateral approach added additional challenge to the procedure over a standard infrarenal AAA repair. In addition, the need to place the stents from a contralateral approach limited applicability of the fenestrated technique in patients without bilateral access. Towards these ends, and as suggested by Krassi Ivancev (Sweden), a novel preloaded delivery system (Fig. 1.7) was developed with its first use by Dr. Brendan Stanley in Perth, in May 2007, closely followed by Drs. Greenberg (USA), Ivancev (Sweden), Ferreira (Brazil), and Haulon (France), all of whom recognized the potential of the system to simplify procedures and contributed to its development. Rather than relying on contralateral access for targeting branch vessels, ports were added to the fenestrated delivery system to allow ipsilateral access with preloaded guide wires and sheaths for cannulation of target vessels and placement of the branch stents. The added inherent stability and control offered by the system simplifies vessel cannulation and placement of stents through the fenestrations.

The preloaded delivery system facilitated the most recent evolution of fenestrated repair: an off-the-shelf device to treat short-neck AAA, juxta-renal AAA, and pararenal AAA. Planning, manufacturing, and delivery of a fenestrated device built for a specific patient can take several weeks.



Fig. 1.3 The first clinical implant of a fenestrated stent using the Cook Zenith platform was performed by Dr. John Anderson in Adelaide, Australia. This illustration based on the actual case depicts a single left renal fenestration. The patient had been previously treated for a high-grade left renal stenosis by placement of a bare metal stent, which was carefully deployed inside the vessel. Note that the fenestration was non-reinforced and was not aligned by stent. By permission of Mayo Foundation for Medical Education and Research. All rights reserved

This delay limits the potential for this technology in patients who experience a rupture, are symptomatic, or have a large aneurysm. The Zenith p-Branch is an off-the-shelf fenestrated device. The device includes a large scallop for the celiac artery, a standard fenestration for the superior mesenteric artery, and two pivot fenestrations for the renal arteries (Fig. 1.8). The device is deployed as a standard fenestrated graft, with focus on alignment of the SMA fenestration with its target. The dome-shaped pivot fenestrations are designed to allow for offset of the renal arteries from the renal fenestrations. In this way, a singular device can be used to treat a range of patient anatomies. The additional stability and control afforded by the preloaded fenestration delivery system, which is part of the p-Branch package, help to offset possible challenges in cannulation of renal arteries from the fenestrations. Tim Resch followed by Stephan Haulon completed the first p-Branch cases in 2011 [4, 5] and pre-approval clinical studies are currently under way (see Fig. 1.8).

Preservation of Normal Anatomy

Another key philosophy from surgery translated into endovascular techniques is the preservation of normal anatomy whenever possible. It is possible to restore blood flow to critical branches via surgical bypasses in combination with standard endovascular grafts that cover and occlude blood flow the native vessel ostia or via so-called parallel grafts. Although such "hybrid techniques" were a critical step in treating more patients by endovascular approaches, they most definitely do not preserve normal anatomy and hybrid techniques have the further downside of necessitating surgical intervention in combination with the endovascular repair. Fenestrations are the foremost example of preservation of normal anatomy in endovascular aortic repair that incorporate blood flow to branch vessels. In fenestrated repair, the structure of the combined endovascular graft and covered bridging stent placed in the branch vessel often replicates the

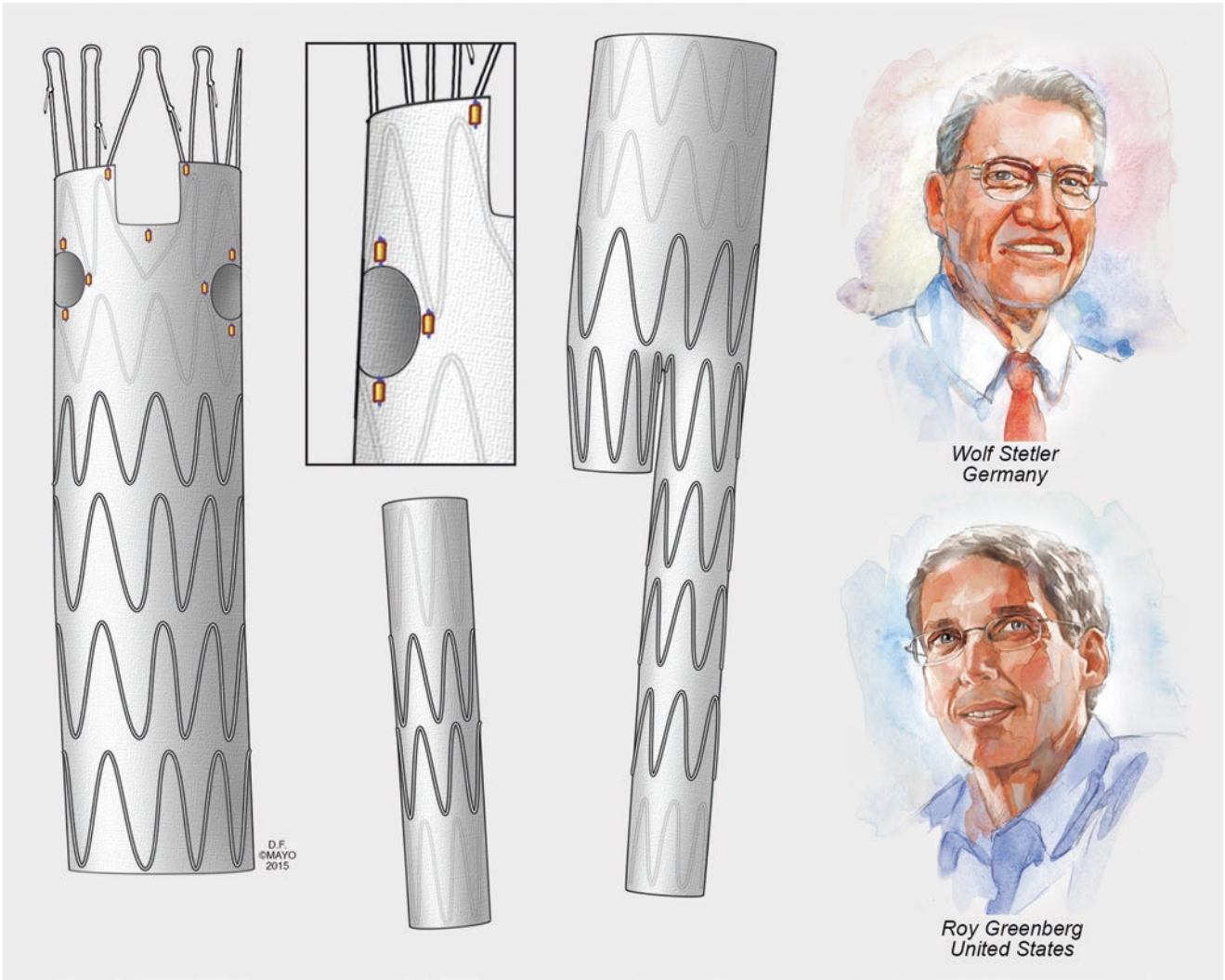


Fig. 1.4 Progress in the design of the fenestrated graft is credited to Wolf Stelter in Germany who suggested the concept of a separate tubular component with the fenestrations and a distal bifurcated component. Roy Greenberg in the USA is credited with applying the technology to wide clinical use, treating complex anatomy with multiple fenestrations and scallops in a large number of patients. The fenestrations at this point were not reinforced, but the design had evolved to avoid struts across the fenestrations, with the intention to align the fenestration to the target vessel with an "alignment" stent. By permission of Mayo Foundation for Medical Education and Research. All rights reserved

native anatomy to within a millimeter or two. In some instances, blood flow may even be optimized as any stenosis in the orifice may be resolved by the stents. Angulation and tortuosity of branches may provide additional challenges to branch stent conformance to the anatomy leading to distortion at the junction of the stents with the arteries or kinking of the stents. In practice, additional self-expanding stents are often added to help address these transitions and to provide long-term branch patency. The transition at the end of the distal end of the connecting stent in the target vessels remains a challenge with some of these procedures.

Directional Branches

Endovascular branched grafts used to maintain blood flow to critical aortic branches were not an independent innovation but rather a continued evolution of previous designs. The Chuter unibody bifurcated abdominal aortic graft in 1993 was the first example of a branch device, to preserve native anatomy and patency of both iliac arteries, when the common practice at the time was to employ an aorto-uniiliac graft and a surgical fem-fem crossover procedure. This was followed by modular bifurcated branch devices with off-the-

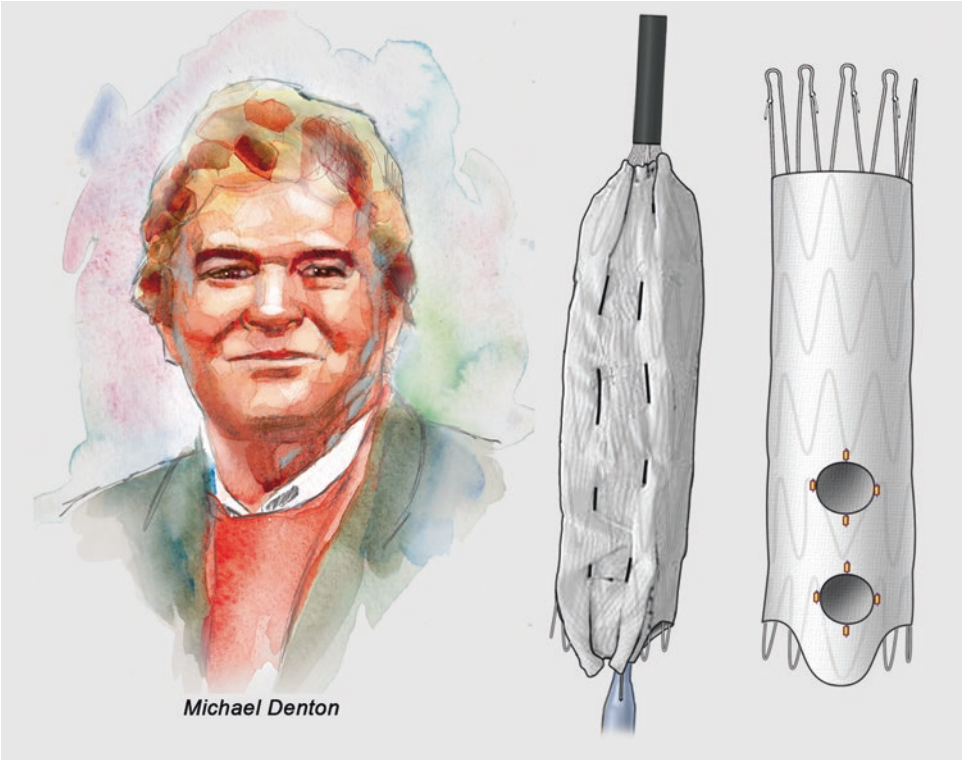


Fig. 1.5 Michael Denton collaborated with initial experience using the fenestrated stent to treat a distal thoracoabdominal aneurysm. By permission of Mayo Foundation for Medical Education and Research. All rights reserved

shelf components to accommodate a wide range of iliac artery anatomy and simplified the procedure by allowing implantation in a staged fashion. When the use of fenestrated grafts to save renal arteries began in 1997, it was a small step forward to use a covered stent in the fenestration, and turn it into what was effectively a side branch.

However, for the sake of clarity, branched endovascular grafts are now distinguished from their fenestrated counterparts by having a tubular protrusion arising from the main lumen of the endovascular graft. The rationale for using such a connecting structure is that when self-expanding bridging stents are used to bridge the gap across an aneurysm space, it provides more surface area for seal and security. It can also direct the bridging stents, aligning them towards the target vessel in a direction that matches native anatomy, and allows more latitude in the positioning of these bridging stents.

Initial development of branched endovascular grafts was focused in two areas: (1) a branch for the internal iliac artery in patients with iliac or aorto iliac aneurysms and (2) branches for the visceral vessels in patients with extensive TAAA. Today, branched stent grafts have evolved to include the treatment of aortic arch disease.

Iliac Branch Device

The first use of an iliac branch device to maintain flow to the internal iliac artery was performed successfully by Dr. Marcel Goodman in 2001 (Perth, WA). Professor Wolf Stelter (Frankfurt, Germany), also involved in the development of the iliac branch device (Fig. 1.9), completed the first large series of cases soon after that [6]. Initial attempts at iliac branch repair paralleled early approaches to complete infrarenal AAA repair with a unibody (single piece) bifurcated endovascular prosthesis. Similar to the experience with AAA repair, the device implantation was simpler and the required device sizes required to treat varying patient anatomy were reduced by a modular approach.

Ultimately, the graft design was similar to that of a standard iliac leg extension with a small branch added a few centimeters from the proximal end of the graft. Two unique versions of the device were developed. The first version had a straight branch that was designed to be used in combination with a balloon-expandable covered stent to bridge to the internal iliac artery. The second version, pioneered by Roy Greenberg (see Fig. 1.9), had a helical branch that intended to align the branch with the internal iliac and use a self-expandable covered stent to connect to the internal iliac. The philosophy behind the helical device was to better manage the often angulated takeoff of the internal iliac and narrowing in the iliac bifurcation [7].

The iliac branch device is intended to be the first component placed in the repair. The graft seals distally in the external iliac artery and can land proximally at or below the aortic bifurcation. A preloaded catheter facilitates placement of a femoral-to-femoral through-wire that further

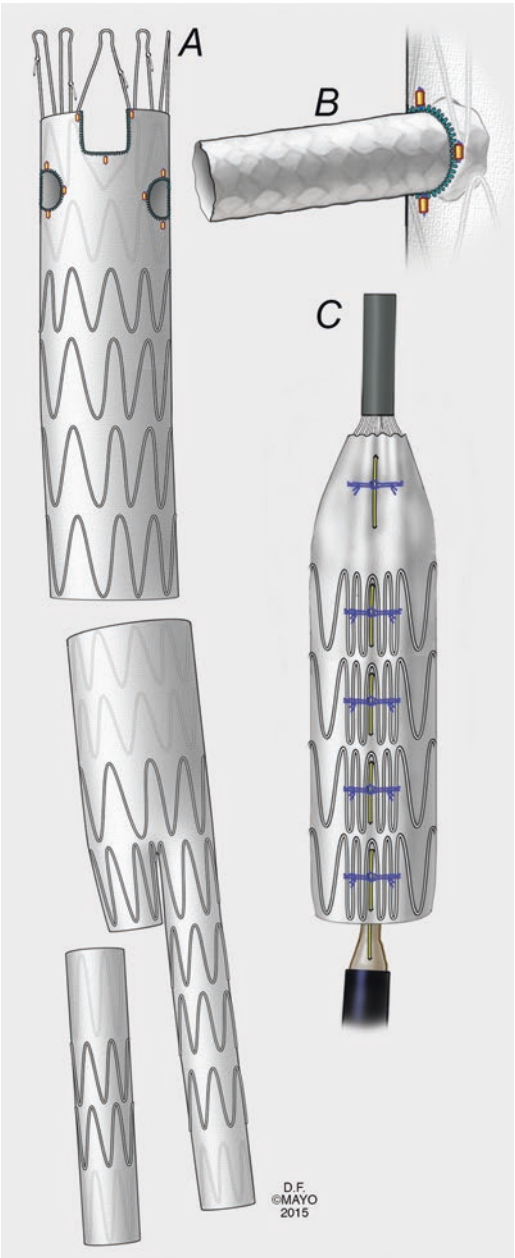


Fig. 1.6 Evolution of the Zenith fenestrated graft included the addition of a nitinol-reinforced ring and gold radiopaque markers (**a**), the use of covered stents to replace bare metal stents for alignment of fenestrations (**b**), and diameter-reducing ties (**c**). By permission of Mayo Foundation for Medical Education and Research. All rights reserved

facilitates access to the branch, stability during cannulation of the internal iliac artery, and placement of the bridging stent from a contralateral approach. The repair is completed with a bifurcated device deployed above the iliac branch device and short limb connecting the short limb of the bifurcated device to the proximal end of the iliac device prosthesis. The Zenith Branch Endovascular Graft was CE marked in 2006 with the helical version approved in 2007. The pivotal US trial completed enrollment in early 2015. FDA approval is expected in 2016.

A third iliac branch device, the bi-branch was developed in collaboration with Dr. Stephen Cheng in Hong Kong and Roy Greenberg and is currently under clinical evaluation at the Cleveland Clinic (see Fig. 1.9). The device incorporates the branch for the internal iliac in the leg of a bifurcated prosthesis rather than in a leg extension. The repair is completed with a proximal cuff landing below the renal arteries and a contralateral iliac leg extension. The concept was originally developed for use in patients with short common iliac arteries, because removal of two modular connections between the aortic graft bifurcation and the internal iliac branch shortened the overall length of the device. The device also found favor in use for preservation of internal iliac arteries in combination with other composite systems such as fenestrated or TAAA repairs. Preservation of internal iliac arteries is critical in TAAA repairs to minimize the risk of paraplegia.

Thoracoabdominal Multibranch Repair

Dr. Tim Chuter (Fig. 1.10) implanted the first multibranched device for TAAA repair [8]. The branched component had four branches (Fig. 1.10a), and was physician-manufactured and constructed of Z-stents sewn to Dacron fabric and remarkably similar to the design of visceral branched grafts manufactured today with two 8 mm braches for the SMA and celiac arteries and two 6 mm branches for the renal arteries.

The first Cook-manufactured side branch was in the form of a short extension (Fig. 1.10b), only a few millimeters long, attached to the outside of a fenestration in a thoracoabdominal fenestrated endovascular graft. This graft was placed by John Anderson in 2002. The axis of these early cuffs was orthogonal to the long axis of the graft but soon evolved in accordance with the principle of the Chuter design to have the cuffs arise from the graft at a lesser angle, nearly parallel to the graft itself (see Fig. 1.10b). In a further development of the original Chuter design, the side branches were manufactured to minimize profile, and strategically placed above each target vessel such that they could be cannulated and stents placed in an antegrade fashion (Fig. 1.10c). The graft evolved to its current design (t-Branch stent graft) with four directional branches as an off-the-shelf alternative (Fig. 1.10d).

An alternative configuration conceived and most commonly used by Roy Greenberg had helical branches to preserve flow to the celiac and SMA and fenestrations with covered stents to provide flow to the renal arteries. Although use of helical branches in the treatment of TAAA is less common than straight branches, device strategies that primarily combine branches for the SMA and celiac and fenestrations for the renal arteries are commonplace today.

Key design principles for the ideal branch are as follows: the branches should be short in length, long-overlap is essential for a stable repair and long-term durability, and the trajectory of

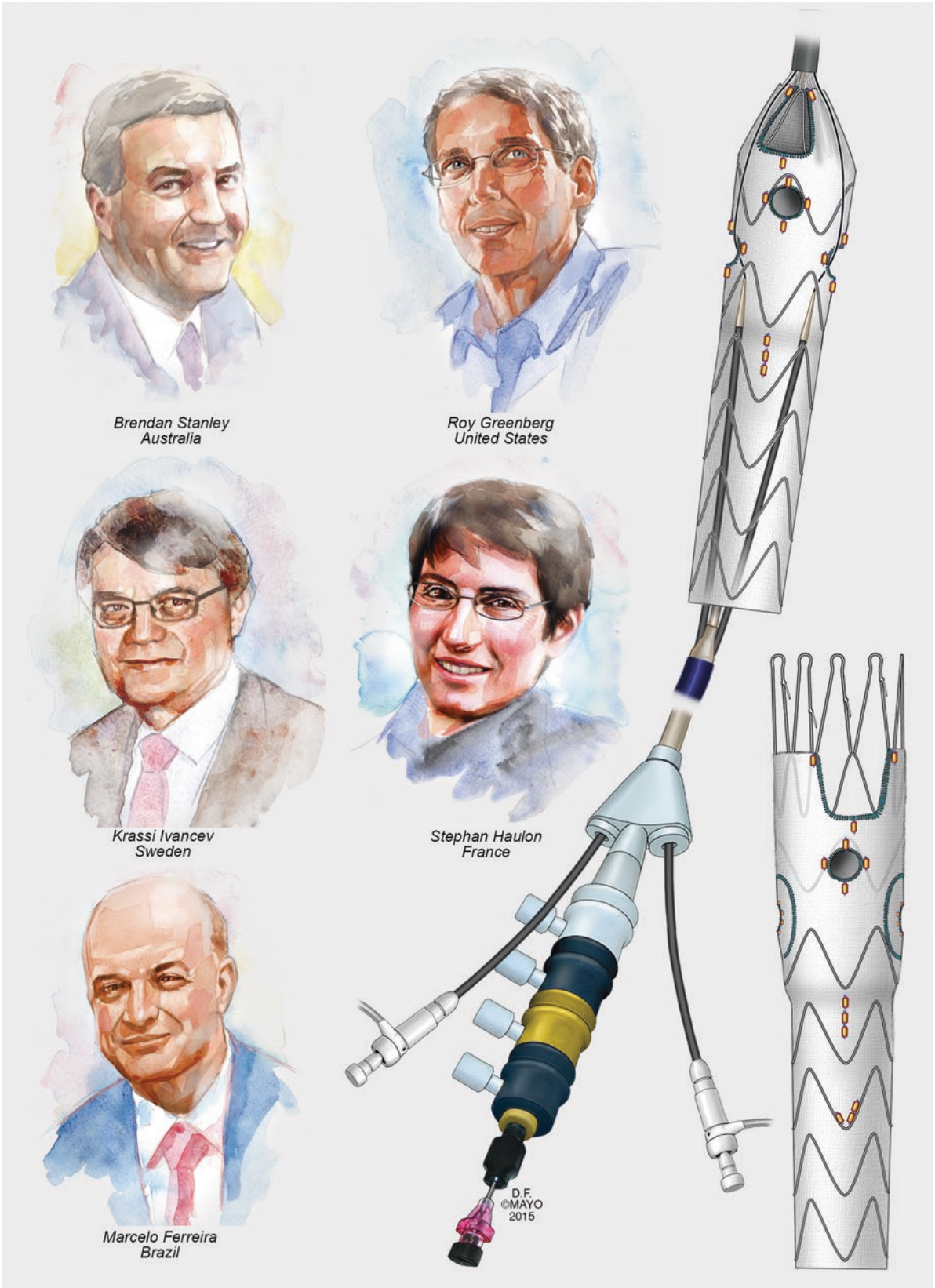


Fig. 1.7 Development of the preloaded delivery system to facilitate fenestrated repair was first suggested by Ivancev, and became a collaboration of multiple investigators including Drs. Stanley (Australia), Greenberg (USA), Ivancev (Sweden), Haulon (France), and Ferreira (Brazil). By permission of Mayo Foundation for Medical Education and Research. All rights reserved

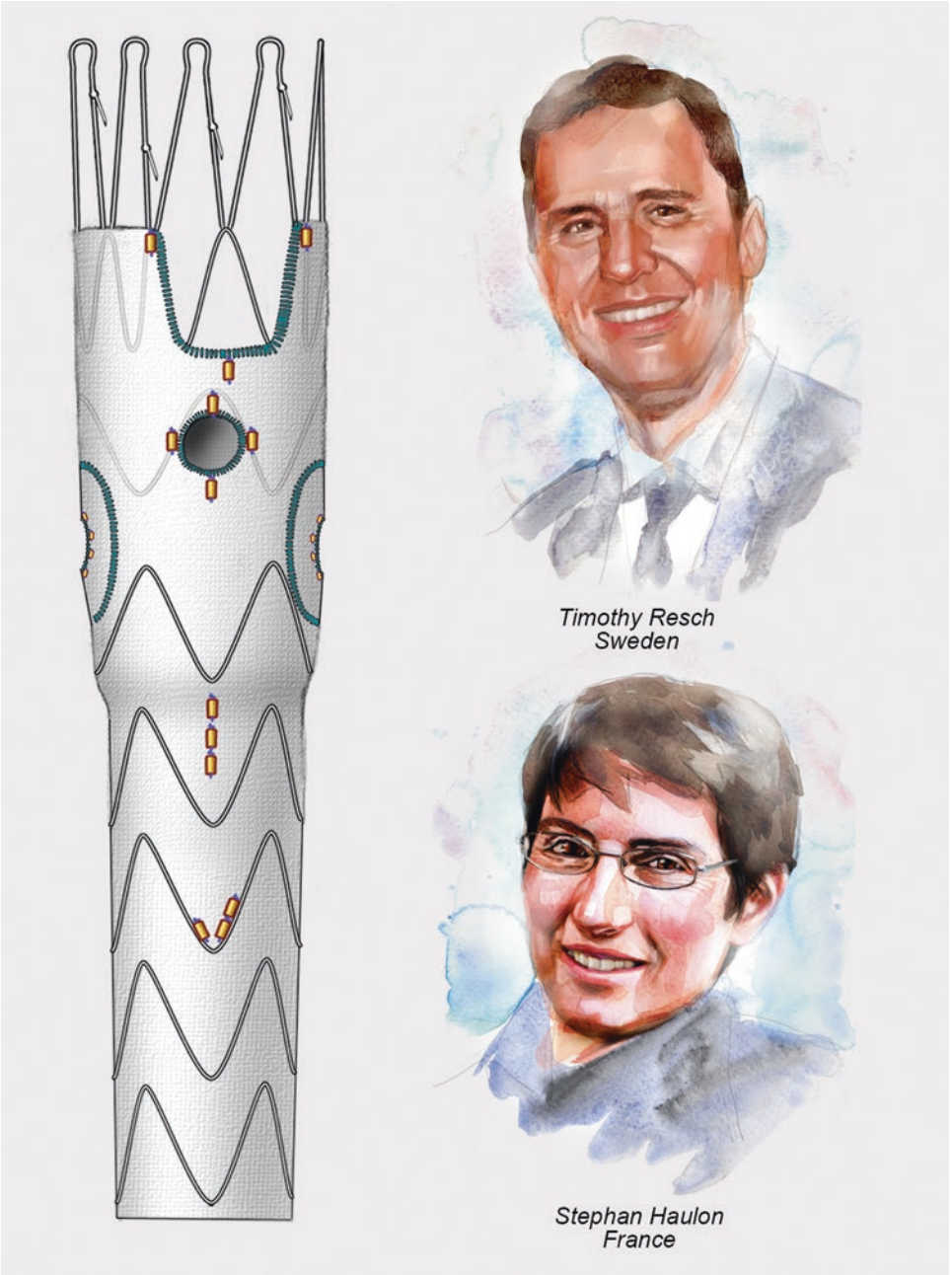


Fig. 1.8 The p-Branch fenestrated graft evolved as an off-the-shelf alternative to treat juxta-renal abdominal aortic aneurysms. The device has a double-wide scallop for the celiac axis, a fenestration for the superior mesenteric artery, and two pivot fenestrations for the renal arteries. The initial clinical experience was by Tim Resch in Sweden and Stephan Haulon in France. By permission of Mayo Foundation for Medical Education and Research. All rights reserved

the branch as it arises from the graft should be aligned with the target vessel. In this way, angulation of the branch stent and tendency towards kink is greatly reduced. Regardless of branch configuration, these principles provide a solid foundation for design of fenestrated and branched endovascular repairs.

In theory, endovascular branches spanning an aneurysmal space allow some flexibility in offset of the branch from the target vessel. Taking advantage of this property, Tim Chuter's suggestion to the research team in 2008 proposed a standardized design for a TAAA branched graft [9]. This analysis determined that a majority of patient's visceral vessel anatomy could be accommodated with a single four-branch configuration, something that could potentially be available off the shelf. Ultimately the Zenith t-Branch, an off-the-shelf four-branch device to treat TAAA was CE marked in 2012 (see Fig. 1.10d).

In spite of the availability of an off-the-shelf solution, a significant portion of endovascular TAAA repairs are still completed using grafts manufactured for specific patients. Advantages to this approach include tailoring branch and potentially fenestration locations and branch graft dimensions

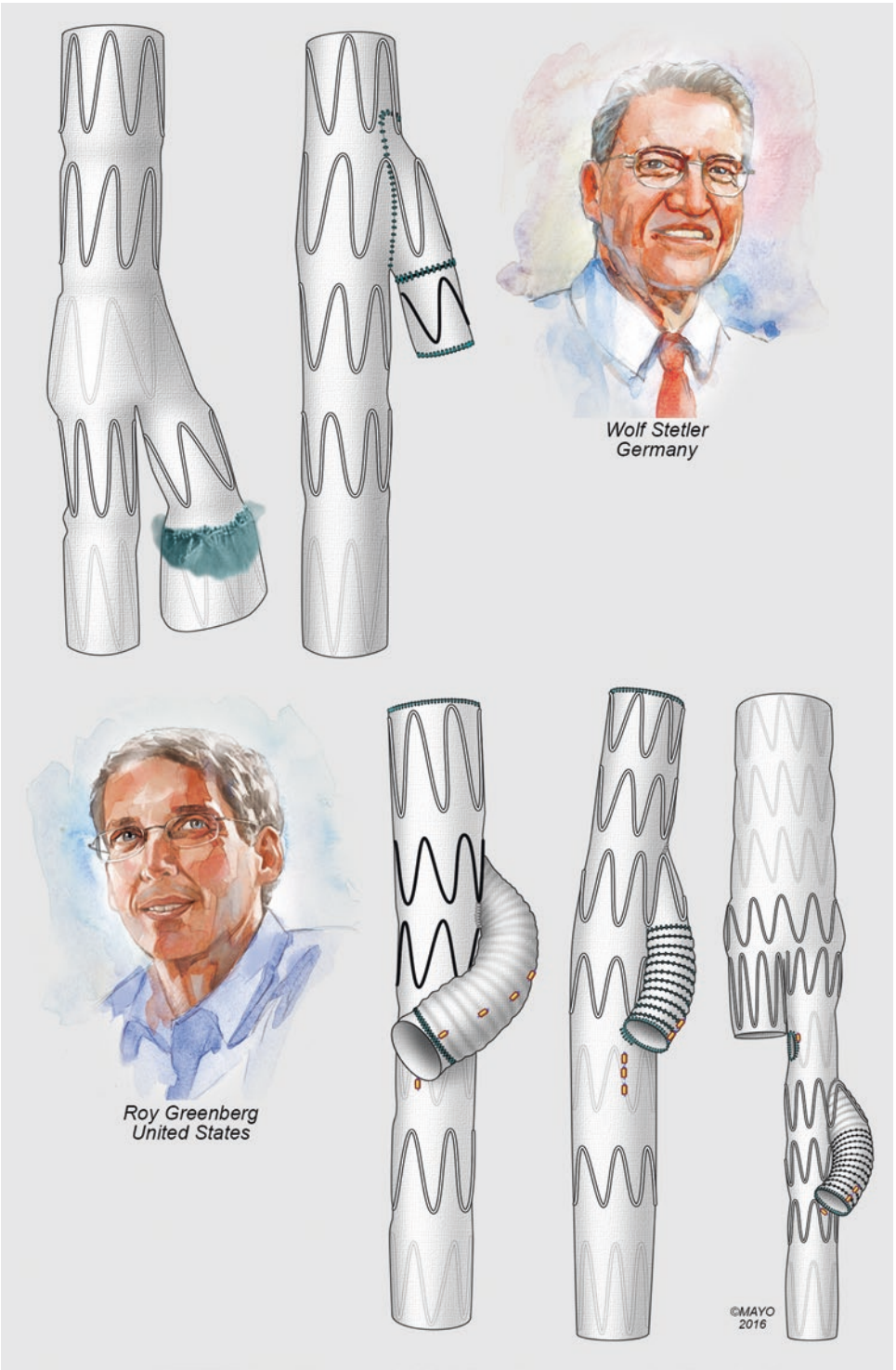


Fig. 1.9 Evolution of endovascular repair to extend the landing zone into the external iliac artery required creation of an iliac branch device. The initial case by Marcel Goodman (Australia) and a larger clinical experience by Wolf Stelter (Germany) using the prototype depicted in the illustration, which evolved later into the straight iliac branch device currently utilized. The helical branch pioneered by Roy Greenberg later evolved into a bifurcated-bifurcated device with a helical branch. By permission of Mayo Foundation for Medical Education and Research. All rights reserved

to fit an individual patient's anatomy. Branches can even be included that have an upwards orientation if such a design will be a better match for the target vessel anatomy. Branch/fenestration locations that accurately match a patient's anatomy have the potential to simplify deployment and improve outcomes. Custom tailoring of graft dimensions may also reduce the number of components required for the repair and limit the amount of coverage in the thoracic aorta. For these reasons, device usage for TAAA repair remains a split between off-the-shelf designs and grafts built for a specific patient.

The first low-profile TAAA repair was completed in early 2011 by Tim Chuter at the University of California, San

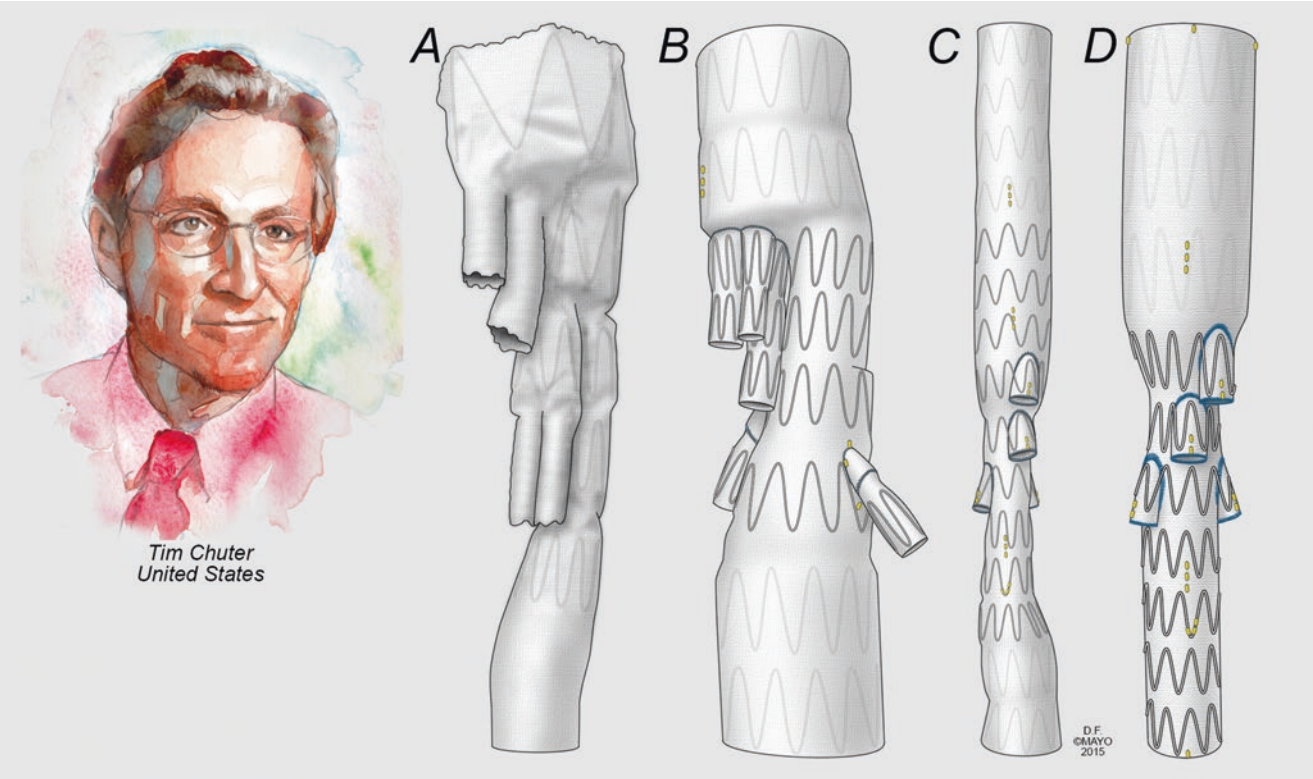


Fig. 1.10 Tim Chuter is credited for the development and first clinical use of a multibranched thoracoabdominal device. The illustration depicts evolution of the device based on photographs of the first implant (**a**), first versions of a manufactured device (**b**, **c**), and current off-the-shelf t-branch stent graft (**d**). By permission of Mayo Foundation for Medical Education and Research. All rights reserved

Francisco. The graft had four downward-facing branches similar to the Zenith t-Branch. Delivery sheath profile was reduced by 4 Fr from 22Fr to 18Fr. Low-profile systems may provide the biggest benefit in the thoracic aorta as graft delivery systems are often larger to begin with and TAAA occur at a higher rate in women who often present with access challenges.

Arch Branch Device

As with short-necked infrarenal aortic aneurysms, where fenestrations and scallops were used to move the seal to a more proximal region, the same concept was applied in thoracic grafts, with scallops and fenestrations used to extend the sealing zone proximally to the level of the innominate, left common carotid and left subclavian arteries (Fig. 1.11a). The first clinical case performed by Dr. Peter Mossop and Ian Nixon in Melbourne, Australia, occurred in 2000 and had a fenestration to preserve the flow in a left subclavian artery.

This approach required extreme accuracy in deployment to align fenestrations and scallops with target vessels. Deployment of the graft in the arch from a femoral approach makes precise positioning a challenge. Preloaded catheters were used to assist in alignment of fenestrations and scallops to the vessels, but this technique still provided a challenge especially in difficult anatomy, even for very skilled operators.

The first case of a branched endovascular graft involving all of the branches in the arch was described by Tim Chuter in 2003 [10]. This approach relied on debranching of the arch, including carotid-carotid and carotid-subclavian bypasses. The branch graft was delivered through the right carotid artery and sealed proximally in the ascending aorta and in the innominate trunk (Fig. 1.11b). A single large-diameter branch directed to the distal arch. A standard thoracic graft delivered from a femoral approach, landing in this branch, completed the repair. A primary limitation of this technique was the requirement of a large-caliber delivery sheath for the branch graft through the right carotid artery.

Early endovascular approaches described above and experience from hybrid techniques where cervical debranching and a bypass arising from the ascending aorta are used in combination with standard thoracic endograft sealing proximally in the distal ascending aorta provided the initial experience with endografts in the ascending aorta and arch. Combined, these techniques clearly demonstrated the potential benefits but also the primary challenges associated with arch endovascular repair:

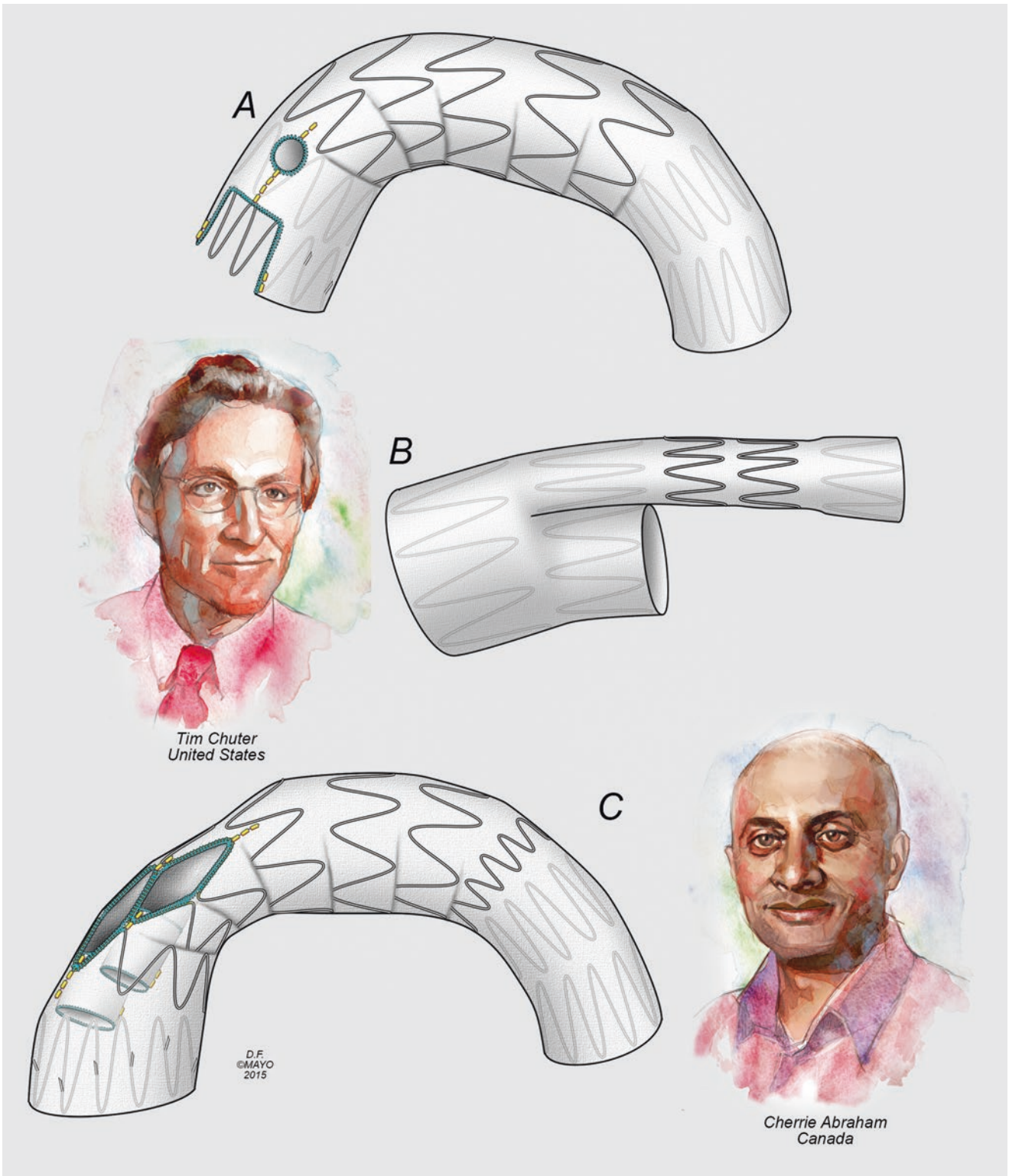


Fig. 1.11 Evolution of the arch branch device from initial experience using fenestrations and scallops (**a**) to the first full arch repair by Tim Chuter (**b**). The first clinical use of the third-generation device with diamond-shaped fenestrations is credited to Cherrie Abraham (**c**). By permission of Mayo Foundation for Medical Education and Research. All rights reserved

accuracy in landing, conformance to the aorta, access challenges, morbidity from surgical bypasses, mortality, and stroke.

In late 2009, the first multibranched graft for a total arch repair was implanted by Cherrie Abraham (Fig. 1.11c) in Montreal, Canada, who also described the initial experience with the technique [11]. Cases soon followed using a slightly modified design including completely internal cuffs and branches with Tim Chuter, Roy Greenberg, Krassi Ivancev, Stephan Haulon, and Brendan Stanley contributing to the design. The graft is intended to land in the ascending aorta and eliminates the need for precise positioning with respect to the branches of the arch. Moreover, the introducer is designed to rotationally align the branches to the outer curve of the arch. The branches are internal to the endograft and incorporate a wide, diamond-shaped opening to facilitate retrograde cannulation. Although it was initially applied to patients with arch aneurysms, the technique has found applicability in patients with chronic type A dissection [12]. Patients with prior surgical repair of the ascending aorta often present with the need to repair the remainder of the arch. The surgical graft provides an excellent landing zone for an endovascular repair. Iterative improvements are still under way. One such modification to the delivery system allows treatment of patients with a mechanical aortic valve [13]. Results with the latest versions have been generally better than previous approaches, but clinical evaluation is still under way [14].

Dissemination of the Technique

It is important to note the significance of a global, collaborative, multidisciplinary team to translate their philosophies, ideas, and technologies into viable new devices and therapies for patients. The original collaborators were not from a single specialty. Many of the innovators undertook multidisciplinary training programs in vascular surgery and interventional radiology. One example of many is the Malmo experience where Krassi Ivancev contributed his enthusiasm and interventional radiology skills and knowledge together with the vascular surgery specialty to form a multidisciplinary endovascular unit. A measure of the success of this approach is that the unit attracted visitors such as those with the talents of Tim Chuter, and Roy Greenberg, who, along with many others trained, benefited, and contributed to the development of the technology. The global team importantly included innovative engineers and technicians who not only applied their skills in prototype manufacture development and testing, but because of their close involvement, and understanding of the clinical, technical, and regulatory requirements and opportunities, contributed significantly to the concept and detailed specification of devices for clinical research programs in countless locations around the world. Even after the field of endovascular surgery became established, embarking on repairs of the aortic arch involved collaboration with cardiac and thoracic surgeons. As a result of this collaboration, branched and fenestrated devices are now capable, in many instances of treating aneurysms and dissections of the entire aorta.

The philosophy of fenestrated and branched stent graft technology is based on a common set of fundamental principles: achieving seal in healthy aorta, matching the native anatomy whenever possible, and optimizing the endovascular repair for long-term durability. Although initially theoretical, these design philosophies have been validated with clinical data that has enabled extension of the technology from the initial treatment of a limited number of patients under compassionate use to commercially available devices that are used to treat thousands of patients each year. In summary the initial fenestrated experience from Australia [15] provided the impetus to disseminate the techniques, particularly in Europe, with CE-marked devices. In the USA, Roy Greenberg was the primary driver of clinical studies for branched and fenestrated endovascular grafts with now over 1000 patients enrolled in the studies he initiated in prospective clinical trials at the Cleveland Clinic [15, 16]. His large database and his willingness to share his experience contributed significantly in the acceptance of these techniques internationally. The many he trained, including Matt Eagleton, Stephan Haulon, Tara Mastracci, Gustavo Oderich, and Tim Resch, not only continue his studies, but have also developed comprehensive endovascular research programs around the globe (Fig. 1.12). In parallel, Eric Verhoeven has developed the largest European experience approaching 1000 fenestrated and branched cases in his centers and cases proctored in other centers. Experienced physicians proctoring new users of the technology have been critical in dissemination of fenestrated and branched devices. Finally, multicenter, prospective clinical studies have also been completed in the case of Zenith Fenestrated with more studies progressing. In aggregate, these studies prove that when designed appropriately, branched and fenestrated repairs can be safe, effective, and durable. It remains to build on these designs and further disseminate the technology so more patients may benefit in the future.



Fig. 1.12 Dissemination of endovascular experience with fenestrated and branched endografts around the globe. Eric Verhoeven is credited with the largest clinical experience in Europe. Graduates of the Cleveland Clinic Aortic Program later developed extensive clinical experience and research programs, including Stephan Haulon (Lille, France), Tim Resch (Malmo,Sweden), Gustavo Oderich (Rochester, USA), Matt Eagleton (Cleveland, USA), and Tara Mastracci (London, UK). By permission of Mayo Foundation for Medical Education and Research. All rights reserved

References

1. Browne TF, Hartley D, Purchas S, Rosenberg M, Van Schie G, Lawrence-Brown M. A fenestrated covered suprarenal aortic stent. Eur J Vasc Endovasc Surg. 1999;18(5):445–9.
2. Mohabbat W, Greenberg RK, Mastracci TM, Cury M, Morales JP, Hernandez AV. Revised duplex criteria and outcomes for renal stents and stent grafts following endovascular repair of juxtarenal and thoracoabdominal aneurysms. J Vasc Surg. 2009;49(4):827–37.
3. Oderich GS, Greenberg RK, Farber M, Lyden S, Sanchez L, Fairman R, et al. Results of the United States multicenter prospective study evaluating the Zenith fenestrated endovascular graft for treatment of juxtarenal abdominal aortic aneurysms. J Vasc Surg. 2014;60(6):1420–8.
4. Resch TA, Dias NV, Sobocinski J, Sonesson B, Roeder B, Haulon S. Development of off-the-shelf stent grafts for juxtarenal abdominal aortic aneurysms. Eur J Vasc Endovasc Surg. 2012;43(6):655–60.
5. Kitagawa A, Greenberg RK, Eagleton MJ, Mastracci TM. Zenith p-branch standard fenestrated endovascular graft for juxtarenal abdominal aortic aneurysms. J Vasc Surg. 2013;58(2):291–300.

6. Ziegler P, Avgerinos ED, Umscheid T, Perdikides T, Erz K, Stelter WJ. Branched iliac bifurcation: 6 years experience with endovascular preservation of internal iliac artery flow. J Vasc Surg. 2006;46(2):204–10.
7. Wong S, Greenberg RK, Brown CR, Mastracci TM, Bena J, Eagleton MJ. Endovascular repair of aortoiliac aneurysmal disease with the helical iliac bifurcation device and the bifurcated-bifurcated iliac bifurcation device. J Vasc Surg. 2013;58(4):861–9.
8. Chuter TA, Gordon RL, Reilly LM, Pak LK, Messina LM. Multibranched stent-graft for type III thoracoabdominal aortic aneurysm. J Vasc Interv Radiol. 2001;12(3):391–2.
9. Sweet MP, Hiramoto JS, Park KH, Reilly LM, Chuter TA. A standardized multi-branched thoracoabdominal stent-graft for endovascular aneurysm repair. J Endovasc Ther. 2009;16(3):359–64.
10. Chuter TA, Schneider DB, Reilly LM, Lobo EP, Messina LM. Modular branched stent graft for endovascular repair of aortic arch aneurysm and dissection. J Vasc Surg. 2003;38(4):859–63.
11. Lioupis C, Corriveau MM, MacKenzie KS, Obrand DI, Steinmetz OK, Abraham CZ. Treatment of aortic arch aneurysms with a modular transfemoral multibranched stent graft: initial experience. Eur J Vasc Endovasc Surg. 2012;43(5):525–30.
12. Spear R, Kaladji A, Roeder B, Haulon S. Endovascular repair of a chronic arch dissecting aneurysm with a branched endograft. Ann Thor Surg. 2013;96(2):e39–41.
13. Spear R, Azzaoui R, Maurel B, Sobocinski J, Roeder B, Haulon S. Total endovascular treatment of an aortic arch aneurysm in a patient with a mechanical aortic valve. Eur J Vasc Endovasc Surg. 2014;48(2):144–6.
14. Haulon S, Greenberg RK, Spear R, Eagleton M, Abraham C, Lioupis C, Verhoeven E, et al. Global experience with an inner branched arch endograft. J Thorac Cardiovasc Surg. 2014;148(4):1709–16.
15. Anderson JL, Berce M, Hartley DE. Endoluminal Aortic Grafting with Renal and Superior Mesenteric Artery Incorporation by Graft Fenestration. J Endovasc Ther. 2001;8(1):3–15.
16. Mastracci TM, Eagleton MJ, Kuramochi Y, Bathurst S, Wolski K. Twelve-year results of fenestrated endografts for juxtarenal and group IV thoracoabdominal aneurysms. J Vasc Surg. 2015; 61(2):355–64.
17. Eagleton MJ, Follansbee M, Wolski K, Mastracci T, Kuramochi Y. Fenestrated and branched endovascular aneurysm repair outcomes for type II and III thoracoabdominal aortic aneurysms. J Vasc Surg.2016;63(4):930–42.

Mechanisms of Disease and Natural History

2

Bulat A. Ziganshin and John A. Elefteriades

Introduction

Aortic diseases represent a variety of conditions from clinically silent to acutely symptomatic, which affect virtually any part of the aorta (Fig. 2.1). In-depth studies of the mechanisms of aortic disease (via clinical observations, genetic studies, molecular biology research, and bioengineering modeling) conducted increasingly over the past two decades have significantly enhanced our understanding that the aorta is an active living organ and not just a passive hollow conduit that transports blood [1, 2]. Understanding how the aorta functions under normal circumstances as well as under pathologic conditions is critical for predicting its behavior in order to allow effective and timely management of patients with aortic disease.

Aneurysms of the thoracic aorta are among the most challenging conditions to detect and treat, primarily because of their silent yet virulent nature [1]. Patients who harbor an aneurysm in the chest are often unaware until the "silent killer" [3] strikes, producing either death or a serious complication that is likely to lead to death, such as aortic rupture or dissection [4]. Therefore, the main goals of physicians treating thoracic aortic aneurysm (TAA) are first to identify those individuals harboring or at risk of developing an aneurysm, and second to predict accurately the likely behavior of the diseased aorta in these individuals.

TAAs are often identified incidentally during diagnostic imaging procedures performed for other purposes. However, active identification of affected patients can be achieved by screening relatives of patients with known aortic disease and by detecting certain conditions that have been shown to be associated with thoracic aortic disease (TAD). These conditions include bicuspid aortic valve [5], intracranial aneurysm [6], aortic arch anomalies (such as bovine aortic arch, isolated left vertebral artery, and aberrant right subclavian artery) [7, 8], abdominal aortic aneurysm [9], temporal arteritis [10], simple renal cysts [11], inguinal hernias [12], among others. Accordingly, we recommend a "guilt-by-association" approach for detecting individuals either harboring a TAA or at risk of developing a TAA in the future (Fig. 2.2) [13].

In this chapter we review in detail the second component—the mechanism of development and natural history (or behavior) of TAD as a means for predicting behavior of the diseased aorta.

Most Common Types of Thoracic Aortic Pathology

It is important to define the various types of thoracic aortic pathology whose mechanisms and natural history are discussed throughout this chapter. For the purpose of this chapter we selected the following clinically relevant types of TAD:

1. *Aortic aneurysm*—is an enlargement of the aorta to greater than 1½ times its normal size [14]. Depending on the involvement of the aortic root and the ascending aorta in the disease process, aneurysms in this proximal anatomic region can be classified as being supra-coronary (involvement of the ascending aorta only, with the aortic root normal in size), Marfanoid (predominant involvement of the aortic root only, while much of the ascending

B.A. Ziganshin
Yale University School of Medicine, Aortic Institute at Yale-New Haven Hospital,
789 Howard Avenue, Clinic Building CB317, New Haven, CT 06519, USA

Department of Surgical Diseases 2, Kazan State Medical University, 49 Butlerov Street, Kazan 420012, Russia
e-mail: bulat.ziganshin@yale.edu

J.A. Elefteriades (✉)
Yale University School of Medicine, Aortic Institute at Yale-New Haven Hospital,
789 Howard Avenue, Clinic Building CB317, New Haven, CT 06519, USA
e-mail: john.elefteriades@yale.edu

© Mayo Foundation for Medical Education and Research 2017

G.S. Oderich (ed.), *Endovascular Aortic Repair*, DOI 10.1007/978-3-319-15192-2_2

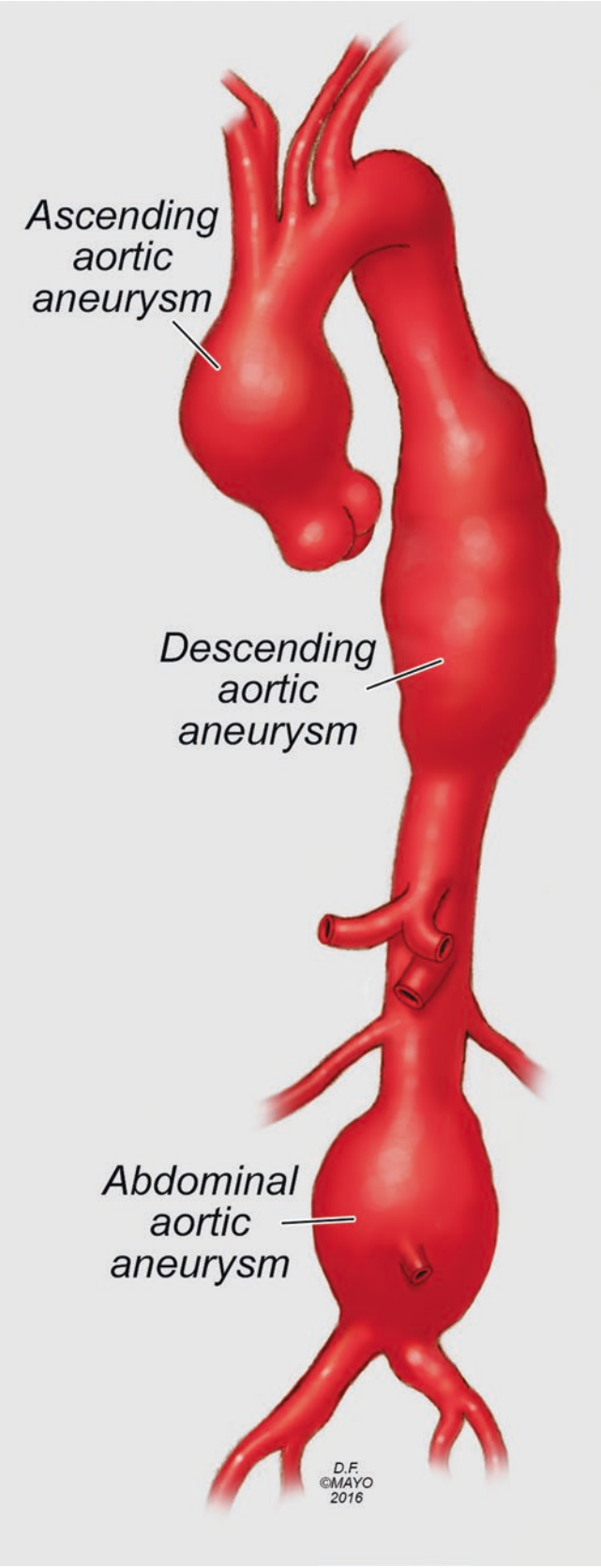


Fig. 2.1 Aortic aneurysm disease can affect virtually any part of the aorta—the ascending and arch portion, the descending thoracic, and the abdominal segments. By permission of Mayo Foundation for Medical Education and Research. All rights reserved

aorta is normal in size), and tubular (involvement of both the aortic root and ascending aorta). See Fig. 2.3 (please note that the aorta may have a "Marfanoid" configuration in the absence of clinical Marfan's disease in the patient). Aneurysms located in the descending thoracic and thoracoabdominal segments of the aorta are categorized using the original Crawford classification system [15] (Fig. 2.4):

(a) *Type I*—involves the majority of the descending thoracic aorta and the suprarenal part of the abdominal aorta.
(b) *Type II*—involves the entire descending thoracic aorta and the entire abdominal aorta down to the aortoiliac bifurcation.
(c) *Type III*—involves the lower (distal) part of the descending thoracic aorta and the entire abdominal aorta down to the aortoiliac bifurcation.
(d) *Type IV*—involves the abdominal aorta below the diaphragm and down to the aortoiliac bifurcation.
(e) *Type V* (*Safi modification* [16])—involves the lower (distal) part of the descending thoracic aorta and the suprarenal part of the abdominal aorta.

2. *Acute aortic syndrome* is a collective term that includes the following heterogeneous group of painful, emergent, and potentially life-threatening conditions (Fig. 2.5):
   (a) *Aortic dissection*—splitting of the layers of the aortic wall, usually occurring within the medial layer of the aorta with an evident intimal tear, allowing longitudinal propagation of a false lumen filled with blood [4].
   (b) *Intramural hematoma*—a concentric, circumferentially oriented collection of thrombus in the aortic wall, without the discrete transluminal flap typical of aortic dissection.
   (c) *Penetrating aortic ulcer*—localized perforation of the medial layer of the aortic wall beneath an atherosclerotic plaque (Figs. 2.5 and 2.6).
   (d) Any of the three above-mentioned conditions can lead to another acute condition called *aortic rupture* (as can a severely enlarged aneurysm), which is a self-explanatory term.
3. *Aortic transection* is usually traumatic in etiology. A transection is a disruption of the continuity of the aortic wall, without a propagating dissection (Fig. 2.7). Contrary to aortic dissection, the aortic wall is intrinsically normal and resistant to the dissection process [2].

Pathophysiology Involved in the Development of Aortic Aneurysm

For decades significant efforts have been undertaken to elucidate the pathophysiology of thoracic and abdominal aortic aneurysm formation [4, 17–22]. This process is complex and includes multiple components, such as inflammation, proteolysis, matrix injury, and dysfunction and necrosis of smooth muscle cells in the aortic wall (Fig. 2.8) frequently in the

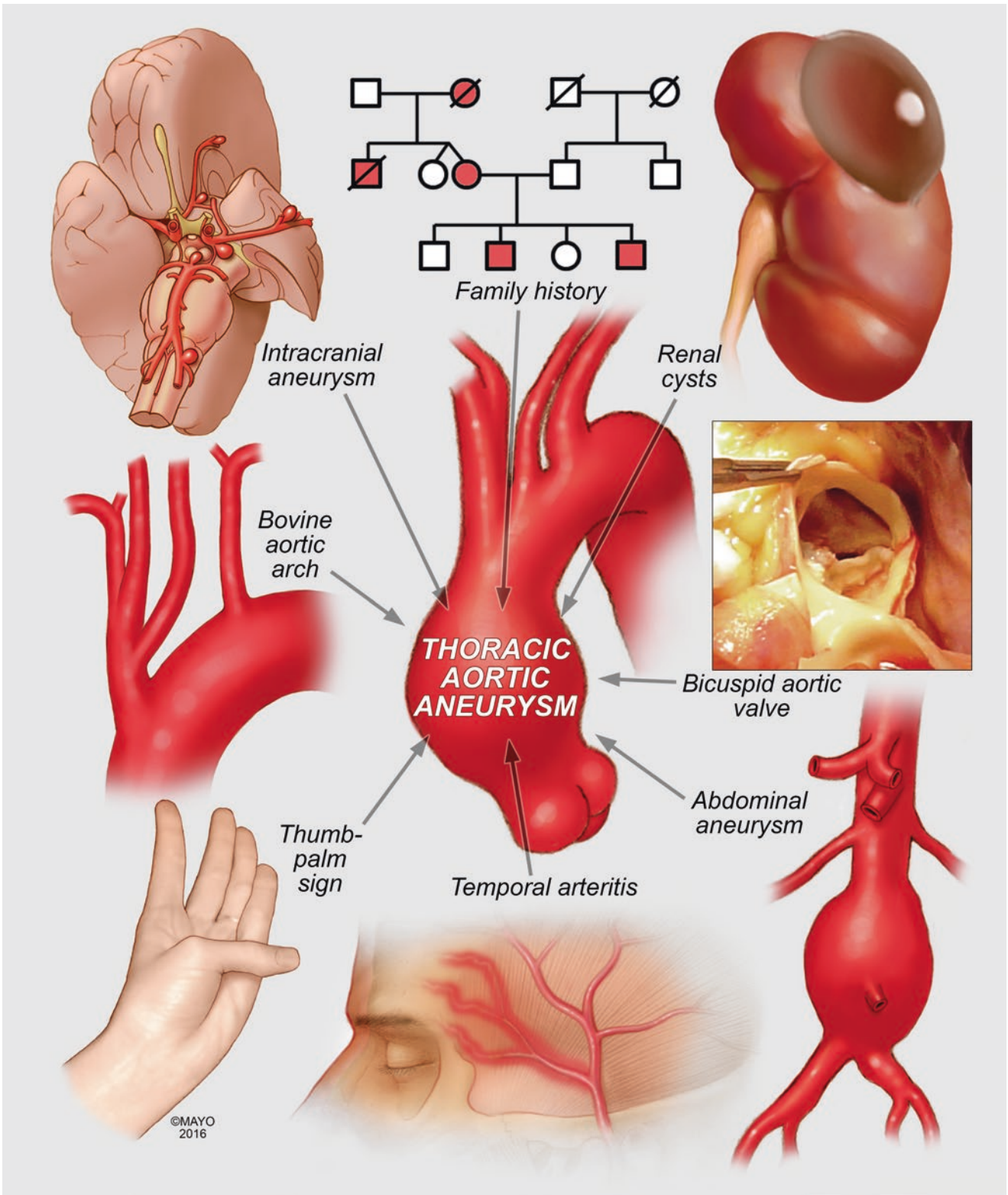


Fig. 2.2 Paradigm of "guilt by association" for detection of silent thoracic aortic aneurysm. By permission of Mayo Foundation for Medical Education and Research. All rights reserved

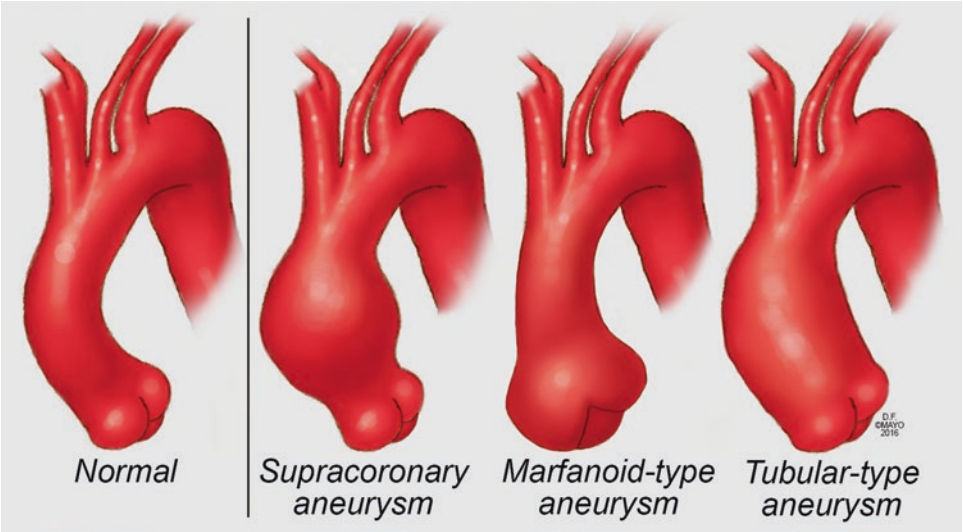


Fig. 2.3 A schematic illustration comparing the normal ascending aorta to three common patterns of ascending aortic aneurysmal disease: supracoronary, annuloaortic ectasia (also known as Marfanoid-type aneurysm), and tubular. By permission of Mayo Foundation for Medical Education and Research. All rights reserved

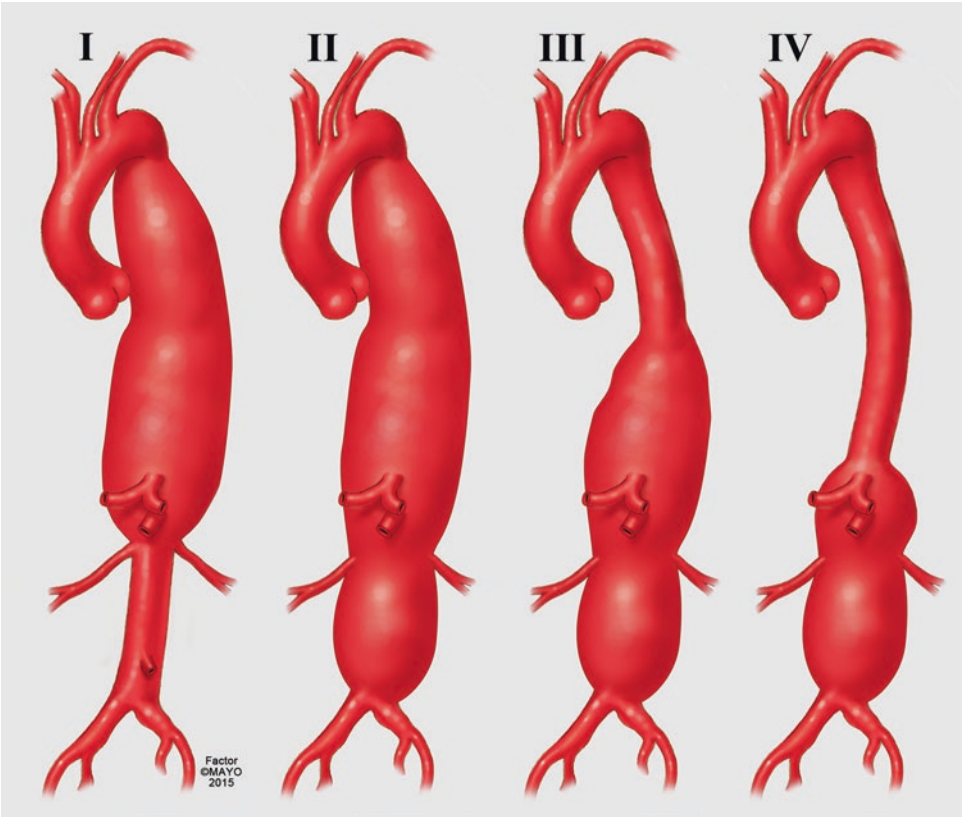


Fig. 2.4 Classification of thoracoabdominal aortic aneurysms. See text for details. By permission of Mayo Foundation for Medical Education and Research. All rights reserved

setting of fundamental genetic abnormalities [23]. It is the interplay of all these varying cellular and molecular mechanisms that leads to the disintegration of the medial layer of the aortic wall, producing an aneurysm (please see Fig. 2.9 for a histologic image of an aneurysmal aorta showing a complete loss of the medial layer).

A family of proteolytic enzymes called matrix metalloproteinases (MMPs) has been implicated as a major player in the deleterious medial degeneration process. MMPs are zinc-dependent enzymes that degrade elastin, fibrillin, and collagen—the main structural proteins of the aortic wall [22]. Such medial degradation is part of a physiological

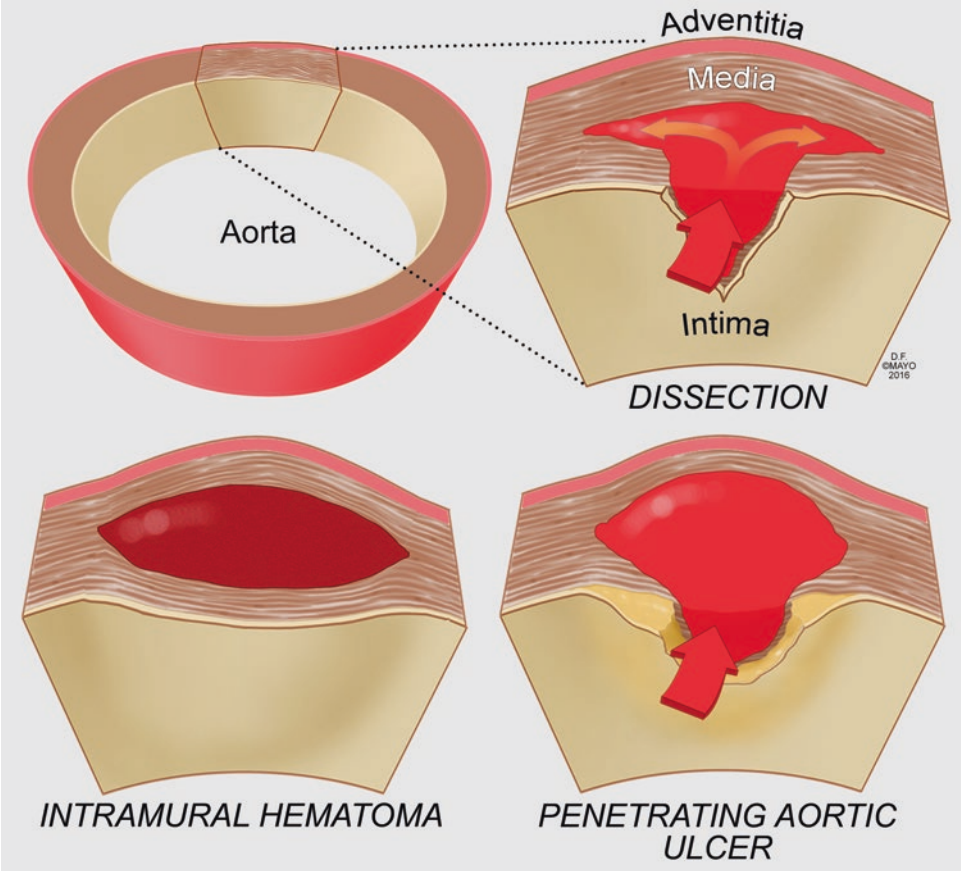


Fig. 2.5 Acute aortic syndromes [107]: Typical aortic dissection with a flap traversing the lumen; intramural hematoma involves a circumferential collection of blood in the aortic wall, but without a frank flap; penetrating ulcer of the aortic closely resembles duodenal ulcer in its overall appearance. By permission of Mayo Foundation for Medical Education and Research. All rights reserved

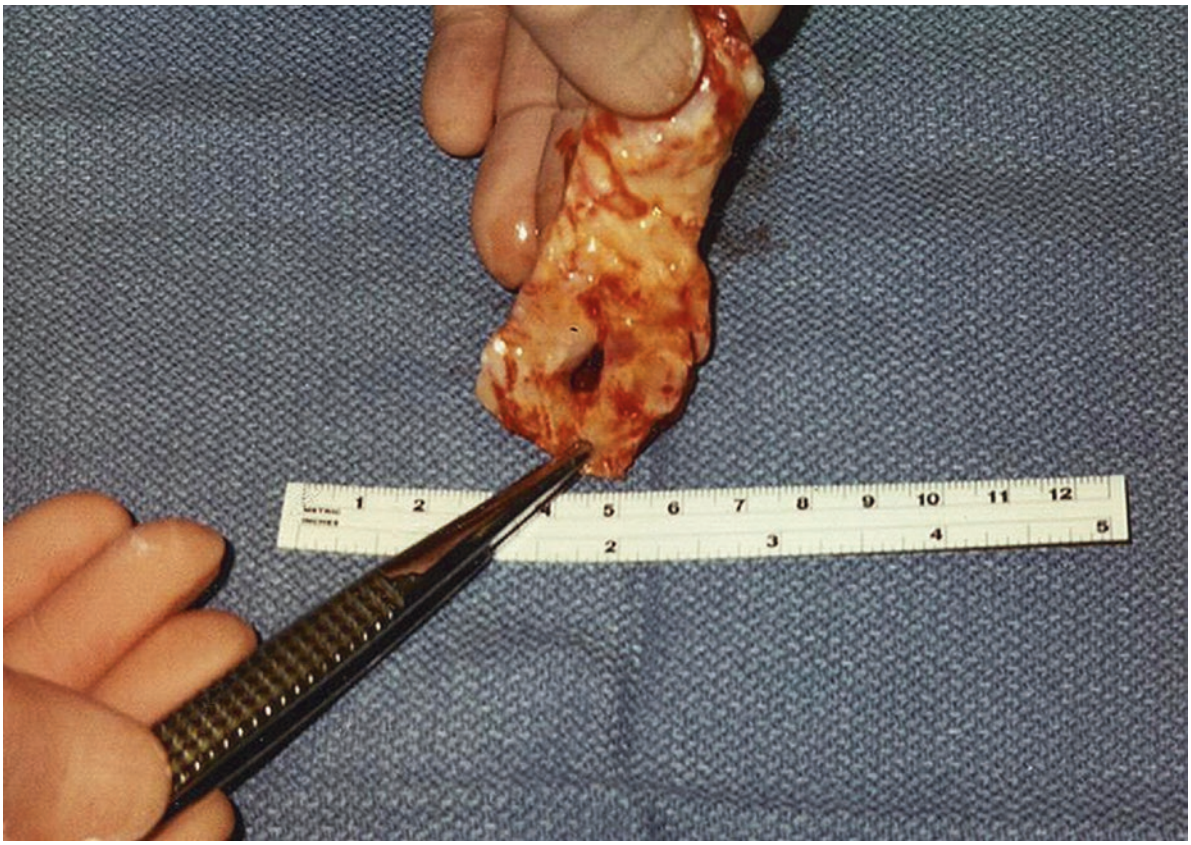


Fig. 2.6 Gross macroscopic image of a resected penetrating ulcer. Reproduced with permission from Coady M, Elefteriades JA. The Natural History of Thoracic Aortic Aneurysms: Etiology, Pathogenesis, and Evidence-Based Decision Making for Surgical Intervention. In: Elefteraides JA, ed. Acute Aortic Disease. New York, NY: Informa Healthcare USA; 2007:173–203 [107]

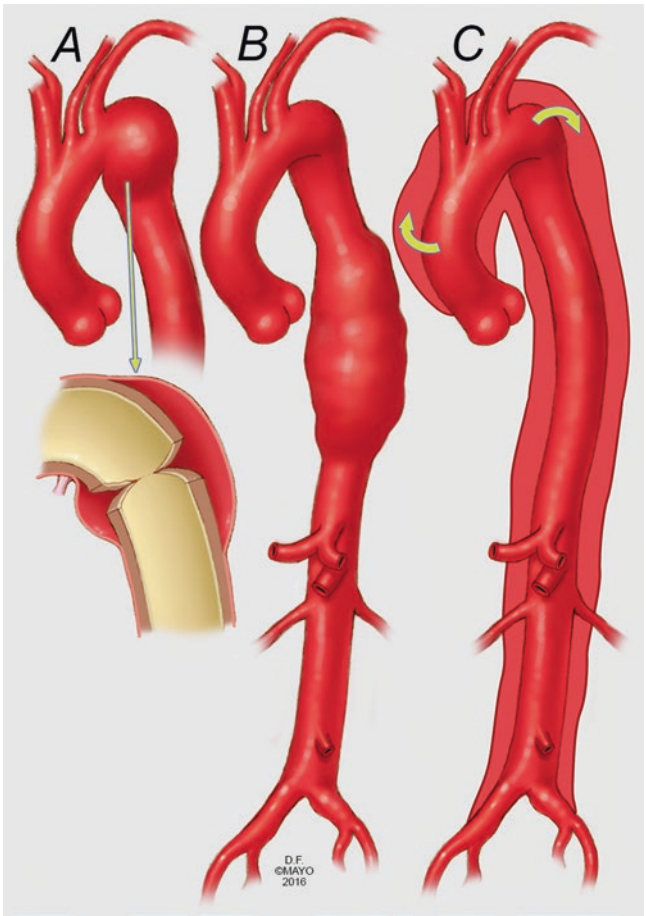


Fig. 2.7 Three commonly confused disorders: (**a**)—acute aortic transection; (**b**)—"atherosclerotic" aneurysm of the descending aorta; (**c**)—acute aortic dissection. By permission of Mayo Foundation for Medical Education and Research. All rights reserved

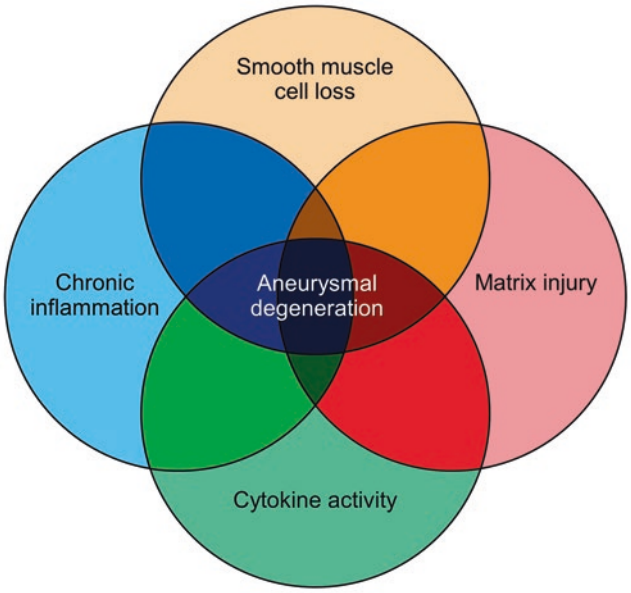


Fig. 2.8 Diagram illustrating multiple pathophysiological components that overlap and contribute to aortic aneurysm formation. By permission of Mayo Foundation for Medical Education and Research. All rights reserved

matrix turnover process, regulated primarily by macrophages [22]. Under normal conditions, MMP tissue activity is regulated by coexisting tissue inhibitors of metalloproteinases (TIMPs), which prevent excess degradation of aortic wall proteins. However, in the diseased aorta, activity of the MMPs is markedly elevated, while the activity of TIMPs may be reduced. This leads to a significant imbalance between synthesis and degradation of the extracellular matrix of the aorta (favoring proteolysis), which subsequently leads to weakening of the aortic wall and aneurysm formation.

Currently, MMPs have been proven to play an important role in the development of both abdominal [24, 25] and thoracic aortic aneurysms [22, 26–30]. The family of MMPs includes more than two dozen enzymes. However, MMP types 1, 2, 3, 9, 12, 13, and 14 have been most prominently associated with aortic disease [4]. In investigations conducted by our group, we looked specifically at the profiles of proteolytic enzymes and their tissue inhibitors in the aortic wall of aneurysm patients and compared these profiles to those of normal individuals. We found a marked elevation of two subtypes of MMPs—2 and 9—and a marked depression of the inhibitory enzymes (TIMPs) in ascending aortic aneurysms and dissections (Fig. 2.10) [29, 30]. Our current belief is that aneurysm patients are genetically programmed to manifest excessive MMP activity, leading ultimately to degradation and thinning of the aortic wall [31]. This is shown in Fig. 2.11, where the wall of a patient's aorta became so thin in a 6 cm aneurysm that a ruler placed behind the wall can be seen clearly through the tissue. It is hard to imagine how such a thin structure was maintaining the main blood flow to all organs of the body and not rupturing under arterial pressure. The recognition of pathophysiologic mechanisms of aneurysm development raises the potential for innovative drug therapies, such as administration of matrix protease inhibitors, in order to produce a slowing or halting of the evolution of thoracic aneurysm disease.

Another important contributor to the pathophysiology of aortic aneurysm is inflammation [32]. Specimens of surgically removed aneurysmal aortic tissue often show powerful excess of inflammatory cells within the aortic media and adventitia [23, 33], including macrophages, monocytes, plasma cells, B-lymphocytes, and T-lymphocytes. However, the exact role of each of these cell types in the process of aneurysm formation remains unclear, although some studies have identified T-helper 1 and T-helper 2 lymphocytes as important participants in the immune responses leading to aortic aneurysm formation [33, 34].

Inflammatory cytokines (IL-1β, IL-6, IL-8, INF-γ, and others) and loss of smooth muscle cells have also been shown to contribute to the process of aneurysm development [4, 23]. Inflammatory cytokines act by attracting and

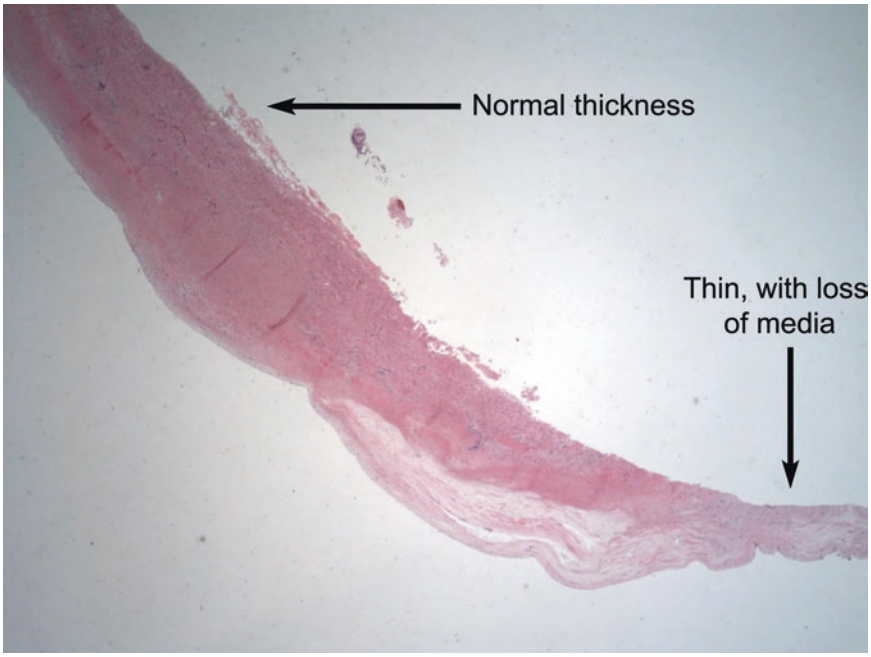


Fig. 2.9 Microscopic image of a cross section of the aortic wall. A clear transition from a normal to an abnormally thin aorta is seen, which is due to complete loss of the medial layer of the blood vessel. This causes aneurysmal dilation of the aorta and ultimately leads to dissection and/or rupture

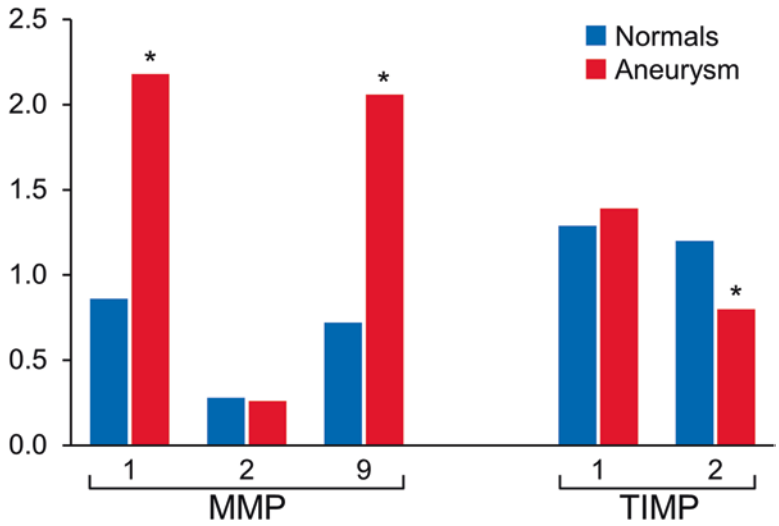


Fig. 2.10 Graph depicting matrix metalloproteinase (MMP) and tissue inhibitor of metalloproteinase (TIMP) expression scores in aneurysms and controls (*asterisk* indicates statistical significance). Adapted with permission from [30]. By permission of Mayo Foundation for Medical Education and Research. All rights reserved

activating macrophages and other immune cells, which in response release MMPs. In situations when such activation of inflammatory cells is excessive, an abundance of MMPs are released, leading to excessive medial degeneration. The loss of smooth muscle cells (as seen also in Fig. 2.9) has been shown in abdominal aortic aneurysms, where a 75 % loss was seen in aneurysmal aortas compared to normal abdominal aortas [35]. Two primary mechanisms that are thought to contribute to smooth muscle cell loss [23] are the following:

1. First, increased apoptosis in aneurysm smooth muscle cells, possibly due to release of inflammatory cytokines and mediators from inflammatory cells, which initiate programmed cell death. Previous studies have shown a threefold increase in apoptosis in aortic aneurysms [36–38].
2. Second, reduced growth capacity of smooth muscle cells in diseased aortas (based on observations of the abdominal aorta) [39].

In summary, proteolysis via MMPs, inflammation with participation of various cell types and inflammatory cytokines, matrix injury, and loss of normally functioning smooth muscle cells are all important contributing factors in the pathophysiology of aortic aneurysm development.

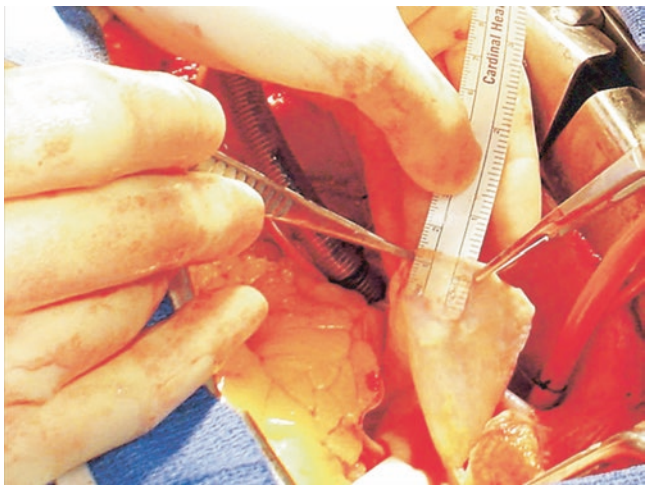


Fig. 2.11 An intraoperative image of a 6.0 cm ascending aorta, which became so thin that the writing on a ruler can be read directly through the aortic wall. It is sobering to think that this was all the tissue restraining the bloodstream and blood pressure in this patient. It is presumed that MMPs) participated in the underlying destruction of the aortic wall that resulted in such loss of substance. Reproduced with permission from Elefteriades JA. Thoracic aortic aneurysm: reading the enemy's playbook. Curr Probl Cardiol 2008;33:203–277

Ascending and Descending Aortic Aneurysm Are Two Different Diseases

For many years, arteriosclerosis was considered the primary etiologic factor in aortic aneurysm development [40, 41], although several early studies questioned whether dilatative diseases of the aorta shared any etiologic similarities with occlusive aortic disease [42, 43]. Over the past decade more and more evidence has been accumulating suggesting that aortic aneurysm, particularly in the ascending aorta and arch, has little to do with arteriosclerosis [1, 44, 45]. In fact, it appears that ascending and descending aortic aneurysms are fundamentally different in the mechanism of disease development and morphological appearance. Ascending aneurysms are smooth, without significant calcium deposits, debris, or clot, and are not related to traditional arteriosclerotic risk factors. On the contrary, descending aortic aneurysms are irregular, calcified, arteriosclerotic, and full of debris and clot, and patients usually present with the classic risk factors (such as hypertension, smoking, and dyslipidemia). Therefore, it appears that the separation point between these two different diseases is approximately at the *ligamentum arteriosum* (Fig. 2.12) [1]. It is conceivable that such differences between ascending and descending aortic aneurysms are due to different embryologic origins of the corresponding anatomic locations of the aorta: the ascending aorta develops from the tissues of the neural crest, while the descending aorta is a product of the mesoderm (Fig. 2.13) [21, 46–48].

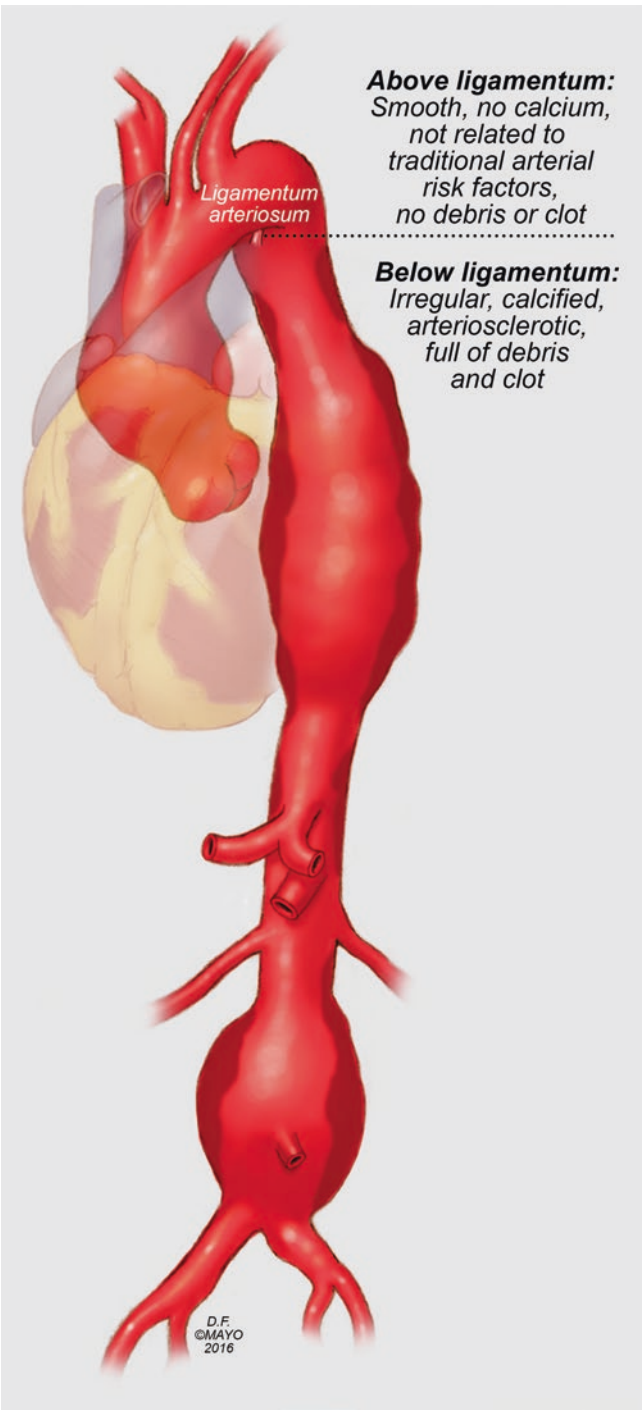


Fig. 2.12 Aortic aneurysm is really two diseases: Ascending/arch disease differs markedly from descending/abdominal disease. By permission of Mayo Foundation for Medical Education and Research. All rights reserved

Clinical observations into this phenomenon have revealed that ascending aortic aneurysms appear to be protective against systemic arteriosclerosis [1, 49]. This has been shown in studies that evaluated the total body calcium score [49], the carotid intimal thickness [50], and even the prevalence of myocardial infarctions [51] in patients with

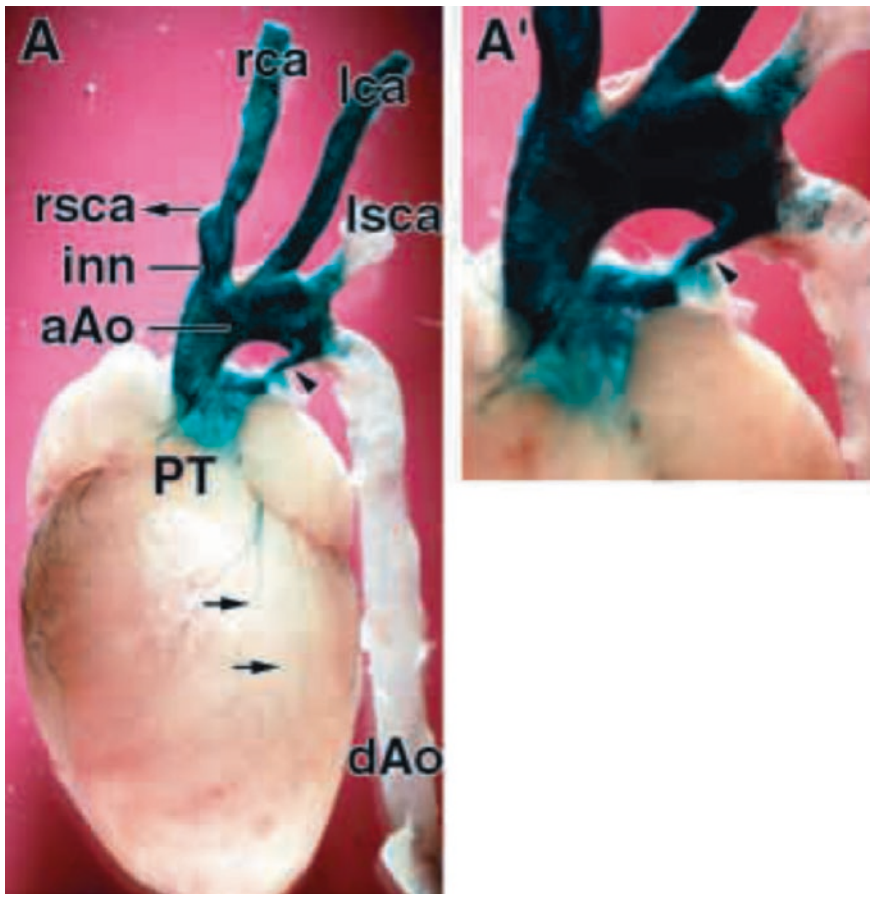


Fig. 2.13 Staining of neural crest cells in a 7-week adult heart. Note the extensive staining in the ascending aorta and the arch of the aorta, in the innominate and left and right carotid arteries, but not in the dorsal aorta or in the left subclavian artery. Reproduced with permission from Jiang X, Rowitch DH, Soriano P, McMahon AP, Sucov HM. Fate of the mammalian cardiac neural crest. Development 2000;127:1607–1616

ascending aortic aneurysm. It is possible that certain specific MMPs play a dual role in ascending aneurysm formation: *pro-aneurysmal* and *antiatherogenic* [52, 53].

Thoracic Aortic Aneurysm Is a Genetic Disease

The role of genetics and family history of aortic disease was first described by Tilson and colleagues for abdominal aortic aneurysm in the mid-1980s [54, 55]. However, for the thoracic aorta the knowledge lagged behind. The genetics of the well-appreciated Marfan syndrome were known: an autosomal dominant disorder, first described in 1896, characterized by dolichostenomelia (long, thin extremities), ligamentous redundancy or laxity, ectopia lentis, ascending aortic dilation, and incompetence of the aortic or mitral valves (or both) [56]. However, Marfan syndrome explained fewer than 5 % of all cases of thoracic aortic aneurysm, while many other cases seemed clinically to run in families [57, 58]. It was not until the late 1990s when two independent centers utilizing Mendelian genetic techniques nearly concurrently reported a 21 % incidence of familial non-syndromic thoracic aortic disease, with one or more affected relatives in a family in addition to the proband (Fig. 2.14) [59, 60]. These two studies laid the foundation for numerous further intense investigations of the genetics of TAD. Current "genetic" classification separates thoracic aortic aneurysm into two separate categories: syndromic (that is, with manifestations in other organs besides the aorta) and non-syndromic cases (that is, without extra-aortic manifestations) [57, 58]. Syndromic causes of TAD include Marfan syndrome [61, 62], and other rare syndromes such as Ehlers-Danlos [63, 64], Turner [65, 66], and Loeys-Dietz [67, 68]. In these patients the aortic dilation is just one of many features and extra-aortic manifestations of connective tissue abnormalities are abundant. Syndromic conditions are often inherited and run in families. Patients with syndromic thoracic aortic pathology usually have a positive "thumb-palm sign," the ability to cross the thumb across and beyond the edge of a flat palm as shown in Fig. 2.15. All syndromic cases put together still constitute little more than 5 % of all cases of TAD seen in the population. The non-syndromic category is much larger and includes two subcategories—familial and sporadic. Familial cases of TAD are proven to run in families, but, in contrast to syndromic aortic disease, aortic pathology is the only manifestation of the disease. Sporadic forms of thoracic aortic dissection are the most common type and likely represent the first presentation of TAD in a given family.

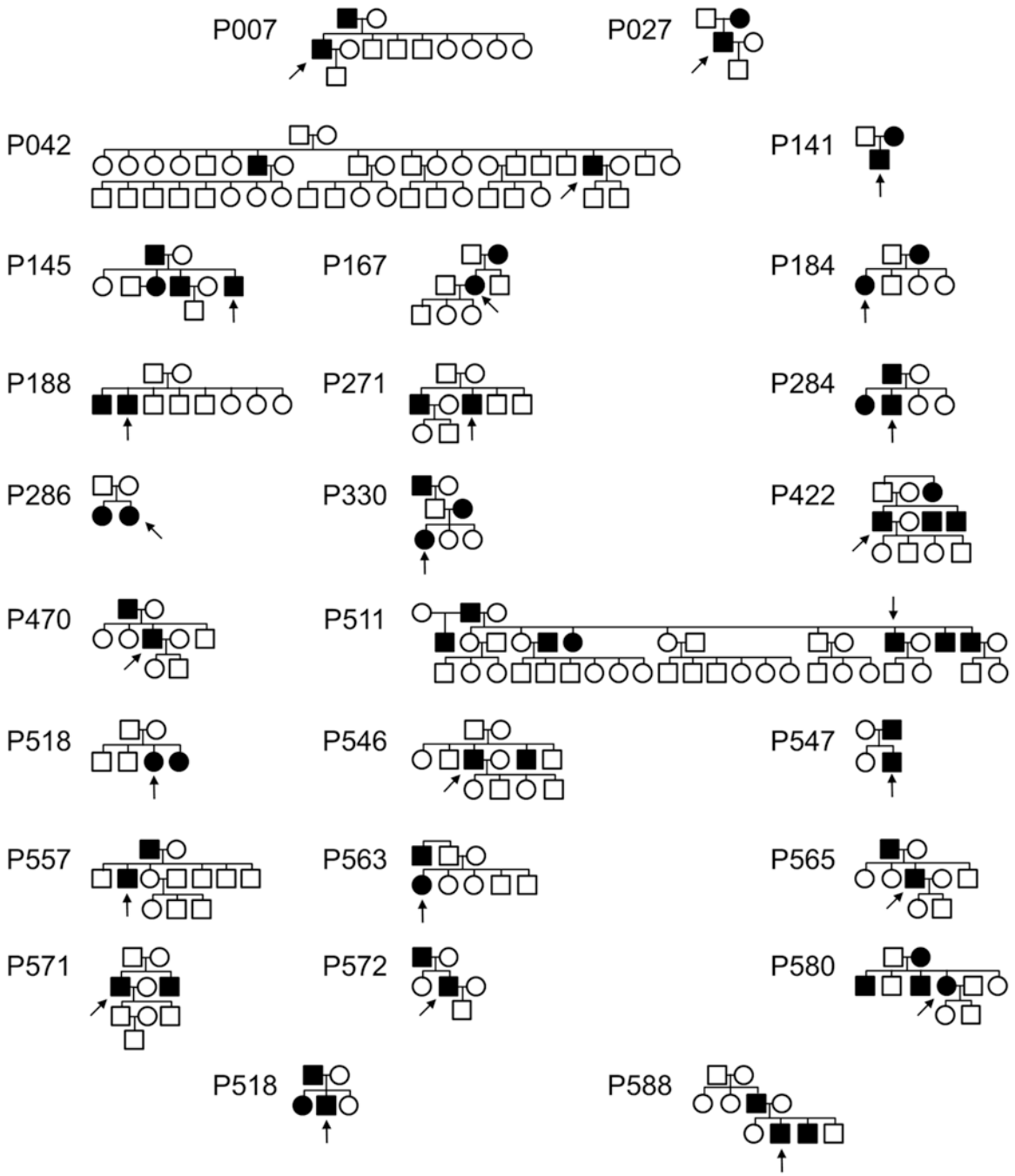


Fig. 2.14 Among the authors' first 100 constructed pedigrees, 21 were positive for a family pattern. These 21 positive pedigrees are displayed here. Reproduced with permission from Coady MA, Davies RR, Roberts M, et al. Familial patterns of thoracic aortic aneurysms. Arch Surg 1999;134:361–367

In-depth investigation of the genetic patterns of TAD has revealed that autosomal dominant inheritance is far and away the most common pattern in patients with this disease [69]. Other modes of inheritance (recessive, X-linked) have also been identified, but less commonly [69]. Furthermore, patients with an ascending aortic aneurysm are more likely to have a relative with an ascending aortic aneurysm, while patients with a descending thoracic aortic aneurysm are much more likely to have a relative with an abdominal aortic aneurysm (Fig. 2.16) [69]. (This finding substantiates the division of aortic disease into two zones by the ligamentum arteriosum.)

Currently investigations into the genetics of TAD have shifted to the molecular genetic level. At the time that this

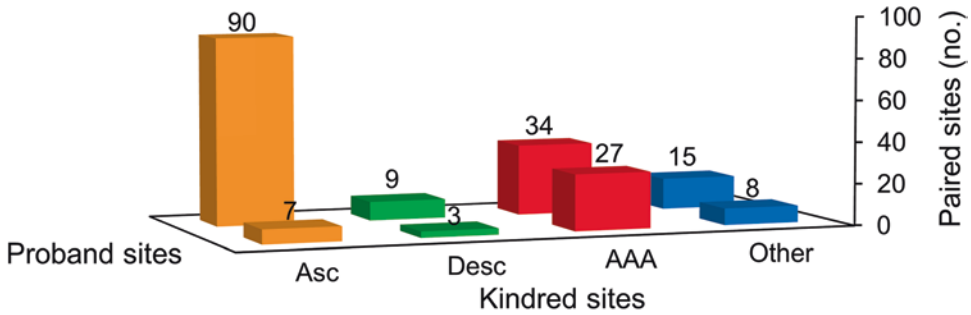
chapter is being written, as many as 21 genes have been implicated to be causative of thoracic aortic aneurysm and dissection (this includes genes that cause both syndromic and non-syndromic cases of TAD) (Fig. 2.17). These encode molecules that regulate the extracellular matrix (FBN1, FBN2, COL1A1, COL1A2, COL3A1), the cytoskeleton of smooth muscle cells (ACTA2, MYH11, MYLK), and the TGF-β signaling pathway (TGFβ2, TGFBR1, TGFBR2, SMAD3, SLC2A10). New genes responsible for this disease are being discovered regularly and it is likely that many more new genes will be identified in connection to TAD.



Fig. 2.15 Patient with a positive "thumb-palm" sign for connective tissue disease. Being able to cross the thumb beyond the edge of the palm indicates that the long bones are excessive and the joints are lax. By permission of Mayo Foundation for Medical Education and Research. All rights reserved

There are certain genes that influence substantially the natural history of thoracic aortic disease. For example, some mutations are exclusively involved in aortic dissection without aneurysm formation (MYLK gene [70]), or cause aortic dissection at small aortic sizes (ACTA2 gene [71, 72]). These mutations in part explain the phenomenon of aortic dissection occurring at a smaller aortic size than the current surgical criterion [73]. Patients who harbor these mutations are a challenge in terms of timely surgical intervention, because the dissection can occur before any significant enlargement is noted.

Current US guidelines on the management of patients with thoracic aortic disease recommend screening first- and second-degree relatives of patients with a known aneurysm or dissection via imaging studies (echocardiography, CT, or MRI) [74]. However, in the era of molecular genetics, genetic testing of patients and their relatives may offer some advantages in comparison to screening solely by conventional imaging techniques. For example, if an index patient (proband) is identified as a carrier of a pathogenic genetic defect that causes TAD, all family members can also be tested to determine whether they also carry the pathogenic abnormality or not. Such testing is beneficial for both carriers of the mutation, as it provides the opportunity for advanced and regular screening and subsequent timely prophylactic surgery, and noncarriers since it removes the need for regular imaging and the emotional burden of potential aneurysm disease. Such genetic testing can be accomplished using panels of genes or next-generation sequencing techniques, such as



		Kindred sites				
Proband sites		**Asc**	**Desc**	**AAA**	**Other**	**Total paired sites**
Asc	106	90	9	34	15	148
Desc	25	7	3	27	8	45
						193

Fig. 2.16 Distribution of sites of arterial aneurysms and dissections in kindred of familial probands. Adapted with permission from [69]. By permission of Mayo Foundation for Medical Education and Research. All rights reserved

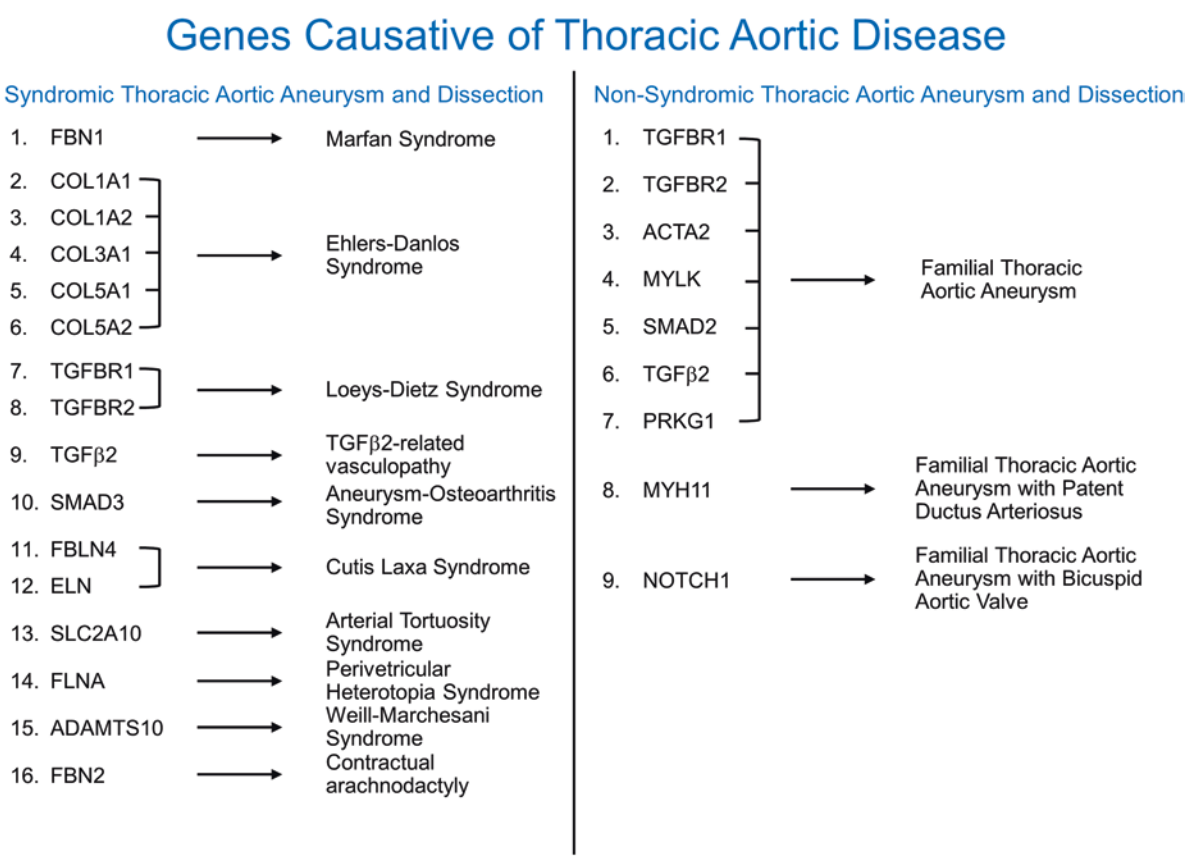


Fig. 2.17 Genes that are currently known to cause syndromic and non-syndromic thoracic aortic aneurysm and dissection. Adapted with permission from [76]. By permission of Mayo Foundation for Medical Education and Research. All rights reserved

whole-exome sequencing (Fig. 2.18) [75]. A clinical experience with routine whole-exome sequencing in patients with thoracic aortic aneurysm and dissection has recently been reported [76]. Follow-up testing of relatives for an identified particular variant/mutation can be conducted via single-site (Sanger) sequencing. Advanced genetic testing of patients with TAD provides the opportunity for personalized management of patients tailored to the specifics of the genetic mutation.

Natural History of Thoracic Aortic Disease

How Big Is the Normal Aorta?

Much analysis of the natural history of the thoracic aorta is based on aortic size. Before moving on to discuss size criteria and growth rates, it is useful to review aortic size under normal conditions. Recent reports from the Multi-Ethnic Study of Atherosclerosis that analyzed the size of the ascending aorta in 3500 individuals identified the mean diameter of the ascending aorta to be 3.2 ± 0.4 cm [77, 78]. The diameter of the aortic arch is not much different from the ascending aorta. The proximal portion of the descending aorta is about 2–2.3 cm and the abdominal aorta narrows further to 1.7–1.9 cm.

Where Should We Measure the Aorta?

Since accurate sizing of aortic diameter in patients with TAA is essential to enable preemptive surgical intervention before rupture and other complications occur, our group has proposed a system of uniform measurements of the aortic size at eight levels (Fig. 2.19) [79]: (1) aortic annulus, (2) sinuses of Valsalva, (3) sinotubular junction, (4) widest portion of the vertical ascending aorta (at any specific level), (5) the widest diameter in the aortic arch region between the takeoff of the innominate artery and the distal margin of the left subclavian artery, (6) widest portion of the vertical descending aorta (at any specific level), (7) suprarenal portion of the abdominal aorta, and (8) infrarenal portion of the abdominal aorta.

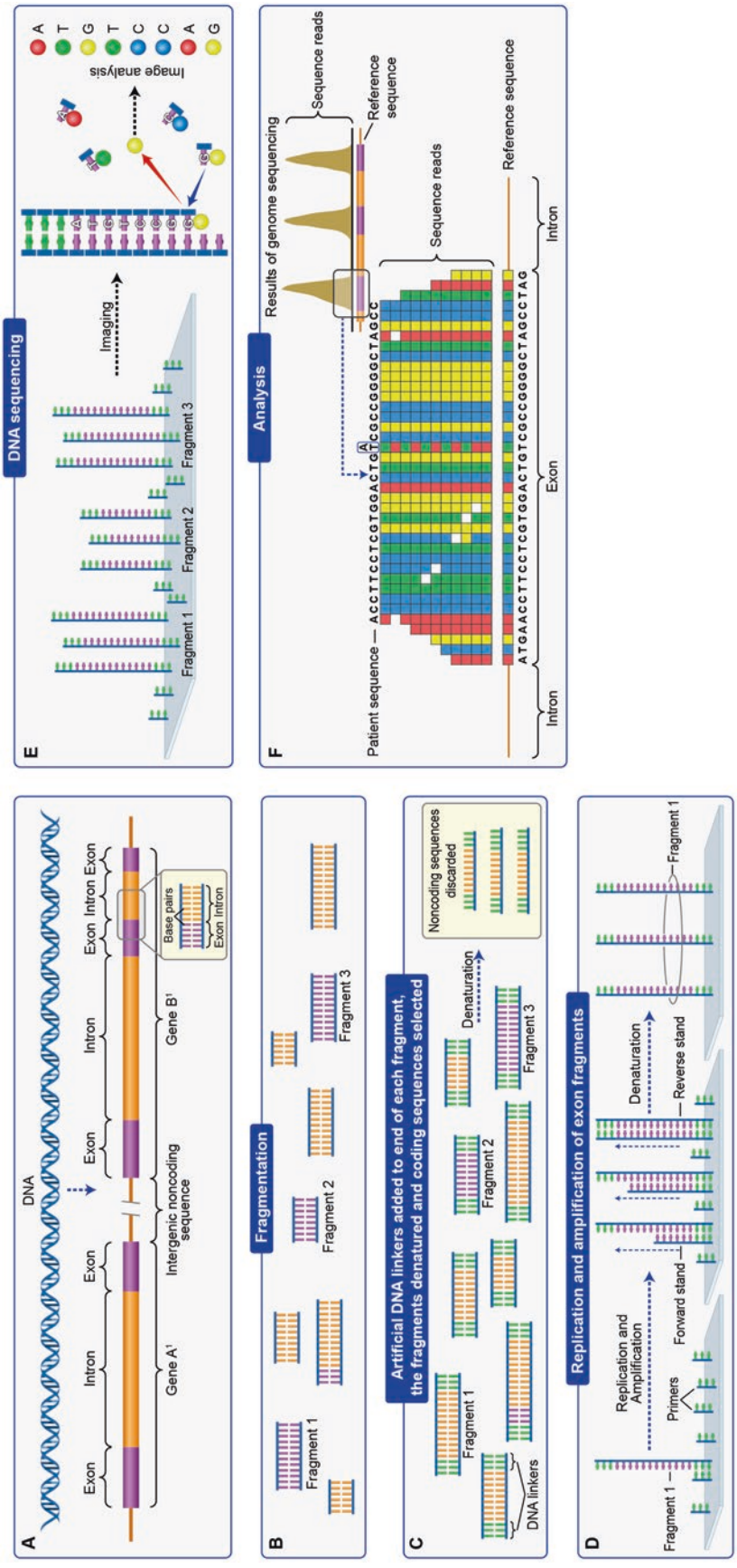


Fig. 2.18 Schematic overview of exome sequencing. Exome sequencing targets the approximately 1 % of the genome that is made up of exons, which encode protein sequence. The DNA from the patient (*Panel A*) is isolated and broken into fragments (*Panel B*); the DNA fragments are coupled to artificial DNA linker segments (*Panel C*), and the fragments are selected with the use of artificial DNA or RNA baits that are complementary to targeted DNA (not shown). The sequencing process starts with the binding of the end of each DNA fragment to a solid matrix and in situ amplification (*Panel D*), and the DNA fragments are then sequenced on the slide in a series of reactions in which a complementary nucleotide with one of the four colored fluorescent dyes is added to each cluster of identical molecules (*Panel E*). The identity of the colored fluorescent indicator of each cluster is imaged with a laser and a camera coupled to a microscope, the fluorescent indicator is removed, and the cycle is repeated to generate a nucleotide sequence read that is 75–150 nucleotides in length. The sequence reads are aligned to a reference DNA sequence (*Panel F*), and a genotype call for each position is made. In this example, most of the positions are homozygous reference sequence, but one position is called as heterozygous A/T. Adapted with permission from [75]. By permission of Mayo Foundation for Medical Education and Research. All rights reserved

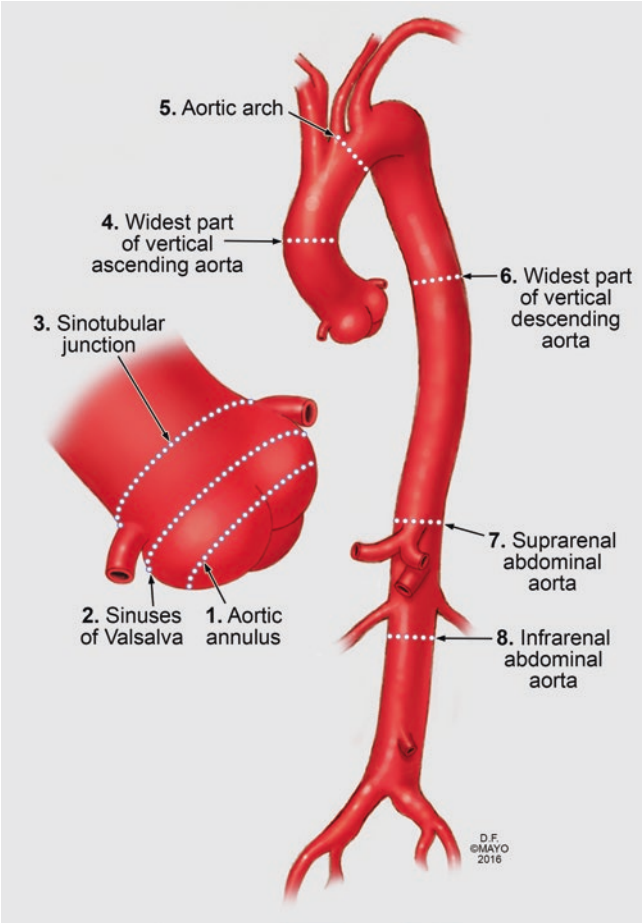


Fig. 2.19 Eight locations for uniform measurement and reporting of aortic diameter. By permission of Mayo Foundation for Medical Education and Research. All rights reserved

Growth Rate of the Thoracic Aorta

One of the most important parameters that defines the natural history of aortic disease is the rate of growth of the aorta. Estimating aortic growth rate is not a simple calculation of the difference in aortic size at the same anatomic location between two time points divided by the time between these points. Many different factors need to be accounted and controlled for, such as imaging modality, interobserver variability, and measurement error, among others. Therefore, sophisticated statistical methods have been developed to accurately assess the rate of aortic growth [80, 81]. Our early studies revealed that the aneurysmal aorta grows slowly—at a mean rate of 0.10 cm/year [82–84]. This figure is an incidence-weighted average of the 0.07 cm/year growth rate of the ascending aorta and a 0.19 cm/year rate for the descending aorta [82–84]. However, our more recent study on a larger number of patients from the same institution showed higher growth rates: 0.20, 0.26, and 0.23 cm/year for the ascending aorta and arch, descending aorta, and thoracoabdominal aorta, respectively [85]. Another notable finding is that the growth rate of the aorta increases with an increase in the size of the aorta in all three anatomic locations (Fig. 2.20) [85]. In other words, the larger the aneurysm, the faster it grows. This observation vividly emphasizes the dangers of a large aortic size, as the enlargement process intensifies in a vicious cycle. Epidemiologic studies of aortic growth rates may be hindered by two specific types of selection biases. First, patients seen at major referral centers may be different from the general population of TAD patients. This type of bias might lead to overestimating the growth rates since referral centers see more advanced aortic disease than that of the general population [80]. The second type of selection bias stems from the fact that patients with larger aneurysms (which might be fast growers) are selected out for prophylactic surgery quicker than patients with smaller aneurysms (slow growers). Such a bias would lead to underestimation of the true aortic rate of growth [80].

The current US guidelines recommend considering prophylactic surgical intervention if the size of the ascending aorta increases by more than 0.5 cm/year (class 1 recommendation, level of evidence C) [74]. We feel that increases of this magnitude are often spurious, based on oblique imaging planes or comparison of non-concordant segments [1]. Such large-diameter changes may be real in the unusual setting of clinically silent intercurrent aortic dissection—between the times of the two measurements.

Risk of Adverse Events

The other very important characteristic of the natural history of TAD concerns the risk of developing adverse events, such as rupture or dissection (or death from either of these) at different aortic sizes. This can be presented as either the lifetime risk of adverse events or the yearly risk.

Analysis of the lifetime risk of manifesting an aortic catastrophe showed that for the ascending aorta 34 % of patients will have suffered a rupture or a dissection by the time the size of the aorta reaches 6.0 cm (Fig. 2.21a) [82, 83, 86]. For the descending aorta the lifetime risk of an adverse event is dramatically increased as the aorta reaches the 7.0 cm point. At this size, 43 % of patients will have suffered rupture or a dissection (Fig. 2.21b) [82, 83, 86]. These sizes of the ascending and descending aorta represent "hinge points." Prophylactic surgical interventions should be carried out prior to the aorta reaching this size in order to prevent potentially lethal complications.

Yearly risk of rupture, dissection, or death is also a very useful indicator. The annual risk of adverse event with an aneurysm of a certain size is an easier concept for discussion with patients. Analysis of the yearly risk of adverse events showed a stepwise increase in risk with increasing aortic size (Fig. 2.22) [86]. The maximal risk is

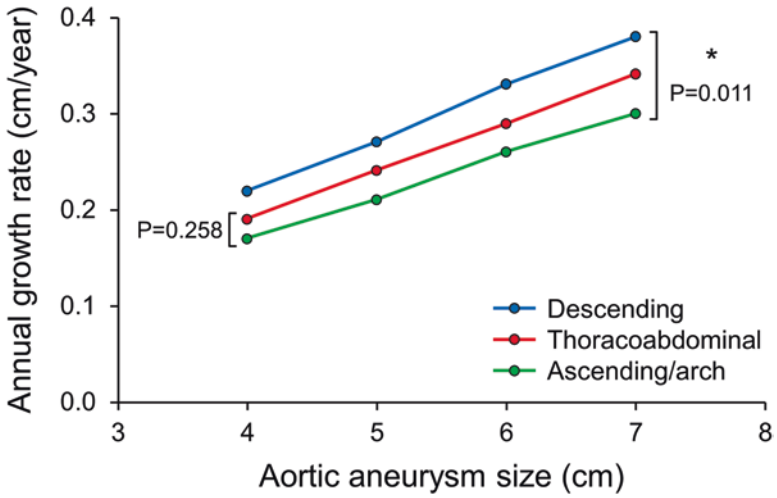


Fig. 2.20 Rates of annual growth of the thoracic aorta at three anatomic levels: the ascending aorta, the descending aorta, and the thoracoabdominal aorta. Note that growth rate increases as the aorta grows. Adapted with permission from [85]. By permission of Mayo Foundation for Medical Education and Research. All rights reserved

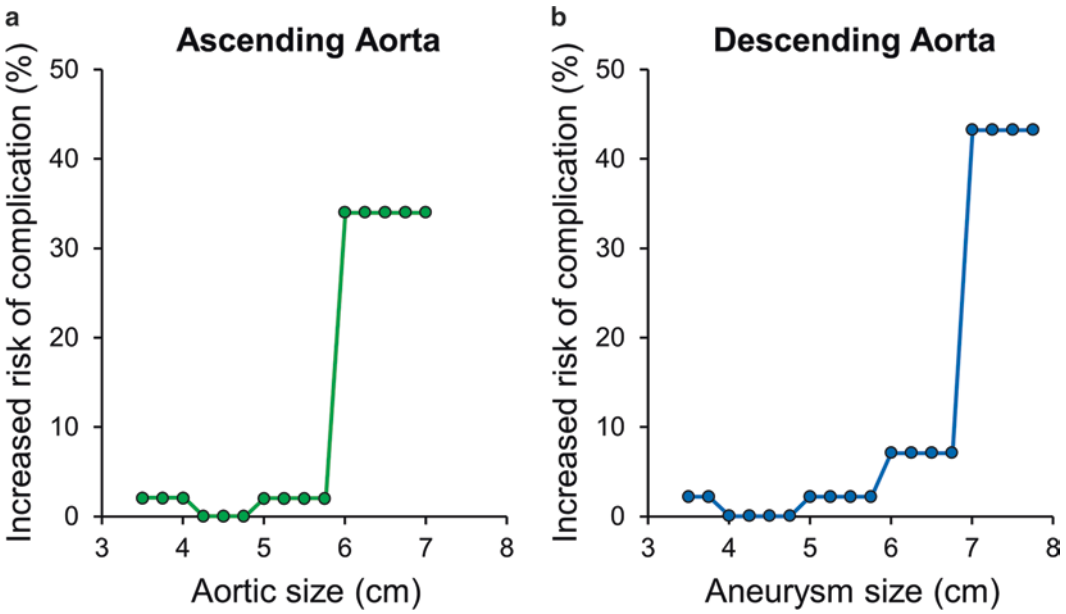


Fig. 2.21 The increase in risk of rupture or dissection as the thoracic aorta enlarges to specific dimensions. Note the abrupt hinge point at 6 cm for the ascending aorta (*Panel A*) and at 7 cm for the descending aorta (*Panel B*). Adapted with permission from [82]. By permission of Mayo Foundation for Medical Education and Research. All rights reserved

found in aortas greater than 6.0 cm. At 6 cm, the yearly risk of rupture, dissection, or death in patients with ascending aortic aneurysms is as high as 14.1 % [86]. (Of course, not all these deaths are aortic related, but for many the aorta is the cause.)

Based on these studies describing the risk of adverse events for patients with TAD, evidence-based intervention criteria have been developed that are still in use today and included in the most recent US guidelines for managing patients with TAD. For the ascending aorta, prophylactic surgery is recommended when the aorta reaches 5.5 cm, and for the descending aorta at 6.5 cm [84, 87]. When surgery can be delivered at low risk, it is appropriate to drop these criteria to 5.0 cm for ascending and 6.0 cm for descending aneurysm. All these criteria likely will be "personalized" based on specific causative mutation within the next decade. For patients with Marfan syndrome and other connective tissue disorders the recommended criteria are slightly lower—5.0 and 6.0 cm for the ascending and descending aorta, respectively (Fig. 2.23) [84, 87].

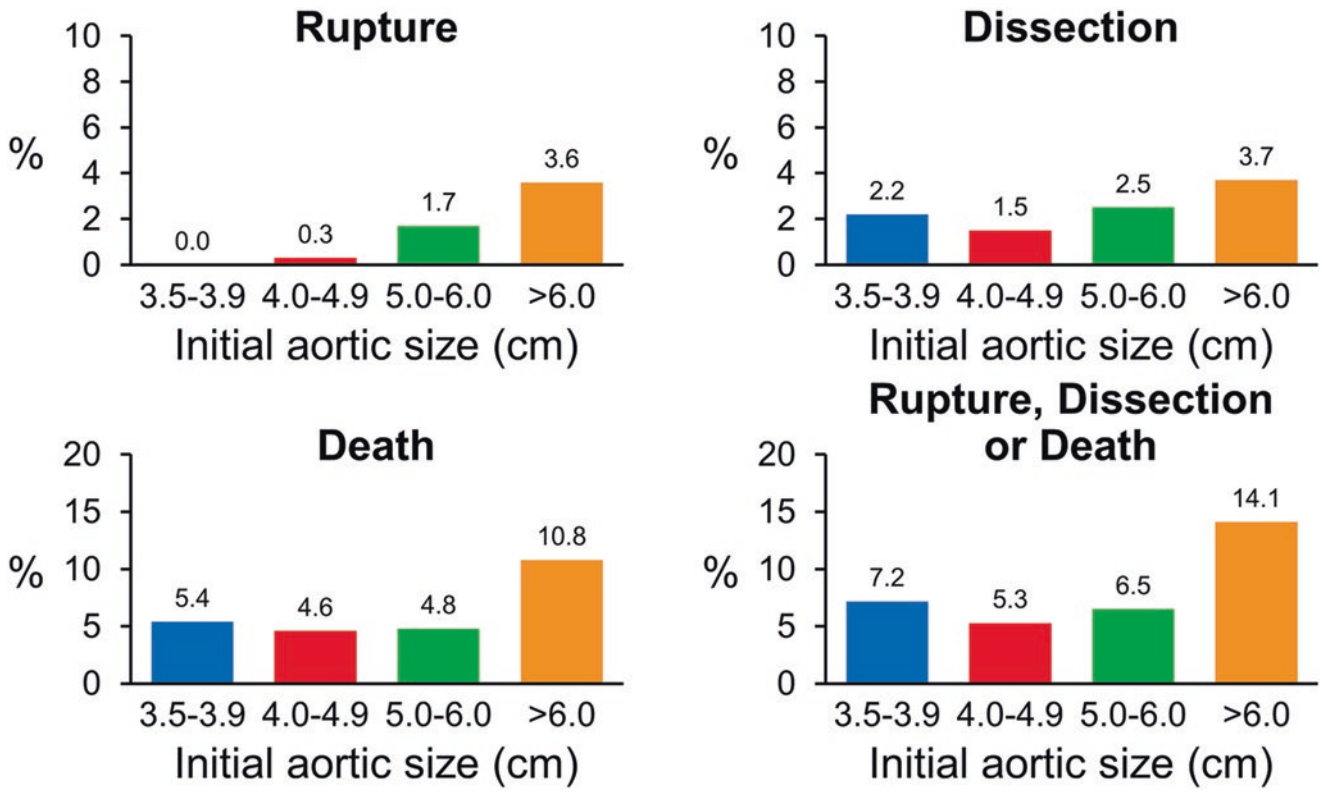


Fig. 2.22 These graphs illustrate the yearly rates of rupture, dissection, and combined end point of death and rupture dissection or death as the aorta enlarges. Adapted with permission from [4]. By permission of Mayo Foundation for Medical Education and Research. All rights reserved

The Yale Center for Thoracic Aortic Disease Recommended Surgical Intervention Criteria for Thoracic Aortic Aneurysms

1. Rupture
2. Acute aortic dissection
   a. Ascending requires urgent operation
   b. Descending requires a "complication-specific approach"
3. Symptomatic states
   a. Pain consistent with rupture and unexplained by other causes
   b. Compression of adjacent organs, especially trachea, esophagus, or left stem bronchus
   c. Significant aortic insufficiency in conjunction with ascending aortic aneurysm
4. Documented enlargement
   a. Growth ≥1 cm/yr or substantial growth and aneurysm is rapidly approaching absolute size criteria
5. Absolute size (cm)

	Marfan's	Non-Marfan's
Ascending	5.0 cm	5.5 cm
Descending	6.0 cm	6.5 cm

Fig. 2.23 Size algorithm for intervention for asymptomatic thoracic aortic aneurysm. Adapted with permission from [87]. By permission of Mayo Foundation for Medical Education and Research. All rights reserved

Role of Body Surface Area

Although the intervention criteria mentioned above are designed to be used generally, we realized that adjustments are necessary for extremes of body size. For example, for a 7-foot-tall basketball player an ascending aorta of 4.4 cm might actually be within the normal size range, given the large body and commensurate circulatory demand. On the other hand, a 4.4 cm aorta for a petite 5-foot-tall lady might be very significant and put her at high risk for adverse aortic events. Therefore, it became apparent that body surface area had to be included into the risk calculations for adverse events. Table 2.1 shows the corresponding risk for patients of varying sizes based on their body surface area [88]. The risk is stratified as either being low (~4% annual risk), medium (~8% annual risk), or high (~20% annual risk) [88]. This data provides important information that will make it possible to "fine-tune" the traditional intervention criteria that are routinely used in practice based on the person's body size.

Mechanical Properties of Thoracic Aorta Underlie Its Natural History

It is important to note that the natural history data described above, which are based on imaging studies and clinical observations, are largely supported and confirmed by concurrent bioengineering studies that assess the mechanical properties of the thoracic aorta. These studies have shown that the biomechanical properties of the thoracic aorta markedly deteriorate as the aortic size reaches 6 cm—the exact same size at which the natural history studies show the risk of adverse events to increase significantly. As the aorta enlarges and reaches 6 cm in diameter, it loses its distensibility (Fig. 2.24) and elasticity, thereby resembling a non-distensible rigid tube that has been stretched to its limits [89]. Therefore, in a large, noncompliant aorta the entire force of each cardiac contraction is directly translated into wall stress, since the aneurysmal aortic wall cannot stretch elastically [89]. The larger the aorta gets, the higher is the wall stress (please see the stepwise increase in wall stress in Fig. 2.25),

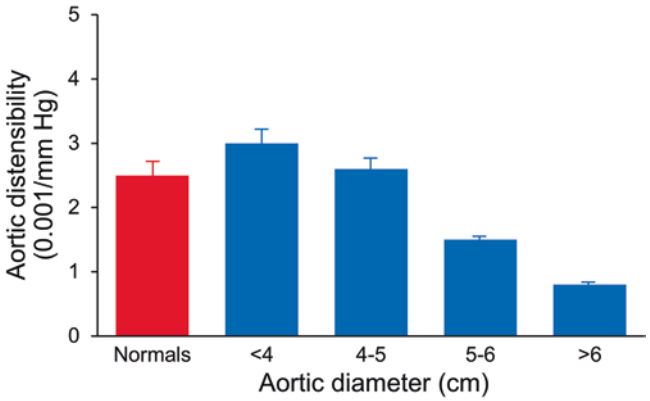


Fig. 2.24 Distensibility values in normal aortas and aortic aneurysms of different diameters. Distensibility of ascending aortic aneurysms decreases rapidly as diameter increases, to very low values at dimensions greater than 6 cm. Adapted with permission from [89]. By permission of Mayo Foundation for Medical Education and Research. All rights reserved

Table 2.1 Risk of complication in aortic aneurysm as a function of aortic diameter (horizontal axis) and patient body surface area (vertical axis)[a]
[a]Adapted from [88]

	Aortic size (cm)									
	3.5	4.0	4.5	5.0	5.5	6.0	6.5	7.0	7.5	8.0
BSA										
1.30	2.69	3.08	3.46	3.85	4.23	4.62	5.00	5.38	5.77	6.15
1.40	2.50	2.86	3.21	3.57	3.93	4.29	4.64	5.00	5.36	5.71
1.50	2.33	2.67	3.00	3.33	3.67	4.00	4.33	4.67	5.00	5.33
1.60	2.19	2.50	2.80	3.13	3.44	3.75	4.06	4.38	4.69	5.00
1.70	2.05	2.35	2.65	2.94	3.24	3.53	3.82	4.12	4.41	4.71
1.80	1.94	2.22	2.50	2.78	3.06	3.33	3.61	3.89	4.17	4.44
1.90	1.84	2.11	2.37	2.63	2.89	3.16	3.42	3.68	3.95	4.22
2.00	1.75	2.00	2.25	2.50	2.75	3.00	3.25	3.50	3.75	4.00
2.10	1.67	1.90	2.14	2.38	2.62	2.86	3.10	3.33	3.57	3.80
2.20	1.59	1.82	2.05	2.27	2.50	2.72	2.95	3.18	3.41	3.64
2.30	1.52	1.74	1.96	2.17	2.39	2.61	2.83	3.04	3.26	3.48
2.40	1.46	1.67	1.88	2.08	2.29	2.50	2.71	2.92	3.13	3.33
2.50	1.40	1.60	1.80	2.00	2.20	2.40	2.60	2.80	3.00	3.20

= low risk (~4% per year) = moderate risk (~8% per year) = severe risk (~20% per year)

and at 6 cm the wall stress of the aorta has the potential to exceed the ultimate tensile limits of the aorta if the blood pressure reaches 200 mmHg, which would result in dissection and/or rupture [1, 89]. Overall, these sophisticated bioengineering studies are consonant with the natural history findings and provide additional scientific justification for the current size criteria for prophylactic aortic replacement.

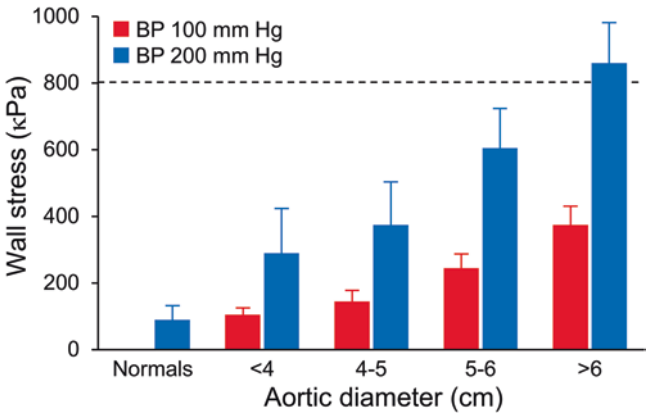


Fig. 2.25 In vivo mechanical properties of human ascending aorta. Exponential relationship between wall stress and aneurysm size in ascending aortic aneurysms. The *red columns* represent a blood pressure of 100 mmHg, and the *blue columns* represent a blood pressure of 200 mmHg. The lines at 800–1000 kPa represent the range of maximum tensile strength of the human aorta. Adapted with permission from [1]. By permission of Mayo Foundation for Medical Education and Research. All rights reserved

How Does Aortic Dissection Pick a Particular Time to Occur?

Although the studies on the natural history of aortic disease give an accurate estimate of the size at which a dilated aorta is likely to dissect or rupture, until recently the precipitating events that cause a dissection to occur at a particular time were unknown. In fact, aortic dissection was previously considered to be a completely random event that can occur practically on any day and at any time. However, there is evidence that occurrence of aortic dissection is not random and that certain predisposing and inciting factors and conditions need to be met for a dissection to occur at a particular time. In Fig. 2.26 we provide a schematic (based on many clinical observations and studies) that depicts our current understanding of the mechanism of how an aortic dissection is likely to occur [1, 4, 90]. This includes a sequence of five important components: (1) genetic predisposition to TAD; (2) degeneration of the medial layer of the aorta (via MMP action); (3) weakening of the aortic wall and aneurysm formation; (4) an acute hypertensive episode (sudden spike in blood pressure); and (5) aortic dissection.

Most of the abovementioned components were previously discussed in this chapter. However, the hypertensive episode deserves a more detailed analysis. The importance of blood pressure increase in inciting aortic dissection is currently well accepted, with antihypertensive drugs being the first line of medical management for patients at risk.

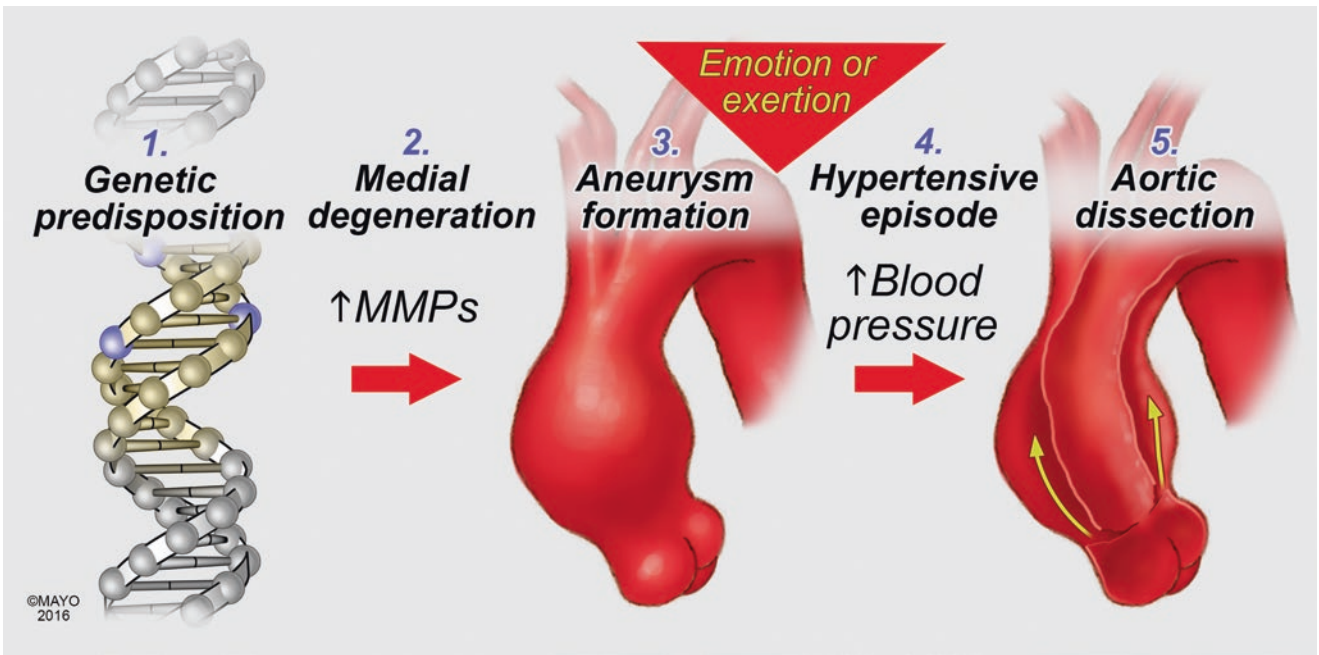


Fig. 2.26 Schematic presentation of possible relationships underlying the instigation of an acute aortic dissection at one particular time. By permission of Mayo Foundation for Medical Education and Research. All rights reserved

However, this relationship was not as obvious a decade ago until the phenomenon of aortic dissection was discovered in weightlifters [91, 92]. Through an experimental study on volunteers, our group was able to show that during severe weightlifting the arterial blood pressure can exceed 300 mmHg (Fig. 2.27) [31]. Such extreme blood pressures are not commonly seen even in such acute environments as the cardiac intensive care unit, where hypertension is a very common condition. Furthermore, the significance of a hypertensive episode in aortic dissection was further supported by a study that showed that extreme physical exertion (moving furniture, shoveling snow, etc.) or emotional stress (loss of a loved one, news of an illness, extreme work-related stress, etc.) preceded aortic dissection in 67 % of patients with this condition (Fig. 2.28) [90]. Although not as intuitive as physical exercise, emotional stress too can provoke a serious spike in blood pressure, enough to incite aortic dissection [93]. The role of hypertension in inciting aortic dissection is also evidenced by studies that have found a higher rate of occurrence of these events in the winter months and in the morning periods of the day, when the blood pressure is known to be highest [94–97].

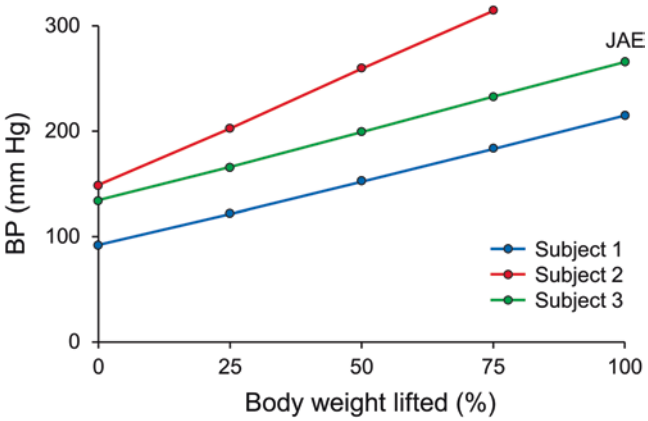


Fig. 2.27 Determination of instantaneous blood pressure during a weight-lifting exercise. Blood pressure during lifting was related to percent of body weight lifted in the bench press exercise. Subject 1 was a healthy 16-year-old athlete; he reached a blood pressure exceeding 200 mmHg at 100 % body weight lifted. Subject 2 was a prior athlete, now sedentary; his lifting was stopped when he attained a blood pressure of 320 mmHg at 75 % of his body weight. Subject 3, the senior author, an experienced weight lifter, reached a blood pressure of 250 mmHg at 100 % of body weight lifted. Adapted with permission from [4]. By permission of Mayo Foundation for Medical Education and Research. All rights reserved

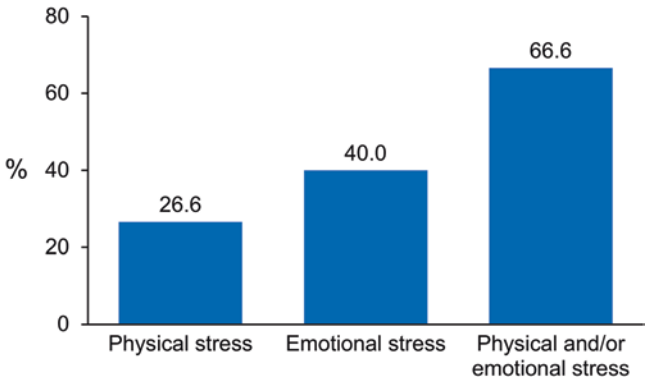


Fig. 2.28 Emotional or exertional events immediately preceding the onset of the pain of acute aortic dissection. Adapted with permission from [90]. By permission of Mayo Foundation for Medical Education and Research. All rights reserved

The hypothesis depicted in Fig. 2.26 is based on the widely accepted assumption that the dissection starts with a tear in the intimal layer of the aorta. However, this assumption has recently been challenged by Humphrey and colleagues [98, 99], who have postulated an alternative hypothesis that the dissection actually starts within the medial layer of the aorta via pooling of glycosaminoglycans and proteoglycans (Fig. 2.29). This in turn initiates a delamination process within the medial layer, which biomechanically promotes aortic dissection. In this scenario the intimal tear is the result of an initial degradative process within the media, rather than being the initial event of the dissection [98, 99].

Why Do Some Aortic Dissections Occur at Small Sizes?

In 2007 the International Registry of Acute Aortic Dissection (IRAD) made an important observation that almost half of all cases of aortic dissection occur at a size of the aorta that falls below the currently used intervention criteria [73]. This study might lead the readers to believe that the guidelines are not correct in their assessment of risk and need to be revised with a leftward shift (i.e., recommended prophylactic surgical intervention at smaller aortic size). However, the IRAD authors wisely did not make this recommendation based on the "size paradox" that they found.

How can this paradox be explained? The IRAD data were only able to assess the occurrence of dissection events (numerator), but were not able to estimate the actual risk of dissection at a certain aortic size, because the number of individuals at risk in each size category (denominator) remained unknown. From the MESA database [77, 78] we know that the size of the ascending aorta follows a nearly typical bell-shaped distribution curve (Fig. 2.30). This means that, at the right "tail" of the curve, the number of individuals with smaller aortas is manyfold greater than individuals with larger aortas. This in turn means that the risk of a patient developing an aortic dissection at a small aortic size is significantly lower, because of the large number of susceptible patients with aortas of this size. Using this numerator/denominator data, we were able to calculate the

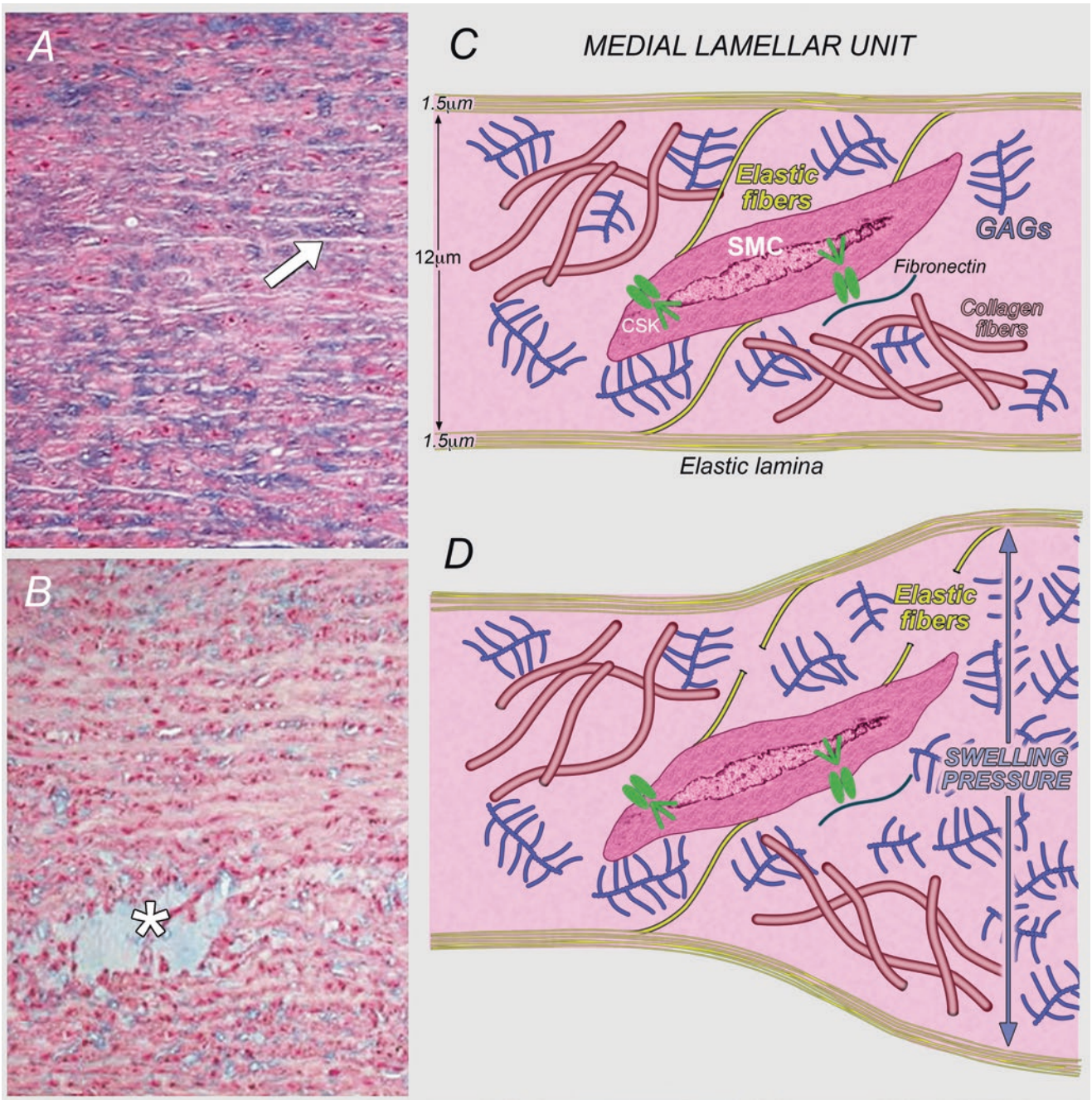


Fig. 2.29 This comparative illustration summarizes the hypothesis that pools of glycosaminoglycans/proteoglycans initiate the dissection from within. (*Panels A and B*) Sections of the medial layer of the human ascending aorta stained with alcian blue (which stains glycosaminoglycans blue) for both a normal (*panel A*) and an aneurysmal (*panel B*) aortic wall. Reproduced with permission from Borges LF, Touat Z, Leclercq A, et al. Tissue diffusion and retention of metalloproteinases in ascending aortic aneurysms and dissections. Hum Pathol 2009;40:306–13 [108]. (*Panel C*) Schematic drawing of a normal aortic medial lamellar unit consisting of paired elastic laminae (at the *top and bottom*) with an embedded smooth muscle cell (SMC) as well as collagen fibers, adhesion molecules (e.g., fibronectin), and glycosaminoglycans (GAGs) (not to scale). Shown, too, are thin "radially oriented" elastic fibers (i.e., elastin and associated microfibrils, predominately fibrillin-1) that may provide direct mechanical connections between the elastic laminae and smooth muscle cell and thus a mechanosensory capability beyond the typical cytoskeletal (CSK)–integrin–extracellular matrix (fibronectin/collagen) axis. It is possible that negatively charged GAGs sequester water and may thereby contribute a normal intralamellar pressure that could help maintain the thin elastic fibers in tension. (*Panel D*) This schematic drawing depicts a localized accumulation of GAGs, on the right side of the medial lamellar unit, which results in an increased swelling pressure, which in turn helps to separate the elastic laminae and possibly disrupt connections between the SMCs and either thin elastic fibers or the collagenous matrix. Such effects could initiate a local delamination and/or altered mechanosensitive cellular response leading to dysregulated wall homeostasis. *Panels C and D* courtesy of Professor Jay Humphrey, Yale School of Engineering and Applied Sciences and Yale University School of Medicine

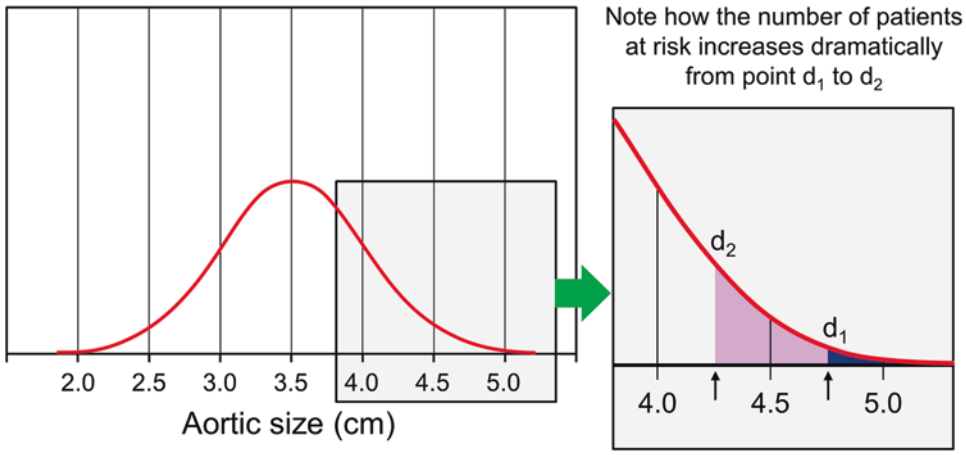


Fig. 2.30 The aortic size follows a modified bell curve distribution. The population at risk increases dramatically moving leftward from the right "tail" of the bell curve. The corollary of this observation is that, at small aortic sizes, a huge population is at risk; therefore, although dissections do occur, the relative risk is very low compared with the huge "at-risk" population. Adapted with permission from [1]. By permission of Mayo Foundation for Medical Education and Research. All rights reserved

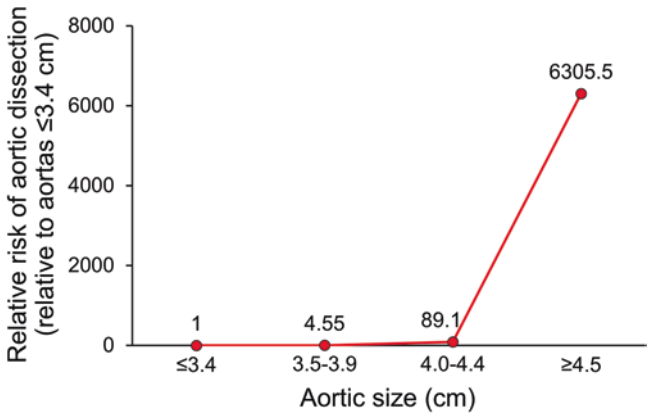


Fig. 2.31 The graph illustrates that the relative risk of aortic dissection is >6000-fold higher for large aortas than for small ones (calculated based on published data from IRAD and MESA databases). Adapted with permission from [78]. By permission of Mayo Foundation for Medical Education and Research. All rights reserved

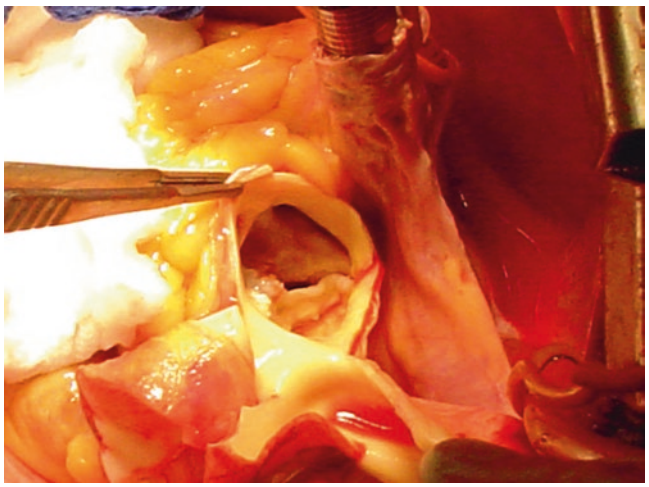


Fig. 2.32 Intraoperative image of a heavily calcified bicuspid aortic valve. Reproduced with permission from Friedman T, Mani A, Elefteriades JA. Bicuspid aortic valve: clinical approach and scientific review of a common clinical entity. Expert Rev Cardiovasc Ther 2008;6:235–248

relative risk of an aortic dissection occurring in a large aorta; we found this to be a full 6000 times higher than in small aortas (Fig. 2.31). Thus, comparing the observed number of dissections with the actual number of patients at risk who harbor an aneurysm of the corresponding size confirms the validity of the surgical intervention criteria that are being used today.

Thoracic Aortic Disease in the Setting of a Bicuspid Aortic Valve

Bicuspid aortic valve (BAV) is the most common congenital cardiac anomaly and is estimated to affect 1–2 % of the population (Fig. 2.32) [100–102]. Many patients with BAV also develop ascending aortic aneurysm (as part of bicuspid aortopathy, Fig. 2.33). Although the exact frequency of aneurysm formation in BAV patients is hard to determine, multiple studies estimate this figure to be in the broad range of 20–84 % [102]. A study from the International Bicuspid Aortic Valve Consortium found that the risk of aneurysm development is 80 times higher than in the general population [103]. There is some equivocal evidence in the literature to suggest that thoracic aortic aneurysms in patients with a BAV behave in a more malignant way than regular aneurysms. They grow faster—0.19 cm/year vs. 0.13 cm/year—for patients with a trileaflet aortic valve (Fig. 2.34) [5] and are known to play a major role in the causation of aortic dissection [104, 105]. Also, a higher proportion of BAV patients require surgery for their aneu-

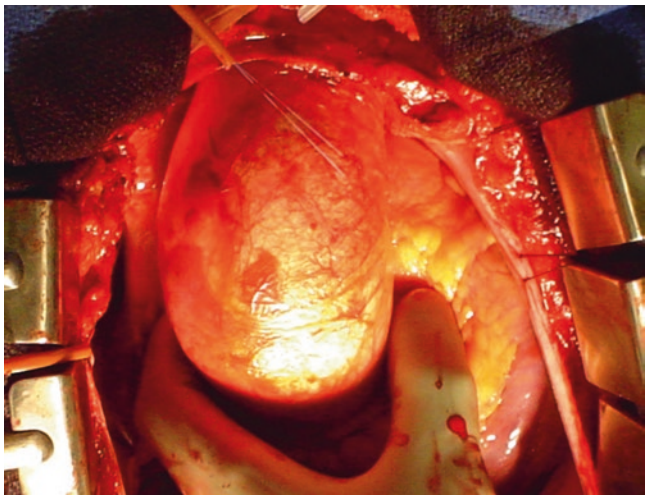


Fig. 2.33 Intraoperative image of an ascending aortic aneurysm in a patient with a bicuspid aortic valve (shown in Fig. 2.32)

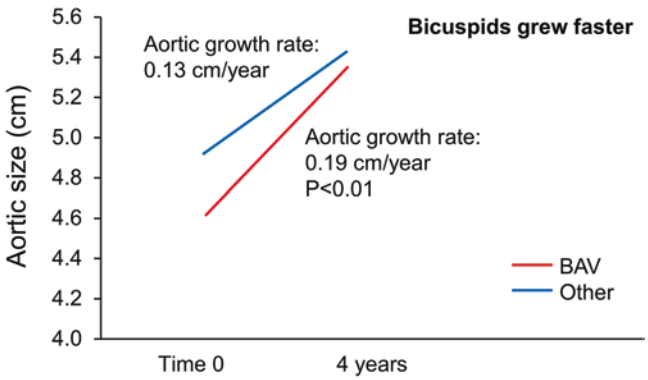


Fig. 2.34 Aortic growth rate chart, illustrating a faster growth of aneurysms for patients with a bicuspid aortic valve than in patients with non-BAV-related aneurysms. Adapted with permission from [101]. By permission of Mayo Foundation for Medical Education and Research. All rights reserved

rysmal aortas (72.8 % vs. 44.8 %) at a significantly younger age (48.9 vs. 63.1 years) [5]. Despite the seemingly more aggressive course of aortic disease in BAV patients, recent studies have demonstrated that with appropriate diagnosis and care the outlook for patients with a BAV is no different from the general population [106–108].

Conclusion

The pieces of the puzzle in the playbook of thoracic aortic aneurysm are coming together (Fig. 2.35):

- A genetic abnormality predisposes to aneurysm development.
- The MMPs participate significantly in a complex aneurysm pathophysiology.
- Definite family patterns prevail.
- Mechanical properties of the aorta are dramatically altered.
- Aortic dissection and rupture tend to occur at or above 5 cm aortic diameter.
- Exertion or emotion are acute inciting factors for aortic dissection
- Specific genetic mutations (including single base change) are being identified in individual patients via modern whole-exome sequencing.

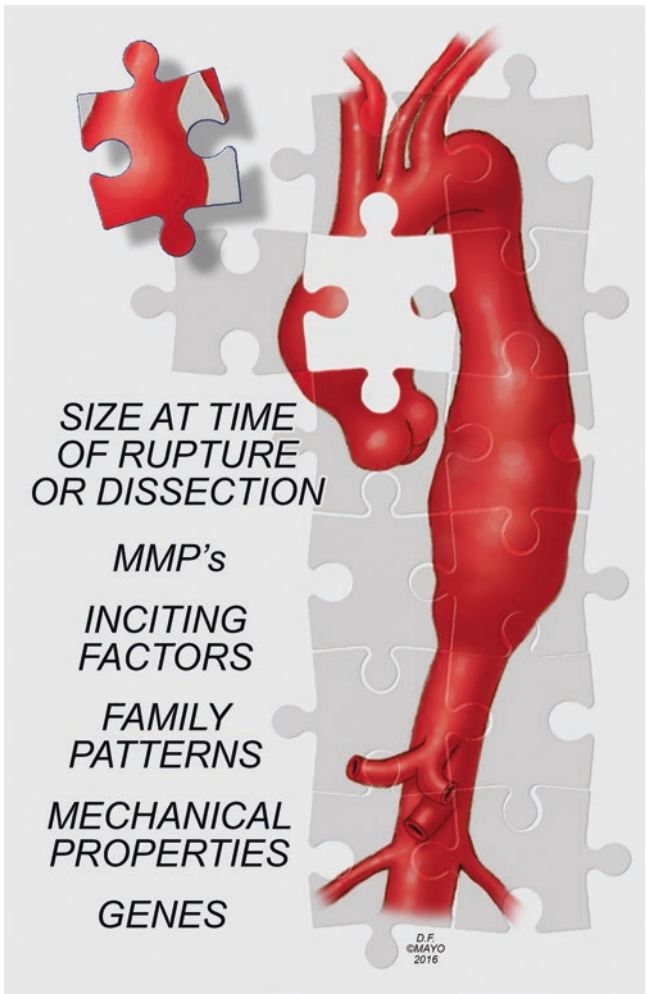


Fig. 2.35 Pieces in the puzzle of the playbook of thoracic aortic aneurysm. By permission of Mayo Foundation for Medical Education and Research. All rights reserved

These advances in understanding put aortic specialists in a better position than ever before to combat the silent, virulent, and capricious disease of thoracic aortic aneurysm.

References

1. Elefteriades JA, Farkas EA. Thoracic aortic aneurysm clinically pertinent controversies and uncertainties. J Am Coll Cardiol. 2010;55:841–57.
2. Ziganshin BA, Elefteriades JA. Thoracic aortic disease. In: Stergiopoulos K, Brown DL, editors. Evidence-based cardiology consult. 1st ed. London: Springer; 2014. p. 331–53.
3. Elefteriades JA. Beating a sudden killer. Sci Am. 2005;293: 64–71.
4. Elefteriades JA. Thoracic aortic aneurysm: reading the enemy's playbook. Curr Probl Cardiol. 2008;33:203–77.
5. Davies RR, Kaple RK, Mandapati D, Gallo A, Botta Jr DM, Elefteriades JA, et al. Natural history of ascending aortic aneurysms in the setting of an unreplaced bicuspid aortic valve. Ann Thorac Surg. 2007;83:1338–44.
6. Kuzmik GA, Feldman M, Tranquilli M, Rizzo JA, Johnson M, Elefteriades JA. Concurrent intracranial and thoracic aortic aneurysms. Am J Cardiol. 2010;105:417–20.
7. Hornick M, Moomiaie R, Mojibian H, Ziganshin B, Almuwaqqat Z, Lee ES, et al. 'Bovine' aortic arch—a marker for thoracic aortic disease. Cardiology. 2012;123:116–24.
8. Dumfarth J, Chou AS, Ziganshin BA, Bhandari R, Peterss S, Tranquilli M, et al. Atypical aortic arch branching variants: a novel marker for thoracic aortic disease. J Thorac Cardiovasc Surg. 2015;149:1586–92.
9. Hultgren R, Larsson E, Wahlgren CM, Swedenborg J. Female and elderly abdominal aortic aneurysm patients more commonly have concurrent thoracic aortic aneurysm. Ann Vasc Surg. 2012;26: 918–23.
10. Robson JC, Kiran A, Maskell J, Hutchings A, Arden N, Dasgupta B, et al. The relative risk of aortic aneurysm in patients with giant cell arteritis compared with the general population of the UK. Ann Rheum Dis. 2015;74:129–35.
11. Ziganshin BA, Theodoropoulos P, Salloum MN, Zaza KJ, Tranquilli M, Mojibian HR, et al. Simple renal cysts as markers of thoracic aortic disease. J Am Heart Assoc. 2016;5:e002248.
12. Olsson C, Eriksson P, Franco-Cereceda A. Association between thoracic aortic disease and inguinal hernia. J Am Heart Assoc. 2014;3. pii: e001040.
13. Elefteriades JA, Sang A, Kuzmik G, Hornick M. Guilt by association: paradigm for detecting a silent killer (thoracic aortic aneurysm). Open Heart. 2015;2:e000169.
14. Johnston KW, Rutherford RB, Tilson MD, Shah DM, Hollier L, Stanley JC. Suggested standards for reporting on arterial aneurysms. Subcommittee on Reporting Standards for Arterial Aneurysms, Ad Hoc Committee on Reporting Standards, Society for Vascular Surgery and North American Chapter, International Society for Cardiovascular Surgery. J Vasc Surg. 1991;13: 452–8.
15. Crawford ES, Coselli JS. Thoracoabdominal aneurysm surgery. Semin Thorac Cardiovasc Surg. 1991;3:300–22.
16. Safi HJ, Miller III CC. Spinal cord protection in descending thoracic and thoracoabdominal aortic repair. Ann Thorac Surg. 1999;67:1937–9; discussion 1953–1938.
17. McMillan WD, Pearce WH. Inflammation and cytokine signaling in aneurysms. Ann Vasc Surg. 1997;11:540–5.
18. Shah PK. Inflammation, metalloproteinases, and increased proteolysis: an emerging pathophysiological paradigm in aortic aneurysm. Circulation. 1997;96:2115–7.
19. Alexander JJ. The pathobiology of aortic aneurysms. J Surg Res. 2004;117:163–75.
20. Ailawadi G, Eliason JL, Upchurch Jr GR. Current concepts in the pathogenesis of abdominal aortic aneurysm. J Vasc Surg. 2003;38: 584–8.
21. Ruddy JM, Jones JA, Ikonomidis JS. Pathophysiology of thoracic aortic aneurysm (TAA): is it not one uniform aorta? Role of embryologic origin. Prog Cardiovasc Dis. 2013;56:68–73.
22. Barbour JR, Spinale FG, Ikonomidis JS. Proteinase systems and thoracic aortic aneurysm progression. J Surg Res. 2007;139:292–307.
23. Hackmann AE, Thompson RW, LeMaire SA. Long-term suppressive therapy: clinical reality and future prospects. In: Elefteriades JA, editor. Acute aortic disease. New York: Informa Healthcare; 2007. p. 309–30.
24. Thompson RW, Parks WC. Role of matrix metalloproteinases in abdominal aortic aneurysms. Ann N Y Acad Sci. 1996;800: 157–74.
25. McMillan WD, Pearce WH. Increased plasma levels of metalloproteinase-9 are associated with abdominal aortic aneurysms. J Vasc Surg. 1999;29:122–7; discussion 127–129.
26. LeMaire SA, Wang X, Wilks JA, Carter SA, Wen S, Won T, et al. Matrix metalloproteinases in ascending aortic aneurysms: bicuspid versus trileaflet aortic valves. J Surg Res. 2005;123:40–8.
27. Ikonomidis JS, Jones JA, Barbour JR, Stroud RE, Clark LL, Kaplan BS, et al. Expression of matrix metalloproteinases and endogenous inhibitors within ascending aortic aneurysms of patients with Marfan syndrome. Circulation. 2006;114:I365–70.
28. Ikonomidis JS, Jones JA, Barbour JR, Stroud RE, Clark LL, Kaplan BS, et al. Expression of matrix metalloproteinases and endogenous inhibitors within ascending aortic aneurysms of patients with bicuspid or tricuspid aortic valves. J Thorac Cardiovasc Surg. 2007;133:1028–36.
29. Koullias GJ, Korkolis DP, Ravichandran P, Psyrri A, Hatzaras I, Elefteriades JA. Tissue microarray detection of matrix metalloproteinases, in diseased tricuspid and bicuspid aortic valves with or without pathology of the ascending aorta. Eur J Cardiothorac Surg. 2004;26:1098–103.
30. Koullias GJ, Ravichandran P, Korkolis DP, Rimm DL, Elefteriades JA. Increased tissue microarray matrix metalloproteinase expression favors proteolysis in thoracic aortic aneurysms and dissections. Ann Thorac Surg. 2004;78:2106–10; discussion 2110–2101.
31. Elefteriades JA. Thoracic aortic aneurysm: reading the enemy's playbook. Yale J Biol Med. 2008;81:175–86.
32. El-Hamamsy I, Yacoub MH. Cellular and molecular mechanisms of thoracic aortic aneurysms. Nat Rev Cardiol. 2009;6:771–86.
33. Tang PC, Yakimov AO, Teesdale MA, Coady MA, Dardik A, Elefteriades JA, et al. Transmural inflammation by interferon-gamma-producing T cells correlates with outward vascular remodeling and intimal expansion of ascending thoracic aortic aneurysms. FASEB J. 2005;19:1528–30.
34. Schonbeck U, Sukhova GK, Gerdes N, Libby P. T(H)2 predominant immune responses prevail in human abdominal aortic aneurysm. Am J Pathol. 2002;161:499–506.
35. Lopez-Candales A, Holmes DR, Liao S, Scott MJ, Wickline SA, Thompson RW. Decreased vascular smooth muscle cell density in medial degeneration of human abdominal aortic aneurysms. Am J Pathol. 1997;150:993–1007.
36. Jacob MP, Badier-Commander C, Fontaine V, Benazzoug Y, Feldman L, Michel JB. Extracellular matrix remodeling in the vascular wall. Pathol Biol (Paris). 2001;49:326–32.
37. Rowe VL, Stevens SL, Reddick TT, Freeman MB, Donnell R, Carroll RC, et al. Vascular smooth muscle cell apoptosis in aneurysmal, occlusive, and normal human aortas. J Vasc Surg. 2000;31:567–76.
38. Henderson EL, Geng YJ, Sukhova GK, Whittemore AD, Knox J, Libby P. Death of smooth muscle cells and expression of mediators of apoptosis by T lymphocytes in human abdominal aortic aneurysms. Circulation. 1999;99:96–104.
39. Liao S, Curci JA, Kelley BJ, Sicard GA, Thompson RW. Accelerated replicative senescence of medial smooth muscle cells derived from abdominal aortic aneurysms compared to the adjacent inferior mesenteric artery. J Surg Res. 2000;92:85–95.

40. Zarins CK, Glagov S, Vesselinovitch D, Wissler RW. Aneurysm formation in experimental atherosclerosis: relationship to plaque evolution. J Vasc Surg. 1990;12:246–56.
41. Reed D, Reed C, Stemmermann G, Hayashi T. Are aortic aneurysms caused by atherosclerosis? Circulation. 1992;85:205–11.
42. Tilson MD. Aortic aneurysms and atherosclerosis. Circulation. 1992;85:378–9.
43. Tilson MD, Stansel HC. Differences in results for aneurysm vs occlusive disease after bifurcation grafts: results of 100 elective grafts. Arch Surg. 1980;115:1173–5.
44. Agmon Y, Khandheria BK, Meissner I, et al. Is aortic dilatation an atherosclerosis-related process? Clinical, laboratory, and transesophageal echocardiographic correlates of thoracic aortic dimensions in the population with implications for thoracic aortic aneurysm formation. J Am Coll Cardiol. 2003;42:1076–83.
45. Silence J, Collen D, Lijnen HR. Reduced atherosclerotic plaque but enhanced aneurysm formation in mice with inactivation of the tissue inhibitor of metalloproteinase-1 (TIMP-1) gene. Circ Res. 2002;90:897–903.
46. Jiang X, Rowitch DH, Soriano P, McMahon AP, Sucov HM. Fate of the mammalian cardiac neural crest. Development. 2000;127:1607–16.
47. Cheung C, Bernardo AS, Trotter MW, Pedersen RA, Sinha S. Generation of human vascular smooth muscle subtypes provides insight into embryological origin-dependent disease susceptibility. Nat Biotechnol. 2012;30:165–73.
48. Gittenberger-de Groot AC, DeRuiter MC, Bergwerff M, Poelmann RE. Smooth muscle cell origin and its relation to heterogeneity in development and disease. Arterioscler Thromb Vasc Biol. 1999;19:1589–94.
49. Achneck H, Modi B, Shaw C, Rizzo J, Albornoz G, Fusco D, et al. Ascending thoracic aneurysms are associated with decreased systemic atherosclerosis. Chest. 2005;128:1580–6.
50. Hung A, Zafar M, Mukherjee S, Tranquilli M, Scoutt LM, Elefteriades JA. Carotid intima-media thickness provides evidence that ascending aortic aneurysm protects against systemic atherosclerosis. Cardiology. 2012;123:71–7.
51. Chau K, Elefteriades JA. Ascending thoracic aortic aneurysms protect against myocardial infarctions. Int J Angiol. 2014;23:177–82.
52. Chau KH, Bender JR, Elefteriades JA. Silver lining in the dark cloud of aneurysm disease. Cardiology. 2014;128:327–32.
53. Curtis A, Smith T, Ziganshin BA, Elefteriades JA. Ascending aortic proaneurysmal genetic mutations with antiatherogenic effects. Int J Angiol. 2015;24:189–97.
54. Tilson MD, Seashore MR. Fifty families with abdominal aortic aneurysms in two or more first-order relatives. Am J Surg. 1984;147:551–3.
55. Tilson MD, Seashore MR. Human genetics of the abdominal aortic aneurysm. Surg Gynecol Obstet. 1984;158:129–32.
56. Marfan AB. Un cas de deformation congenitale des quatre membres, plus prononce des extremites, caracterise par r allongement des coeur avec un certain degre d'amincissement. Bull Mem Soc Med Hop Paris. 1896;13:220–6.
57. Elefteriades JA, Pomianowski P. Practical genetics of thoracic aortic aneurysm. Prog Cardiovasc Dis. 2013;56:57–67.
58. Pomianowski P, Elefteriades JA. The genetics and genomics of thoracic aortic disease. Ann Cardiothorac Surg. 2013;2:271–9.
59. Coady MA, Davies RR, Roberts M, Goldstein LJ, Rogalski MJ, Rizzo JA, et al. Familial patterns of thoracic aortic aneurysms. Arch Surg. 1999;134:361–7.
60. Biddinger A, Rocklin M, Coselli J, Milewicz DM. Familial thoracic aortic dilatations and dissections: a case control study. J Vasc Surg. 1997;25:506–11.
61. Milewicz DM, Hariyadarshi P, Avidan N, Guo DC, Tran-Fadulu V. Genetic basis of thoracic aortic aneurysms and dissections. In: Elefteriades JA, editor. Acute aortic disease. New York: Informa Healthcare USA; 2007. p. 99–121.
62. Loeys BL, Dietz HC, Braverman AC, Callewaert BL, De Backer J, Devereux RB, et al. The revised Ghent nosology for the Marfan syndrome. J Med Genet. 2010;47:476–85.
63. Callewaert B, Malfait F, Loeys B, De Paepe A. Ehlers-Danlos syndromes and Marfan syndrome. Best Pract Res Clin Rheumatol. 2008;22:165–89.
64. De Paepe A, Malfait F. The Ehlers-Danlos syndrome, a disorder with many faces. Clin Genet. 2012;82:1–11.
65. Lin AE, Lippe B, Rosenfeld RG. Further delineation of aortic dilation, dissection, and rupture in patients with Turner syndrome. Pediatrics. 1998;102:e12.
66. Sybert VP, McCauley E. Turner's syndrome. N Engl J Med. 2004;351:1227–38.
67. Loeys BL, Chen J, Neptune ER, Judge DP, Podowski M, Holm T, et al. A syndrome of altered cardiovascular, craniofacial, neurocognitive and skeletal development caused by mutations in TGFBR1 or TGFBR2. Nat Genet. 2005;37:275–81.
68. Loeys BL, Schwarze U, Holm T, Callewaert BL, Thomas GH, Pannu H, et al. Aneurysm syndromes caused by mutations in the TGF-beta receptor. N Engl J Med. 2006;355:788–98.
69. Albornoz G, Coady MA, Roberts M, Davies RR, Tranquilli M, Rizzo JA, et al. Familial thoracic aortic aneurysms and dissections—incidence, modes of inheritance, and phenotypic patterns. Ann Thorac Surg. 2006;82:1400–5.
70. Wang L, Guo DC, Cao J, Gong L, Kamm KE, Regalado E, et al. Mutations in myosin light chain kinase cause familial aortic dissections. Am J Hum Genet. 2010;87:701–7.
71. Guo DC, Pannu H, Tran-Fadulu V, Papke CL, Yu RK, Avidan N, et al. Mutations in smooth muscle alpha-actin (ACTA2) lead to thoracic aortic aneurysms and dissections. Nat Genet. 2007;39:1488–93.
72. Guo DC, Papke CL, Tran-Fadulu V, Regalado ES, Avidan N, Johnson RJ, et al. Mutations in smooth muscle alpha-actin (ACTA2) cause coronary artery disease, stroke, and Moyamoya disease, along with thoracic aortic disease. Am J Hum Genet. 2009;84:617–27.
73. Pape LA, Tsai TT, Isselbacher EM, Oh JK, O'gara PT, Evangelista A, et al. Aortic diameter >or = 5.5 cm is not a good predictor of type A aortic dissection: observations from the International Registry of Acute Aortic Dissection (IRAD). Circulation. 2007;116:1120–7.
74. Hiratzka LF, Bakris GL, Beckman JA, Bersin RM, Carr VF, Casey DE Jr, et al. 2010 ACCF/AHA/AATS/ACR/ASA/SCA/SCAI/SIR/STS/SVM guidelines for the diagnosis and management of patients with thoracic aortic disease. A report of the American College of Cardiology Foundation/American Heart Association Task Force on Practice Guidelines, American Association for Thoracic Surgery, American College of Radiology, American Stroke Association, Society of Cardiovascular Anesthesiologists, Society for Cardiovascular Angiography and Interventions, Society of Interventional Radiology, Society of Thoracic Surgeons, and Society for Vascular Medicine. J Am Coll Cardiol. 2010;55:e27–129.
75. Biesecker LG, Green RC. Diagnostic clinical genome and exome sequencing. N Engl J Med. 2014;370:2418–25.
76. Ziganshin BA, Bailey AE, Coons C, Dykas D, Charilaou P, Tanriverdi LH, et al. Routine genetic testing for thoracic aortic aneurysm and dissection in a clinical setting. Ann Thorac Surg. 2015;100:1604–11.
77. Turkbey EB, Jain A, Johnson C, Redheuil A, Arai AE, Gomes AS, et al. Determinants and normal values of ascending aortic diameter by age, gender, and race/ethnicity in the Multi-Ethnic Study of Atherosclerosis (MESA). J Magn Reson Imaging. 2014;39:360–8.

78. Paruchuri V, Salhab KF, Kuzmik G, Gubernikoff G, Fang H, Rizzo JA, et al. Aortic size distribution in the general population: explaining the size paradox in aortic dissection. Cardiology. 2015;131:265–72.
79. Berger JA, Elefteriades JA. Toward uniformity in reporting of thoracic aortic diameter. Int J Angiol. 2012;21:243–4.
80. Rizzo JA, Coady MA, Elefteriades JA. Procedures for estimating growth rates in thoracic aortic aneurysms. J Clin Epidemiol. 1998;51:747–54.
81. Rizzo JA, Coady MA, Elefteriades JA. Interpreting data on thoracic aortic aneurysms. Statistical issues. Cardiol Clin. 1999;17:797–805. x.
82. Coady MA, Rizzo JA, Hammond GL, Mandapati D, Darr U, Kopf GS, et al. What is the appropriate size criterion for resection of thoracic aortic aneurysms? J Thorac Cardiovasc Surg. 1997;113:476–91; discussion 489–491.
83. Coady MA, Rizzo JA, Goldstein LJ, Elefteriades JA. Natural history, pathogenesis, and etiology of thoracic aortic aneurysms and dissections. Cardiol Clin. 1999;17:615–35. vii.
84. Coady MA, Rizzo JA, Hammond GL, Kopf GS, Elefteriades JA. Surgical intervention criteria for thoracic aortic aneurysms: a study of growth rates and complications. Ann Thorac Surg. 1999;67:1922–6; discussion 1953–1928.
85. Elefteriades JA, Ziganshin BA, Rizzo JA, Fang H, Tranquilli M, Paruchuri V, et al. Indications and imaging for aortic surgery: size and other matters. J Thorac Cardiovasc Surg. 2015;149:S10–3.
86. Davies RR, Goldstein LJ, Coady MA, Tittle SL, Rizzo JA, Kopf GS, et al. Yearly rupture or dissection rates for thoracic aortic aneurysms: simple prediction based on size. Ann Thorac Surg. 2002;73:17–27; discussion 27–18.
87. Coady MA, Rizzo JA, Elefteriades JA. Developing surgical intervention criteria for thoracic aortic aneurysms. Cardiol Clin. 1999;17:827–39.
88. Davies RR, Gallo A, Coady MA, Tellides G, Botta DM, Burke B, et al. Novel measurement of relative aortic size predicts rupture of thoracic aortic aneurysms. Ann Thorac Surg. 2006;81:169–77.
89. Koullias G, Modak R, Tranquilli M, Korkolis DP, Barash P, Elefteriades JA. Mechanical deterioration underlies malignant behavior of aneurysmal human ascending aorta. J Thorac Cardiovasc Surg. 2005;130:677–83.
90. Hatzaras IS, Bible JE, Koullias GJ, Tranquilli M, Singh M, Elefteriades JA. Role of exertion or emotion as inciting events for acute aortic dissection. Am J Cardiol. 2007;100:1470–2.
91. Elefteriades JA, Hatzaras I, Tranquilli MA, Elefteriades AJ, Stout R, Shaw RK, et al. Weight lifting and rupture of silent aortic aneurysms. JAMA. 2003;290:2803.
92. Hatzaras I, Tranquilli M, Coady M, Barrett PM, Bible J, Elefteriades JA. Weight lifting and aortic dissection: more evidence for a connection. Cardiology. 2007;107:103–6.
93. Feldman M, Elefteraides JA. Triggers of aortic dissection. In: Boudoulas H, Stefanadis C, editors. The aorta: structure, function, dysfunction, and diseases. New York: Informa Healthcare; 2009; xi, 259 p.
94. Mehta RH, Manfredini R, Hassan F, Sechtem U, Bossone E, Oh JK, et al. Chronobiological patterns of acute aortic dissection. Circulation. 2002;106:1110–5.
95. Manfredini R, Boari B, Gallerani M, Salmi R, Bossone E, Distante A, et al. Chronobiology of rupture and dissection of aortic aneurysms. J Vasc Surg. 2004;40:382–8.
96. Sumiyoshi M, Kojima S, Arima M, Suwa S, Nakazato Y, Sakurai H, et al. Circadian, weekly, and seasonal variation at the onset of acute aortic dissection. Am J Cardiol. 2002;89:619–23.
97. Hata T, Ogihara T, Maruyama A, Mikami H, Nakamaru M, Naka T, et al. The seasonal variation of blood pressure in patients with essential hypertension. Clin Exp Hypertens A. 1982;4:341–54.
98. Humphrey JD. Possible mechanical roles of glycosaminoglycans in thoracic aortic dissection and associations with dysregulated transforming growth factor-beta. J Vasc Res. 2013;50:1–10.
99. Roccabianca S, Ateshian GA, Humphrey JD. Biomechanical roles of medial pooling of glycosaminoglycans in thoracic aortic dissection. Biomech Model Mechanobiol. 2014;13:13–25.
100. Hoffman JI, Kaplan S. The incidence of congenital heart disease. J Am Coll Cardiol. 2002;39:1890–900.
101. Friedman T, Mani A, Elefteriades JA. Bicuspid aortic valve: clinical approach and scientific review of a common clinical entity. Expert Rev Cardiovasc Ther. 2008;6:235–48.
102. Verma S, Siu SC. Aortic dilatation in patients with bicuspid aortic valve. N Engl J Med. 2014;370:1920–9.
103. Michelena HI, Prakash SK, Della Corte A, Bissell MM, Anavekar N, Mathieu P, et al. Bicuspid aortic valve: identifying knowledge gaps and rising to the challenge from the International Bicuspid Aortic Valve Consortium (BAVCon). Circulation. 2014;129:2691–704.
104. Ward C. Clinical significance of the bicuspid aortic valve. Heart. 2000;83:81–5.
105. Januzzi JL, Isselbacher EM, Fattori R, Cooper JV, Smith DE, Fang J, et al. Characterizing the young patient with aortic dissection: results from the International Registry of Aortic Dissection (IRAD). J Am Coll Cardiol. 2004;43:665–9.
106. Michelena HI, Desjardins VA, Avierinos JF, Russo A, Nkomo VT, Sundt TM, et al. Natural history of asymptomatic patients with normally functioning or minimally dysfunctional bicuspid aortic valve in the community. Circulation. 2008;117:2776–84.
107. Coady M, Elefteraides JA. The natural history of thoracic aortic aneurysms: etiology, pathogenesis, and evidence-based decision making for surgical intervention. In: Elefteraides JA, editor. Acute aortic disease. New York: Informa Healthcare USA; 2007. p. 173–203.
108. Borges LF, Touat Z, Leclercq A, Zen AA, Jondeau' G, Franc B, et al. Tissue diffusion and retention of metalloproteinases in ascending aortic aneurysms and dissections. Hum Pathol. 2009;40:306–13.

Genetic Considerations in Patients with Aortic Disease

3

Sherene Shalhub

Introduction

The development of aortic endovascular repair has been a major advance in the treatment of aortic aneurysms and dissections. The use of stent-grafts to treat patients with connective tissue disease has been limited due to concerns for device failure and they have been intentionally excluded from FDA trials. These patients form a subset of a larger group of patients with genetically triggered aortic disease. The aim of this chapter is to summarize the current body of knowledge about the genetics of syndromic (including connective tissue disease) and non-syndromic genetically triggered aortic aneurysms and dissections, diagnosis, current management, and role of endovascular repair in this population. Having a working knowledge of the known mutations leading to aortic aneurysms and dissections will allow the vascular surgeon to identify these patients and will facilitate early diagnosis and treatments tailored to the affected individuals [1].

Prevalence of Genetically Triggered Aortic Disease

The phenomenon of familial clustering of aneurysms and dissections is well described. These patients tend to present with aneurysms and dissections at a relatively young age, and are frequently described as having fragile tissues and a more aggressive growth rate of their aneurysm than patients with sporadic disease [2]. It is estimated that 21 % of the non-syndromic thoracic aortic aneurysms and dissections and 15–20 % of abdominal aortic aneurysms are familial [2–4]. While each mutation has a unique phenotype, patients are at an increased risk for the early onset of aortic aneurysms and dissections, which are the most common cause of death in this population.

The most well-studied genes have been the ones affecting the formation of ascending aortic aneurysms and subsequent dissection. These have been collectively called “aneurysms involving the ascending thoracic aorta leading to acute aortic dissections” (TAAD). TAAD may occur in association with a syndrome or, as demonstrated more recently, in a familial pattern with few to no additional clinical findings—non-syndromic (FTAAD). Syndromic TAAD have striking features and therefore have been a focus of study for several decades. The cause is usually a connective tissue disease (CTD). A CTD is a genetic disease in which the primary target is either collagen or elastin protein assembly, in which disruption leads to an inherent predisposition to loss of structural integrity, degeneration, and consequent aneurysm formation, and/or spontaneous vascular dissection and rupture. The most extensively studied syndromic CTD affecting the aorta is Marfan syndrome (MFS), which is also the most common mutation leading to syndromic FTAAD. Other syndromic conditions known to affect the aorta and arteries include vascular Ehlers-Danlos syndrome (VEDS), aneurysms osteoarthritis syndrome (AOS), Loeys-Dietz syndrome (LDS), and arterial tortuosity syndrome (ATS). With the exception of VEDS, these syndromes are characterized by increased transforming growth factor (TGF)-β signaling in the arterial wall. The increased TGFβ signaling is thought to disrupt the balance of inflammatory-mediated extracellular matrix production and degradation during pathological remodeling of the aortic wall, leading to aneurysmal degeneration [5]. The less common non-syndromic manifestation of FTAAD includes a group of mutations which affect one of the two pathways: the TGFβ pathway or genes affecting smooth muscle cell contractile proteins.

Descending thoracic aorta and abdominal aortic aneurysms (AAA) also occur in syndromic and non-syndromic

S. Shalhub (✉)
Department of Surgery, Division of Vascular Surgery,
University of Washington, 1959 NE Pacific Street, Box 356410,
Seattle, WA 98195, USA
e-mail: shalhub@uw.edu

© Mayo Foundation for Medical Education and Research 2017

G.S. Oderich (ed.), *Endovascular Aortic Repair*, DOI 10.1007/978-3-319-15192-2_3

FTAAD, but most familial AAAs appear to be unrelated to specific genetic syndromes. An estimated 25 % are inherited in autosomal dominant manner and the rest are inherited in an autosomal recessive manner [4].

In the absence of familial history, the proportion of thoracic and abdominal aortic aneurysms and dissections resulting from a genetic predisposition is still unknown and is an area of active investigation given that many mutations can arise in a de novo manner. Identification of a patient's underlying gene mutation can have significant implications for vascular screening, management, and choice of operative repair, including decisions about endovascular repair. This chapter offers an overview of the presentation of patients with genetically triggered aortic aneurysms and dissections and a description of their phenotype (physical appearance, arterial and aortic involvement), along with a discussion of the endovascular therapeutic implications in these populations.

Marfan Syndrome

MFS is an autosomal dominant heritable CTD that affects the cardiovascular, ocular, and musculoskeletal systems (Fig. 3.1). The syndrome is named after Antoine-Bernard Marfan, who first described a 5-year-old child with arachnodactyly in 1896. Estimates indicate that about 1 in 3000–5000 individuals have MFS. There is no known role of gender or ethnicity [6].

Mutations

The underlying mutations for MFS are mutations in the fibrillin-1 (*FNB1*) gene on chromosome 15, discovered in 1991 [7]. The mutation is inherited in an autosomal dominant manner with high penetrance and varying phenotypic expression leading to great clinical variability [7]. The gene encodes fibrillin-1 glycoprotein, which is essential for the formation of elastic fibers found in connective tissue, provides a scaffold for elastin deposition in the extracellular matrix (Fig. 3.2). This is fundamental to maintaining the integrity of the vessel wall and serves as a regulator of TGFβ signaling (Fig. 3.3). The TGFβ signaling pathway is important in regulation of cellular proliferation, differentiation, embryogenesis, and apoptosis. The altered extracellular matrix is believed to lead to aortic dilation and dissection. Approximately 25 % of patients with MFS have a de novo mutation.

Diagnosis

The diagnosis of MFS relies on defined clinical criteria, known as the Ghent criteria, first reported in 1996 and revised in 2010 [8]. These criteria were outlined through the international expert opinion of a panel with extensive experience in applying the diagnostic criteria, the differential diagnosis of MFS, and the strengths and limitations of molecular genetic testing. The diagnostic criteria include disease manifestations in numerous body systems including the skeletal, ocular, cardiovascular, and pulmonary systems, the dura, and the integument. The presence of aortic root aneurysm or dissection and ectopia lentis are the cardinal clinical features of MFS. In the absence of any family history, the presence of aortic root aneurysm or dissection and ectopia lentis manifestations is sufficient for the unequivocal diagnosis of MFS. If none of these two features are present, the presence of an *FBN1* mutation or a combination of systemic manifestations is required. The clinical diagnosis has proven consistent with genetic data, as improved molecular techniques have allowed confirmation of the diagnosis in up to 97 % of patients [9]. The current revised Ghent criteria are as follows:

1. Aortic diameter at the sinuses of Valsalva above ≥2 *Z*-score or aortic root dissection AND ectopia lentis
2. Aortic diameter at the sinuses of Valsalva above ≥2 *Z*-score or aortic root dissection AND *FBN1* mutation
3. Aortic diameter at the sinuses of Valsalva above >2 *Z*-score or aortic root dissection AND scoring of systemic features (listed below) >7
4. Ectopia lentis AND *FBN1* mutation with known aortic root dissection
5. Ectopia lentis AND a family history of MFS (as defined above)
6. Scoring of systemic features (listed below) ≥7 AND a family history of MFS (as defined above)
7. Aortic diameter at the sinuses of Valsalva above ≥2 *Z*-score if age is above 20 years old or ≥3 *Z*-score if age is 3 years old and below 20 years AND a family history of MFS

(For (1), (3), (6), and (7) the caveat is that this applies as long as it is without discriminating features of Shprintzen Goldberg syndrome, LDS, and VEDS, AND after *TGFβR1/2*, collagen biochemistry, *COL3A1* testing if indicated AND with the knowledge that other conditions/genes will emerge with time.)

The following are the systemic features that are assigned a point value used in scoring of the overall systemic features (maximum total: 20 points; score >7 indicates systemic involvement):

1. Wrist AND thumb sign—3 points (wrist OR thumb sign—1 point): The wrist sign is positive when the tip of the thumb covers the entire fingernail of the fifth finger when wrapped around the contralateral wrist. The thumb sign is positive when the entire distal phalanx of the adducted thumb extends beyond the ulnar border of the palm with or without the assistance of the patient or examiner to achieve maximal adduction. Three points are assigned to the combination of wrist and thumb

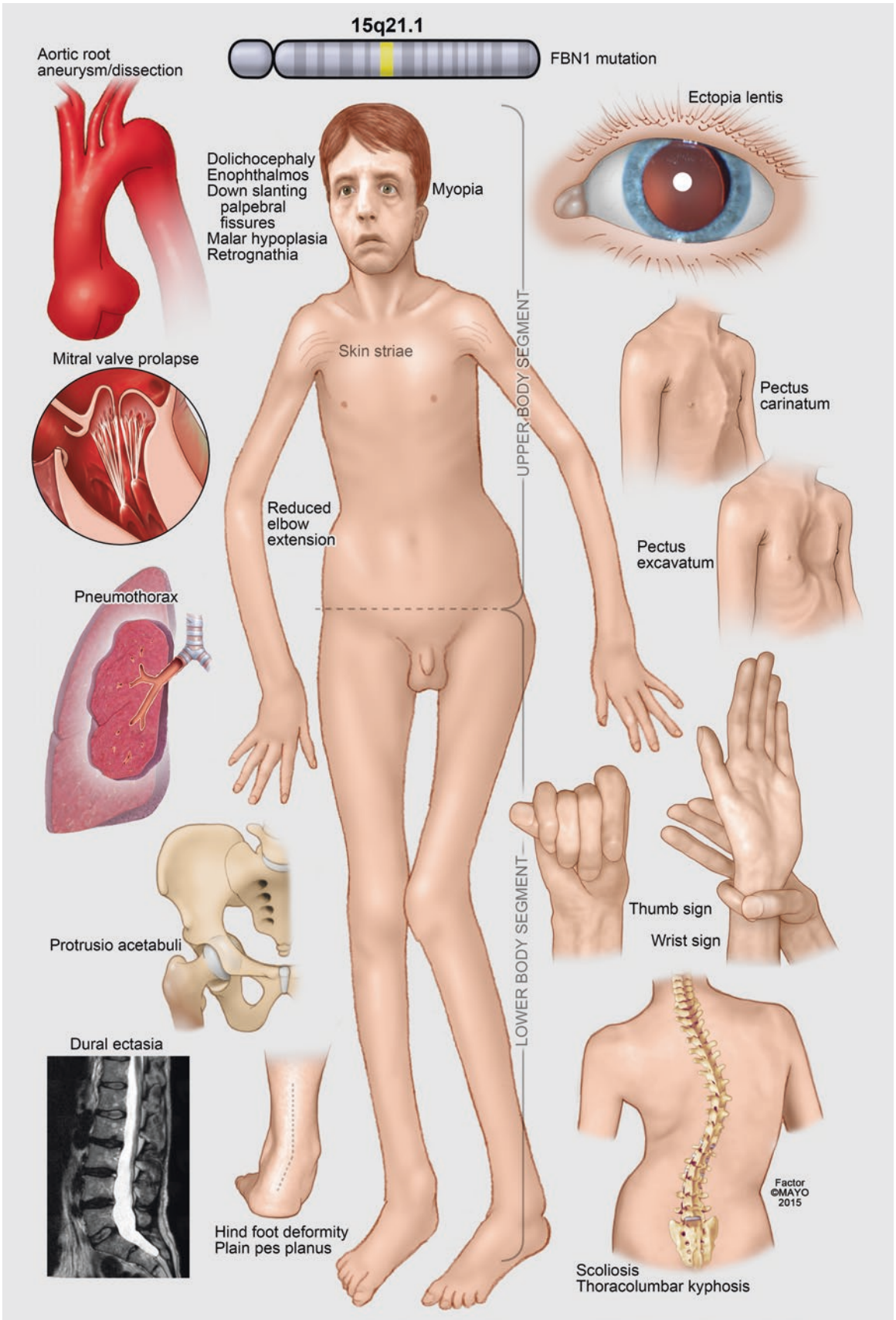


Fig. 3.1 FDN1 mutation in the chromosome 15q21.1 and clinical spectrum of findings in patients with Marfan syndrome. By permission of Mayo Foundation for Medical Education and Research. All rights reserved

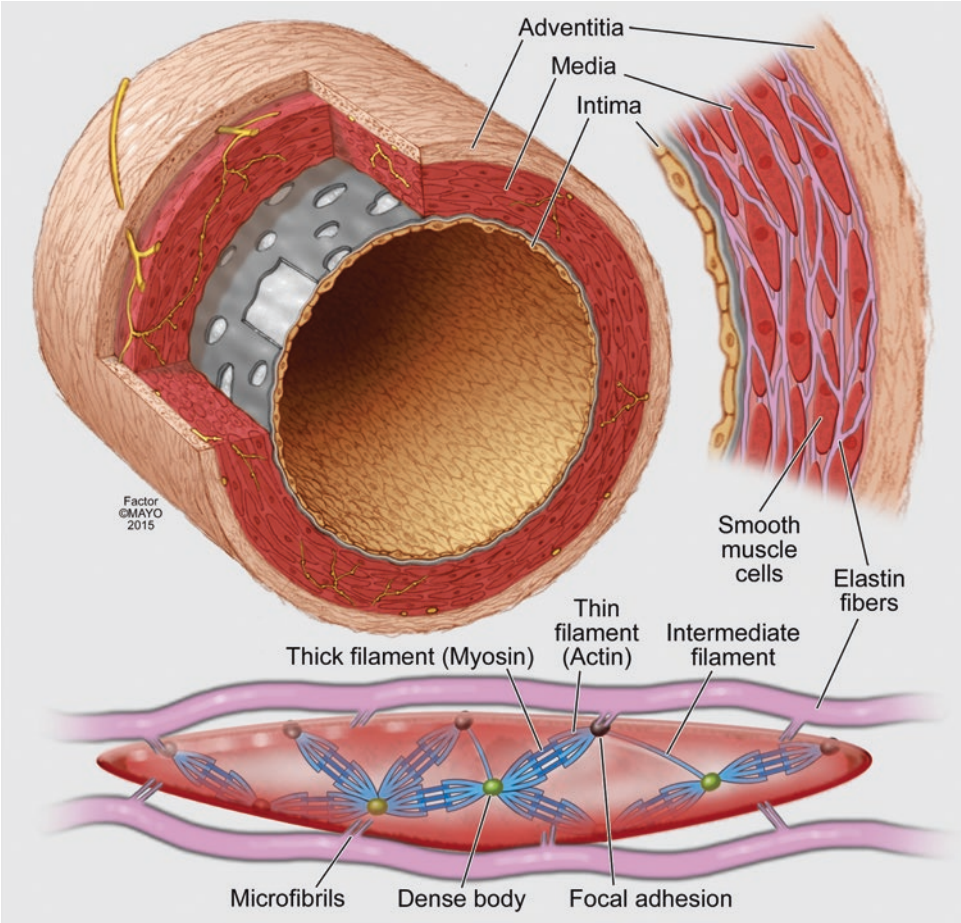


Fig. 3.2 The aortic wall structure is a muscular organ where the tensile strength and elasticity reside in the medial layer, which is composed of concentrically arranged elastic fibers and smooth muscle cells. By permission of Mayo Foundation for Medical Education and Research. All rights reserved

signs. If either of the two signs is absent, only one point is assigned.

2. Pectus carinatum deformity—2 (pectus excavatum or chest asymmetry—1): Pectus carinatum is believed to be more specific for MFS than pectus excavatum and is assigned two points.
3. Hind foot deformity—2 points (plain pes planus—1 point)
4. Pneumothorax—2 points
5. Dural ectasia—2 points
6. Protrusio acetabuli—2 points
7. Reduced upper segment/lower segment ratio AND increased arm/height AND no severe scoliosis—1 point
8. Scoliosis or thoracolumbar kyphosis—1 point
9. Reduced elbow extension—1 point
10. Facial features (3/5)—1 point (dolichocephaly, enophthalmos, down slanting palpebral fissures, malar hypoplasia, retrognathia)
11. Skin striae—1 point
12. Myopia >3 diopters—1 point
13. Mitral valve prolapse (all types)—1 point

Maximum total: 20 points; score >7 indicates systemic involvement. Joint hypermobility, highly arched palate, and recurrent or incisional hernia were removed from the revised Ghent criteria because of lack of perceived specificity.

The role of genetic testing in establishing a diagnosis of MFS remains limited and is included as part of the clinical criteria testing. This is because more than 1300 mutations have been identified in the *FBN1* gene and 90 % of the mutations are unique within a pedigree. Even within families in which the same mutation is shared, phenotypic variation is prominent. Thus, exacting a genotype–phenotype correlation has been a challenge [9]. Moreover, an estimated 10 % of the mutations in the *FBN1* gene that cause MFS are missed by conventional screening methods [10]. Therefore, the diagnosis of MFS currently rests primarily on physical clinical assessment based on the Ghent criteria.

Differential Diagnosis

It is important to understand that features of MFS overlap with those of other genetic syndromes. Several conditions present with aortic aneurysms and overlapping clinical manifestations with MFS, such as LDS, bicuspid aortic valve, VEDS, ATS, and FTAAD.

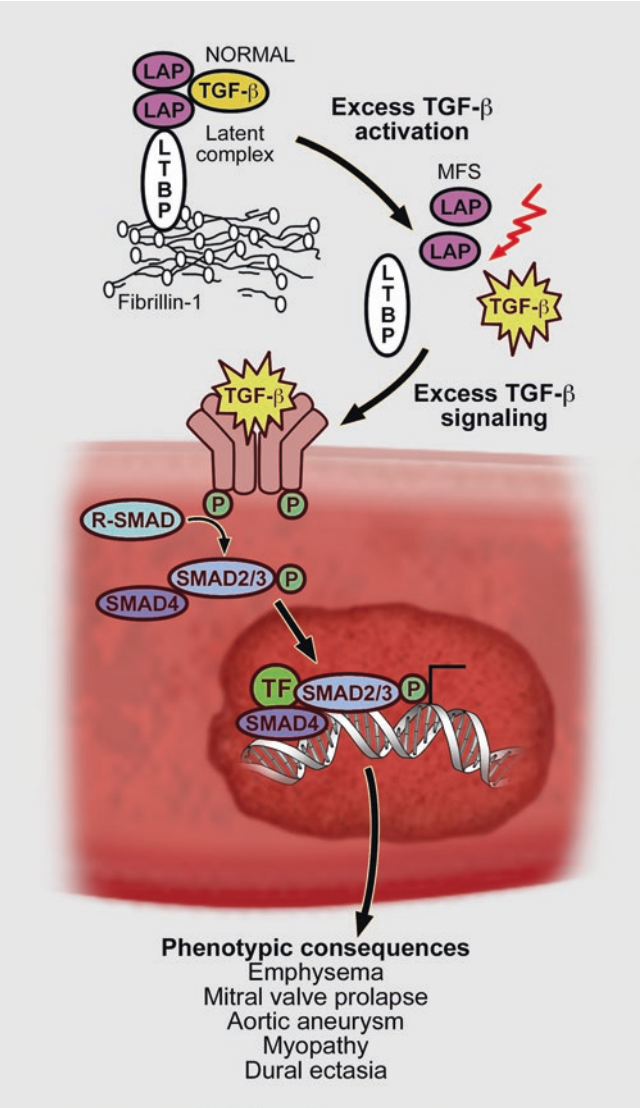


Fig. 3.3 Excess activation of transforming growth factor β (TGFβ) causes many of the features of syndromic familial thoracic aneurysm and dissection. Normal TGFβ metabolism requires binding of the cytokine to several proteins, including microfibrils, to prevent excess signaling. In Marfan syndrome, lack of normal microfibrillar assembly allows TGFβ to remain unsequestered in the extracellular space. As a consequence, excess TGFβ signaling can occur on the cell surfaces of TGFβ receptors. Once the TGFβ binds to its receptor, downstream receptor-associated SMAD proteins translocate to the nucleus to modulate transcriptional activity, alter protein expression, and yield phenotypic change. *LAP* latency-associated peptide, *LTBP* latent TGFβ-binding protein, *MFS* Marfan syndrome, *Nml* normal, *TF* tissue factor. By permission of Mayo Foundation for Medical Education and Research. All rights reserved

Surgical Management

Aortic Root

Root dilatation at the sinuses of Valsalva represents the most common cardiovascular manifestation requiring surgery in MFS patients. The natural history of the disease includes a high frequency of dissection and rupture once the aortic diameter reaches 6 cm. Elective aortic root replacement, first reported by Bentall in 1967, was introduced to prevent this complication. In adults, prophylactic aortic root and ascending aorta repair to prevent aortic rupture and dissection is recommended when its greatest diameter exceeds 50 mm [11]. The prophylactic root repair has been showed to be a safe operation in MFS with a 30-day mortality rate of 0.6 % [12, 13]. As a consequence, life expectancy with MFS has risen dramatically in the last 30 years from a median of 48 years in 1972 to a median of 72 years by 1993 [14, 15]. Because of the requirement for lifelong anticoagulation with warfarin, efforts were directed at maintaining the native aortic valve. This valve-sparing root replacement approach has the additional benefit of avoiding warfarin embryopathy in women with MFS who may later desire pregnancy. A prospective, international registry study was initiated to provide contemporary comparative data on short-term clinical outcomes after aortic valve-sparing and aortic valve-replacing root operations in patients with MFS. Early results demonstrate no differences in survival or valve-related morbidity; however, long-term results are necessary to assess the mid- and long-term durability of the two operations [12].

Descending Thoracic and Abdominal Aorta

The first successful replacement of the thoracoabdominal aorta in a patient with MFS was performed in the 1980s by Crawford [16]. Prolonged survival after successful aortic root replacement has led to a substantial increase in surviving MFS patients who require secondary interventions on the descending thoracic aorta or thoracoabdominal aorta due to new or residual dissections, distal aneurysm formation, and rupture [17–20]. These patients frequently require staged replacement of the entire aorta. One series demonstrated that 50 % of patients required descending aorta repair after aortic root replacement over a mean period of 26 years [17–20]. Additionally, there remains a segment of the population without prophylactic root repair who are at risk for type A aortic dissections. The incidence of reoperations is significantly higher in this sub-cohort than in those with dilatation only [18, 21].

Medical Management

Beta-blockers and angiotensin II blockade are advocated to slow the progression of aortic dilation in order to prevent acute ascending thoracic aortic dissection [22, 23]. Currently, a prospective, collaborative meta-analysis based on individual patient data from all randomized trials in MFS of ARBs versus placebo or open-label control and ARBs versus beta-blockers is under way (Marfan Treatment Trialists' Collaboration) [24].

Vascular Ehlers-Danlos Syndrome

Ehlers-Danlos syndrome is an autosomal dominant heterogeneous group of heritable CTDs, characterized by joint hypermobility, skin hyperextensibility, and tissue fragility affecting the skin, ligaments, joints, blood vessels, and internal organs (Fig. 3.4). Vascular Ehlers-Danlos syndrome (VEDS) is a subtype of Ehlers-Danlos syndrome due to defective type III collagen. Type III collagen is especially abundant in the skin, blood vessels, and hollow organs such as the bowel and uterus. The defective collagen production leads to a loss of tissue integrity most pronounced in the skin, arteries, and intestines. VEDS is estimated to occur at a rate of 1 in 90,000, but this estimate is likely to be low [25]. The prevalence is likely to increase over time due to improvements in molecular diagnosis and recognition of mutations that lead to a milder phenotype [25]. The median survival in patients with VEDS is 51 years of age, with mortality largely due to vascular rupture [25].

Mutations

VEDS occurs due to autosomal dominant heterozygous mutations in *COL3A1*, which encodes the procollagen peptide for type III collagen [26]. Over 700 mutations in *COL3A1* have been identified. In approximately 50 % of the cases, the mutation occurs as a de novo mutation without antecedent family history [27]. Some mutations result in failure to secrete type III procollagen from fibroblasts and accumulation of the protein in the rough endoplasmic reticulum

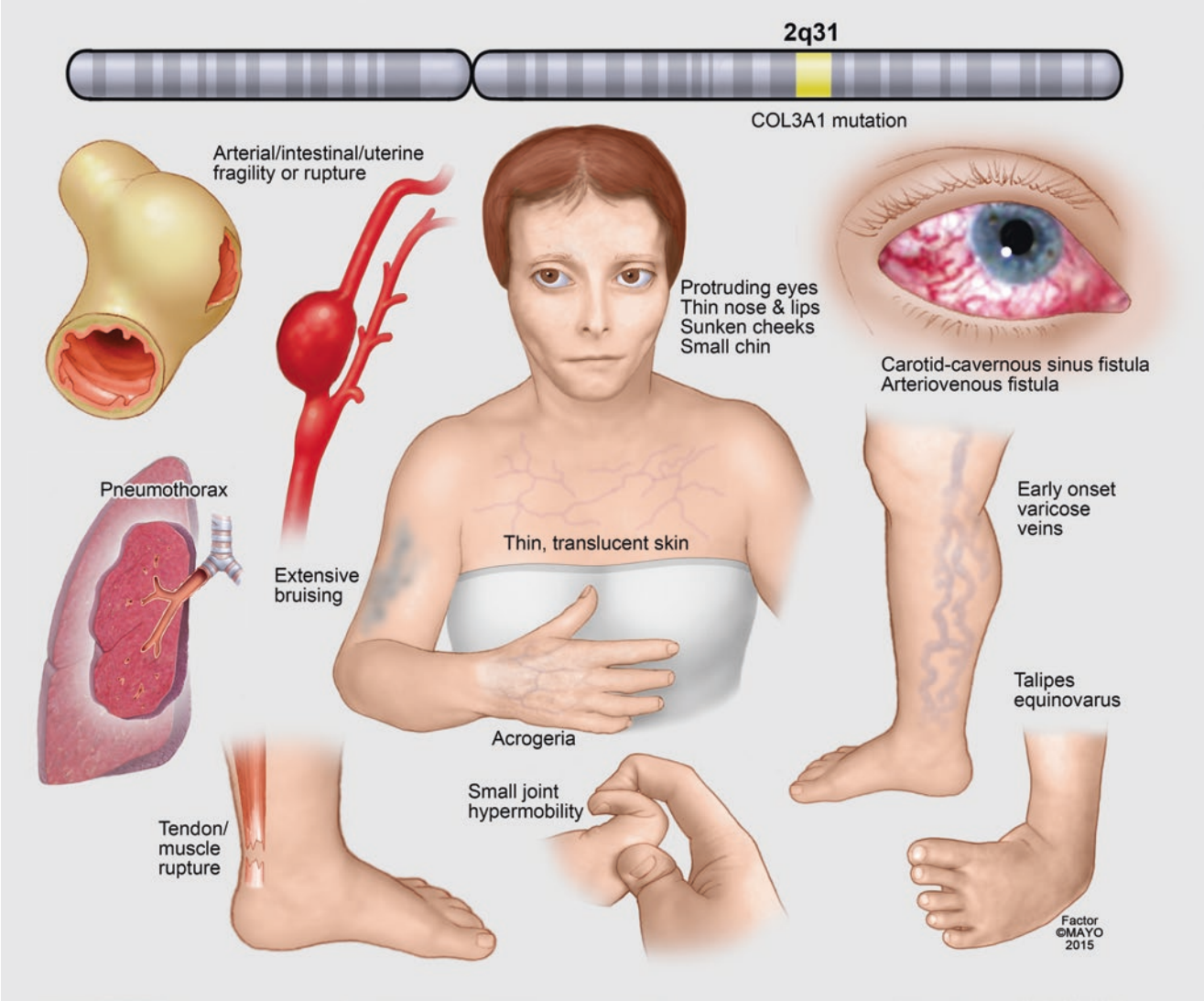


Fig. 3.4 COL3A1 mutation in the chromosome 2q31 and clinical spectrum of findings in patients with vascular Ehlers-Danlos syndrome. By permission of Mayo Foundation for Medical Education and Research. All rights reserved

while other mutations lead to haploinsufficiency-type mutation that results in production of normal collagen but at half the amount of normal. Patients with haploinsufficiency mutations have a milder disease phenotype with a delayed onset of complications and longer life expectancy [28].

Confirmation of the underlying molecular diagnosis of a *COL3A1* mutation is important for the counseling and care of VEDS patients on two levels. First, it allows the physician to differentiate VEDS from other syndromes that have several phenotypic features in common such as LDS syndrome which has a similar distribution of arterial aneurysms and a similar age at presentation [29]. Second, prior knowledge of the mutation allows for surgical planning that could potentially improve survival [30].

Diagnosis and Clinical Features

Unlike patients with other forms of Ehlers-Danlos syndrome, VEDS patients have skin that is soft but not overly stretchy. The clinical diagnosis of VEDS is made on the basis of "major" and "minor" criteria established by an expert group in 1997 [31]. The diagnostic criteria are as follows:

Major Diagnostic Criteria

1. Thin, translucent skin (veins are visible beneath the skin particularly on the chest and abdomen)
2. Arterial/intestinal/uterine fragility or rupture
3. Extensive bruising
4. Characteristic facial appearance (protruding eyes, a thin nose and lips, sunken cheeks, and a small chin)

Minor Diagnostic Criteria

1. Acrogeria (cutaneous condition characterized by premature aging with fragile, thin skin on the hands and feet)
2. Hypermobility of small joints
3. Tendon and muscle rupture
4. Talipes equinovarus (clubfoot)
5. Early-onset varicose veins
6. Arteriovenous, carotid–cavernous sinus fistula
7. Pneumothorax/pneumohemothorax
8. Gingival recession
9. Positive family history, sudden death in one or more close relatives

The minor criteria findings are not seen all in individuals with VEDS [30] and, for that reason, in most individuals, especially in the absence of a family history, the diagnosis is not suspected until arterial aneurysm and/or dissection, bowel perforation, or organ rupture occurs.

In terms of arterial involvement, dissection or rupture typically occurs in medium-sized arteries, although aortic involvement is sometimes observed. There is no particular predisposition at the aortic root [25].

Treatment

Management of vascular pathology associated with VEDS remains a clinical challenge. Celiprolol, a β1 antagonist with a β2 agonist action, has been the one treatment of choice to reduce the incidence of vascular ruptures in patients with VEDS. The use of celiprolol was assessed in a multicenter randomized trial of 53 patients with the clinical diagnosis of VEDS randomly assigned to celiprolol or no treatment. Celiprolol decreased the incidence of arterial rupture or dissection by three times, over a median follow-up of 47 months (20 % vs. 50 % in the control group) [32]. The study was criticized for the fact that the patients were diagnosed according to clinical criteria and thus the cohort might have included patients with different mutations who shared a similar phenotype, such as LDS [33]. Prophylactic measures to control blood pressure and reduce atherosclerotic risk factors remain the mainstay of medical management.

Most experience with surgical treatment is based on case reports and case series [30, 34, 35]. In a recent systematic literature review of 231 patients with VEDS, mortality was 30 % after open surgical repair and 24 % after endovascular procedures with a median age of death at 31 years [36]. A multicenter review of 68 VEDS patients with arterial pathology and confirmed molecular diagnosis *COL3A1* mutation demonstrated that postoperative complications were highest when the diagnosis of VEDS was not known at the time of surgical repair (62 % vs. 14 %) and when operative repairs were undertaken in an emergency setting (5 % vs. 55 %). Thus, establishing the molecular diagnosis is recommended for confirmation of VEDS diagnosis, and the traditional practice of avoiding surgery until complications develop is being modified in select cases [35]. The latter change in practice is based on the more contemporary experience where selected VEDS were treated on an elective basis. The overall perioperative bleeding rate and mortality were greatly reduced when compared to surgical repairs performed on an emergency basis [37].

Loeys-Dietz Syndrome

Loeys-Dietz syndrome (LDS) is an autosomal dominant heritable CTD characterized by the triad of craniofacial abnormality with bifid uvula/cleft palate (90 %), hypertelorism (widely spaced in eyes, 90 %), and/or arterial tortuosity with ascending aortic aneurysm/dissection (98 %, Fig. 3.5). Other

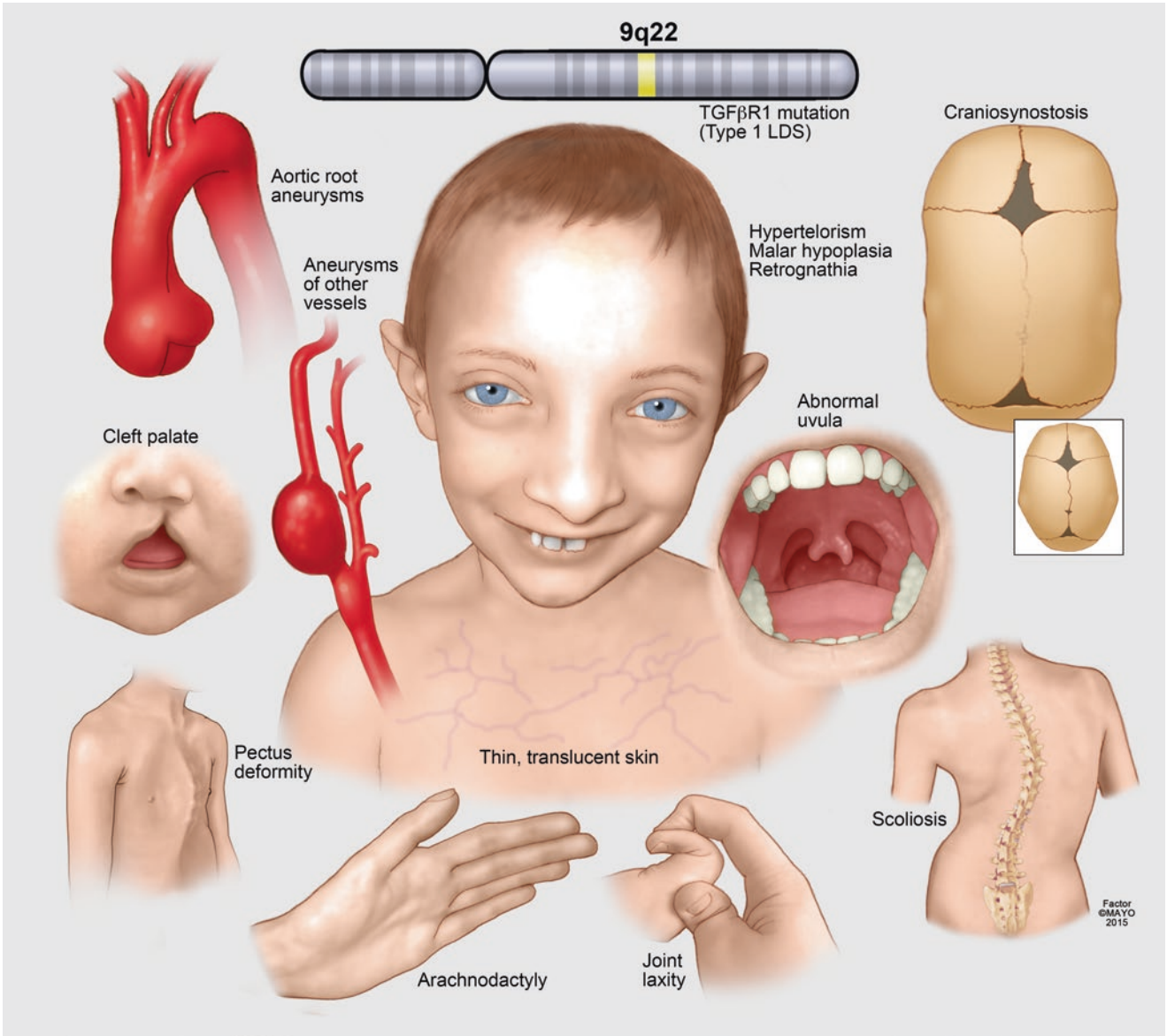


Fig. 3.5 TGFβR1 mutation in the chromosome 9q22 and clinical spectrum of findings in patients with Loeys-Dietz syndrome type 1. By permission of Mayo Foundation for Medical Education and Research. All rights reserved

more variable clinical features that distinguish LDS from MFS include craniosynostosis (one or more of the fibrous sutures in an infant skull prematurely ossifies), Chiari malformation, clubfoot deformity, congenital heart disease, cervical spine instability, easy bruising, dystrophic scarring, translucent skin, and, most importantly, a high risk of aneurysm and dissection throughout the arterial tree. Patients with LDS are not typically inappropriately tall and do not exhibit disproportionally long extremities, although arachnodactyly is observed. Some patients with *TGFβR1/2* mutations lack overt craniofacial features despite an equal or greater severity of vascular or systemic findings. Importantly, the natural history of patients with LDS tends to be more aggressive than those with MFS or VEDS. In LDS, aortic dissections often occur at a younger age or at smaller aortic dimensions (<40 mm) compared to MFS, and the incidence of pregnancy-related complications is especially high [38].

Mutations

The heterozygous autosomal dominant mutations leading to LDS are found in the transforming growth factor beta-receptor genes 1 and 2 (*TGFβR1/TGFβR2*) [29]. *TGFβR1/TGFβR2* mutations lead to increased TGFβ signaling in the aorta resulting in overproduction of collagen, loss of elastin, and disarray of elastic fibers. The mutations display reduced penetrance and variable expressivity and the majority (75 %)

occur de novo. Missense mutations in the serine threonine kinase domain of *TGFβR1/TGFβR2* appear to account for the majority of mutations leading to LDS.

Diagnosis

The phenotype associated with *TGFβR1/TGFβR2* mutations can be variable, even within families and can be associated with skeletal features of MFS leading to overlapping phenotypes. Molecular testing should be strongly considered because it influences clinical management, especially given the aggressive nature of LDS. It allows physicians to identify the patients who are at great risk of arterial complications and who might benefit from early surgical intervention [8]. Due to the limited number of patients reported to date, the full spectrum of patients with LDS is likely to evolve as additional patients are identified.

Clinical Features

The emerging phenotypes of LDS are divided into two types. Type 1 LDS is a Marfan-like condition associated with severe craniofacial features (craniosynostosis, malar hypoplasia, retrognathia, cleft palate, or abnormal uvula and hypertelorism), aortic root aneurysms, and aneurysm of other vessels, arterial tortuosity, arachnodactyly, pectus deformity, scoliosis, joint laxity, and developmental delay [38].

Type 2 LDS lacks the severe craniofacial features of type 1 LDS. It mimics VEDS in terms of arterial dissections, diffuse arterial aneurysms, arterial tortuosity, and catastrophic complications of pregnancy. Patients do not have cleft palate, hypertelorism, or craniosynostosis [38].

Differential Diagnosis of LDS

Because of the early age of appearance of dramatic pathology, VEDS and ATS are often considered along with LDS. It is critical to differentiate between LDS and VEDS because surgical management and tissue fragility are dramatically more challenging in patients with VEDS than in those with LDS.

Treatment

Overall, the median survival of LDS patients is 37 years (in contrast to 48 years for VEDS and 70 years for MFS). Mortality is from thoracic or abdominal aortic dissection, rupture, or cerebral hemorrhage. Mean age for the first vascular surgical procedure is about 20 years. The majority will have aneurysms distal to the aortic root. Dissection can occur without marked arterial dilatation (in contrast to MFS but similar to VEDS). Perioperative vascular surgical mortality is only 1.7 % (in contrast to 45 % for VEDS) [39, 40]. These results prompt early surgical intervention in patients with LDS. Prophylactic repair of adult patients with LDS has been suggested at aortic diameters of 4.0 cm. The medical management recommendations and surveillance are similar to the beta-blockade recommended for patients with MFS.

Aneurysms-Osteoarthritis Syndrome

Aneurysms-osteoarthritis syndrome (AOS) is autosomal dominant heritable CTD characterized by the presence of arterial aneurysms and tortuosity, and osteoarthritis at a young age [41]. The aneurysms occur throughout the arterial tree with a high risk of early dissection/rupture, resembling patients with LDS. The early-onset joint abnormalities including osteoarthritis, intervertebral disc degeneration, osteochondritis dissecans, and meniscal anomalies are present in almost all patients with AOS. Additional findings include skin abnormalities (velvety skin, easy bruising, striae), skeletal abnormalities (arachnodactyly, scoliosis, pes planus), and craniofacial abnormalities (hypertelorism, high-arched palate, dental malocclusion) [41].

AOS is due to heterozygous autosomal dominant mutations in the *SMAD3* gene which encodes SMAD3, the protein involved in downstream cellular signaling initiated by TGFβ binding to its receptors (TGFβR1 and TGFβR2) [41, 42]. Carriers of the mutation have phenotypic features that significantly overlap with findings in TGFβR1/TGFβR2-related LDS and, to some extent, with VEDS.

The most frequent vascular findings are aneurysms of the aorta, at the level of the sinuses of Valsalva. Patients also present with abdominal aortic aneurysms, cerebrovascular aneurysms, and arterial tortuosity. Cardiovascular abnormalities were documented in 89 % of patients identified in one study with sudden death from aortic dissections, with the most common presentation being aortic aneurysms and severe mitral valve insufficiency [41].

Arterial Tortuosity Syndrome

Arterial tortuosity syndrome (ATS) is a rare autosomal recessive heritable CTD, characterized by severe tortuosity of large- and middle-sized arteries including the aorta, carotid, renal, and pulmonary arteries. Arterial aneurysms and stenosis of the pulmonary arteries and the aorta are also characteristic features and ventricular hypertrophy is often present [43]. Facial features include an elongated face with down-slanting palpebral

fissures and micrognathia (undersized jaw). The majority of patients have congenital involvement of the skin, with softness and hyperextensibility but not easy bruising. Other features include arachnodactyly and inguinal and/or umbilical hernia.

ATS is due to autosomal recessive inheritance of loss-of-function mutations in *SLC2A10*, the gene encoding the facilitative glucose transporter GLUT10 [44]. It is the only CTD known to arise from defective glucose metabolism. GLUT10 deficiency is associated with upregulation of TGFβ in the arterial wall that leads to medial degeneration of elastic fibers, followed by elongation, stenosis, tortuosity, and eventual aneurysm formation [44]. The condition is lethal in infancy in a subset of patients, but some survive into adulthood and seem to do well [45].

Familial Thoracic Aortic Aneurysms and Dissections

Non-syndromic familial thoracic aortic aneurysms and dissection (FTAAD) mutations account for 20% of non-syndromic patients with thoracic aortic aneurysms and dissections. These mutations are mostly associated with ascending aorta aneurysm and dissection. Non-syndromic FTAAD have only been recently described when compared to the genes leading to the better known syndromic CTDs. FTAAD mutations lead to a clinically heterogeneous group of disorders where thoracic aortic disease predominates with variable expression with respect to disease presentation, age of onset, and associated features that include variable or subtle systemic manifestations of a CTD [2]. Patients with FTAAD present at a younger age than those with sporadic thoracic aortic aneurysms (mean age, 58.2 vs. 65.7 years) [46]. FTAAD can occur due to mutations also affecting the TGFβ pathway but additionally can occur due to mutations in genes affecting smooth muscle cell contractile proteins. Table 3.1 presents a summary of FTAAD genes.

FTAAD Mutations Affecting the TGFβ Pathway

TGFβR2 Mutations

Mutations in *TGFβR2* cause LDS; however, these mutations can also cause TAAD in the absence of features of LDS in large multigenerational families. These mutations are responsible for 2% of FTAAD. Patients with this mutation present with ascending aortic dissections at aortic diameters less than 5 cm. Additionally, they are at increased risk for aneurysms and dissections of other vessels and cerebral aneurysms [47–49].

TGFβ2 Mutations

TGFβ2 encodes TGFβ2. Mutations in this gene are inherited in an autosomal dominant manner and are predicted to cause haploinsufficiency for TGFβ2; thus the defective gene leads to the production of a TGFβ2 protein with little or no function. As a result, the protein cannot bind to its receptor and paradoxically leads to an increase in TGFβ2 production in the diseased aorta. The exact mechanism responsible for the increase in signaling is unclear. The mutation leads to predisposition for ascending thoracic aortic aneurysms leading to acute aortic dissections [48].

SMAD3 Mutations

Mutations in *SMAD3* cause AOS; however, autosomal dominant mutations in *SMAD3* can also cause TAAD in the absence of features of LDS in large multigenerational families. Non-syndromic *SMAD3* mutations are responsible for 2% of FTAAD. Patients present with ascending thoracic aortic aneurysms leading to aortic dissections and intracranial artery aneurysms with subarachnoid hemorrhage, along with abdominal aortic and bilateral iliac artery aneurysms. In terms of aortic dissections, type A dissection is more common than type B dissections with an average age of onset of dissection of 42 years (range 25–54 years) [42]. Imaging of the cerebrovascular for aneurysms in mutation carriers is recommended in addition to the entire aorta and its branches [50].

FTAAD Mutations Affecting the Smooth Muscle Cell Contractile Apparatus

ACTA2 Mutations

Heterozygous missense mutations *ACTA2* are responsible for up to 16% of FTAAD. .*ACTA2* encodes the vascular smooth muscle cell-specific isoform of alpha-actin ACTA2 which is a major component of the contractile apparatus in the smooth muscle cells located throughout the arterial system. In addition to aortic aneurysms and dissections, other associated variable features occur including iris flocculi, livedo reticularis (mottled reticulated vascular pattern that appears as a lacelike purplish discoloration of the skin), bicuspid aortic valve, and patent ductus arteriosus. Interestingly, patients with ACTA2 mutations can present with premature ischemic strokes (including Moyamoya disease), cerebral aneurysms, and premature coronary artery disease. This has been attributed to increased proliferation of smooth muscle cell leading to occlusive disease in small arteries [51].

In a study of 277 individuals with 41 various *ACTA2* mutations, an aortic event occurred in 48% of these individuals, with the vast majority presenting with thoracic aortic dissections. Type A dissections were more common than type B dissections (54% vs. 21%), but the median age of onset of type B dissections was significantly earlier than type A dissections (27 years vs. 36 years) [52, 53].

Table 3.1 A summary of FTAAD genes, including year of discovery, number of discovered mutations within the gene, affected protein, and associated connective tissues disorders and syndromes

Gene	Year of discovery	No. of mutations	Protein	Associated syndrome	Associated pathology
Mutations affecting the TGFβ signaling pathway					
FBN1	1991	1300	Fibrillin-1	MFS	Ocular, skeletal involvement
TGFβR1/TGFβR2	2005	110	TGFβ receptors 1 and 2	LDS	Skeletal manifestations, craniofacial abnormalities, tortuous arteries, cutaneous anomalies
SMAD3	2011	11	SMAD3	AOS	Arterial aneurysms/tortuosity, mild craniofacial, skeletal, cutaneous anomalies, early-onset osteoarthritis
TGF-β2	2012	14	TGFβ2		Intracranial aneurysms, subarachnoid hemorrhages
SLC2A10	2006	19	Glucose transporter GLUT10	ATS	
Mutations affecting collagen					
Col3A1	1986	700	Procollagen III	VEDS	Risk of bowel and uterine rupture
Mutations affecting smooth muscle cell proteins					
ACTA2	2009	30	ACTA2		Early-onset coronary artery disease, strokes, Moyamoya disease, livedo reticularis
MYH11	2006		MYH11		Patent ductus arteriosus
MLCK	2010		Myosin light-chain kinase		
PRKG1	2013		PKGI		

MFS Marfan syndrome, *LDS* Loeys-Dietz syndrome, *AOS* aneurysms-osteoarthritis syndrome, *ATS* arterial tortuosity syndrome, *VEDS* vascular Ehlers-Danlos syndrome

MYH11 Mutations

Autosomal dominant MYH11 mutations account for approximately 2% of cases of FTAAD [54]. MYH11 is a major contractile protein specific to smooth muscle cells. These mutations provided the first example of direct changes in a contractile protein produced specifically in smooth muscle cells, leading to an inherited arterial disease. Affected individuals with MYH11 mutations have marked aortic stiffness and a decrease in aortic compliance. They develop aneurysms of the ascending aorta but spare the sinuses of Valsalva (unlike MFS) and have an associated patent ductus arteriosus (PDA) [55, 56].

MYLK Mutations

MYLK gene encodes the kinase that controls smooth muscle cell contractile protein myosin light chain. The mutation is a heterozygous loss-of-function mutation. The phenotype is characterized by acute aortic dissection with little to no enlargement of the aorta [57].

PRKG1 Mutations

Autosomal dominant *PRKG1* c.530G>A (p.Arg177Gln) mutation is a gain-of-function mutation predicted to cause decreased contraction of vascular smooth muscle cells. *PRKG1* encodes type I cGMP-dependent protein kinase (PKG-1), which is activated upon binding of cGMP and controls smooth muscle cell relaxation. The majority of affected individuals presented with acute aortic dissections (63%) at relatively young ages (mean 31 years, range 17–51 years) [58].

Familial Abdominal Aortic Aneurysms

The initial publication describing familial abdominal aortic aneurysms (AAAs) in 1977 focused on three brothers all reported to have AAA. Since this report, AAA clustering within specific families has been described, and it is estimated that 15–20% of AAAs are familial [3, 4]. Studies suggest that patients with familial AAA are significantly more likely to be female and younger, and have fewer cardiovascular risk factors such as hypertension and diabetes mellitus [59]. Another study confirmed the younger age of aortic disease presentation, and, interestingly, demonstrated an increased number of aneurysmal segments, greater likelihood of developing aneurysmal disease proximal to the infrarenal aorta, increased occurrence of bilateral common iliac and unilateral internal iliac artery aneurysms, and a higher frequency of previous aortic repairs [60]. These

observations have been reported recently and likely have implications for subsequent endovascular repair failures.

Endovascular Repair and Genetically Triggered Aortic Diseases

FDA trials for endovascular devices have intentionally excluded patients with CTDs. The current consensus statement of the Society of Thoracic Surgeons (STS) and European guidelines on diagnosis and treatment of aortic diseases recommends strongly against endovascular repair in patients with CTDs unless operative risk has been deemed truly prohibitive by a center experienced in management of complex aortic disease, and in emergency situations, in order to stabilize the patient as a bridge to definitive surgical therapy [1, 61].

The concern for stent graft failure stems from the knowledge that the entire aorta is affected in patients with CTDs such as MFS. MFS patients frequently need staged replacement of the entire aorta [17–19]. This natural history suggests that device failure would occur, as the available fixation zones for the stent grafts are prone to future dilatation due to the chronic outward radial force exerted by the stent grafts. Ultimately this would lead to loss of seal and development of endoleaks, device migration or erosion (Fig. 3.6), and subsequent need for reoperation to remove the device and re-repair the aorta [62]. In the absence of device failure post-TEVAR, it has been observed that MFS patients experience continued dilatation of the distal thoracic and abdominal aorta post-TEVAR. This has been addressed with distal extension by supplemental stent grafting and where necessary hybrid extra-anatomical bypass or branch/fenestrated stent graft technology to maintain aortic branch perfusion [63, 64]. To date a total of 69 patients with MFS treated with TEVAR have been described in the literature from different case series with a mean follow-up of 32 months. Of those, 20.3 % required additional endovascular interventions and 21.7 % required open repair, which is substantially higher as compared to patients without genetically triggered thoracic aortic disease who were treated with TEVAR [62–68].

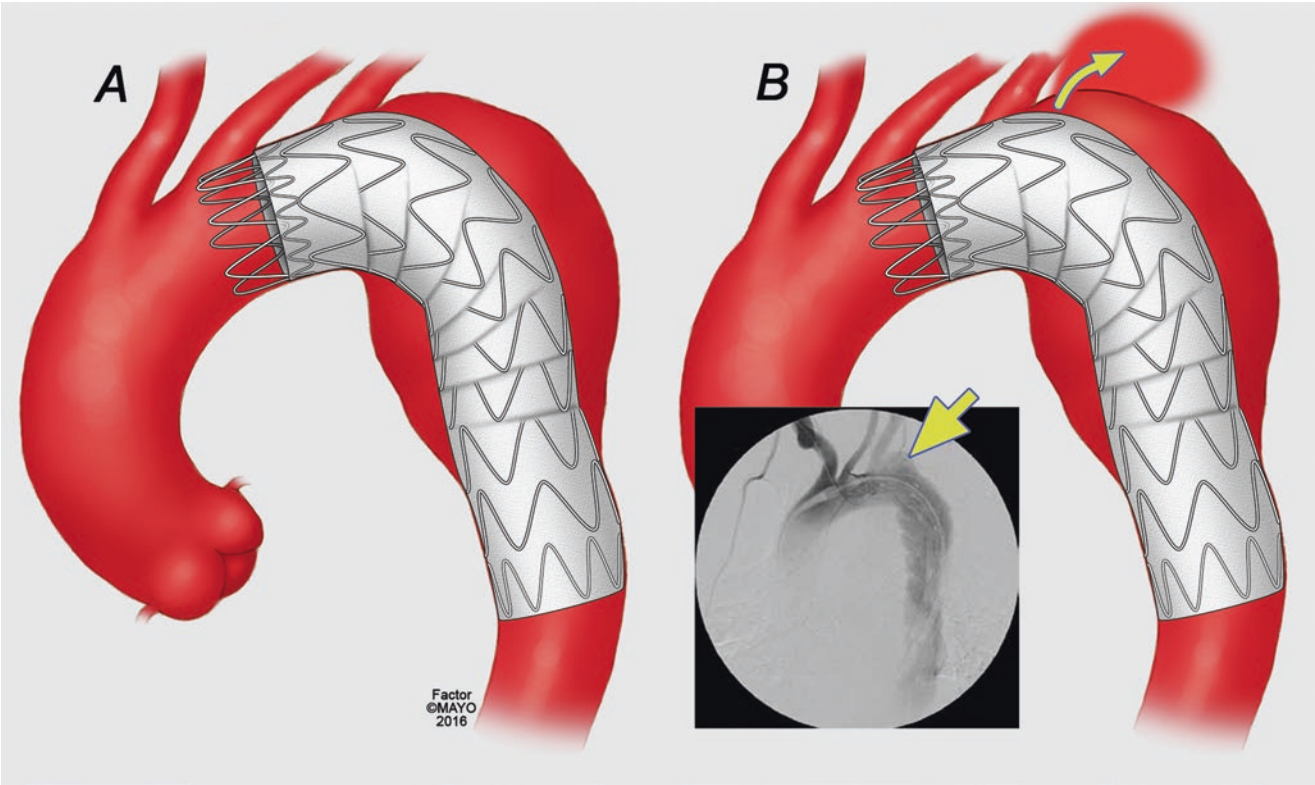


Fig. 3.6 Thoracic endovascular aortic repair was successfully performed in a Marfan patient with complicated ruptured thoracic dissection (**a**). Follow-up presentation with constrained ruptured aneurysm in the proximal thoracic aorta due to erosion of the stent through the aortic wall (**b**). By permission of Mayo Foundation for Medical Education and Research. All rights reserved

Another major concern is retrograde aortic dissection post-stent graft placement. It has been proposed that stiff stent grafts can cause further aortic tears in patients with CTDs. In a large series of TEVAR for type B aortic dissection, 8 patients of 443 developed retrograde aortic dissection post-TEVAR (1.8 %) compared to 3 of 11 patients with MFS (27.3 %) [69]. The occurrence of new entry tears at the distal edge of the stent graft can occur as well. A report examined 12 patients with MFS treated with TEVAR for dissection of the descending thoracic aorta after previous open aortic root/arch surgery; 25 % of the patients developed new dissection either retrograde dissection into the arch or distally into the abdominal aorta at a mean follow-up period of 31 months [65]. In a large series of 650 patients with type B aortic dissection treated with TEVAR, 22 events of new stent graft induced tears with an incidence of 33 % in patients with MFS compared to only 3 % in the rest of the population. The investigators concluded that this was due to a stress-induced injury of the TEVAR against the fragile aortic wall [66, 69].

VEDS deserves special attention in terms of use of endovascular treatment due to the especially fragile arterial wall. Diagnostic angiography should be avoided as severe morbidity and the risk of vessel dissection or perforation (or both) during selective catheterization or from the puncture site itself has been demonstrated to be as high as 67 % with 12 % mortality [70]. In a more contemporary series, endovascular approaches for coil embolization of aortic branch vessels and other medium-sized arteries have been performed successfully in patients with known VEDS, with consideration of open femoral artery exposure and repair, as percutaneous access can precipitate femoral rupture and pseudoaneurysm formation, especially when large devices are necessary [35]. While rare stent graft therapy for aortic aneurysms has been reported, the reports were retrospective reviews lacking sufficient detail and follow-up. Certainly durability concerns and the risk to the fixation zones in the setting of chronic outward radial force may increase the frequency of device failure and secondary interventions. Thus the general recommendation of avoiding stent graft therapy in patients with CTDs applies.

Assessment of endovascular repair in patients with nonsyndromic FTAAD remains lacking, and consensus recommendation is not available. Until more details are available, the same recommendation for avoiding the use of aortic stent grafts in patients with CTDs has been extrapolated to all genetically triggered aortic disease.

Endovascular repair may be well suited for specific problems in the population of patients with genetically triggered aortic aneurysms and dissections, such as excluding focal pseudoaneurysms when an existing aortic graft can be used for the proximal and distal landing zones, or in the setting of prior repairs where the proximal and distal landing zones are inside previously placed Dacron grafts such as fixation of TEVAR in an "elephant trunk" graft after previous arch repair, the extension of a device distally from a secure thoracic replacement, or for patients with prohibitive operative risk or in cases of aortic rupture (Fig. 3.7). These repairs are recommended at medical centers with sufficient expertise and resources for both open and endovascular aortic repairs as well as close follow-up post-repair to address endovascular treatment failures in a timely manner [19, 71].

These recommendations do not appear to be applicable to patients with familial AAA unrelated to CTDs. Two recent investigations evaluate the use of EVAR in patients with familial AAA. In both series, there was a higher rate of endovascular repair-related complications in familial AAA patients when compared with patients with sporadic AAA. Patients with familial AAA who underwent EVAR had significantly more AAA-related complications and secondary interventions than patients with sporadic AAA despite similar AAA morphology at baseline. Familial AAA patients are at an increased risk of developing a delayed endoleak following EVAR with postoperative imaging demonstrating type I endoleaks in 6 % of the cases and type II endoleaks in 18 %, compared to 1 % and 11 % type I and II endoleaks, respectively, in patients with sporadic AAA. The majority of secondary interventions undertaken were embolization performed for type II endoleak and reintervention for graft limb stenosis/occlusion. These findings suggest that while EVAR is safe and effective, patients with a familial form of AAA may benefit from closer surveillance post-EVAR [72, 73].

Conclusion

Significant advances have improved the understanding of the association of genetics and aortic aneurysmal disease. The disorders discussed above include most of the aortic disease in younger patients. There remain unknown underlying genetic defects and aberrant molecular pathways and the varying levels of expression and penetrance make detection a challenge.

The isolation of new genes and elucidation of their correlations with genetic syndromes allow not only the understanding of the pathophysiology involved in the genesis of the aortic aneurysms, but also pave the development of better clinical management and surgical repair methodology in affected individuals.

It is anticipated that future stratification of patients by genetic etiology will help to refine phenotypic descriptions and inform patient counselling and management, allowing personalization of care to those with aortic aneurysms and dissections.

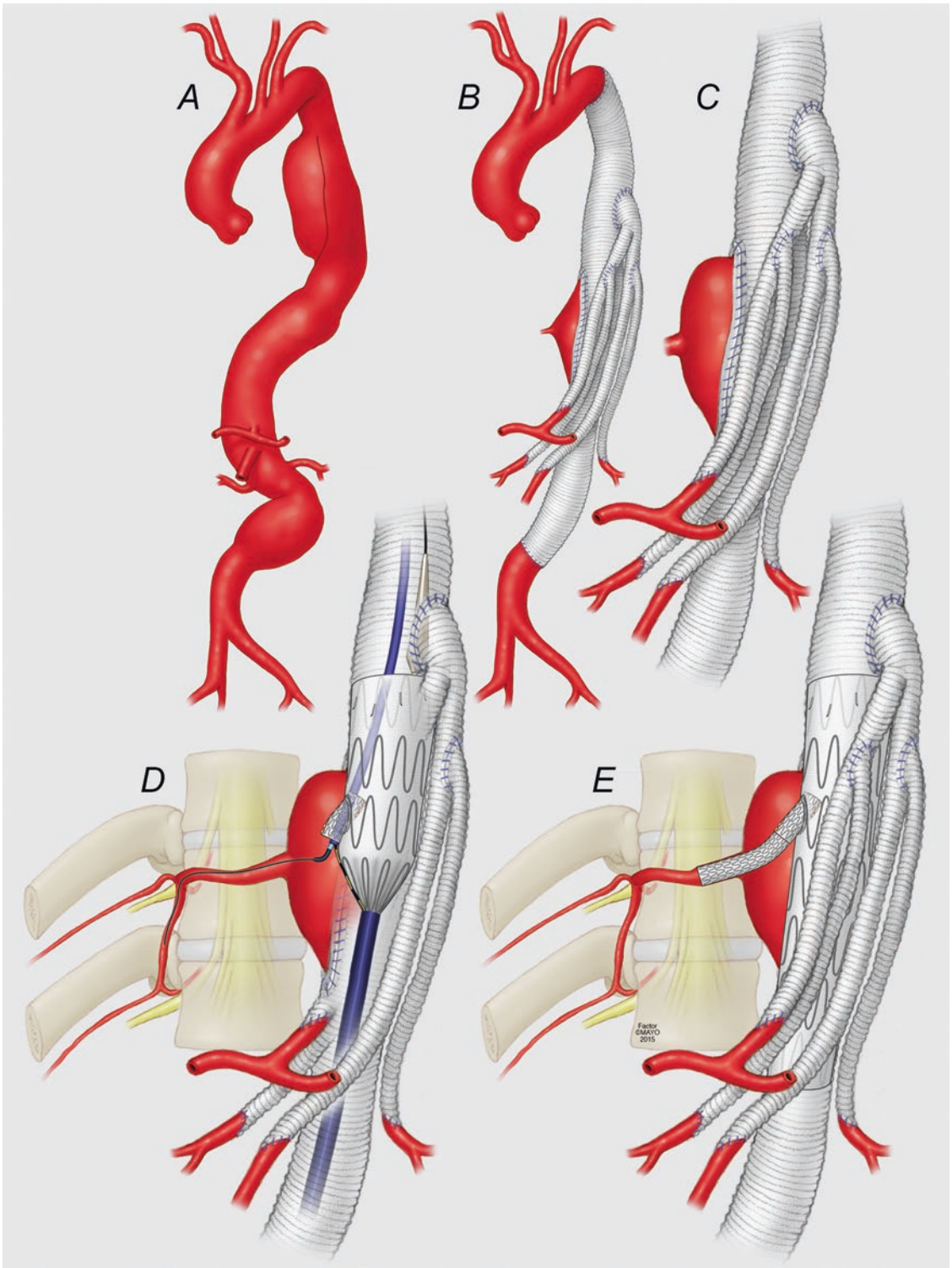


Fig. 3.7 Extensive aortic aneurysm and dissection in a 28-year-old patient with Loeys-Dietz syndrome (**a**) treated by open repair with a patch to incorporate segment intercostal artery (**b**). At 2-year follow-up the patient presented with symptomatic, rapidly expanding patch aneurysm (**c**). Endovascular repair using a physician-modified endograft with single branch to incorporate the intercostal artery (**d**). Branch incorporation using a Viabahn stent graft (**e**). Test balloon occlusion revealed no changes in motor-evoked potential. Note that the thoracic endograft is anchored in surgical grafts. By permission of Mayo Foundation for Medical Education and Research. All rights reserved

References

1. Hiratzka LF, Bakris GL, Beckman JA, Bersin RM, Carr VF, Casey DE Jr, et al. 2010 ACCF/AHA/AATS/ACR/ASA/SCA/SCAI/SIR/STS/SVM guidelines for the diagnosis and management of patients with Thoracic Aortic Disease: a report of the American College of Cardiology Foundation/American Heart Association Task Force on Practice Guidelines, American Association for Thoracic Surgery, American College of Radiology, American Stroke Association, Society of Cardiovascular Anesthesiologists, Society for Cardiovascular Angiography and Interventions, Society of Interventional Radiology, Society of Thoracic Surgeons, and Society for Vascular Medicine. Circulation. 2010;121(13):e266–369.
2. Albornoz G, Coady MA, Roberts M, Davies RR, Tranquilli M, Rizzo JA, et al. Familial thoracic aortic aneurysms and dissections—incidence, modes of inheritance, and phenotypic patterns. Ann Thorac Surg. 2006;82(4):1400–5.
3. Tilson MD, Seashore MR. Fifty families with abdominal aortic aneurysms in two or more first-order relatives. Am J Surg. 1984;147(4):551–3.
4. Kuivaniemi H, Shibamura H, Arthur C, Berguer R, Cole CW, Juvonen T, et al. Familial abdominal aortic aneurysms: collection of 233 multiplex families. J Vasc Surg. 2003;37(2):340–5.
5. Jones JA, Spinale FG, Ikonomidis JS. Transforming growth factor-beta signaling in thoracic aortic aneurysm development: a paradox in pathogenesis. J Vasc Res. 2009;46(2):119–37.
6. Judge DP, Dietz HC. Marfan's syndrome. Lancet. 2005;366(9501):1965–76.
7. Dietz HC, Pyeritz RE, Hall BD, Cadle RG, Hamosh A, Schwartz J, et al. The Marfan syndrome locus: confirmation of assignment to chromosome 15 and identification of tightly linked markers at 15q15-q21.3. Genomics. 1991;9(2):355–61.
8. Loeys BL, Dietz HC, Braverman AC, Callewaert BL, De BJ, Devereux RB, et al. The revised Ghent nosology for the Marfan syndrome. J Med Genet. 2010;47(7):476–85.
9. Loeys B, Nuytinck L, Delvaux I, De BS, De PA. Genotype and phenotype analysis of 171 patients referred for molecular study of the fibrillin-1 gene FBN1 because of suspected Marfan syndrome. Arch Intern Med. 2001;161(20):2447–54.
10. Loeys B, De BJ, Van AP, Wettinck K, Pals G, Nuytinck L, et al. Comprehensive molecular screening of the FBN1 gene favors locus homogeneity of classical Marfan syndrome. Hum Mutat. 2004;24(2):140–6.
11. Gott VL, Greene PS, Alejo DE, Cameron DE, Naftel DC, Miller DC, et al. Replacement of the aortic root in patients with Marfan's syndrome. N Engl J Med. 1999;340(17):1307–13.
12. Coselli JS, Volguina IV, LeMaire SA, Sundt TM, Connolly HM, Stephens EH, et al. Early and 1-year outcomes of aortic root surgery in patients with Marfan syndrome: a prospective, multicenter, comparative study. J Thorac Cardiovasc Surg. 2014;147(6):1758–66, 1767.
13. Cameron DE, Alejo DE, Patel ND, Nwakanma LU, Weiss ES, Vricella LA, et al. Aortic root replacement in 372 Marfan patients: evolution of operative repair over 30 years. Ann Thorac Surg. 2009;87(5):1344–9.
14. Silverman DI, Burton KJ, Gray J, Bosner MS, Kouchoukos NT, Roman MJ, et al. Life expectancy in the Marfan syndrome. Am J Cardiol. 1995;75(2):157–60.
15. Gott VL, Cameron DE, Alejo DE, Greene PS, Shake JG, Caparrelli DJ, et al. Aortic root replacement in 271 Marfan patients: a 24-year experience. Ann Thorac Surg. 2002;73(2):438–43.
16. Crawford ES. Marfan's syndrome. Broad spectral surgical treatment cardiovascular manifestations. Ann Surg. 1983;198(4):487–505.
17. Niinami H, Aomi S, Tagusari O, Hashimoto A, Koyanagi H. Extensive aortic reconstruction for aortic aneurysms in Marfan syndrome. Ann Thorac Surg. 1999;67(6):1864–7.
18. Carrel T, Beyeler L, Schnyder A, Zurmuhle P, Berdat P, Schmidli J, et al. Reoperations and late adverse outcome in Marfan patients following cardiovascular surgery. Eur J Cardiothorac Surg. 2004;25(5):671–5.
19. Milewicz DM, Dietz HC, Miller DC. Treatment of aortic disease in patients with Marfan syndrome. Circulation. 2005;111(11):e150–7.
20. Girdauskas E, Kuntze T, Borger MA, Falk V, Mohr FW. Distal aortic reinterventions after root surgery in Marfan patients. Ann Thorac Surg. 2008;86(6):1815–9.
21. Song HK, Kindem M, Bavaria JE, Dietz HC, Milewicz DM, Devereux RB, et al. Long-term implications of emergency versus elective proximal aortic surgery in patients with Marfan syndrome in the Genetically Triggered Thoracic Aortic Aneurysms and Cardiovascular Conditions Consortium Registry. J Thorac Cardiovasc Surg. 2012;143(2):282–6.
22. Brooke BS, Habashi JP, Judge DP, Patel N, Loeys B, Dietz III HC. Angiotensin II blockade and aortic-root dilation in Marfan's syndrome. N Engl J Med. 2008;358(26):2787–95.
23. Shores J, Berger KR, Murphy EA, Pyeritz RE. Progression of aortic dilatation and the benefit of long-term beta-adrenergic blockade in Marfan's syndrome. N Engl J Med. 1994;330(19):1335–41.
24. Pitcher A, Emberson J, Lacro RV, Sleeper LA, Stylianou M, Mahony L, et al. Design and rationale of a prospective, collaborative meta-analysis of all randomized controlled trials of angiotensin receptor antagonists in Marfan syndrome, based on individual patient data: a report from the Marfan Treatment Trialists' Collaboration. Am Heart J. 2015;169(5):605–12.
25. Pepin MG, Schwarze U, Rice KM, Liu M, Leistritz D, Byers PH. Survival is affected by mutation type and molecular mechanism in vascular Ehlers-Danlos syndrome (EDS type IV). Genet Med. 2014;16(12):881–8.
26. Pope FM, Narcisi P, Nicholls AC, Germaine D, Pals G, Richards AJ. COL3A1 mutations cause variable clinical phenotypes including acrogeria and vascular rupture. Br J Dermatol. 1996;135(2):163–81.
27. Pepin MG, Byers PH. Ehlers-Danlos syndrome type IV. 1993.
28. Leistritz DF, Pepin MG, Schwarze U, Byers PH. COL3A1 haploinsufficiency results in a variety of Ehlers-Danlos syndrome type IV with delayed onset of complications and longer life expectancy. Genet Med. 2011;13(8):717–22.
29. Loeys BL, Chen J, Neptune ER, Judge DP, Podowski M, Holm T, et al. A syndrome of altered cardiovascular, craniofacial, neurocognitive and skeletal development caused by mutations in TGFBR1 or TGFBR2. Nat Genet. 2005;37(3):275–81.
30. Shalhub S, Black III JH, Cecchi AC, Xu Z, Griswold BF, Safi HJ, et al. Molecular diagnosis in vascular Ehlers-Danlos syndrome predicts pattern of arterial involvement and outcomes. J Vasc Surg. 2014;60(1):160–9.
31. Beighton P, De PA, Steinmann B, Tsipouras P, Wenstrup RJ. Ehlers-Danlos syndromes: revised nosology, Villefranche, 1997. Ehlers-Danlos National Foundation (USA) and Ehlers-Danlos Support Group (UK). Am J Med Genet. 1998;77(1):31–7.
32. Ong KT, Perdu J, De BJ, Bozec E, Collignon P, Emmerich J, et al. Effect of celiprolol on prevention of cardiovascular events in vascular Ehlers-Danlos syndrome: a prospective randomised, open, blinded-endpoints trial. Lancet. 2010;376(9751):1476–84.
33. Brooke BS. Celiprolol therapy for vascular Ehlers-Danlos syndrome. Lancet. 2010;376(9751):1443–4.
34. Oderich GS, Panneton JM, Bower TC, Lindor NM, Cherry KJ, Noel AA, et al. The spectrum, management and clinical outcome of Ehlers-Danlos syndrome type IV: a 30-year experience. J Vasc Surg. 2005;42(1):98–106.
35. Lum YW, Brooke BS, Arnaoutakis GJ, Williams TK, Black III JH. Endovascular procedures in patients with Ehlers-Danlos syndrome: a review of clinical outcomes and iatrogenic complications. Ann Vasc Surg. 2012;26(1):25–33.
36. Bergqvist D, Bjorck M, Wanhainen A. Treatment of vascular Ehlers-Danlos syndrome: a systematic review. Ann Surg. 2013;258(2):257–61.

37. Brooke BS, Arnaoutakis G, McDonnell NB, Black III JH. Contemporary management of vascular complications associated with Ehlers-Danlos syndrome. J Vasc Surg. 2010;51(1):131–8.
38. Loeys BL, Schwarze U, Holm T, Callewaert BL, Thomas GH, Pannu H, et al. Aneurysm syndromes caused by mutations in the TGF-beta receptor. N Engl J Med. 2006;355(8):788–98.
39. Williams JA, Loeys BL, Nwakanma LU, Dietz HC, Spevak PJ, Patel ND, et al. Early surgical experience with Loeys-Dietz: a new syndrome of aggressive thoracic aortic aneurysm disease. Ann Thorac Surg. 2007;83(2):S757–63.
40. Williams JA, Hanna JM, Shah AA, Andersen ND, McDonald MT, Jiang YH, et al. Adult surgical experience with Loeys-Dietz syndrome. Ann Thorac Surg. 2015;99(4):1275–81.
41. van de Laar IM, Oldenburg RA, Pals G, Roos-Hesselink JW, de Graaf BM, Verhagen JM, et al. Mutations in SMAD3 cause a syndromic form of aortic aneurysms and dissections with early-onset osteoarthritis. Nat Genet. 2011;43(2):121–6.
42. Regalado ES, Guo DC, Villamizar C, Avidan N, Gilchrist D, McGillivray B, et al. Exome sequencing identifies SMAD3 mutations as a cause of familial thoracic aortic aneurysm and dissection with intracranial and other arterial aneurysms. Circ Res. 2011;109(6):680–6.
43. Wessels MW, Catsman-Berrevoets CE, Mancini GM, Breuning MH, Hoogeboom JJ, Stroink H, et al. Three new families with arterial tortuosity syndrome. Am J Med Genet A. 2004;131(2):134–43.
44. Coucke PJ, Willaert A, Wessels MW, Callewaert B, Zoppi N, De BJ, et al. Mutations in the facilitative glucose transporter GLUT10 alter angiogenesis and cause arterial tortuosity syndrome. Nat Genet. 2006;38(4):452–7.
45. Callewaert BL, Willaert A, Kerstjens-Frederikse WS, De BJ, Devriendt K, Albrecht B, et al. Arterial tortuosity syndrome: clinical and molecular findings in 12 newly identified families. Hum Mutat. 2008;29(1):150–8.
46. Pannu H, Avidan N, Tran-Fadulu V, Milewicz DM. Genetic basis of thoracic aortic aneurysms and dissections: potential relevance to abdominal aortic aneurysms. Ann N Y Acad Sci. 2006;1085:242–55.
47. Inamoto S, Kwartler CS, Lafont AL, Liang YY, Fadulu VT, Duraisamy S, et al. TGFBR2 mutations alter smooth muscle cell phenotype and predispose to thoracic aortic aneurysms and dissections. Cardiovasc Res. 2010;88(3):520–9.
48. Boileau C, Guo DC, Hanna N, Regalado ES, Detaint D, Gong L, et al. TGFB2 mutations cause familial thoracic aortic aneurysms and dissections associated with mild systemic features of Marfan syndrome. Nat Genet. 2012;44(8):916–21.
49. Tran-Fadulu V, Pannu H, Kim DH, Vick III GW, Lonsford CM, Lafont AL, et al. Analysis of multigenerational families with thoracic aortic aneurysms and dissections due to TGFBR1 or TGFBR2 mutations. J Med Genet. 2009;46(9):607–13.
50. Regalado E, Medrek S, Tran-Fadulu V, Guo DC, Pannu H, Golabbakhsh H, et al. Autosomal dominant inheritance of a predisposition to thoracic aortic aneurysms and dissections and intracranial saccular aneurysms. Am J Med Genet A. 2011;155A(9):2125–30.
51. Guo DC, Papke CL, Tran-Fadulu V, Regalado ES, Avidan N, Johnson RJ, et al. Mutations in smooth muscle alpha-actin (ACTA2) cause coronary artery disease, stroke, and Moyamoya disease, along with thoracic aortic disease. Am J Hum Genet. 2009;84(5):617–27.
52. Regalado ES, Guo DC, Prakash S, Bensend TA, Flynn K, Estrera A, et al. Aortic disease presentation and outcome associated with ACTA2 mutations. Circ Cardiovasc Genet. 2015;8(3):457–64.
53. Milewicz DM, Ostergaard JR, Ala-Kokko LM, Khan N, Grange DK, Mendoza-Londono R, et al. De novo ACTA2 mutation causes a novel syndrome of multisystemic smooth muscle dysfunction. Am J Med Genet A. 2010;152A(10):2437–43.
54. Guo DC, Pannu H, Tran-Fadulu V, Papke CL, Yu RK, Avidan N, et al. Mutations in smooth muscle alpha-actin (ACTA2) lead to thoracic aortic aneurysms and dissections. Nat Genet. 2007;39(12):1488–93.
55. Zhu L, Vranckx R, Van Khau KP, Lalande A, Boisset N, Mathieu F, et al. Mutations in myosin heavy chain 11 cause a syndrome associating thoracic aortic aneurysm/aortic dissection and patent ductus arteriosus. Nat Genet. 2006;38(3):343–9.
56. Pannu H, Tran-Fadulu V, Papke CL, Scherer S, Liu Y, Presley C, et al. MYH11 mutations result in a distinct vascular pathology driven by insulin-like growth factor 1 and angiotensin II. Hum Mol Genet. 2007;16(20):2453–62.
57. Wang L, Guo DC, Cao J, Gong L, Kamm KE, Regalado E, et al. Mutations in myosin light chain kinase cause familial aortic dissections. Am J Hum Genet. 2010;87(5):701–7.
58. Guo DC, Regalado E, Casteel DE, Santos-Cortez RL, Gong L, Kim JJ, et al. Recurrent gain-of-function mutation in PRKG1 causes thoracic aortic aneurysms and acute aortic dissections. Am J Hum Genet. 2013;93(2):398–404.
59. van de Luijtgaarden KM, Bastos GF, Hoeks SE, Valentijn TM, Stolker RJ, Majoor-Krakauer D, et al. Lower atherosclerotic burden in familial abdominal aortic aneurysm. J Vasc Surg. 2014;59(3):589–93.
60. Brown CR, Greenberg RK, Wong S, Eagleton M, Mastracci T, Hernandez AV, et al. Family history of aortic disease predicts disease patterns and progression and is a significant influence on management strategies for patients and their relatives. J Vasc Surg. 2013;58(3):573–81.
61. Erbel R, Aboyans V, Boileau C, Bossone E, Bartolomeo RD, Eggebrecht H, et al. 2014 ESC guidelines on the diagnosis and treatment of aortic diseases: document covering acute and chronic aortic diseases of the thoracic and abdominal aorta of the adult. The Task Force for the Diagnosis and Treatment of Aortic Diseases of the European Society of Cardiology (ESC). Eur Heart J. 2014;35(41):2873–926.
62. Ince H, Rehders TC, Petzsch M, Kische S, Nienaber CA. Stent-grafts in patients with Marfan syndrome. J Endovasc Ther. 2005;12(1):82–8.
63. Nordon IM, Hinchliffe RJ, Holt PJ, Morgan R, Jahangiri M, Loftus IM, et al. Endovascular management of chronic aortic dissection in patients with Marfan syndrome. J Vasc Surg. 2009;50(5):987–91.
64. Geisbusch P, Kotelis D, von Tengg-Kobligk H, Hyhlik-Durr A, Allenberg JR, Bockler D. Thoracic aortic endografting in patients with connective tissue diseases. J Endovasc Ther. 2008;15(2):144–9.
65. Botta L, Russo V, La PC, Rosati M, Di BR, Fattori R. Stent graft repair of descending aortic dissection in patients with Marfan syndrome: an effective alternative to open reoperation? J Thorac Cardiovasc Surg. 2009;138(5):1108–14.
66. Waterman AL, Feezor RJ, Lee WA, Hess PJ, Beaver TM, Martin TD, et al. Endovascular treatment of acute and chronic aortic pathology in patients with Marfan syndrome. J Vasc Surg. 2012;55(5):1234–40.
67. Marcheix B, Rousseau H, Bongard V, Heijmen RH, Nienaber CA, Ehrlich M, et al. Stent grafting of dissected descending aorta in patients with Marfan's syndrome: mid-term results. JACC Cardiovasc Interv. 2008;1(6):673–80.
68. Eid-Lidt G, Gaspar J, Melendez-Ramirez G, Cervantes SJ, Gonzalez-Pacheco H, Damas de Los Santos F, et al. Endovascular treatment of type B dissection in patients with Marfan syndrome: mid-term outcomes and aortic remodeling. Catheter Cardiovasc Interv. 2013;82(7):E898–905.
69. Dong ZH, Fu WG, Wang YQ, Guo DQ, Xu X, Ji Y, et al. Retrograde type A aortic dissection after endovascular stent graft placement for treatment of type B dissection. Circulation. 2009;119(5):735–41.

70. Cikrit DF, Miles JH, Silver D. Spontaneous arterial perforation: the Ehlers-Danlos specter. J Vasc Surg. 1987;5(2):248–55.
71. Kitagawa A, Greenberg RK, Eagleton MJ, Mastracci TM, Roselli EE. Fenestrated and branched endovascular aortic repair for chronic type B aortic dissection with thoracoabdominal aneurysms. J Vasc Surg. 2013;58(3):625–34.
72. van de Luijtgaarden KM, Bastos GF, Hoeks SE, Majoor-Krakauer D, Rouwet EV, Stolker RJ, et al. Familial abdominal aortic aneurysm is associated with more complications after endovascular aneurysm repair. J Vasc Surg. 2014;59(2):275–82.
73. Ryer EJ, Garvin RP, Thomas B, Kuivaniemi H, Franklin DP, Elmore JR. Patients with familial abdominal aortic aneurysms are at increased risk for endoleak and secondary intervention following elective endovascular aneurysm repair. J Vasc Surg. 2015;62(5):1119–24.e9.

Normal Aortic Anatomy and Variations of Its Branches

4

Randall R. DeMartino

Introduction

The vascular system evolves from an iterative process during development that includes the aorta and all of its major branches. As such, although normal arterial circulation predominates, specific variations exist and are commonly encountered in clinical practice. Understanding these variations is critical for identification and treatment planning for complex aortic repair. The goal of this chapter is to review the normal branch patterns of the aorta and to describe common and critical variations that should be identified.

Aorta and Aortic Arch Branches

The thoracic aorta consists of three segments: the ascending aorta, aortic arch, and the descending aorta. Of these, only the aortic arch develops branches that ultimately supply the upper extremities, upper chest, head, and neck via a complex development process. By the fourth week of development, the paired dorsal aortae fuse for much of their length and the six sets of paired aortic arches begin their development. By the fifth week of development, the first, second, and fifth arches have largely regressed. The roots of the third arches will form the common carotid arteries as the external carotid arties migrate to their position as new branches from the aortic sac. The left fourth arch will ultimately persist in most cases as the left-sided aortic arch and the right fourth arch will develop into the right subclavian artery as the right dorsal aorta regresses. The right sixth arch will also regress and the left side will become the ductus arteriosus [1]. Given the numerous steps of aortic development, variation in arch anatomy can occur with any variation of this sequence.

R.R. DeMartino (✉)
Division of Vascular and Endovascular Surgery, Department of Surgery, Mayo Clinic, 200 First St. SW, Rochester, MN 555905, USA
e-mail: demartino.randall@mayo.edu

The normal aortic arch pattern from proximal to distal includes the brachiocephalic trunk (also referred to as the innominate artery), the left common carotid artery, and the left subclavian artery. The brachiocephalic artery divides after several centimeters into the right subclavian and right common carotid artery (Fig. 4.1a). This pattern occurs 65 % of the time. Alternatively, the most common variation (22–27 % of the time) involves the left common carotid artery originating with the brachiocephalic artery as a common orifice off the arch (AKA bovine arch). Alternatively, the left common carotid artery may originate off the mid/distal segment of the brachiocephalic artery (see Fig. 4.1b). In both of these settings, the left subclavian artery is a separate branch off the arch. The third most common variant (1.2–2.5 % of patients) is a four-vessel arch where the left vertebral artery originates from the arch between the left common carotid artery and the left subclavian artery (see Fig. 4.1c). Less common patterns include bilateral brachiocephalic trunks (see Fig. 4.1d) or any combination of two or three vessel common trunks involving the right and left subclavian and carotid arteries (see Fig. 4.1e–j). Finally, an important variant involves an aberrant right subclavian artery that originates distal to the left subclavian artery and passes retropharyngeal (Figs. 4.2a and 4.3). This may cause compressive symptoms termed "dysphagia lusoria." Importantly, the origin of the aberrant subclavian is commonly enlarged and is prone to aneurysmal degeneration, termed a diverticulum of Kommerell (see Fig. 4.2b) [1–3].

The arch itself can have variation. If both aortic arches persist, there will be a double-aortic arch forming a "vascular ring" around the trachea and esophagus (see Fig. 4.4b). Regression of the left aortic arch will produce a right aortic arch (see Figs. 4.4c and 4.5a, b). The reader is referred to other sources for extensive classification of these uncommon vascular rings and arch malformations [4]. In addition to the variations above, the aortic arch also undergoes conformational changes with age due to elongation. The brachiocephalic artery origin moves forward and the origins of the arch branches become more acute. These are classified as

© Mayo Foundation for Medical Education and Research 2017

G.S. Oderich (ed.), *Endovascular Aortic Repair*, DOI 10.1007/978-3-319-15192-2_4

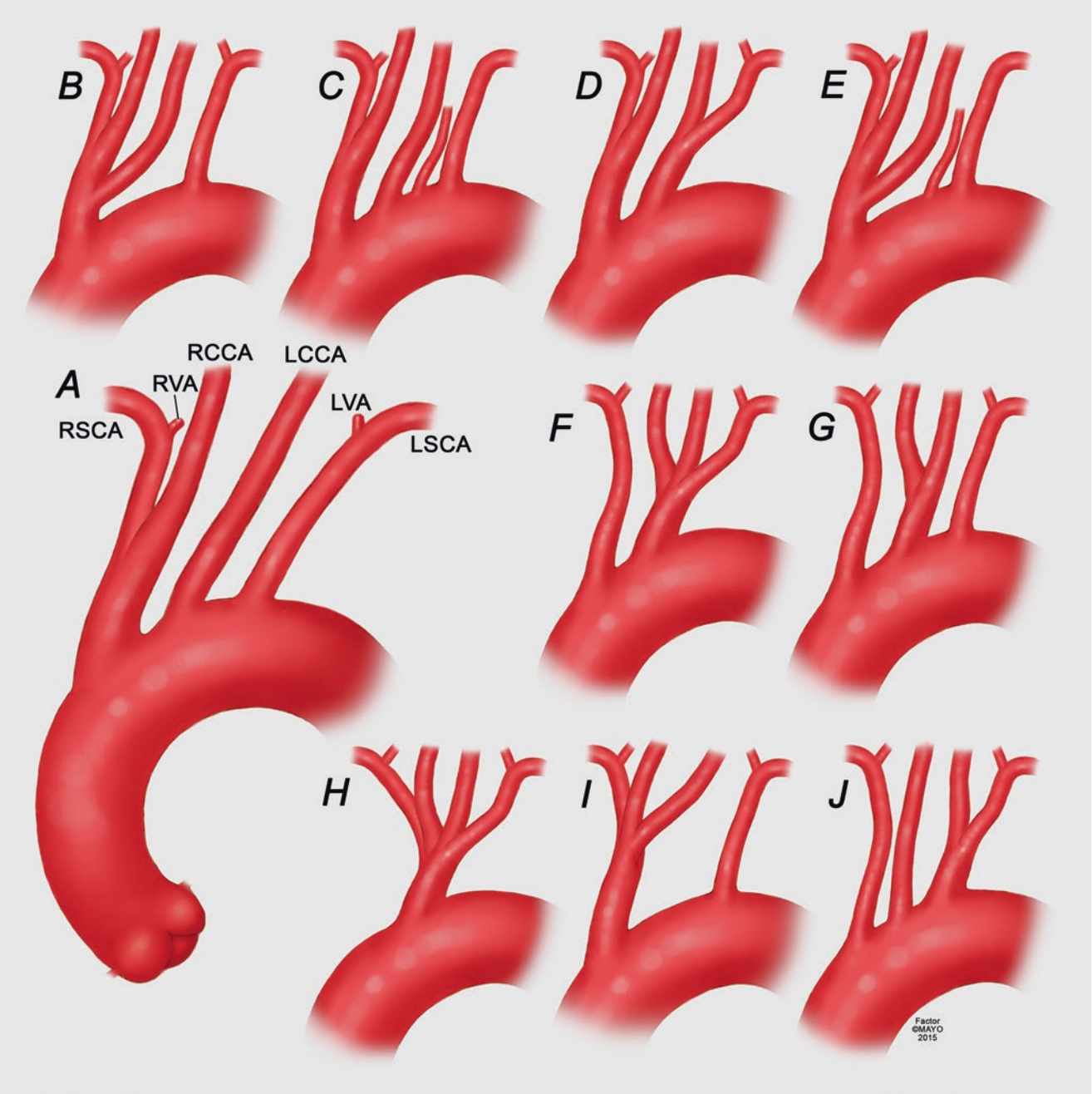


Fig. 4.1 Normal and variations of the aortic arch branches. *RSCA* right subclavian artery, *RVA* right vertebral artery, *RCCA* right common carotid artery, *LCCA* left common carotid artery, *LVA* left vertebral artery, *LSCA* left subclavian artery. By permission of Mayo Foundation for Medical Education and Research. All rights reserved

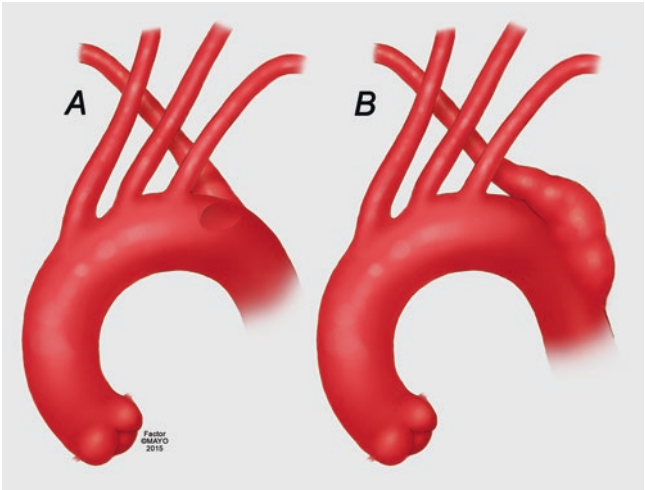


Fig. 4.2 Aberrant right subclavian artery. (**a**) Aberrant right subclavian artery; (**b**) with aneurysmal diverticulum of Kommerell. By permission of Mayo Foundation for Medical Education and Research. All rights reserved

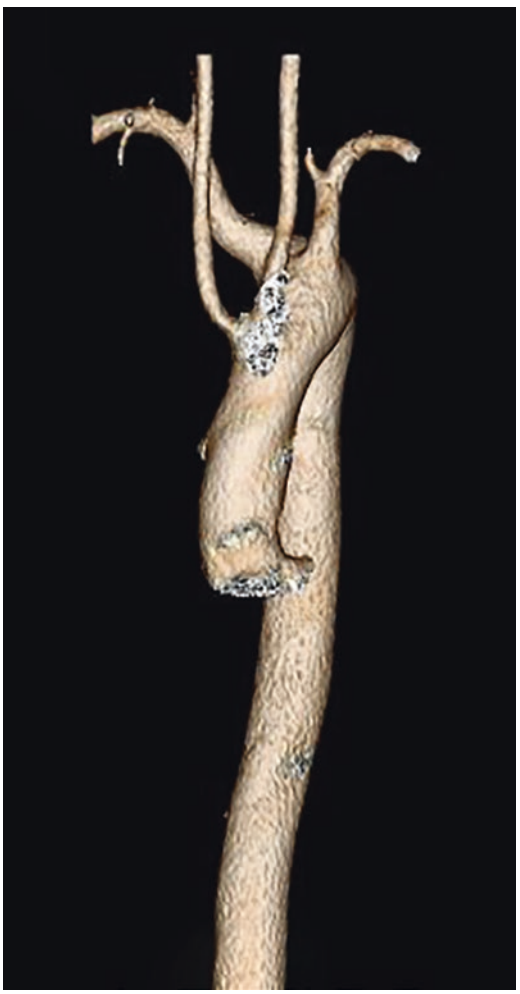


Fig. 4.3 Computed tomographic angiogram of an aberrant right subclavian artery. By permission of Mayo Foundation for Medical Education and Research. All rights reserved

types I–III arch patterns (Fig. 4.6a–c). The more progressive the arch pattern (type III being the most progressive), the more difficult cannulation of each vessel becomes as well as attaining good opposition of an endograft on the lesser curve (common cause for "bird beaking").

Mesenteric Branches

The celiac axis, superior mesenteric artery (SMA), and inferior mesenteric artery (IMA) represent the major mesenteric branches of the aorta and are the derivatives of the fused 10th, 13th, and 21st ventral segmental arteries of the developing embryo, respectively. The ventral orientation of these three main mesenteric branches is the most common configuration. There is little variation of the IMA in regard to presence, position, and origin. IMA variation typically occurs in the collateralization to the SMA and internal iliac arteries and its branching pattern in the mesentery, but not of the main branch itself [5].

However, the celiac trunk and SMA branches can have several variations that are important to recognize. The "normal" celiac trunk and SMA configuration consist of the celiac trunk with a left gastric, splenic, and common hepatic artery and the SMA is a separate branch (Fig. 4.7a). This occurs in 55–89 % in series of anatomic dissections and arteriograms performed over the last 50 years [1, 6, 7]. In <10 % of cases, the common hepatic artery originates separate from the aorta while the left gastric and splenic arteries form a common origin (gastrosplenic trunk; see Fig. 4.7b). Less commonly, a hepatosplenic (see Fig. 4.7c) or hepatogastric trunk (see Fig. 4.7d) is formed, with the remaining branch coming from the aorta. In rare circumstances, the

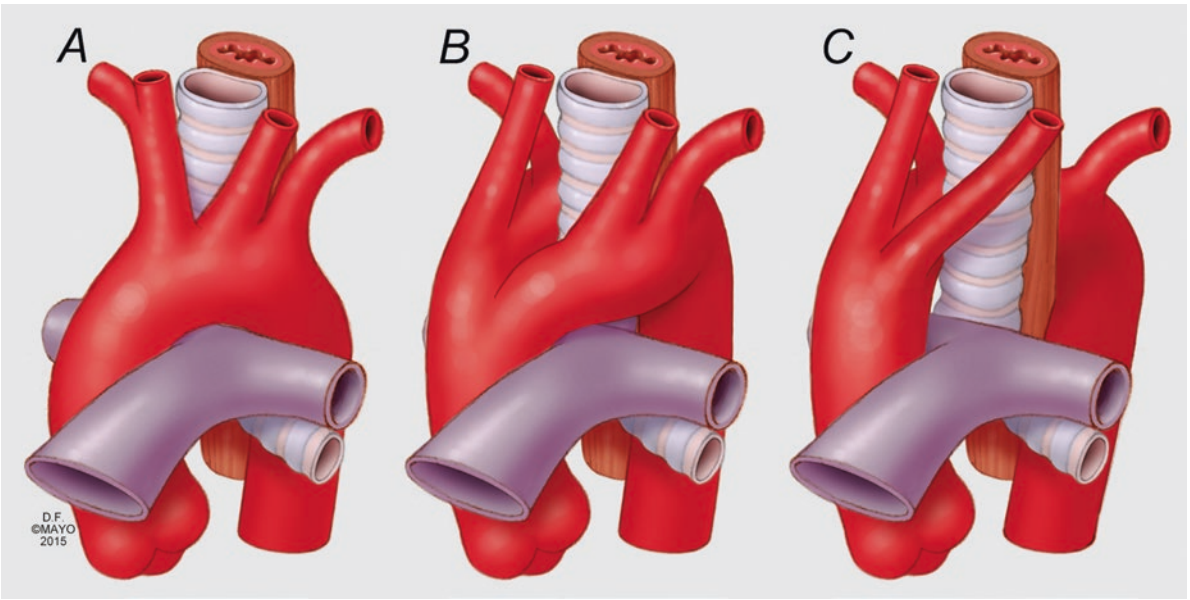


Fig. 4.4 Aortic arch variations. (**a**) Normal aortic arch; (**b**) double-aortic arch; (**c**) right-sided arch. By permission of Mayo Foundation for Medical Education and Research. All rights reserved



Fig. 4.5 (**a**) Arteriogram of a right-sided aortic arch. (**b**) Computed tomographic angiogram of a right-sided aortic arch. By permission of Mayo Foundation for Medical Education and Research. All rights reserved

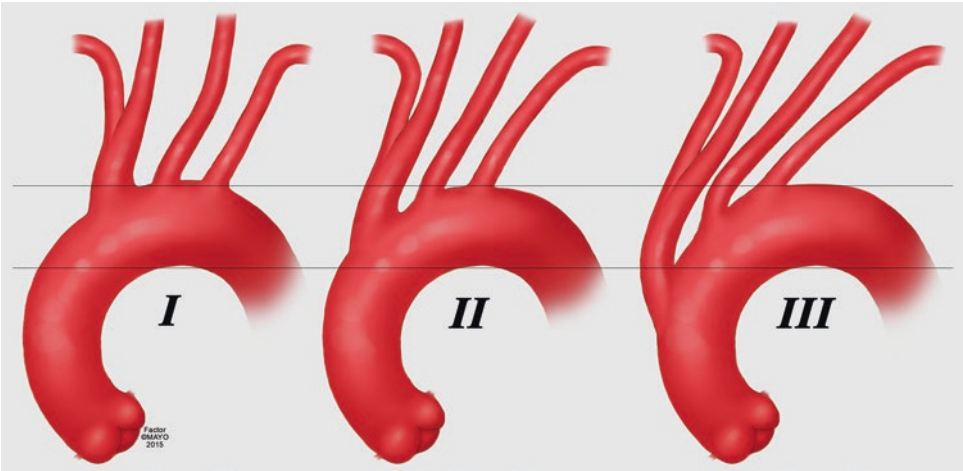


Fig. 4.6 Aortic arch types *I*, *II*, and *III*. By permission of Mayo Foundation for Medical Education and Research. All rights reserved

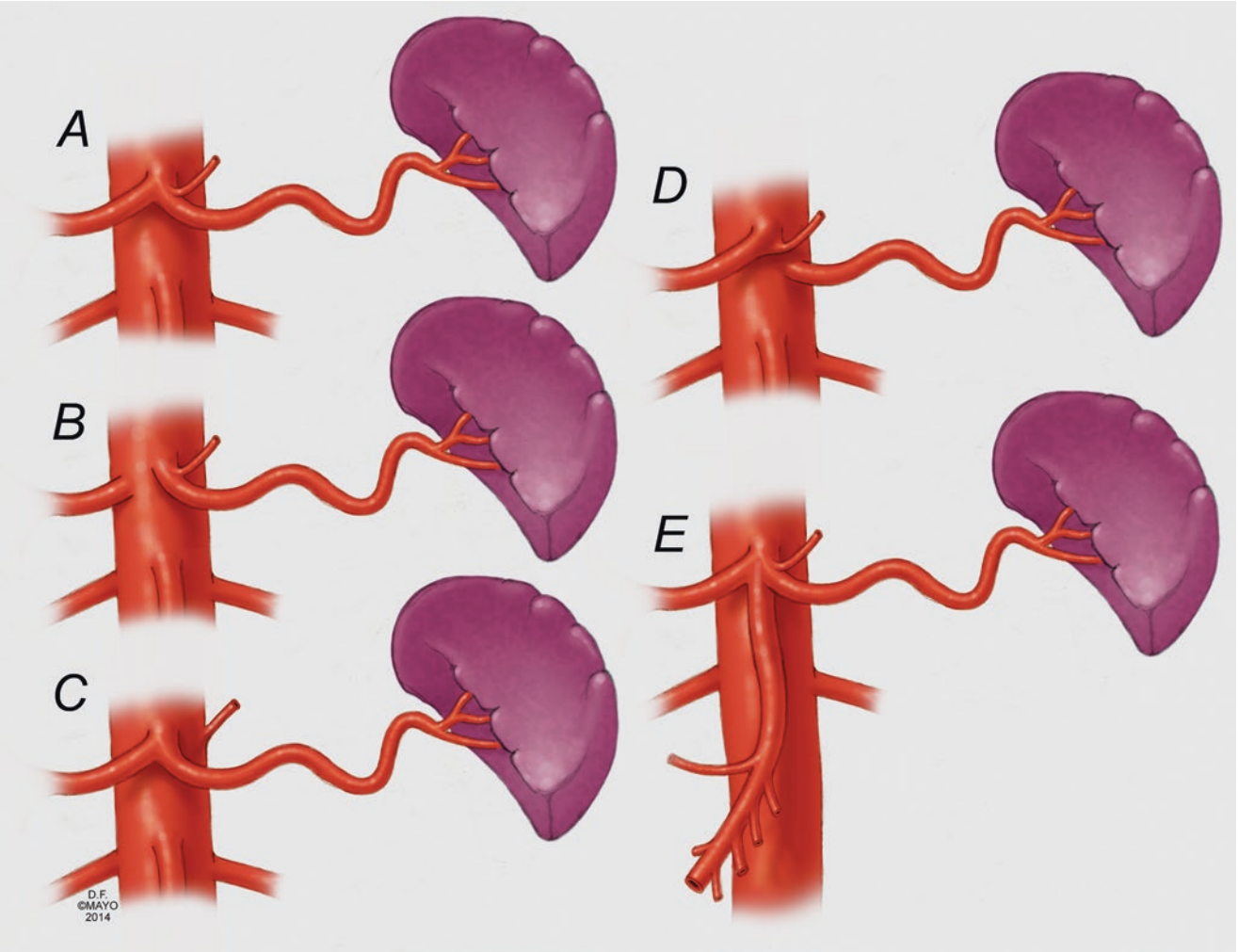


Fig. 4.7 Variations of mesenteric aortic branches. By permission of Mayo Foundation for Medical Education and Research. All rights reserved

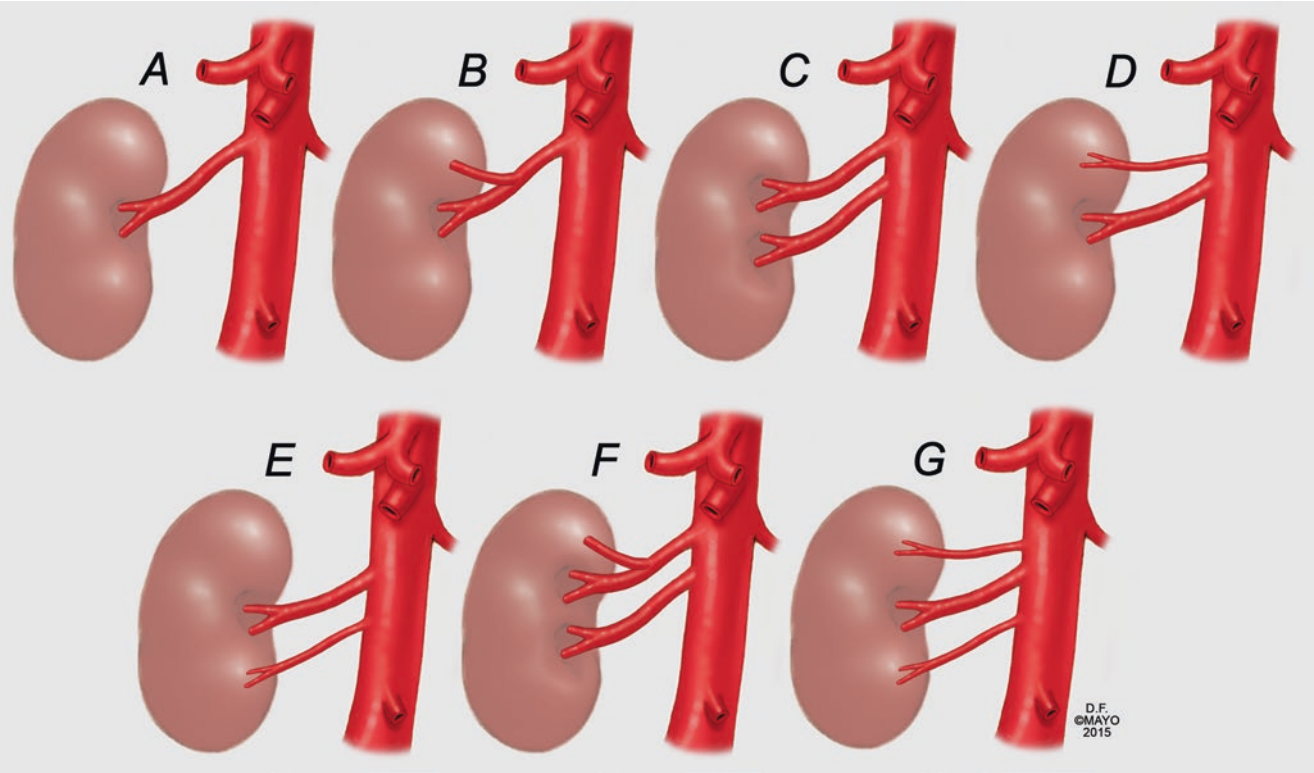


Fig. 4.8 Variations of renal artery branches. By permission of Mayo Foundation for Medical Education and Research. All rights reserved

SMA originates from the celiac artery as a common celiacomesenteric axis (see Fig. 4.7e) [1]. The left gastric artery is a relatively constant structure. However, it may give rise to an accessory left hepatic artery (1–16 % of cases) or a replaced left hepatic artery 10 % of the time [6–8]. The splenic artery may be part of anomalous permutations of the celiac artery as discussed previously. The splenic artery can originate from the SMA as opposed to the celiac artery. It may also be duplicated with one or both branches originating from the aorta. Additionally, it may give rise to the left gastric, middle colic, or left hepatic artery [1]. The SMA may provide any combination of hepatic arteries (commonly a replaced right hepatic artery), or accessory gastric, splenic, or pancreatic vessels.

Renal Branches

The mature kidney results from rostral migration of the metanephros of the developing embryo starting at week 7 of development. These metanephric kidneys eventually derive their blood supply from several lateral segmental arteries that ultimately will fuse to form the renal arteries. These fuse at the L1–L2 lumbar vertebral body level 1–2 cm below the SMA [3, 9] and often with a slight oblique course where the right renal artery is more anterior. Due to the iterative development of the renal vasculature, notable variation can exist. It is important to remember that the term "accessory renal" artery is a misnomer as these are end-organ vessels that perfuse a specific segment of the kidney and coverage or ligation will result in renal infarction. However, it is unlikely that renal function will decline if vessels <3 mm are not incorporated in open or endovascular repair of pararenal or thoracoabdominal repairs. Variations of renal perfusion require careful consideration for endovascular repair, but do not preclude advanced branched or fenestrated options [10].

In a review of nearly 11,000 kidneys, approximately 72 % of kidneys have a single renal artery (Fig. 4.8a). The most common variations are either a single renal artery with an early upper pole branch (13 %) or two hilar renal arteries (11 %; see Fig. 4.8b, c). Less commonly there is a hilar branch and either a separate upper pole (6 %) or lower pole vessel (3 %; see Fig. 4.8d, e). Finally, two vessels with an upper pole branch (2.7 %) and three vessels (1.7 %) are the least common variations (see Fig. 4.8f, g) [2].

Failure of the kidney to completely migrate rostrally may result in either a pelvic kidney (Fig. 4.9) or, if the

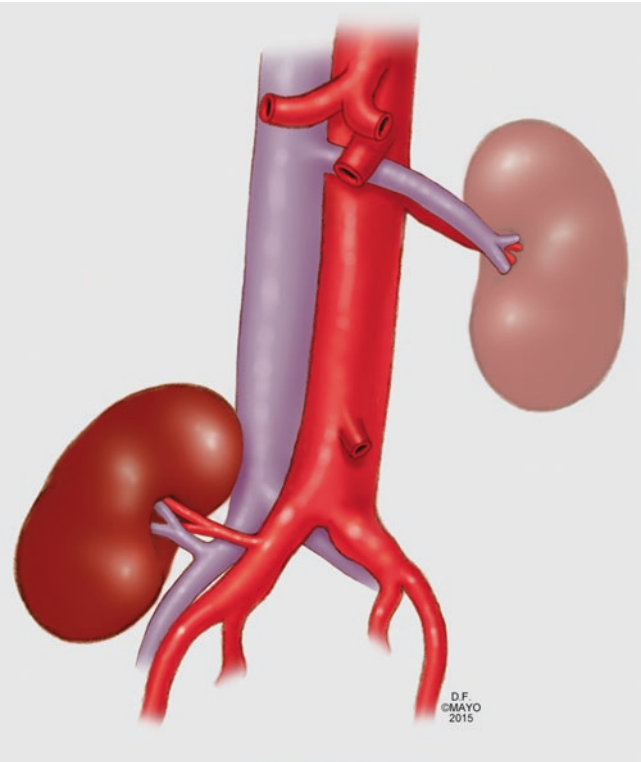


Fig. 4.9 Right-sided pelvic kidney. By permission of Mayo Foundation for Medical Education and Research. All rights reserved

lower poles fuse, a horseshoe kidney. Either of these situations typically results in variations in the normal renal arterial pattern that can involve one to three renal arteries on each side and may originate anywhere along the infra-mesenteric abdominal aorta or common iliac arteries. The kidneys may reside in the pelvis, span the abdomen, or be rotated to either side. The horseshoe kidney may have one of six common arterial patterns originally described by Graves [11]. In resin injection, he identified that each renal artery supplied a specific segment (upper, middle, lower) of the kidney and there was no collateralization. Importantly, several variations involve arterial supply from the distal aorta or common iliac arteries (Fig. 4.10).

Iliac Branches

The bifurcation of the aorta into the right and left common iliac arteries occurs around the fourth lumbar vertebra and is without major branches. The aortic bifurcation and common iliac configuration are responsible for the bilateral pelvis and lower extremity perfusion and have little variability. However, the length of the common iliac artery is variable and in an extremely rare case it may be absent with the external and internal iliac arteries originating at the aortic bifurcation. Occasionally, as noted above, the lower pole of an ectopic pelvic kidney may originate from the common iliac artery as well as smaller lumbar, sacral, and gonadal arteries. Rarely, the middle colic, umbilical, obturator, or circumflex iliac branch will originate from the common iliac artery [1]. The external iliac artery also has little variability, but may be tortuous and have several branches near the inguinal ligament. In the case of a persistent sciatic artery, it may be reduced or absent.

Although variability of the common and external iliac artery is rare, variability of the internal iliac (hypogastric) artery is common. There is usually a 4 cm trunk, followed by the typical division into an anterior and posterior division in only 57–77 % of the population. Absence of the internal iliac artery is rare, and more likely to be occluded due to atherosclerosis if not visualized on CT scan. The anterior division of the internal iliac artery is primarily responsible for perfusion of the bladder, uterus, rectum, and vagina. The posterior division typically is responsible for perfusion of the bones, muscles, and nerves, specifically the superior gluteal artery that will supply the gluteus maximus. Although perfusion is variable, branched grafts to the posterior division are preferable to minimize buttock claudication for this reason. Important variants of internal iliac artery anatomy involve the branch pattern of the superior and inferior gluteal and pudendal arteries. The most common configuration (59 %) involves a separate superior gluteal artery with the internal pudendal and inferior gluteal arteries sharing a common trunk (Fig. 4.11a). Less commonly, in 23 % of the population there is sequential branching of the superior gluteal, inferior gluteal, and internal pudendal (see Fig. 4.11b) or a common gluteal trunk with a separate internal pudendal branch (15 % of the population; see Fig. 4.11c). Rarely, there is a common

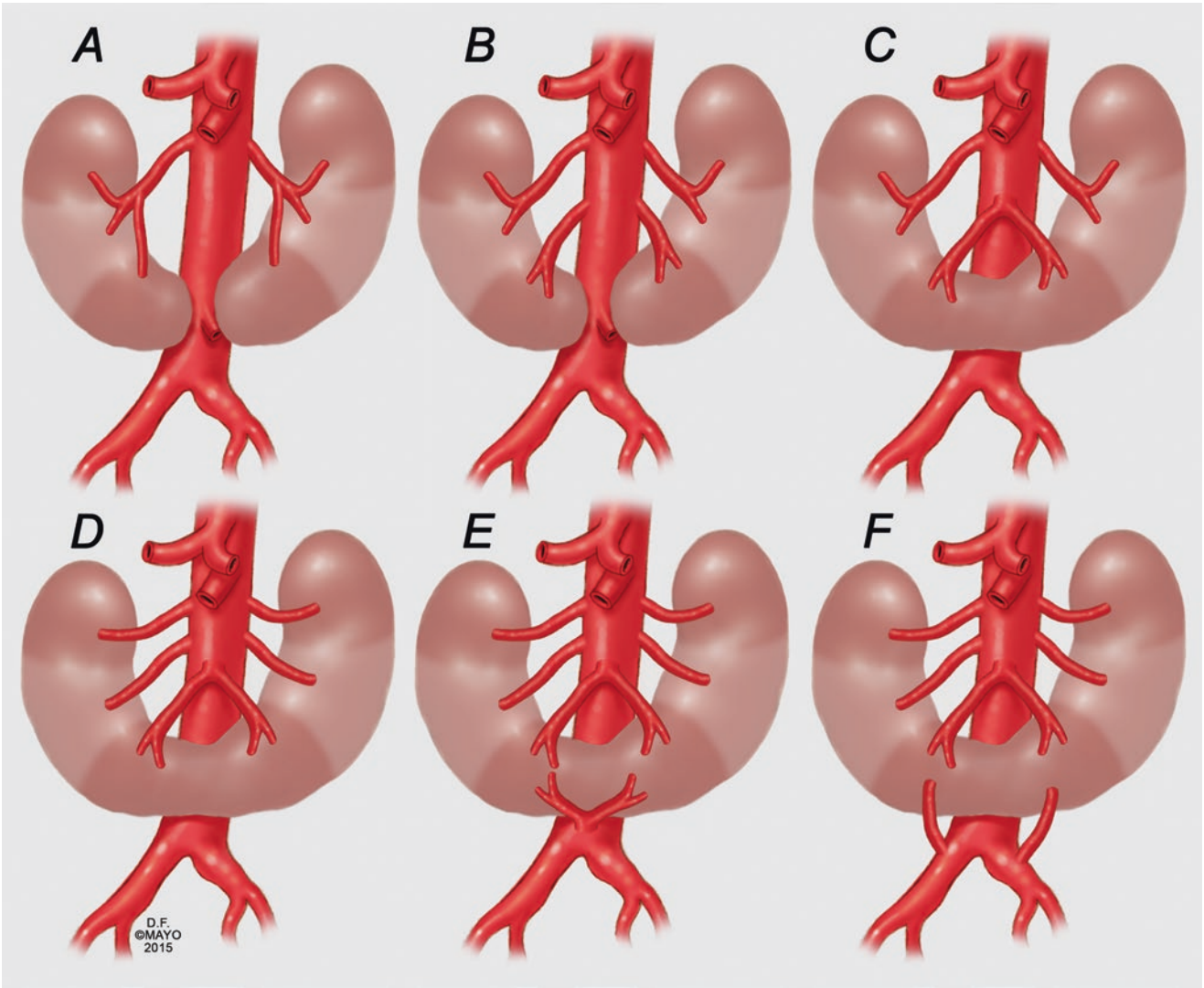


Fig. 4.10 Arterial supply classification of the horseshoe kidney. By permission of Mayo Foundation for Medical Education and Research. All rights reserved

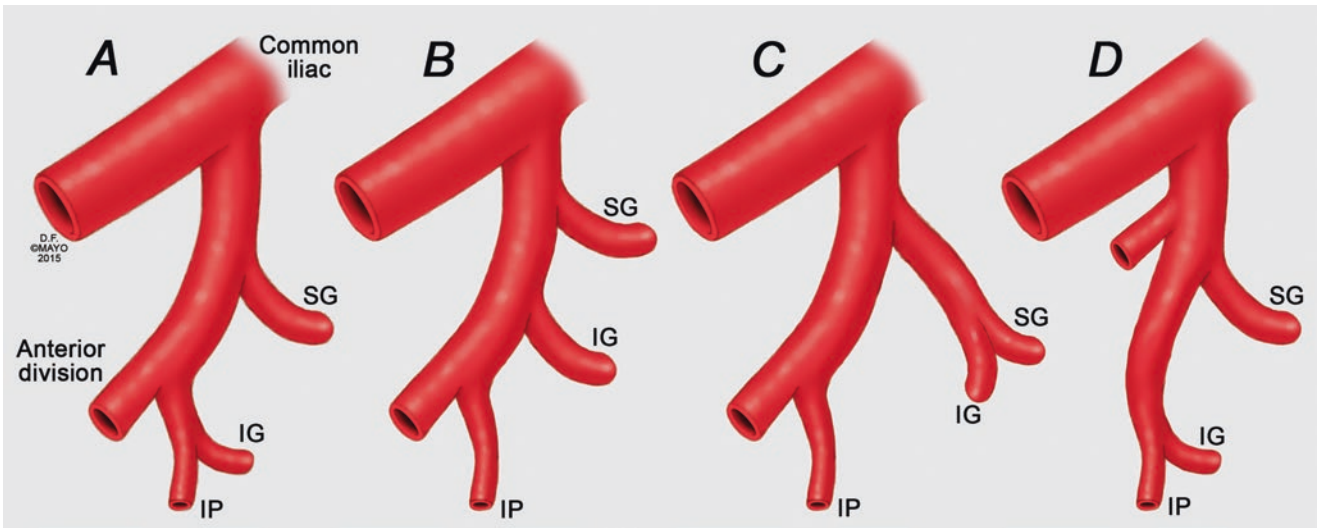


Fig. 4.11 Internal iliac artery branch variation. *SG* superior gluteal, *IG* inferior gluteal, *IP* internal pudendal. By permission of Mayo Foundation for Medical Education and Research. All rights reserved

trunk for all three branches with early origin of the superior gluteal artery (see Fig. 4.11d).

References

1. Valentine RJ, Wind GG. Anatomic exposures in vascular surgery. 2nd ed. Philadelphia: Lippincott Williams & Wilkins; 2003. xiii, 577 pp.
2. Bergman RA. Compendium of human anatomic variation: text, atlas, and world literature. Baltimore: Urban & Schwarzenberg; 1988. xiv, 593 pp.
3. Uflacker R, Selby JB. Atlas of vascular anatomy: an angiographic approach. 2nd ed. Philadelphia: Lippincott Williams & Wilkins; 2007. xiv, 905 pp.
4. Stewart JR. An atlas of vascular rings and related malformations of the aortic arch system. Springfield: Charles C Thomas; 1964. xi, 171 pp.
5. Oderich GS. Mesenteric vascular disease. New York: Springer; 2014.
6. Covey AM, Brody LA, Maluccio MA, Getrajdman GI, Brown KT. Variant hepatic arterial anatomy revisited: digital subtraction angiography performed in 600 patients. Radiology. 2002;224(2):542–7.
7. Hiatt JR, Gabbay J, Busuttil RW. Surgical anatomy of the hepatic arteries in 1000 cases. Ann Surg. 1994;220(1):50–2.
8. De Cecco CN, Ferrari R, Rengo M, Paolantonio P, Vecchietti F, Laghi A. Anatomic variations of the hepatic arteries in 250 patients studied with 64-row CT angiography. Eur Radiol. 2009;19(11):2765–70.
9. Cronenwett JL, Johnston KW. Rutherford's vascular surgery. 8th ed. Two volumes. Philadelphia: Saunders/Elsevier; 2014.
10. Spear R, Maurel B, Sobocinski J, Perini P, Guillou M, Midulla M, et al. Technical note and results in the management of anatomical variants of renal vascularisation during endovascular aneurysm repair. Eur J Vasc Endovasc Surg. 2012;43(4):398–403.
11. Graves FT. The arterial anatomy of the congenitally abnormal kidney. Br J Surg. 1969;56(7):533–41.

Classification Systems Relevant to Complex Endovascular Aortic Repair

5

Gustavo S. Oderich and Tiziano Tallarita

Introduction

Endovascular aortic repair (EVAR) has become the first treatment option for most patients with aortic aneurysms and dissections. Anatomical constraints for EVAR include presence of suboptimal necks, angulation, and aneurysm involvement of side branches. In the last decade, technical developments have focused on branch incorporation using a variety of techniques including fenestrations, directional branches, and parallel stent grafts. Specifically designed fenestrated and branched stent grafts were introduced as a minimally invasive alternative to treat complex aneurysms, allowing proximal extension of the stent graft without compromising seal and aneurysm exclusion [1]. This chapter focuses on description of definitions and classification systems which are pertinent to use of complex endovascular techniques to treat aortic aneurysms and dissections [2].

Types of Repair

Branch incorporation has been performed using a variety of methods. In essence the aortic stent-graft component is connected to a specific target vessel by means of a bridging stent, but the specific connecting mechanism varies. The classification of stent design takes into consideration that connecting mechanism and the quality or actual diameter of the aorta at the level of the side branch. It is important to acknowledge that definitions represent the most common terminology used in the literature and by pioneers, but these terms have not yet been validated by society reporting standards.

Fenestrated and Branched Stent Grafts

The term *fenestrated endovascular repair* is applied when a fenestrated stent graft is used to repair an aneurysm with inadequate or short infrarenal neck (Fig. 5.1a), yet the target vessels (e.g., renal arteries) arise from normal aorta. There is no gap between the fenestration and the target vessel. Alignment stents are typically used to prevent vessel occlusion or stenosis from misalignment between the fenestration and the origin of the target vessel.

Branched endovascular repair is the term used to describe endovascular repair of aneurysms with frank involvement of side branches. The target vessel originates from the aneurysm and there is a gap between the main stent graft and the aortic wall. Branched stent grafts are currently performed using one of the two approaches. *Fenestrated branches* are based on reinforced fenestrations bridged by balloon-expandable covered stents (Fig. 5.1b). *Directional or cuffed branches* are based on pre-sewn cuffs (Fig. 5.1c), which can be straight, helical, downgoing, upgoing, internal, or external. These branches are bridged by self-expandable stent grafts.

Parallel Stent Grafts

Parallel stent-graft techniques have been widely used as bail out or as primary treatment in patients with compromised aortic necks. This broad term includes a variety of techniques. Chimneys or snorkel stent grafts imply the use of stents placed from brachial access with downgoing orientation (Fig. 5.2a). The technique was first described by

G.S. Oderich (✉) • T. Tallarita
Division of Vascular and Endovascular Surgery,
Department of Surgery, Mayo Clinic, 200 First Street SW,
Rochester, MN 55905, USA
e-mail: oderich.gustavo@mayo.edu; tallaritat@gmail.com

© Mayo Foundation for Medical Education and Research 2017

G.S. Oderich (ed.), *Endovascular Aortic Repair*, DOI 10.1007/978-3-319-15192-2_5

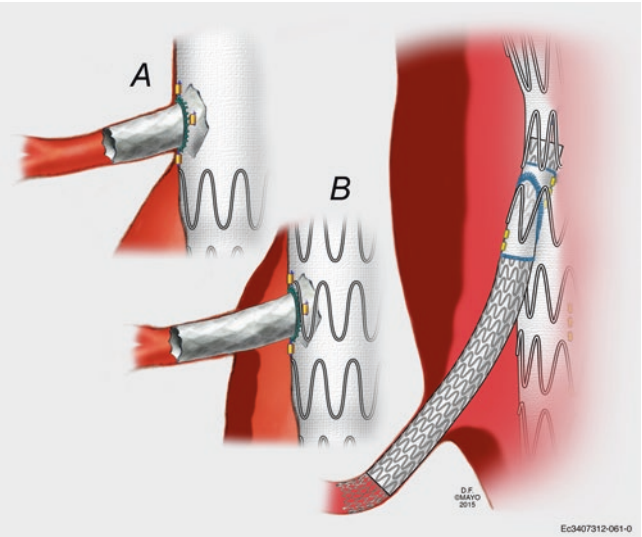


Fig. 5.1 Classification of type of repair includes fenestrated repair (**a**), fenestrated branched repair (**b**), and directional branched repair. By permission of Mayo Foundation for Medical Education and Research. All rights reserved

Roy Greenberg and popularized by Frank Criado. Larger clinical experience has been accumulated by the Zurich (Mario Lachat), Muenster (Giovanni Torsello), and Stanford groups (Jason Lee). Upgoing branches placed from femoral approach define periscope technique (Fig. 5.2b). The use of aortic components and multiple parallel branches anchored into limbs of bifurcated aortic devices as initially described by Kasirajan from Emory University in 2011 (Fig. 5.2c). The use of parallel stents between aortic components was described and popularized by Armando Lobato from Sao Paulo as the sandwich technique (Fig. 5.2d).

Hybrid Endovascular Repair

Hybrid techniques represented the first step towards extending endovascular repair to complex anatomy (Fig. 5.3). The first hybrid endovascular repair was described by William Quinones-Baldrich from the

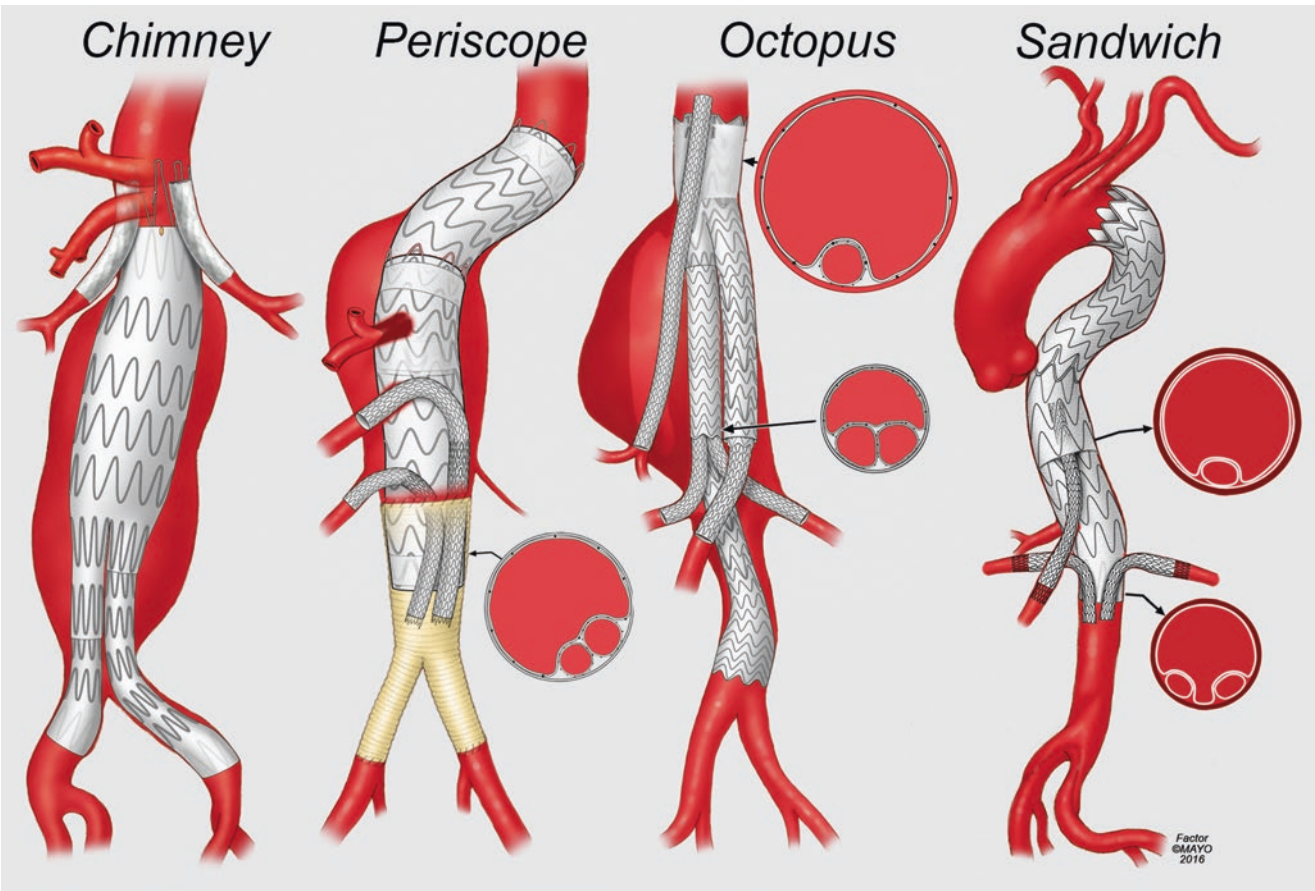


Fig. 5.2 Parallel stent-graft techniques. By permission of Mayo Foundation for Medical Education and Research. All rights reserved

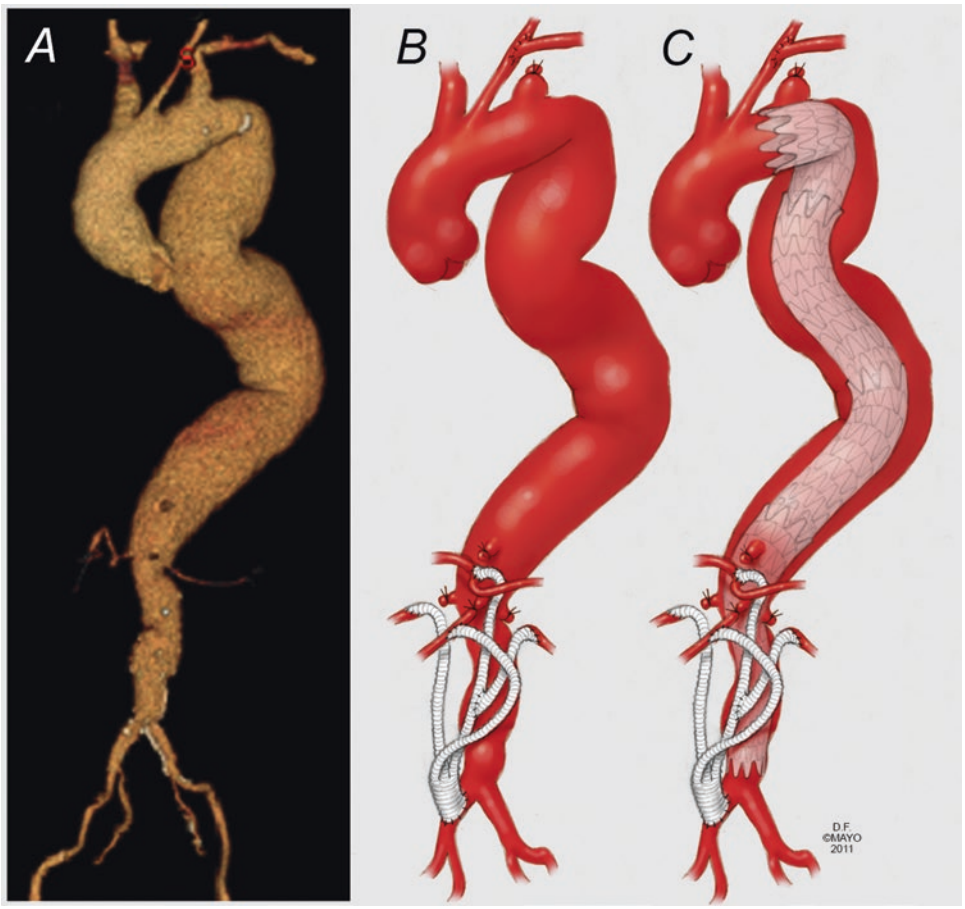


Fig. 5.3 Hybrid technique illustrated in a patient treated for Extent II TAAA (**a**) using staged visceral debranching (**b**) followed by stent-graft placement (**c**). By permission of Mayo Foundation for Medical Education and Research. All rights reserved

University of California, Los Angeles, in 1999 to treat a high-risk patient with Extent IV thoracoabdominal aortic aneurysm. The technique has been widely applied to treat aortic arch, thoracoabdominal, pararenal, and aortoiliac aneurysms. Aortic debranching implies the use of extra-anatomical bypasses based in the aorta, iliac, and visceral arteries or within an aortic graft.

Spectrum of Aortic Disease

Aortic aneurysmal disease is the 13th most common cause of death in the USA and is increasingly diagnosed since the introduction of screening programs. The pathogenesis of aortic aneurysms is complex and not completely defined. Aortic wall degeneration induced by atherosclerosis, proteolytic enzyme activation, and inflammatory processes are the leading hypothesis; other theories include infectious, connective tissue disorders from genetic predisposition, and hemodynamic influences. It is likely that aneurysm formation is multifactorial rather than a single process.

Atherosclerotic Aneurysms

The association of aortic aneurysm with aortic atherosclerosis has long been recognized. Most patients with an abdominal aortic aneurysm have evidence of atherosclerosis in other vascular beds, notably the coronary, carotid, and/or peripheral arteries. The pathogenesis of atherosclerosis is a complex and dynamic process involving cellular proliferation and migration, intimal lipid deposition, inflammation, fibrosis, and necrosis with dystrophic calcification [3]. This has led to the theory that aortic aneurysmal disease is part of the atherosclerosis process involving the aorta. Therefore, aortic aneurysms are commonly referred as atherosclerotic, although this is likely an oversimplification of the actual pathogenesis. A characteristic feature of atherosclerosis is plaque deposition in the intima of the arterial wall. Atherosclerotic intimal plaques cause thinning of the adjacent media, leading to weakening of the arterial wall. The media is the major structural unit of the aorta and is composed of layers of musculo-elastic fascicles, or lamellar units. The elastic fibers distribute mural tensile stresses and

provide recoil during the cardiac cycle, while the collagen network prevents over-distention, disruption, and enlargement. Proteolytic activation with increased amounts of collagenase, elastase, and metalloproteinases have been associated with aneurysm development and risk of rupture.

Macrophages are consistently found in the adventitial layer of aneurysms as well as in association with atherosclerotic plaques. Many proteinases are released by macrophages, including a number of important matrix metalloproteinases (MMPs). These include the interstitial collagenase (MMP-1), stromelysin (MMP-3), a 72 kDa gelatinase/type IV collagenase (MMP-2), and a 92 kDa gelatinase/type IV collagenase (MMP-9). All these MMPs have the capacity to degrade all the major connective tissue components of the aortic wall, including collagen, elastin, proteoglycans, fibronectin, and laminin. These proteinases are inhibited by tissue inhibitor of metalloproteinase (TIMP), which is also produced by macrophages.

Inflammatory Aneurysms

Inflammatory aneurysms account for approximately 5 % of abdominal aortic aneurysms. Their characteristic feature is chronic inflammatory infiltrate of varying degree in the outer layers of the media and adventitia. Inflammatory cells are also seen in non-atherosclerotic aortic aneurysms such as those caused by various types of aortitis, including giant cell arteritis, rheumatoid arthritis, systemic lupus erythematosus, polyarteritis nodosa, syphilis, and Takayasu's, Behcet's, and Kawasaki's diseases. This suggests that the possibility that inflammatory cells, through the release of proteolytic enzymes, may play a primary role in either the causation or the exacerbation of aneurysmal dilation. Macrophages, along with T and B lymphocytes, are the major cellular components of chronic inflammation. Inflammatory aneurysms of the abdominal aorta tend to encase the ureters causing hydronephrosis. Renal insufficiency may result from hydronephrosis and this may be the primary manifestation.

Genetically Triggered Aortic Diseases

Genetically triggered aortic diseases are discussed in detail in Chaps. 2 and 3. It is well recognized that a positive family history (first-degree relative) increases the risk of aortic aneurysm. Several specific genetic abnormalities have been identified in "non-atherosclerotic" aneurysm groups, such as fibrillin gene abnormalities in patients with Marfan's syndrome and procollagen type III defects in patients with vascular Ehlers-Danlos syndrome.

Classification of Blunt Aortic Traumatic Injuries

Traumatic aortic injury is the second most common cause of death among victims of blunt trauma. In a cohort of 275 patients with traumatic rupture, Parmley et al. [1], [4] reported that 88 % of the patients with traumatic aortic injuries die within the first hour, and only 2 % survive long enough to develop a chronic aneurysm. The classification of traumatic aortic injury is depicted in Fig. 5.4. The classification is based on imaging and pathology evaluation as depicted in Fig. 5.5, [5]. These injuries are often result of transection of the descending thoracic aorta at the level of the ligamentum arteriosum, a point of fixation of the mobile aortic arch, but can also occur in the distal thoracic or abdominal aorta (Fig. 5.6). The mechanism of injury involves a combination of increased shear stress due to rapid deceleration and acute increases in intraluminal pressure. Little is known about the management and long-term outcomes of chronic traumatic thoracic aortic aneurysms [6, 7].

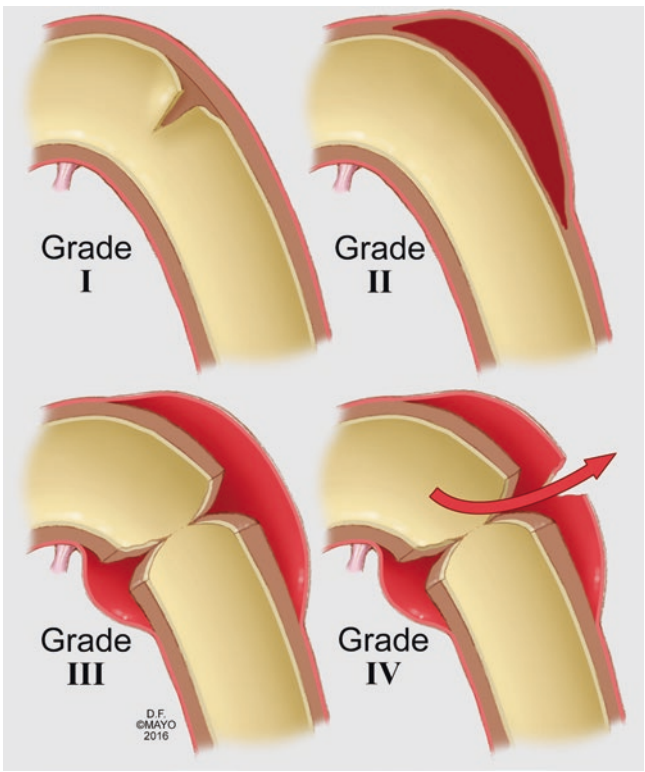


Fig. 5.4 Classification of traumatic aortic blunt injury. By permission of Mayo Foundation for Medical Education and Research. All rights reserved

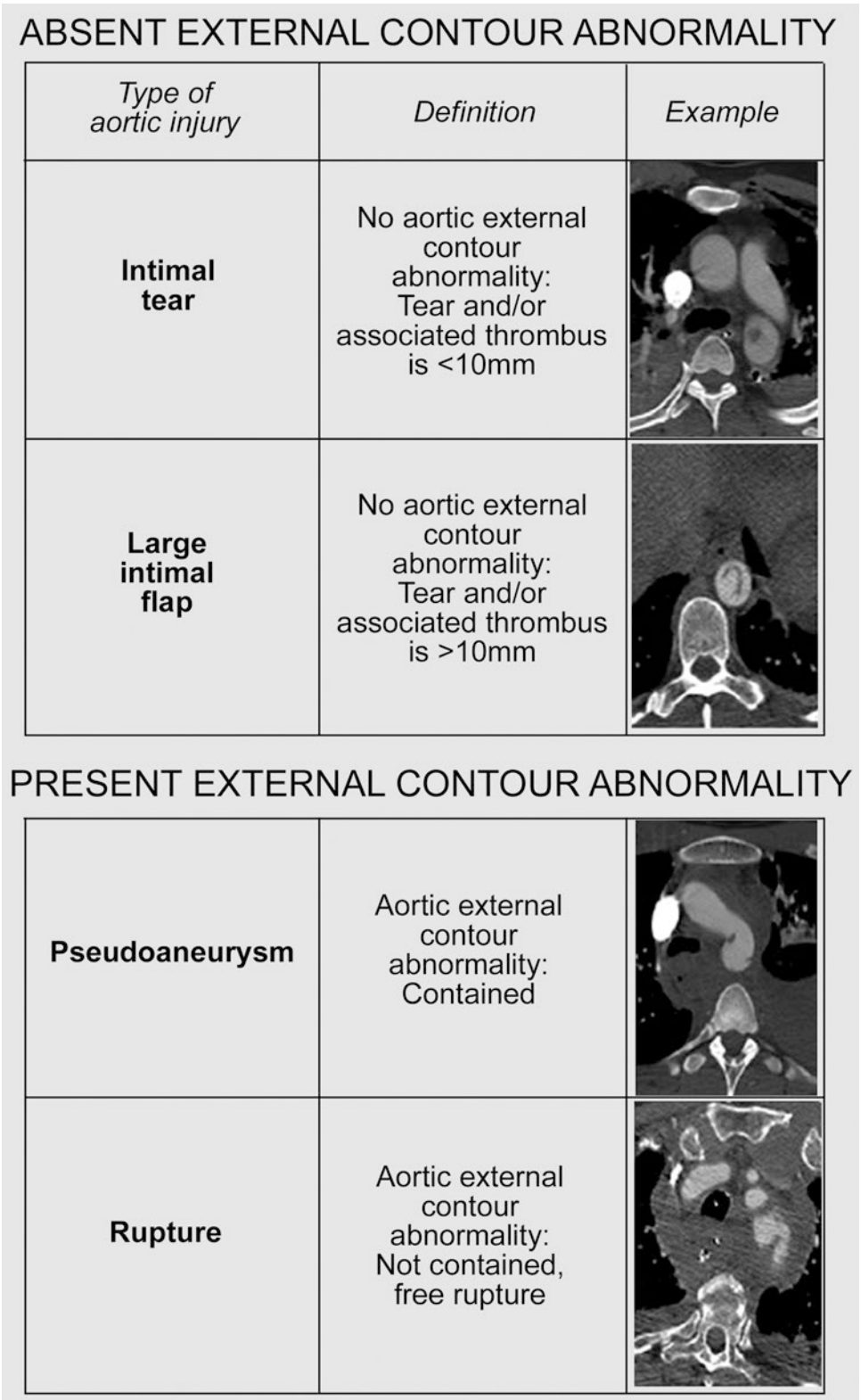


Fig. 5.5 Imaging findings of traumatic aortic blunt injury. Reprinted from Journal of Vascular Surgery, 55(1), Starnes BW, Lundgren RS, Gunn M, Quade S, Hatsukami TS, Tran NT, et al., A new classification scheme for treating blunt aortic injury, 47–54, Copyright 2012, with permission from Elsevier

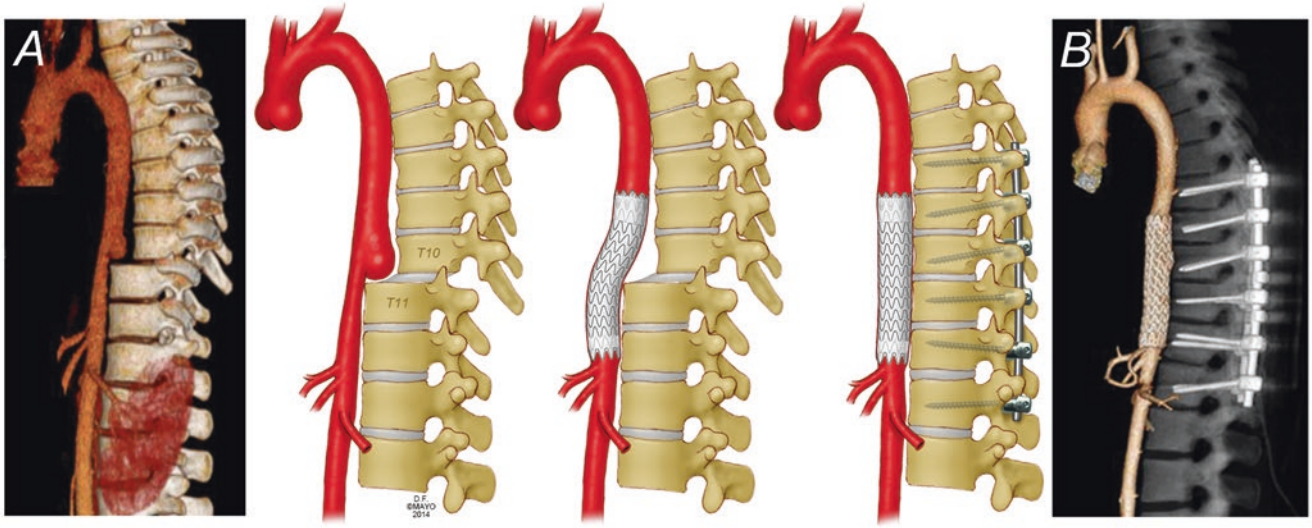


Fig. 5.6 Traumatic blunt aortic injury associated with fracture-dislocation of lower thoracic spine (**a**) was treated by endovascular repair and reduction of dislocation (**b**). By permission of Mayo Foundation for Medical Education and Research. All rights reserved

Classification of Aortic Coarctation

Aortic coarctation is a congenital arch disease that is anatomically described in relationship to the ductus arteriosus (ligamentum arteriosum). The narrowing can be preductal, ductal, or postductal. Most commonly, in adults an aortic coarctation is immediately distal to the atrophied ductus (postductal), but such cases are often associated with a hypoplastic, more proximal aortic arch. Rarely in adults, the arch or the descending aorta is completely interrupted. This defect can occur between the left subclavian artery and descending thoracic aorta (type A), the left subclavian and carotid arteries (type B), or the left carotid and brachiocephalic arteries (type C).

Classification of Aortic Aneurysms

Ascending Aorta and Arch

Aneurysms of the ascending aorta are commonly classified as supracoronary, annuloaortic ectasia (alsoknown as Marfanoid type), and tubular. Arch aneurysms can be isolated or representing proximal extension of a thoracic aortic aneurysm or distal extension of ascending aortic aneurysm (Fig. 5.7).

Descending Thoracic Aneurysms

Thoracic endovascular aortic repair (TEVAR) has become the first treatment option for most aneurysms and for acute type B aortic dissections that are complicated. A classification scheme has been proposed to describe the extent of coverage during repair of descending thoracic aortic (DTA) aneurysms (Fig. 5.8). This classification includes type A DTAs from the left subclavian artery to T6, type B DTAs from T6 to the diaphragmatic hiatus, and type C DTAs from above T6 or the left subclavian artery to the diaphragmatic hiatus.

Thoracoabdominal Aortic Aneurysms

The first report of open surgical repair of a TAAA in the USA was by Etheredge in 1955 [8]. The same year, Charles Rob, an English surgeon, also reported on his experience of 33 abdominal aortic aneurysms, six of which required lower thoracic aortic clamping via thoracoabdominal incision. Cooley and DeBakey's initial report of repair of a descending thoracic aortic aneurysm in 1953 predated Etheredge's report, but there was no direct reconstruction of the visceral arteries [9]. Shortly thereafter, DeBakey reported four cases of TAAA repair using aortic homograft and in a subsequent report in 1965 he included 42 patients treated by knitted Dacron grafts, marking the beginning of a new era of open surgical reconstruction of the thoracoabdominal aorta using prosthetic grafts [10].

Stanley E. Crawford is credited with pioneering techniques of TAAA repair by adding intra-aortic anastomosis after longitudinal division of the sac. The origins of the celiac axis, superior mesenteric artery, and right renal artery were included as a Carrel patch, followed by left renal anastomosis by reim-

plantation or separate graft. In his first report he had a single death among 23 consecutive cases. Along with the utilization of cardiopulmonary bypass and hypothermic circulatory arrest, Crawford's approach most resembles contemporary techniques performed at major centers today.

In 1986, Crawford (Fig. 5.9) described the first TAAA classification scheme based on the anatomic extent of the aneurysm [11]. Extent I involves most of the descending thoracic aorta from above T6 to the level of the renal arteries but not including the infrarenal aorta. Extent II is the most extensive from, starting above T6 in the thoracic aorta and extending distally into the infrarenal aorta or aortic bifurcation. Extent III involves the distal thoracic aorta below T6 with variable distal extension to the renal arteries or beyond. Extent IV TAAA was described above as a more proximal extension of complex abdominal aortic aneurysm above the level of the celiac axis.

Based on this classification, Crawford stratified outcomes for 1509 patients who underwent 1679 TAAA repairs between 1960 and 1991 [12]. The report included 378 Extent I (25 %), 442 Extent II (29 %), 343 Extent III (23 %), and 346 Extent IV (23 %) TAAAs. The 30-day mortality was 8 % and was influenced by age, renal function, concurrent proximal aortic aneurysms, coronary artery disease, chronic lung disease, and total aortic clamp time. Spinal cord injury was noted in 16 % of patients and was associated with clamp time, extent of aorta repaired, rupture, age, and history of chronic kidney disease [12].

Hazin Safi reported a modification of the Crawford classification (Fig. 5.10) to describe the distal aortic involvement of Extent III TAAAs. In his classification, Extent I, II, and IV remain unchanged. A fifth type was added to describe disease starting below T6 and extending up to the renal arteries but not beyond [13].

Abdominal Aortic Aneurysms

Approximately 80 % of the aortic aneurysms are located in the abdominal aorta. Of these, the majority of aneurysms are infrarenal, which imply treatment by open repair using infrarenal clamp and reconstruction or endovascular repair with infrarenal fixation and a minimum aortic neck of 10 mm in length. Aneurysms that do not meet the criteria of infrarenal fixation and require incorporation of at least one of the renal arteries are termed complex abdominal aortic aneurysms. The anatomic classification (Fig. 5.11) of complex abdominal aortic aneurysms includes short-neck infrarenal (<10 and >4 mm infrarenal neck), juxtarenal aneurysms (0–4 mm infrarenal neck), and suprarenal aneurysms. The latter group is subdivided into pararenal aneurysms, which involve at least one renal artery and extend up to superior mesenteric artery (SMA) and paravisceral aneurysms, which involve the renal arteries and the SMA but extend not beyond the celiac axis. A type IV TAAA represents cranial extension of aortic aneurysm above the celiac axis and into the diaphragmatic hiatus. This anatomical classification has been widely utilized in reports dealing with open conventional repair with reasonably good correlation between location of the healthy aorta and extent of open surgical reconstruction (Fig. 5.12).

Iliac Artery Aneurysms

Iliac aneurysms have been previously classified as (a) isolated unilateral, (b) isolated bilateral, and (c) aortoiliac aneurysm. The latter group (c) represents the majority of the iliac aneurysms [14]. A more contemporary classification has taken into account endovascular alternatives and divided iliac aneurysms into one of the five broad categories based on feasibility of endovascular or open treatment (Fig. 5.13) [15].

In this classification, patients with isolated CIA aneurysms who have adequate proximal and distal landing zones within the CIA are classified as type A. A minimum landing zone of 10 mm with no thrombus or calcification is considered adequate. Type B aneurysms include those with adequate proximal CIA neck but distal extension into the CIA bifurcation. Patients with adequate proximal neck in the CIA but who have aneurysm extension into the external iliac artery, which is uncommon, are classified as type C. In practical terms, type B and C aneurysms are treated identically in most cases. Type D consists of patients with solitary IIA aneurysms and normal CIA. Finally, patients with either a CIA with an inadequate proximal neck (aneurysm involving CIA ostium or aortic bifurcation), or bilateral CIA aneurysms, or CIA and abdominal aortic aneurysms are classified as type E [15] (see Fig. 5.13).

Classification of Aortic Dissections

Aortic dissection is more common in men (3:1) and is associated with long-standing hypertension, cocaine use, connective tissue disorders (e.g., the Marfan syndrome), and congenital anomalies (e.g., bicuspid aortic valve and aortic coarctation). Other genetic and autoimmune disorders,

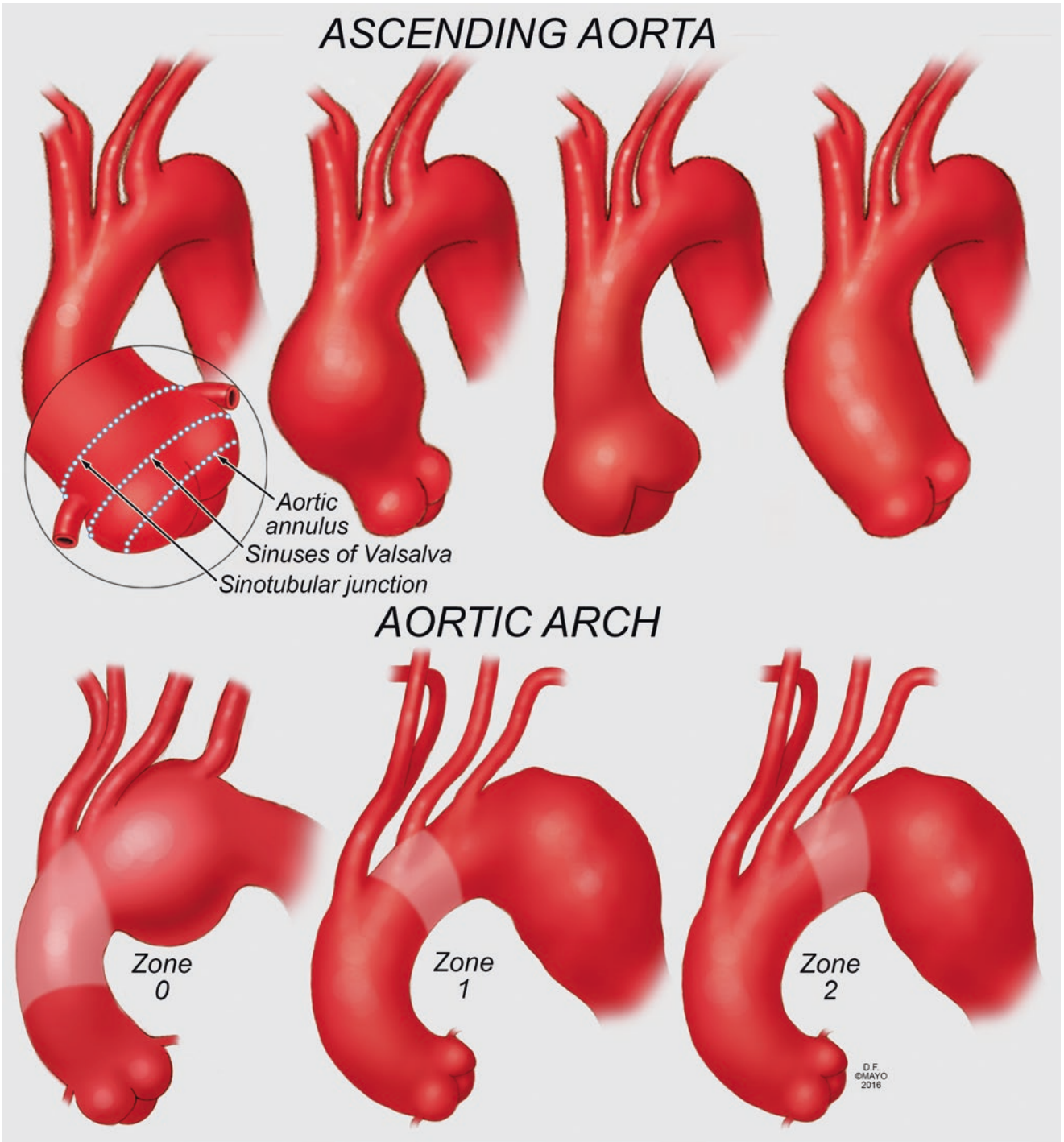


Fig. 5.7 A schematic illustration comparing the normal ascending aorta to three common patterns of ascending aortic aneurysmal disease: supracoronary, annuloaortic ectasia (also known as Marfanoid-type aneurysm), and tubular. Arch aneurysm classification using zones of Ishimura. By permission of Mayo Foundation for Medical Education and Research. All rights reserved

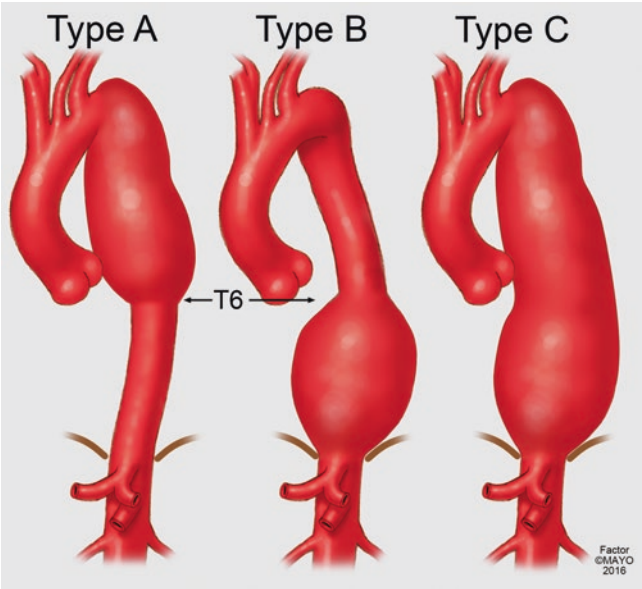


Fig. 5.8 Classification of descending thoracic aortic aneurysm repair using endovascular stent grafts. By permission of Mayo Foundation for Medical Education and Research. All rights reserved

such as Turner's syndrome, Noonan's syndrome, polycystic kidney disease, giant-cell aortitis, systemic lupus, and relapsing polychondritis, are associated with aortic dissection. Iatrogenic aortic dissection can also occur from aortic cross-clamp placement, aortotomy, or endovascular manipulations. Aortic dissections have been classified anatomically with respect to location of entrance site and its distal extension.

DeBakey's Classification

The DeBakey's classification system (Fig. 5.14) published in 1956 provides more detailed description of the distal extension of the dissection with respect to the thoracic and abdominal aorta [16]. The classification includes three types. DeBakey type I dissections originate in the ascending aorta or arch, proximal to the left subclavian artery, with distal extension to the aortic arch and often beyond it distally. These are most often seen in patients less than 65 years of age and represent the most lethal form of the disease. DeBakey type II dissections originate in ascending aorta and are confined to the ascending aorta with no involvement of the distal aortic arch or descending thoracic aorta. DeBakey type III dissections originate in descending thoracic aorta, and are further subdivided into IIIa (distal extension to the diaphragmatic hiatus) or IIIb (distal extension into the abdomen or iliacs).

Stanford Classification

The *Stanford classification* was introduced 1 year after DeBakey classification and is divided into two groups, A and B, depending on whether the ascending aorta is involved (Fig. 5.15) [17]. Stanford type A involves the ascending aorta and/or the aortic arch, with or without distal extension to the descending thoracic aorta and beyond. The tear can originate in the ascending aorta, the aortic arch, or, more rarely, the descending aorta with retrograde extension. A Stanford type B dissection involves the descending thoracic aorta or the arch (distal to the left subclavian artery), without involvement of the ascending aorta.

Aortic Arch Dissections

Involvement of the aortic arch by dissection is further classified based on the location of the entry intimal tear either proximal or distal to the innominate artery. Tears in the aortic arch can be classified into five groups (Fig. 5.16). Class I tears (10 %) are located just above the aortic root and cause the classic two lumen dissection with a flap or septum in between. Class II tears are those with intramural hematoma not identifiable on CTA because of the clot and always seen at the time of the operation. Class III tears are rare localized intimal tears, most commonly in the ascending aorta in patients with Marfan's syndrome that do not cause dissection. Class IV tears are associated with penetrating ulcers. It is not infrequent to see associated calcifications or atheromatous ulcer. The dissection plan penetrates into the medial layer and causes an intramural hematoma. Class V tears are those associated with iatrogenic maneuvers such as cardiac catheterization and aortic stenting.

Endovascular Classification Schemes

Endovascular classification schemes have been based largely on the location of the landing zone, anatomical configuration, or extent of reconstruction, which is based on the number of vessels requiring incorporation by fenestrations, branches, or parallel grafts. The extent of endovascular repair does not always correlate with the proposed anatomical classifications that are used for open surgical repair. For example, a paravisceral aortic aneurysm that can be treated using a transabdominal approach with clamping above the SMA may require four fenestrations with an extent IV TAAA approach if treated by endovascular means. The Society for Vascular Surgery (SVS) proposed a classification system based on landing zones.

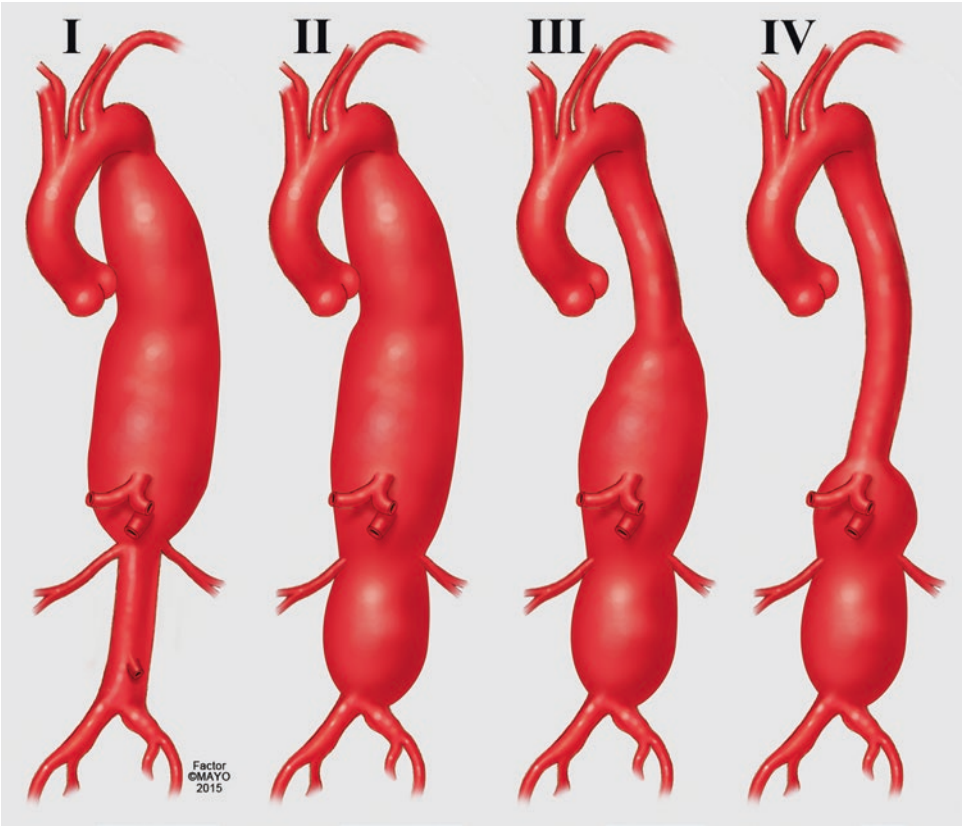


Fig. 5.9 Classification of thoracoabdominal aortic aneurysms proposed by Stanley E. Crawford. By permission of Mayo Foundation for Medical Education and Research. All rights reserved

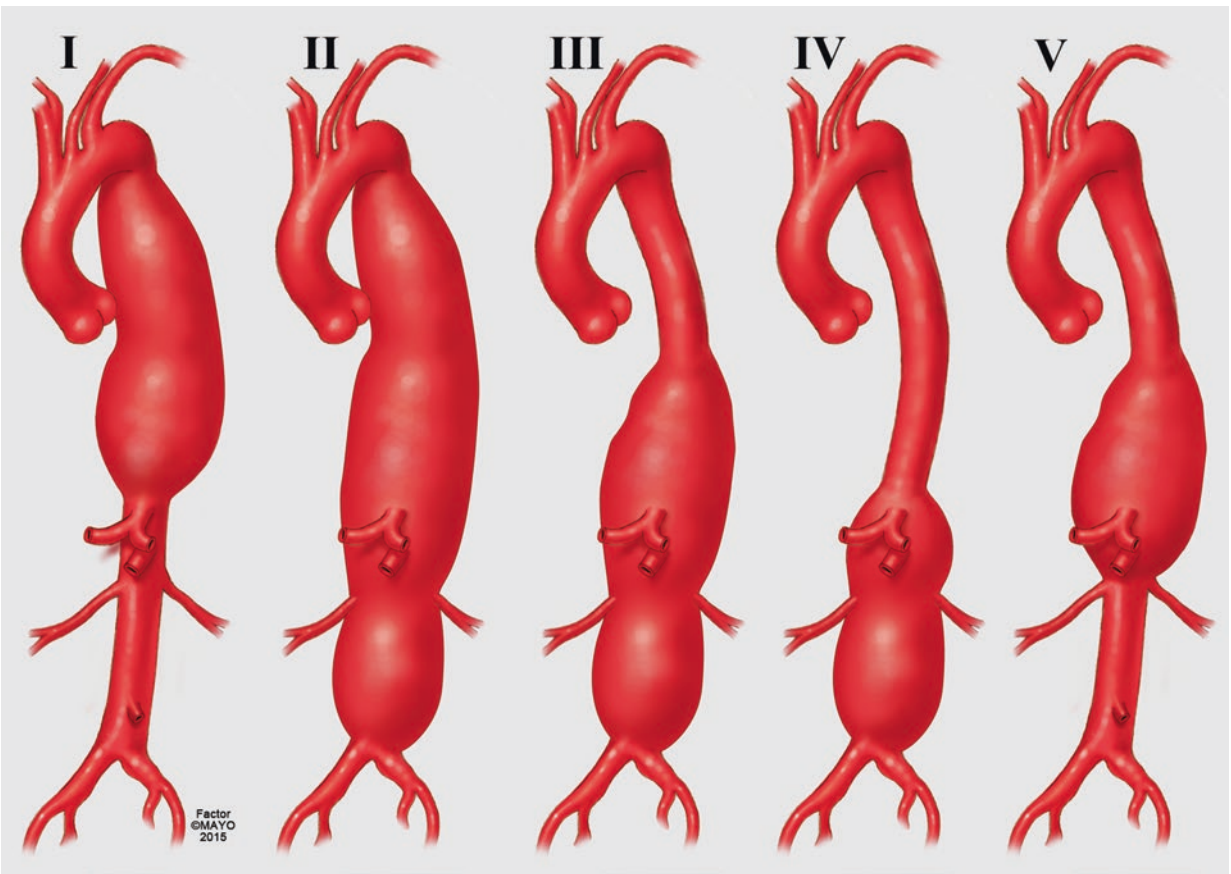


Fig. 5.10 Classification of thoracoabdominal aortic aneurysms proposed by Hazin Safi. By permission of Mayo Foundation for Medical Education and Research. All rights reserved

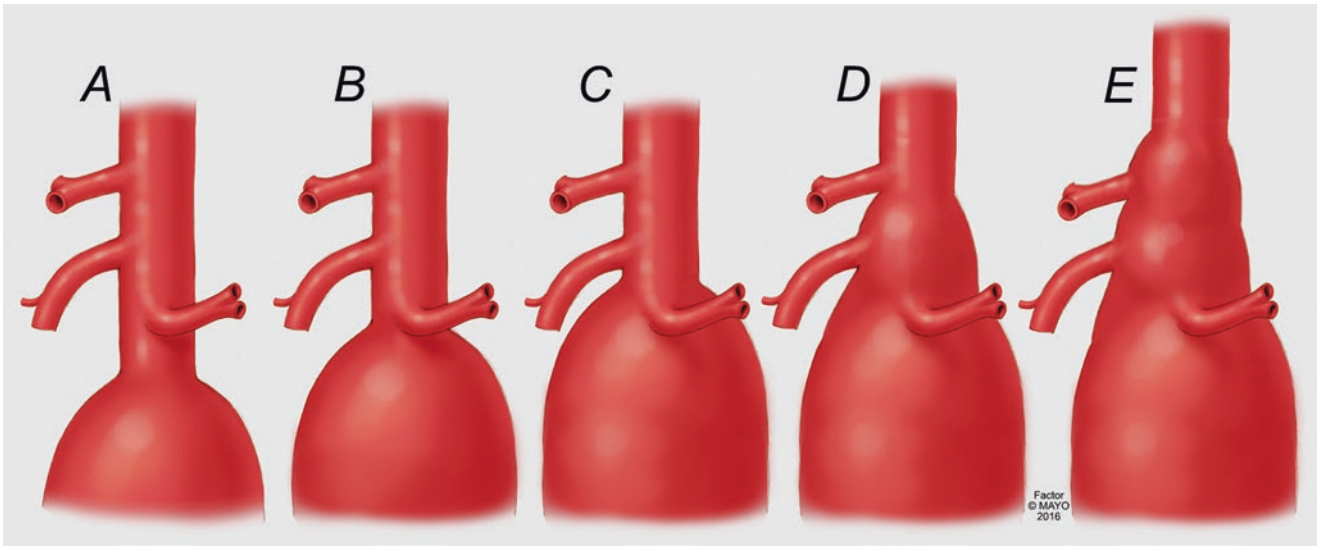


Fig. 5.11 Anatomical classification of complex abdominal aortic aneurysms includes short neck infrarenal (**a**), juxta-renal (**b**), pararenal (**c**), paravisceral (**d**), and type IV TAAA (**e**). By permission of Mayo Foundation for Medical Education and Research. All rights reserved

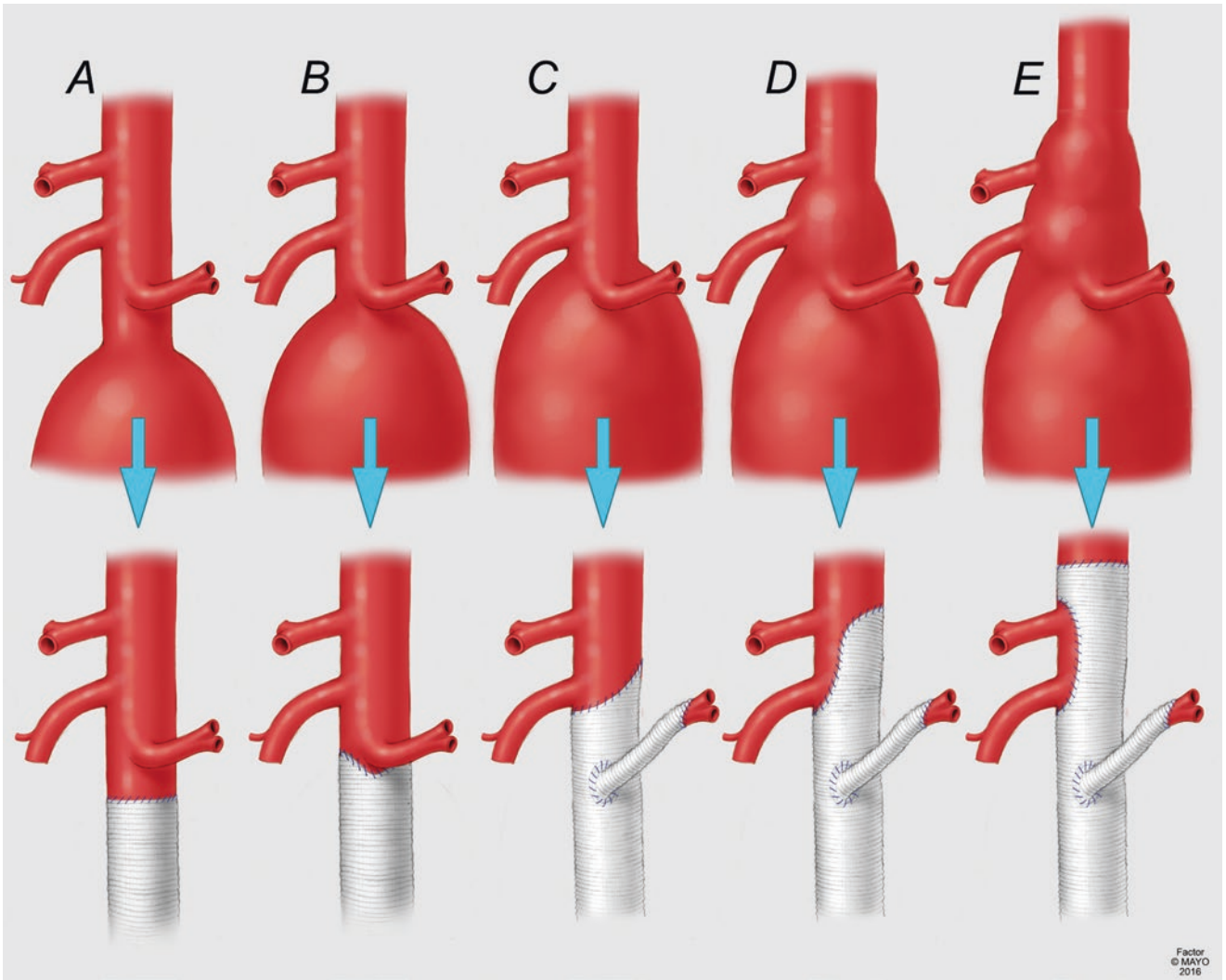


Fig. 5.12 Correlation of complexity of open repair of complex abdominal aortic aneurysms for short neck infrarenal (**a**), juxtarenal (**b**), pararenal (**c**), paravisceral (**d**), and type IV TAAA (**e**). By permission of Mayo Foundation for Medical Education and Research. All rights reserved

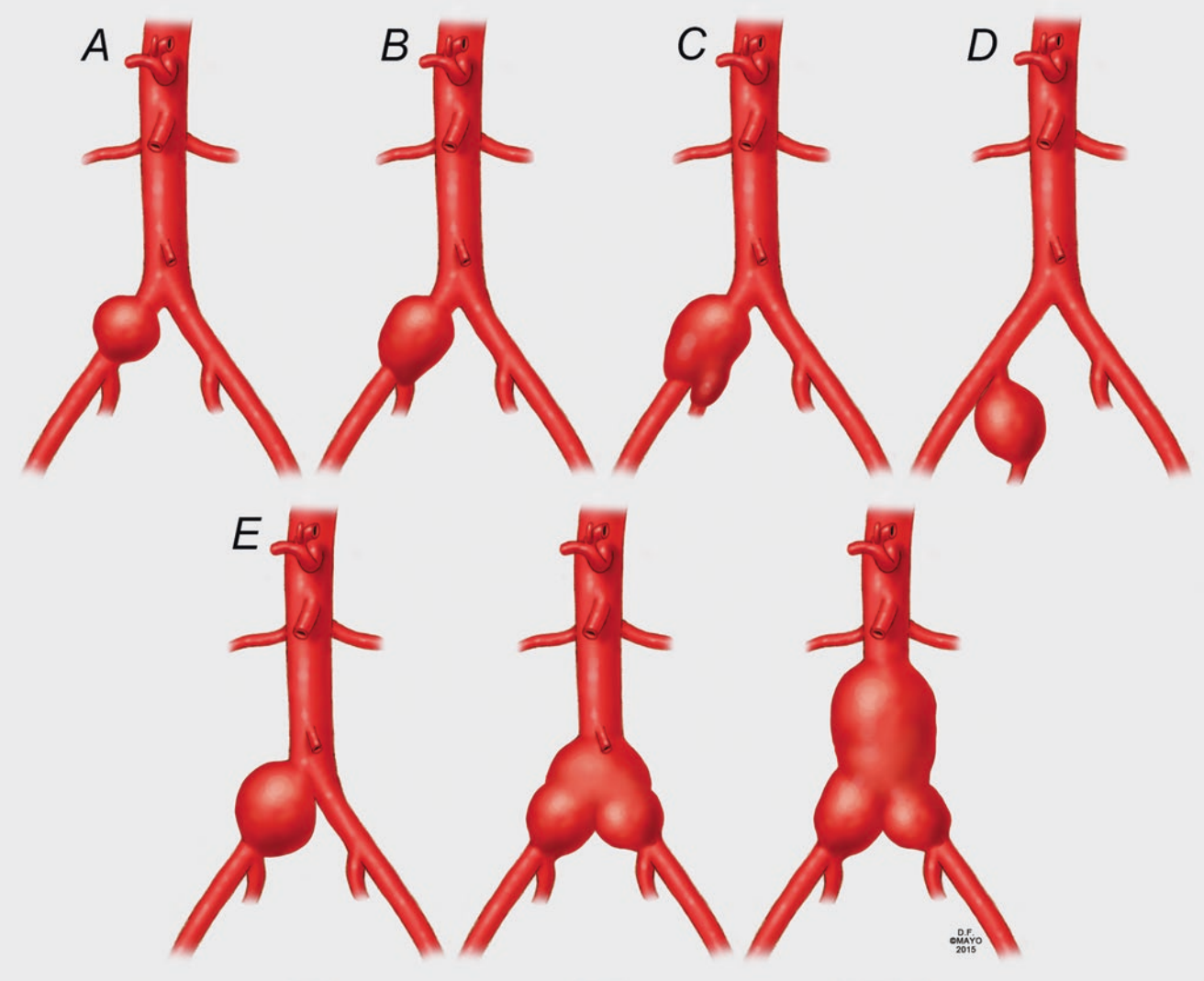


Fig. 5.13 Classification of iliac artery aneurysms (**a**–**e**). By permission of Mayo Foundation for Medical Education and Research. All rights reserved

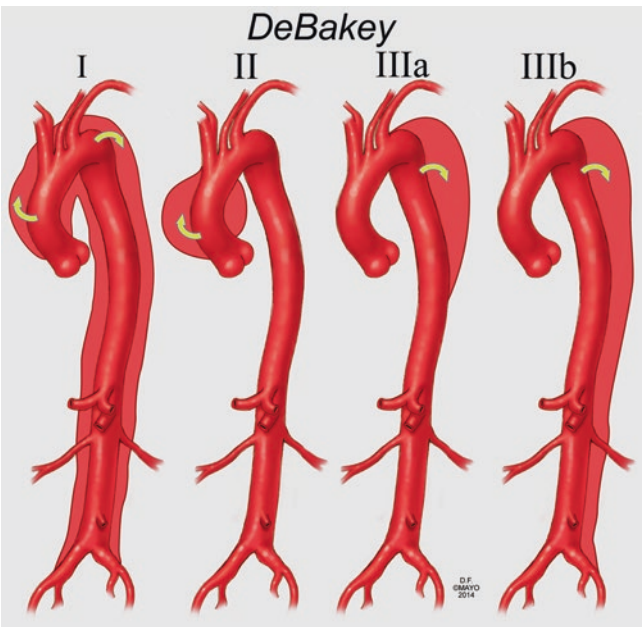


Fig. 5.14 DeBakey classification of aortic dissections. By permission of Mayo Foundation for Medical Education and Research. All rights reserved

Aortic Arch Type

The classification of the types of arch into one of the three types is widely utilized to grade technical difficulties and assist with patient selection for procedures requiring arch manipulations (Fig. 5.17). With aging there is migration of the supra-aortic vessels towards the ascending aorta, which leads to increasing angulation in the aortic arch. The classification scheme uses imaginary lines traced in the outer and inner curvature of the aortic arch. Origin of the innominate artery above the outer line describes a type I arch, where the vessels are centered in the dome or top of the aortic arch, which is commonly seen in the younger individual. Origin of the innominate artery between the upper (outer curvature) and lower (inner curvature) line describes a type II aortic arch, which is the most common type among patients with aortic aneurysms. Further proximal migration of the innominate artery with origin proximal to the lower line (inner curvature) defines a type III aortic arch, which increases technical difficulty for selective catheterization of the supra-aortic trunks, particularly the innominate artery.

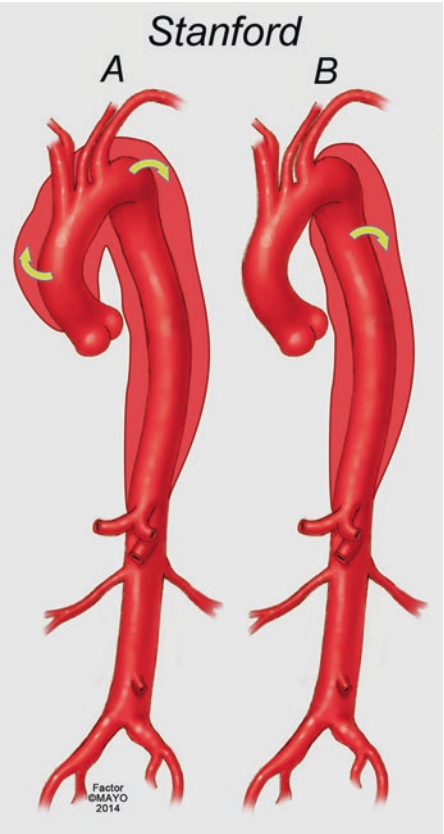


Fig. 5.15 Stanford classification of aortic dissections. By permission of Mayo Foundation for Medical Education and Research. All rights reserved

Ishimura Zones of Implantation

A classification system proposed by Ishimura describes the zones of implantation within the aortic arch based on location of normal aortic segment relative to the supra-aortic trunks (Fig. 5.18) [14, 15, 18, 19]. Ideally, segments of normal aorta are selected for placement of endografts with minimum of 2.0 cm length of "normal" parallel aortic wall without excessive thrombus or atherosclerotic debris. Inadequate landing zones are the single most frequent cause of persistent endoleaks leading to sac growth or rupture. Selection of the landing zone in relationship with the aortic curvature is important to anticipate problems related to lack of apposition of the stent-graft and inner aortic curvature.

The Ishimura classification includes four aortic arch zones, which have been incorporated in the SVS reporting standards classification previously described. Zone 0 extends from the sino-tubular junction to distal to the innominate artery or a bovine trunk. Zone 1 extends from the innominate artery to distal to the left carotid artery. Zone 2 extends from distal to the left common carotid artery to distal to the left subclavian artery. Zone 3 extends from distal to the left subclavian artery to the most proximal curvature of the descending thoracic aorta, typically 2–4 cm distal to the left subclavian artery. Zone 4 involves most of the descending thoracic aorta.

In practical terms, novel designs of arch branch endografts are placed either proximal or distal to the innominate artery, as there is rarely enough length between the left common carotid artery and the innominate artery in Zone 1. A simplified classification proposed by Oderich divides the arch into two zones: *proximal arch*, which includes the ascending aorta and innominate artery and distal arch, which implies placement of endografts distal to the innominate artery (Fig. 5.19) and *distal arch*, which involve placement of the endograft most often into zone 2 or rarely in zone 1. This classification facilitates greatly the comparison with hybrid techniques, which require median sternotomy for proximal arch or only cervical approach for distal arch lesions.

Society for Vascular Surgery Zones of Implantation

The reporting standards for endovascular repair of abdominal and thoracic aortic aneurysms proposed a standardized classification system based on the location of the proximal landing zone (Fig. 5.20). In essence, this classification extends the zones of Ishimura into the thoracic and abdominal aorta. The proximal attachment zones (0–4) have already been described. Zone 4, or the transition zone, implies placement of the endograft at least 2 cm distal to the left subclavian artery extending distally up to T6. Zone 5 starts in the distal half of the descending thoracic aorta beyond T6 and extends to proximal edge of the celiac artery origin. Zone 6 extends from the proximal edge of the celiac origin to the proximal edge of the superior mesenteric artery (SMA). Zone 7 extends from the proximal edge of the highest renal artery. Zone 8 extends from the proximal edge of the highest renal artery to the distal edge of the lowest renal artery. Zone 9 involves the entire infrarenal aorta from the distal edge of the lowest renal artery to the aortic bifurcation. The distal attachment zones are usually located in Zone 9 for distal extension of TAAAs or in the iliac arteries. Zone 10 extends from the aortic bifurcation to the common iliac artery bifurcation. Zone 11 implies placement of the endograft into the external iliac artery, covering the origin of the internal iliac artery [20].

Mayo Clinic Endovascular Complex Abdominal Aneurysm Classification

The correlation between an anatomical and endovascular classification was studied in 490 patients treated for complex abdominal aortic aneurysms at the Mayo Clinic between 2000 and 2010. Because of the wide variation in

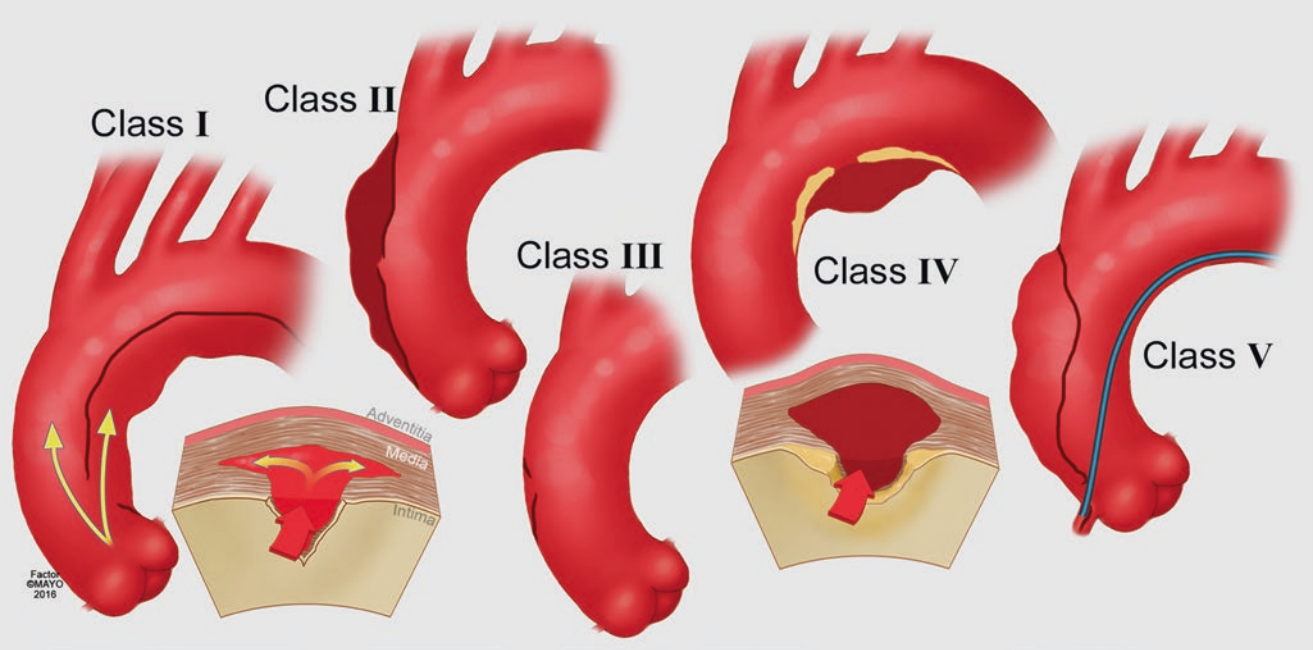


Fig. 5.16 Classification of aortic arch dissections. By permission of Mayo Foundation for Medical Education and Research. All rights reserved

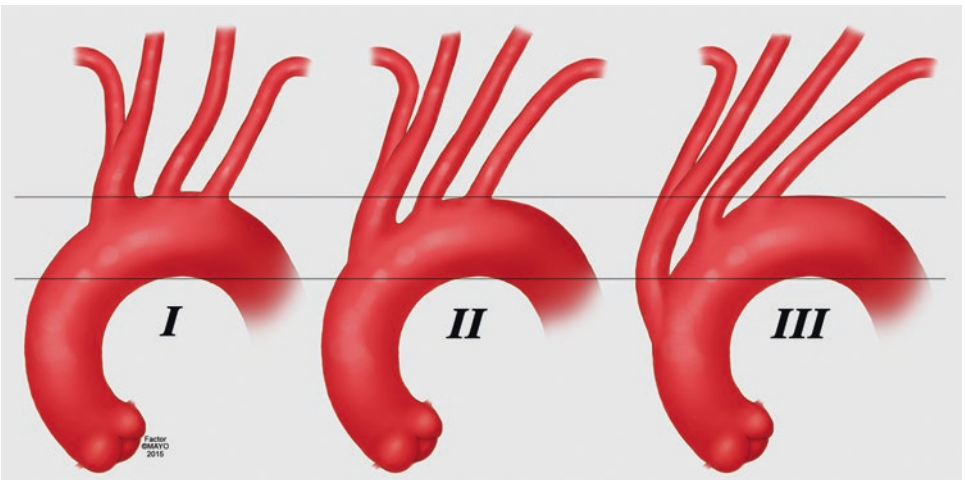


Fig. 5.17 Classification of aortic arch types. By permission of Mayo Foundation for Medical Education and Research. All rights reserved

open surgical techniques and potential discrepancy between the extent of open repair and the number of vessels that need incorporation by endovascular repair, this classification was devised as a means to standardize reporting of fenestrated and branched endografts. For example, a juxtarenal aortic aneurysm (Fig. 5.21) can be repaired with one, two, three, or even four fenestrations depending on relative length of the landing zone in relation to the origins of all four renal-mesenteric arteries. In general, the anatomical extent of aortic disease based on location of healthy aortic segment has linear correlation with the number of vessels requiring incorporation (Fig. 5.22). Therefore, for a juxtarenal aneurysm, most repairs would be done using an infrarenal or juxtarenal surgical graft (with "fish-mouth" anastomosis) and two renal fenestrations and an SMA scallop, whereas for a type IV TAAA the standard endovascular repair would be a four-vessel design (Fig. 5.23). An endovascular classification was proposed based on the minimum number of vessels requiring incorporation by fenestrations and/or branches (Fig. 5.24) assuming a proximal landing

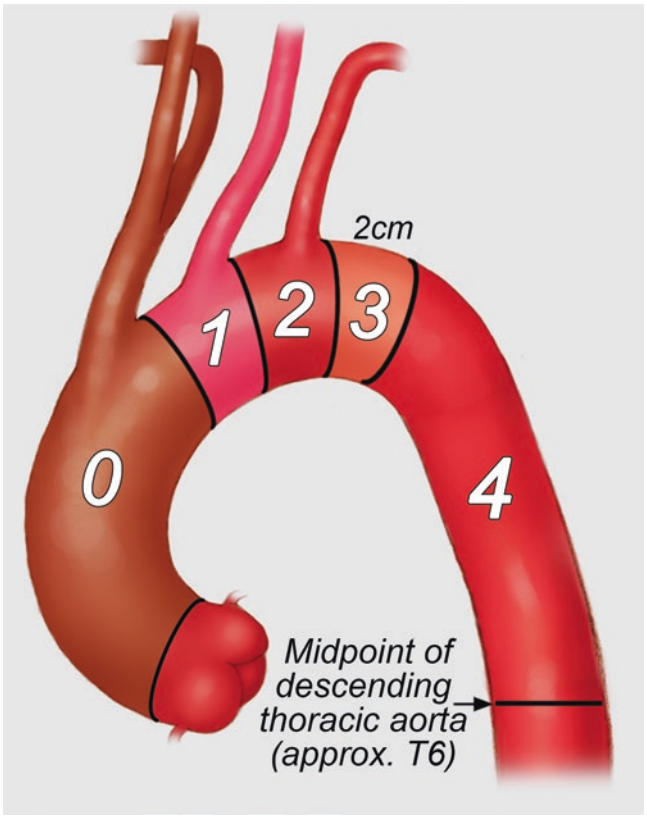


Fig. 5.18 Classification of zones of implantation in the aortic arch. By permission of Mayo Foundation for Medical Education and Research. All rights reserved

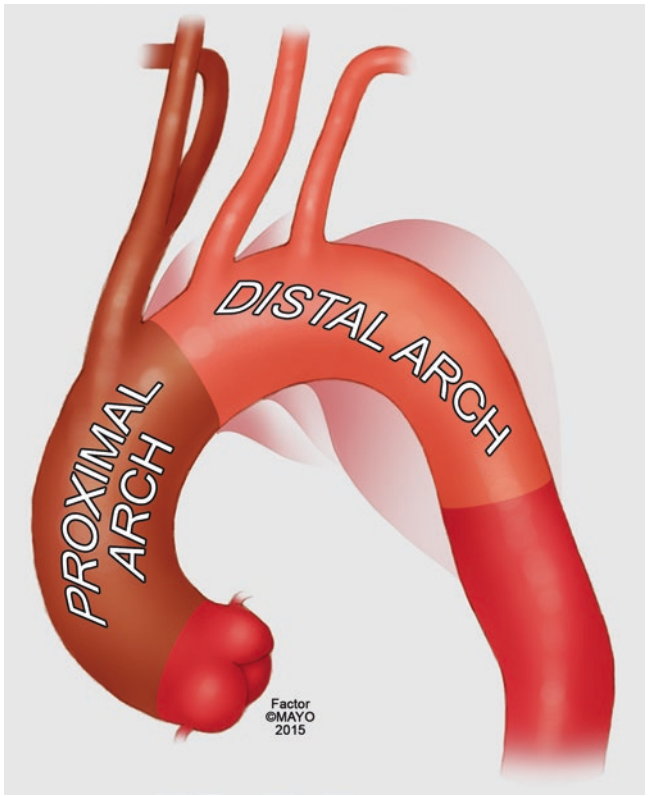


Fig. 5.19 Simplified classification of zones of implantation in the aortic arch. By permission of Mayo Foundation for Medical Education and Research. All rights reserved

zone of >2 cm based on healthy aortic segment with parallel aortic wall. A type I endovascular repair would imply one renal fenestration with or without one scallop to the contralateral renal artery or SMA. This design is rarely utilized in current practices. A type II repair included two fenestrations with or without a scallop. A type III repair implies three fenestrations with or without a scallop and a type IV repair four or more fenestrations or branches. The highest variation in the extent of endovascular repair was observed for suprarenal aneurysms.

Mayo Clinic Supra-celiac Coverage Classification

Banga and associates presented at the 2015 European Vascular Meeting a new classification concept to analyze outcomes of fenestrated and branched endografts based on supra-celiac sealing zones. A 4 cm line (equivalent to two sealing stents) was used above the upper aspect of the celiac artery origin to define high supra-celiac coverage (Fig. 5.25). Infra-celiac coverage designs include two or three fenestrations (Fig. 5.26), whereas supra-celiac coverage implies use of four fenestrations, branches, or combinations of fenestrations and branches.

Conclusion

Endovascular repair has gained widespread acceptance. Novel techniques and results continued to be compared to open surgical repair. It is critical that standardized classification systems are used to allow meaningful comparison of results with both modalities.

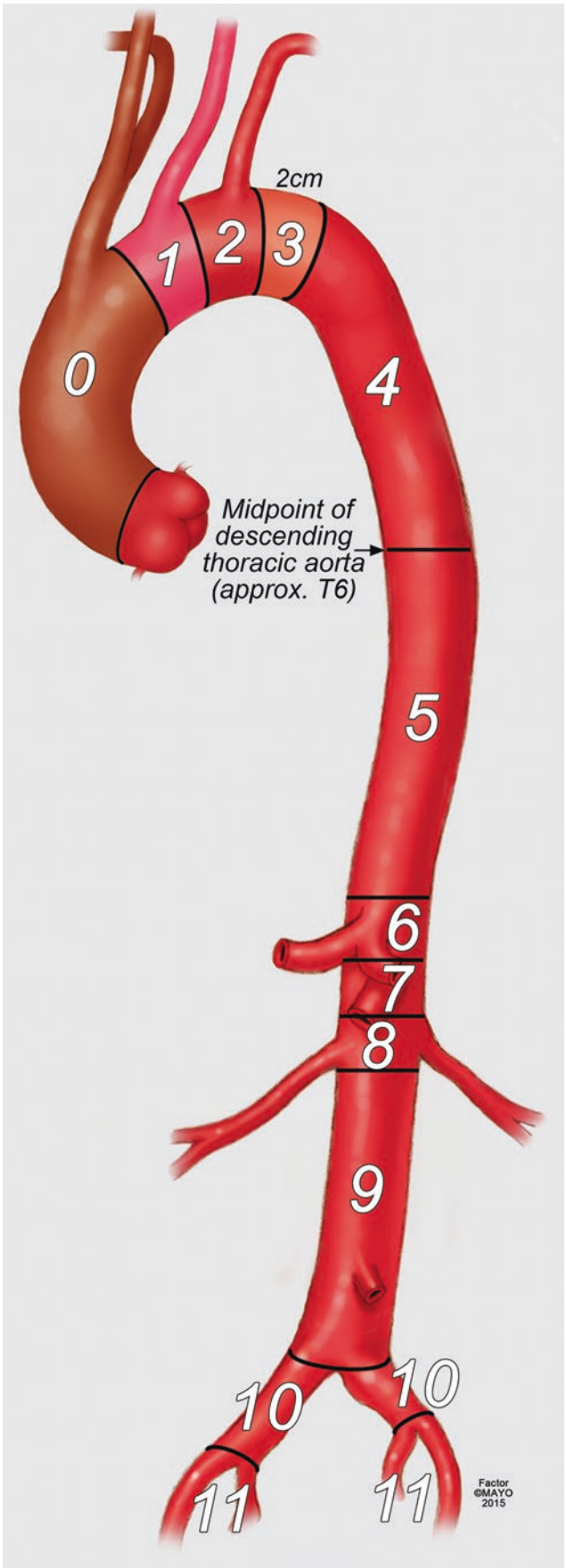


Fig. 5.20 Society for vascular surgery classification of zones of implantation. By permission of Mayo Foundation for Medical Education and Research. All rights reserved

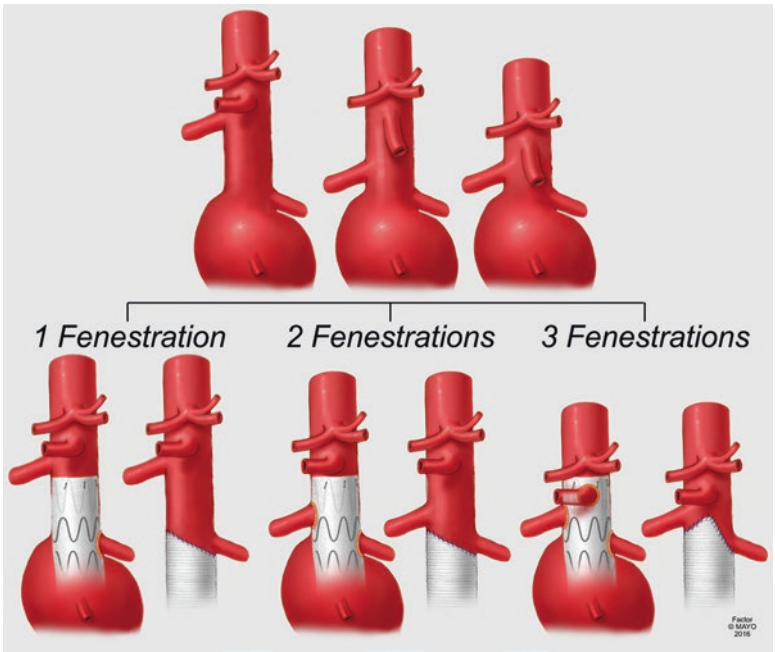


Fig. 5.21 Variations of stent-graft design and open repair options for juxtarenal aortic aneurysms. By permission of Mayo Foundation for Medical Education and Research. All rights reserved

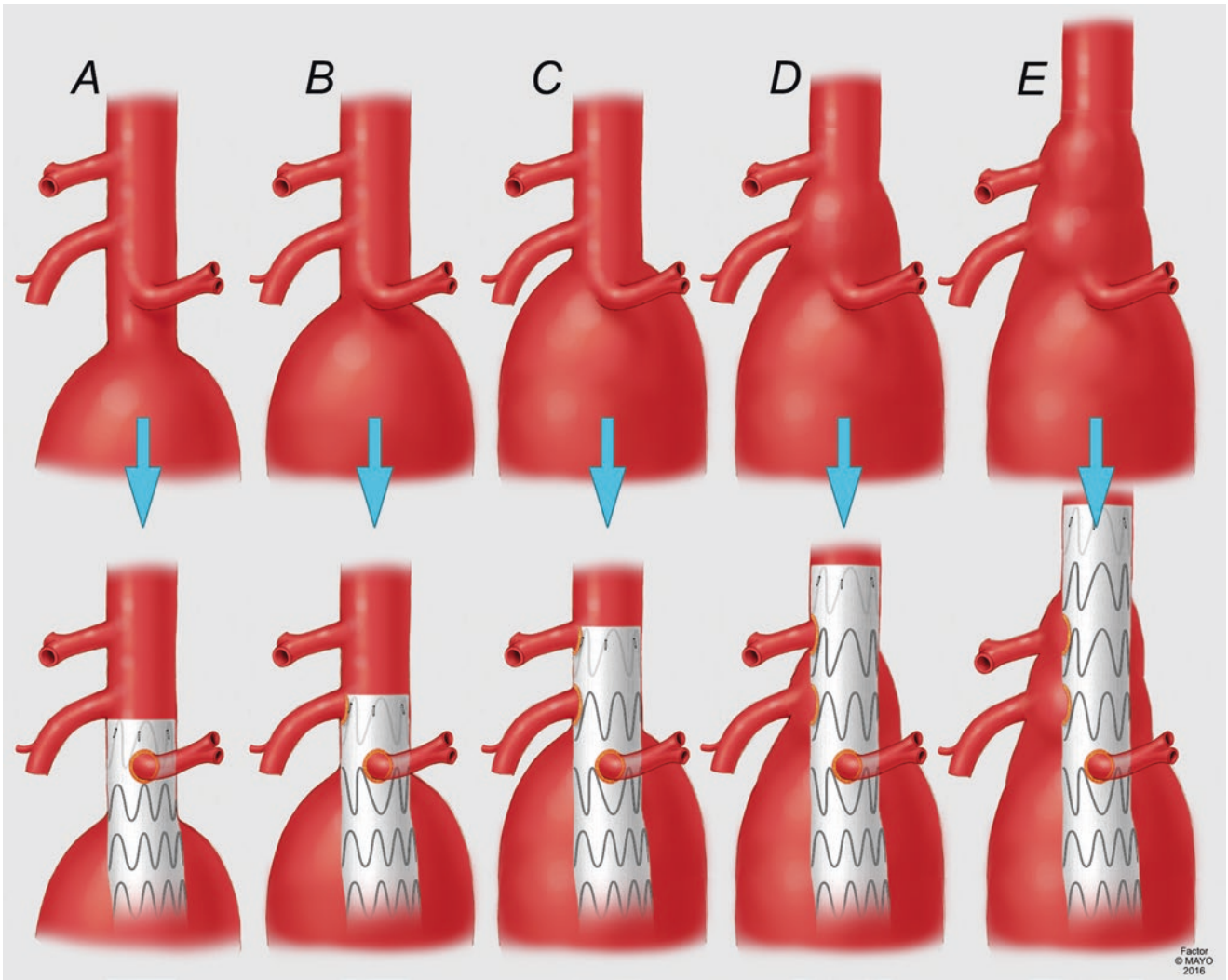


Fig. 5.22 Correlation of complexity of endovascular repair of complex abdominal aortic aneurysms for short-neck infrarenal (**a**), juxtarenal (**b**), pararenal (**c**), paravisceral (**d**), and type IV TAAA (**e**). By permission of Mayo Foundation for Medical Education and Research. All rights reserved

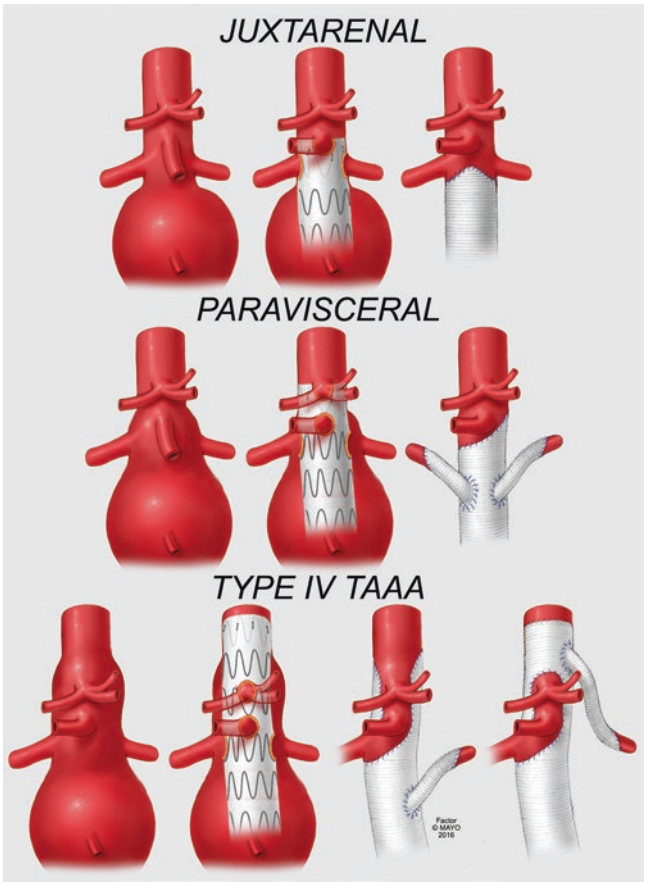


Fig. 5.23 Most common types of endovascular and open repair configuration for juxtarenal, paravisceral, and type IV TAAAs. By permission of Mayo Foundation for Medical Education and Research. All rights reserved

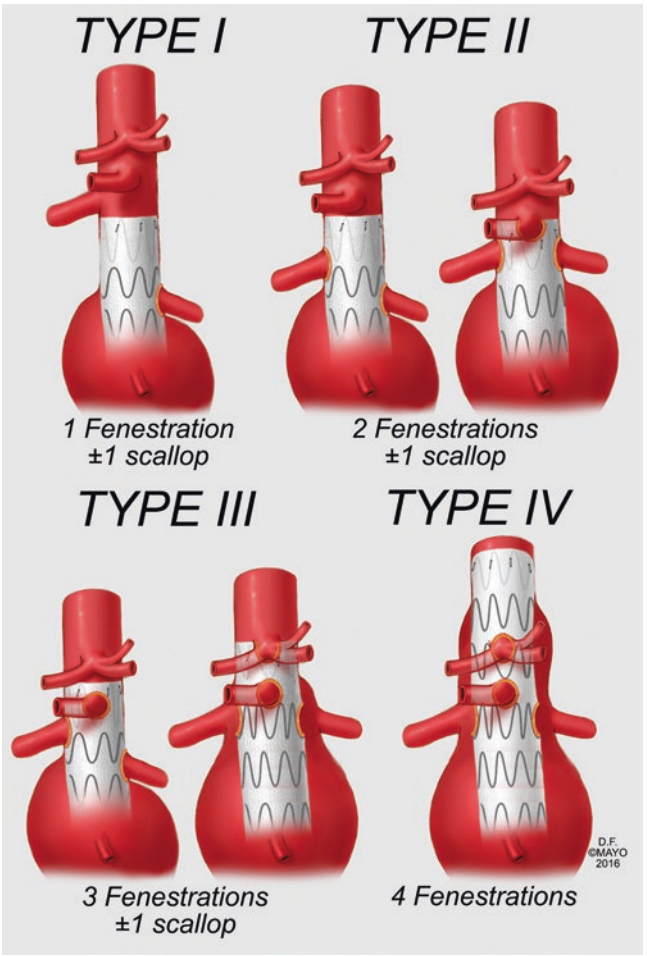


Fig. 5.24 Mayo Clinic endovascular classification of fenestrated and branched repair of complex abdominal aortic aneurysms. By permission of Mayo Foundation for Medical Education and Research. All rights reserved

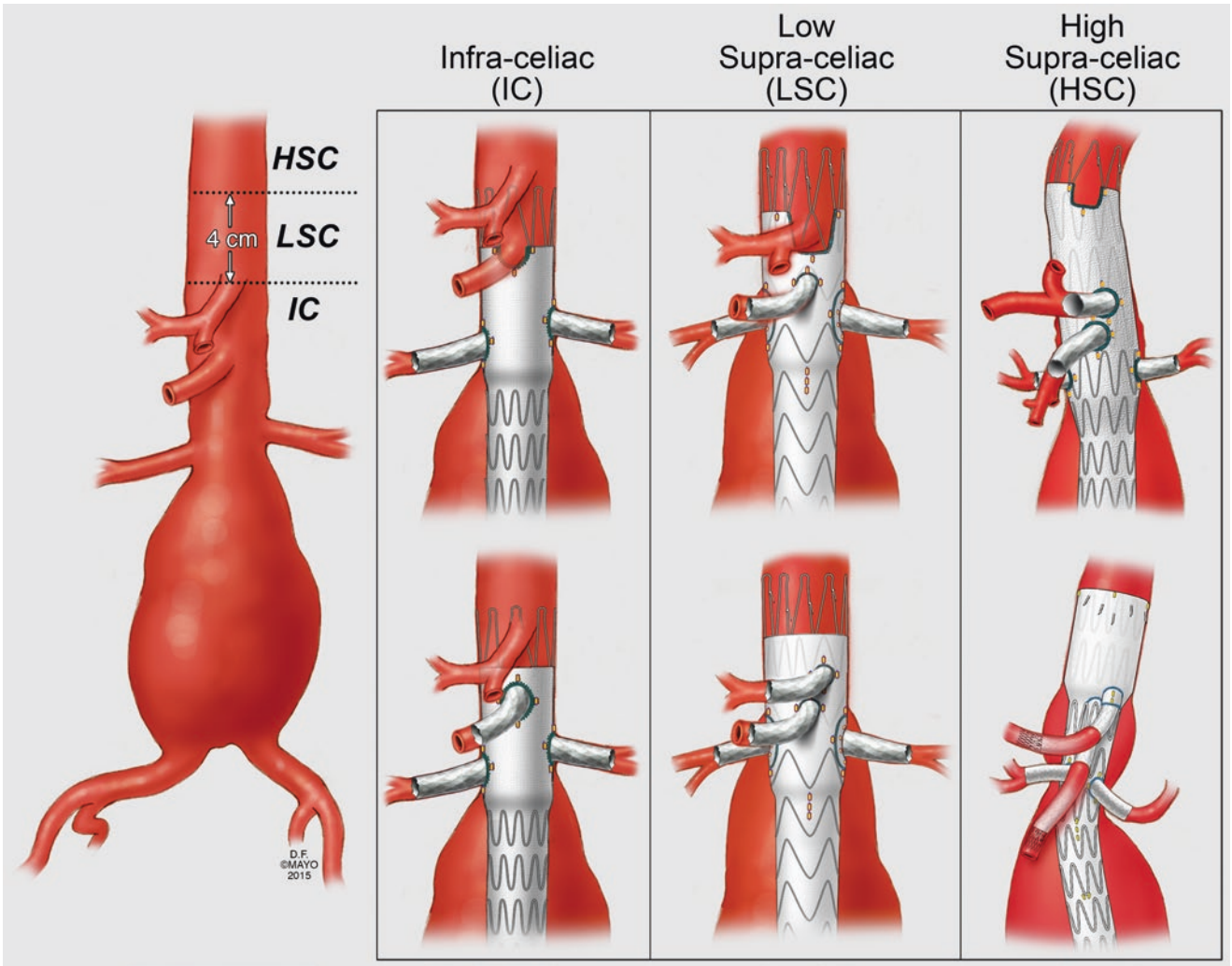


Fig. 5.25 Mayo Clinic endovascular classification of supra-celiac sealing zones for fenestrated and branched endografts. By permission of Mayo Foundation for Medical Education and Research. All rights reserved

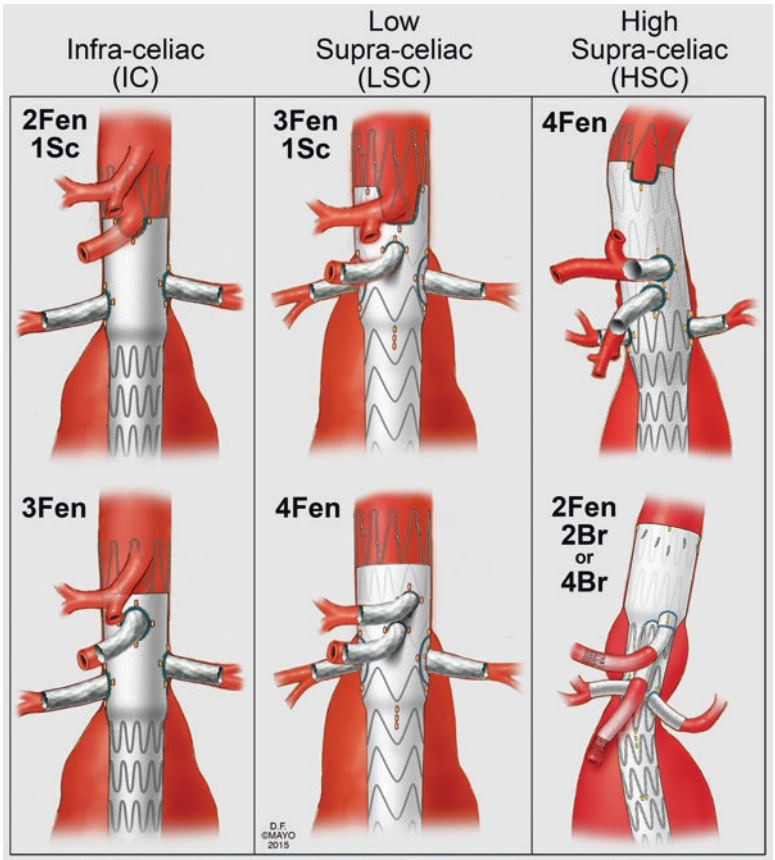


Fig. 5.26 Mayo Clinic endovascular coverage classification based on anatomical location of the aneurysm. By permission of Mayo Foundation for Medical Education and Research. All rights reserved

References

1. Sveinsson M, Sobocinski J, Resch T, Sonesson B, Dias N, Haulon S, et al. Early versus late experience in fenestrated endovascular repair for abdominal aortic aneurysm. J Vasc Surg. 2015;61(4):895–901. doi:10.1016/j.jvs.2014.11.007. Epub 2015 Jan 13.
2. Mendes BC, Oderich GS, Macedo TA, Pereira AA, Cha S, Duncan AA, et al. Anatomic feasibility of off-the-shelf fenestrated stent grafts to treat juxtarenal and pararenal abdominal aortic aneurysms. J Vasc Surg. 2014;60(4):839–47, discussion 847–8.
3. Zarins CK, Glagov S. Artery wall pathology in atherosclerosis. In: Rutherford RB, editor. Vascular surgery, vol. 1. 5th ed. Philadelphia: WB Saunders; 2000. p. 313–33.
4. Parmley LF, Mattingly TW, Manion WC, Jahnke Jr EJ. Nonpenetrating traumatic injury of the aorta. Circulation. 1958;17:1086–101.
5. Starnes BW, Lundgren RS, Gunn M, Quade S, Hatsukami TS, Tran NT, et al. A new classification scheme for treating blunt aortic injury. J Vasc Surg. 2012;55(1):47–54.
6. Szostek MM, Jakuczun W, Alagbari A, Pogorzelski R, Szostek M, Osęka M, et al. Chronic traumatic thoracic aortic aneurysms—results of endovascular treatment. 14-years single centre experience. Int Angiol. 2015;34(6):506–13. Epub 2014 Nov 14.
7. Lee WA, Matsumura JS, Mitchell RS, Farber MA, Greenberg RK, Azizzadeh A, et al. Endovascular repair of traumatic thoracic aortic injury: clinical practice guidelines of the society for vascular surgery. J Vasc Surg. 2011;53(1):187–92.
8. Etheredge SN, Yee J, Smith J, Schonberger S, Goldman MJ. Successful resection of a large aneurysm of the upper abdominal aorta and replacement with homograft. Surgery. 1955;38:1071–81.
9. Cooley DA, De Bakey ME. Surgical consideration of excisional therapy for aortic aneurysms. Surgery. 1953;34(6):1005–20.
10. De Bakey ME, Cooley DA. Treatment of aneurysms of the aorta by resection and restoration of continuity with aortic homograft. Angiology. 1954;5(3):251–4.
11. Crawford ES, Crawford JL, Safi HL, Coselli JS, Hess KR, Brooks B, et al. Thoracoabdominal aortic aneurysms: preoperative and intraoperative factors determining immediate and long term results of operations in 605 patients. J Vasc Surg. 1986;3:389–404.
12. Svensson LG, Crawford ES, Hess KR, Coselli JS, Safi HJ. Experience with 1509 patients undergoing thoracoabdominal aortic operations. J Vasc Surg. 1993;17(2):357–68. Discussion 368–70.
13. Safi HJ, Miller III CC. Spinal cord protection in descending thoracic and thoracoabdominal aortic repair. Ann Thorac Surg. 1999;67(6):1937–9.
14. Huang Y, Gloviczki P, Duncan AA, Kalra M, Hoskin TL, Oderich GS, et al. Common iliac artery aneurysm: expansion rate and results of open surgical and endovascular repair. J Vasc Surg. 2008;47:1203–11.
15. Sandhu R, Pipinos I. Isolated iliac artery aneurysms. Semin Vasc Surg. 2005;18:209–15.
16. DeBakey ME, Henly WS, Cooley DA, Morris Jr GC, Crawford ES, Beall Jr AC. Surgical management of dissection aneurysms of the aorta. J Thorac Surg. 1965;49:130–49.

17. Daily PO, Trueblood HW, Stinson EB, Wuerflein RD, Shumway NE. Management of acute aortic dissections. Ann Thorac Surg. 1970;10(3):237–47.
18. Ishimura S. Endografting of the aortic arch. J Endovasc Ther. 2004;11 Suppl 2:II62.
19. Mitchell RS, Ishimura S, Ehrlich MP, Iwase T, Lauterjung L, Shimono T, et al. First International Summit on Thoracic Aortic Endografting: roundtable on thoracic aortic dissection as an indication for endografting. J Endovasc Ther. 2002;9 Suppl 2:II98.
20. Fillinger MF, Greenberg RK, McKinsey JF, Chaikof EL. Society for Vascular Surgery Ad Hoc Committee on TEVAR Reporting Standards. Reporting standards for thoracic endovascular aortic repair (REVAR). J Vasc Surg. 2010;52(4):1022–38.

Intravascular Ultrasound to Guide Complex Endovascular Aortic Repair

6

David E. Timaran, Martyn Knowles, and Carlos H. Timaran

Introduction

The endovascular treatment of complex aortic lesions requires the use of imaging techniques for operative planning and execution of the procedures. Intravascular ultrasonography (IVUS) allows real-time imaging of the vessel and is ideally suited for aortic interventions [1–5]. IVUS provides accurate imaging to assess access of, location of, and distances between branch vessels; vessel size for endograft sizing; associated lesions; and other pathology, which facilitates complex aortic endovascular procedures. Moreover, the use of IVUS reduces the need of contrast and radiation doses in most procedures, as it replaces angiography in many instances.

The use of IVUS during fenestrated endovascular aortic aneurysm repair (FEVAR) is of particular utility as it provides accurate imaging of the visceral segment of the aorta for the location of target vessels, identification of thrombus or calcification, and aortic sizing. Most importantly, however, IVUS allows fluoroscopic marking of the visceral vessel origins. These saved images can be used as a reference, based on bony landmarks, for the correct deployment of the fenestrated endograft using the graft radiopaque markers. This allows minimal manipulation via torquing or pushing/pulling for successful vessel cannulation and stenting. Pre-cannulation of visceral vessels prior to endograft placement can then be avoided, which could decrease fluoroscopic time, contrast dose, and the possibility of vessel injury.

This chapter describes the use of IVUS for FEVAR, and the shift in technique away from pre-cannulation of vessels with the addition of IVUS, as well as the ability of IVUS to identify the location of visceral vessels and their clock position.

Intravascular Ultrasound

IVUS is a catheter-based imaging modality that provides high-resolution cross-sectional images of vessels, enabling measurements of luminal and vessel diameters and areas. First introduced in 1988, grayscale IVUS has been the mainstay coronary assessment in equivocal lesions for over two decades [6]. Plaque morphology and constituents may be identified and quantified by the amplitude and frequency of reflected ultrasound signals that correspond to normal tissue, fibrosis, calcium, and necrotic core. The axial resolution is 100–200 μm and lateral resolution is 250 μm with frequencies of 20–40 MHz.

IVUS has been primarily used for the quantification of coronary and peripheral lesions and stenosis [1, 7, 8]. IVUS algorithms accurately measure minimum luminal area (MLA), a more accurate dimension than luminal diameter. The main limitation of IVUS is ensuring imaging in a coaxial position. IVUS is an excellent method for determining plaque volume and can be of particular utility in situations in which angiographic imaging is considered unreliable, such as the presence of ostial lesions or segments with multiple overlapping vessels [9]. IVUS may provide an optimal assessment of bifurcation lesions, which are particularly difficult to assess by angiography because side branches frequently obscure the lesion.

D.E. Timaran
Department of Surgery, University of Texas Southwestern Medical Center, 5323 Harry Hynes Blvd, Dallas, TX 75093-9157, USA
e-mail: david.timaran@utsouthwestern.edu

M. Knowles
Department of Surgery, University of North Carolina Rex Hospital, 4414 Lake Boone Trail, Ste.108, Raleigh, NC 27607, USA
e-mail: Martyn.Knowles@unchealth.unc.edu

C.H. Timaran (✉)
Division of Vascular and Endovascular Surgery, Department of Surgery, University of Texas Southwestern Medical Center, 5909 Harry Hines Blvd, Dallas, TX 75390-9157, USA
e-mail: carlos.timaran@utsouthwestern.edu

© Mayo Foundation for Medical Education and Research 2017
G.S. Oderich (ed.), *Endovascular Aortic Repair*, DOI 10.1007/978-3-319-15192-2_6

Aortic IVUS

With the increasing use of endovascular therapies for the treatment of vascular diseases, vascular imaging has become the cornerstone to guide and complete most vascular intervention. IVUS provides real-time imaging during aortic interventions, which is mandatory in the evaluation and treatment of aortic pathologies, including aneurysms, dissection, and penetrating ulcers (PAU) [1]. IVUS allows the anatomic definition of the target vessels and the relationship of branch vessels to the lesion, which are critical in the confirmation of the diagnosis, the endograft selection and successful endovascular treatment. IVUS is particularly helpful in situations in which accurate measurements may be difficult to obtain or unreliable with standard imaging techniques, such as CT or digital subtraction angiography, as it relies on immediate and live image acquisition. Severe tortuosity, angulation, and reverse tapered configurations are anatomic challenges in which IVUS may allow more accurate anatomic determinations, including measurements and target vessel location [1].

IVUS is useful for assessment of access vessels, proximal and distal fixation sites and the accurate vessel sizing for endograft selection during endovascular abdominal aortic aneurysm repair (EVAR) and thoracic endovascular aortic aneurysm repair (TEVAR). Important anatomic structures can be identified and located, including the left subclavian artery for TEVAR and the renal arteries for EVAR. IVUS can then provide imaging data that otherwise could only be obtained with angiography, thereby reducing the radiation dose and contrast load, of particular importance in patients with compromised renal function. Endograft apposition after deployment can also be confirmed with IVUS, although fixation and attachment site endoleaks can only be assessed with angiography. IVUS is indeed of utmost relevance in defining the location and characteristic of true and false lumen as well as entry and reentry sites during the treatment of aortic dissections.

IVUS and Fenestrated EVAR

IVUS to guide FEVAR is usually performed after initial groin access has been obtained. In our practice, we usually use a "preclose" technique with Perclose Proglide (Abbott Vascular, Redwood City, CA) devices. The sheaths are usually upsized to 11 Fr, and a stiff wire is advanced through the planned side for endograft placement. At a minimum, an 8 Fr sheath is necessary to advance the catheter required for aortic IVUS. We usually use the Volcano Visions 8.2 catheter (Volcano, San Diego, Calif.) (Fig. 6.1). The access vessels are interrogated for size, calcification, and pathology (Fig. 6.2). The need for dilators or endovascular/open conduits is then entertained, if applicable at this time. In general, in instances of inadequate access secondary to aortoiliac occlusive disease or small arteries, staged endoconduit creation with iliac stenting is performed to avoid arterial access injury. Such injuries usually occur at the end of the covered stents because of the frailty of the vessels after the "pave and crack" technique. IVUS can assist with the identification of the origin of the hypogastric artery, which should be preserved if patent to maintain this collateral network for spinal cord perfusion. IVUS can also be used to assess the degree of expansion and apposition of the covered stents and the need of additional dilatation. Additional information may be gathered relating to the aorta in the anticipated proximal landing zone, although 3-D reconstructions are particularly good at sizing and diagnosis of pathology. Large differences could influence the need to alter the operative plan, particularly when endograft fixation is located in areas of aortic angulation or tortuosity. This may be of particular utility when there is a need to place a proximal endograft to the fenestrated device, as the latter is either premanufactured or off-the-shelf and cannot be modified in most instances. Sizing the aneurysm itself is usually not feasible as this is generally limited by the parameters of the catheter.

Aortic IVUS for FEVAR primarily focuses on the visceral segment of the aorta (Fig. 6.3). The left renal vein is used for orientation, as long as it is not retroaortic in the preoperative CT angiogram, and the images are rotated to place the left renal vein at 12 o'clock (see Fig. 6.2). The vessels are then individually identified and attention is paid to identifying any potential pathology such as calcification, ostial stenosis, and proximity of the stiff wire to the visceral vessels. Each vessel ostium is then identified on IVUS and the IVUS tip is marked fluoroscopically. In this manner, each vessel is marked in fluoroscopic single shots, labeled, and saved by the radiology technician, including the celiac axis (see Fig. 6.3), superior mesenteric artery (Fig. 6.4), and left (Fig. 6.5) and right renal arteries (Fig. 6.6). Further reference to these vessels can then be accomplished using bony landmarks of the vertebrae, ribs, surgical clips, or other identifying features.

Importantly, prior to IVUS labeling of the target vessels with fluoroscopy, centering of the image on the visceral aorta and the removal of all cranio-caudal and lateral orientation is prudent. 3-D CT angiography reconstructions and other 3-D roadmapping techniques based on integration of preoperative CT angiograms, such as overlay or fusion, may assist further regarding visceral vessel location with reference to bony landmarks. Moreover, manual manipulation of the fusion and overlay images may enhance the accuracy of



Fig. 6.1 Hybrid endovascular room with fixed imaging unit and either a fixed or mobile aortic intravascular ultrasound (IVUS) systems. The Volcano IVUS catheter IVUS aortic catheter is 9 Fr 0.035 in. guide wire compatible with 90 cm working length, over-the-wire design, and maximum imaging diameter of 60 mm. Recent version includes markers to measure lengths in centimeters. The system is compatible with GE, Philips, Siemens, and Toshiba X-ray equipment. With Volcano integrated into the procedure suite, a dedicated IVUS monitor with control panel is available for the interventionist or an assistant. By permission of Mayo Foundation for Medical Education and Research. All rights reserved

these techniques by cross reference of the live IVUS images with the CTA reconstructions to ensure the target vessel is correctly identified, located and marked. Other details such as the aortic bifurcation may be also marked using IVUS as appropriate. Of note, IVUS is of limited utility in cases of large thoracoabdominal aortic aneurysms with minimal thrombus as the limitations in the range of the current ultrasound beam of the aortic IVUS catheter does not allow interrogation of areas greater than 60 mm in diameter. IVUS is, however, not as necessary for branched EVAR because precise alignment with the target vessels is not required. In fact, branched devices are usually used for aneurysms with large intravascular lumen; thus the need for accurate location of the visceral vessels is less critical.

Once the IVUS interrogation of the aorta and access vessels is completed, the access sites are upsized to the

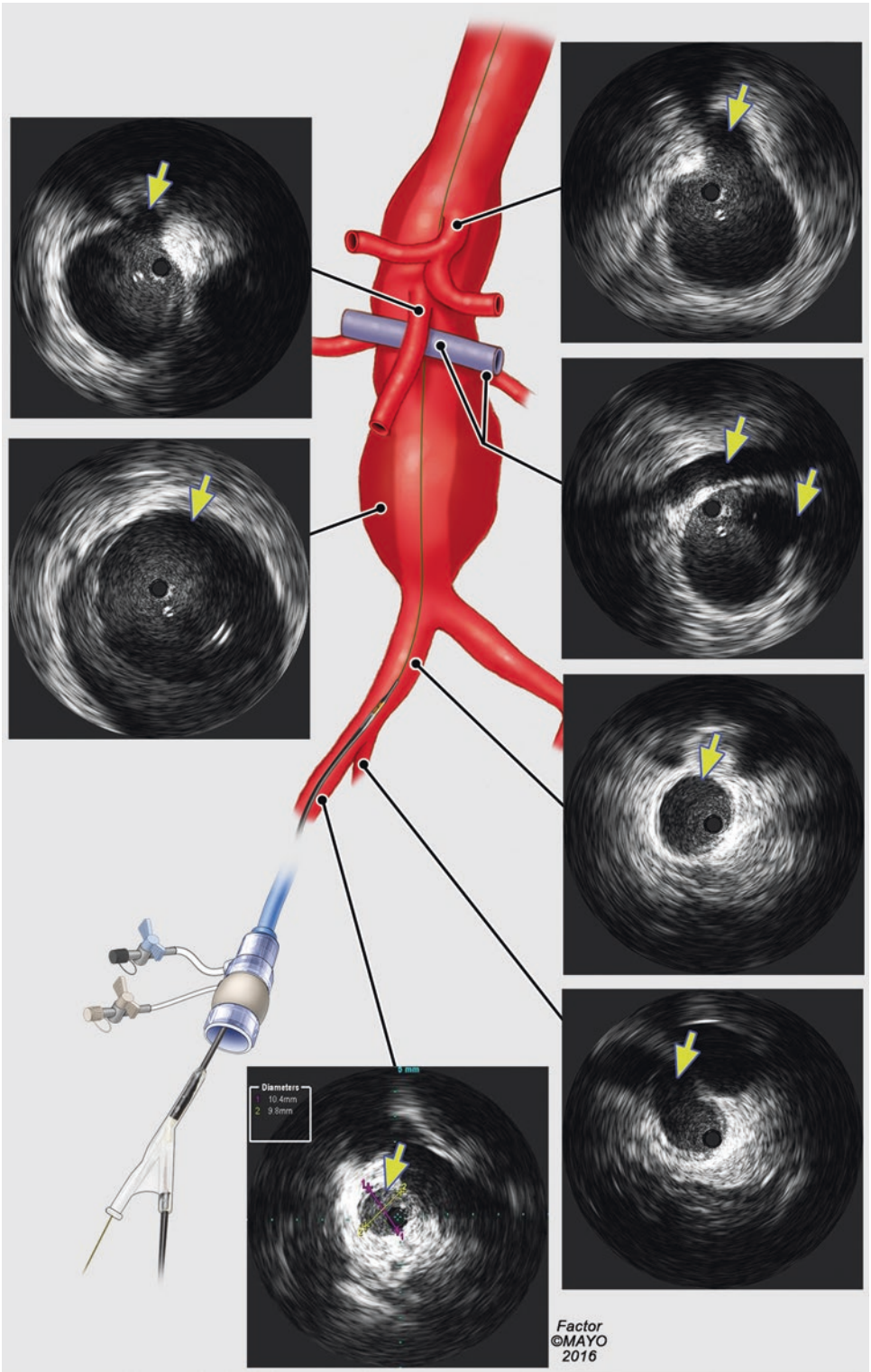


Fig. 6.2 Intravascular ultrasound aortic imaging starts with interrogation of the iliac arteries to measure the inner vessel diameter of the external iliac artery, which needs to have minimum diameter to allow an 18–24 Fr sheath. IVUS imaging may visualize possible occlusive lesions and calcium at the access site. Advancement to the common iliac artery allows visualization of the internal iliac artery origin. The proximal and distal landing zones are evaluated to confirm measurements, configuration, and presence of plaque, calcification, and/or thrombus. At the visceral segment of the aorta, the left renal vein is located and placed at the 12 o'clock position to allow proper orientation of the vessels. In the illustration, IVUS demonstrates the origins of the celiac axis, superior mesenteric artery and left renal arteries, as well as the large aneurysm sac. By permission of Mayo Foundation for Medical Education and Research. All rights reserved

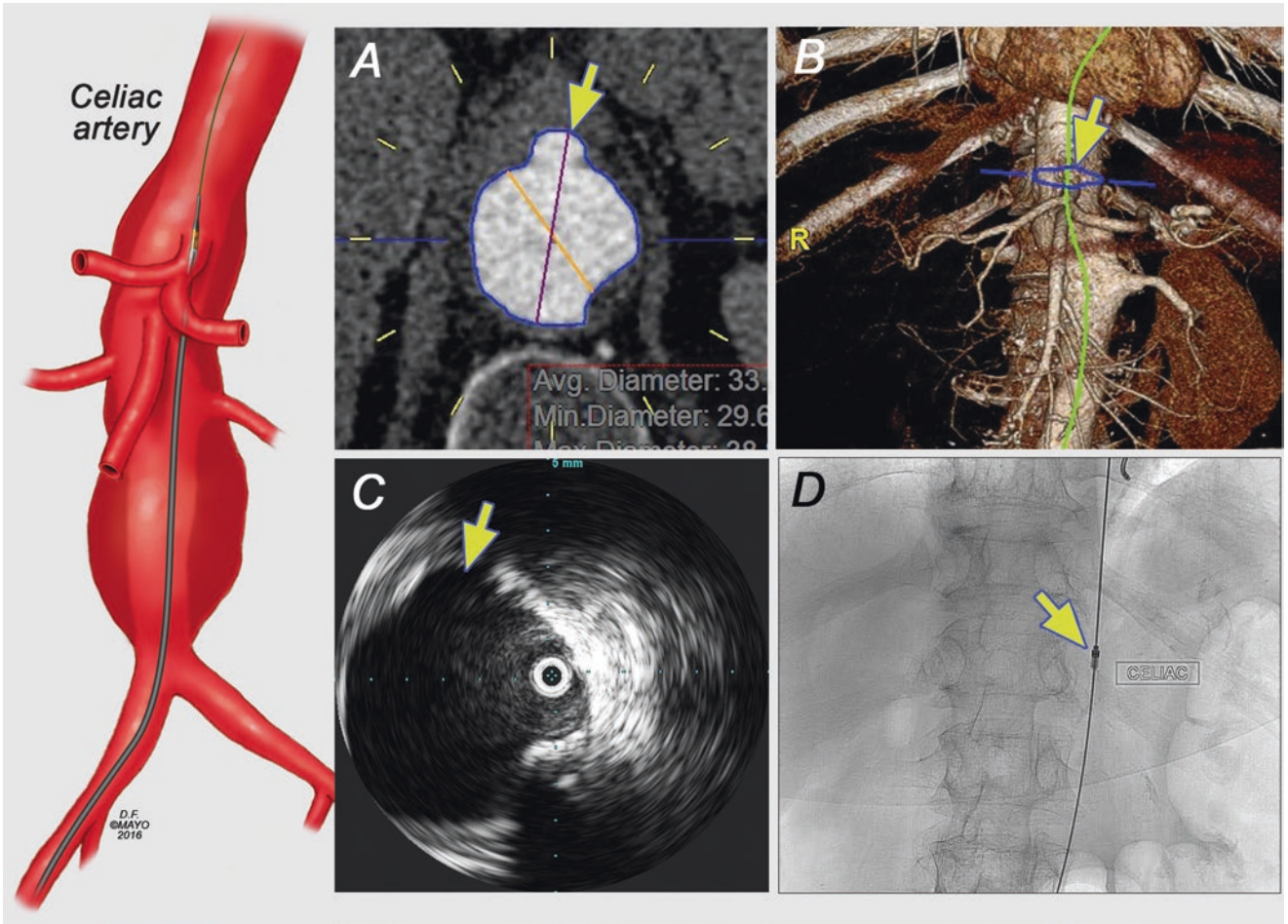


Fig. 6.3 Preoperative computed tomography angiography identification of the location of the celiac axis (**a**, **b**) with respect to bony landmarks, particularly the spine, is confirmed by intravascular ultrasound in real time during fenestrated EVAR procedure (**c**, **d**). By permission of Mayo Foundation for Medical Education and Research. All rights reserved

appropriate sheath size and the fenestrated endograft is advanced into the aorta. The referenced image, typically the SMA, is placed on the stored image screen for reference alongside the live image. Matched magnification and position comparing bony landmarks of the reference image and the live image is performed. The endograft is then advanced into position, and cranio-caudal and lateral c-arm orientation is utilized to open up the vessel for an angiogram if felt to be needed prior to deployment of the graft. In our practice, we rarely obtain angiograms prior to endograft deployment. For location of the target vessels, we rely almost exclusively on IVUS, 3-D reconstructions of the preoperative CT angiogram, and, lately, 3-D roadmapping based on fusion or overlay techniques. The first angiogram is usually obtained once the fenestration has been catheterized for confirmation of the target vessel location (Fig. 6.7). With orientation lined and correct anterior-posterior orientation checked with the endograft, partial deployment is initiated. Sequential cannulation of the fenestrations using brachial access and deployment of the endograft is then performed. Complete deployment of the endograft is only performed if cannulation is to be directed solely from femoral access.

One of the most useful features of IVUS is the examination of the "true" center line, i.e., the path the endograft will take through the visceral segment. Although 3-D reconstructions allow tracing a centerline, this is only based on an estimation of where the wire will likely run through the visceral

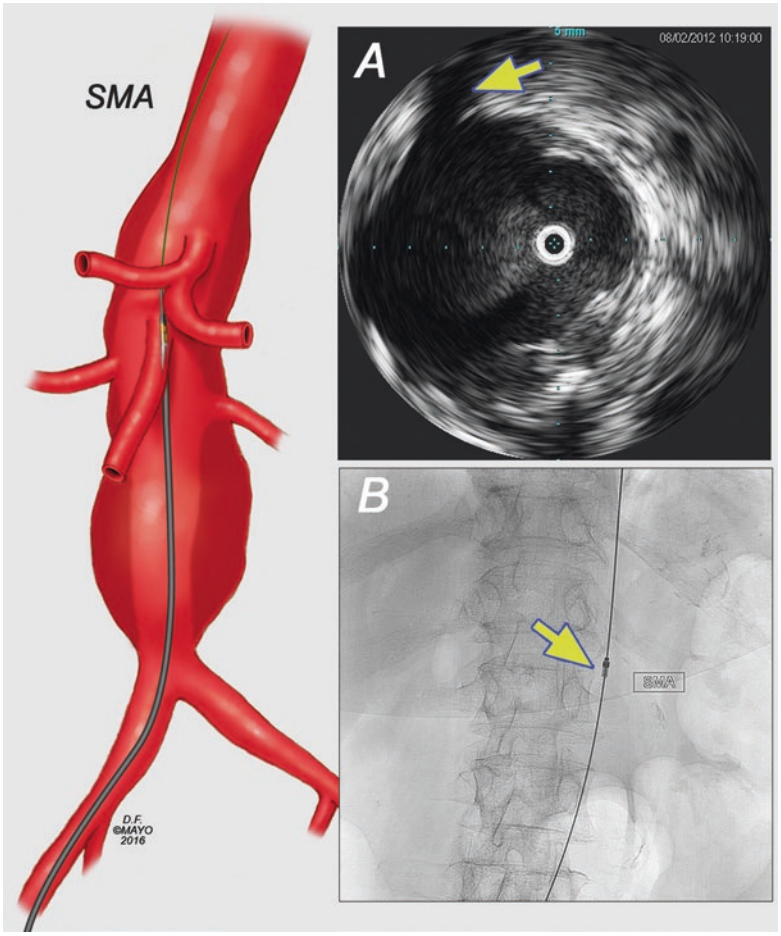


Fig. 6.4 The superior mesenteric artery is visualized with intravascular ultrasound (**a**). The location of the origin of the vessel is marked with fluoroscopy using the IVUS catheter tip (**b**, *yellow arrow*) as reference. By permission of Mayo Foundation for Medical Education and Research. All rights reserved

segment. Angulation in either anterior-posterior or lateral orientation, visceral segment aneurysmal degeneration, and length and tortuosity of access vessels may determine variation in where the centerline may likely lie. IVUS allows a real-time analysis over a stiff wire that likely simulates the "true" centerline and planned course of the endograft, and can identify proximity to vessels that may change the course of the operation. A Cook Lunderquist (Cook Medical, Bloomington, IN) wire is used and the IVUS is advanced over this wire through the planned side for endograft deployment. Identification of the proximity to vessel ostia is important for case planning. Proximity to vessel ostia that were going to have stents placed, ballooned and flared may place the patient at risk for deformation of the flared portion of the stents with subsequent passage of the lengthy tip of the bifurcated device. In such situations, the bifurcated device may be placed prior to stent deployment to avoid crushing of the visceral stent close to the stiff wire.

Although we have abandoned chimney graft repairs of paravisceral and thoracoabdominal aortic aneurysm because of dismal outcomes, the same principles outlined above for identification and location of the target vessel can be implemented during chimney endograft repair. Moreover, because of the risk of endograft compression among the chimney grafts, IVUS can be particularly useful to assess graft expansion, apposition, and residual stenosis due to compression. Peripheral IVUS catheters may be necessary for this purpose. If significant compression is evident, further ballooning or adjunct stenting using balloon-expandable or self-expanding stents may be necessary.

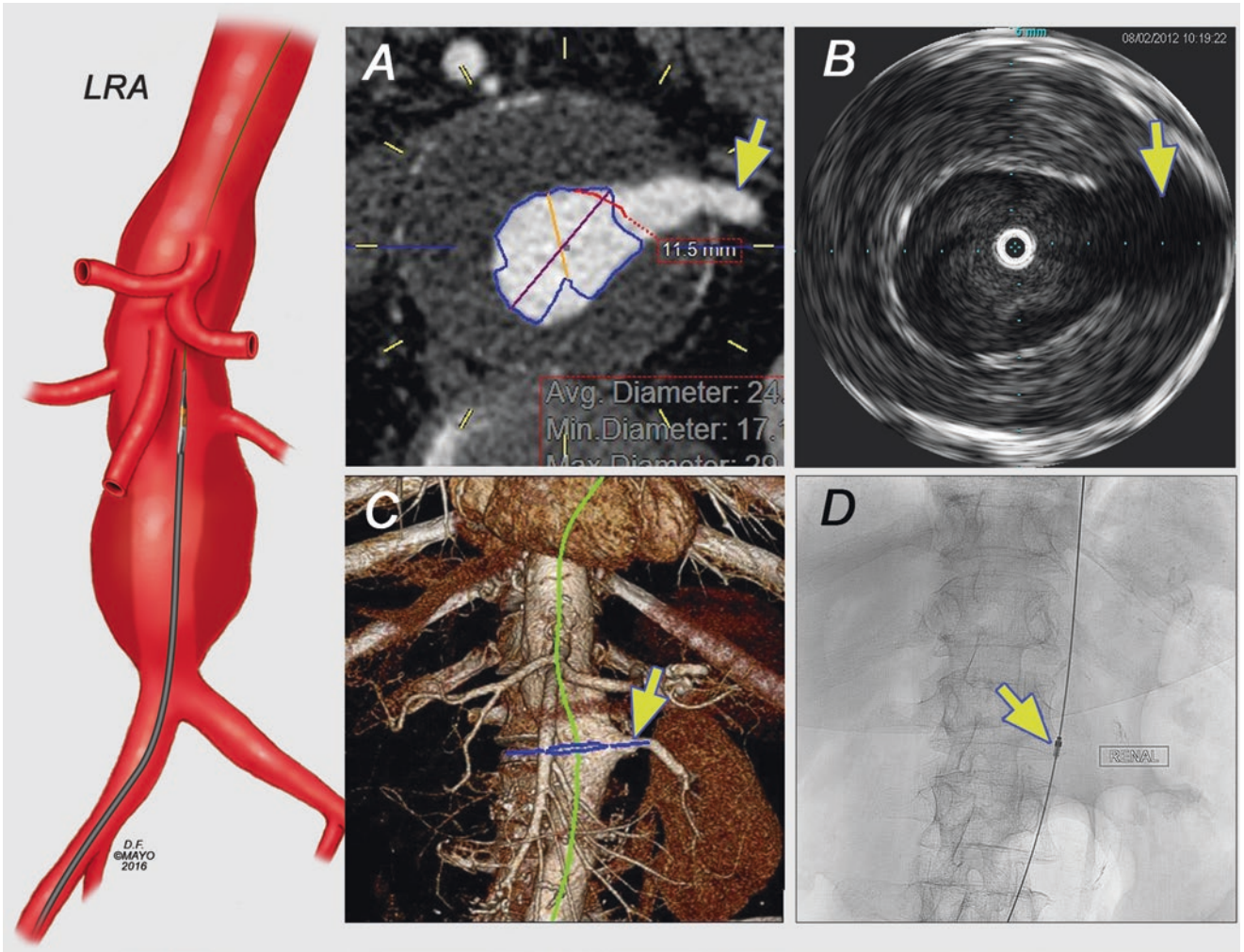


Fig. 6.5 Preoperative computed tomography angiography (**a**) demonstrates a large aneurysm with the left renal artery origin at 2:45 o'clock position. Intravascular ultrasound (**b**) tip marking the origin of the left renal artery, which is marked with fluoroscopy and correlated with preoperative computed tomography angiography imaging and reconstructions (**c**, **d**). By permission of Mayo Foundation for Medical Education and Research. All rights reserved

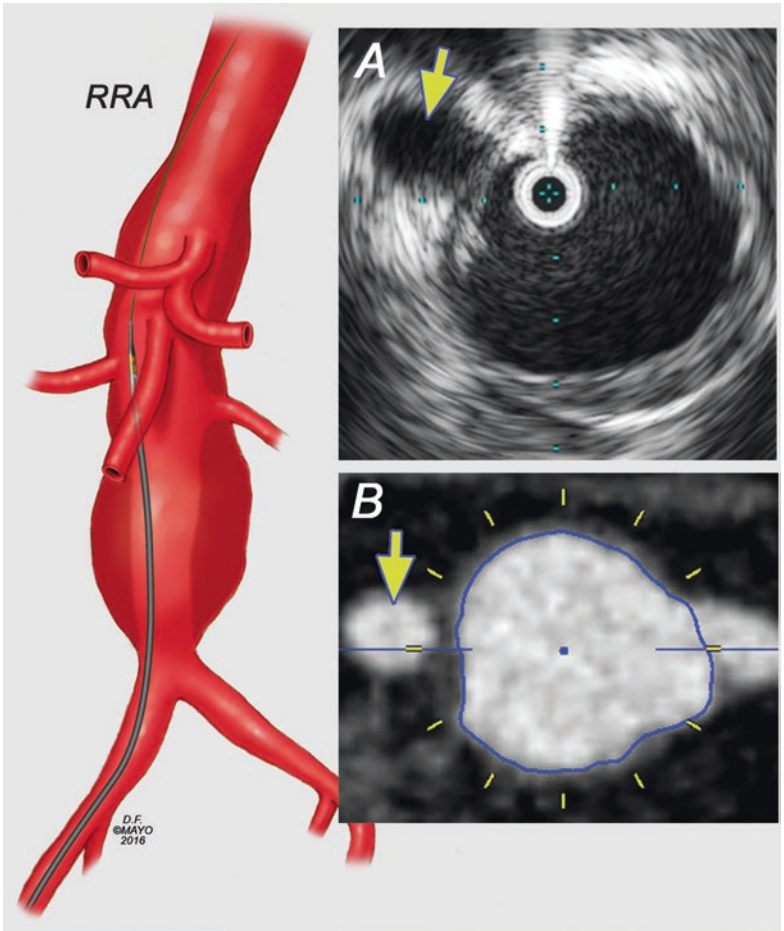


Fig. 6.6 The right renal artery is identified at the origin using intravascular ultrasound (**a**). Note the excellent correlation with the patients' preoperative computed tomography angiography (**b**). By permission of Mayo Foundation for Medical Education and Research. All rights reserved

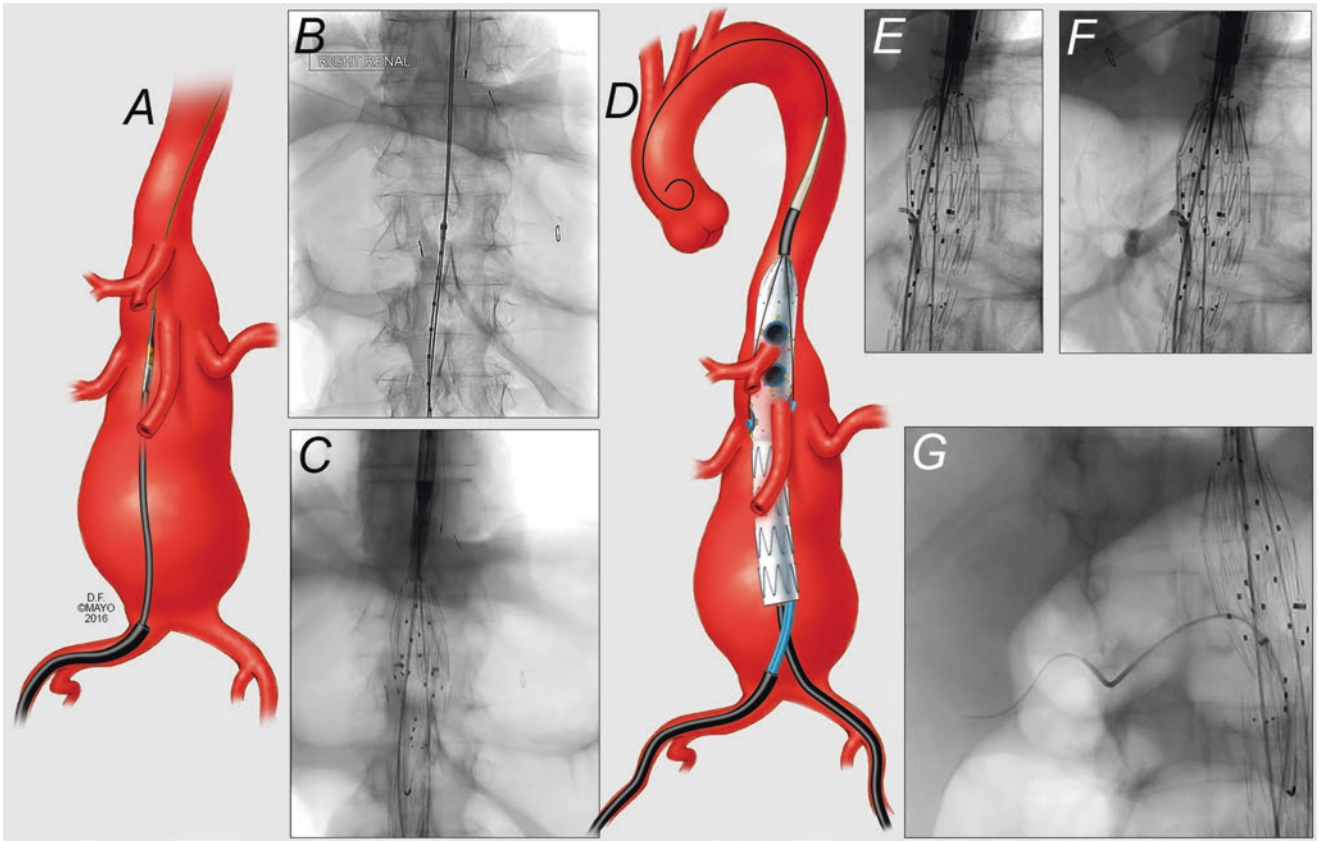


Fig. 6.7 Sequential IVUS identification and assisted catheterization of the right renal artery (**a**). Once the IVUS is positioned at the origin of the right renal artery, a single shot X-ray is obtained to mark the tip of the IVUS at the origin of the right renal artery (**b**). The right renal artery fenestration is aligned with the fluoroscopically marked origin of the right renal artery using bony landmarks for reference (**c**, **d**). A diagnostic catheter is advanced through the right renal artery fenestration (**e**), and selective angiography confirms opacification of the right renal artery (**f**). Successful catheterization of the right renal artery is performed through the fenestration (**g**). By permission of Mayo Foundation for Medical Education and Research. All rights reserved

References

1. Pearce BJ, Jordan Jr WD. Using IVUS during EVAR and TEVAR: improving patient outcomes. Semin Vasc Surg. 2009;22:172–80.
2. Marty B, Tozzi P, Ruchat P, Haesler E, von Segesser LK. Systematic and exclusive use of intravascular ultrasound for endovascular aneurysm repair—the Lausanne experience. Interact Cardiovasc Thorac Surg. 2005;4:275–9.
3. von Segesser LK, Marty B, Ruchat P, Bogen M, Gallino A. Routine use of intravascular ultrasound for endovascular aneurysm repair: angiography is not necessary. Eur J Vasc Endovasc Surg. 2002;23:537–42.
4. Hoshina K, Kato M, Miyahara T, Mikuriya A, Ohkubo N, Miyata T. A retrospective study of intravascular ultrasound use in patients undergoing endovascular aneurysm repair: its usefulness and a description of the procedure. Eur J Vasc Endovasc Surg. 2010;40:559–63.
5. Garret Jr HE, Abdullah AH, Hodgkiss TD, Burgar SR. Intravascular ultrasound aids in the performance of endovascular repair of abdominal aortic aneurysm. J Vasc Surg. 2003;37:615–8.
6. Das P, Meredith I. Role of intravascular ultrasound in unprotected left main percutaneous coronary intervention. Expert Rev Cardiovasc Ther. 2007;5:81–9.
7. Ben-Dor I, Torguson R, Deksissa T, Bui AB, Xue Z, Satler LF, et al. Intravascular ultrasound lumen area parameters for assessment of physiological ischemia by fractional flow reserve in intermediate coronary artery stenosis. Cardiovasc Revasc Med. 2012;13:177–82.
8. Nishioka T, Amanullah AM, Luo H, Berglund H, Kim CJ, Nagai T, et al. Clinical validation of intravascular ultrasound imaging for assessment of coronary stenosis severity: comparison with stress myocardial perfusion imaging. J Am Coll Cardiol. 1999;33:1870–8.
9. Puri R, Kapadia SR, Nicholls SJ, Harvey JE, Kataoka Y, Tuzcu EM. Optimizing outcomes during left main percutaneous coronary intervention with intravascular ultrasound and fractional flow reserve: the current state of evidence. JACC Cardiovasc Interv. 2012;5:697–707.

The Spinal Cord Collateral Network: Implications for Endovascular Aortic Repair

7

Sarah Geisbüsch, Gabriele Di Luozzo,
Eva Botstein Griepp, and Randall B. Griepp

Introduction

Endovascular repair of aortic aneurysms has evolved as the primary treatment strategy for many patients suffering from infrarenal aortic pathologies, and already represents an alternative treatment for patients with aortic aneurysms involving the thoracic and visceral segment of the aorta. With the implementation of fenestrated and branched stent grafts, we are now facing different complications than were usually encountered after open repair, but certain issues remain unsolved. Among these, paraplegia as a consequence of spinal cord ischemic damage has an incidence as high as 30 % in some reports, is the most devastating complication to patients and most dreaded by surgeons. Paraplegia results in dramatic life changes and often in early mortality, encouraging us in the quest for ways to minimize its risk.

S. Geisbüsch (✉)
Department of Vascular and Endovascular Surgery, Klinikum rechts der Isar der Technischen Universität München, Ismaninger Str. 22, Munich 81675, Germany
e-mail: sarahgeisbuesch@hotmail.com

G. Di Luozzo
Department of Cardiac Surgery, Hackensack University Medical Center, 30 Prospect Avenue, Hackensack, NY 07601, USA
e-mail: gdiluozzo@HackensackUMC.org

E.B. Griepp • R.B. Griepp
Department of Cardiothoracic Surgery, The Mount Sinai School of Medicine, New York, NY, USA
e-mail: ebgriepp@aol.com; randallgriepp@msnyuhealth.org

Background

Anatomy

To understand the anatomy of the spinal cord vasculature and its physiological mechanisms as a reaction to critical changes in spinal cord perfusion is a vital first step toward improved treatment. The spinal cord is nourished by three major arteries: the anterior spinal artery (ASA) feeds the anterior two-thirds of the spinal cord, and two posterior spinal arteries provide blood flow to the posterior third. Arising from the aorta, intercostal and lumbar arteries give off branches to the spinal arteries: the anterior and posterior radicular–medullary arteries (ARMA, Fig. 7.1).

The traditional teaching that there exists one dominant artery which feeds the spinal cord, the artery of Adamkiewicz, has dominated the thinking of surgeons seeking to safeguard spinal cord perfusion, and many attempts have been made to identify and preserve this elusive vessel preoperatively and intraoperatively, recently using high-resolution computed tomographic angiography (CTA). Unfortunately, however, valiant attempts to re-implant SAs associated with prominent radicular arteries have been frustrated by lack of improvement in paraplegia rates. We have shown in a review of hundreds of TAAA resections that there is no unique SA whose interruption results in cord ischemia [1, 2]. Lazorthes et al. were among the first to question the idea of a single dominant artery, and they described the importance of additional inflow into the spinal cord circulation provided by the subclavian and hypogastric arteries [3–5]. The occlusion of a large number of segmental arteries when replacing a long segment of the aorta by open or endovascular means results in immediate loss of blood flow to the cord through intercostal and lumbar arteries, and this immediate ischemia results in recruitment and development of additional sources.

Pathophysiology

Serial examination of spinal cord blood flow (SCBF) using fluorescent microspheres in experimental pig studies has

© Mayo Foundation for Medical Education and Research 2017

G.S. Oderich (ed.), *Endovascular Aortic Repair*, DOI 10.1007/978-3-319-15192-2_7

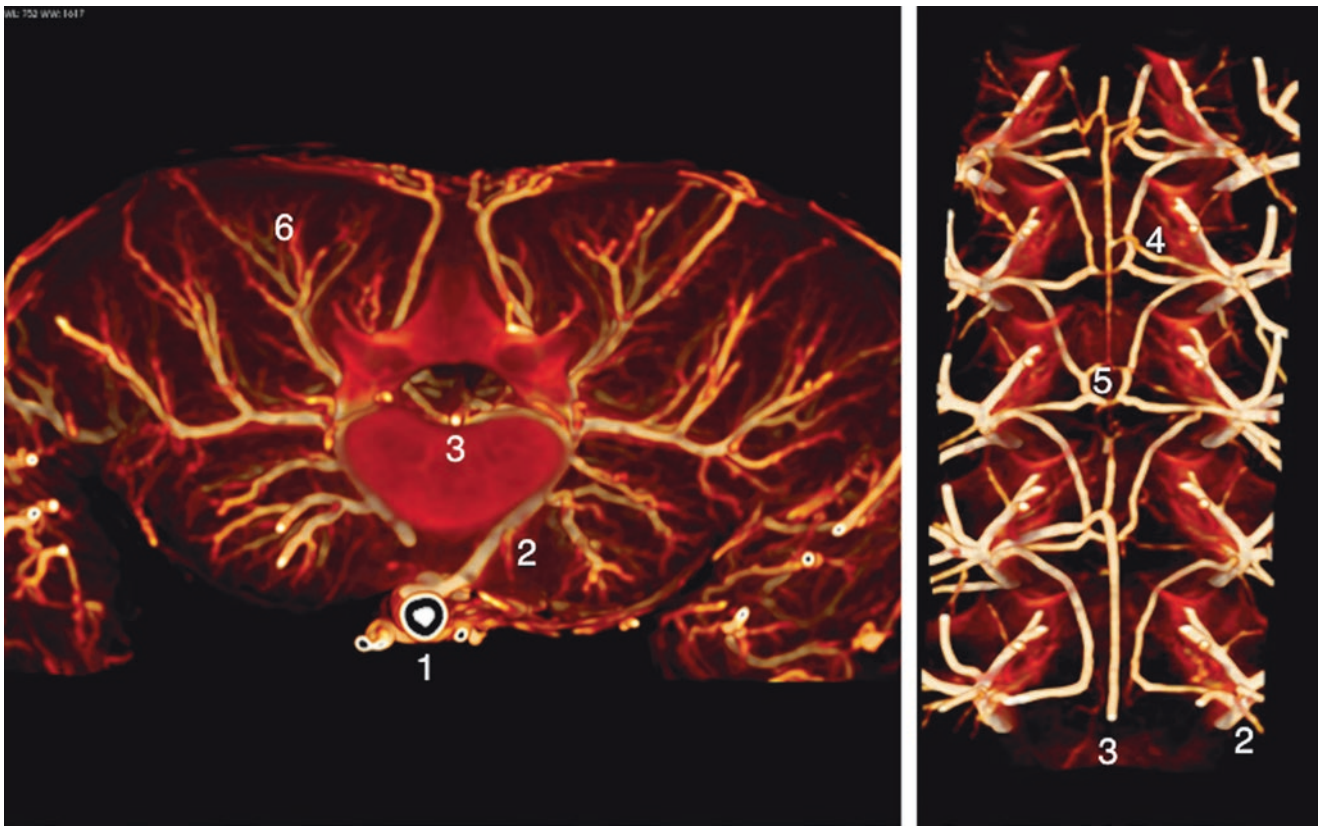


Fig. 7.1 High-resolution CT scan of the vasculature. The aorta (1) gives rise to the segmental arteries (2), which run around the vertebral bodies and connect to the anterior spinal artery (3) through the anterior radicular–medullary arteries (4), and give off branches to the epidural arcades (5). Its connections with the dense vasculature within the paraspinous muscles can also be seen (6). Reprinted from The Journal of Thoracic and Cardiovascular Surgery, 144(6), Geisbusch S, Schray D, Bischoff S, Lin HM, Griepp RB, Di Luozzo G, Imaging of vascular remodeling after simulated thoracoabdominal aneurysm repair, 1471–8, Copyright 2012, with permission from Elsevier

shown that the lowest flow occurs within 5 h after extensive SA ligation, at a time when sham-operated pigs demonstrate hyperemia. Pigs that recover from SA ligation with normal hind limb function show a return to baseline SCBF at the 5-h time point, whereas those that suffer paraplegia do not reach baseline until 72 h after SA sacrifice (Fig. 7.2) [6].

Monitoring of the actual spinal cord perfusion pressure (SCPP) via a catheter inserted in the stump of a ligated SA confirms that the most severe drop in pressure occurs also at 5 h, with recovery even in paraplegic animals by 72 h (Fig. 7.3). In patients as in pigs, SCPP is a fraction of mean arterial pressure (MAP): in hypertensive patients, MAP must be maintained at preoperative levels during and after operation in order to avoid spinal cord ischemic injury [7, 8].

The explanation for the physiological patterns of spinal cord perfusion after sacrifice of SAs has been provided by several anatomic studies. The blood supply to the spinal cord is part of an extensive network of vessels within and surrounding the cord and the vertebrae, extending into the paraspinous muscles, which is interconnected with major arteries: the subclavian, hypogastric, and internal thoracic. The most surprising finding of our initial anatomic studies—carried out using acrylic casts of the vascular system in the pig—is the dominance of the vasculature of the paraspinal muscles over the much less extensive arterial supply of the spinal cord (Fig. 7.4) [9].

There are multiple longitudinal interconnections between the blood supply of the muscles, an extensive epidural system, and the anterior spinal artery, with numerous anastomoses at every thoracic and lumbar level between these various components of the network. A reconstruction based on several casts of the paraspinal and intrathecal vessels is shown in Fig. 7.5 [9].

Following sacrifice of all SAs from level T4 to S1 through simulated TAAA repair in a pig model, an increase in the diameter of the ASA can be seen already at 24 h after operation. By 48 h and especially 120 h, there is also a significant increase in the volume and diameter of the epidural arteries, and evidence of proliferation of small arterioles within the muscles surrounding the cord as well as enlargement of those which were present before SA ligation [1, 9].

The proliferation of small vessels as well as enlargement of major collateral arteries after SA ligation has been

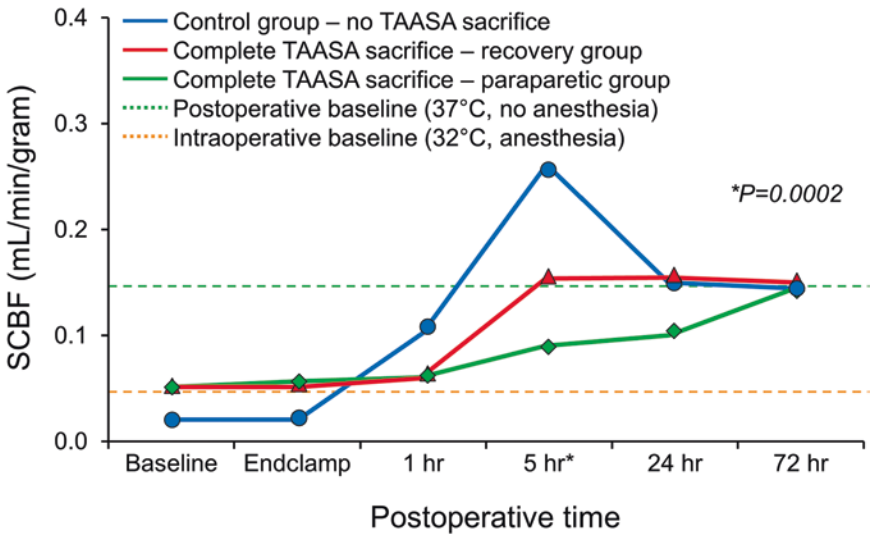


Fig. 7.2 Spinal cord blood flow (SCBF) drops after sacrifice of all thoracoabdominal segmental arteries and returns to baseline 5 h after the operation in pigs that recover without impairment of hind limb function. In paraparetic pigs, it takes up to 72 h to return to baseline levels. By permission of Mayo Foundation for Medical Education and Research. All rights reserved

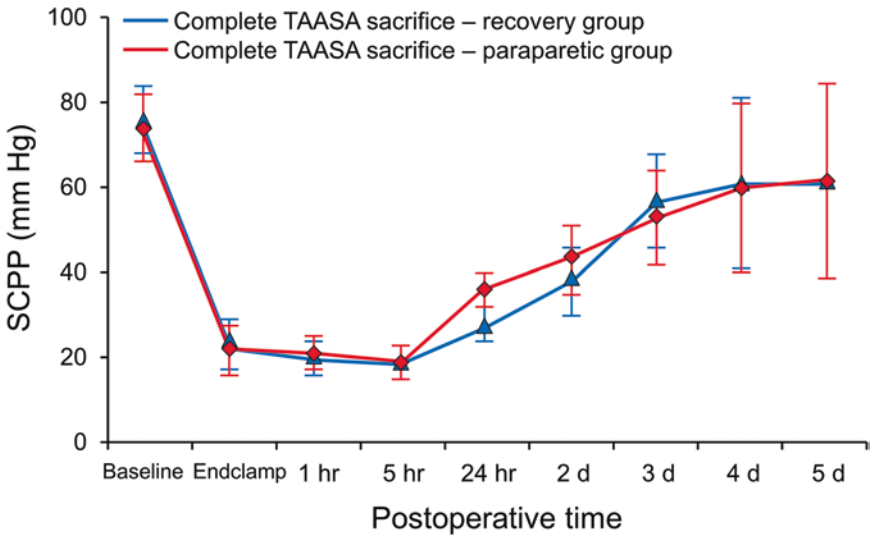


Fig. 7.3 Spinal cord perfusion pressure (SCPP) drops immediately after sacrifice of all segmental arteries and shows complete recovery even in paraparetic animals. By permission of Mayo Foundation for Medical Education and Research. All rights reserved

confirmed by studies using a barium latex infusion viewed by means of CT scanning [1]. One of the most striking findings is the extensive anterior-posterior collateralization, which develops between the internal thoracic and intercostal arteries. The dramatic proliferation of the network is easily appreciated visually, and can be confirmed by morphometric studies. Figure 7.6 shows a native pig compared with a pig 24 h and 5 days after complete SA ligation. The latex-barium method permits analysis of the vessels in situ, in contrast with the need for digestion of the tissue around the acrylic vascular cast, a process, which destroys many small and fragile vessels.

Histological findings have made it clear that necrosis of the spinal cord neurons is most prominently seen in the lower thoracic region (T9-T13), the part of the cord where input from cranial and caudal sources is limited when direct blood flow through SAs is interrupted (Fig. 7.7) [10].

After simulated TAAA repair in experimental models, there is also a striking reorientation of vessels within the musculature, from a random pattern (top) to one more parallel to the cranio-caudal axis (bottom), suggesting that this is a mechanism to augment flow along the longitudinal axis and provide both cranial and caudal input to the central region of a spinal cord which has been deprived of its direct blood supply (Fig. 7.8) [11].

The Impact of the Collateral Network on Endovascular Repair

Although its incidence is gradually diminishing, paraplegia following repair of aortic aneurysms is a formidable complication and continues to be disturbingly high even in the hands of experts, especially in cases where the aneurysm

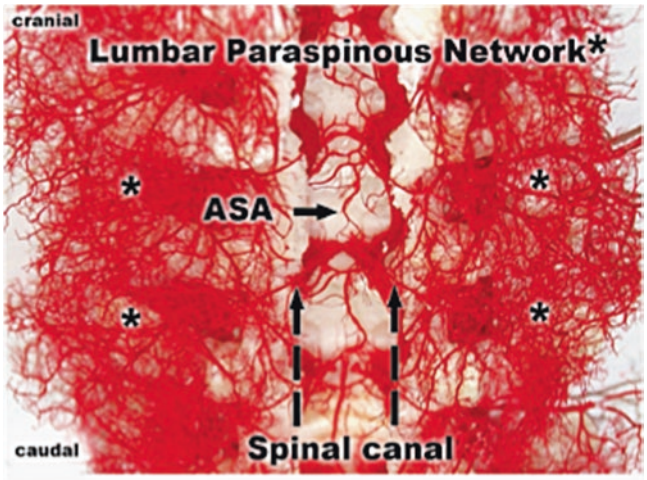


Fig. 7.4 Casting of the vasculature using acrylic resin revealed a dense network within the paraspinous muscles. Reprinted from The Journal of Thoracic and Cardiovascular Surgery, 141(4), Etz CD, Kari FA, Mueller CS, Silovitz D, Brenner RM, Lin HM, et al., The collateral network concept: a reassessment of the anatomy of spinal cord perfusion, 1020–8, Copyright 2011, with permission from Elsevier

spans most of the thoracic and thoracoabdominal aorta. The number of SAs to be sacrificed during an operation—equivalent to the extent of the aneurysm—and the presence of additional compromise of input resulting from previous or concomitant occlusion of the subclavian or hypogastric arteries are the major factors in assessing the risk of paraplegia or paraparesis [12–14]. Current surgical strategies to reduce the risk of cord ischemia include reimplantation of SAs and use of cardiopulmonary bypass to increase intraoperative flow, and deep hypothermia to decrease the nutritional demand of the spinal cord, but these techniques are of limited relevance in endovascular repair, where intraoperative cord ischemia is much less of a problem. Other surgical adjuncts, such as drainage of cerebrospinal fluid (CSF) and maintenance of mean arterial pressure (MAP) at high normal levels, are part of the routine perioperative management in both surgical and endovascular repair to assure adequate SCPP. In addition, monitoring tools such as motor-evoked potentials (MEPs) or somatosensory-evoked potentials (SSEPs) help to immediately detect changes and adjust treatment in anaesthetized patients, but are not feasible once they awaken, making us rely on clinical assessments of spinal cord function.

The impact of the collateral network on recovery from endovascular aortic repair becomes apparent when we look at results of clinical as well as experimental studies in which extensive aortic replacement has been carried out in two stages. There is an undeniable decrease in the incidence of postoperative paraplegia after staged repair [15–17], notwithstanding the ongoing controversy over the impact of previous aortic repair as a risk factor for paraplegia: the detrimental effect of previous surgery may well be a consequence of hypogastric or subclavian artery sacrifice. Experiments in which various numbers of SAs T4–S1 were sacrificed have shown that the incidence of spinal cord ischemia corresponds to the number of sacrificed vessels. Further studies have shown that pigs in which the subclavian and/or the hypogastric arteries had been ligated prior to SA sacrifice had a worse outcome than those in which these other sources of blood flow were intact: in the absence of an intact subclavian or hypogastric blood supply, fewer SAs could be sacrificed without spinal cord injury [18].

Taking into account what we have learned about spinal cord anatomy and physiology, it is likely that the first step of a two-stage procedure provides an ischemic stimulus which stimulates the collateral network to develop small new vessels (angiogenesis) and to transform existing small vessels into larger ones (arteriogenesis) and to reorient them. All of these changes serve to augment spinal cord blood flow to compensate for diminished direct SA input. Patients in whom recruitment of collateral input sources is compromised by previous occlusion of subclavian or hypogastric vessels are therefore at higher risk of spinal cord ischemia following SA sacrifice during aneurysm repair.

With constant improvement of endovascular strategies including fenestrated and branched stent grafts, innovative concepts to prevent spinal cord ischemia after complete endovascular repair have been developed, with the idea of promoting enhancement of the collateral network before occlusion of all segmental vessels. First published in 2010, temporary aneurysm sac perfusion (TASP) after branched thoracic endovascular aortic repair (bEVAR) is a technique which involves leaving two or more branches open at the time of initial repair, and performing side branch completion in a second stage procedure days to weeks later. TASP has shown promising results in a case report and two series of 10 and 40 patients [19–22]. Although spinal cord perfusion is dramatically reduced by implanting a thoracoabdominal stent graft, leaving some branches open seems to assure sufficient cord perfusion until the collaterals have had time to develop, while placing the stent graft immediately reduces the risk of rupture by minimizing flow into the aneurysm sac.

Endovascular occlusion of a number of SAs prior to simulated TAAA repair has shown excellent results in an experimental study: no paraplegia in pigs that had coil occlusion of two or more SAs 1 week prior to sacrifice of all SAs, in contrast to a 60 % rate of spinal cord injury in controls without pretreatment [10]. The first clinical cases report successful application in patients at high risk [23]. Coiling of a few SAs seems to stimulate collateral development prior to subsequent simulated TAAA endovascular repair in healthy pigs without being harmful to spinal cord integrity: histologic

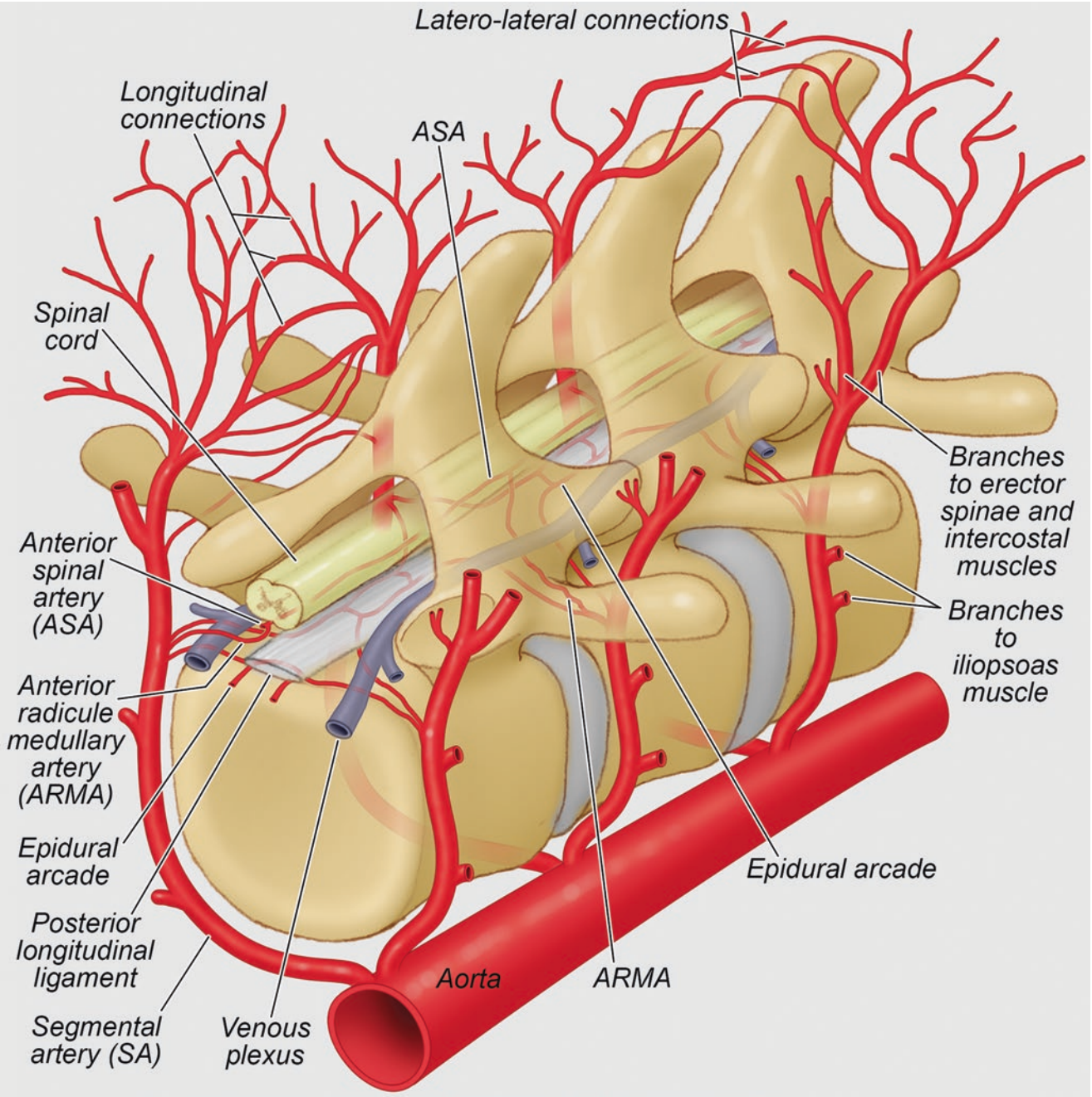


Fig. 7.5 Spinal cord anatomy with longitudinal interconnections at every thoracic and lumbar level between various components of the network. By permission of Mayo Foundation for Medical Education and Research. All rights reserved

ischemic damage, quantified as necrosis of grey and white matter, was significantly reduced after preparatory coiling ($p = 0.001$) (Fig. 7.9).

TASP and coiling of SAs seem to have real potential clinical utility, although some issues pose concerns. In patients with degenerative aneurysms, some of the SAs may already be occluded by thrombus, and so the coiling of additional arteries could then itself lead to spinal cord ischemia [19]. Test balloon occlusion in the awake patient may be a way of dealing with this problem: in the absence of neurological symptoms, permanent coils could be placed, or implantation of the branch to complete bEVAR could be performed. In addition, catheter manipulation during the coiling procedure carries a risk of atheroembolization from plaque and mural thrombus and should be performed by an experienced interventionalist or surgeon. The imaging of patent intercostal

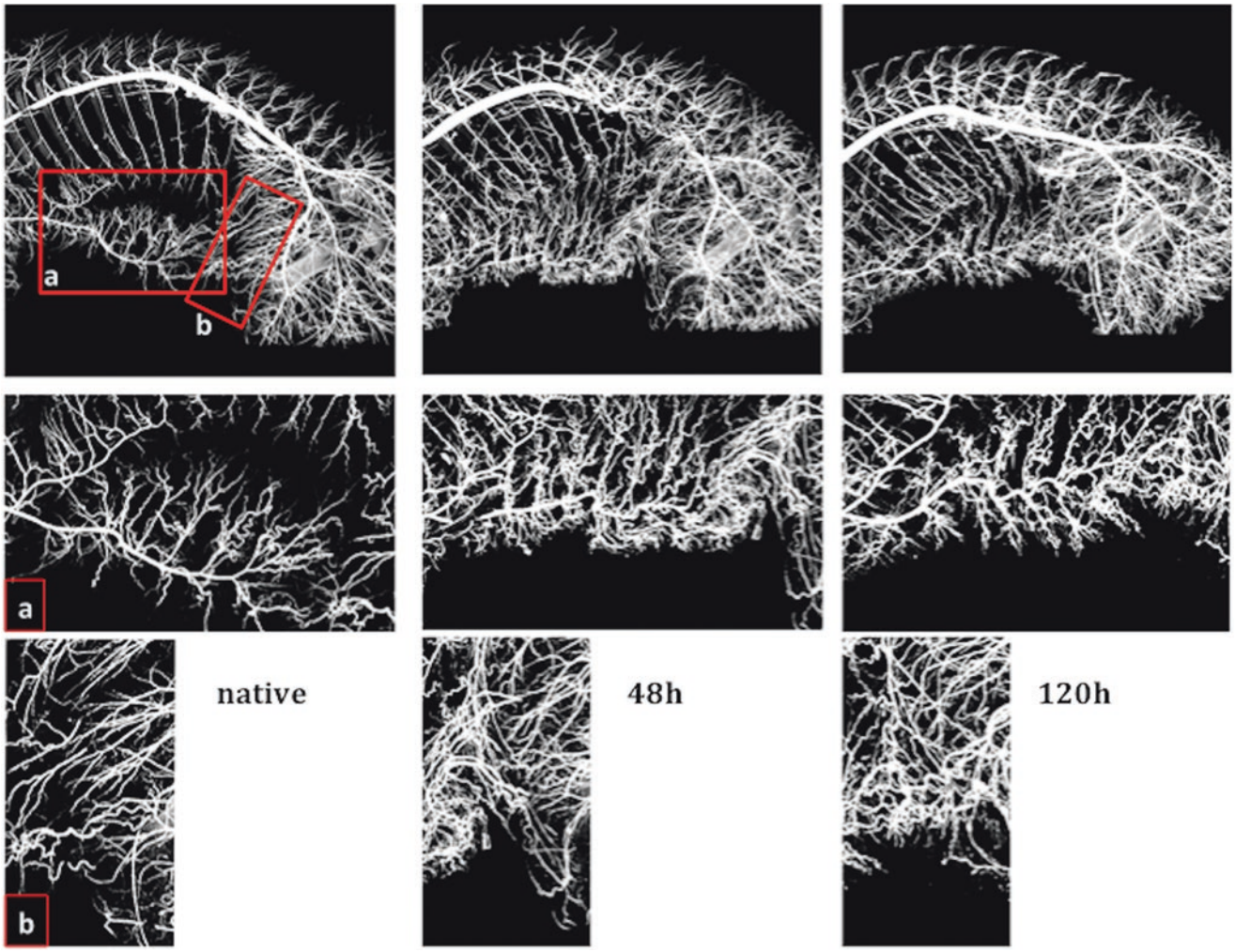


Fig. 7.6 High-resolution CT scans of a native pig, and pigs 48 and 120 h after complete SA sacrifice (simulated TAAA repair). It can easily be appreciated that a dense network of collaterals develops, and that an increase in vessel diameter occurs as early as 48 h after the operation. Reprinted from The Journal of Thoracic and Cardiovascular Surgery, 144(6), Geisbusch S, Schray D, Bischoff S, Lin HM, Griepp RB, Di Luozzo G, Imaging of vascular remodeling after simulated thoracoabdominal aneurysm repair, 1471–8, Copyright 2012, with permission from Elsevier

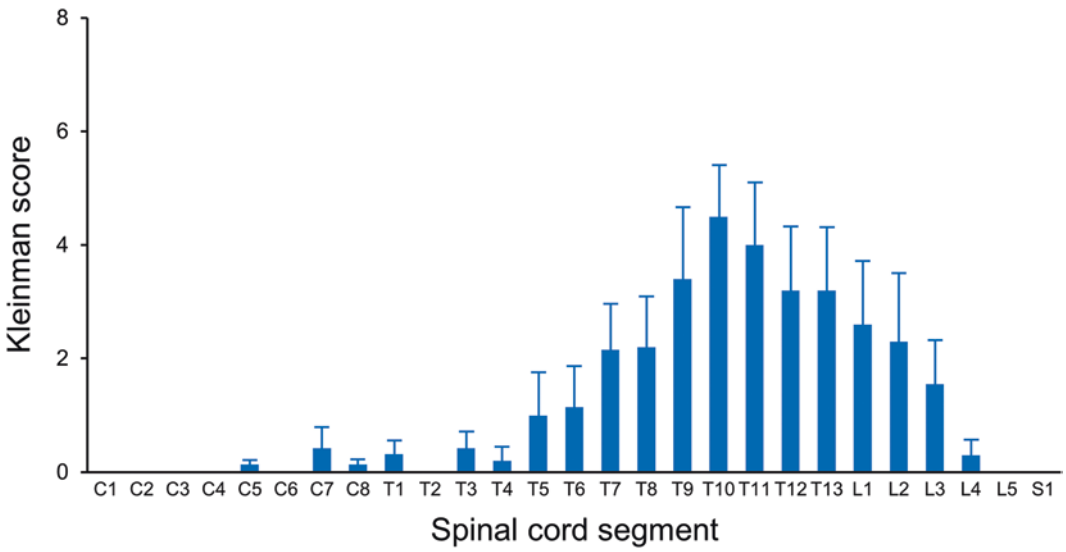


Fig. 7.7 In experimental studies, the ischemic damage within the spinal cord was graded on an 8-point scale after complete SA sacrifice from T4–S1. Necrosis was most prominently seen from T9 to T13, the region farthest away from supportive cranial and caudal input when direct inflow is interrupted. By permission of Mayo Foundation for Medical Education and Research. All rights reserved

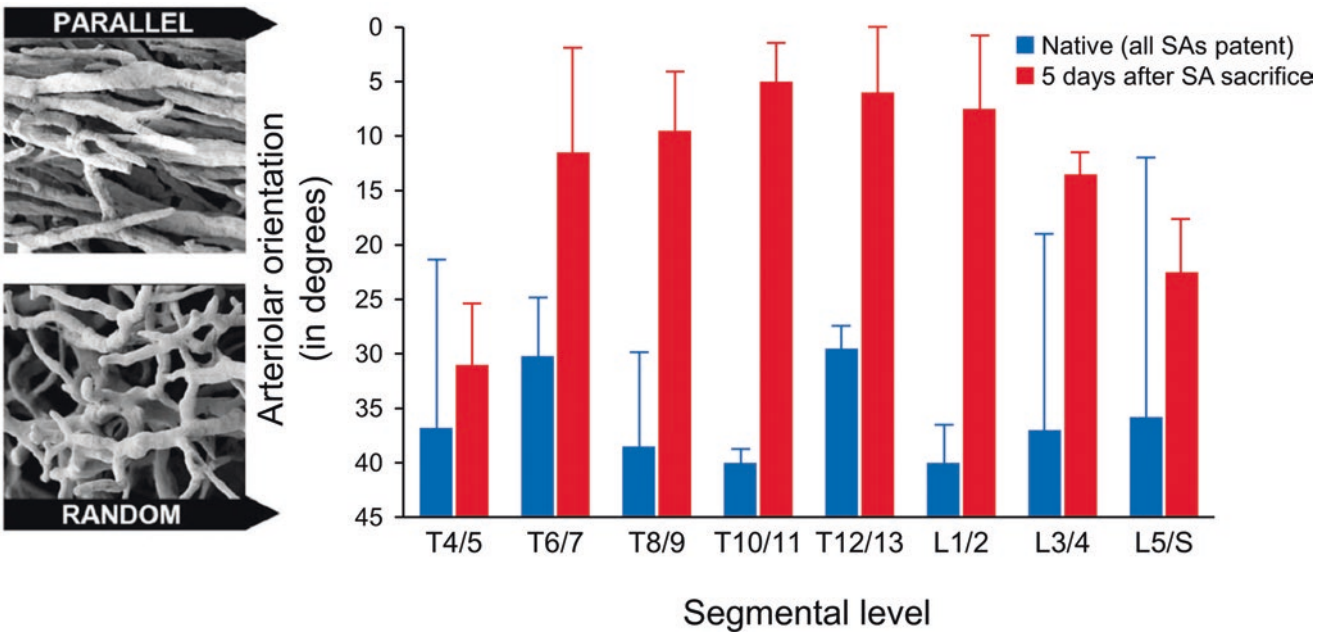


Fig. 7.8 The reorientation of the smallest vessels within the collateral network, most likely to direct flow to the central region of the cord. Reprinted from The Journal of Thoracic and Cardiovascular Surgery, 141(4), Etz CD, Kari FA, Mueller CS, Brenner RM, Lin HM, Griepp RB, The collateral network concept: remodeling of the arterial collateral network after experimental segmental artery sacrifice, 1029–36, Copyright 2011, with permission from Elsevier

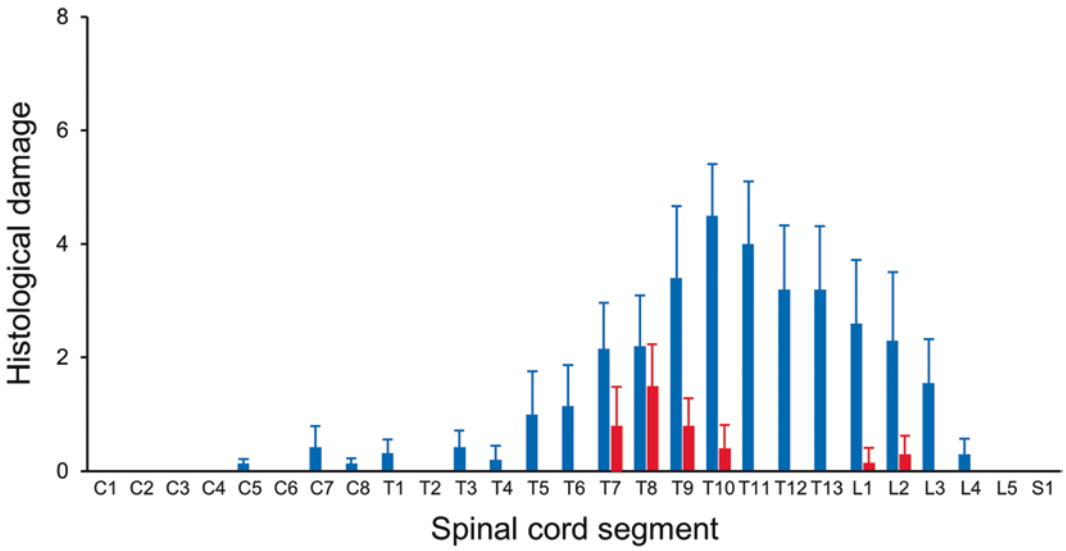


Fig. 7.9 As opposed to the pattern of spinal cord necrosis after simulated TAAA repair (*blue bars*), the extent of ischemic cell damage is marginal in the T9-T13 region after coiling of two or more SAs in this region of the cord (*red bars*), $p=0.001$. The ischemic stimulus likely activates the dilatation of existing vessels and the development of small new vessels that compensate for the loss of inflow after subsequent TAAA repair [10]. By permission of Mayo Foundation for Medical Education and Research. All rights reserved

arteries and thrombus formation by angiography, CT or MRI is a helpful tool in planning the procedure [24, 25].

Revascularization of the left subclavian artery via a bypass graft should be considered in each patient in whom coverage of the artery with a stent graft is inevitable, and when additional risk factors—such as previous aortic repair with sacrifice of the hypogastric artery—are present.

Finally, it should be pointed out that some patients are not eligible for a two-stage procedure, TASP or coiling: those with symptoms or imminent rupture, rapid aneurysm

progression over a short period of time, or large aneurysm diameters. For these patients, the risk of paraplegia with extensive aneurysm repair remains high, and should be minimized using careful monitoring and supportive adjuncts during the first few days following the endovascular procedure.

In summary, minimally invasive endovascular repair of complex extensive aortic pathologies still carries a high risk of postoperative paraplegia, but innovative endovascular strategies in combination with currently accepted management may improve outcome and reduce paraplegia to a rare complication.

References

1. Geisbusch S, Schray D, Bischoff S, Lin HM, Griepp RB, Di Luozzo G. Imaging of vascular remodeling after simulated thoracoabdominal aneurysm repair. J Thorac Cardiovasc Surg. 2012;144(6):1471–8 [Research Support, N.I.H., Extramural].
2. Etz CD, Halstead JC, Spielvogel D, Shahani R, Lazala R, Homann TM, et al. Thoracic and thoracoabdominal aneurysm repair: is reimplantation of spinal cord arteries a waste of time? Ann Thorac Surg. 2006;82(5):1670–7.
3. Lazorthes G, Gouaze A, Zadeh JO, Santini JJ, Lazorthes Y, Burdin P. Arterial vascularization of the spinal cord. Recent studies of the anastomotic substitution pathways. J Neurosurg. 1971;35(3):253–62 [Review].
4. Lazorthes G, Poulhes J, Bastide G, Roulleau J, Chancholle AR. [Research on the arterial vascularization of the medulla; applications to medullary pathology]. Bull Acad Natl Med. 1957;141(21–23):464–77.
5. Lazorthes G, Poulhes J, Bastide G, Roulleau J, Chancholle AR. Arterial vascularization of the spine; anatomic research and applications in pathology of the spinal cord and aorta. Neurochirurgie. 1958;4(1):3–19.
6. Etz CD, Homann TM, Luehr M, Kari FA, Weisz DJ, Kleinman G, et al. Spinal cord blood flow and ischemic injury after experimental sacrifice of thoracic and abdominal segmental arteries. Eur J Cardiothorac Surg. 2008;33(6):1030–8.
7. Etz CD, Zoli S, Bischoff MS, Bodian C, Di Luozzo G, Griepp RB. Measuring the collateral network pressure to minimize paraplegia risk in thoracoabdominal aneurysm resection. J Thorac Cardiovasc Surg. 2010;140(6 Suppl):S125–30. [Research Support, N.I.H., Extramural]; discussion S42–S46.
8. Etz CD, Di Luozzo G, Zoli S, Lazala R, Plestis KA, Bodian CA, et al. Direct spinal cord perfusion pressure monitoring in extensive distal aortic aneurysm repair. Ann Thorac Surg. 2009;87(6):1764–73; discussion 73–4.
9. Etz CD, Kari FA, Mueller CS, Silovitz D, Brenner RM, Lin HM, et al. The collateral network concept: a reassessment of the anatomy of spinal cord perfusion. J Thorac Cardiovasc Surg. 2011;141(4):1020–8 [Research Support, N.I.H., Extramural].
10. Geisbusch S, Stefanovic A, Koruth JS, Lin HM, Morgello S, Weisz DJ, et al. Endovascular coil embolization of segmental arteries prevents paraplegia after subsequent thoracoabdominal aneurysm repair: an experimental model. J Thorac Cardiovasc Surg. 2014;147(1):220–6 [Research Support, N.I.H., Extramural].
11. Etz CD, Kari FA, Mueller CS, Brenner RM, Lin HM, Griepp RB. The collateral network concept: remodeling of the arterial collateral network after experimental segmental artery sacrifice. J Thorac Cardiovasc Surg. 2011;141(4):1029–36 [Research Support, N.I.H., Extramural].
12. Czerny M, Eggebrecht H, Sodeck G, Verzini F, Cao P, Maritati G, et al. Mechanisms of symptomatic spinal cord ischemia after TEVAR: insights from the European Registry of Endovascular Aortic Repair Complications (EuREC). J Endovasc Ther. 2012;19(1):37–43 [Multicenter Study].
13. Eagleton MJ, Shah S, Petkosevek D, Mastracci TM, Greenberg RK. Hypogastric and subclavian artery patency affects onset and recovery of spinal cord ischemia associated with aortic endografting. J Vasc Surg. 2014;59(1):89–94 [Clinical Trial Research Support, Non-U.S. Gov't].
14. Zoli S, Roder F, Etz CD, Brenner RM, Bodian CA, Lin HM, et al. Predicting the risk of paraplegia after thoracic and thoracoabdominal aneurysm repair. Ann Thorac Surg. 2010;90(4):1237–44; discussion 45.
15. Zoli S, Etz CD, Roder F, Brenner RM, Bodian CA, Kleinman G, et al. Experimental two-stage simulated repair of extensive thoracoabdominal aneurysms reduces paraplegia risk. Ann Thorac Surg. 2010;90(3):722–9.
16. Etz CD, Zoli S, Mueller CS, Bodian CA, Di Luozzo G, Lazala R, et al. Staged repair significantly reduces paraplegia rate after extensive thoracoabdominal aortic aneurysm repair. J Thorac Cardiovasc Surg. 2010;139(6):1464–72.
17. Bischoff MS, Scheumann J, Brenner RM, Ladage D, Bodian CA, Kleinman G, et al. Staged approach prevents spinal cord injury in hybrid surgical-endovascular thoracoabdominal aortic aneurysm repair: an experimental model. Ann Thorac Surg. 2011;92(1):138–46. [Comparative Study Research Support, N.I.H., Extramural]; discussion 46.
18. Strauch JT, Spielvogel D, Lauten A, Zhang N, Shiang H, Weisz D, et al. Importance of extrasegmental vessels for spinal cord blood supply in a chronic porcine model. Eur J Cardiothorac Surg. 2003;24(5):817–24.
19. Harrison SC, Agu O, Harris PL, Ivancev K. Elective sac perfusion to reduce the risk of neurologic events following endovascular repair of thoracoabdominal aneurysms. J Vasc Surg. 2012;55(4):1202–5.
20. Kasprzak PM, Gallis K, Cucuruz B, Pfister K, Janotta M, Kopp R. Editor's choice—temporary aneurysm sac perfusion as an adjunct for prevention of spinal cord ischemia after branched endovascular repair of thoracoabdominal aneurysms. Eur J Vasc Endovasc Surg. 2014;48(3):258–65.
21. Lioupis C, Corriveau MM, Mackenzie KS, Obrand DI, Steinmetz OK, Ivancev K, et al. Paraplegia prevention branches: a new adjunct for preventing or treating spinal cord injury after endovascular repair of thoracoabdominal aneurysms. J Vasc Surg. 2011;54(1):252–7 [Case Reports].
22. Reilly LM, Chuter TA. Reversal of fortune: induced endoleak to resolve neurological deficit after endovascular repair of thoracoabdominal aortic aneurysm. J Endovasc Ther. 2010;17(1):21–9 [Case Reports Research Support, Non-U.S. Gov't].
23. Etz CD, Debus ES, Mohr FW, Kolbel T. First-in-man endovascular preconditioning of the paraspinal collateral network by segmental artery coil embolization to prevent ischemic spinal cord injury. J Thorac Cardiovasc Surg. 2015;149(4):1074–9.
24. Schurink GW, Nijenhuis RJ, Backes WH, Mess W, de Haan MW, Mochtar B, et al. Assessment of spinal cord circulation and function in endovascular treatment of thoracic aortic aneurysms. Ann Thorac Surg. 2007;83(2):S877–81; discussion S90–2.
25. Williams GM, Roseborough GS, Webb TH, Perler BA, Krosnick T. Preoperative selective intercostal angiography in patients undergoing thoracoabdominal aneurysm repair. J Vasc Surg. 2004;39(2):314–21.

Role of Fusion Cone-Beam Computed Tomography Imaging During Complex Aortic Procedures

8

Timothy A. Resch, Per Törnqvist, and Nuno V. Dias

Introduction

Since the introduction of endovascular aneurysm repair (EVAR), imaging has come to play an increasingly important role to guide the treatment of abdominal aortic aneurysms [1]. During the pre- and postoperative imaging phases, thin-slice computed tomographic angiography (CTA) has become the gold standard for planning procedures and evaluating short and long-term outcome. The volume data acquired with a CTA examination is most often transferred into a dedicated imaging workstation where the imaging data can be processed. This allows evaluation using 3D rendering techniques as well as maximum-intensity projections (MIP) and multiplanar reconstructions (MPR) to get detailed picture of the aortic anatomy as well as the different components of an implanted EVAR device. With the increased use of EVAR for complex aortic pathology, including thoracoabdominal aortic aneurysms (TAAA) and aortic dissection (AD), the preoperative planning and postoperative evaluation have become increasingly important.

The rapid development of imaging techniques in the preoperative and postoperative phases has been paralleled by improvement also in intraoperative imaging when performing EVAR. Increasingly, operating rooms are being converted into dedicated hybrid operating rooms combining high-quality intraoperative imaging with high-end angiographic equipment with a fully sterile and functional operating room environment. The versatility of dedicated angiographic systems provides excellent intraoperative fluoroscopic guidance during endovascular procedures in addition to allowing a reduction of contrast and radiation exposure to patients and operators. However, for a number of years, intraoperative imaging was dominated by use of conventional fluoroscopy and angiographic imaging both for guidance and final imaging. In contrast to the advanced 3D techniques in the pre- and postoperative imaging phases, these intraoperative techniques do not fully utilize the full potential of the imaging acquired.

The increasing use of endovascular procedures for complex aortic pathology has raised awareness regarding iodine and radiation exposure to patients and operators and has simultaneously increased the demands further on the intraoperative imaging to detect and prevent endograft failure. This has pushed the development of intraoperative imaging techniques that take advantage of 3D imaging in the intraoperative setting as well.

This chapter aims to describe the current use of intraoperative cross-sectional cone-beam computed tomography (CBCT) as a tool for procedure guidance and evaluation.

Cone-Beam Computed Tomography

CBCT uses the C-arm to provide a CT in the operating room [2, 3]. There are currently four commercially available systems of CBCT: DynaCT (Siemens medical Solutions, Forchheim, Germany), XperCT (Phillips Medical Systems, Eindhoven, The Netherlands), 3D-CT (Toshiba Medical Systems, Edinburgh, UK), and Innova CT (GE Healthcare, Waukesha, Wisconsin, USA). The C-ram is rotated approximately 200° around the patient (Fig. 8.1a) during a single breath-hold. The rotation time, number of projections acquired, image quality, and time required for reconstruction vary depending on the system used. The image acquisition can be performed with or without contrast administered by a coordinated power injector at a preset infusion rate. The acquired image set is automatically transferred to the corresponding post-processing workstation allowing the volume data to be viewed in desired format (axial, MIP, MPR, 3D rendering).

T.A. Resch (✉) • P. Törnqvist • N.V. Dias
Vascular Center, Skane University Hospital,
Ruth Lundskogs gata 10, Malmö 205 02, Sweden
e-mail: timothyresch@gmail.com

© Mayo Foundation for Medical Education and Research 2017

G.S. Oderich (ed.), *Endovascular Aortic Repair*, DOI 10.1007/978-3-319-15192-2_8

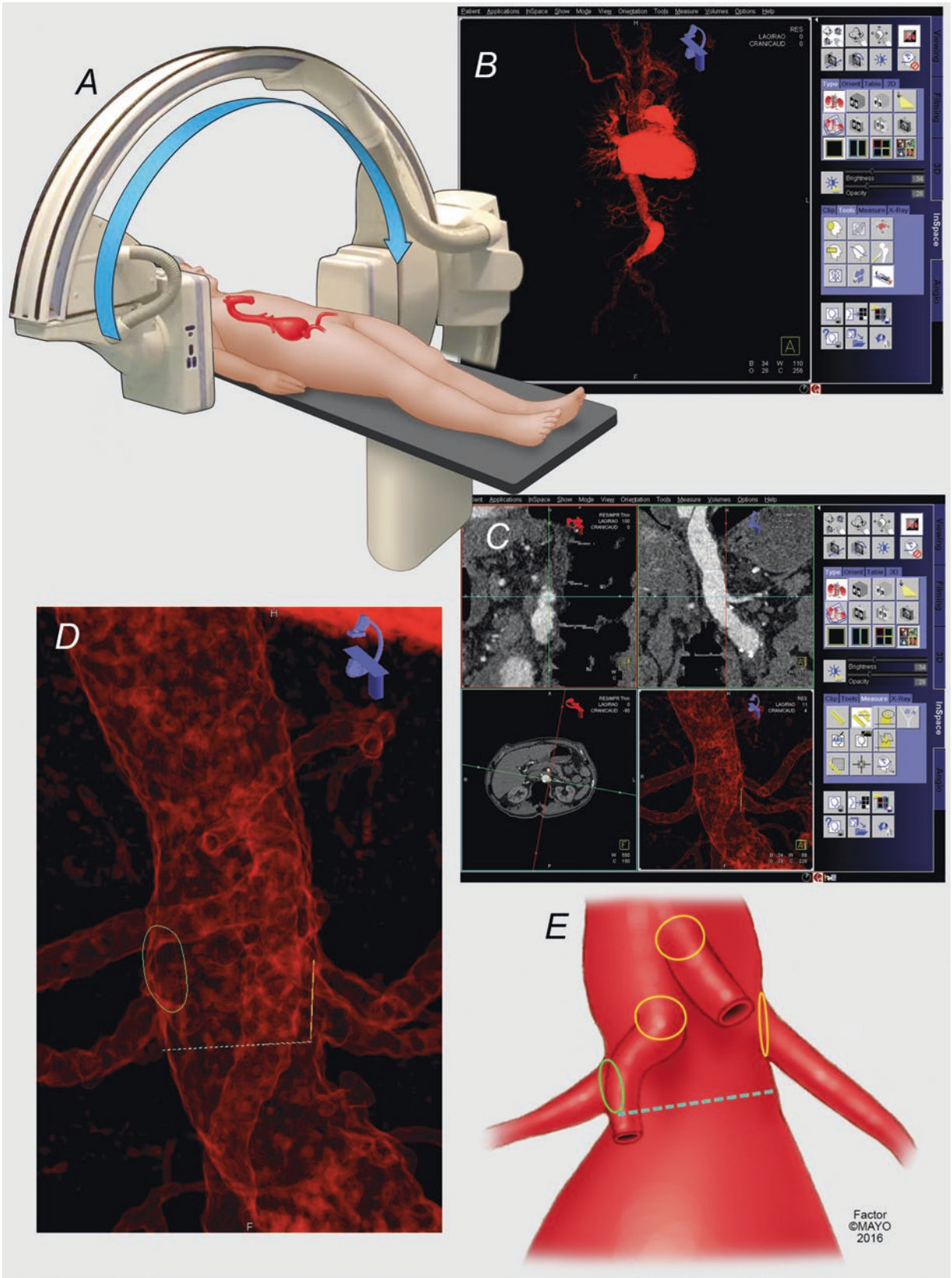


Fig. 8.1 Fusion imaging using the Siemens Zee system is depicted in the illustration. The C-ram is rotated (**a**) to allow creating a template for intraoperative guidance. The CT scans are automatically processed (**b**) using MPR reconstructions (**c**) to outline the branches which are marked with rings (**d**, **e**). By permission of Mayo Foundation for Medical Education and Research. All rights reserved

Fusion Imaging

Fusion imaging involves four steps to achieve optimal intraoperative guidance: processing of preoperative CTA, intraoperative volume acquisition using CBCT, registration of preoperative CTA, and CBCT and intraoperative adjustment.

Processing of Preoperative CTA

The concept of fusion imaging involves using the preoperative imaging (usually CTA data) as a template for intraoperative guidance [4]. The CT scans are automatically processed to obtain a transparent volume rendering reconstruction of the aortic lumen and its side branches (Fig. 8.1b). This can be used directly for the subsequent overlay on the fluoroscopy. However, further post processing can be beneficial. Using MPR reconstructions (Fig. 8.1c) the branch vessels of the aorta are outlined with ring markers. The process of preoperative marking can be performed in advance of the procedure, as it usually requires some time to get an optimal result. Areas of interest can be marked including target vessel origins, the aortic bifurcation, internal iliac bifurcations, as well as planned landing zones for the stent graft (Fig. 8.1d). These markings serve as guides to minimize the use of contrast during the procedure. Placement of a maker ring outlining the aorta immediately below the renal arteries (Fig. 8.1e) is very useful to allow for precise endograft positioning during deployment while avoiding parallax. Even in standard infrarenal EVAR, we find it beneficial to mark the renal arteries, the aortic bifurcation as well as the iliac bifurcations (Fig. 8.2a). Standardized markers can be created for the arch, visceral, iliac, and infrarenal segments (Fig. 8.2b–e).

Intraoperative Volume Acquisition: CBCT

Once the patient is placed on the operating table a CBCT run without contrast is performed. The CBCT images are then transferred to the workstation and used to register the intraoperative imaging onto the processed, preoperative CT data with markers. The fusion process can also be achieved by using a 2D registration of bony landmarks only utilizing an anterio-posterior and lateral single fluoroscopic image (so-called 2D to 3D registration). The latter will reduce the overall radiation exposure compared to using CBCT. As the 2D-3D fusion is not yet widely available and approved on all systems, the process described in this chapter will refer to 3D-3D fusion.

Registration of Preoperative CTA and CBCT

Figure 8.3 depicts the CBCT acquired volume seen as a white box overlay on the preoperative CTA. Note that the CBCT acquired volume is significantly smaller than the preoperative CTA volume. This is due to the fact that the CBCT acquired volume is limited by the size of the image intensifier on the angiographic system. In most systems, a volume of about 25 cm length cranio-caudal can be obtained, which is usually sufficient to cover an area from the above the visceral arteries down to the iliac bifurcations. However, since the registration process relies on the alignment of the bony structures, it is usually beneficial to include the distal lumbar and upper pelvis in the CBCT. The overlay is projected over the CTA volume in lateral, AP and axial projections. As is seen in Fig. 8.3a (lower right panel) the imported overlay has been automatically placed much to cephalad in relation to the preoperative CTA. By using the automatic registration feature in the software (Fig. 8.3b–d), a reasonable match can often be achieved within seconds. Once the top of the pelvic bones and lumbar vertebrae are almost in perfect alignment, the arterial anatomy is aligned with the preoperative CTA imaging to allow fusion. Further refinement is achieved by manual matching of bony landmarks as well as identifying markers of the aorta such as calcium deposits in the aortic wall or branch vessel orifices (3D-to-3D registration) as depicted in Fig. 8.4a, which shows the overlay in an AP view where calcium deposits in the aortic wall do not exactly match those of the preoperative CTA. By manually adjusting the overlay a perfect match can be achieved in all planes (Fig. 8.4b).

Intraoperative Adjustment

Once the process of registration and marking is done, the processed dataset can be used to aid intraoperative navigation and vessel deployment. An issue that must not be overlooked is the possibility for a mismatch in registration intraoperatively caused by the introduction of the stent graft in the aorta as well as the patient's different position between the CBCT (arms down) compared to the CTA (arms above the head). Moreover, there is also the possibility of patient movement on the table after the intraoperative volume has been acquired. The former has been studied in the clinical setting and it has indeed been shown that there is a significant displacement of the main aortic branches after insertion of rigid materials into the aorta [5, 6]. Thus, the fusion application must be designed to allow for both control and adjustment of the overlay during the aortic procedure.

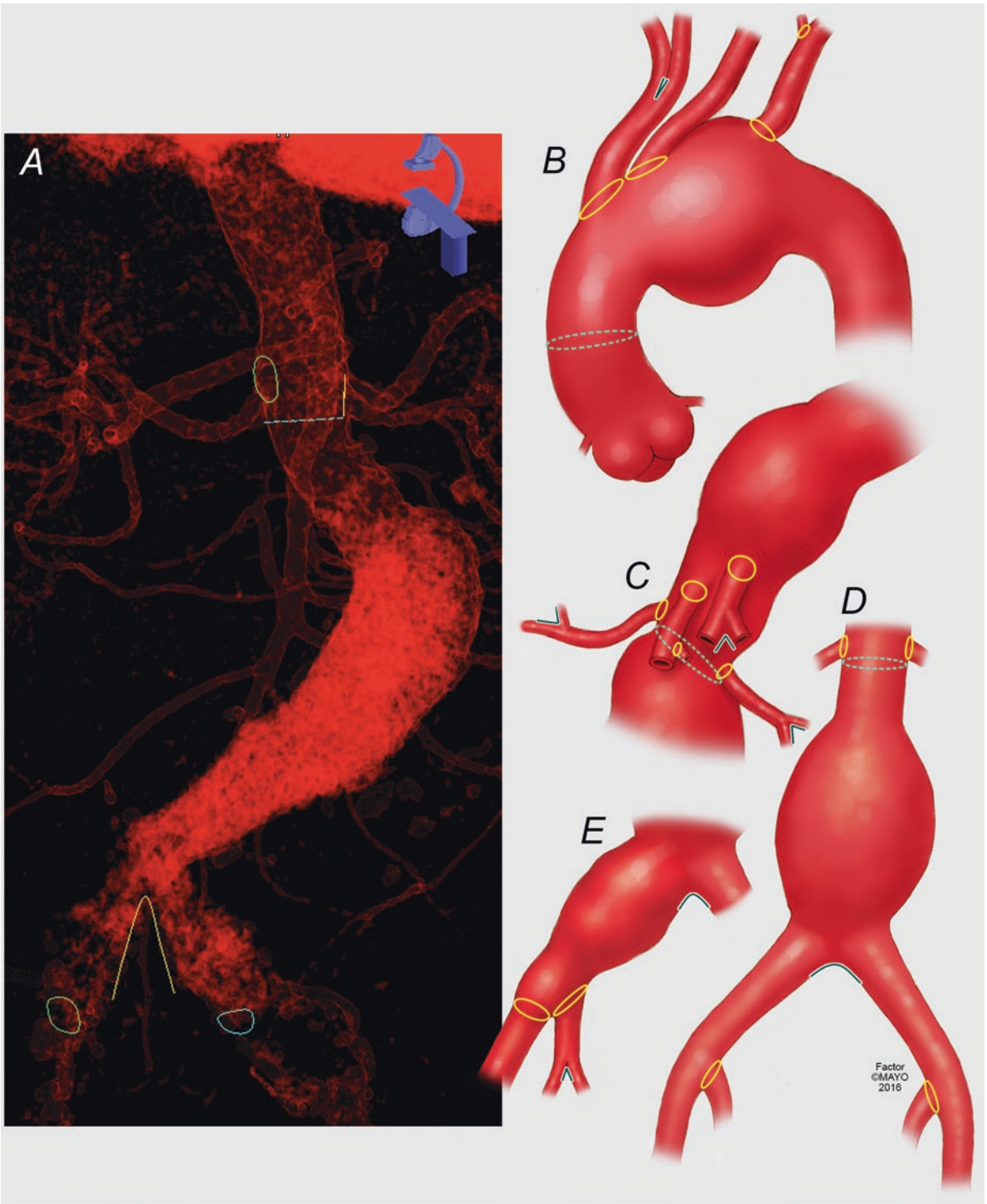


Fig. 8.2 Markers used for standard EVAR (**a**) and for procedures involving the arch (**b**), visceral (**c**), iliac (**d**), and infrarenal segments (**e**). By permission of Mayo Foundation for Medical Education and Research. All rights reserved

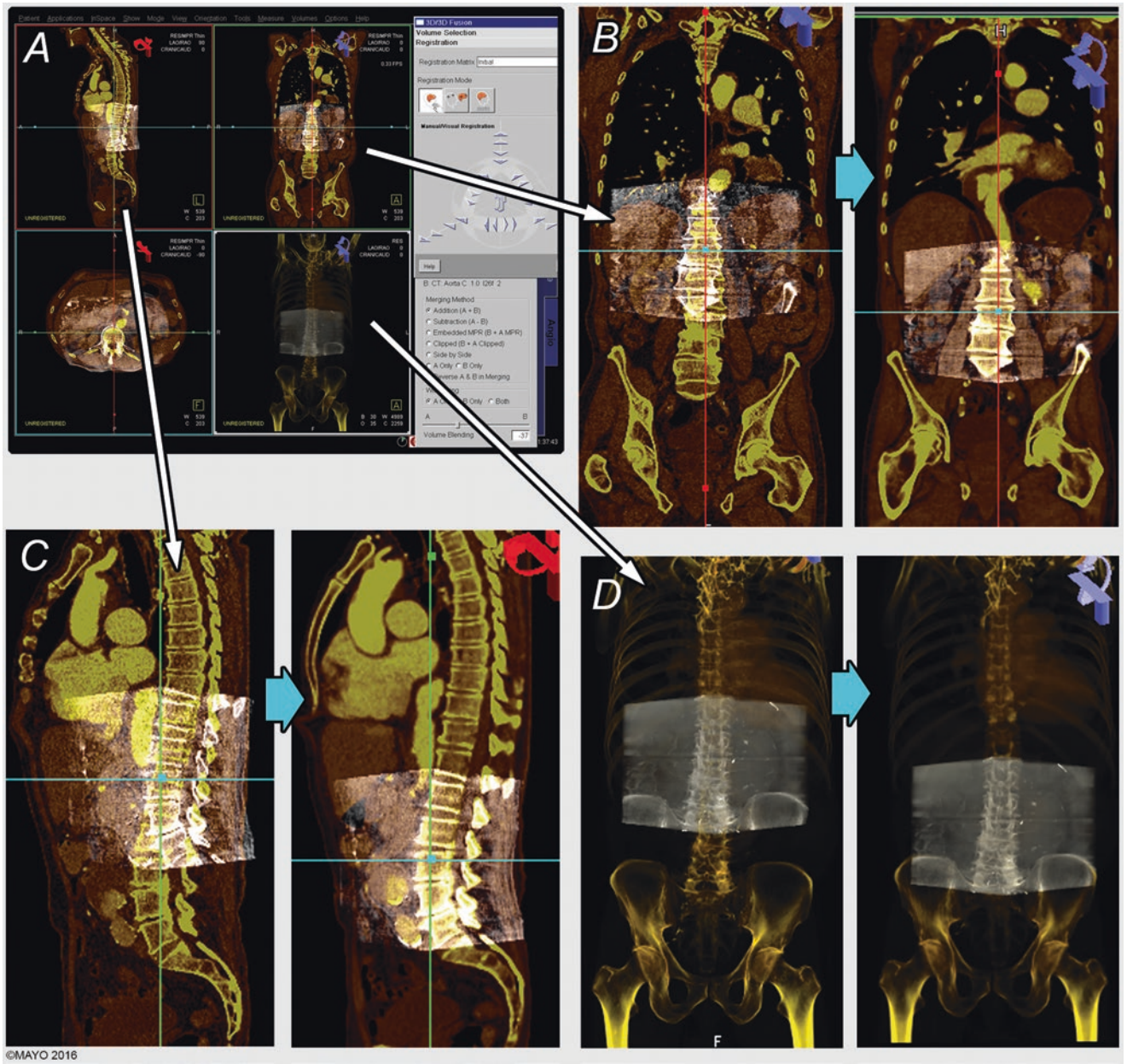


Fig. 8.3 CBCT acquired volume is significantly smaller than the preoperative CTA volume (**a**). Since the registration process relies on the alignment of the bony structures it is usually beneficial to include the distal lumbar and upper pelvis in the CBCT (**b**). The overlay is projected over the CTA volume in lateral (**c**), AP (**d**) and axial projections. A reasonable match can often be achieved within seconds. By permission of Mayo Foundation for Medical Education and Research. All rights reserved

It is advisable to perform a control of the fusion even before the endograft has been inserted, to allow for positioning of the graft. One way of achieving this is to place a marking catheter in one or two of the target vessels to determine if the placements of the ring markers are correct. Figure 8.5a shows a patient treated for type 3 TAAA using a two-stage approach. In the first stage, the patient was treated by a proximal TEVAR stent graft that was placed under fusion guidance (Fig. 8.5b), which allowed location of the left subclavian artery orifice (*yellow ring marker*) and intended distal landing zone (*turquoise ring*). During the second stage (Fig. 8.5c), which was performed 2 weeks later, the thoracoabdominal repair was completed using image fusion of the visceral segment of the aorta to locate the target vessels. Marker rings are placed for the celiac artery (*upper green ring*), the celiac artery division (*yellow line*), superior mesenteric artery (*yellow ring*), the main right renal artery (*purple ring*), left renal artery (*blue ring*), and a small polar right renal artery (*lower green ring*). The latter was planned for intraoperative embolization. Note

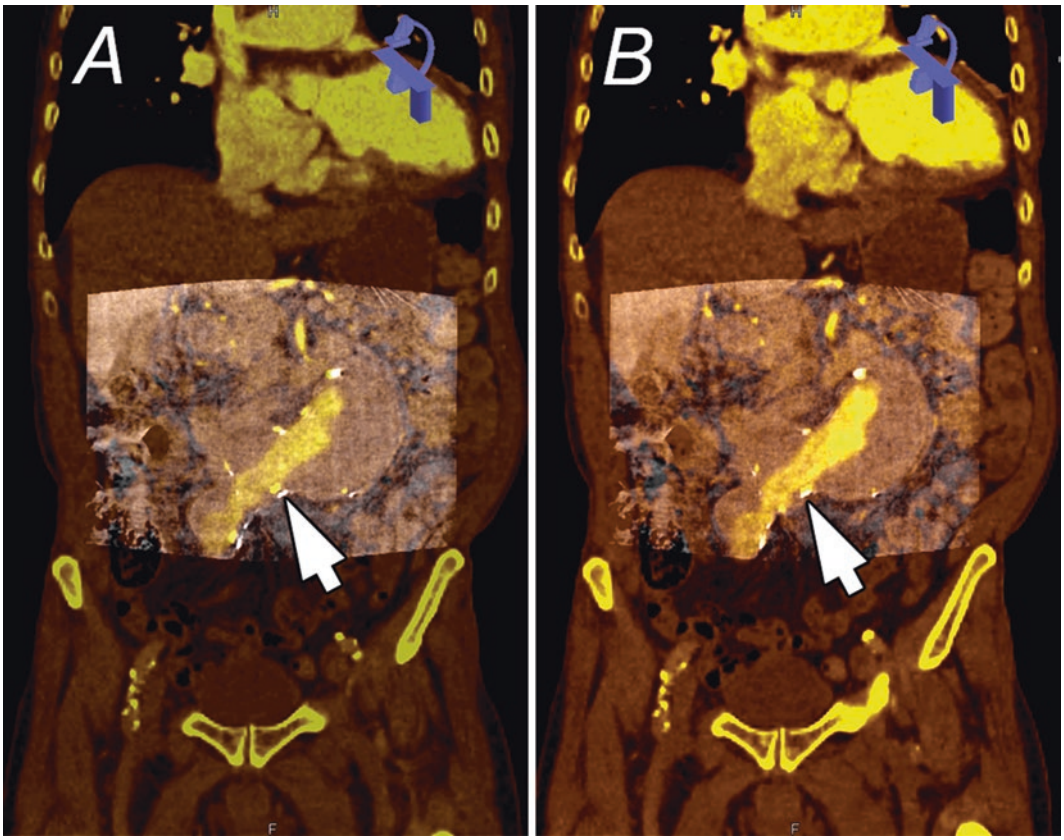


Fig. 8.4 Further refinement is achieved by manual matching of bony landmarks as well as identifying markers of the aorta such as calcium deposits (**a**, *white arrow*). By manually adjusting the overlay a perfect match can be achieved in all planes (**b**). By permission of Mayo Foundation for Medical Education and Research. All rights reserved

that CO_2 is used to provide an angiogram to determine if the placement of the rings is correct. The TAAA stent-graft containing two visceral branches and two renal fenestrations is then placed with marker guidance only (Fig. 8.6a, b). This allows for both longitudinal and rotational adjustment of the graft during deployment without the use of contrast. After the stent graft has been fully deployed, the ring markers are used to guide the catheterization of the target vessels (Fig. 8.6c), as noted by the lateral fluoroscopic projection of the deployed stent graft. Mating stents have been placed in the renal arteries (blue and purple rings) and the SMA (yellow ring). The celiac artery orifice is marked with a green ring and the celiac bifurcation marked with an orange line to allow for precise placement of the mating stent. The sheath in the celiac branch as well as the wire in the celiac artery is clearly seen but note how the stiff wire in the artery deflects the orifice from the green ring marker. Moreover, the breathing-related movements of the distal part of the visceral arteries cannot be compensated in the dynamic overlay of the fusion, but the relative relationship is quite constant. Figure 8.7 illustrates another example where CO_2 angiography is used to adjust the fusion overlay after the stent-graft has been introduced into position, which is currently our preferred option. Initial angiography (Fig. 8.7a) demonstrates the purple ring and line have been placed at the celiac artery origin and division respectively whereas the yellow ring marks the SMA orifice. After correct adjustment of position (Fig. 8.7b) CO_2 angiography confirms that the ring markers are in the correct position. Finally, the fusion overlay (Fig. 8.8) can be used to correct for parallax during deployment of the stent graft. Significant cranial angulation (Fig. 8.8a) is noted by misalignment of the red marker. After C-arm rotation the aortic ring is seen as a perpendicular ring indication a correct view without parallax (Fig. 8.8b, c). The fenestrated stent graft is again positioned using marker guidance only (Fig. 8.8c) and all four target vessels can be catheterized successfully (Fig. 8.8d). In some instances it can also be useful to add the full fusion overlay (Fig. 8.9) to see not only the orifices of the target vessels but also their specific anatomic characteristics to help catheterization. The overlay can be faded in and out on the live fluoroscopic image during navigation. However, we most often we prefer to overlay only the markers in order to avoid any shadowing of the fluoroscopy by the overlay of the 3D volume, which in turn allows the use of even lower dose fluoroscopy.

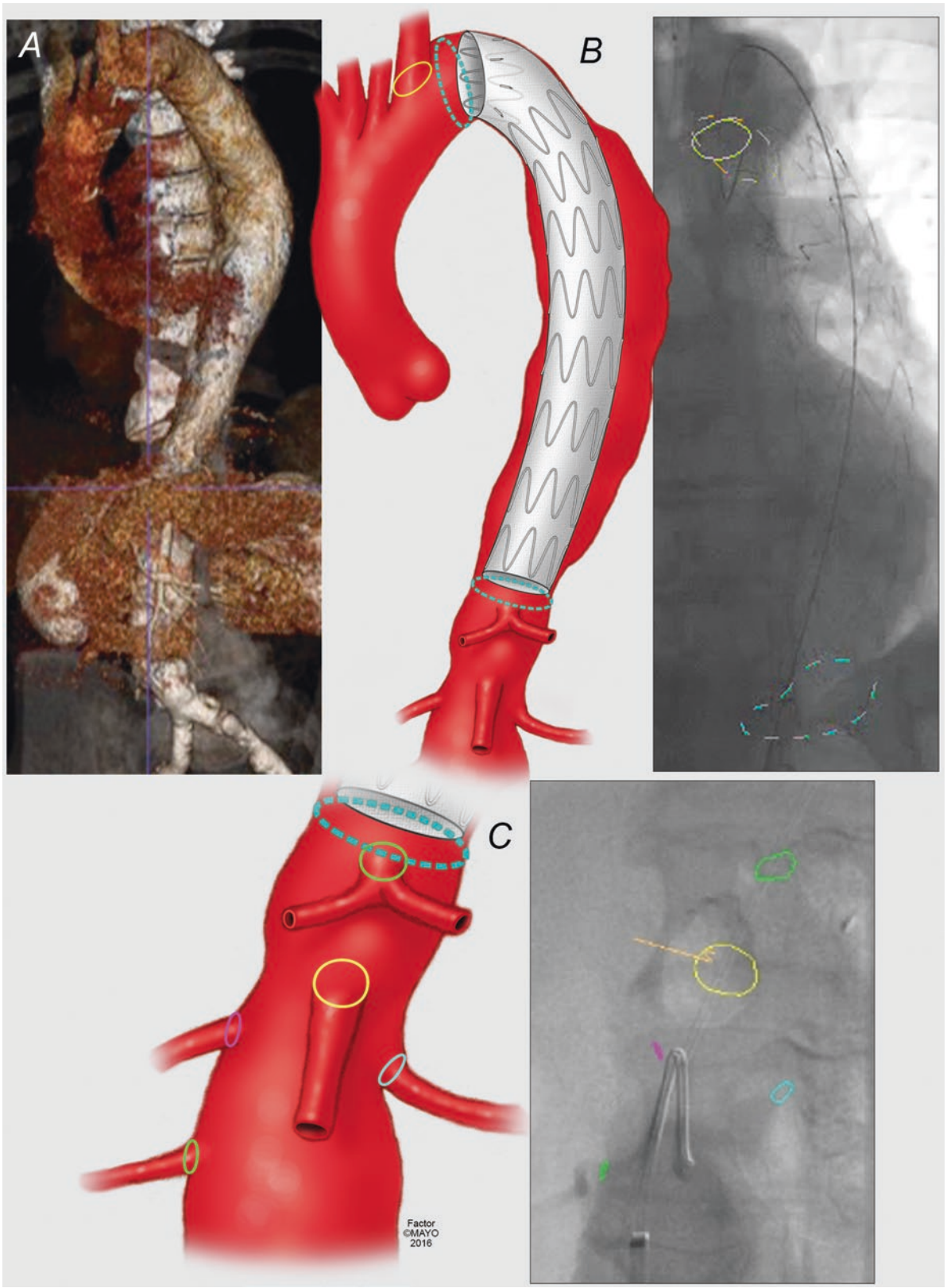


Fig. 8.5 Patient treated for type 3 TAAA (**a**) using a two-stage approach, first with proximal TEVAR stent graft (**b**) and as a second stage (**c**) with visceral branches. By permission of Mayo Foundation for Medical Education and Research. All rights reserved

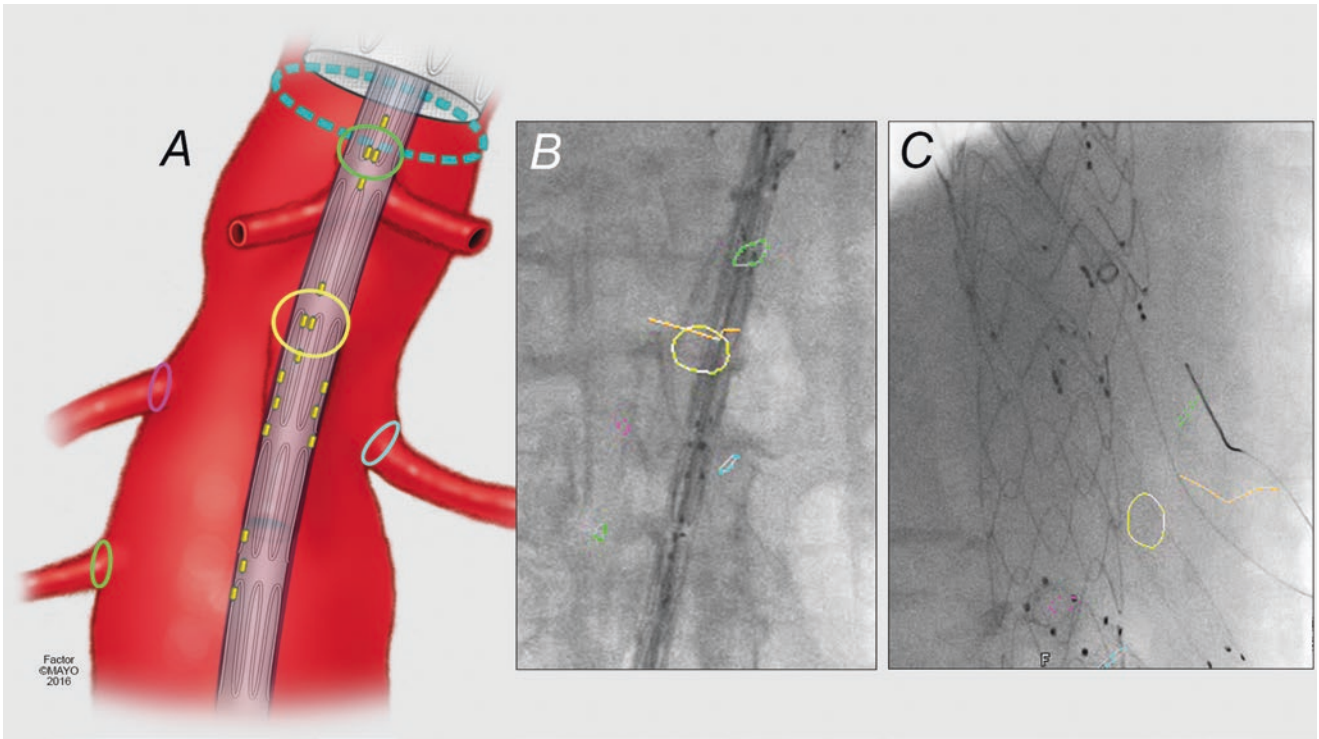


Fig. 8.6 TAAA stent graft is deployed using the markers (**a**) without the use of contrast (**b**). After deployment (**c**), ring markers are used to guide the catheterization. By permission of Mayo Foundation for Medical Education and Research. All rights reserved

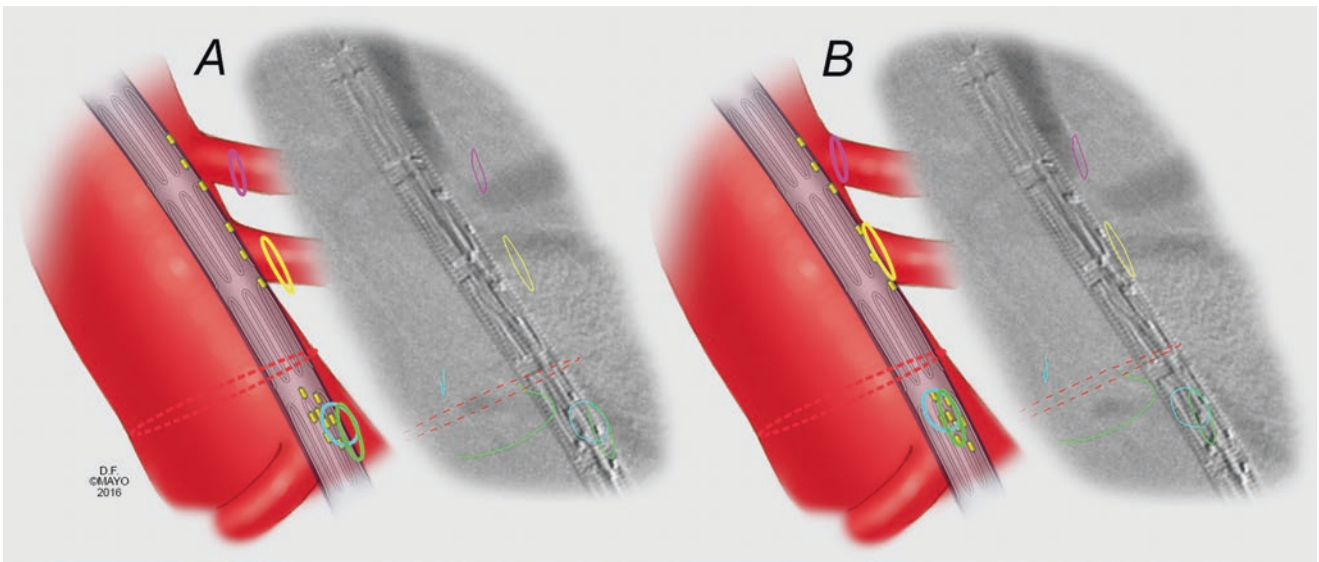


Fig. 8.7 CO_2 angiography (**a**) is used to adjust the fusion overlay. After correct adjustment of position (**b**) CO_2 angiography confirms that the ring markers are in the correct position. By permission of Mayo Foundation for Medical Education and Research. All rights reserved

CBCT for Intra-procedural Evaluation

Traditionally, intraoperative angiography has been the imaging of choice to evaluate the final operative result after EVAR. In the setting of standard infrarenal EVAR this is often sufficient. However, multiple projections of the treated segment might be required to properly evaluate both the integrity of the iliac limbs and the origins of possible endoleaks. This requires multiple contrast injections that obviously increase the overall contrast load of the procedure and can

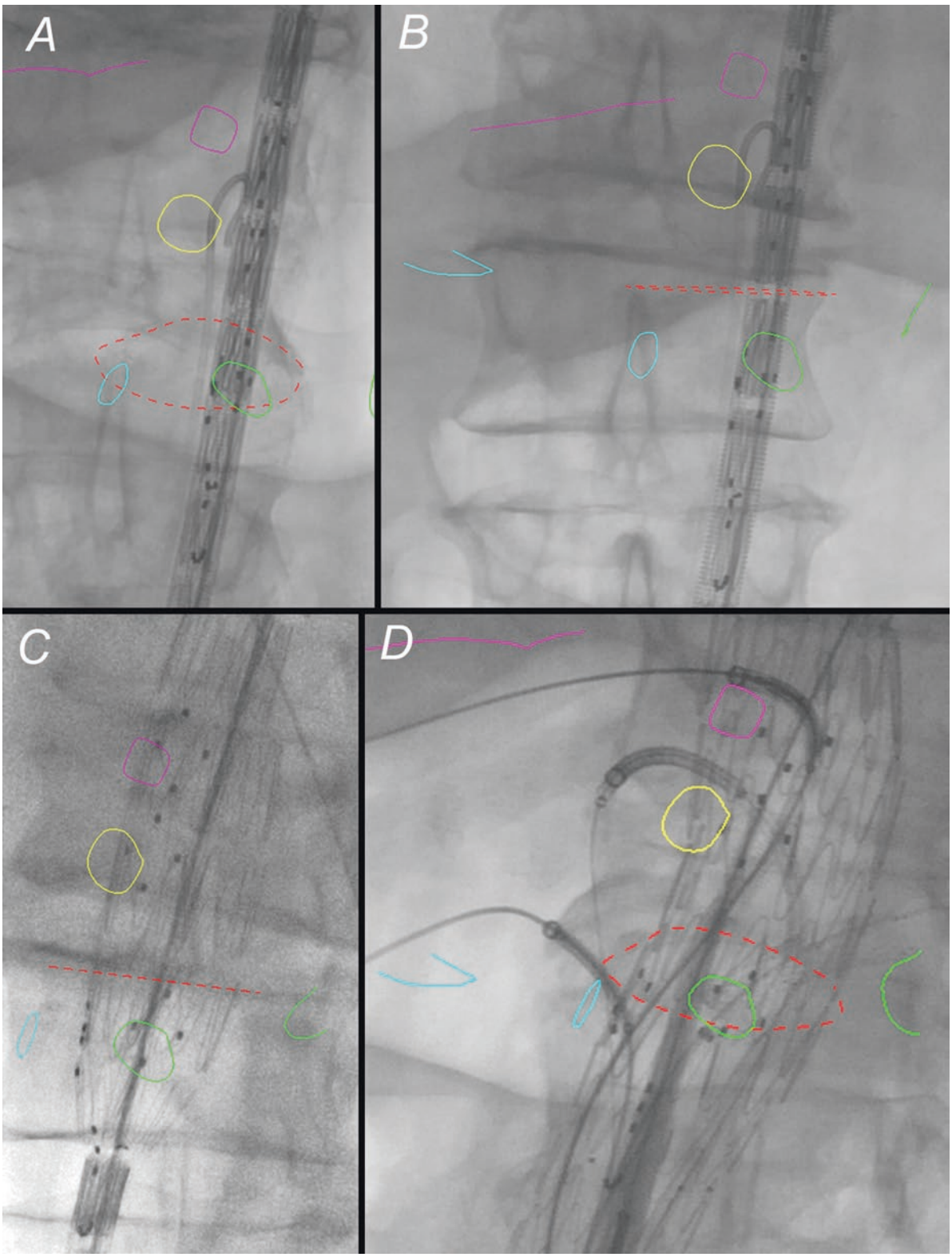


Fig. 8.8 Fusion overlay can be used to correct for parallax, noted by misalignment of the red marker (**a**), which is corrected without parallax (**b**). The fenestrated stent graft is again positioned using marker guidance only (**c**) and all four target vessels can be catheterized successfully (**d**)

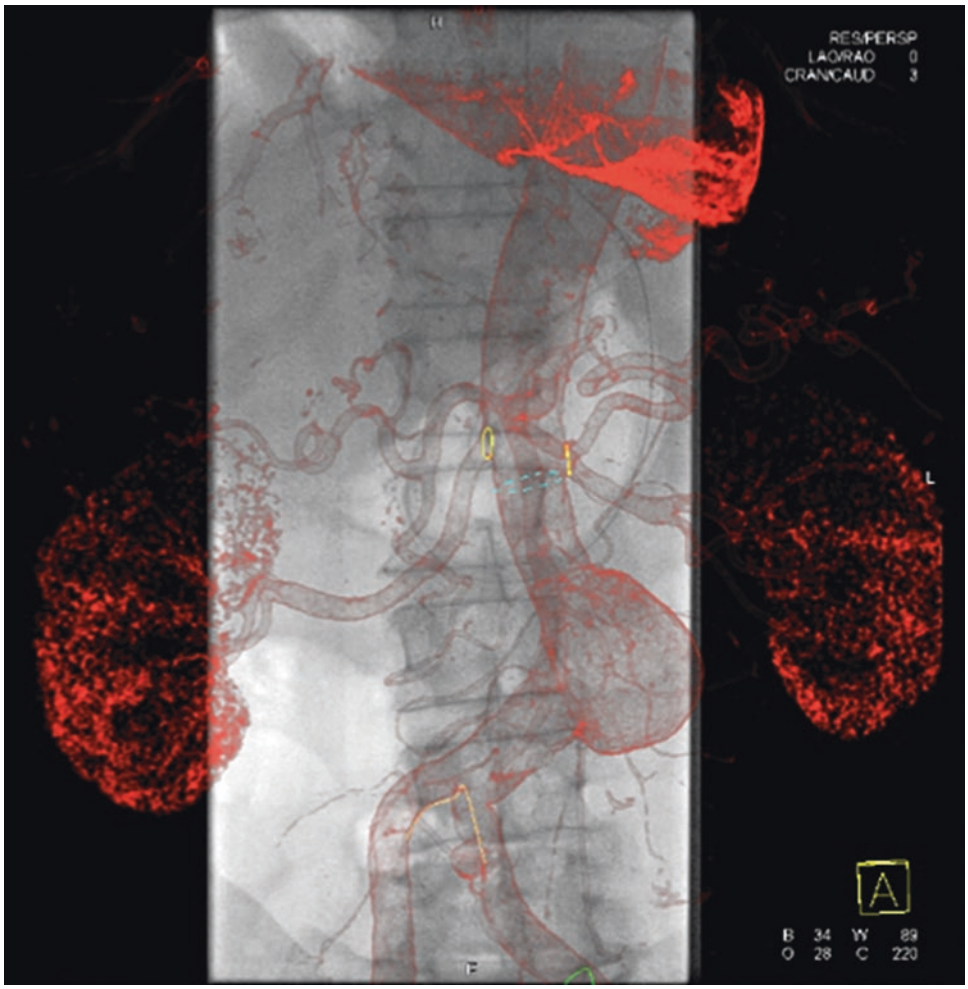


Fig. 8.9 Fusion overlay and markers. By permission of Mayo Foundation for Medical Education and Research. All rights reserved

have detrimental effect on renal function. In situations where the intraoperative angiography is inconclusive, a common practice is to perform a pre-discharge CTA to properly evaluate the operative result. Indeed, many protocols still mandate a pre-discharge CTA regardless of the perioperative findings. Unfortunately, a significant finding on postoperative CTA, will necessitate a return to the operating theater or angiosuite for an adjunctive procedure.

With the introduction of complex EVAR this situation becomes even more relevant as the multitude of branches, fenestrations, and mating stents make the perioperative evaluation with angiography even more cumbersome. This pitfall with final angiography is clearly reflected in a very high number of early adjunctive procedures occurring after EVAR.

CBCT has the potential to overcome some of these issues as it offers an intraoperative evaluation producing volumetric data that can be reformatted and analyzed in a workstation before the patient leaves the operating room [6]. Thus, additional procedures such as balloon angioplasty and stent extensions can be performed in the same setting, limiting the need to bring the patient back to the operating room in the early postoperative phase [7, 8]. A final angiography can sometimes have difficulties detecting stenoses in the iliac limbs of an EVAR and multiple projections can be necessary to determine if a there is significant limb compression. CBCT is superior in detecting these lesions and may reveal a compressed iliac limb, prompting immediate intervention. Further reconstructions can be made directly in the operating room or after exporting the DICOM dataset to a dedicated 3D workstation. The technique for performing CBCT as a final control is identical to that used for the 3D-3D fusion described above. The examination can be used with or without contrast enhancement depending on the clinical situation. Obviously, contrast is required to see any endoleaks, but in situations where contrast use is contraindicated, CBCT without contrast can still be a valuable adjunct to detect kinks or compressions of limbs or mating stents.

Sometimes an endoleak is seen on final angiography (Fig. 8.10a) and CBCT can be used to make a closer characterization of that particular endoleak and its origin (Fig. 8.10b). Whereas angiography demonstrates endoleak in the proximal portion of the stent graft it remains unclear whether this is a type 1 or type 2 endoleak. Further decision regarding treatment relies

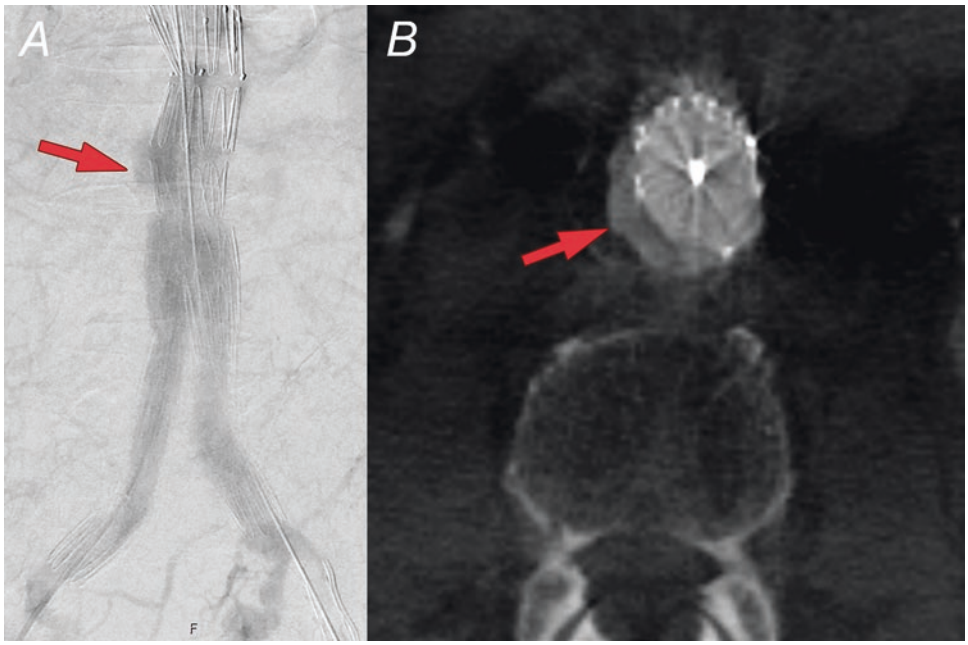


Fig. 8.10 Endoleak seen on final angiography (**a**, *red arrow*) and by CBCT (**b**). By permission of Mayo Foundation for Medical Education and Research. All rights reserved

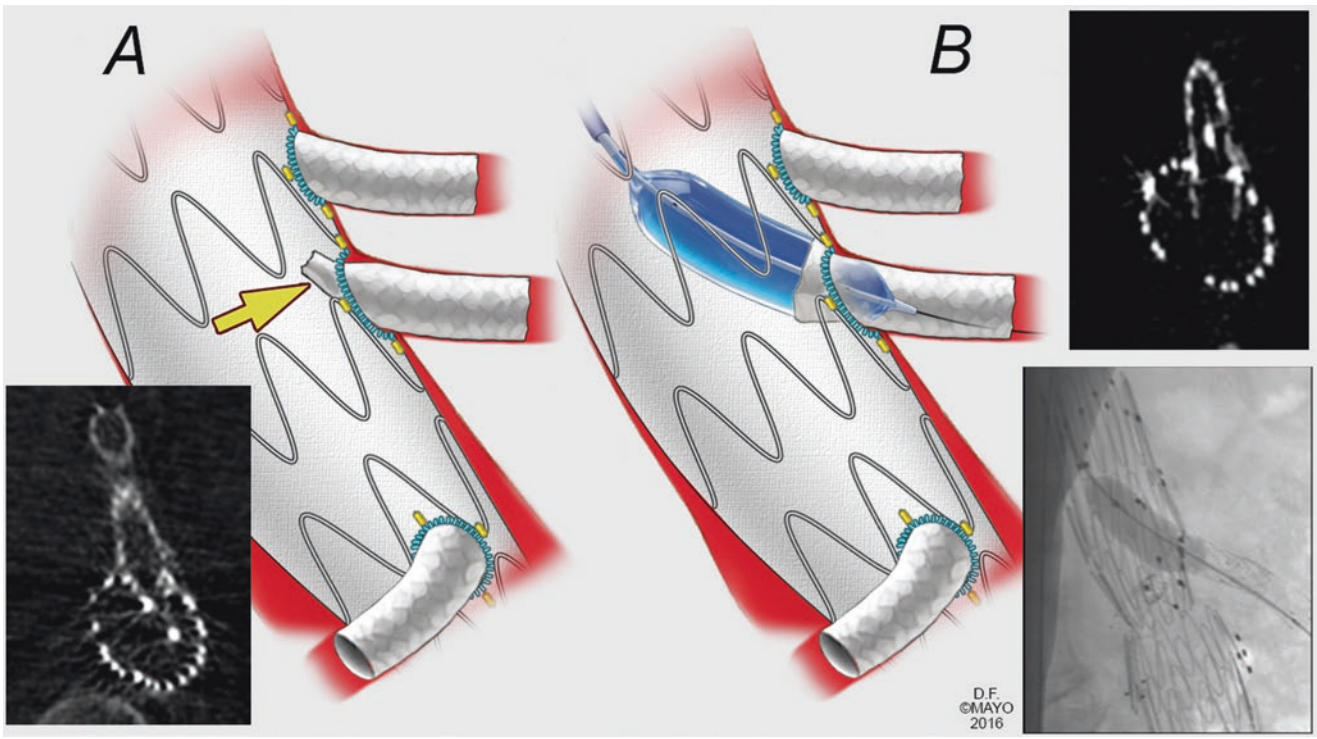


Fig. 8.11 CBCT intraoperatively reveals significant stent compression (**a**), which is immediately resolved by simple balloon angioplasty (**b**). By permission of Mayo Foundation for Medical Education and Research. All rights reserved

heavily on this information. In the illustration, the CBCT demonstrates a proximal type 1 endoleak, which requires immediate treatment.

The integrity of mating stents in fenestrated and branched stent-grafts is perhaps the most difficult to detect on plain films and angiography. A completely normal angiography following placement of a stent-graft with fenestrations for the SMA and both renal arteries shows good flow to all target vessels and no evidence of endoleaks. A CBCT intraoperatively reveals significant compression of the portion of the SMA stent protruding into the main aortic endograft (Fig. 8.11a). This compression could be immediately

resolved by simple balloon angioplasty (Fig. 8.11b). The control CBCT without contrast shows that the compressed SMA stent has been fully opened by the angioplasty.

Conclusion

Imaging plays a pivotal role in all phases of EVAR planning, delivery and follow-up. Whereas advanced imaging applications have become routine for the planning and follow-up phases after complex EVAR procedures in particular, angiography and fluoroscopy have remained the intraoperative imaging techniques of choice for many years. The introduction of advanced intraoperative imaging for guidance and procedural control has the potential to reduce perioperative use of contrast and radiation, improve intraoperative success, and reduce the need for postoperative secondary interventions [2–4, 8–11]. The use of these techniques requires advanced imaging equipment in the operating room.

References

1. Tornqvist P, Dias NV, Resch T. Optimizing imaging for aortic repair. J Cardiovasc Surg (Torino). 2015;56(2):189–95.
2. Dijkstra ML, Eagleton MJ, Greenberg RK, Mastracci T, Hernandez A. Intraoperative C-arm cone-beam computed tomography in fenestrated/branched aortic endografting. J Vasc Surg. 2011;53(3):583–90.
3. Tornqvist P, Dias N, Sonesson B, Kristmundsson T, Resch T. Intra-operative cone beam computed tomography can help avoid reinterventions and reduce CT follow up after infrarenal EVAR. Eur J Vasc Endovasc Surg. 2015;49(4):390–5.
4. Tacher V, Lin M, Desgranges P, Deux JF, Grunhagen T, Becquemin JP, et al. Image guidance for endovascular repair of complex aortic aneurysms: comparison of two-dimensional and three-dimensional angiography and image fusion. J Vasc Interv Radiol. 2013;24(11):1698–706. Pubmed Central PMCID: 3888792.
5. Maurel B, Hertault A, Gonzalez TM, Sobocinski J, Le Roux M, Delaplace J, et al. Evaluation of visceral artery displacement by endograft delivery system insertion. J Endovasc Ther. 2014;21(2):339–47.
6. Kauffmann C, Douane F, Therasse E, Lessard S, Elkouri S, Gilbert P, et al. Source of errors and accuracy of a two-dimensional/three-dimensional fusion road map for endovascular aneurysm repair of abdominal aortic aneurysm. J Vasc Interv Radiol. 2015;26(4):544–51.
7. Biasi L, Ali T, Hinchliffe R, Morgan R, Loftus I, Thompson M. Intraoperative DynaCT detection and immediate correction of a type Ia endoleak following endovascular repair of abdominal aortic aneurysm. Cardiovasc Intervent Radiol. 2009;32(3):535–8.
8. Biasi L, Ali T, Ratnam LA, Morgan R, Loftus I, Thompson M. Intraoperative DynaCT improves technical success of endovascular repair of abdominal aortic aneurysms. J Vasc Surg. 2009;49(2):288–95.
9. Hertault A, Maurel B, Sobocinski J, Martin Gonzalez T, Le Roux M, Azzaoui R, et al. Impact of hybrid rooms with image fusion on radiation exposure during endovascular aortic repair. Eur J Vasc Endovasc Surg. 2014;48(4):382–90.
10. Maurel B, Hertault A, Sobocinski J, Le Roux M, Gonzalez TM, Azzaoui R, et al. Techniques to reduce radiation and contrast volume during EVAR. J Cardiovasc Surg (Torino). 2014;55(2 Suppl 1):123–31.
11. McNally MM, Scali ST, Feezor RJ, Neal D, Huber TS, Beck AW. Three-dimensional fusion computed tomography decreases radiation exposure, procedure time, and contrast use during fenestrated endovascular aortic repair. J Vasc Surg. 2015;61(2):309–16. Pubmed Central PMCID: 4308450.

3D Printing to Create Templates for Patient-Specific Fenestrated Stent Grafts

9

Benjamin W. Starnes and Daniel F. Leotta

Introduction

Physician-modified endovascular grafts (PMEGs), with fenestrations added to accommodate major branch vessels, provide a means for endovascular treatment of juxta-renal abdominal aortic aneurysms. Manual measurements of vessel origin locations from computed tomography images, however, take time and can lead to errors in the positions of the fenestrations. To make the fenestration process faster and more accurate, we have developed a procedure to create custom templates that serve as patient-specific guides for graft fenestration. We use a three-dimensional printer to create a clear rigid sleeve that replicates the patient's aorta and includes holes placed precisely at the locations of the branch vessels. The sleeve is placed over the graft, the locations of the openings are marked with a sterile pen, and the fenestrations are created after the sleeve is removed. Custom fenestration templates can potentially save procedural costs and make minimally invasive aortic aneurysm repair available to many more patients.

Minimally invasive endovascular repair of abdominal aortic aneurysms (AAAs) has been shown to reduce morbidity and mortality associated with open repair [1]. Unfortunately, a large percentage of patients presenting with AAAs are not candidates for endovascular repair [2]. The reasons for exclusion predominantly involve lack of a healthy suitable proximal aortic neck, which is required for stable fixation without covering major branch vessels. Multibranched or fenestrated endografts [3–5] offer one solution to this problem but generally with increased costs and long manufacture/delivery times.

On-site physician modification of endovascular grafts for branch vessel preservation is an alternative treatment strategy for juxta-renal AAAs [6, 7]. In these cases, fenestrations are added to standard commercial stent grafts to accommodate patient-specific vessel origin sites. The opening locations are determined from the vessel origins visualized in computed tomography (CT) images. Longitudinal distances are measured on the graft, and the relative angular locations are specified as "clock" positions relative to a reference point. However, potential barriers to wider use of physician-modified endovascular grafts are (1) preoperative planning time for measuring the fenestration locations from CT data, (2) time in the operating room required to map the opening locations on the endograft, (3) accuracy of the placement of the openings, and (4) optimum location of all openings to avoid stent struts. To address these issues, we have developed a method to create patient-specific fenestration templates that allow for faster and more accurate endograft modification.

3D Printing Methodology

We use a patient's CT image data to create a three-dimensional (3D) printed rigid sleeve that replicates the proximal neck of the subjects aorta, including openings at the locations of the branch vessel origins. The creation of a custom fenestration template for a patient with a juxta-renal AAA is presented in Figs. 9.1, 9.2, and 9.3. This is performed under a protocol approved by the University of Washington Institutional Review Board and with the patient's informed consent.

B.W. Starnes (✉)
Division of Vascular Surgery, Department of Surgery, University of Washington, 325 Ninth Avenue, Seattle, WA 98104, USA
e-mail: starnes@uw.edu

D.F. Leotta
Applied Physics Laboratory, University of Washington, Box 355640, Seattle, WA 98195, USA
e-mail: leotta@uw.edu

© Mayo Foundation for Medical Education and Research 2017

G.S. Oderich (ed.), *Endovascular Aortic Repair*, DOI 10.1007/978-3-319-15192-2_9

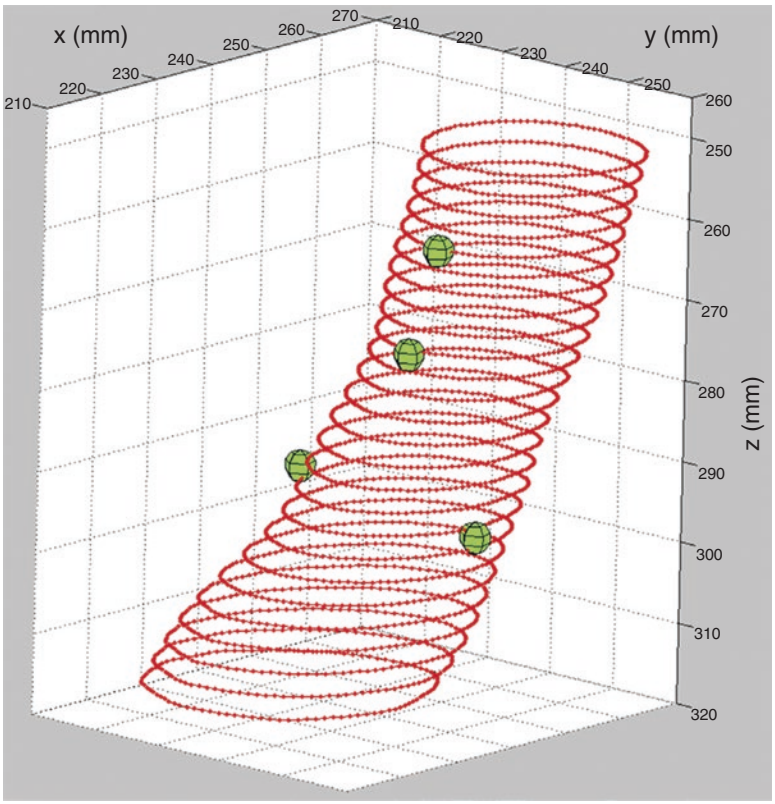


Fig. 9.1 Three-dimensional (3D) display of the traced lumen contours of the abdominal aortic aneurysm (AAA) proximal neck for the demonstration data set. The branch vessel origin locations are displayed as spheres. Reprinted from Journal of Vascular Surgery, 61(6), Leotta DF, Starnes BW, Custom fenestration templates for endovascular repair of juxtarenal aortic aneurysms, 1637–41, Copyright 2015, with permission from Elsevier

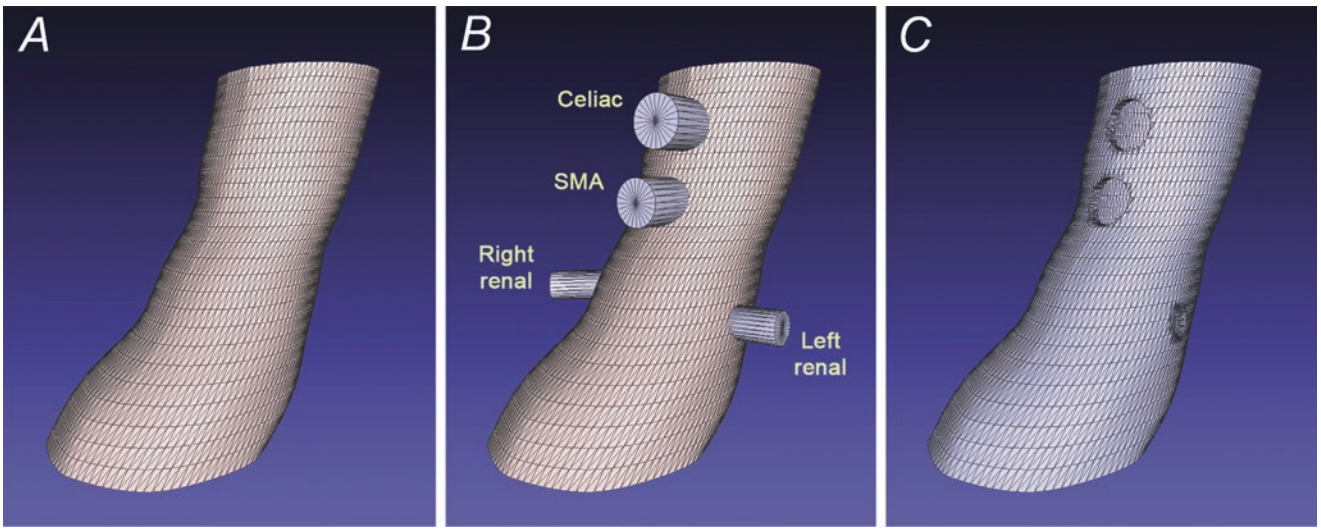


Fig. 9.2 Fenestration template computer-assisted design model. The lumen contours shown in Fig. 9.1 were converted to a solid model format compatible with a three-dimensional (3D) printer. (**a**) Polygon model of the aneurysm proximal neck. (**b**) Combined display of the proximal neck model and cylinders at each of the branch vessel origins. The cylinder diameters are set to match the branch vessel opening diameters as measured from the original computed tomography (CT) images. *SMA* superior mesenteric artery. (**c**) The result of the Boolean difference between the proximal neck object and each cylinder is a hole in the aorta model at the location of each of the branch vessel origins. Reprinted from Journal of Vascular Surgery, 61(6), Leotta DF, Starnes BW, Custom fenestration templates for endovascular repair of juxtarenal aortic aneurysms, 1637–41, Copyright 2015, with permission from Elsevier



Fig. 9.3 Three-dimensional (3D)-printed fenestration template. (**a**) Computer model of the template. (**b**) Solid printed model of the template created using a stereolithography 3D printer with clear resin. (**c**) An endovascular graft inserted in the template. A reprinted from Journal of Vascular Surgery, 61(6), Leotta DF, Starnes BW, Custom fenestration templates for endovascular repair of juxtarenal aortic aneurysms, 1637–41, Copyright 2015, with permission from Elsevier. B and C by permission of Mayo Foundation for Medical Education and Research. All rights reserved

A custom software developed at the University of Washington Cardiovascular Research and Training Center outlines the aorta in a patient's CT image data set [8, 9]. The aorta lumen is manually traced, and point markers are placed at specific 3D locations to indicate the origins of the branch vessels (Fig. 9.1).

Next, custom software [10] developed in the MATLAB programming environment (The MathWorks, Natick, MA) is used to convert the lumen outlines into a computer model that defines a sleeve whose inner surface represents the aorta lumen (Fig. 9.2a). The holes at the locations of the branch vessels are created by first constructing cylindrical objects in 3D space that are centered at the branch origin points (Fig. 9.2b). Rhinoceros 5 computer-aided design software (Robert McNeel & Associates, Seattle, WA) is then used to subtract the sections of the aorta mesh that are intersected by the cylinders, effectively "punching holes" in the aorta mesh model. The result is a computer mesh model with openings at the branch vessel origin locations (Fig. 9.2c).

Finally, a stereolithography 3D printer (4D Parts Direct, Broadview Heights, Ohio) is used to produce a clear rigid sleeve that includes holes placed precisely at the locations of the branch vessels (Fig. 9.3). The clear printing material allows visualization of the stent struts during positioning of the graft in the template (Fig. 9.3c).

This template-based fenestration procedure was validated by deploying a custom fenestrated graft in an aorta phantom. The phantom was created by embedding a commercially available flexible AAA model (Aortic Aneurysm 1808-2; Pacific Research Laboratories, Vashon Island, WA) in an agar block (Fig. 9.4a, b). The phantom was scanned by CT (Fig. 9.4c), and a template was designed and printed to match the four branch vessels. This custom template was used to create fenestrations in a standard Zenith Flex endovascular graft (Cook Medical, Bloomington, Indiana). The sleeve was slipped over the unsheathed graft and rotated to optimize the positions of the holes relative to the stent struts. The locations of the openings were marked with a pen (Fig. 9.5a), and the fenestrations were cut with an electrocautery device after the sleeve was removed (Fig. 9.5b). The graft was resheathed and then deployed in the phantom under visual guidance using alignment of the simulated celiac artery and superior mesenteric artery origins for reference.

Alignment of the fenestrations was verified by performing continuous fluoroscopy as each branch was targeted with a guide-wire introduced through the right iliac branch of the

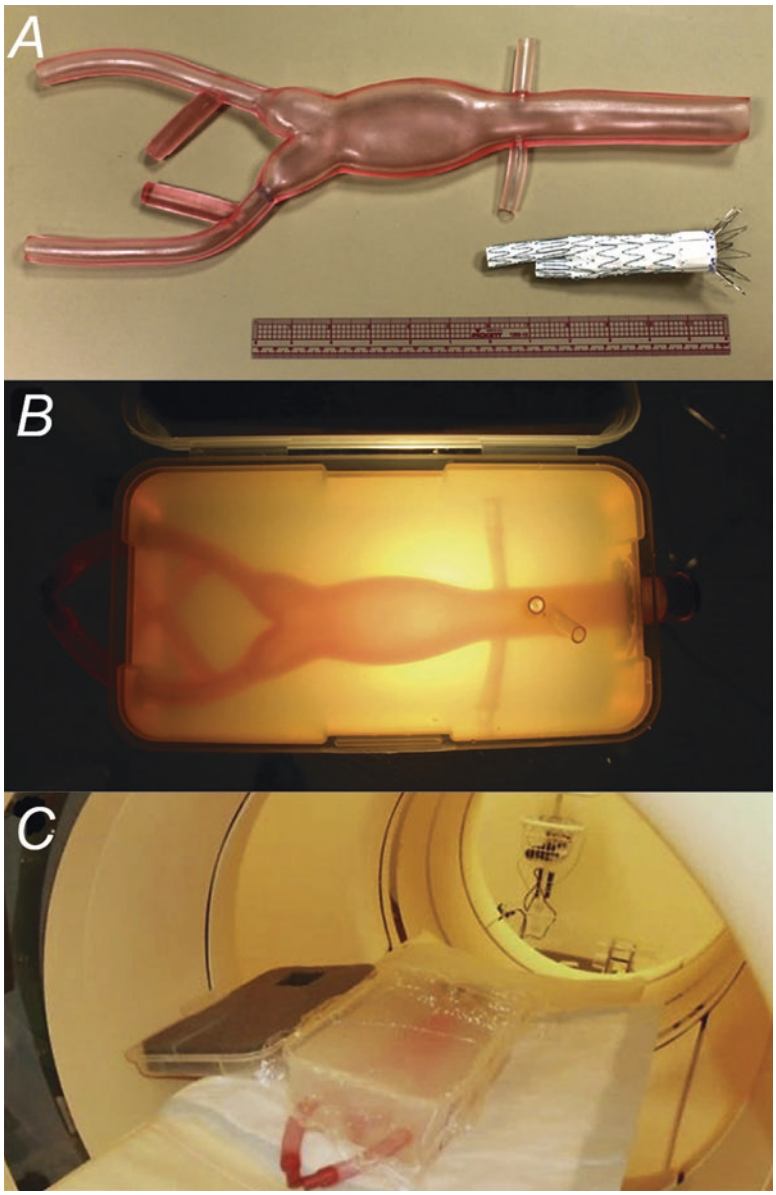


Fig. 9.4 Phantom for fenestration template validation. (**a**) An off-the-shelf model of an abdominal aortic aneurysm (AAA) that includes the renal arteries. (**b**) Tubes were attached to the AAA phantom to represent the celiac artery and the superior mesenteric artery, and the phantom was embedded in agar in a plastic container. (**c**) The phantom was imaged with a standard computed tomography (CT) scanner. Reprinted from Journal of Vascular Surgery, 61(6), Leotta DF, Starnes BW, Custom fenestration templates for endovascular repair of juxtarenal aortic aneurysms, 1637–41, Copyright 2015, with permission from Elsevier

phantom. Guide-wires were successfully introduced in each of the four branch vessels (Fig. 9.6), confirming that the graft fenestrations specified by the 3D-printed template were properly aligned with the phantom branch vessel origins.

Clinical Implications

We have demonstrated a procedure to create a template based on each patient's anatomy that provides a simple and accurate guide for on-site placement of graft fenestrations. Without the template, fenestration planning time for physician-modified grafts varies with experience and case complexity [7]. Early in the experience of one coauthor (B.W.S.), the time required for workstation measurements was 1–2 h. After performing >150 physician-modified endograft procedures, this planning time has decreased to <30 min per case. In the operating room, manual measurement of fenestration locations on the graft takes <15 min.

The template preproduction time, including manual outlining of the aorta and the subsequent computer processing steps, currently takes <30 min. This time could be reduced

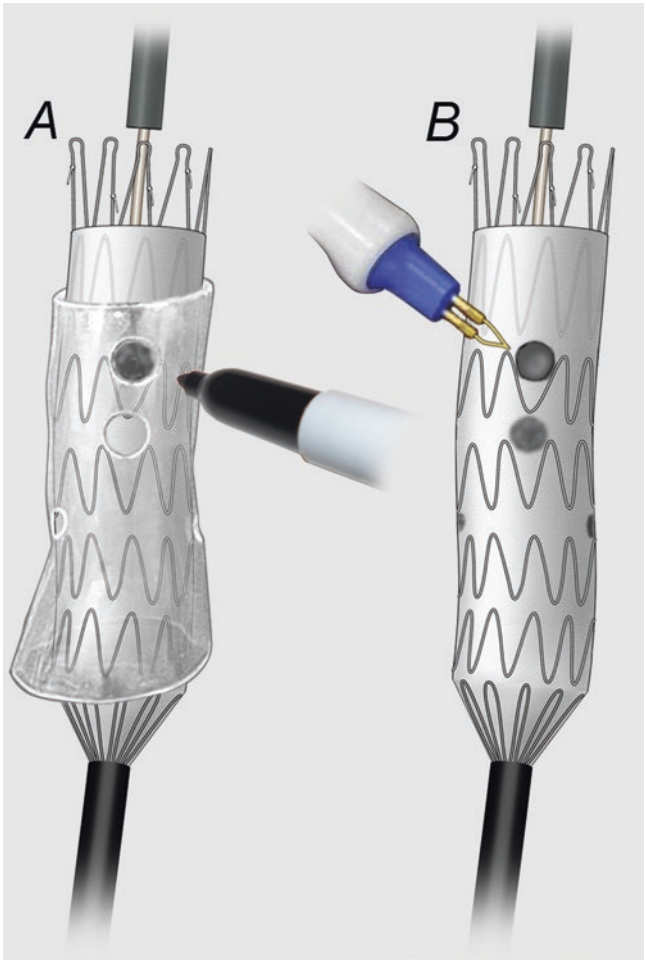


Fig. 9.5 Graft fenestration and deployment for validation. (**a**) An unsheathed graft is inserted in the fenestration template and the branch vessel origins are marked with a pen. (**b**) Fenestrations are cut with an electrocautery device after removal of the template. By permission of Mayo Foundation for Medical Education and Research. All rights reserved

by incorporating automated image segmentation to generate the lumen outlines. Printing time for the template shown in Fig. 9.3 (6.3 cm long, 2 mm wall thickness) was 4 h, which would allow production of a template for use the next day. Although this current printing time makes the template method impractical for patients with a ruptured AAA, it would still be applicable to symptomatic patients. Also, printing times will likely decrease in the future as 3D printing technology matures.

Use of the template saves time in the operating room because all of the relative distances of the fenestrations are established by the template; the surgeon is not required to perform any measurements at the time of device deployment. The template transparency allows for rapid assessment of the fenestration locations relative to the stent struts, and, most importantly, the potential for measurement errors is eliminated. Certain commercially available endografts harbor wide amplitude stents in the aortic seal zone providing more available graft "real estate" for placement of strut-free fenestrations.

Another benefit offered by the 3D-printed template is the potential to shift the preoperative planning steps from the surgeon to an outside provider. Manufacture at a centralized processing facility, based on electronically transferred images, would make template guides available to any clinical site performing endovascular repair of AAAs. The raw image data could be sent to the service provider, and the fenestration guide could be shipped back to the surgery site. Clear printing materials are available that are compatible with gas sterilization methods, so templates could be sterilized before shipment or at the clinical site. Therefore, individual clinical sites would not require expertise with image segmentation, computer-assisted design software, or 3D printing. This approach could lead to wider use of fenestrated endografts for elective repairs and treatment of symptomatic AAAs.

Conclusion

Custom fenestration templates provide for fast and accurate placement of all fenestrations, without the need for manual measurements. The use of the fenestration template with a standard graft provides an off-the-shelf solution for endovascular treatment of juxta-renal AAAs. Pending US Food and Drug Administration approval, this technique has the potential to save procedural costs and make minimally invasive AAA repair available to more patients with challenging anatomy.

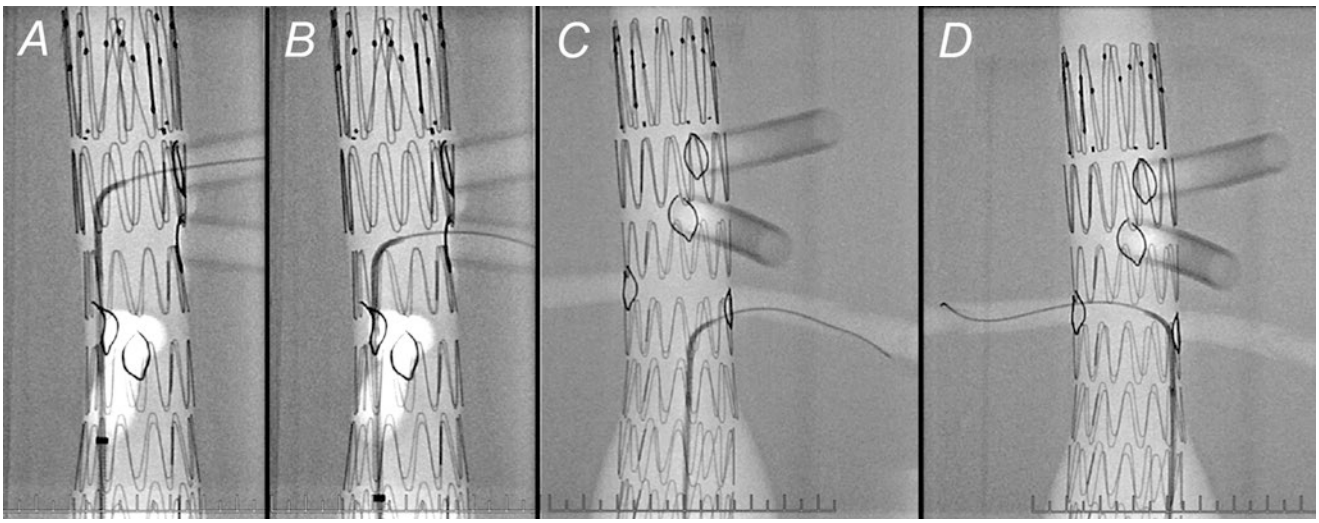


Fig. 9.6 Fluoroscopic confirmation of proper alignment of the graft fenestrations with each of the branch vessels in the abdominal aortic aneurysm (AAA) phantom. A guide-wire was successfully deployed through the openings in the fenestrated graft into each of the branch vessels. Gold markers sewn around the graft openings are visible for each fenestration. (**a**) Celiac artery; (**b**) superior mesenteric artery; (**c**) left renal artery; (**d**) right renal artery. Reprinted from Journal of Vascular Surgery, 61(6), Leotta DF, Starnes BW, Custom fenestration templates for endovascular repair of juxtarenal aortic aneurysms, 1637–41, Copyright 2015, with permission from Elsevier

References

1. United Kingdom EVAR Trial Investigators, Greenhalgh RM, Brown LC, Powell JT, Thompson SG, Epstein D, Sculpher MJ. Endovascular versus open repair of abdominal aortic aneurysm. N Engl J Med. 2010;362:1863–71.
2. Schanzer A, Greenberg RK, Hevelone N, Robinson WP, Eslami MH, Goldberg RJ, et al. Predictors of abdominal aortic aneurysm sac enlargement after endovascular repair. Circulation. 2011;123:2848–55.
3. Higashiura W, Nagata T, Tabayashi N, Itoh H, Sakaguchi S, Taniguchi S, et al. Initial experience of branched endovascular graft for abdominal aortic aneurysm with complex anatomy of proximal neck: planning and technical considerations. Jpn J Radiol. 2010;28:66–74.
4. Nordon IM, Hinchliffe RJ, Manning B, Ivancev K, Holt PJ, Loftus IM, et al. Toward an "off-the-shelf" fenestrated endograft for management of short-necked abdominal aortic aneurysms: an analysis of current graft morphological diversity. J Endovasc Ther. 2010;17:78–85.
5. Resch T, Sonesson B, Malina M. Incidence and management of complications after branched and fenestrated endografting. J Cardiovasc Surg (Torino). 2010;51:105–13.
6. Starnes BW. Physician-modified endovascular grafts for the treatment of elective, symptomatic, or ruptured juxtarenal aortic aneurysms. J Vasc Surg. 2012;56:601–7.
7. Starnes BW, Tatum B. Early report from an investigator-initiated investigational device exemption clinical trial on physician-modified endovascular grafts. J Vasc Surg. 2013;58:311–7.
8. Legget ME, Leotta DF, Bolson EL, McDonald JA, Martin RW, Li XN, et al. System for quantitative three dimensional echocardiography of the left ventricle based on a magnetic field position and orientation sensing system. IEEE Trans Biomed Eng. 1998;45:494–504.
9. Causey MW, Jayaraj A, Leotta DF, Paun M, Beach KW, Kohler TR, et al. Three-dimensional ultrasonography measurements after endovascular aneurysm repair. Ann Vasc Surg. 2013;27:146–53.
10. Leotta DF, Primozich JF, Beach KW, Bergelin RO, Strandness Jr DE. Serial measurement of cross-sectional area in peripheral vein grafts using three-dimensional ultrasound. Ultrasound Med Biol. 2001;27:61–8.

Preoperative Evaluation and Clinical Risk Assessment

10

Ying Huang and Gustavo S. Oderich

Introduction

Since the first report by Parodi and colleagues in 1991 [1], endovascular aortic repair (EVAR) has gained widespread acceptance owing to its minimal invasiveness, early survival benefit, decreased risk of complications, and quick recovery. The use of EVAR in the USA has increased from 5.2 % in 2000 to 74 % in 2010 [2]. At our institution, the proportion of EVAR for elective AAA repairs reached 73 % in 2011 [3]. EVAR has also been increasingly utilized for ruptured AAA repairs [4].

Anatomical factors remain the most important determinant of eligibility to EVAR. Parallel graft techniques were introduced as a "bail out" in patients with inadvertent coverage of side branches or short necks, but its use is now accepted for elective treatment of complex aortic aneurysms in many centers [5, 6]. Fenestrated grafts were first reported using device modifications in 1996 [7] and later further developed by a dedicate group of physicians in Western Australia and worldwide (see Chap. 1). These specially designed grafts allowed total endovascular approaches to be applied in the aortic arch, thoracoabdominal and aortoiliac segments [8–12]. Endovascular techniques are now routinely used not only for aneurysms, but also for dissections, intramural hematoma, penetrating ulcers, trauma, coarctation, and infection.

Patients with complex aortic pathology are often elderly and have widespread atherosclerosis affecting numerous vascular beds. Therefore, a thorough preoperative evaluation is needed prior to embarking in any aortic reconstruction, regardless of whether an endovascular or open surgical technique is selected. Several studies have shown that patients with aortic pathology have high incidence of cardiovascular, cerebrovascular, renal, and peripheral arterial disease (PAD), accounting for most mortality and morbidity during early and late follow-up. Aortic aneurysm and dissection were the 15th cause of death in the USA in 2011, with 77 % of patients aged 65 years and older [13]. The abdominal aorta is affected more often and, the prevalence of AAA is as high as 9 % in people 65 to 85 years of age [14]. This chapter summarizes the preoperative evaluation and clinical risk assessment as well as proposed guidelines in patients necessitating open and endovascular repair of aortic aneurysms and dissections.

General Assessment

According to 2014 American College of Cardiology/American Heart Association (ACC/AHA) [15] and European Society of Cardiology/European Society of Anesthesiology (ESC/ESA) [16] guidelines on noncardiac surgery, endovascular interventions of aorta or major branch arteries including mesenteric, renal, and iliac arteries are considered intermediate risk, and open surgical reconstruction of the aorta or major branch vessels is regarded as high-risk procedure. These guidelines did not take into consideration recent advancements in fenestrated and branched techniques, and mostly refer to infrarenal and thoracic repair with standard endografts. Because endovascular repair of more complex aortic aneurysms including arch aneurysms and thoracoabdominal aortic aneurysms (TAAAs) carries substantial risk of morbidity and mortality, we consider patients undergoing these types of procedures as high risk, thereby recommending the same work-up and assessment that is needed with an open surgical repair. The estimated 30-day incidence of cardiac events including cardiovascular death or nonfatal myocardial infarction was 1–5 % and >5 %, respectively, for intermediate-risk and high-risk procedures [15].

Y. Huang
Department of Vascular Surgery, Mayo Clinic,
200 First Street SW, Rochester, MN 55905, USA
e-mail: huang.ying@mayo.edu

G.S. Oderich (✉)
Division of Vascular and Endovascular Surgery,
Department of Surgery, Mayo Clinic, 200 First Street SW,
Rochester, MN 55905, USA
e-mail: oderich.gustavo@mayo.edu

© Mayo Foundation for Medical Education and Research 2017

G.S. Oderich (ed.), *Endovascular Aortic Repair*, DOI 10.1007/978-3-319-15192-2_10

Table 10.1 Pre-procedural checklist for all patients undergoing elective endovascular interventions

	Description
History	● Age
	● Gender
	● Functional capacity
	● Past medical and surgical history
	● Present and past medication use
	● Smoking status
	● Allergies
	● Alcohol misuse
	● Illicit drug use
	● History of trauma
	● Family history of aneurysm or dissection
	● Marfan's syndrome
	● Connective tissue disorders
	● Aortic dissection
	● Others
Physical examination	● Vital signs
	● Carotid bruit
	● Heart sounds and murmur
	● Lung fields and sounds
	● Abdominal examination
	● Pulse examination
Laboratory studies	● Complete blood count
	● Blood urea nitrogen (BUN) and serum creatinine (Cr)
	● Serum electrolyte values
	● Blood glucose
	● Prothrombin time (PT), activated partial thromboplastin time (aPTT), international normalized ratio (INR)
Resting 12-lead ECG	
Ankle-brachial index test	
Imaging studies	● Chest radiograph
	● Computed tomographic angiography (CTA) chest, abdomen, and pelvis
Informed consent	

Table 10.2 Estimated energy required for various activities (functional capacity)[a]

Functional capacity	Examples of activity
Excellent (>10 METs)	Strenuous sports such as football, basketball, singles tennis, karate, jogging 10 min mile or greater, chopping wood
Good (7–10 METs)	Doubles tennis, calisthenics without weights, golfing without cart
Moderate (4–6 METs)	Climbing a flight of stairs or walking up a hill, running a short distance, heavy housework (scrubbing floors or moving furniture)
Poor (1–3 METs)	Eating, walking at 2–3 miles per hour, getting dressed, light housework (washing dishes)

MET metabolic equivalent unit

[a]Reprinted from Journal of Vascular Surgery, 50 (4 Suppl), Chaikof EL, Brewster DC, Dalman RL, Makaroun MS, Illig KA, Sicard GA, et al., The care of patients with an abdominal aortic aneurysm: the Society for Vascular Surgery practice guidelines, S2–49, Copyright 2009, with permission from Elsevier

All patients undergoing elective endovascular interventions should have a preoperative assessment with the exception of those who need emergency (<6 h) or urgent (6–24 h) procedures. The initial assessment should include clinical evaluation, laboratory studies and imaging of the aorta and its branches (Table 10.1) [17]. A multidisciplinary team (MDT) is often needed, including consultations with cardiology, pulmonology, nephrology, endocrinology, anesthesiology, radiology, or other specialty. An estimation of the functional capacity [18] (Table 10.2) is of paramount importance to determine cardiac and overall perioperative risk, as measured by metabolic equivalents (METs). One important indicator of poor functional status and an increased risk of postoperative cardiopulmonary complications after major noncardiac surgery is walk four blocks [19], or the inability to climb two flights of stairs [20].

In addition to laboratory studies listed in Table 10.1, disease-specific laboratory studies should be considered in select patients such as those with Marfan's syndrome, connective tissue disorders, infection, or rheumatologic disorders. An overall assessment of health can be quantified using two modalities:

American Society of Anesthesiology (ASA) Physical Status Classification [21]

This classification (Table 10.3) is simple and universal for risk stratification for all patients undergoing surgery, but it may have inter-rater reliability even among anesthesiologists [22, 23].

Society for Vascular Surgery/American Association for Vascular Surgery (SVS/AAVS) Comorbidity Score [24]

In this scoring model, cardiac, pulmonary, and renal risk factors are considered major components, whereas hypertension and age are used as minor components (Table 10.4). The results of established screening tests, such as the dipyridamole thallium perfusion scan and ejection fraction are included as well. A combined comorbidity severity score is calculated based on risks in both early and late mortality after open or endovascular procedure, with a highest weighting for cardiac risk, which accommodates to the prevalence of cardiac comorbidities in patients with vascular disease (Table 10.5).

Table 10.3 American Society of Anesthesiologists' (ASA) physical status classification[a]

Class	Description	Examples (including, but not limited to)
I	A normal healthy patient	Healthy, nonsmoking, no or minimal alcohol use
II	A patient with mild systemic disease; no functional limitation	Current smoker, social alcohol drinker, pregnancy, obesity (30 < BMI < 40), well-controlled DM or HTN, mild lung disease
III	Severe systemic disease; definite functional limitation	One or more moderate-to-severe diseases: poorly controlled DM or HTN, COPD, morbid obesity (BMI ≥ 40), active hepatitis, alcohol dependence or abuse, implanted pacemaker, moderate reduction of ejection fraction, ESRD undergoing regularly scheduled dialysis, premature infant PCA <60 weeks, history of MI (>3 months), CVA, TIA, or CAD/stents
IV	Severe systemic disease that is constant threat to life	Recent MI (<3 months), CVA, TIA, or CAD/stents, ongoing cardiac ischemia or severe valve dysfunction, severe reduction of ejection fraction, sepsis, DIC, ARD, or ESRD not undergoing regularly scheduled dialysis
V	Moribund patient; unlikely to survive 24 h with or without operation	Ruptured abdominal/thoracic aneurysm, massive trauma, intracranial bleed with mass effect, ischemic bowel in the face of significant cardiac pathology or multiple organ/system dysfunction

The addition of "E" denotes emergency surgery
ARD acute respiratory distress, *BMI* body mass index, *CAD* coronary artery disease, *COPD* chronic obstructive pulmonary disease, *CVA* cerebrovascular accident, *DIC* disseminated intravascular coagulation, *DM* diabetes mellitus, *ESRD* end-stage renal disease, *HTN* hypertension, *MI* myocardial infarction, *PCA* postconceptional age, *TIA* transient ischemic attack
[a]Reproduced with permission from the American Society of Anesthesiologists. ASA physical status classification system. 2014 [cited 2015 August 6]; Available from: http://www.asahq.org/resources/clinical-information/asa-physical-status-classification-system

Table 10.4 SVS/AAVS medical comorbidity grading system[a]

Score	Description
Major components	
Cardiac status	
0	Asymptomatic, with normal electrocardiogram
1	Asymptomatic but with either remote myocardial infarction by history (6 months), occult myocardial infarction by electrocardiogram, or fixed defect on dipyridamole thallium or similar scan
2	Any one of the following: stable angina, no angina but significant reversible perfusion defect on dipyridamole thallium scan, significant silent ischemia (1 % of time) on Holter monitoring, ejection fraction 25–45 %, controlled ectopy or asymptomatic arrhythmia, or history of congestive heart failure that is now well compensated
3	Any one of the following: unstable angina, symptomatic or poorly controlled ectopy/arrhythmia (chronic/recurrent), poorly compensated or recurrent congestive heart failure, ejection fraction less than 25 %, myocardial infarction within 6 months
Pulmonary status	
0	Asymptomatic, normal chest radiograph, pulmonary function tests within 20 % of predicted
1	Asymptomatic or mild dyspnea on exertion, mild chronic parenchymal radiograph changes, pulmonary function tests 65–80 % of predicted
2	Between 1 and 3
3	Vital capacity less than 1.85 L, FEV_1 less than 1.2 L or less than 35 % of predicted, maximal voluntary ventilation less than 50 % of predicted, PCO_2 greater than 45 mmHg, supplemental oxygen use medically necessary, or pulmonary hypertension
Renal status	
0	No known renal disease, normal serum creatinine level
1	Moderately elevated creatinine level, ≤2.4 mg/dL
2	Creatinine level, 2.5–5.9 mg/dL
3	Creatinine level ≥6.0 mg/dL, or on dialysis or with kidney transplant
Minor components	
Hypertension	
0	None (diastolic pressure <90 mmHg)
1	Controlled (diastolic pressure <90 mmHg) with single drug
2	Controlled with two drugs
3	Requires more than two drugs or is uncontrolled
Age	
0	<55 years
1	55–69 years
2	70–79 years
3	≥80 years

SVS/AAVS Society for Vascular Surgery/American Association for Vascular Surgery
[a]Reprinted from Journal of Vascular Surgery, 35(5), Chaikof EL, Fillinger MF, Matsumura JS, Rutherford RB, White GH, Blankensteijn JD, et al., Identifying and grading factors that modify the outcome of endovascular aortic aneurysm repair, 1061–6, Copyright 2002, with permission from Elsevier

Table 10.5 Combined medical comorbidity severity scoring scheme[a]

Risk factor	Weighting	Score
Cardiac	×4	12
Pulmonary	×2	6
Renal	×2	6
Hypertension	×1	3
Age	×1	3
Maximum score		30

[a]Reprinted from Journal of Vascular Surgery, 35(5), Chaikof EL, Fillinger MF, Matsumura JS, Rutherford RB, White GH, Blankensteijn JD, et al., Identifying and grading factors that modify the outcome of endovascular aortic aneurysm repair, 1061–6, Copyright 2002, with permission from Elsevier

Scores can be divided by 10 to yield a comorbidity severity score on a 3-point scale, where grades of 0–3 correspond to absent, mild, moderate, and severe. The SVS reporting standards also propose an anatomical risk classification system which is beyond the scope of this chapter [24].

Cardiac Risk Assessment

Cardiac deaths, related primarily to coronary artery disease (CAD), are the dominant cause of early and late mortality after open and endovascular repair of aortic aneurysms [25–27]. Recent systematic review showed that the prevalence of AAA among patients who had coronary angiography and coronary artery bypass grafting was 9.5 % for men and 0.35 % for women [28], reaching 14.4 % among men with three-vessel disease [29]. Thus preoperative cardiac risk evaluation may indicate undiagnosed heart disease and decrease the risk of perioperative cardiac complications and death. This is especially important in the patient with complex aortic disease who necessitates extensive aortic reconstructions.

Active Cardiac Conditions

Active cardiac conditions indicate major clinical risk. These patients who have one or more active cardiac conditions generally will need intensive management, which typically results in delay or cancellation of procedure unless the procedure is emergent (Table 10.6) [30, 31].

Table 10.6 Active cardiac conditions requiring evaluation and treatment before endovascular procedure[a]

	Description
Unstable coronary syndromes	● Angina symptoms with everyday living activities or inability to perform any activity without angina or angina at rest
	● Myocardial infarction within 30 days
Decompensated heart failure	● New York Heart Association functional class IV
	– Unable to carry on any physical activity without discomfort
	– Symptoms of heart failure at rest
	– If any physical activity is undertaken, discomfort increases
	● Worsening heart failure
	● New-onset heart failure
Significant arrhythmias	● High-grade atrioventricular block
	● Mobitz II atrioventricular block
	● Third-degree atrioventricular heart block
	● Symptomatic ventricular arrhythmias
	● Supraventricular arrhythmias (including atrial fibrillation) with uncontrolled ventricular rate (HR >100 bpm at rest)
	● Symptomatic bradycardia
	● Newly recognized ventricular tachycardia
Severe valvular disease	● Severe aortic stenosis
	– Symptomatic (exertional dyspnea or decreased exercise tolerance, exertional angina, exertional syncope or presyncope, heart failure, angina, syncope or presyncope)
	– Mean pressure gradient >40 mmHg
	– Aortic valve area <1.0 cm^2
	– Maximum aortic velocity >4.0 m/s
	● Symptomatic mitral stenosis
	– Decreased exercise tolerance
	– Exertional dyspnea

[a]Adapted from Fleisher et al., ACCF/AHA [30] and Nishimura et al., AHA/ACC [31] practice guidelines

Recommendations on Perioperative Cardiovascular Assessment

Guidelines regarding evaluation and management of cardiac risk in patients undergoing intermediate- and high-risk noncardiac surgery have been reported by the 2009 American College of Cardiology Foundation/American Heart Association (ACCF/AHA), 2014 ACC/AHA and 2014 ESC/ESA [15, 30, 32]. The recommendations for preoperative cardiovascular assessment prior to endovascular procedures are summarized in Table 10.7. Different recommendations in the guidelines are also provided for patients who had prior percutaneous coronary interventions (Table 10.8) or coronary artery bypass grafts (Table 10.9). Supplemental tests prior to endovascular repair are also recommended in Table 10.10. It is important to highlight that the guidelines recommendations have been established prior to widespread use of more complex endovascular techniques such as branched TAAA repair, and that the level of complexity and rates of cardiac events are significantly higher with these procedures compared to standard EVAR.

Table 10.7 Recommendations for perioperative cardiac assessment before endovascular procedure[a]

Scenario	Recommendations	COR	LOE
Patients who need emergency procedure	Proceed to the operating room, continue perioperative surveillance, postoperative risk stratification, and risk factor management	I	C
Patients with active cardiac conditions	Evaluated and treated according to guideline-directed medical therapy, elective procedure should be postponed or cancelled	I	B
Patients with poor (<4 METs) or unknown functional capacity and no clinical risk factors[b]	Proceed with planned procedure	I	B
Patients with functional capacity ≥4 METs without symptoms	Proceed with planned procedure	IIa	B
Patients with poor (<4 METs) or unknown functional capacity and ≥3 clinical risk factors[b] who are scheduled for endovascular procedure	Proceed with planned surgery with heart rate control	IIa	B
Patients with poor (<4 METs) or unknown functional capacity and ≥3 clinical risk factors[b] who are scheduled for vascular surgery	Consider further testing if it will change management	IIa	B
Patients with poor (<4 METs) or unknown functional capacity and 1–2 clinical risk factors[b] who are scheduled for vascular or endovascular surgery	Proceed with planned surgery with heart rate control	IIa	B
Patients with poor (<4 METs) or unknown functional capacity and ≥3 clinical risk factors[b] who are scheduled for endovascular procedure	Consider noninvasive testing if it will change management	IIb	B
Patients with poor (<4 METs) or unknown functional capacity and 1 or 2 clinical risk factors[b] who are scheduled for vascular or endovascular surgery	Consider noninvasive testing if it will change management	IIb	B

Class I recommendations suggest that procedures/treatments should be performed/administered; Class IIa recommendations suggest that it is reasonable to perform the procedure/treatment; Class IIb recommendations imply that the procedure/treatment may be considered; and in Class III the procedure/treatment should not be performed because it may not be helpful or there is no proven benefit, and may potentially be harmful to the patient

Level of evidence: *A* data derived from multiple randomized clinical trials or meta-analyses; *B* data derived from a single randomized clinical trial or nonrandomized studies; *C* only consensus opinion of experts, case studies, or standard of care

COR class of recommendations, *LOE* level of evidence, *MET* metabolic equivalents

[a]Adapted from Fleisher et al., ACCF/AHA [30] and ACC/AHA [15] practice guidelines

[b]History of ischemic heart disease, history of compensated or prior heart failure, history of cerebrovascular disease, diabetes mellitus, and renal insufficiency (creatinine>2 mg/dL)

Table 10.8 ACC/AHA recommendations on timing of elective noncardiac surgery in patients with previous percutaneous coronary intervention (PCI)[a]

Recommendations	COR	LOE
Endovascular procedure without angiographic evaluation is not recommended in asymptomatic patients who have undergone CABG in the past 6 years, except for high-risk patients	I	B
Endovascular procedure should be delayed 30 days after BMS implantation	I	B
Endovascular procedure should be performed at a minimum of 4 weeks and ideally 3 months after BMS implantation	IIa	B
Endovascular procedure should be delayed 14 days after balloon angioplasty[b]	I	C
Endovascular procedure should optimally be delayed 365 days after DES implantation[b]	I	B
A consensus decision as to the relative risks of discontinuation or continuation of antiplatelet therapy can be useful	IIa	C
Elective endovascular procedure after DES implantation may be considered after 180 days if the risk of further delay is greater than the expected risks of ischemia and stent thrombosis	IIb	B

BMS bare-metal stent, *DAPT* dual-antiplatelet therapy, *DES* drug-eluting stent, *PCI* percutaneous coronary intervention

[a]Adapted from Fleisher et al., ACC/AHA practice guidelines [15] and Kristensen et al. ESC/ESA guidelines [32]

[b]Class IIa recommendation and B level of evidence in 2014 ESC/ESA guidelines

Therefore, one should use caution when generalizing the recommendations of suggested guidelines to more complex procedures. In our practice, we regard complex endovascular repair with similar risk as a major open aortic reconstruction [15, 30, 32].

Cardiac Risk Models

Standardization of cardiac risk has been used for decades since the pioneer work of Goldman, Eagle, and others. Cardiac risk evaluation is based on clinical characteristics

Table 10.9 Recommendations for supplemental testing before endovascular procedure[a]

Testing	Scenario	Recommendations	COR	LOE
Resting 12-lead ECG	Patients who have risk factor(s) and are scheduled for intermediate- or high-risk surgery	Recommended	I	C
	Patients with known coronary heart disease, significant arrhythmia, peripheral arterial disease, cerebrovascular disease, or other significant structural heart disease	Reasonable	IIa	B
	Asymptomatic patients without known coronary heart disease	May be considered	IIb	B
	Patients with no risk factors and age >65 years who are scheduled for endovascular procedure	May be considered	IIb	C
Assessment of LV function	Patients with dyspnea of unknown origin to undergo preoperative	Reasonable	IIa	C
	Patients with HF with worsening dyspnea or other change in clinical status	Reasonable	IIa	C
	Clinically stable patients	Reassessment of LV function may be considered if there has been no assessment within a year	IIb	C
		Routine preoperative evaluation of LV function is not recommended	III: No Benefit	B
Stress testing				
Exercise stress testing	Patients with elevated risk and excellent (>10 METs) functional capacity	Reasonable to forgo and proceed to endovascular procedure	IIa	B
	Patients with elevated risk and unknown functional capacity	May be reasonable if it will change management	IIb	B
	Patients undergoing elevated risk procedures and unknown functional capacity	May be considered	IIb	B
	Patients with elevated risk and moderate-to-good (≥4 METs to 10 METs) functional capacity	May be reasonable to forgo and proceed to endovascular procedure	IIb	B
	Patients with elevated risk and poor or unknown (<4 METs) functional capacity	May be reasonable to perform exercise testing with cardiac imaging to assess for myocardial ischemia	IIb	C
Noninvasive pharmacological stress testing	Patients at elevated risk and poor (<4 METs) functional capacity	Reasonable to undergo either DSE or MPI if it will change management	IIa	B
Preoperative coronary angiography		Routine preoperative coronary angiography is not recommended exclusively to reduce perioperative cardiac events	III: No Benefit	B

Class I recommendations suggest that procedures/treatments should be performed/administered; Class IIa recommendations suggest that it is reasonable to perform the procedure/treatment; Class IIb recommendations imply that the procedure/treatment may be considered; and in Class III the procedure/treatment should not be performed because it may not be helpful or there is no proven benefit, and may potentially be harmful to the patient

Level of evidence: *A* data derived from multiple randomized clinical trials or meta-analyses; *B* data derived from a single randomized clinical trial or nonrandomized studies; *C* only consensus opinion of experts, case studies, or standard of care

ACC/AHA the American College of Cardiology/American Heart Association, *CCS* Canadian Cardiovascular Society, *COR* class of recommendation, *CVD* cerebrovascular disease, *DSE* dobutamine stress echocardiogram, *ECG* electrocardiogram, *HF* heart failure, *LOE* level of evidence, *LV* left ventricular, *MET* metabolic equivalent, *MI* myocardial infarction, *MPI* myocardial perfusion imaging, *NSTE-ACS* non-ST-segment elevation acute coronary syndromes, *PAD* peripheral arterial disease

[a]Adapted from Fleisher et al., ACC/AHA practice guidelines [15] and Kristensen et al. ESC/ESA guidelines [32]

Table 10.10 ACC/AHA recommendations for coronary revascularization before endovascular procedure[a]

Recommendations	COR	LOE
Revascularization before endovascular procedure is recommended when indicated by existing clinical practice guidelines	I	C
Revascularization is not recommended before endovascular procedure exclusively to reduce perioperative cardiac events	III: no benefit	B

[a]Adapted from Fleisher et al., ACC/AHA practice guidelines [15]

and urgency of procedure, and then extended to laboratory and noninvasive assessments. Among many cardiac risk predicting models, the revised cardiac risk index (RCRI) [33], the American College of Surgeons National Surgical Quality Improvement Program Myocardial Infarction Cardiac Arrest Calculator (ACS NSQIP MICA) [34], ACS NSQIP Surgical Risk Calculator [35], and Vascular Surgery Group Cardiac Risk Index (VSG-CRI) [36] can be applied to predict adverse events in patients undergoing vascular surgery;

however, renal risk factor is included in each model. Different from the old models, patients who have been managed with more current standards of care have been included in these models, the ACS NSQIP MICA outperforms the RCRI in some circumstances, and both ACS NSQIP surgical risk calculator and VSG-CRI are procedure specific. ACS NSQIP MICA, ACS NSQIP surgical risk calculator and VSG-CRI are available online for calculation. It should be noted that these models are not exclusively for patients undergoing EVAR with fenestrated, branched or parallel stent grafts, as the original study population for each model included open or endovascular procedures for carotid artery disease, PAD, or aortic aneurysms, mostly infrarenal AAA repairs. In addition, the NSQIP-based calculators have not been validated in an external population outside the NSQIP, and the definition of myocardial infarction (MI) includes only ST-segment MIs or troponin level >3 times normal that occur in symptomatic patients.

Revised Cardiac Risk Index [33]

The RCRI is a six-point index score (Table 10.11) for assessing the risk of major cardiac complications including MI, pulmonary edema, ventricular fibrillation or primary cardiac arrest, and complete heart block following noncardiac surgery. It is simple, has been extensively validated, and provides a good estimate of the preoperative risk. However, the RCRI does not discriminate between low- and high-risk patients undergoing vascular surgery, who generally carry increased perioperative cardiac risk [37].

The ACS NSQIP MICA [34]

Target cardiac complications (Table 10.12) of the ACS NSQIP MICA were defined as cardiac arrest or MI. This model was further tested using 2008 NSQIP data of patients undergoing aortic or other vascular surgery ($n=26{,}183$); the C statistic of the model was 0.746.

Table 10.11 Revised cardiac risk index (RCRI)[a]

Risk factor	Points
Ischemic heart disease	1
History of congestive heart failure	1
Creatinine >2 mg/dL (177 μmol/L)	1
Insulin-dependent diabetes	1
History of cerebrovascular disease	1
High-risk surgery (intrathoracic, intra-abdominal, or suprainguinal vascular surgery)	1

Rates of major cardiac complication: Class I (0 point): 0.4 %; Class II (1 point): 1 %; Class III (2 points): 7 %
Class IV (≥3 points): 11 %
[a]Adapted from [33]

ACS NSQIP Surgical Risk Calculator [38]

This is a decision-support tool based (Table 10.13) on reliable multi-institutional data, which includes 21 patient-specific variables. The estimated surgery-specific risk of cardiac complications, mortality, and six additional complications can be calculated. However, ACS NSQIP hospitals perform approximately 30 % of all operations in the USA, and only clinical preoperative variables collected by ACS NSQIP could be used in risk models.

VSG-CRI Scoring System [36]

The Vascular Surgery Group Cardiac Risk Index (VSG-CRI) can more accurately (Table 10.14) predict the actual risk of major cardiac events across four procedures including EVAR for both low- and higher risk groups than the RCRI. The composite endpoints were MI, arrhythmia, or congestive heart failure (CHF). When the VSG-CRI was used to score patients, six categories of risk ranging from 2.6 to 14.3 % (score of 0–3 to 8) were discernible.

Table 10.12 The American College of Surgeons National Surgical Quality Improvement Program Myocardial Infarction Cardiac Arrest Calculator (ACS NSQIP MICA)[a]

Risk factor
● Increasing age
● Creatinine >1.5 mg/dL
● Partially or completely dependent functional status
● ASA physical status class
● Type of surgery
– Anorectal
– Aortic
– Bariatric
– Brain
– Breast
– Cardiac
– Ear, nose, and throat
– Foregut/hepatopancreatobiliary
– Gallbladder/adrenal/appendix/spleen
– Intestinal
– Neck
– Obstetric/gynecological
– Orthopedic
– Other abdomen
– Peripheral vascular
– Skin
– Spine
– Thoracic
– Vein
– Urologic

ASA American Society of Anesthesiologists
[a]Adapted from [34]

Table 10.13 The American College of Surgeons National Surgical Quality Improvement Program (ACS NSQIP) variables used in the new universal surgical risk calculators[a]

Variable	Categories
Age group, years	● <65
	● 65–74
	● 75–84
	● ≥85
Sex	● Male
	● Female
Functional status	● Independent
	● Partially dependent
	● Totally dependent
Emergency case	Yes, no
ASA class	● 1
	● 2, 3, 4
	● 5
Steroid use for chronic condition	Yes, no
Ascites within 30 days preoperatively	Yes, no
System sepsis within 48 h preoperatively	● None
	● SIRS
	● Sepsis
	● Septic shock
Ventilator dependent	Yes, no
Disseminated cancer	Yes, no
Diabetes	● No
	● Oral
	● Insulin
Hypertension requiring medication	Yes, no
Previous cardiac event	Yes, no
Congestive heart failure in 30 days preoperatively	Yes, no
Dyspnea	Yes, no
Current smoker within 1 year	Yes, no
History of COPD	Yes, no
Dialysis	Yes, no
Acute renal failure	Yes, no
BMI class	● Underweight
	● Normal
	● Overweight
	● Obese 1
	● Obese 2
	● Obese 3
CPT-specific linear risk	2805 values

ASA American Society of Anesthesiologists, *ACS NSQIP* the American College of Surgeons National Surgical Quality Improvement Program, *BMI* body mass index, *COPD* chronic obstructive pulmonary disease, *CPT* current procedural terminology, *SIRS* systemic inflammatory response syndrome

[a]Reprinted from Journal of the American College of Surgeons, 217(5), Karl Y. Bilimoria, Yaoming Liu, Jennifer L. Paruch, Lynn Zhou, Thomas E. Kmiecik, Clifford Y. Ko, Mark E. Cohen, Development and Evaluation of the Universal ACS NSQIP Surgical Risk Calculator: A Decision Aid and Informed Consent Tool for Patients and Surgeons, 833–842.e3, Copyright 2013, with permission from Elsevier

Table 10.14 Vascular Surgery Group Cardiac Risk Index (VSG-CRI) scoring system[a]

VSG-CRI risk factors	Points
Age ≥80	4
Age 70–79	3
Age 60–69	2
CAD	2
CHF	2
COPD	2
Creatinine >1.8 mg/dL	2
Smoking	1
Insulin-dependant diabetes	1
Long-term β-blockers	1
History of CABG or PCI	-1

CABG coronary artery bypass grafting, *CAD* coronary artery disease, *CHF* congestive heart failure, *COPD* chronic obstructive pulmonary disease, *PCI* percutaneous coronary intervention

[a]Reprinted from Journal of Vascular Surgery, 52(3), Bertges DJ, Goodney PP, Zhao Y, Schanzer A, Nolan BW, Likosky DS, et al., The Vascular Study Group of New England Cardiac Risk Index (VSG-CRI) predicts cardiac complications more accurately than the Revised Cardiac Risk Index in vascular surgery patients, 674–683.e3. Copyright 2010, with permission from Elsevier

Biomarkers

A meta-analysis showed that the performance of the RCRI can be significantly improved by further stratification using the preoperative serum concentration of B-type natriuretic peptides in vascular patients. B-type natriuretic peptides outperform the RCRI at predicting postoperative major adverse cardiac events (MACE) [39, 40]. However, data from prospective, controlled trials on the use of preoperative biomarkers are sparse.

Hypertension

Most hypertensive patients are not at increased perioperative risk as long as the hypertension is not severe and serum electrolytes and renal function are normal, with the exception of pheochromocytoma. Elective surgery should be postponed in patients with blood pressures (BP) above 170/110 mmHg, unless an urgent surgery is required and patient should be treated with parenteral antihypertensive agents. The ideal circumstance is to normalize BP (<140/90 mmHg) for several months prior to elective surgery. Patients with well-controlled hypertension preoperatively are less likely to experience intraoperative blood pressure lability and postoperative complications than patients with poorly controlled

Table 10.15 Recommendations for management of hypertension[a]

Recommendation	COR
In the general population aged ≥60 years, initiate pharmacologic treatment to lower BP at SBP ≥150 mmHg or DBP ≥90 mmHg and treat to a goal SBP <150 mmHg and goal DBP <90 mmHg	A
In the general population <60 years, initiate pharmacologic treatment to lower BP at DBP ≥90 mmHg and treat to a goal DBP <90 mmHg	A: ages 30–59 years E: ages 18–29 years
In the general population <60 years, initiate pharmacologic treatment to lower BP at SBP ≥140 mmHg and treat to a goal SBP <140 mmHg	E
In the population aged ≥18 years with CKD, initiate pharmacologic treatment to lower BP at SBP ≥140 mmHg or DBP ≥90 mmHg and treat to goal SBP <140 mmHg and goal DBP <90 mmHg	E
In the population aged ≥18 years with diabetes, initiate pharmacologic treatment to lower BP at SBP ≥140 mmHg or DBP ≥90 mmHg and treat to a goal SBP <140 mmHg and goal DBP <90 mmHg	E
In the general nonblack population, including those with diabetes, initial antihypertensive treatment should include a thiazide-type diuretic, CCB, ACEI, or ARB	B

ACEI angiotensin-converting enzyme inhibitor, *ARB* angiotensin receptor blocker, *BP* blood pressure, *CCB* calcium channel blocker, *CKD* chronic kidney disease, *COR* class of recommendation (*A* strong, *B* moderate, *E* expert opinion), *DBP* diastolic blood pressure, *SBP* systolic blood pressure
[a]Adapted from [59]

Table 10.16 2014 ESC/ESA recommendations on arterial hypertension before noncardiac surgery[a]

Scenario	Recommendations	COR	LOE
Patients with a new diagnosis of hypertension preoperatively	Patients should be screened for end-organ damage and cardiovascular risk factors	I	C
Patients with hypertension	Large perioperative fluctuations in blood pressure should be avoided	IIa	B
Patients with grade 1 or 2 hypertension (SBP <180 mmHg; DBP <110 mmHg)	May consider not deferring noncardiac surgery	IIb	B

DBP diastolic blood pressure, *SBP* systolic blood pressure
[a]Adapted from [32]

Table 10.17 Stages of chronic kidney disease[a]

Stage	Description	GFR (mL/min/1.73 m^2)
1	Kidney damage with normal or increased GFR	≥90
2	Kidney damage with mild decreased GFR	60–89
3	Moderate decreased GFR	30–59
4	Severe decreased GFR	15–29
5	Kidney failure	<15 or dialysis

GRF glomerular filtration rate
[a] Reprinted from American Journal of Kidney Diseases, 41, I. Introduction, S11–S21. Copyright 2003, with permission from Elsevier

hypertension [41]. When hypertension has caused end-organ disease such as CHF and renal insufficiency, the probability of adverse cardiac outcome in the perioperative period increases significantly [42]. In patients with suspected secondary hypertension, a diagnostic evaluation prior to elective surgery is suggested. In SVS comorbidity scoring system, hypertension is considered as minor component [24]. Table 10.15 summarizes the 2014 Evidence-Based Guideline for the Management of High Blood Pressure in Adults Report from the Panel Members Appointed to the Eighth Joint National Committee (JNC 8). 2014 ESC/ESA recommendations on arterial hypertension before noncardiac surgery are shown in Table 10.16.

Renal Risk Assessment

Patients receiving endovascular aortic repair are usually old and have higher rates of comorbidities compared with those treated by open surgical repair [3, 11, 43]. Contrast-induced acute kidney injury (CI-AKI), which is defined as a rise of serum creatinine of 0.5 mg/dL (44 mmol/L) or a 25 % relative rise from baseline at 48 h (or 5–10 % at 12 h) following contrast administration, remains a major concern. For complex procedures, several mechanisms account for rise in creatinine, including not only contrast use but also catheter manipulations and end-organ ischemia. In addition, several medications including angiotensin-converting enzyme inhibitor (ACEI), angiotensin II receptor blockers (ARB), diuretics, nonsteroidal anti-inflammatory drugs, which used chronically for cardiovascular disease, and some antibiotics used preoperatively, such as aminoglycosides and vancomycin, may cause renal adverse effects. Study from Italy showed that an in-hospital AKI rate of 14 % among 171 patients undergoing TEVAR of the descending thoracic or thoracoabdominal aorta, preoperative poor renal function, the extent of thoracoabdominal aortic disease, along with postoperative blood transfusions, were the most important predictors for AKI [44]. In another study of 350 TEVAR patients, the AKI rate was 17 % [45]. Preoperative renal assessment is important to identify patients with risk factors of developing postoperative renal complications, and those with chronic kidney disease (CKD), which is a risk factor for AKI (Table 10.17). Definitions of AKI are summarized in Table 10.18. In such patients, preventive measures including hydration, control of underlying risk factors, minimization of nephrotoxic contrast agents, and medications with renal side effects.

Table 10.18 Definitions of acute kidney injury (AKI)[a]

	AKIN stage		KDIGO stage		RIFLE class	
Urine output	Serum creatinine		Serum creatinine		Serum creatinine/GFR	
<0.5 mL/kg/h for 6 h	I	≥150–200 % (1.5–2-fold) increase from baseline, or ≥0.3 mg/dL (≥26.4 μmol/L) increase	I	1.5–1.9 times baseline or ≥0.3 mg/dL (≥26.5 mmol/L) increase	Risk	Increase in serum creatinine × 1.5 or decrease in GFR >25 %
<0.5 mL/kg/h for 12 h	II	>200–300 % (>2–3-fold) increase from baseline	II	2.0–2.9 times baseline	Injury	Increase in serum creatinine × 2 or decrease in GFR >50 %
<0.3 mL/kg/h for 24 h or anuria for 12 h	III	>300 % (>3-fold) from baseline, ≥4.0 mg/dL [≥354 μmol/L] with an acute increase of at least 0.5 mg/dL [44 μmol/L]), or initiation of RRT	III	3.0 times baseline or increase in serum creatinine to ≥4.0 mg/dL (≥353.6 mmol/L) or initiation of RRT	Failure	Increase in serum creatinine × 3 or decrease in GFR >75 %, or if baseline serum creatinine ≥353.6 μmol/L (≥4 mg/dL) increase in serum creatinine >44.2 μmol/L (>0.5 mg/dL)
					ESRD	Complete loss of kidney function >3 months

AKI acute kidney injury; *AKIN* Acute Kidney Injury Network; *ESRD* end-stage renal disease; *GFR* glomerular filtration rate; *KDIGO* Kidney Disease: Improving Global Outcomes; *RIFLE* risk, injury, failure, loss, end-stage renal disease; *RRT* renal replacement therapy
[a]Adapted from [32, 48, 60, 61]

Table 10.19 Risk factors of acute kidney injury in patients undergoing endovascular procedure[a]

- Chronic kidney disease (adults with an eGFR <40 mL/min/1.73 m^2 are at particular risk)
- Diabetes but only with chronic kidney disease (adults with an eGFR <40 mL/min/1.73 m^2 are at particular risk)
- Heart failure
- Renal transplant
- Age ≥ 65 years
- Hypovolemia
- Increasing volume of contrast agent
- Intra-arterial administration of contrast agent
- Emergency surgery, especially when the patient has sepsis or hypovolemia
- Intraperitoneal surgery
- Liver disease
- Use of drugs with nephrotoxic potential in the perioperative period
- Susceptibilities
  - Female gender
  - Black race
  - Cancer
  - Anemia

[a]Adapted from [46] and [47]

Table 10.20 RIFLE classification[a]

	Urine output	Serum creatinine/GFR
Risk	<0.5 mL/kg/h for 6 h	Increase in serum creatinine × 1.5 or decrease in GFR >25 %
Injury	<0.5 mL/kg/h for 12 h	Increase in serum creatinine × 2 or decrease in GFR >50 %
Failure	<0.3 mL/kg/h for 24 h or anuria for 12 h	Increase in serum creatinine × 3 or decrease in GFR >75 %, or if baseline serum creatinine ≥353.6 μmol/L (≥4 mg/dL) increase in serum creatinine >44.2 μmol/L (>0.5 mg/dL)
Loss		Complete loss of kidney function >4 weeks
ESRD		Complete loss of kidney function >3 months

ESRD end-stage renal disease; *GRF* glomerular filtration rate; *RIFLE* risk of renal dysfunction, injury to the kidney, failure of kidney function, loss of kidney function and end-stage kidney disease
[a]Reprinted from Bellomo R, Ronco C, Kellum JA, Mehta RL, Palevsky P. Acute renal failure—definition, outcome measures, animal models, fluid therapy and information technology needs: the Second International Consensus Conference of the Acute Dialysis Quality Initiative (ADQI) Group. Crit Care. 2004;8(4):R204–12. © Bellomo et al.; licensee BioMed Central Ltd. 2004

Risk factors of AKI before endovascular procedure, adapted from KDIGO and NICE guidelines [46, 47], are listed in Table 10.19. Renal function can be evaluated using RIFLE classification, namely, risk of renal dysfunction, injury to the kidney, failure of kidney function, loss of kidney function, and end-stage kidney disease (Table 10.20) [48]. The ESC/ESA guidelines on renal function before endovascular procedure are summarized in Table 10.21 [16].

Pulmonary Risk Assessment

Postoperative pulmonary complications are an important source of perioperative morbidity and mortality in elderly patients. Rates of pulmonary complications are high with complex open repair and are significantly lower with standard and complex EVAR. Studies have shown that the presence of an aortic aneurysm and male gender were associated with a higher risk of airway obstruction (odds ratio: 2.93; 95 %

confidence interval [CI], 1.72–4.98; odds ratio: 1.62, 95 % CI: 1.06–2.50, respectively) [49]; chronic obstructive pulmonary disease (COPD) was more prevalent in aneurysm patients (44 %; 98/221) than in PAD patients (20 %; 17/87) (adjusted odds ratio: 3.0, 95 % CI: 1.6–5.5, $P < .001$), and a major proportion of AAA patients was newly diagnosed with COPD [50]. A combination use of Global Initiative for Chronic Obstructive Lung Disease (GOLD) classification, the Modified British Medical Research Council (mMRC) questionnaire on breathlessness, and the COPD Assessment Test (CAT) is recommended to assess the severity of COPD (Table 10.22) [51]. To prevent postoperative pulmonary complications, patients with COPD) should be optimally treated before surgery, and surgery should be postponed if an exacerbation is present. Exacerbation risk can be assessed by GOLD classification or history of two or more exacerbations in the preceding year [51].

There are three models predicting postoperative pulmonary complications used in clinical settings, the Assess Respiratory Risk in Surgical Patients in Catalonia (ARISCAT, Canet) developed in Europe [52], and two Gupta calculators derived from NSQIP data [53, 54].

Table 10.21 2014 ESC/ESA recommendations on renal function before noncardiac surgery[a]

Scenario	Recommendations	COR	LOE
Patients undergoing endovascular procedures	Should be assessed for risk of CI-AKI	IIa	C
Patients with moderate or moderate-to-severe CKD	Hydration with normal saline before administration of contrast medium	I	A
	Use of LOCM or IOMC	I	A
	The volume of contrast media should be minimized	I	B
	Hydration with sodium bicarbonate should be considered before administration of contrast medium	IIa	A
	Short-term high-dose statin therapy should be considered	IIa	B
Patients with severe CKD	In patients with stage 4 or 5 CKD, prophylactic hemofiltration may be considered before complex intervention or high-risk surgery	IIb	B
	In patients with stage 3 CKD, prophylactic hemodialysis is not recommended	III	B

CI-AKI contrast-induced acute kidney injury, *CKD* chronic kidney disease, *GFR* glomerular filtration rate, *IOMC* iso-osmolar contrast medium, *LOCM* low-osmolar contrast medium
[a]Adapted from Kristensen et al. ESC/ESA guidelines [32]

ARISCAT

In this model, preoperative pulmonary risk index predicts three levels of postoperative pulmonary complications, by assigning a weighted point score to seven independent risk factors [52]. Nevertheless, the endpoints of this model also include minor complications.

The Gupta Calculator

This model uses multiple preoperative factors to predict risk of postoperative respiratory failure to wean from mechanical ventilation within 48 h of surgery or unplanned intubation/reintubation postoperatively. It is derived from the ACS NSQIP 2007 data set (211,410 patients for training) and 2008 data set (257,385 patients for validation) using logistic regression techniques to determine the weight of preoperative predictors [53].

Similarly, the Gupta model is derived in a similar manner to the Gupta calculator for postoperative respiratory failure [54]. Both Gupta risk calculators need to be downloaded to a personal device to perform the calculations [16].

The ACC/AHA and ESC/ESA recommendations on patients with pulmonary or pulmonary vascular disease before endovascular procedure are shown in Table 10.23 [15, 32].

Table 10.22 Combined chronic obstructive pulmonary disease (COPD) assessment[a]

Group	GOLD score	GOLD description	No. of exacerbations per year	mMRC grade	CAT score
Low risk					
Less symptoms (A)	1–2	Mild: $FEV_1 \geq 80$ % predicted, or moderate: 50 % ≤ FEV_1 < 80 % predicted	0–1	0–1	<10
More symptoms (B)				≥2	≥10
High risk					
Less symptoms (C)	3–4	Severe: 30 % ≤ FEV_1 < 50 % predicted, or very severe: FEV_1 < 30 % predicted	≥2, or ≥1 hospitalized exacerbation	0–1	<10
More symptoms (D)				≥2	≥10

CAT COPD assessment test, *COPD* chronic obstructive pulmonary disease, *FEV_1* forced expiratory volume in the first second, *GOLD* Global Initiative for Chronic Obstructive Lung Disease, *mMRC* modified British Medical Research Council
[a]Adapted from [51]

Table 10.23 Recommendations on patients with pulmonary and pulmonary vascular disease before endovascular procedure[a]

Scenario	Recommendations	COR	LOE
Patients with PAH	Continue chronic pulmonary vascular targeted therapy unless contraindicated or not tolerated	I	C
Patients with PAH, particularly for those with features of increased perioperative risk including:	Preoperative evaluation by a pulmonary hypertension specialist can be beneficial, unless the risks of delay outweigh the potential benefits	IIa	C
1. Diagnosis of Group 1 pulmonary hypertension			
2. Other forms of pulmonary hypertension associated with high pulmonary pressures (pulmonary artery systolic pressures >70 mmHg) and/or moderate or greater right ventricular dilatation and/or dysfunction and/or pulmonary vascular resistance >3 Wood units)			
3. World Health Organization/New York Heart Association class III or IV symptoms attributable to pulmonary hypertension			
Patients with severe PAH, who are undergoing elective surgery	Patients should be managed in a center with appropriate expertise	I	C
High-risk patients with PAH	Interventions should be planned by the multidisciplinary pulmonary hypertension team	I	C
Patients with PAH	An optimized treatment regimen is recommended before any nonemergency surgical intervention	I	C
Patients receiving PAH-specific treatment	Continuation of this treatment in the perioperative period without interruption	I	C
Patients with COPD	Smoking cessation >2 months before procedure	I	C
Patient with severe right heart failure who is not responsive to supportive therapy	Temporary administration of pulmonary vasodilators (inhaled and/or intravenous) under the guidance of a physician experienced in PAH	I	C
Patients at high risk of OHS	Consider additional specialist investigation before major elective surgery	IIa	C

COPD chronic obstructive pulmonary disease, *PAH* pulmonary artery hypertension, *OHS* obesity hypoventilation syndrome
[a]Adapted from Fleisher et al., ACC/AHA practice guidelines [15] and Kristensen et al. ESC/ESA guidelines [32]

Diabetes

Although patients with diabetes have an increased incidence of cardiovascular disease, type 2 diabetes was revealed inversely associated with AAA (adjusted hazard ratio [HR]: 0.46; 95% CI: 0.35–0.59) in a population-based study [55]. Data from the NSQIP (1999–2004) showed that preoperative or perioperative mean serum glucose concentrations of 150 mg/dL and higher were associated with an increased risk of postoperative infection in diabetic patients undergoing noncardiac surgery [56]. However, the relationship of diabetes and postoperative cardiac adverse events and infection is not well defined in patients undergoing endovascular procedures.

2014 ESC/ESA recommendations on blood glucose control before noncardiac surgery [16] are listed in Table 10.24. Determination of the type of diabetes is essential, since type 1 diabetic patients are at much higher risk of diabetic ketoacidosis and must have basal insulin supplied at all times. The key aspect of the perioperative diabetes management is glycemic control. According to the American Association of Clinical Endocrinologists/American College of Endocrinology clinical practice guidelines, inpatient glucose targets for nonpregnant general medicine and surgery adult patients in non-ICU settings: a premeal glucose target <140 mg/dL and a random blood glucose <180 mg/dL are recommended (recommendation grade: weak; level of evidence: weak, Table 10.25) [57, 58].

Table 10.24 2014 ESC/ESA recommendations on blood glucose control before noncardiac surgery[a]

Scenario	Recommendations	COR	LOE
Patients at high surgical risk	Consider screening for elevated HbA_{1c} before major surgery and improving preoperative glucose control	IIa	C

HbA_{1c} glycosylated hemoglobin
[a]Adapted from Kristensen et al. ESC/ESA guidelines [32]

Addendum

Comparison of cardiac risk predictive factors is summarized in Table 10.26.

Medications

Recommendations of perioperative medications are shown in Table 10.27.

Table 10.25 Recommendations on diabetic patients who undergo endovascular procedure, according to Endocrine Society clinical practice guideline on hyperglycemia in hospitalized patients in noncritical care setting[a]

Scenario	Recommendations	Grade[b]	QOE[c]
All patients with type 1 diabetes	Patients receive either continuous insulin infusion or subcutaneous basal insulin with bolus insulin as required to prevent hyperglycemia during the perioperative period	1	A
Patients with diabetes who develop hyperglycemia during the perioperative period	Discontinuation of oral and noninsulin injectable antidiabetic agents before procedure with initiation of insulin therapy	1	D

[a]Adapted from [58]
[b]*1* Strong recommendations use the phrase "we recommend"; *2* weak recommendations use the phrase "we suggest"
[c]*A* high quality, *B* moderate quality, *C* low quality, *D* very low quality

Table 10.26 Comparison of the Vascular Surgery Group Cardiac Risk Index (VSG-CRI) [36], the revised cardiac risk index (RCRI) [33, 37], the American College of Surgeons National Surgical Quality Improvement Program Myocardial Infarction Cardiac Arrest Calculator (ACS NSQIP MICA) [53], and the ACS NSQIP Surgical Risk Calculator [38]

RCRI		ACS NSQIP MICA	ACS NSQIP surgical risk calculator	VSG-CRI	
Risk factor	Points	Risk factor	Risk factor	Risk factor	Points
		Increasing age	Age	Age ≥80	4
				Age 70–79	3
				Age 60–69	2
Creatinine >2 mg/dL	1	Creatinine >1.5 mg/dL	Acute renal failure	Creatinine >1.8 mg/dL	2
CHF	1			CHF	2
			COPD	COPD	2
				CAD	2
			Smoker	Smoking	1
Insulin-dependent diabetes	1		Diabetes	Insulin-dependent diabetes	1
				Long-term β-blockers	1
				History of CABG or PCI	-1
Cerebrovascular disease	1				
Ischemic heart disease	1		Previous cardiac event		
High-risk surgery (intrathoracic, intra-abdominal, or suprainguinal vascular surgery)	1	Type of surgery (aortic, peripheral vascular, vein, and others	Procedure (CPT Code)		
		Partially or completely dependent functional status	Functional status		
		ASA physical status class	ASA physical status class		
			Sex		
			BMI		
			Hypertension		
			Dyspnea		
			Ventilator dependent		
			Dialysis		
			Acute kidney injury		
			Ascites		
			Systemic sepsis		
			Disseminated cancer		
			Wound class		
			Steroid use		
			Emergency case		

(continued)

Table 10.26 (continued)

RCRI		ACS NSQIP MICA	ACS NSQIP surgical risk calculator	VSG-CRI	
Risk factor	Points	Risk factor	Risk factor	Risk factor	Points
	Beta-blocker therapy should not be started on the day of procedure	III: Harm	B		
Statins	Continue statins in patients currently taking statins	I	B		
	Perioperative initiation of statin use is reasonable in patients undergoing vascular surgery	IIa	B		
	Perioperative initiation of statins may be considered in patients with a clinical risk factor who are undergoing elevated-risk procedures	IIb	C		
Alpha-2 agonists	Not recommended for prevention of cardiac events	III: No benefit	B		
ACE inhibitors	Continuation of ACE inhibitors or ARBs is reasonable perioperatively	IIa	B		
	If ACE inhibitors or ARBs are held before surgery, it is reasonable to restart as soon as clinically feasible postoperatively	IIa	C		
Antiplatelet agents	Continue DAPT in patients undergoing urgent vascular surgery during the first 4–6 weeks after BMS or DES implantation, unless the risk of bleeding outweighs the benefit of stent thrombosis prevention	I	C		
	In patients with stents undergoing surgery that requires discontinuation $P2Y_{12}$ inhibitors, continue aspirin and restart the $P2Y_{12}$ platelet receptor inhibitor as soon as possible after surgery	I	C		
	Management of perioperative antiplatelet therapy should be determined by consensus of treating clinicians and the patient	I	C		
	In patients undergoing elective vascular surgery without prior coronary stenting, it may be reasonable to continue aspirin when the risk of increased cardiac events outweighs the risk of increased bleeding	IIb	B		

ACE indicates angiotensin-converting enzyme, *ARB* angiotensin-receptor blocker, *BMS* bare-metal stent, *CAD* coronary artery disease, *DAPT* dual-antiplatelet therapy, *DES* drug-eluting stent, *HF* heart failure, *RCRI* revised cardiac risk index

[a]Adapted from Fleisher et al., ACC/AHA practice guidelines [15]

Table 10.27 Recommendations on cardiovascular medications before endovascular procedure[a]

Therapy	Recommendations	COR	LOE
Beta-blockers	Continue beta-blockers in patients who are on beta-blockers chronically	I	B
	Guide management of beta-blockers after surgery by clinical circumstances, independent of when the agent was started	IIa	B
	In patients with ≥3 RCRI factors[b], it may be reasonable to begin beta-blockers before endovascular procedure	IIb	B
	Initiating beta-blockers in the perioperative setting as an approach to reduce perioperative risk is of uncertain benefit in those with a long-term indication but no other RCRI risk factors	IIb	B
	It may be reasonable to begin perioperative beta-blockers long enough in advance to assess safety and tolerability, preferably >1 day before surgery	IIb	B
	In patients with intermediate- or high-risk myocardial ischemia noted in preoperative risk stratification tests, it may be reasonable to begin perioperative beta-blockers	IIb	C
	Beta-blocker therapy should not be started on the day of procedure	III: Harm	B
Statins	Continue statins in patients currently taking statins	I	B
	Perioperative initiation of statin use is reasonable in patients undergoing vascular surgery	IIa	B
	Perioperative initiation of statins may be considered in patients with a clinical risk factor who are undergoing elevated-risk procedures	IIb	C
Alpha-2 agonists	Not recommended for prevention of cardiac events	III: No Benefit	B
ACE inhibitors	Continuation of ACE inhibitors or ARBs is reasonable perioperatively	IIa	B
	If ACE inhibitors or ARBs are held before surgery, it is reasonable to restart as soon as clinically feasible postoperatively	IIa	C
Antiplatelet agents	Continue DAPT in patients undergoing urgent vascular surgery during the first 4–6 weeks after BMS or DES implantation, unless the risk of bleeding outweighs the benefit of stent thrombosis prevention	I	C
	In patients with stents undergoing surgery that requires discontinuation $P2Y_{12}$ inhibitors, continue aspirin and restart the $P2Y_{12}$ platelet receptor inhibitor as soon as possible after surgery	I	C
	Management of perioperative antiplatelet therapy should be determined by consensus of treating clinicians and the patient	I	C
	In patients undergoing elective vascular surgery without prior coronary stenting, it may be reasonable to continue aspirin when the risk of increased cardiac events outweighs the risk of increased bleeding	IIb	B

ACE indicates angiotensin-converting enzyme, *ARB* angiotensin-receptor blocker, *BMS* bare-metal stent, *CAD* coronary artery disease, *DAPT* dual-antiplatelet therapy, *DES* drug-eluting stent, *HF* heart failure, *RCRI* revised cardiac risk index

[a]Adapted from Fleisher et al., ACC/AHA practice guidelines [15]

[b]Including diabetes mellitus, HF, CAD, renal insufficiency, and cerebrovascular accident

Conclusion

A comprehensive evaluation of cardiac, pulmonary, and renal performance is crucial to optimize patient selection. These operations are often indicated in the sickest patient. The evaluation should include noninvasive cardiac stress test (DSE or sestamibi study), pulmonary function tests, and carotid ultrasound. It is important to highlight that none of the criteria suggested in this chapter has been validated prospectively in patients undergoing complex aortic surgery. Nonetheless, guidelines should be followed and tailored taking into account institutional experience with these types of repairs and anticipated morbidity and mortality.

References

1. Parodi JC, Palmaz JC, Barone HD. Transfemoral intraluminal graft implantation for abdominal aortic aneurysms. Ann Vasc Surg. 1991;5(6):491–9.
2. Dua A, Kuy S, Lee CJ, Upchurch Jr GR, Desai SS. Epidemiology of aortic aneurysm repair in the United States from 2000 to 2010. J Vasc Surg. 2014;59(6):1512–7.
3. Huang Y, Gloviczki P, Oderich GS, Duncan AA, Kalra M, Fleming MD, et al. Outcome after open and endovascular repairs of abdominal aortic aneurysms in matched cohorts using propensity score modeling. J Vasc Surg. 2015;62(2):304–11. e2.
4. Park BD, Azefor N, Huang CC, Ricotta JJ. Trends in treatment of ruptured abdominal aortic aneurysm: impact of endovascular repair and implications for future care. J Am Coll Surg. 2013;216(4):745–54; discussion 54–5.
5. Patel RP, Katsargyris A, Verhoeven EL, Adam DJ, Hardman JA. Endovascular aortic aneurysm repair with chimney and snorkel grafts: indications, techniques and results. Cardiovasc Intervent Radiol. 2013;36(6):1443–51.
6. Wilson A, Zhou S, Bachoo P, Tambyraja AL. Systematic review of chimney and periscope grafts for endovascular aneurysm repair. Br J Surg. 2013;100(12):1557–64.
7. Park JH, Chung JW, Choo IW, Kim SJ, Lee JY, Han MC. Fenestrated stent-grafts for preserving visceral arterial branches in the treatment of abdominal aortic aneurysms: preliminary experience. J Vasc Interv Radiol. 1996;7(6):819–23.
8. Kitagawa A, Greenberg RK, Eagleton MJ, Mastracci TM. Zenith p-branch standard fenestrated endovascular graft for juxtarenal abdominal aortic aneurysms. J Vasc Surg. 2013;58(2):291–300.

9. Panuccio G, Bisdas T, Berekoven B, Torsello G, Austermann M. Performance of bridging stent grafts in fenestrated and branched aortic endografting. Eur J Vasc Endovasc Surg. 2015;50(1):60–70.
10. Oderich GS, Greenberg RK, Farber M, Lyden S, Sanchez L, Fairman R, et al. Results of the United States multicenter prospective study evaluating the Zenith fenestrated endovascular graft for treatment of juxtarenal abdominal aortic aneurysms. J Vasc Surg. 2014;60(6):1420–8.e1–5.
11. Cochennec F, Kobeiter H, Gohel M, Leopardi M, Raux M, Majewski M, et al. Early results of physician modified fenestrated stent grafts for the treatment of thoraco-abdominal aortic aneurysms. Eur J Vasc Endovasc Surg. 2015;50(5):583–92.
12. Mastracci TM, Eagleton MJ, Kuramochi Y, Bathurst S, Wolski K. Twelve-year results of fenestrated endografts for juxtarenal and group IV thoracoabdominal aneurysms. J Vasc Surg. 2015;61(2):355–64.
13. Heron M. Deaths: leading causes for 2011. Natl Vital Stat Rep. 2015;64(7):1–96.
14. Sakalihasan N, Limet R, Defawe OD. Abdominal aortic aneurysm. Lancet. 2005;365(9470):1577–89.
15. Fleisher LA, Fleischmann KE, Auerbach AD, Barnason SA, Beckman JA, Bozkurt B, et al. 2014 ACC/AHA guideline on perioperative cardiovascular evaluation and management of patients undergoing noncardiac surgery: a report of the American College of Cardiology/American Heart Association Task Force on Practice Guidelines. Circulation. 2014;130(24):e278–333.
16. Kristensen SD, Knuuti J, Saraste A, Anker S, Botker HE, Hert SD, et al. 2014 ESC/ESA guidelines on non-cardiac surgery: cardiovascular assessment and management: The Joint Task Force on non-cardiac surgery: cardiovascular assessment and management of the European Society of Cardiology (ESC) and the European Society of Anaesthesiology (ESA). Eur Heart J. 2014;35(35):2383–431.
17. Eagleton MJ, Kang J. Preoperative management. In: Cronenwett JL, Johnston KW, editors. Rutherford's vascular surgery. 8th ed. Philadelphia: Saunders; 2014. p. 466–79.
18. Chaikof EL, Brewster DC, Dalman RL, Makaroun MS, Illig KA, Sicard GA, et al. The care of patients with an abdominal aortic aneurysm: the Society for Vascular Surgery practice guidelines. J Vasc Surg. 2009;50(4 Suppl):S2–49.
19. Reilly DF, McNeely MJ, Doerner D, Greenberg DL, Staiger TO, Geist MJ, et al. Self-reported exercise tolerance and the risk of serious perioperative complications. Arch Intern Med. 1999;159(18):2185–92.
20. Girish M, Trayner Jr E, Dammann O, Pinto-Plata V, Celli B. Symptom-limited stair climbing as a predictor of postoperative cardiopulmonary complications after high-risk surgery. Chest. 2001;120(4):1147–51.
21. American Society of Anesthesiologists. ASA physical status classification system. 2014. http://www.asahq.org/resources/clinical-information/asa-physical-status-classification-system. [Cited 6 Aug 2015].
22. Mak PH, Campbell RC, Irwin MG. The ASA Physical Status Classification: inter-observer consistency. American Society of Anesthesiologists. Anaesth Intensive Care. 2002;30(5):633–40.
23. Aronson WL, McAuliffe MS, Miller K. Variability in the American Society of Anesthesiologists Physical Status Classification Scale. AANA J. 2003;71(4):265–74.
24. Chaikof EL, Fillinger MF, Matsumura JS, Rutherford RB, White GH, Blankensteijn JD, et al. Identifying and grading factors that modify the outcome of endovascular aortic aneurysm repair. J Vasc Surg. 2002;35(5):1061–6.
25. Golden MA, Whittemore AD, Donaldson MC, Mannick JA. Selective evaluation and management of coronary artery disease in patients undergoing repair of abdominal aortic aneurysms. A 16-year experience. Ann Surg. 1990;212(4):415–20. discussion 20-3.
26. Van Kuijk JP, Flu WJ, Dunckelgrun M, Bax JJ, Poldermans D. Coronary artery disease in patients with abdominal aortic aneurysm: a review article. J Cardiovasc Surg (Torino). 2009;50(1):93–107.
27. Smetana GW. Preoperative medical evaluation of the healthy patient. 2015. http://www.uptodate.com. [updated 10 Aug 2015; cited 13 Aug 2015].
28. Hernesniemi JA, Vanni V, Hakala T. The prevalence of abdominal aortic aneurysm is consistently high among patients with coronary artery disease. J Vasc Surg. 2015;62(1):232–40. e3.
29. Durieux R, Van Damme H, Labropoulos N, Yazici A, Legrand V, Albert A, et al. High prevalence of abdominal aortic aneurysm in patients with three-vessel coronary artery disease. Eur J Vasc Endovasc Surg. 2014;47(3):273–8.
30. Fleisher LA, Beckman JA, Brown KA, Calkins H, Chaikof EL, Fleischmann KE, et al. 2009 ACCF/AHA focused update on perioperative beta blockade incorporated into the ACC/AHA 2007 guidelines on perioperative cardiovascular evaluation and care for noncardiac surgery: a report of the American College of Cardiology Foundation/American Heart Association Task Force on practice guidelines. Circulation. 2009;120(21):e169–276.
31. Nishimura RA, Otto CM, Benow RO, et al. 2014 AHA/ACC guidelines for the management of patients with valvular heart disease: a report of the American College of Cardiology/American Heart Association Task Force on Practice Guidelines. J Am Coll Cardiol. 2014;63(22):2438–88.
32. Kristensen SD, Knuuti J. New ESC/ESA guidelines on non-cardiac surgery: cardiovascular assessment and management. Eur Heart J. 2014;35(35):2344–5.
33. Lee TH, Marcantonio ER, Mangione CM, Thomas EJ, Polanczyk CA, Cook EF, et al. Derivation and prospective validation of a simple index for prediction of cardiac risk of major noncardiac surgery. Circulation. 1999;100(10):1043–9.
34. Gupta PK, Gupta H, Sundaram A, Kaushik M, Fang X, Miller WJ, et al. Development and validation of a risk calculator for prediction of cardiac risk after surgery. Circulation. 2011;124(4):381–7.
35. Cohen ME, Ko CY, Bilimoria KY, Zhou L, Huffman K, Wang X, et al. Optimizing ACS NSQIP modeling for evaluation of surgical quality and risk: patient risk adjustment, procedure mix adjustment, shrinkage adjustment, and surgical focus. J Am Coll Surg. 2013;217(2):336–46.e1.
36. Bertges DJ, Goodney PP, Zhao Y, Schanzer A, Nolan BW, Likosky DS, et al. The Vascular Study Group of New England Cardiac Risk Index (VSG-CRI) predicts cardiac complications more accurately than the Revised Cardiac Risk Index in vascular surgery patients. J Vasc Surg. 2010;52(3):674–83, 83.e1–83.e3.
37. Ford MK, Beattie WS, Wijeysundera DN. Systematic review: prediction of perioperative cardiac complications and mortality by the revised cardiac risk index. Ann Intern Med. 2010;152(1):26–35.
38. Bilimoria KY, Liu Y, Paruch JL, Zhou L, Kmiecik TE, Ko CY, et al. Development and evaluation of the universal ACS NSQIP surgical risk calculator: a decision aid and informed consent tool for patients and surgeons. J Am Coll Surg. 2013;217(5):833–42.e1–3.
39. Rodseth RN, Lurati Buse GA, Bolliger D, Burkhart CS, Cuthbertson BH, Gibson SC, et al. The predictive ability of pre-operative B-type natriuretic peptide in vascular patients for major adverse cardiac events: an individual patient data meta-analysis. J Am Coll Cardiol. 2011;58(5):522–9.
40. Biccard BM, Lurati Buse GA, Burkhart C, Cuthbertson BH, Filipovic M, Gibson SC, et al. The influence of clinical risk factors on pre-operative B-type natriuretic peptide risk stratification of vascular surgical patients. Anaesthesia. 2012;67(1):55–9.
41. Fleisher LA. Preoperative evaluation of the patient with hypertension. JAMA. 2002;287(16):2043–6.
42. Eagle KA, Berger PB, Calkins H, Chaitman BR, Ewy GA, Fleischmann KE, et al. ACC/AHA guideline update for perioperative

cardiovascular evaluation for noncardiac surgery--executive summary: a report of the American College of Cardiology/American Heart Association Task Force on Practice Guidelines (Committee to Update the 1996 Guidelines on Perioperative Cardiovascular Evaluation for Noncardiac Surgery). J Am Coll Cardiol. 2002;39(3):542–53.
43. Schermerhorn ML, O'Malley AJ, Jhaveri A, Cotterill P, Pomposelli F, Landon BE. Endovascular vs. open repair of abdominal aortic aneurysms in the Medicare population. N Engl J Med. 2008;358(5):464–74.
44. Piffaretti G, Mariscalco G, Bonardelli S, Sarcina A, Gelpi G, Bellosta R, et al. Predictors and outcomes of acute kidney injury after thoracic aortic endograft repair. J Vasc Surg. 2012;56(6):1527–34.
45. Drews JD, Patel HJ, Williams DM, Dasika NL, Deeb GM. The impact of acute renal failure on early and late outcomes after thoracic aortic endovascular repair. Ann Thorac Surg. 2014;97(6):2027–33. discussion 33.
46. Kidney Disease: Improving Global Outcomes (KDIGO). Acute Kidney Injury Work Group. KDIGO clinical practice guideline for acute kidney injury. Kidney Int Suppl. 2012;2:1–138.
47. Acute kidney injury: prevention, detection and management up to the point of renal replacement therapy. London: National Clinical Guideline Centre; 2013.
48. Bellomo R, Ronco C, Kellum JA, Mehta RL, Palevsky P. Acute renal failure—definition, outcome measures, animal models, fluid therapy and information technology needs: the Second International Consensus Conference of the Acute Dialysis Quality Initiative (ADQI) Group. Crit Care. 2004;8(4):R204–12.
49. Sakamaki F, Oya H, Nagaya N, Kyotani S, Satoh T, Nakanishi N. Higher prevalence of obstructive airway disease in patients with thoracic or abdominal aortic aneurysm. J Vasc Surg. 2002;36(1):35–40.
50. Meijer CA, Kokje VB, van Tongeren RB, Hamming JF, van Bockel JH, Moller GM, et al. An association between chronic obstructive pulmonary disease and abdominal aortic aneurysm beyond smoking: results from a case-control study. Eur J Vasc Endovasc Surg. 2012;44(2):153–7.
51. Vestbo J, Hurd SS, Agusti AG, Jones PW, Vogelmeier C, Anzueto A, et al. Global strategy for the diagnosis, management, and prevention of chronic obstructive pulmonary disease: GOLD executive summary. Am J Respir Crit Care Med. 2013;187(4):347–65.
52. Canet J, Gallart L, Gomar C, Paluzie G, Valles J, Castillo J, et al. Prediction of postoperative pulmonary complications in a population-based surgical cohort. Anesthesiology. 2010;113(6):1338–50.
53. Gupta H, Gupta PK, Fang X, Miller WJ, Cemaj S, Forse RA, et al. Development and validation of a risk calculator predicting postoperative respiratory failure. Chest. 2011;140(5):1207–15.
54. Gupta H, Gupta PK, Schuller D, Fang X, Miller WJ, Modrykamien A, et al. Development and validation of a risk calculator for predicting postoperative pneumonia. Mayo Clin Proc. 2013;88(11):1241–9.
55. Shah AD, Langenberg C, Rapsomaniki E, Denaxas S, Pujades-Rodriguez M, Gale CP, et al. Type 2 diabetes and incidence of cardiovascular diseases: a cohort study in 1.9 million people. Lancet Diabetes Endocrinol. 2015;3(2):105–13.
56. King Jr JT, Goulet JL, Perkal MF, Rosenthal RA. Glycemic control and infections in patients with diabetes undergoing noncardiac surgery. Ann Surg. 2011;253(1):158–65.
57. Handelsman Y, Bloomgarden ZT, Grunberger G, Umpierrez G, Zimmerman RS, Bailey TS, et al. American Association of Clinical Endocrinologists and American College of Endocrinology—clinical practice guidelines for developing a diabetes mellitus comprehensive care plan—2015. Endocr Pract. 2015;21 Suppl 1:1–87.
58. Umpierrez GE, Hellman R, Korytkowski MT, Kosiborod M, Maynard GA, Montori VM, et al. Management of hyperglycemia in hospitalized patients in non-critical care setting: an endocrine society clinical practice guideline. J Clin Endocrinol Metab. 2012;97(1):16–38.
59. James PA, Oparil S, Carter BL, Cushman WC, Dennison-Himmelfarb C, Handler J, et al. 2014 Evidence-based guideline for the management of high blood pressure in adults report from the panel members appointed to the Eighth Joint National Committee (JNC 8). JAMA. 2014;311(5):507–20.
60. Mehta RL, Kellum JA, Shah SV, Molitoris BA, Ronco C, Warnock DG, Levin A, Acute Kidney Injury Network. Acute Kidney Injury Network: report of an initiative to improve outcomes in acute kidney injury. Crit Care. 2007;11(2):R31.
61. Mehta RL. Kidney disease: improving global outcomes (KDIGO) acute kidney injury workgroup. KDIGO clinical practice guideline for acute kidney injury. Kidney Int Suppl. 2012;2:1–138.

11 Computed Tomography/Computed Tomography Angiography for Evaluation, Planning, and Surveillance of Complex Endovascular Repair

Terri J. Vrtiska, Thanila A. Macedo, and Gustavo S. Oderich

Introduction

Endovascular aortic repair (EVAR) has become the first treatment option in most patients with thoracic and abdominal aortic aneurysms. EVAR is also used for other indications including acute aortic syndrome (e.g., dissections, penetrating ulcers, intramural hematomas), coarctation, infection, vasculitis, and traumatic aortic injury. In the last decade, indications for EVAR have been extended to patients with aneurysms and dissections involving the aortic arch, thoracoabdominal, and iliac arteries. This has been possible with development of techniques of branch vessel incorporation using fenestrations, branches, and parallel grafts. Computed tomography (CT) and computed tomography angiography (CTA) are essential to plan aortic repair using either open or endovascular techniques. Its utility in planning endovascular procedures relies on the accurate assessment of etiology, extent of disease, involvement of side branches, adequacy of access vessels, and presence of extra-vascular diseases that might affect treatment selection and approach. However, CT/CTA should not simply be ordered with the expectation that an adequate and informative study will appear at the fingertips of the clinician. Imaging studies often require tailoring the examination to a specific indication and establishing pre-existing protocols in collaboration with radiology colleagues. Communication between multiple specialties, including the radiologist performing the study, is critical to properly address specific questions.

The vast majority of current CT scanners use two-dimensional multi-detector elements (MDCT). The term *CAT scan*, coined in the 1980s to denote *Computed Axial Tomography*, coined a linear array of detector element, which has been replaced by the more advanced MDCT scanner technology. The detectors are mounted in a gantry, which is positioned opposite to the x-ray source. The gantry rotates at a predefined speed continuously in the same direction, while the table moves in a continuous linear fashion through the gantry while it is rotating. The images are obtained in a helical manner over the desired anatomy. This portion of the study is termed acquisition phase, and the data obtained in this phase define the ultimate quality of the study.

The acquired data are then reconstructed into a format that is desired for clinical analysis including the width of slice increments impacting the resolution of the CT examination. Pre-established protocols are useful to standardize imaging in clinical practice to fit specific indications. Post-processing of the source images allows production of many types of images including off-axis multi-planar display and volume-rendered reconstructions that provide a means for clinicians to perform complex measurements and analysis. This chapter summarizes the critical aspects of CT imaging for evaluation, planning, and follow-up of complex endovascular repair in patients with aortic aneurysms and dissections.

Imaging Data

CT imaging data are constructed from small square image elements termed pixels, which are identified by a position in the *x*- and *y*-planes as well as a quantitative radio-density (or Hounsfield unit) in the gray scale color spectrum. The

T.J. Vrtiska (✉)
Section of Vascular CT, Department of Diagnostic Radiology, Mayo Clinic, 200 First Street SW, Rochester, MN 55905, USA
e-mail: vrtiska.terri@mayo.edu

T.A. Macedo
Department of Diagnostic Radiology, Mayo Clinic, 200 First Street SW, Rochester, MN 55905, USA
e-mail: Macedo.Thanila@mayo.edu

G.S. Oderich
Division of Vascular and Endovascular Surgery, Mayo Clinic, 200 First Street SW, Rochester, MN 55905, USA
e-mail: oderich.gustavo@mayo.edu

© Mayo Foundation for Medical Education and Research 2017

G.S. Oderich (ed.), *Endovascular Aortic Repair*, DOI 10.1007/978-3-319-15192-2_11

Hounsfield unit (HU) scale is bounded on one end by air, which is represented by black (negative numbers), and on the other end by bone, which is represented by white (positive numbers). Water is neutral and defined as 0 HU. Typically, the *x*–*y* resolution of a CT scan is 0.4–0.6 mm in the axial plane. However, when data are obtained in a helical volumetric format using MDCT, each pixel is also extended in the *z*-plane direction, and represented by a volume rather than planer unit. The volume unit is termed *voxel*. Each voxel has an *x*, *y*, and *z* coordinate and a resolution in the *x*–*y* and *z*-plane. When the resolution in the *x*–*y* and *z* planes is equal, the term *isotropic resolution* is used. Post-processing of reconstructed imaging is most accurate when a scan is acquired and reconstructed as close to isotropic resolution as possible.

Vascular imaging requires a technique to visualize blood-filled structures (arteries and veins) typically represented in a HU spectrum of + 30–45 and separate them from adjacent structures with a similar HU spectrum. To create a larger HU gradient between blood and the adjacent structures, administration of iodinated intravenous contrast provides an HU of +130 or greater in the opacified blood vessel. Ultimately, the ability to discriminate between two voxels depends upon the spatial resolution and the gradient between neighboring voxels based on their relative HU. Many examinations can be acquired using multiphase technique including an acquisition before and after the administration of iodinated contrast material. The pre-contrast acquisition provides an accurate assessment of the vessel wall and can be used to differentiate intramural hematomas from inflammation, as well as assessment of calcification patterns. The arterial, or contrast enhanced phase of the study, best depicts the lumen of the vessel and the early opacification of end organs with contrast. A delayed acquisition can be included to demonstrate regions of the vasculature or organ parenchyma enhancement that opacifies more slowly with contrast, such as an aneurysm sac filled by a retrograde endoleak from the lumbar arteries or a parenchymal infarct involving the spleen or kidneys.

Scan Parameters

The quantity and quality of energy that is generated by the x-ray source of the CT scanner is termed the tube voltage and is measured in peak kilo-voltage (kVp). A high kVp penetrates tissues better, but it has the effect of decreasing gradient of HU between voxels. Therefore, an obese patient requires a high kVp simply to provide enough energy to penetrate the thicker tissue but may result in less optimal tissue separation. A lower kVp can be used in thinner patients or in children, and results in a lower radiation exposure and better contrast differences between tissues. The rate of x-ray production delivered by the x-ray tube per second is represented by milliampere/second (mAs). A higher mAs translates into sharper images because more photons are reaching the detector to create the image. However, as the mAs increases, so does the radiation dose. Most often kVp and mAs are linked and dictated by specific protocols (Table 11.1), but modifications can be made to the acquisition parameters if indicated to optimize image quality dependent on the patient size and examination type.

Table 11.1 Abdominal aortic computed tomography angiogram example of acquisition parameters

Scan type	Spiral
Rotation time (s)	0.5
Collimation	64×0.6
Pitch	1.2
Reference kV	120
Quality reference mAs	240
CARE dose 4D	ON
Breath-hold	Inspiration

Other important factors during MDCT studies are the collimation, which allows regulation of the thickness of the x-ray beam and the table speed or how fast a patient moves through the gantry. Table speed, collimation, and the speed that the gantry rotates define the pitch of the helical data that are acquired. If the table quickly advances a patient through a slowly spinning gantry, the scan will be fast, but the *z*-plane resolution will be poor. Alternatively, if the gantry speed is increased or the table speed is decreased, a tighter spiral of data will be obtained, improving the *z*-plane resolution. Similarly, if a thinner collimation is used, finer data cuts are acquired. In general a pitch less than one is optimal for subsequent image reconstructions, but newer MDCT scanners use alternative reconstruction algorithms that do not allow a simple calculation of the pitch.

In some locations such as the aortic valve or ascending aorta, the temporal resolution of scans is important because of the dynamic nature of the vascular beds impacted by hemodynamic forces and pulsatility. Electrocardiography (ECG) gating is a technique that allows the acquisition of data during a specific phase of the cardiac cycle (usually during diastole) or during multiple points during a cardiac cycle. Although technological advancements have minimized the need to slow heart rates during ECG-gated MDCT, it is important that patients are not tachycardic. Irregular heart rate can also make cardiac gating challenging and result in image degradation. These scans often have higher radiation exposure and limited scan length, which reduces its utilization in patients with thoracic and thoracoabdominal aortic disease. Its primary indications are for patients with involvement of the aortic valve, the ascending aorta and aortic arch. Multiphase studies can be acquired that depict data throughout the cardiac cycle (as many as 20 phases) and illustrate four-dimensional anatomy, with change in the cardiac anatomy over time being the fourth dimension. Thus specific

measurements can be made during peak systole and end diastole establishing a range of diameters of the vessel over the cardiac cycle.

Reconstruction

The data acquired from an MDCT scan are reconstructed into two-dimensional axial images with a slice thickness. The thickness of the slices may overlap, so that the same point in three-dimensional (3D) space on the patient is represented on two different slices. This method optimizes the spatial resolution of the study and helps to improve the accuracy of volumetric 3D-reconstruction. Multi-planar reformatting (MPR) is the most common method used to display a CT scan today (Fig. 11.1), and it typically consists of a panel that depicts the axial, coronal, and sagittal reconstructions. However, because the data exist in three dimensions, the angle of each planar reconstruction can be modified, allowing the clinician to interpret the specific relationships among the various structures.

Maximum intensity projections (MIPs) are created by projecting the voxels created up to a maximum value into a visualization plane. The voxels are grouped and projected at a uniform HU value that is equal to the highest HU value within the grouping of points. This connects the high-intensity regions of contrast-enhanced vessels in three dimensions, which can then be viewed from any projection. As vessels that pass back and forth between planes, they can be viewed by scrolling through any one of the imaging sets. Alternatively, a curved MPR can be created that allows interpretation of a specific vascular bed. This is done by creating a reconstruction of the images along the centerline of flow (CLF) of a vessel (Fig. 11.2).

MIP images define the borders of a vessel, allowing the geometric center to be calculated. The dots representing the center of the vessel lumen in 3D space are connected to form the CLF. The vessel can be projected along a curved CLF or a straightened CLF. Although there is some debate into which is the best method to measure vessel diameter, most experts use CLF projections (Fig. 11.3). An image is reconstructed that is perpendicular to the CLF, and the diameter of

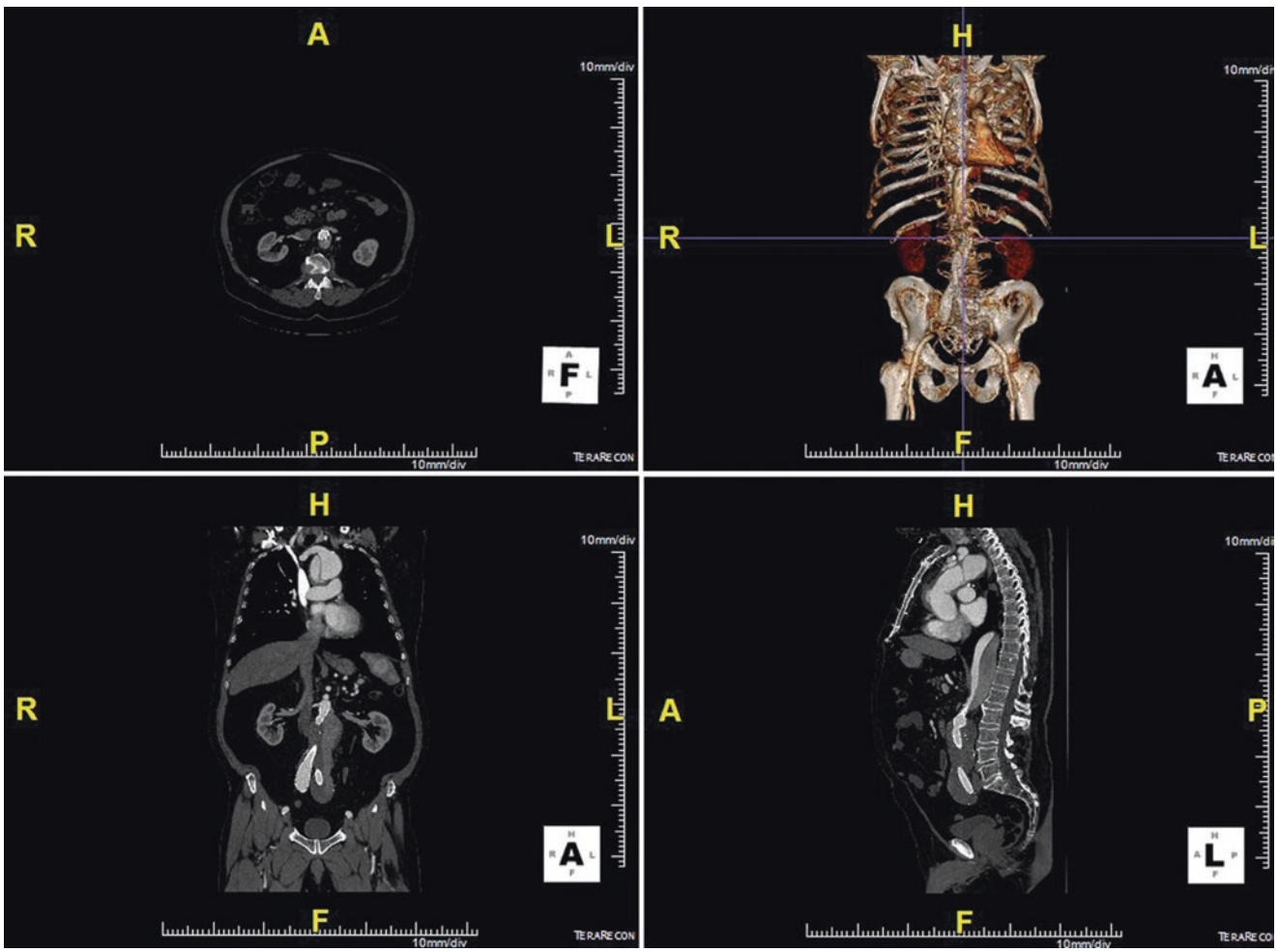


Fig. 11.1 Multi-planar reformatting (MPR) typically includes a panel that depicts the axial, coronal, and sagittal reconstructions. By permission of Mayo Foundation for Medical Education and Research. All rights reserved



Fig. 11.2 The tortuous aorta (**a**) is evaluated using centerline of flow analysis (CLF, **b**). A curved multi-planar reformatting (MPR) image is created to analyze specific segments of the vessel (**c**). The straightened CLF is used for measurements of lengths and to assess the extent of aortic disease (**d**). By permission of Mayo Foundation for Medical Education and Research. All rights reserved

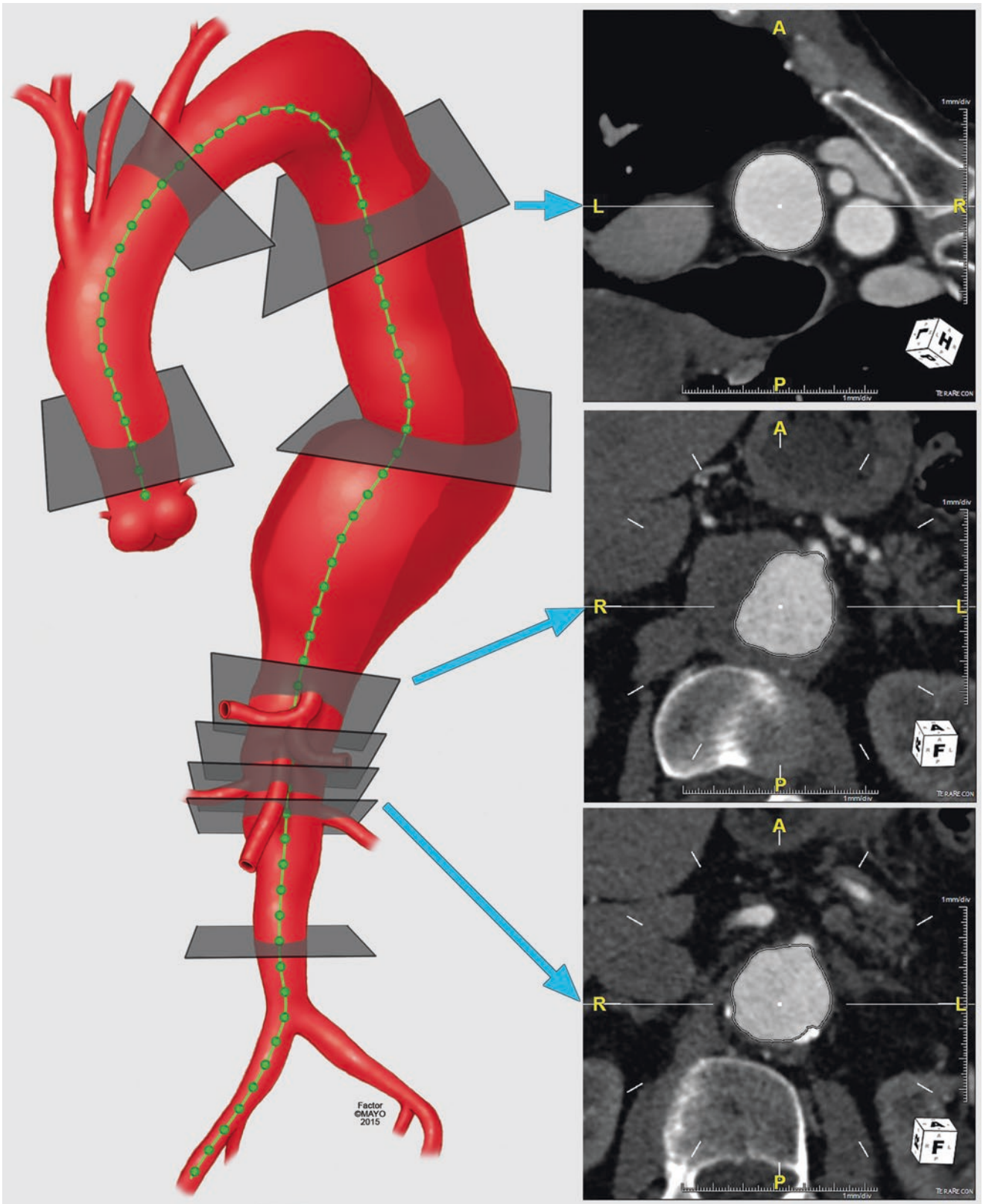


Fig. 11.3 Use of centerline of flow to evaluate aortic diameters in each specific segment. By permission of Mayo Foundation for Medical Education and Research. All rights reserved

Table 11.2 Scanning protocols for abdominopelvic CT and CT angiography (CTA) examinations[a]

	CT		CTA	
Parameter	Routine	Liver or pancreas	Thoracic, abdominal, extremity	Renal artery
Scan type	Spiral	Spiral	Spiral	Spiral
Rotation time (s)	0.5	0.5	0.5	0.5
Collimation (mm)	128×0.6	128×0.6	128×0.6	128×0.6
Pitch	0.8	0.8	0.4 for extremities, 0.6 for others	0.6
Reference tube potential (kV)	120	120	120	120
Quality reference mAs	240	350	250	350
CARE kV	On	On	On	On
CARE kV strength	8	6	11	11
CARE dose 4D	On	On	On	On

[a]Adapted from Yu L, Fletcher JG, Grant KL, Carter RE, Hough DM, Barlow JM, Vrtiska TJ, et al. Automatic selection of tube potential for radiation dose reduction in vascular and contrast-enhanced abdominopelvic CT. AJR Am J Roentgenol. 2013 August; 201 (2): 297–306
Reprinted with permission from the American Journal of Roentgenology

the vessel is measured from this image. This obviates the need to obtain the maximum/minimum diameters of vessels from images that may cut obliquely through a vessel, which create an inconsistent and less accurate way to measure the diameter of aneurysms or stenosis.

Standardized Protocols

CT angiogram acquisitions are adapted according to the clinical question as well as potential interventions. Typically the examinations are performed on state-of-the-art scanner technology (128-MDCT scanners or greater) in order to provide the optimal image resolution at the lowest radiation dose. The examinations are acquired with a spiral technique and a rotation time of 0.5 s. A typical detector configuration is 128×0.6 mm with a pitch of <1. Traditionally, 120 kVp has been used for the average-sized patients, however, using newer technologies such as auto-kV accompanied with technological scanner advances allow the scans to be acquired at a lower kVp without compromising image quality. Automatic exposure control (AEC) is also an advanced technique used in all CT angiogram studies in order to adjust the tube current based on the specific size and shape of the patient resulting in considerable radiation dose reduction (40–60 %) compared to earlier CT acquisitions without AEC. Administration of iodinated intravenous contrast material volume is also adjusted to the patient size typically using 80–140 ml of contrast material although recent scanner advancement allows consistent arterial opacification with volumes as low as 40–50 ml. The rate of contrast injection for an arterial study most commonly is performed at 4–5 ml/s followed by 25 ml of normal saline in order to flush the contrast material from the arm veins and use the full contrast bolus in the CTA acquisition. Examples of standard CT angiogram acquisitions are given in Table 11.2.

Special Protocols

Low Radiation

A regular requirement for CT scanning is optimization of radiation dose to follow the ALARA principle, or As Low As Reasonably Achievable. This requirement is applied to every CTA study but is especially important when considering examinations in young patients, patients undergoing repetitive examinations or multiphase CT acquisitions. Current CT scanners have been optimized to use the radiation dose most efficiently from the electronic components as well as decreasing noise within the CT examinations. Automatic exposure control is now established as a necessary addition to nearly all CT examinations and individualizes the tube current to each patient. Other radiation lowering techniques include Auto kV, which typically lowers the kilovolts for the patient based on the patient size. A simple way to also lower the radiation dose for every examination is to limit the acquisition coverage and number of acquisitions to only those needed for the specific study. For example, only scanning the length of an endovascular stent in follow-up can markedly reduce the radiation dose rather than "over-scanning" the entire chest, abdomen and pelvis, if not clinically indicated. Finally, ongoing advancements in iterative reconstruction (IR) techniques allow CT examinations to be obtained at a lower dose (e.g., greater noise), which are then processed to improve the visualization of vascular and other structures to match examinations that would have been obtained at a higher radiation dose.

Low Contrast

Using lower volumes of iodinated contrast material (renal-sparing protocols) is possible with the latest CT technology (Fig. 11.4). For example, the amount of iodinated contrast

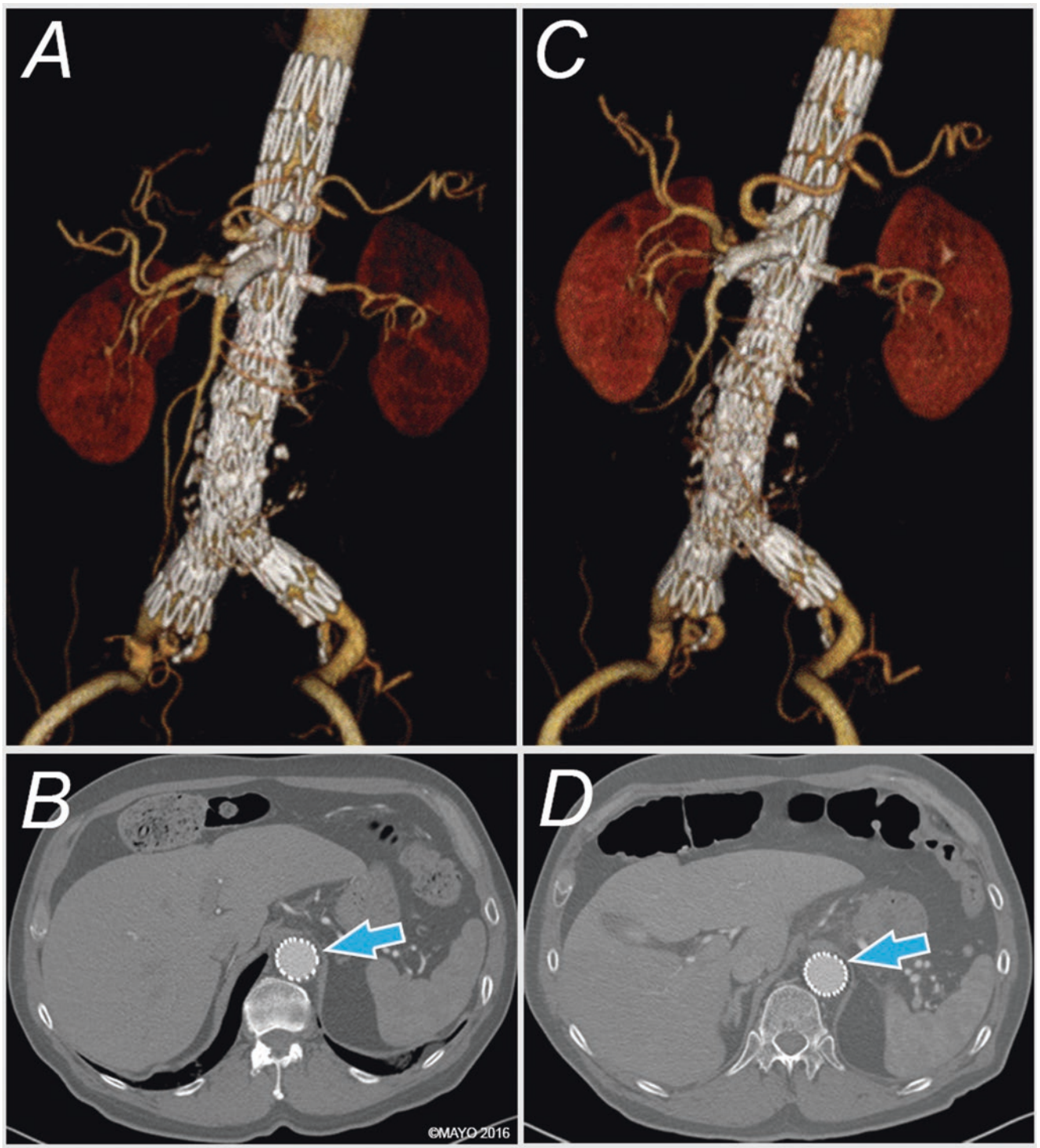


Fig. 11.4 A 74-year-old male with two postoperative CT angiograms. (**a**, **b**) A volume-rendered image and axial CTA acquired on the third-generation dual-source dual-energy CT scanner required only 50 ml of IV contrast material. (**c**, **d**) A traditional CT angiogram obtained 4 months later used a full-contrast bolus of 140 ml of IV contrast. Note that there is no change in the aortic enhancement using the smaller amount of IV contrast (*arrows*). By permission of Mayo Foundation for Medical Education and Research. All rights reserved

material can be markedly reduced in the third-generation dual source CT scanners (SOMATOM FORCE; Siemens Healthcare, Malvern, PA) through improvements in the x-ray tube, which has a smaller focal spot accompanied by a larger x-ray generator. The impact of these changes allows low kV scanning to be performed. There is improved visualization of iodine at lower doses of IV contrast and at a lower kV. Using these newest CT scanners, IV contrast volumes can be reduced to 30 % of prior IV contrast injections (e.g., 50 ml or less), with acceptable image quality and confidence in

diagnostic review. The ability to give the smaller doses of contrast material is especially useful in patients with poor renal function who may undergo multiple catheter interventions as well as multiple CT angiograms for preoperative and postoperative assessment.

Intra-arterial Injection

Approximately one-third of the patients with complex aortic aneurysms have Stage III or greater chronic kidney disease. Contrast-induced nephropathy continues to be a controversial topic, and to generate significant anxiety from patients and physicians. Prior to use of low-contrast CT protocols specified above, we have evaluated intra-arterial contrast injection for CTA to plan endovascular repair with fenestrated and branched endografts in patients with severe renal dysfunction. This was used selectively in a few patients with Stage IIIb or IV chronic kidney disease. The IA-CTA protocol required placement of a 5Fr transfemoral flush catheter, which was positioned in the proximal descending thoracic aorta. IA-CTA was obtained using helical MDCT scanner with total of 40 ml of non-ionic contrast agent diluted in 80 ml of normal saline and injected at 8 ml/s for 15 s (Fig. 11.5). Although the quality of the studies was considered satisfactory to plan the procedures, the need for placement of intra-arterial catheter under fluoroscopy and the added cost represented major limitations. More recently, the availability of third-generation dual source CT scanners (SOMATOM FORCE; Siemens Healthcare, Malvern, PA) and low-contrast protocols eliminated the need for IA-CTA.

Initial Aortic Assessment

All patients with aortic pathology need assessment of the entire aorta using CT, CTA, magnetic resonance imaging (MRI) or magnetic resonance angiography (MRA), irrespective of the disease extent, or whether the primary problem is an aneurysm, dissection, or other aortic disorder (Fig. 11.6). The importance of a thorough imaging evaluation relies on the incidence of concomitant multi-segment disease in 10–25 % of patients, and the need to assess the arch and iliofemoral arteries to evaluate the risk of stroke and anticipate access challenges. A single-phase CTA is typically performed of the chest, abdomen, and pelvis for the initial examination. However, the study can be adapted to include pre-contrast or delayed images depending on the specific indication. If the proximal aorta is not diseased, the subsequent CTAs are tailored to image only the relevant anatomy such as the abdomen and pelvis, and the number of phases and longitudinal extent of the examination is decreased to limit the radiation dose. In patients who have arterial wall thickening identified on CTA, the pre-contrast phase is used to ascertain the presence of blood (hematoma) in the aortic wall rather than inflammation that may be associated with rapid growth or an arteritis. The non-contrast phase also provides an assessment of calcifications.

The aorta and its branches are evaluated for stenosis or dilatation on the optimal phase of arterial enhancement. This should be done in a systematic manner, usually relying upon the axial images. Scrolling through the axial images, the aorta is inspected first, followed by each of the main aortic branches, including the supra-aortic trunks, the celiac, superior mesenteric artery (SMA), renals, and internal iliac arteries. When pathology is noted and specific measurements are needed, one can rely upon MIP images and the creation of CLF for the assessment of luminal narrowing, and the projection of images perpendicular to the CLF for measurements of the outer wall diameter. These data are used to establish a diagnosis and assist with the planning of treatment for patients with aortic disease.

Analysis of Disease Extent

Arteries are cylindrical and have decreasing diameter as they travel distally through the circulation. Disease assessment is performed using surrogates such as changes in diameter or presence of arterial wall abnormalities such as calcium, thrombus, debris, or thickening. The vessel wall, in the absence of any pathology, is difficult to accurately quantify on most CT studies. A vessel wall that appears thick or is lined by atherosclerotic debris indicates pathology and should be further evaluated. Aortic aneurysms are traditionally classified according to which specific segment and side branches they involve. Figures 11.7 and 11.8 summarize proposed nomenclature based on extent of disease by CTA for complex abdominal and thoracoabdominal aortic aneurysms. Aortic disease moves cranially with progressive involvement of side branches. Therefore, it is not infrequent that very large aneurysms have signs of disease affecting the renal and mesenteric arteries, or the aorta in the chest. CTA imaging has revolutionized assessment of extent of aortic disease, which plays a critical role on selection of treatment method or extent of aortic replacement.

CLF studies provide the greatest amount of information when carefully assessing the aorta. The area of aortic dilatation can be readily identified, compared with adjacent segments, and evaluated for specific vessel involvement. When evaluating the results of treatment, the extent of disease and presence of specific complications such as endoleaks, device integrity issues, stenosis, occlusions, migration, or disconnections,

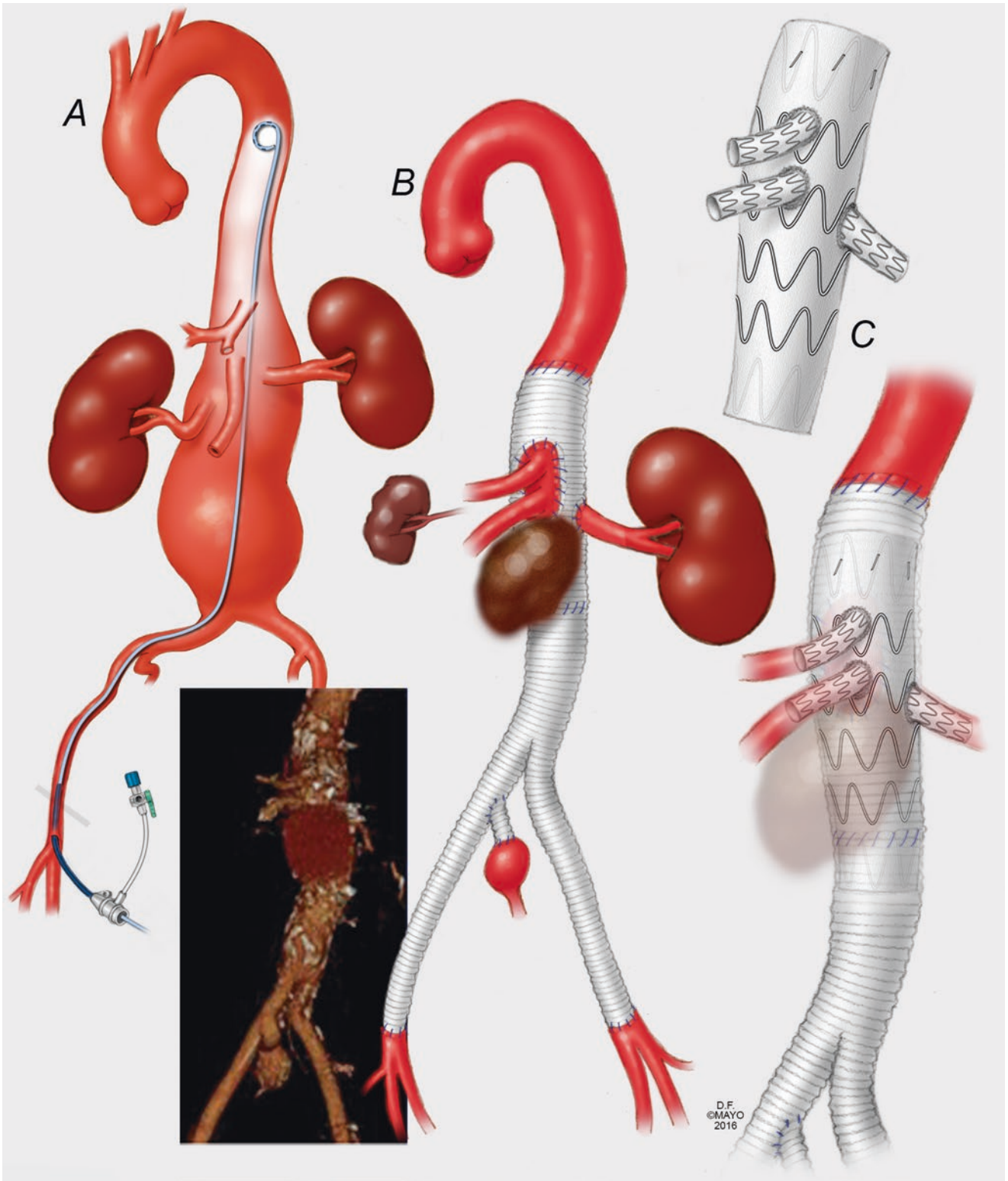


Fig. 11.5 Technique of intra-arterial contrast injection for computed tomography angiography (IA-CTA). Using trans-femoral arterial access, a flush diagnostic catheter with no radiopaque markers is positioned in the proximal thoracic aorta (**a**). In the case presented, a patient with severe renal dysfunction and a large acute pseudo-aneurysm at the level of the mesenteric arteries (**b**) is evaluated by IA-CTA and immediately taken to the hybrid endovascular room for emergency repair using a modified fenestrated graft (**c**). By permission of Mayo Foundation for Medical Education and Research. All rights reserved

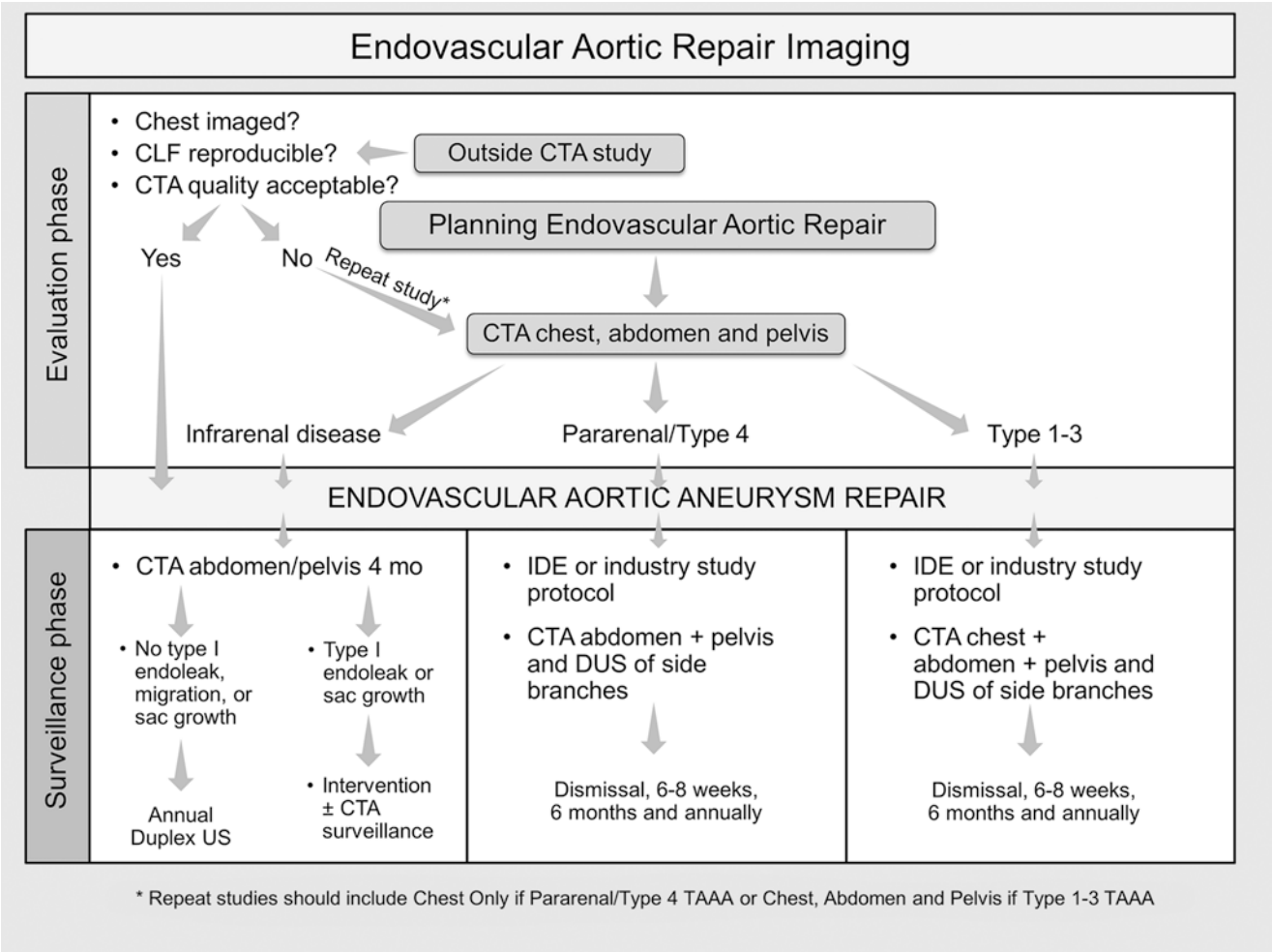


Fig. 11.6 Mayo Clinic protocol of computed tomography angiography evaluation prior to endovascular repair according to extent of aortic disease. By permission of Mayo Foundation for Medical Education and Research. All rights reserved

should be interpreted and categorized in accordance with the published reporting standards of the Society of Vascular Surgery for reports dealing with abdominal aortic aneurysms, thoracic, and thoracoabdominal aortic aneurysms.

Aneurysm Size Measurements

Significant progress has been made since the time where aneurysms were measured using very rudimentary techniques. Early CT scans were used to evaluate the aorta, but vessel tortuosity posed some challenges. Because the aorta is often tortuous in aneurysmal segments, slices from nonhelical CT studies provide an elliptical section of the vessel, which most often represents the obliquity of the plane intersecting with the vessel rather than an unusually shaped aorta. Clinicians generally agree that the minimal diameter of the vessel in a given slice of a CT scan most closely represents the maximal diameter of the aneurysm. Current reconstruction techniques make aneurysm size assessment both simpler and more reproducible, allowing analysis of the aneurysm morphology and selection of optimal location, projection, and technique to measure the largest aneurysm diameter. This requires analysis of imaging in the axial, coronal, sagittal planes as well as CLF (see Fig. 11.3).

In general, diameter measurements should always be made perpendicular to the CLF. This can be done manually using MPR projections, by aligning two of the three planes orthogonal to the measurement plane, or using automated technique and CLF with an orthogonal image projection. CLF measurements of maximum diameter allow any unusual vessel morphology to be accurately depicted on the reconstructed image. Volume calculation can also be obtained and may be a more accurate representation for assessment of aneurysm sac enlargement, given that any maximal aneurysm diameter measurement is representative of a single location. However,

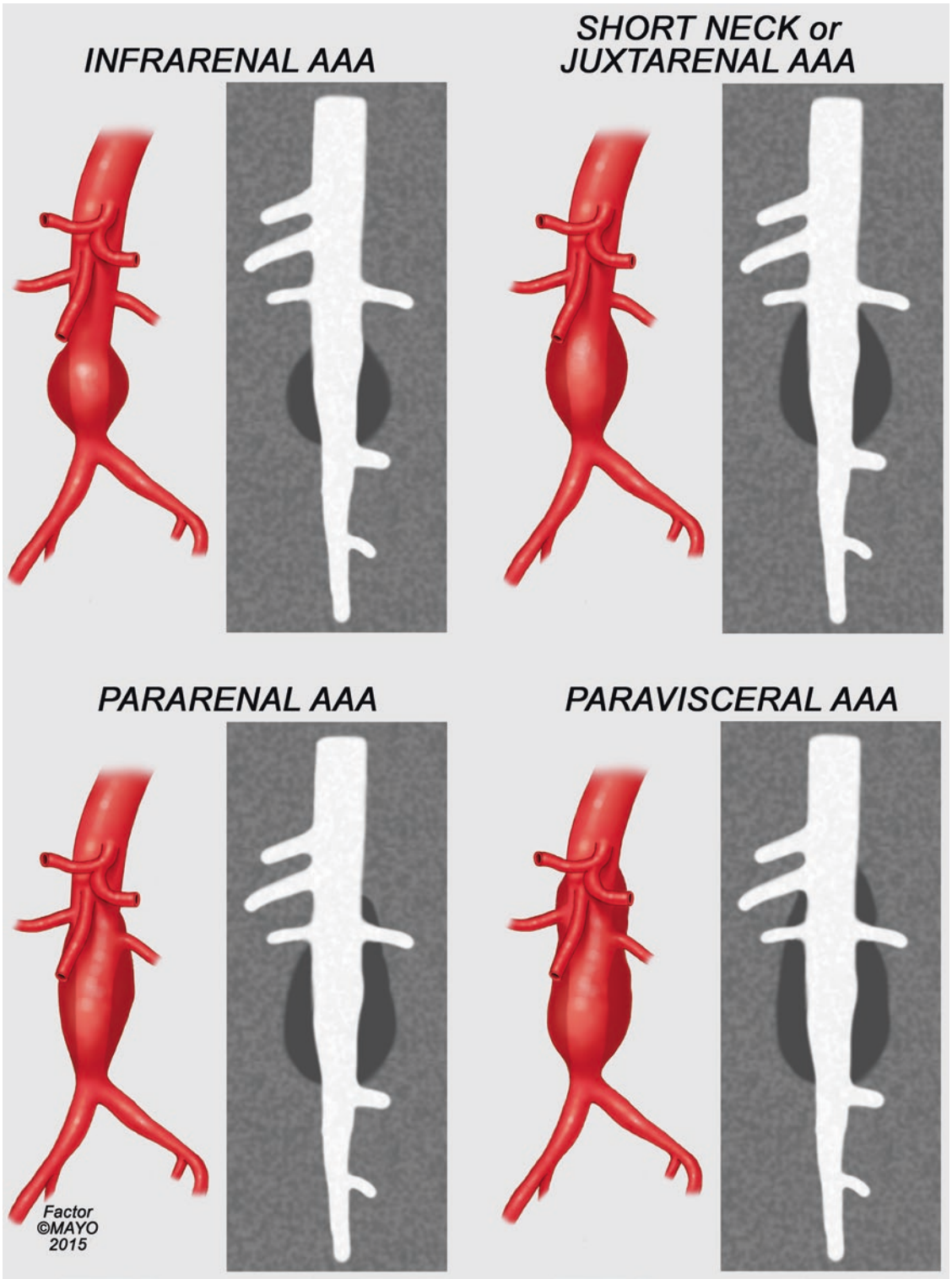


Fig. 11.7 Proposed nomenclature for complex abdominal aortic aneurysms based on analysis of parallel aortic wall by computed tomography angiography. By permission of Mayo Foundation for Medical Education and Research. All rights reserved

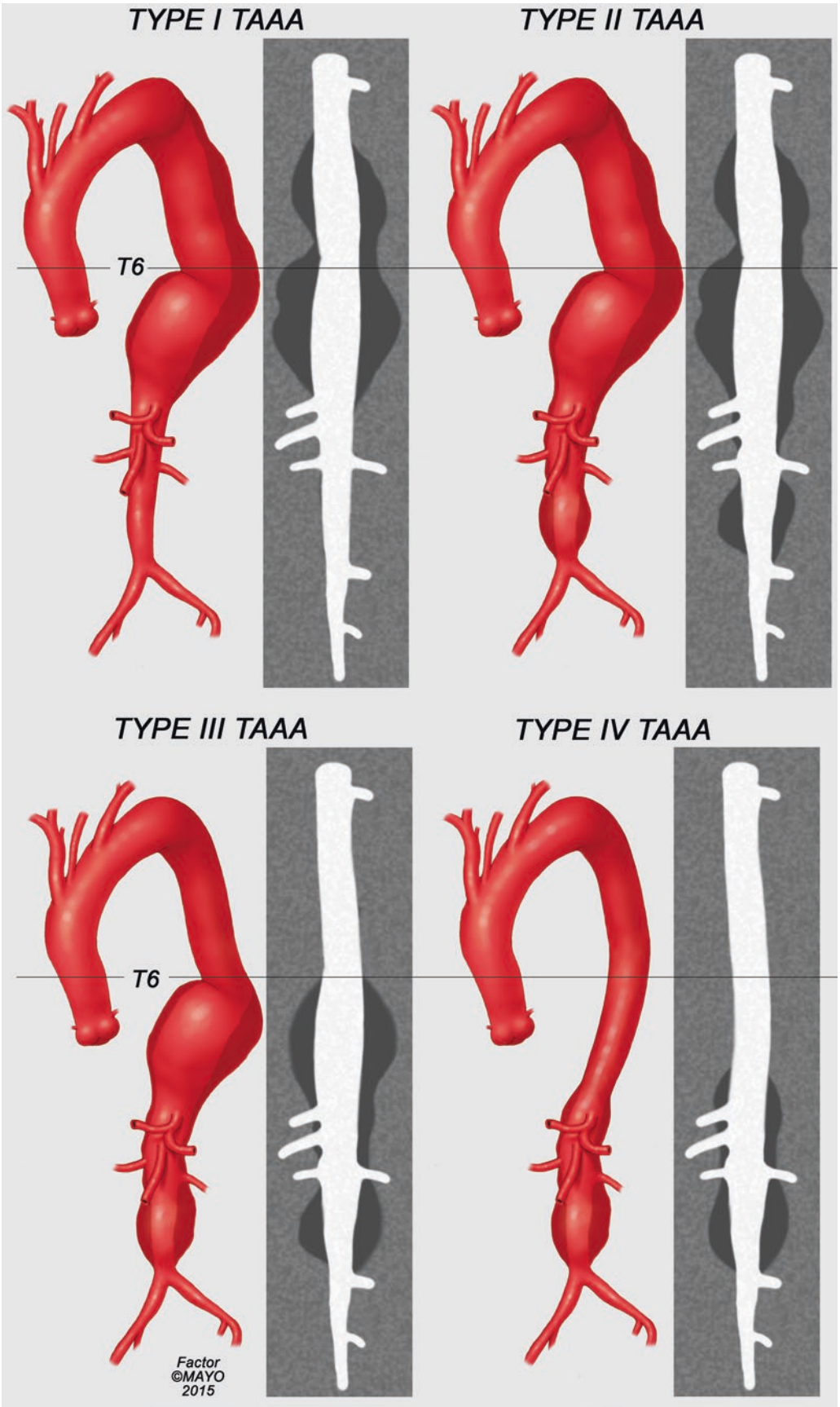


Fig. 11.8 Proposed nomenclature for thoracoabdominal aortic aneurysms based on analysis of parallel aortic wall by computed tomography angiography. By permission of Mayo Foundation for Medical Education and Research. All rights reserved

natural history studies that describe estimates of rupture risk are uniformly based on diameter and not on volume.

Measurement of aneurysm volume is performed with identification of the outer wall of the aneurysm sac. Given that vessel wall, atheroma, adjacent psoas musculature, and inferior vena cava have similar HUs, automated calculations are challenging or practically impossible. Several software programs provide volume measurements. It remains to be determined whether volume is important with regard to the initial assessment of an aneurysm, but few would argue that volume assessment is more sensitive at detecting size changes following treatment of aneurysms with endovascular devices. The necessity of such measurements is questioned, but when they are readily available, they are potentially useful.

Recent reports have also analyzed the effect of specific aneurysm morphology with respect to rupture risk. The use of complex engineering calculations termed *finite element analysis* can determine regions of high wall stress, which may be more prone to rupture. This is often in the posterior lateral wall of the aorta, which correlates clinically with the most common location for aneurysm rupture.

Assessment of Landing Zones

The most important strategic decision on planning any open surgical or endovascular aortic repair is the selection of the proximal and distal anastomotic or landing sites. For open repair, the surgeon identifies areas that are safe for placement of a clamp, and are relatively free of calcification and thrombus, and ideally free of aortic disease. Although the graft can be anastomosed to areas of relative mild aortic enlargement, for endovascular stents a normal segment needs to be selected given that there is continued neck growth after placement of a self-expandable stent (Fig. 11.9). Endovascular repair therefore requires a length of healthy aorta or iliac artery to allow circumferential stent-graft apposition to the vessel wall, creating a seal zone and allowing adequate fixation of the device by active mechanism.

Analysis of neck morphology is one of the most important surrogates in selection of healthy aorta (Fig. 11.10). Areas that have extreme tortuosity or that appear conical, non-cylindrical, and segments that contain atheromatous debris, thrombus or calcification are not considered safe regions to clamp, sew a graft or to fix and seal endovascular devices. Ideally, assessment of landing zones is best done using CLF projections (Fig. 11.11). A segment that is reasonably straight and that appears otherwise healthy and without calcification, thrombus or significant change in diameter (>10 % variation), and that is smaller than adjacent proximal aortic segments, is considered normal aorta for placement of endograft.

Open surgical grafts can be tailored intra-operatively depending on specific anatomy. For endovascular repair, planning needs to be completed pre-operatively to allow selection of all anticipated modular devices. Patient-specific thoracoabdominal devices also tailored to the anatomy with respect to the number and location of fenestrations and branches, changes in stent diameter, and location of sealing zones. Longitudinal distance measurements can be obtained from CLF projections, including the straightened or stretched view, and diameter measurements are obtained from orthogonal projections. Each of the commercially available endografts has identified minimum length and diameter requirements for the proximal and distal landing zones, which are based upon their analysis of the device behavior in vivo and in vitro. This information is available in the instructions for use of each type of device. Additionally, many processing imaging software vendors have specific programs that aid with the planning and sizing of devices.

Tortuosity

Aneurysms grow in diameter and in length, which accounts for varying degrees of tortuosity in certain segments of the aorta. Because the supra-aortic trunks and the renal-mesenteric arteries represent fixating points in the aorta, the most frequent areas of significant tortuosity are in the mid segment of the thoracic aorta and in the infra-renal aorta adjacent to the renal arteries. In general, larger aneurysms tend to be associated with more tortuosity compared to smaller aneurysms. It is difficult to define tortuosity using 3D imaging. Any 3D projection can be reduced to 2D, and the maximal angle can be calculated. Although this technique is what was used to define proximal neck angulation in most studies of AAA endografts, the information is of limited use. Iliac tortuosity is even more difficult to quantify. This is usually done with a scale of mild, moderate, and severe.

The arch represents a special challenge because of its natural curved geometry and the differences in length between the greater and the lesser curvatures of the arch. The location of the supra-aortic trunks can be variable in 25 % of the patients, and arch curvature changes with age.

Branch Assessment

Complex aortic aneurysms by definition involve side branches. The presence of concomitant occlusive or aneurysmal disease of the aortic branches is critical to determine candidacy to fenestrated and branch grafts and the specific design and approach. Minimum requirements are diameters from 4 to 11 mm and absence of early vessel bifurcation (Fig. 11.12). Qualitative assessment can be made from careful inspection of imaging, and when suspicion arises, more detailed imaging processing is helpful. Images perpendicular to the vessel are most helpful, and this can be obtained manually using MPR projections or with CLF. Arterial narrowing, diameter measurements, and

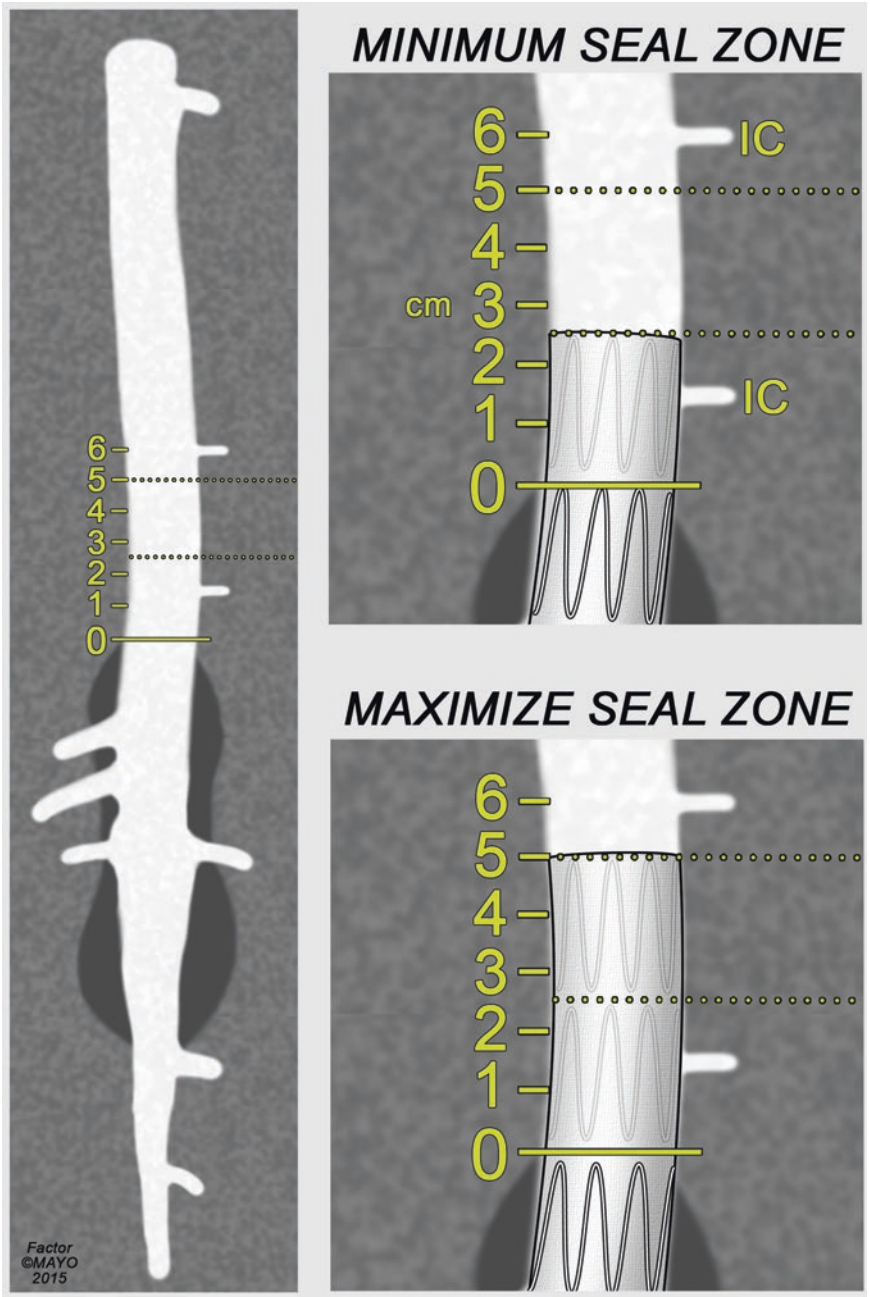


Fig. 11.9 Selection of minimal proximal landing zone based on parallel aortic wall. Note a landing zone of 2.5 cm is selected, but this is extended proximally just below the next intercostal arterial station to maximize seal at the proximal attachment site. By permission of Mayo Foundation for Medical Education and Research. All rights reserved

assessment of branch vessel length before bifurcations can be obtained using these techniques. The same criteria that are applied to determine the quality of the aorta and its sealing zones are used to establish vessel involvement by aneurysm or atherosclerotic disease. A cylindrical vessel with proper distal tapering of diameter and absence of atheromatous debris indicate normal anatomy. Also calcifications can be determined from pre-contrast studies or by using a window leveling technique. Volumetric analysis of the renal parenchyma is done to assess estimate of volume in patients with large accessory renal arteries or early branch bifurcation (Fig. 11.13).

Branch Vessel Geometry

The development of specially designed stents to incorporate aortic side branches has created a need to assess and accurately describe the 3D geometry of the aorta around the renal-mesenteric arteries. Vessel triangulation or the special relationship between the origins of all four visceral arteries allows precise planning of fenestrated and branched endografts. A CLF projection is used and the proximal sealing and fixation section of the aorta is chosen upon the appearance of healthy aortic tissue as previously described. The distance between the center of

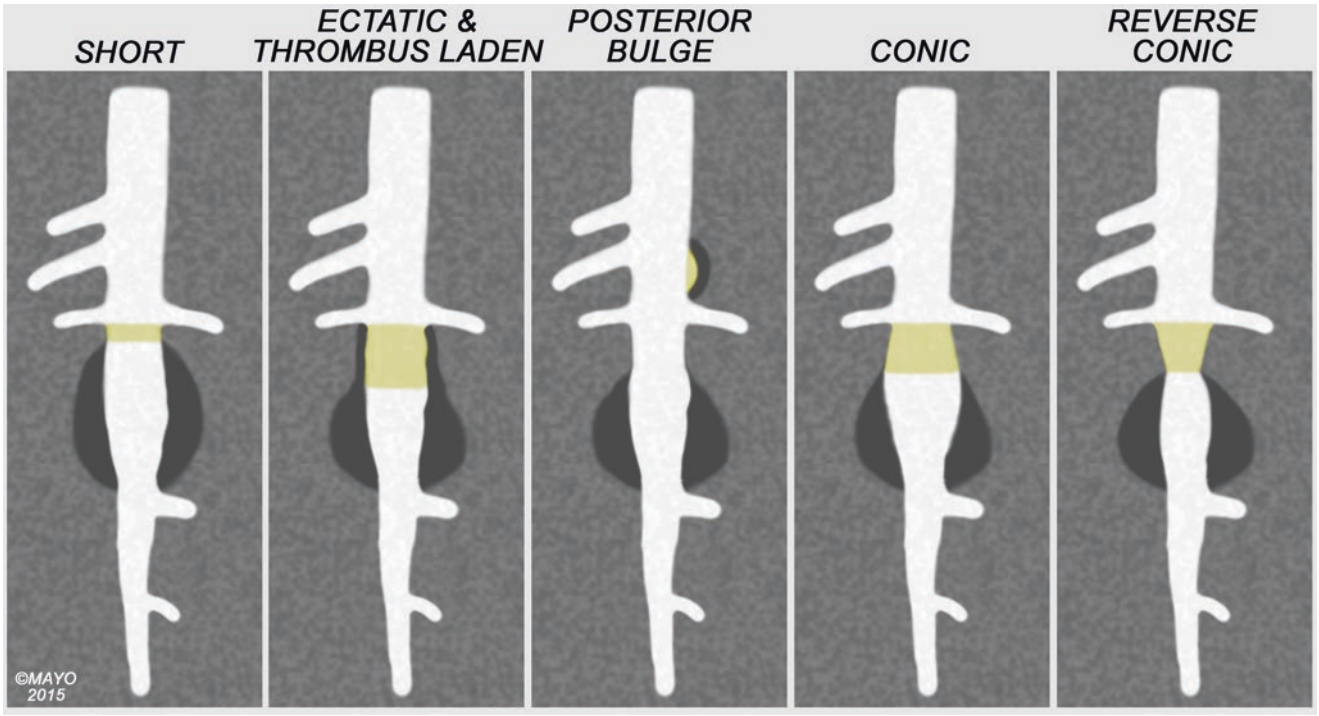


Fig. 11.10 Unsuitable landing zones for endovascular aortic repair include short, ectatic or thrombus laden aorta, posterior bulge, conic or reverse conic necks. By permission of Mayo Foundation for Medical Education and Research. All rights reserved

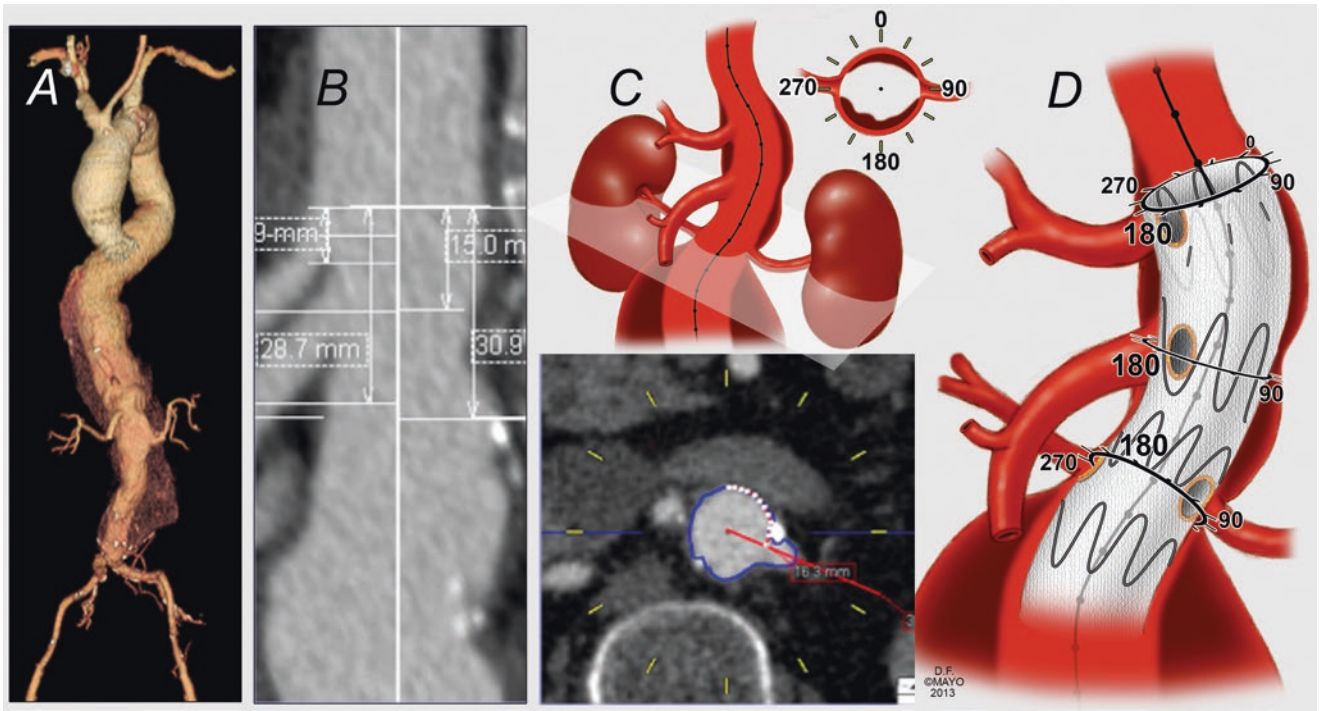


Fig. 11.11 Computed tomography angiography (**a**) is analyzed using centerline of flow (**b**). The proximal landing zone is selected above the celiac axis (**c**). Vessel triangulation technique using length measurements (**b**) coupled with axial clock orientation of each target (**c**) allows precise planning of fenestrated endografts (**d**). By permission of Mayo Foundation for Medical Education and Research. All rights reserved

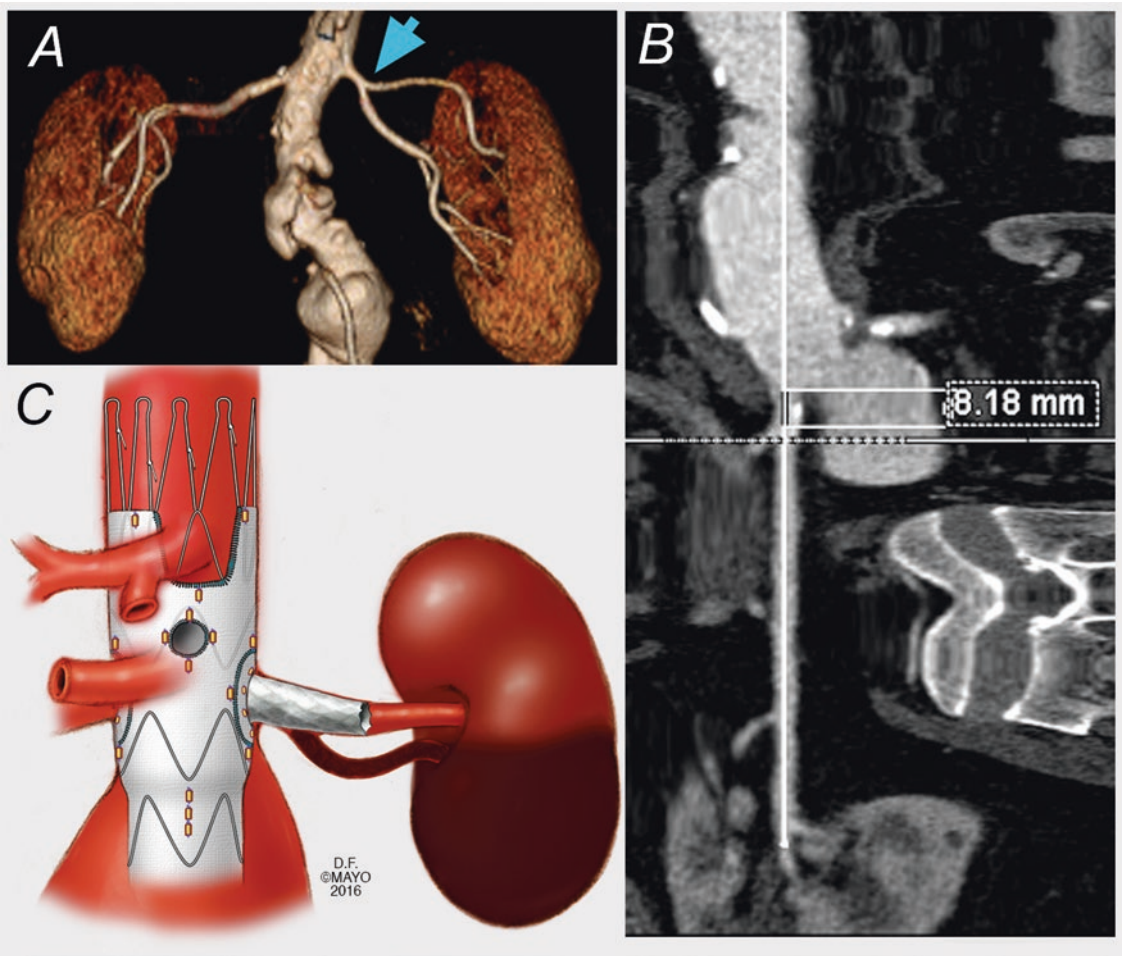


Fig. 11.12 Branch vessel analysis is critical to plan these procedures. Computed tomography angiography of a patient with juxta-renal aortic aneurysms shows early bifurcation of the left main renal artery (**a**, *arrow*). This is measured using centerline of flow analysis (**b**). Branch vessel stenting in this patient would result in large infarct of the lower pole of the left kidney (**c**). By permission of Mayo Foundation for Medical Education and Research. All rights reserved

each aortic branch ostium and the proximal seal is then measured from the straightened view of the CLF, allowing precise calculation of the location of a fenestration in the longitudinal axis (Fig. 11.14). The straightened view of the CLF is then rotated such that the visceral segment is properly aligned with the vertebral bodies. Usually this means the superior mesenteric and celiac arteries are oriented anteriorly, and the renal arteries are directed laterally.

By assessing each imaging orthogonal to the CLF at the midpoint of the vessel origin, the radial position of the branch ostium can be described (Fig. 11.15). This is typically done as a clock position, angle (0°–360°), or it can be more accurately described as an arc length from the 12:00 o'clock position. Figure 11.16 summarizes the sequence of measurements for planning definitive repair. Most common factors limiting suitability of repair are multiple small renal arteries, excessive angulation, early vessel bifurcation, and excessive atherosclerotic debris (Fig. 11.17).

Surveillance Protocols

Surveillance using periodic cross-sectional imaging remains an essential part of continued care after endovascular aortic repair. In the setting of open surgery, baseline imaging is obtained to establish the appearance of the aorta following the repair, in addition to the presence or absence of concurrent arterial disease. More specific questions are raised after an endovascular aortic repair. Potential problems include stent migration, the presence of endoleaks into the aneurysm sac, and the integrity of the prostheses form.

Follow-up CTA studies include typically a pre-contrast, contrast, and delayed phase. The pre-contrast image provides information on regions of calcification that may be confused with endoleaks and the relationship and metallic integrity of all modular stent-graft components. If there are specific questions about the graft integrity, the source CT data can be

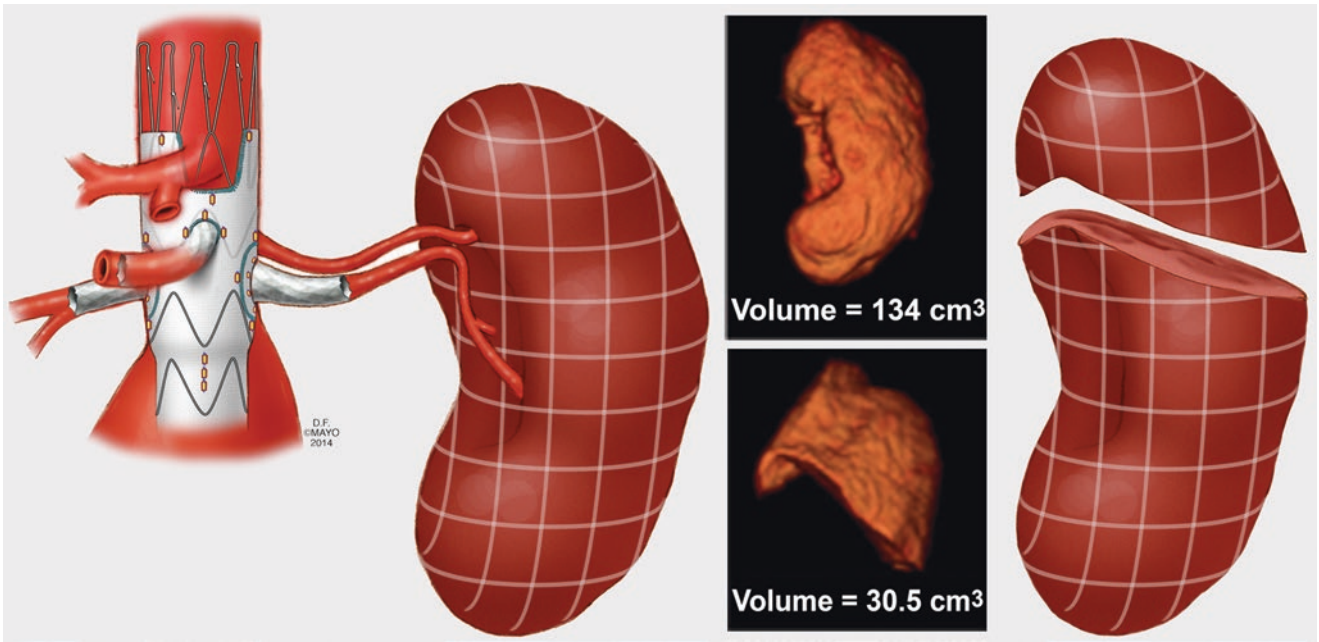


Fig. 11.13 Technique of volumetric analysis in patients with early renal artery bifurcation has been used to select patients for branch vessel stenting. By permission of Mayo Foundation for Medical Education and Research. All rights reserved

reconstructed using alternative algorithms. During the post-processing analysis, a hardware mask can be applied to the data set to help illustrate the metallic structures involved in the repair. Contrast studies are used to assess endoleak, migration, stenosis, occlusion, or thrombus. The timeline of potential problems that can occur after fenestrated and branched repair is summarized in Fig. 11.18. Endoleak assessment requires review of the contrast phase images side-by-side as compared to the pre-contrast images so that the patterns of calcification will not be confused with endoleaks. The CLF model is used to assess the maximal aortic diameter and to calculate aneurysm volume. The delayed phase studies are used to assess the sac for subtle evidence of endoleak. This is best done by comparing two or three of the phases of the studies side-by-side in assessing the HU in any area of question.

Although surveillance paradigms have evolved for standard EVAR from routine CTA to duplex ultrasound, fenestrated and branched endografts continue to be followed using a rigid regime. This is largely explained by its investigational nature and by the potential risk for other failure mechanisms involving not only the main aortic component but its side branches. Therefore, we continue to recommend a CT/CTA at dismissal, within 1–2 months, 6 months, and yearly thereafter. Duplex ultrasound is performed to assess side branch patency in addition to CTA. There is considerable debate regarding the benefit of such extensive protocols after EVAR. One must remember that aside from the financial cost, there is exposure to radiation and contrast.

Endoleaks

Endoleak classification has been well established by the reporting standards of the SVS for standard EVAR. Although this classification has not been officially modified for more complex repairs, an ongoing SVS taskforce headed by the author is proposing a new classification system to address additional sites of endoleak that can occur with fenestrated, branched, and parallel stent-grafts (Fig. 11.19). This classification maintains the standard definitions of Type Ia (Figs. 11.20, 11.21, and 11.22), Ib, II, and IV endoleaks. However, it adds detail pertinent to side branch involvement such as type Ic endoleak (Figs. 11.23 and 11.24), which is defined by an endoleak originating from the sealing site of a branch stent or fenestration. In addition, Type III or inter-component endoleak (Figs. 11.25 and 11.26) is further classified to address the specific origin. As such, Type IIIa endoleak specifies the attachment of the fenestrated and branch component with its bifurcated device, IIIb iliac limb and IIIc side branch component endoleaks (Fig. 11.27). Type IIId endoleak occurs due to integrity issues such as tear, perforation or fracture in the stent-graft or branches (Fig. 11.28).

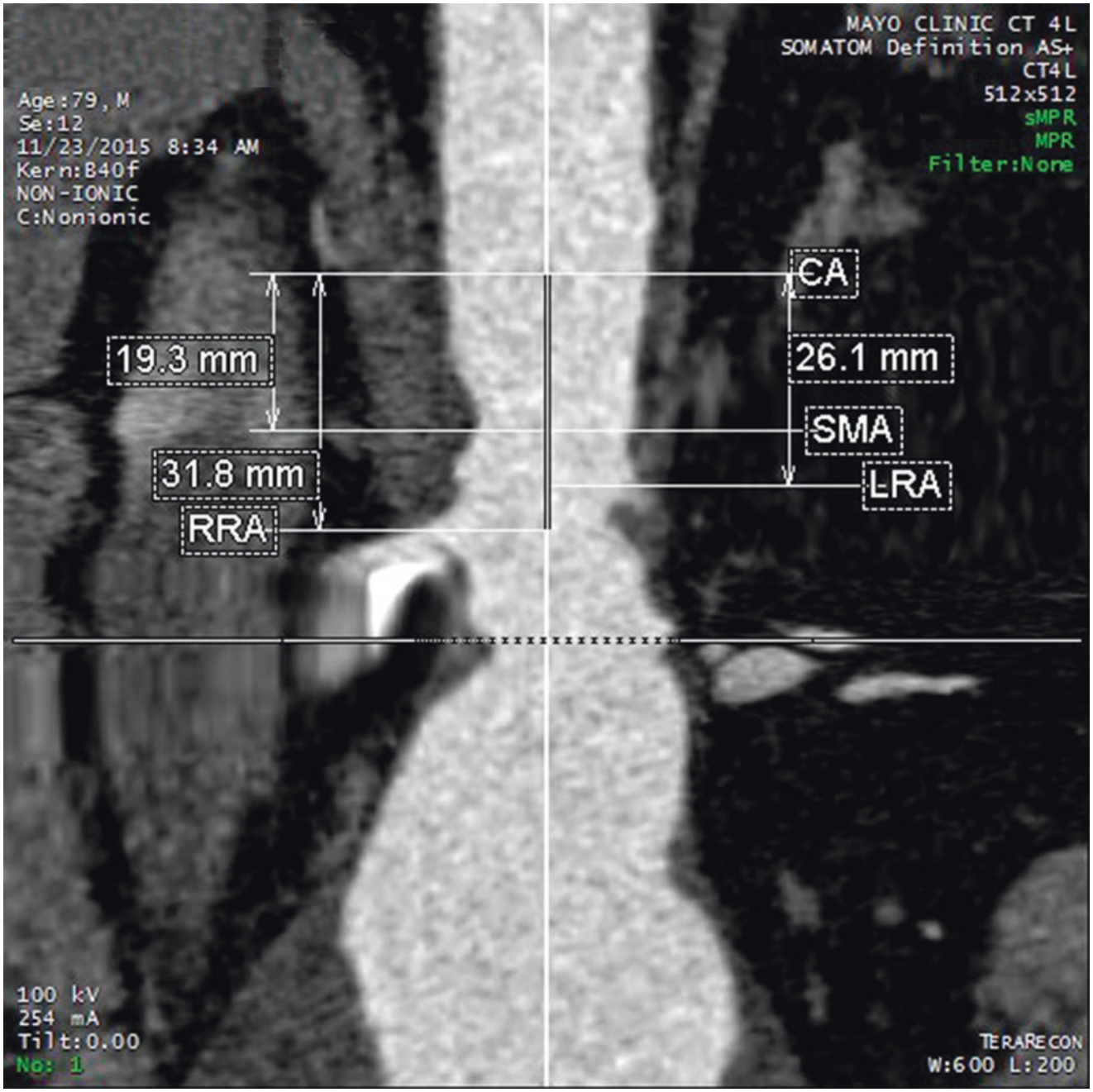


Fig. 11.14 After selection of a healthy landing zone in a patient with paravisceral aortic aneurysm, lengths are measured between the each of the vessels. By permission of Mayo Foundation for Medical Education and Research. All rights reserved

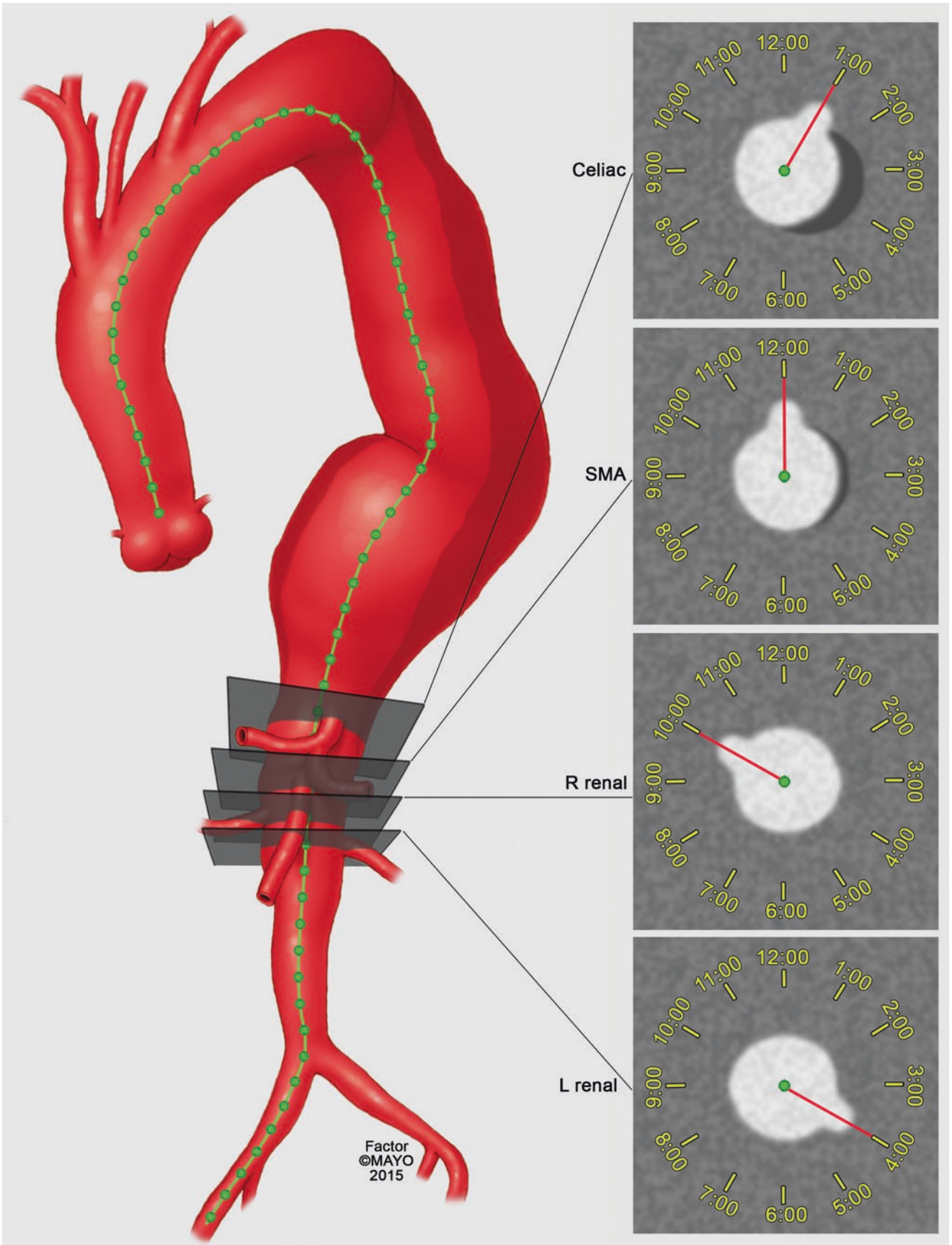


Fig. 11.15 Measurement of clock positions for the renal-mesenteric arteries. By permission of Mayo Foundation for Medical Education and Research. All rights reserved

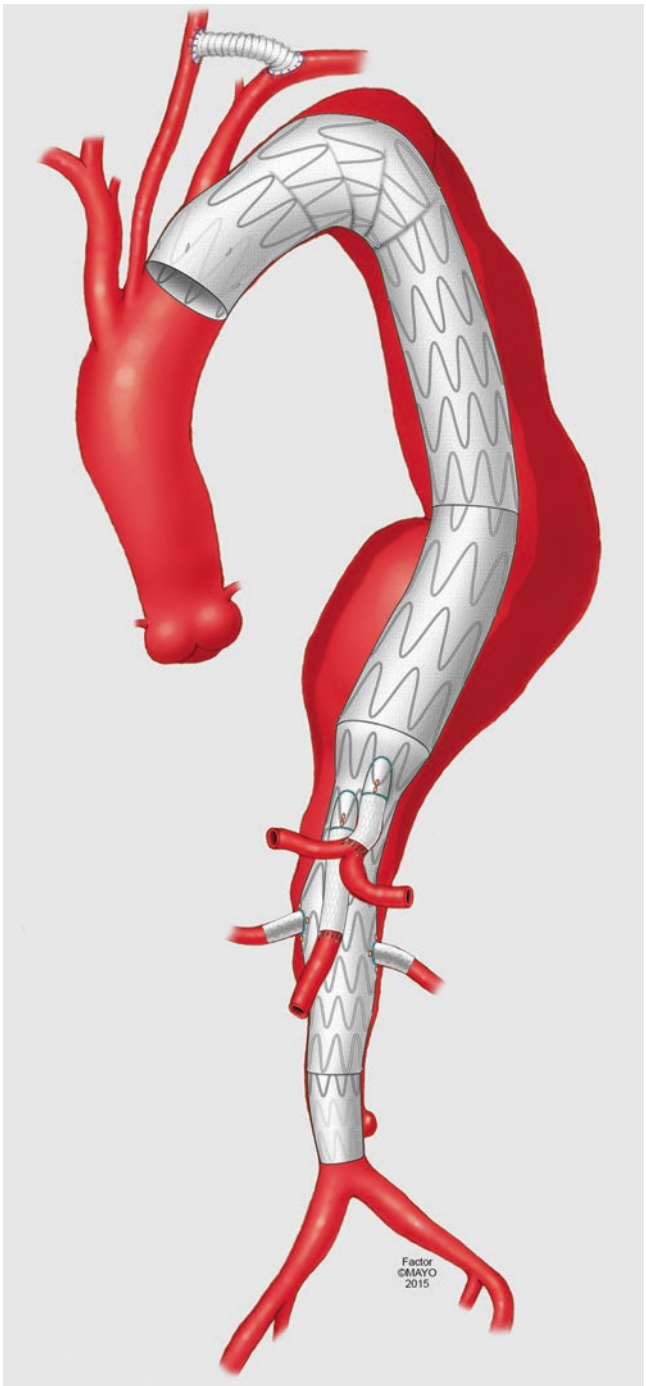


Fig. 11.16 Summary of sequence of measurements for planning fenestrated and branched endovascular repair in a patient with type I thoracoabdominal aortic aneurysm. By permission of Mayo Foundation for Medical Education and Research. All rights reserved

Type IV endoleak is ubiquitous intra-operatively and usually resolves with reversal of anticoagulation. Finally, specific mechanisms of branch-related endoleaks are also clarified in the classification.

Branch Stenosis, Kink, or Occlusion

Placement of side branch stents to incorporate the renal-mesenteric arteries is associated with potential risk of stenosis or occlusion from kinks, intimal hyperplasia, thrombus formation, or atherosclerotic disease. Assessment of side branch stenosis by CTA alone can be difficult because of extensive metallic artifact (Fig. 11.29) for stainless steel stents and numerous radiopaque markers. For fenestrated alignment stents, the leaflets of the stent should be flared into the aortic lumen, protruding 2–5 mm (Figs. 11.30 and 11.31). Compression of the stent can result from intra-procedural maneuvers such as advancement of a large dilator to place an iliac limb extension (Figs. 11.32 and 11.33). Assessment of the side branches by CT may help prevent avoidable occlusions from unrecognized stent compression. In patients with scallops not aligned by stents, the ostia of the vessel should be assessed for fabric coverage which can result in occlusion or branch malperfusion (Fig. 11.34). Finally, intimal hyperplasia is a common cause of stent stenosis in bare metal stent segments as depicted in Figs. 11.35 and 11.36.

Solid Organ Embolization

Embolization of atherosclerotic debris, plaque, or thrombus is a major source of morbidity and mortality after fenestrated and branched repair (Fig. 11.37). Ribeiro and associates created a score system to assess the impact of atherosclerotic debris on embolic events (Fig. 11.38). Using this classification, presence of higher thrombus burden was associated with renal function deterioration and solid organ embolization in the liver, spleen and kidneys.

Component Separations

Inter-component separation can occur in any of the modular joints, including the side branches (Fig. 11.39), the fenestrated and distal bifurcated stent (Fig. 11.40) or the iliac limbs. Because the fenestrations and iliac limbs represent fixation points that relatively resistant to migration, the junction of the bifurcated distal stent and fenestrated stent is particularly susceptible to component separation.

Stent Infolding

Aortic stent-grafts are typically oversized 10–20 % relative to its intended aortic diameter. For fenestrated grafts the landing zone is typically selected at the level of the celiac

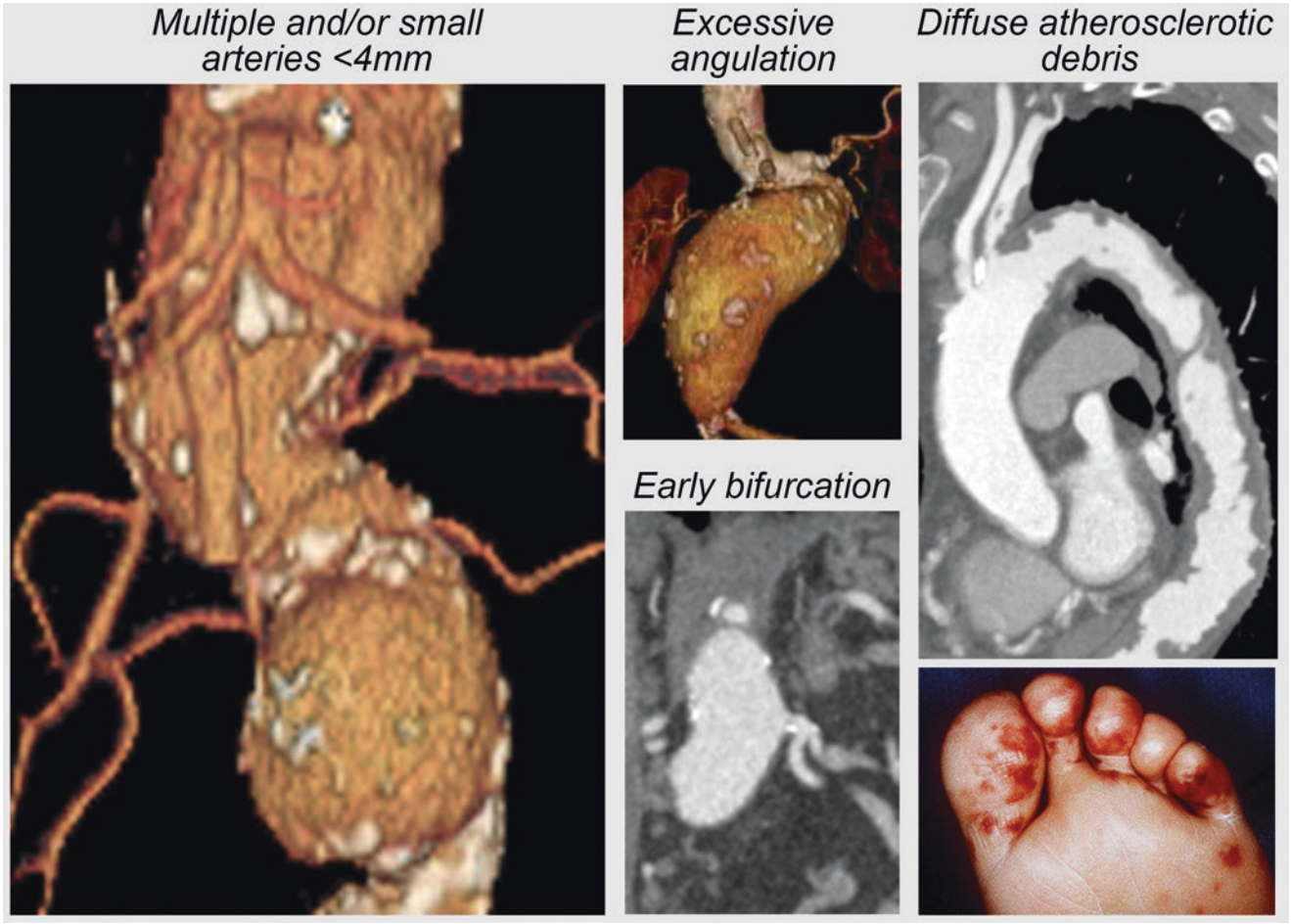


Fig. 11.17 Factors limiting suitability for fenestrated and branched endovascular repair. By permission of Mayo Foundation for Medical Education and Research. All rights reserved

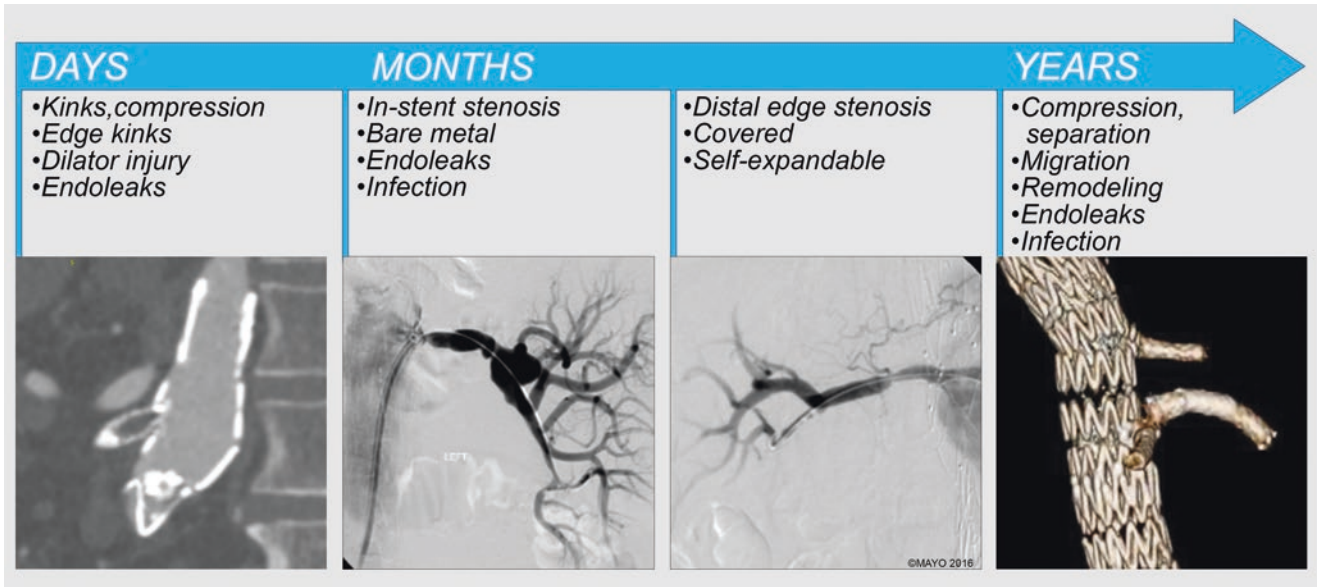


Fig. 11.18 Timeline of failure mechanisms for fenestrated and branched endovascular repair. By permission of Mayo Foundation for Medical Education and Research. All rights reserved

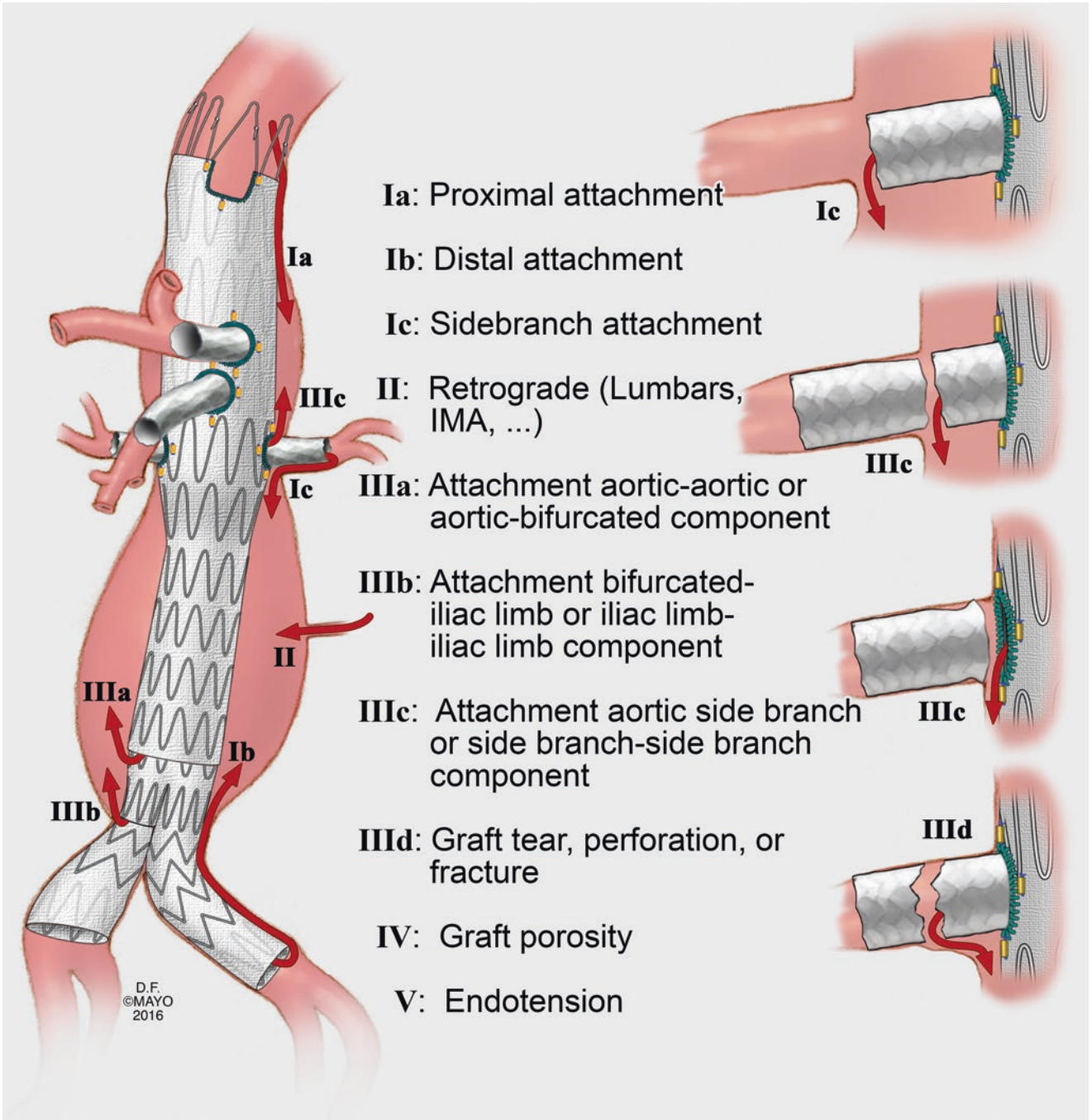


Fig. 11.19 New proposed classification for endoleaks in patients with complex aortic repairs. By permission of Mayo Foundation for Medical Education and Research. All rights reserved

axis, and there may be significant discrepancy in diameter relative to the renal arteries. Excessive oversizing around the renal arteries may predispose to stent infolding (see Fig. 11.21), which is a relatively infrequent complication but can lead to type Ia endoleak and branch compromise.

Progression of Aortic Disease

Aortic disease progression may be a cause of migration or loss of seal in the proximal landing zone (Fig. 11.41). Although migration of fenestrated stents is relatively infrequent with

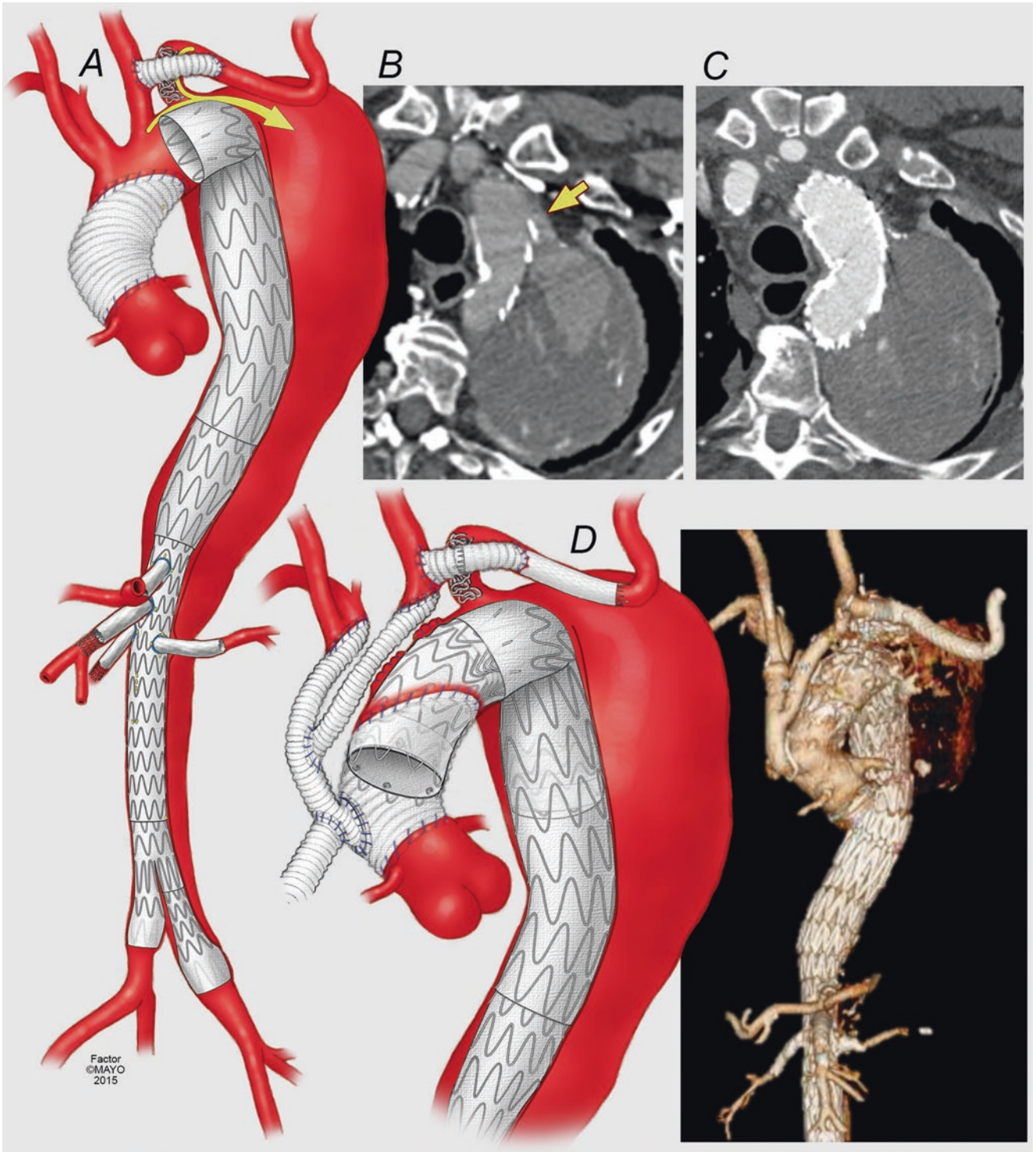


Fig. 11.20 Patient treated for chronic aortic dissection with a proximal Type Ia endoleak in the thoracic stent (**a**). Note the axial view of computed tomography angiography depicts lack of apposition between the stent-graft and aortic wall, indicative of Type Ia endoleak (**b**, *arrow*). The patient was treated by aortic arch debranching procedure (**d**), with resolution of the proximal endoleak. By permission of Mayo Foundation for Medical Education and Research. All rights reserved

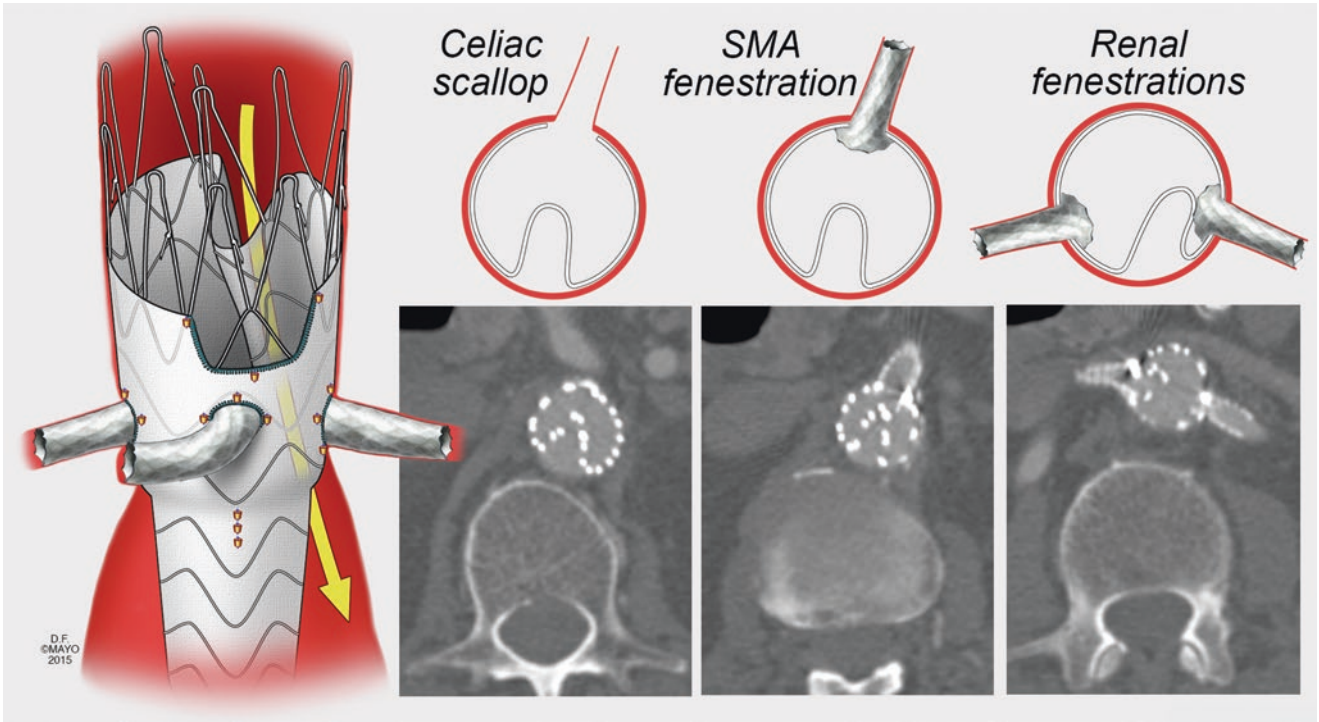


Fig. 11.21 Infolding of fenestrated stent-graft due to excessive oversizing caused a Type I endoleak. By permission of Mayo Foundation for Medical Education and Research. All rights reserved

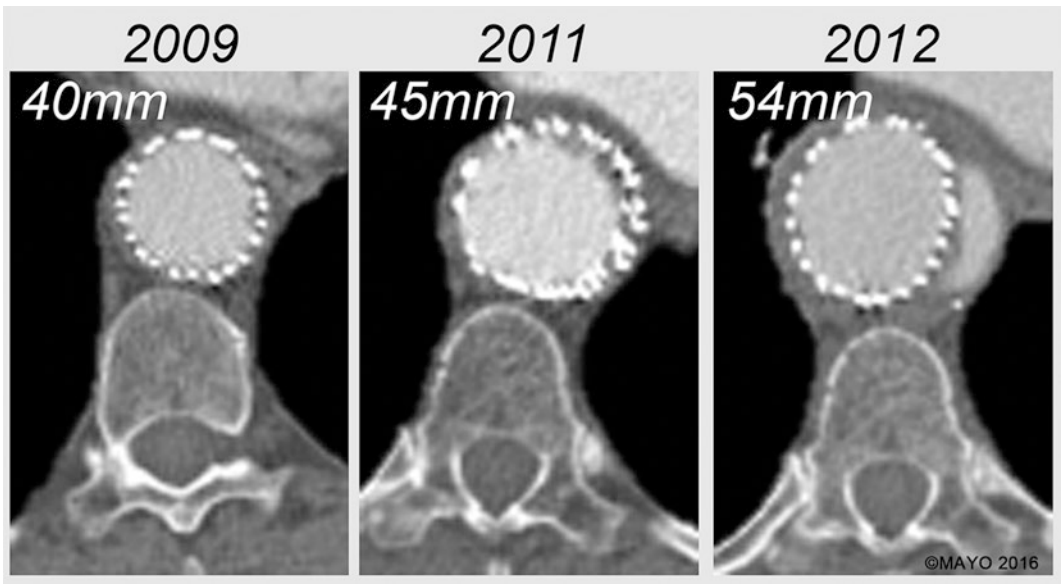


Fig. 11.22 Development of Type I endoleak due to progressive aortic disease affecting the proximal landing zone. By permission of Mayo Foundation for Medical Education and Research. All rights reserved

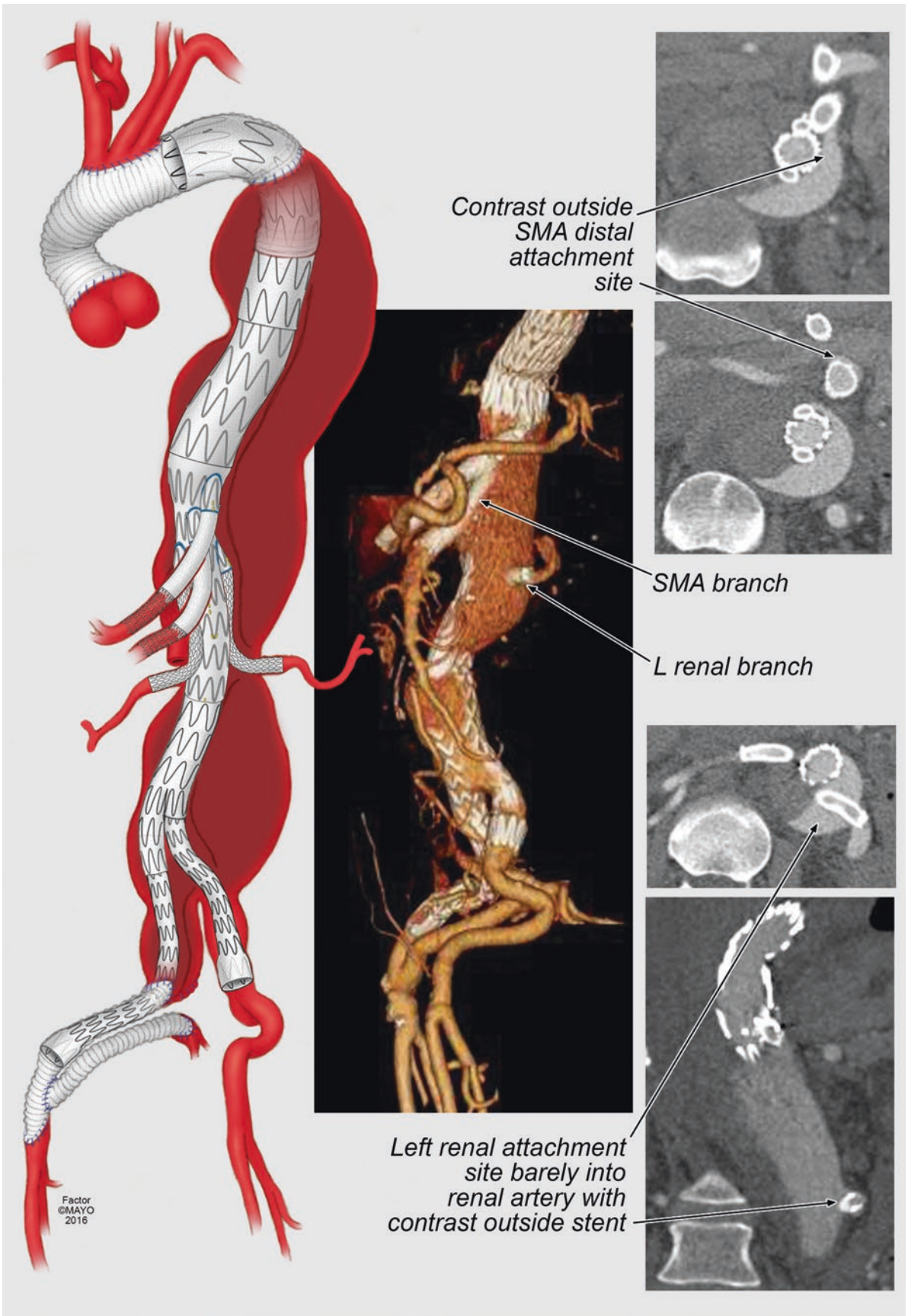


Fig. 11.23 Illustration of aortic repair in a patient with chronic dissection depicts a complex endoleak with origin from the distal sealing sites of the SMA and left renal stents (Type Ic). By permission of Mayo Foundation for Medical Education and Research. All rights reserved

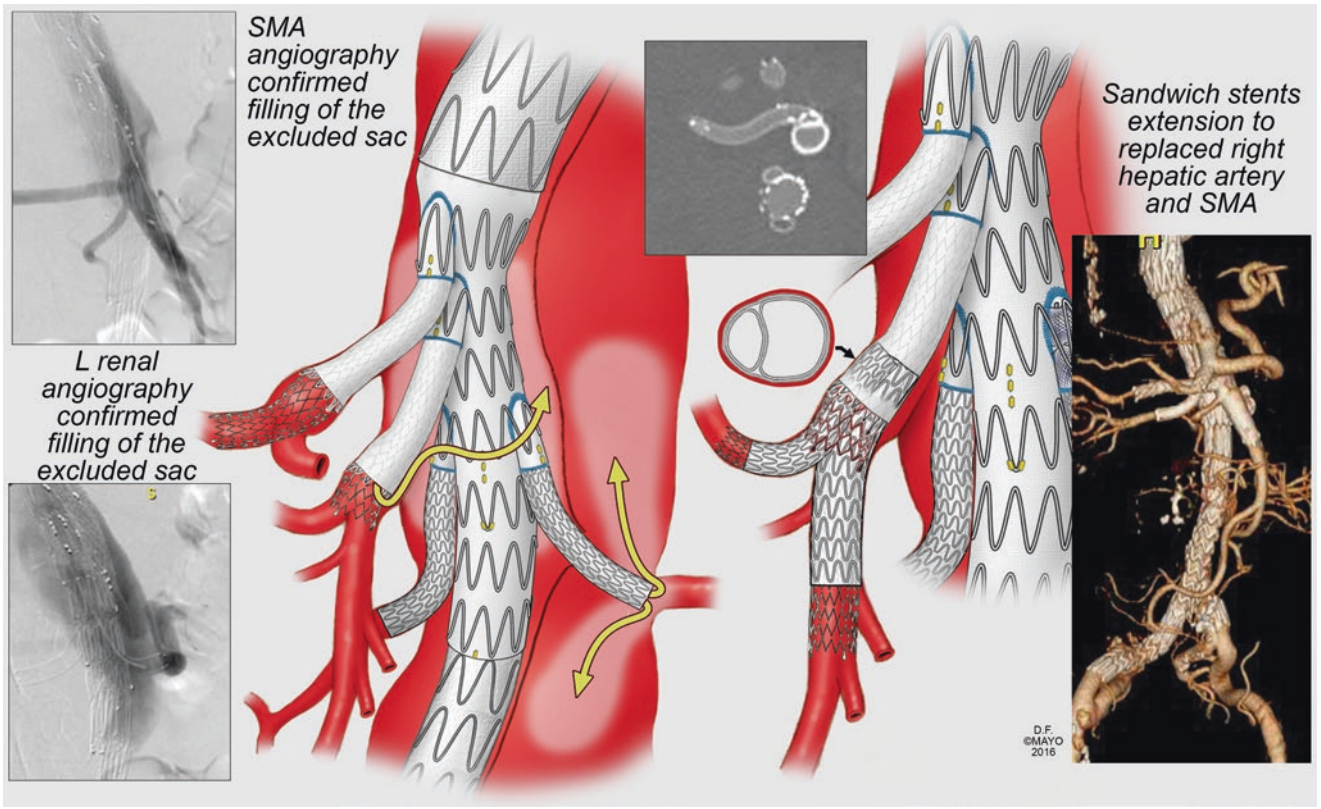


Fig. 11.24 Intraoperative angiography confirms Type Ic endoleak. Illustration depicts treatment by parallel branch graft in the SMA and occlusion of the left renal branch in this patient who was on chronic hemodialysis. By permission of Mayo Foundation for Medical Education and Research. All rights reserved

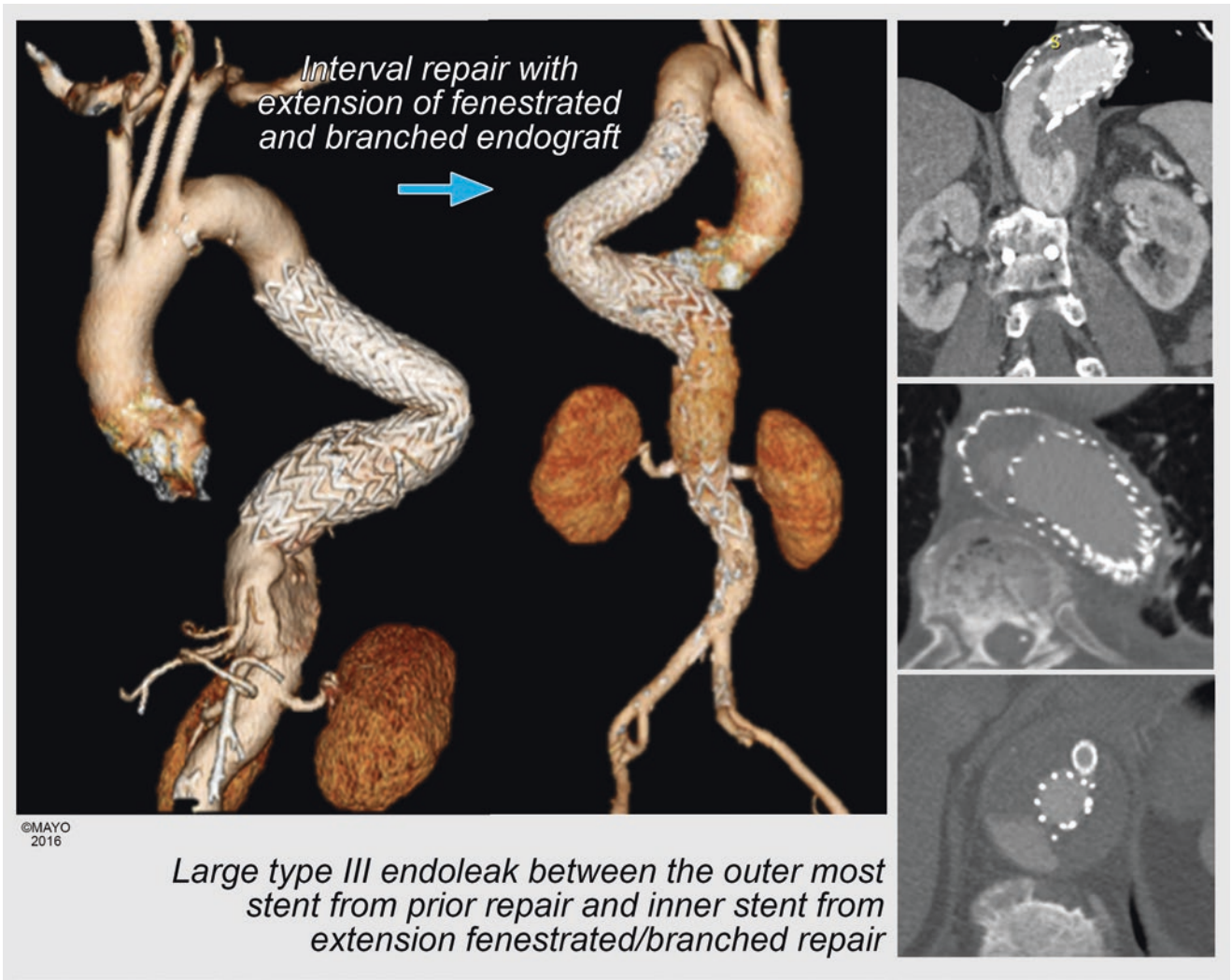


Fig. 11.25 Patient with prior thoracic endograft was treated by distal thoracoabdominal fenestrated–branched endograft with development of a large Type III endoleak at the overlap segment of the proximal and distal stents due to excessive tortuosity. By permission of Mayo Foundation for Medical Education and Research. All rights reserved

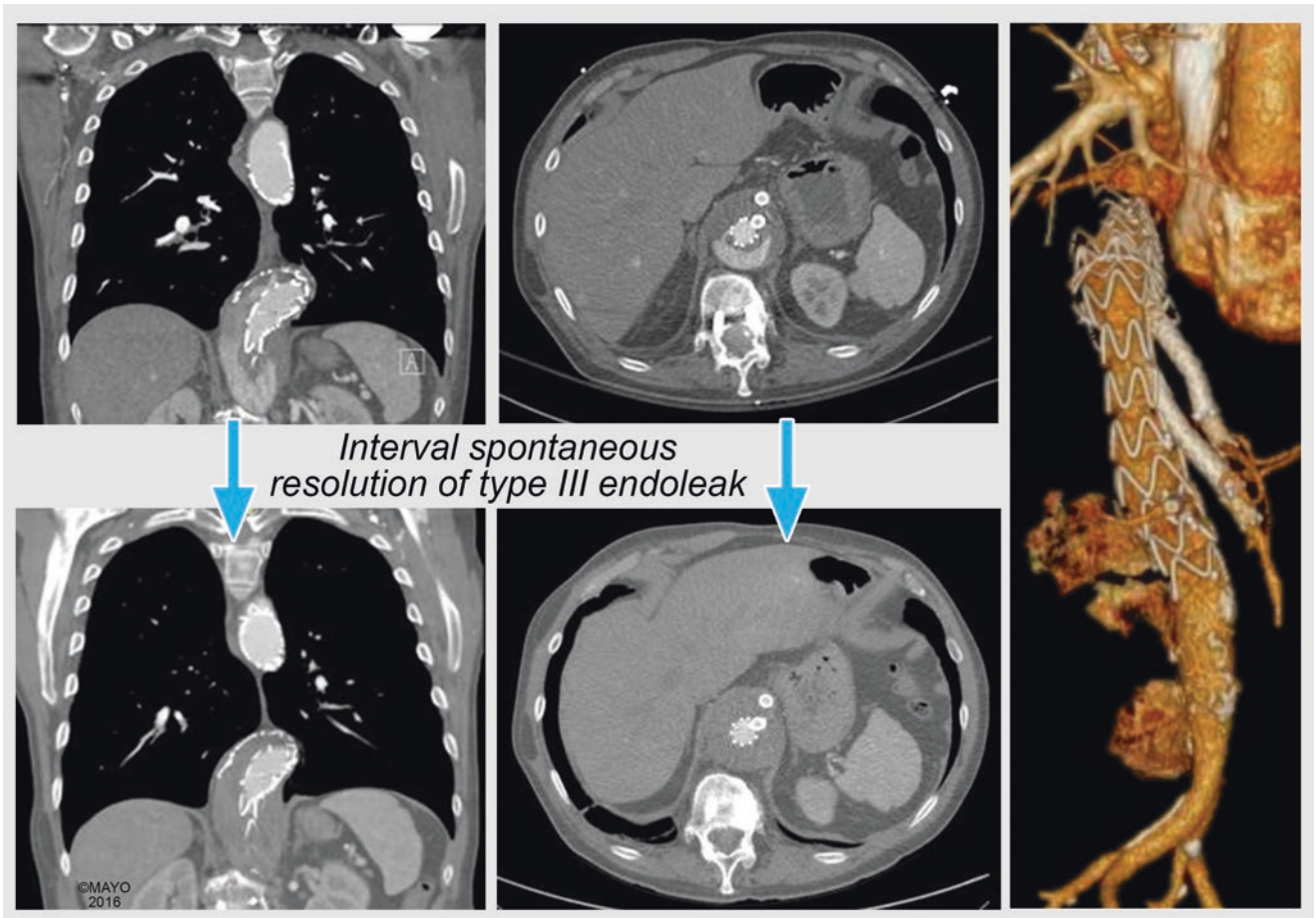


Fig. 11.26 Spontaneous resolution of the Type III endoleak depicted in Fig. 11.25. By permission of Mayo Foundation for Medical Education and Research. All rights reserved

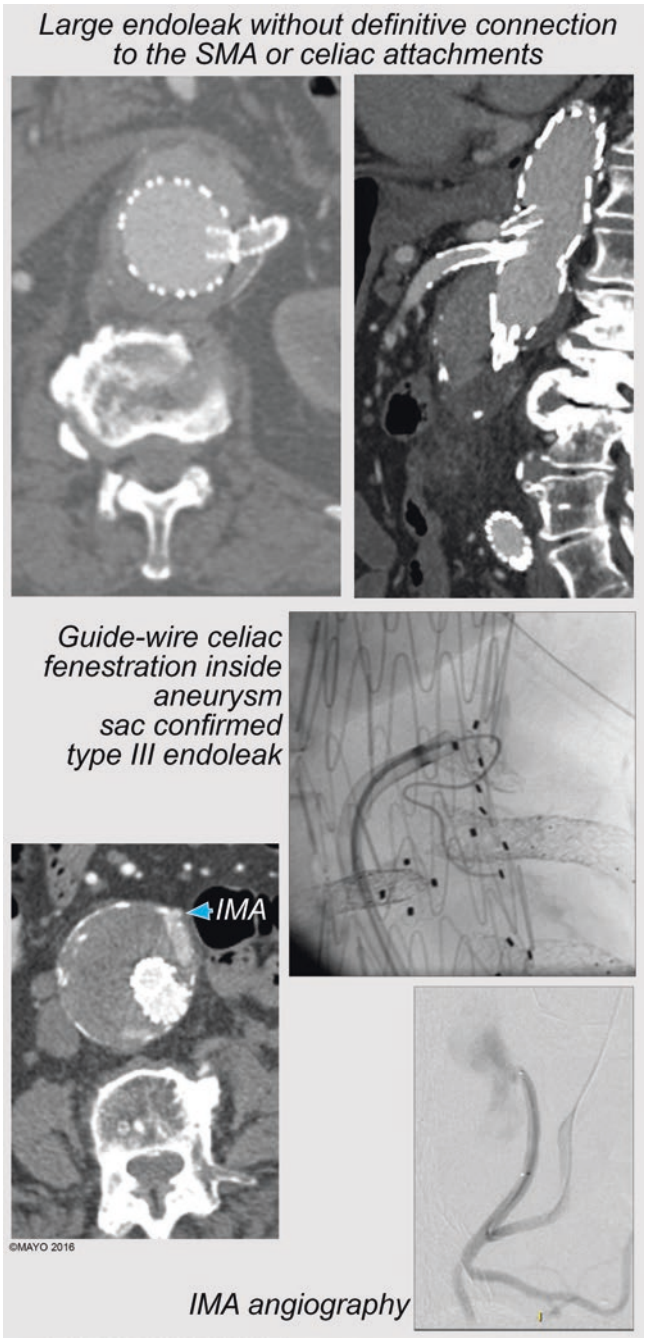


Fig. 11.27 Patient with type IIIc endoleak from the celiac fenestrated-branch. Note that the guide-wire exits through the fenestration. The patient also had a type II endoleak from the inferior mesenteric artery. By permission of Mayo Foundation for Medical Education and Research. All rights reserved

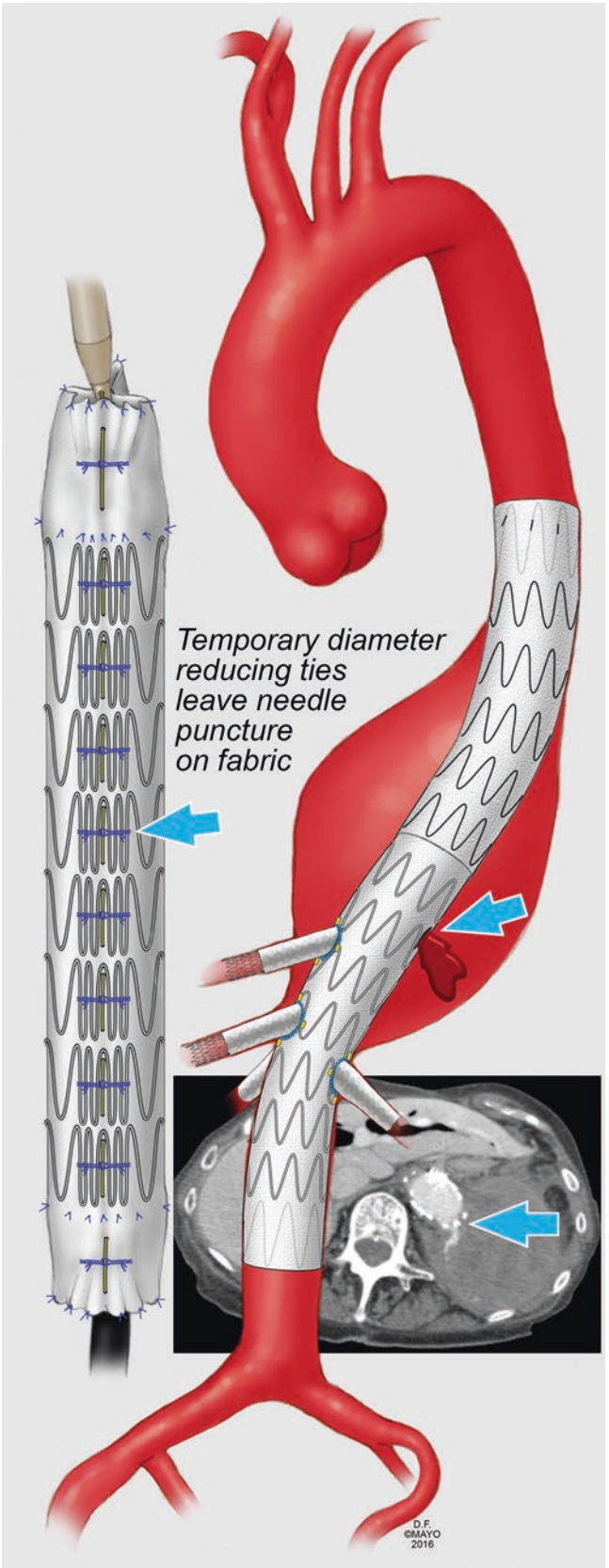


Fig. 11.28 Type IIId endoleak from fabric tear likely in the location of the diameter reducing ties. By permission of Mayo Foundation for Medical Education and Research. All rights reserved

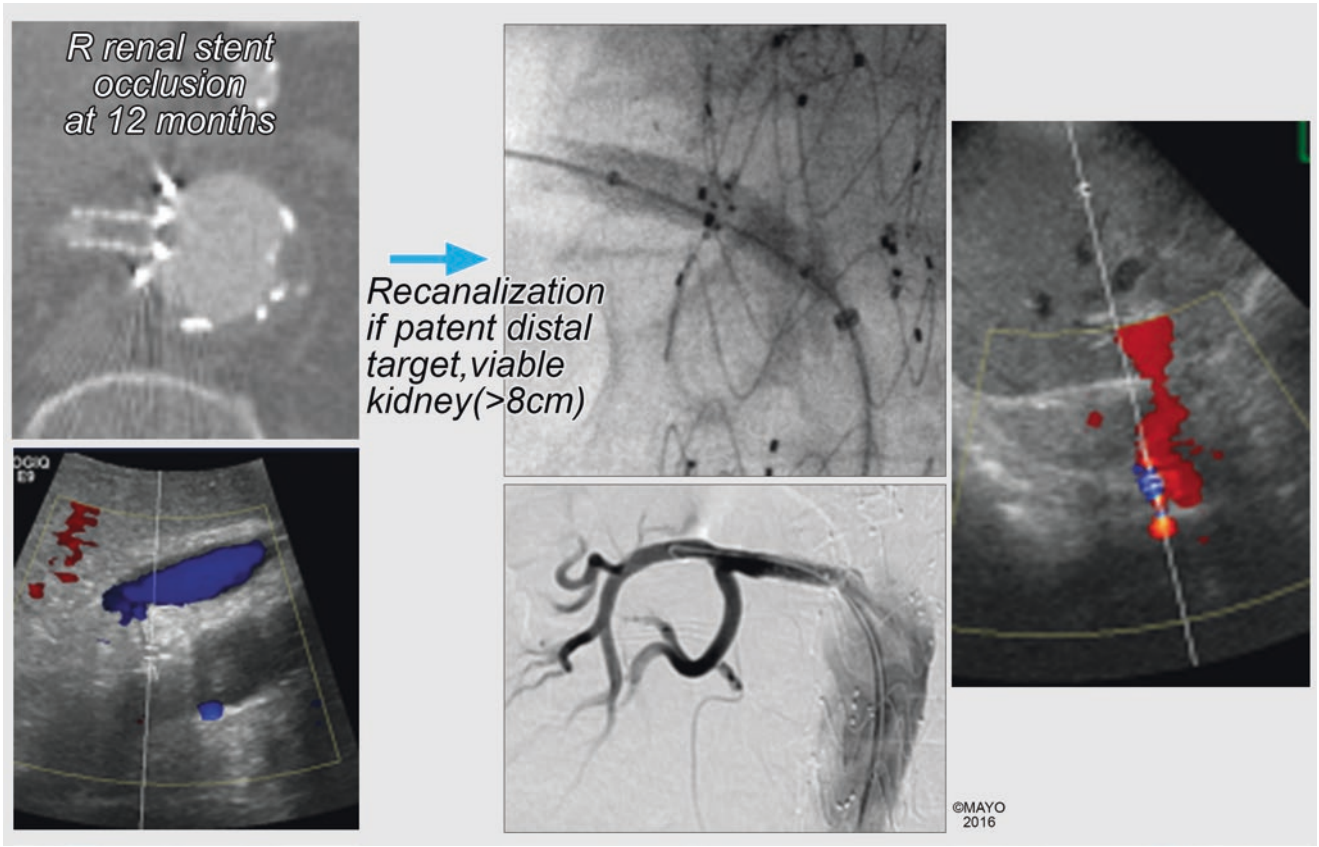


Fig. 11.29 Right renal artery occlusion is shown by CTA despite metallic artifact and is confirmed by duplex ultrasound. The patient was successfully treated by recanalization. By permission of Mayo Foundation for Medical Education and Research. All rights reserved

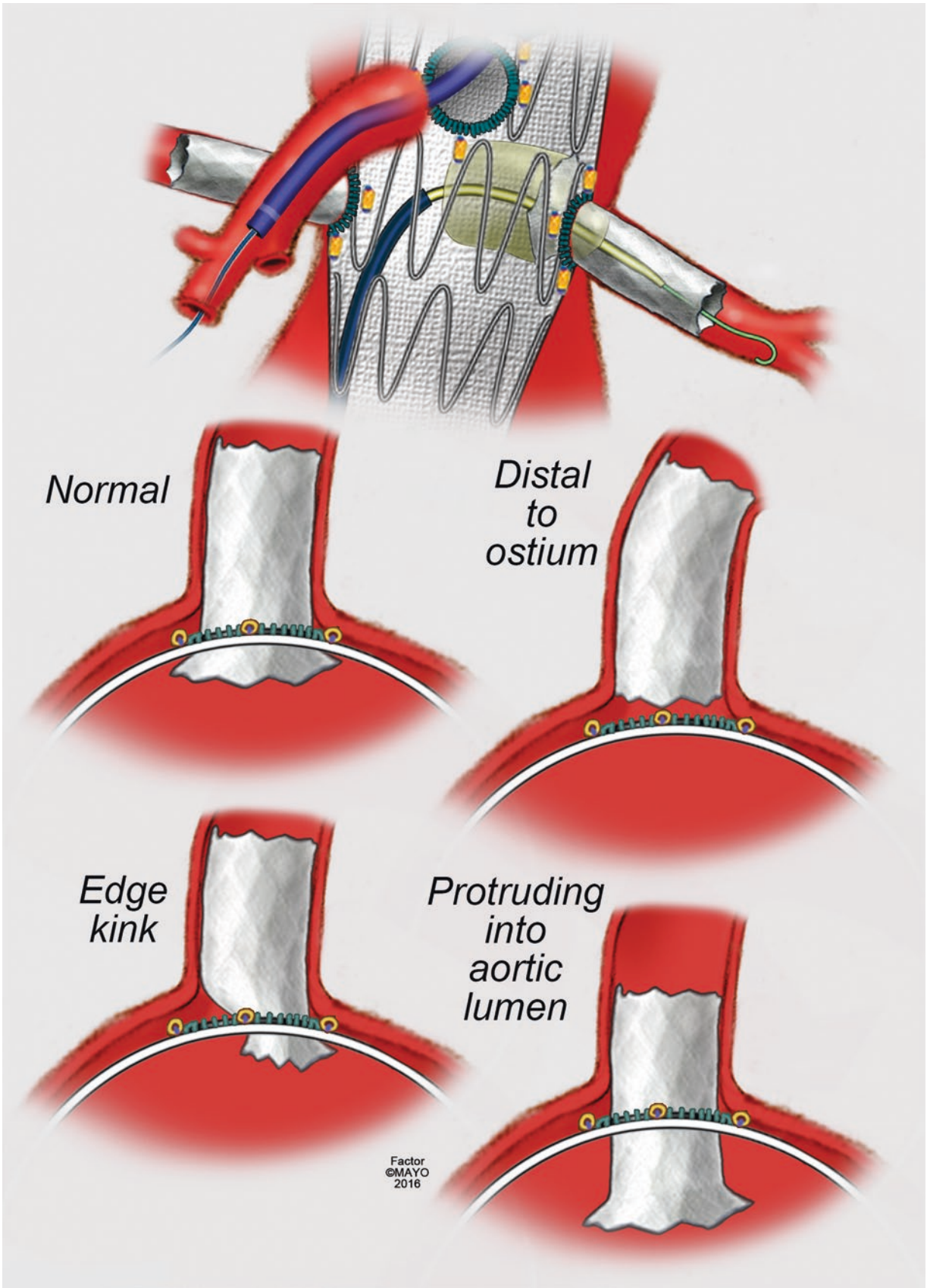


Fig. 11.30 The stent leaflets should be carefully evaluated by computed tomography angiography. These are flared with a large 10-mm balloon and should be located 2–5 mm into the aorta. Computed tomography angiography is critical to identify malposition and kink. By permission of Mayo Foundation for Medical Education and Research. All rights reserved

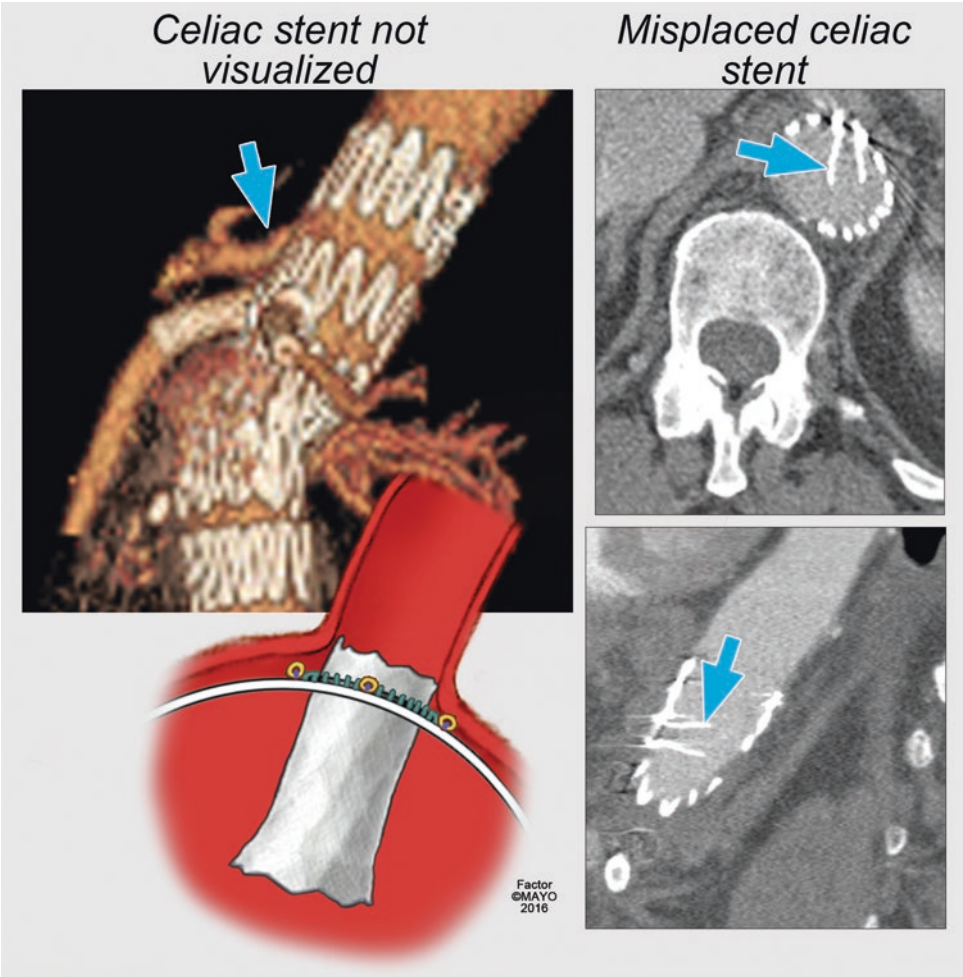


Fig. 11.31 The celiac stent migrated into the aortic lumen, likely during excessive flaring. This was detected by CTA and revised by removing the stent and relocating in one of the iliac limbs. The celiac artery was re-stented. By permission of Mayo Foundation for Medical Education and Research. All rights reserved

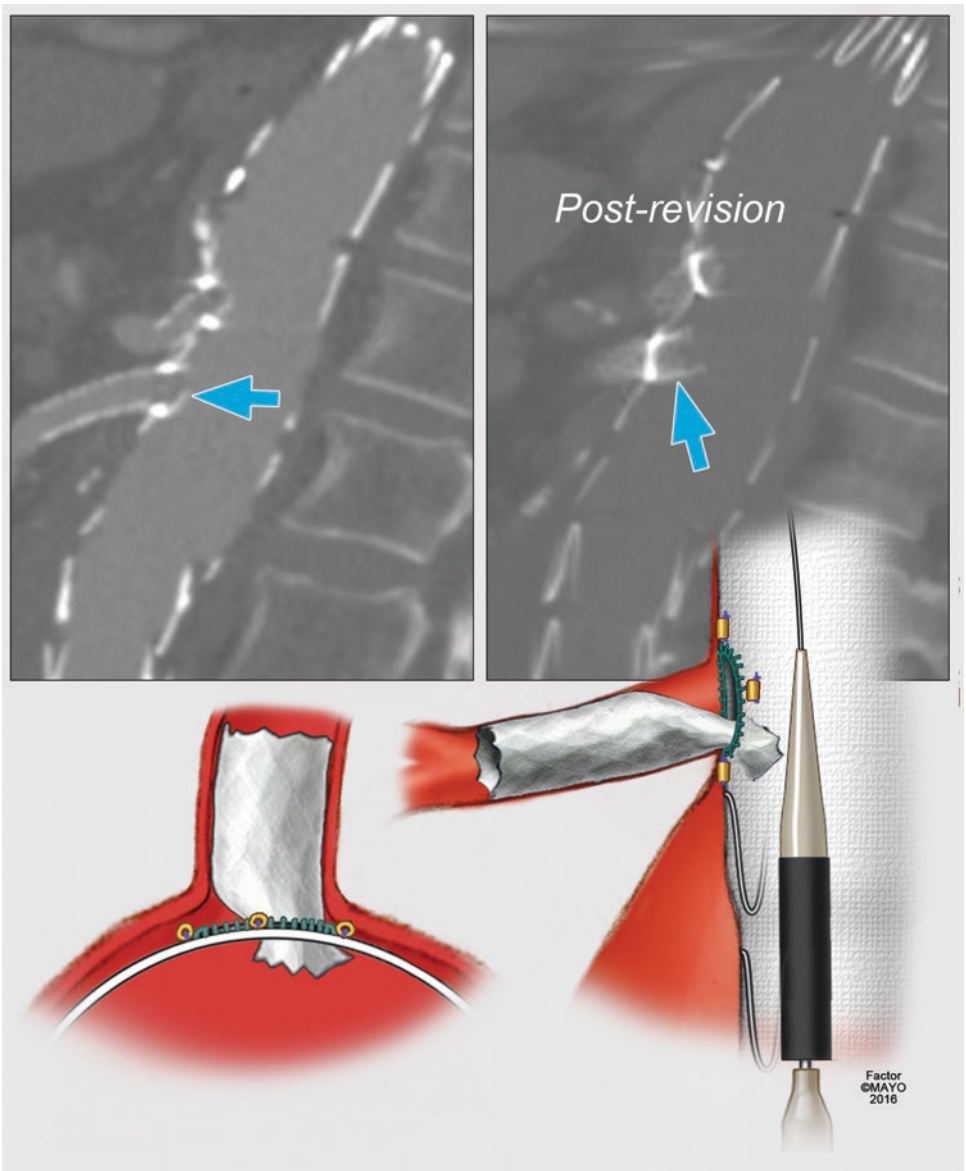


Fig. 11.32 The inferior leaflet of the stent is shifted upwards due to compression from the dilator tip. This was identified and revised with placement of additional stent and flaring. By permission of Mayo Foundation for Medical Education and Research. All rights reserved

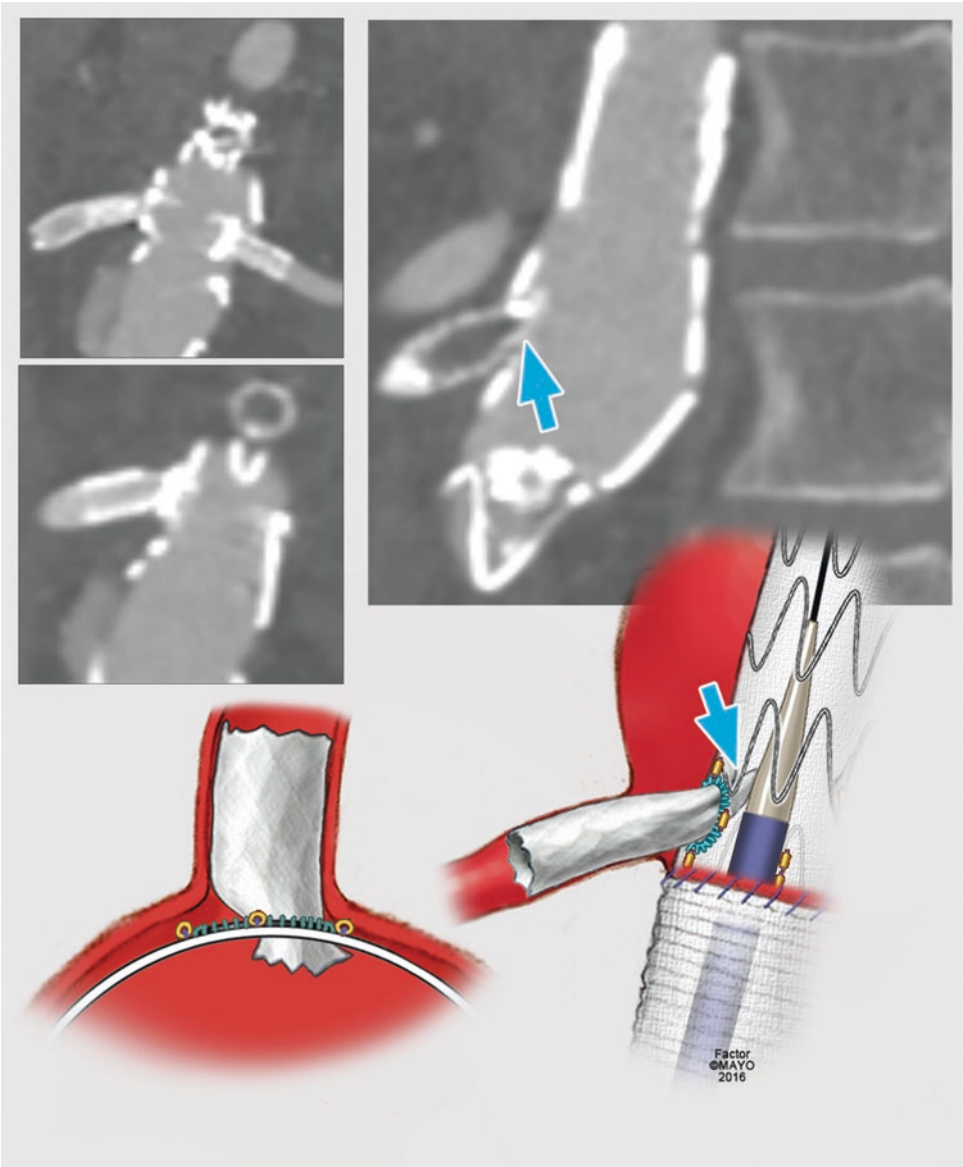


Fig. 11.33 Occlusion of the SMA stent also from compression by the dilator tip. This was successfully treated by recanalization of the stent. By permission of Mayo Foundation for Medical Education and Research. All rights reserved

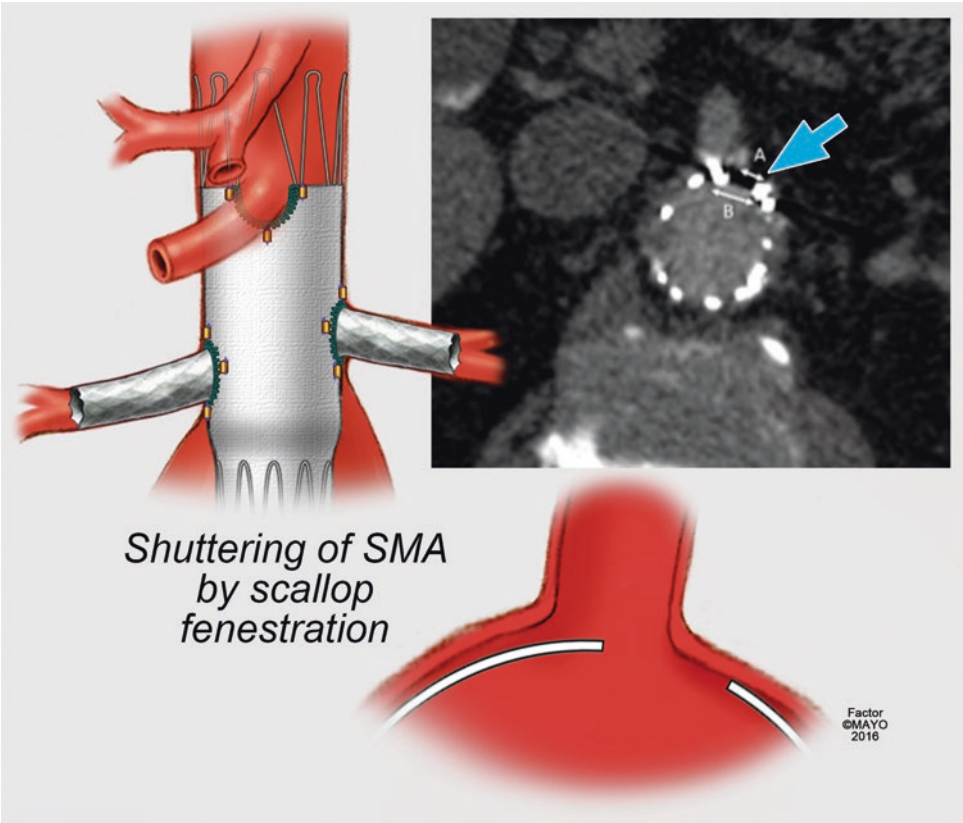


Fig. 11.34 Scallops are often not aligned by stent. It is important to evaluate shuttering of the origin of the vessel cause by misalignment of the scallop and target vessel. By permission of Mayo Foundation for Medical Education and Research. All rights reserved

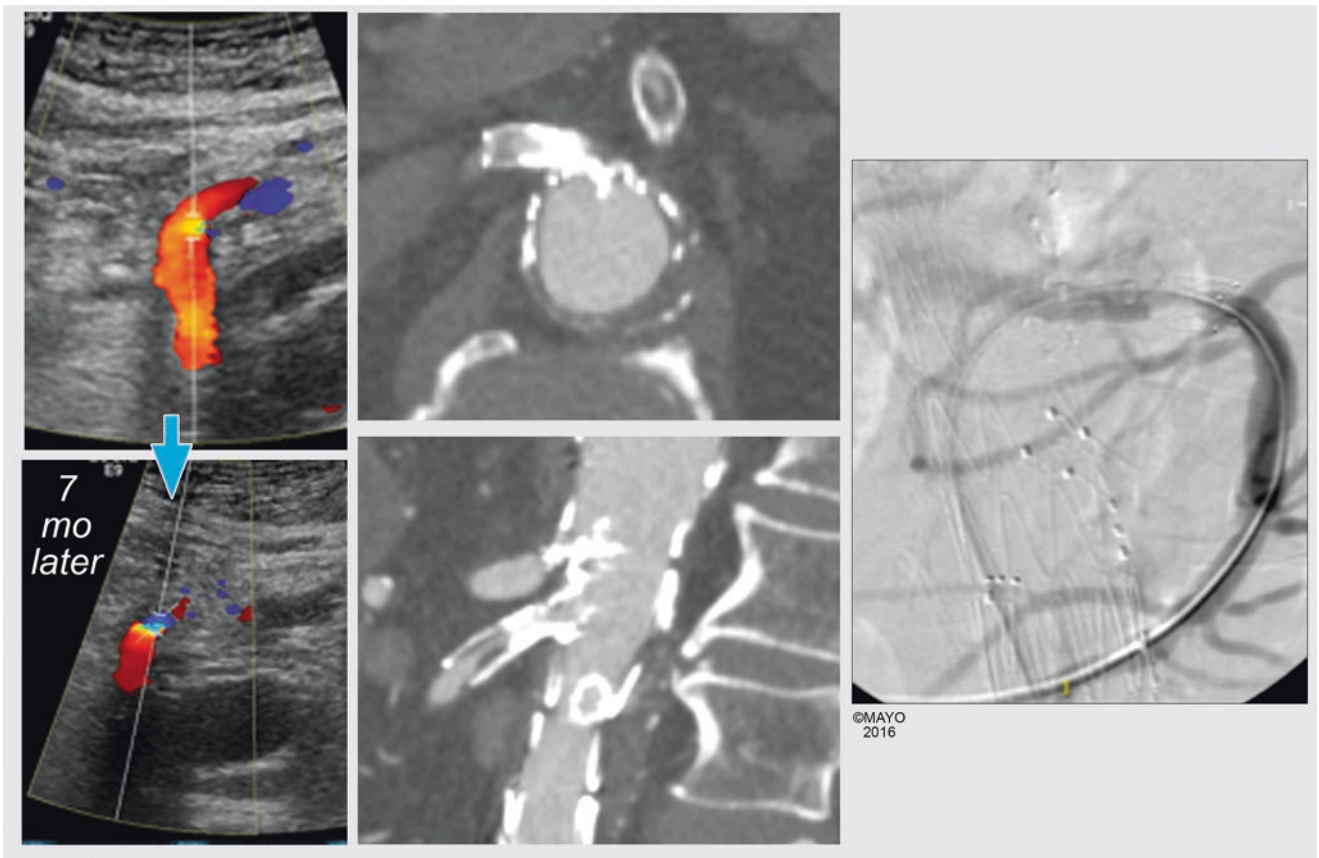


Fig. 11.35 Duplex ultrasound reveals high-grade stenosis of the stented SMA in the bare metal stent segment. This was confirmed by angiography and treated by redo stent placement. By permission of Mayo Foundation for Medical Education and Research. All rights reserved

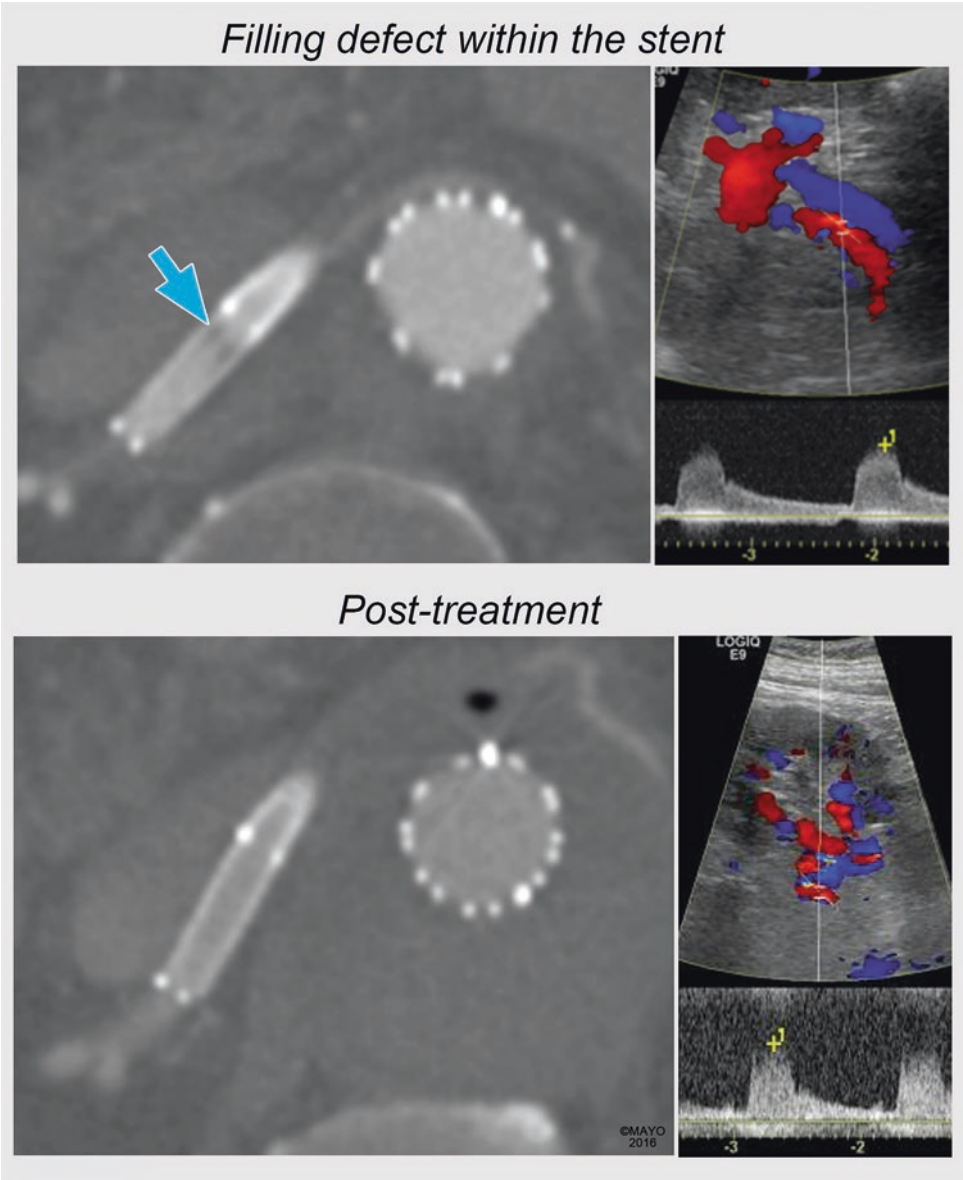


Fig. 11.36 Intimal hyperplasia causing stenosis of a right renal artery branch in the bare metal stent segment (*arrow*). This was successfully treated by placement of a self-expandable stent-graft. By permission of Mayo Foundation for Medical Education and Research. All rights reserved

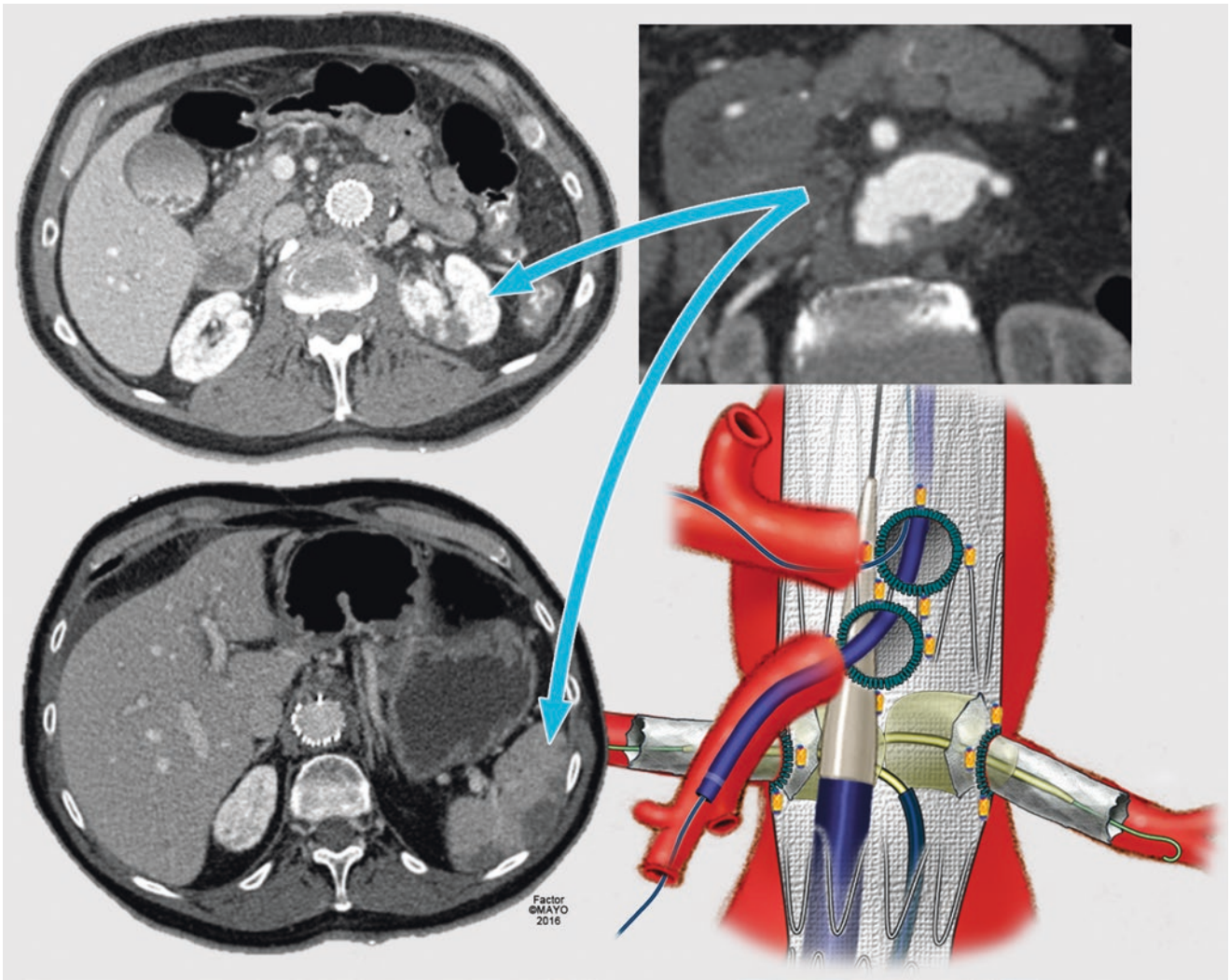


Fig. 11.37 Embolization to the kidney and spleen is noted on CTA in a patient with significant aortic debris. By permission of Mayo Foundation for Medical Education and Research. All rights reserved

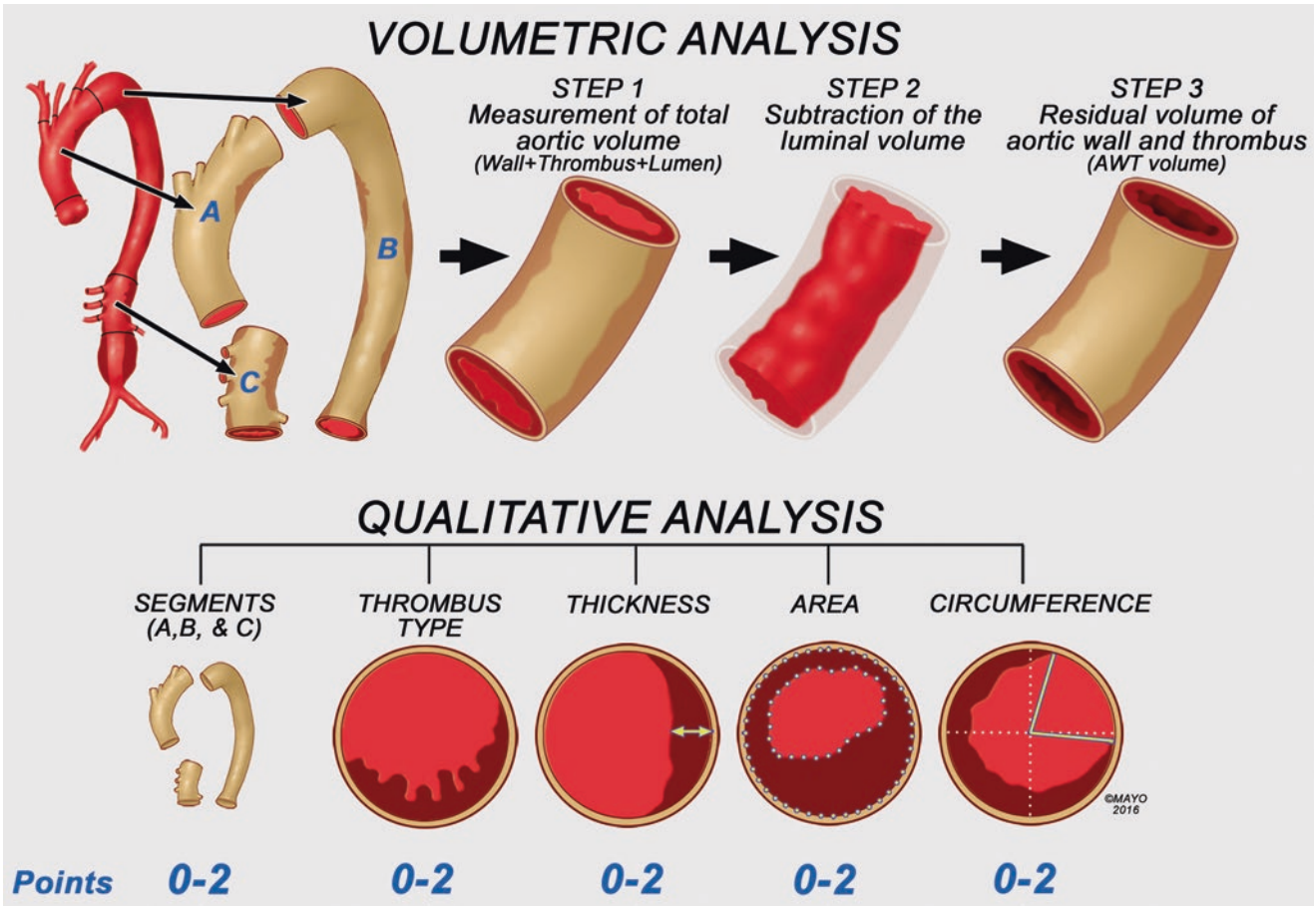


Fig. 11.38 Proposed Mayo Clinic grading system for assessment of aortic debris using volumetric and qualitative analysis using computed tomography angiography. By permission of Mayo Foundation for Medical Education and Research. All rights reserved

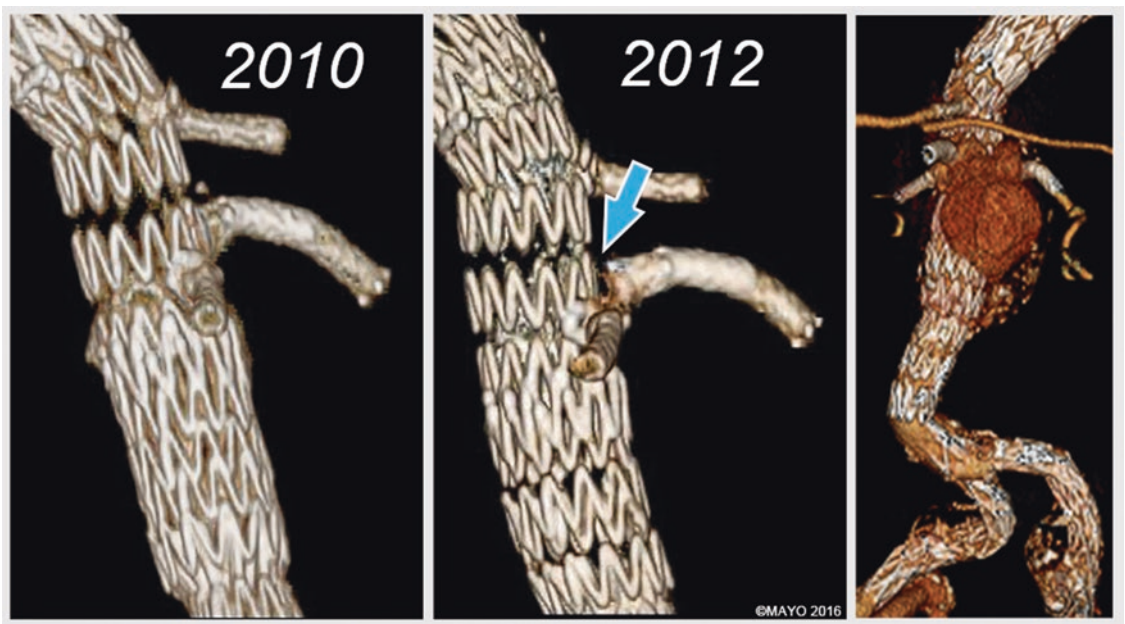


Fig. 11.39 Separation of components in a SMA fenestrated–branched stent caused a large Type IIIc endoleak, which was treated by redo stenting. By permission of Mayo Foundation for Medical Education and Research. All rights reserved

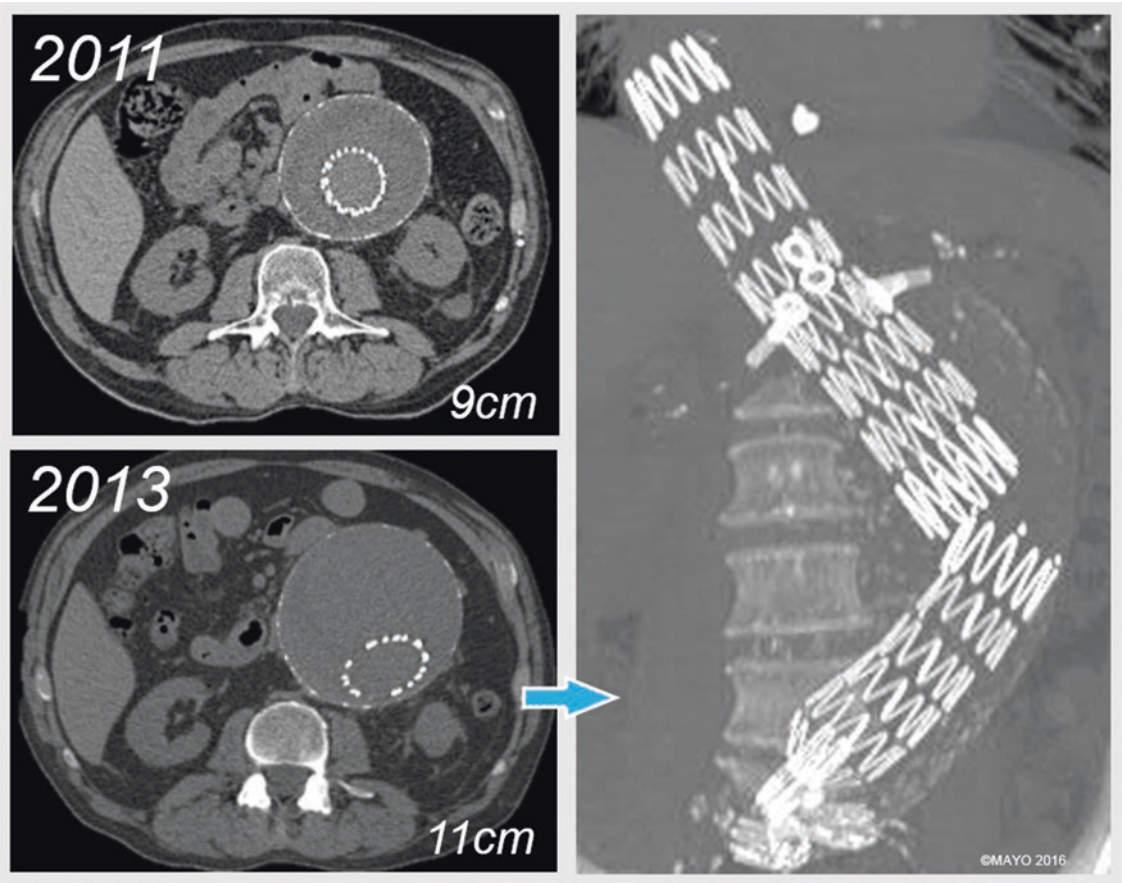


Fig. 11.40 Separation of distal bifurcated and proximal fenestrated components was treated by placement of tubular stent-graft. By permission of Mayo Foundation for Medical Education and Research. All rights reserved

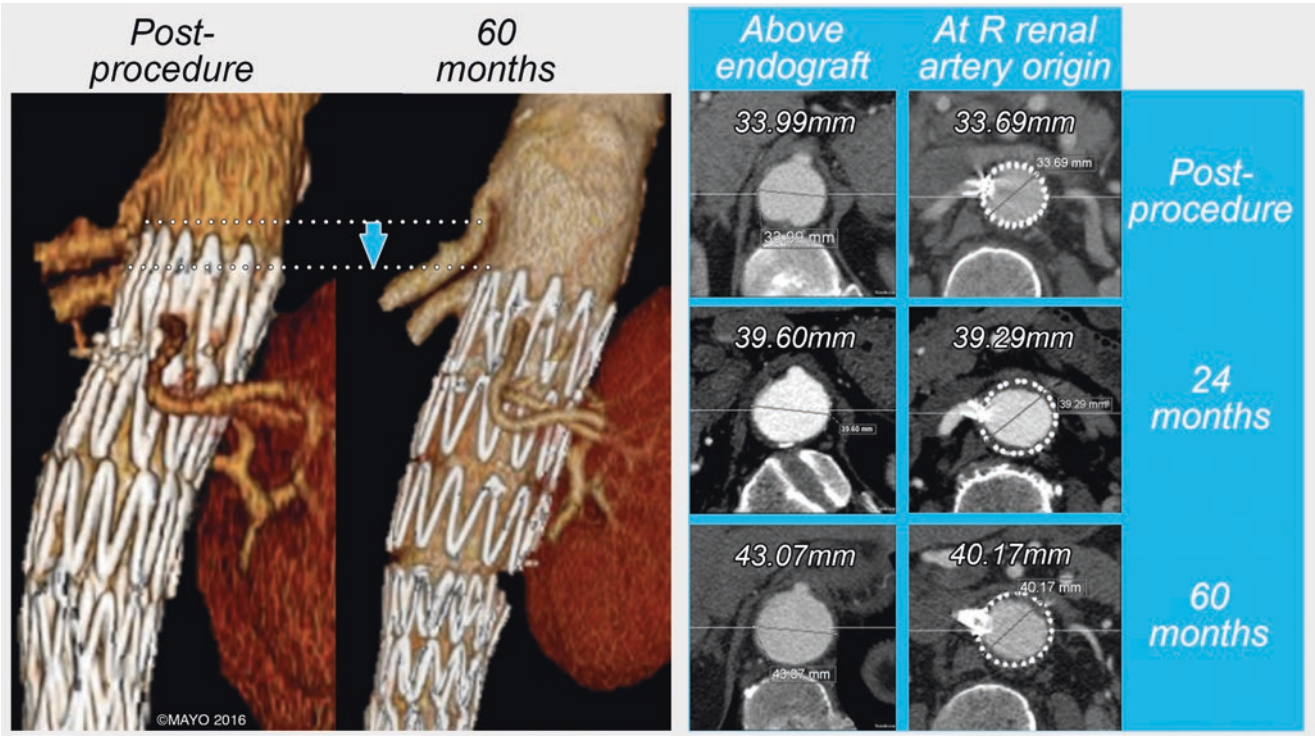


Fig. 11.41 Progression of aortic disease caused migration of the fenestrated stent-graft (*arrow*). By permission of Mayo Foundation for Medical Education and Research. All rights reserved

proper design, it can have devastating complications if not recognized. Progressive compression, dislodgement and loss of the renal stents can occur.

Device Integrity Issues

Device integrity failures are fortunately infrequent but can occur in the fabric (see Fig. 11.28) or metallic structure of the stent. These problems are manifested by endoleaks, complete graft disintegration, migration, and loss of seal zones.

Conclusion

CT angiography is an extremely powerful tool that provides a means to develop a detailed preoperative plan and detect any complications during follow-up before an issue manifests clinically. However, a clear understanding of the basics of CT scans and the methods of reconstruction and postprocessing techniques is required to accomplish these tests properly. Clinicians should be facile using postprocessing programs allowing the generation of MIPS, CLF reconstructions, and other tools that help define the vascular anatomy and pathology without an incision or an intervention.

Suggested Reading

1. Picel AC, Kansal N. Essentials of endovascular abdominal aortic aneurysm repair imaging: preprocedural assessment. AJR Am J Roentgenol. 2014;203(4):W347–57.
2. Picel AC, Kansal N. Essentials of endovascular abdominal aortic aneurysm repair imaging: postprocedure surveillance and complications. AJR Am J Roentgenol. 2014;203(4):W358–72.
3. Rossi M, Iezzi R. Cardiovascular and Interventional Radiological Society of Europe guidelines on endovascular treatment in aortoiliac arterial disease. Cardiovasc Intervent Radiol. 2014;37(1):13–25.
4. Wadgaonkar AD, Black III JH, Weihe EK, Zimmerman SL, Fishman EK, Johnson PT. Abdominal aortic aneurysms revisited: MDCT with multiplanar reconstructions for identifying indicators of instability in the pre- and postoperative patient. Radiographics. 2015;35(1):254–68.
5. Kalva SP, Dill KE, Bandyk DF, et al. ACR Appropriateness Criteria(R) nontraumatic aortic disease. J Thorac Imaging. 2014;29:W85–8.
6. Ambler GK, Coughlin PA, Hayes PD, Varty K, Gohel MS, Boyle JR. Incidence and outcomes of severe renal impairment following ruptured abdominal aortic aneurysm repair. Eur J Vasc Endovasc Surg. 2015;50(4):443–9.
7. Goldfarb S, McCullough PA, McDermott J, Gay SB. Contrast-induced acute kidney injury: specialty-specific protocols for interventional radiology, diagnostic computed tomography radiology, and interventional cardiology. Mayo Clin Proc. 2009;84:170–9.
8. McDonald RJ, McDonald JS, Carter RE, et al. Intravenous contrast material exposure is not an independent risk factor for dialysis or mortality. Radiology. 2014;273:714–25.
9. Yu L, Fletcher JG, Grant KL, Carter RE, Hough DM, Barlow JM, et al. Automatic selection of tube potential for radiation dose reduction in vascular and contrast-enhanced abdominopelvic CT. AJR Am J Roentgenol. 2013;201(2):W297–306.
10. McCollough CH, Primak AN, Braun N, Kofler J, Yu L, Christner J. Strategies for reducing radiation dose in CT. Radiol Clin North Am. 2009;47:27–40.
11. Yu L, Li H, Fletcher JG, McCollough CH. Automatic selection of tube potential for radiation dose reduction in CT: a general strategy. Med Phys. 2010;37:234–43.
12. Buls N, Van Gompel G, Van Cauteren T, et al. Contrast agent and radiation dose reduction in abdominal CT by a combination of low tube voltage and advanced image reconstruction algorithms. Eur Radiol. 2015;25:1023–31.
13. Winklehner A, Goetti R, Baumueller S, et al. Automated attenuation-based tube potential selection for thoracoabdominal computed tomography angiography: improved dose effectiveness. Invest Radiol. 2011;46:767–73.
14. Petersilka M, Bruder H, Krauss B, Stierstorfer K, Flohr TG. Technical principles of dual source CT. Eur J Radiol. 2008;68:362–8.
15. Megibow AJ, Sahani D. Best practice: implementation and use of abdominal dual-energy CT in routine patient care. AJR Am J Roentgenol. 2012;199:S71–7.
16. Sommer WH, Graser A, Becker CR, et al. Image quality of virtual non-contrast images derived from dual-energy CT angiography after endovascular aneurysm repair. J Vasc Interv Radiol. 2010;21(3):315–21.
17. Flors L, Leiva-Salinas C, Norton PT, Patrie JT, Hagspiel KD. Endoleak detection after endovascular repair of thoracic aortic aneurysm using dual-source dual-energy CT: suitable scanning protocols and potential radiation dose reduction. AJR Am J Roentgenol. 2013;200(2):451–60.
18. Chandarana H, Godoy MC, Vlahos I, et al. Abdominal aorta: evaluation with dual-source dual-energy multidetector CT after endovascular repair of aneurysms—initial observations. Radiology. 2008;249(2):692–700.
19. Stolzmann P, Frauenfelder T, Pfammatter T, et al. Endoleaks after endovascular abdominal aortic aneurysm repair: detection with dual-energy dual-source CT. Radiology. 2008;249(2):682–91.
20. Ascenti G, Mazziotti S, Lamberto S, et al. Dual-energy CT for detection of endoleaks after endovascular abdominal aneurysm repair: usefulness of colored iodine overlay. AJR Am J Roentgenol. 2011;196(6):1408–14.
21. Maturen KE, Kaza RK, Liu PS, Quint LE, Khalatbari SH, Platt JF. "Sweet spot" for endoleak detection: optimizing contrast to noise using low keV reconstructions from fast-switch kVp dual-energy CT. J Comput Assist Tomogr. 2012;36(1):83–7.
22. Albrecht MH, Scholtz JE, Husers K, et al. Advanced image-based virtual monoenergetic dual-energy CT angiography of the abdomen: optimization of kiloelectron volt settings to improve image contrast. Eur Radiol. 2016;26(6):1863–70.

12 Duplex Ultrasound for Evaluation and Surveillance of Fenestrated, Branched, and Parallel Stent-Grafts

Thanila A. Macedo and Gustavo S. Oderich

Introduction

Fenestrated and branched stent-grafts have been increasingly utilized to treat complex aortic aneurysms offering a less invasive option. However lifelong surveillance is required to monitor for complications that can threat stent durability. Computed tomography angiography (CTA) is the most widely used modality to follow-up patients after endovascular procedure; however, it is associated with risks from iodinated contrast injection, radiation, and higher costs. Ultrasound is an attractive imaging alternative due to its low cost, wide availability, lack of ionizing radiation, or use of iodinated contrast. It is limited by inferior sensitivity and specificity to identify endoleaks [1], although recent literature has demonstrated that the use of ultrasound contrast can overcome this limitation. Ultrasound still suffers from operator dependency and its inability to reliably detect morphologic complications such as stent fracture or migration. Nonetheless, this modality can promptly diagnose branch vessel occlusion, stenosis, and endoleaks, which can adversely affect patient outcomes.

Our protocol typically includes a baseline study prior to stent-graft implantation, followed by target vessel ultrasound at 6–8 weeks, 6 months, and yearly after the operation. This chapter focuses on technical aspects of duplex ultrasound of renal-mesenteric arteries, diagnostic interpretation criteria, and examples of normal and abnormal findings in patients with fenestrated and/or branched endografts.

T.A. Macedo
Department of Diagnostic Radiology, Mayo Clinic,
200 First Street SW, Rochester, MN 55905, USA
e-mail: Macedo.Thanila@mayo.edu

G.S. Oderich (✉)
Division of Vascular and Endovascular Surgery, Mayo Clinic,
200 First Street SW, Rochester, MN 55905, USA
e-mail: oderich.gustavo@mayo.edu

Technique

The same basic principles applied for standard evaluation of the renal and mesenteric arteries are used to evaluate patients with fenestrated and branched stent-grafts. Duplex ultrasound evaluation of the renal and mesenteric circulation can be technically challenging. In experienced hands, the time for examination completion range between 40 and 60 min depending on patient's characteristics and on the number of vessels to be interrogated. Besides experience and knowledge of the vascular anatomy and the specific stent-graft design used in the patient, some factors can potentially contribute to increased difficulty. Obesity, previous abdominal surgery, dressings, anatomic variants, respiratory motion, and excessive bowel gas are the main factors contributing to a suboptimal examination. Modern and efficient equipment, experienced sonographer, and appropriate patient selection are keys to success.

Patients are asked to fast for 8–12 h prior to the examination with a low-fiber dinner the night before the examination to minimize bowel gas. Furthermore, the established criteria currently used to diagnose mesenteric artery disease are based on fasting velocities.

Prior to the examination, review of surgical or procedure notes and correlation with CTA studies is helpful to define stent-graft designs and which specific vessels were target by fenestrations or branches, as well as bridging stent length and configuration.

The examination is typically performed with the patient in supine position and transducer at the midline or coronal window through the liver (Fig. 12.1). When bowel gas prevents adequate visualization of the vessels, patients may be turned to a lateral oblique or lateral decubitus, which may provide a better window. Patient cooperation with breath hold is critical to record adequate Doppler spectral samples. We most commonly use the C1-5 curved transducer with starting frequency of 4.5 MHz and on patients with challenging body habitus we use the

© Mayo Foundation for Medical Education and Research 2017

G.S. Oderich (ed.), *Endovascular Aortic Repair*, DOI 10.1007/978-3-319-15192-2_12

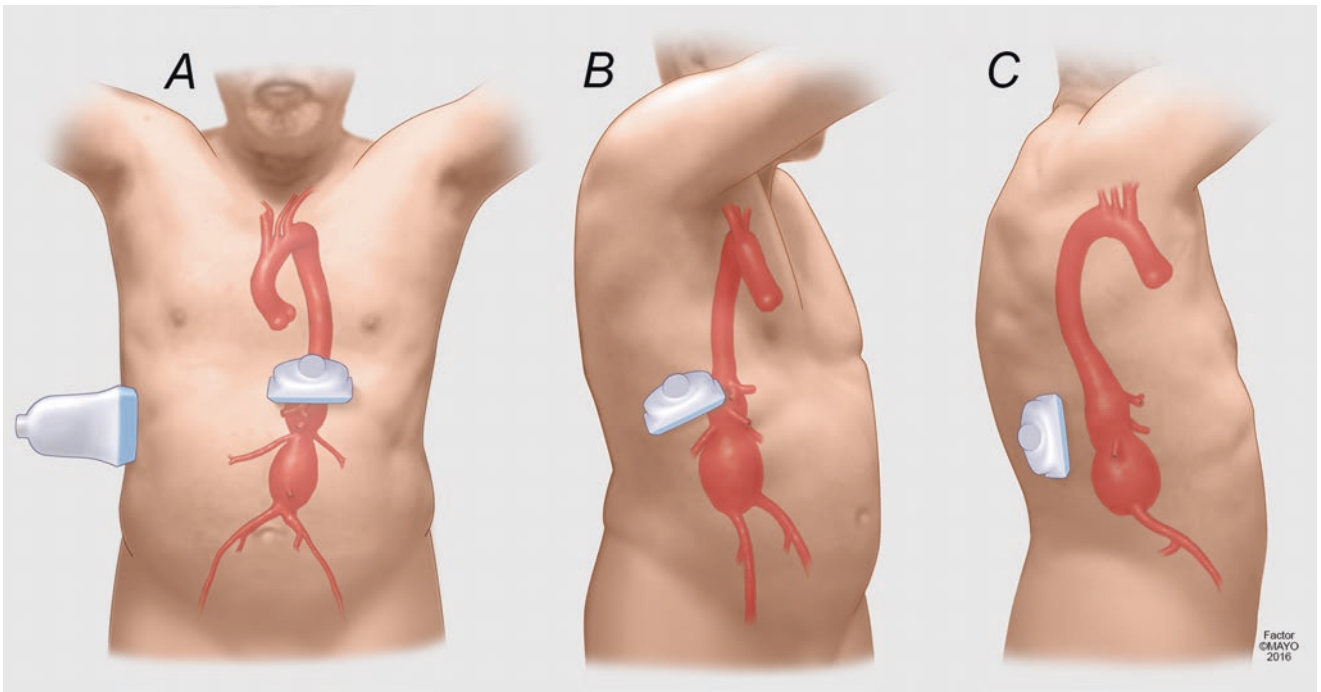


Fig. 12.1 Patient positioning for duplex ultrasound. Patient typically lies supine and transducer is located in the midline or lateral upper abdomen (**a**). Oblique (**b**) and lateral (**c**) decubitus are frequently used if better visualization is needed. Occasionally, the liver is used for window to obtain coronal images of the mesenteric and renal arteries (**c**). By permission of Mayo Foundation for Medical Education and Research. All rights reserved

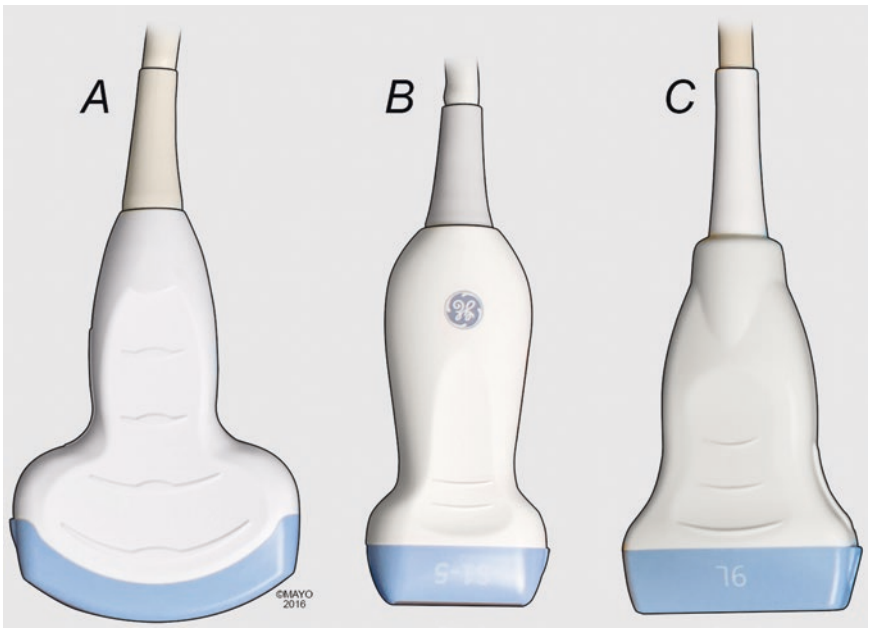


Fig. 12.2 Transducers used for duplex evaluation of renal and mesenteric arteries prior to fenestrated and branched endovascular procedure. Most commonly used is the C1-5 MHz (**a**). In patients with large body habitus, the S1-5 vector transducer (**b**) is often used. Occasionally, the 9L linear transducer (**c**) is an excellent choice for patients with slim body habitus. By permission of Mayo Foundation for Medical Education and Research. All rights reserved

S1-5 MHz vector transducer with lower frequency of 2 MHz. Occasionally, in small patients we are able to use the 9 MHz linear transducer with high frequencies up to 9 MHz (Fig. 12.2). Sonographers are instructed to use the smallest possible Doppler angle of insonation, which should always be less than 60°. It has been well documented the variations of peak systolic velocity measurement as a function of angle of insonation [2]. This should be kept in mind especially in follow-up comparison examinations where similar Doppler angle should be used to minimize velocity variations that may be incorrectly attributed to disease progression.

Suggested Minimum Scanning Routine **All PW waveforms should be performed at <60 degrees and have PSV and EDV measurements**	
Images	**Label**
1. Aorta Images	
PSV and EDV in Aorta at Renal arts	Aorta at Renal arts
2. Mesenteric Arteries	
Celiac Artery	
CA Color	CA
CA PSV/EDV Org	CA ORG
CA PSV/EDV Prx	CA Prx
CA PSV/EDV Dst	CA DST
Superior Mesenteric Artery	
SMA Color	SMA
SMA PVS/EDV Org	SMA Org
SMA PSV/EDV Prx	SMA Prx
SMA PSV/EDV Mid	SMA Mid
SMA PSV/EDV DST	SMA Dst
3. Renal Arteries	
RRA/LRA Color	RRA/LRA
RRA/LRA PSV/EDV Org	RRA/LRA Org
PRA/LRA PSV/EDV Prx	RRA/LRA Prx
RRA/LRA PSV/EDV Mid	RRA/LRA Mid
RRA/LRA PSV/EDV Dst	RRA/LRA Dst
RT/LT Seg Art Upper and Lower RI	RT/LT Upper/Lower Seg A
**Note – Please review V&IRAD report/images looking for and Accessory renal arteries. All accessory renal arteries must be imaged completely. If patient has accessory renal arteries, please perform the above images and label accordingly. ie: LT/RT Access. Art Org/stent, prox/stent, mid, dist.	
4. Kidneys	
Long RT Kidney w/ measurement	Long RT Kidney
Trans Rt Kidney	Trans RT Kidney
Long LT Kidney w/ measurement	Long LT Kidney
Trans Lt Kidney	Trans Lt Kidney

Suggested Minimum Scanning Routine **All PW waveforms should be performed at <60 degrees and have PSV and EDV measurements**	
Images	**Label**
1. Aorta Images	
PSV and EDV in Aorta at Renal arts	Aorta at Renal arts
2. Mesenteric Arteries	
Celiac Artery – label stent if present	
CA Color	CA
CA PSV/EDV Org (stent)	CA ORG
CA PSV/EDV Prx (stent)	CA Prx
CA PSV/EDV Dst	CA DST
Superior Mesenteric Artery – label stent if present	
SMA Color	SMA
SMA (stent) PVS/EDV Org	SMA Org
SMA (stent) PSV/EDV Prx	SMA Prx
SMA PSV/EDV Mid	SMA Mid
SMA PSV/EDV DST	SMA Dst
3. Renal Arteries – label stent if present	
RRA/LRA Color	RRA/LRA
RRA/LRA PSV/EDV Org (stent)	RRA/LRA Org
PRA/LRA PSV/EDV Prx (stent)	RRA/LRA Prx
RRA/LRA PSV/EDV Mid	RRA/LRA Mid
RRA/LRA PSV/EDV Dst	RRA/LRA Dst
RT/LT Seg Art Upper and Lower RI	RT/LT Upper/Lower Seg A
**Note – Please review V&IRAD report/images looking for and Accessory renal arteries. All accessory renal arteries must be imaged completely. If patient has accessory renal arteries, please perform the above images and label accordingly. ie: LT/RT Access. Art Org/stent, prox/stent, mid, dist.	
4. Kidneys	
Long RT Kidney w/ measurement	Long RT Kidney
Trans Rt Kidney	Trans RT Kidney
Long LT Kidney w/ measurement	Long LT Kidney
Trans Lt Kidney	Trans Lt Kidney

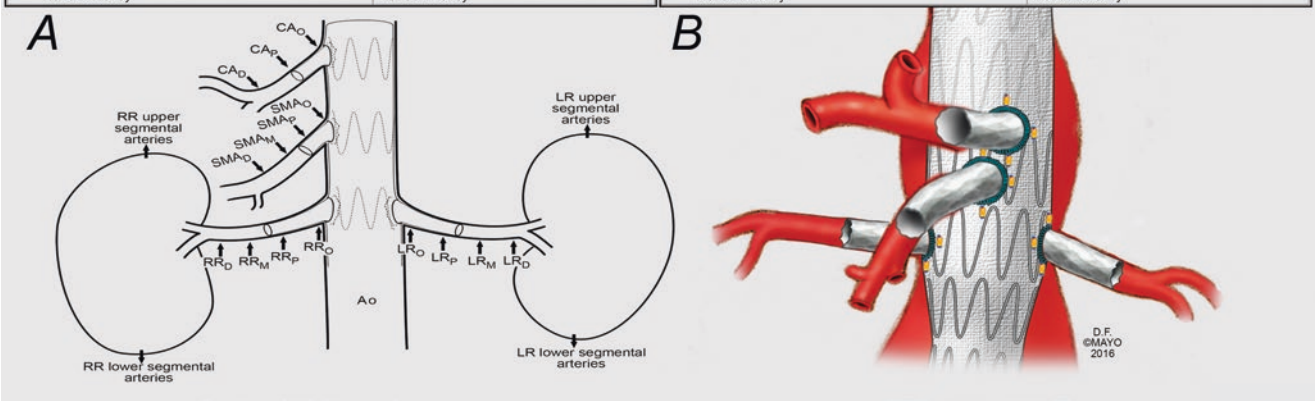


Fig. 12.3 Protocol for duplex ultrasound scanning of the renal and mesenteric arteries prior (**a**) and post procedure (**b**). By permission of Mayo Foundation for Medical Education and Research. All rights reserved

Images are acquired following a standard protocol (Fig. 12.3). Initially, the abdominal aorta is identified in transverse and sagittal planes, paying attention to diameter and atherosclerotic involvement. Spectral Doppler waveform is obtained with peak systolic velocity (PSV) and end diastolic velocity (EDV) measurements. Next, attention is turned to mesenteric and renal arteries. Color Doppler is used to identify the arteries and to guide sample volume placement for spectral Doppler analysis. The stents are occasionally discretely identified, mostly in patients with favorable body habitus (Fig. 12.4). The superior mesenteric artery (SMA) and the celiac axis (CA) are best identified in the sagittal plane, arising from the anterior aspect of the aorta (Fig. 12.5). The CA branches (hepatic and splenic) are best viewed in transverse orientation. The celiac artery is a short vessel and velocities are obtained at the origin, proximal, and distal segment during tidal breathing. In specific cases, measurements can be obtained in deep inspiration and expiration for evaluation of median arcuate ligament compression Spectral Doppler sampling with PSV and EDV measurements are obtained at the origin and at the proximal, mid, and distal SMA. Shortly after the origin, the SMA will curve inferiorly and course almost parallel to the aorta for several centimeters where it may be difficult to obtain a Doppler angle of <60°. The inferior mesenteric artery (IMA) is not routinely evaluated, but can be evaluated when specifically requested. It is best identified using the transverse plane, arising from the anterior or slightly anterolateral aspect of the aorta, generally a few centimeters above the aortic bifurcation. Measurements of PSV and EDV are obtained at the origin and distally as far as visible. Generally, only a short segment of the IMA near the origin is visualized and because of its inferior trajectory nearly parallel to the aorta, optimal angle of insonation can be challenging. Vessel identification is typically not an issue except in recent postoperative stage when there is abundant bowel gas and lack of patient cooperation. In published

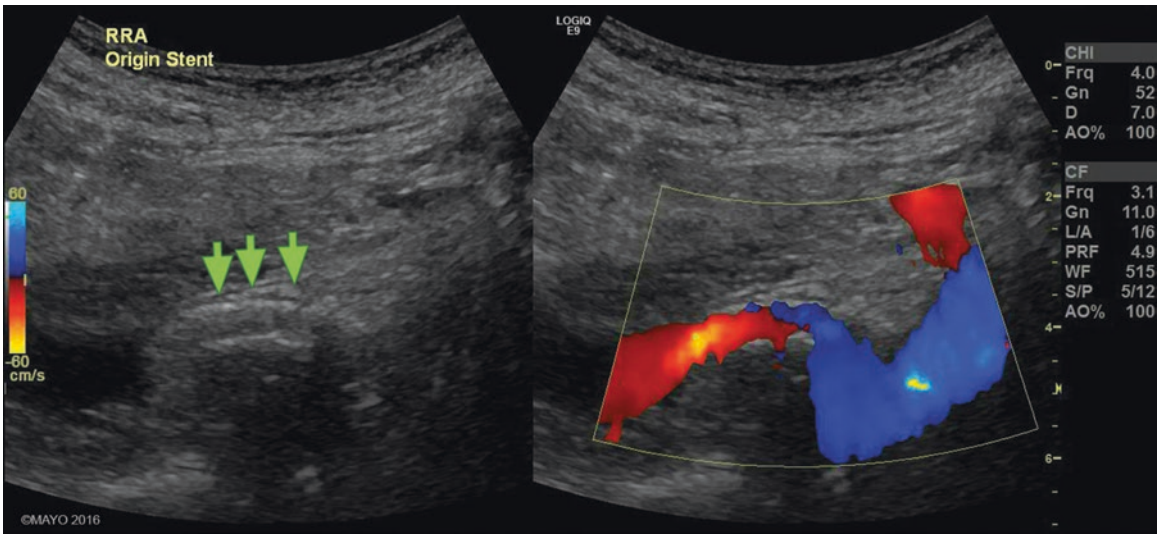


Fig. 12.4 Gray scale and color flow Doppler ultrasound of the right renal artery. Occasionally, the stent can be discretely visualized in gray scale as hyperechoic lines delineating the metallic struts (*arrows*). Color flow Doppler confirms patency of the stent. By permission of Mayo Foundation for Medical Education and Research. All rights reserved

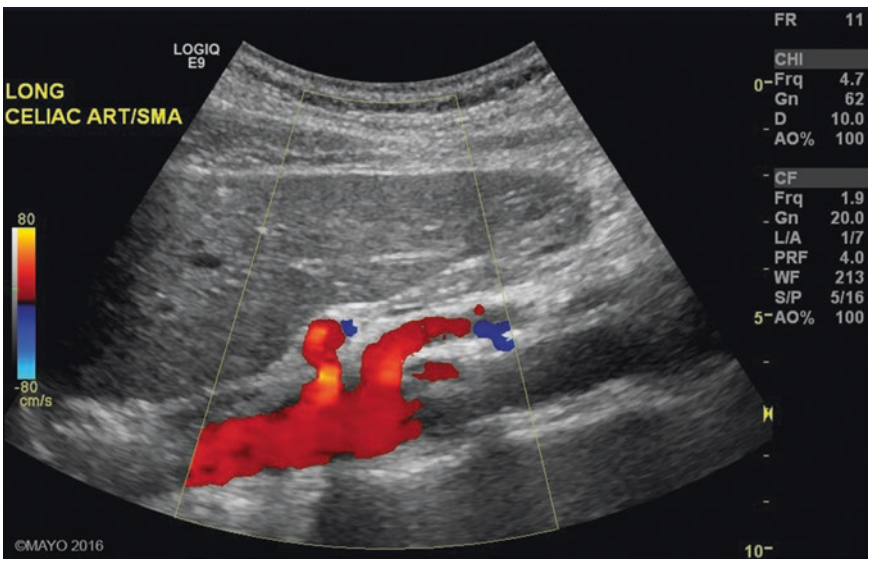


Fig. 12.5 Color Doppler ultrasound of the mesenteric arteries. The celiac and superior mesenteric arteries are best identified in the midline longitudinal plane using color Doppler. By permission of Mayo Foundation for Medical Education and Research. All rights reserved

series of ultrasound evaluation for mesenteric artery disease, the mesenteric arteries have been successfully identified in 83–98 % of patients [3–5].

The renal arteries arise from the lateral wall of the aorta about 1–2 cm below the SMA. The right renal artery originates from the anterolateral wall and subsequently courses behind the IVC. Occasionally, it may be difficult to obtain optimal Doppler angle from an anterior approach as the artery courses perpendicular to the beam, and a lateral approach may be necessary for better Doppler angle of insonation. The left renal artery typically has its origin from the posterolateral aorta. A helpful landmark is the left renal vein which usually lies anterior to the renal artery. The "banana peel" view optimally demonstrates the renal artery origin from a coronal plane using the liver as a window (Fig. 12.6). Accessory renal arteries are a challenge for ultrasound evaluation because of its small size and are not infrequently missed. Otherwise, the renal arteries are identified in most patients referred for evaluation, with studies quoting visualization in 84–90 % of patients [6]. With experienced sonographers who are highly skilled, this number should be in the higher end of the spectrum. From a lateral approach, segmental renal artery waveforms are obtained and resistive of indices (RIs) are calculated. Screening views of the kid-

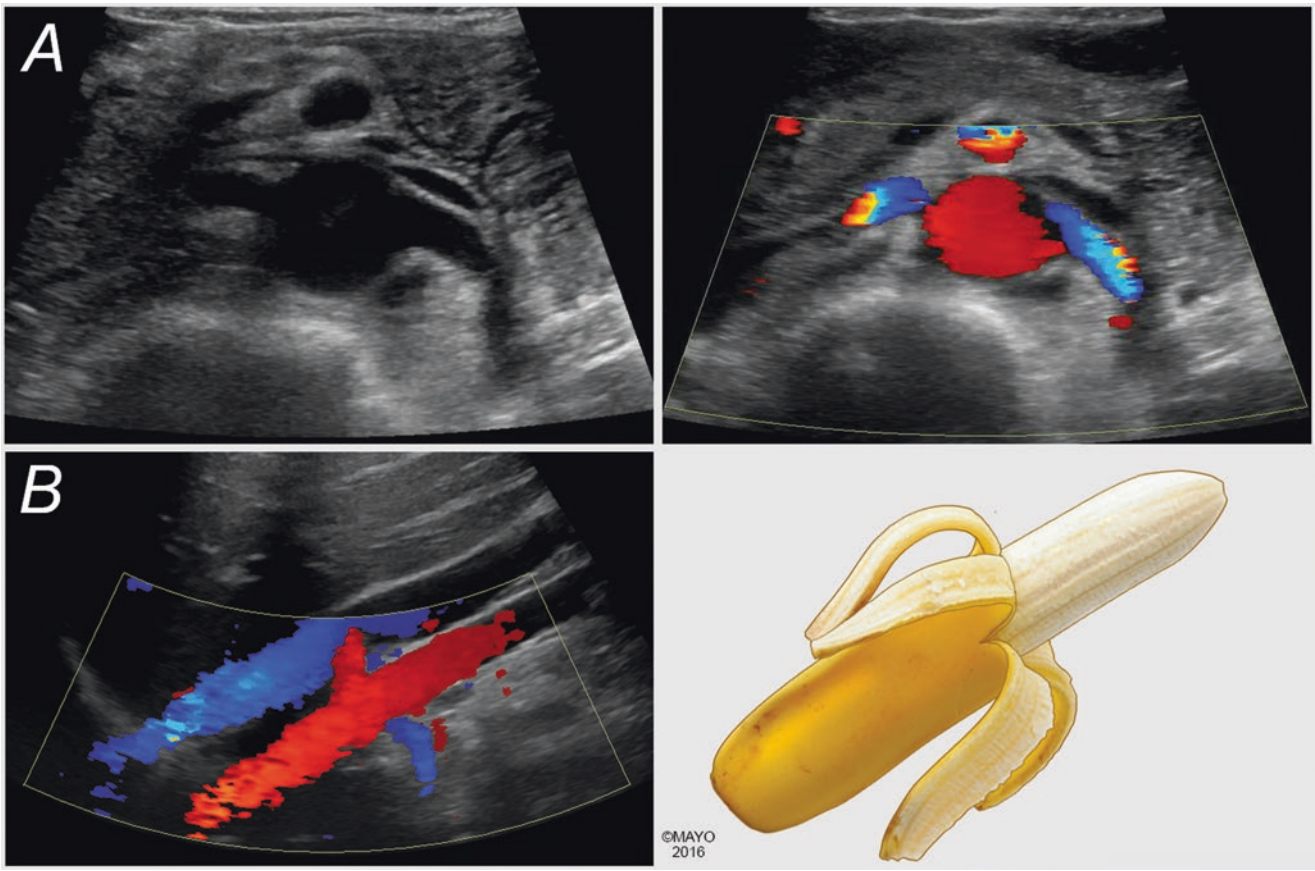


Fig. 12.6 Gray scale and color Doppler of the renal arteries origin. The renal arteries origin can be found with the transducer in transverse plane midline (**a**). Alternatively, the coronal plane using the liver as a window can be used to obtain the coveted "banana peel" image where the renal arteries origin from the aorta resemble peeling of a banana (**b**). By permission of Mayo Foundation for Medical Education and Research. All rights reserved

neys are obtained to evaluate for renal mass, renal size and hydronephrosis. Measurements of PSV and EDV are obtained at the origin, proximal, mid, and distal segments. When a stent is present, at least two velocities are obtained at the origin and proximal segment.

Mesenteric Arteries

The normal celiac artery and SMA have distinct waveforms reflecting the different end-organ blood supply requirements (Fig. 12.7). The major branches of the celiac artery supply the liver and spleen. These organs have a high demand for arterial flow resulting in a low resistance arterial waveform with substantial flow throughout diastole. The SMA supplies the small bowel and proximal colon. In the fasting state, the Doppler waveform is high-resistance with diminished flow during diastole. In the post-prandial state, due to the normal hyperemic response, the end-organ resistance is decreased, and blood flow is increased for adequate food absorption, resulting in low resistance arterial waveform similar to the celiac artery and increased diameter. The IMA supplies the distal colon and upper rectum, and therefore has a high-resistance waveform, similar to the SMA. The IMA is usually not affected by meals unless this vessel provides important compensatory collateral flow to the SMA

Anatomic variations in the origin of the hepatic arteries, which occur in approximately 20 % of the population, can account for a normal low resistance arterial waveform in the SMA during fasting state. The most common variation is a replaced right hepatic artery originating from the SMA, which occurs in up to 17 % of individuals. In these cases, the typical waveform has lower resistance pattern in the SMA, resembling the waveform of a CA. Confirmation with the patient that fasting directions were followed, along with a normal PSV and the finding of a non-turbulent waveform with a clear systolic window favor the diagnosis of an anatomic anomaly.

In 1991, Moneta and colleagues reported the first retrospective study evaluating the role of duplex scanning of splanchnic arteries to identify SMA and CA stenosis in patients undergoing abdominal aortography [7]. In that study, a PSV of

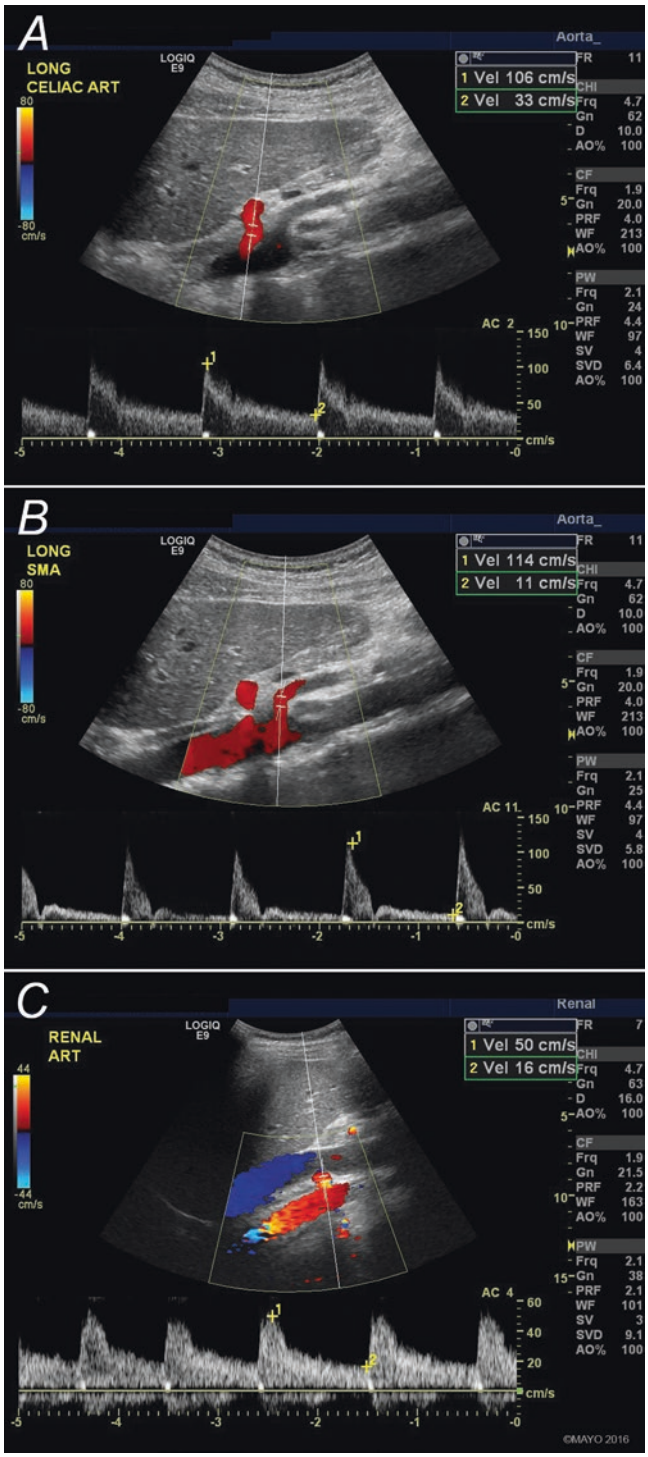


Fig. 12.7 Normal mesenteric and renal spectral Doppler waveform. The celiac artery has a low resistance waveform reflecting the constant high blood supply to the liver and spleen with persistent flow throughout diastole (**a**). The superior mesenteric artery has a high resistance waveform in fasting state with diminished flow through diastole (**b**) and a low resistance waveform during post-prandial state reflecting the increased blood flow necessary for food absorption. Similarly to the liver, the kidneys require constant high blood flow, consequently the normal renal artery waveform will have a low resistance pattern (**c**). By permission of Mayo Foundation for Medical Education and Research. All rights reserved

>275 cm/s for the SMA and >200 cm/s for the CA accurately detected stenosis greater than 70 %. It also suggested that PSV was a better predictor than EDV, and that an aorto-mesenteric ratio had no significant improvement in the ability to diagnose a significant stenosis. A few years later, the same group validated their findings in a prospective study of 100 patients who underwent duplex ultrasound and abdominal aortography, including 13 patients who had investigation for chronic mesenteric ischemia. Using the previously described PSV criteria, these authors found a sensitivity of 92 %, specificity of 96 %, positive predictive value (PPV) of 80 %, negative predictive value (NPV) of 99 %, and accuracy of 96 % to diagnose 70 % or greater stenosis. For the CA, the same parameters were 87 %, 80 %, 63 %, 94 %, and 82 %, respectively [3]. At the Mayo Clinic, we use the same criteria for the SMA, but have adjusted the celiac artery criteria to 250 cm/s to improve diagnostic accuracy.

Other velocity criterion has been proposed in the literature. A retrospective study has identified EDV greater than 45 cm/s as the most accurate predictor of a greater than 50 % SMA stenosis [8]. The same group later published a prospective study validating this finding with sensitivity of 90 % and specificity of 91 %. The same parameters for a greater than 50 % stenosis in CA are, respectively, 93 % and 100 % [5].

More recently, a retrospective study of 153 patients who underwent angiography to evaluate chronic mesenteric ischemia reported the best PSV criteria to diagnose >50 % and >70 % SMA stenosis were 295 cm/s (accuracy of 88 %) and 400 cm/s (accuracy of 85 %) and for the celiac were 240 cm/s (accuracy of 86 %) and 320 cm/s (accuracy of 85 %), respectively. Differences in velocity criteria in these studies need to be interpreted carefully given distinct methodology, equipment, and patient demographics [9].

Only a few studies have validated the criteria for IMA stenosis given its limited relevance in clinical practice. A PSV higher than 200 cm/s was found to diagnose a greater than 50 % stenosis with a specificity of 90 % and specificity of 97 % [4]. In another study an IMA PSV of 250 cm/s predicted greater than 50 % stenosis with 95 % of accuracy or 270 cm/s could predict a greater than 70 % stenosis with accuracy of 92 %. In our laboratory, we use 275 cm/s to diagnose 70 % or greater stenosis based on our previous experience review [10]. The data concerning previous studies and the established criteria for SMA, CA, and IMA stenosis are summarized in Tables 12.1, 12.2, and 12.3.

There are no available studies validating duplex ultrasound criteria for mesenteric fenestrations or branches. Identification of stenosis and kinks is of paramount importance to identify target vessels at risk for occlusion. Because fenestrated and branched stent-grafts have multiple radiopaque markers to help guide accurate device deployment, computed tomography angiography often allows limited evaluation of branch-vessel stenosis due to associated metallic artifact and small

Table 12.1 Most accurate cutoff points to diagnose stenosis of the superior mesenteric artery in different studies

–	Design	Stenosis grade	Cutoff (cm/s)	Sb (%)	St (%)	PPV (%)	NPV (%)	Ac (%)
Moneta (1993) [3]	Prospective	≥70 %	PSV ≥ 275	92	96	80	99	96
Zwolak (1998) [5]	Prospective	≥50 %	PSV ≥ 300	60	100	100	73	81
AbuRahma (2012) [9]	Retrospective	≥70 %	PSV ≥ 400	72	93	84	85	85
			PSV ≥ 410	68	95	88	84	85
			EDV ≥ 70	65	95	89	82	84
		≥50 %	PSV ≥ 295	87	89	91	84	88
			EDV ≥ 45	79	79	84	72	79

Sb sensibility, *St* specificity, *PPV* positive predictive value, *NPV* negative predictive value, *Ac* accuracy, *PSV* peak systolic velocity, *EDV* end-diastolic velocity

Table 12.2 Most accurate cutoff points to diagnose stenosis of the celiac artery in different studies

–	Design	Stenosis grade	Cutoff (cm/s)	Sb (%)	St (%)	PPV (%)	NPV (%)	Ac (%)
Moneta (1993) [3]	Prospective	≥70 %	PSV ≥ 200	87	80	63	94	82
Zwolak (1998) [5]	Prospective	≥50 %	PSV ≥ 200	93	94	96	88	93
			EDV ≥ 55	93	100	100	89	95
AbuRahma (2012) [9]	Retrospective	≥70 %	PSV ≥ 320	80	89	84	86	85
			EDV ≥ 100	58	91	83	74	77
			EDV ≥ 110	56	92	85	74	77
			EDV ≥ 120	53	95	89	73	77
		≥50 %	PSV ≥ 240	87	83	93	72	86
			EDV ≥ 40	84	48	80	54	73
			EDV ≥ 45	80	58	82	53	73

Sb sensibility, *St* specificity, *PPV* positive predictive value, *NPV* negative predictive value, *Ac* accuracy, *PSV* peak systolic velocity, *EDV* end-diastolic velocity

Table 12.3 Most accurate cutoff points to diagnose stenosis of the inferior mesenteric artery in different studies

–	Design	Stenosis grade	Cutoff[a]	Sb (%)	St (%)	PPV (%)	NPV (%)	Ac (%)
Pellerito (2009) [4]	Retrospective	≥50 %	PSV ≥ 200	90	97	90	97	95
			EDV ≥ 25	40	91	57	83	79
			MAR ≥ 2.5	80	88	67	93	86
AbuRahma (2012) [9]	Retrospective	≥50 %	PSV ≥ 250	90	96	90	96	95
			PSV ≥ 260	85	98	94	95	95
			EDV ≥ 80	60	100	100	83	96
			EDV ≥ 80	60	100	100	83	96
			MAR ≥ 4	75	100	100	92	93
			MAR ≥ 4.5	75	100	100	92	93

Sb sensibility, *St* specificity, *PPV* positive predictive value, *NPV* negative predictive value, *Ac* accuracy, *PSV* peak systolic velocity, *EDV* end-diastolic velocity, *MAR* mesenteric/aortic velocity ratio
[a]PSV and EDV in cm/s; MAR is a ratio

vessel size. In most practices, correlation of CTA and duplex ultrasound is used for surveillance. There is no well-established criterion to identify in-stent stenosis within renal and/or mesenteric fenestrated branches. Similarly, there is no consensus on which duplex criteria should be used to define significant recurrent stenosis that requires re-intervention.

There is evidence in the literature that the duplex criterion used to diagnose stenosis in native arteries may overestimate stenosis in stented vessels. This has been more extensively studied in the carotid arteries. One of the possible explanations is that the stent may reduce vessel wall compliance, resulting in higher velocities in the absence of stenosis. A retrospective study compared mean PSV before and after stenting of the SMA and found post-stenting PSVs higher than 275 cm/s, despite reduction in pressure gradients and satisfactory arteriographic image [11]. Similar findings were published by Baker et al. [10]. In our experience [12], we have found optimal criteria to identify 50 % or greater stenosis in stented superior mesenteric artery to be PSV of 350 cm/s (100 % sensitivity, 76 % specificity, and 79 % accuracy) and in the celiac artery 270 cm/s (100 % sensitivity, 77 % specificity, and 80 % accuracy, Figs. 12.8 and 12.9). This is similar to

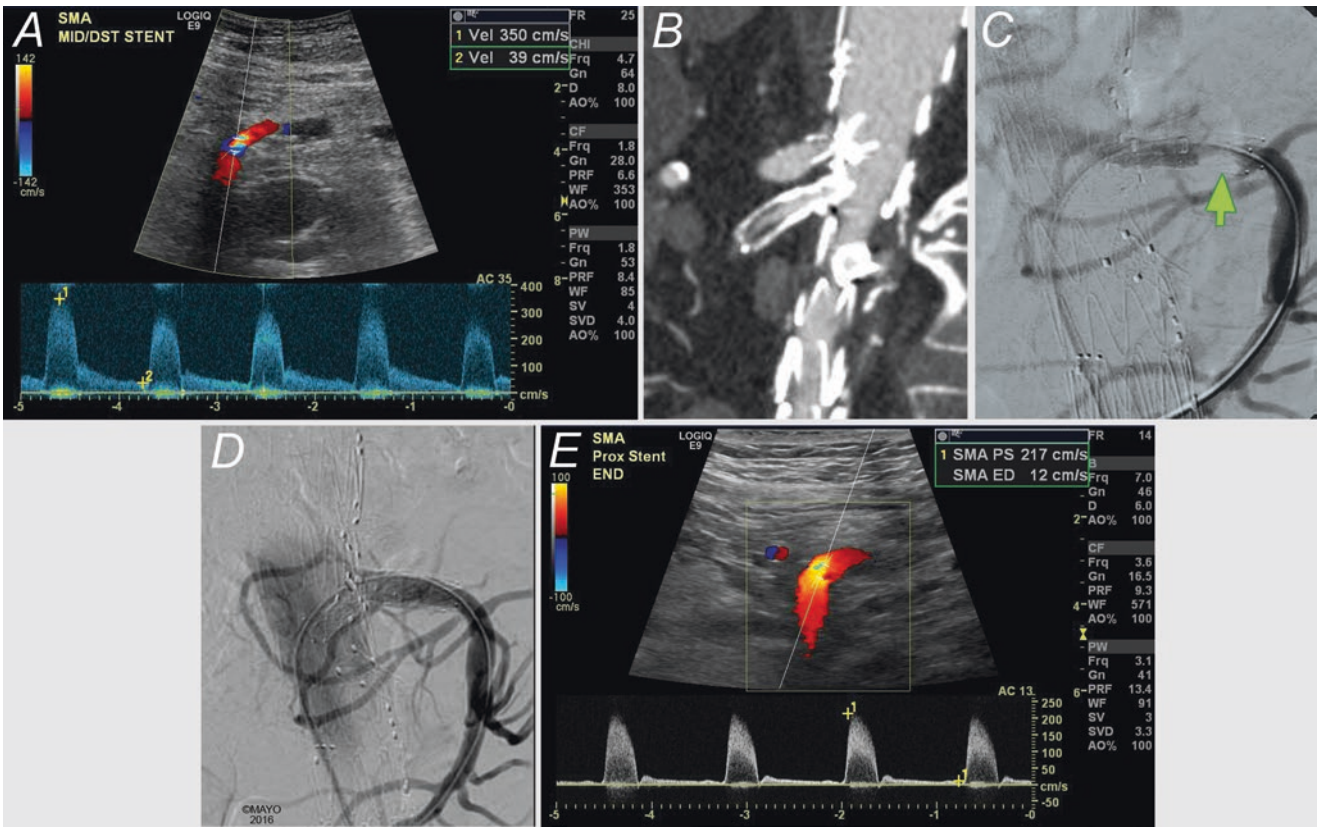


Fig. 12.8 Duplex ultrasound of fenestrated endograft with a superior mesenteric artery stent showing elevated velocities consistent with in-stent stenosis (**a**). Correlation with CTA (**b**) and catheter angiogram (**c**) confirmed a significant stenosis. Angiogram post angioplasty and redo stenting shows resolution of stenosis with widely patent SMA stent (**d**) and normal velocities on ultrasound (**e**). By permission of Mayo Foundation for Medical Education and Research. All rights reserved

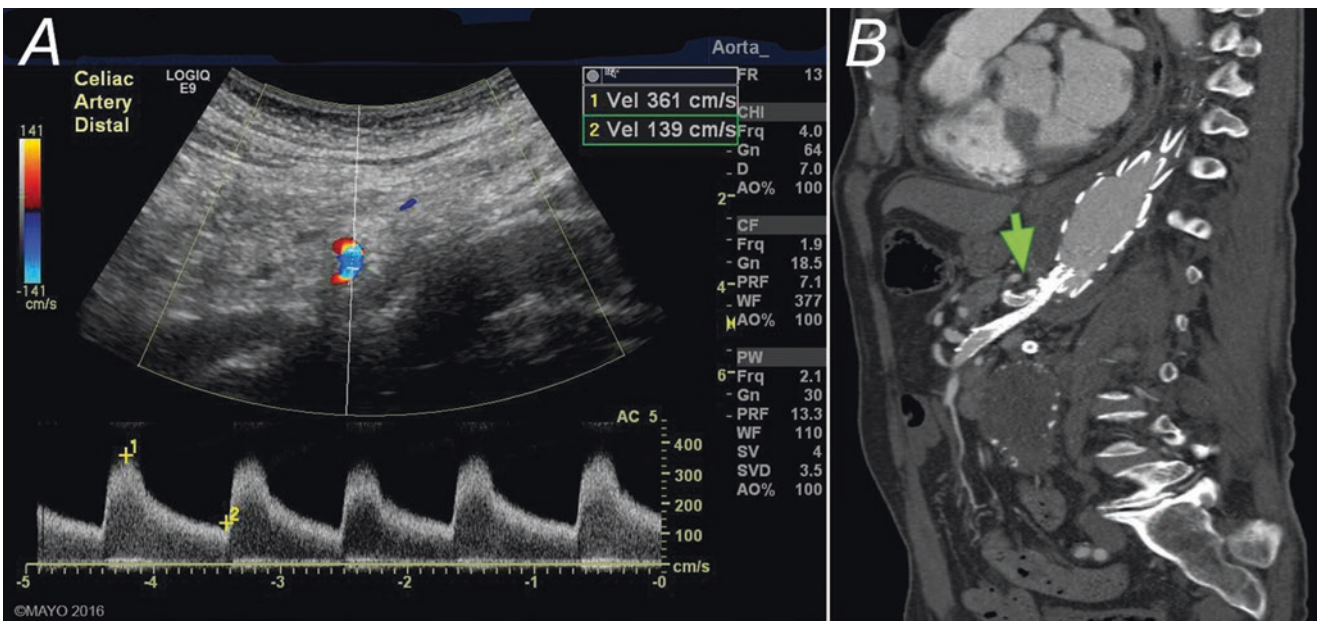


Fig. 12.9 Duplex ultrasound and computed tomography angiography (CTA) of fenestrated endograft with a celiac artery stent. Spectral Doppler demonstrates elevated peak systolic velocity of 361 cm/s associated with turbulence and color aliasing (**a**). In our experience, elevated velocity greater than 270 cm/s is indicative of 50 % or greater stenosis. Correlation with CTA in sagittal view confirmed stent kink and luminal narrowing (*arrow*) at the site of high velocities (**b**). By permission of Mayo Foundation for Medical Education and Research. All rights reserved

previously reported findings proposing a PSV over 325 cm/s to detect >50 % stenosis in stented SMA (89 % of sensitivity, 100 % of specificity, 91 % of accuracy) and 274 cm/s in the celiac artery (96 % of sensitivity, 86 % of specificity, 93 % of accuracy) [13]. Interestingly, in our experience the majority of patients with less than 50 % in-stent stenosis had velocities in the normal range, with a mean stented superior mesenteric artery PSV of 260 cm/s.

Renal Arteries

The general principles of renal duplex scanning are similar to those for other sites. The renal artery can be visualized with B-mode and color-flow imaging. Spectral Doppler waveforms for velocity measurements are obtained within the stent and native artery to characterize flow pattern and identify stenosis. The stent can be discretely identified in some patients with favorable body habitus. Similar to the mesenteric arteries, a localized flow disturbance with elevated velocity is indicative of high-grade stenosis. One of the main challenges in renal duplex scanning is to locate the renal artery and to obtain a satisfactory pulsed Doppler evaluation. These vessels are especially difficult to visualize because of its small size, deep location, and variable anatomy. As previously discussed, the study can be limited in the presence of obesity, bowel gas, limited scanning window, and respiratory motion.

The normal renal artery waveform reflects low vascular resistance in the renal bed with persistent flow throughout diastole (see Fig. 12.7). Presence of renal artery stenosis results in focally increased renal artery peak systolic velocity. Normal renal arteries typically have a PSV of less than 180 cm/s. Several studies have published the criteria to diagnose greater than 60 % renal artery stenosis suggesting a threshold velocity of 180 cm/s and 200 cm/s with high sensitivity and specificity [14, 15]. The renal artery to aortic ratio (RAR) can also be used to diagnose renal artery stenosis. A RAR of 3.5 or greater has been reported to diagnose renal artery stenosis with high sensitivity. At the Mayo Clinic, criteria for native renal artery stenosis greater than 60 % include primarily a PSV >200 cm/s. In patients with PSV between 180 and 200 cm/s, stenosis is suggested if other suspicious findings are present such as elevated aortorenal ratio, post-turbulent waveform, significant drop in velocity at the mid and distal segment and/or tardus parvus waveform in segmental arteries. Renal artery occlusion is indicated by absence of flow in a visualized segment of renal artery (Fig. 12.10). Occlusion is suspected when the renal arteries cannot be discretely identified despite adequate visualization of the expected area.

Duplex scanning of the renal artery hilum is used to identify tardus parvus waveforms with delayed systolic upstroke, which may be associated with a hemodynamically significant renal artery stenosis. Using a flank approach, pulsed Doppler waveforms are relatively easy and quick to be obtained in the renal artery hilum. Several renal artery hilar parameters have been described including acceleration time (AT), acceleration index (AI), early systolic peak (ESP), and tardus/parvus pattern. The specificity for hilar parameters is greater than 90 % in most reports, but sensitivity varies greatly between 32 and 93 % [16, 17].

Ultrasound evaluation of the renal parenchyma has also been used to predict clinical outcomes of renal revascularizations. Measurements of kidney length and evaluation of parenchymal flow patterns are utilized frequently as surrogate markers of renal parenchymal disease. Doppler waveforms taken from segmental arteries reflect renovascular resistance. Some of the parameters that have been used to quantify renovascular resistance include end-diastolic ratio (EDR: end-diastolic velocity/peak systolic velocity) and the renal-resistive index (RRI: peak systolic velocity—end-diastolic velocity/peak systolic velocity). Elevated renal parenchymal resistance is associated with low EDR and high RRI and correlates with severe renovascular parenchymal disease, which predicts less favorable results with renal artery revascularization. Rademarcher and associates reported on the use of RRI to predict outcomes of renal artery angioplasty and stenting in a prospective study. RRI greater than 0.80 was associated with no improvement in renal function, blood pressure or kidney survival, thereby identifying patients who were unlikely to respond to revascularization [18].

Similar to the mesenteric arteries, criterion for stented renal arteries has not been established. Controversy remains whether the criterion for native artery is adequate to evaluate restenosis in stented renal arteries (Fig. 12.11). A study in patients treated with fenestrated stent-grafts has proposed a revised criterion for renal artery stenosis (>60 %) consisting of PSV >280 cm/s, with sensitivity of 93 % and specificity of 100 %. For RAR, the proposed criterion was a ratio of >4.5, which had sensitivity of 83 % and specificity of 89 % [19].

An important aspect to consider when evaluating post-stent examinations is stability over time. In the absence of validated established criteria, an examination shortly after the procedure is helpful to establish a baseline, which serves for comparison with future studies. Given the limitations of available studies and controversy regarding optimal criteria to identify in-stent restenosis, it is prudent to use caution interpreting elevated velocities on duplex ultrasound examinations.

Contrast-Enhanced Ultrasound

Contrast-enhanced ultrasound (CEUS) is an emerging technique with potential advantages over standard color Doppler ultrasound. The contrast media utilized consists of stabilized

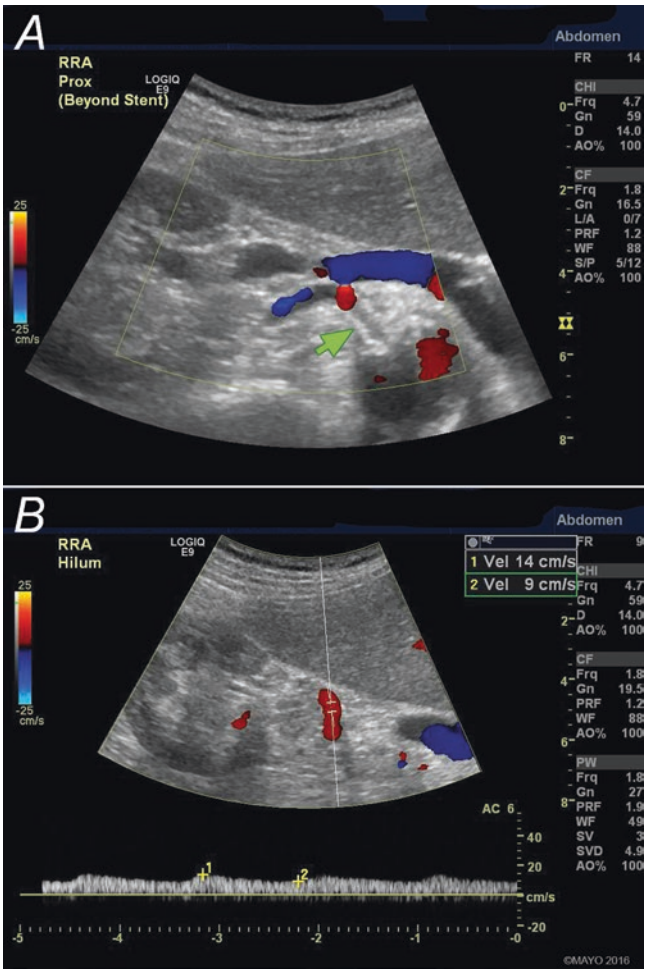


Fig. 12.10 Color Doppler ultrasound of an occluded renal artery stent. Color Doppler demonstrates the absence of flow within a well depicted renal artery stent (**a**, *arrow*). Color flow is demonstrated in the distal renal artery with low velocity and a tardus parvus waveform (**b**) which are secondary findings associated with a proximal occlusion. By permission of Mayo Foundation for Medical Education and Research. All rights reserved

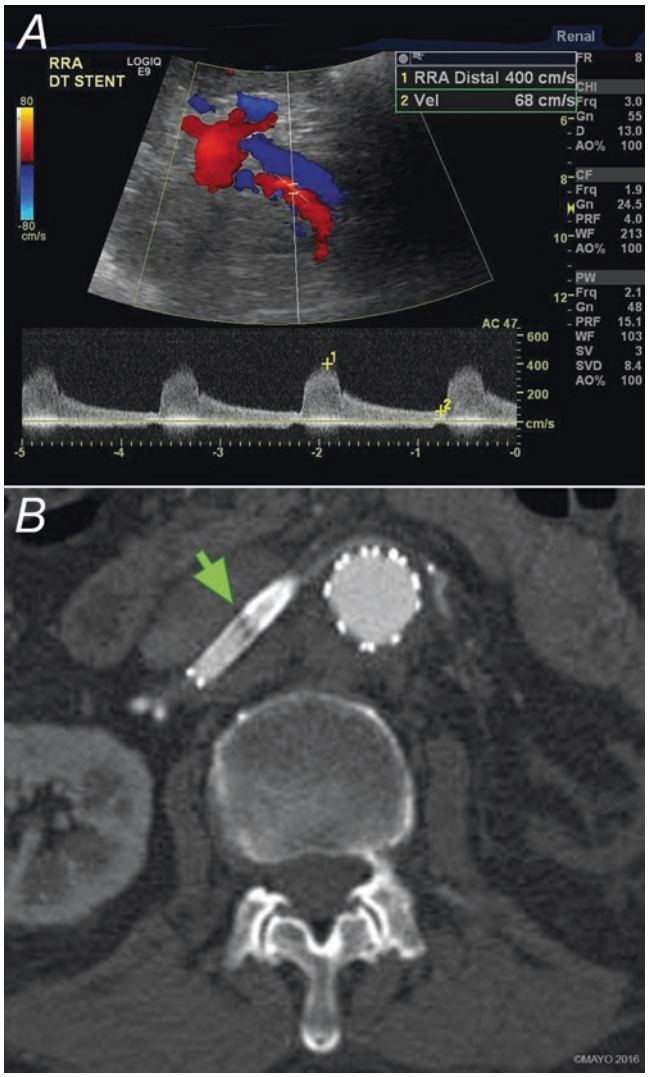


Fig. 12.11 Duplex ultrasound and CTA of a right renal artery stent in a patient with fenestrated endograft. Elevated velocity in the distal right renal artery stent up to 400 cm/s (**a**) is indicative of recurrent in-stent stenosis. CTA demonstrates stenosis with filling defect (**b**, *arrow*) in the stent corresponding to the area of high velocity. By permission of Mayo Foundation for Medical Education and Research. All rights reserved

microspheres of sulfur hexafluoride or perfluorocarbon encapsulated by phospholipid shell. These are blood pool agents without extravascular distribution excreted by the respiratory system. It does not affect the kidneys and therefore can be safely used in patients with renal impairment. Typical dose administered is between 1 and 2.5 ml followed by a 5 ml saline bolus. It is important to point out that ultrasound contrast is not FDA-approved for use in endograft evaluation. It has been used for cardiac evaluation and recently approved for evaluation of liver lesions. The intravascular contrast is believed to improve detection of endoleaks. It has been shown to be as accurate as CTA or some showing even superior results with the added information regarding flow direction and hemodynamics to better understand the endoleak. It is also comparable to CTA for aneurysm diameter measurement and evaluation of target vessels during surveillance [20–22].

Other Issues

Median Arcuate Ligament Compression

Median arcuate ligament compression can affect velocity measurements in the celiac axis and cause compression, fracture, or dislodgement of celiac stents. During expiration, there is dynamic compression of the celiac artery which resolves or significantly improves during inspiration. The unclear pathophysiology and significance of the anatomic

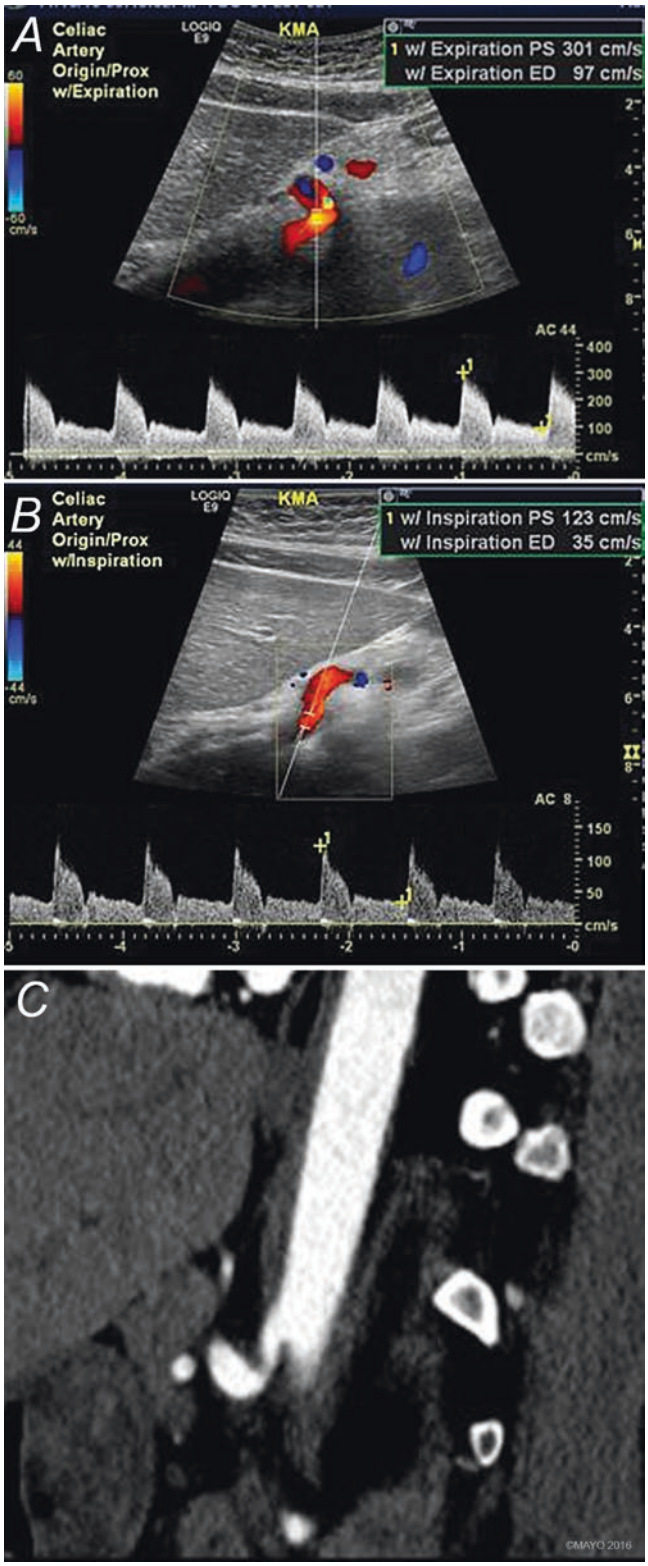


Fig. 12.12 Duplex ultrasound shows dynamic compression of the celiac artery during expiration (**a**) and normalization during inspiration (**b**). CT correlation (**c**) confirms the typical "hook" appearance related to median arcuate ligament compression during expiration. These findings in the appropriate clinical context are suggestive of median arcuate ligament compression syndrome. By permission of Mayo Foundation for Medical Education and Research. All rights reserved

finding in this entity is supported by the fact that asymptomatic individuals in the general population have celiac axis compression, between 24 and 57% expiration [23, 24]. Furthermore, although immediate relief has been widely reported with surgical decompression, the long-term success is poor with high recurrence rates. Irrespective of these controversies, duplex ultrasound has been widely applied to screen patients with suspected median arcuate ligament syndrome. The variations in celiac artery compression related to respiration can be well documented with duplex ultrasound. Typical finding is elevated PSV during expiration, above 250 cm/s, with improvement or resolution during inspiration (Fig. 12.12). Occasionally, the velocity during inspiration diminishes but remains above the threshold for significant stenosis indicating an underlying degree of fixed stenosis, which can develop overtime. Commonly, another imaging modality such as CTA or magnetic resonance angiography (MRA) is used to anatomically delineate and confirm the diagnosis.

Conclusion

Duplex examination is widely used in the diagnosis and follow-up of mesenteric and renal artery disease and in patients undergoing fenestrated, branched and parallel grafts. It is well accepted as the first screening study in patients with symptoms of chronic mesenteric ischemia and renal artery stenosis and is widely used for pre and post evaluation of patients undergoing endovascular treatment of complex aortic aneurysm repair. It is safe, noninvasive, low-cost without ionizing radiation and readily accessible. While well-established criteria are available for native vessel disease, caution should be used with elevated velocities in the stented arteries.

References

1. Raman KG, Missig-Carroll N, Richardson T, Muluk SC, Makaroun MS. Color-flow duplex ultrasound scan versus computed tomographic scan in the surveillance of endovascular aneurysm repair. J Vasc Surg. 2003;38(4):645–51.
2. Park MY, Jung SE, Byun JY, Kim JH, Joo GE. Effect of beam-flow angle on velocity measurements in modern Doppler ultrasound systems. AJR Am J Roentgenol. 2012;198:1139–43.
3. Moneta GL, Lee RW, Yeager RA, Taylor Jr LM, Porter JM. Mesenteric duplex scanning: a blinded prospective study. J Vasc Surg. 1993;17(1):79–84; discussion 5–6. Epub 1993/01/01.
4. Pellerito JS, Revzin MV, Tsang JC, Greben CR, Naidich JB. Doppler sonographic criteria for the diagnosis of inferior mesenteric artery stenosis. J Ultrasound Med. 2009;28(5):641–50. Epub 2009/04/25.
5. Zwolak RM, Fillinger MF, Walsh DB, LaBombard FE, Musson A, Darling CE, et al. Mesenteric and celiac duplex scanning: a validation study. J Vasc Surg. 1998;27(6):10787; discussion 88. Epub 1998/07/04.

6. Granata A, Fiorini F, Andrulli S, Logias F, Gallieni M, Romano G, et al. Doppler ultrasound and renal artery stenosis: an overview. J Ultrasound. 2009;12(4):133–43.
7. Moneta GL, Yeager RA, Dalman R, Antonovic R, Hall LD, Porter JM. Duplex ultrasound criteria for diagnosis of splanchnic artery stenosis or occlusion. J Vasc Surg. 1991;14(4):511–8.
8. Bowersox JC, Zwolak RM, Walsh DB, Schneider JR, Musson A, LaBombard FE, et al. Duplex ultrasonography in the diagnosis of celiac and mesenteric artery occlusive disease. J Vasc Surg. 1991;14(6):780–6.
9. AbuRahma AF, Stone PA, Srivastava M, Dean LS, Keiffer T, Hass SM, et al. Mesenteric/celiac duplex ultrasound interpretation criteria revisited. J Vasc Surg. 2012;55(2):428–36.e6; discussion 35–6. Epub 2011/12/27.
10. Baker AC, Chew V, Li CS, Lin TC, Dawson DL, Pevec WC, et al. Application of duplex ultrasound imaging in determining in-stent stenosis during surveillance after mesenteric artery revascularization. J Vasc Surg. 2012;56(5):1364–71.
11. Mitchel EL, Chang EY, Landry GJ, Liem TK, Keller FS, Moneta GL. Duplex criteria for native superior mesenteric artery stenosis overestimate stenosis in stented superior mesenteric arteries. J Vasc Surg. 2009;50(2):335–40.
12. May EJ, Macedo TM, Lewis BD. Optimal duplex ultrasound criteria in stented mesenteric arteries. Abstract presented at Society of Radiologists in Ultrasound, Chicago, IL, Oct 2013.
13. AbuRahma AF, Mousa AY, Stone PA, Hass SM, Dean LS, Keifer T. Duplex velocity criteria for native celiac/superior mesenteric artery stenosis vs in-stent stenosis. J Vasc Surg. 2012;55(3):730–8.
14. Olin JW, Piedmonte MR, Young JR, DeAnna S, Grubb M, Childs MB. The utility of duplex ultrasound scanning of the renal arteries for diagnosing significant renal artery stenosis. Ann Intern Med. 1995;122:833–8.
15. Hoffman U, Edwards JM, Carter S, Goldman ML, Harley JD, Zaccardi MJ, et al. Role of duplex scanning for the detection of atherosclerotic renal artery disease. Kidney Int. 1991;39(6):1232–9.
16. Motew SJ, Cherr GS, Craven TE, Travis JA, Wong JM, Reavis SW, et al. Renal duplex sonography: main renal artery versus hilar analysis. J Vasc Surg. 2000;32(3):462–9.
17. Stavros AT, Parker SH, Yakes WF, Chantelois AE, Burke BJ, Meyers PR, et al. Segmental stenosis of the renal artery: pattern recognition of tardus and parvus abnormalities with duplex sonography. Radiology. 1992;184(2):487–92.
18. Radermacher J, Chavan A, Bleck J, Vitzthum A, Stoess B, Gebel MJ, et al. Use of Doppler ultrasonography to predict the outcome of therapy for renal-artery stenosis. N Engl J Med. 2001;344:410–7.
19. Mohabbat W, Greenberg RK, Mastracci TM, Cury M, Morales JP, Hernandez AV. Revised duplex criteria and outcomes for renal stents and stent grafts following endovascular repair of juxtarenal and thoracoabdominal aneurysms. J Vasc Surg. 2009;49(4):827–37.
20. Perini P, Ibrahim S, Midulla M, Delsart P, Gautier C, Haulon S. Contrast-enhanced ultrasound vs. CT angiography in fenestrated EVAR surveillance: a single-center comparison. J Endovasc Ther. 2012;19:648–55.
21. Gurthler VM, Sommer WH, Meimarakis G, Kopp R, Weidenhagen R, Reiser MF, et al. A comparison between contrast-enhanced ultrasound imaging and multislice computed tomography in detecting and classifying endoleaks in the follow-up after endovascular aneurysm repair. J Vasc Surg. 2013;58(2):340–5.
22. Cantisani V, Ricci P, Grazhdani H, Napoli A, Fanelli F, Catalano C, et al. Prospective comparative analysis of colour-Doppler ultrasound, contrast-enhanced ultrasound, computed tomography and magnetic resonance in detecting endoleak after endovascular abdominal aortic aneurysm repair. Eur J Vasc Endovasc Surg. 2011;41(2):186–92.
23. Levin DC, Baltaxe HA. High incidence of celiac axis narrowing in asymptomatic individuals. Am J Roentgenol Radium Ther Nucl Med. 1972;116(2):426–9.
24. Lee VS, Morgan JN, Tan AG, Pandharipande PV, Krinsky GA, Barker JA, et al. Celiac artery compression by the median arcuate ligament: a pitfall of end-expiratory MR imaging. Radiology. 2003;228(2):437–42.

13 Magnetic Resonance Angiography for the Initial Assessment and Follow-Up of Acute Aortic Syndromes

Eric Y. Yang, Adeline Schwein, Dipan Shah, and Jean Bismuth

Introduction

Early diagnosis and assessment of acute aortic syndromes are critical to both short-term and long-term survival of patients suffering from these lethal disorders [1]. Acute aortic syndrome is the modern term including aortic dissection, intramural hematoma, and penetrating aortic ulcer [2, 3]. Per multi-society guidelines released in 2010, imaging studies have become central for confirmation of the diagnosis, extent of involvement and classification, indicators of emergency, pre-surgical or interventional planning, and follow-up surveillance [3]. Multiple imaging modalities are often employed in the same patient [4]. Furthermore, societal guidelines stress that if a high clinical suspicion exists for acute aortic dissection but initial aortic imaging is negative, a second imaging study should be obtained [3].

E.Y. Yang
Baylor College of Medicine, Houston, TX, USA

Department of Medicine, Houston Methodist Hospital, 6565 Fannin Street, STE B160/MS-A601, Houston, TX 77030, USA

Department of Cardiovascular Imaging, DeBakey Heart and Vascular Center, Houston Methodist Hospital, 6565 Fannin Street, STE B160/MS-A601, Houston, TX 77030, USA
e-mail: eyyang@houstonmethodist.org

A. Schwein • J. Bismuth (✉)
Department of Vascular Surgery, DeBakey Heart and Vascular Center, Houston Methodist Hospital, 6550 Fannin Street, Smith Tower, Suite 1401, Houston, TX 77030, USA
e-mail: aschwein@houstonmethodist.org; jbismuth@houstonmethodist.org

D. Shah
Cardiovascular MRI Laboratory, DeBakey Heart and Vascular Center, Houston Methodist Hospital, 6550 Fannin Street, #677, Houston, TX 77401, USA
e-mail: djshah@houstonmethodist.org

While magnetic resonance imaging (MRI) has been the least used modality for initial assessment, it remains the most accurate imaging modality with the highest sensitivity for aortic dissections and the modality of choice to evaluate disease progression during follow-up [4–7]. MRI techniques have made possible the non-invasive assessment of anatomical structures and dynamic flow information, through magnetic resonance angiography (MRA). Thus, the modality is well suited for the assessment of complex aortic cases. Its use has been limited by availability of scanners, and expertise for study acquisition and interpretation at medical centers. Further issues include patient tolerability due to longer scan times (e.g., hemodynamic instability, claustrophobia) or safety (e.g., ferromagnetic metal implants, bullets, or shrapnel) [8].

Additionally, the use of gadolinium contrast agents is contraindicated in advanced renal disease (glomerular filtration rate <30 mL/min/1.73 m^2) [8], due to the risk of nephrogenic systemic fibrosis. However, iron-based contrast agents, such as off-label use of ferumoxytol, may be considered as an alternative for contrast imaging in appropriate patients [9]. Further, an entire class of non-contrast MRA techniques to be discussed can still be used for vascular assessment.

In this chapter, we will present a brief overview of MRI techniques and possible technical issues, examples of its use in acute aortic syndromes, factors to consider in surgical planning, and guideline recommendations on surveillance.

Overview of Magnetic Resonance Angiographic Techniques

A variety of MRI techniques have been developed for non-invasive visualization of the vascular system. A full discussion of the physical principles underlying these techniques is beyond the scope of this chapter. The interested reader is referred to the cited review articles for further reading [10, 11].

© Mayo Foundation for Medical Education and Research 2017

G.S. Oderich (ed.), *Endovascular Aortic Repair*, DOI 10.1007/978-3-319-15192-2_13

Table 13.1 Magnetic resonance imaging pulse sequences for aortic dissection imaging and their associated purpose

Pulse sequence		Purpose
ECG-gated two-dimensional SSFP (single-shot acquisition)	Radiologic views (axial, coronal, sagittal)	General structural anatomy with blood appearing bright
	Oblique sagittal views	Aortic focused view along entire thoracic course, "candy cane" views allowing visualization of supra-aortic trunk
	Oblique axial views	Visualization of aortic dissection extent and possible entry/exit tears
ECG-gated dark blood single-shot TSE (axial)		Suppression of moving blood as black, evaluation of vessel walls
Axial cines of aortic arch and arch vessel origins		Evaluation of dissection extension into and obstruction at origin of arch vessels
Cines of celiac, superior mesenteric, and renal arteries		Evaluation for dynamic obstruction
Contrast/post-contrast sequences		
Time resolved contrast-enhanced MRA		Three-dimensional volumetric dataset of entire aorta for "off-line" analysis of aortic dimensions. Time-resolved nature allows assessment of true and false lumen filling patterns, done during contrast first pass
Three-dimensional FGE (with fat suppression) during breath-hold		Imaging with contrast equilibrium. Provides 3-D volumetric dataset of entire aorta for "off-line" analysis of aortic dimensions and allows visualization of mural thrombus. Also aids in assessment of contrast uptake by vessel wall
ECG-gated single-shot inversion recovery with long inversion time (TI600 or TI1000)		Detection of vessel wall thrombi (no delayed uptake of contrast by thrombus and hence long inversion recovery [TI] times)
Cardiac assessment[a] (optional; should not delay intervention if acute type A dissection is found)		
Myocardial delayed enhancement (short-axis, long-axes)		Detection of prior myocardial infarcts, possibly due to coronary compromise from aortic root involvement
Cine (short-axis, long-axes)		Chamber quantification, systolic function assessment
High-resolution aortic valve		Assessment of aortic root and valve morphology, detection of valve involvement
Flow assessment		
Phase velocity encoding (valvular, entry/exit)		Requires encoding in one of three dimensions for a given two-dimensional slice, allows quantitative measurement and assessment of flow

Sequences are listed in order of acquisition
SSFP steady state free precession, *TSE* turbo spin echo, *FGE* fast gradient echo, *MRA* magnetic resonance angiography
[a]Except myocardial delayed enhancement imaging, all of the following imaging sequences can be done without gadolinium contrast agents

A list of sequences used at our institution and their corresponding purpose can be found in Table 13.1.

MRA utilizes vascular contrast to distinguish vessels from surrounding tissues in a number of ways. The simplest involves intravenous administration of a gadolinium contrast agent (GCA). GCA shortens both T1 and T2 relaxation times of surrounding tissues. At commonly used concentrations in blood, this effect results in the blood pool appearing bright on T1-weighted images (Fig. 13.1).

Most GCA are of the extravascular, extracellular form. Upon injection the GCA will go through a "first pass" phase initially transiting through the arterial and then venous systems before eventually extravasating from the vessels into the surrounding tissues and achieving equilibrium throughout the entire volume of distribution (vascular system and extravascular tissue). Thus, timing of MR image acquisition must be considered to enhance only the vascular system of interest. Two techniques have been commonly used to achieve accurate timing of MRA acquisition: the test bolus method and MR fluoroscopy.

The test bolus involves administration of a small GCA dose and rapidly imaging multiple slices in the region of interest to determine timing of the contrast appearance. The technologist can then set the MRA acquisition to start at a calculated time after the full GCA infusion has begun. For MR fluoroscopy, the full GCA infusion is started while MR fluoroscopy is used to detect appearance of the contrast proximal to the region of interest. On detection of GCA arrival, the scanner will have been pre-programmed to switch modes from MR fluoroscopy to full MRA acquisition.

Flow assessment can also be conducted using phase velocity encoding techniques. Briefly, RF pulse sequences



Fig. 13.1 Anterior–posterior maximal intensity projection of a magnetic resonance angiogram obtained during the first-pass arterial phase of contrast

can be applied to de-phase and re-phase everything in a 2D slice in one direction. Blood flowing within a slice and along that de-phasing/re-phasing direction will not completely re-phase. The lack of re-phasing will predictably be a function of the blood flow velocity. The maximum velocity detectable can be set through the strength of the de-phasing/re-phasing gradients. Thus, flow patterns and volumes through valves and through vessels can be assessed and measured. Four-dimensional (4D) flow sequences are being developed to capture flow information in all three dimensions in one

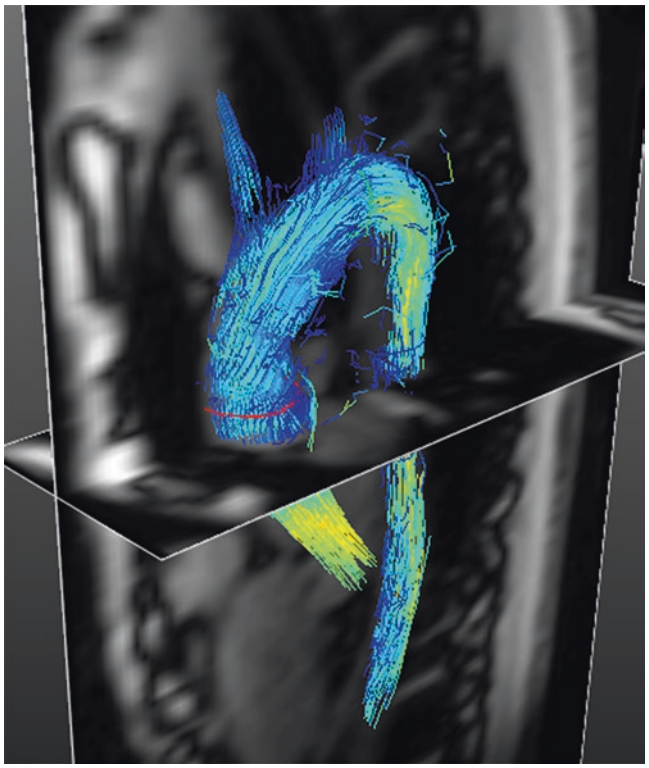


Fig. 13.2 Aortic flow path lines computed from four-dimensional flow data acquired during non-contrast magnetic resonance angiography

acquisition for a body volume of interest (Fig. 13.2). However, these sequences have been limited to clinical research use due to lengthy acquisition and complex, intensive post-processing. New 4D flow sequences may allow more rapid acquisition of flow information and hold promise for clinical vascular assessment in the future.

Acute Aortic Syndromes

Normal Anatomical Variants

Recognition of variants in aortic anatomy is necessary for accurate reporting of vessel involvement in an acute aortic syndrome and for subsequent interventional planning. Only variants affecting vessel origins from the aorta will be discussed, exclusive of coronary artery variants. Assuming normal arch anatomy, the ascending thoracic aorta involves the segment proximal to the right innominate artery. The descending thoracic aorta involves the segment distal to the left subclavian artery.

For the aortic arch, a report from Dumfarth et al. screened imaging data of 556 patients with reported thoracic aortic disease and reported on anatomic variants of the supra-aortic trunk [12]. The majority (66.5 %) of the patients had normal arch vessel anatomy: innominate, left common carotid, and

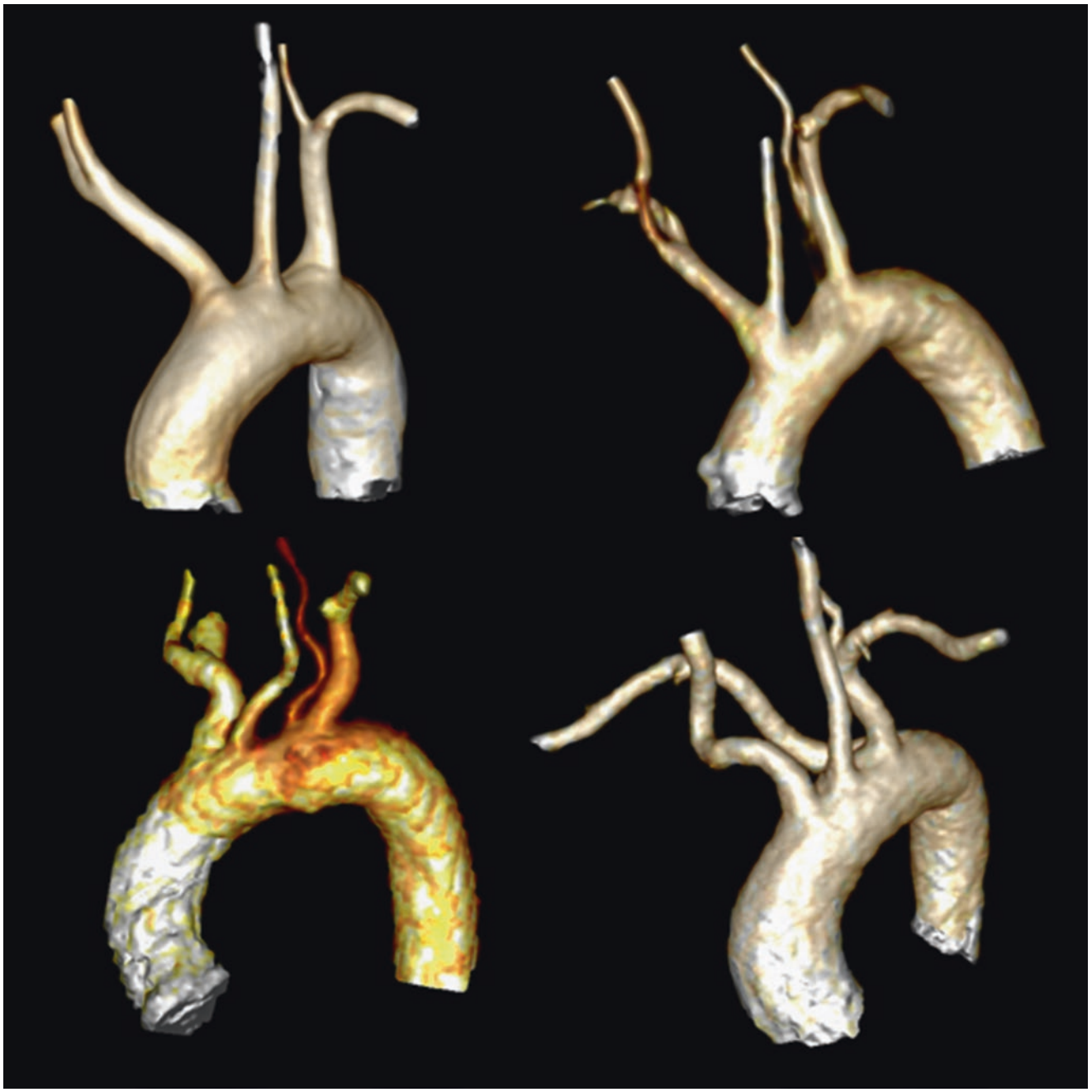


Fig. 13.3 Segmented volume renderings of aortic arches from magnetic resonance angiography showing normal (*upper left*), "bovine" arch (*upper right*), isolated left vertebral artery (*lower left*), and aberrant right subclavian artery (*lower right*)

left subclavian artery all originating from the arch (Fig. 13.3). Additional variants in decreasing order of frequency included "bovine" aortic arch or single origin of the right innominate and left common carotid artery (24.6 %), isolated left vertebral artery (6.3 %), and aberrant right subclavian artery (1.8 %) (see Fig. 13.3).

For the celiac axis, Song et al. examined imaging data from 5002 patients and reported that 13 of 15 possible variants were present, including normal anatomy [13]. Of the 5002 patients, 4457 (89.1 %) had normal anatomy: a separate hepatogastrosplenic celiac trunk and superior mesenteric artery trunk originating from the aorta (Fig. 13.4). The second most common variant was reported to be separate origin of the left gastric artery directly from the aorta (221 [4.42 %]); and the third most common variant, shared origin of the hepatic artery and the superior mesenteric artery (132 [2.64 %]).

For the renal arteries, Ozkan et al. examined angiographic data from 855 consecutive patients for origin and variations of the renal arteries [14]. Of these patients, 650 (76 %) had a



Fig. 13.4 Segmented volume rendering from magnetic resonance angiography of the abdominal aorta (*left*) showing a normal celiac axis (hepatic, gastric, splenic branches), superior mesenteric artery, and single renal arteries to each kidney. Two right renal accessory arteries are seen on the *right*

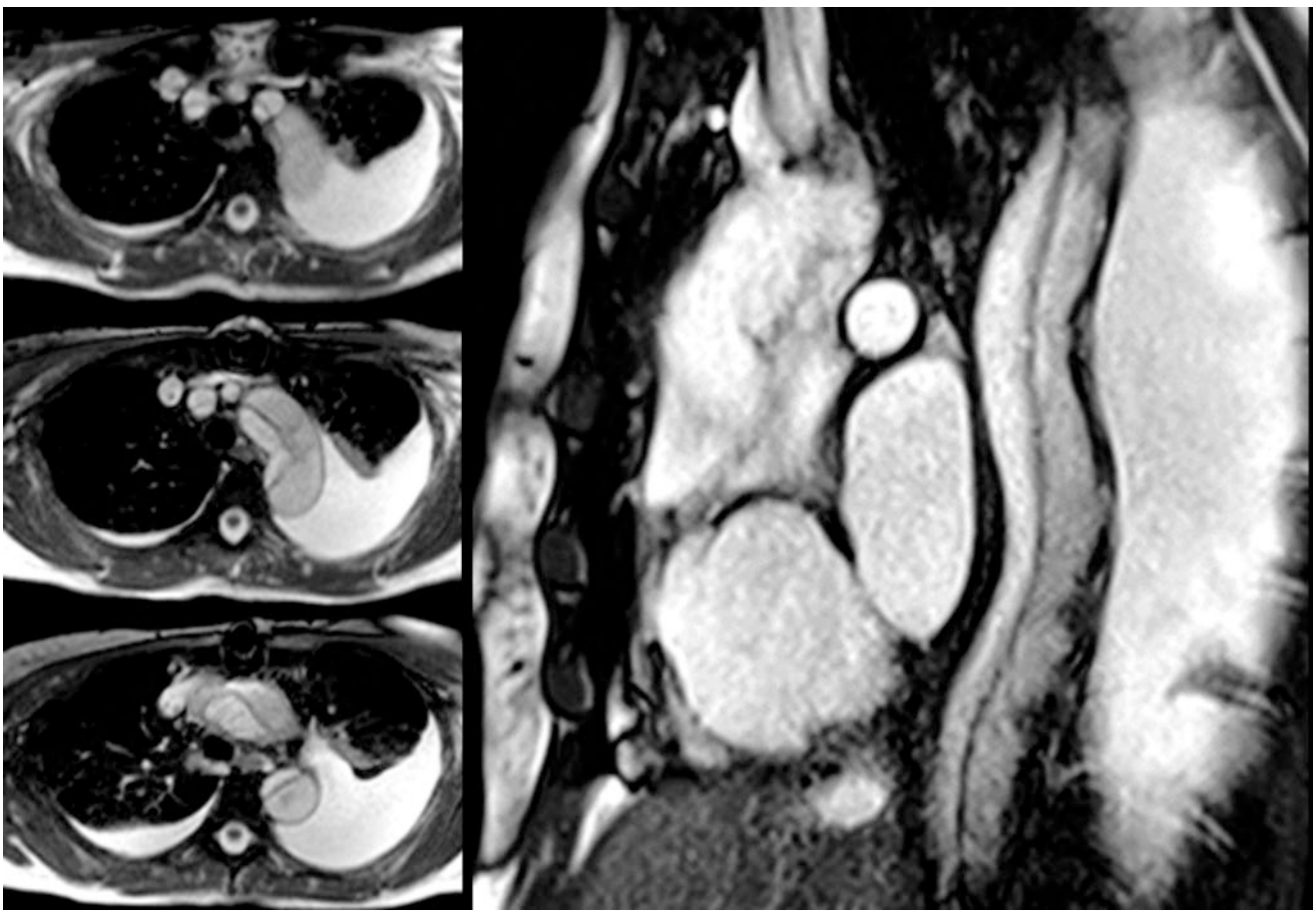


Fig. 13.5 Axial bright blood slices through the aortic arch (*left panels*) demonstrate a type I aortic dissection involving not only the arch but also the right innominate and left subclavian arteries. An oblique sagittal slice taken from cines (*right panel*) shows extension of the dissection into the abdominal aorta

single renal artery for each kidney (see Fig. 13.4). Multiple arteries (both accessory, or to the hilum, and aberrant, or to a kidney pole) were observed for the right kidney in 135 (16%) and for the left kidney in 113 (13%), with 46 (5%) having multiple arteries for both kidneys.

Aortic Dissections

In 1965 DeBakey et al. put forward the three-category classification system of acute aortic dissections, a system endorsed in multi-society guidelines for thoracic aorta disease management [15]. This classification is based on both the location of the entry tear and extent of the dissection flap.

- Type I dissections originate in the ascending aorta and propagate distally to include at least the aortic arch and typically the descending aorta (Fig. 13.5).
- Type II dissections originate in the ascending aorta and is confined to the ascending aorta (Fig. 13.6).
- Type III dissections originate in the descending aorta and propagate distally (Fig. 13.7).
  - Type III dissections are often subdivided into IIIa, limited to the descending thoracic aorta,
  - and IIIb, extending below the diaphragm.

The Stanford classification divides aortic dissections into two categories, based on the extent of the disease, regardless the location of the entry tear.

- Type A dissections gather all dissections involving the ascending aorta (equivalent to DeBakey type I and II)
- Type B dissections gather all dissections not involving the ascending aorta (equivalent to DeBakey type III)

There is currently no consensus regarding which classification is ideal and should be preferred. For the sake of clarity, we will be using the Stanford classification in the rest of this chapter.

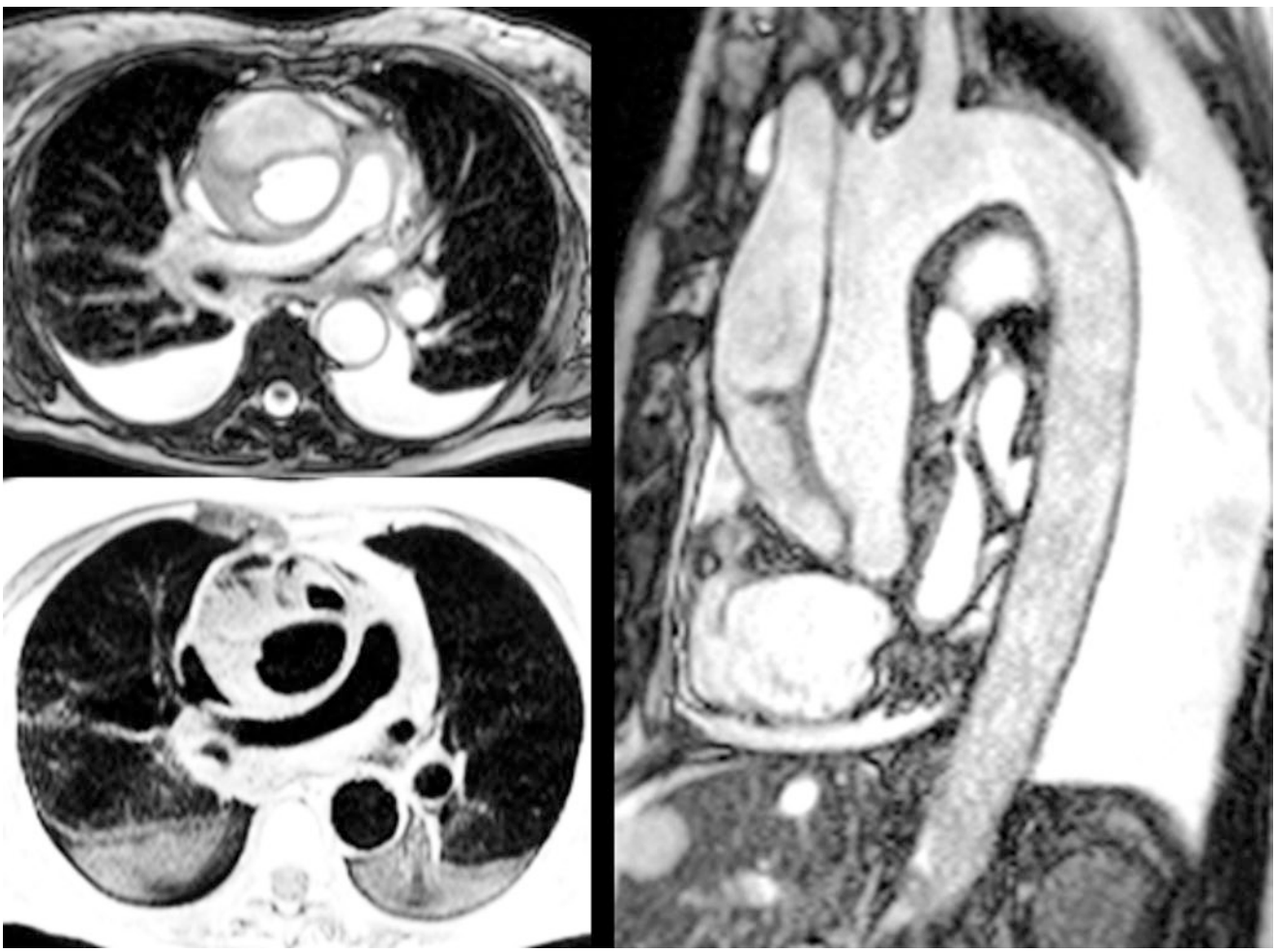


Fig. 13.6 Axial bright blood (*left top panel*) and dark blood (*left bottom panel*) are shown demonstrating a nearly circumferential aortic dissection in the ascending aorta. An oblique sagittal slice taken from cines (*right panel*) shows involvement of the right innominate artery by the type II dissection

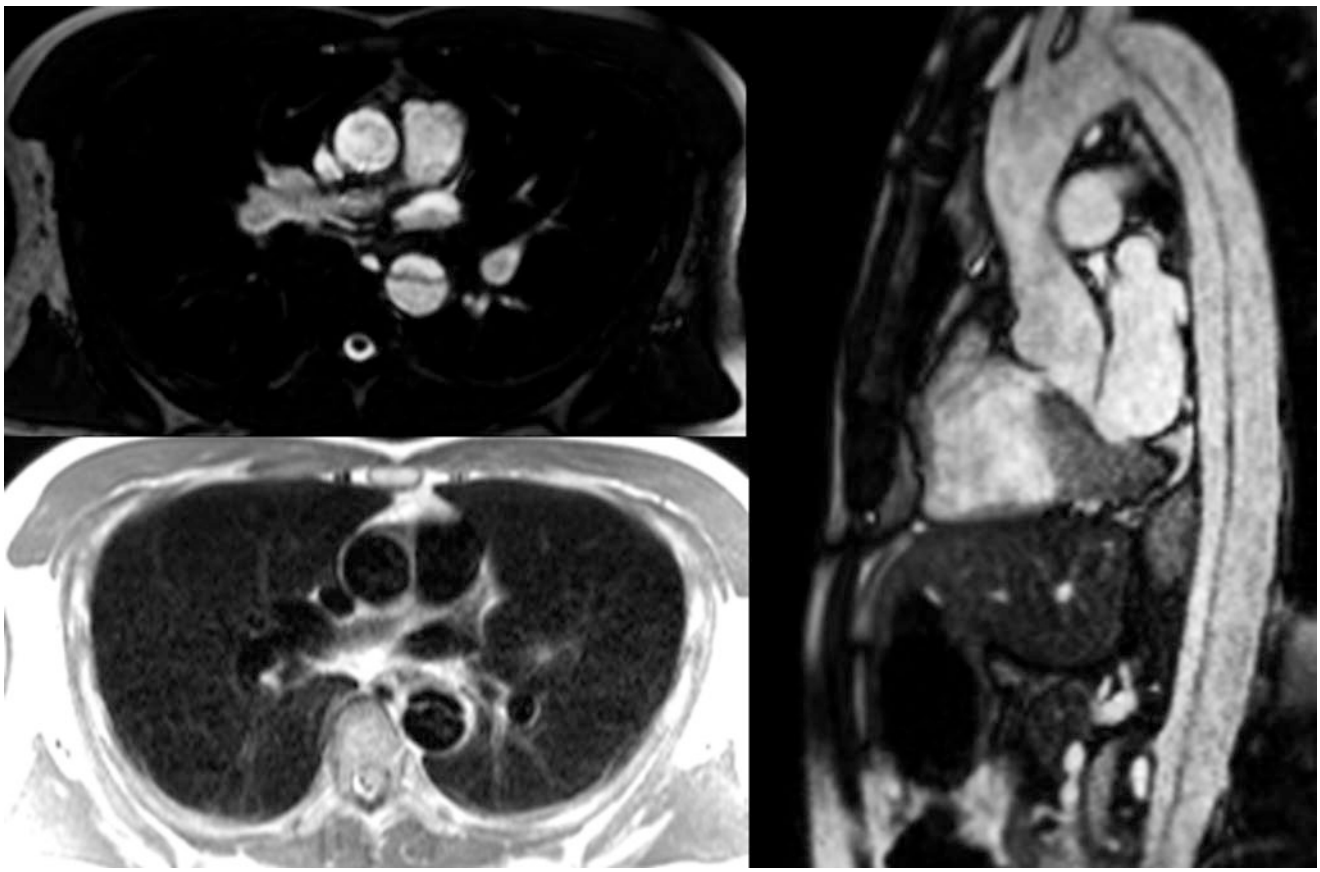


Fig. 13.7 Axial bright blood (*left top panel*) and dark blood (*left bottom panel*) are shown demonstrating a type III aortic dissection in the descending aorta. An oblique sagittal slice taken from steady-state free precession cines (*right panel*) shows extension of the dissection into the abdominal aorta

Type A dissections usually necessitate emergent open surgical intervention due to their associated high mortality, and thus unrepaired type A dissections are infrequently referred for MRA. If no acute complications are occurring, type B dissections may be managed medically. The presence of refractory pain, uncontrolled hypertension, critical aneurysmal dilation, or organ malperfusion is an indication for intervention, which mostly involves endovascular management.

Intramural Hematomas

A publication by Krukenberg has been regarded as one of the earliest descriptions of intramural hematomas (IMH), described as a dissection without intimal rupture [16]. With modern non-invasive imaging techniques such as MRI, antemortem visualization of such lesions has established IMH as an acute process [17]. Despite advances and progresses in imaging techniques, there are still many controversies surrounding the definition of IMH, its pathophysiology and relationship with aortic dissection. Some authors have described that IMH do actually show small intimal defects, particularly in the type B IMH group [18]. The intraoperative finding of confirmed intimal tears associated with IMH also contributes to the theory that IMH and dissection may actually be the same disease, at different stages [19]. Regardless of the postulated mechanism, the basic criteria on imaging are based on appearance of fresh thrombus within the aortic wall [3]. In MRA, thrombus would not be expected to take up gadolinium contrast and thus should have long recovery times relative to blood and tissues. Long inversion time pulse sequences, typically ~600 ms or ~1000 ms, will result in thrombus appearing dark and surrounding tissue appearing bright (Fig. 13.8). Surveillance of patients with IMH is important, as these lesions may expand and convert to a classic acute aortic dissection, especially with ascending aorta involvement [3].

There is no general consensus concerning the management of IMH. According to the last ESC guidelines on the diagnosis and treatment of aortic diseases [20], emergent open repair is usually indicated with ascending aorta involvement (type A). Concerning type B IMH, the occurrence of complications such as refractory pain, progression to aortic

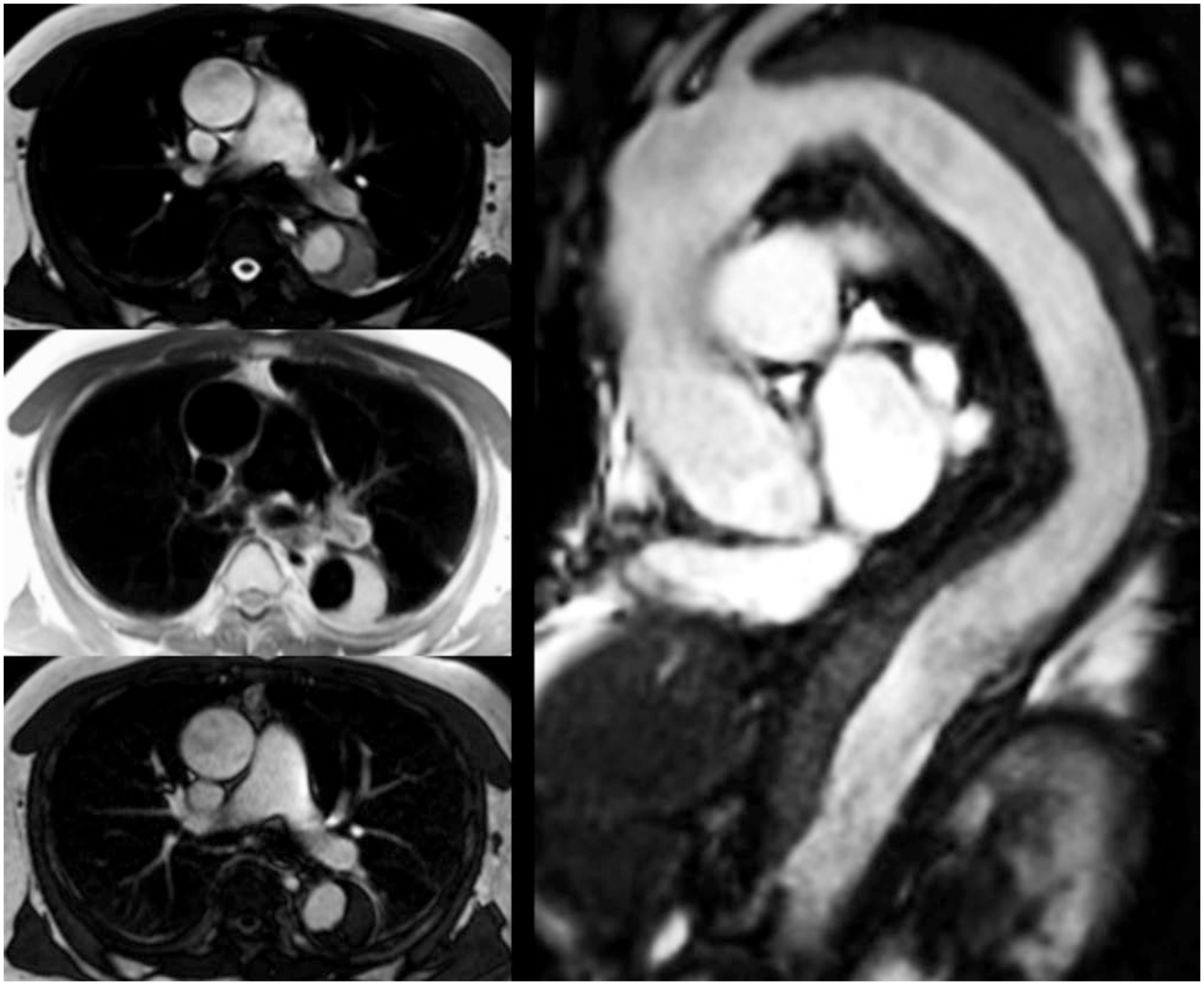


Fig. 13.8 An intramural hematoma is seen in the descending thoracic aorta. The thrombus appears gray on axial bright blood (*left top panel*) and dark blood sequences (*left middle panel*) and dark on post-contrast TI600 sequences (*left bottom panel*). An oblique sagittal view of the aorta shows involvement of the entire descending thoracic aorta (*right panel*)

dissection or rapidly increasing extension or thickness of the IMH lead to surgical treatment, through an usual endovascular approach. Uncomplicated type B IMH are usually treated medically with close imaging and clinical surveillance.

Penetrating Atherosclerotic Ulcers

In the context of atherosclerosis, lipid deposition within the sub-intimal layer of the aorta leads to formation of aortic plaque atheromas [21, 22]. Plaque rupture results in intimal plaque ulceration that can penetrate into the medial layer, the classic description of a penetrating atherosclerotic ulcer (PAU). In their case series, Stanson et al. likened its angiographic appearance to that of peptic ulcers seen in the stomach on barium examination [21]. On MRA, PAU is seen as an ulceration within a thickened aortic wall on dark blood or contrast-enhanced sequences (Fig. 13.9). One limitation of MRA compared to computed tomography angiography (CTA) might be the lack of visualization of calcifications in the PAU's surrounding area.

There is again no general consensus on the management of PAU. Type A PAUs usually undergo emergent open repair. Uncomplicated type B PAUs require optimal initial medical treatment with regular imaging surveillance to detect evolution toward IMH, aortic rupture, pseudo-aneurysms, or aortic dissections. Symptoms or complications including rapid PAU progression, refractory pain or signs of contained rupture (associated periaortic hematoma, pleural effusion) should lead toward surgical management, mostly endovascular repair [20].

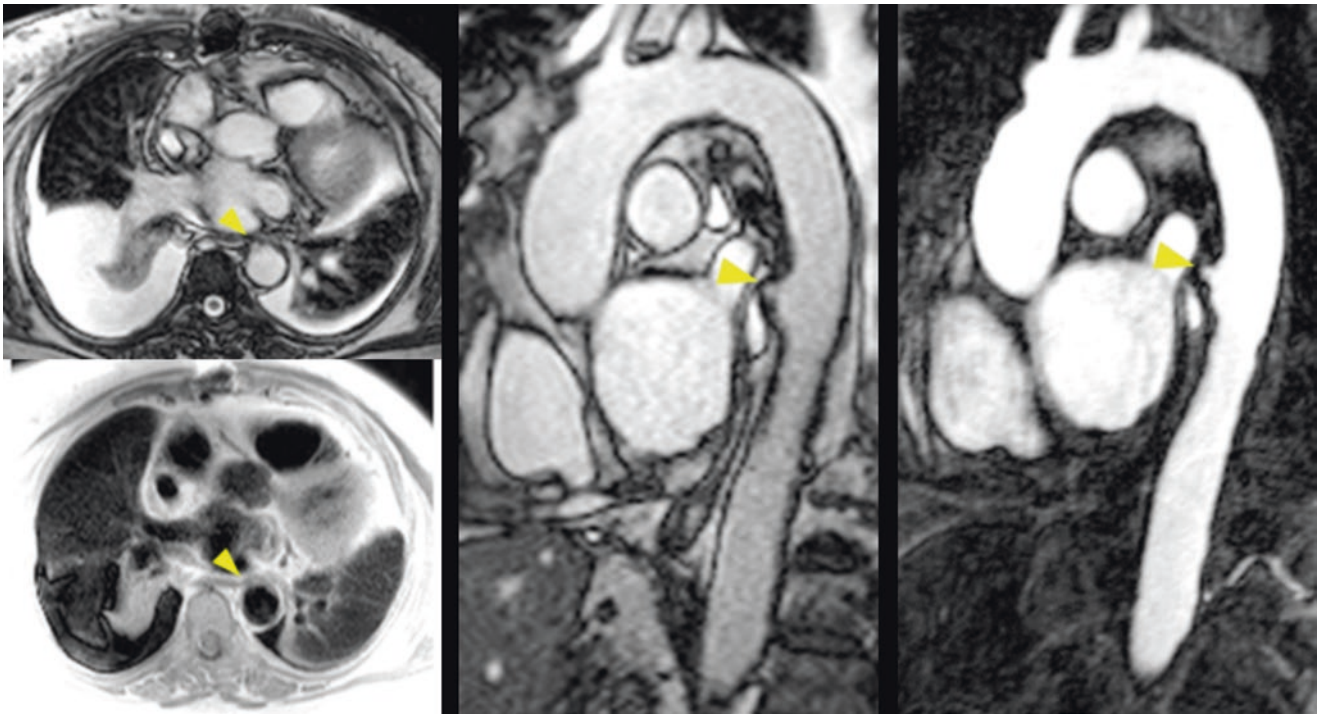


Fig. 13.9 Axial bright blood (*left top panel*) and dark blood (*left bottom panel*) scans

Surgical Planning

MRA sequences have allowed us certain perspectives that have not been previously appreciated. Our goal in the following section is not to give management guidelines for a particular acute aortic syndrome type, but rather to give some insight into MRA findings that may be especially relevant in planning an intervention.

Entry and Re-entry Tears

The location of the entry tear and possible major re-entry tears is important to appreciate since they may influence the extent of aortic coverage. Most of the time, the entry tear of a type B aortic dissection is located close to the origin of the left subclavian artery. The typical endovascular treatment consists in covering this proximal entry tear with a short stent graft, avoiding thus long aortic coverage and major risks for spinal ischemia. Nevertheless, the presence of a large re-entry tear located in a more distal segment of the descending thoracic aorta will make the surgeon consider extending distally the aortic coverage to make sure to close this major re-entry tear and thus promote optimal aortic remodeling.

One limitation of MRA compared to CTA might be its resolution for the detection of small entry or re-entry tears. With 2-mm resolution on usual clinical MRAs, we observed in our practice some cases where entry tears seen on diagnostic CTA could not be precisely seen on diagnostic MRA.

Distance from Branches

Endovascular treatment requires specific anatomical features to allow optimal deployment of the stent graft, especially adequate lengths for both proximal and distal landing zones. According to the manufacturer instructions for use, a 1–1.5 cm landing zone is required. Like CTA, MRA is an adequate imaging tool to evaluate the length between an entry/re-entry tear and the origin of aortic branches to consider (left subclavian artery, celiac trunk), thus permitting optimal device sizing.

False Lumen Flow Assessment

One particularly interesting value of MRA for surgical planning is its capability for flow assessment. MRA allows dynamic imaging studies of both the true and false aortic lumen, permitting to assess the chronology of blood filling and flushing within both lumens. Using contrast-enhanced time-resolved MRA techniques, we can identify antero-grade and retrograde filling patterns of the false lumen, relative to the aortic true lumen (Fig. 13.10). Identification of these filling patterns may better inform clinicians of the location of re-entry tears of the false lumen. However, the

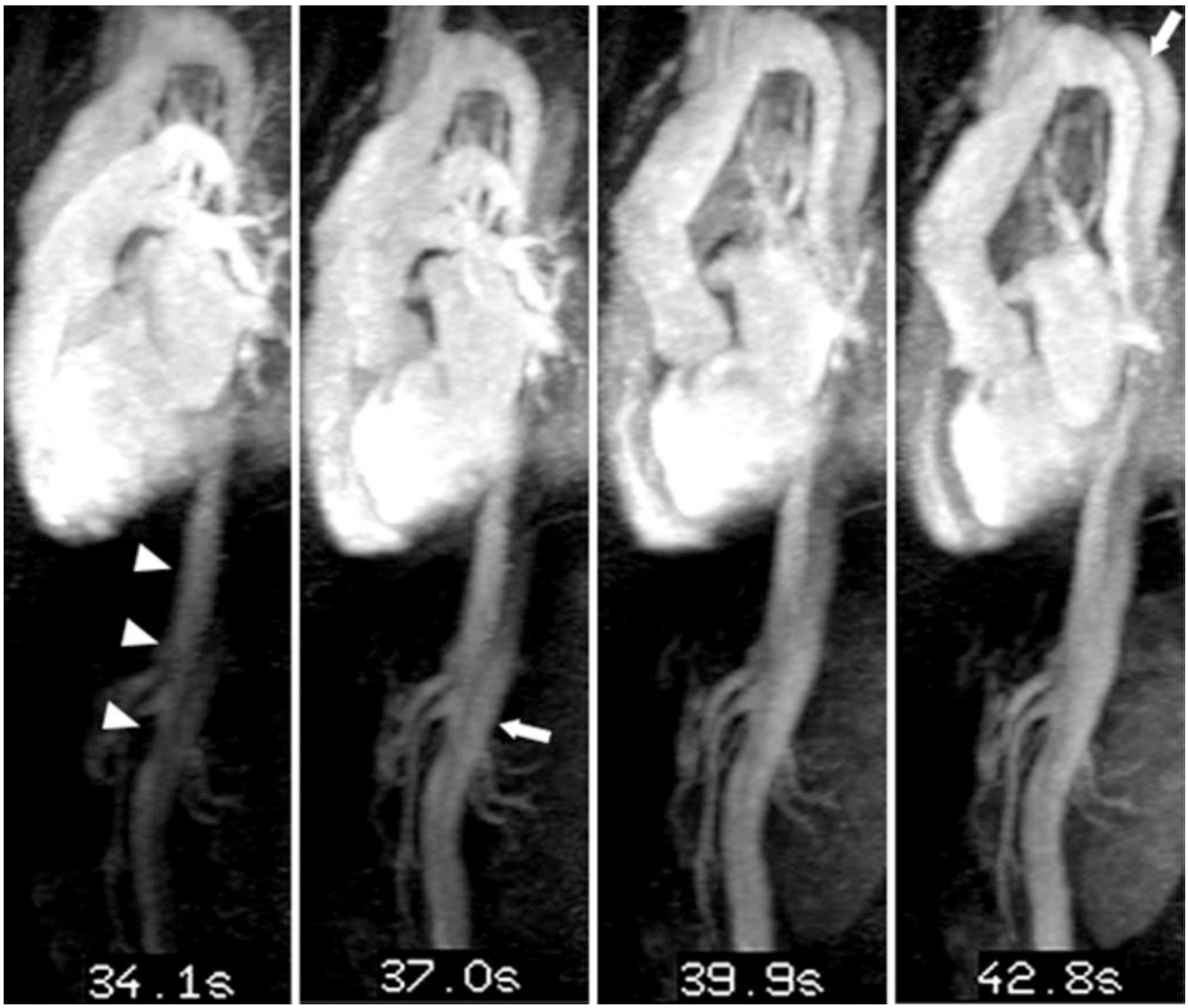


Fig. 13.10 Sagittal maximal intensity projections showing timing of contrast arrival in different portions of the aorta in a patient with type B dissection. The left most panel shows initial contrast enhancement of the true lumen (*arrowheads*). Subsequent times show retrograde enhancement of the false lumen beginning at the abdominal aorta and extending back into the proximal descending thoracic aorta (*arrows*)

exact significance of the filling patterns to flow dynamics and further aortic remodeling currently remains under investigation.

Branch Involvement, Static Versus Dynamic Obstructions

One last particular advantage of MRA for surgical indications is its capability to assess dynamic obstruction of aortic branches. It is possible to observe the flap motion at the particular level of an aortic branch, through an entire cardiac cycle (Fig. 13.11). We have used this information as an element of our decision making as far as treating or not. This information has been particularly useful in atypical presentations of dissections. For example, patients can present with acute aortic dissection involving the visceral aorta and nonspecific abdominal pain, without laboratory or static cross-sectional imaging evidence of organ malperfusion. In our practice, if such a patient should have MRA findings of dynamic obstruction of a visceral artery in systole, we would elect to treat him with an endovascular approach, before waiting for signs of organ ischemia. The concept here is to obviate tissue loss by visceral or renal compromise.

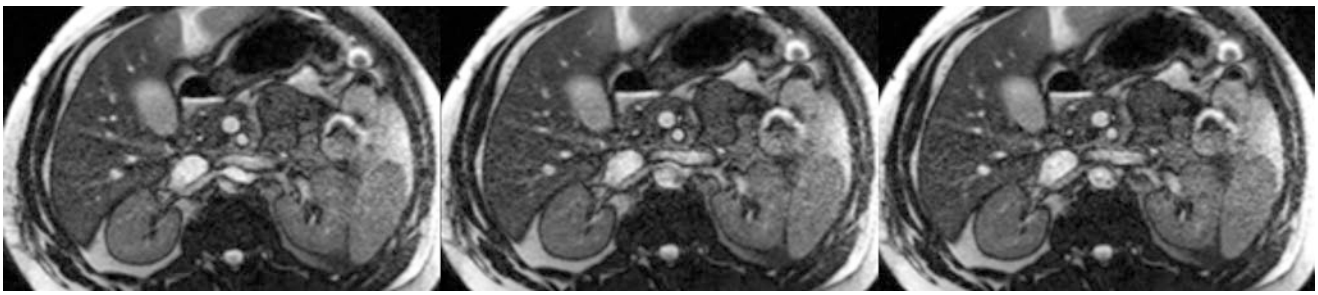


Fig. 13.11 Axial slices at the level of the renal bifurcation demonstrating a patent true lumen communicating with both renal arteries in diastole (*left*) and dynamic obstruction of both renal arteries in early (*mid panel*) and late (*right panel*) systole via false lumen expansion

Surveillance

Long-term imaging surveillance of both untreated and treated acute aortic syndromes has been a corner stone of their good management [3]. Imaging surveillance of untreated IMH and PAU should be recurrent in the early phase of the disease to detect possible evolution toward aortic rupture or aortic dissection. Following treatment of acute dissection CT or MRI is recommended for surveillance prior to discharge and post-discharge at 1 month, 6 months, and then annually [3]. Following treatment of acute IMH or PAU, the same authors recommended a similar surveillance schedule with additional follow-up at 3 months post-discharge [3]. The presence of pseudoaneurysm, suture aneurysm, or further dilatation of non-intervened aortic segments should be promptly recognized, as further treatment may be indicated.

Given the need of lifelong aortic imaging, guidelines give some preference to MR over CT, thus avoiding repeated exposure to iodinated contrast agent and the risk for associated contrast-induced nephropathy. Furthermore, in patients with non-paramagnetic metallic stents of the aorta, MRI does not suffer from beam hardening artifacts seen with CT and may be a better imaging modality for follow-up after endovascular management.

Conclusion

Magnetic resonance angiography is the most sensible imaging modality for the diagnostic of acute aortic syndrome, where appropriate. In addition to morphological information, it provides highly valuable assessment of dynamic flow and filling patterns, dissection flap mobility, and dynamic obstruction, which may impact clinical management. Finally, avoiding the use of iodinated contrast agent. MRA is particularly suitable for long-term follow-up imaging, minimizing nephrotoxicity and radiation exposure.

References

1. Tsai TT, Nienaber CA, Eagle KA. Acute aortic syndromes. Circulation. 2005;112(24):3802–13.
2. Vilacosta I, Roman JA. Acute aortic syndrome. Heart. 2001;85(4):365–8.
3. Hiratzka LF, Bakris GL, Beckman JA, Bersin RM, Carr VF, Casey DE Jr, et al. 2010 ACCF/AHA/AATS/ACR/ASA/SCA/SCAI/SIR/STS/SVM guidelines for the diagnosis and management of patients with thoracic aortic disease: a report of the American College of Cardiology Foundation/American Heart Association Task Force on Practice Guidelines, American Association for Thoracic Surgery, American College of Radiology, American Stroke Association, Society of Cardiovascular Anesthesiologists, Society for Cardiovascular Angiography and Interventions, Society of Interventional Radiology, Society of Thoracic Surgeons, and Society for Vascular Medicine. Circulation. 2010;121(13):e266–369.
4. Hagan PG, Nienaber CA, Isselbacher EM, Bruckman D, Karavite DJ, Russman PL, et al. The International Registry of Acute Aortic Dissection (IRAD): new insights into an old disease. JAMA. 2000;283(7):897–903.
5. Nienaber CA, von Kodolitsch Y, Nicolas V, Siglow V, Piepho A, Brockhoff C, et al. The diagnosis of thoracic aortic dissection by noninvasive imaging procedures. N Engl J Med. 1993;328(1):1–9.
6. Moore AG, Eagle KA, Bruckman D, Moon BS, Malouf JF, Fattori R, et al. Choice of computed tomography, transesophageal echocardiography, magnetic resonance imaging, and aortography in acute aortic dissection: International Registry of Acute Aortic Dissection (IRAD). Am J Cardiol. 2002;89(10):1235–8.
7. Baliga RR, Nienaber CA, Bossone E, Oh JK, Isselbacher EM, Sechtem U, et al. The role of imaging in aortic dissection and related syndromes. JACC Cardiovasc Imaging. 2014;7(4):406–24.
8. Ocazionez D, Dicks DL, Favinger JL, Shroff GS, Damani S, Kicska GA, et al. Magnetic resonance imaging safety in cardiothoracic imaging. J Thorac Imaging. 2014;29(5):262–9.
9. Bashir MR, Bhatti L, Marin D, Nelson RC. Emerging applications for ferumoxytol as a contrast agent in MRI. J Magn Reson Imaging. 2015;41(4):884–98.
10. Ridgway JP. Cardiovascular magnetic resonance physics for clinicians: part I. J Cardiovasc Magn Reson. 2010;12:71.
11. Biglands JD, Radjenovic A, Ridgway JP. Cardiovascular magnetic resonance physics for clinicians: part II. J Cardiovasc Magn Reson. 2012;14:66.
12. Dumfarth J, Chou AS, Ziganshin BA, Bhandari R, Peterss S, Tranquilli M, et al. Atypical aortic arch branching variants: a novel marker for thoracic aortic disease. J Thorac Cardiovasc Surg. 2015;149(6):1586–92.

13. Song SY, Chung JW, Yin YH, Jae HJ, Kim HC, Jeon UB, et al. Celiac axis and common hepatic artery variations in 5002 patients: systematic analysis with spiral CT and DSA. Radiology. 2010;255(1):278–88.
14. Ozkan U, Oguzkurt L, Tercan F, Kizilkilic O, Koc Z, Koca N. Renal artery origins and variations: angiographic evaluation of 855 consecutive patients. Diagn Interv Radiol. 2006;12(4):183–6.
15. Debakey ME, Henly WS, Cooley DA, Morris Jr GC, Crawford ES, Beall Jr AC. Surgical management of dissecting aneurysms of the aorta. J Thorac Cardiovasc Surg. 1965;49:130–49.
16. Krukenberg E. Beiträge zur frage des aneurysma dissecans. Beitr Pathol Anat Allg Pathol. 1920;67:329–51.
17. Yamada T, Tada S, Harada J. Aortic dissection without intimal rupture: diagnosis with MR imaging and CT. Radiology. 1988;168(2):347–52.
18. Kitai T, Kaji S, Yamamuro A, Tani T, Kinoshita M, Ehara N, et al. Detection of intimal defect by 64-row multidetector computed tomography in patients with acute aortic intramural hematoma. Circulation. 2011;124(11 Suppl):S174–8.
19. Uchida K, Imoto K, Karube N, Minami T, Cho T, Goda M, et al. Intramural haematoma should be referred to as thrombosed-type aortic dissection. Eur J Cardiothorac Surg. 2013;44(2):366–9; discussion 9.
20. Erbel R, Aboyans V, Boileau C, Bossone E, Bartolomeo RD, Eggebrecht H, et al. 2014 ESC guidelines on the diagnosis and treatment of aortic diseases: document covering acute and chronic aortic diseases of the thoracic and abdominal aorta of the adult. The Task Force for the Diagnosis and Treatment of Aortic Diseases of the European Society of Cardiology (ESC). Eur Heart J. 2014;35(41):2873–926.
21. Stanson AW, Kazmier FJ, Hollier LH, Edwards WD, Pairolero PC, Sheedy PF, et al. Penetrating atherosclerotic ulcers of the thoracic aorta: natural history and clinicopathologic correlations. Ann Vasc Surg. 1986;1(1):15–23.
22. Movsowitz HD, Lampert C, Jacobs LE, Kotler MN. Penetrating atherosclerotic aortic ulcers. Am Heart J. 1994;128(6):1210–7.

Part II

Building Advanced Endovascular Aortic Programs

Managing Endovascular Inventory

14

Jesse M. Manunga, Gustavo S. Oderich, Karl E. Bjellum, and Karen M. Bjellum

Introduction

Endovascular technology continues to evolve in a fast pace with newer developments to facilitate procedures of increasing complexity. For practices performing complex endovascular procedures such as fenestrated, branched, and parallel endografts, a robust endovascular inventory is needed to deal with all variations in anatomy and unanticipated problems that can occur during procedures. It is critical that this inventory is maintained up to date to avoid disappointments and problems from unavailability of an important tool in the middle of a case. A wide range of wires, catheters, balloons, stents, stent grafts, and other ancillary tools is needed to safely and successfully complete complex procedures. Since most patients undergoing these procedures also have multiple comorbidities, the operation must be simplified as much as possible and operative time needs to be minimized. This includes having a comprehensive endovascular inventory in close proximity to the endovascular or hybrid room, and having well trained staff that is familiar with specific devices. Management of the inventory requires a coordinator that is well familiar with all aspects of available devices, including its specific manufacturer, clinical need, in-service training, and cost. It is also imperative that surgeons and interventionists in the practice have thorough understanding of the inventory and anticipate which tools will be required to complete the procedure. Unfamiliarity with ones own inventory leads to delays in the care and likely add cost. In addition to having the proper tools, physicians performing these procedures need to master endovascular skills and often use their creativity on how to further simplify steps of the operation. In this chapter, we hope to give the reader a complete list of tools needed to successfully complete the complex endovascular aortic repair.

Endovascular Coordinator

The single most important aspect of the endovascular inventory is its coordinator. Because endovascular tools are rapidly evolving and differ completely from open surgical tools, these individuals are not easy to identify and should be passionate about their jobs. A thorough knowledge about the specifics of each device is critical so the individual can anticipate usage prior to procedures, provide feedback to physicians on how to minimize waist, help organize in-service training and rapidly contact manufacturer representatives on and off regular hours. The coordinator responsibility includes bringing in and out new tools, organizing shelf space in a logical fashion, color coding devices by cost, and communicating regularly with physicians. Because complex cases often come in the last minute of a busy day, the coordinator serves as the liaison between the hospital and the manufacturer, making sure that every tool is available to complete the operation. The inventory needs to be kept up to date at all times to allow use in emergency cases. In busy institutions, it is recommended to appoint one physician member as the liaison between the group and the coordinator. Weekly or biweekly meetings are often needed to optimize the inventory to ones practice. It is important to constantly question the utility and usage of balloons, catheters and stents, and to replace and optimize the

J.M. Manunga
University of Minnesota, Minneapolis, MN, USA

Department of Vascular and Endovascular Surgery,
Abbott Northwestern Hospital/Minneapolis Heart Institute,
920 E 28th Street, Suite 300, Minneapolis, MN 55407, USA
e-mail: Jesse.manunga@allina.com; Jmanunga@gmail.com

G.S. Oderich (✉) • K.M. Bjellum
Division of Vascular and Endovascular Surgery, Mayo Clinic,
200 First Street SW, Rochester, MN 55905, USA
e-mail: oderich.gustavo@mayo.edu; Mensink.karen@mayo.edu

K.E. Bjellum
Division of Vascular and Endovascular Surgery and Division of
Thoracic Surgery, Mayo Clinic, 200 First Street SW, Rochester,
MN 55905, USA
e-mail: Bjellum.karl@mayo.edu

© Mayo Foundation for Medical Education and Research 2017

G.S. Oderich (ed.), *Endovascular Aortic Repair*, DOI 10.1007/978-3-319-15192-2_14

inventory to avoid waist. This often includes eliminating specific tools that are not being utilized and bringing new developments to the attention of physicians.

Space Management

Since space is a high commodity in the operating room and organization of tools is a critical aspect of a successful inventory, space management becomes a major issue. The space needs to be clean, organized, and preferentially locked to avoid usage of tools that are unaccounted by the ancillary staff (Fig. 14.1). The space has to be in close proximity, preferentially within or adjacent to the endovascular or hybrid room where the procedures are being performed. In an emergency situation (vessel disruption or perforation), access to a stent-graft, balloon, or coil has needs to be immediate with no delays. Familiarity of the staff with the organization of the endovascular inventory space is therefore very important. Endovascular tools can be organized in locked rooms with shelves, cabinets, or mobile carts. It is useful to have all these three aspects and keep the tools that are anticipated within the procedure room in a mobile cart, but return the tools to the locked space immediately after the case is completed.

Labeling

Many of the ancillary staff are not completely familiar with every tool, so proper identification by labeling is critical (Fig. 14.2). This can also serve to grade tools by cost: green for less expensive, yellow for intermediate and red for very expensive. Cabinets with glass windows and clear labels help organization. Use of infrared or barcoding can be extremely helpful in keeping the inventory up to date.

Specific Ancillary Tools

The "Buyers Guide" issue published yearly by *Endovascular Today* is a very useful source if one needs a broader review of what tools are available in the market and how to reach the manufacturer. As previously stated, building and maintaining a successful endovascular complex aortic aneurysm program requires not only advanced skills in endovascular aneurysm repair but also a complete endovascular inventory. A wide range of wires, catheters, sheaths, balloons, stents, and stent grafts is needed to complete these procedures and deal with all variations in anatomy and techniques.



Fig. 14.1 Shelf space organization at the Saint Mary's Hospital Endovascular Core, Mayo Clinic, Rochester, MN. By permission of Mayo Foundation for Medical Education and Research. All rights reserved

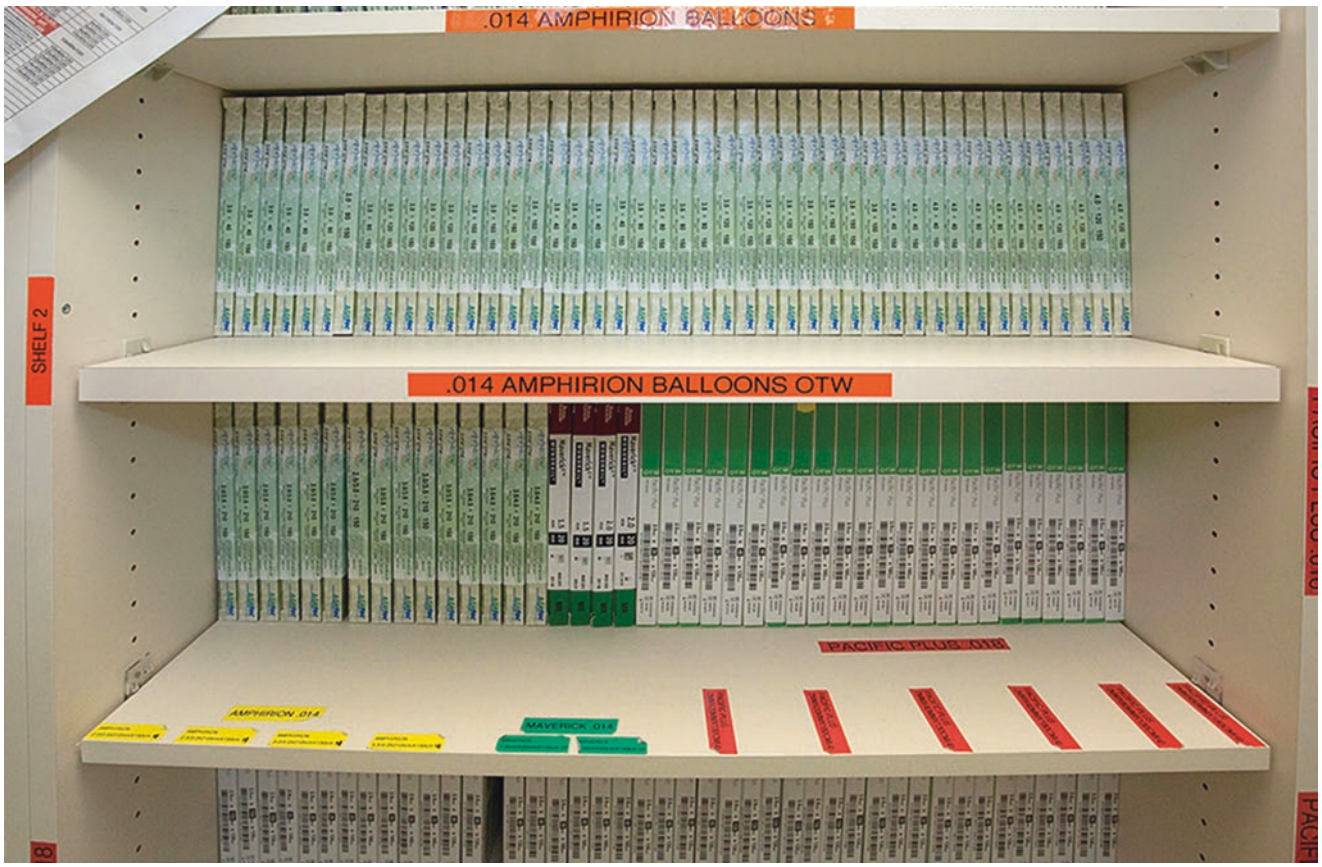


Fig. 14.2 Labeling of balloons and color coding at the Saint Mary's Hospital Endovascular Core, Mayo Clinic, Rochester, MN. By permission of Mayo Foundation for Medical Education and Research. All rights reserved

Table 14.1 Sheaths/guiding sheaths

Sheath	Manufacturer	Application
6 Fr, 23 cm	Multiple	Initial access
7–10 Fr, 23 cm	Multiple	Upsize after perclose/proglide placement
7 Fr, 55 or 70 cm Ansel	Cook Medical, Inc.	Visceral artery stenting
7 Fr, 55 cm Destino Twist Steerable	Oscor, Inc.	Visceral artery stenting
12 Fr, 45 cm Ansel	Cook Medical, Inc.	Visceral artery stenting
16–24 Fr, 25, 40 and 65 cm Check Flo	Cook Medical, Inc.	Femoral artery access
Dryseal 12–26 Fr, 28 cm	L.W. Gore	Femoral artery access
AlSeal 14–26 Fr, 14 and 30 cm	AlSeal	Femoral artery access
SOLOPATH Balloon Expendable, 14–21 Fr, 25 and 35 cm	Terumo	Femoral artery access

Sheaths

Just like any other endovascular procedure, complex endovascular aortic aneurysm repair begins with gaining arterial access (Table 14.1). The choice of percutaneous versus open repair depends on multiple factors. Presence of calcifications in the femoral artery is the most important determinant of feasibility of a total percutaneous approach [1]. For the brachial artery, surgical exposure is recommended to avoid hematoma and compression of the median nerve. Percutaneous access of any vessel is always done with ultrasound guidance using a micropuncture set (Cook, Inc., Bloomington, Indiana, USA; Fig. 14.3). The 0.018-in. micro-puncture wire is exchanged to a 0.035-in. system and a short 6Fr Pinnacle sheath (Terumo, Somerset, NJ, USA; Fig. 14.3) is introduced over a Benson wire (Cook, Inc., Bloomington, IN, USA). Glide-wires and a supporting catheter are used to cross the aneurysm and aorta up to the arch, allowing exchange to a stiff guide-wire system (e.g., Lunderquist, Cook Medical, Bloomington, IN, USA), which is needed for introduction of large diameter sheaths.

Large sheaths are needed to allow introduction of smaller sheaths for multi-branch catheterization. This can be done using either 20-24Fr Check-Flo sheaths (Cook Medical, Cook Medical, Bloomington, IN, USA; Fig. 14.4a), which

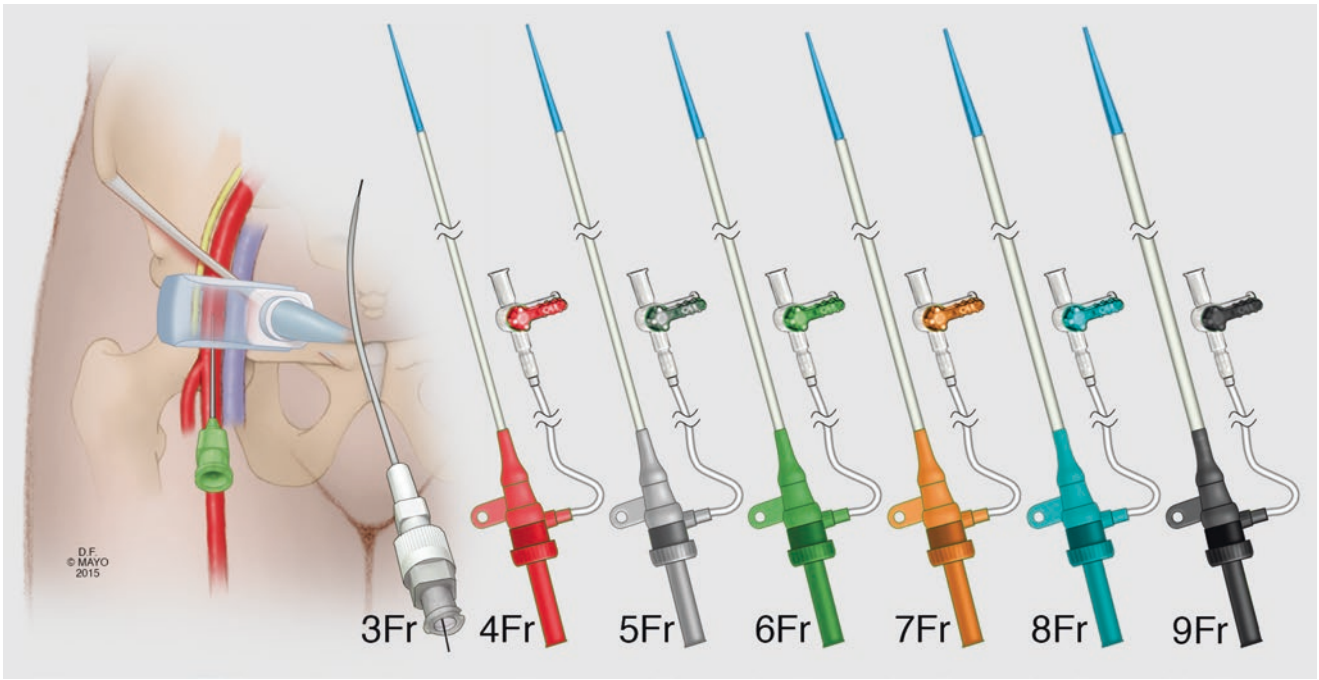


Fig. 14.3 Micropuncture set and color coding of sheaths by French size. By permission of Mayo Foundation for Medical Education and Research. All rights reserved

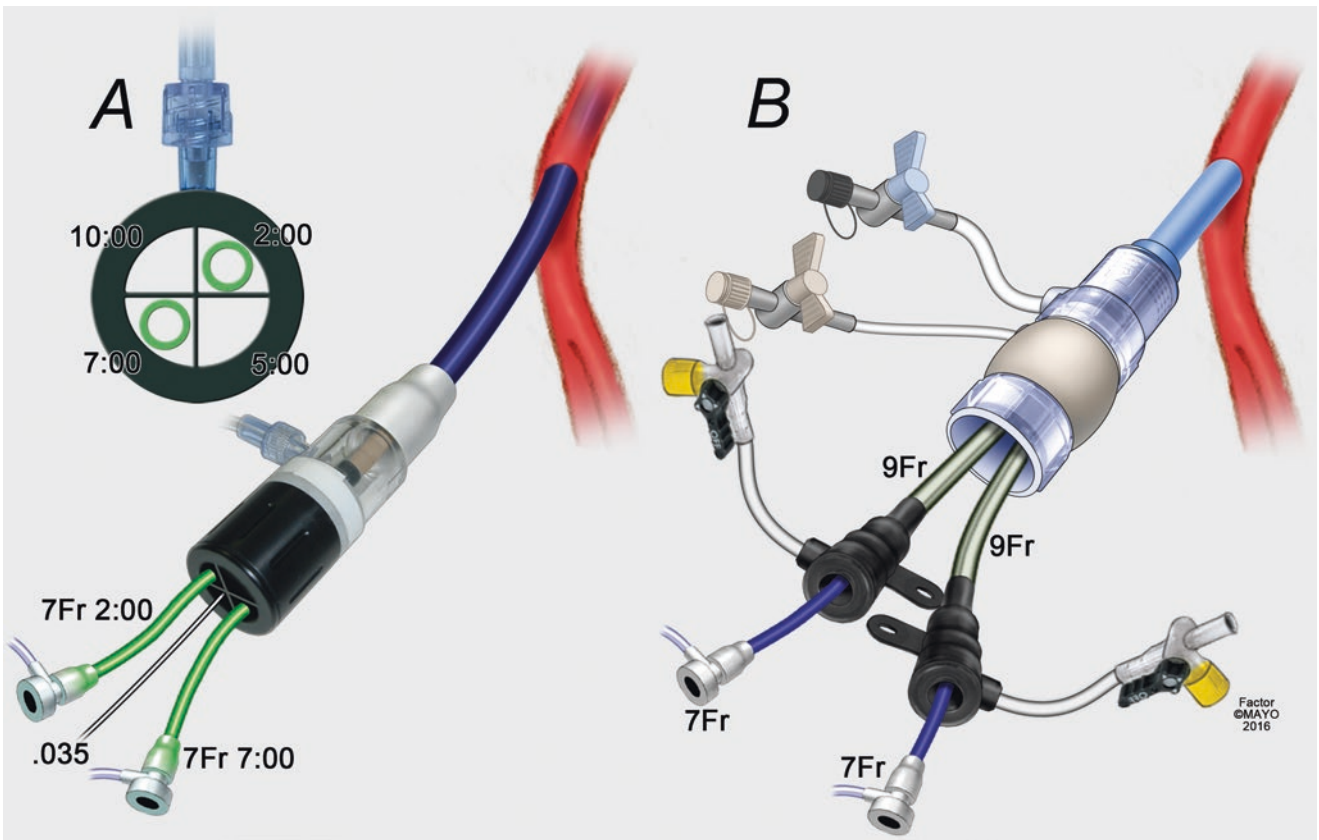


Fig. 14.4 Large vessel access for fenestrated endografts using Cook Check Flo sheaths (**a**, sizes range from 16- to 24-French) or Gore DrySeal sheaths (**b**). By permission of Mayo Foundation for Medical Education and Research. All rights reserved

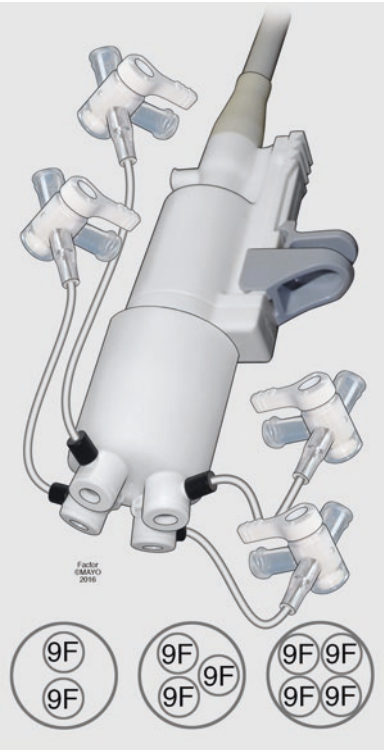


Fig. 14.5 AlSeal sheath with size ranging from 14- to 26-French and comes in two lengths: 14 cm and 30 cm. The sheath has one dynamic hemostatic valve that allows for complete hemostasis whether a wire or another sheath is introduced through it. Additionally, its multiple access converter is able to convert one insertion into the main sheath into multiple access (up to 4) ports making it extremely attractive for fenestrated stent graft procedures. By permission of Mayo Foundation for Medical Education and Research. All rights reserved

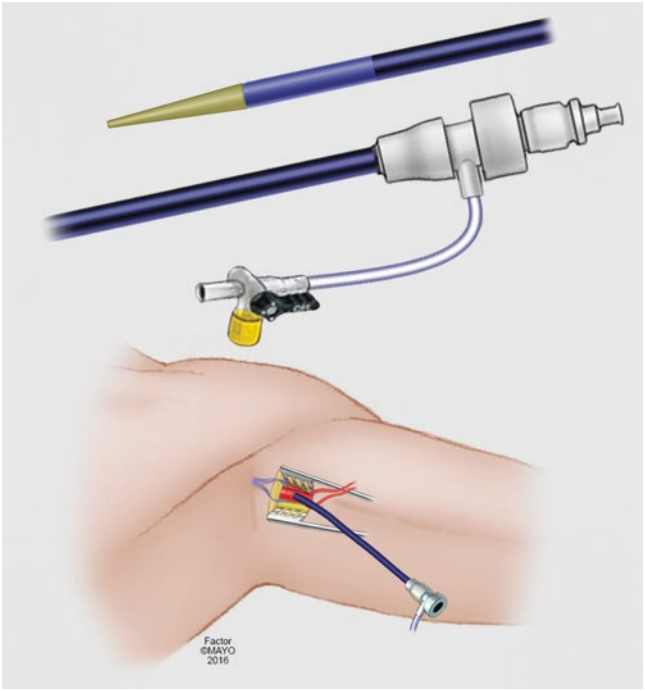


Fig. 14.6 Ansel Sheaths (Cook, Inc. IN, USA) with hyperflex dilators are useful for visceral artery stenting during fenestrated stent graft implantation. In tortuous arch, the 12-Fr, 55 cm, Ansel sheath can be inserted into the brachial artery and serve as a conduit to for stenting of visceral arteries from above. By permission of Mayo Foundation for Medical Education and Research. All rights reserved

have four silicon valve leaflets that can be punctured on each quadrant for introduction of smaller sheaths. It is important to note that the valve of the purple 16 or 18Fr sheaths is not adequate to maintain hemostasis. In general, the 20-Fr check-Flo sheath is optimal for 2-vessel and a 22-Fr sheath for 3-vessel catheterization. A major disadvantage of this setup is the constant dripping of blood that, over the course of a long case, can become significant. As such, the use of a cell saver is recommended especially in long cases. Other alternative is to use a DrySeal sheath (Gore, Flagstaff, AZ, USA; Fig. 14.4b), but the attrition of one sheath over the other can be bothersome during exchanges. This can be avoided by using a 9Fr pinnacle sheath first, and then introducing the 7Fr Ansel sheath into the pinnacle, instead of directly into the DrySeal valve. The DrySeal sheath comes in sizes ranging from 12- to 26-Fr and is 26 cm long. It contains a dilator and a hemostatic valve that can be inflated with a 2.5 ml valve inflation syringe. Most recently, the AlSeal (Alseal, Inc., Besancon, France) sheath was designed by Claudio Mialle especially for fenestrated cases (Fig. 14.5). This has been approved by the Food and Drug administration (FDA) in February 2014 and combines the function of the Check-Flo and DrySeal sheaths.

Branch vessel stenting requires hydrophilic braided sheaths that are kink-resistant. This is best done using 7-Fr Ansel 55-cm long sheaths (Cook, Inc., Bloomington, IN, USA) with flexible dilator (Fig. 14.6) if femoral approach, or 7–9Fr Raabe of Flexor sheaths (Cook Medical, Bloomington, IN, USA) if brachial approach. The Ansel sheath is well suited for stenting visceral arteries via femoral access. A 12 French 45-cm Ansel sheath is available with soft dilator for brachial access during thoracoabdominal repair or femoral access during iliac branch repair. For difficult visceral artery catheterization and stenting, we find the 7-Fr Destino™ Twist steerable sheath to be most useful (Oscor Inc., Palm Harbor, FL, USA; Fig. 14.7). The sheath handle can be twisted and the tip guided toward the previously marked visceral artery.

Selective stenting via the brachial approach requires 70-cm or 90-cm sheaths that are hydrophilic and braided. Our preference has been to use a 7 or 8-French 90 cm Raabe sheath (Cook Medical, Inc., IN, USA) depending on the diameter of the bridging stent. A 9-Fr 70-cm Flexor sheath may be needed for vessels stented with self-expandable



Fig. 14.7 Destino™ Twist steerable (Oscor Inc.) can be useful for difficult to cannulate visceral arteries after placement of the stent graft. By permission of Mayo Foundation for Medical Education and Research. All rights reserved

stent-grafts. It is also recommended to have available 4 and 5-Fr 110-cm tibial Shuttle sheaths and 5-Fr 90 cm Shuttle sheaths (Cook Medical, Bloomington, IN, USA) for difficult catheterizations requiring flexible systems.

Catheters and Guide-Catheters

Tables 14.2 and 14.3 summarize the most commonly used catheters and guiding catheters in our practice. Catheter selection is dependent on physician preference, approach (arm or femoral), vessel angulation and shape (Fig. 14.8). In general, our preference has been to use simple catheters such as 4 or 5Fr Kumpe, Vertebral or Berenstein catheters for most of the work. Four French systems track better on difficult curves but are more prone to kinks and provide less support. Guide catheters are very useful to provide support and allow advancement of catheters into the target vessel (Fig. 14.9). The 7Fr LIMA and MPA guides (Cook Medical, Bloomington, IN, USA) are most useful when working from the femoral and brachial approach, respectively. For navigating the aortic arch from the arm, a Cobra 1 catheter is ideal in most cases, but rarely a SOS or VS1 catheter is needed with more angulated anatomy. Vessel catheterization from above is usually done using MPA, Kumpe, Vertebral or Van Schie 3 catheter (Fig. 14.10). The Van Schie 3 is optimal because it provides a 90° angle with short reach, allowing one to work on tight spaces, which is often the case when a fenestration is misaligned or a branch is compressed against the anterior aortic wall.

Table 14.2 Catheters used for endovascular complex aneurysm repairs

Catheter	Manufacturer	Application
5 F Kumpe catheter (65 cm)	Multiple	Selective vessel catherization
5 F Kumpe catheter (100 cm)	Multiple	Selective vessel catherization
5 F SOS catheter (65 cm)	Multiple	Selective vessel catherization
5 F VS1 catheter (80 cm)	Multiple	Selective vessel catherization
5 F C1 catheter (100 cm)	Multiple	Selective vessel catherization
4 F Vertebral catheter (125 cm)	Multiple	Selective vessel catherization
5 F Van Schie 3 catheter (65 cm)	Cook, Inc	Selective vessel catherization
5 F Van Schie 4 catheter (65 cm)	Cook, Inc	Selective vessel catherization
5 F Simmons I catheter (100)	Multiple	Selective vessel catherization
5 F MPA catheter (125 cm)	Multiple	Selective vessel catherization
5 F MPB catheter (100 cm)	Multiple	Selective vessel catherization (SVC)
5 F Diagnostic flush catheter (100 cm)	Multiple	Diagnostic angiography (DA)
5 F Diagnostic pigtail catheter (100 cm)	Multiple	DA and SVC
Quick-Cross catheter 0.014–0.035 inc (90 and 150 cm)	Spectranetics Corporation	Selective vessel catheterization
Renagade catheter (150 cm)	Boston Scientific Corporation	Selective vessel catheterization

Table 14.3 Guide catheters used for endovascular complex aneurysms repair

7 F LIMA guide (55 cm)	Cordis Corporation	Precatherization
7 F Internal mammary guide (100 cm)	Multiple	Selective vessel catherization
7 F MPA guide (100 cm)	Multiple	Selective vessel catherization

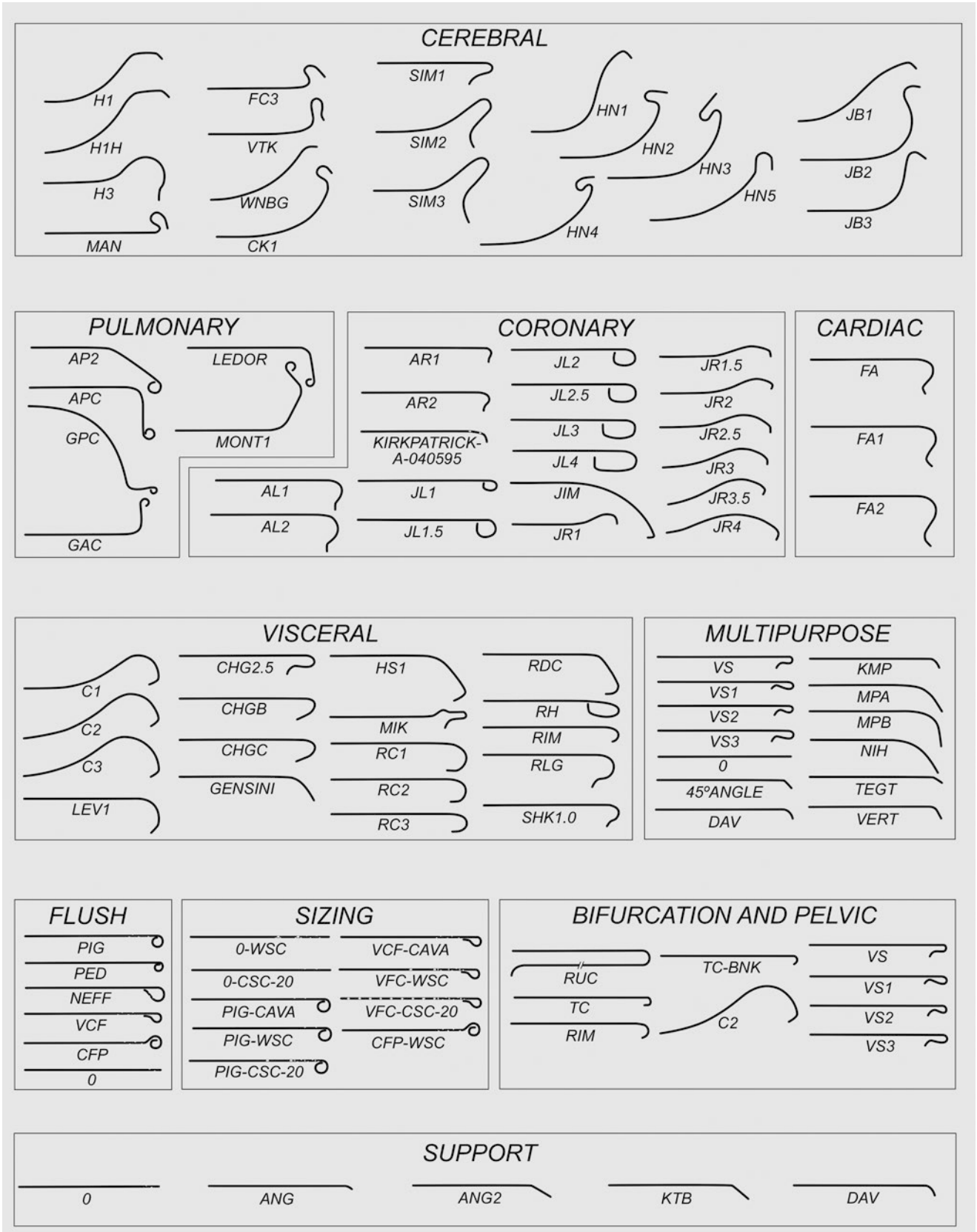


Fig. 14.8 Wide range of catheter shapes. Courtesy of Cook Medical Inc., Bloomington, IN

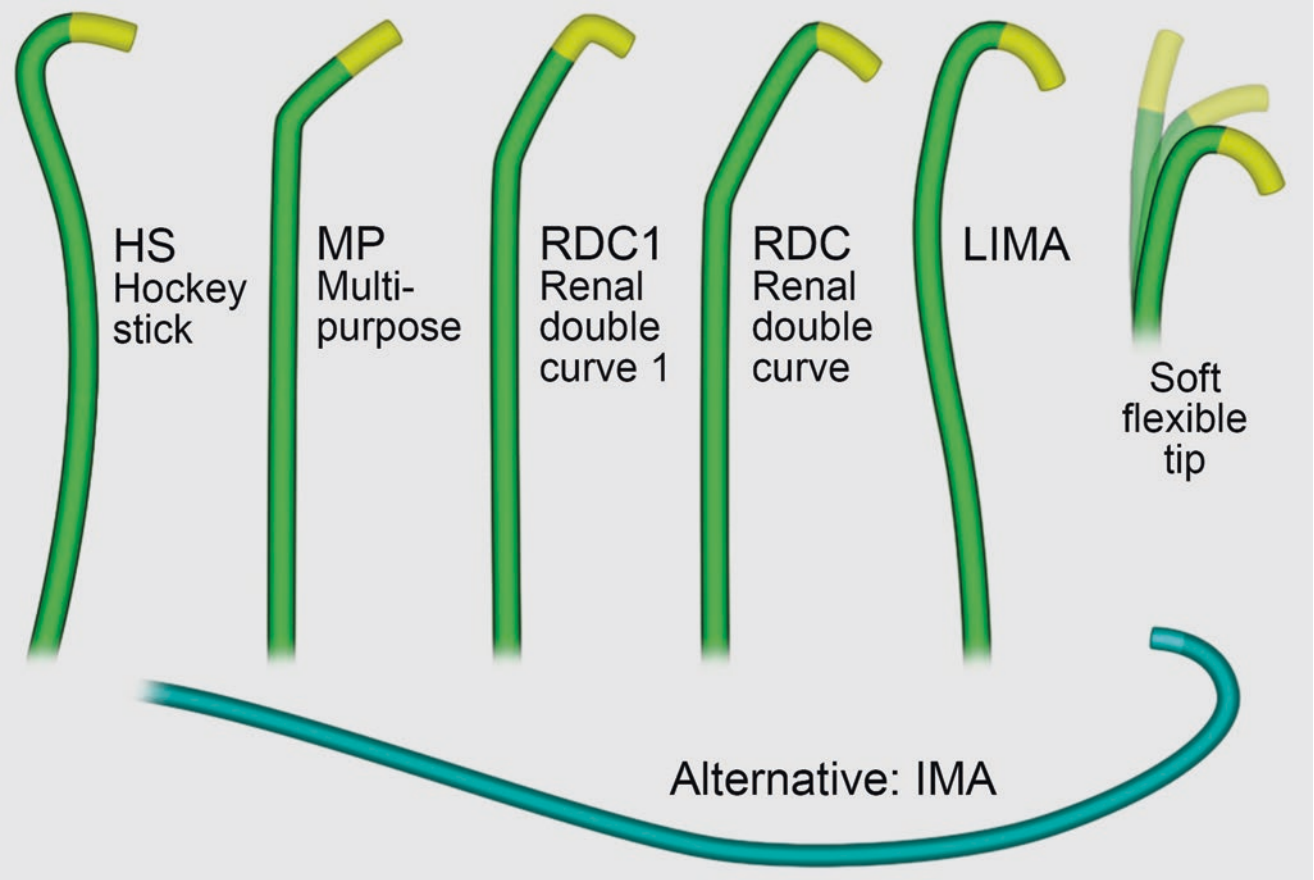


Fig. 14.9 Wide range of guide catheter shapes. By permission of Mayo Foundation for Medical Education and Research. All rights reserved

Guide-Wires

The guide-wire system is the trail that carries tools to the target vessel. Physicians need to master the skills of building stiff and soft systems that are needed with variable anatomy. In general, for carrying large diameter sheaths and stents a stiff system is needed. However, a floppy or soft system is equally important when there is no catheter support to get to the distal target, or when navigating tortuous anatomy in small vessels, such as during embolization of a type II endoleak. Three guide-wire platforms are commonly used: 0.035, 0.018, and 0.014-in. In general, 0.035-in. system is used and 0.014–18-in. is reserved for special situations such as difficult access or limited space in a sheath. Most cases can be completed with choice of five or six guide-wires. The Benson wire is used for initial access but should not be used to navigate the aorta. A floppy glide-wire is the workhorse for getting into places; a stiff glide-wire should also be available but is avoided due to risk of perforating smaller branches or causing vessel dissections. The main aortic components are advanced over a curly doubled curve Lunderquist guide-wire, which should be positioned in the ascending aorta, while the contra-lateral sheath and iliac extensions are advanced over a straight Lunderquist guide-wire positioned in the descending thoracic aorta. For branch stenting from the brachial approach, the short 1-cm tip Amplatz guide-wire is selected for the celiac axis and SMA, while Rosen guide-wires are preferred for the renal arteries from femoral or brachial approach. Table 14.4 summarizes the most commonly used guide-wires in our practice, their manufacturer and their respective application [2].

Balloons

A wide range of 0.035 and 0.014–18 balloons are needed to complete these procedures. Historically, the first fenestrated cases were aligned by placement of balloons through the fenestrations and into the target vessels prior to removal of diameter reducing ties. While some experts continue to do

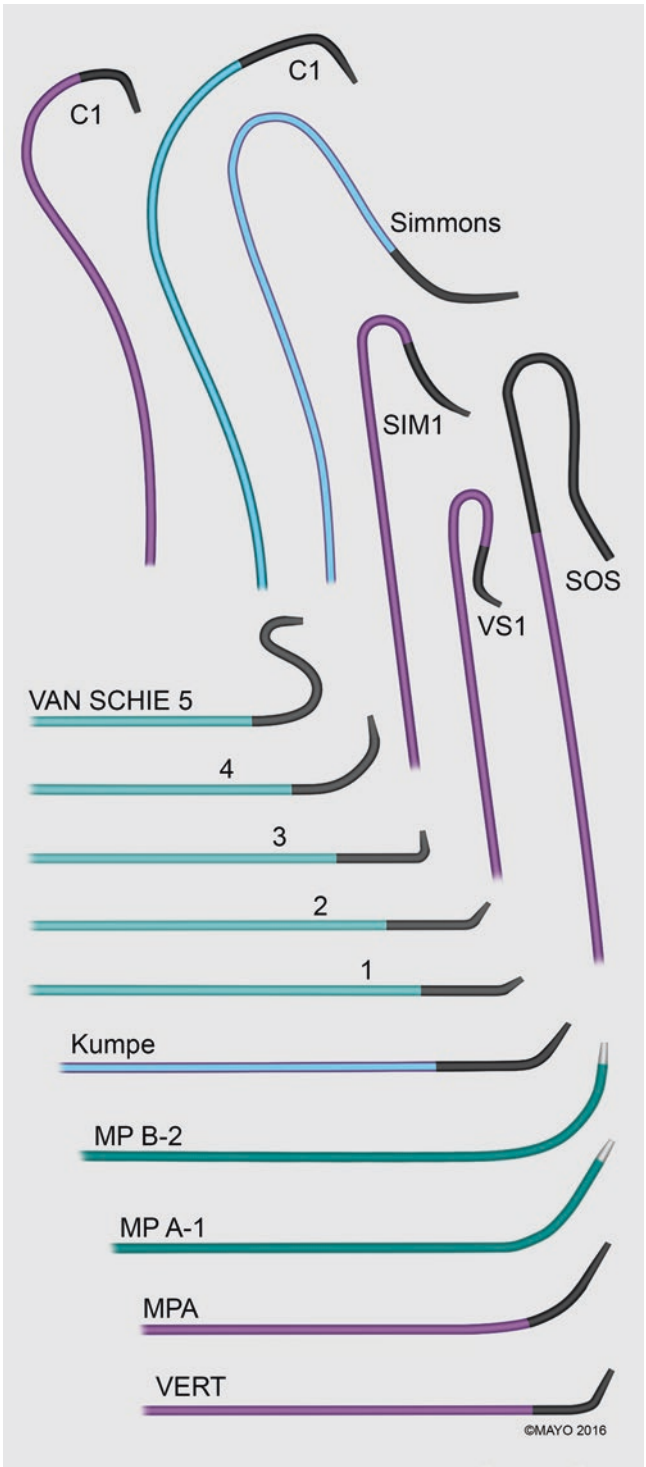


Fig. 14.10 Most frequently utilized catheter shapes for fenestrated and branched endografts. By permission of Mayo Foundation for Medical Education and Research. All rights reserved

this, the author does not use this routinely and gain access with hydrophilic sheaths only. Balloons are needed typically for angioplasty of stenosed vessels (access or targets), for flaring of bridging stents against fenestrations or branches and for advancement of sheaths (Fig. 14.11). All fenestrations should be aligned to the target using balloon expandable stents, with superior patency for covered compared to bare metal stents. Flaring of the stent is routinely done using a 10 mm × 2-cm balloon (Fig. 14.11a). Our preference is to use the Mustang balloon (Boston Scientific, Bloomington, MN, USA), but any balloon can be utilized. Smaller diameter balloons may be needed for pre-dilation and various indications (Fig. 14.11b). For stenting small vessels (4 or 5 mm) flaring with the 10-mm balloon can be problematic and should be done carefully to avoid vessel disruption by balloon shoulders that protrude beyond the stent edges. A balloon that can be useful in select cases is the Flash Ostial System Dual Balloon Angioplasty catheter (AccessClosure Inc., Santa Clara, CA, USA; Fig. 14.11c). Limitations to routine use of this balloon are the high cost and 0.014-in. guide-wire system, which is not optimal for fenestrated cases. However, this is a good balloon for re-interventions or when flare of a small vessel is needed. Finally, although 0.035-in. balloons are the most commonly used ones, it is important to have rapid exchange 0.014–18 balloons when dealing with difficult or small vessels, or when using the balloon to advance sheaths over stenosed vessels or fabric edges of the main aortic stent-graft. Balloons are often critical to advance sheaths in difficult anatomy (Fig. 14.11d) and for optimal flaring (Fig. 14.11e). Table 14.5 outlines the list of commonly balloons used in our practice [2].

Stents

Stents are needed to bridge the aortic components to the target vessels and also to deal with difficult access, kinks and vessel complications. For fenestrations, the Atrium-Maquet Icast® (Hudson, NH, USA) covered stent is most frequently utilized. For directional branches, stenting is done preferentially with a self-expandable stent-graft. The Fluency® (Bard, Tempe, AZ, USA) has the advantages of wider length availability (40, 50, 60, 80 mm, flared options and smaller profile on the larger diameter options (9Fr)), but is more prone to kinks and needs reinforcement at the distal end by placement of additional self-expandable bare metal stents. The Viabahn® stent (Gore, Flagstaff, AZ, USA) is very flexible and comes with radiopaque markers and 50 or 100 mm length, although the 75 mm length is available to us for investigational use and will soon come to market. The newer stent has radiopaque markers to facilitate visualization. Stenting of directional branches can also be achieved with balloon expandable stents. Options are the atrium iCAST® and the upcoming Gore balloon-expandable Viabahn® or VBX® (Fig. 14.12). A self-expandable stent may be needed after placement of the covered stent to prevent kinks at the

Table 14.4 Guide-wire used for endovascular complex aneurysms repair

Wire	Manufacturer	Application
0.035 in. Benson wire (150 cm)	Multiple	Initial access
0.035 in. Soft Glidewire (260 cm)	Terumo Interventional System	Target vessel catherization
0.035 in. Rosen wire (260 cm)	Multiple	Branch artery stenting
0.035 in., 1-cm tip Amplatz (260 cm)	Multiple	Branch artery stenting
0.035 in., Lunderquist (260 cm)	Multiple	Aortic Stent graft delivery
0.018 in. Glidewire Gold (180 cm)	Terumo Interventional Systems	Target vessel catherization

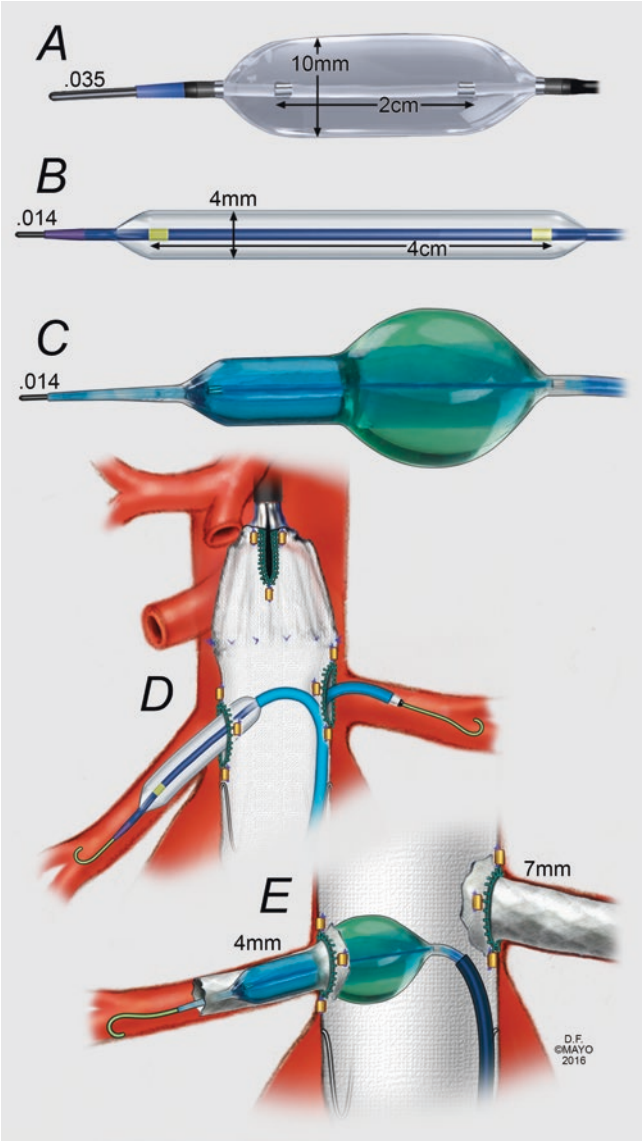


Fig. 14.11 Most frequently utilized balloons for fenestrated endografts. By permission of Mayo Foundation for Medical Education and Research. All rights reserved

distal edge, to add more radial force or to deal with vessel complications such as a flow limiting dissection distal to the stent edge. A wide range of 5–14 mm diameter by 20, 40, 60, or 80 mm lengths are needed. Since the introduction of Zilver PTX (Cook Medical, Inc., IN, USA) in the market, some providers have transition to using this stent in the hopes of increasing patency rate although this has not been used routinely to align target vessels due to high cost and need for Clopidogrel immediately after its placement. Table 14.6 outlines the list of most commonly used bare metal and covered stents [2].

Aortic Stent-Graft Components

A wide range of commercially approved thoracic (Fig. 14.13) and abdominal (Fig. 14.14) components are needed (Tables 14.7 and 14.8). The specific investigational components needed for complex procedures are discussed in other sections of this book. It is important for centers to have access to more than one device option to adapt to different anatomical requirements. The number of device manufacturers continues to increase and it is impossible to have every single device available. In general, basic principles are to keep all components in the same line of stents given that testing and clinical experience is not available for mixing components of different manufacturers. Ideally, options of supra and infra-renal fixation devices are needed to address all types of anatomical variations. Most advanced endografts are still in the investigational phase and are briefly discussed below.

Arch Aneurysms

Arch endografts need to address the hostile anatomic and hemodynamic environment that is imposed by proximity to the

Table 14.5 Balloons used for complex endovascular aneurysm repair

Balloon	Manufacturer	Application
Coda (32 and 40 cm^3)	Cook Medical, Inc.	Ballooning of leaning zones
10-mm × 2-cm angioplasty balloon	Multiple	Proximal stent flaring
12-mm × 2-cm angioplasty balloon	Multiple	Proximal stent flaring
5-mm × 2-cm angioplasty balloon	Multiple	Advance sheath over balloon

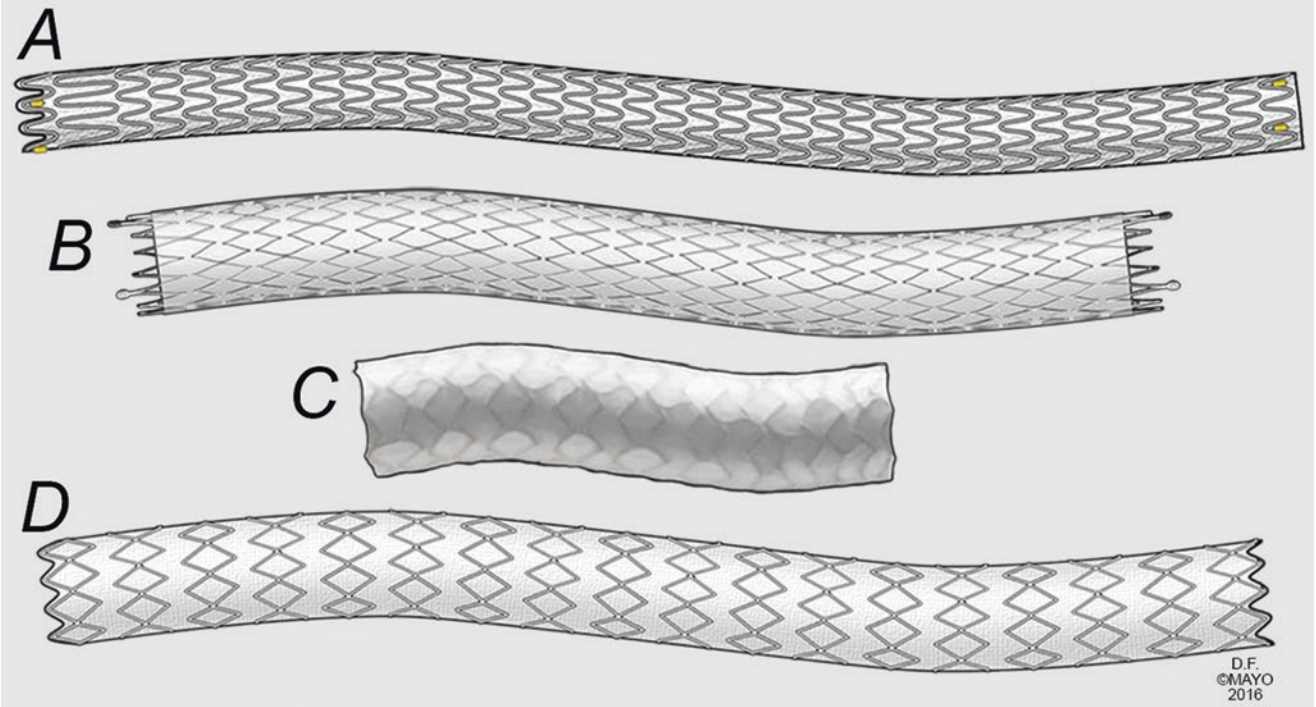


Fig. 14.12 Vessel stenting is done using covered stents. Self-expandable stents include the Gore Viabahn (**a**), Bard Fluency (**b**). Balloon expandable stents include the iCAST (**c**) and Viabahn VBX (**d**). By permission of Mayo Foundation for Medical Education and Research. All rights reserved

Table 14.6 Bare metal and covered stents

Stent	Manufacturer	Application
iCast stent graft 5–10 mm	Maquet getinger group	Branch artery stenting
Viabahn	LW Gore & associate, Inc.	Branch artery stenting
Fluency 6–13.5	Bard Medical	Branch artery stenting
0.035 in. balloon-expendable stents	Multiple	Branch artery stenting/reinforcement
0.035 in. self-expendable stents	Multiple	Distal branch artery stenting
0.014 in. self-expendable stents	Multiple	Distal branch artery stenting

coronary artery, aortic valve and sino-tubular junction, presence of supra-aortic trunks, sharp inner arch curvature, hemodynamic forces and wall pulsatility and respiratory motion. A current update on available devices that are currently under clinical investigation is outlined below (Fig. 14.15):

Bolton Medical

The Bolton Arch device is designed to treat complete aortic arch with the options of a single or double antegrade inner branches that are intended to be catheterized retrograde via the supra-aortic trunks.

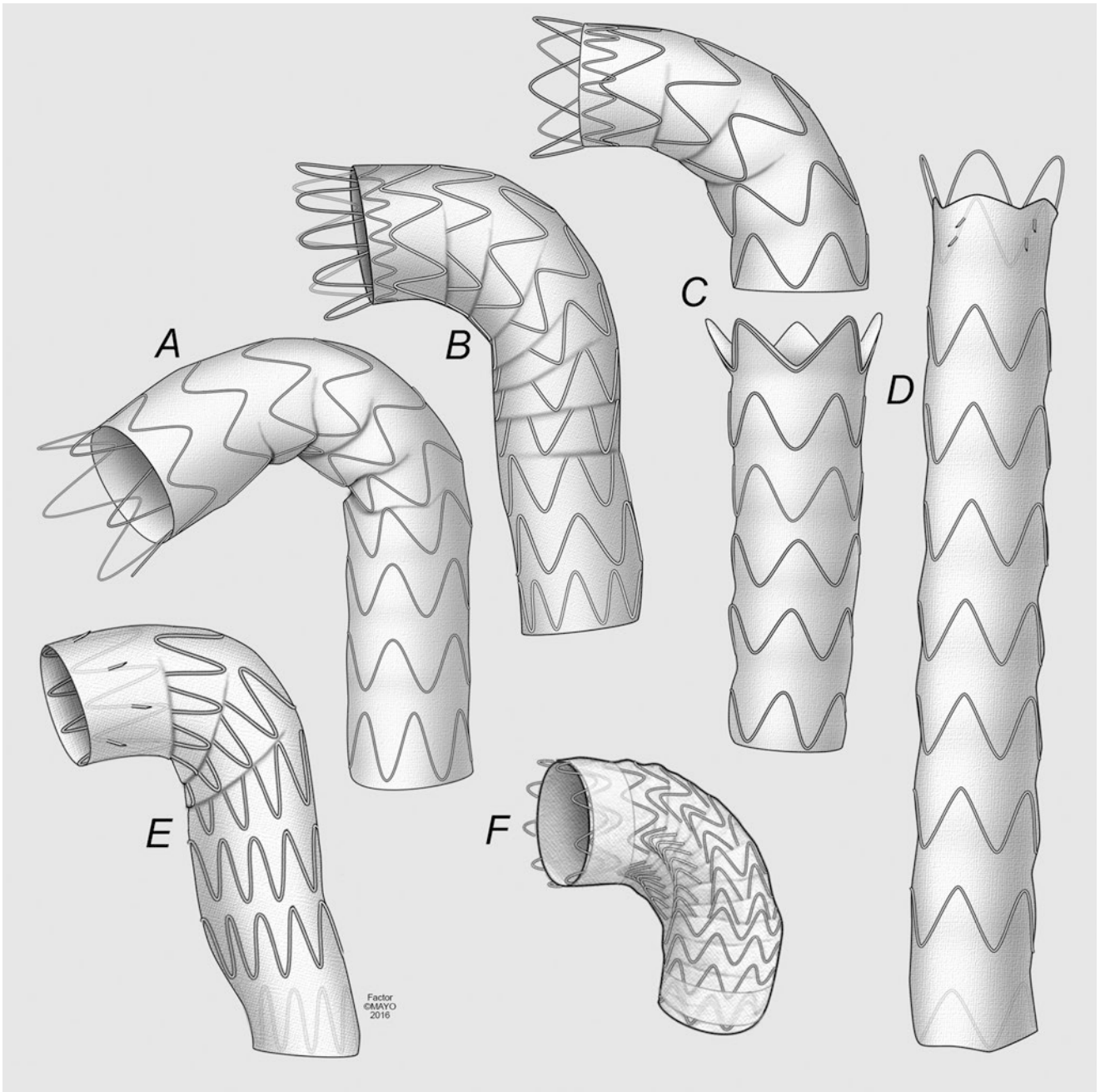


Fig. 14.13 Approved thoracic stent-grafts include the Bolton Relay (**a**), Medtronic Talent Thoracic (**b**) and Medtronic Valiant Thoracic (**c**), Cook Low Profile TX2 (**d**), Cook Standard Profile TX2 (**e**) and Gore C-TAG (**f**). By permission of Mayo Foundation for Medical Education and Research. All rights reserved

Cook a-Branch and Fenestrated Platform

Cook Medical has pioneered fenestrated and branched endografts from the arch to the iliac arteries. A fenestrated platform has been used with patient-specific arch devices in select centers. A final iteration of a double inner arch branch is also available under investigation.

Gore Thoracic Branch Endoprosthesis (TBE)

The Gore device has completed a feasibility study for Zone 2 placement and is starting Pivotal study in the United States. The device is intended for placement in either Zone 0 or Zone 1–2 with a single retrograde portal and a pre-catherized guide-wire system. The sealing stent for the Zone

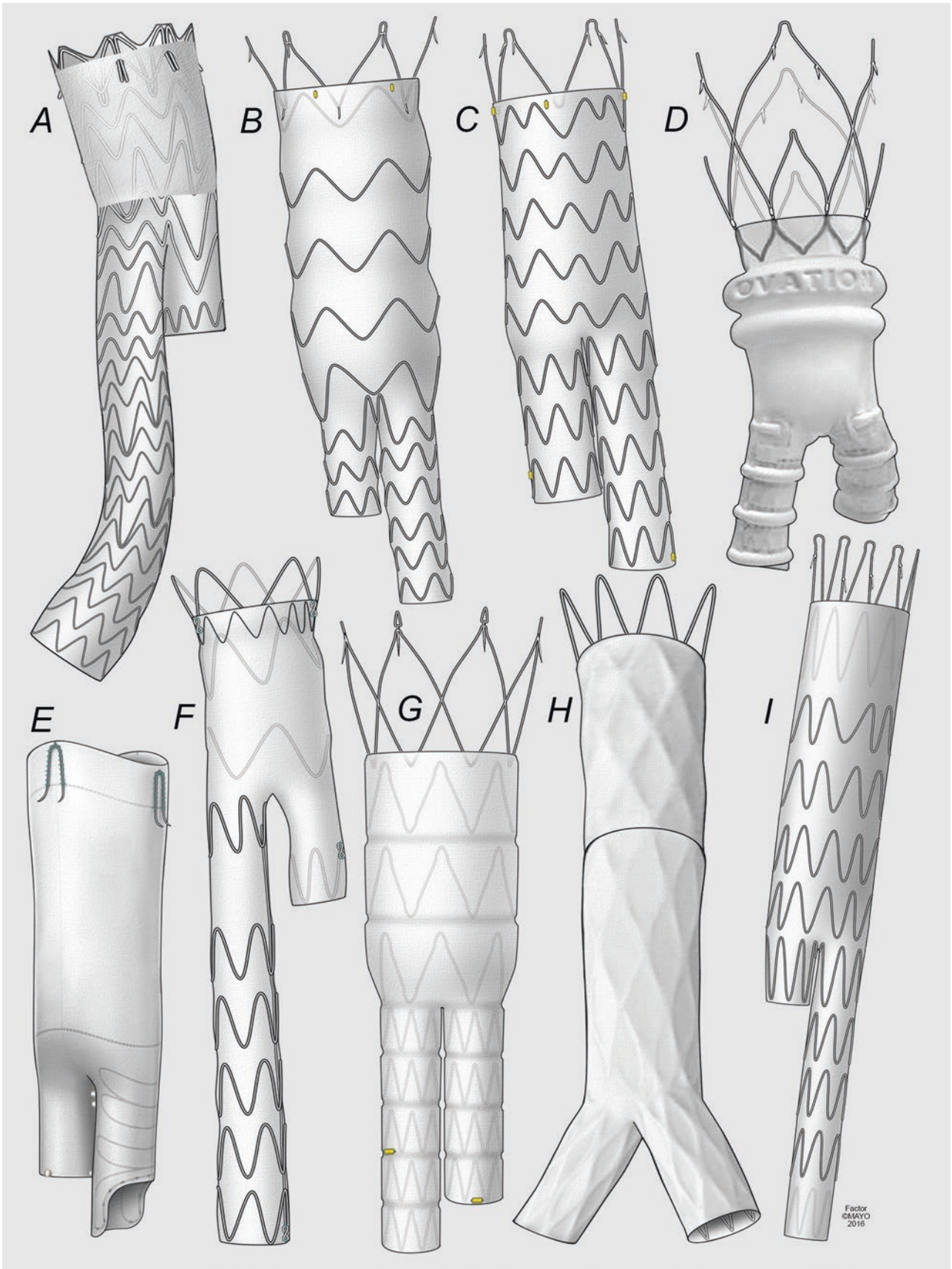


Fig. 14.14 Approved abdominal stent-grafts include the Gore Excluder (**a**), Bolton Abdominal (**b**), Medtronic Endurant (**c**), Trivascular Ovation (**d**), Vascutek Anaconda (**e**), Medtronic Talent (**f**), Cordis Incraft (**g**), Endologix Powerlink (**h**), and Cook Zenith (**i**). By permission of Mayo Foundation for Medical Education and Research. All rights reserved

Table 14.7 FDA-approved AAA devices

Device	Sheath size OD (F)	Main body diameter (mm)	Main body length (cm)	Iliac sizes (mm)
Cook Zenith	20, 22, 24	22, 24, 26, 28, 30, 32, 36	8.2, 9.5, 11.1, 11.3, 12.5,13.1, 14.0, 14.9	**L:** 39, 56, 74, 90, 107, 122
				D: 9, 11, 13, 16, 20, 24
Endologix	17	22, 25, 28	4, 6, 7, 8, 9, 10, 11,12	**L:** 30, 40, 55
				D: 13, 16, 20
Aorfix AAA Endovascular Stent graft	22	24, 27, 31, 34	8.1, 9.6, 11.1, 12.6	**L:** 56, 64, 73, 81, 90, 98, 106
				D: 12, 14, 16, 18, 20
Gore Excluder	18.6, 20.4	23, 26, 28.5, 31, 35	12, 13, 14, 15, 16, 17, 18	**L:** 95, 100, 115, 120, 135, 140
				D: 10, 12, 14.5, 16, 18, 20, 23, 27
Endurant AAA Stent Graft System	18, 20	23, 25, 28, 32, 36	12, 14.5, 17	L: 80, 95, 120
				D: 10, 13, 16, 20, 24, 28
Endurant II AAA Stent Graft System	18, 20	23, 25, 28, 32, 36	12.4, 14.5, 16.6	**L:** 82, 93, 124, 156, 199
				D: 10, 13, 16, 20, 24, 28
Endurant II AUI Stent Graft System	18, 20	23, 25, 28, 32, 36	10.2	**L:** 82, 93, 124, 156, 199
				D: 10, 13, 16, 20, 24, 28
Ovation iX Abdominal Stent Graft System	14, 15	20, 23, 26, 29, 34	8	**L:** 80, 100, 120, 140, 160
				D: 10, 12, 14, 16, 18, 22, 28

Table 14.8 FDA-approved thoracic aortic devices

Device	Sheath size OD (F)	Main body diameter (mm)	Main body length (cm)
RelayPlus (Bolton Medical, Inc)	22, 23, 24, 25, 26	22, 24, 26, 28, 30, 32, 34, 38, 40, 42, 44, 46	10, 15, 25
		4-mm taper: 28, 32, 34, 36, 38, 40, 42, 44, 46	Tapered: 15, 20, 25
TX2 (Cook Medical)	20, 22	Proximal 28–42; tapered proximal: 32–42; Distal: 28–42; Proximal extension: 28–42; distal extensions: 28–42	Proximal: 12–21.6; tapered proximal: 15.2–20.8; distal:13.6–20.7; proximal extensions: 7.7–8.1; distal extensions: 7.7–8.1
Zenith Alpha Thoracic (Cook Medical0	16, 18, 20	Proximal: 18–46; tapered proximal: 26–46; distal: 28–46; distal extension: 22–46	Proximal: 10.5–23.3; tapered proximal 10.5–23.3; distal 14.2–21.1; distal extension: 9.1–11.2
Gore TAG Thoracic Endoprosthesis	18, 20, 22, 24	21, 26, 28, 31, 34, 37, 40, 45; tapered: 26×21, 31×26	10, 15, 20
Valiant Thoracic Stent Graft on Captivia Delivery System (Medtronic)	22, 24, 25	22, 24, 26, 28, 30, 32, 24, 36, 38, 40, 42, 44, 46; tapered: 26, 28, 30, 32, 34, 36, 38, 40, 42, 44, 46	10, 15, 20

0 device is longer to accommodate anatomical requirements of the proximal arch. A specially designed bridging stent is also available.

Medtronic Valiant Mona LSA

The Medtronic Valiant Mona LSA has a funnel side branch port that is pre-catheterized and intended to be stented to the left subclavian artery with a specially designed side stent.

Najuta Next-Gen Fenestrated TEVAR and Innoue Stent

Asian experience has been reported with a customized device that is not available in the United States. It comes pre-curved and does not have bridging stents. It requires a proximal landing zone of greater or equal to 10 mm and an adequate proximal seal zone between supra-aortic branches and lesion on aortic wall.

Pararenal and Thoracoabdominal Aneurysms

Cook Patient-Specific and Off-the-Shelf Fenestrated and Branched Platforms

The Zenith fenestrated stent-graft has become commercially approved in the United States in April of 2012, providing an alternative in patients with short neck or juxtarenal aneurysms. The stent has been approved with maximum of three fenestrations, although options of more fenestrations are available worldwide and in US centers with PS-IDE protocols (Fig. 14.16). Cook also has off-the-shelf

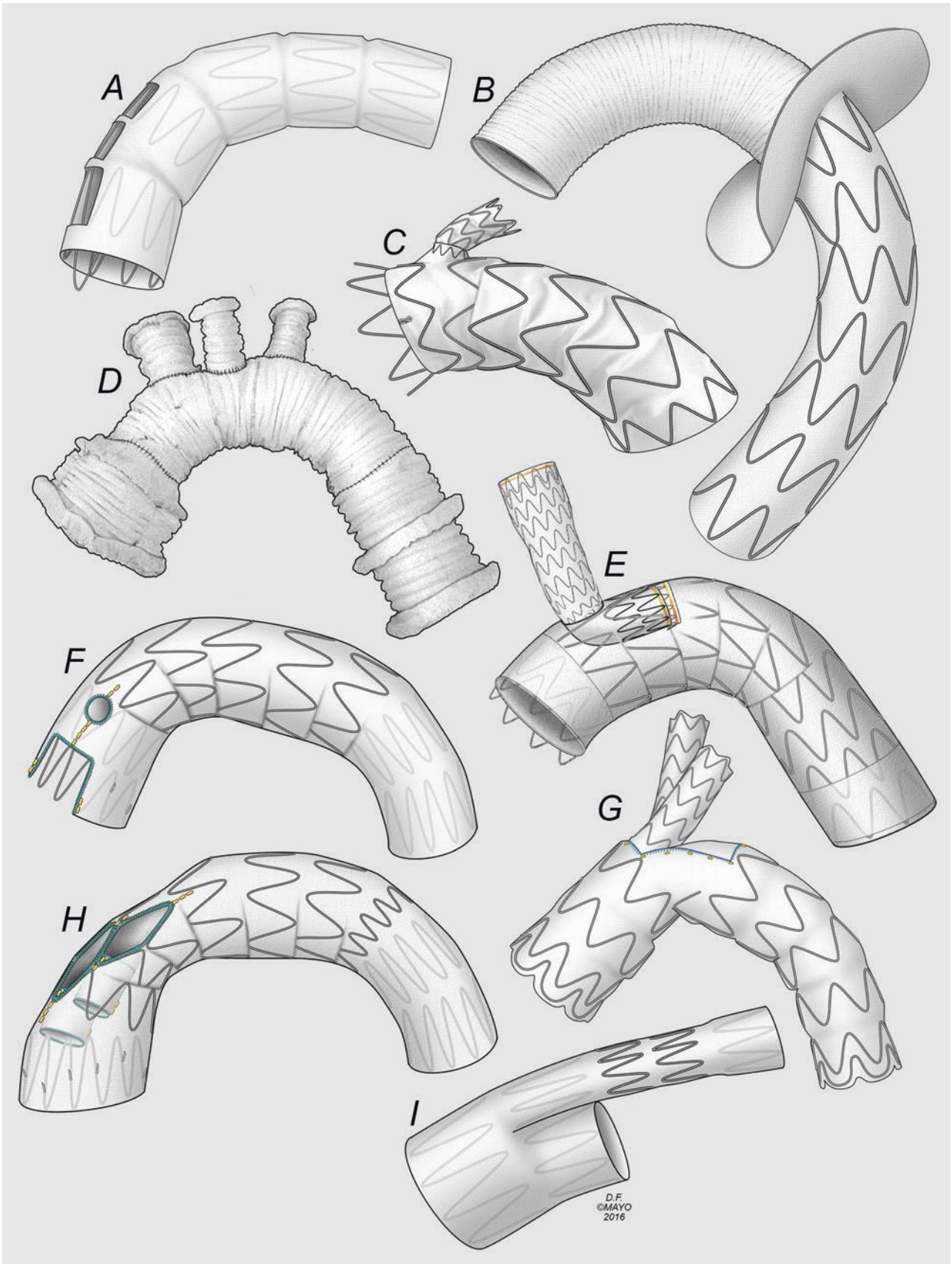


Fig. 14.15 Arch devices include the Najuta arch device (**a**), Evita Hybrid Stent-Graft (**b**), Medtronic MonaLSA (**c**), Innoue arch device (**d**), Gore Thoracic Branch Endoprosthesis (**e**), Cook Arch fenestrated (**f**), Bolton Arch Branch (**g**), Cook A-Branch device (**h**), and Cook first generation Chuter arch device (**i**). By permission of Mayo Foundation for Medical Education and Research. All rights reserved

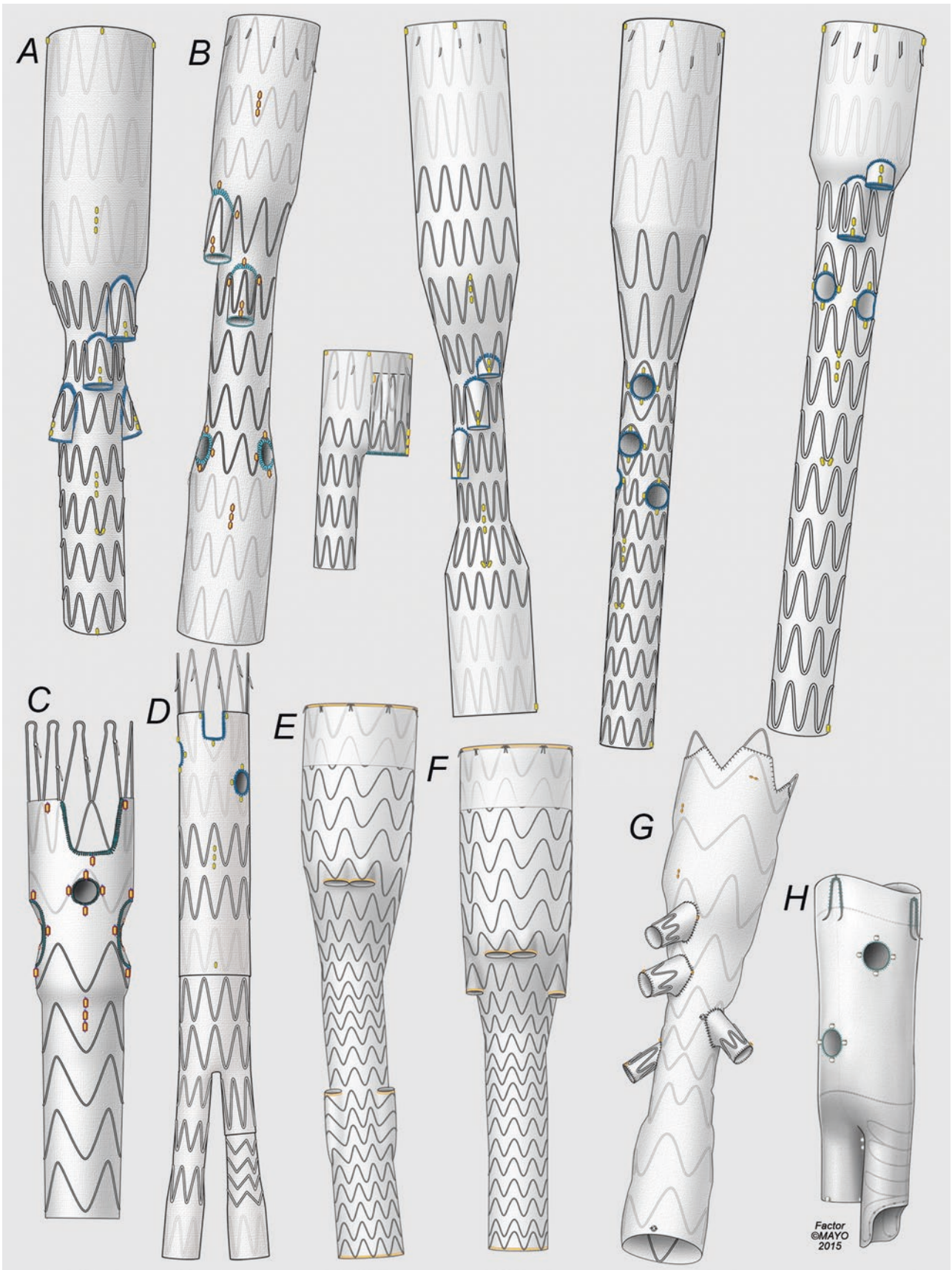


Fig. 14.16 Visceral incorporation devices include the Cook t-Branch (**a**), Cook patient-specific thoracoabdominal platform (**b**), Cook p-Branch (**c**), Cook ZFEN (**d**), Gore TAMBE retrograde (**e**), Gore TAMBE antegrade (**f**), Jotec TAAA branched (**g**), and Vascutek fenestrated (**h**). By permission of Mayo Foundation for Medical Education and Research. All rights reserved

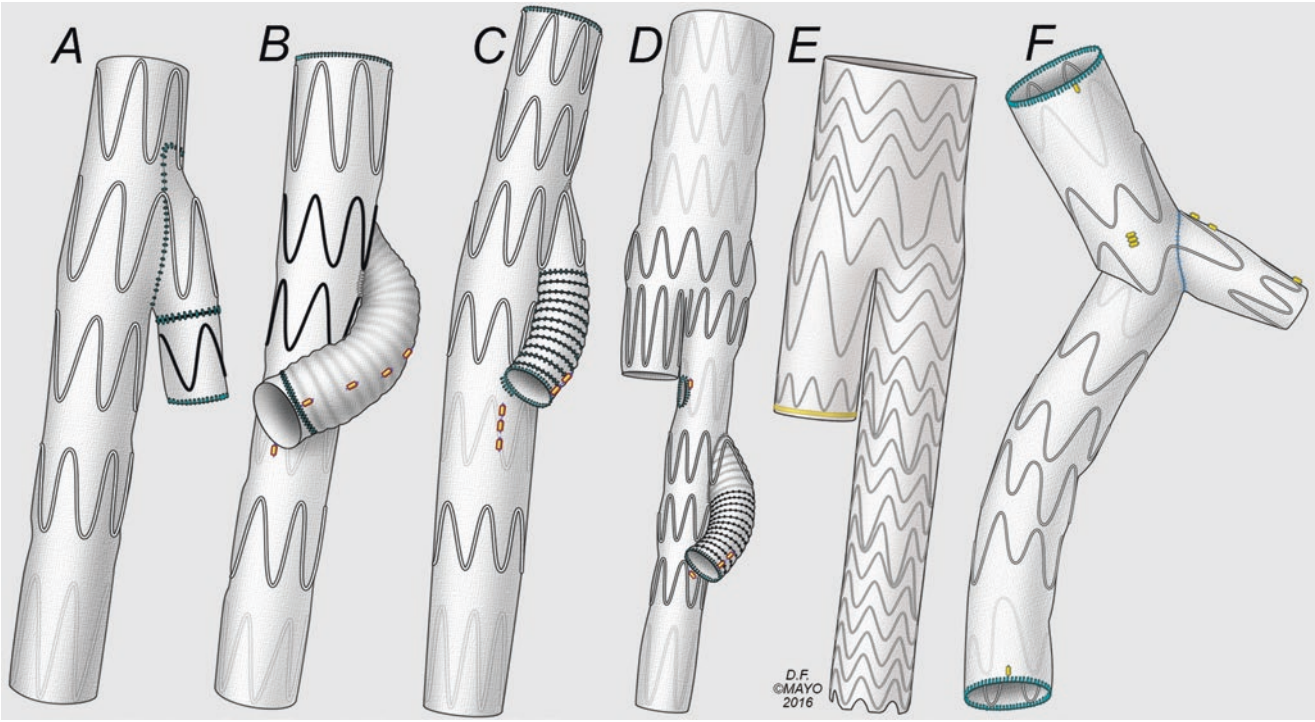


Fig. 14.17 Iliac branch devices include the Cook straight branch (**a**), helical branch (**b**, **c**), bifurcated-bifurcated branch (**d**), Gore IBE (**e**), and Jotec Iliac branch (**f**). By permission of Mayo Foundation for Medical Education and Research. All rights reserved

options for pararenal (p-branch®) and thoracoabdominal aneurysms (t-branch®) that are discussed at length in other chapters.

Gore TAMBE® (Thoracoabdominal Multi-Branch Endoprosthesis)

The TAMBE device is currently under clinical investigation in the United States. The first worldwide in man implant of the retrograde branch was done by Pierre Galvani Silveira in Brazil (November 2014) and the first US implant by Gustavo Oderich (December 2015). The first worldwide in man implant of the antegrade TAMBE was done by Gustavo Oderich at the Mayo Clinic in March 2016.

Anaconda Fenestrated

The Vascutek anaconda fenestrated offers a patient-specific device with fenestrations for Juxta- and Pararenal aneurysms

Jotec Multi-Branch Thoracoabdominal Device

Jotec from Germany provides an option of multi-branched endograft for thoracoabdominal aneurysms

Iliac Aneurysms

Iliac branch devices are available by Cook medical, WL Gore, and Jotec (Fig. 14.17). The WL Gore device was the first to achieve commercial approval in the United States in March 2016.

References

1. Manunga JM, Gloviczki P, Oderich GS, Kalra M, Duncan AA, Fleming MD, Bower TC. Femoral artery calcification as a determinant of success for percutaneous access for endovascular abdominal aortic aneurysm repair. J Vasc Surg. 2013;58(5):1208–12.
2. Oderich GS. Fenestrated stent graft repair for complex aneurysms. EV Today 2013; 16–26.

Integration of Clinical Practice, Research, Innovation, and Education

15

Gustavo S. Oderich and Jesse M. Manunga

Introduction

Modern aortic programs require integration of clinical practice, research, innovation, and education (Fig. 15.1). It is critical for physicians to develop collaborations between multiple specialties, engineers, and industry. More important is the need to constantly assess outcomes and to identify weaknesses and strengths. Changes in a procedure, methodology, or concept require analysis of outcomes and dedicated time to develop a team approach to address complex problems. This is well exemplified by the experience and legacy of Dr. Roy Greenberg (1964–2013), our friend, teacher, and a pioneer in fenestrated and branched techniques. This chapter summarizes the evolution of Dr. Greenberg's major contributions to modern aortic therapy, and how his influence affected the development of advanced clinical and research programs at Cleveland Clinic and worldwide.

Dr. Roy Greenberg's Legacy

Investing in Education

A fundamental aspect is the time invested in education and training, which cannot be shortened to achieve outstanding results. Despite being a gifted technician, Dr. Greenberg sought himself specialized training, well beyond the traditional paradigms for early 1990s. His background included biomedical engineering (Cornell University, 1987), a Medical Degree (University of Cincinnati, 1992), and general surgery training (University of Rochester, 1997). He realized the importance of mastering endovascular skills and sought an interventional radiology fellowship in Sweden (1998) before obtaining his vascular surgery training at the University of Rochester (1999).

Early Years

Dr. Greenberg joined the staff of the Cleveland Clinic in 1999. His initial approach was to generate an exceptionally busy clinical practice (Fig. 15.2) that consisted largely of complex aortic problems, while coupling this with his efforts in research and development. He contributed significantly to the dissemination of advanced endovascular techniques, including numerous landmark publications (Table 15.1), research grants, and over 50 published patents [1–16]. Some of his most important contributions ranged from novel stent-graft designs to mathematical modeling of three-dimensional imaging and numerous aspects of fenestrated and branched endograft techniques.

Identifying Clinical Need

Roy developed several physician-sponsored investigational device exemption (IDE) protocols, which allowed him to have access to technology not yet commercially approved in the United States, while conducting high-quality prospective clinical trials to evaluate outcomes of fenestrated and branched stent-grafts. As a result, he accumulated the largest worldwide experience in essentially every advanced aortic technique. In addition to a robust clinical experience, Dr. Greenberg research laboratory focused among other things on the development of more durable branch stent-grafts. His designs incorporated features that he felt would mitigate the

G.S. Oderich (✉)
Division of Vascular and Endovascular Surgery, Mayo Clinic, 200 First Street SW, Rochester, MN 55905, USA
e-mail: oderich.gustavo@mayo.edu

J.M. Manunga
University of Minnesota, Minneapolis, MN, USA

Department of Vascular and Endovascular Surgery, Abbott Northwestern Hospital/Minneapolis Heart Institute, 920 E 28th Street, Suite 300, Minneapolis, MN 55407, USA
e-mail: Jesse.manunga@allina.com; Jmanunga@gmail.com

© Mayo Foundation for Medical Education and Research 2017

G.S. Oderich (ed.), *Endovascular Aortic Repair*, DOI 10.1007/978-3-319-15192-2_15

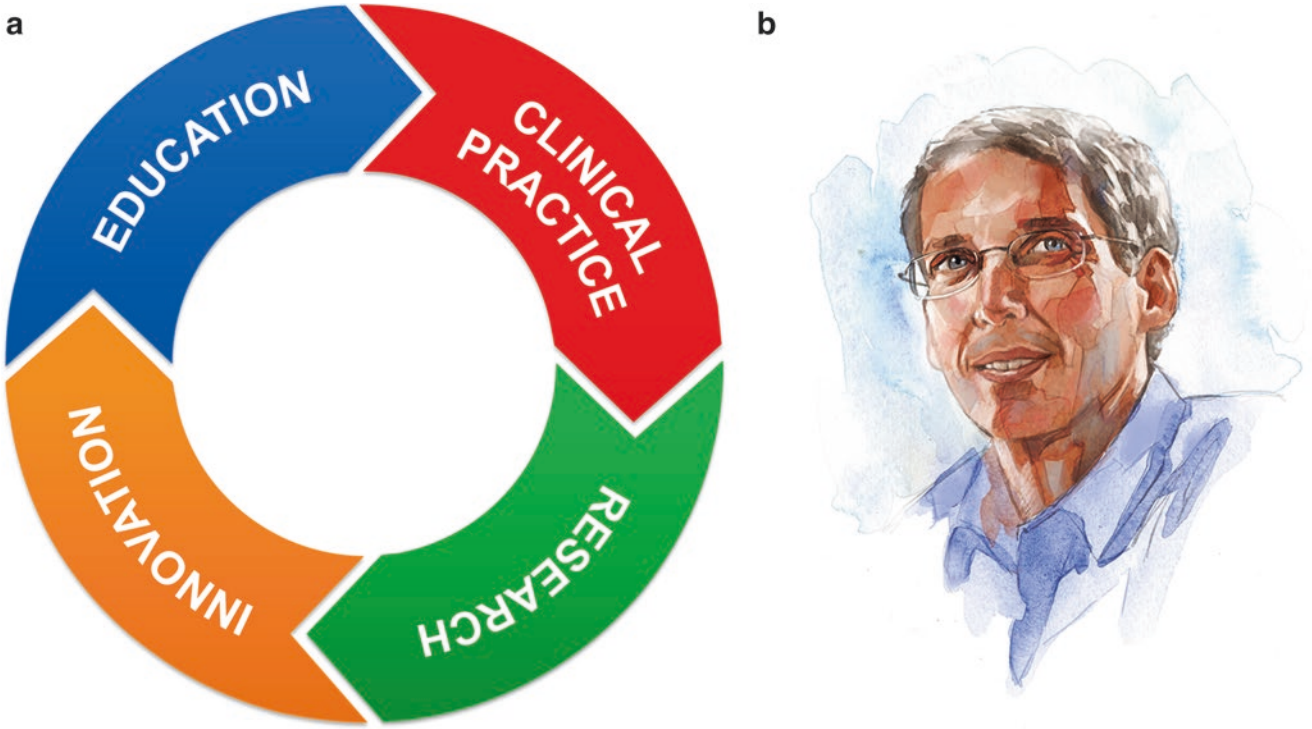


Fig. 15.1 An integrated aortic program with clinical practice, research, innovation, and education (**a**) as modeled by Dr. Roy K. Greenberg at the Cleveland Clinic (**b**). By permission of Mayo Foundation for Medical Education and Research. All rights reserved

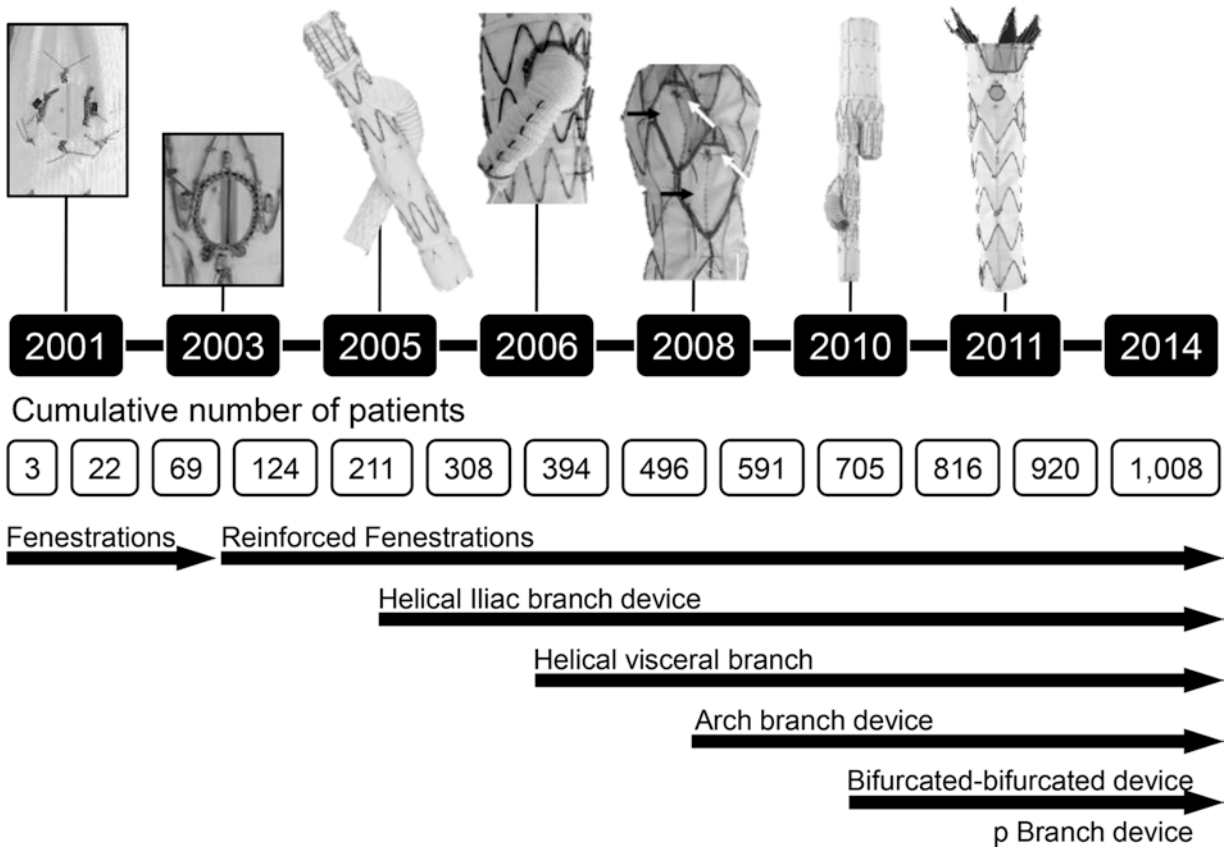


Fig. 15.2 Progress of clinical practice and branch incorporation in Dr. Greenberg's physician-sponsored investigational device exemption protocols. Reproduced with permission from Oderich GS. New Horizons in Aortic Disease The Lasting Legacy of a Visionary Innovator. J Endovasc Ther. 2015; 22(1): 139–145

Table 15.1 Selected landmark publications on fenestrated and branched techniques by Dr. Greenberg and colleagues[a]

First author (year)	Study design	Main message
Greenberg [3] (2004)	Prospective study of fenestrated repair for juxtarenal AAAs	• Fenestrated repair is safe and effective • Low rate of type I endoleak (<1 %)
Haddad [1] (2005)	Renal outcomes during fenestrated EVAR	• Renal function deterioration occurred in 32 % of patients with plateau at 3 months
O'Neill [2] (2006)	Prospective study of fenestrated repair for juxtarenal AAAs	• Fenestrated repair is safe (1 % mortality) and effective at midterm follow-up of 17 months
Goel [6] (2008)	Mathematical analysis of DICOM datasets	• Automated mathematical model is feasible and reproducible to calculate inter-renal distances compared to experienced operator
Dowdall [8] (2008)	Separation of components in fenestrated and branch endovascular repair	• Intercomponent movement (>10 mm) was noted in 14 devices, 8 of which had <2-stent overlap per IFU • Rate of type III endoleak was <1 % • 4-stent overlap was protective in all patients
Mohabbat [7] (2009)	Renal fenestration patency and duplex velocity criteria for stenosis	• Peak systolic velocity of 250 cm/s and renal-aortic ratio >4.5 suggested as criteria for renal stenosis >60 % • Covered stents associated with improved patency rates
Conway [17] (2010)	Renal implantation angles in TAAAs	• Type IV TAAAs more often have downward-going renal arteries • Types II and III TAAAs more often have orthogonally oriented renal arteries • Data support use of fenestrated branches for renal arteries
Bub [20] (2011)	Cardiac events during fenestrated and branched endovascular repair	• Atrial fibrillation in 9 %, myocardial infarction in 7 %, ventricular arrhythmias in 3 %, and cardiac death in 2 % • Troponin elevation in 12 % • Preoperative stress was not predictive
Dijkstra [11] (2011)	Cone-beam CT in fenestrated endografts	• Decreased contrast dose and fluoroscopy time • Immediate detection of technical problems may decrease rate of reinterventions
Pannucio [12] (2011)	Indirect vs. direct radiation doses during fenestrated TAAA repair	• Fluoroscopy time is unreliable to measure radiation exposure • Effective radiation dose of TAAA repair is equivalent to 2 CT studies and a single operator can perform 300 cases before reaching maximum operator dose
Brown [13] (2013)	Family history of aortic disease	• Family history predicted higher rates of aneurysm in every segment of the aorta • Patients with family history are younger and over 50 % ultimately developed suprarenal involvement
Mastracci [16] (2013)	Branch durability	• 89 % freedom from any branch-related reintervention at 5 years • Death from branch-related complications is rare (<0.5 %) • Renal occlusion is infrequent (<1.7 %) with renal fenestrated branches
Qureshi [19] (2012)	Outcomes of fenestrated repair in patients with COPD	• Severe COPD associated with decreased long-term survival • Patients with COPD had lower endoleak rates and more sac shrinkage
Oderich [17] (2014)	United States Zenith Fenestrated Pivotal Trial	• First multicenter study leading to commercial approval of the Zenith fenestrated device in April 2012 • 30-day mortality of 1.5 % with no rupture, dialysis, conversion, or early type I endoleak • Renal occlusion was 3 % • One late type I endoleak occurred at 3 years from progression of aortic disease

AAA abdominal aortic aneurysm, *EVAR* endovascular aneurysm repair, *DICOM* Digital Imaging and Communications in Medicine, *IFU* instructions for use, *TAAA* thoracoabdominal aortic aneurysm, *CT* computed tomography, *COPD* chronic pulmonary obstructive disease

[a]Reproduced with permission from Oderich GS. New Horizons in Aortic Disease The Lasting Legacy of a Visionary Innovator. J Endovasc Ther. 2015; 22(1): 139–145

risk of late failure, such as short length, long overlap, and vector alignment (Fig. 15.3). The concept of helical branches incorporated all these features by allowing alignment to the target vessel and longer overlap at the cuff. Later, this clinical experience was reported by Mastracci and colleagues (Fig. 15.4), who demonstrated 89 % freedom from any branch-related event at 5 years and remarkably low renal branch occlusion (<2 %) [2].

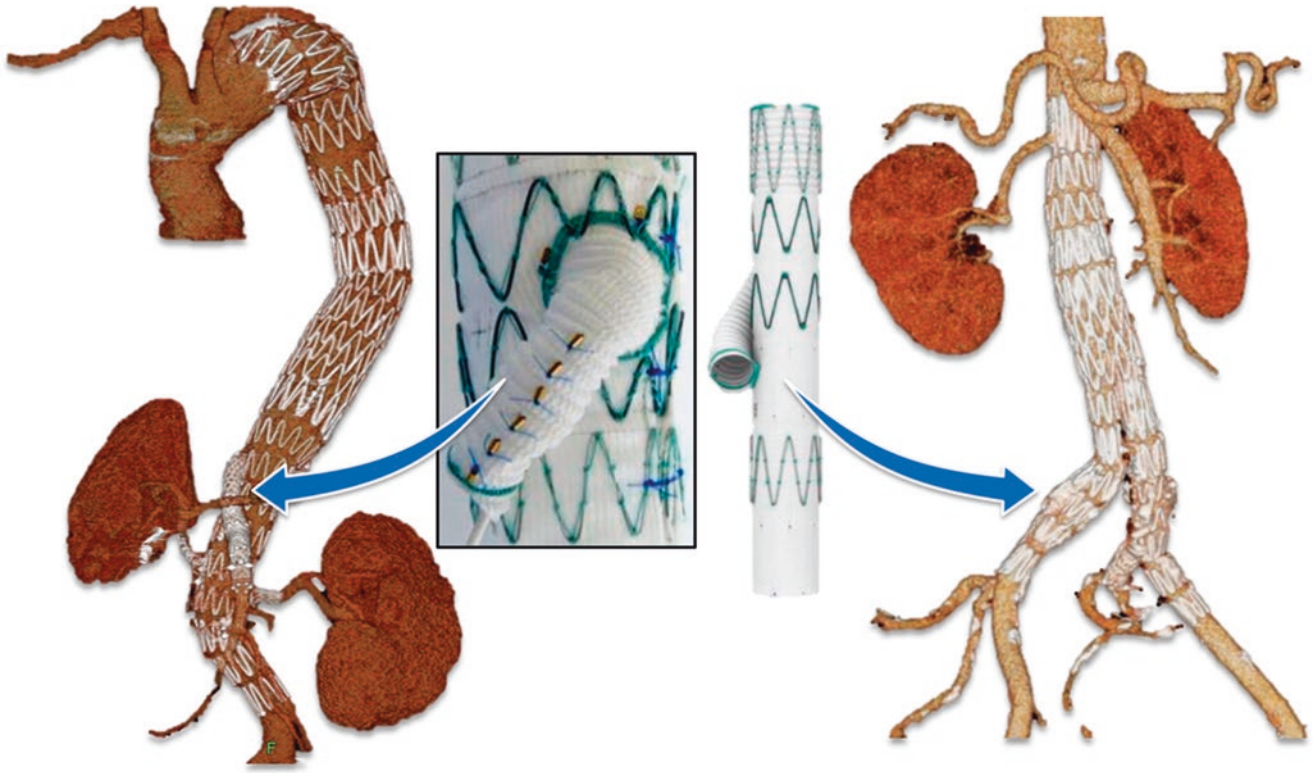


Fig. 15.3 Helical branch designs for the visceral arteries and iliac arteries. Dr. Greenberg's design for thoracoabdominal aortic aneurysms most often consisted of helical branches for the celiac axis and superior mesenteric artery with short renal fenestrated branches. Reproduced with permission from Oderich GS. New Horizons in Aortic Disease The Lasting Legacy of a Visionary Innovator. J Endovasc Ther. 2015; 22(1): 139–145

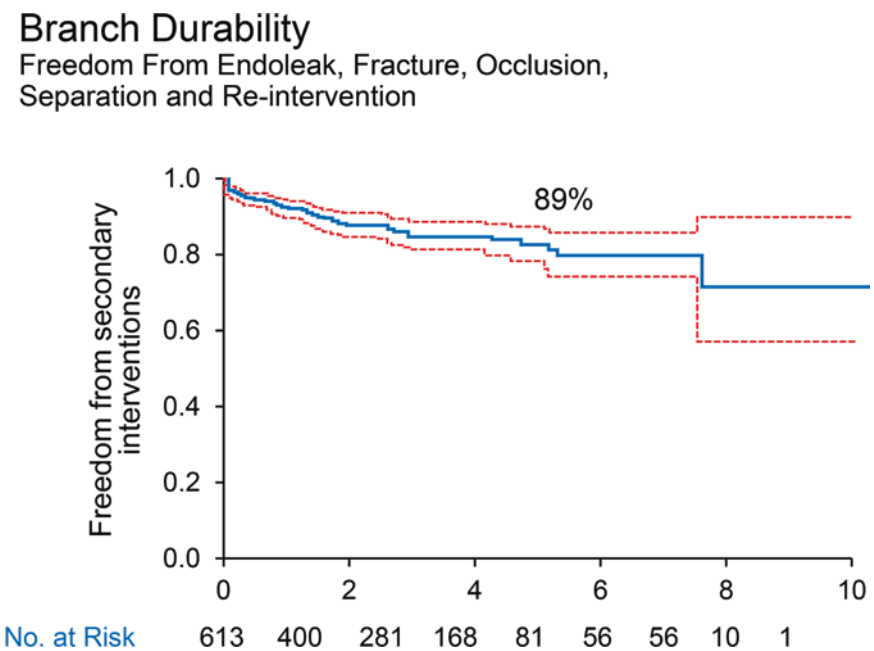


Fig. 15.4 Kaplan–Meier estimates of survival free of any branch-related complications or reinterventions including a composite of disconnection, endoleak, kink, stenosis, or occlusion. Reproduced with permission from Oderich GS. New Horizons in Aortic Disease The Lasting Legacy of a Visionary Innovator. J Endovasc Ther. 2015; 22(1): 139–145

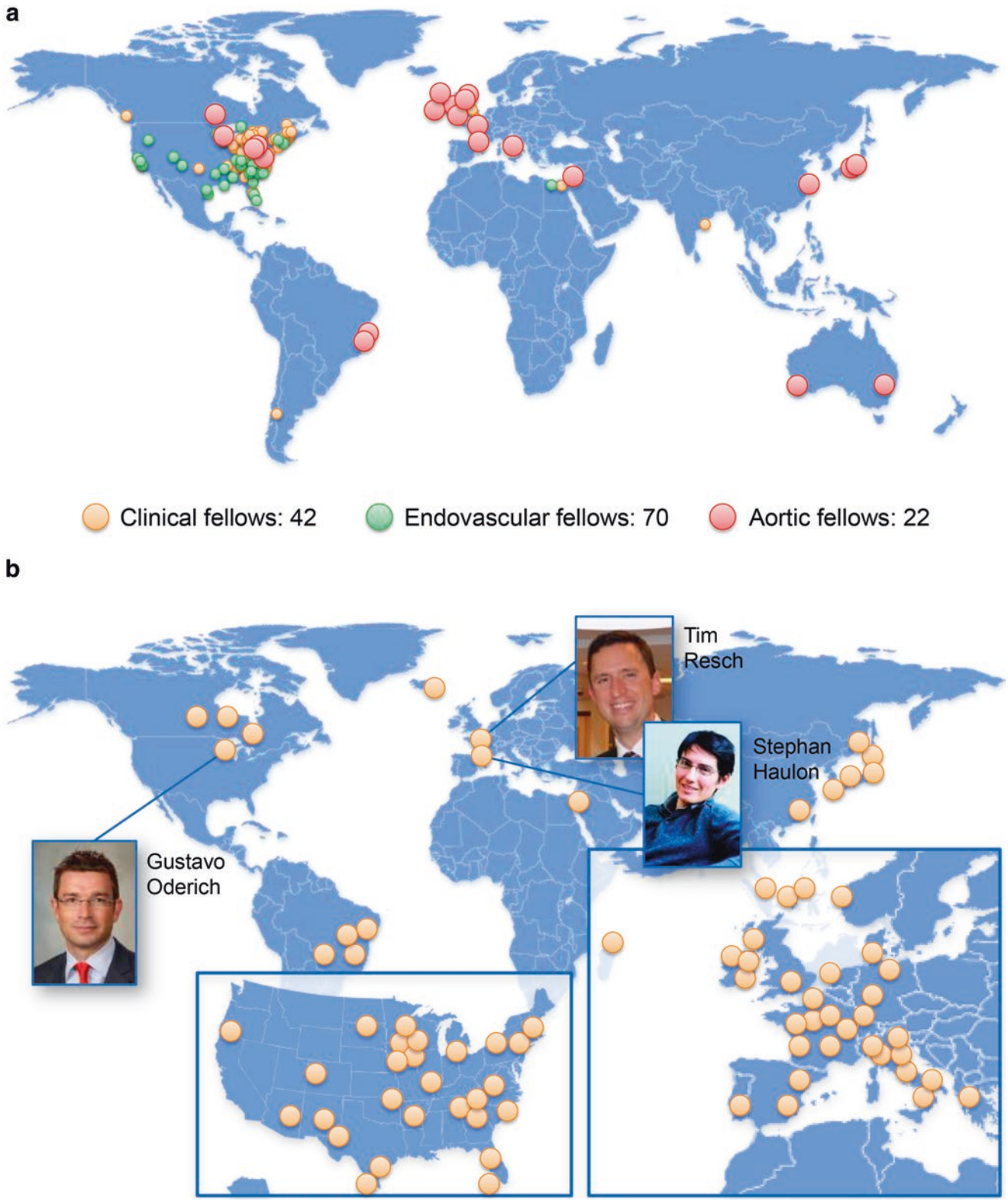


Fig. 15.5 Distributions of graduates of vascular and endovascular training programs at the Cleveland Clinic (**a**) and subsequent exponential effect on training by three of his graduates (**b**). By permission of Mayo Foundation for Medical Education and Research. All rights reserved

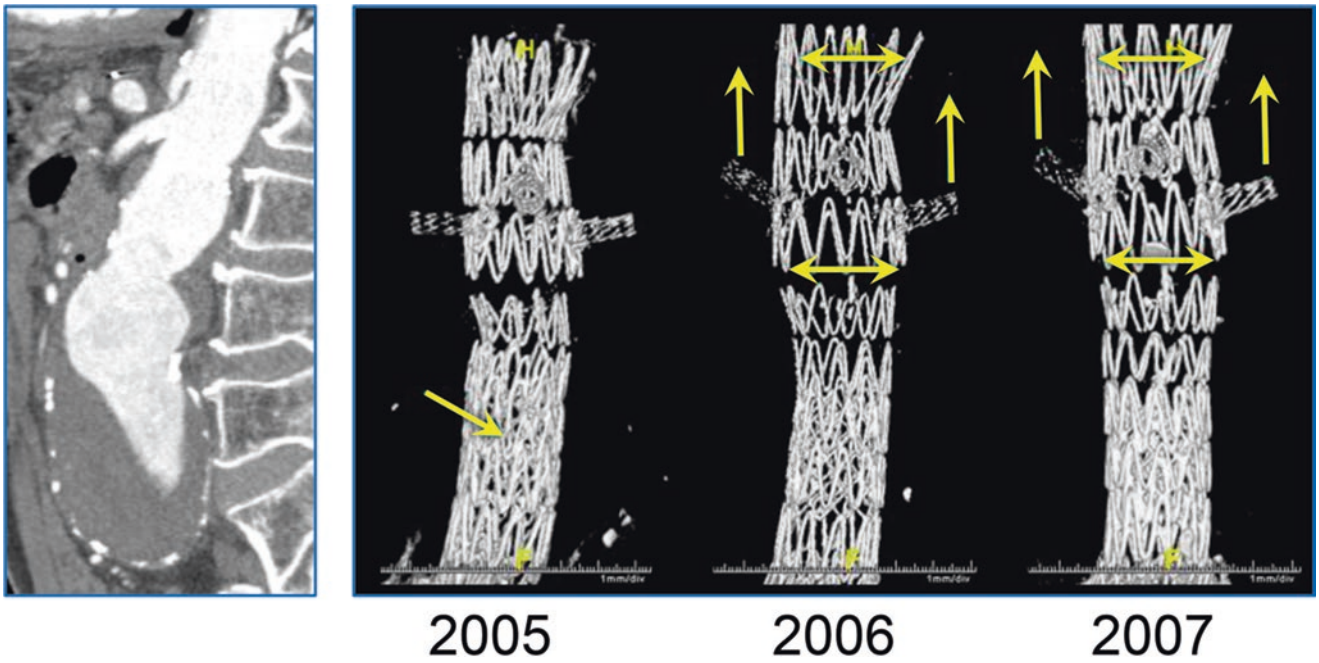


Fig. 15.6 Disease progression in a patient treated by fenestrated endovascular repair. By permission of Mayo Foundation for Medical Education and Research. All rights reserved

Dissemination of Endovascular Education

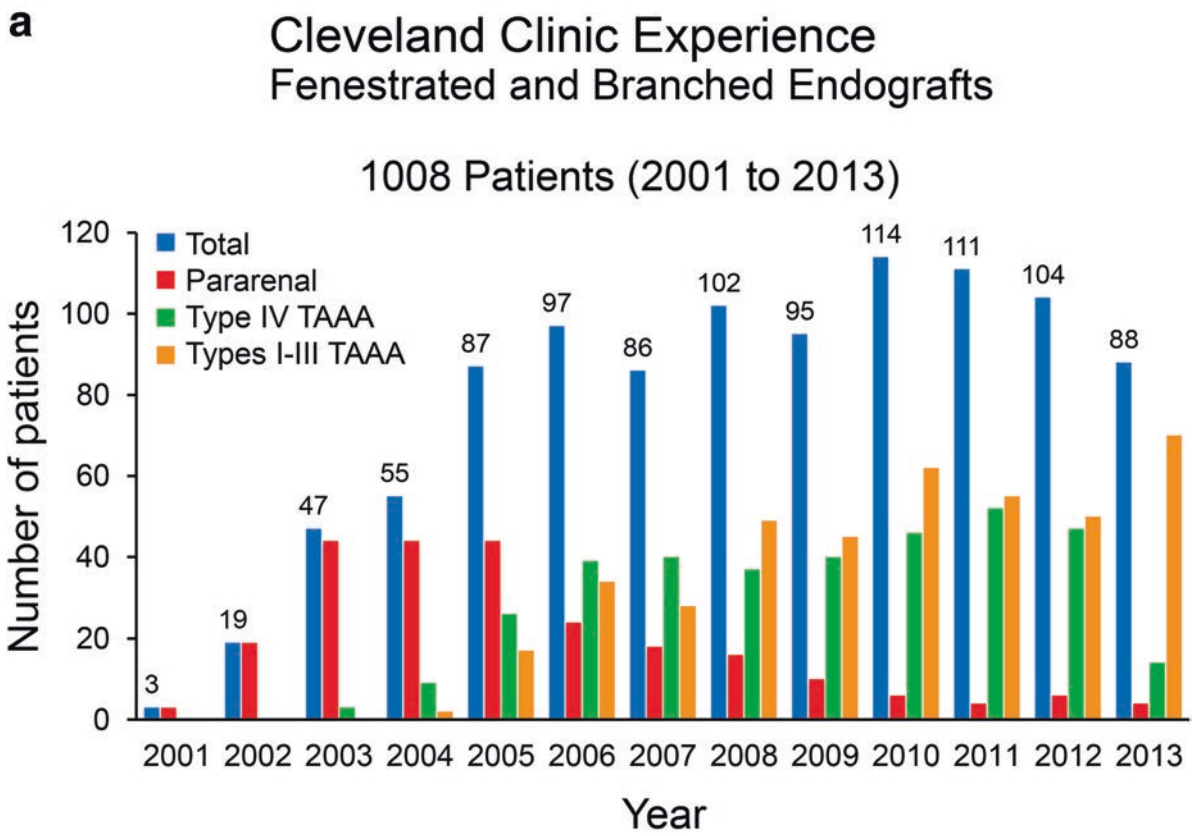
Dr. Greenberg's major long-lasting legacy was his contribution to education and dissemination of complex endovascular techniques. As pointed out by Dr. Ken Ouriel "An excellent surgeon enhances the lives of many patients one patient at a time, but an excellent teacher improves the lives of countless of patients in an exponential fashion". In the course of a decade, Dr. Greenberg had a direct hand in the training of 133 fellows, including 42 clinical fellows, 70 endovascular fellows, and 22 aortic fellows from all over the world (Fig. 15.5). The effect of his influence in endovascular education spread exponentially worldwide.

Focus on Durability

Dr. Greenberg always emphasized the importance of planning a durable repair that would last the patient's lifespan, well beyond 5–10 years. Based on extensive clinical experience, Dr. Greenberg recognized that placement of endografts in vulnerable aortic segments (Fig. 15.6) would be prone to late failure due to progression of aortic disease leading to device migration or loss of attachment seal. Similar to other pioneers, Dr. Greenberg's clinical practice evolved with the notion that fenestrated endografts had to be placed in more stable aortic segments, often above the celiac axis, thereby providing a more durable repair and also an alternative for future treatment in the event of failure. Based on his experience and of others, seal zones have been extended more proximally to incorporate all four vessels into a more stable aortic segment, particularly in those patients with long life-expectancy, family history of aortic disease, multiple affected segments in the aorta, prior failed open or endovascular repair, or diseased, ecstatic, or thrombus-laden necks [3, 4].

Impact on Advanced Endovascular Aortic Programs Worldwide

The Cleveland Clinic experience led by Dr. Greenberg serves as a model of modern aortic practice where clinical excellence, research, innovation, and education work synchronously. Successful programs have build their clinical experiences in a stepwise fashion with increase in the level of complexity of device design and extent of repair, higher number of TAAAs and 4-vessel designs (Fig. 15.7). It is important to learn the basic tenets of fenestrated and branched techniques in the lower risk territories (e.g., aortoiliac and pararenal aorta), and then have the courage to advance therapy to patients with more complex anatomy (e.g., thoracoabdominal aorta and arch). The extensive experience accumulated by the Cleveland Clinic group and others have demonstrated that the incremental challenge in device design complexity from two- to four-vessel fenestrations was not associated with added risk of mortality.



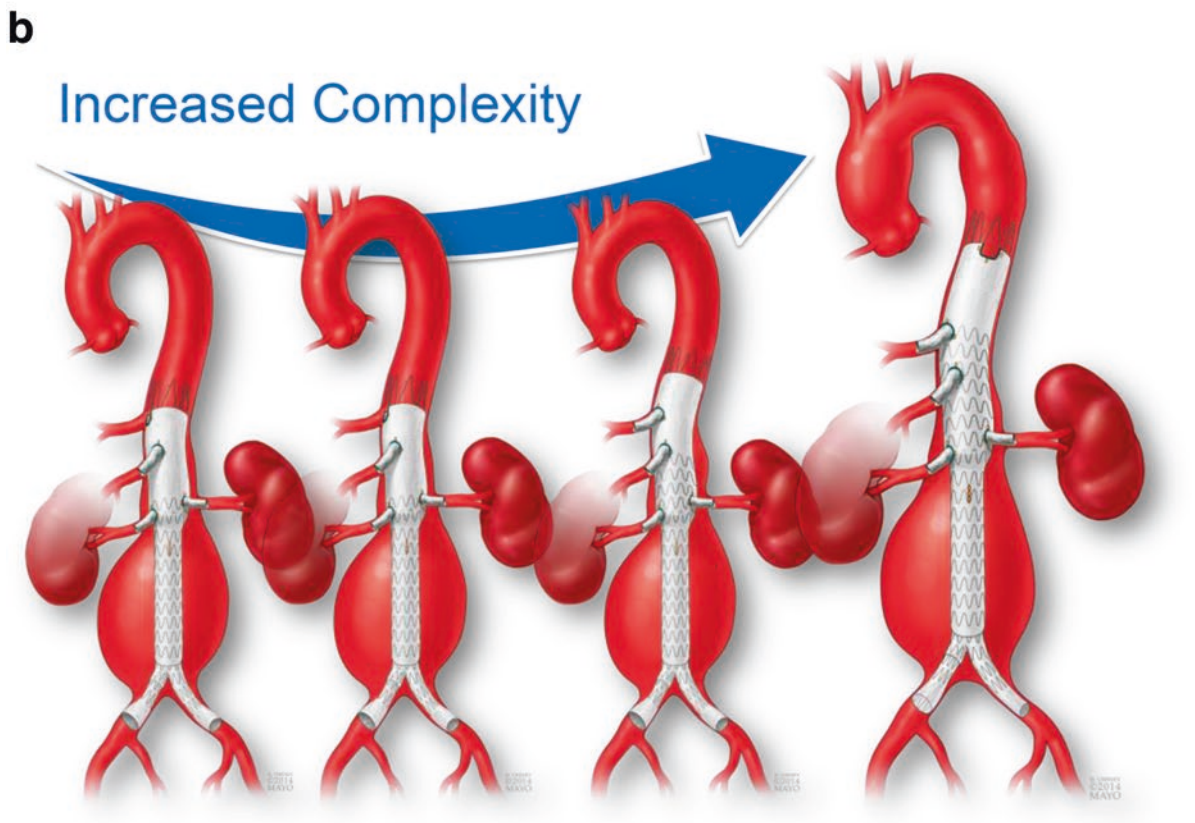


Fig. 15.7 Increasing fenestrated-branched design complexity over the years of experience at the Cleveland Clinic Foundation (**a**). For the same extent aneurysm, four-vessel designs have been used preferentially to seal the aneurysm in a more stable aortic segment (**b**). By permission of Mayo Foundation for Medical Education and Research. All rights reserved

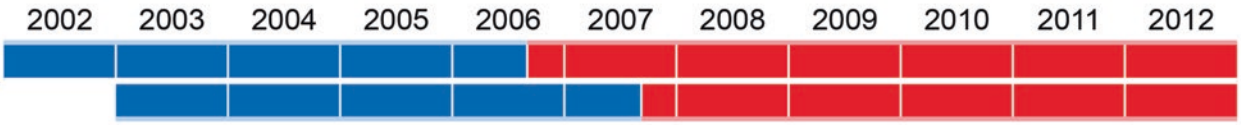
The importance of a dedicated and intensive training program in fenestrated and branched techniques is reflected by the excellent clinical results achieved by several of Dr. Greenberg's aortic fellows, who went to develop specialized aortic centers with focus on these techniques. Drs. Haulon (France) and Resch (Sweden) are examples of successful trainees who became leaders in the field [6]. In a recent report, Resch and Haulon compared outcomes of their first 50 patients treated by fenestrated endografts for juxtarenal abdominal aortic aneurysms with their contemporary experience (Fig. 15.8). There was a significant increase in utilization of three- and four-vessel designs over time. In that study, despite the increments in complexity of device design, there was significant decrease in fluoroscopy time, contrast volume, and no change in mortality (2%).

The Mayo Clinic fenestrated program started April 11, 2007, a week after the author returned from the Cleveland Clinic for specialized endovascular training. Since then, a total of 300 patients were treated using fenestrated and branched endografts for pararenal aneurysms in 45% and TAAAs in 55%. There was significant increase in complexity of aneurysm extent and device design over time, which is reflected by the higher number of TAAAs and 4-vessel designs in recent years. Despite this, 30-day mortality was 2.3% for the entire cohort, 0.6% for pararenal, and 4.4% for TAAAs, with no increase in mortality associated with more complex designs. In a recent analysis of the first 110 patients enrolled in a prospective non-randomized study (65% TAAAs), there was no mortality, conversion, or aneurysm rupture.

The Mayo Clinic experience started with physician-modified endovascular grafts. Device modifications used the same principles of sizing, design, and implantation applied for manufactured devices. A limitation of the technique was the lack of a reinforced nitinol ring, which is available in manufactured devices. Lack of a reinforced nitinol ring can lead to enlargement of the fenestrations and

Lille-Malmo Experience
Fenestrated Endografts for Juxtarenal AAAs

288 Patients (2002-2012)
Early experience with first 50 patients (~4.7 yr)



Early experience Late experience

	Early experience n=100	Late experience n=188	
Fenestrations	2.7±0.8	3.2±0.8	0.001
2 fen	35	11	
4 fen	7	30	

	Early experience (%) n=100	Late experience (%) n=188	
Fenestrations	2.7±0.8	3.2±0.8	0.001
Fluoroscopy	84 min	65 min	0.05
Contrast volume	254 ml	184 ml	0.05
30-day Mortality (%)	2	2	NS

Fig. 15.8 Results of early experience with fenestrated stent-grafts for juxtarenal abdominal aortic aneurysms in Lille, France and Malmo, Sweden. By permission of Mayo Foundation for Medical Education and Research. All rights reserved

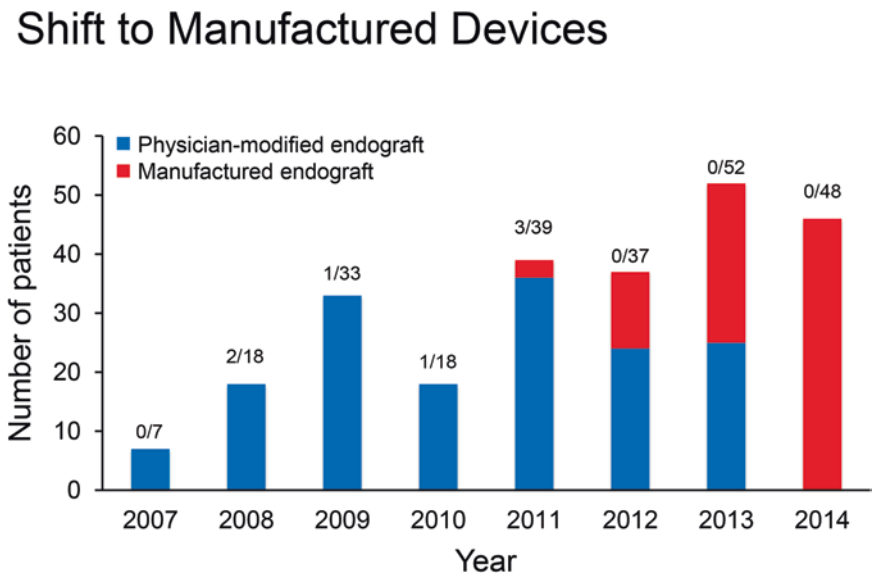


Fig. 15.9 Increasing utilization of manufactured devices has replaced physician-modified fenestrated endografts at the Mayo Clinic. By permission of Mayo Foundation for Medical Education and Research. All rights reserved

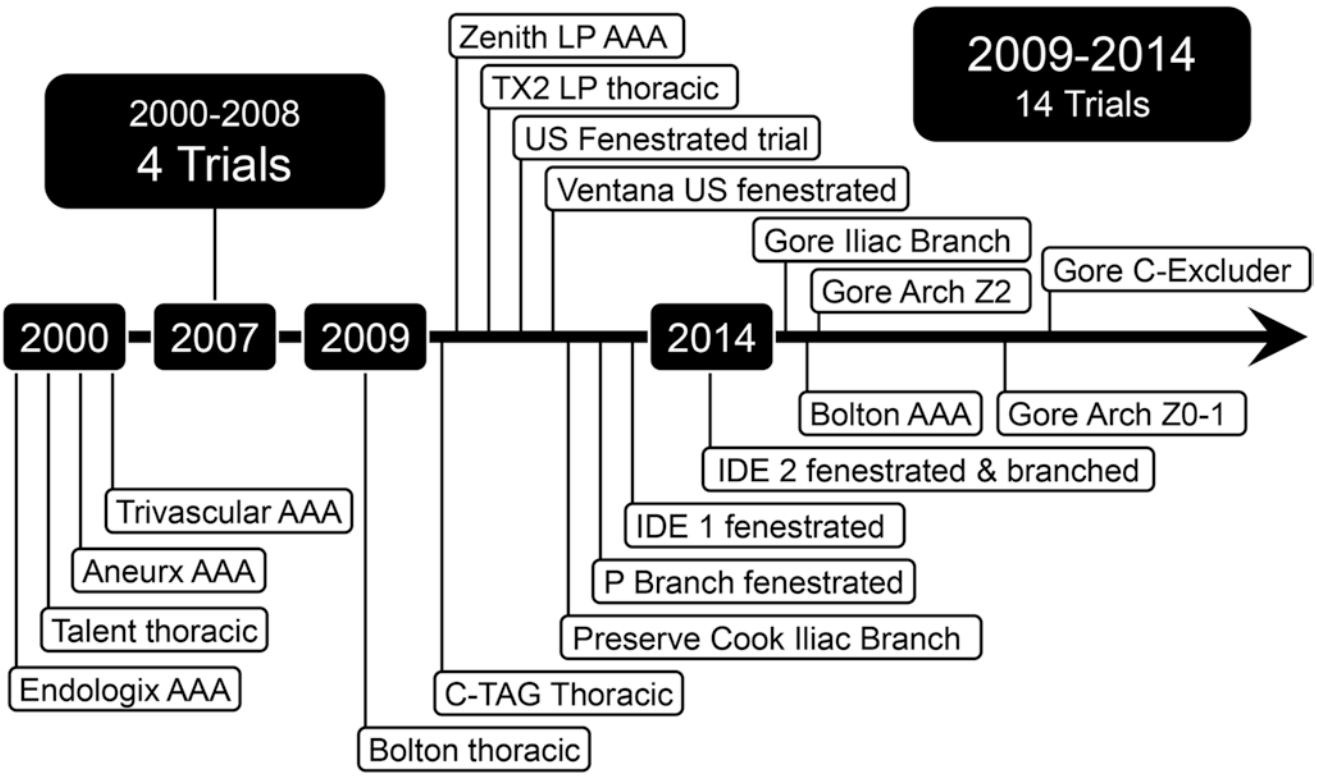
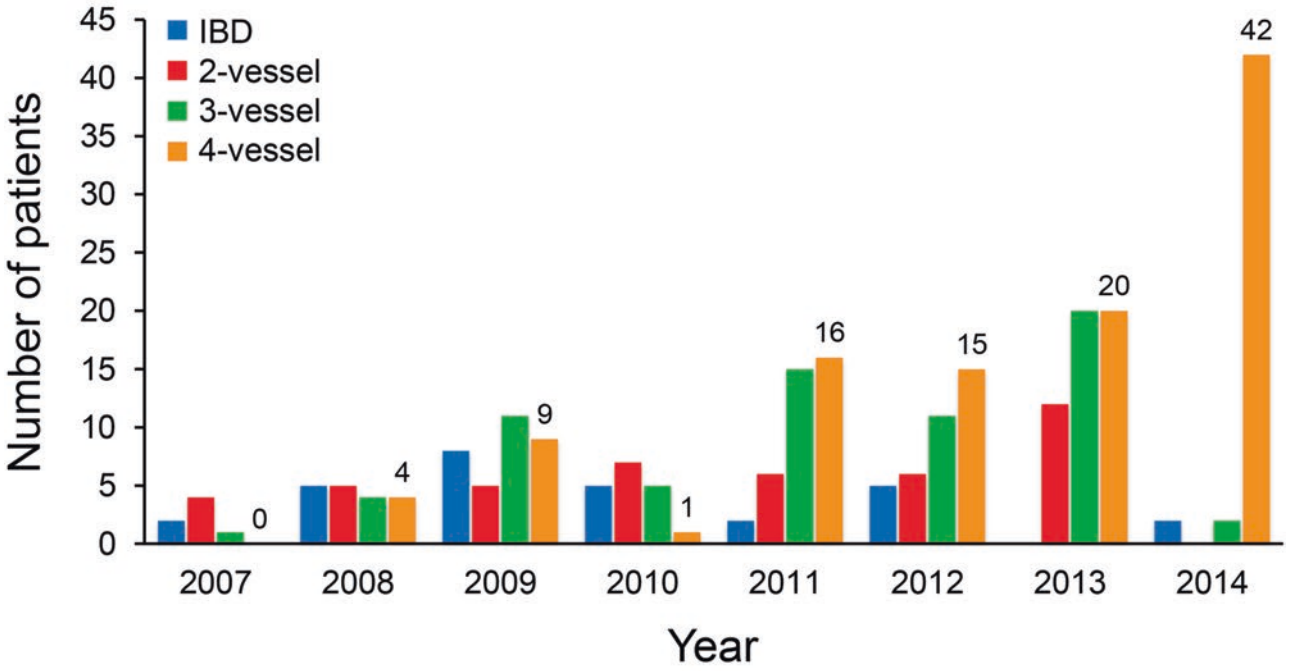


Fig. 15.10 Development of clinical trial section has been possible with collaboration with industry sponsors and engineers. By permission of Mayo Foundation for Medical Education and Research. All rights reserved

poor apposition with alignment stents, predisposing to component separations and type III endoleaks. Other important limitations of PMEGs include the lack of quality control, added cost of using multiple devices, time required for modifications, limited reimbursement, and questionable long-term durability. Therefore, our practice shifted from PMEGs to utilization of manufacture devices (Fig. 15.9, online only) under a prospective physician-sponsored investigational device exemption protocol (IDE). Following the example of Dr. Greenberg, we also developed a robust clinical research program, which currently includes over 20 clinical trials evaluating complex aortic devices (Fig. 15.10). These trials

a



b

Learning Curve

	Patient			P
	1 to 80	81 to 160	161 to 240	
Pararenal (%)	70	74	38	0.01
TAAA (%)	30	26	62	0.01
Vessels (no.)	2.4±1.06	3.04±1.02	3.54±0.75	0.001
2-vessel (%)	50	29	10	0.001
4-vessel (%)	19	41	65	0.001
Fluoroscopy (min)	117±61	84±38	72±23	0.05
Contrast (ml)	237±99	163±73	138±75	0.001
30-day mortality	5 (6%)	2 (3%)	0	0.12

Fig. 15.11 Increasing device complexity at the Mayo Clinic fenestrated-branched program in 250 consecutive cases was associated with more thoracoabdominal aneurysms and more four-vessel designs (**a**) and with decrease in fluoroscopy time and contrast volume (**b**). By permission of Mayo Foundation for Medical Education and Research. All rights reserved

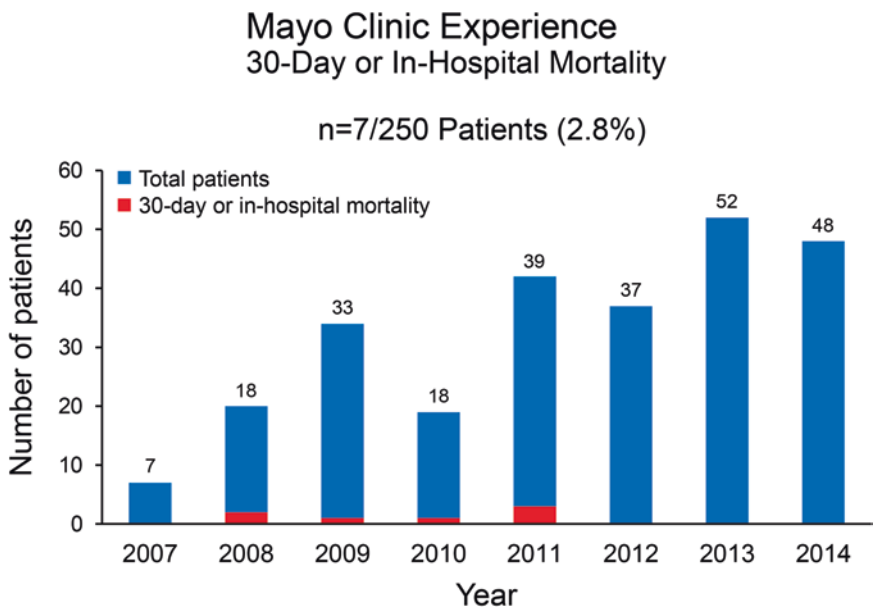


Fig. 15.12 Despite the increase in complexity of repair using more four-vessel fenestrated designs, mortality has decreased over the years. By permission of Mayo Foundation for Medical Education and Research. All rights reserved

also include IDE protocols evaluating outcomes and quality of life measures of patients treated for complex aneurysms, allowing treatment of pararenal and thoracoabdominal aneurysms and dissections with the options of an off-the-shelf multi-branched design (t-branch stent-graft) or custom-made devices with combination of fenestrations and branches. Similar to other centers, we also noted increase in device design complexity (Fig. 15.11) and a trend toward operative mortality in the last few years (Fig. 15.12).

References

1. Haddad F, Greenberg RK, Esteban W, Nally J, O'Neill S, Kolin G, et al. Fenestrated endovascular grafting: the renal side of the story. J Vasc Surg. 2005;41:181–90.
2. O'Neill S, Greenberg RK, Haddad F, Resch T, Sereika J, Katz E. A prospective analysis of fenestrated endovascular grafting: intermediate-term outcomes. Eur J Vasc Endovasc Surg. 2006;32:115–23.
3. Greenberg RK, Haulon S, O'Neill S, Lyden S, Ouriel K. Primary endovascular repair of juxtarenal aneurysms with fenestrated endovascular grafting. Eur J Vasc Endovasc Surg. 2004;27(5):484–91.
4. Greenberg RK, West K, Pfaff K, Foster J, Skender D, Haulon S, et al. Beyond the aortic bifurcation: branched endovascular grafts for thoracoabdominal and aortoiliac aneurysms. J Vasc Surg. 2006;43:879–86.
5. Haulon S, Greenberg RK, Pfaff K, Francis C, Koussa M, West K. Branched grafting for aortoiliac aneurysms. Eur J Vasc Endovasc Surg. 2007;33:567–74.
6. Goel VR, Greenberg RK, Greenberg DP. Mathematical analysis of DICOM CT datasets: can endograft sizing be automated for complex anatomy? J Vasc Surg. 2008;47:1306–12.
7. Mohabbat W, Greenberg RK, Mastracci TM, Cury M, Morales JP, Hernandez AV. Revised duplex criteria and outcomes for renal stents and stent grafts following endovascular repair of juxtarenal and thoracoabdominal aneurysms. J Vasc Surg. 2009;49:827–37.
8. Dowdall JF, Greenberg RK, West K, Moon M, Lu Q, Francis C, et al. Separation of components in fenestrated and branched endovascular grafting—branch protection or a potentially new mode of failure. Eur J Vasc Endovasc Surg. 2008;36(1):2–9.
9. Greenberg RK, Sternbergh C, Makaroun M, Ohki T, Chuter T, Bharadwaj P, et al. Intermediate results of a United States multicenter trial of fenestrated endograft repair for juxtarenal abdominal aortic aneurysms. J Vasc Surg. 2009;50:730–7.
10. Greenberg RK, Eagleton M, Mastracci T. Branched endografts for thoracoabdominal aneurysms. J Thorac Cardiovasc Surg. 2010;140:S171–8.
11. Dijkstra ML, Eagleton MJ, Greenberg RK, Mastracci T, Hernandez A. Intraoperative C arm cone-bean computed tomography in fenestrated/branched endografting. J Vasc Surg. 2011;53:583–90.
12. Panuccio G, Greenberg RK, Wunderle K, Mastracci TM, Eagleton M, Davros W. Comparison of indirect radiation dose estimates with directly measured radiation dose for patients and operators during complex endovascular procedures. J Vasc Surg. 2011;53:885–94.
13. Brown CR, Greenberg RK, Wong S, Eagleton M, Mastracci T, Hernandez AV, et al. Family history of aortic disease predicts disease patterns and progression and is a significant influence on management strategies for patients and their relatives. J Vasc Surg. 2013;58:573–81.
14. Wong S, Greenberg RK, Brown CR, Mastracci TM, Bena J, Eagleton MJ. Endovascular repair of aortoiliac aneurysmal disease with the helical iliac bifurcation device and the bifurcated-bifurcated iliac bifurcation device. J Vasc Surg. 2013;58:861–9.
15. Mohapatra A, Greenberg RK, Mastracci TM, Eagleton MJ, Thornsberry B. Radiation exposure to operating room personnel and patients during endovascular procedures. J Vasc Surg. 2013;58:702–9.
16. Mastracci TM, Greenberg RK, Eagleton MJ, Hernandez AV. Durability of branches and fenestrated endografts. J Vasc Surg. 2013;57:926–33.
17. Oderich GS, Greenberg RK, Farber M, Lyden S, Sanchez L, Fairman R, et al. Results of the United States multicenter prospective study evaluating the Zenith fenestrated endovascular graft for treatment of juxtarenal abdominal aortic aneurysms. J Vasc Surg. 2014; 1420–8.e1–5.

Endovascular Training and Learning Curve for Complex Endovascular Procedures

16

Jesse M. Manunga and Gustavo S. Oderich

Introduction

From its early days of apprenticeship pioneered by Edwin J. Wylie, MD to the recent introduction of the 0–5 integrated training programs, vascular surgical education in the United States has undergone major transformations [1]. Arguably, this evolution has been fuelled by advancements in endovascular therapy. While significant strides have been made in the management of peripheral arterial disease, the most impressive changes have occurred in the management of abdominal and thoracic aortic aneurysms. It is estimated that more than 80 % of all elective abdominal aortic aneurysms in the United States are now repaired by endovascular means [2]. In addition, complex aortic aneurysms involving side branches can now be treated using fenestrations, branches, or parallel grafts. Therefore, the indications of endovascular aortic repair (EVAR) have been broadened to include aneurysms involving the aortic arch, thoracoabdominal aorta, and iliac bifurcation.

As with any new procedure, there is a learning curve associated with mastering the technique. The increasing complexity of fenestrated, branched, and parallel graft techniques requires dedicated training to learn all facets of these procedures from planning, implantation, and follow up. In this chapter, we review the importance of novel training paradigms, learning curve, and factors affecting outcomes of complex endovascular aneurysm repair.

J.M. Manunga
University of Minnesota, Minneapolis, MN, USA

Department of Vascular and Endovascular Surgery,
Abbott Northwestern Hospital/Minneapolis Heart Institute,
920 E 28th Street, Suite 300, Minneapolis, MN 55407, USA
e-mail: Jesse.manunga@allina.com; Jmanunga@gmail.com

G.S. Oderich (✉)
Division of Vascular and Endovascular Surgery, Mayo Clinic,
200 First Street SW, Rochester, MN 55905, USA
e-mail: oderich.gustavo@mayo.edu

Training Paradigms

Since the initial description of EVAR by Juan Parodi and colleagues in 1991, vascular surgeons immediately recognized and embraced endovascular therapy. In the early years, training was in the form of collaboration with other specialties (e.g., interventional radiology, cardiology) and mini-fellowship programs spearheaded by the Society of Vascular Surgery and key pioneering physicians. In the year 2000, the Residency Review Committee in Surgery (RRC-S) approved the incorporation of endovascular therapy in training of vascular surgeons. The committee also set minimum volume requirements for certification in vascular surgery. The introduction of endovascular techniques into the vascular curriculum prompted the addition of an extra year, from 1 to a 2-year program, to the vascular surgery fellowship [1].

Training and credentialing of existing vascular surgeons was another challenge that needed to be addressed. In 1993, the Society for Vascular Surgery/International Society for Cardiovascular Surgery published a document with the recommended number of procedures needed for credentialing existing vascular surgeons. This document, amended in 1998, recommended that a surgeon performed a minimum of 100 catheterizations, 50 angiograms, and 50 interventions [3].

When EVAR was first introduced in the 1990s, most vascular surgeons lacked guide-wire and catheter skills. At most institutions, interventional radiologists performed these procedures and their practices were largely based on referrals by vascular surgeons. The collaboration between the two specialties was a necessity because surgeons were needed to expose the femoral arteries to allow introduction of larger profile devices. Surgeons also served as a “back up” in case of an emergency requiring conversion of the procedure to an open repair and had the knowledge of the pathology accumulated from years of open aortic repairs. Basic EVAR skills were often acquired in industry-sponsored workshops of 2–3

© Mayo Foundation for Medical Education and Research 2017

G.S. Oderich (ed.), *Endovascular Aortic Repair*, DOI 10.1007/978-3-319-15192-2_16

days, which were organized to introduce new devices approved by the FDA. Endovascular experts who pioneered these techniques typically proctored the initial cases and workshops. In less than a decade, vascular surgeons became leaders in endovascular aortic therapy and device development. Several innovations led to improved procedures and expanded indications to a point that over 80 % of aortic aneurysms are currently treated by EVAR in the United States, and most of these procedures are done independently by vascular surgeons [2].

Currently, the Accreditation Council for Graduate Medical Education (ACGME) requires fellows to complete a minimum of 20 endovascular aneurysm repairs, 80 endovascular therapeutic procedures, 100 endovascular diagnostic procedures, 10 complex, 45 peripheral, 25 cerebrovascular, and 30 abdominal procedures in order to graduate the program and sit for qualifying board examination in vascular surgery. However, most programs do not allow adequate experience in complex endovascular techniques with fenestrated and branched endografts because of limited access to these devices. Training in these procedures therefore has been obtained in the form of learning with own experience, workshops, mini-fellowships, and aortic fellowships.

Credentialing Process

The Joint Commission for Accreditation for Health Care Organizations requires every hospital in the United States to delineate specific privileges for each medical staff member. This organization places the onus on hospitals to insure the appropriateness of care delivered by a given physician and emphasizes that there be a mechanism in place to assess new technology before it is incorporated in daily patient care. For EVAR and other surgical procedures, this requires being proctored for a number of cases and deemed competent to perform them without supervision. Additionally, surgeons are given the opportunity to voluntarily report outcomes of procedures as the hospital sees it fit.

Different ways exist of acquiring the skillset needed for credentialing by health care systems. Generally, people graduating from accredited programs already possess the necessary skills. New technologies are learned through supervised preceptorships or postgraduate training courses. The Food and Drug Administration plays an important role in controlling the number of investigators involved in evaluating new technologies, often through the use of physician or industry-sponsored Investigational Device Exemption (IDE). Once the technology is proven safe, effective, and durable, it is then disseminated around with the original investigators serving as preceptors.

Hospital and Surgeon Volume and Outcomes

Patients with complex aortic aneurysms are often elderly and have multiple comorbidities, and operations to treat these aneurysms have been traditionally associated with high morbidity and mortality rates. Patient selection, meticulous technique, and patient care are critical factors determining outcomes. Each of these steps requires a steep learning curve that needs to be mastered; and learning from others is important to avoid “reinventing the wheel” and repeating the same mistakes. The skillset acquired and needed to safely get these patients through various operations serve surgeons well when it comes to learning new technologies. Mastering the necessary skills to perform these procedures require practice, volume, patience, and dedication.

A number of reports have shown the association between surgeon and hospital volume for almost every major operation; the classic examples are CABG, arch reconstructions, aortic aneurysm repair, esophagectomy, duodenopancreatectomy, but even minor operations are affected by volume. Dimick and colleagues reported on outcomes of open AAA repair and found significantly higher mortality in low volume hospitals and for procedures performed by low-volume surgeons (Fig. 16.1). Moreover, in that study the best results were achieved by vascular surgeons as compared to surgeons with cardiac or general surgery training (Fig. 16.2). The impact of hospital and surgeon volume is even greater for repair of TAAAs, with doubling in mortality rates for procedures performed in low volume hospitals and by low volume surgeons (Fig. 16.3). For major procedures, coordinated care involves multiple disciplines including the surgeon, operating room staff, anesthesia, critical care, nursing, and social services. Each of these entities works cohesively to ensure optimal care.

Hockenberry and colleagues analyzed mortality among 27,463 patients undergoing coronary artery bypass grafting (CABG) in Taiwan according to surgeon and hospital volume. High volume surgeons and hospitals had a significantly lower mortality compared to low volume surgeons and hospitals [4]. Lapar et al. examined the effect of surgeon volume on risk-adjusted mortality after off-pump coronary artery bypass grafting using data from the Nationwide Inpatient Sample database. Authors used hierarchic generalized linear regression modeling with spline functions for annual individual operating surgeon volume to assess the relationship between annual surgeon volume and inpatient mortality after adjusting for various confounders. In this study, surgeons who performed more than 50 off-pump coronary artery bypass grafting per year had a significantly lower mortality than their low volume counterparts [5]. Birkmeyer and colleagues used information from the

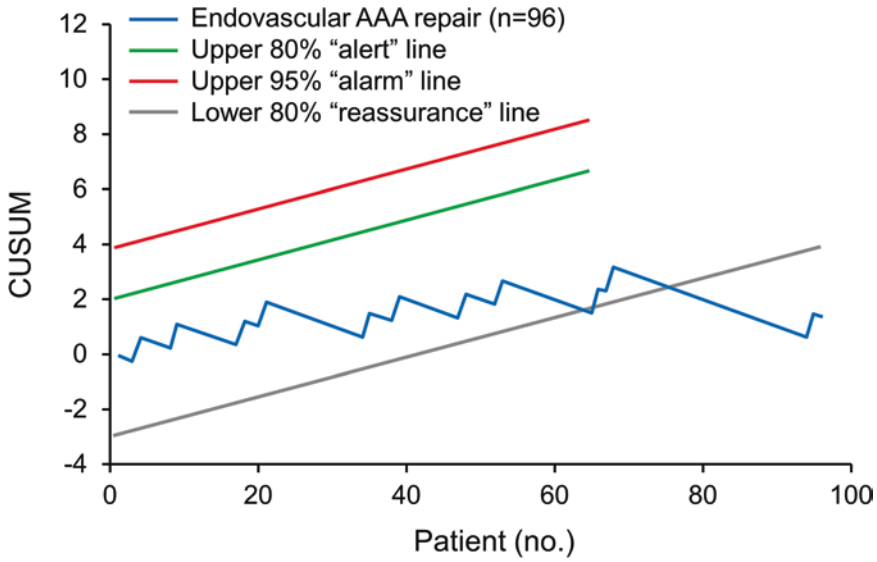


Fig. 16.1 CUSUM analysis of initial clinical success. Note the downward slope of the curve after 60 patients indicating improved outcomes. Based on [18]. By permission of Mayo Foundation for Medical Education and Research. All rights reserved

national Medicare claims database and nested regression models to examine the relationship between surgeon volume and mortality among 474,108 patients who underwent one of eight cardiovascular procedures or cancer resection. Patients undergoing lung resection for cancer, cystectomy, esophagectomy, pancreatic resection, aortic valve replacement, coronary artery bypass grafting, carotid endarterectomy, and abdominal aortic aneurysm repair were analyzed. The authors found that the lower hospital mortality observed at high volume centers was driven primarily by surgeon volume. Analysis by these investigators brought into light the importance of surgeon volume as they concluded "patients can often improve their chances of survival substantially, even at high-volume hospitals, by selecting surgeons who perform the operations frequently" [6]. These findings are not unique to cardiac surgery or procedures reported above. There is a large body of work in the literature supporting similar findings in cancer operations, Whipple procedure and a variety of vascular procedure [7–10].

Failure to Rescue

Ghaferi et al. reviewed outcomes of six different procedures in Medicare patients—pancreatectomy, esophagectomy, abdominal aortic aneurysm repair, aortic valve replacement, mitral valve replacement, and coronary artery bypass grafting. Hospitals performing these procedures were ranked in five groups based on adjusted mortality. Failure to rescue, or the ability to overcome complications after the procedure, was compared between the top 20 % and bottom 20 % hospitals. Authors found a significantly higher failure to rescue rate at bottom tier when compared to top tier hospitals (16.7 % vs. 6.8%) [11]. Without a doubt, top tier hospitals have more resources in terms of specialized services and high technological equipment and training, all of which play an important role in providing patients with the best chance to survive post-operative complications.

Ilonzo and colleagues analyzed 491,779 Medicare patients undergoing elective AAA repair and found that failure to rescue decreased overtime (2.68 % in 2000 and 1.58 % in 2011) was lower in high volume medical centers and was less likely to occur among patients treated by endovascular repair compared to open repair [11].

Learning Curve

Minimally Invasive Cardiovascular Procedures

Learning curve has been studied for a variety of cardiovascular procedures. It is clear that surgeon-team combination plays an important role determining outcomes. And as novel techniques are introduced into the hospital system, time and dedication are needed to overcome the learning curve of these procedures. Holzhey et al. reviewed outcomes of 17 cardiac surgeons performing minimally invasive mitral valve surgery and found that 8 out of 17 surgeons exhibited the classic learning curve where their outcomes improved with increasing experience (Fig. 16.4). The number of cases (75–125) required to reach the turning point varied drastically in this group. In addition, authors found that surgeons who per-

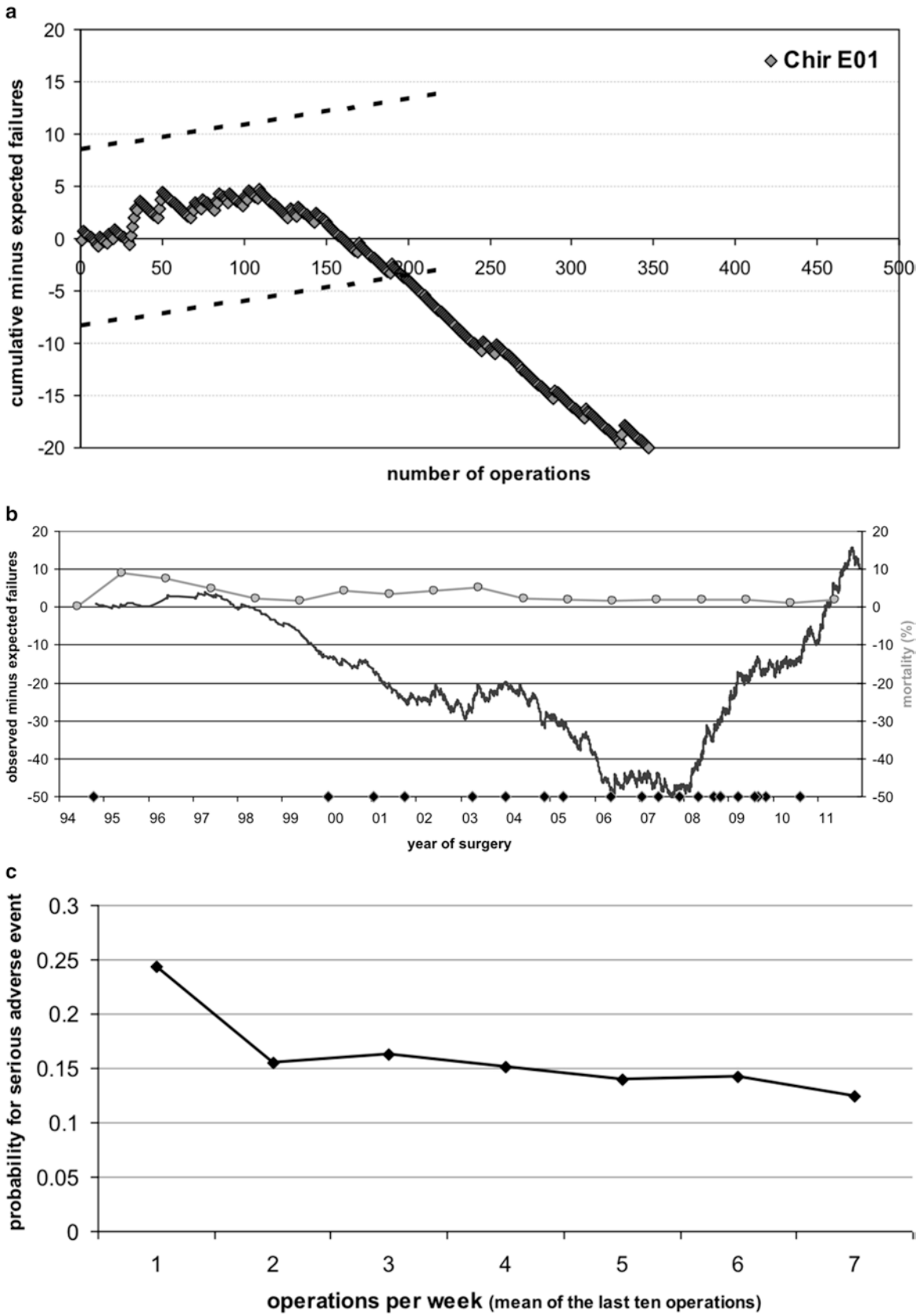


Fig. 16.2 Mortality is affected by surgeon background training and is lower for vascular surgeons in high volume hospitals (**a**). Note the impact of mortality is less for simpler endovascular repairs, but still significantly less for higher volume hospitals (**b**). By permission of Mayo Foundation for Medical Education and Research. All rights reserved. (**a**) Learning curve for 8 of 17 surgeons performing minimally invasive mitral valve surgery at a single institution. Note that complications decreased as experience was gained over time. From Holzhey et al. (**b**) Institutional learning curve for the development of complications in patients undergoing minimally invasive mitral valve surgery. The *gray line* depicts the average mortality per year while the *black dots* on the *x*-axis depict new surgeons being introduced to the group. Note that complications increased with the introductions of new surgeons to the group. From Holzhey et al. (**c**) Dependency of complication rate on operation frequency for a given surgeon performing minimally invasive mitral valve operations. Complications are lower for surgeon performing the procedure more frequently. From Holzhey et al.

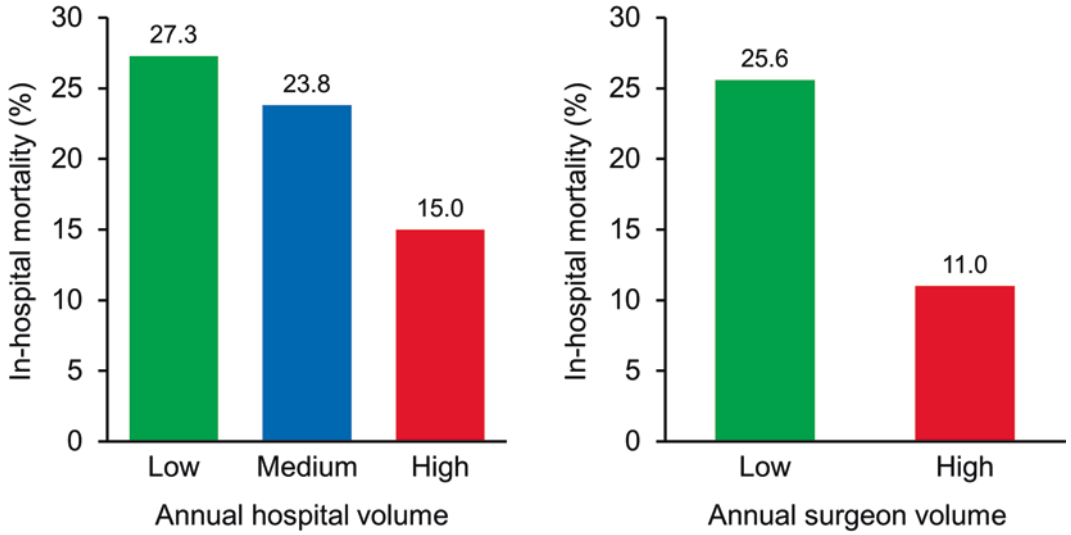


Fig. 16.3 Open TAAA repair mortality is significantly affected by hospital and surgeon volume with nearly doubling in mortality for procedures performed in low volume centers and by low volume surgeons. By permission of Mayo Foundation for Medical Education and Research. All rights reserved

formed the operation at least twice per week had better outcome. While the overall complication rate decreased as experience was gained, there was a spike in complications as new surgeons were added to the group, outlining the importance of learning curve and of a concentrated experience [12].

Since being approved by the Food and Drug Administration (FDA) in November 2011, the number of trans-catheter aortic valve replacement (TAVR) being performed across the United States has increased significantly. The TAVR experience, in more ways than one, parallels that of EVAR techniques and provides large number of procedures for analysis of learning curve. Investigators in the PARTNER-I trail reviewed results of over 1500 patients undergoing trans-femoral TAVR. Authors used institution-specific patient sequence number, interval between procedures and institutional trial entry date to determine the learning curve of technical performance metrics. They found that as the number of cases performed by a given institution increased, the average procedure time and fluoroscopy time decreased significantly. The procedure time plateaued after 25 cases at an average of 83 min per case [13]. Institutions enrolled in the trial at later dates saw a shorter initial procedure time compared to those who enrolled earlier perhaps underlining the value of learning from other people experience. McCarthy et al. recently reported similar outcomes in patients treated by TAVR in clinical trial hospitals compared to those treated at non-trial hospitals [14].

Standard EVAR

The learning curve of EVAR in the 1990s reflected the acquisition of basic guide-wire skills and also the use of first-generation devices that were technically more difficult to manage. While evaluating their experience with the first 277 patients, Lobato and colleagues found that 55 EVARs were needed to obtain optimal results, ideally with less than 10 days between cases [15]. In 2002, Lee and colleagues reported the outcomes of their first 150 EVARs using the AneuRx device (Medtronic, Santa Rosa, CA). In that study, there was no difference in technical success between the early and late experience, but more experienced operators had lower fluoroscopy time and less need for proximal cuff extension and femoral artery reconstructions [16]. The importance of case volume was also reported by the EUROSTAR investigators in 2002. While the rate of aneurysm rupture did not change between teams, more experienced operators had lower mortality and fewer complications necessitating a secondary intervention. The study suggested that surgeon experience with 38 patients was needed to result in lower mortality, and 92 patients to result in less re-interventions [17].

Retrospective studies based on analysis of case volume may not be ideal to evaluate learning curve. Forbes and associates proposed the use of cumulative sum failure method (CUSUM), which factors time and experience, to analyze learning curve using retrospective data. A predetermined acceptable failure rate of 10 % is considered acceptable. The authors found that 60 patients (or 20 using a single device) were needed in order to see improved results with respect to the target failure rate of 10 % [18].

Complex EVAR

Since these early years, vascular surgeons and many vascular specialists have mastered techniques of basic

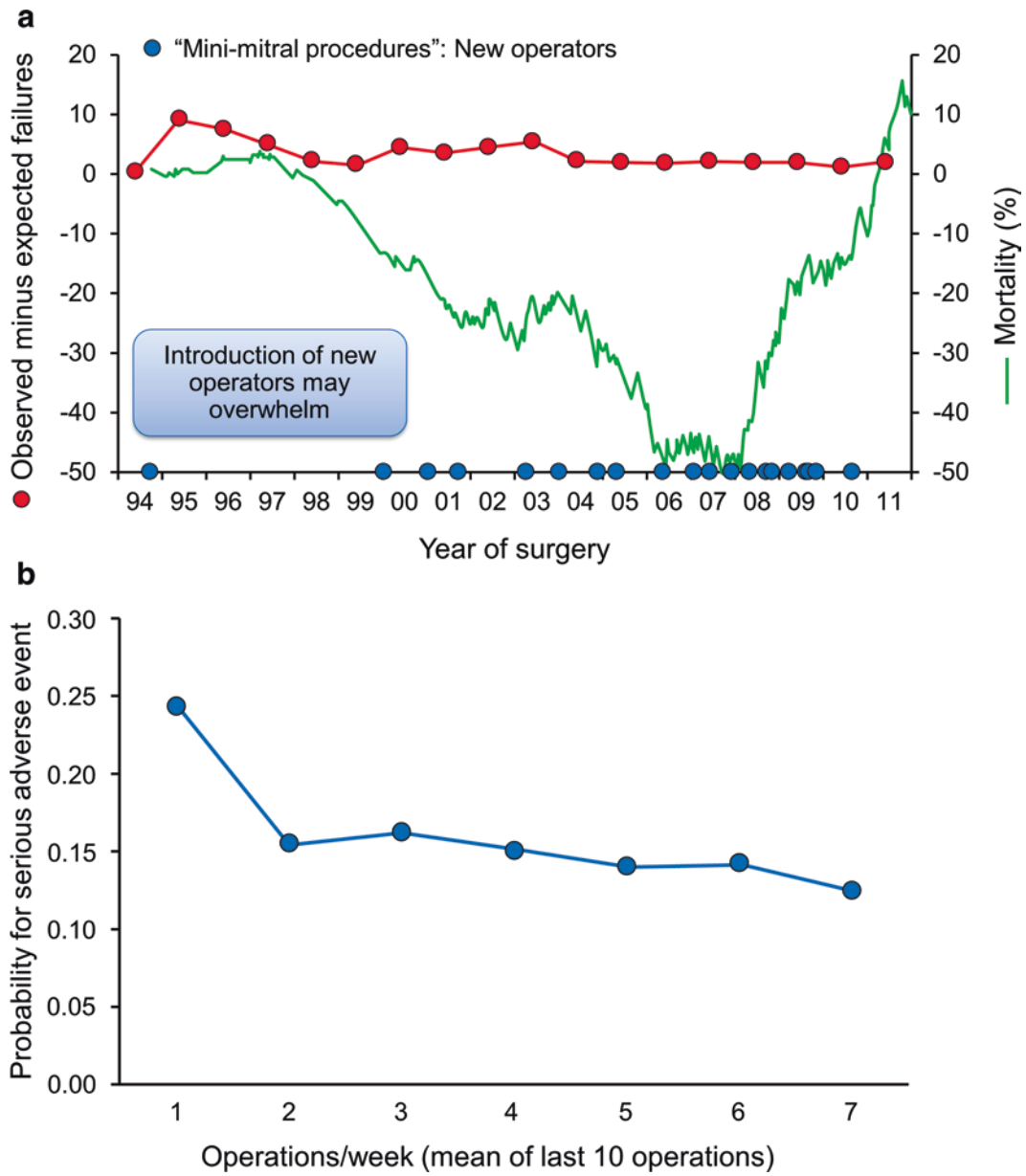


Fig. 16.4 Institutional learning curve for the development of complications in patients undergoing minimally invasive mitral valve surgery. The *green line* depicts the average mortality per year while the *blue dots* on the *x*-axis depict new surgeons being introduced to the group. Note that after improvement in mortality by trained surgeons the mortality increased with the introductions of new surgeons to the group (**a**). Mortality was highly dependent on number of procedures performed weekly (**b**). Based on [12]. By permission of Mayo Foundation for Medical Education and Research. All rights reserved

EVAR. Better patient selection, more refined guide-wire skills, improved imaging and lower profile devices have all played major role in improving outcomes and decreasing conversion rates. In most large center experiences, mortality of EVAR is 0.1–1 %. However, complex aortic procedures require longer operating time and catheter manipulation of multiple vessels, increasing the potential for intra-procedural complications and mortality. Learning these techniques requires at the minimum extensive experience with basic EVAR and TEVAR, renal and mesenteric stenting, and knowledge of "bail out" maneuvers, tips and tricks on how to get out of problems using an endovascular solution. Ideally, surgeons and specialists who want to invest in developing an advanced endovascular program need dedicated training beyond standard EVAR to develop the skills needed in complex techniques. Unfortunately, most start doing cases on their own and learn from mistakes that can potentially be avoided by spending a period of training under experienced

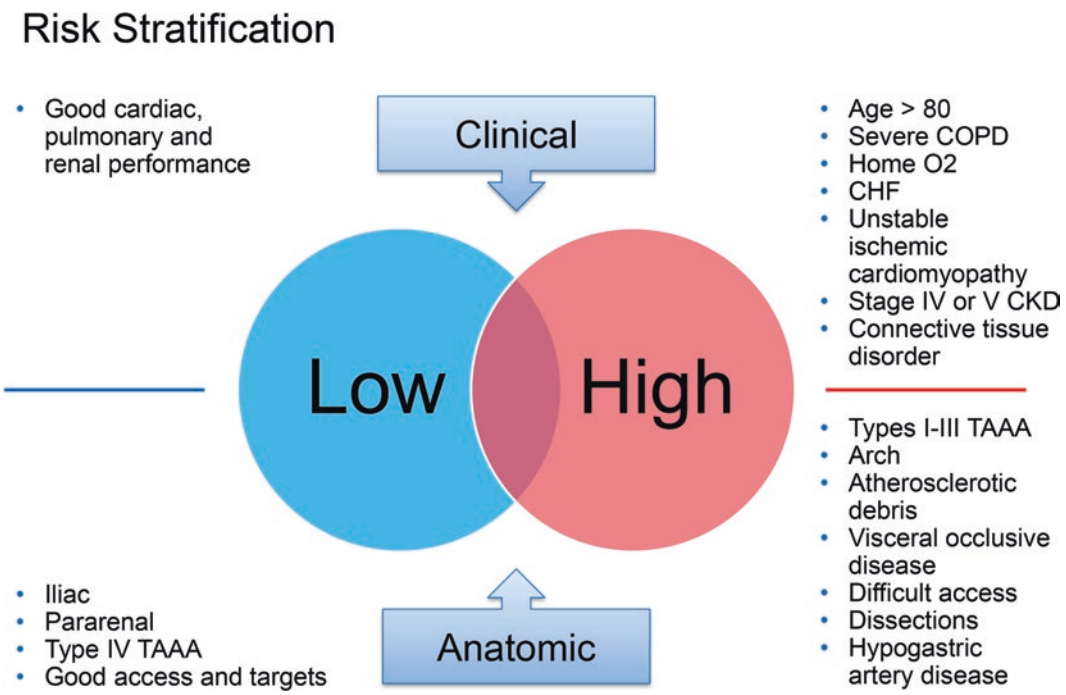


Fig. 16.5 Selection of patients for fenestrated and branched endograft procedures stratified by clinical and anatomical risk. By permission of Mayo Foundation for Medical Education and Research. All rights reserved

operators who already mastered these techniques. It is prudent to start first with lower risk groups (e.g., iliac branch, renal fenestrations, 1–2 vessel incorporation, Figs. 16.4 and 16.5) and then to expand the indications to higher risk groups (e.g., mesenteric fenestrations, 3–4 vessel incorporation and arch). The following are common avoidable problems at the beginning of ones experience with fenestrated and branched endografts:

- Selecting too high-risk patients who have limited life expectancy
- Selecting diseased segments of the aorta to land the graft
- Inadequate use of centerline techniques resulting in errors of graft design
- Inadequate implantation techniques resulting in prolonged lower extremity ischemia and excessive contrast use and catheter manipulation
- Branch-related intra-procedural complications such as vessel perforation or dissections

Fenestrated and Branched Stent-Grafts

The use of fenestrated stent-graft to treat abdominal aortic aneurysm was born in 1999 from the need to expand EVAR indications to patients with short necks and poor infra-renal sealing zones. Over the years, surgeons have grown more confident in their ability to treat patients with complex anatomy and planning these procedures has changed from 1–2 to 3–4 vessel designs. Experience has been gained about the long-term durability of these devices and the most suitable graft configuration needed to treat various anatomies [19, 20].

Roy K Greenberg pioneered several of these techniques and was instrumental in the application of fenestrated and branched endografts to more complex anatomy, development of helical branches and dissemination of the technique via numerous presentations, landmark publications, and training of several physicians. Since 2001, the Cleveland Clinic group has treated over 1100 patients using fenestrated and branched endografts, an experience that is second to none (Fig. 16.6). Dr. Greenberg wrote extensively about the endovascular treatment of aortic aneurysm with these grafts. His contribution to the field of endovascular surgery cannot be overstated and much of what we know today about these devices comes from his experience. Despite the significant clinical experience at the Cleveland Clinic with hundreds of repairs, modifications of the technique in their late experience with the addition of pre-loaded catheters and on lay fusion CT resulted in decrease in operative time, fluoroscopy time, and contrast use (Fig. 16.7a). Operative mortality for most extensive type II TAAA also decreased after the introduction of staged techniques (Fig. 16.7b).

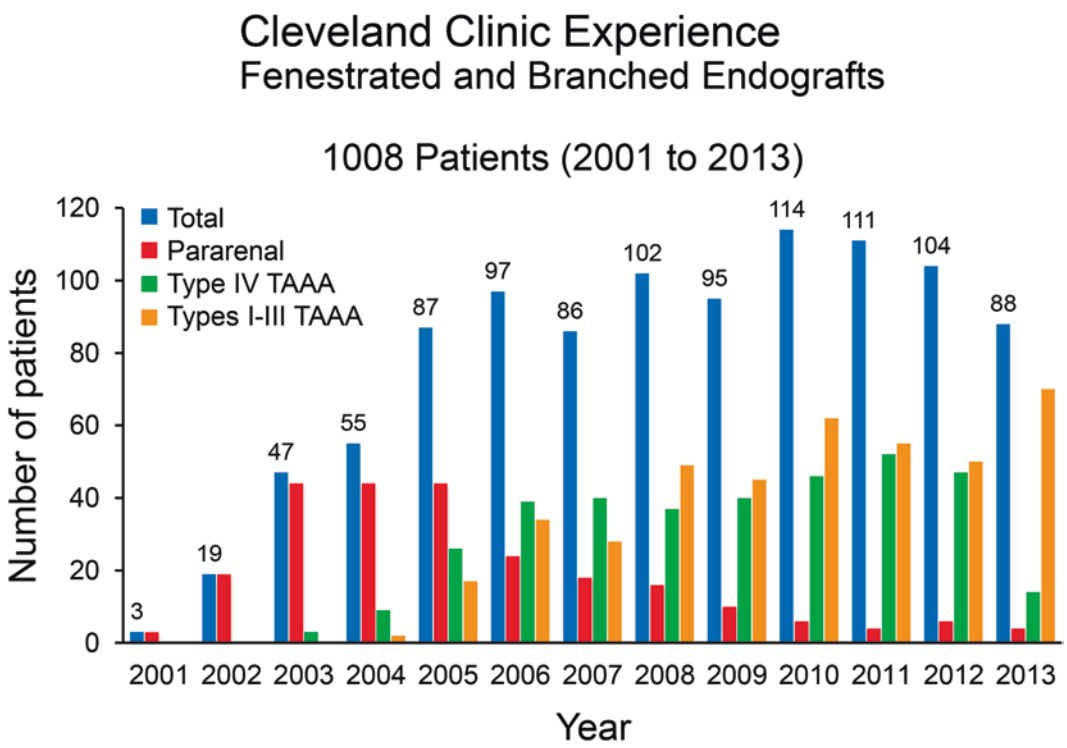


Fig. 16.6 Cleveland Clinic experience with fenestrated and branched endografts from 2001 to 2014. Note increasing complexity of procedures. Courtesy of Dr. Matthew Eagleton

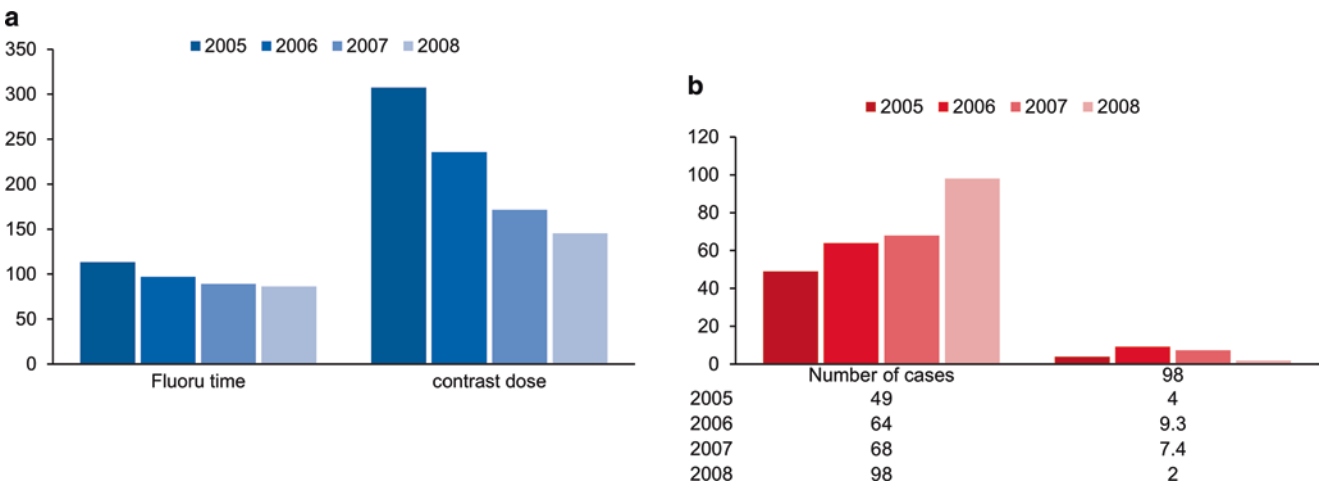
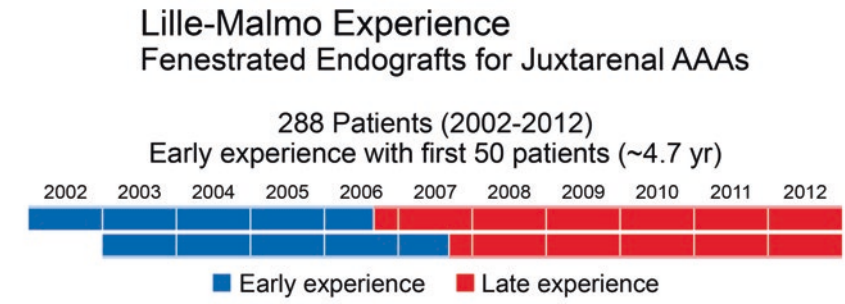


Fig. 16.7 Cleveland Clinic experience with repair of extent II TAAAs. Note decreasing fluoroscopy time and contrast dose (**a**) despite the significant clinical experience. The introduction of staged repairs in 2008 also reduced mortality and paraplegia rates (**b**). Courtesy of Dr. Matthew Eagleton

Timothy Resch and Stephan Haulon recently reported their early and late experiences with fenestrated and branched endografts. The authors used a cutoff of 50 patients per center (100 total patients) in defining early experience and included 188 patients in the late experience (Fig. 16.8). Each center took approximately 5 years to accumulate the first 50 patients. The authors found that complexity (number of fenestrations per patient treated) of cases increased over time while the volume of contrast used and fluoroscopy time decreased significantly with mortality being the same between the two groups [21].

The Mayo Clinic complex endovascular aneurysm program started in 2007 (Table 16.1). To date, approximately 350



	Early experience n=100	Late experience n=188	
Fenestrations	2.7±0.8	3.2±0.8	0.001
2 fen	35	11	
4 fen	7	30	

	Early experience (%) n=100	Late experience (%) n=188	
Fenestrations	2.7±0.8	3.2±0.8	0.001
Fluoroscopy	84 min	65 min	0.05
Contrast volume	254 ml	184 ml	0.05
30-day Mortality (%)	2	2	NS

Fig. 16.8 Learning curve of fenestrated endografts in Malmo and Lille. Based on [21]. By permission of Mayo Foundation for Medical Education and Research. All rights reserved

patients have been treated by fenestrated and branched endografts. An analysis of the first 250 patients included 103 TAAAs, 127 pararenal, and 20 aortoiliac aneurysms. Similar to the experience of Lille-Malmo, the complexity of cases has increased overtime, but mortality, fluoroscopy time, and contrast volume decreased as more experience has been gained (Figs. 16.9). After graduating from the Mayo Clinic program with dedicated aortic training, the author (JM) joined the Abbott Northwestern Hospital and started a fenestrated aortic program on December 17, 2013. A total of 41 patients (36 pararenal, 2 thoracoabdominal, and 3 aortoiliac) have been treated with fenestrated endografts. The average SVS/AAVS comorbid score was 17 [4–10, 13, 14, 19, 20, 22] with 76% of patients having a score of 15 or over. Two-thirds of the patients did not meet the anatomical requirement of >4-mm infra-renal neck for the Zenith fenestrated endograft. Technical success was 100%. A total of 97 vessels (76 renals, 20 SMA, and 1 celiac) were incorporated by fenestrations, with only 2 renal artery occlusions due to inability to place an alignment stent or discontinuation of anti-platelet therapy. One patient required temporary dialysis, with subsequent recovery of renal function. Thirty-day mortality was 2.4%. This occurred in one patient who became paraplegic post procedure and eventually went into multi-system organ failure. With increasing experience, we have noticed a decrease in the amount of contrast, operative, and fluoroscopy time in our own practice. Training in aortic fenestrated and branched procedures at the Mayo Clinic was essential for the successful start of our program.

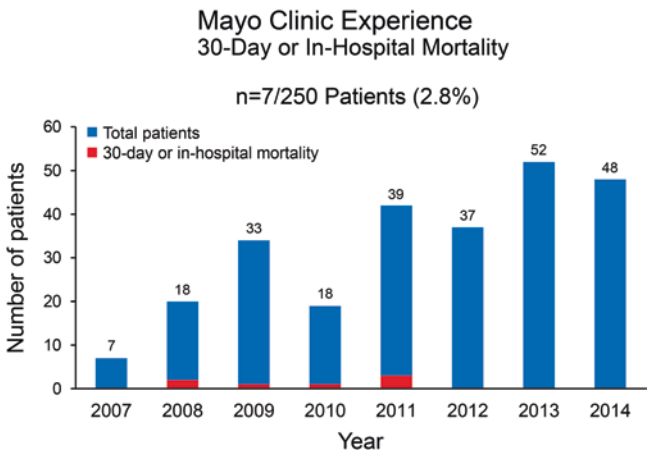


Fig. 16.9 Annual 30-day mortality rate (*red*) in the first 250 fenestrated-branched repairs at the Mayo Clinic. Unpublished data. By permission of Mayo Foundation for Medical Education and Research. All rights reserved

The Washington University group also reported their initial experience with fenestrated endografts. Using linear regression analysis (Lowess smoothing), there was significant reduction in mean operative time from 280 to 140 min (Fig. 16.10) and reduction in fluoroscopy time from 80 to 35 min (Fig. 16.11). Contrast volume also decreased in the first 60 cases, reaching a plateau after that (Fig. 16.12).

Table 16.1 The Mayo Clinic fenestrated experience

	Patient			*P* value
	1–80	81–160	161–240	
Pararenal	80 %	74 %	38 %	0.01
TAAA	30 %	26 %	62 %	0.01
No. of vessels	2.4 ± 1.06	3.04 ± 1.02	3.54 ± 0.75	0.001
2-vessel	50 %	29 %	10 %	0.001
4-vessel	19 %	41 %	65 %	0.001
Fluoroscopy (min)	117 ± 61	84 ± 38	72 ± 23	0.05
Contrast (ml)	237 ± 99	163 ± 73	138 ± 75	0.001
30-Day mortality	5(6 %)	2(3 %)	0	0.12

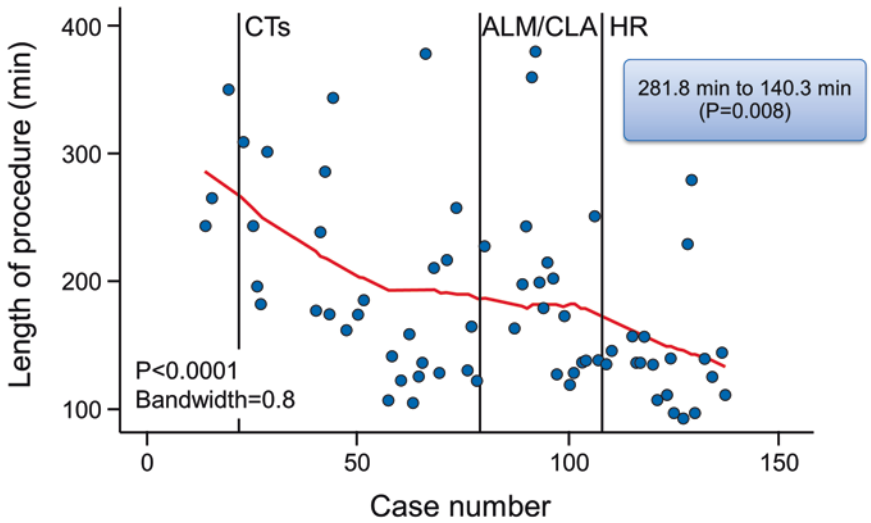


Fig. 16.10 Operative time in three-vessel fenestrated repair at the Washington University. By permission of Mayo Foundation for Medical Education and Research. All rights reserved

The most important lesson from large fenestrated and branched experiences is on the impact of learning curve on graft design and durability (Fig. 16.13). Durability, as defined by prevention of aneurysm rupture and branch-related events, is directed not only to adequate planning of the first procedure but also to routine surveillance and aggressive intervention of endoleaks, branch stenosis, disconnections, and other potential problems. And undoubtedly, durability of fenestrated and branched repair is negatively impacted by progression of aortic disease and device failure. The importance of aortic degeneration is reflected in large experiences by the increasing use of more complex graft designs with three or four vessels (Fig. 16.14). Selection of the supraceliac aorta for landing zone unquestionably provides a more stable repair. Most repair failures and endoleaks start after the third or fifth year of follow-up. The increasing utilization of more complex designs resulted in a significant reduction of endoleaks and endoleak-related re-interventions (Fig. 16.15) [23].

Conclusion

Vascular surgery has emerged as one of the most rapidly changing field in medicine, largely due to the embracement, by vascular surgeons of endovascular therapy. With increased longevity, it is safe to assume that vascular surgeons will be called upon to treat patients with increasing comorbidities.

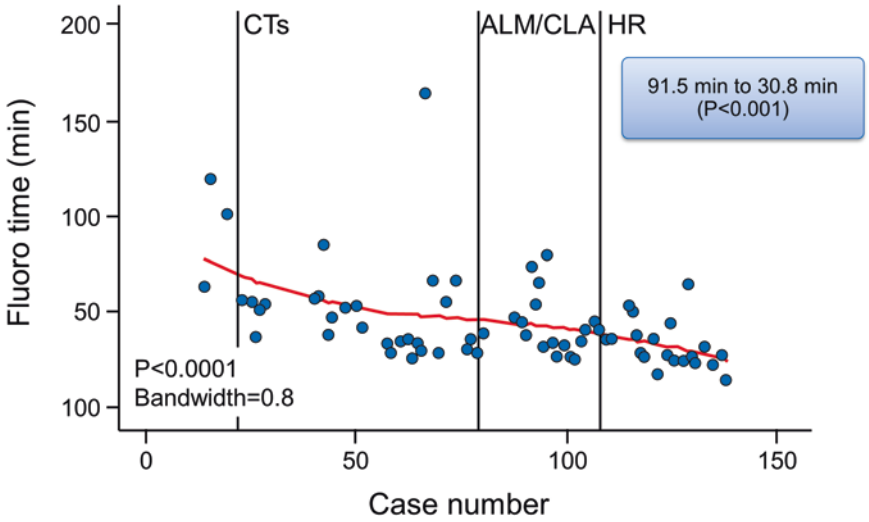


Fig. 16.11 Fluoroscopy time in three-vessel fenestrated repair at the Washington University. By permission of Mayo Foundation for Medical Education and Research. All rights reserved

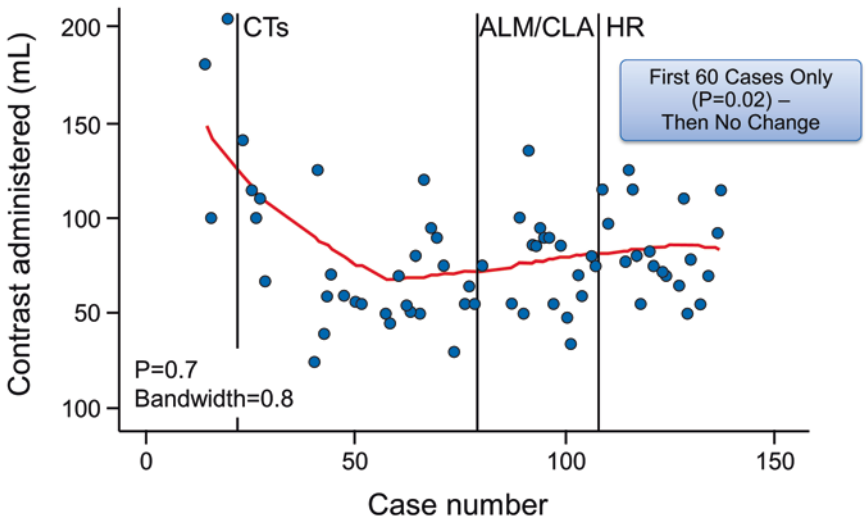


Fig. 16.12 Contrast dose in three-vessel fenestrated repair at the Washington University. By permission of Mayo Foundation for Medical Education and Research. All rights reserved

Surgeons will undoubtedly rely heavily on endovascular therapy to manage fragile patients with complex aneurysms. Fenestrated stent-grafts have emerged as an acceptable alternative to open surgical repair and is posed to become the standard of care in a very foreseeable future. Even with this minimally invasive approach, complications are bound to happen. When they do, experience predicts that patients who have their procedures performed by high volume surgeons at high volume hospitals will tend to have better outcomes, underlining the importance of multidisciplinary approach to the management of the aging vascular patient.

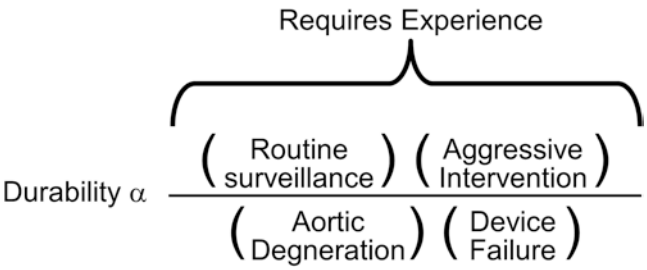


Fig. 16.13 Durability equation. Courtesy of Dr. Tara Mastracci

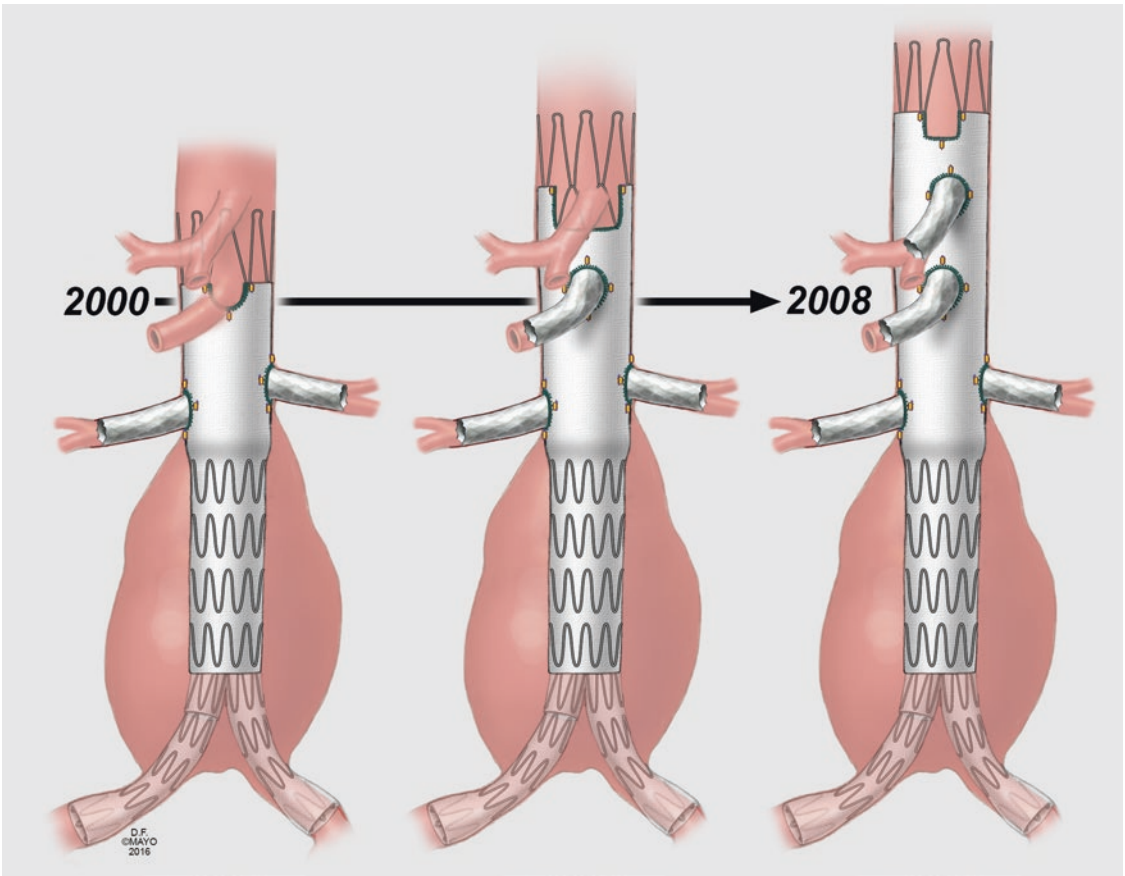


Fig. 16.14 Increasing complexity of endovascular repairs to improve durability. By permission of Mayo Foundation for Medical Education and Research. All rights reserved

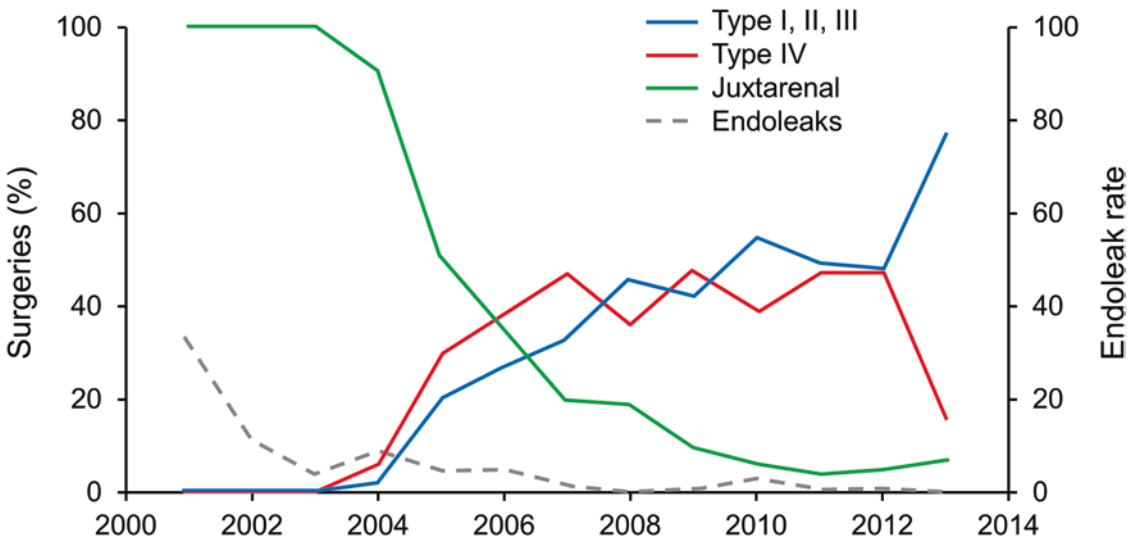


Fig. 16.15 Decline in endoleak rates with more complex repairs. Based on [23]. By permission of Mayo Foundation for Medical Education and Research. All rights reserved

References

1. Mills JL. Vascular surgery training in the United States: a half-century of evolution. J Vasc Surg. 2008;48:90S–7.
2. Lederle FA, Freichlag JA, Kyriakides TC, Matsumura JS, Padberg Jr FT, Kohler TR, et al. Long-term comparison of endovascular and open repair of abdominal aortic aneurysm. N Engl J Med. 2012;367:1988–97.
3. White RA, Hodgson KJ, Ahn SS, HobsonII RW, Veith FJ. Endovascular interventions training and credentialing for vascular surgeons. J Vasc Surg. 1999;29:177–86.
4. Hockenberyy JM, Lien HM, Chou SY. Surgeon and hospital as quality indicators for CAGB in Taiwan: examining hazard to mortality and accounting for unobserved heterogeneity. Health Serv Res. 2010;45:1168–87.
5. Lapar DJ, Mery CM, Kozower BD, Kern JA, Kron IL, Stukenborg GJ, Ailawadi G. The effect of surgeon volume on mortality for off-pump coronary artery bypass grafting. J Thorac Cardiovasc Surg. 2012;143:854–63.
6. Birkmeyer JD, Stukel TA, Siewers AE, Goodney PP, Wennberg DE, Lucas FL. Surgeon volume and operative mortality in the United States. N Engl J Med. 2003;349:2117–27.
7. Siemens DR, Mackillop WJ, Peng Y, Berman D, Elharram A, Rhee J, Booth CM. Processes of care and the impact of surgical volumes on cancer-specific survival: a population-based study in bladder cancer. Urology. 2014;84(5):1049–57.
8. Enomoto LM, Gusani NJ, Dillon PW, Hollenbeak CS. Impact of surgeon and hospital volume, length of stay, and cost of pancreaticoduodenectomy. J Gastrointest Surg. 2014;18(4):690–700.
9. Dardik A, Lin JW, Gordon TA, Williams GM, Perler BA. Results of elective abdominal aortic aneurysm repair in the 1990s: a population-based analysis of 2335 cases. J Vasc Surg. 1999;30:985–95.
10. Tu JV, Austin PC, Johnston KW. The influence of surgical specialty training on the outcomes of elective abdominal aortic aneurysm surgery. J Vasc Surg. 2001;33(3):447–52.
11. Ilonzo N, Egorova NN, Mckinsey FJ, Nowygrod R. Failure to rescue trends in elective abdominal aortic aneurysm repair between 1995 and 2011. J Vasc Surg. 2014;60:1473–80.
12. Holzhey MD, Seeburger J, Misfeld M, Borger AM, Mohr WF. Learning minimally invasive mitral valve surgery: a cumulative sum sequential probability analysis of 3895 operations from a single high-volume center. Circulation. 2013;128:483–91.
13. Alli O, Rihal CS, Suri RM, Greason KL, Waksman R, Minha S, Torguson R, Pichard AD, et al. Learning curves for transfemoral transcatheter aortic valve replacement in the PARTNER-I trial: technical performance. Catheter Cardiovasc Interv. 2016;87(1):154–62. doi:10.1002/ccd.26120.
14. McCarthy FH, Groeneveld PW, Kobrin D, McDermott KM, Wirtalla C, Desai ND. Effect of clinical trial experience on transcatheter aortic valve replacement outcomes. Circ Cardiovasc Interv. 2015;8(9). pii: e002234.
15. Lobato AC, Rodiguez-Lopez J, Diethrich EB. Learning curve for endovascular abdominal aortic aneurysm repair: evaluation of a 277 patient single-center experience. J Endovasc Ther. 2002;9:262–8.
16. Lee WA, Wolf YG, Hill BB, Cipriano P, Fogarty TJ, Zarins CK. The first 150-endovascular AAA repairs at a single institution: how steep is the learning curve? J Endovasc Ther. 2002;9:269–76.
17. Laheij RJF, van Marrewijk CJ, Buth J, Harris PL. The influence of team experience on outcomes of endovascular stenting of abdominal aortic aneurysms. Eur J Vasc Endovasc Surg. 2002;24:128–33.
18. Forbes LT, DeRose G, Kribs WS, Harris AK. Cumulative sum failure analysis of the learning curve with endovascular abdominal aortic aneurysm repair. J Vasc Surg. 2004;39:201–8.
19. Mastracci TM, Greenberg RK, Eagleton MJ, Hernandez AV. Durability of branches in branched and fenestrated endografts. J Vasc Surg. 2013;57:926–33; discussion 933.
20. Verhoeven EL, Vouliotakis G, Bos WT, Tielliu IF, Zeebregts CJ, Prins TR, et al. Fenestrated stent grafting for short-necked and juxtarenal abdominal aortic aneurysm: an 8-year single-centre experience. Eur J Vasc Endovasc Surg. 2010;39:529–36.
21. Sveinsson M, Sobocinski J, Resch T, Sonesson B, Dias N, Haulon S, Kristmundsson T. Early versus late experience in fenestrated endovascular repair for abdominal aortic aneurysm. J Vasc Surg. 2015;61:895–901.
22. Mastracci MT, Eagleton JM, Kuramochi Y, Bathurst S, Wolski K. Twelve-year results of fenestrated endografts for juxtarenal and group IV thoracoabdominal aneurysms. J Vasc Surg. 2015;61:355–64.
23. O'Callaghan A, Greenberg RK, Eagleton JM, Bena J, Mastracci MT. Type Ia endoleaks after fenestrated and branched endografts may lean to component instability and increased aortic mortality. J Vasc Surg. 2015;61:908–14.
24. Mell WM, Bartels C, Kind A, Smith AM. Failure to rescue: physician specialty and mortality after reoperation for abdominal aortic aneurysm (AAA) repair. J Vasc Surg. 2011;54:346–52.
25. Ghaferi AA, Birkmyer JD, Dimick JB. Complications, failure to rescue, and mortality with major inpatient surgery in Medicare patients. Ann Surg. 2009;250:1029–34.

17 Regulatory Pathway for Physician-Sponsored Studies Evaluating Endovascular Aortic Repair

Dorothy Abel, Karen Ulisney, Fabienne J. Santel, and Jose Pablo Morales

Introduction

Access to new technology in the US is often achieved through participation in clinical studies. 21 CFR Part 812, the Investigational Device Exemptions (IDE) regulations, applies to these clinical studies or investigations, with submission of an IDE application required for the study of a significant risk device. The purpose of these regulations is to encourage development of useful devices while providing protection of public health and safety. An approved IDE exempts sponsors from certain provisions of the Food Drug & Cosmetic Act for the purpose of conducting a clinical investigation, for example, the requirement to have premarket approval to allow for lawful shipment of a device for the purpose of conducting a clinical investigation.

An IDE can be sponsored by a manufacturer or by an individual physician (termed sponsor-investigator or SI). For an SI IDE, the physician usually authors and will assume the responsibilities of both the sponsor and the primary investigator. These responsibilities include submission of the IDE application, oversight of data collection and reporting, appropriate study monitoring, and obtaining regulatory approval (http://www.fda.gov/MedicalDevices/DeviceRegulationandGuidance/HowtoMarketYourDevice/InvestigationalDeviceExemptionIDE/ucm046702.htm).

There are multiple advantages of conducting SI IDE studies. Compliance with FDA's IDE regulations provides enhanced protection of the rights, safety, and welfare of study subjects. SI IDEs often treat patients that are not included in industry-sponsored IDEs, and these studies can advance treatment by capturing information that can be used to improve procedures and encourage device innovation in collaboration with industry partners. Also, since SI IDE studies collect patient-level data, SI IDE studies may be used to develop performance goals for industry-sponsored studies or can provide supportive data for a marketing application.

This chapter provides a general overview of the IDE regulations and the processes for IDE preparation, application, and conduct for physicians who are considering sponsoring an IDE with the intent to: (1) explain when an IDE is needed; (2) assist in the preparation and submission of an IDE application, and (3) clarify the responsibilities of sponsor-investigators. The information included in this chapter reflects past and current experiences with endovascular graft SI IDEs and information regarding good clinical practices and human subject protections as applied to these studies. This chapter is not intended to provide official FDA regulatory guidance.

When Is an IDE Needed?

The IDE regulations apply to clinical investigations to evaluate the safety and effectiveness of medical devices. Submission of an IDE may be needed for a clinical study depending on the device's approval status; the intended clinical use; and whether it is a significant risk or non-significant risk device.

The clinical study of a legally marketed device (e.g., an approved device) *may be* subject to the IDE regulations; the study of a device that is not marketed in the US *is always* subject to the IDE regulations because an IDE is the primary

D. Abel • J.P. Morales (✉)
Division of Cardiovascular Devices, Office of Device Evaluation, Center for Devices and Radiological Health, United States Food and Drug Administration, 10903 New Hampshire Avenue, Silver Spring, MD 20993, USA
e-mail: Dorothy.Abel@fda.hhs.gov; Jose.Morales@fda.hhs.gov

K. Ulisney
Clinical Trials Program, Office of Device Evaluation, Center for Devices and Radiological Health, United States Food and Drug Administration, 10903 New Hampshire Avenue, Silver Spring, MD 20993, USA
e-mail: Karen.Ulisney@fda.hhs.gov

F.J. Santel
Office of Compliance, Center for Devices and Radiological Health, United States Food and Drug Administration, 10903 New Hampshire Avenue, Silver Spring, MD 20993, USA
e-mail: Fabienne.Santel@fda.hhs.gov

© Mayo Foundation for Medical Education and Research 2017

G.S. Oderich (ed.), *Endovascular Aortic Repair*, DOI 10.1007/978-3-319-15192-2_17

mechanism to obtain access to a device that is not legally marketed in the US.

Some studies are exempted from the IDE regulations, for example, the study of a marketed device that is being used in accordance with its labeling. If a study is not exempted from the IDE regulations, a determination as to whether it is a significant risk device is needed, as non-significant risk (NSR) device studies do not need an IDE application submitted to FDA. A NSR device is considered to have an approved IDE after being granted Institutional Review Board (IRB) approval and the SI follows the abbreviated IDE regulations.

A significant risk device may be an implant; a life-supporting or life-sustaining device; or a device of substantial importance in diagnosing curing, mitigating, or treating disease, or in otherwise preventing impairment of human health. Thus, significant risk devices are those that present the potential for serious risk to the health, safety, or welfare of a subject. A clinical study of a significant risk device that is subject to the IDE regulations (i.e., that is not exempt) requires prior FDA approval, through the submission of an IDE application to FDA, and IRB approval before initiating study subject enrollment.

Figure 17.1 summarizes when an IDE is needed. Any time a physician is systematically collecting safety or effectiveness data on a device (i.e., conducting a clinical study), the applicability of the IDE regulations and the need for an IDE must be considered. The IDE regulations apply to clinical studies or investigations of safety and effectiveness of all devices that are not legally marketed in the US and studies of marketed devices that are not exempted from the IDE regulations. Submission of an IDE application to FDA is needed for all significant risk studies that are subject to the IDE regulations. With respect to endovascular grafts, by definition all are categorized as significant risk devices and their clinical investigation to evaluate safety and effectiveness in the US requires an approved IDE and IRB approval if the studies are not exempted from the IDE regulations [1].

Content of an IDE Application

In order to gain FDA approval of an IDE, an investigator must provide adequate information to justify the proposed study, including, but not limited to reports of prior investigations of the device and an explanation as to how risks to the subjects will be minimized. The clinical protocol should also be designed to collect valid scientific evidence. Additional information is needed to ensure that the investigator will generate appropriate records and reports, distribution of the investigational device will be controlled, the study will be adequately monitored, and informed consent will be obtained from all subjects participating in the clinical study.

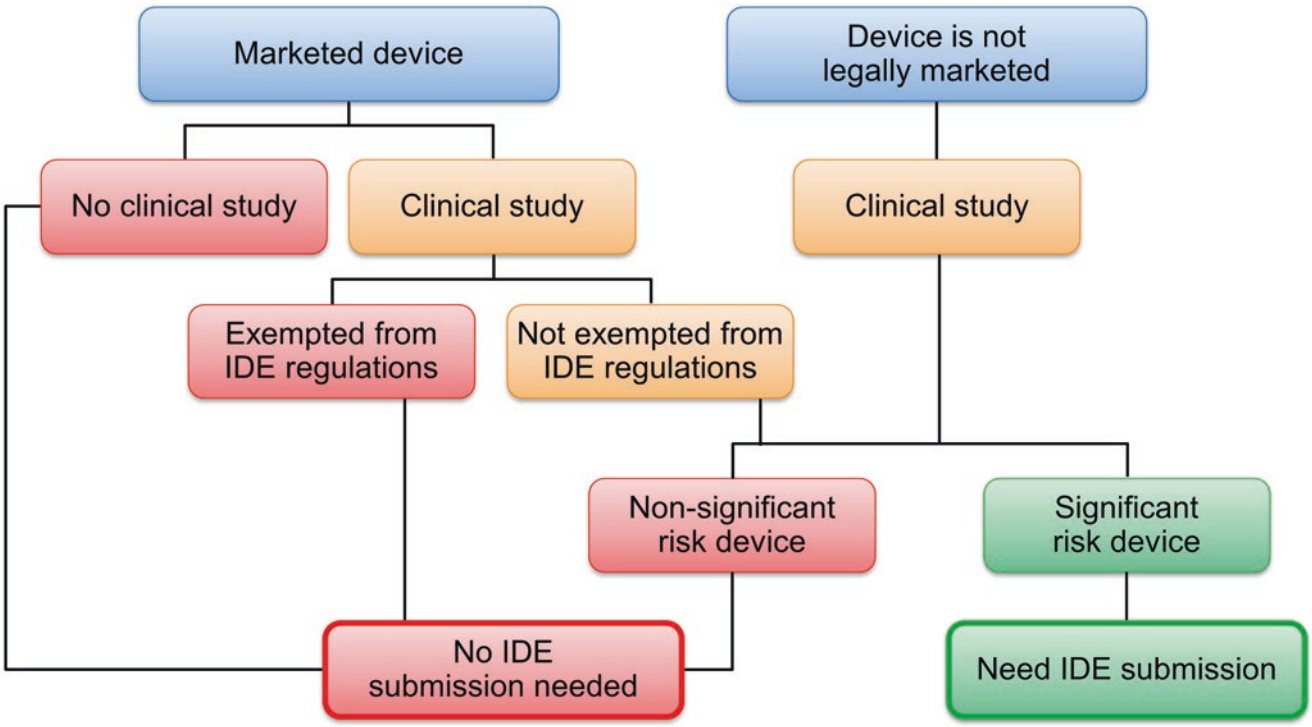


Fig. 17.1 When an IDE submission is needed

Table 17.1 Example of basic content for an SI IDE

1. Cover letter requesting to initiate a study
(a) Statement that it is an original IDE application
(b) Type of study
• Feasibility
• Pivotal
• Other study requiring IDE
(c) Study title
(d) Indications for use
• Type of lesions to be treated
• Extent of aorta to be treated
• Anatomical limitations
(e) Devices to be used
• Whether devices will be modified by the physician
• Manufacturer names and addresses
(f) Risk level of study subjects (e.g., standard risk, high risk)
(g) Number of sites and study subjects
(h) Pre-submission number (if applicable)
(i) Referenced files
(j) Contact information for all persons who may be contacted regarding the IDE (e.g., study sponsor, study coordinator, manufacturer representative)
(k) Attach the CDRH Premarket Review Submission Cover Sheet[a]
2. Table of contents
3. Cover sheet with basic information
(a) Study title
(b) Name and address of sponsor
(c) Contact information
(d) Investigational device(s)
(e) Intended use
(f) Study monitor
4. Report of Prior Investigations (§ 812.27)
5. Investigational Plan (§812.25)
6. Manufacturing information
7. Certification of investigators (or certification that all investigators will sign the investigator agreement)
8. Reviewing Institutional Review Board information
9. Device charges (i.e., the amount, if any, to be charged for the device and an explanation of why sale does not constitute commercialization)
10. Labeling (§ 812.5)
11. Appendices
(a) Copies of relevant references
(b) Test reports (if applicable)
(c) Investigator agreement (§ 812.43)
(d) Case report forms
(e) Draft informed consent form (21 CFR 50, Protection of Human Subjects)

[a]See the following link for a copy of the form: http://www.fda.gov/downloads/AboutFDA/ReportsManualsForms/Forms/UCM080872.pdf

The complete list of information that must be included in an IDE application for the investigation of a significant risk device is outlined in the IDE regulations (21 CFR 812.20, available on the FDA website at http://www.fda.gov/MedicalDevices/DeviceRegulationandGuidance/HowtoMarketYourDevice/InvestigationalDeviceExemptionIDE). Table 17.1 provides an example of the basic contents for an SI IDE for the evaluation of an endovascular graft, based on prior IDE submissions.

Additional information regarding the key elements for an endovascular graft SI IDE follows.

The Report of Prior Investigations (RPI) includes reports of all relevant nonclinical and clinical testing of the device(s), and a description of any additional information intended to support study initiation and as outlined in the IDE regulations (21 CFR 812.27). Based on prior reviews of SI endovascular graft IDEs, the justification for the study may include the clinical expertise of the individual submitting the IDE, historical information on the development of the techniques proposed, and a description of the benefits and risks of alternative treatment options. Clinical mitigation strate-

gies (i.e., strategies included in the clinical protocol intended to minimize the frequency or severity of potential adverse events) have also been critical to support the study, particularly when limited nonclinical testing is available, consistent with the guidance provided in the Early Feasibility Study Guidance. As for all IDEs, the rationale for the conduct of the study should be tailored to the specific patient population to be enrolled, for example, patients at high risk for complications if treated with open surgical repair.

Examples of valuable information that has been submitted in the RPI specific to a proposed investigation include background information on the lesions to be treated and the alternative treatment options for the patients to be enrolled in the study, including the anatomy and pathophysiology and the benefits and risks of alternative treatments. As for all IDEs, the RPI should be specific to the patients to be enrolled, providing a justification for the subject selection criteria. An RPI for an SI IDE has historically included the investigator's experience and training, which can be described, along with the experience and support capabilities of the investigational site. A detailed description of the proposed device has helped to explain the applicability of any previous evaluations to the proposed study, with reference to regulatory submissions for nonclinical testing information and any prior clinical use of the device helping to describe the potential benefits and risks of the study device(s). This approach is consistent with the use of master files to support a study submitted by someone other than the owner of the master file. Particularly for early feasibility studies, and consistent with that guidance, clinical mitigation strategies have been described to help explain how the risks may be mitigated in the clinical study. It has been beneficial for the RPI to be wrapped up with a synopsis of the information available to support study initiation.

The clinical protocol for an SI endovascular graft IDE should contain information similar to that provided under manufacturer-sponsored IDEs. For an SI IDE, it has been helpful to be clear and consistent on the following aspects throughout the IDE submission:

- The patients to be enrolled in the study (e.g., suitable candidates for open surgical repair, at elevated risk of morbidity and mortality with open surgical repair);
- The lesion types to be treated (e.g., aneurysm, acute dissections, chronic dissections);
- The location and extent of aorta that may be treated (e.g., juxtarenal, pararenal, paravisceral, types of thoracoabdominal aneurysms);
- All devices to be used in the study (e.g., devices used in constructing the modified endovascular graft, covered stents, bare stents) and how the endovascular graft will be modified, if applicable;
- The anatomical limitations for the devices to be used (e.g., minimum length of landing zones, minimum and maximum vessel diameters, allowed angulation);
- The duration of the study (most endovascular graft IDEs specify 5-year follow-up for each patient);
- The potential risks that may be associated with the treatment and how the risks will be minimized; and
- The data to be captured, differentiating between protocol-required data and optional information.

The informed consent document for an SI IDE study as required by 21 CFR Part 50 Subpart B, Informed Consent of Human Subjects can be found in http://www.fda.gov/RegulatoryInformation/Guidances/ucm404975.htm. For these studies, it has been particularly important for prospective study subjects to be informed of potential benefits and risks that may be associated with study participation and that there could be unforeseeable risks due to limitations in available data and experience with the device. The benefits and risks associated with the standard of care (e.g., open surgical repair) should also be addressed.

Incorporation of appropriate monitoring and oversight will be important and may include the use of a clinical events committee and a data and safety monitoring board. Detailed information regarding the data monitoring committee may be found in FDA's Guidance for Clinical Trial Sponsors, The Establishment and Operation of Clinical Trial Data Monitoring Committees for Clinical Trial Sponsors, published in March 2006 (http://www.fda.gov/RegulatoryInformation/Guidances/ucm127069.htm).

How to Apply for an IDE?

Information on how to prepare and submit an IDE application as outlined in the IDE regulations can be found at http://www.fda.gov/MedicalDevices/DeviceRegulationandGuidance/HowtoMarketYourDevice/InvestigationalDeviceExemptionIDE/ucm046164.htm. The preparation of an IDE application and the conduct of an IDE study can be challenging, requiring a skilled research staff. Consultation with the device manufacturer and physicians who have experience with the IDE process may be helpful. In addition, it is recommended that a sponsor-investigator interact with the FDA through the Pre-Submission process when preparing the IDE application. This process allows for discussion and feedback from FDA to address key components that need to be included or revised in the IDE submission regarding nonclinical and clinical testing strategies, study design, or application preparation. Information on the pre-submission process may be found in the guidance "Medical Devices: The Pre-Submission Program and Meetings with FDA Staff" at http://www.fda.gov/downloads/MedicalDevices/DeviceRegulationandGuidance/GuidanceDocuments/UCM311176.pdf.

Please note that an electronic copy (eCopies) will be required for a Pre-Submission or an IDE. See the following link for gen-

eral guidance on the preparation of eCopies: http://www.fda.gov/MedicalDevices/DeviceRegulationandGuidance/HowtoMarketYourDevice/ucm370879.htm.

Common Mistakes Identified During Review of IDEs

Avoiding the frequently made mistakes in drafting an IDE can reduce delays in obtaining IDE approval. One of the most common mistakes is a lack of consistency throughout the IDE application (e.g., in the RPI, clinical protocol, and case report forms). For example, the RPI may support the use of the device in patients with juxtarenal aortic aneurysm; however, the eligibility criteria outlined in the investigational plan include patients with other aortic pathologies (e.g., dissections).

Sponsor-investigators often only identify the branched or fenestrated aortic component as the investigational device. For any IDE, however, devices not being used in accordance with their labeling need to be identified and addressed as investigational devices. As the use of multiple devices (e.g., renal or superior mesenteric artery stents) is required to complete an endovascular repair, all devices intended to be used during the procedure need to be specified as investigational devices. The use of each device needs to be justified in the RPI and appropriate information captured on the case report forms regarding the device use and performance.

Endovascular repair of complex aortic aneurysms often requires extensive aortic coverage and staged procedures may be used to decrease the incidence of paraplegia [2]; however, staging is often not addressed in the IDE. For any IDE, it is necessary to clearly describe the procedure and address any associated risks. Based on experience with previous SI IDEs, this would include staged procedures and therefore, to appropriately evaluate the potential benefits and risks associated with the endovascular treatment, considerations for staging and capturing data on the complete repair (i.e., both procedures) or incomplete repair (i.e., if the second procedure could not be performed) should be incorporated in the clinical protocol, case report forms, and informed consent form. Particularly for an early feasibility study, the use of staged procedures may also be identified as a risk mitigation strategy for paraplegia.

Another common mistake seen with SI IDEs is being too prescriptive which can lead to protocol violations. Since the devices used under SI IDE often have endovascular grafts tailored to the patient anatomy and pathology, and there is significant variability from patient to patient, it may be beneficial to be less prescriptive (e.g., include options when possible and appropriate for both the devices to be used and the procedures for placing the devices). For example, a sponsor could propose that the selection criteria allow for the use of a vascular conduit for access, rather than only requiring a specific access vessel size. As for any IDE, to avoid protocol deviations, it is helpful to distinguish between data that are required to monitor patient safety and device performance under the IDE from additional information that may be of interest to capture.

With the intent to offer patients specialized and personalized medical care, sponsor-investigators tend to be overly ambitious with their proposed clinical studies. For example, the IDE may request a large number of patients, when adequate information is only available to justify a smaller initial study. Commonly an SI will not propose to start with patients that do not have good treatment options or will not include strategies to minimize risks by starting with less complicated anatomies and expanding treatment to more complex anatomies after successful treatment of the first patients. As for any IDE, it is important for IDE applicants to be able to justify their proposed study, which may involve presenting a conservative approach to enrolling subjects under their IDE. Notably, supplements can be submitted to an IDE to modify or expand the clinical study (e.g., patient selection criteria and numbers) after information is available to support the proposal.

Finally, delays can be minimized when sponsor-investigators submit their IDE application after the spelling, grammar, formatting, and consistency are properly checked.

What It Takes to Run an IDE

Overview of Good Clinical Practices

FDA regulations that apply to the conduct of clinical investigations are based on the principles of Good Clinical Practices (GCP). Even beyond FDA, GCPs are the foundation upon which clinical investigations are developed and executed worldwide. Therefore, as a sponsor-investigator, a clear and thorough understanding of GCP and the practical implementation of these principles during the planning and conduct of the clinical investigation is just as important as possessing the scientific and clinical expertise in the disease or condition being investigated. It is, in fact, the combination of these two factors, scientific expertise and a thorough understanding of GCP that will help ensure that the clinical investigator will be successful in not only following FDA regulatory requirements, but most importantly help ensure the safety of the subjects enrolled in the investigation as well as provide valid and reliable data to FDA.

What Do We Mean When We Say GCP?

FDA regulations define GCP as "a standard for the design, conduct, performance, monitoring, auditing, recording, analysis, and reporting of clinical trials in a way that provides

Table 17.2 Summary of GCP principles as per ICH E6

• Clinical trials should be conducted in accordance with the ethical principles that have their origin in the Declaration of Helsinki, and that are consistent with GCP and the applicable regulatory requirement(s)
• Before a trial is initiated, foreseeable risks and inconveniences should be weighed against the anticipated benefit for the individual trial subject and society. A trial should be initiated and continued only if the anticipated benefits justify the risks
• The rights, safety, and well-being of the trial subjects are the most important considerations and should prevail over interests of science and society
• The available nonclinical and clinical information on an investigational product should be adequate to support the proposed clinical trial
• Clinical trials should be scientifically sound, and described in a clear, detailed protocol
• A trial should be conducted in compliance with the protocol that has received prior institutional review board (IRB)/independent ethics committee (IEC) approval/favorable opinion
• The medical care given to, and medical decisions made on behalf of, subjects should always be the responsibility of a qualified physician or, when appropriate, of a qualified dentist
• Each individual involved in conducting a trial should be qualified by education, training, and experience to perform his or her respective task(s)
• Freely given informed consent should be obtained from every subject prior to clinical trial participation
• All clinical trial information should be recorded, handled, and stored in a way that allows its accurate reporting, interpretation, and verification
• The confidentiality of records that could identify subjects should be protected, respecting the privacy and confidentiality rules in accordance with the applicable regulatory requirement(s)
• Investigational products should be manufactured, handled, and stored in accordance with applicable good manufacturing practice (GMP). They should be used in accordance with the approved protocol
• Systems with procedures that assure the quality of every aspect of the trial should be implemented

assurance that the data are credible and accurate and that the rights, safety, and well-being of trial subjects are protected" (21 CFR 312.120(a)(1)(i)). The principles of GCP can also be found in the International Conference on Harmonization of Technical Requirements for Registration of Pharmaceuticals for Human Use E6 Good Clinical Practice [3]. In that document, commonly known as ICH E6, the principles of GCP are summarized in Table 17.2.

In addition to ICH E6, there are other globally recognized documents that further describe the importance, principles, and practices of GCP. These include:

- "***Ethical and Policy Issues in International Research: Clinical Trials in Developing Countries***," published by the National Bioethics Advisory Commission, 2001
- "***International Ethical Guidelines for Biomedical Research Involving Human Subjects***," prepared by the Council for International Organizations of Medical Sciences (CIOMS), in collaboration with the World Health Organization 2002
- ISO 14155:2011 "***Clinical Investigation of Medical Devices for Human Subjects-Good Clinical Practice***," issued by the International Organization for Standardization

It is important to note that ISO 14155:2011, unlike the other documents mentioned, is specific to medical devices and therefore it is intended to address the unique challenges that one may encounter when conducting a trial on medical devices that are not typically seen in trials of drugs and biologics.

The numerous documents and standards on GCP published by the various global health agencies and organizations give evidence to the fact that GCP is a critically important concept worldwide and is at the foundation of what it means to conduct a clinical investigation ethically by upholding the rights of study subjects and ensuring their safety and welfare. While it is not necessary for a clinical investigator to read and analyze all of these documents to remain in compliance with FDA regulations, it is important for him/her to recognize the importance of GCP and the general globally accepted concepts and principles that make up GCP.

Another reason why adherence to GCP is so important for FDA as well for regulators globally is because, in the not so distant past, the idea that human subjects in clinical trials should be afforded certain rights and protections was not given. As a result, there are numerous examples of clinical trials that were not conducted ethically and the rights of the human subjects were not considered. Not surprisingly, many of these trials resulted in significant injury or even the death of some of the human subjects involved. One of the earliest examples of violations of the rights of human subjects resulted in the Nuremberg War Crimes Trials.

During these trials, 23 physicians were charged with crimes against humanity due to their performing experiments on the prisoners in concentration camps without their knowledge and/or consent. These trials resulted in the formulation of the "Nuremberg Code" that effectively set basic rules for clinical trials. These are that consent should be voluntary; benefits should outweigh the risks, and that the subject should be able to terminate participation at any time. Unfortunately, despite the existence of the Nuremberg code,

there continued to be instances of human subject protection violations. Some of these include:

- The Thalidomide tragedy: The experimental drug, Thalidomide, was prescribed to thousands of pregnant women without informing them of the risks of the drug and the fact that it was experimental. The drug was found to be teratogenic, causing limb deformities in the fetus. Expectant mothers were not informed of the risks associated with thalidomide or that it was an experimental drug. Additionally, patients did not volunteer nor did they give consent to participate in the research. It is thought that some 12,000 babies were born with birth defects due to Thalidomide. In 1960, Dr. Francis Oldham Kelsey, a physician at FDA refused to approve Thalidomide for use in the U.S. due to reports of side effects, despite pressure from manufacturers. For her service to public health, Dr. Kelsey was awarded the President's Award for Distinguished Federal Civilian Service in 1962 by President John F. Kennedy (Fig. 17.2).
- The story of Henrietta Lacks: a 31-year-old African-American female from Maryland who sought treatment at Johns Hopkins for cervical cancer. She eventually died from the disease; however, during the course of her treatment before her death, her physicians at Hopkins had taken samples of her tissues, both healthy and malignant, to use for research purposes without her knowledge or consent. These cells would later be known as "HeLa" cells (Fig. 17.3) and they are referred to in more than 74,000 scientific publications and would eventually be used in the development of a number of medical advances, including the polio vaccine, tamoxifen, chemotherapy, gene mapping, in vitro fertilization, and treatments for influenza, leukemia, and Parkinson's disease. Her family became aware of this in 1973 and petitioned to have some say in the use of their relative's tissues. However, it was only recently in 2013 that the family regained some control over how Henrietta Lacks' genome is used [4] through an agreement reached with the National Institutes of Health.
- The Tuskegee Syphilis Experiment, 1932–1972 [5]: The experiment, sponsored by U.S. Public Health Service was proposed as an observational study of the effects of untreated syphilis. The clinical investigators recruited 600 poor, African-American males in Macon County, Alabama to participate in the study. Three hundred and ninety-nine (399) men had syphilis and 201 did not. These men's rights were violated from the very beginning. Some of the violations included the fact that the men were not told the purpose of the study; as a result no informed consent was obtained; they were lied to and were told that they were being treated for "bad blood"; they were offered free meals and payment of burial expenses as an incentive to participate; and finally the men who were known to have syphilis were not treated with Penicillin despite its availability in 1947. The Tuskegee Syphilis Study (Fig. 17.4) did set the stage for important U.S. legislation geared toward ensuring the protection of study subjects involved in clinical trials. Most specifically the Belmont Report [6] was drafted to provide important guidelines to help develop U.S. Regulations, including FDA GCP regulations, for the ethical conduct of clinical trials.



Fig. 17.2 Dr. Francis Oldham Kelsey receiving the President's Award for Distinguished Federal Civilian Service in 1962 by President John F. Kennedy

The Sponsor-Investigator and Good Clinical Practice

The clinical investigator of a trial has numerous responsibilities. The specific responsibilities as required by regulation will be discussed later in the chapter. If the clinical investigator is also the one manufacturing the device and/or initiating the clinical investigation, he/she therefore becomes the trial's sponsor-investigator (SI's). For those who choose to be SI's, the responsibilities increase significantly since they are accountable for following the FDA regulations that dictate both the sponsor's and the clinical investigator's responsibility. As stated earlier, FDA regulations for device trials are based on the principles of GCP—the design, conduct, performance, monitoring, auditing, recording, analysis, and reporting of clinical trials. The SI's is ultimately responsible

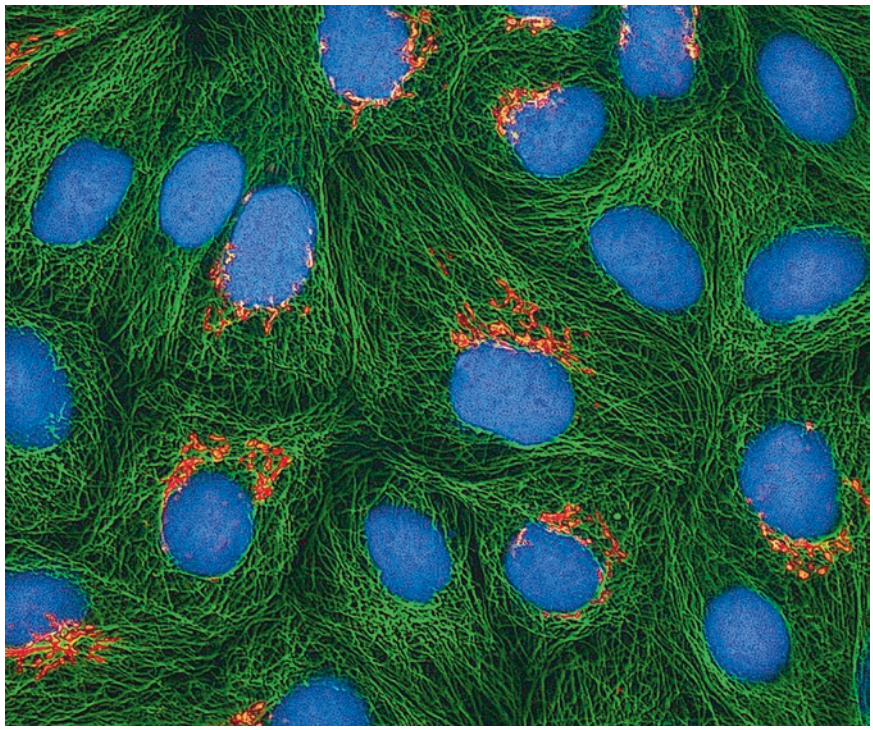


Fig. 17.3 Multiphoton fluorescence image of cultured HeLa cells *Tom Deerinck.* http://www.nih.gov/news-events/news-releases/nih-lacks-family-reach-understanding-share-genomic-data-hela-cells. NIH, Lacks family reach understanding to share genomic data of HeLa cells



Fig. 17.4 U.S. Public Health Service Syphilis Study at Tuskegee

for making sure that all of these principles are met. This may seem at first burdensome; however, in order to prevent any recurrences of the ethical violations presented earlier on in this chapter, it is essential that the SI acknowledges and accepts that the principles of GCP must be upheld through their understanding and compliance with FDA regulations. The NIH GCP training/certificate resource (http://www.cc.nih.gov/training/training/crt.html) is accepted by all IRBs and includes a module for FDA oversight of clinical research.

Adhering to GCP and conducting a trial successfully involves a team approach. For FDA, the trial's clinical investigator, sponsor, CRO, IRB, and FDA are all on the same team where communication is key and the responsibility to conduct the trial in accordance with GCP is shared.

Not unlike being the head of a surgical team, the SI should realize that successful conduct of a clinical trial at his/her site also involves a team approach where he/she is also the team leader. As the team leader, the SI's goal should be to recognize that each member of his/her team has their own set of responsibilities that must be fulfilled. Therefore, as the team leader the SI should make sure that, for example, his/her sub-investigators are properly trained and have knowledge of the protocol, including any amendments; that the person getting informed consent from subjects knows that they must use the most updated version and the form must be signed and dated in all of the required fields; and that the person reporting the adverse events is aware of when the report needs to be submitted if delineated by the protocol. In essence, the SI should ensure that members of the team are qualified to fulfill their role; are properly trained clinically, but also have knowledge of the protocol and what is required. The SI should also make it a practice to perform regular checks on the team members to ensure that they are performing their roles adequately. Regularly scheduled study team meetings are a great venue to communicate study updates and discuss study progress and challenges.

Overview of Sponsor-Investigator Roles and Responsibilities

The regulations define the dual role of the sponsor and investigator (SI's) as an individual who both initiates and actually conducts the study (21 CFR 812.3(o)). Examples of SI's include: inventor/innovator, academic researcher, sponsor sur-

rogate, physician/surgeon interested in a new use of an already approved device, or any combination of these examples. FDA regulations clearly define the role and responsibilities of those involved in FDA-regulated clinical investigations. It is important to have a full understanding of the SI role and associated responsibilities because this becomes a legal responsibility for which one is held accountable by regulatory authorities. Wearing both hats can be challenging and requires a skilled research team. Consultation with a device manufacturer with research experience and colleagues who have experience with the IDE application process and conduct of an IDE study can be helpful. Academic SI's may find it useful to consider the resources available within your institutions. For example, most academic institutions have regulatory resources available through the Research Department or Ethics Office of the University. Additionally, it is recommended that an SI interact with the FDA through the pre-submission process when preparing the IDE application. FDA also provides online resources that can assist the SI in their role and responsibilities. The following links will provide you with detailed information regarding device advice, basics of an IDE, and several case studies:

- http://www.fda.gov/MedicalDevices/DeviceRegulationandGuidance/HowtoMarketYourDevice/InvestigationalDeviceExemptionIDE/default.htm
- http://fda.yorkcast.com/webcast/Play/696d857b34334d5389364ed8c2db3ded1d
- http://www.fda.gov/Training/CDRHLearn/default.htm

As discussed earlier, the SI's are responsible for following the regulations of the Sponsor and Clinical Investigator (CI) as defined in the FDA IDE regulations (21 CFR 812.40 and 812.100). The clinical investigator conducts the investigation and oversees the use or administration of the investigational device in a patient. In the event of an investigation being conducted by a team of individuals, "investigator" refers to the responsible leader of that team. It is important to note that the FDA considers the principal investigator and the sub-investigators "investigators" who are held responsible for complying with the investigator responsibilities in the regulation.

The sponsor is an individual, company, institution, or organization that takes responsibility for the initiation, management, and may finance a clinical investigation. The sponsor-investigator responsibilities include all of those listed above for the investigator plus the sponsor responsibilities presented in Table 17.3.

Building Quality Into Sponsor-Investigator Clinical Studies of Medical Devices

There are resources available to assist SI's with incorporating quality early in the study design [7]. A well-designed and -executed study protocol is the most important tool for ensuring high-quality data and human subjects protections. Interactions with FDA during the design phase and throughout the study conduct is recommended as well as selecting qualified study personnel and working with a skilled research staff. It is advisable to consult with the device manufacturer when appropriate and other SI's who have experience with IDE studies. Additionally, obtain feedback from study staff early and often on the protocol requirements. Poorly designed or difficult to execute protocols and poor study monitoring can introduce errors leading to unreliable study data and may place study subjects at risk for harm. Study-specific training of site staff and the development of an adequate study monitoring plan is one of the best upfront investments to ensure data quality, integrity, and subject safety.

Site staff training is provided before study initiation and recommended when essential study staff are replaced, there are significant changes in the device or protocol, or monitoring visits reveal problems. Important areas to cover during training include: the study protocol, study expectations, procedures unique to the device or its use in the study, regulatory requirements, clinician vs. investigator responsibilities, and the importance of following the informed consent process, reporting of adverse events, and protocol deviations.

Clinical study monitoring is the development of a plan used to oversee the study conduct and reporting of data from a clinical investigation. The focus of study monitoring should be on the processes that are critical to protecting human subjects, maintaining the integrity of study data and compliance with applicable regulations.

Monitoring is intended to identify and correct practices that could result in inadequate patient protections and poor data quality. Regular data audits also avoid numerous site queries and costly late database cleanup.

FDA regulations are not specific about how sponsors are to conduct monitoring of clinical investigations. The regulations do require the selection of qualified, trained, and experienced monitors to monitor the study in accordance with the IDE and other applicable FDA regulations (21 CFR 812.43). For example, a medical monitor can be a physician independent of the study team who routinely provides this service through the university or academic research office. It is not advisable to select a colleague or physician who is not experienced in the role of a study monitor or able to commit to the study monitoring responsibilities. Monitoring services can also be provided through qualified third-party contract research organizations (CROs). Although sponsors can transfer responsibilities for monitoring to a third party, they are ultimately responsible for ensuring adequate study monitoring. The monitor assists the SI in study activities such as the development of the study monitoring plan, adverse event adjudication, data and site audits and initiation of corrective action early in the study conduct to catch problems before they become repetitive and data integrity is compromised.

Table 17.3 Summary of key components of an IDE as per CFR

21 CFR Part	Area	Description
812.40	General	Select qualified investigators and provide them with the information needed to conduct the investigation properly. Ensure proper monitoring of the investigation and IRB review and approval, submit an IDE application to FDA for significant risk device studies, and inform the IRB and FDA promptly of any significant new information about the investigation
812.42	FDA and IRB approval	Cannot begin an investigation or any part of an investigation until an IRB and FDA have both approved the application or supplemental application
812.43	Selecting investigators	Select qualified, trained, experienced investigators to investigate the device
812.43	Selecting monitors	Select qualified, trained, experienced monitors to monitor the investigational study in accordance with the IDE and other applicable FDA regulations
812.43	Device control	Can ship investigational devices only to qualified investigators participating in the investigation
812.43	Investigator agreements	Must obtain a signed agreement from each participating investigator as required by the regulation
812.45	Informing investigators	Must supply all participating investigators with copies of the investigational plan and a report of prior investigations of the device
812.46	Monitoring	Must secure investigator compliance, evaluate unanticipated adverse device effects, and follow-up on subsequent actions as required. Must seek IRB and FDA approval for the resumption of terminated studies
812.140	Sponsor records	Must maintain accurate and complete investigation records
812.150	Sponsor reports	Must provide reports in a timely manner to FDA, the IRB, and/or investigators
812.5	Labeling	An investigational device or its immediate package must bear a label with the prescribed information
812.7	Promotion of investigational devices	A sponsor, investigator, or any person acting for or on behalf of a sponsor or investigator cannot promote, test market, commercialize, etc., investigational devices

Source: U.S. Food and Drug Administration—Case Study (2014). http://www.fda.gov/downloads/Training/CourseMaterialsforEducators/NationalMedicalDeviceCurriculum/UCM404249.pdf

Typically, monitoring visits occur early to ensure site readiness and as frequent as necessary (i.e., every 4–8 weeks) to meet the needs of the specific study. Monitoring should focus on activities related to evaluation of study data and study conduct or processes. Suggestions for what should be monitored in an IDE study include:

- Data critical to the reliability of the study findings (i.e., source to case report form verification of data that support primary and secondary endpoints);
- Data critical to subject safety (i.e., protocol deviations/violations, subject eligibility criteria, serious and unanticipated adverse events, deaths and withdrawals particularly when related to an adverse event);
- Processes critical to subject safety and ethical treatment (i.e., verification that proper informed consent is obtained, appropriate medical consultation for significant clinical or lab findings and documentation of device accountability and administration of the investigational product); and
- Processes critical to data integrity (i.e., timely review of specified events for adjudication).

The goal at the end of the study is to have accurate and reliable clinical data and assurance that the rights, safety, and welfare of the subjects participating in the clinical investigation were protected.

FDA conducts on-site inspections to assess the protection and safety of subjects participating in clinical investigations and to determine the integrity and quality of data submitted to the agency. FDA's inspection program includes inspections of Sponsors, Clinical Investigators, CROs, and Institutional Review Boards (IRBs). An SI can be cited for non-compliance of both the sponsor and investigator regulations. Based on data from FDA inspections [8], some of the more common SI citations or deficiencies include:

- Failure to follow the investigational plan, investigator agreement or protocol (e.g.., changes made to the study without amending the protocol);
- Failure to obtain adequate informed consent (e.g., not re-consenting subjects when substantive revisions were made to the initial approved protocol and informed consent or consenting subjects with the incorrect version of the informed consent document);

- Not submitting an IDE application to FDA (e.g., SI not aware their study required an IDE);
- Inadequate study Monitoring (e.g., SI served as their study monitor and failed to catch many of their own mistakes);
- Not providing adequate progress reports to FDA and IRB (e.g., IRB halted the SI IDE study and the SI did not report to FDA); and
- Not having accurate, current, and complete records (e.g., SI focused on the science of the study and not enough on the importance of good documentation).

Historically, studies that have been initiated and conducted by physician-scientists or physician-inventors have been at the cornerstone of medical device innovation and development. We recognize that physicians and/or scientists who wish to pursue SI IDEs are required to take on a significant amount of responsibly as there are many rules and regulations to follow. However, FDA is committed to supporting and guiding those who wish to pursue SI IDEs in order to improve the public health by getting safe and effective medical devices to those who need them.

References

1. Abel D, Farb A. Application of Investigational Device Exemptions regulations to endograft modification. J Vasc Surg. 2013;57:823–5.
2. O'Callaghan A, Mastracci TM, Eagleton MJ. Staged endovascular repair of thoracoabdominal aortic aneurysms limits incidence and severity of spinal cord ischemia. J Vasc Surg. 2015;61(2):347–54. e1. doi: 10.1016/j.jvs.2014.09.011. Epub 2014 Oct 23.
3. http://www.fda.gov/downloads/Drugs/…/Guidances/ucm073122.pdf. Note: the ICH E6 currently published is being revised
4. Zimmer C. A family consents to a medical gift, 62 years later. The New York Times. 7 Aug 2013.
5. http://www.cdc.gov/tuskegee/timeline.htm
6. http://www.hhs.gov/ohrp/humansubjects/guidance/belmont.html
7. http://www.ctti-clinicaltrials.org/toolkit/qbd/learn-about-qbd
8. http://www.fda.gov/ScienceResearch/SpecialTopics/RunningClinicalTrials/ucm261409.htm

Resources/Useful Links

Device Advice: Investigational Device Exemption (IDE). http://www.fda.gov/MedicalDevices/DeviceRegulationandGuidance/HowtoMarketYourDevice/InvestigationalDeviceExemptionIDE/default.htm

Selected FDA GCP/Clinical Trial Guidance Documents. http://www.fda.gov/ScienceResearch/SpecialTopics/RunningClinicalTrials/GuidancesInformationSheetsandNotices/ucm219433.htm

2015 Case Studies. http://www.fda.gov/Training/CourseMaterialsforEducators/NationalMedicalDeviceCurriculum/ucm404245.htm

Building Quality Into Clinical Trial Design. http://www.ctti-clinicaltrials.org/toolkit/qbd/learn-about-qbd

Clinical Trials and Human Subject Protection. http://www.fda.gov/ScienceResearch/SpecialTopics/RunningClinicalTrials/default.htmPre-Submission Program. http://www.fda.gov/downloads/MedicalDevices/DeviceRegulationandGuidance/GuidanceDocuments/UCM311176.pdf

Ecopy. http://www.fda.gov/downloads/medicaldevices/deviceregulationandguidance/guidancedocuments/ucm313794.pdf

Early Feasibility. http://www.fda.gov/downloads/medicaldevices/deviceregulationandguidance/guidancedocuments/ucm279103.pdf

CDRH Learn. http://www.fda.gov/Training/CDRHLearn/

18 Developing Physician-Sponsored Investigational Device Exemption Protocols

Benjamin W. Starnes

The pace of medical device innovation in vascular surgery has exploded in the last two decades. Physician-modified and "custom-made" endovascular devices are becoming commonplace in a modern climate where innovation outpaces regulated technological advancement. Off-label use of medical devices occurs on a daily basis throughout many institutions across the United States and when performed by physicians, is both legal and unregulated. The purpose of this chapter is to review the regulatory, compliance, and legal issues regarding the practice of medical device modification and to offer advice on obtaining investigational device exemption (IDE) protocols in the United States. At the time of this writing, there exist only ten IDEs registered with clinicaltrials.gov for managing complex aortic disease with fenestrated and branched stent-grafts. Two of these are at the University of Washington and none involve the use of parallel stent-grafts.

Immediate stent-graft modification with fenestrations was initially described in 2006 by Krasi Ivancev and colleagues in a series of three patients [1]. In April of 2007, we began treating patients with asymptomatic, symptomatic, or ruptured juxtarenal aortic aneurysms by modifying a Food and Drug Administration (FDA)-approved medical device (Zenith Flex; Cook, Inc, Bloomington, Ind) with the creation of fenestrations to maintain branch vessel patency (Fig. 18.1). These procedures were performed on patients who were deemed not to be suitable candidates for open surgical repair and had no other treatment options [2]. The purpose of this chapter is to review the regulatory, compliance, and legal issues regarding the practice of medical device modification.

Off-label use of medical devices occurs on a daily basis throughout many institutions across the United States and when performed by physicians, is both legal and unregulated. This is according to the "practice of medicine doctrine," which was explicitly articulated in the Food and Drug Administration Modernization Act of 1997 [3].

> *"Nothing in this chapter shall be construed to limit or interfere with the authority of a health care practitioner to prescribe or administer any legally marketed device to a patient for any condition or disease within a legitimate health care practitioner-patient relationship."* [3]

What actually composes a "legitimate health care practitioner-patient relationship" is poorly defined in the current literature. Just because off-label use by a physician is legal and unregulated does not necessarily mean that it is safe, smart, well-justified, or legal with respect to billing practices. The defense of an "unsafe" off-label use would actually be an ex post facto liability matter, not a regulatory matter. The author will address the separate but equally important topic of product liability later in this article.

According to the FDA, device modifications are a regulated activity [3], although within the FDA's regulatory discretion, it has not actively pursued in-house device modifications. A critically important feature of regulatory discretion is that it can change without notice, and/or be exercised sporadically. If everything goes well, the FDA will not become interested, but if something bad happens, the FDA will become interested and have unlimited authority to act. They could very well find the practitioner out of compliance even though they had no previous interest in the provider's activities. The Food and Drug Administration Modernization Act of 1997 further states that its provisions do nothing to limit the existing FDA regulatory powers [3].

In general, the FDA has the authority over a device and any person or facility where anyone is engaged in the manufacture, preparation, propagation, compounding, assembly, or processing of a device intended for human use (21 CFR 807.20). Title 21 CFR 807.81 makes it crystal clear that anyone introducing a medical device into commercial distribution must meet the existing premarket requirements. However, physicians who produce or alter a device for use within their own practice are exempted from the premarket notification requirement (21 CFR 807.65(d)), but they are not exempted from the premarket approval requirements for a class III medical device. Even though physicians may modify a device and have a good outcome, the Center for Medicaid

B.W. Starnes (✉)
Division of Vascular Surgery, Department of Surgery, University of Washington, 325 Ninth Avenue, Seattle, WA 98104, USA
e-mail: starnes@u.washington.edu; starnes@uw.edu

© Mayo Foundation for Medical Education and Research 2017

G.S. Oderich (ed.), *Endovascular Aortic Repair*, DOI 10.1007/978-3-319-15192-2_18

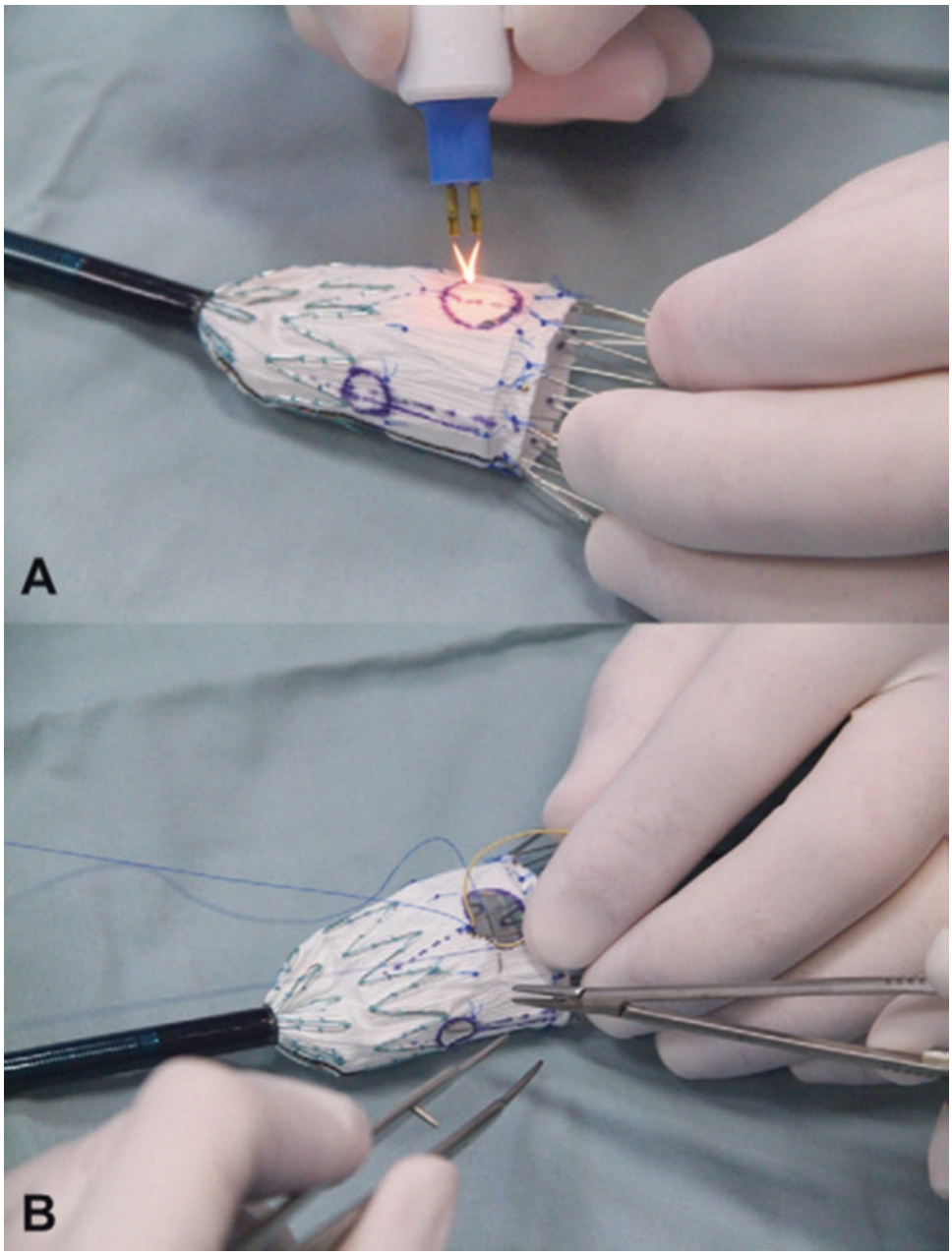


Fig. 18.1 Physician modification of a currently available Food and Drug Administration-approved stent-graft. (**a**) Creation of a fenestration for the superior mesenteric artery with an ophthalmic bovie. (**b**) Suturing of a radio-opaque marker around the same fenestration to aid in fixation and visibility. This device was modified under an investigator-sponsored investigational device exemption

and Medicare Services (CMS), a sister governmental organization to the FDA without any reciprocal influence, may choose not to reimburse the practitioner or the institution for the procedure, citing that the device modifications are "investigational."

Furthermore, it is considered fraudulent to bill the CMS for services that are investigational without formal prior approval from CMS. This is exactly what happened at the University of Washington in 2009 (CMS chose not to reimburse our institution for the procedures), after carrying out dozens of physician-modified endovascular graft (PMEG) procedures beginning in April 2007. The only recourse to continue to treat patients with PMEG was to pursue a formal investigational device exemption with oversight from the FDA.

The issue of product liability is germane to this topic. Many people have had medical devices used to better their health only to suffer injuries related to the use of that same device. Sometimes, these injuries serve as the basis for a product liability claim on behalf of the treated patient. All defective product liability claims come in three varieties. Product liability claims resulting from defective medical devices are based on one or more of the following three entities:

1. Defectively manufactured medical devices. These are devices that were manufactured improperly or somehow damaged during the manufacturing process. This may have happened because of an error in the manufacturing

process, a problem with shipping of the device, or an error that occurs in the hospital setting during device implantation or use (failure of quality control).
2. Medical devices with a defective design. These are devices that were properly manufactured but have an inherently and unreasonably dangerous design that results in injury. Sometimes, the device will have been on the market for a long period of time but then fails in some way and causes serious injury.
3. Defectively marketed medical devices. "Marketing" of a medical device refers to any recommendation, warning, lack of warning, or instruction concerning the use of that device by a potential defendant. This claim category involves anything from a failure to provide adequate or accurate warnings regarding the danger posed by the medical device to a failure to provide adequate instructions regarding its safe and appropriate use [4].

Every person or entity involved in the "chain of distribution" of a medical device (the path the medical device took from the manufacturer to the consumer) is potentially liable for the claim. This includes the manufacturer, the medical sales representative who counsels and makes recommendations to the treating physician, the doctor, and the hospital [5]. The use of a new FDA-approved device in the hands of an inexperienced operator can also lead to potential liability. With PMEG, since the device had been modified after the manufacturing process and used outside the instructions for use, the manufacturer essentially became exempt from any product liability claim. It is therefore extremely prudent on the part of the physician, in this case practicing PMEG, to initiate an IDE for the proper study of the safety and effectiveness of the technique. An investigator-initiated IDE requires extensive regulatory and compliance knowledge on the part of the principal investigator. As an IDE holder, the physician is not simply a site investigator but also the sponsor of the clinical study.

Sponsor responsibilities are considerably different than site investigator responsibilities. When our team finally decided to move forward with the application process for an IDE, we had no concept of the amount of work that would eventually be required to win approval and sustain the entire process. The cost of running an IDE is considerable and includes a research coordinator's salary and monitoring service fees. Staffing requirements, secure database management, clinical events committees, data safety monitoring boards, reporting of adverse events and deviations from the predescribed study plan, and annual progress reports add up to a mountain of work for even the most motivated of individuals. Essentially, there are three entities that revolve around the investigator: the FDA, the investigator's Institutional Review Board (IRB), and the Center for Medicare and Medicaid Services (CMS). None of these groups will talk directly to the other but communicate entirely through the investigator who is considered precisely in the center and responsible for documenting and tracking all communications. A list of steps for obtaining an IDE at our institution is listed in Table 18.1.

Table 18.1 Steps for obtaining an IDE at the University of Washington

1.	Review FDA website for the appropriate submission format to use http://www.fda.gov/MedicalDevices/default.htm
2.	Write protocol, obtain references, and justification for why this study is being proposed
3.	Request trusted colleagues to review the protocol for accuracy and readability
4.	After protocol is written, write CRFs
5.	Submit protocol to IRB and at the same time, request an in-person meeting to present directly to them. With non-sponsored studies, the IRB may have many questions and it is easier to answer them in person rather than have delay of approval by a back-and-forth dialog. This may not be possible with all IRBs, but it does help pave the way to approval
6.	Obtain "conditional approval" from the IRB meaning that the study cannot begin until FDA approval is obtained and the FDA-amended protocol is resubmitted to the IRB
7.	Submit an IRB conditional approval letter and pre-IDE application to the FDA. Follow the guidelines on the FDA.gov website. The FDA is very good about informal communications and can help guide the submission process
8.	Once comments and suggestions are received back from the FDA, submit full IDE application to the FDA. One must follow new IDE submission requirements or one will have a delay in getting approval
9.	The budget can be done at any time. If one needs buy-in from the host institution, start this process after the protocol and case report forms are written (the coordinator/budget personnel will have a better idea of the time involved if they have these two sets of documents). In truth, one really needs the institutional buy-in before even starting the protocol-writing process
10.	Once FDA approval is received, submit this approval letter to the IRB for their final approval. One may get approval to start the study, but there may be requested changes or corrections to make to the protocol
11.	Once final IRB approval is received, submit this document back to the FDA. The initial FDA approval letter will state that the investigator can begin the study after the FDA has received the final approval from the host institution IRB, and they (the FDA) have acknowledged receipt of this approval
12.	Submit to CMS part A and B. Currently, part A can be submitted electronically, but part B needs to be sent in paper form. Part B will not be approved until part A approval is received (We recommend simultaneously submitting part A electronically and part B in paper form. Once part A approval is received, the part A approval letter can be sent to part B personnel)

CRF Case report form, *FDA* Food and Drug Administration, *IDE* investigational device exemption, *IRB* institutional review board. Investigators should check the FDA website, their individual IRB requirements, and their regional Medicare submission requirements

Furthermore, we quickly realized after receiving approval to conduct the IDE that our team was subject to inspection by the FDA at any time. Interestingly, the author used to believe that the FDA was a prohibitive entity, but after working closely with this organization for over 5 years, we now believe the FDA to be incredibly facilitative. The FDA sincerely promotes the message that they want to help physicians successfully treat their patients.

In conclusion, the practice of device modification is legal and unregulated in most instances. However, the FDA has wide and unlimited authority to intervene when patient safety or effectiveness of the device becomes a concern. The CMS, depending on the regional carrier, may choose to fully compensate or pay absolutely nothing for these cases based on an assessment of "investigational use." Any practitioner who chooses to modify an existing FDA-approved medical device outside of an IDE should weigh heavily the ramifications of a product liability claim and/or a criminal or civil liability claim, as the manufacturer becomes exempt once the device has been modified. It is the author's opinion that physicians performing device modification of the nature described herein are obliged to obtain an IDE.

References

1. Uflacker R, Robison JD, Schonholz C, Ivancev K. Clinical experience with a customized fenestrated endograft for juxtarenal abdominal aortic aneurysm repair. J Vasc Interv Radiol. 2006;17:1935–42.
2. Starnes BW. Physician-modified endovascular grafts for the treatment of elective, symptomatic, or ruptured juxtarenal aortic aneurysms. J Vasc Surg. 2012;56:601–7.
3. Food and Drug Administration Modernization Act of 1997. The National Academies. http://www7.nationalacademies.org/ocga/laws/PL105_115.asp. Accessed 18 Aug 2012.
4. Gee T. Impact of modifying FDA regulated devices. http://medical-connectivity.com/2009/10/25/impact-of-modifying-fda-regulated--devices. Accessed 25 Oct 2009.
5. Brown OW. Legal implications of pushing the endovascular envelope. J Vasc Surg. 2012;56:273–4.

Part III

Techniques of Implantation and Adjunctive Procedures to Minimize Complications

Principles of Side Branch Incorporation and "Bail Out" Maneuvers

19

Aaron C. Baker and Gustavo S. Oderich

Introduction

Branch vessel catheterization and incorporation is a critical step when dealing with complex aortic repair involving fenestrated, branched, and parallel stent-grafts. Adequate planning, finesse, and attention to detail are of paramount importance to avoid complications. Excessive catheter and guide-wire manipulation can result in a number of complications including atheroembolization, prolonged visceral ischemia from stent-graft coverage, and inadvertent dissection or vessel perforation. Key maneuvers outlined in other chapters will detail how to set up sheaths, catheters, and guide-wires for efficient side branch incorporation. This chapter focuses on basic principles used for placement of side stent and how to troubleshoot and "bail out" from unexpected intra-procedural complications during complex endovascular repair (Table 19.1).

Pre-procedure Planning

A thorough review of the patient anatomy is paramount to anticipate difficulties with side branch placement. The presence of tortuosity, ostial disease, plaque, debris, small vessel diameter, and early branch bifurcation all increase technical difficulty for placement of bridging stents. Therefore, preoperative case planning remains critical to successful execution of these procedures. A thin slice compute tomography angiogram (CTA) of chest, abdomen, and pelvis best determines target vessel orientation and choice of ideal approach—femoral or brachial. As a general rule, down-going vessels are more easily approached from above using antegrade branches of fenestrations with preloaded catheter or wire systems. Likewise, use of the brachial approach allows earlier restoration of lower limb perfusion, which may be associated with improved pelvic and spinal cord perfusion. Most complications described below can be anticipated on the basis of careful review of pre-operative imaging.

Alignment of Fenestrations and Fenestrated-Branches

Since the initial reports of fenestrated endografts in the early 2000s, it has become evident that all fenestrations should be aligned by stent placement. Proper alignment of fenestrations of the main aortic stent graft requires accurate identification of the target vessels using angiography, pre-catheterization, fusion imaging or iGuide. Selective catheterization of the fenestrations and target vessels is then required via the aortic device. Manufactured fenestrated stent-grafts undergo extensive quality control and are typically designed to precisely fit the patient's anatomy. Sizing and planning by experienced physicians and by the company's design team allows little room for errors of design. Nonetheless, neck angulation, tortuosity, and errors of design can lead to misalignment between the fenestration and the intended vessel.

"Bail out" maneuvers for errors of design or deployment may be needed if the fenestration is not properly aligned with the target. Regaining access into the target vessel via the fenestration even with a constrained stent-graft is almost always possible. Leaving a stiff guide-wire between the main aortic stent-graft and the aortic wall can serve well in case of severe misalignment when there is not enough space

A.C. Baker
Division of Vascular Surgery, Department of Surgery, Mayo Clinic, 200 First Street, SW, Rochester, MN 55905, USA
e-mail: aaron.c.baker@kp.org

G.S. Oderich (✉)
Division of Vascular and Endovascular Surgery, Mayo Clinic, 200 First Street SW, Rochester, MN 55905, USA
e-mail: oderich.gustavo@mayo.edu

© Mayo Foundation for Medical Education and Research 2017

G.S. Oderich (ed.), *Endovascular Aortic Repair*, DOI 10.1007/978-3-319-15192-2_19

Table 19.1 Intra-procedural complications, predisposing factors, preventive measures, and bail-out strategies

Complication	Predisposing factors	Preventive measures	Bail-out strategies
Misalignment of fenestrations	Excessive neck angulation	Adequate size planning	Use of curved catheters (e.g., VS1 or SOS) for down-going vessels or micro-catheters for selective vessel catheterization
	Tortuosity	Gentle anterior rotation of fenestrations	Balloon displacement of the main stent-graft providing more room for catheter manipulations
	Design errors		
	Posterior displacement of fenestrations by diameter-reducing ties		
Branch perforation or dissection	Small vessel diameter	Meticulous technique	Immediate recognition and treatment
	Atherosclerotic occlusive disease	Avoid excessive manipulation	Balloon reintroduction and inflation in the perforated branch stent
	Early vessel bifurcation	Constant visualization of the tip of the wire	Micro-catheter/Glidewire Gold wire access and coiling of perforated branch
		Avoid positioning wire in terminal branches	Placement of self-expandable stents for dissections
Endoleaks	Inadequate landing zone selection	Adequate neck and size planning	Re-dilation of proximal neck (with protection of alignment stents with separate balloons)
	Design errors	Precise stent-graft deployment	Additional stent-graft implantation
	Inadequate flare	Optimal stent overlap (>2 full-length stents)	
	Lack of stent apposition		
	Use of bare metal stents		
	Inadequate bridging stents length into the aorta		
Stent kinks or narrowing	Vessel tortuosity	Careful review of vessel anatomy	Self-expandable stent placement
	Use of long stents	Use of short stents (<2 cm) to avoid distal bends	Angioplasty or stenting with second balloon-expandable stent
	Right renal artery posterior orientation		
	Inadequate flare		
	Strut compression		
	Ostial disease		

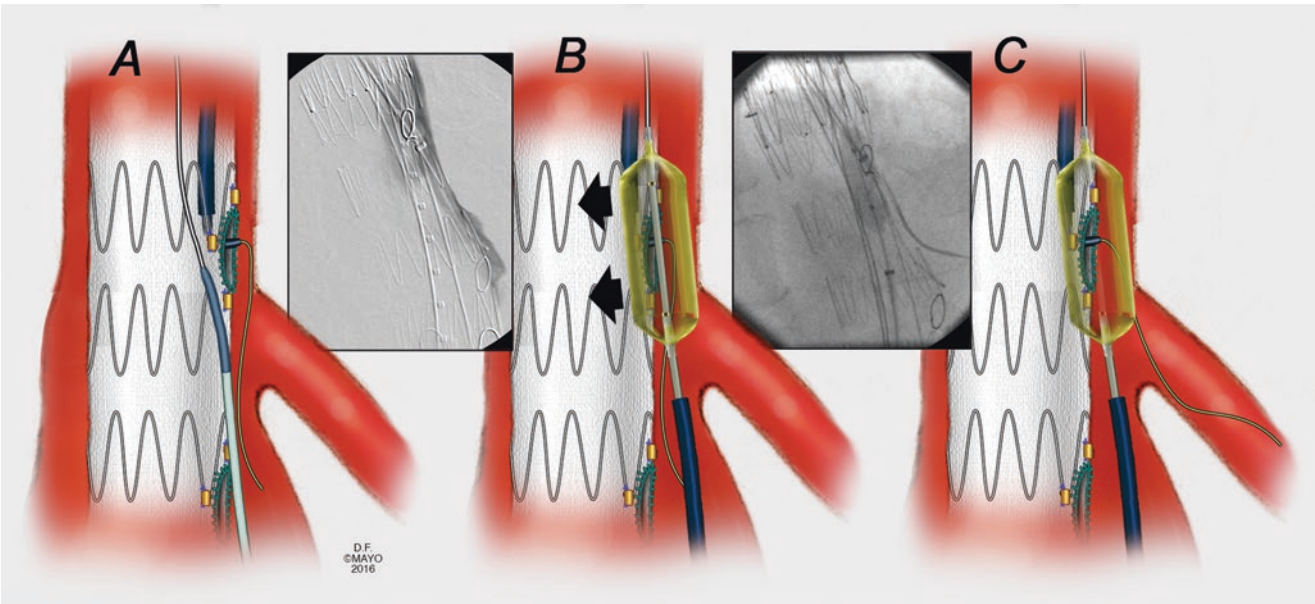


Fig. 19.1 Technique of graft displacement for severe misalignment of fenestrations. Note that the fenestration is above the anticipated target (**a**) with no contrast opacification of the vessel. A balloon is advanced and inflated outside the aortic stent displacing it from the aortic wall (**b**) and allowing enough space for successful branch vessel catheterization (**c**). By permission of Mayo Foundation for Medical Education and Research. All rights reserved

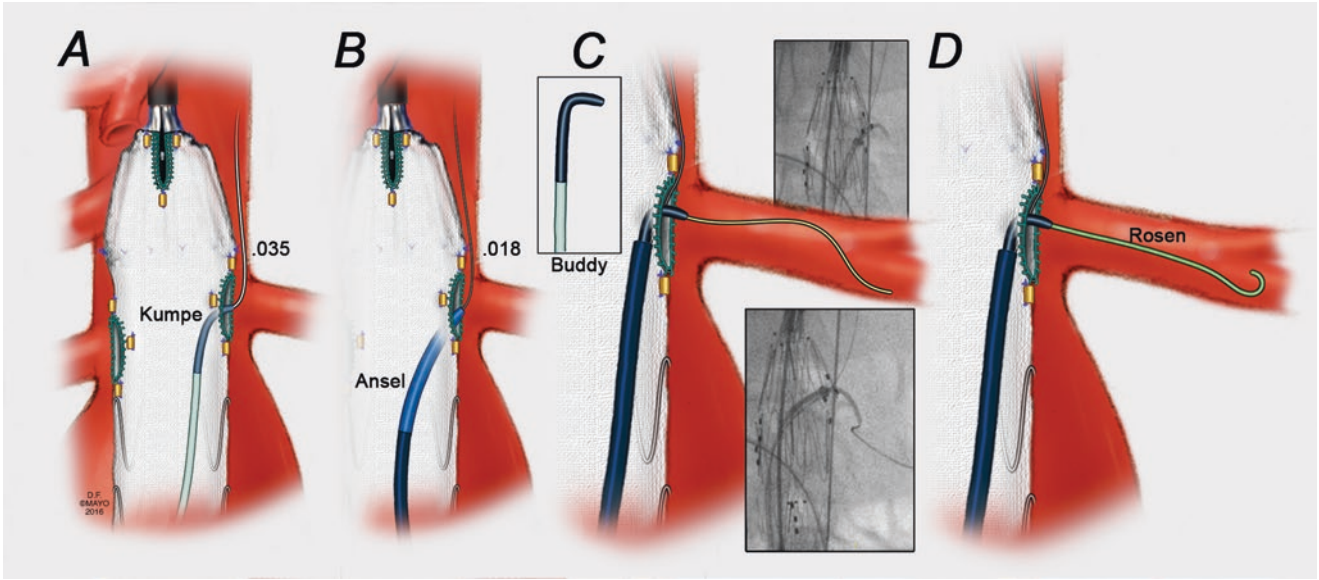


Fig. 19.2 A renal fenestration is accessed and a 0.035-in. guide-wire is advanced into the aorta (**a**), which is exchanged for a 0.018-in. system (**b**) to allow use of a buddy catheter (**c**), which is advanced into the target vessel (**d**). By permission of Mayo Foundation for Medical Education and Research. All rights reserved

to manipulate catheters. In these cases, a simple maneuver is to advance and inflate a balloon between the stent-graft and aortic wall. The inflated balloon displaces the stent-graft away from the aortic wall, which allows enough space to cannulate the fenestration and target vessel (Fig. 19.1). If the fenestration can be catheterized and a wire can be advanced between the aortic wall and the stent-graft, a "buddy" wire system should be used. This can be done using a 7Fr sheath coupled with 0.018-in. or an 8Fr sheath coupled with a 0.035-in. guide-wire system. The "buddy" wire system provides support while securing the sheath within the fenestration, while a "buddy" catheter is to selective catheterize the target vessel (Fig. 19.2). A Van-Schie 3 catheter has a 90° angle which is ideal for working on tight spaces. Alternatively, a micro-catheter coupled with a 0.018-in. Glidewire Gold (45° or 70°) or a deformable guide catheter may be required.

Diameter-reducing ties typically reduce graft diameter by 30 % and are based in the posterior aspect of the aortic stent-graft component. Therefore, the posterior crimping of fabric results in natural displacement of the fenestrations, which are pulled more posterior from its intended location (Fig. 19.3). One of the first maneuvers in these cases is to rotate each fenestration more anteriorly, based on assessment of the target catheters in relation to each of the fenestration. One of the fenestrations is catheterized, a hydrophilic sheath is advanced of a Rosen guide-wire, the graft is rotated in the opposite direction, and the contralateral renal artery is catheterized. Other maneuvers are rarely needed. A secondary curved catheter (e.g., VS1 or SOS) may be used to catheterize down-going vessels or vessels that are originating from the lower part of the fenestration. Balloon displacement of the main stent-graft as previously described is rarely needed, but may provide more room for catheter manipulations (see Fig. 19.1).

Kinks

Most kinks can be anticipated on careful review of preoperative imaging. Because the renal arteries often have a posterior orientation in patients with large aneurysm, one can almost always anticipate a kink at the distal edge of a balloon expandable stent, particularly If the stent is long (Fig. 19.4a). Kinks should be immediately recognized and prevented, as these remain one of the main causes of secondary interventions. Review of CTA anatomy is often more useful than the selective angiography which is done after branch stenting. A useful tip is to keep the length of the stents short (<2 cm), which avoid bends and minimizes the effects from respiratory, which is greater in the distal renal artery. The right renal artery often has a more posterior orientation from its course behind the inferior vena cava. If a kink is anticipated by CTA or is noted on completion angiography, a self-expandable stent should be used to allow a

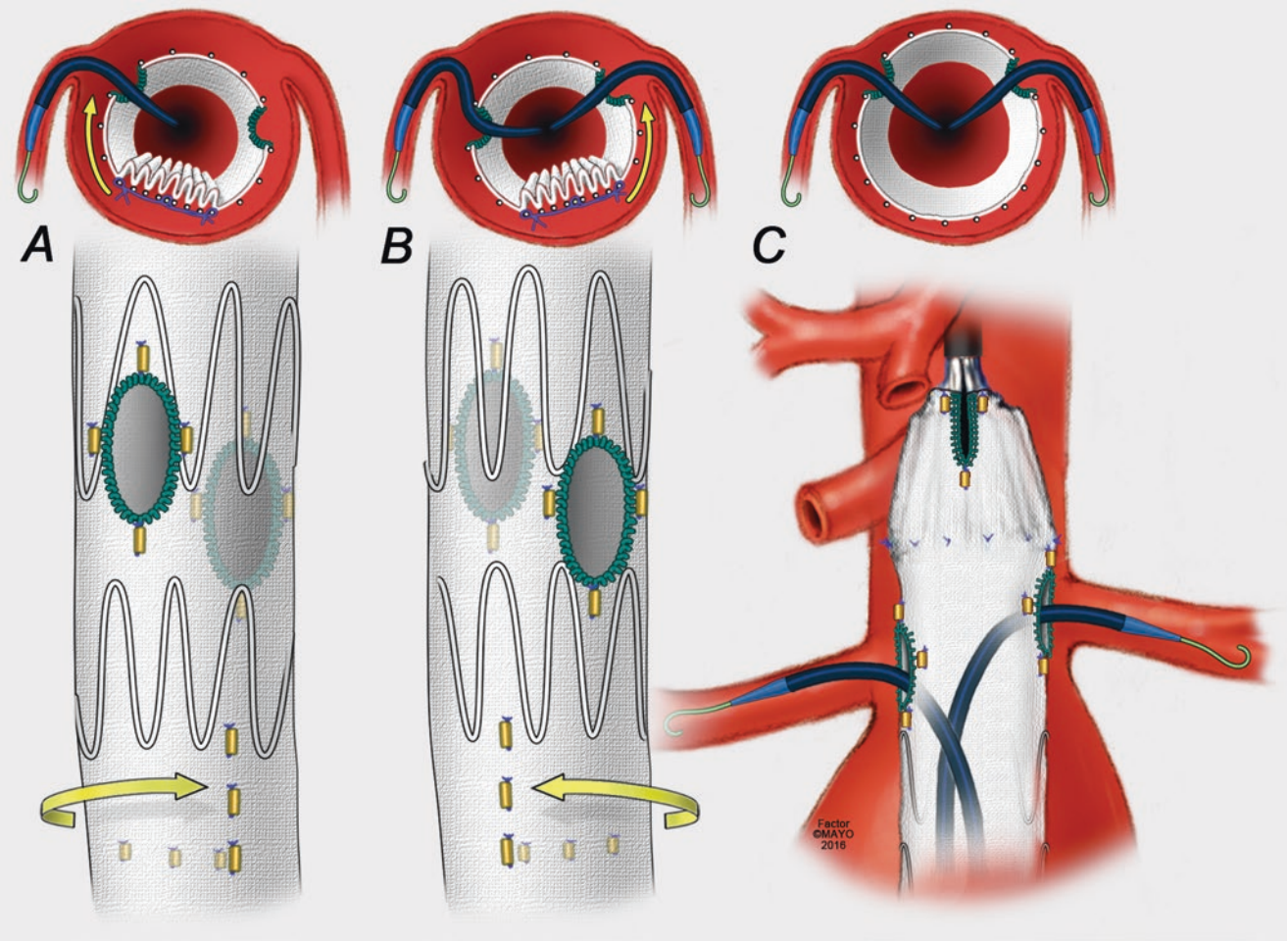


Fig. 19.3 Natural posterior displacement of the fenestrations occurs because of posterior diameter reducing ties. The device is rotated clockwise for access to the right renal artery (**a**) and counter clockwise for the left renal artery (**b**). Hydrophilic sheaths are advanced into both renal arteries over Rosen wires (**c**). By permission of Mayo Foundation for Medical Education and Research. All rights reserved

smooth transition between the balloon-expandable stent and the target vessel (Fig. 19.4b). Other points of potential kink or strain are at the reinforced ring, struts within large fenestrations or in patients who failed devices with supra-renal fixation and the origin of the vessel from the aorta (Fig. 19.5). For these, placement of a second balloon expandable stent may be needed to increase radial force.

Vessel Perforation or Dissection

Attention to detail is critical to avoid complications. This is also a reason why branch stenting should be done one at a time, rather than two vessels done by different operators simultaneously. With finesse, proper technique and good patient selection, vessel perforation or dissections are infrequent. Guide-wire selection is the first step. For the renal arteries, one should avoid stiff guide-wires such as Amplatz short tip or CTO guide-wires such as v18. Instead, the Rosen guide-wire or a braided tip 0.014–18 wire are ideal to prevent complications. The tip of the guide-wire should not be positioned into small terminal branches, which are prone to perforation or dissection. Most importantly, the tip of the guide-wire should be visualized during manipulations, and the guide-wire should be stabilized during exchanges, avoiding forward or retrograde movement. If a guide-wire ventures into a visceral or renal branch unexpectedly, the wire should be left in place instead of removed. A catheter should be advanced into the branch to allow immediate and precise access to the potential perforation. The occurrence of a perforation should be immediately treated, and should not be observed in the hopes that it will seal off on its own. In the unfortunate event of major renal branch perforation, a 0.035 balloon should be inflated in the renal stent to minimize bleeding. The 0.035-in. guide-wire is removed to allow angiography to be performed via the lumen of the balloon shaft (Fig. 19.6). For more distal

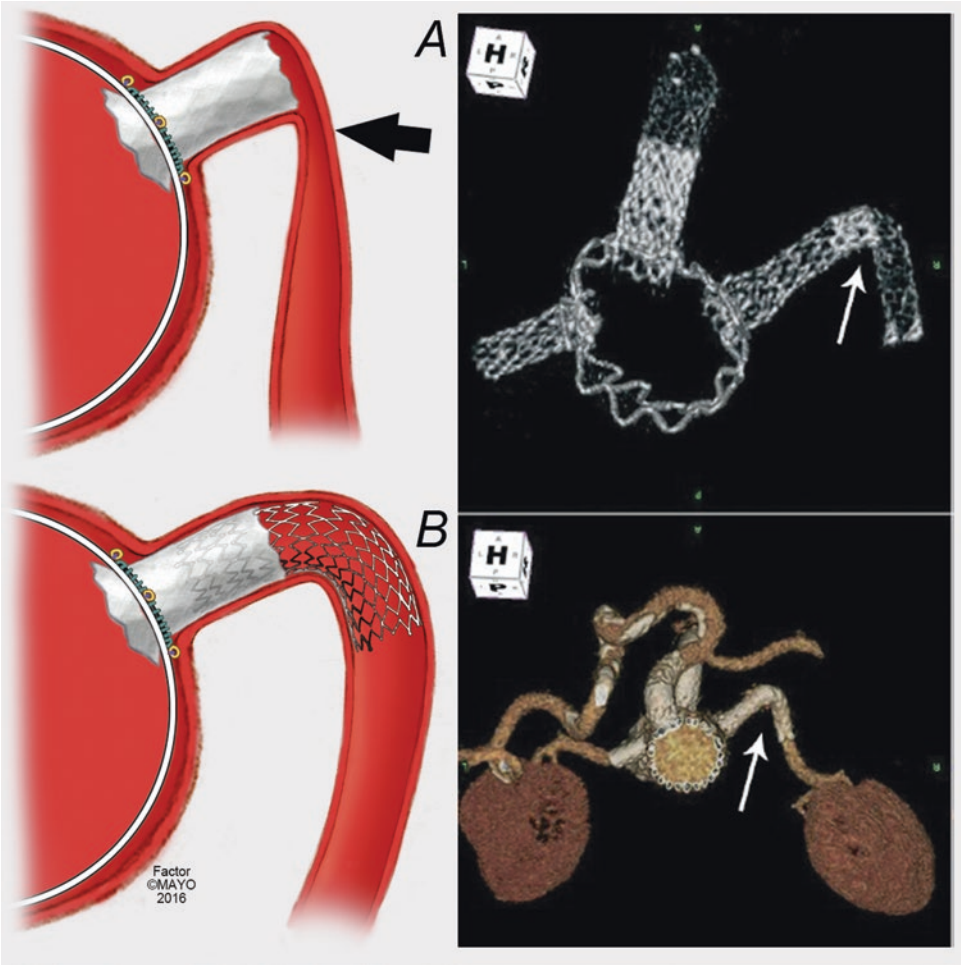


Fig. 19.4 Renal arteries with posterior orientation are prone to kink at the distal edge of the balloon expandable stents (A), which can be treated by placement of a self-expandable stent (B). By permission of Mayo Foundation for Medical Education and Research. All rights reserved.

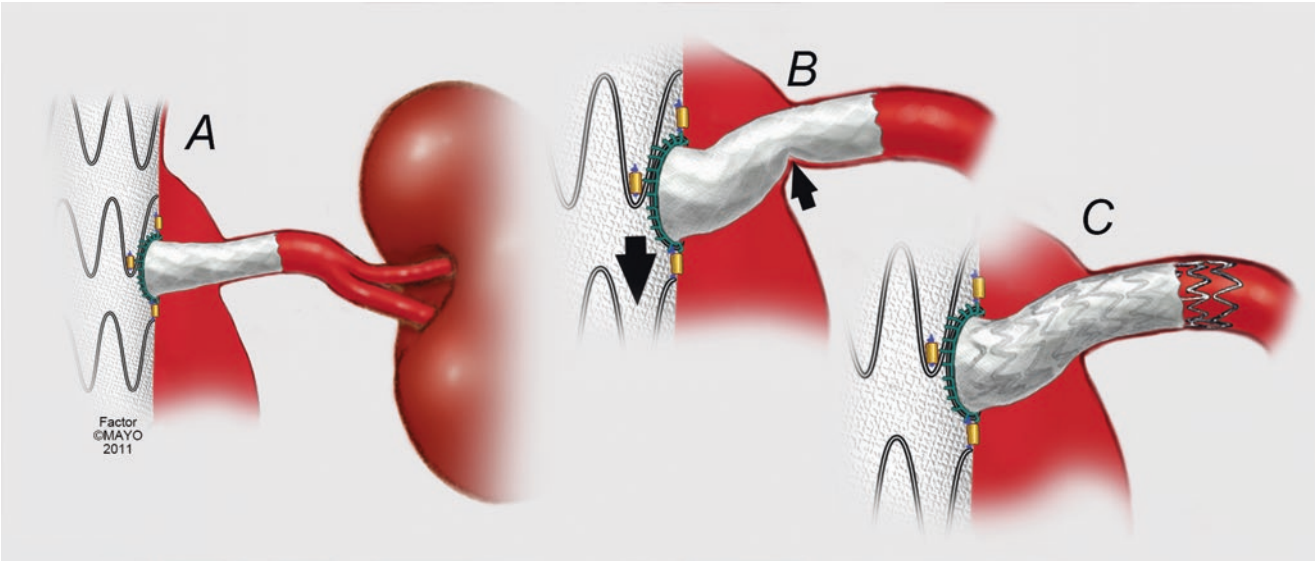


Fig. 19.5 Fenestrated branches are subjected to excessive force at the reinforced fenestration and origin of the vessel (**a**). If a kink is noted due to displacement of the stent (**b**) this can be reinforced by placement of additional balloon-expandable stent (**c**). By permission of Mayo Foundation for Medical Education and Research. All rights reserved

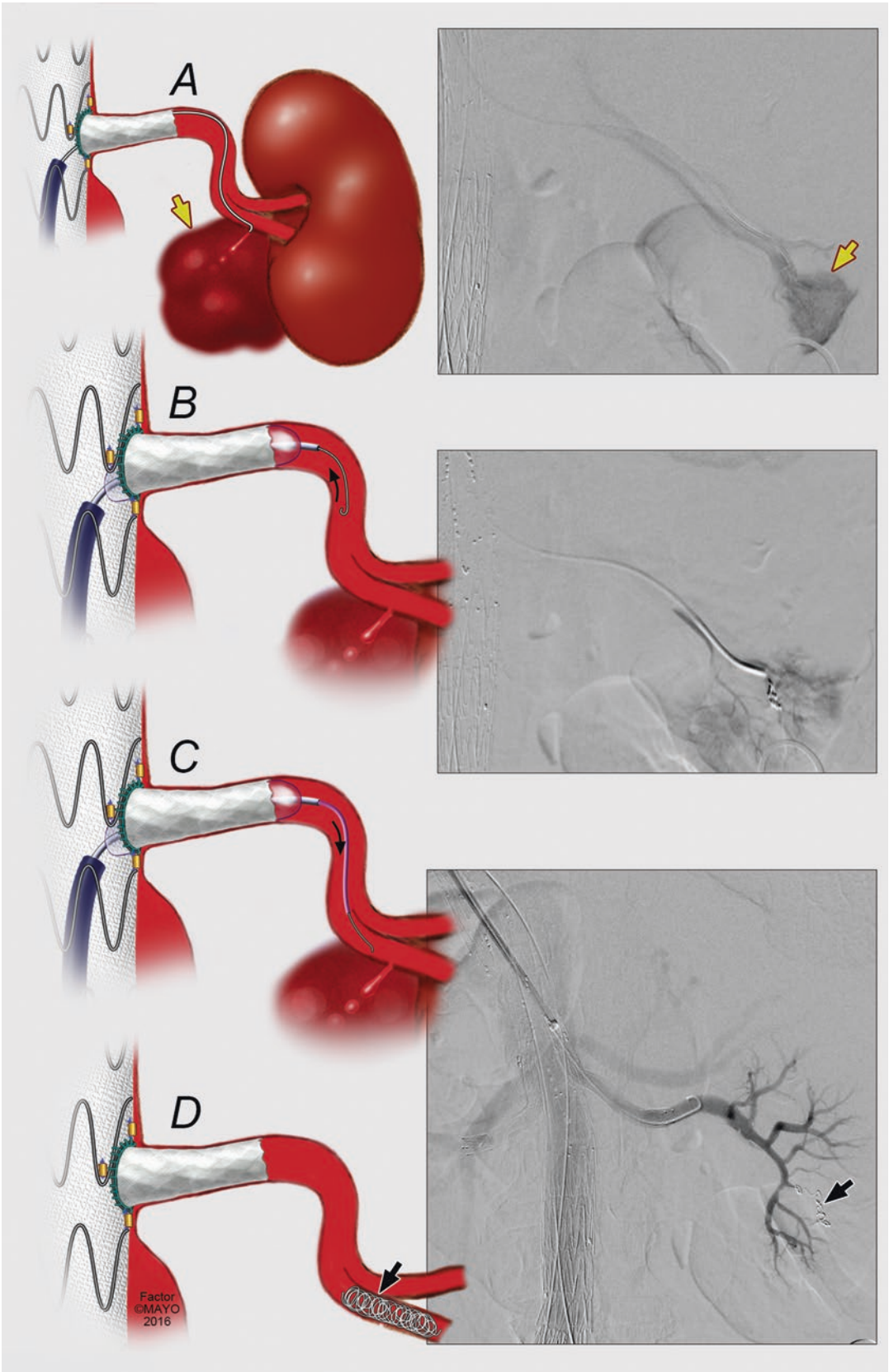


Fig. 19.6 Inadvertent perforation of a side branch should be immediately recognized (**a**) by completion angiography. The balloon is re-inflated in the bridging stent (**b**) and angiography is obtained via the balloon catheter (**c**). A micro-catheter can be advanced through the inflated balloon and the distal perforated vessel is coil embolized (**d**). By permission of Mayo Foundation for Medical Education and Research. All rights reserved

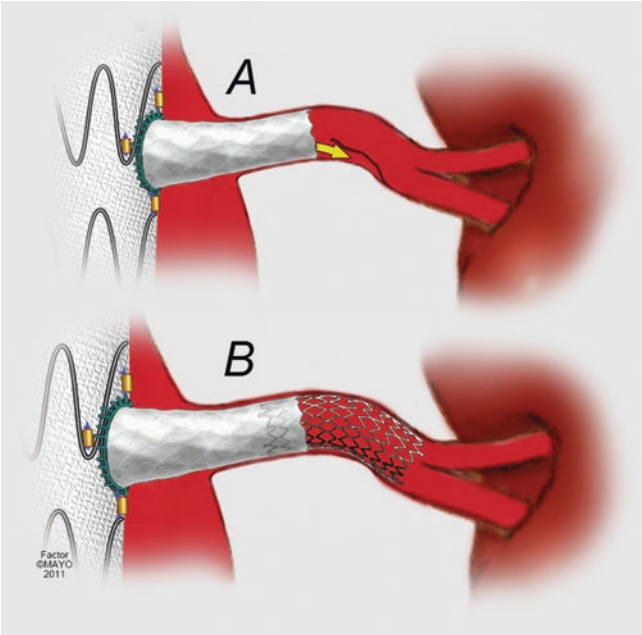


Fig. 19.7 Treatment of branch vessel dissection (**a**) with placement of bare metal self-expandable stent (**b**). By permission of Mayo Foundation for Medical Education and Research. All rights reserved

branches, access to the vessel with a micro-catheter should be maintained throughout all the aforementioned steps to avoid time to re-access the branch. Additionally, the catheter within the branch can temporize bleeding while coils are prepared. Coils can then be delivered through the catheter (Fig. 19.6). If access to the branch needs to be reestablished, a micro-catheter and 0.018-in. soft glide-gold wire are useful to catheterize the perforated branch, which is coiled using 0.018-in. coils. Dissections within the main renal artery can be treated by placement of an additional self-expandable stent. A devastanting complication can occur if there is total disruption of the vessel beyond a short fenestrated stent. It is imperative that access is not lost and the balloon should be immediately reintroduced and inflated in the stent. If salvage is not possible and the vessel needs to be sacrificed, it is best to extend the stent first by placement of a longer stent into the retro-peritoneum, and then to pack the stent with coils and plugs. A dissection distal to the bridging stent should be recognized and treated using a self-expandable bare metal stent to prevent vessel occlusion (Fig. 19.7).

Dissection of the hepatic artery can be difficult (Fig. 19.8a), but may be managed by loop technique to allow retrograde access via the superior mesenteric artery and gastroduodenal collaterals (Fig. 19.8b). Once the glide-wire is advanced into the celiac branch it is snared (Fig. 19.8c), and a loop is established to allow of a 4Fr catheter and exchange for a 0.035-in. guide-wire, which is positioned in the non-dissected segment of the celiac axis. Celiac stenting is completed with placement of a self-expandable stent across the dissected segment (Fig. 19.8e, f).

Endoleaks

The higher number of stent-graft components that is needed to repair complex aneurysms increases the potential for failure of one of the attachment sites. In general, endoleaks are frequent at the completion angiography but most are due to combination of type IV and II endoleaks from extensive stent-graft coverage and fabric perforation at the diameter-reducing ties and multiple retrograde branches. Type I endoleaks are exceedingly uncommon with proper planning and long landing zones [1–3]. In the US fenestrated trial, there were no patients with type I or III endoleaks [4]. In the event of a type I endoleak, repeat dilatation of the proximal neck may be needed using a Coda balloon. In these cases, all alignment stents need to be protected by balloon inflation (Fig. 19.9). Type III endoleaks may occur from lack of alignment stent apposition, use of bare-metal stent or inadequate length into the aorta. These may require repeat dilatation or placement of a second covered stent.

Type III endoleaks can occur at the attachment of balloon expandable stents with reinforced fenestrations. To avoid these endoleaks, proper flaring of the stent is needed using a 10 mm balloon. In patients with small renal arteries, flaring has to be done carefully to avoid risk of perforation. Until proven otherwise, an endoleak adjacent to a renal fenestration is a type III endoleak, and if this is noted it should be revised immediately by additional flaring or placement of additional covered stent. These endoleaks can also occur late in follow-up due to material fatigue or undocking of the target vessel stent. Regaining access to these damaged stents can be challenging. One technique involves use of 0.018 in. wire used as a rail to align the sheath with the target fenestration and stent. After the rail has been established, buddy catheter and wire can be used to localize the stent lumen. Ballooning of the stent and relining with additional stents can then easily be performed.

Infolding of the Aortic Stent

The proximal fenestrated component is often sized for the diameter of the aortic neck located above the mesenteric vessels with tapering of the fabric below the renal arteries. However, there is often a natural narrowing of the aorta at the level of the renal arteries, creating potential for excessive oversizing and infolding of the aortic stent. While this is a

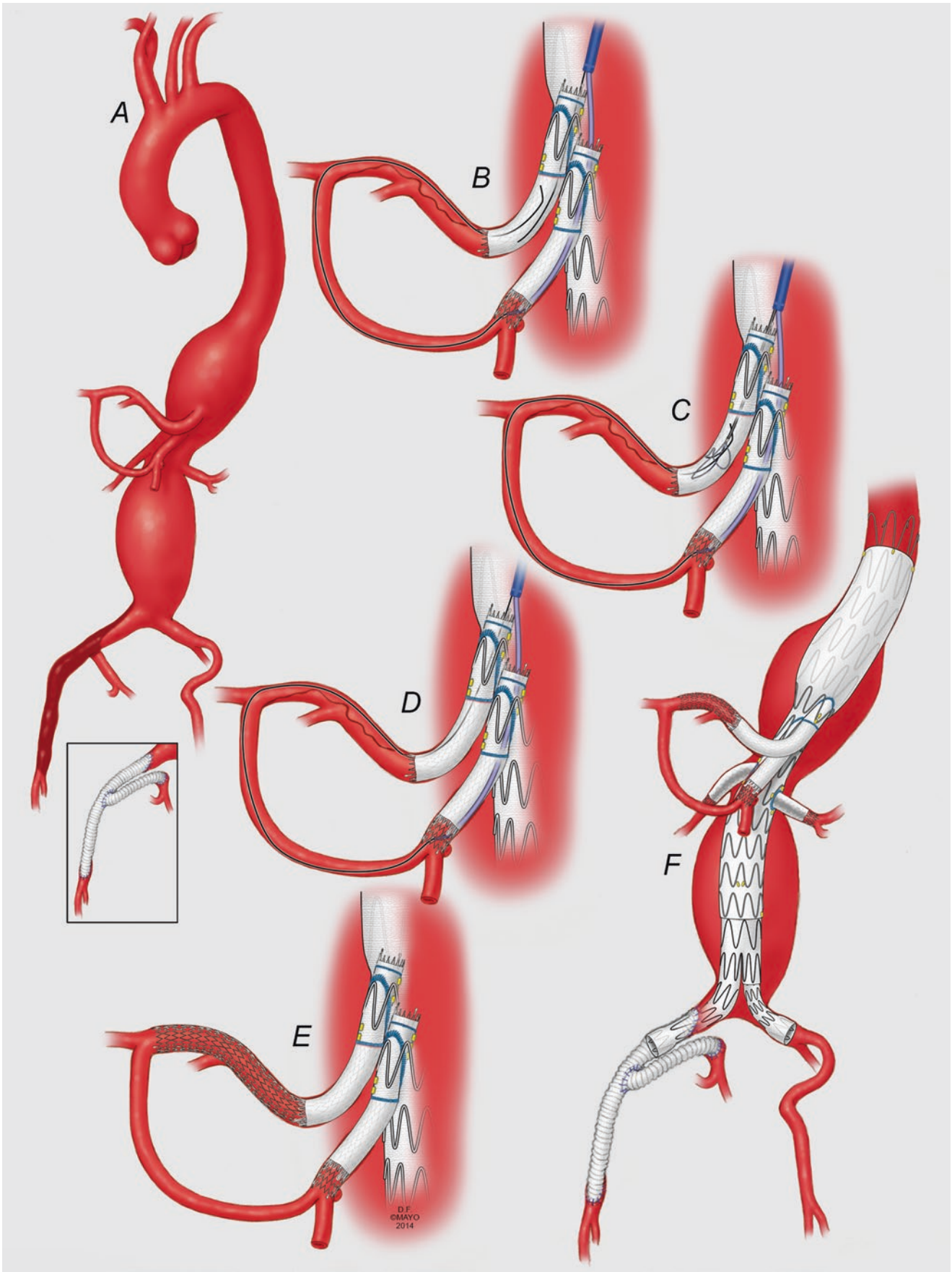


Fig. 19.8 Loop technique for access into the celiac axis via SMA collateral branches (**a**–**f**). By permission of Mayo Foundation for Medical Education and Research. All rights reserved

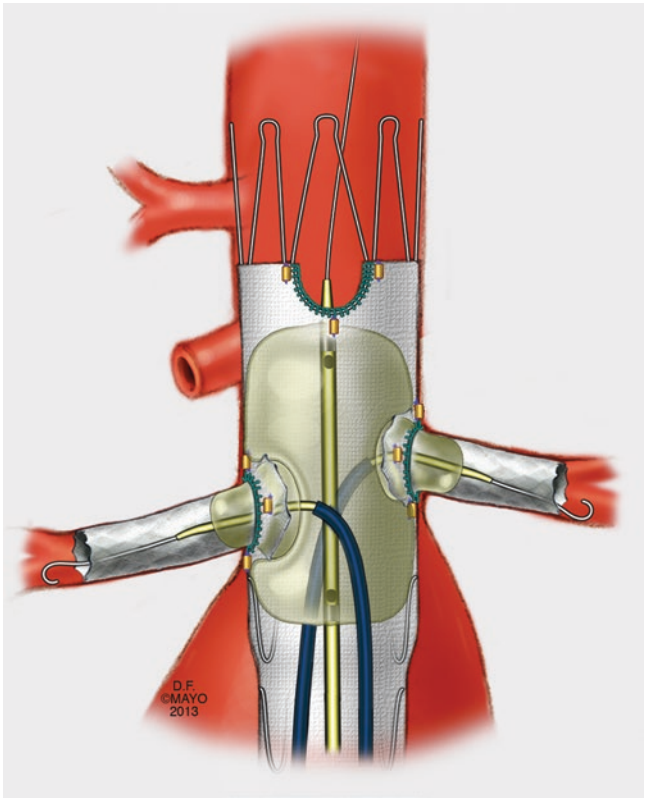


Fig. 19.9 Balloon dilatation of the sealing zone after placement of bridging stents requires protection of each stent by separate balloons. By permission of Mayo Foundation for Medical Education and Research. All rights reserved

rare complication, it should be immediately recognized by observing the behavior of the aortic stent during balloon inflation or obtaining a cone beam CT at completion of the case (Fig. 19.10). The infolded graft is often a cause of a type Ia endoleak and may cause outflow obstruction and/or compression of nearby target vessel stents (Fig. 19.10a). Overall, the sequelae can be catastrophic resulting in increased risk of graft or target vessel thrombosis.

Management of infolded grafts is complex as illustrated in Fig. 19.10. Excessive ballooning must be done with caution to avoid rupture of the aorta or avulse a side branch. In the event that infolding occurs in proximity to a stented side branch, each target vessels needs to be re-assessed with a guide-wire, sheath, and balloon prior to any aggressive ballooning (Fig. 19.10b). If ballooning alone is unsuccessful to undo the infolding, additional radial force may be needed to smooth proximal sealing stent. A Palmaz stent can be deployed in the proximal aspect of the graft using a non-compliant balloon (Fig. 19.10c). After balloon protection is placed within nearby stents, the Palmaz stent is deployed and aggressive ballooning can safely be performed. The aortic balloon is carried distally across the branched vessels to fully expand the aortic stent (Fig. 19.10d). Following deflation of the aortic balloon and successful resolution of the infolding, each side stent is flared into its original configuration by inflation of 10 mm angioplasty balloons (Fig. 19.10e). The aortic balloon can be inflated again (Fig. 19.10f), but it is important that this is deflated before the side branch balloons, allowing complete expansion of the aortic stent with adequately flared side stents (Fig. 19.10g). Intraoperative cone beam CT or rotational angiography can help identify and prevent these defects before completion of the procedure.

Stenotic Target Vessels

Preoperative imaging typically identifies stenosis of target vessels. In general, we avoid stenting these vessels prior to proceeding with the fenestrated stent because of risk of having the branch stent protruding into the aorta. If stenting is performed this should be done carefully by placement of the branch stent inside the vessel and using preferentially a covered stent. More commonly, the author's preference is to leave a balloon loaded over a 0.014-in. guide-wire, which can be used after deployment of the fenestrated stent to predilate the lesion. In the event the target vessel stenosis can be crossed with the 0.035-in. angled glide-wire, a 4 Fr Kumpe with guide sheath support can be used in a "drilling" motion to cross the renal artery stenosis (Fig. 19.11). The glide-wire can then be exchanged for a Rosen wire to perform a pre-ballooning angioplasty before advancing the sheath into place.

Stent Dislodgement

The first generation of iCAST covered stents were more prone to moving in the balloon so that stent dislodgement was not infrequent. This should be immediately recognized to avoid having a stent "floating" in the aorta or target vessel. If the sheath needs to be repositioned after a stent is advanced, the stent should be removed and the balloon shaft should be examined to assure that the stent is not inside the sheath. If this is not recognized and the dilator and sheath are re-advanced, the stent will be advanced over the wire without the balloon (Fig. 19.12a). In these cases it is best to re-access the fenestration from brachial or femoral approach and advance a small 5 Fr sheath into the vessel along with a snare (Fig. 19.12b). The "floating" stent is snared (Fig. 19.12c), and a 0.035-in. quickcross catheter is advanced across the stent (Fig. 19.12d). The 0.035-in. wire is exchanged for

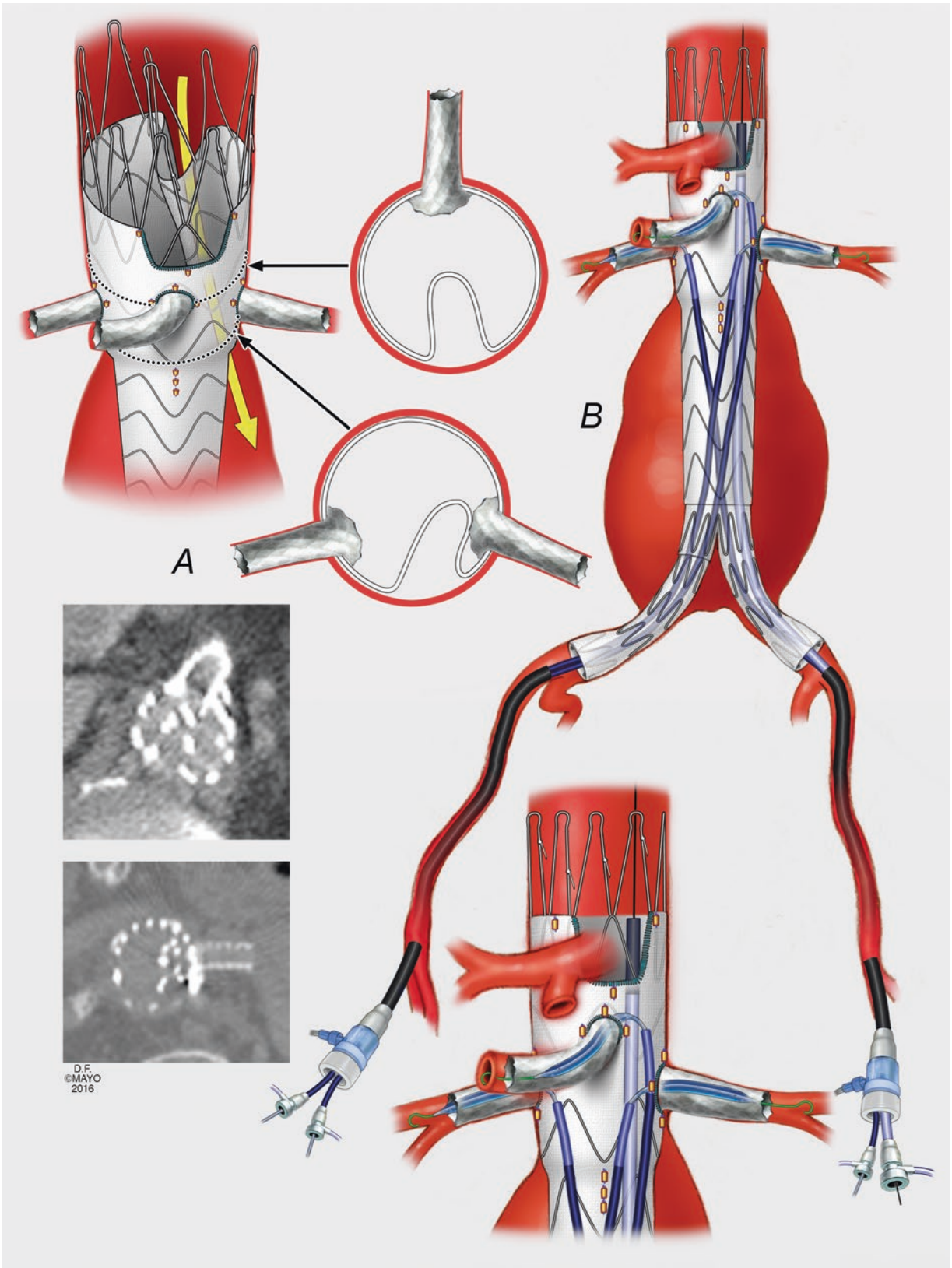


Fig. 19.10 Infolded aortic stent across the fenestrated segment (**a**) requires protection of each of the side stents by sheath and balloon (**b**). Placement of a Palmaz stent in the proximal sealing stent (**c**), followed by dilatation of the visceral segment of the graft (**d**), balloon dilatation of each side stent (**e**), and the aorta (**f**) allows complete expansion of the aortic graft (**g**). By permission of Mayo Foundation for Medical Education and Research. All rights reserved

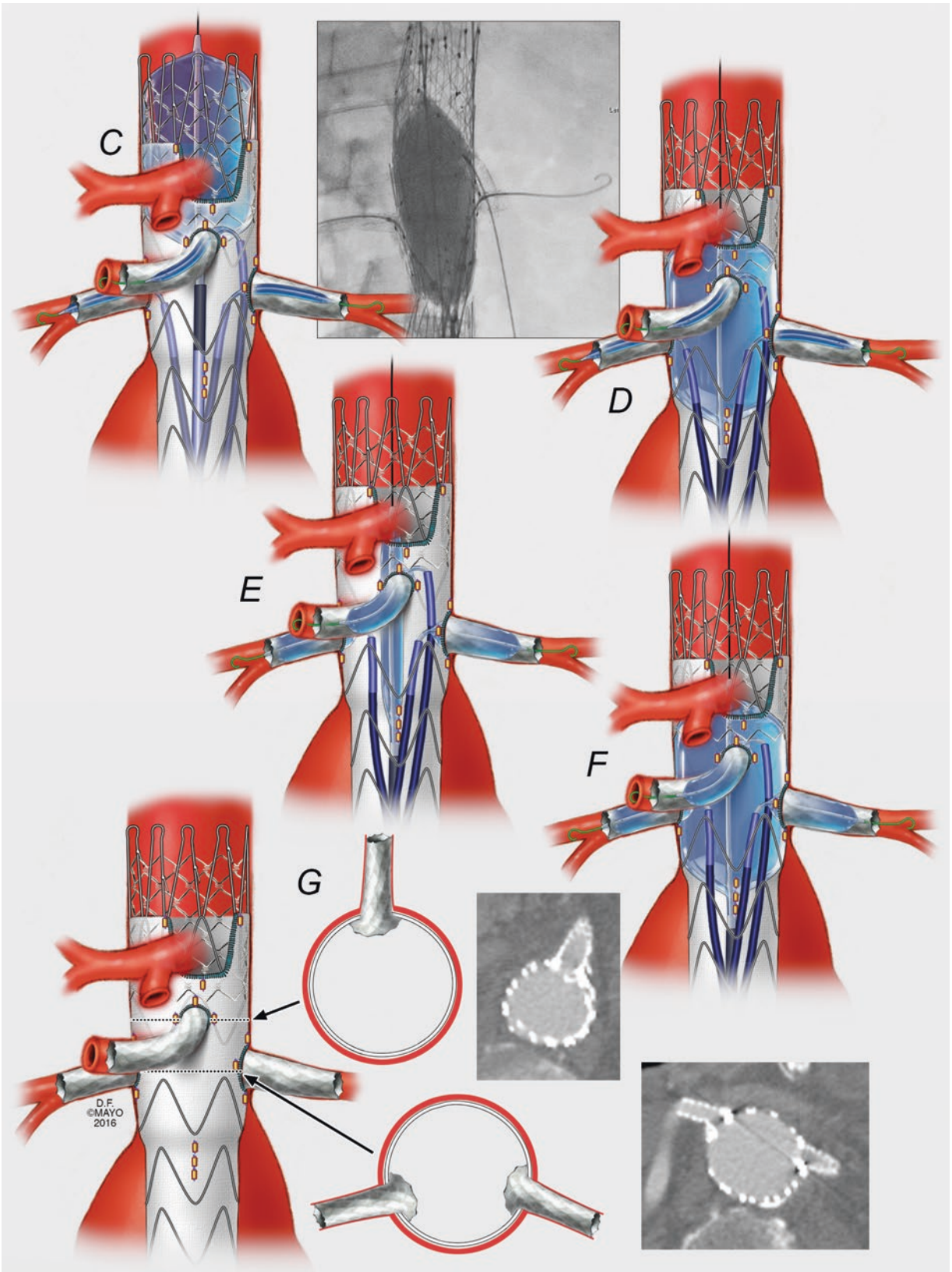


Fig. 19.10 (continued)

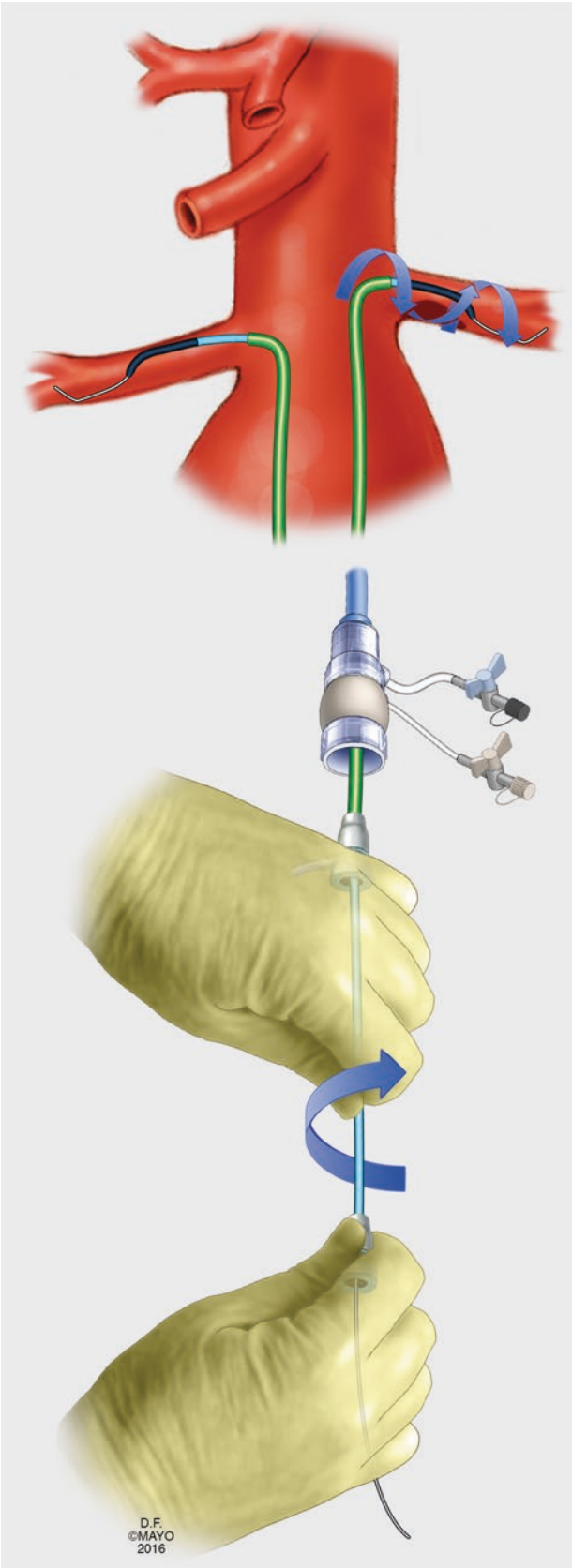


Fig. 19.11 Technique of advancement of Kumpe catheter across tortuous or stenotic vessels. By permission of Mayo Foundation for Medical Education and Research. All rights reserved

smaller 0.018-in. system (Fig. 19.12e), a small undersized balloon is inflated in the stent (Fig. 19.12f), which is deployed in neutral position within the target vessel (Fig. 19.12g). A new bridging stent is then placed to complete the repair (Fig. 19.12h).

Viabahn stent-grafts are deployed using a cord mechanism from tip to hub (Fig. 19.13a). Rapid deployment may result in inadvertently pulling the stent out of the target vessel (Fig. 19.13b). To avoid this complication, it is important that Viabahn stents are deployed slowly while keeping the sheath in the middle segment of the stent (Fig. 19.13c). The sheath is then progressively withdrawn while the stent is deployed into the cuff of the directional branch (Fig. 19.13d, e). If the stent requires additional radial force at the attachment of the cuff, a balloon expandable covered stent can be added (Fig. 19.13f).

Preventing Compression of Side Stents

The bifurcated stent and iliac limbs delivery device can damage previously placed stents in the target vessels (Fig. 19.14a, b). Delivery systems can inadvertently crush a renal or SMA stent during advancement. Direct fluoroscopic visualization adds one layer of visualization, but protection with balloon insufflation within the stents of concern is the only definitive guarantee the stent is not compromised (Fig. 19.14c, d). Additionally, if any reintervention is required, balloon protection of the renal and visceral vessels should be considered to avoid any inadvertent stent compression resulting in inability to access the stent altogether.

Sheath Advancement

Down-going renal arteries may be difficult to access via the femoral approach. One of the first maneuvers that can be used is to advance the catheter to the top of the device and into the target vessel, allowing guide-wire exchange for a Rosen wire (Fig. 119.5a). If a sheath with soft dilator cannot be advanced into the vessel (Fig. 19.15b), a useful maneuver is to inflate a balloon, which is used as dilator for the sheath (Fig. 19.15c). The sheath is advanced into the target vessel while the balloon is deflated (Fig. 19.15d).

Crossing Dissection Flaps

Fenestrated and branched endografts have been increasingly applied to treat complex anatomy including chronic dissections. In these cases fenestrations are preferentially used in segments of narrow aortic diameter and branches are reserved for larger diameter lumens or for vessels which

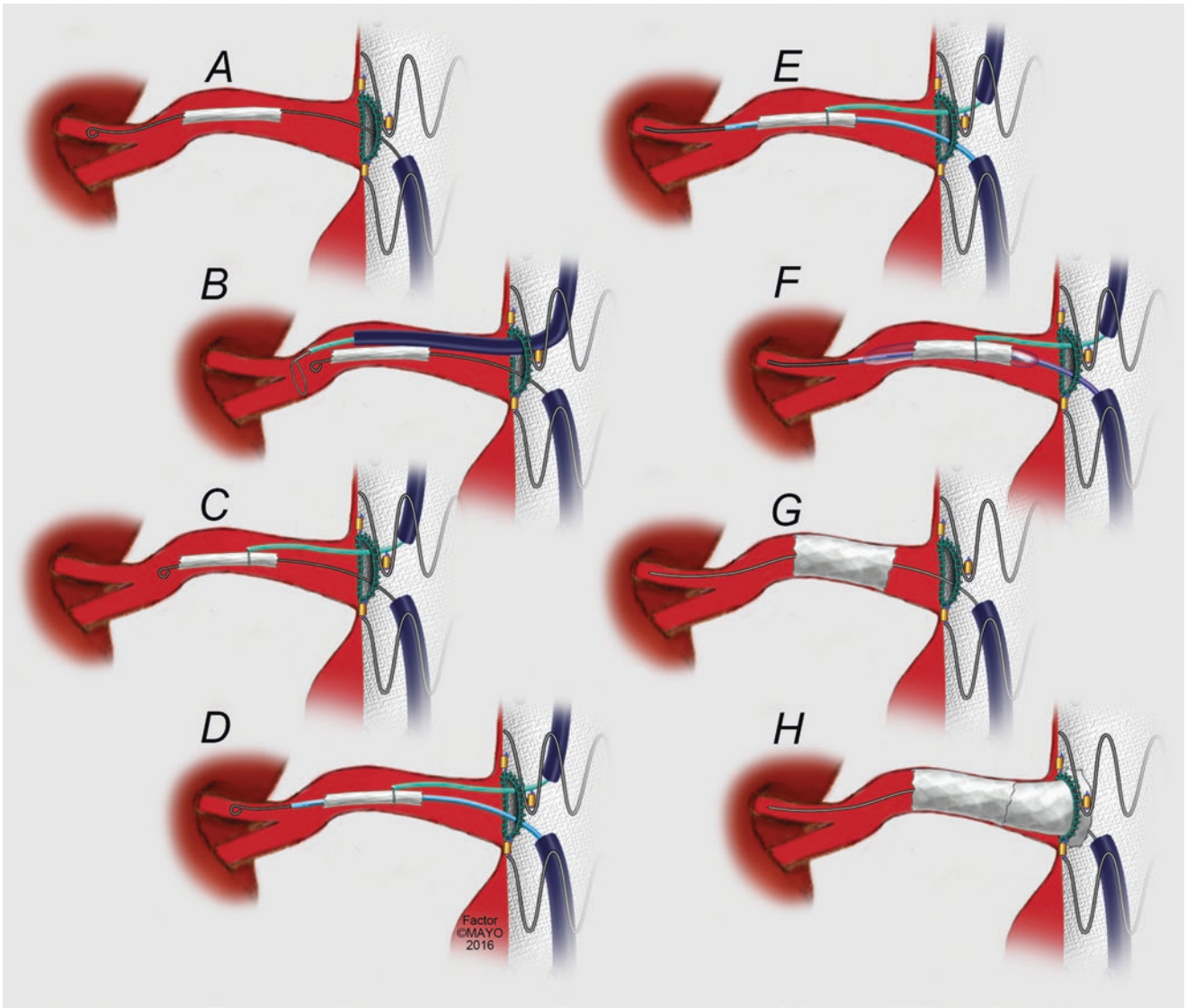


Fig. 19.12 Technique of dealing with displaced floating stents is described in detail (**a**–**h**). By permission of Mayo Foundation for Medical Education and Research. All rights reserved

originate from an isolated false lumen (Fig. 19.16a, b). Staged coverage of the aorta is preferred for extensive aneurysms to minimize risk of paraplegia (Fig. 19.16c). Following placement of the distal fenestrated and branched component and successful stenting of all fenestrations (Fig. 19.16d), the branch is catheterized and septum is crossed using an outback reentrance catheter (Fig. 19.16e). Access into the false lumen is confirmed and the septum is dilated with a balloon (Fig. 19.16f) to facilitate exchanges. A catheter is advanced into the target vessel (Fig. 19.16g) and the procedure is completed by placement of the bridging stent across the false lumen.

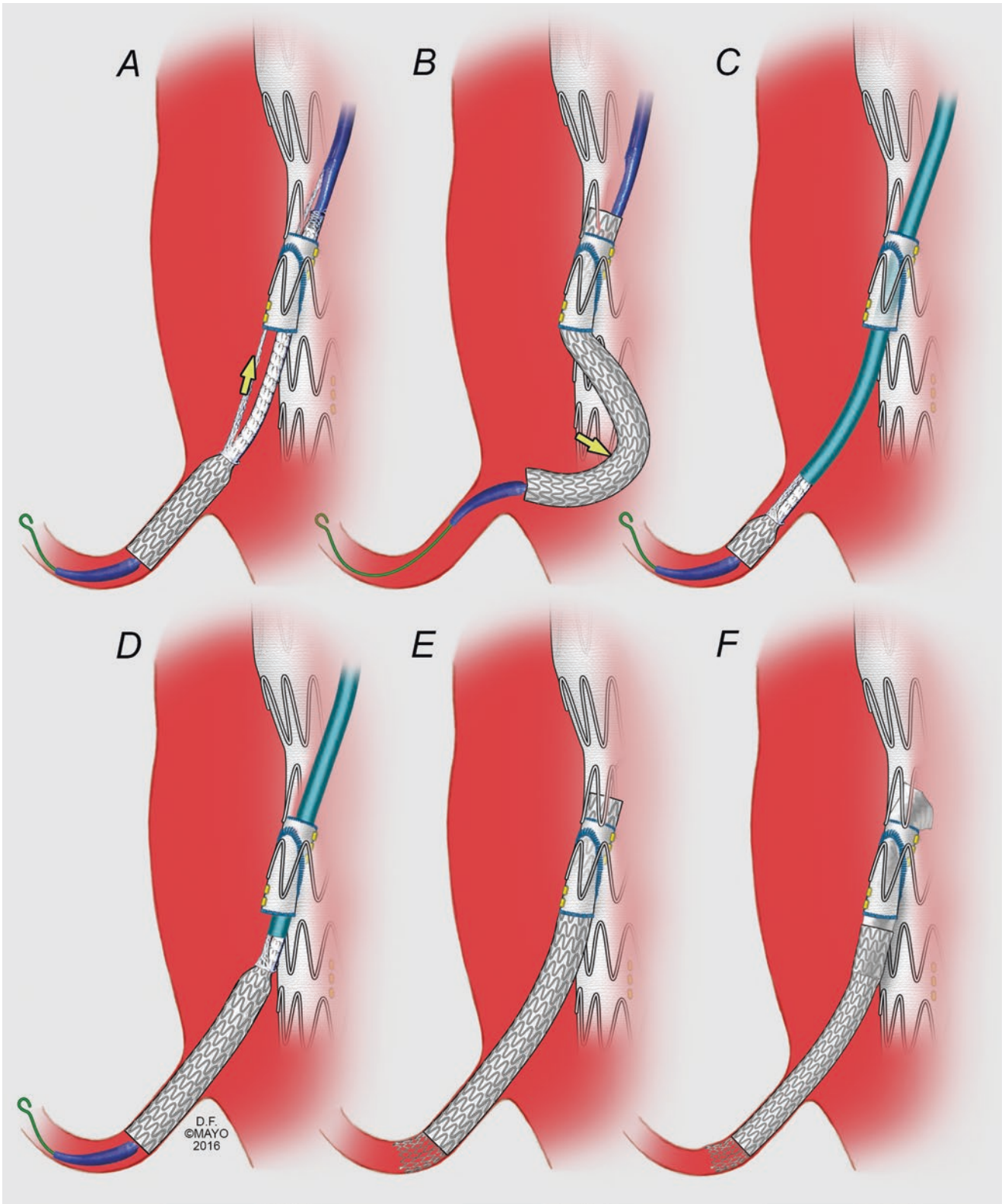


Fig. 19.13 Technique of deployment of Viabahn stent-graft to avoid displacement (**a**–**f**). By permission of Mayo Foundation for Medical Education and Research. All rights reserved

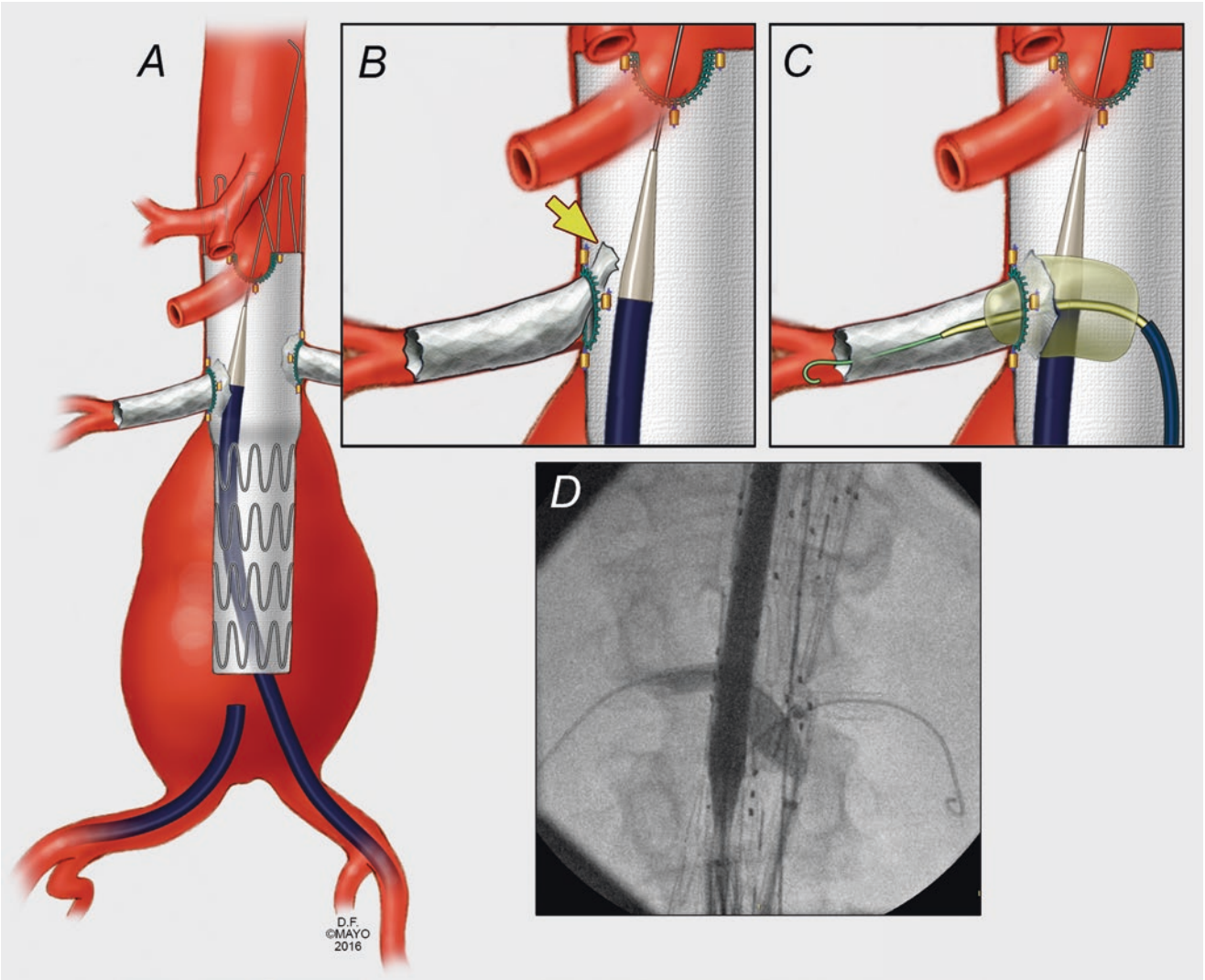


Fig. 19.14 Compression of side branch stent by placement of distal component (**a**, **b**) can be avoided by inflation of a balloon to protect the side branch (**c**, **d**). By permission of Mayo Foundation for Medical Education and Research. All rights reserved

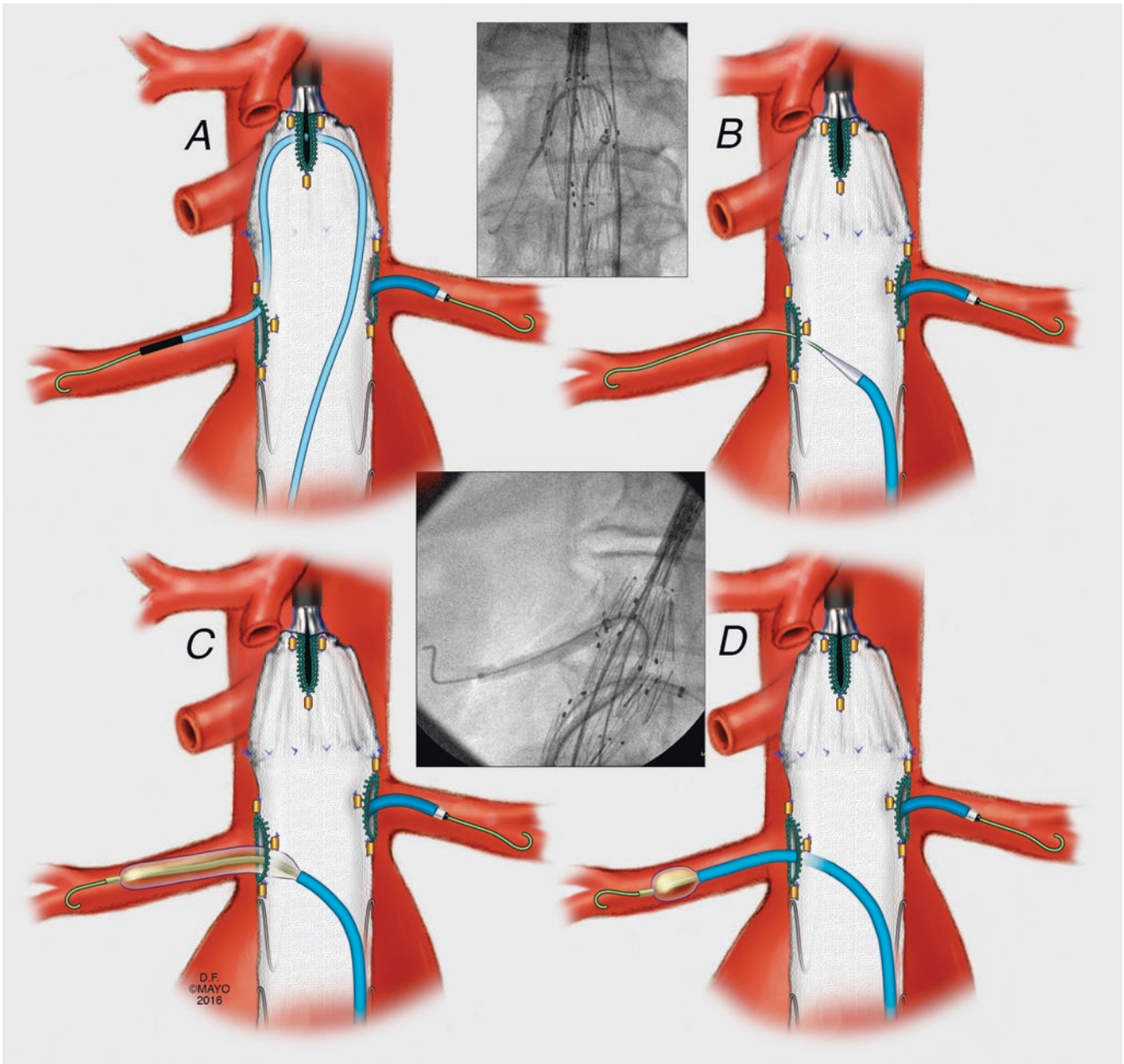


Fig. 19.15 Sheath advancement using the top part of the fenestrated stent (**a**, **b**) and a balloon to replace the dilator of the sheath (**c**, **d**). By permission of Mayo Foundation for Medical Education and Research. All rights reserved

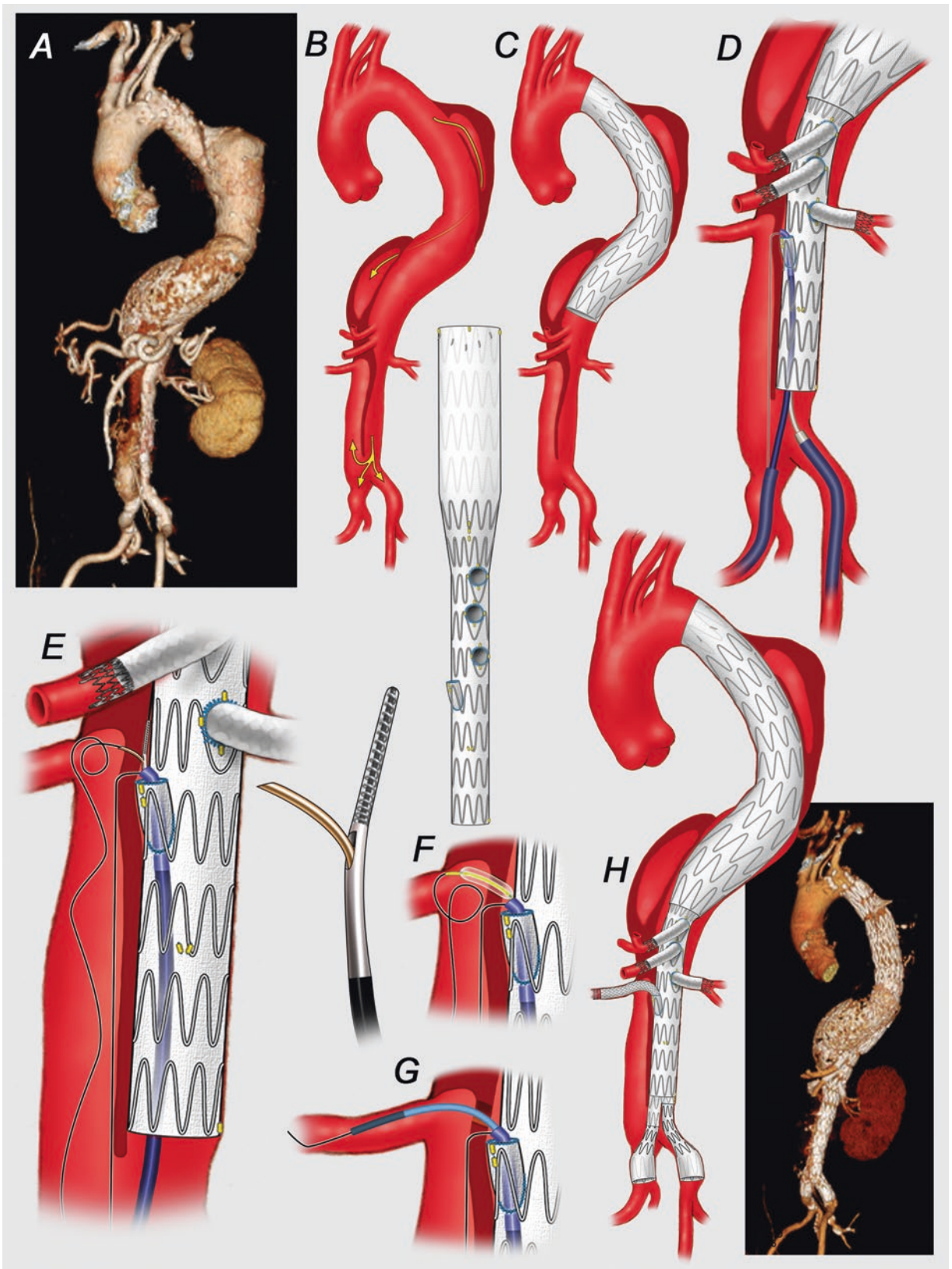


Fig. 19.16 Technique of branch vessel stenting in patients with chronic aortic dissections with vessels originating from an isolated false lumen (**a**–**h**). By permission of Mayo Foundation for Medical Education and Research. All rights reserved

Suggested Reading

1. Greenberg R, Eagleton M, Mastracci T. Branched endografts for thoracoabdominal aneurysms. J Thorac Cardiovasc Surg. 2010;140(6 Suppl):S171–8.
2. Guillou M, Bianchini A, Sobocinski J, Maurel B, D'Elia P, Tyrrell M, et al. Endovascular treatment of thoracoabdominal aortic aneurysms. J Vasc Surg. 2012;56(1):65–73.
3. Haulon S, Amiot S, Magnan PE, Becquemin JP, Lermusiaux P, Koussa M, et al. An analysis of the French multicentre experience of fenestrated aortic endografts: medium-term outcomes. Ann Surg. 2010;251(2):357–62.
4. Greenberg RK, Sternbergh III WC, Makaroun M, Ohki T, Chuter T, Bharadwaj P, et al. Intermediate results of a United States multicenter trial of fenestrated endograft repair for juxtarenal abdominal aortic aneurysms. J Vasc Surg. 2009;50(4):730–7.e1.
5. Conway BD, Greenberg RK, Mastracci TM, Hernandez AV, Coscas R. Renal artery implantation angles in thoracoabdominal aneurysms and their implications in the era of branched endografts. J Endovasc Ther. 2010;17(3):380–7.
6. Dowdall JF, Greenberg RK, West K, Moon M, Lu Q, Francis C, et al. Separation of components in fenestrated and branched endovascular grafting—branch protection or a potentially new mode of failure? Eur J Vasc Endovasc Surg. 2008;36(1):2–9.
7. Martin-Gonzalez T, Pincon C, Maurel B, Hertault A, Sobocinski J, Spear R, et al. Renal outcomes following fenestrated and branched endografting. Eur J Vasc Endovasc Surg. 2015;50(4):420–30.
8. Mastracci TM, Eagleton MJ, Kuramochi Y, Bathurst S, Wolski K. Twelve-year results of fenestrated endografts for juxtarenal and group IV thoracoabdominal aneurysms. J Vasc Surg. 2015;61(2):355–64.
9. Mohabbat W, Greenberg RK, Mastracci TM, Cury M, Morales JP, Hernandez AV. Revised duplex criteria and outcomes for renal stents and stent grafts following endovascular repair of juxtarenal and thoracoabdominal aneurysms. J Vasc Surg. 2009;49(4):827–37; discussion 37.
10. Oderich GS, Correa MP, Mendes BC. Technical aspects of repair of juxtarenal abdominal aortic aneurysms using the Zenith fenestrated endovascular stent graft. J Vasc Surg. 2014;59(5):1456–61.
11. Oderich GS, Greenberg RK, Farber M, Lyden S, Sanchez L, Fairman R, et al. Results of the United States multicenter prospective study evaluating the Zenith fenestrated endovascular graft for treatment of juxtarenal abdominal aortic aneurysms. J Vasc Surg. 2014;60(6):1420–8.e1–5.
12. Oderich GS, Mendes BC, Correa MP. Preloaded guidewires to facilitate endovascular repair of thoracoabdominal aortic aneurysm using a physician-modified branched stent graft. J Vasc Surg. 2014;59(4):1168–73.
13. Oderich GS, Mendes BC, Kanamori KS. Technique of implantation and bail-out maneuvers for endovascular fenestrated repair of juxtarenal aortic aneurysms. Perspect Vasc Surg Endovasc Ther. 2013;25(1-2):28–37.
14. Park JH, Chung JW, Choo IW, Kim SJ, Lee JY, Han MC. Fenestrated stent-grafts for preserving visceral arterial branches in the treatment of abdominal aortic aneurysms: preliminary experience. J Vasc Interv Radiol. 1996;7(6):819–23.
15. Uflacker R, Robison JD, Schonholz C, Ivancev K. Clinical experience with a customized fenestrated endograft for juxtarenal abdominal aortic aneurysm repair. J Vasc Interv Radiol. 2006;17(12):1935–42.

Strategies to Minimize Risk of Spinal Cord Injury During Complex Endovascular Aortic Repair

20

Gustavo S. Oderich, Aaron C. Baker, and Peter Banga

Introduction

Endovascular treatment of thoracoabdominal aortic aneurysms (TAAAs) has greatly evolved in the last decade. Improvements in device design, techniques of implantation, adjunctive measures, and better perioperative care have resulted in substantial improvements in morbidity and mortality [1]. Contemporary reports by experienced operators indicate that 30-day mortality ranges from 5 to 9 %, which compares favorably to the largest open surgical experiences in centers with over thousands of repairs [1–5]. Nonetheless, spinal cord injury (SCI) continues to be the most devastating complication of these procedures with rates reaching up to 35 % in some series [1].

Paraplegia is a devastating complication for the patient, family and medical team and has been associated with significantly shortened survival [6]. Although the etiology of SCI is multifactorial, arterial embolization, coverage of large aortic segments, insufficient collaterals, and systemic hypotension are the main predisposing factors during endovascular TAAA repair [2, 7–9]. The importance of an extensive spinal collateral network has been discussed in Chap. 7. These collaterals include the carotid, subclavian, vertebral, intercostal, lumbar, hypogastric, and deep femoral arteries (Fig. 20.1) [2, 5, 10, 11]. As such, pre-operative, intra-operative, and post-operative strategies can be applied to maximize spinal cord perfusion and decrease risk of SCI.

Risk Stratification

The risk of spinal cord injury is variable depending on a number of predisposing risk factors. Extent of aortic coverage is the single-most important predictor with the highest rates observed for Type II (10–20 %) and Type I TAAAs and the lowest rates for Type IV TAAAs (1–5 %). The risk of spinal cord injury is higher among patients who need aortic coverage ≥4 cm above the celiac axis. Presence of occluded collateral network (hypogastric and/or vertebral artery) is associated with higher rate of immediate paraplegia and lack of improvement in motor function. Other determinants include prior aortic replacement and severe atherosclerotic debris. In general, our approach has been to routinely apply a protocol for spinal cord injury prevention in all patients undergoing TAAA) repair with ≥4 cm (or two sealing stents) above the celiac axis. This protocol is described in detail below.

Mechanisms of Injury

Spinal cord ischemia can result from multiple insults, which may occur in combination or as isolated events. Although many reports have identified risk factors for spinal cord injury, the specific causes have not been well described. Some of the recognized factors are hemodynamic deterioration leading to spinal cord infarction secondary to loss of intercostal arteries coupled with insufficient collateral network; reperfusion injury and spinal cord edema; and microembolization from catheter or device manipulations. Traditionally, embolization has been considered a relatively uncommon cause. However, since the widespread use of adjunctive measures to improve spinal cord perfusion during open aortic repair (e.g., distal perfusion, interscostal reimplantation,

G.S. Oderich (✉) • A.C. Baker
Division of Vascular and Endovascular Surgery,
Department of Surgery, Mayo Clinic, 200 First Street, SW,
Rochester, MN 55905, USA
e-mail: oderich.gustavo@mayo.edu aaron.c.baker@kp.org

P. Banga
Department of Vascular Surgery, Cardiovascular Center, Semmelweis University, Városmajor u. 68., Budapest 1122, Hungary
e-mail: bapevi@hotmail.com

© Mayo Foundation for Medical Education and Research 2017

G.S. Oderich (ed.), *Endovascular Aortic Repair*, DOI 10.1007/978-3-319-15192-2_20

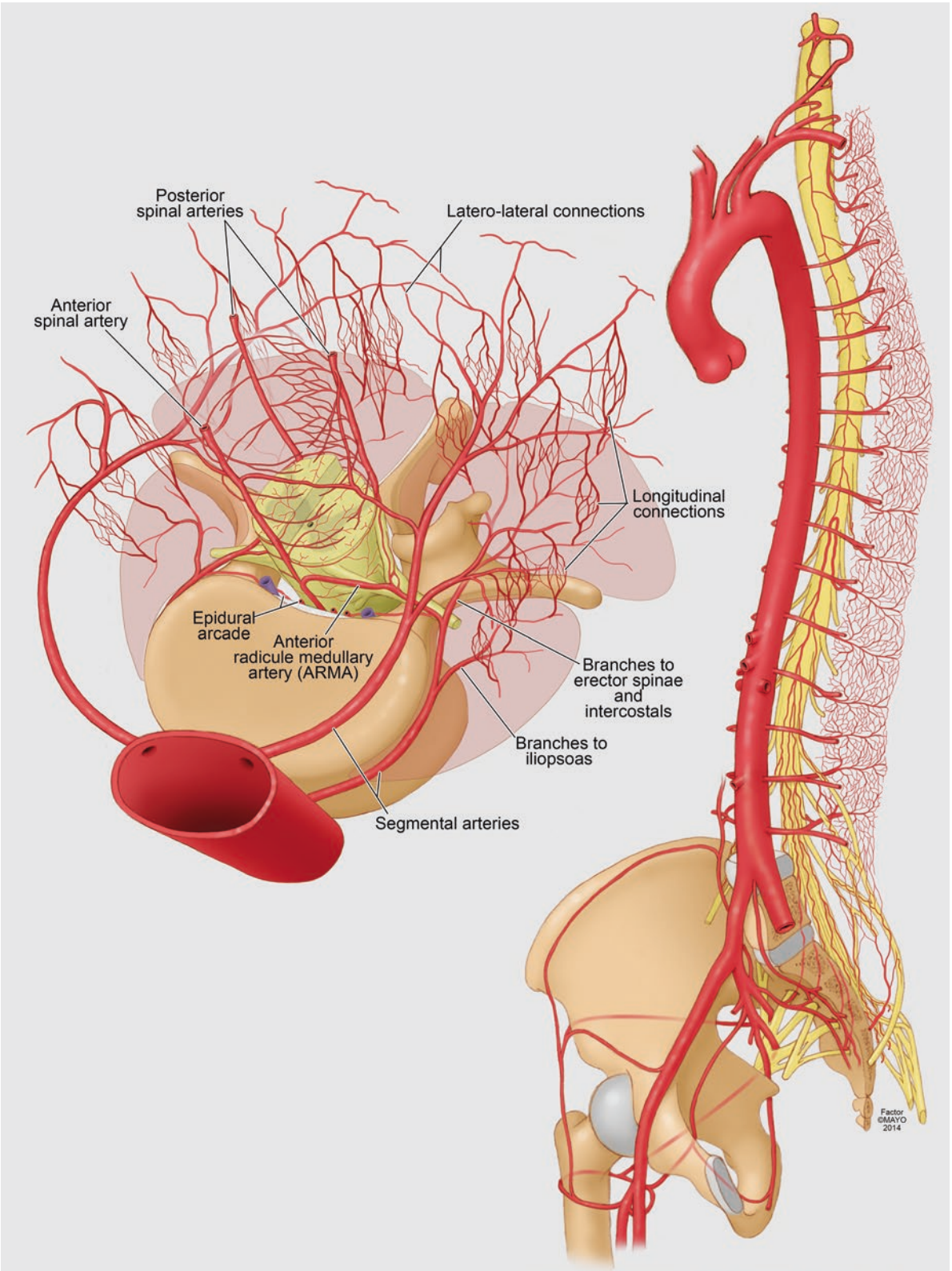


Fig. 20.1 Perfusion is provided via extensive segmental intercostal arteries, vertebral, hypogastric and para-spinal and intra-spinal collateral networks. By permission of Mayo Foundation for Medical Education and Research. All rights reserved

hypothermia, CFS drainage), the most common etiology of spinal cord ischemia may have shifted from hemodynamic deterioration to micro-emboli. Tanaka and associates reported the results of MRI to evaluate mechanisms of spinal cord injury after aortic repair. In that study, diffuse infarction around the artery radicularis magna, which is consistent with hemodynamic deterioration, was observed in only 20 % of patients with injury. The remaining 80 % of patients had scattered or focal MRI lesions corresponding to infarction from microembolization.

Neuromonitoring has been extensively used during open surgical repair to help identify ischemia in the anterior and lateral spinal columns, which are sensitive to decreases in oxygen supply [15, 16]. During open TAAA repair, this technique has helped guide selective intercostal artery reimplantation and intra-operative maneuvers designed to improve spinal cord perfusion. Because signal changes can result from dysfunction in any of the recorded pathways, including the brain, peripheral nerves, receptors or muscles, as well as technical issues, interpretation requires correlation with the clinical scenario. During endovascular procedures, early detection of these changes may ultimately help identify patients at increased risk of spinal cord injury and in whom hemodynamic deterioration may be prevented or reversed by use of sequential maneuvers designed to optimize spinal cord perfusion pressure (SCPP) by augmentation of mean arterial pressure (MAP) and reduction of cerebrospinal fluid (CSF) pressure (SCPP = MAP − CSF pressure). These maneuvers raise traditional targets currently applied to endovascular procedures (MAP of 80 mmHg; CSF pressure of 10 mmHg, or maintaining a SCPP > 70 mmHg) and include early restoration of flow to the pelvis and lower extremities. In contrast to open aortic procedures, endovascular procedures do not allow for direct incorporation of intercostal arteries.

Prolonged lower extremity ischemia during complex endovascular procedures has been associated with more complications and increased risk of spinal cord injury. The large sheaths, which are needed for delivery of the aortic and target vessel stents, occlude inflow to the lower extremity and pelvis by covering the origin of the profunda femoris and internal iliac arteries. The surgeon needs to be attentive to lower extremity ischemia and its deleterious consequences including acidosis, pelvic and spinal ischemia and lower extremity compartment syndrome. Ideally, lower extremity perfusion should be restored within <2 h or as soon as possible.

Recent experimental and clinical studies have shown that staged segmental arterial coverage of the aorta allows rapid recruitment of the spinal collateral networks, decreasing mortality and SCI during endovascular TAAA repair. Moritz S. Bischoff, Randall Griepp, and associates reported no spinal cord injury in pigs randomized to staged coverage, compared to 50 % rate of paraplegia in pigs treated in a single stage. Subsequently, the Cleveland Clinic group reported that internal iliac artery occlusion was an independent predictor of immediate spinal cord injury and lack of recovery, while staged thoracoabdominal aortic repair reduced early mortality and rates of paraplegia. The benefits of staged repair for thoracoabdominal aneurysm may go beyond the optimization of collaterals. It is possible that a faster, simpler, second-stage procedure with earlier restoration of pelvic and lower extremity blood flow is associated with improved spinal cord perfusion, or that prior stent-graft coverage of the proximal thoracic aorta results in lower rates of micro-embolization during the second-stage procedure or a less pronounced systemic inflammatory response during the second-stage procedure. Although further clinical experiences are needed to confirm these results, current evidence suggests that a staged repair with segmental coverage of the aorta can allow rapid recruitment of the spinal collateral networks, decreasing mortality and SCI during endovascular TAAA repair [12–14].

Spinal Cord Injury Prevention Protocol

A standardized protocol to reduce risk of spinal cord injury is applied in all patients undergoing endovascular TAAA repair. Procedures are performed by a dedicated endovascular team under total intravenous general endotracheal anesthesia using fixed imaging in a hybrid endovascular room. The anesthetic management is discussed in detail in Chap. 22 and consists of propofol and fentanyl or sufentanil infusion at the discretion of the anesthesiologist with avoidance of non-depolarizing muscle relaxants. Succinylcholine is used as the muscle relaxant of choice for induction of anesthesia.

Staging

Staged endovascular approach is used in all patients with extent type I or II TAAAs (Fig. 20.2). Several staging strategies have been utilized. Our preference is to proceed with coverage of the proximal thoracic aorta from the landing zone to just above the celiac axis, leaving a distal Ib endoleak with completion repair in 6–8 weeks or earlier in patients with rapid expansion of very large aneurysms who are suitable candidates for off-the-shelf devices (Fig. 20.3). Temporary sac perfusion branches can be designed into the main aortic stent, which are left patent in the initial procedure with plan of subsequent occlusion. In these cases (Fig. 20.4), the perfusion branch(es) is occluded in a few days using an amplatzer plug, which can be deployed under local anesthesia. The patient is kept heparinzed and observed for 2–4 h with the

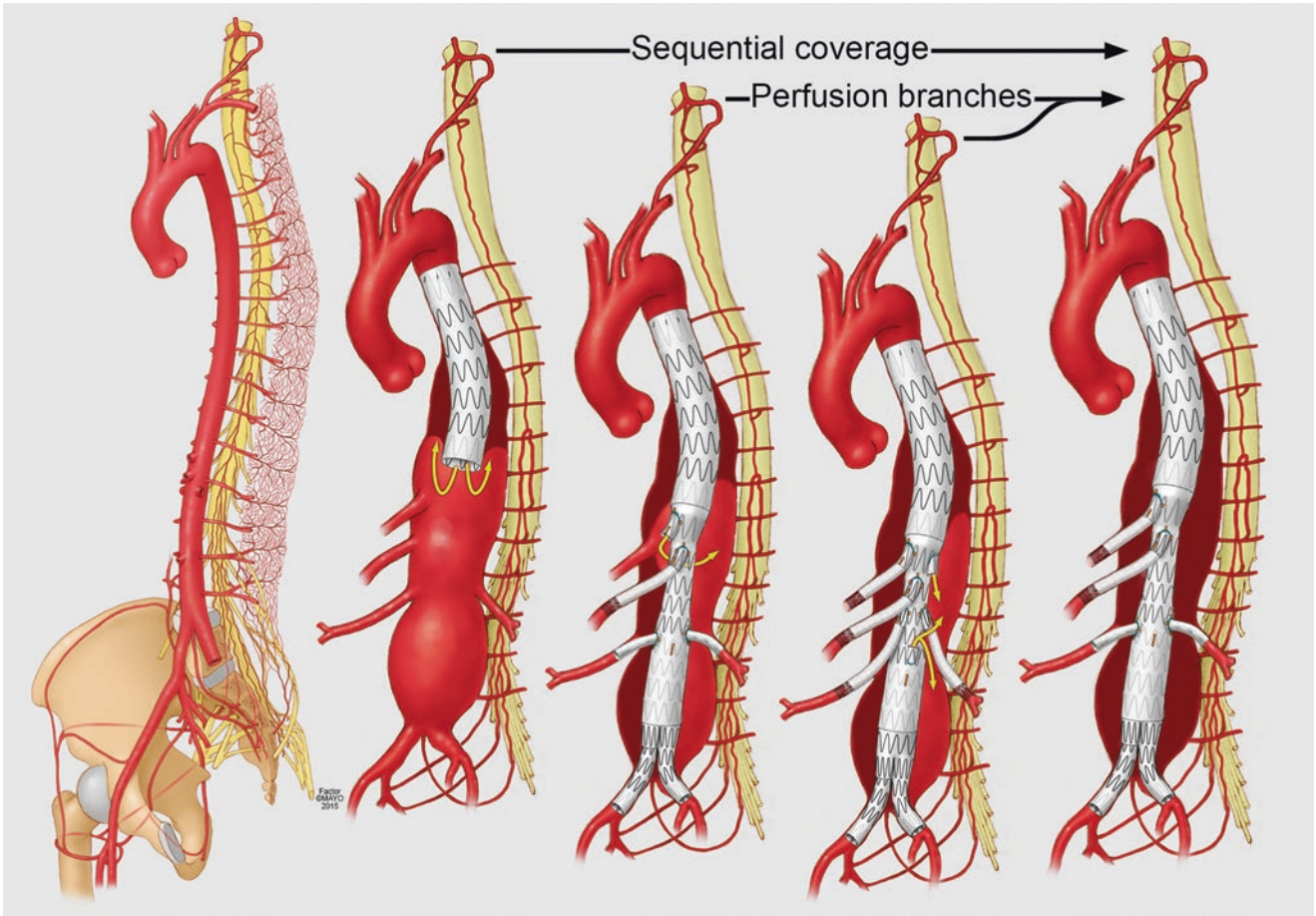


Fig. 20.2 Optimization of the extensive spine collateral network including vertebral, intercostal, lumbar, and hypogastric arteries forms the basis for staged endovascular repair of complex aneurysms. Strategies include coverage of the proximal thoracic aorta up to the celiac axis, followed by visceral branch stenting in a second stage. Alternatively, the sac can be perfused via perfusion branches or unstented celiac axis or contra-lateral iliac limb. By permission of Mayo Foundation for Medical Education and Research. All rights reserved

plug still connected to the delivery system. If there are no changes on examination, the plug is disconnected and heparinization is reversed. Alternatively, the repair can be left incomplete by not placing the contra-lateral iliac limb extension or one of the bridging stents (e.g., celiac stent). Limitations of perfusion branches are the potential risks of increased sac pressure due to poor outflow via small segmental arteries and disseminated intra-vascular coagulopathy from large endoleak into a blind sac. Over time, our technique has evolved and now utilizes sequential aortic coverage by first placing thoracic stent-grafts starting distal to the left subclavian artery and covering up to the celiac artery.

Blood Pressure Management

Calcium channel blockers and angiotensine-inhibitors are discontinued a week prior to the operation and up to 4–6 weeks after the procedure unless systolic blood pressures are >160 mmHg. The goal mean arterial pressure is targeted at ≥80 mmHg intra-operatively and for the first 72 h after the operation. Blood pressure goals are titrated according to intra-operative neuromonitoring or post-operative examination. If there are changes in neuromonitoring detected during the operation or neurological changes observed on post-operative physical examination, MAP goals are incrementally raised up to 100 mmHg. In addition, transfusion of blood products is indicated in the first 48 h after the procedure to keep a target hemoglobin ≥10 mg/dL and normal coagulation profile prior to removal of the spinal drain.

Cerebrospinal Fluid Drainage

Routine CSF drainage is used in all patients with ≥4 cm stent-graft coverage (or two sealing stents) above the celiac axis. This is the minimum extent of coverage used for all

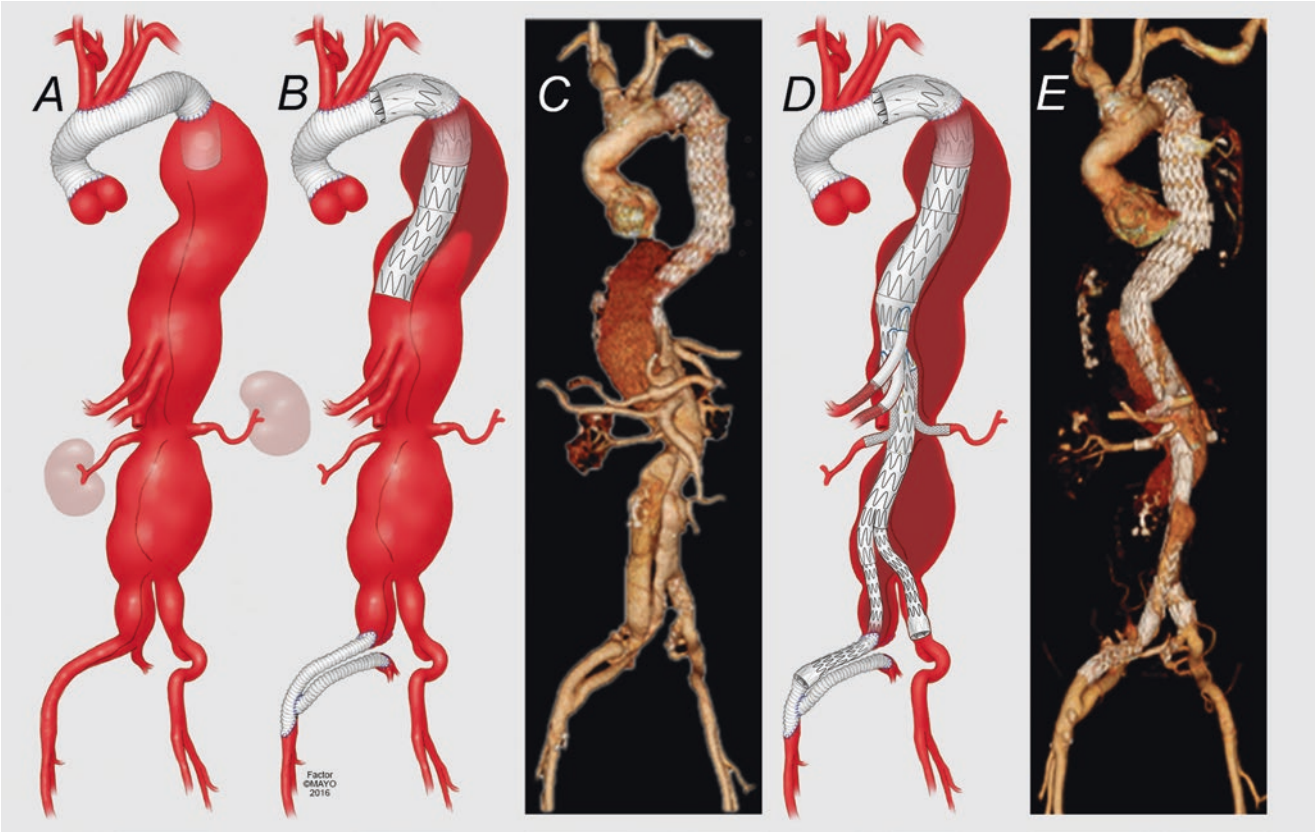


Fig. 20.3 Illustration of a patient treated by elephant trunk procedure (**a**) for extensive aortic dissection and thoracoabdominal aortic aneurysm. The patient was treated in a staged fashion (**b**) with coverage of the proximal thoracic aorta and surgical revascularization of the right internal iliac artery. Computed tomography angiography shows thrombosis of the false lumen adjacent to the thoracic stent (**c**). A completion endovascular repair was performed using four-vessel directional branched stent-graft (**d**) with exclusion of the aneurysm and presence of persistent type II endoleak (**e**). By permission of Mayo Foundation for Medical Education and Research. All rights reserved

type IV TAAAs. Spinal fluid pressure is set at a baseline of 10 mmHg. The spinal drain is opened for 15 min every hour with a maximum drainage of 20 mL per hour, after which the drain is clamped for the remaining of the hour. A maximum of 150 mL of drainage is accepted for 24 h. If there are changes in neuromonitoring or neurological examination, CSF pressure is decreased to 5 mmHg or 0 mmHg. CSF pressure is raised to 10 mmHg once neuromonitoring or examination improved. Spinal fluid drainage is continued for 24 h in patients with extent type IV TAAA, and for 48–72 h in those with extent type I–III TAAAs. The CSF drain is removed in patients who had stable hemodynamics and neurological examination after a 6-h clamping trial.

Neuromonitoring

Neuromonitoring with continuous motor-evoked potential (MEP) and somatosensory-evoked potential (SSEP) has been widely applied during open TAAA repair to guide reimplantation of intercostal arteries and to optimize distal aortic perfusion. In contrast to open repair, endovascular incorporation of intercostal arteries is not feasible. Nonetheless, immediate recognition of ischemia using neuromonitoring may allow introduction of maneuvers to optimize spinal cord and lower extremity (LE) perfusion and decrease the rate of SCI. Total intravenous anesthesia is used to allow intra-operative neurophysiological monitoring of MEP and SSEPs. A ≥75% reduction from baseline-evoked potential amplitude is considered to be significant (Fig. 20.5). Cadwell Elite machines and Cascade software is used to collect data (Cadwell Laboratories, Kennewick, WA) by electromyography (EMG) technologists. Electrical charges sent to the motor cortex through C3, C4 scalp electrodes evoke motor-evoked potentials (MEP) through the motor pathway (Fig. 20.6) which are recorded down the cord over multiple muscles in the upper and lower extremities for at least every 10–15 min. An upper extremity muscle (*Extensor Digitorum Communis*) is recorded to help differentiate neurogenic impairment such as spinal and lower limb ischemia from non-specific changes.



Fig. 20.4 Illustration of a patient with extent II thoracoabdominal aortic aneurysm (**a**) and prior infra-renal aortic repair. The patient was treated by four-vessel branched endograft with a temporary perfusion branch (**b**). The perfusion branch was occluded 1 week later using Amplatzer plug (**c**) with resolution of the intentional endoleak (**d**). By permission of Mayo Foundation for Medical Education and Research. All rights reserved

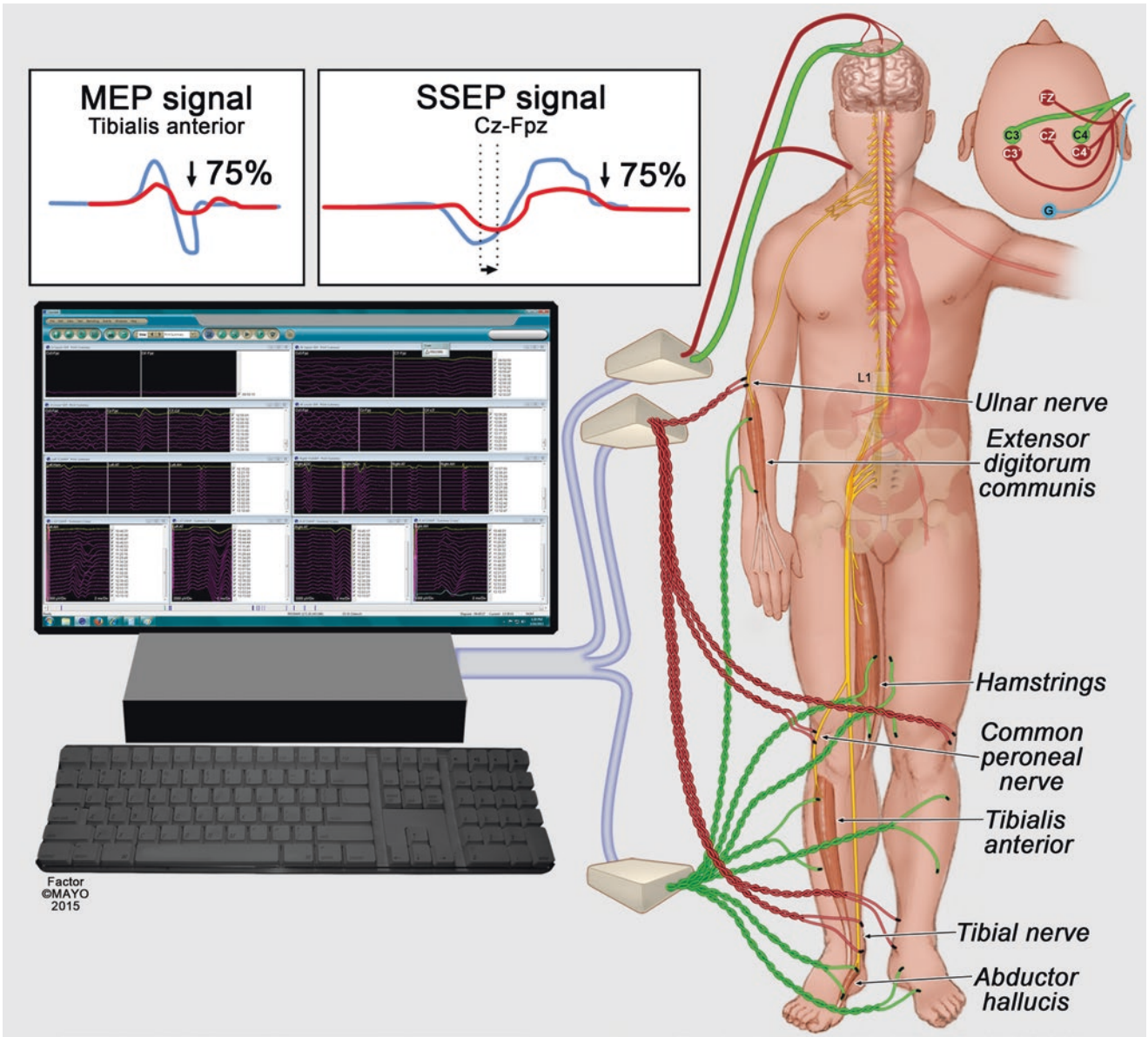


Fig. 20.5 Illustration depicting placement of electrodes for monitoring of motor-evoked (MEP) and somatosensory-evoked potentials (SSEP) during complex endovascular aortic repair. A significant change is defined by greater than 75 % decline in amplitude in MEP or SSEPs. By permission of Mayo Foundation for Medical Education and Research. All rights reserved

Bilateral lower extremity muscles are recorded using subdermal EEG electrodes placed in the *hamstring, tibialis anterior, and abductor hallucis muscles*. In addition, somatosensory-evoked potentials (SSEPs) consisting of electrical stimulus generated at the ulnar or tibial nerve that travels from the distal extremity were recorded over the neck and scalp (see Fig. 20.6). In patients where the lower extremity tibial SSEP are not present at the ankle, subdermal EEG electrodes can be positioned behind the knee. In addition, a compound muscle action potential (CMAP) is performed (Fig. 20.7) by stimulating the peroneal nerve and posterior tibialis nerve. The CMAP is important to help differentiate peripheral nerve and spinal cord ischemia.

Limb Perfusion

Large trans-femoral sheaths are associated with limb and pelvic ischemia (Fig. 20.8a), which may aggravate spinal cord ischemia because of compromised collateral networks.

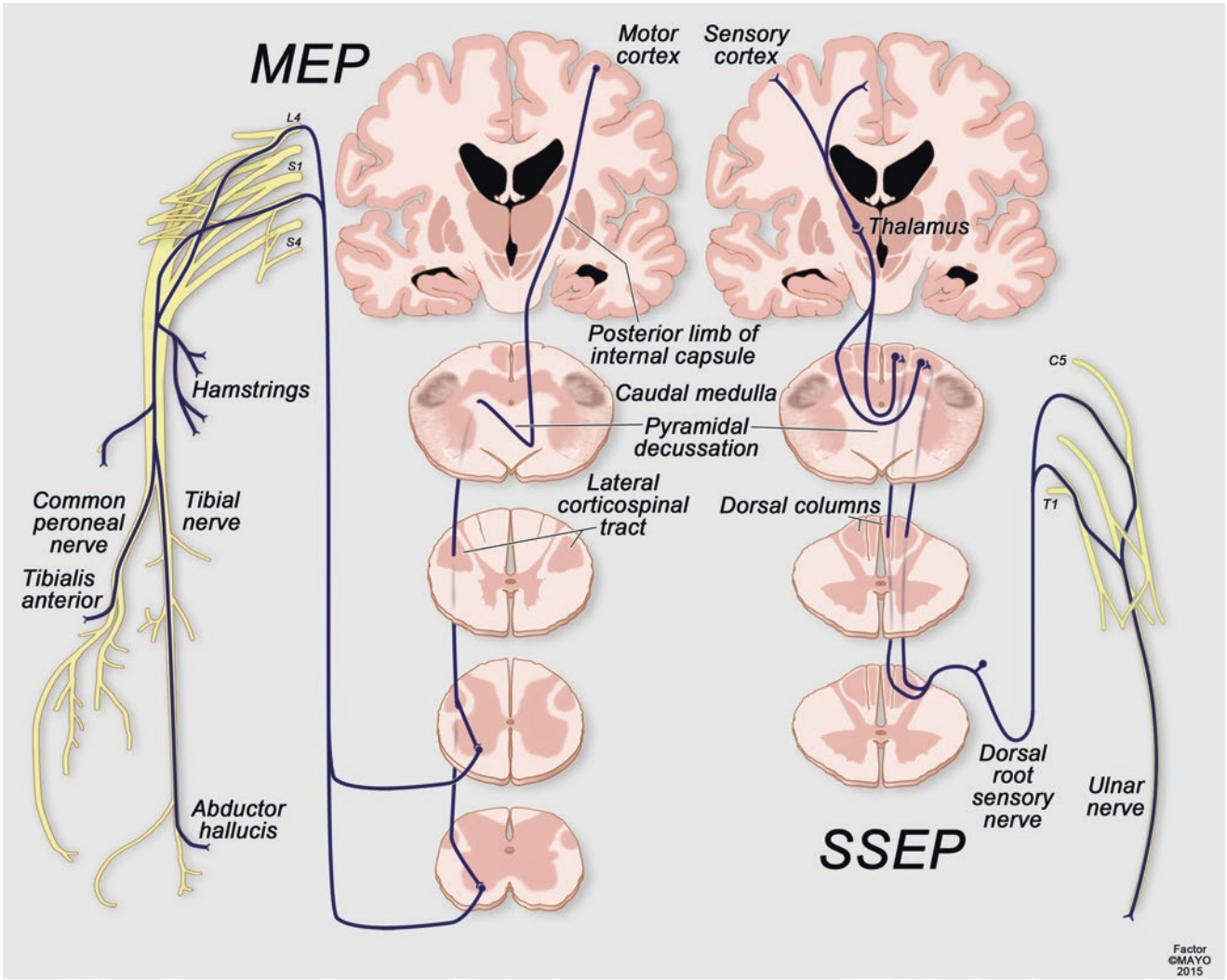


Fig. 20.6 Illustration depicting of motor-evoked (MEP) and somatosensory-evoked potential (SSEP) pathways. By permission of Mayo Foundation for Medical Education and Research. All rights reserved

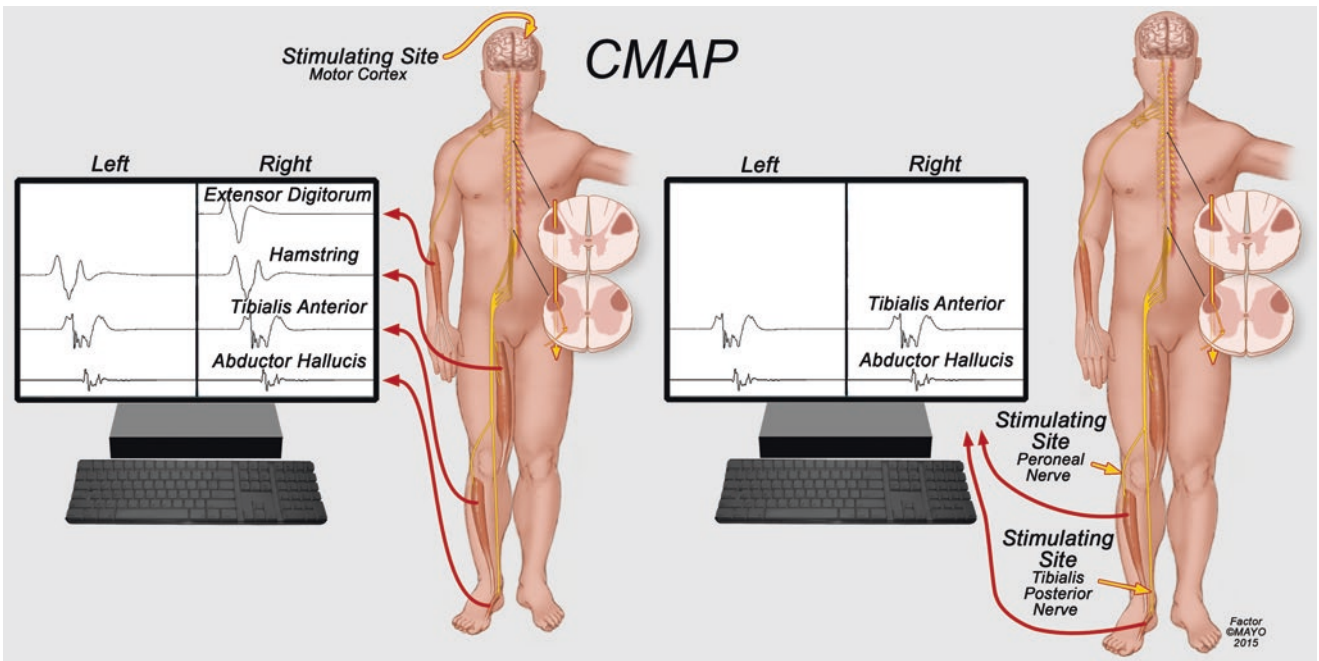


Fig. 20.7 Compound muscle action potentials help differentiate peripheral from spinal cord ischemia. By permission of Mayo Foundation for Medical Education and Research. All rights reserved

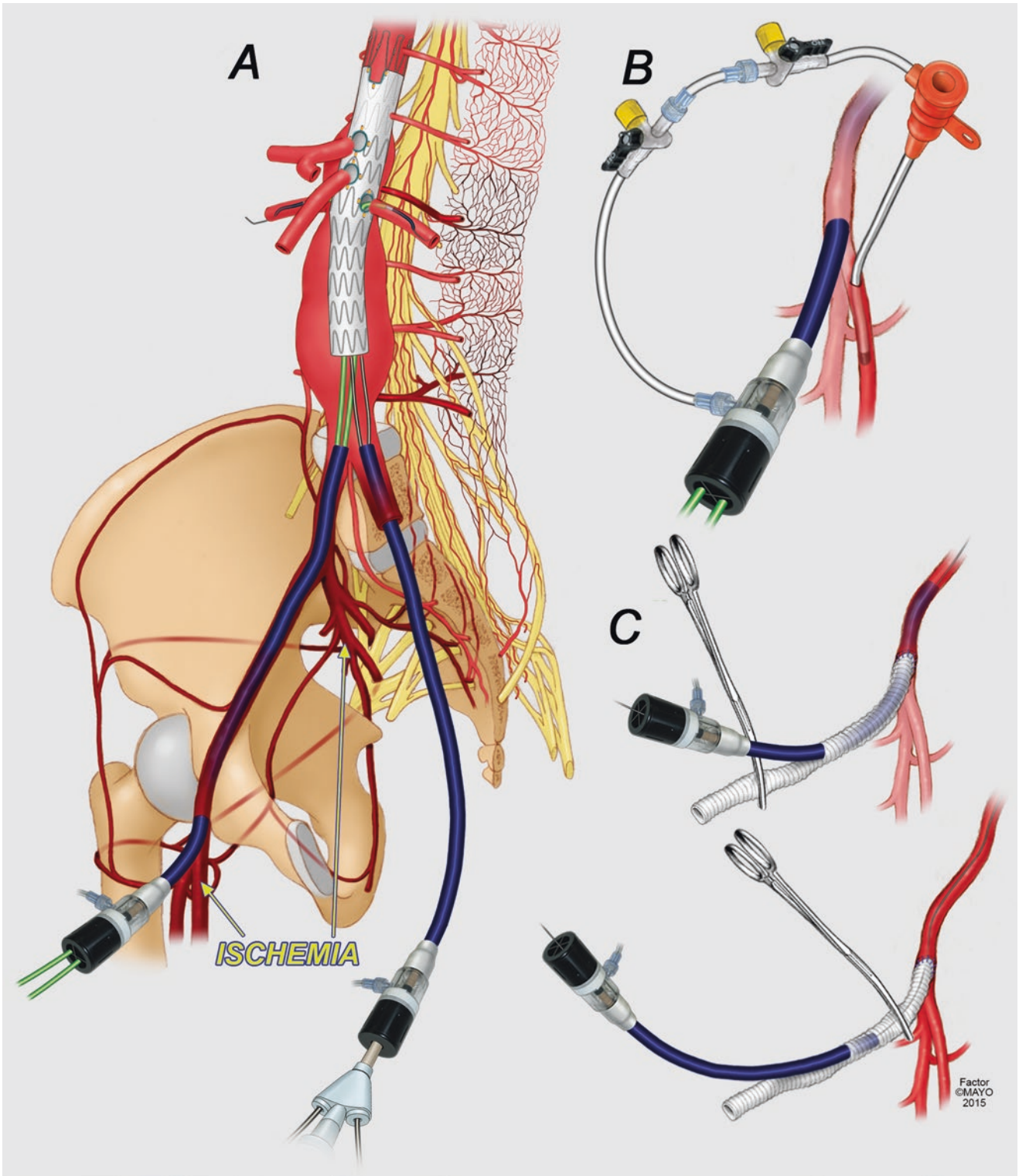


Fig. 20.8 Mechanism of pelvic and lower extremity ischemia due to large trans-femoral sheaths (**a**). Use of superficial femoral artery sheath (**b**) and femoral conduits (**c**) to minimize leg ischemia. By permission of Mayo Foundation for Medical Education and Research. All rights reserved

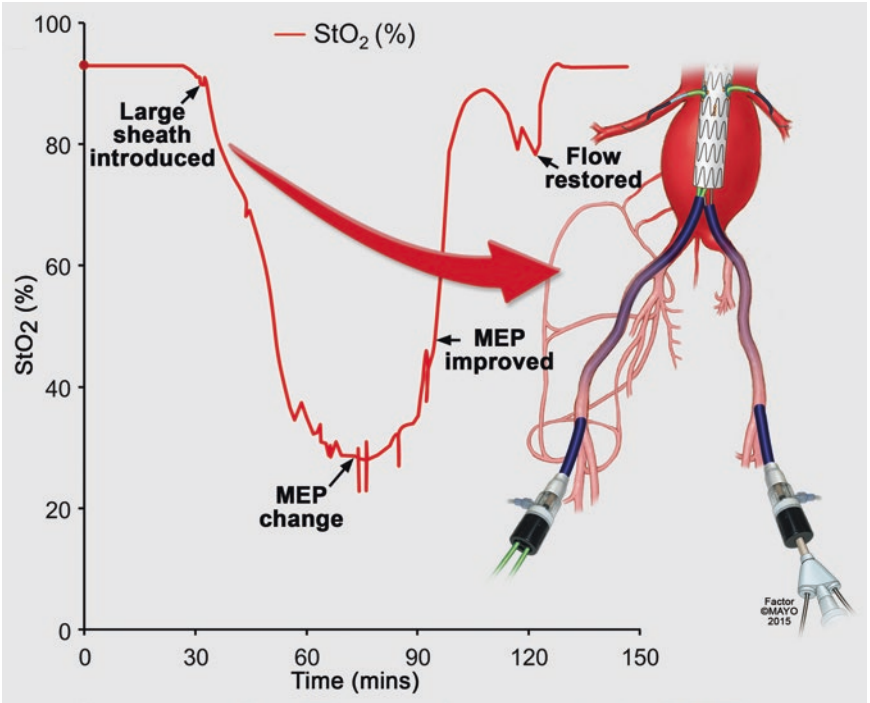


Fig. 20.9 Graph demonstration of correlation between decline in lower extremity (LE) trans-cutaneous oxygen saturation (StO_2) with placement of large diameter sheaths in the ilio-femoral arteries during complex endovascular aortic repair. Note that drop in StO_2s start immediately after the sheath is introduced, reaching its nadir within 60 min. Once changes in motor-evoked potential (MEP) are noted, maneuvers to optimize flow were started with increase in StO_2 and improvement in MEP. After flow is restored to the LE, StO_2 return to baseline values. By permission of Mayo Foundation for Medical Education and Research. All rights reserved

Increasing evidence indicates that minimizing lower limb and pelvic ischemia may improve outcomes of complex endovascular repair including lower risk of paraplegia (Fig. 20.9). This can be done by several adjunctive measures. The superficial femoral artery may be accessed using a small sheaths, which can be connected into the larger trans-femoral sheath creating a shunt (Fig. 20.8b). However, this technique can be cumbersome and also does not address the occlusion of the internal iliac and profunda femoris arteries, which are the main collateral networks to the spine. Our preference has been to use a temporary iliac artery conduit in patients with small iliac arteries, severe occlusive disease of the aorto-iliac arteries or when technical challenge with prolonged (>2 h) ischemia time is anticipated. A femoral conduit anastomosed end-to-side to the common femoral artery (Fig. 20.8c) to allow restoration of lower extremity flow. The use of femoral conduit minimizes lower extremity ischemia during visceral branch stenting by allowing the aortic device sheath to be retracted into the conduit (Fig. 20.10). More frequently, we prefer to use total percutaneous femoral approach whenever the common femoral arteries are not calcified and a straightforward case is anticipated (Fig. 20.11). In these cases, the aortic device, renal fenestrated-branches, bifurcated device, and iliac limbs are performed using the femoral approach first. Flow is restored into both lower extremities (<2 h) and the procedure is completed via the left arm by placement of the superior mesenteric and celiac artery stents.

Intra-operative Maneuvers

Our protocol uses neuromonitoring to trigger intra-operative maneuvers to optimize spinal cord perfusion. A decrease in MEP/SSEPs triggers introduction of sequential standardized maneuvers as depicted in Fig. 20.12. These maneuvers include incremental changes in MAP and CSF pressure as previously described. The MAP goals are raised from 80 mmHg up to 100 mmHg with norepinephrine and/or vasopressin infusion along with simultaneous decrease in CSF drain pressure from 10 mmHg to 5 or 0 mmHg. Response to these maneuvers is recorded and the MAP and CSF pressure parameters are readjusted accordingly. In patients with improvement after maneuvers, the procedure

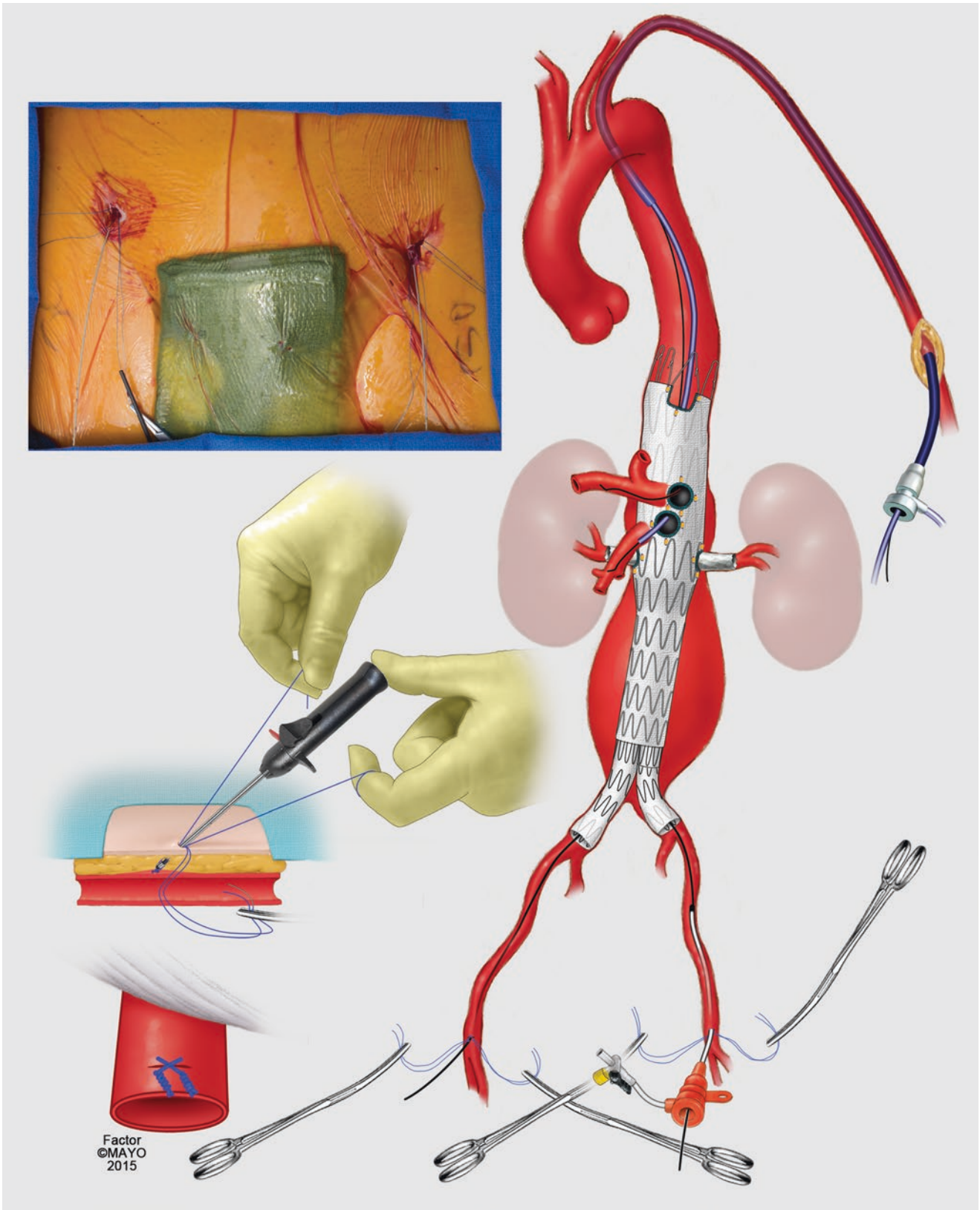


Fig. 20.10 Technique of percutaneous femoral approach with early lower limb reperfusion. By permission of Mayo Foundation for Medical Education and Research. All rights reserved

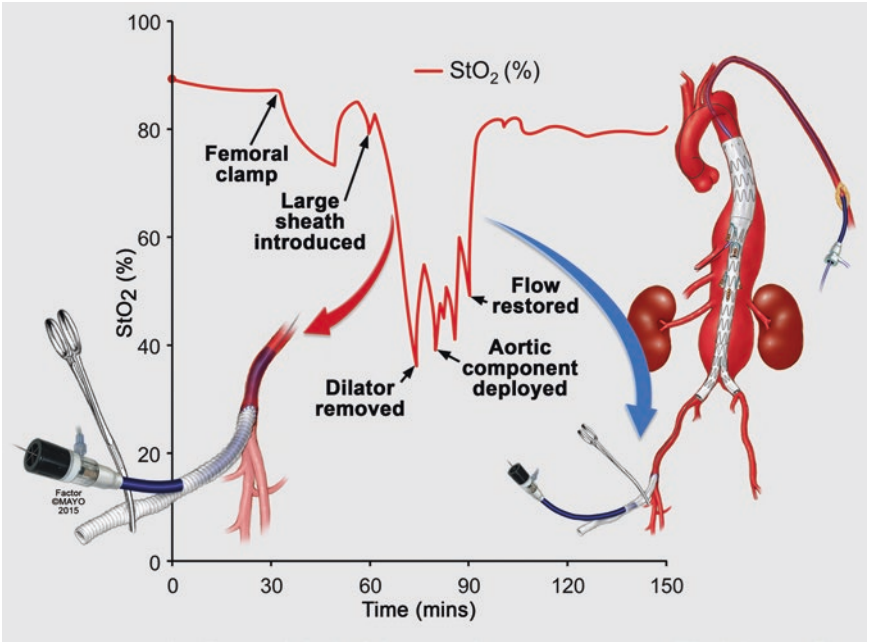


Fig. 20.11 Temporary femoral conduits anastomosed end-to-side to the common femoral artery were used selectively as an adjunct to optimize lower extremity (LE) flow during difficult cases. This graph illustrates the decline in LE trans-cutaneous oxygen saturation (StO_2) with placement of large diameter sheaths in the ilio-femoral arteries. After the dilator is retracted to the femoral conduit, StO_2 returns to baseline values. In this patient there were no changes observed in neuromonitoring, despite the complex anticipated anatomy. By permission of Mayo Foundation for Medical Education and Research. All rights reserved

is completed in standard fashion. In those with no change or deterioration in neuromonitoring, flow is restored to the pelvis and LEs as fast as possible by changing the sequence of target vessel stenting as depicted in Fig. 20.12. In patients with normalization of MEP/SSEPs after lower extremity flow is restored, the procedure is completed. If changes persist, the procedure is left incomplete with flow into the sac via the celiac branch or contra-lateral iliac limb whenever possible (Fig. 20.13).

Peri-operative Management

Post-operative, all patients are closely monitored in a closed cardiovascular intensive care unit by a dedicated critical care team. Spinal fluid pressure is set at a baseline of 10 mmHg as previously described. The spinal drain is opened for 15 min every hour with a maximum drainage of 20 mL per hour, after which the drain is clamped for the remaining of the hour. Similar adjunctive maneuvers are utilized in the post-operative setting if neurological changes are observed on physical examination. MAP goals are incrementally raised up to 100 mmHg. In addition, transfusion of blood products is performed to keep a target hemoglobin ≥10 mg/dL and normal coagulation profile should the need to reposition or replace a spinal drain be required. CSF pressure is decreased to 5 or 0 mmHg. CSF pressure is raised to 10 mmHg once neuromonitoring or examination improves. Spinal fluid drainage is continued for 24 h in patients with extent type IV TAAA, and for 48–72 h in those with extent type I–III TAAAs. The CSF drain was removed in patients who had stable hemodynamics and neurological examination after a 6-h clamping trial.

Delayed Neurologic Deficit

Most spinal cord injuries (>2/3) after complex endovascular repair are delayed, likely due to hemodynamic compromise. Safi and colleagues described the COPS protocol, which we have incorporated into our practice to manage delayed injury. The protocol includes the following:

– **C** for CSF drain status: malfunction of drain is management by immediate replacement; for functioning drains,

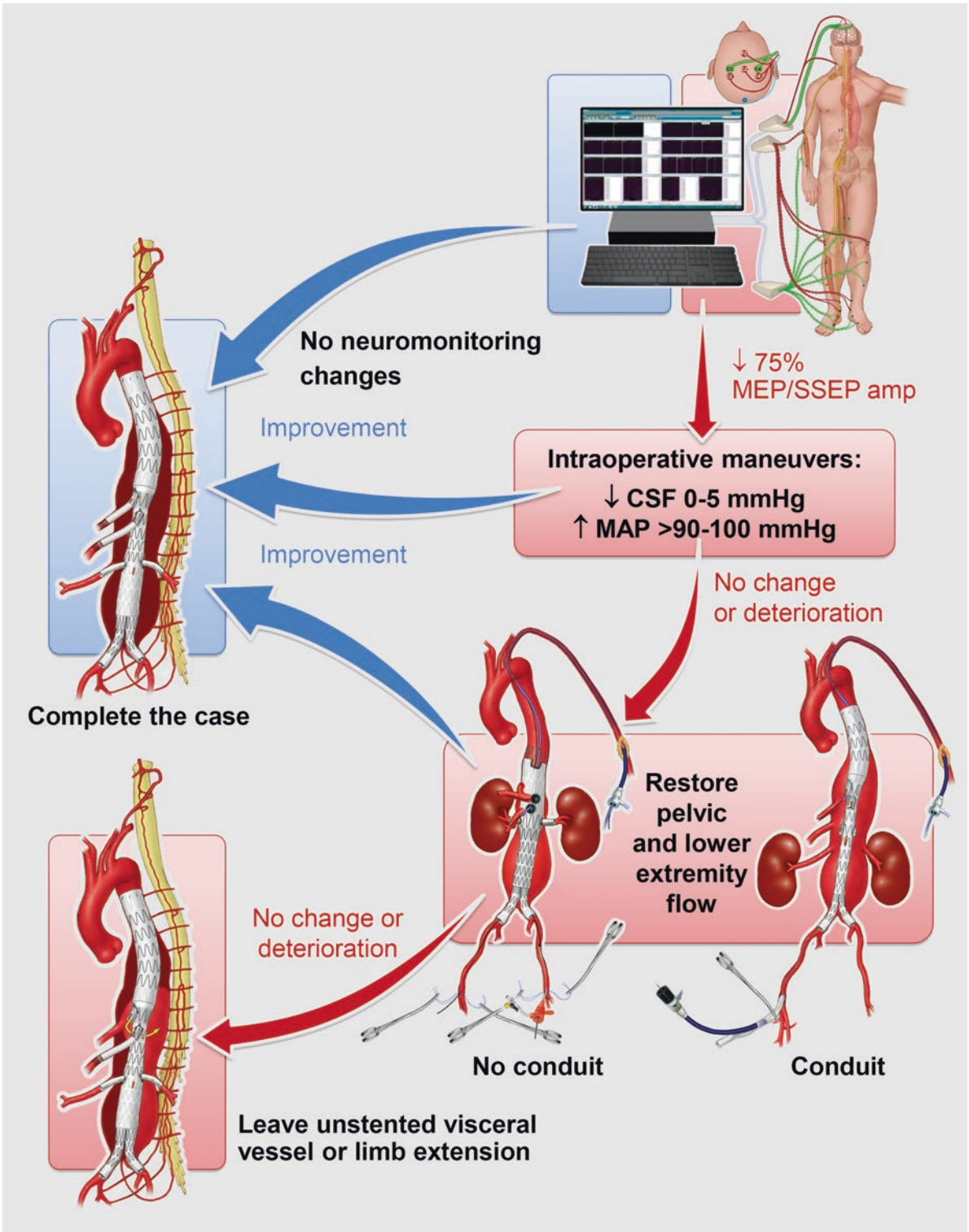


Fig. 20.12 Standardized maneuvers and protocol triggered by changes in motor and somato-sensory-evoked potentials. By permission of Mayo Foundation for Medical Education and Research. All rights reserved

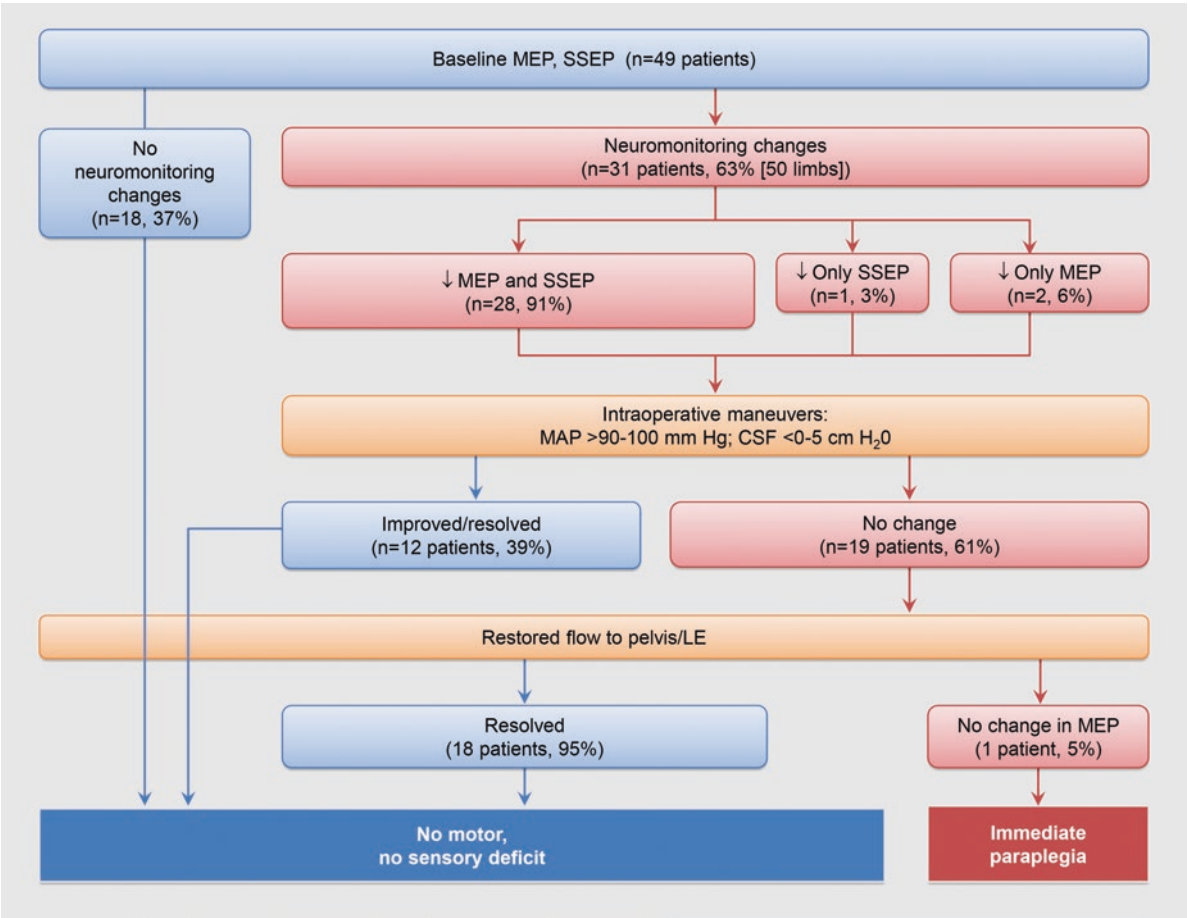


Fig. 20.13 Description of changes in motor-evoked and somatosensory-evoked potentials (MEP and SSEP) during complex endovascular repair in 49 patients. Note changes in MEP and SSEP and response to maneuvers outlined in Fig. 20.4. By permission of Mayo Foundation for Medical Education and Research. All rights reserved

pressure is decreased to <5 mmHg with patient maintained flat and with continued drainage for 7 days.

- **O** for Oxygen delivery: low oxygen delivery is avoided and reversed by optimizing O_2 saturations (>90 %), hemoglobin (>12 mg/dL) and cardiac index (>2.5 L/min/BSA).
- **PS** for Patient Status: any cardiac or systemic complication is immediately diagnosed and managed, with special attention to cardiac, pulmonary, and septic complications; a target mean arterial pressure of 90–100 mmHg is recommended, spinal cord perfusion pressure >80 mmHg and avoidance of bloody CSF drainage.

Results

Please see Tables 20.1 and 20.2.

Table 20.1 Demographics, clinical, and anatomical characteristics in 49 patients treated for descending thoracic (DTA) or thoracoabdominal aortic aneurysms (TAAA)[a]

Variable	*n* = 49	%
Male gender	38	78
Age (years old)	75 ± 8	
Cardiovascular risk factors, No. (%)		
Hypertension	43	88
Cigarette smoking	42	86
Hyperlipidemia	40	82
Coronary artery disease	32	65
Chronic pulmonary disease	21	43
Chronic kidney disease (Stage IIIb to V)	18	37
Peripheral arterial disease	12	24
Diabetes	9	18
Stroke/TIA	4	8
Aneurysm characteristics		
Type C DTA	5	10
TAAA	44	90
Type I	2	4
Type II	8	16
Type III	11	22
Type IV	23	47
Aneurysm maximum diameter (mm)	65 ± 10	
Visceral targets /patient	3.9 ± 0.6	
Extent of aortic coverage (%)	64 ± 18	
Staged TAAA repair	16	33
Previous thoracic aortic repair	11	22
Open thoracic repair	6	12
TEVAR	5	10
Perfusion branch	5	10
Arch repair or cervical debranching	3	6
Conduits		
Permanent conduits	5	10
Iliofemoral bypass	4	8
Endovascular conduit	1	2
Temporary conduits	14	28
Iliac temporary conduits	5	10
Femoral temporary conduits	9	18

TIA transient ischemic attack, *TEVAR* thoracic endovascular aortic repair
[a]Adapted from [17]

Table 20.2 Early outcomes in 49 patients treated for descending thoracic (DTA) or thoracoabdominal aortic aneurysms (TAAA)[a]

Variable	*n* = 49	%
30-Day mortality (aneurysm type/cause)	2	4
Type B dissection/ruptured DTAA, hemorrhage	1	2
Symptomatic type II TAAA/multiple strokes	1	2
Major adverse events (MAE)	17	35
EBL > 1000 mL at index procedure	12	24
Renal failure (dialysis or Cr > 0.5 mg/dL)	4	8
Myocardial infarction	3	6
Respiratory failure[b]	3	6
Paraplegia[c]	2	4
Stroke	1	2
Bowel ischemia[d]	1	2
Other complications	7	14
Atrial fibrillation/arrhythmia	4	8
Vascular or access	4	8
Pneumonia	1	2
Urinary tract infection	1	2
Coagulopathy	1	2
Spinal cord ischemia	3	6
Immediate paraplegia (Type IV TAAA, Intra-op)[c]	1	Permanent
Delayed paraplegia (Type II TAAA, day 3)[c]	1	Permanent
Delayed paresis (Type II TAAA, day 14)	1	Resolved
Length of hospital stay median (days)	4 (IQR 3–7)	8

EBL estimated blood loss
[a]Adapted from [17]
[b]Required >24 h of ventilation support that is not anticipated
[c]Including patients in below
[d]Requiring intensification of medical therapy or surgical therapy

References

1. Greenberg RK, Lu Q, Roselli EE, Svensson LG, Moon MC, Hernandez AV, et al. Contemporary analysis of descending thoracic and thoracoabdominal aneurysm repair: a comparison of endovascular and open techniques. Circulation. 2008;118(8):808–17.
2. Eagleton MJ, Shah S, Petkosevek D, Mastracci TM, Greenberg RK. Hypogastric and subclavian artery patency affects onset and recovery of spinal cord ischemia associated with aortic endografting. J Vasc Surg. 2014;59(1):89–94.
3. Safi HJ, Estrera AL, Miller CC, Huynh TT, Porat EE, Azizzadeh A, et al. Evolution of risk for neurologic deficit after descending and thoracoabdominal aortic repair. Ann Thorac Surg. 2005;80(6):2173–9; discussion 9.
4. Coselli JS, Bozinovski J, LeMaire SA. Open surgical repair of 2286 thoracoabdominal aortic aneurysms. Ann Thorac Surg. 2007;83(2):S862–4; discussion S90–2.
5. Maurel B, Delclaux N, Sobocinski J, Hertault A, Martin-Gonzalez T, Moussa M, et al. The impact of early pelvic and lower limb reperfusion and attentive peri-operative management on the incidence of spinal cord ischemia during thoracoabdominal aortic aneurysm endovascular repair. Eur J Vasc Endovasc Surg. 2015;49(3):248–54.
6. Svensson LG, Crawford ES, Hess KR, Coselli JS, Safi HJ. Experience with 1509 patients undergoing thoracoabdominal aortic operations. J Vasc Surg. 1993;17(2):357–70.
7. Tanaka H, Minatoya K, Matsuda H, Sasaki H, Iba Y, Oda T, et al. Embolism is emerging as a major cause of spinal cord injury after descending and thoracoabdominal aortic repair with a contemporary approach: magnetic resonance findings of spinal cord injury. Interact Cardiovasc Thorac Surg. 2014;19(2):205–10.
8. Etz DC, Luehr M, Aspern KV, Misfeld M, Gudehus S, Ender J, et al. Spinal cord ischemia in open and endovascular thoracoabdominal aortic aneurysm repair: new concepts. J Cardiovasc Surg. 2014;55(2 Suppl 1):159–68.
9. Etz CD, Weigang E, Hartert M, Lonn L, Mestres CA, Di Bartolomeo R, et al. Contemporary spinal cord protection during thoracic and thoracoabdominal aortic surgery and endovascular aortic repair: a position paper of the vascular domain of the European Association for Cardio-Thoracic Surgery†. Eur J Cardiothorac Surg. 2015;47(6):943–57.
10. O'Callaghan A, Mastracci TM, Eagleton MJ. Staged endovascular repair of thoracoabdominal aortic aneurysms limits incidence and severity of spinal cord ischemia. J Vasc Surg. 2015;61(2):347–54. e1.
11. Etz CD, Debus ES, Mohr FW, Kolbel T. First-in-man endovascular preconditioning of the paraspinal collateral network by segmental artery coil embolization to prevent ischemic spinal cord injury. J Thorac Cardiovasc Surg. 2015;149(4):1074–9.
12. Etz CD, Kari FA, Mueller CS, Brenner RM, Lin HM, Griepp RB. The collateral network concept: remodeling of the arterial collateral network after experimental segmental artery sacrifice. J Thorac Cardiovasc Surg. 2011;141(4):1029–36.

13. O'Callaghan A, Eagleton MJ, Mastracci TM, Bena J. Staged endovascular repair of thoraco-abdominal aneurysms (TAA) protects against spinal cord injury. J Vasc Surg. 2014;59(6 Suppl):22S.
14. Bischoff MS, Brenner RM, Scheumann J, Zoli S, Di Luozzo G, Etz CD, et al. Staged approach for spinal cord protection in hybrid thoracoabdominal aortic aneurysm repair. Ann Cardiothorac Surg. 2012;1(3):325–8.
15. Achouh PE, Estrera AL, Miller III CC, Azizzadeh A, Irani A, Wegryn TL, et al. Role of somatosensory evoked potentials in predicting outcome during thoracoabdominal aortic repair. Ann Thorac Surg. 2007;84(3):782–7; discussion 7–8.
16. Jacobs MJ, Meylaerts SA, de Haan P, de Mol BA, Kalkman CJ. Strategies to prevent neurologic deficit based on motor-evoked potentials in type I and II thoracoabdominal aortic aneurysm repair. J Vasc Surg. 1999;29(1):48–57; discussion 57–9.
17. Banga PV, Oderich GS, Reis de Souza L, Hofer J, Cazares Gonzalez ML, Pulido JN, et al. Neuromonitoring, cerebrospinal fluid drainage, and selective use of iliofemoral conduits to minimize risk of spinal cord injury during complex endovascular aortic repair. J Endovasc Ther. 2016;23(1):139–49.

Strategies to Minimize Risk of Acute Kidney Injury During Complex Endovascular Aortic Repair

21

Mark A. Farber and Raghuveer Vallabhaneni

Introduction

Renal complications occur in as many as 30 % of patients undergoing complex aortic aneurysm repair. Development in endovascular techniques and devices enables the repair of complex aneurysms, which can potentially reduce complications such as renal failure and insufficiency after aortic repair. Acute kidney injury can be the result of several factors and strategies to minimize the risk should be undertaken in the preoperative and postoperative periods as well as during the procedure. Recent publications suggest that the incidence of renal failure and renal ischemic events can be reduced with proper endovascular techniques.

One of the most underappreciated risks associated with complex aortic repair is acute kidney injury. Historically, renal complications occur in approximately 15–30 % of patients who undergo open surgical repair of their infrarenal aortic aneurysm and it is considered the most critical complication associated with open repair [1]. The percentage of patients with renal compromise associated with repair may also be higher in individuals with more complex repairs such as juxtarenal or suprarenal aneurysms or in those patients with preexisting chronic kidney disease [2]. While serum creatinine levels are generally utilized when evaluating renal function, they are notoriously insensitive. Estimated glomerular filtration rate (eGFR) provides a slightly better assessment of renal function; however, it is also highly inaccurate. Accurate GFR is best obtained using 24-h urine collection specimens.

The incidence or renal insufficiency after open repair has been fairly well documented over the past three decades. During this time period, rates have trended downward and vary between 15 and 32 % [1–3]. The degree of injury is directly related to the duration of renal ischemia and reports suggest that each additional 5 min of renal ischemia doubles the risk of postoperative renal dysfunction. Renal failure requiring dialysis after open repair has also been reported and is estimated to be between 6 % and 11.5 % [3]. Other factors may also play a role in developing periprocedural ischemic injury including prolonged hypotension, hypovolemia, renal ischemic time, renal vein division, and atheroemboli from aortic clamping. This includes clamps placed above, below or at distant sites from the renal arteries [2, 4].

Renal Outcomes After Complex Endovascular Aneurysm Repair

Fenestrated and branched repairs involving patient-specific manufactured devices currently provide the longest results with respect to branch vessel outcomes immediately and long-term after complex aortic repair. A large series has shown technical success of 96 % with postoperative renal insufficiency in 29 % of FEVAR and BEVAR patients. EGFR decline was noted in 14 % of the patients at 3 years. At 1 month and 5 years the freedom from renal occlusion was not statistically different between branched and fenestrated repairs (99.5 % vs. 94.5 %) [1]. When compared to open repair, FEVAR does not appear to impair renal function in juxtarenal aortic aneurysms. Shahverdyan et al. reported renal insufficiency in the open and FEVAR cohorts of 15 and 9 % (p 0.05) with each group experiencing dialysis in 3 % of the patients [5]. In most cases renal insufficiency persists after FEVAR for the initial 6 months with GFR returning to within 30 % of baseline in the majority of patients [13].

Other techniques involving snorkel parallel grafts or a variation thereof have also been used to protect complex aortic aneurysms from rupture. There are currently no clinical trial results and most studies are derived from single center experience. Single center institutions have reported their

M.A. Farber (✉)
Department of Surgery and Radiology, UNC Aortic Center, University of North Carolina,
3025 Burnett-Womack, Chapel Hill, NC 27599, USA
e-mail: mark_farber@med.unc.edu

R. Vallabhaneni
Division of Vascular Surgery, Department of Surgery, University of North Carolina-Chapel Hill, Chapel Hill, NC, USA

© Mayo Foundation for Medical Education and Research 2017

G.S. Oderich (ed.), *Endovascular Aortic Repair*, DOI 10.1007/978-3-319-15192-2_21

renal outcomes however. Lee examined 43 patients undergoing snorkel EVAR for JRAA (14). Renal patency at 2 years was 95 %. Almost one-third of the patients experienced some sort of acute kidney injury based upon the RIFLE criteria. During follow-up 35 % of the patients had renal function decline of one stage and 5.4 % by two stages.

Measurement of Renal Function and Acute Kidney Injury

As previously mentioned eGFR is an insensitive means of measuring renal function. More recently Cyst C (Cystatin C) has shown some clinical value in determining renal function. Cystatin C is a plasma protein that is produced by nucleated human cells and more sensitive to renal injury than serum creatinine and GFR. Its use however is rarely realized in clinical practice [7, 8].

Evaluation of Cyst C as a marker for renal complications after EVAR has contradicting reports with some showing no impact or decreasing levels of this low molecular weight protein suggesting improvement in renal function [9, 10]. In an evaluation of Cyst C after EVAR and FEVAR, levels were shown to increase after EVAR and FEVAR, which is contrary to previous reports; however, the population studied had elevated baseline Cyst C values. Increased levels of Cyst C persisted for up to 12 months after repair despite serum creatinine and GFR values remaining stable. This suggests that Cyst C may be a more sensitive indicator of minor renal damage [11].

Factors Associated with Acute Kidney Injury

Several factors play a role in acute kidney injury related to endovascular procedures including systemic factors, ischemic time, contrast induced nephropathy, atheroembolism, renal artery ostial disease, technical injury to the renal artery, and inflammatory reaction associated with the procedure (Fig. 21.1). Other factors that may potentially impact outcomes include the type of bridging stent used in the renal arteries, flow dynamics thru the stent and the anatomic configuration of the renal arteries themselves. A number of reports have been published detailing the impact on renal function with fenestrated and branched endovascular aortic repair (Figs. 21.2, 21.3, and 21.4). One single center publication detailed a comparison between open and FEVAR repair [5]. FEVAR demonstrated an advantage with only 9 % versus 27 % new onset renal insufficiency with 3 % requiring dialysis in both groups; however, this difference did not persist. During the 2-year follow-up there was a small increase in both groups (12 % vs. 6 %) without statistical difference. Similarly, a systemic review article demonstrated a minimal difference (14 % vs. 11 %, respectively) [6].

Attempts at reducing renal complications have included adjuvants such as renal perfusate, preoperative medication involving free radical scavengers and cooling either intravascularly or packing the kidney with ice. The latter strategies however are not possible during fenestrated or branched EVAR. In the following sections we concentrate on the preprocedural, intraoperative, and postoperative techniques and strategies which have demonstrated some benefit in reducing renal complication associated with complex endovascular aortic repair.

Preoperative Measures

Implantation of endovascular devices typically requires detailed imaging and administration of nephrotoxic contrast agents. Patients with normal or mildly elevated creatinine (<1.8 mg/dl) can withstand a reduced contrast load CT scan in conjunction with hydration with minimal risks. In those patients with more severe renal disease catheter directed CT scans have been obtained safely [12] and newer imaging techniques are on the horizon with advanced CT scan protocols.

Data suggest that preoperative hydration reduces the risks associated with nephrotoxic agents administered during contrast interventions. Both 0.9 % normal saline and sodium bicarbonate have been shown to significantly reduce post-procedure renal dysfunction, but there is no advantage of a fluid over another (Fig. 21.5) [26]. In patients with normal renal function the impact of pre-hydration is less dramatic. However, in patients with preexisting chronic renal insufficiency pre-hydration has been shown to be beneficial [15, 16]. In fact, either IV or PO hydration can confer a benefit when done pre operatively (Fig. 21.6) [27]. Some studies have suggested that there is a beneficial effect of hydration and *N*-acetylcysteine in reducing the incidence of radiographic contrast-induced nephropathy (Fig. 21.7) [28]. However, other studies showed there was no added benefit to those patient receiving in-patient hydration [17]. Perioperative administration of N-acetylcysteine also did not attenuate the effect on renal function in patients undergoing EVAR [18]. Multi-antioxidant supplementation demonstrated a brief period of higher creatinine clearance [19] but no impact on serum creatinine impact after open aneurysm repair. Mannitol administered during open aortic aneurysm repair has been demonstrated to reduce subclinical renal injury [20]. The administration of mannitol along with hydration during the procedure has been shown to provide a small benefit to patients undergoing EVAR in a randomized trial [21]. However, in a much larger review of the literature mannitol in the setting of open repair has not been shown to be beneficial [22].

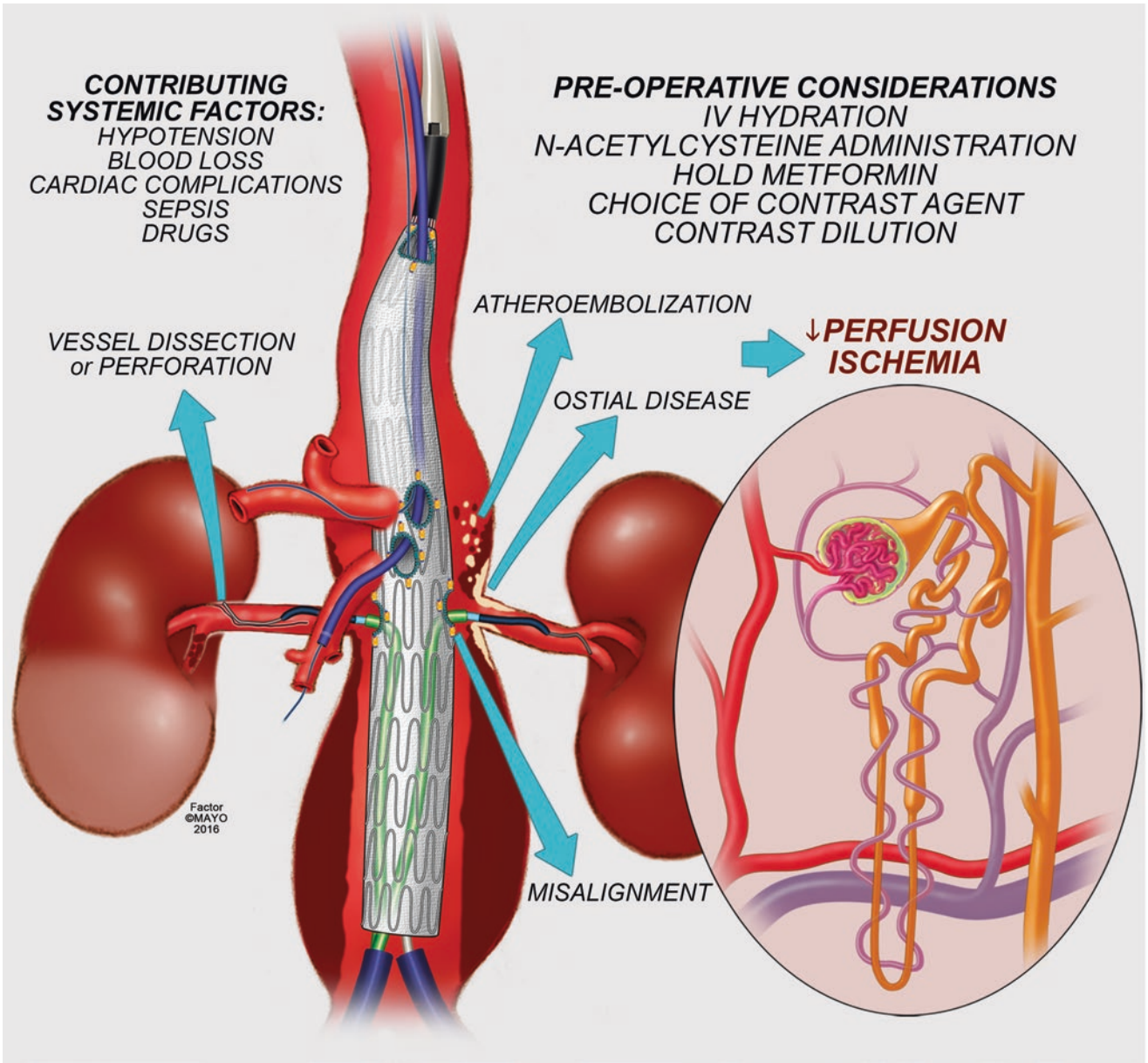


Fig. 21.1 Contributing factors to acute kidney injury during complex endovascular procedures. By permission of Mayo Foundation for Medical Education and Research. All rights reserved

The effects of additional pharmacological adjuncts have been studied in renal protection, but have not overwhelmingly or consistently demonstrated routine use (see Fig. 21.7).

While some post-procedural acute kidney injury may be related to atheroemboli there is no data on the role of preoperative antiplatelet therapy. Since a proportion of these patients may need an intrathecal catheter, clopidogrel is generally avoided preoperatively and most if not all patients are taking aspirin for its cardiac benefit.

Metformin, a common oral hypoglycemic agent, need special consideration when combined with IV contrast. Metformin is excreted by the kidneys, and impaired clearance in the setting of renal dysfunction results in lactic acidosis. Low osmolality contrast agents should be used in this scenario. A number of oral hypoglycemic agents contain metformin in combination with other medications, and attention to these medications is warranted. Holding metformin

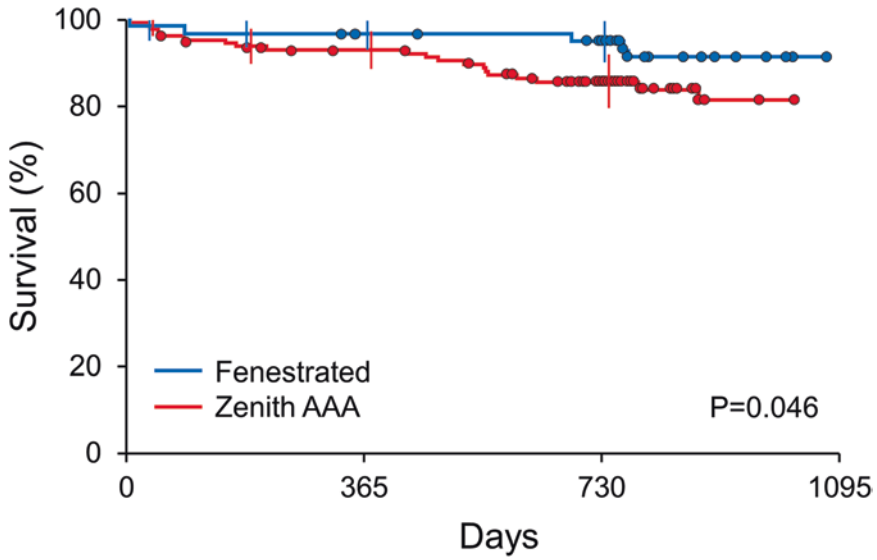


Fig. 21.2 Kaplan–Meier survival estimates of freedom from renal function deterioration in patients enrolled in the prospective US Zenith fenestrated (*blue line*) and in the Zenith infrarenal (*red line*) pivotal trials. By permission of Mayo Foundation for Medical Education and Research. All rights reserved

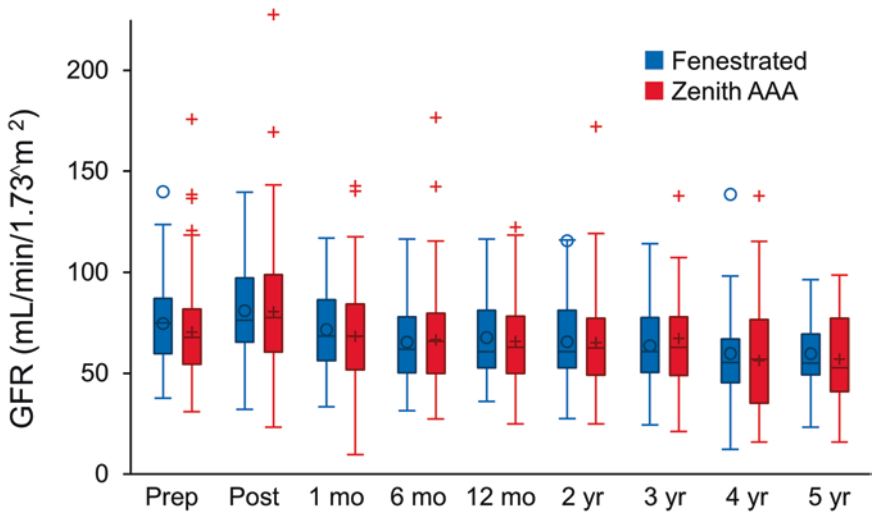


Fig. 21.3 Changes in estimated glomerular filtration rate in patients enrolled in the prospective US Zenith Fenestrated (*blue line*) and in the Zenith infrarenal (*red line*) Pivotal Trials. By permission of Mayo Foundation for Medical Education and Research. All rights reserved

either before or after the angiographic procedure should be strongly considered.

Intraoperative Measures

Meticulous planning and technique of implantation are essential to minimize the risk of injury to the renal artery and kidney parenchyma. Because of the complexity of these repairs, multiple steps can be associated with deleterious effects to the kidney. Misalignment of fenestrations relative to its target, or a renal sheath across a renal artery stenosis can limit perfusion and result in prolonged ischemia. Embolization or large or microscopic debris can occur during device orientation, deployment and branch vessel stenting. Because these devices require larger profile system, using filter is not a practical alternative. Excessive use of contrast media can be associated with added risk of nephrotoxicity. Finally, selective catheterization and stenting of renal target should be done with meticulous technique to avoid inadvertent perforation or dissection, which results in partial or total renal loss.

The results of fenestrated and branched endografts have been previously described. Studies evaluating patient-specific devices have 5–8 years follow-up and have shown

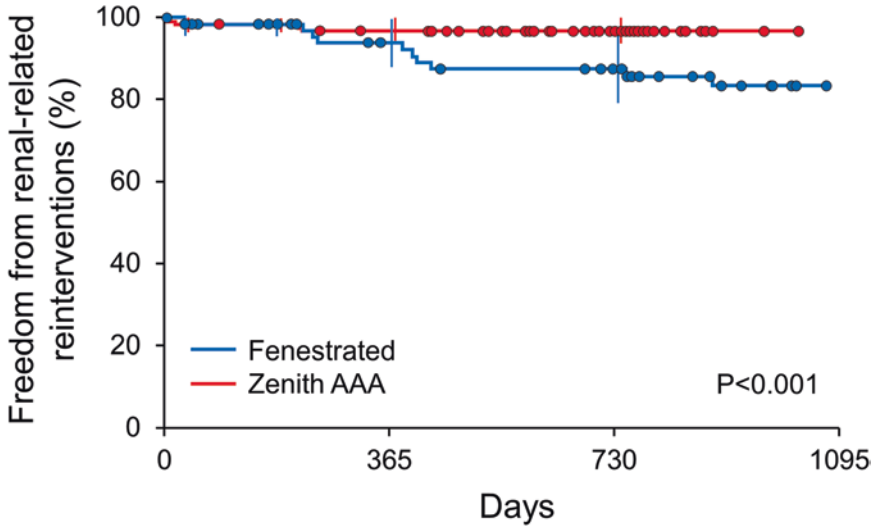


Fig. 21.4 Kaplan-Meier survival estimates of freedom from renal reinterventions in patients enrolled in the prospective US Zenith Fenestrated (*blue line*) and in the Zenith infrarenal (*red line*) Pivotal Trials. By permission of Mayo Foundation for Medical Education and Research. All rights reserved

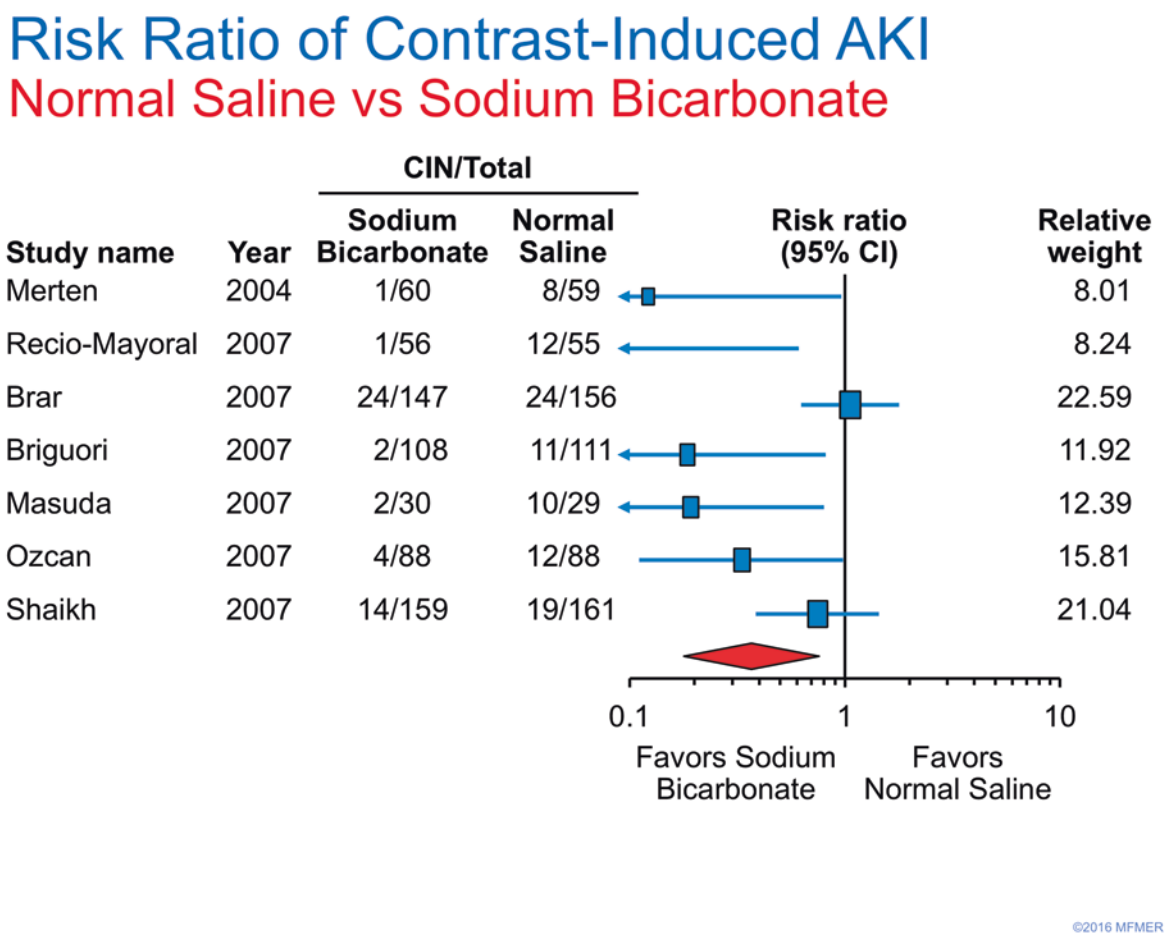


Fig. 21.5 Meta-analysis results comparing preoperative IV hydration utilizing normal saline or sodium bicarbonate to prevent contrast-induced nephropathy. Based on [26]. By permission of Mayo Foundation for Medical Education and Research. All rights reserved

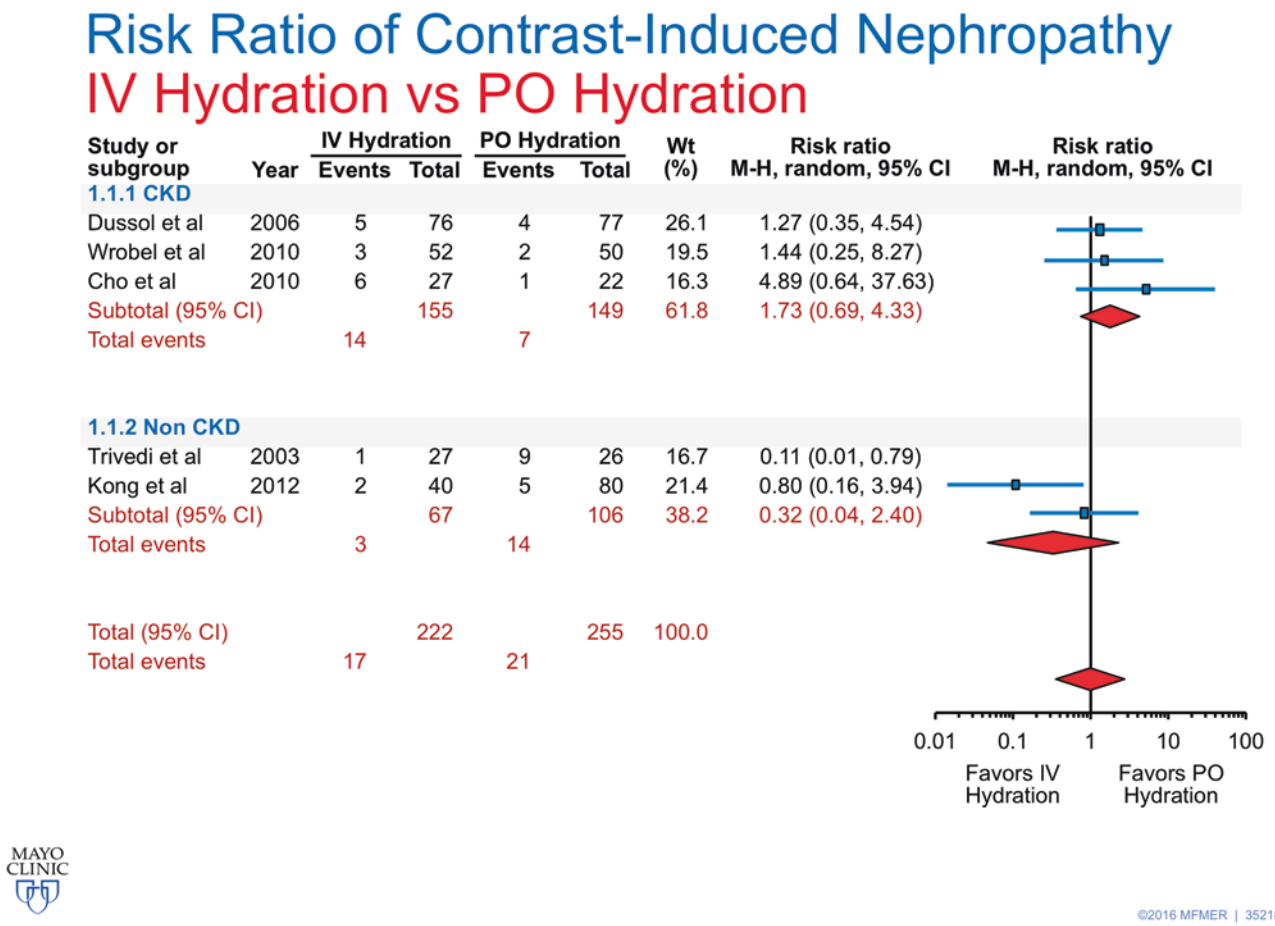


Fig. 21.6 Meta-analysis results comparing oral hydration and IV hydration to prevent contrast-induced hydration. Based on [27]. By permission of Mayo Foundation for Medical Education and Research. All rights reserved

high technical success and freedom from any branch related event approaching 90 % in 5 years. Other techniques involving snorkel or parallel grafts have also been used to repair complex aortic aneurysms. There are currently no clinical trials evaluating outcomes of parallel grafts and most studies are derived from single center experiences. Lee examined 43 patients undergoing snorkel EVAR for JRAA [14]. Renal patency at 2 years was 95 %. Almost one-third of the patients experienced some sort of acute kidney injury based upon the RIFLE criteria. During follow-up 35 % of the patients had renal function decline of one stage and 5.4 % by two stages.

There is no substitute for meticulous procedural technique to avoid renal complications associated with F/BEVAR. Careful attention to the position of the renal wires as well as identification of potential side branch positions and accurate placement of stent is critical in avoiding renal complications. Excessive manipulations especially when there is orificial renal disease can result in atheroembolic events (see Fig. 21.1). Branched devices may require more intra-aortic manipulation compared to fenestrated devices. Renal complications appear to be more common earlier in practitioners experience in reported series [13]. To begin, careful procedural planning to limit these manipulations is paramount. Often ptotic renal arteries may be catheterized from a cephalad approach using the brachial artery to help minimize manipulations and possible injury. In order to accomplish this, an access scallop is often required at the proximal aspect of the device to allow cannulation from a more proximal position. The size of the intended branch or fenestration is also important. Small renal arteries less than 5 mm that have calcified origins may be better treated with a small 6×6 fenestration rather than an 8×6 fenestration. Trying to over dilate the proximal renal artery to prevent a type III endoleak at the fenestration junction may be particularly difficult in these conditions. Renal arteries treated with small stents (<5 mm) have a higher occlusion rate and should be avoided if at all possible. Preoperative planning will also help determine where the intended stiff balloon expandable stent will be positioned. When the distal aspect of the stent is positioned within a curved renal artery kink-

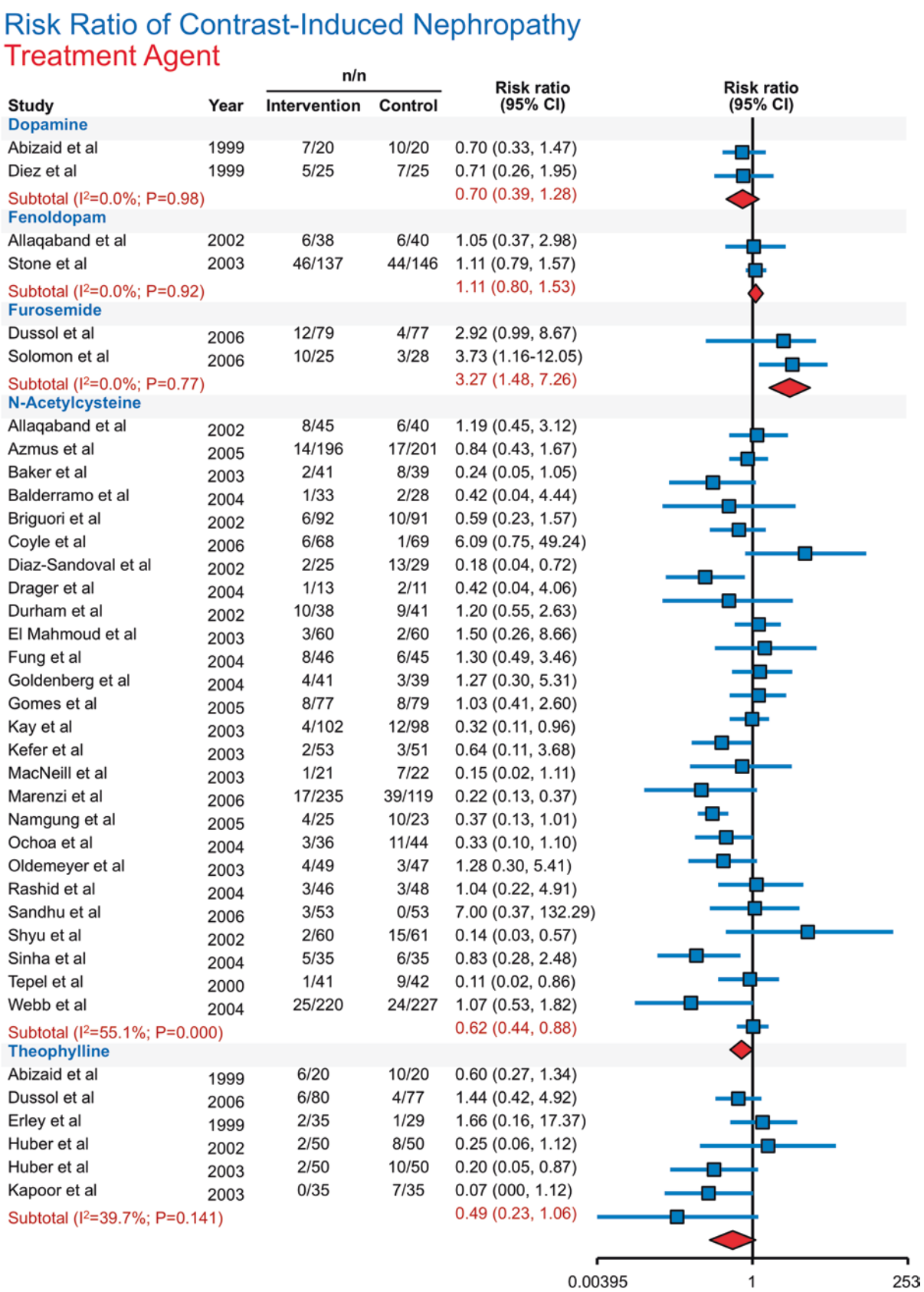


Fig. 21.7 Meta-analysis results comparing various pharmacologic agents in prevention of contrast-induced nephropathy. Based on [28]. By permission of Mayo Foundation for Medical Education and Research

Table 21.1 Characteristics of commonly used contrast agents

Product (manufacturer)	Generic name	Ionicity	Iodine content (mg/ml)	Osmolality (mOsm/kg H_2O)
Omnipaque™ 140 (GE Healthcare)	Iohexol 302	Nonionic	140	322
Conray™ 30 (Covidien)	Iothalamate (300)	Ionic	141	600
Ultravist® 150 (Bayer HealthCare)	Iopromide	Nonionic	150	328
Omnipaque™ 180 (GE Healthcare)	Iohexol (388)	Nonionic	180	408
Isovue®-200 (Bracco)	Iopamidol (408)	Nonionic	200	413
Conray™ 43 (Covidien)	Iothalamate (430)	Ionic	202	1000
Omnipaque™ 240 (GE Healthcare)	Iohexol (518)	Nonionic	240	520
Optiray™ 240 (Mallinckrodt)	Ioversol (509)	Nonionic	240	502
Ultravist® 240 (Bayer Healthcare)	Iopromide	Nonionic	240	483
Isovue® 250 (Bracco)	Iopamidol (510)	Nonionic	250	524
Visipaque™ 270 (GE Healthcare)	Iodixanol (550)	Nonionic	270	290
Conray™ (Covidien)	Iothalamate (600)	Ionic	282	1400
Isovue® 300 (Bracco)	Iopamidol (612)	Nonionic	300	616
Omnipaque™ -300 (GE Health- care)	Iohexol (647)	Nonionic	300	672
Optiray™ 300 (Mallinckrodt)	Ioversol (640)	Nonionic	300	651
Oxilan® 300 (Guerbet)	Ioxilan (623)	Nonionic	300	610
Ultravist® 300 (Bayer Healthcare)	Iopromide	Nonionic	300	607
Hexabrix™ (Guerbet)	Ioxaglate meglumine/sodium (589)	Ionic	320	≈600
Optiray™ 320 (Mallinckrodt)	Ioversol (680)	Nonionic	320	702
Visipaque™ 320 (GE Healthcare)	Iodixanol (652)	Nonionic	320	290
Optiray™ 350 (Mallinckrodt)	Ioversol (740)	Nonionic	350	792
Omnipaque™ 350 (GE Healthcare)	Iohexol (755)	Nonionic	350	844
Oxilan® 350 (Guerbet)	Ioxilan (727)	Nonionic	350	721
Isovue® 370 (Bracco)	Iopamidol (755)	Nonionic	370	796
MD-76™ R (Mallinckrodt)	Diatrizoate/meglumine/sodium (760)	Ionic	370	1551
Ultravist® 370 (Bayer Healthcare)	Ioprokoi98mide	Nonionic	370	774
Cholografin® (Bracco)	Iodipamide (520)	Ionic	257	664

ing can occur resulting in eventual renal target vessel occlusion. In these situations, a self-expanding stent can be used to transition thru the kinked region. In the author's experience, these are more commonly needed in the right renal artery as it courses more posteriorly behind the inferior vena cava, but can also occur in the left renal artery. Kinks in the renal arteries are difficult to appreciate during the procedure because the stiff renal cannulation wire distorts the natural curvature. As previously mentioned it is therefore important to pay particular attention to this preoperatively while planning the procedure.

During the procedure, additional time should be spent positioning and flaring the renal stents. Obtaining orthogonal views to the fenestration and placing the stent approximately 5 mm into the aortic endoprosthesis allows for sufficient overlap and flaring. In most cases 6 or 7 mm Atrium (Maquet) stents are used for fenestrations and require an 8–10 mm balloon for flaring. Compression and occlusion of visceral vessel stents can occur with insertion or removal of additional stent-graft components. It more commonly occurs on the contralateral renal artery with respect to the device insertion side. If suspected, protection with a balloon during device manipulation is helpful in avoiding proximal renal stent injury. Occasionally crushing of the renal stent can occur in an anterior-posterior orientation making it impossible to detect with traditional intraoperative fluoroscopy. If suspected 3D rotational angiography such as DynaCT (Siemens) can be helpful in its recognition prior to leaving the operating room. Even if detected it may be difficult to recannulate when severe crushing of the proximal stent occurs.

Inaccurate device positioning can result in excessive device manipulation and potentially increase the risk of injury to the renal arteries from atheroemboli and added manipulations. The duration of the procedure should also not be overlooked. Lower extremity ischemia from iliac and femoral artery occlusion longer than 3 h can occur and has been reported as a cause of renal complication after open thoracoabdominal aortic repair [23]. Close monitoring of urine output postoperatively as well as hydration and possible bicarbonate administration may be helpful in avoiding renal injury from elevated levels of creatine kinase.

Lastly, it should be noted that reduction of contrast administration during the procedure can be beneficial in decreasing the incidence of contrast induced nephropathy. During injections half and one-third strength contrast dilution can help minimize the contrast load and currently most cases can be

completed with less than 50–60 cc of contrast load. Different contrast agents are available (Table 21.1). Lower risk of contrast induced nephropathy has been suggested with lower osmolality agents when compared to high osmolality agents. Since the contrast agent is filtered without reabsorption by the glomerulus, an increased osmotic gradient and increased tubular pressure can ensue. The net result is one of afferent arteriolar vasoconstriction, decreased filtration and ultimately renal ischemia.

Use of newer imaging fusion techniques can help better localize the target vessels and also may reduce the number of manipulations during the procedure. Use of intravascular ultrasound to facilitate alignment of the graft with the fusion imaging may help reduce extra manipulations caused from pre-cannulation as well. While gadolinium and carbon dioxide have been used to reduce the risk with contrast angiography they are not without inherent risks. Gadolinium has been associated with serious complication when administered to patients with renal insufficiency resulting in nephrogenic systemic fibrosis [24]. Carbon dioxide use above the level of the diaphragm should be avoided due to the risk of gas embolism to various vascular territories.

Postoperative Measures

During the postoperative period volume status is closely correlated to renal function. Those patients who experience significant hypotension associated with hypovolemia develop a temporary rise in serum creatinine which may result in permanent or persistent decline in renal function. Urine sediment evaluation as well as duplex ultrasound may help to determine the cause of abnormally elevated creatinine in the postoperative period. If renal parenchymal perforation has occurred resulting in a perinephric hematoma decreased renal perfusion can occur from elevated perinephric pressure. Severe renal injury can occur if not corrected by incision of Gerota's fascia. Close inspection of the renal stent by duplex ultrasound can detect possible renal stent issues during the follow-up period. Evaluation is undertaken approximately every 6 months during the first 2 years and then yearly thereafter. For fenestrated grafts criteria has been recently defined to help detect significant lesions [25] (see Chap. 12 on follow-up duplex ultrasound).

Conclusion

In summary complex endovascular aortic repair is associated with a 20–30 % risk of acute kidney injury from the procedure. Fortunately, renal failure requiring dialysis occurs in only 1–3 % of patients treated at high volume centers. Meticulous preoperative planning with appropriate hydration can help reduce these risks in especially in patients with preexisting renal insufficiency. During the procedure, the use of advanced imaging techniques along with limited manipulations, judicious IV contrast administration, and careful protection of the stents during device implantations helps minimize the risk of injury. Patient require routine follow-up to detect renal complications during the postoperative period with the 40 % of patients recovering after the acute renal insult to within 30 % of their baseline.

References

1. Martin-Gonzalez T, Pinçon C, Hertault A, Maurel B, Labbé D, Spear R, et al. Renal outcomes analysis after endovascular and open aortic aneurysm repair. J Vasc Surg. 2015;62(3):569–77.
2. Jeyabalan G, Park T, Rhee RY, Makaroun MS, Cho J-S. Comparison of modern open infrarenal and pararenal abdominal aortic aneurysm repair on early outcomes and renal dysfunction at one year. J Vasc Surg. 2011;54(3):654–9.
3. Tallarita T, Sobreira ML, Oderich GS. Results of open pararenal abdominal aortic aneurysm repair: Tabular review of the literature. Ann Vasc Surg. 2011;25(1):143–9.
4. Wartman SM, Woo K, Yaeger A, Sigman M, Huang SG, Ham SW, et al. Early and late outcomes after abdominal aortic aneurysm repair requiring a suprarenal cross-clamp. J Vasc Surg. 2014;60:893–9.
5. Shahverdyan R, Majd MP, Thul R, Braun N, Gawenda M, Brunkwall J. F-EVAR does not impair renal function more than open surgery for juxtarenal aortic aneurysms: single centre results. Eur J Vasc Endovasc Surg. 2015 Oct;50(4):432–41.
6. Rao R, Lane TRA, Franklin IJ, Davies AH. Open repair versus fenestrated endovascular aneurysm repair of juxtarenal aneurysms. J Vasc Surg. 2015;61(1):242–55.
7. Deinum J, Derkx FH. Cystatin for estimation of glomerular filtration rate? Lancet. 2000;356(9242):1624–5.
8. Tian S, Kusano E, Ohara T, Tabei K, Itoh Y, Kawai T, et al. Cystatin C measurement and its practical use in patients with various renal diseases. Clin Nephrol. 1997;48(2):104–8.
9. Aho PS, Niemi T, Lindgren L, Lepäntalo M. Endovascular vs open AAA repair: similar effects on renal proximal tubular function. Scand J Surg. 2004;93(1):52–6.
10. Davey P, Peaston R, Rose JD, Jackson RA, Wyatt MG. Impact on renal function after endovascular aneurysm repair with uncovered supra-renal fixation assessed by serum cystatin C. Eur J Vasc Endovasc Surg. 2008;35(4):439–45.
11. Abdelhamid MF, Davies RS, Vohra RK, Adam DJ, Bradbury AW. Assessment of renal function by means of cystatin C following standard and fenestrated endovascular aneurysm repair. Ann Vasc Surg. 2013;27(6):708–13.
12. Isaacson AJ, Burke LM, Vallabhaneni R, Farber MA. Ultralow Iodine Dose Transarterial Catheter-Directed CT Angiography for Fenestrated Endovascular Aortic Repair Planning. Ann Vasc Surg. May 2016. Electronic publication.
13. Haddad F, Greenberg RK, Walker E, Nally J, O'Neill S, Kolin G, et al. Fenestrated endovascular grafting: the renal side of the story. J Vasc Surg. 2005;41(2):181–90.
14. Lee JT, Varu VN, Tran K, Dalman RL. Renal function changes after snorkel/chimney repair of juxtarenal aneurysms. J Vasc Surg. 2014;60(3):563–70.
15. Solomon R, Werner C, Mann D, D'Elia J, Silva P. Effects of saline, mannitol, and furosemide to prevent acute decreases in renal function induced by radiocontrast agents. N Engl J Med. 1994;331(21):1416–20.

16. Taylor AJ, Hotchkiss D, Morse RW, McCabe J. PREPARED: Preparation for Angiography in Renal Dysfunction: a randomized trial of inpatient vs outpatient hydration protocols for cardiac catheterization in mild-to-moderate renal dysfunction. Chest. 1998;114(6):1570–4.
17. Lawlor DK, Moist L, DeRose G, Harris KA, Lovell MB, Kribs SW, et al. Prevention of contrast-induced nephropathy in vascular surgery patients. Ann Vasc Surg. 2007;21(5):593–7.
18. Moore NN, Lapsley M, Norden AG, Firth JD, Gaunt ME, Varty K, et al. Does N-acetylcysteine prevent contrast-induced nephropathy during endovascular AAA repair? A randomized controlled pilot study. J Endovasc Ther. 2006;13(5):660–6.
19. Wijnen MHWA, Vader HL, Van Den Wall Bake AWL, Roumen RMH. Can renal dysfunction after infra-renal aortic aneurysm repair be modified by multi-antioxidant supplementation? J Cardiovasc Surg. 2002;43(4):483–8.
20. Nicholson ML, Baker DM, Hopkinson BR, Wenham PW. Randomized controlled trial of the effect of mannitol on renal reperfusion injury during aortic aneurysm surgery. Br J Surg. 1996;83(9):1230–3.
21. Kalimeris K, Nikolakopoulos N, Riga M, Christodoulaki K, Moulakakis KG, Dima C, et al. Mannitol and renal dysfunction after endovascular aortic aneurysm repair procedures: a randomized trial. J Cardiothorac Vasc Anesth. 2014;28(4):966–71.
22. Hersey P, Poullis M. Does the administration of mannitol prevent renal failure in open abdominal aortic aneurysm surgery? Interact Cardiovasc Thorac Surg. 2008;7(5):906–9.
23. Miller III CC, Grimm JC, Estrera AL, Azizzadeh A, Coogan SM, Walkes J-CM, et al. Postoperative renal function preservation with nonischemic femoral arterial cannulation for thoracoabdominal aortic repair. J Vasc Surg. 2010;51(1):38–42.
24. Khawaja AZ, Cassidy DB, Shakarchi Al J, McGrogan DG, Inston NG, Jones RG. Revisiting the risks of MRI with Gadolinium based contrast agents-review of literature and guidelines. Insights Imaging. 2015;6(5):553–8.
25. Mohabbat W, Greenberg RK, Mastracci TM, Cury M, Morales JP, Hernandez AV. Revised duplex criteria and outcomes for renal stents and stent grafts following endovascular repair of juxtarenal and thoracoabdominal aneurysms. J Vasc Surg. 2009;49(4):827–37. Discussion.
26. Hogan S, L'Allier P, Chetcut S, Grossman PM, Nallamothu BK, Duvernoy C, et al. Current role of sodium bicarbonate-based preprocedural hydration for the prevention of contrast-induced acute kidney injury: a meta-analysis. Am Heart J. 2008;156:414–21.
27. Agarwal SK, Mohareb S, Patel A, Yacoub R, DiNicolantonio JJ, Konstantinidis I, et al. Systematic oral hydration with water is similar to parenteral hydration for prevention of contrast-induced nephropathy: an updated meta-analysis of randomised clinical data. Open Heart. 2015;2:e000317. doi:10.1136/openhrt-2015-000317.
28. Kelly AM, Dwamena B, Cronin P, Bernstein SJ, Carlos RC. Meta-analysis: effectiveness of drugs for preventing contrast-induced nephropathy. Ann Intern Med. 2008;148:284–94.

Anesthetic Considerations for Complex Endovascular Aortic Repair

22

Juan N. Pulido, Erica D. Wittwer, Aaron C. Baker, and Gustavo S. Oderich

Introduction

The rapid evolution of endovascular therapy for aortic pathology has dramatically changed the field of vascular surgery over the past two decades. In parallel, anesthesiology and perioperative medicine have adapted accordingly to the care of this complex patient population. Newer graft technology has enabled the field to expand the applicability of endovascular aortic aneurysm repair (EVAR) to more challenging anatomy. Patients with complex aneurysms who otherwise are deemed inoperable or with extreme risk of morbidity and mortality are now considered for a less invasive alternative that has paved the way to a new standard of care. Moreover, a number of prospective randomized trials have demonstrated short-term advantages over open aortic repair, including reduced blood loss, operative time, morbidity, and hospital length of stay [1, 2]. The survival advantage of EVAR is maintained at 3 years, but with current techniques, aortic-related reintervention rates are higher compared to open aortic repairs, whereas the latter is associated with more laparotomy-related complications [3, 4]. With the development of hybrid approaches, fenestrated, branched, and parallel graft techniques [5–7], there seems to be no limit to the endovascular treatment of aortic pathology. This chapter focuses on anesthetic and perioperative care considerations for these patients including anesthesia technique, specific hemodynamic and neurologic monitoring, spinal cord protection, and induced hypotension techniques to facilitate proximal aortic graft deployment.

J.N. Pulido
Divisions of Cardiovascular Anesthesiology and Critical Care Medicine, Department of Anesthesiology, Mayo Clinic, 200 First Street SW, Rochester, MN 55905, USA

E.D. Wittwer
Department of Anesthesiology, Mayo Clinic, Rochester, MN, USA

A.C. Baker
Division of Vascular and Endovascular Surgery, Department of Surgery, Mayo Clinic, Rochester, MN, USA

G.S. Oderich (✉)
Division of Vascular and Endovascular Surgery, Mayo Clinic, 200 First Street SW, Rochester, MN 55905, USA
e-mail: oderich.gustavo@mayo.edu

Anesthetic Considerations

Understanding of the aortic anatomy, aneurysm extension and morphology as well as open discussion of the procedural plan with the surgical team are essential. From risk calculation to cardiopulmonary testing, a thorough preoperative evaluation must take place, to determine the need and extent of perioperative hemodynamic and neurologic monitoring, need for spinal drain placement, as well as the most appropriate method for induced hypotension, if required. From the preoperative risk point of view, EVAR is considered an intermediate risk surgical category [8]. However, the risk of complex fenestrated, branched, and hybrid endovascular thoracoabdominal aortic approaches is likely underestimated by nonspecific risk calculators [9, 10] and more aggressive preoperative cardiopulmonary testing may be required.

Anesthesia Technique and Patient Setup

The choice of anesthesia technique is usually guided by baseline comorbidities, hemodynamic status, need for complex neurologic monitoring, aneurysm location, and patient preference. More often, general endotracheal anesthesia is the favored method for complex hybrid and fenestrated approaches. Specifically, if somatosensory (SSEP) or motor evoked potentials (MEP) are used [11], total intravenous anesthesia (TIVA) is the preferred anesthetic technique [12] with propofol (100–200 mcg/kg/min) and opioid (fentanyl, remifentanil, or sufentanil) infusions as traditional inhaled anesthetics at required doses inhibit the evoked potential signal. Muscle relaxants are avoided if MEPs are used. It is important to plan a fast-track anesthesia technique to allow for early postoperative neurologic examination, shortly after

© Mayo Foundation for Medical Education and Research 2017

G.S. Oderich (ed.), *Endovascular Aortic Repair*, DOI 10.1007/978-3-319-15192-2_22

conclusion of the procedure. EVAR in patients with simple anatomy can be performed under monitored anesthesia care (MAC) with local anesthesia.

Cerebrospinal Fluid (CSF) Drainage

The use of CSF drainage to minimize risk of spinal cord injury was pioneered by Larry Hollier at the Mayo Clinic in the late 1980s. Although at that time the technique initially faced resistance and criticism, it is currently widely utilized for complex aneurysms involving risk of paraplegia. Despite the lack of clear prospective data, elective preoperative lumbar CSF drain placement for optimization of spinal cord perfusion (see below in Sect. Spinal Cord Protection) plays an important role in TEVAR [13]. Contraindications for spinal drain insertion include preoperative anticoagulation, intracranial process (tumor or bleeding), and infection at the insertion site (Table 22.1). After standard monitoring is in place, the lumbar drain is usually inserted before induction of anesthesia to allow for patient feedback as the needle is being inserted (Fig. 22.1). However, the timing of insertion after induction of anesthesia is largely dependent on institutional preference and it is described in some series [14, 15]. If using a lumbar CSF drain kit (Integra®, CODMAN®, etc.) the 0.7 mm ID drain is prepared in sterile fashion by flushing it with preservative free normal saline prior to inserting the flexible wire to reduce friction. The wire is then advanced to the catheter tip to provide support for drain insertion. Note the drain markings starting at 10 cm and drainage fenestrations up to 5 cm from the catheter tip. Once optimal patient positioning has been achieved (sitting or lateral decubitus with hip, knee, and neck flexion), using anatomical landmarks, the L4–5 interspace is located at the level of the iliac crest. This is the optimal location to avoid the conus medullaris (Fig. 22.2). Alternative insertion spaces are L3–4 or L5–S1. After standard asepsis with alcohol-based chlorhexidine solution and sterile draping, the 14-G beveled needle (lumbar CSF drain insertion kit) or 17-gauge epidural needle (if using a standard epidural catheter) is inserted and gently advanced between the L4–5 spinous processes into the thecal sac (see Fig. 22.1). The bevel is then rotated towards the head of the patient and the needle stylet is removed allowing for brisk CSF return. Once CSF return is noted, the drain with flexible wire (or epidural catheter) is advanced through the needle into the thecal sac. The catheter should be advanced at least 8 cm (up to 12 cm) into the subarachnoid space to ensure all fenestrations are in the thecal sac for optimal drainage [14, 15]. In some instances, such as presence of lumbar spine pathology (spinal stenosis) or prior spinal surgical procedures, the insertion of the lumbar drain is performed the day before surgery under fluoroscopy and advanced to T9–10 [16]. The distance from the patient's skin to the thecal sac should be noted and added to the length of catheter advanced in the subarachnoid space. The final catheter position secured at the skin should be recorded in the procedural note. If traumatic insertion or bloody return is encountered, discussions with the surgical team should include the possibility of delaying anticoagulation for at least 1 h, delaying the procedure for 1 day, or proceeding maintaining a higher index of suspicion for neuraxial hematoma [18]. After optimal catheter position is established, the wire is removed with gentle but firm traction while securing the drain position at the skin with gentle pressure such that the catheter is not retracted; the drain cap is placed, and secured with a small suture tie. The catheter is then secured at the skin with sterile dressing and the patient is placed in the supine position. Maintenance of adequate CSF drainage is confirmed by gentle aspiration with a 3-cc syringe and general anesthesia is induced. Additional hemodynamic lines are then placed and SSEP and MEP electrodes. During this time, the spinal drain is clamped (Fig. 22.3).

Once all monitors and lines are applied, the drainage system is primed with 10 mL of preservative free normal saline, the spinal drain is attached to the drainage system and the transducer is zeroed and opened to drain at 10 mmHg with a maximum CSF drainage volume of 10 mL/h or 20 mL/h during the ischemic period with avoidance of total drainage >130 mL for the case. There is some controversy regarding the optimal location to zero the transducer to guide spinal fluid drainage. Although there is rationale to use the phlebostatic axis (right atrium) due to the location of spinal cord at risk, there is a higher risk of over drainage and subsequent hemorrhagic complications [16, 17]. Moreover, zeroing at the tragus or external ear meatus (Fig. 22.4) is accurate in the supine position and would protect from over draining in any other position. At our institution, we utilize the tragus, and, if neurologic deficit develops, the patient is maintained supine.

Vascular Access, Hemodynamic and Neurologic Monitoring

Nearly all complex EVAR cases require arterial and central venous access for frequent arterial blood sampling and hemodynamic monitoring as well as large bore venous access for rapid volume administration. The site of arterial access should be discussed with the surgical team, as often, the left brachial artery is accessed for the procedure, limiting peripheral venous access and arterial catheter insertion to the right upper extremity. Depending on the patient's comorbidities and/or the need for rapid ventricular pacing, a pulmonary artery catheter may be required (see Sect. "Induced Hypotension For Precise Graft Deployment"). Transesophageal echocardiography (TEE) may also be required at the discretion of the surgeon or anesthesiologist, depending on location of aneurysm, monitoring wire in proximity of aortic valve and evaluation of dissection flaps.

Table 22.1 Guidelines for lumbar CSF drainage in TEVAR[a]

Subject	Recommendation
Assessment of contraindications/ preoperative considerations	
Current anticoagulation[18]	Ensure that: Platelets >100 K INR <1.3 Normal aPTT No LMWH for 24 h (high dose regimen); 12 h (low dose regimen) No clopidogrel for 7 days No ticlopidine for 10 days No abciximab for 24–48 h No eptifibatide or tirofiban for 4–8 h No dabigatran for 5 days No apixaban for 3 days No rivaroxaban for 3 days
Infection at the site	Consider alternative site or delay surgery
Intracranial process	Avoid drain placement if concern for intracranial hypertension
Potential placement issues	
Spinal pathology (spinal stenosis)	Consider elective fluoroscopic guided lumbar drain placement
Prior lumbar spine surgery	
Positioning limitations	
Drain insertion	Consider insertion prior to induction of anesthesia
Traumatic/blood puncture	Evaluate for delay of surgery for 24 h or anticoagulation delay for > 1 h
Intraoperative management	
Hemodynamics	Avoid hypotension Optimize SCPP
Zero transducer	External ear meatus (Tragus)—patient supine, avoid over drainage
CSF drainage	CSFP <10 mmHg and maintain SCPP >60 mmHg. Drain < 10–20 mL/h Avoid large volumes of CSF drainage Maximal drainage <130 mL
Postoperative management and monitoring complications	
Disposition	Intensive care unit
Neurological checks	Hourly
Early neurologic exam	Allow for fast-track anesthesia and early extubation
Position	Allow for head of the bed 20°–30° elevation if no neurologic deficit If neurologic deficit: supine
Hemodynamics	Avoid hypotension, augment BP if needed with vasoactive agents and fluids
CSF drainage	Monitor CSF drainage and calculate SCPP Open drain every hour for 15 min and record drainage If CSF drainage > 20 cc/15 min—clamp drain
Duration of CSF monitoring/drainage	<72 h to minimize infection risk 24 h if neurologic exam intact and Crawford type IV TAAA 48–72 h if neurologically intact and Crawford type I–III TAAA If neurologic deficit present, weigh risk of infection versus benefit of continued CSF drainage
Bloody CSF drainage	May indicate intracranial bleed, consider CT head and/or spine
Headache	Consider symptomatic intracranial hypotension Stop CSF drainage Consult neurology if neurologic deficit
New onset lower extremity neurologic deficit	Consider SCI vs. neuraxial hematoma Increase SCPP > 80 (MAP 90–100 and CSFP 0–5 mmHg) Consider imaging of neuraxis
DVT prophylaxis	SQ heparin ±SCDs
Drain removal	Stable neurologic exam after 6 h with drain clamped Ensure adequate coagulation profile: similar to insertion guidelines Delay removal 2–4 h after last heparin administration Ensure intact catheter tip (rule out catheter fracture) Hold heparin for 1 h after drain removal

Abbreviations: *LMWH* low molecular weight heparin, *SCPP* spinal cord perfusion pressure, *TAAA* thoracoabdominal aortic aneurysm, *MAP* mean arterial pressure, *CSFP* CSF pressure, *SQ* subcutaneous, *SCDs* sequential compression devices

[a]Modified from [19]

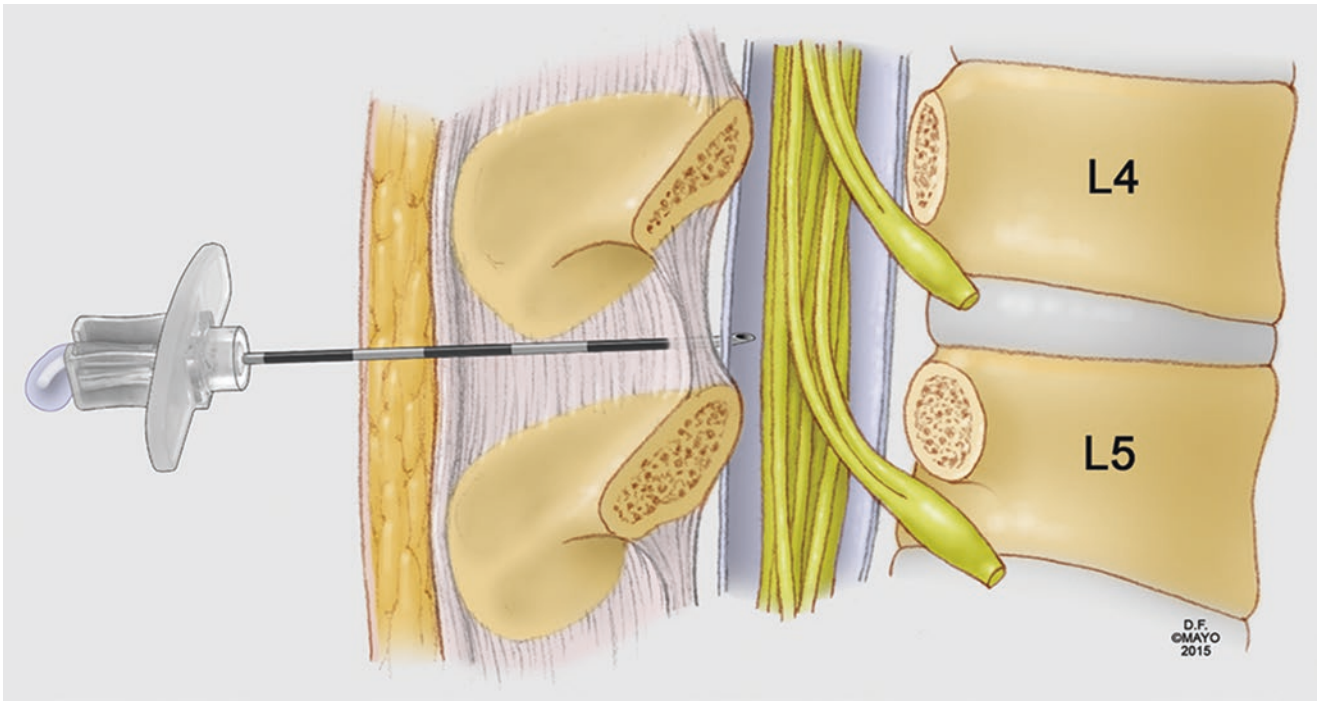


Fig. 22.1 Introduction of access needle in the L4–5 interspace with confirmation of clear cerebrospinal fluid prior to drain insertion. By permission of Mayo Foundation for Medical Education and Research. All rights reserved

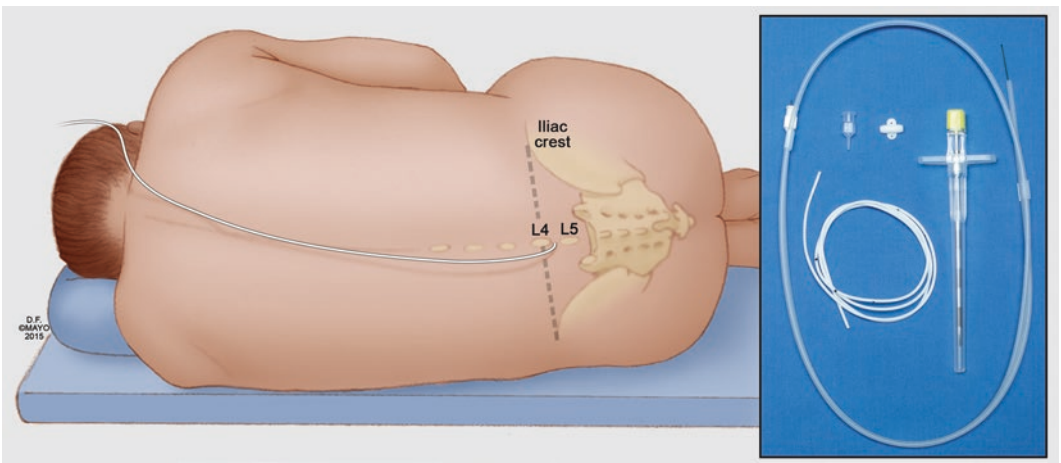


Fig. 22.2 Patient in the left lateral position for CSF drain placement and drain kit with ancillary tools. By permission of Mayo Foundation for Medical Education and Research. All rights reserved

Total intravenous anesthesia (TIVA) is the anesthesia technique of choice whenever SSEPs and MEPs are used to monitor the posterior column sensory proprioceptive and anterior motor pathways (Fig. 22.5). In those circumstances, or at the discretion of the anesthesiologist, a processed EEG monitor is applied in the patient's forehead to monitor anesthesia depth (see Fig. 22.3). The most common technology used is the Bispectral Index (BIS™) targeted anesthesia depth maintaining a BIS range of 40–60. Although TIVA is preferred, low dose inhalation agent (MAC < 0.5) can be used as well with minimal interference of SSEPs and MEPs once a good baseline has been obtained. After induction of anesthesia and placement of invasive hemodynamic monitors, the Intraoperative Neurophysiologic Monitoring (IOM)

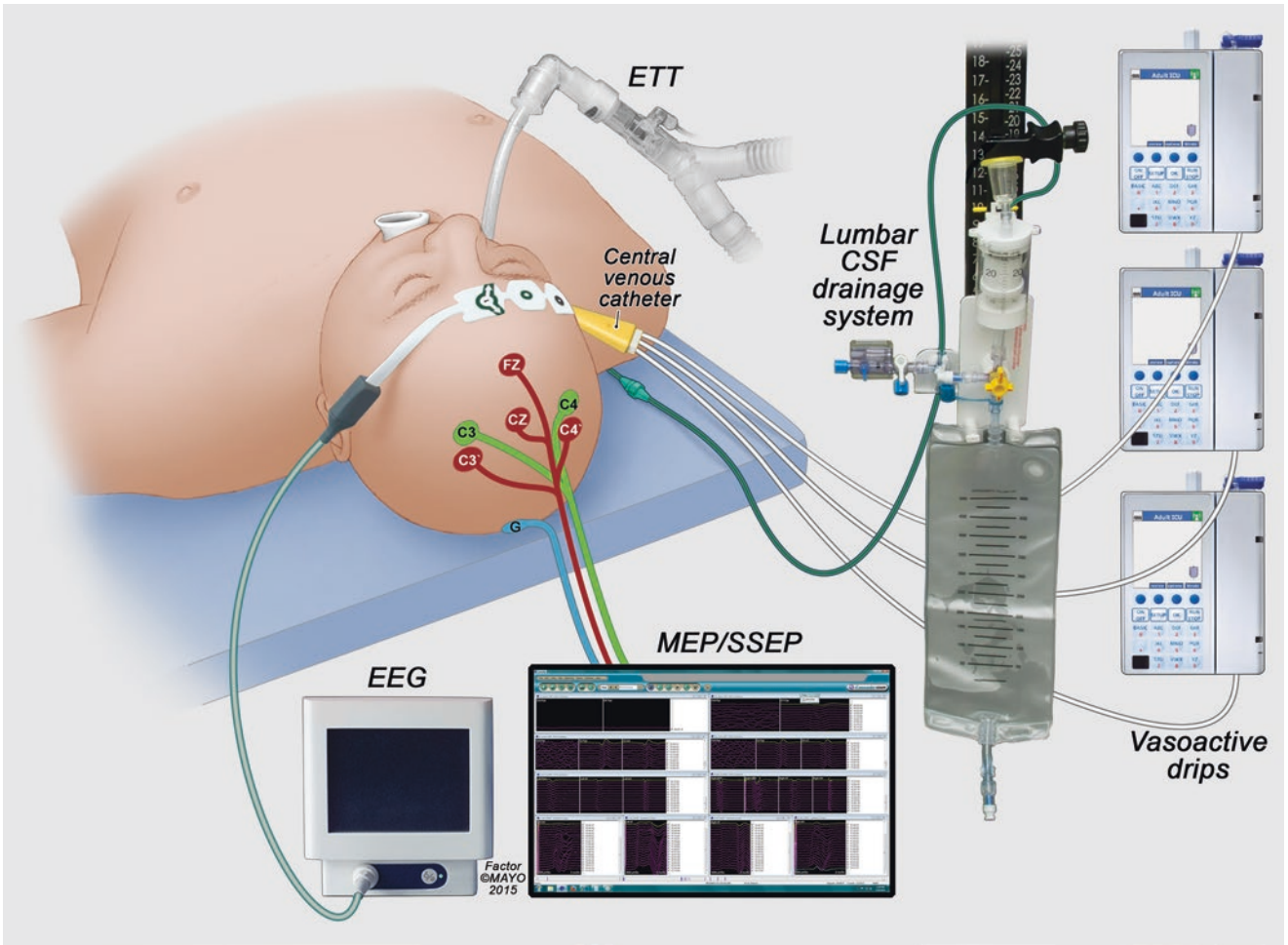


Fig. 22.3 Standardized set for CSF drainage and neuro-monitoring used during complex endovascular aortic procedures. By permission of Mayo Foundation for Medical Education and Research. All rights reserved

technicians place the respective electrodes (see Figs. 22.3 and 22.5). A constant current stimulator is recommended and either standard disk EEG electrodes or sterile subdermal needle electrodes may be used. Disk EEG electrodes should be applied to the scalp with collodion and sealed with tape or sheet to protect them from blood or other fluids. It is important to ensure that the OR personal is aware of the location of electrodes to avoid needle sticks.

During MEPs, electrical charges sent to the motor cortex through C3, C4 scalp electrodes stimulate the motor corticospinal pathway, which are recorded over multiple muscles in the upper and lower extremities at least every 10–15 min. An upper extremity muscle (extensor digitorum communis) is recorded to help differentiate neurogenic impairment such as spinal and lower limb ischemia from nonspecific changes. Bilateral lower extremity muscles are recorded using subdermal EEG electrodes placed in the hamstring, tibialis anterior, and abductor hallucis muscles (see Fig. 22.5). With SSEPs the electrical stimulus is generated at the ulnar or tibial nerve and travels from the distal extremity via the posterior column medial lemniscus pathway and is recorded over the neck and scalp. In patients where the lower extremity tibial SSEP are not present at the ankle, subdermal EEG electrodes can be positioned behind the knee (see Fig. 22.5).

Radiation Safety

The occupational radiation exposure is proportional to the complexity of the procedure and the use of endovascular suites and hybrid operating rooms. The key components of radiation safety include time, distance from radiation source and appropriate shielding. The inverse square law states that radiation scatter will decrease by the square of the distance to source of radiation; therefore, doubling the distance from a point source of radiation will decrease the exposure rate to one-fourth the original exposure rate. Anesthesia providers should practice similar safety to the operating surgical team and wear leaded aprons, thyroid shields and consider leaded eyewear.



Fig. 22.4 Zeroing of CSF drainage for accurate measurement and monitoring. By permission of Mayo Foundation for Medical Education and Research. All rights reserved

Assessing and Managing the Risk for Contrast-Induced Nephropathy

Due to the requirement for iodinated contrast medium during EVAR, preprocedural renal protection strategies are considered for patients with preexisting kidney disease or at risk for acute kidney injury. Although there is no widely accepted definition of contrast-induced nephropathy (CIN), an increase in creatinine of 0.5 mg/dL or 25 % above baseline within 2–3 days from contrast exposure is likely consistent with CIN.

Patents risk factors for CIN include:

- Serum creatinine > 2 mg/dL.
- Congestive heart failure.
- Proteinuria.
- Dehydration.
- Renal transplant.
- Calcineurin inhibitors (cyclopropane, sirolimus, tacrolimus).

Procedural risk factors for CIN include:

- Large volume of contrast agent (>400 mL).

Preoperative hydration with intravenous fluid administration is the primary prevention strategy for contrast induced nephropathy (CIN) [20] and the efficacy of intravenous isotonic bicarbonate as the fluid of choice, or the administration of *N*-acetylcysteine in the prevention of CIN remains unclear despite earlier studies advocating their use [21]. Preprocedure renal optimization includes holding diuretics for 24 h before the procedure, as well as avoiding nephrotoxic medications and cautious periprocedural hydration with normal saline, lactate Ringer's, or isotonic sodium bicarbonate at 100 mL/h for 10 h, unless significant reduction in cardiac reserve or hypervolemia is present.

Spinal Cord Protection

Spinal cord ischemia (SCI) remains an important cause of morbidity after TEVAR [22]. Interestingly, the coverage of the thoracic aorta without revascularization of spinal arteries was expected to produce higher rates of spinal cord ischemia than what is actually observed, challenging traditional anatomical models of spinal cord perfusion [13]. It is important however to consider the extent of coverage of native aorta as an important risk factor for SCI. Despite lower rates of SCI compared with open thoracoabdominal aortic repairs, this phenomenon continues to represent an important cause of morbidity due to the inability to revascularize covered spinal arteries, the presence of hypotension during the procedure, risk of embolization from present atheromatous plaques, and the possibility of compromise of distal perfusion due to large-bore sheaths used for stent graft insertion. Independent risk factors for development of SCI include: perioperative hypotension defined as MAP < 70 mmHg, CSF drainage complications, prior abdominal aortic aneurysm repair (compromise of hypogastric arteries), preoperative kidney disease, left subclavian artery coverage without revascularization, and the use of >3 stent grafts (reflecting on the length and complexity of the procedure as well as the extent of aorta covered) [13]. Notwithstanding, others have demonstrated that the most important risk factor for symptomatic SCI is the simultaneous closure of two independent arterial spinal cord supplying vascular territories in addition to persistent intraoperative hypotension, emphasizing the concept of collateral network in the pathophysiology of this devastating condition [23]. Another important factor to consider is the chronicity of the disease; such as the use of TEVAR in acute aortic dissection compared to chronic aneurysmal atherosclerotic disease, in which a collateral network can be highly variable, including contributions from lumbar and pelvic arteries, with the possibility to compensate for spinal artery compromise [24].

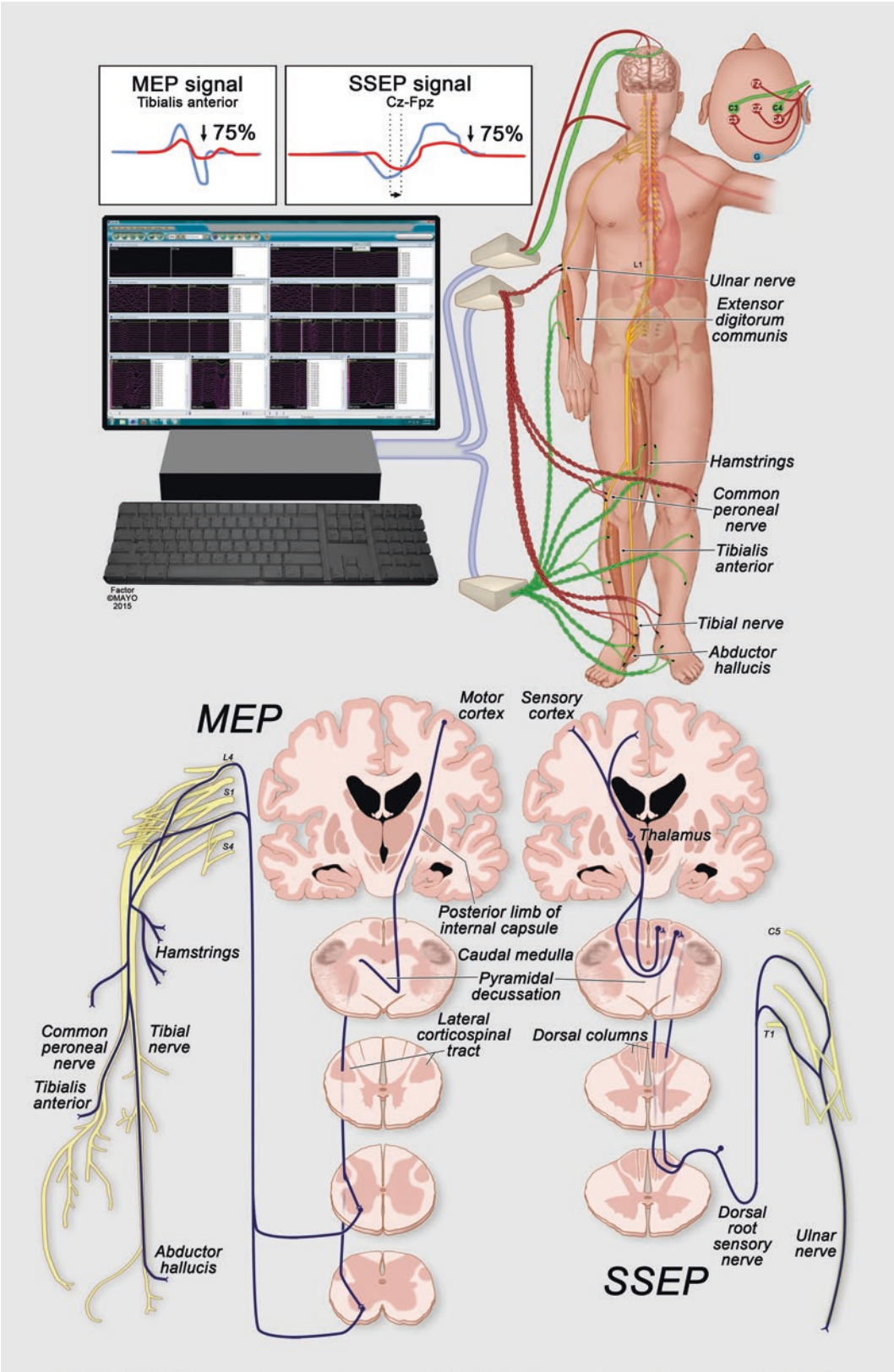


Fig. 22.5 Neuro-monitoring with somatosensory and motor evoked potentials is used routinely during extensive aortic coverage. By permission of Mayo Foundation for Medical Education and Research. All rights reserved

For optimal spinal cord protection, the intraoperative team focuses on strategies to maximize spinal cord perfusion with hemodynamic augmentation and CSF drainage, as well as strategies for early detection and management of SCI.

Strategies to Augment Spinal Cord Perfusion

The main therapeutic strategies to augment spinal cord perfusion aim to increase the collateral network pressure (CNP) and minimize cerebrospinal fluid or venous pressure according to the formula [25–27]:

$$\mathrm{SCPP} = \mathrm{MAP} - \left(\mathrm{CSFP\ or\ CVP}\left[\mathrm{whichever\ higher}\right]\right)$$

where SCPP = spinal cord perfusion pressure; MAP = mean arterial pressure (optimally distal aortic pressure); CSFP = cerebrospinal fluid pressure; and CVP = central venous pressure.

The CNP, which during TEVAR is the main driver of spinal cord perfusion, is only a fraction of the measured MAP (~70 %) [27]. Moreover, the CNP falls significantly more as a percentage of the MAP (~25 %) during the first 24 h after segmental spinal artery occlusion, and proportionally related to the number arteries sacrificed [27]. In general, it is imperative to avoid hypotension, maintain SCPP > 60 mmHg while avoiding large increases of CVP and drain CSF to maintain CSFP at ≤10 mmHg [19] (see Table 22.1). Institutions that perform complex TEVAR usually have protocols approved by the different members of the multidisciplinary team that care for these patients. These protocols vary between institutions from baseline monitoring pressure goals to optimal location to zero the transducer. At our institution, we continuously monitor the CSFP to allow for calculation of SCPP and open the drain to 10 mmHg, avoiding drainage >10 mL/h, or 20 mL/h during the ischemic period. As described above, the transducer is zeroed at the tragus or external ear meatus, which in the supine position correlates with the phlebostatic axis. If there is intraoperative evidence of SCI with changes on SSEPs and/or MEPs, the CSFP is lowered to 5 mmHg or 0 mmHg with care to avoid over draining and increase MAP to 90–100 mmHg (Fig. 22.6) Permissive systemic arterial hypertension is achieved with the use of vasoactive medications depending on cardiac function and hemodynamics. Usually, norepinephrine is initiated as a titratable infusion to increase SCPP >80 mmHg (or MAP 90–100 mmHg), despite paucity of data recommending its use over other vasoactive drugs. The practical advantages of norepinephrine include fast onset–offset of action and ability to titrate up and de-escalate acutely. Although not specific for SCI, at this time, norepinephrine remains the vasopressor of choice for acute neurologic injury [28]. Other adjuncts include vasopressin, a well-recognized and widely used vasopressor in vasodilatory shock. However, at doses >0.04 U/min, the risk of intestinal ischemia outweigh the benefits of permissive hypertension in SCI [29]. Phenylephrine has the potential for tachyphylaxis and therefore its use is limited to the operating room. In patients with significant left ventricular systolic dysfunction, an ionotrope, such as epinephrine or dobutamine with or without the addition of a vasopressor, may be appropriate. The choice of agent is largely dependent on the hemodynamic profile and cardiac function of the patient.

Strategies to Detect and Manage Spinal Cord Ischemia

The use of intraoperative neurologic monitoring (IOM) with SSEPs and MEPs (see Fig. 22.5) allows for detection of spinal cord ischemia and activation of a treatment plan while the patient is under anesthesia. As changes in blood flow correlate with changes in neuronal electrical activity, and there is a finite period of time (3–4 h) in which this can be reversed without permanent neurologic injury, IOM with SSEPs and MEPs has an important role in TEVAR with high risk for SCI [11]. Compared with the sensitivity of the neural tissue of the cerebral cortex to ischemia noted by electroencephalography (~20–30 s), the time for loss of response with ischemia is longer with SSEPs and MEPs (7–18 min and 11–17 min, respectively) [11]. Therefore, the evoked potentials are monitored every 10–15 min. A reduction of 50–75 % from baseline evoke potential amplitude is consider significant to trigger the SCI treatment algorithm (see Fig. 22.6). Once SSEP or MEP has confirmed a significant reduction of potentials, the SCPP is acutely maximized by increasing MAP >90–100 mmHg and decreasing CSFP to 5 mmHg. If these maneuvers improve the MEP and SSEP signals, the procedure is continued in standard fashion. If the optimization of SCPP fails to normalize the MEP/SSEP signals, the flow is restored to the pelvis and lower extremities by rearranging the sequence of target vessel stenting and consideration for arterial conduit is performed vs. staging the procedure.

Induced Hypotension for Precise Graft Deployment

Another important intraoperative technique unique to TEVAR is induced hypotension at the time of endovascular stent graft deployment to prevent the forward flow of blood from the heart causing the graft to move distal to the intended landing zone. Avoiding malposition of the stent graft secondary to pulsatile forces is critical. This is sometimes referred to as the "windsock effect." With newer graft designs and deployment techniques, the need for induced hypotension

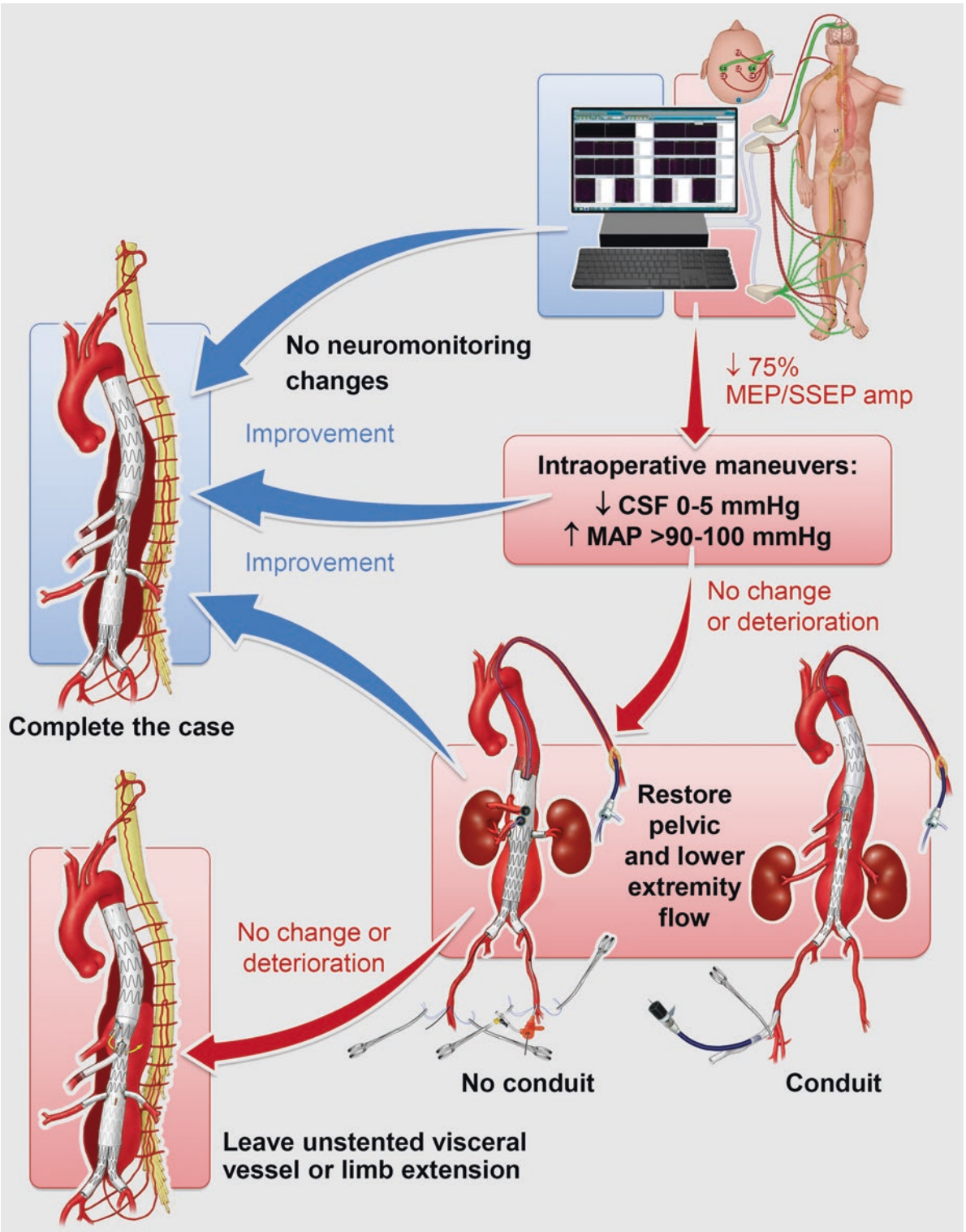


Fig. 22.6 Standardized Mayo Clinic protocol used in conjunction with neuro-monitoring for thoracoabdominal aortic repair. Note maneuvers include lowering CSF pressure and using hemodynamic augmentation to optimize spinal cord perfusion. By permission of Mayo Foundation for Medical Education and Research. All rights reserved

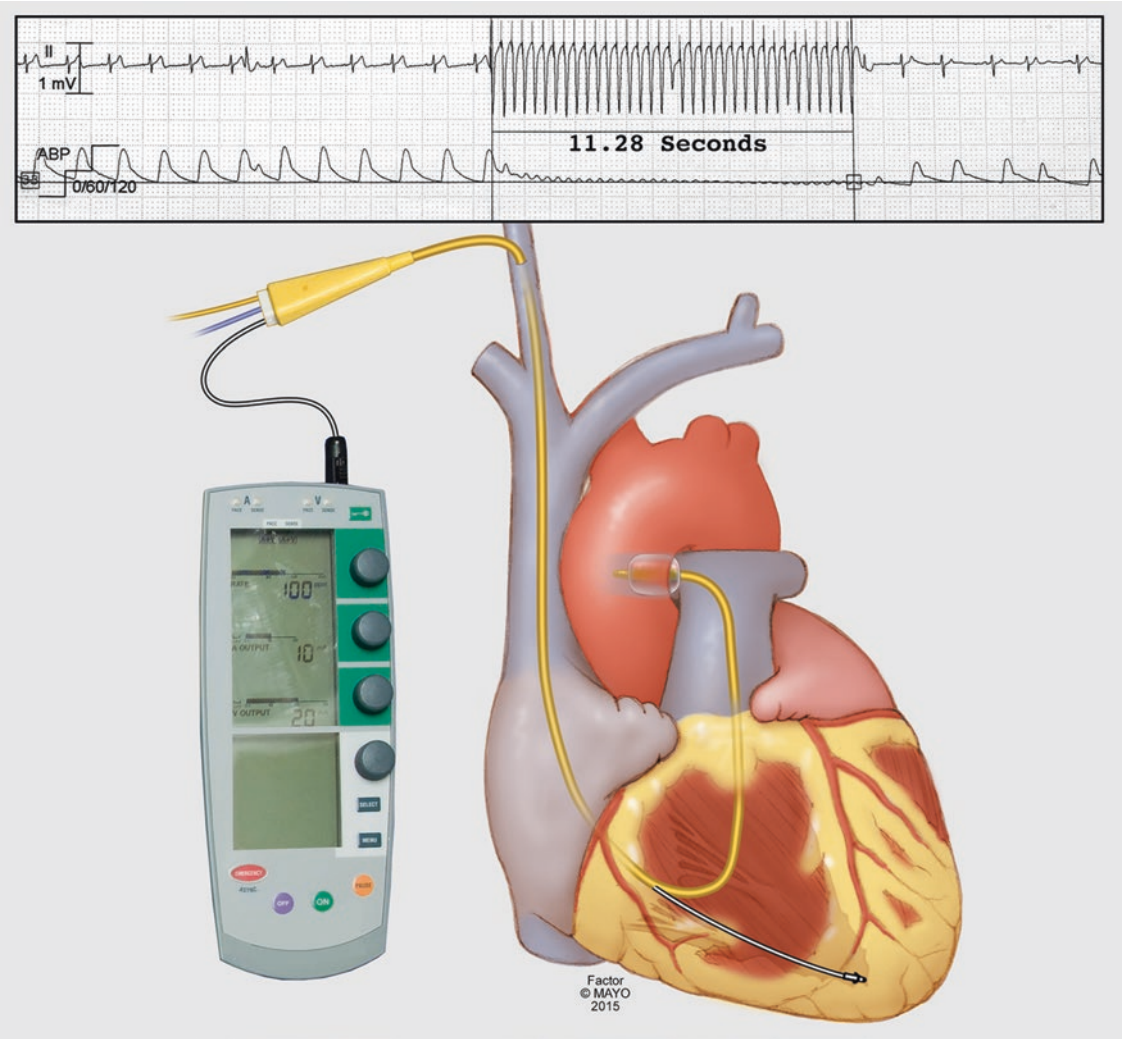


Fig. 22.7 For patients with ascending aortic and arch aneurysms with a landing zone in Zone 0, rapid ventricular pacing is used to allow controlled hypotension during stent deployment. By permission of Mayo Foundation for Medical Education and Research. All rights reserved

has been reduced to the proximal landing zones. Several methods are used to achieve induced hypotension including rapid ventricular pacing, right atrial-IVC balloon occlusion, and medication administration.

Rapid Ventricular Pacing

Rapid ventricular pacing provides a controlled reduction in cardiac output for a precise duration of time with hemodynamics returning to pre-pacing levels when the pacing is terminated. Pacing may be performed via a pulmonary artery catheter [30] (Fig. 22.7, rapid ventricular pacing) or via a transfemoral venous wire [31, 32]. Both cardiologists and anesthesiologist may safely provide rapid ventricular pacing for endograft deployment. Pulmonary artery catheter (PAC) rapid ventricular pacing utilizes a pacing wire placed through the RV pacing port of the catheter (see Fig. 22.7). The wire is deployed after the PAC is appropriately placed utilizing observation of hemodynamic waveforms or fluoroscopy. Capture is generally present when the wire is advanced 5 cm out of the RV pacing port. Regardless of the method of pacing, the pacing wires are tested prior to use for endograft deployment. Immediately prior to deployment pacing is commenced at rates between 160 to 200 beats/min and deployment is initiated when the blood pressure decreases to a mean arterial pressure of 40–50 mmHg and pulsatility is lost on the arterial waveform (see Fig. 22.7). After deployment is complete, pacing is terminated. The heart rate generally returns quickly to baseline, but patients may require temporary pacing at a back-up rate while their hemodynamics fully recovers. This process can be repeated as necessary for additional deployments or stent ballooning provided the patient continues to tolerate the pacing with

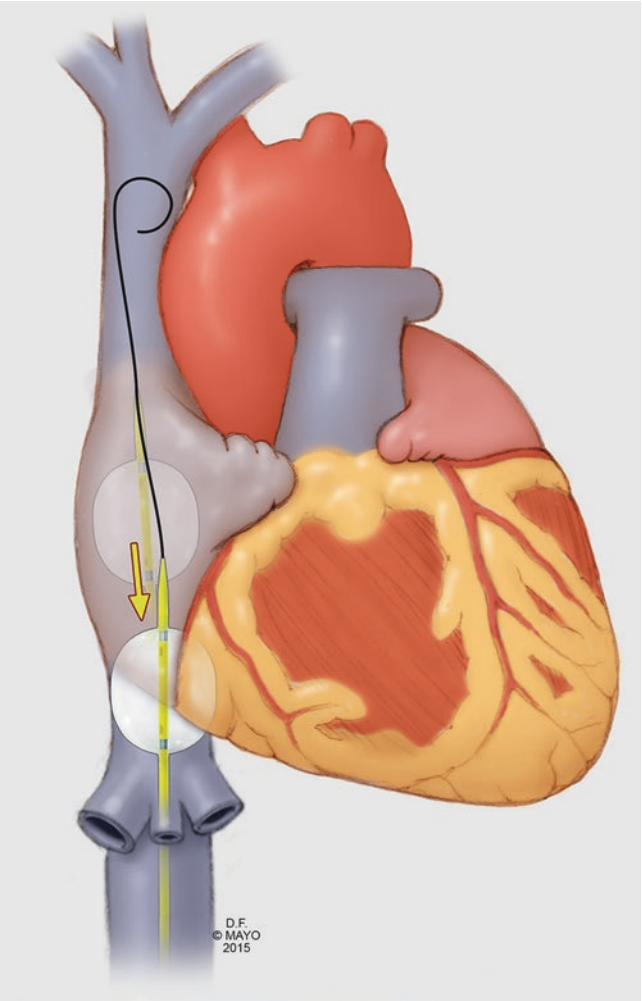


Fig. 22.8 An alternative for induced hypotension is balloon occlusion of the right atrium and caval junction decreasing preload and allowing systemic hypotension for stent deployment. By permission of Mayo Foundation for Medical Education and Research. All rights reserved

good recovery of hemodynamics after each episode. Following the procedure the pacing wire and PAC (if used) are removed.

Right Atrial Inflow Occlusion

Balloon occlusion of the right atrial-IVC junction has been described to decrease cardiac output for endograft deployment by decreasing preload [33, 34] (Fig. 22.8). The common femoral vein is accessed using standard Seldinger technique. Subsequently, a guidewire is advanced from the IVC to the SVC and a 12 Fr introducer sheath is placed (Coda® balloon catheter Cook Medical). The balloon is then advanced into the right atrium with fluoroscopic guidance and inflated. A mixture of contrast and saline may be used for inflation to confirm placement within the atrium. Immediately prior to endograft deployment traction is placed on the balloon pulling it into the IVC-right atrial junction and when resistance is felt the balloon is held in this position preventing blood return to the heart. This decrease in preload causes a decrease in cardiac output. When the deployment is complete the traction on the balloon is released allowing blood to resume flowing from the ICV to the heart and hemodynamics to normalize. It is important to ensure that the balloon is within the atrium at the time it is inflated and to not pull too vigorously on the balloon due to the risk of avulsing the IVC off of the right atrium.

Medications

Lastly, medications can also be used induce hypotension to facilitate endograft deployment. These include adenosine (inducing asystole), intravenous vasodilators (nitroprusside, nitroglycerin), and beta blockers (esmolol). All of these have been used safely to provide adequate conditions for graft deployment [35]. Adenosine-induced asystole results in no cardiac output for the duration of the drug effect; however, the duration is variable between patients. Titration of vasodilators and beta blockers allows for a gradual onset of hypotension and reduced cardiac output. After deployment, the patient is allowed to recover as the medication effects wear off or additional medications may be administered to improve the hemodynamics.

Each technique to alter hemodynamics and facilitate endograft deployment has unique benefits as well as risks. It is important that the team performing the hemodynamic maneuvers understand the physiology of the technique as well as the potential complications. The ability to prevent, recognize, and treat potential complications is paramount.

Postoperative Considerations

The disposition of a patient following endovascular stent graft placement depends on the nature of the procedure, the patient's preoperative state and comorbidities, need for strict neurologic monitoring with optimization of SCPP or development of complications at the time of surgery. At the completion of an endovascular stent graft procedure it is often ideal to evaluate the patient's neurologic status. The patient can either be awakened from anesthesia and extubated or the anesthesia can be lightened to a point where the patient is able to follow commands such as moving all extremities. The decision of whether the patient should be extubated at the end of the procedure should be based on the usual consideration such as hemodynamics, surgical course, and preoperative condition. If the patient is to remain intubated, the patient will go to the intensive care unit (ICU). A patient who is extubated would usually require ICU admission if blood pressure is being augmented by vasoconstrictors or inotropes, if a spinal

drain is in place, or if frequent neurologic monitoring is desired (see Table 22.1).

Complications following endovascular aortic stent grafting include endoleaks, ischemia secondary to inadvertent arterial blockage, other graft-related complications, bleeding, stroke, acute kidney injury, myocardial infarction, and spinal cord ischemia [36]. Spinal cord ischemia may be due to inadequate perfusion following the graft placement or due to spinal cord hematoma secondary to the spinal drain. Spinal cord injury after TEVAR usually occurs in the first 48 h. In a patient with a spinal drain who develops back pain and/or weakness, neuraxial hematoma, although rare, must be considered and appropriate imaging should be performed. More likely, however, new onset postoperative paraplegia is secondary to ischemia from suboptimal spinal cord and collateral network perfusion. At this time, it is appropriate to use the strategies to augment spinal cord perfusion as described above, include augmenting blood pressure with vasoconstricting agents to increase perfusion pressure, placement of a spinal drain if one is not being utilized, or increased CSF drainage in a patient with a functioning spinal drain. Due to the complex nature of these patients, both due to the surgical procedure and comorbidities, close monitoring and quick intervention is crucial to good outcomes.

Conclusion

As newer graft deployment technology is developed, anesthesia and perioperative medicine continues to evolve with the field. It is imperative to have an open discussion about the procedural plan, including the extent of aorta to be covered, the need for induced hypotension for graft deployment, and extremity access needed for graft deployment, as it will dictate the anesthesia technique, hemodynamic and neurologic monitoring required as well as the need for elective spinal drain placement with close vigilance to monitor and manage intraoperative spinal cord ischemia. The postoperative care depends largely on the complexity of the procedure, intraoperative complications, and need for permissive hypertension with vasoactive drips along with frequent neurovascular checks.

References

1. Endovascular aneurysm repair versus open repair in patients with abdominal aortic aneurysm (EVAR trial 1): randomised controlled trial. Lancet. 2005;365(9478):2179–2186.
2. Prinssen M, Verhoeven EL, Buth J, Cuypers PW, van Sambeek MR, Balm R, et al. A randomized trial comparing conventional and endovascular repair of abdominal aortic aneurysms. N Engl J Med. 2004;351(16):1607–18.
3. Chang DC, Parina RP, Wilson SE. Survival after endovascular vs open aortic aneurysm repairs. JAMA Surg. 2015;2:1–7.
4. De Bruin JL, Baas AF, Buth J, Prinssen M, Verhoeven EL, Cuypers PW, et al. Long-term outcome of open or endovascular repair of abdominal aortic aneurysm. N Engl J Med. 2010;362(20):1881–9.
5. Oderich GS, Mendes BC, Gloviczki P, Kalra M, Duncan AA, Bower TC. Current role and future directions of hybrid repair of thoracoabdominal aortic aneurysms. Perspect Vasc Surg Endovasc Ther. 2012;24(1):14–22.
6. Oderich GS, Correa MP, Mendes BC. Technical aspects of repair of juxtarenal abdominal aortic aneurysms using the Zenith fenestrated endovascular stent graft. J Vasc Surg. 2014;59(5):1456–61.
7. de Souza LR, Oderich GS, Banga PV, Hofer JM, Wigham JR, Cha S, et al. Outcomes of total percutaneous endovascular aortic repair for thoracic, fenestrated, and branched endografts. J Vasc Surg. 2015;62(6):1442–9.
8. Fleisher LA, Fleischmann KE, Auerbach AD, Barnason SA, Beckman JA, Bozkurt B, et al. 2014 ACC/AHA guideline on perioperative cardiovascular evaluation and management of patients undergoing noncardiac surgery: a report of the American College of Cardiology/American Heart Association Task Force on practice guidelines. J Am Coll Cardiol. 2014;64(22):e77–137.
9. Zhan HT, Purcell ST, Bush RL. Preoperative optimization of the vascular surgery patient. Vasc Health Risk Manag. 2015;11:379–85.
10. Bertges DJ, Goodney PP, Zhao Y, Schanzer A, Nolan BW, Likosky DS, et al. The Vascular Study Group of New England Cardiac Risk Index (VSG-CRI) predicts cardiac complications more accurately than the Revised Cardiac Risk Index in vascular surgery patients. J Vasc Surg. 2010;52(3):674-683, 683 e671-683 e673.
11. Sloan TB, Edmonds Jr HL, Koht A. Intraoperative electrophysiologic monitoring in aortic surgery. J Cardiothorac Vasc Anesth. 2013;27(6):1364–73.
12. Keyhani K, Miller 3rd CC, Estrera AL, Wegryn T, Sheinbaum R, Safi HJ. Analysis of motor and somatosensory evoked potentials during thoracic and thoracoabdominal aortic aneurysm repair. J Vasc Surg. 2009;49(1):36–41.
13. Etz CD, Weigang E, Hartert M, Lonn L, Mestres CA, Di Bartolomeo R, et al. Contemporary spinal cord protection during thoracic and thoracoabdominal aortic surgery and endovascular aortic repair: a position paper of the vascular domain of the European Association for Cardio-Thoracic Surgery. Eur J Cardiothorac Surg. 2015;47(6):943–57.
14. Estrera AL, Sheinbaum R, Miller CC, Azizzadeh A, Walkes JC, Lee TY, et al. Cerebrospinal fluid drainage during thoracic aortic repair: safety and current management. Ann Thorac Surg. 2009;88(1):9–15. discussion 15.
15. Cheung AT, Pochettino A, McGarvey ML, Appoo JJ, Fairman RM, Carpenter JP, et al. Strategies to manage paraplegia risk after endovascular stent repair of descending thoracic aortic aneurysms. Ann Thorac Surg. 2005;80(4):1280–8. Discussion 1288–1289.
16. Wynn MM, Mell MW, Tefera G, Hoch JR, Acher CW. Complications of spinal fluid drainage in thoracoabdominal aortic aneurysm repair: a report of 486 patients treated from 1987 to 2008. J Vasc Surg. 2009;49(1):29–34. Discussion 34–25.
17. Weaver KD, Wiseman DB, Farber M, Ewend MG, Marston W, Keagy BA. Complications of lumbar drainage after thoracoabdominal aortic aneurysm repair. J Vasc Surg. 2001;34(4):623–7.
18. Horlocker TT, Wedel DJ, Rowlingson JC, Enneking FK, Kopp SL, Benzon HT, et al. Regional anesthesia in the patient receiving antithrombotic or thrombolytic therapy: American Society of Regional Anesthesia and Pain Medicine Evidence-Based Guidelines (third edition). Reg Anesth Pain Med. 2010;35(1):64–101.
19. Fedorow CA, Moon MC, Mutch WA, Grocott HP. Lumbar cerebrospinal fluid drainage for thoracoabdominal aortic surgery: rationale and practical considerations for management. Anesth Analg. 2010;111(1):46–58.
20. Weisbord SD, Palevsky PM. Prevention of contrast-induced nephropathy with volume expansion. Clin J Am Soc Nephrol. 2008;3(1):273–80.

21. Sterling KA, Tehrani T, Rudnick MR. Clinical significance and preventive strategies for contrast-induced nephropathy. Curr Opin Nephrol Hypertens. 2008;17(6):616–23.
22. Greenberg RK, Lu Q, Roselli EE, Svensson LG, Moon MC, Hernandez AV, et al. Contemporary analysis of descending thoracic and thoracoabdominal aneurysm repair: a comparison of endovascular and open techniques. Circulation. 2008;118(8):808–17.
23. Czerny M, Eggebrecht H, Sodeck G, Verzini F, Cao P, Maritati G, et al. Mechanisms of symptomatic spinal cord ischemia after TEVAR: insights from the European Registry of Endovascular Aortic Repair Complications (EuREC). J Endovasc Ther. 2012;19(1):37–43.
24. Jacobs MJ, Elenbaas TW, Schurink GW, Mess WH, Mochtar B. Assessment of spinal cord integrity during thoracoabdominal aortic aneurysm repair. Ann Thorac Surg. 2002;74(5):S1864–1866. Discussion S1892–1868.
25. Mutch WA. Control of outflow pressure provides spinal cord protection during resection of descending thoracic aortic aneurysms. J Neurosurg Anesthesiol. 1995;7(2):133–8.
26. Augoustides JG, Stone ME, Drenger B. Novel approaches to spinal cord protection during thoracoabdominal aortic interventions. Curr Opin Anaesthesiol. 2014;27(1):98–105.
27. Etz CD, Zoli S, Bischoff MS, Bodian C, Di Luozzo G, Griepp RB. Measuring the collateral network pressure to minimize paraplegia risk in thoracoabdominal aneurysm resection. J Thorac Cardiovasc Surg. 2010;140(6 Suppl):S125–130. Discussion S142–S146.
28. Muzevich KM, Voils SA. Role of vasopressor administration in patients with acute neurologic injury. Neurocrit Care. 2009;11(1):112–9.
29. Obritsch MD, Bestul DJ, Jung R, Fish DN, MacLaren R. The role of vasopressin in vasodilatory septic shock. Pharmacotherapy. 2004;24(8):1050–63.
30. Ricotta 2nd JJ, Harbuzariu C, Pulido JN, Kalra M, Oderich G, Gloviczki P, et al. A novel approach using pulmonary artery catheter-directed rapid right ventricular pacing to facilitate precise deployment of endografts in the thoracic aorta. J Vasc Surg. 2012;55(4):1196–201.
31. Nienaber CA, Kische S, Rehders TC, Schneider H, Chatterjee T, Bünger CM, et al. Rapid pacing for better placing: comparison of techniques for precise deployment of endografts in the thoracic aorta. J Endovasc Ther. 2007;14(4):506–12.
32. Chen J, Huang W, Luo S, Yang D, Xu Z, Luo J. Application of rapid artificial cardiac pacing in thoracic endovascular aortic repair in aged patients. Clin Interv Aging. 2014;9:73–8.
33. Lee WA, Martin TD, Gravenstein N. Partial right atrial inflow occlusion for controlled systemic hypotension during thoracic endovascular aortic repair. J Vasc Surg. 2008;48(2):494–8.
34. Cires G, Noll Jr RE, Albuquerque Jr FC, Tonnessen BH, Sternbergh 3rd WC. Endovascular debranching of the aortic arch during thoracic endograft repair. J Vasc Surg. 2011;53(6):1485–91.
35. Nicolaou G, Forbes TL. Strategies for accurate endograft placement in the proximal thoracic aorta. Semin Cardiothorac Vasc Anesth. 2010;14(3):196–200.
36. Bell D, Bassin L, Neale M, Brady P. A review of the endovascular management of thoracic aortic pathology. Heart Lung Circ. 2015;24(12):1211–5.

Techniques of Iliofemoral Conduit for Endovascular Repair

23

Aaron C. Baker and Gustavo S. Oderich

Introduction

Vascular access complications are an important cause of morbidity and mortality during endovascular aortic repair. Iliofemoral conduits are needed in approximately 15–20 % of patients undergoing thoracic or thoracoabdominal repair with device introduction sheaths larger than 20 Fr. Female patients and those with small, narrow, or calcified iliac arteries more often need adjunctive access-related procedures. Inadvertent disruption of the iliac arteries leading to hypotension can be a devastating complication and is associated with added risk of spinal cord injury in patients who have extensive endovascular aortic repair. Review of preoperative imaging is key to plan the endovascular repair and can assist in predicting iliac access difficulties. Computed tomography angiogram findings such as calcification, stenosis/occlusion, small diameter vessels, kinked grafts, and previous stents all can present access challenges during endovascular interventions.

Ideally, iliac artery conduits should be planned prior to the procedure to avoid any inadvertent disruption of the iliofemoral arteries. The most common conduits involve the iliac and femoral arteries, but the aorta, carotids, subclavian, axillary, and left ventricle have all been used as access sites during endovascular procedures. The ideal size diameter of the iliac artery can be determined on the basis of the device selected for the procedure. As a general rule, younger patients have more elastic vessels, which can tolerate more stretching. The same is not true for older patients with calcified vessels or patients with previously placed iliac stents. There are both advantages and disadvantages to open and endovascular conduits, and specific patient anatomy and comorbidities should guide decision-making on selection of the ideal approach to iliac access (Table 23.1).

A.C. Baker
Division of Vascular and Endovascular Surgery,
Department of Surgery, Mayo Clinic, 200 First Street SW,
Rochester, MN 55905, USA

G.S. Oderich (✉)
Division of Vascular and Endovascular Surgery,
Department of Surgery Mayo Clinic, 200 First Street SW,
Rochester, MN 55905, USA
e-mail: oderich.gustavo@mayo.edu

Adjunctive Maneuvers

Several adjunctive maneuvers can be attempted in patients with narrow or small iliac arteries to gauge the need for conduit. Meticulous technique and judgment is required as to not disrupt the iliac artery by excessive force in an attempt to avoid a surgical conduit. The devastating complication of an "iliac-artery-on-a-stick" can be avoided by patient selection and proceeding with conduit prior to arterial disruption (Fig. 23.1). A patient with an excessively tortuous iliac artery may benefit from retroperitoneal mobilization of the external iliac artery via a groin incision with straightening of the redundant iliac artery using the "pull-down" technique. Other maneuvers include using manual compression of the lower abdomen during advancement of the device, or use of the brachial-femoral through-and-through access to provide more support (Fig. 23.2). If the later is selected, it is useful to have a long brachial sheath, which protects the origin of the supra-aortic trunk (e.g., left subclavian artery) in order to prevent the wire from transecting the subclavian-aortic junction or other tortuous arterial segment. A selective angiography of the iliac artery and focal angioplasty with balloon is one of the first steps prior to introduction of a large diameter sheath. Serial dilatation of the iliac artery (Fig. 23.3) with incremental diameter rigid dilators can be attempted, but one needs to recognize that excessive force should not be applied to avoid iliac disruption using this maneuver. A Solopath (Terumo, Somerset, NJ) balloon-expandable sheath can also be used in select cases where tortuosity and plaque is the main limiting factor, yet the iliac vessel diameter accepts a 21 Fr sheath (Fig. 23.4).

© Mayo Foundation for Medical Education and Research 2017

G.S. Oderich (ed.), *Endovascular Aortic Repair*, DOI 10.1007/978-3-319-15192-2_23

Table 23.1 Advantages and disadvantages to open and endovascular conduits

Advantage	Disadvantage
Open surgical conduit	
Internal iliac reperfusion	Longer operative time first stage
Option for larger conduit	Risk of hernia
Decreased operative time second stage	Risk of prosthetic infection
Direct visualization	Increased recovery time from incision
Endovascular conduit	
Less procedural time first stage	Risk of dislodgement second stage
Less invasive procedure	Coverage of internal iliac artery
Faster recovery	Risk of rupture/hematoma

Conduit Selection

Selection of the ideal conduit should take into consideration the patients surgical risk, hostile retroperitoneal or abdominal anatomy, prior iliac stents or surgical grafts and presence of occluded internal iliac artery on at least one of the sides. In general, patent internal iliac arteries should not be sacrificed during complex endovascular aortic repairs in an attempt to perform an endovascular conduit. The rate of paraplegia is significantly higher with inadvertent occlusion of patent internal iliac arteries. If the patient requires internal iliac revascularization or the iliac artery needs to be preserved, a surgical conduit in the iliac artery is the best alternative. This can be a temporary conduit, which is removed at the end of the case, or alternatively a permanent conduit if staged operations are anticipated. Conversely, if the internal iliac artery is chronically occluded, and endovascular conduit is a reasonable alternative.

Surgical Conduits

The most common surgical conduit is performed at the distal common or proximal external iliac artery using a flank retroperitoneal incision. The ideal strategy depends upon the status of the iliac arteries (e.g., calcification, patency of hypogastric arteries, presence of stents) and the surgical risk based on severity of patients comorbidities. Most patients can tolerate a small flank incision and retroperitoneal exposure (Fig. 23.5). However, this is a less ideal option in the patient with hostile anatomy because of stoma, prior surgery or radiation, or in those who are excessively high-risk for any operation.

Temporary Iliofemoral Conduits

Iliac artery conduits and internal iliac artery bypasses are done using a small 10- to 15-cm curvilinear flank incision.



Fig. 23.1 Iliac artery conduits—open surgical or endovascular—should be performed prior to the devastating complication of "iliac artery on a stick," which can be avoided by careful planning and meticulous technique. By permission of Mayo Foundation for Medical Education and Research. All rights reserved

If there is a choice for either side, our preference is to use the right iliac artery for access. It is important not to perform the incision to low in the flank. The aortic bifurcation is typically at the level of the umbilicus and the common iliac bifurcation is 5-cm below this level. It is better to error on a higher than a lower incision (Fig. 23.5a). Dissection is

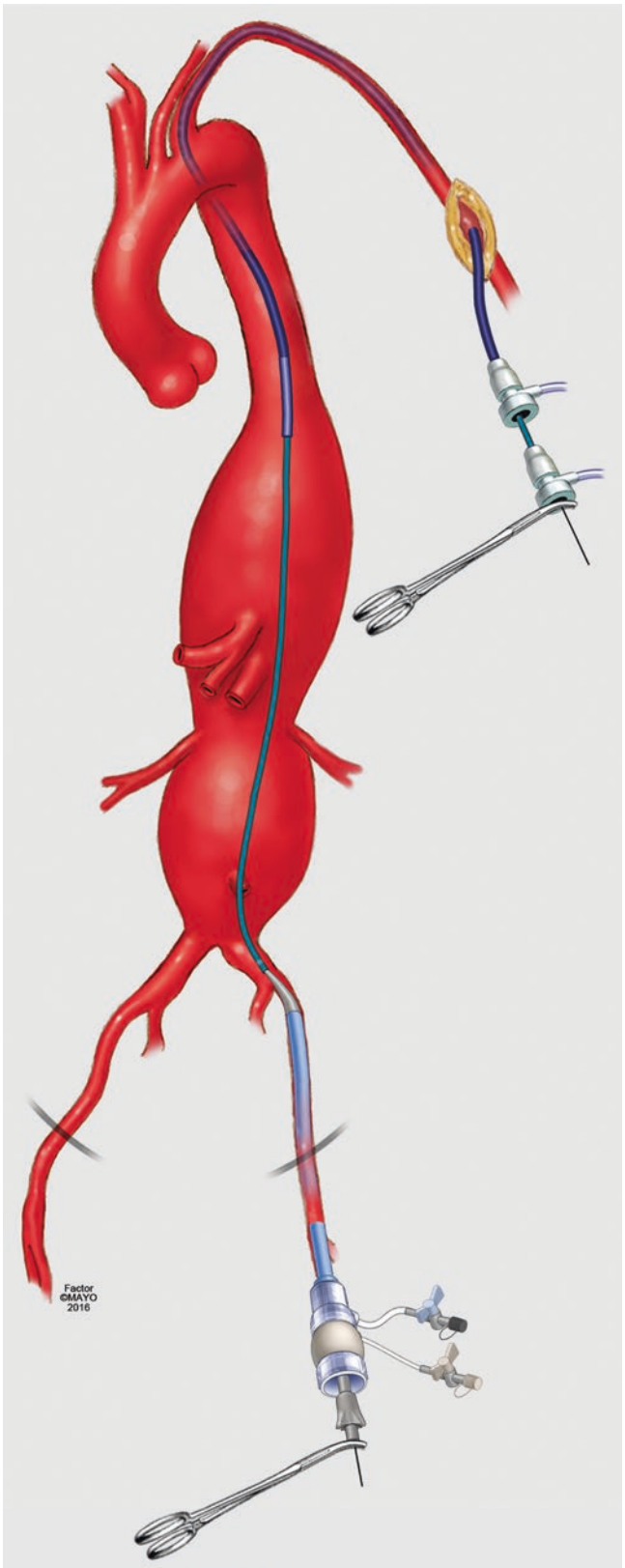


Fig. 23.2 Brachial-femoral access can straighten the iliofemoral arteries and allow introduction of a large sheath. It is important to protect the origin of the supra-aortic trunk by a sheath. The maneuver of hubbing the large sheath into a 7Fr sheath and using two clamps on each end with a "push and pull" maneuver is a very useful technique for difficult access. By permission of Mayo Foundation for Medical Education and Research. All rights reserved

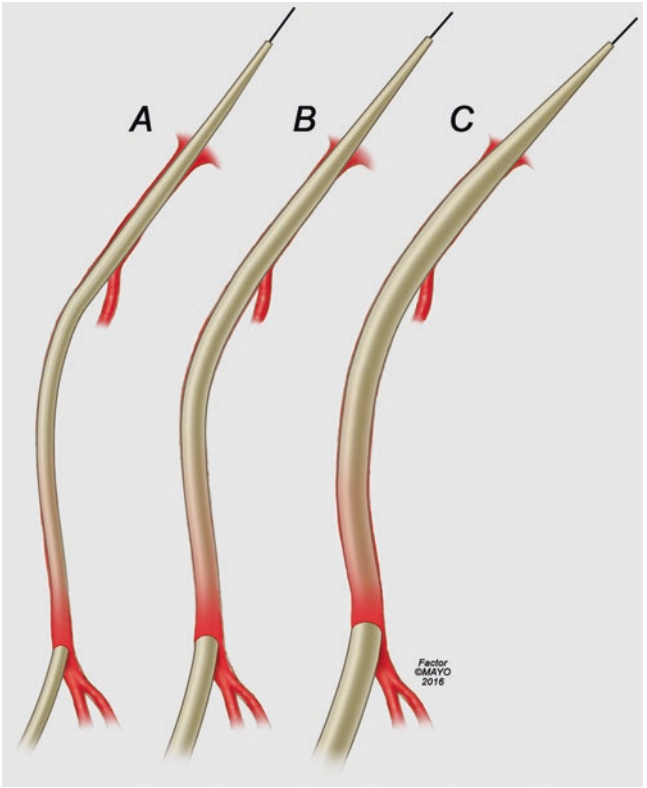


Fig. 23.3 (**a**, **b**, **c**) Sequential dilatation is performed to facilitate access and to gauge the ability to introduce a large sheath. One should not force the dilator. A conduit is indicated if there is difficulty on introduction of the dilator. By permission of Mayo Foundation for Medical Education and Research. All rights reserved

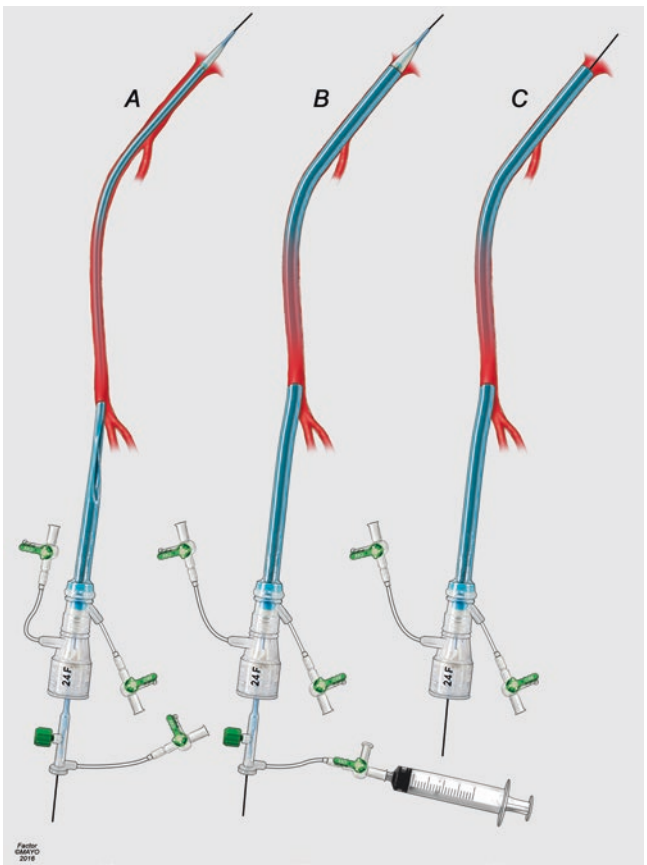


Fig. 23.4 (**a**, **b**, **c**) Solopath balloon expandable sheath (Terumo, Somerset, NJ). By permission of Mayo Foundation for Medical Education and Research. All rights reserved

carried through the skin, soft tissue and external oblique muscle fascia. The abdominis rectus muscle is preserved but the external oblique, internal oblique and transverse abdominis muscles are typically transected to facilitate exposure. If the abdominis muscle is transected, the inferior epigastric vessels should be ligated and divided to prevent postoperative hemorrhage. The retroperitoneal space should be entered carefully to avoid opening the peritoneum. It is easier to start the dissection laterally where there is more preperitoneal fat. Dissection is carried through the retroperitoneal space using blunt maneuver with sponge on a stick or finger dissection. The psoas muscle is encountered first and the dissection is carried medially to expose the external, internal and common iliac arteries. Care should be taken to avoid injuring the iliac veins, which are typically densely adhered to the posterior wall of the common iliac artery, and to avoid excessive dissection or devascularization of the ureter. A self-retaining retractor is useful in the obese patient or those with deep pelvis (Fig. 23.5b). The iliac arteries are controlled with silastic vessel loops and are examined for clamp placement (Fig. 23.5c). The patient is systemically heparizined, and proximal and distal control is obtained in the common, internal and external iliac arteries with silastic vessel loops or surgical clamps (Fig. 23.5d). A longitudinal arteriotomy is made anteriorly extending from the distal common to the external iliac artery. We typically use a 10-mm polyester graft, which is spatulated and anastomosed using 4-0 Prolene sutures with "parachute" technique. If the common iliac artery is excessively calcified, the graft can be loaded into a Fogarty occlusion balloon,

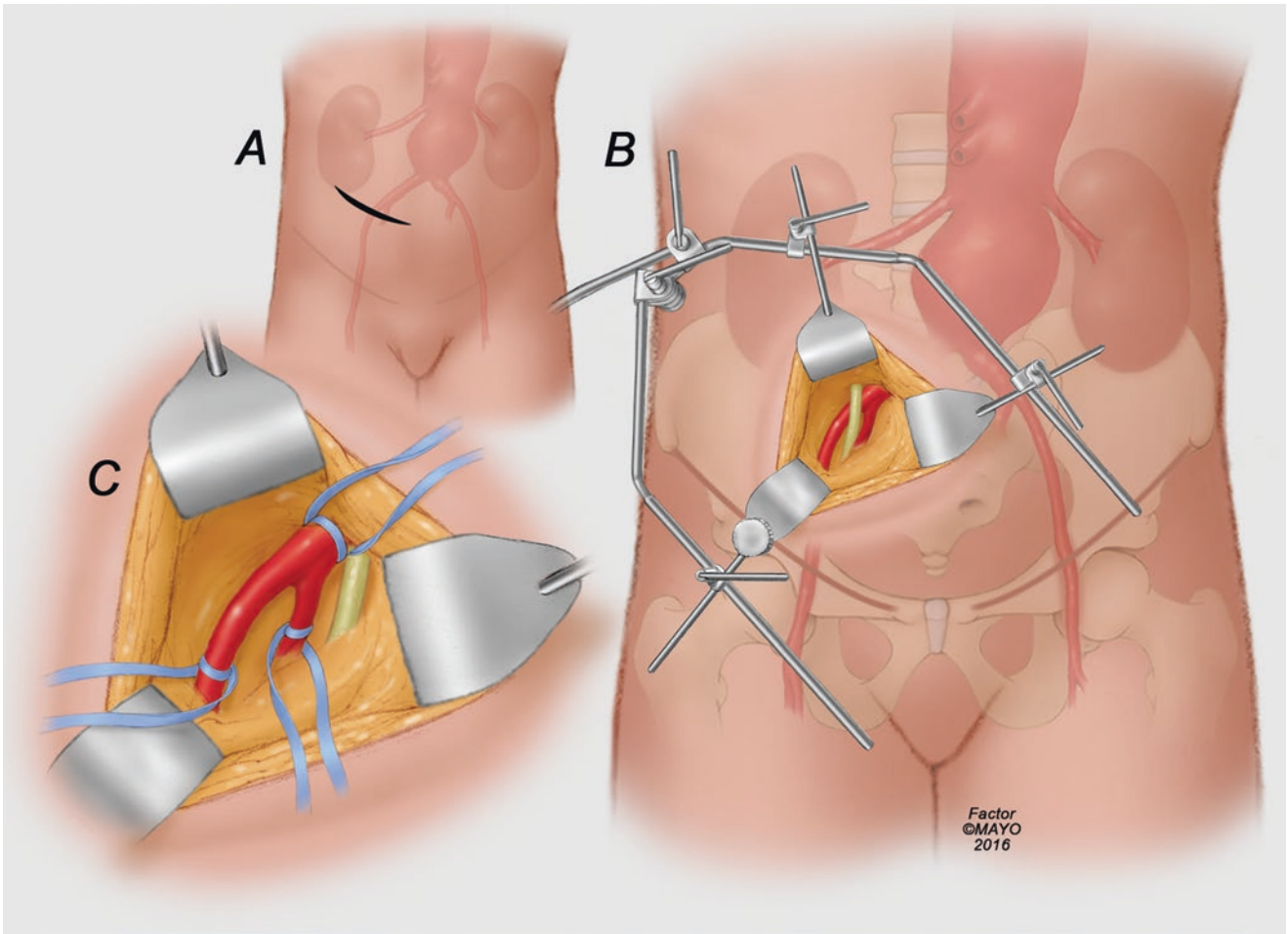


Fig. 23.5 Retroperitoneal exposure for open surgical iliac artery conduits is done using a curvilinear incision (**a**) and self-retaining retractor (**b**) to expose the common, internal and external iliac arteries (**c**). After proximal and distal control is obtained (**d**), a longitudinal arteriotomy is made and 10-mm polyester graft is anastomosed end-to-side using 4-0 Prolene suture. Occasionally balloon occlusion is needed for proximal control if the vessel is calcified (**e**). The conduit is exteriorized via a small counter incision in the groin (**f**). Once the procedure is completed the surgical graft (**g**) is excised leaving a small patch of graft in the iliac arteries (**h**). By permission of Mayo Foundation for Medical Education and Research. All rights reserved

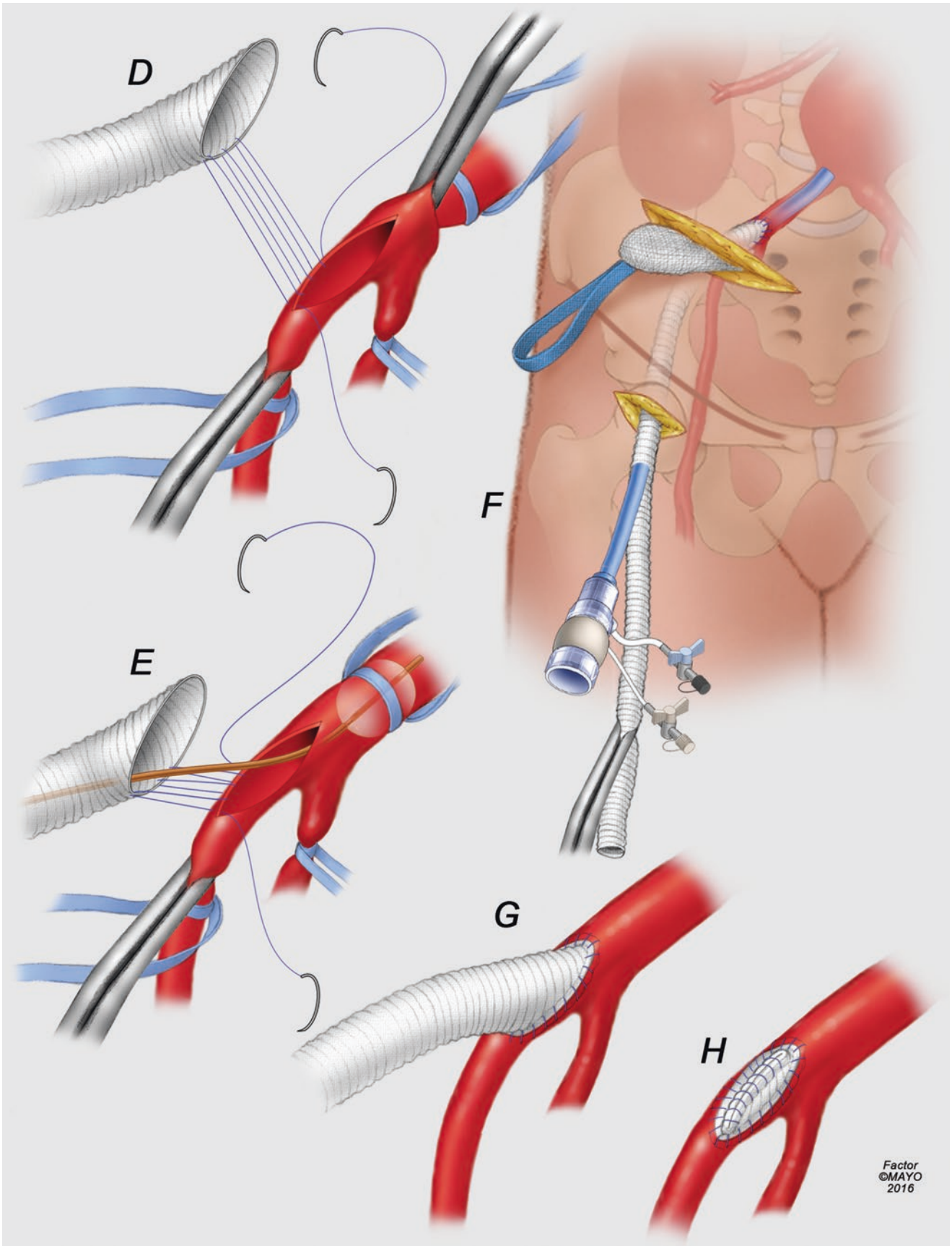


Fig. 23.5 (continued)

which can be used for proximal control (Fig. 23.5e). Alternatively balloon occlusion can be obtained using ipsilateral or contra-lateral femoral access if this is available. We often recommend using a felt strip to do the anastomosis, particularly if there is need for endarterectomy or the artery is thin-walled. Once the anastomosis is completed, the conduit is exteriorized via a small groin incision or a previous groin incision if this has already been done for a prior trans-femoral approach (Fig. 23.5f). Access should be established using a puncture into the polyester graft instead of introducing the sheath via the end of the graft, which leads to poor hemostasis and more bleeding. Once the procedure is completed, the iliac arteries are clamped and the area of the conduit anastomosis (Fig. 23.5g) is partially excised leaving a rim of fabric, which is closed longitudinally leaving a small patch to avoid narrowing (Fig. 23.5h).

A temporary femoral artery conduit can be useful in complex procedures with technical difficulties if one anticipates prolonged lower extremity ischemia time (>2 h). This is also used in patients with severe aorto-iliac and profunda femoral artery disease to minimize lower extremity ischemia. The 10-mm femoral conduit (Fig. 23.6a) is anastomosed end-to-side to the common femoral artery using standard oblique or longitudinal groin incision. The conduit allows withdrawal of the sheath (Fig. 23.6b) to restore flow into the internal iliac, profunda, and lower extremities arteries, while access is maintained with the guide-wire in case there is need for additional intervention. At completion of the case, the conduit is partially excised leaving a small remnant patch.

Permanent Iliofemoral Conduits

Patients who need conduits for staged procedures or extensive thoracoabdominal repairs (Types I to III) are preferentially treated with a permanent iliofemoral conduit to avoid need for redo retroperitoneal exposure and minimize risk of hemorrhage from associated coagulopathy that follows extensive aortic coverage. There are several options on how to fashion the iliofemoral bypass. The common femoral artery is exposed using a small longitudinal groin incision. After the vessels are dissected and the patient is systemically heparinized, the common, internal and external iliac arteries are clamped. The external iliac artery is ligated distally and transected 2-cm distal to the origin. An arteriotomy is carried towards the common iliac artery just proximal to the origin of the internal iliac artery. A 10-mm polyester graft is spatulated and anastomosed end-to-end to the stump of the external iliac artery into the common iliac artery (Fig. 23.7a). The distal anastomosis is done to the proximal common femoral artery just under the inguinal ligament. Access is established directly into the graft while flow is restored to the lower extremity (Fig. 23.7b). Temporary femoral conduits can also be anastomosed end-to-side into the iliofemoral graft if indicated. Alternatively an end-to-end anastomosis to the common iliac artery. The distal stump of the common iliac artery iliac artery is closed primarily and graft is anastomosed distally to the external iliac artery allowing retrograde flow into the internal iliac artery (Fig. 23.7c). Lastly, in order to maintain perfusion to the internal iliac arteries because of inadequate landing zone in the common iliac artery, a separate bypass can be added to the internal iliac artery (Fig. 23.8). This is especially important in patients who need extensive coverage of segmental intercostal or lumbar arteries to minimize risk of spinal cord injury.

Endovascular Conduits

Endovascular conduits were initially described by Yano, Matsumura, and Peterson in a separate publications. This approach has also been popularized by the Malmo Group as the "paving and cracking" technique. It uses endovascular stents or stent-grafts to enlarge the iliac arteries or correct any underlying occlusive disease. A stent-graft is used to over-dilate the artery beyond its normal diameter. This manuever prevents arterial disruption, which can occur with bare metal stents. The technique can be performed with percutaneous femoral access or surgical exposure. The later is preferred if the common femoral arteries are diseased or small size because hemorrhage can occur at the distal end-point of the stent-graft if this is over-dilated with percutaneous approach. After femoral access is established, the iliac arteries are gently dilated with primary angioplasty to allow expansion of the stent-graft (Fig. 23.9a). A covered stent or stent-graft is deployed from the common iliac towards the proximal common femoral artery just across the inguinal ligament (Fig. 23.9b). Following expansion of the stent (Fig. 23.9c), post-dilatation is performed in the covered segment with an 8- or 10-mm angioplasty balloon depending on the diameter sheath that will be utilized (Fig. 23.9d). One needs to be careful not to over-dilate the distal end-point and tear the common femoral artery (Fig. 23.9e). If this occurs, it is best to achieve proximal control with a balloon inflated in the stent and repair the common femoral artery with an interposition graft or a patch.

The choice of the stent for endoconduit is variable. Our preference is to use 11- or 13-mm Viabahn® stent-grafts (Gore, Flagstaff, AZ). If the common iliac artery is larger than 13 mm, a tapered 16-mm to 12-mm Excluder iliac limb (Gore, Flagstaff, AZ) can be used. Covered stents are usually dilated to 9–10 mm in the EIA and 10– 12 mm in the CIA. Over-dilatation does not result in uncontrollable hemor-

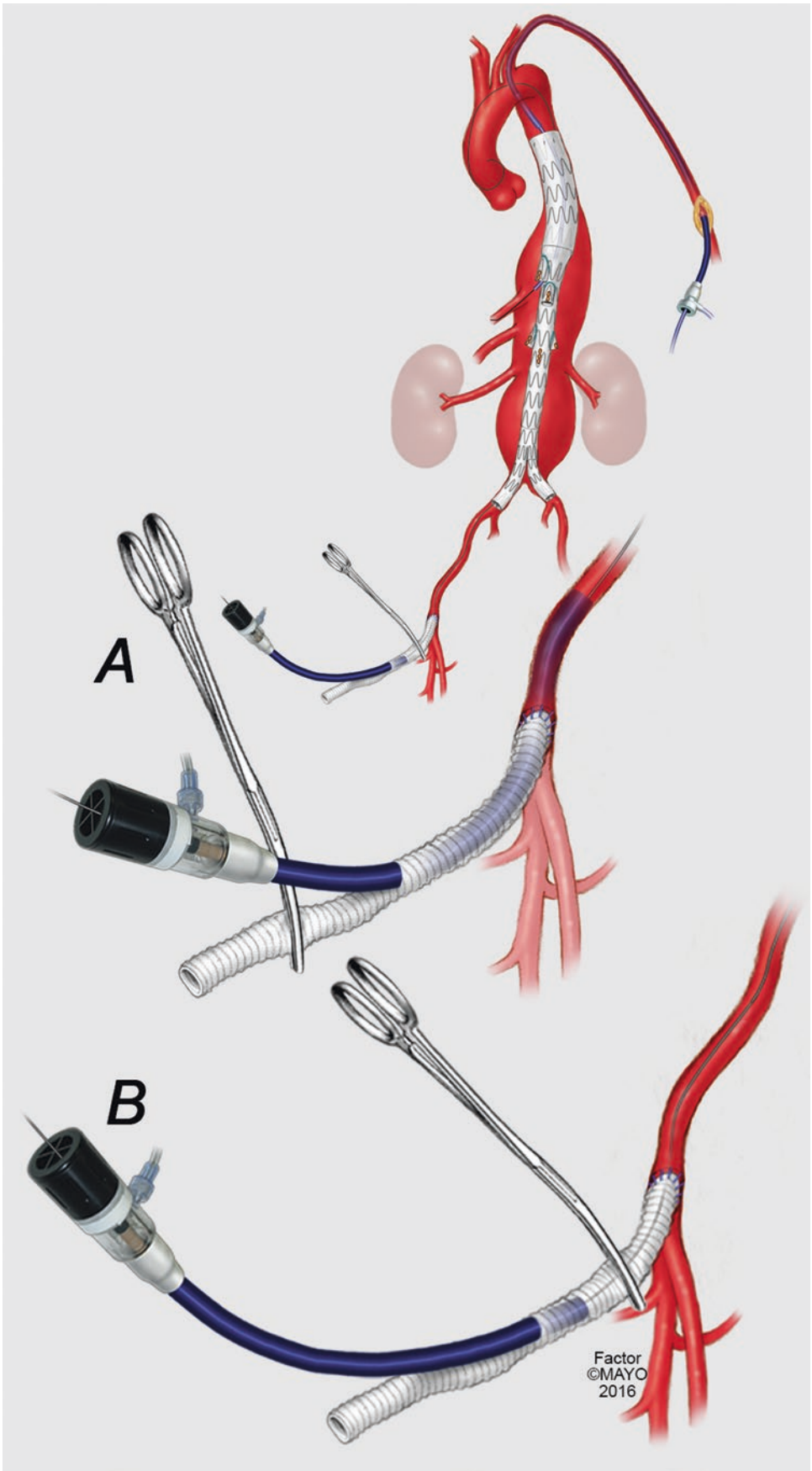


Fig. 23.6 Temporary common femoral conduits are used selectively in patients with extensive thoracoabdominal aneurysms and anticipated technical difficulty to minimize lower extremity ischemia (**a**). The graft is anastomosed end-to-side to the common femoral artery and the sheath is retracted into the graft (**b**) to allow restoration of flow into the limb. By permission of Mayo Foundation for Medical Education and Research. All rights reserved

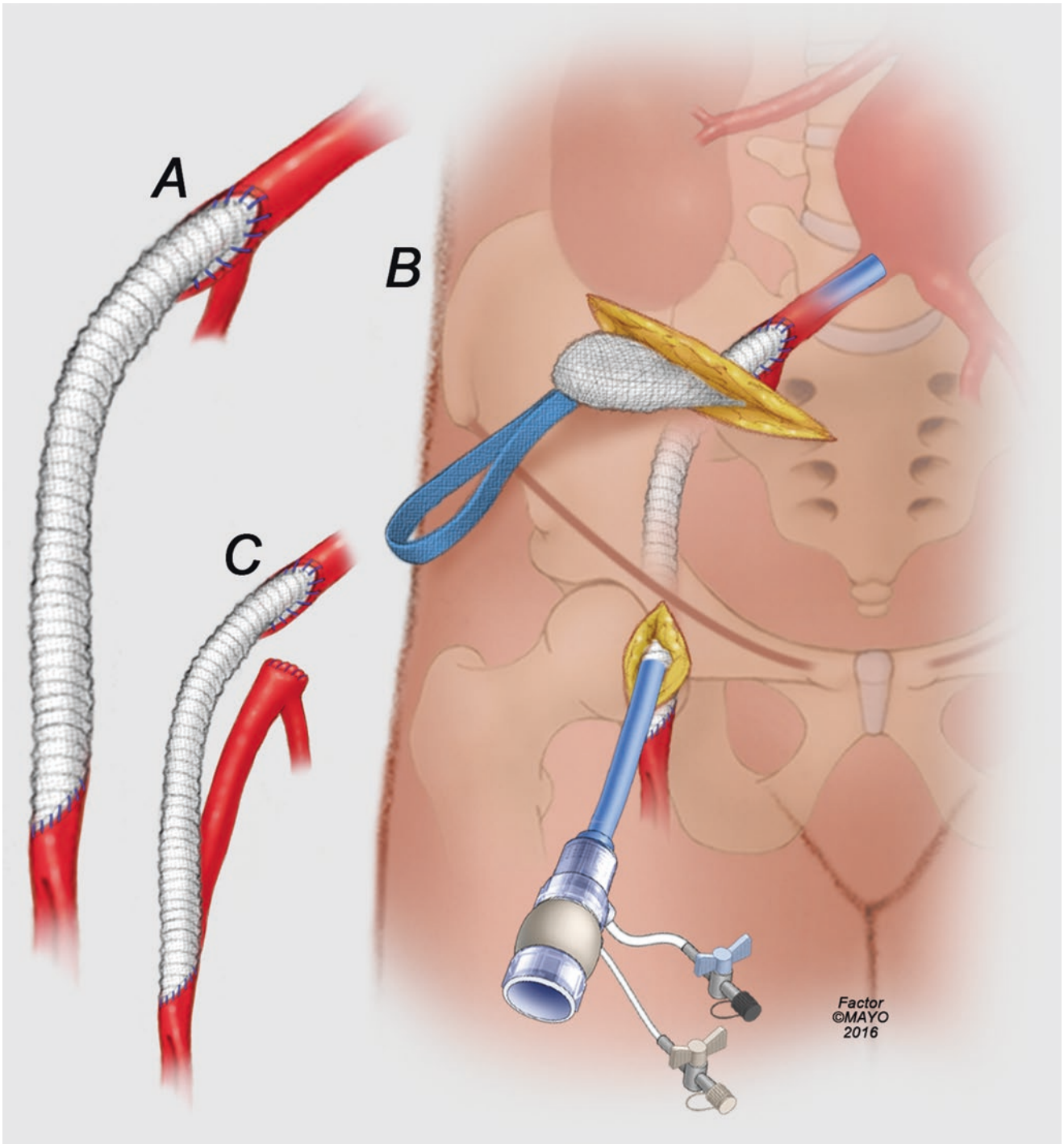


Fig. 23.7 Permanent open surgical conduits can be done using iliofemoral bypass from the distal common-proximal external iliac artery to the proximal common femoral artery (**a**). Access is established into the graft after flow is restored to the lower extremity (**b**). Alternatively the proximal anastomosis is done to the common iliac artery (**c**) while the internal iliac artery is perfused retrograde via the external iliac artery. By permission of Mayo Foundation for Medical Education and Research. All rights reserved

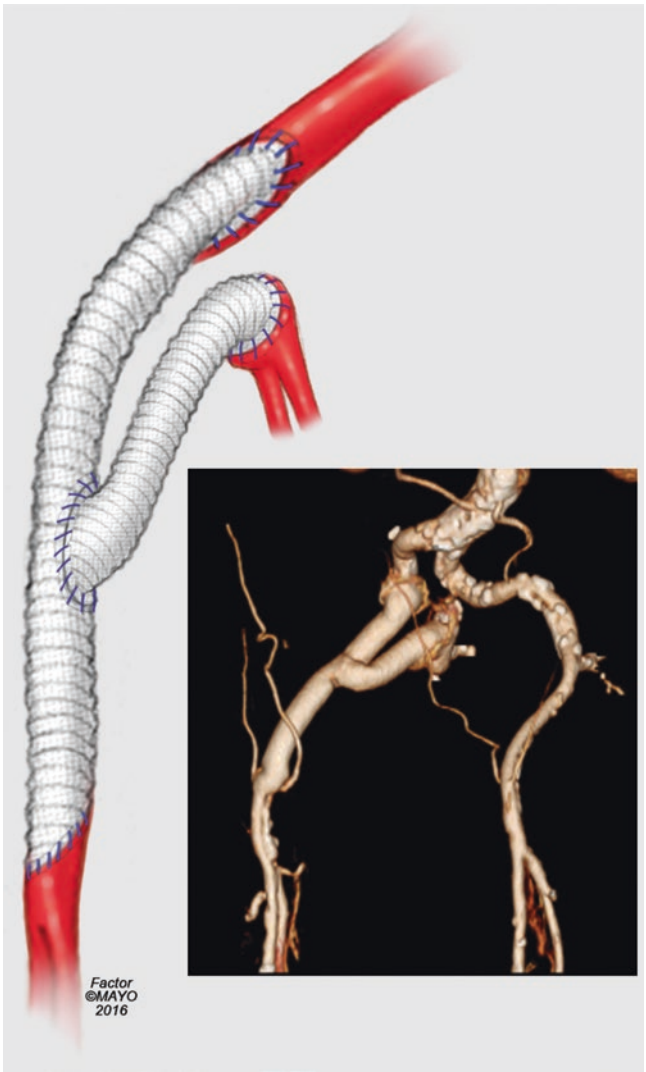


Fig. 23.8 Example of an iliofemoral bypass for conduit with revascularization of the internal iliac artery in a patient with unsuitable access vessels. By permission of Mayo Foundation for Medical Education and Research. All rights reserved

rhage because the stent fabric covers any tears or disruptions. Angioplasty with a 10-mm balloon allows for passage of sheaths up to 22 Fr, and a 12-mm balloon provides room for a 24 Fr sheath. It is important to pass the sheath slowly so that the stent is not dragged with the sheath. If an iliac conduit is going to be used in a patient with patent internal iliac artery (which we do not recommend), it is important to be mindful about the risk of ongoing hemorrhage from the internal iliac artery origin. In these cases it is optimal to coil embolization of the origin of the internal iliac artery prior to controlled arterial disruption. Stenting of iliac access vessels for occlusive lesions or small dissections should ideally be avoided prior to introducing a large diameter sheath, particularly stenting with balloon-expandable bare metal stents. The passage of the larger sheaths could inadvertently dislodge the stent or it may be practically impossible to advancing the sheath.

Axillary Artery Conduits

Complex endovascular procedures requiring multiple sheaths introduced via the axillary approach may benefit from a temporary axillary artery conduit (Fig. 23.10). This is often needed in patients treated by parallel stent-graft technique with more than two vessels accessed from above. The graft is accessed with multiple sheaths, which are advanced across the distal arch.

Conclusion

Complex endovascular aortic repair often requires devices with profile >20 Fr. Approximately 20 % of the patients need a conduit to avoid devastating vascular complications such as disruption, hemorrhage, or dissections. If the internal iliac artery is patent, an open surgical conduit is recommended. Endovascular conduits are preferred in patients with chronically occluded internal iliac arteries.

Suggested Reading

1. Abu-Ghaida AM, Clair DG, Greenberg RK, Srivastava S, O'Hara PJ, Ouriel K. Broadening the applicability of endovascular aneurysm repair: the use of iliac conduits. J Vasc Surg. 2002;36(1):111–7.
2. Lee WA, Berceli SA, Huber TS, Ozaki CK, Flynn TC, Seeger JM. Morbidity with retroperitoneal procedures during endovascular abdominal aortic aneurysm repair. J Vasc Surg. 2003;38(3):459–63. discussion 64–5.
3. May J, White G, Waugh R, Yu W, Harris J. Treatment of complex abdominal aortic aneurysms by a combination of endoluminal and extraluminal aortofemoral grafts. J Vasc Surg. 1994;19(5):924–33.
4. Mehta RH, Honeycutt E, Peterson ED, Granger CB, Halabi AR, Shaw LK, et al. Impact of internal mammary artery conduit on long-term outcomes after percutaneous intervention of saphenous vein graft. Circulation. 2006;114(1 Suppl):I396–401.
5. Oderich GS, Picada-Correa M, Pereira AA. Open surgical and endovascular conduits for difficult access during endovascular aortic aneurysm repair. Ann Vasc Surg. 2012;26(7):1022–9.
6. Peterson BG. Conduits and endoconduits, percutaneous access. J Vasc Surg. 2010;52(4 Suppl):60S–4.
7. Peterson BG, Matsumura JS. Internal endoconduit: an innovative technique to address unfavorable iliac artery anatomy encountered during thoracic endovascular aortic repair. J Vasc Surg. 2008;47(2):441–5.
8. Peterson BG, Matsumura JS. Tips and tricks for avoiding access problems when using large sheath endografts. J Vasc Surg. 2009;49(2):524–7.

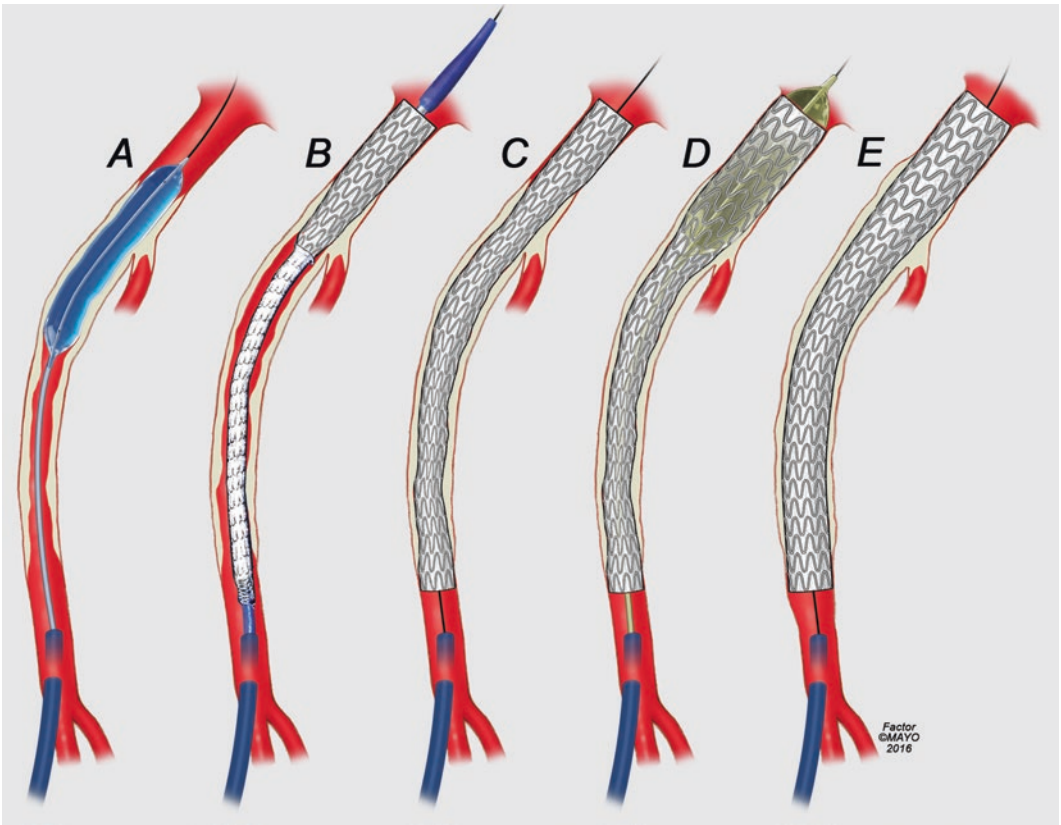


Fig. 23.9 Technique of endovascular conduit requires modest predilatation with angioplasty balloon (**a**), deployment of a Viabahn stent-graft (Gore, Flagstaff, AZ) from the common (**b**) to the external iliac artery (**c**) and post-dilatation (**d**). This is indicated in patients with chronically occluded internal iliac arteries (**e**). By permission of Mayo Foundation for Medical Education and Research. All rights reserved

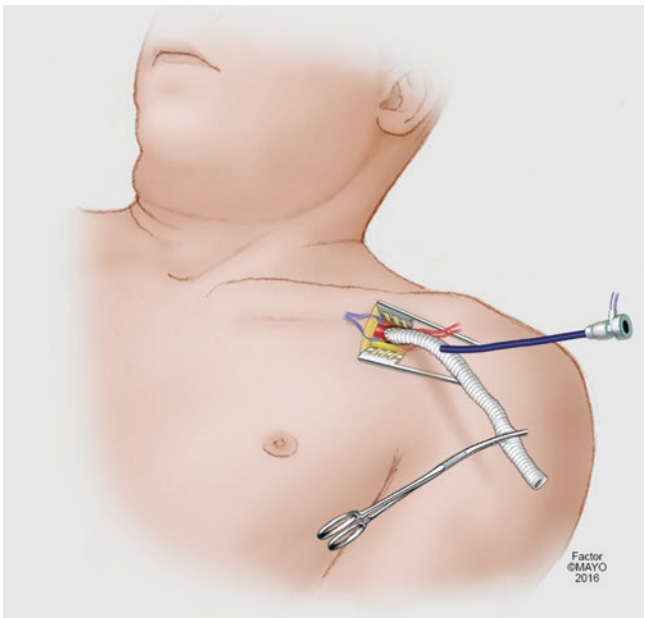


Fig. 23.10 Temporary axillary artery conduit. By permission of Mayo Foundation for Medical Education and Research. All rights reserved

9. van Bogerijen GH, Williams DM, Eliason JL, Dasika NL, Deeb GM, Patel HJ. Alternative access techniques with thoracic endovascular aortic repair, open iliac conduit versus endoconduit technique. J Vasc Surg. 2014;60(5):1168–76.
10. Yano OJ, Faries PL, Morrissey N, Teodorescu V, Hollier LH, Marin ML. Ancillary techniques to facilitate endovascular repair of aortic aneurysms. J Vasc Surg. 2001;34(1):69–75.
11. Hinchliffe RJ, Ivancev K, Sonesson B, Malina M. "Paving and cracking": an endovascular technique to facilitate the introduction of aortic stent-grafts through stenosed iliac arteries. J Endovasc Ther. 2007;14(5):630–3.
12. Carpenter JP. Delivery of endovascular grafts by direct sheath placement into the aorta or iliac arteries. Ann Vasc Surg. 2002;16(6):787–90.
13. Murray D, Ghosh J, Khwaja N, Murphy MO, Baguneid MS, Walker MG. Access for endovascular aneurysm repair. J Endovasc Ther. 2006;13(6):754–61.
14. Fearn SJ, Burke K, Hartley DE, Semmens JB, Lawrence-Brown MM. A laparoscopic access technique for endovascular procedures: surgeon training in an animal model. J Endovasc Ther. 2006;13(3):350–6.
15. Formichi M, Renier JF. A laparoscopic approach to the abdominal aorta for thoracic stent-graft deployment: evaluation in a porcine model. J Endovasc Ther. 2002;9(3):344–9.
16. Wu T, Carson JG, Skelly CL. Use of internal endoconduits as an adjunct to endovascular aneurysm repair in the setting of challenging aortoiliac anatomy. Ann Vasc Surg. 2010;24(1):114.e7–e11.

Part IV

Visceral Artery Incorporation

Current Device Designs to Incorporate Visceral Arteries

24

Bernardo C. Mendes and Gustavo S. Oderich

Introduction

Fenestrated and branched stent grafts were developed to address clinical need in patients with short landing zones or involvement of aortic side branches. The first prototypes were done by clinicians using on table modification of aortic stent grafts with the objective to fit the visceral anatomy of a patient [1]. Custom-made, patient-specific stent grafts were subsequently developed and serially produced by the industry, providing a standardized platform with multiple possibilities to fit a wide array of aortic and visceral vessel morphologies. Extensive clinical experience and analysis of anatomic studies provided a roadmap to the development of novel designs intended to be used off-the-shelf [2–4]. Since the initial use of fenestrated grafts by the Western Australia group, there has been over 15 years of clinical experience and refinements in endovascular technology. While some of the patient-specific designs are reaching its maturity with excellent clinical performance and large experiences worldwide, total endovascular repair is likely in its infancy; future developments on device profile, trackability are likely going to further increase suitability of endovascular procedures and minimize risk of complications. The purpose of this chapter is to describe the current state of the art in fenestrated and branched stent graft designs.

B.C. Mendes • G.S. Oderich (✉)
Division of Vascular and Endovascular Surgery, Mayo Clinic, 200 First Street SW, Rochester, MN 55905, USA
e-mail: mendes.bernardo@mayo.edu; oderich.gustavo@mayo.edu

Visceral Incorporation

Designs for visceral incorporation can be broadly categorized into patient-specific or "custom-made" devices (CMD) and off-the-shelf stent grafts (Table 24.1). The largest body of clinical experience is with the Cook patient-specific platform, which started in the late 1990s with pioneering work in Perth, Western Australia. These devices have been used worldwide and matured with refinements in stent configuration, material, profile, and delivery system. In the last 5 years, several other aortic stent graft manufacturers have expanded research and development to address the visceral segment of the aorta.

Patient-Specific Designs

Cook Zenith Fenestrated and Branched Stent Graft

The Cook Zenith Fenestrated (Cook Medical Inc, Bloomington, IN) stent graft has been used clinically since 1999, as summarized in Chapter 1. The device became available for commercial use in Europe in 2005. In the USA, the Food and Drug Administration (FDA) approved the Zenith Fenestrated device for treatment of patients with short-neck AAAs who do not meet the proposed anatomic criteria for use of standard infrarenal stent grafts and have an infrarenal neck length >4 and <15 mm [5]. The device consists of a proximal fenestrated component, a bifurcated universal component and a contralateral iliac limb extension (Fig. 24.1). The modules are constructed of full-thickness woven polyester fabric sewn to self-expanding stainless steel Cook-Z stents with braided polyester and polypropylene suture. The modules are fully stented. The FDA-approved version of the fenestrated component has a supra-graft bare stent and is custom-made to fit the patient's anatomy with up to three fenestrations, of which two can be of the same type. There

© Mayo Foundation for Medical Education and Research 2017

G.S. Oderich (ed.), *Endovascular Aortic Repair*, DOI 10.1007/978-3-319-15192-2_24

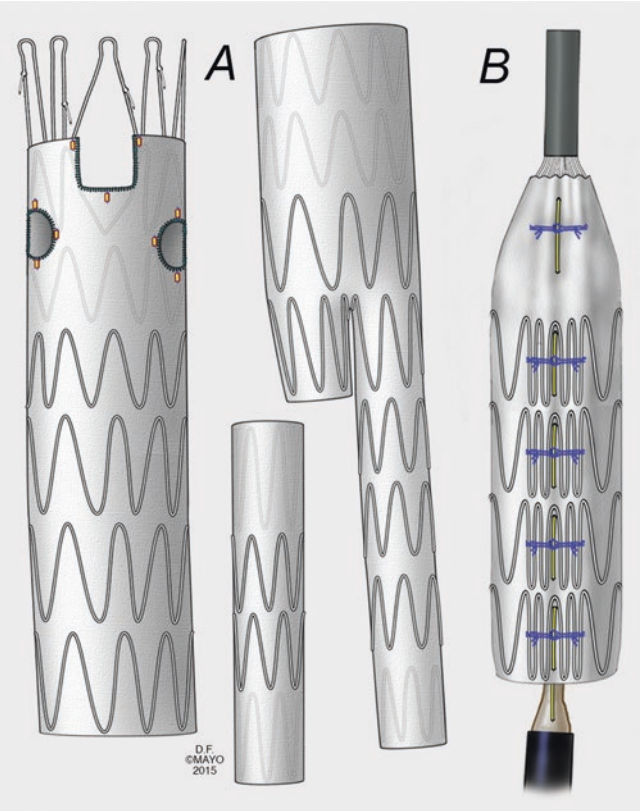


Fig. 24.1 The Cook Zenith fenestrated stent graft currently available in the USA includes a proximal fenestrated tubular component, a distal bifurcated device and iliac limb extensions. The device allows maximum of three fenestrations, two of the same type. The fenestrations include single-wide scallops, small, or large fenestrations and a distal bifurcated device and iliac limbs (**a**). The device has a diameter-reducing tie posteriorly, which constrains the diameter of the fenestrated component (**b**). By permission of Mayo Foundation for Medical Education and Research. All rights reserved

are three types of fenestrations that can be manufactured in the fenestrated component, including small, large, and scallop fenestrations (see Fig. 24.1). Small fenestrations have dimensions of 6×6 or 6×8 mm, do not have struts crossing the middle of the fenestration and are reinforced by a nitinol ring. These fenestrations can be fashioned >15 and <36 mm (for devices 24–32 mm) or <46 mm (for devices 34–36 mm) from the edge of the fabric. Large fenestrations are not reinforced by nitinol ring, measure 8–12 mm in diameter and can be fashioned >10 mm from the edge of the fabric. Large fenestrations have struts crossing at the edge or middle of the fenestration, which limits the ability to place alignment stents. Scallops are openings in the upper edge of the fabric, sized 10 mm wide by 6–12 mm in height.

The Zenith Fenestrated platform has different specifications in the rest of the world. These devices have been widely utilized in Europe, Canada, South America, and Asia, and in the USA through FDA-approved Investigational Device Exemption protocols. While the structure of the stent graft is the same as already described for the US Zenith fenestrated stent graft, including fabric and supporting stents, the limitations regarding number and type of fenestrations are inexistent. The physician can plan and order a stent with any number of fenestrations, which are uniformly reinforced and strut-free, in contrast with a large fenestration in the FDA approved version of the graft. In addition, directional down- or up-going branches can also be added to the structure if needed; these are more often external to the fabric of the main device, but can also be designed as internal branches based on preoperative planning (Fig. 24.2). The option of helical branches and internal branches the option of helical branches and internal branches is also available, with larger clinical experiences by Roy Greenberg and Marcelo Ferreira, respectively (see Fig. 24.2). Finally, these devices have several adjuncts such as tapering of the main body, diameter reducing wires, preloaded wires, or catheters that can be planned to facilitate target vessel cannulation (Fig. 24.3). For patients with short distance between the renal arteries and the aortic bifurcation due to prior endograft or aortoiliac graft, an inverted limb bifurcated device has been designed (Fig. 24.4).

Vascutek Fenestrated Anaconda Endograft

The Fenestrated Anaconda Endograft (Vascutek, Renfrewshire, Scotland) is a trimodular, patient-specific stent graft based on the Anaconda AAA endograft system, which is a three-piece device made of multiple element nitinol stents combined with woven polyester graft material (Fig. 24.5). Also similar to the standard Anaconda AAA system, the top of the Fenestrated device consists of a dual-ring stent design with two to four fixation nitinol hooks, an unsupported graft body in which the nitinol-reinforced fenestrations are contained, and a distal ringed stent. Currently available designs allow up to four fenestrations and can have an "augmented valley" which would compare to a scallop. The fenestrations are located in the unsupported region to maximize the available contact area of the fenestration with the target vessel, in order to facilitate cannulation and minimize planning errors or fenestration–target vessel misalignment. The device is introduced through a 20–23 French delivery system, depending on the diameter; importantly, the deployment system does not have a top cap, which in theory facilitates cannulation of fenestrations via brachial approach. The Fenestrated Anaconda Endograft can be repositioned after full deployment [6].

Table 24.1 Specifications of current designs for visceral artery incorporation using fenestrated and branched endografts

Device	Diameter (mm)	Profile (French)	Length main component (mm)	Off-the-shelf	Graft fabric	Stent material	Number of fenestrations	Scallop	Number of branches
Cook Zenith Fenestrated (USA)	24–36	20–22	97–124	No	Polyester	Stainless steel	0–3	Possible	0
Cook Zenith Fenestrated	b	18 (LP) 22	X	No	Polyester	Stainless steel	Unlimited	Possible	Unlimited
Cook p-Branch	26–36	20	146–151	Yes	Polyester	Stainless steel	3	1	0
Cook t-Branch	34 Tapered to 18	22	202	Yes	Polyester	Stainless steel	0	0	4
WL Gore TAMBE	26–37 Tapered to 20	22	215	Yes	ePTFE	Nitinol	0	0	4
Endologix Ventana	24–36 mm tapered to 28 mm	22	120 and 140 mm	Yes	ePTFE	Cobalt chromium alloy	2	1	0
Vascutek Anacondaa	X-34	20–23	B	No	Polyester	Nitinol	1–4	Possible	0
Jotec E-Xtra Multibranch	24–40 mm	22–24 mm	50–215 mm	No	Polyester	Nitinol	Unlimited	Possible	Unlimited

aCurrently unavailable

Jotec Extra Design Multibranch Stent Graft

The JOTEC E-Xtra Design Engineering Multibranch Stent Graft (Jotec, Hechingen, Germany) is a patient-specific multibranch stent graft based on the E-Vita thoracic 3G stent graft (Fig. 24.6). The main body is tubular with individual nitinol z-stents sewn to a woven polyester fabric. A proximal stent ring is uncovered. The design allows for branches, scallops, and/or reinforced fenestrations; these are preferentially incorporated into a mid-portion of the stent which has a tapered diameter of 16 mm. Branches can have a diameter of 6–10 mm, and can be upward or downward directed, external or internal in the graft; fenestrations diameters are 6–12 mm [7].

Off-the-Shelf Designs

Cook p-Branch

The Cook p-Branch® stent graft is an off-the-shelf modular system with 26–36 mm in diameter. The main component is a tubular device composed of polyethylene terephthalate fabric that has a proximal stainless steel uncovered barbed supraceliac stent, followed by nitinol z-stents with one scallop for the celiac axis, one fixed 8-mm strut-free fenestration for the SMA, and two conical renal artery pivot fenestrations (Fig. 24.7). These pivot fenestrations have an outer diameter of 15 mm and inner diameter of 6 mm, and confer the theoretical ability to catheterize renal arteries within the outer 15 mm diameter range while keeping the inner 6 mm fenestration to provide bridging stent seal. Preloaded wires are present in both renal pivot fenestrations. Immediately distal to the renal fenestrations, a tapered bridging stent reduces the diameter of the device to 24 mm to facilitate mating with a universal distal bifurcated body. A diameter constraining wire is present. Two different renal configurations are available, one with both fenestrations arising at the same longitudinal position (*configuration A*) and one with the left renal artery (LRA) fenestration 4 mm caudal to the right renal artery (RRA) fenestration (*configuration B*). The device is deployed through a 20-French system [3, 8].

Cook t-Branch

The Cook t-Branch stent graft consists of a tapered woven polyester stent graft sutured to a Z-stent stainless steel exoskeleton (Fig. 24.8). The mid-portion of the device contains four short axially oriented, caudally directed cuffs for attachment of covered stents which will be the branches for visceral vessel incorporation. The cuffs are situated in the external surface of the stent graft and located longitudinally 18 mm apart. The device has a diameter of 34-mm at the top and 18-mm at the bottom, with a length of 202 mm. Celiac and superior mesenteric artery cuffs are 8 mm in diameter, 21 and 18 mm in length, and are axially located in the 01:00 and 12:00 positions, respectively. Right and left renal artery cuffs are 6 mm in diameter, 18 mm in length, and located in the 10:00 and 03:00 positions, respectively. The device is delivered through a 22-French system. No preloaded wires or catheters are present in the off-the-shelf t-Branch stent graft [9].

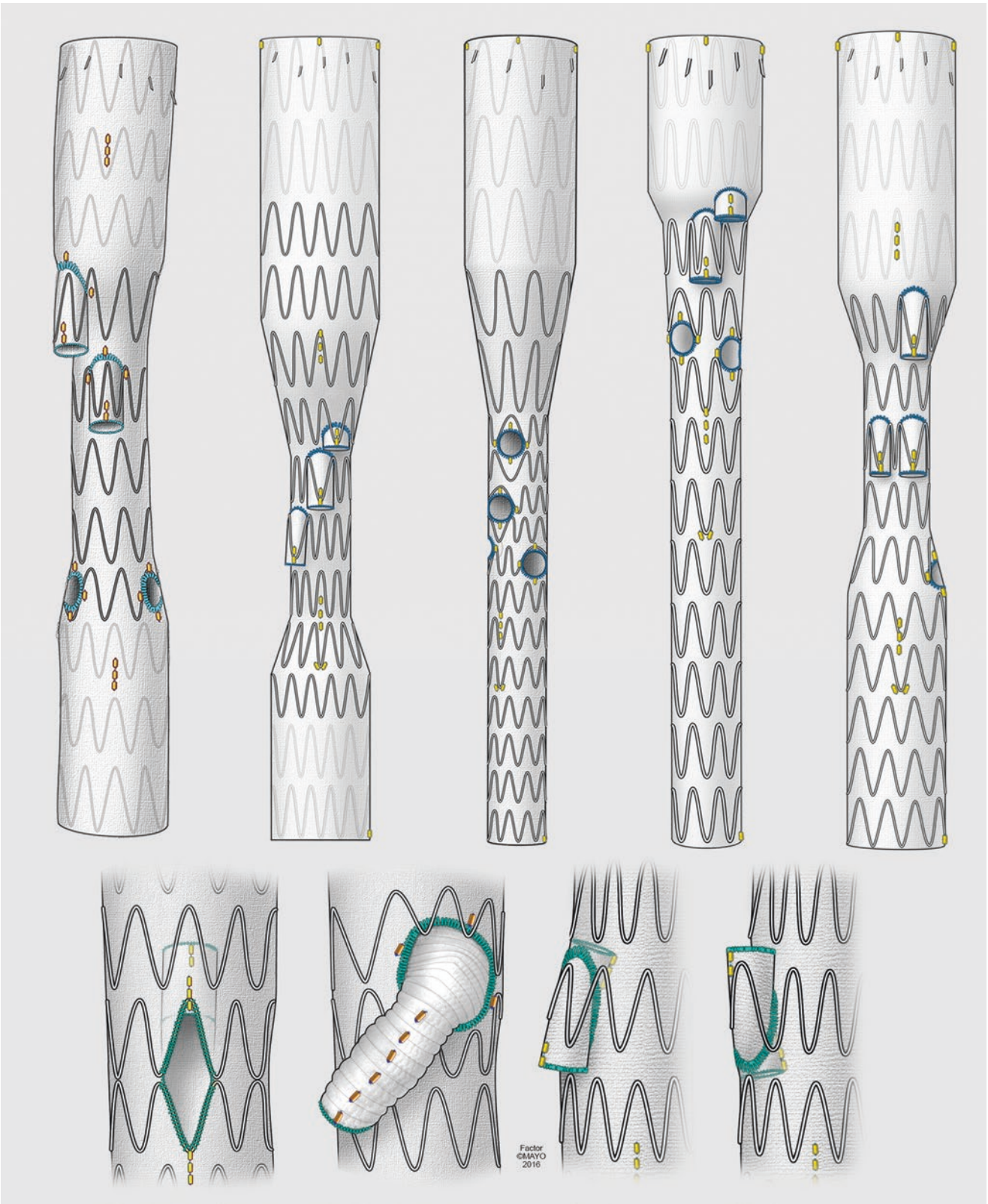


Fig. 24.2 Patient-specific thoracoabdominal devices can be manufactured with any combination of fenestrations or branches, with no limit in the number of vessels that can be incorporated. Devices can be designed with four fenestrations, combinations of fenestrations and branches or only branches. In addition to the fenestrations already described in Fig. 24.1, branches can be straight (down-going or up-going), helical, external or internal. Novel development of internal branch with diamond-shaped fenestration is also available. By permission of Mayo Foundation for Medical Education and Research. All rights reserved

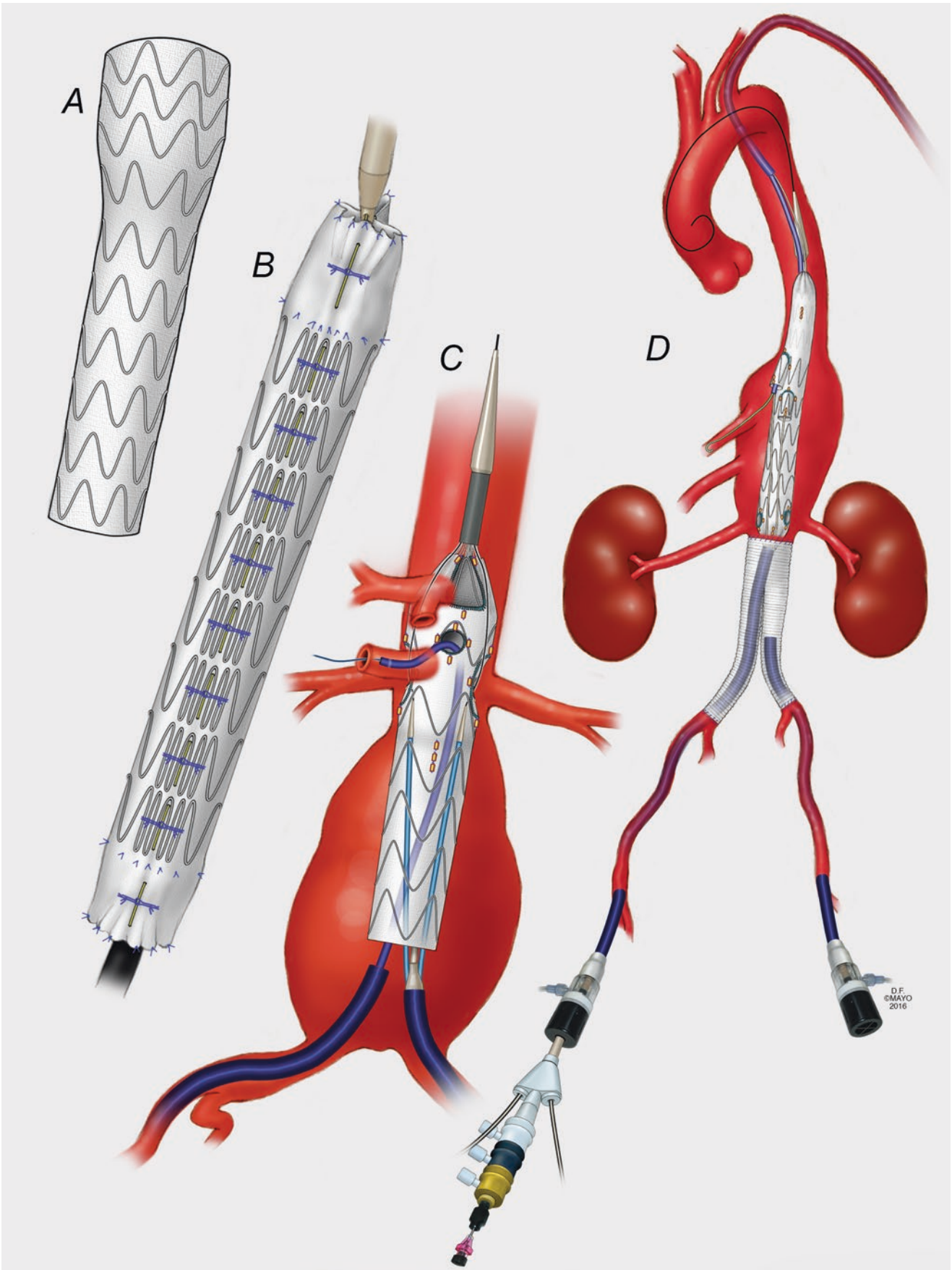


Fig. 24.3 Adjuncts to facilitate the procedure include tapered segments into the device (**a**), diameter-reducing ties (single or double, **b**), preloaded catheters (**c**) and preloaded guide-wires (**d**). By permission of Mayo Foundation for Medical Education and Research. All rights reserved

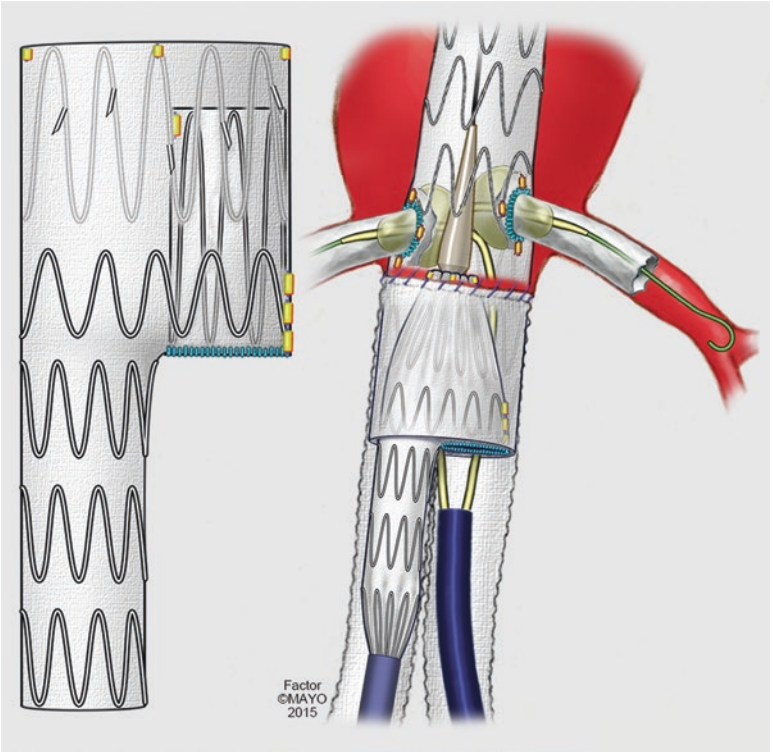


Fig. 24.4 Bifurcated device with inverted iliac limb (**a**) can be used in patients with short length between the renal arteries and the aortic bifurcation (**b**). By permission of Mayo Foundation for Medical Education and Research. All rights reserved

Endologix Ventana

The Endologix Ventana (Endologix Inc, Irvine, CA) stent graft design has a tubular component with self-expanding cobalt chromium alloy endostent and a multilayer expanded polytetrafluoroethylene (ePTFE) graft (Fig. 24.9). The fabric is attached to the stent proximally and distally using nonabsorbable surgical suture; this incorporates an oversized midsection with two fenestrations. There is no stent adjacent to the fenestrations. A large proximal scallop with 4 cm length is intended to incorporate both celiac and superior mesenteric arteries. The available proximal diameters would be able to treat aortic diameters from 18 to 34 mm, with a fixed 28 mm distal diameter. The renal artery fenestrations are movable in situ longitudinally (±30 mm) and circumferentially (90–210°) due to the oversized midsection of the graft fabric; these can be expanded from their nominal 3 mm diameter to 10 mm [3, 10, 11]. The device is delivered through a 22-French system with preloaded guide sheaths for both renal arteries. The Ventana system was planned to receive only the Xpand device (Endologix) as target vessel bridging stent. The US Ventana Pivotal trial was discontinued by the company and the device is currently not available for clinical use.

WL Gore Thoracoabdominal Branched Endoprosthesis (TAMBE)

The GORE® EXCLUDER® Thoracoabdominal Branch Endoprosthesis (WL Gore, Flagstaff, AZ) is an off-the-shelf, modular, multicomponent system composed of a proximal multibranched aortic component, a distal bifurcated component and iliac limb extensions (Fig. 24.10). The TAMBE has been designed with either retrograde or antegrade renal portals. Device dimensions include a proximal diameter of 26, 31, and 37 mm, length of 215 mm, and distal diameter of 20 mm. An alternative option is also available with four antegrade portals, with proximal diameters of 31 and 37 mm, length of 160 mm, and distal diameter of 20 mm. Both options require a 22Fr trans-femoral introducer for the aortic device (with the exception of the 31 mm antegrade configuration, which is 20 Fr) and a 12 Fr brachial or axillary artery introducer for access into the antegrade portals. The aortic component allows for placement of through-and-through preloaded guide-wires. To facilitate placement of the guide-wires and prevent guide-wire wrapping within the aorta, a specially designed triple-lumen catheter is inserted from the brachial approach and exteriorized via the femoral access.

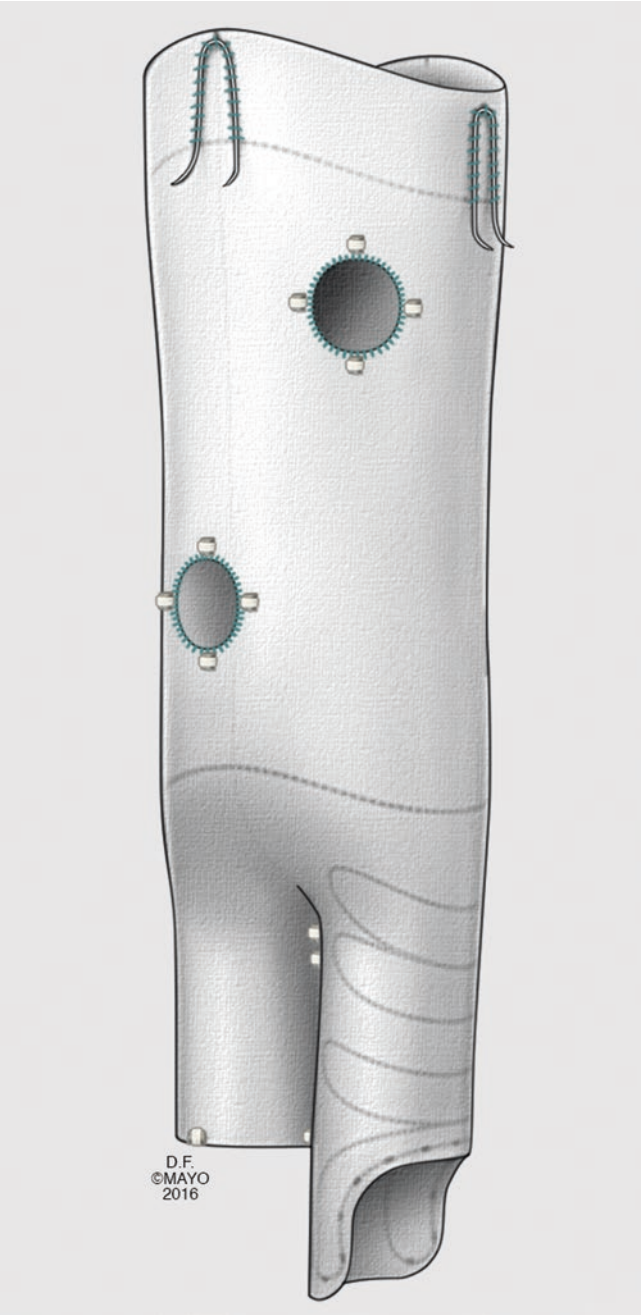


Fig. 24.5 Illustration of the Vascutek fenestrated Anaconda endograft. By permission of Mayo Foundation for Medical Education and Research. All rights reserved

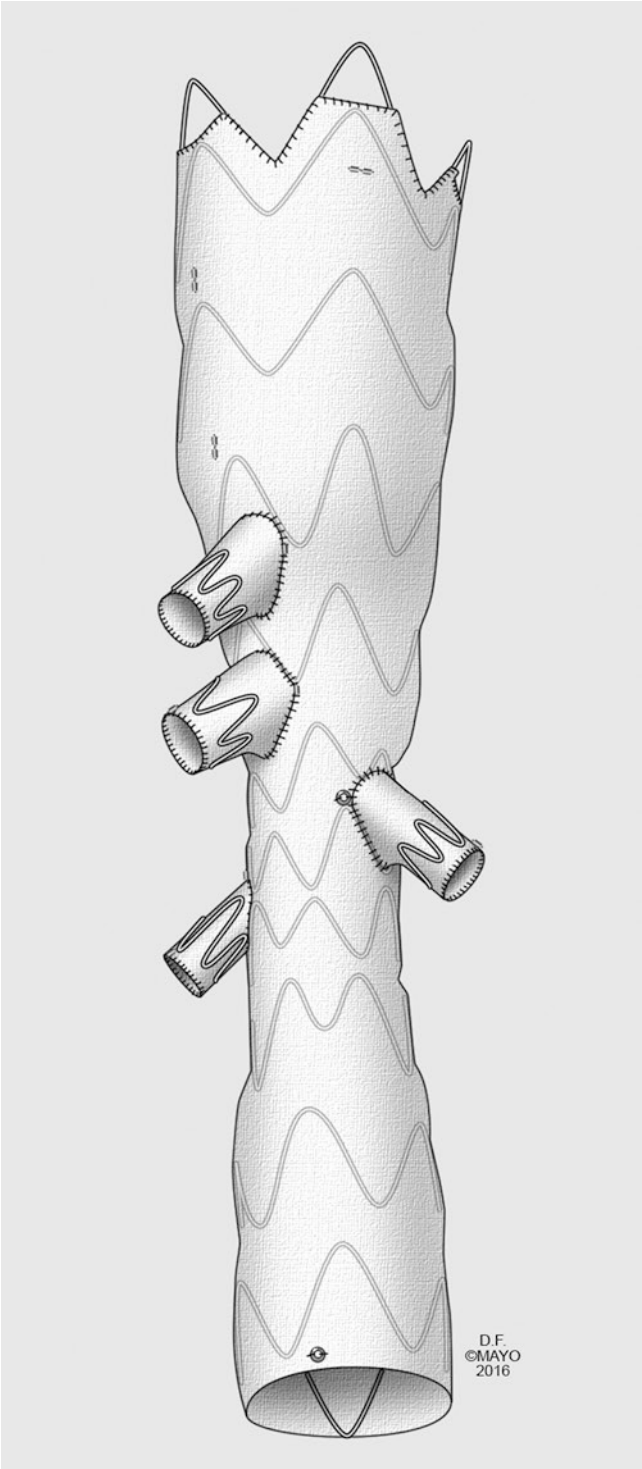


Fig. 24.6 Illustration of the Jotec Extra Design Multibranch Stent Graft. By permission of Mayo Foundation for Medical Education and Research. All rights reserved

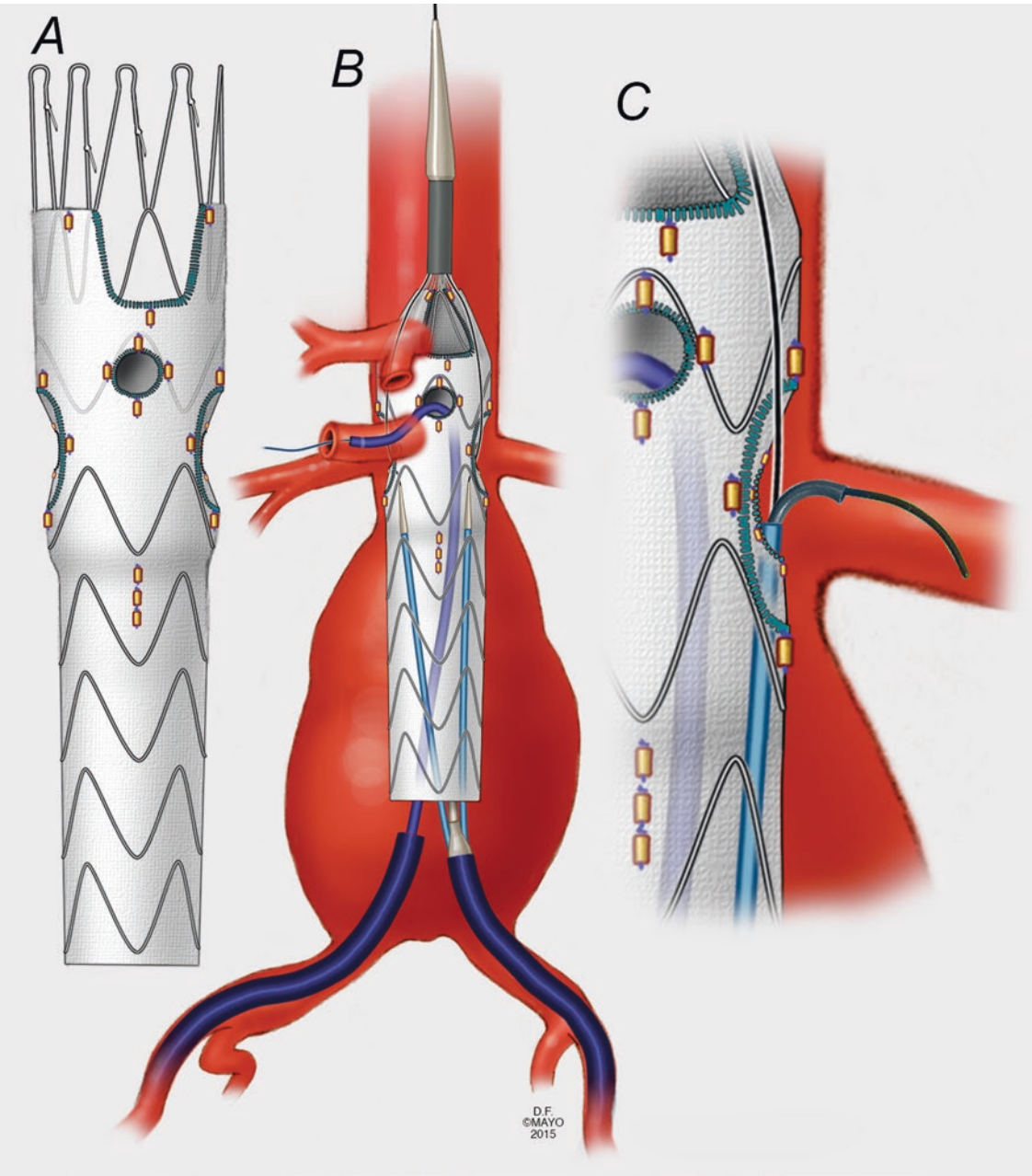


Fig. 24.7 Cook p-Branch stent graft includes a proximal fenestrated component with a doublewide scallop for the celiac axis, large fenestration for the SMA, and pivot fenestrations for the renal arteries (**a**). The device has preloaded guide-wires into the renal fenestrations with a modified delivery system (**b**), allowing immediate access into the renal fenestrations (**c**). By permission of Mayo Foundation for Medical Education and Research. All rights reserved

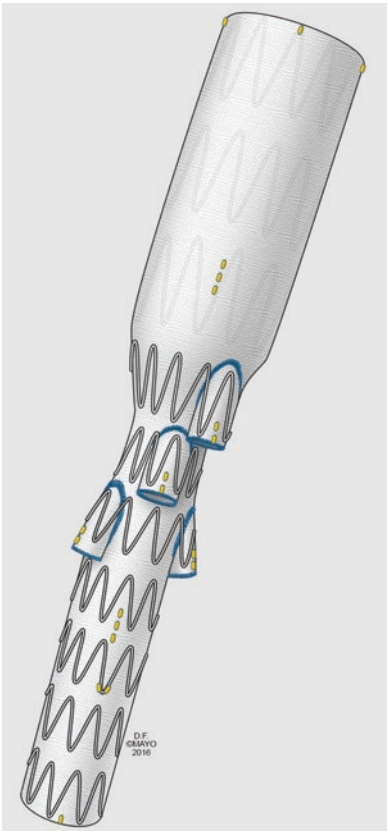


Fig. 24.8 Cook t-branch stent graft has four down-going straight branches for the celiac axis, SMA and both renal arteries. By permission of Mayo Foundation for Medical Education and Research. All rights reserved

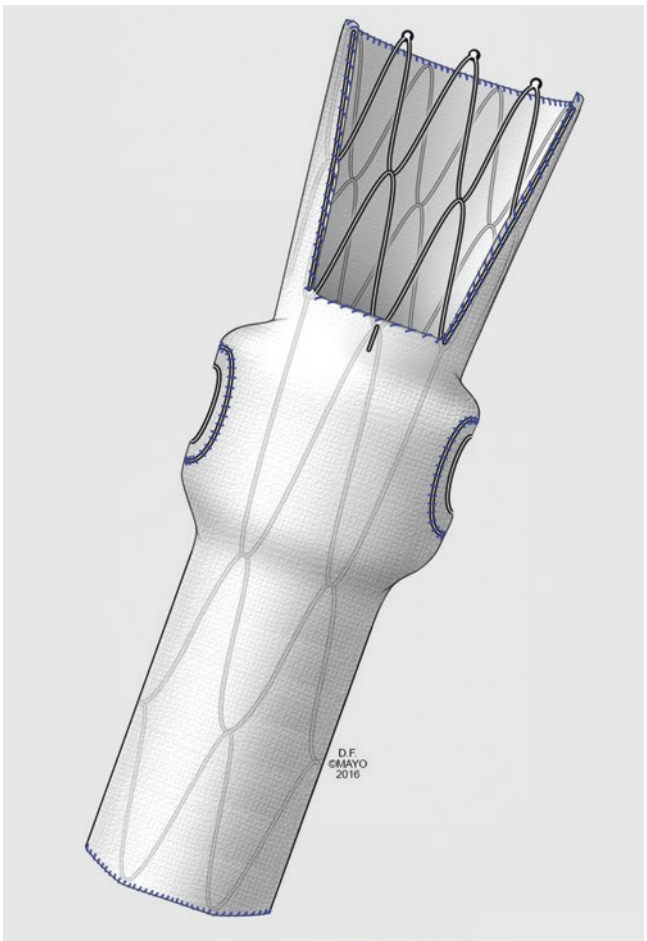


Fig. 24.9 Endologix Ventana is fenestrated stent graft is illustrated for historical purposes since its investigation has been discontinued. The original device had a large scallop for SMA and celiac and movable renal fenestrations. By permission of Mayo Foundation for Medical Education and Research. All rights reserved

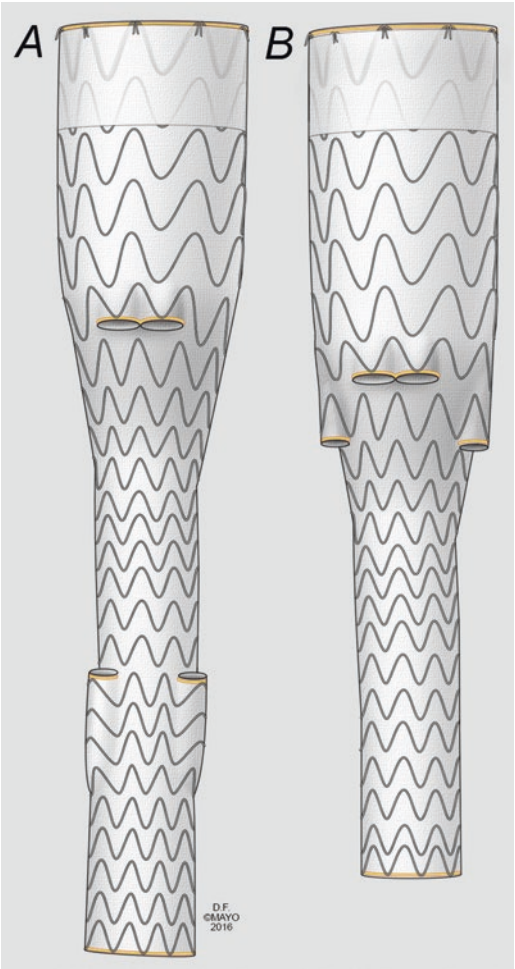


Fig. 24.10 The Gore Excluder Thoracoabdominal Multibranch Endoprosthesis (TAMBE) has four portals with options of either retrograde renal portals (**a**) or antegrade renal portals (**b**). By permission of Mayo Foundation for Medical Education and Research. All rights reserved

References

1. Anderson JL, Berce M, Hartley DE. Endoluminal aortic grafting with renal and superior mesenteric artery incorporation by graft fenestration. J Endovasc Ther. 2001;8(1):3–15.
2. Chuter T, Greenberg RK. Standardized off-the-shelf components for multibranched endovascular repair of thoracoabdominal aortic aneurysms. Perspect Vasc Surg Endovasc Ther. 2011;23(3):195–201.
3. Mendes BC, Oderich GS, Macedo TA, Pereira AA, Cha S, Duncan AA, et al. Anatomic feasibility of off-the-shelf fenestrated stent grafts to treat juxtarenal and pararenal abdominal aortic aneurysms. J Vasc Surg. 2014;60(4):839–47. discussion 847-8.
4. Sobocinski J, d'Utra G, O'Brien N, Midulla M, Maurel B, Guillou M, et al. Off-the-shelf fenestrated endografts: a realistic option for more than 70% of patients with juxtarenal aneurysms. J Endovasc Ther. 2012;19(2):165–72.
5. Oderich GS, Greenberg RK, Farber M, Lyden S, Sanchez L, Fairman R, et al. Results of the United States multicenter prospective study evaluating the Zenith fenestrated endovascular graft for treatment of juxtarenal abdominal aortic aneurysms. J Vasc Surg. 2014;60(6):1420-8.e1–5.
6. Dijkstra ML, Tielliu IFJ, Meerwaldt R, Pierie M, van Brussel J, Schurink GWH, et al. Dutch experience with the fenestrated Anaconda endograft for short-neck infrarenal and juxtarenal abdominal aortic aneurysm repair. J Vasc Surg. 2014;60(2):301–7.
7. Kinstner C, Teufelsbauer H, Neumayer C, Domenig C, Wressnegger A, Wolf F, et al. Endovascular repair of thoracoabdominal aortic aneurysms with a novel multibranch stent-graft design: preliminary experience. J Cardiovasc Surg. 2014;55(4):543–50.
8. Kitagawa A, Greenberg RK, Eagleton MJ, Mastracci TM. Zenith p-branch standard fenestrated endovascular graft for juxtarenal abdominal aortic aneurysms. J Vasc Surg. 2013;58(2):291–300.
9. Chuter TAM, Hiramoto JS, Park KH, Reilly LM. The transition from custom-made to standardized multibranched thoracoabdominal aortic stent grafts. J Vasc Surg. 2011;54(3):660–8.
10. Quinones-Baldrich WJ, Holden A, Mertens R, Thompson MM, Sawchuk AP, Becquemin JP, et al. Prospective, multicenter experience with the Ventana Fenestrated System for juxtarenal and pararenal aortic aneurysm endovascular repair. J Vasc Surg. 2013;58(1):1–9.
11. Mertens R, Bergoeing M, Marine L, Valdes F, Kramer A, Vergara J. Ventana fenestrated stent-graft system for endovascular repair of juxtarenal aortic aneurysms. J Endovasc Ther. 2012;19(2):173–8.

Selection of Optimal Bridging Stents for Fenestrations and Branches

25

Bernardo C. Mendes and Gustavo S. Oderich

Introduction

Fenestrated and branched stent grafts can successfully treat complex aortic aneurysms when used in combination with appropriately sized and precisely deployed bridging stents. All vessels targeted by fenestrations or branches should be aligned by stents to optimize branch perfusion and aneurysm seal. The first fenestrated grafts implanted in Western Australia were not always aligned by stents [1]. Since the early reports, it became clear that vessel shuttering by the fenestration led to occlusion in a few cases. It became routine to align all fenestrations, which initially was done using the available bare metal stents. At the time, wall-grafts (Boston Scientific, Bloomington, MN) were the only commercially available self-expandable stent graft, and were used in the first cases of branched endografts reported by Tim Chuter [2–4]. Nevertheless, as technology has evolved and the spectrum of treated aortic pathology became more extensive, the use of covered stents and stent grafts became routine and is currently the standard of care for all fenestrations and branches [5, 6]. Multiple options are currently available, including balloon-expandable and self-expandable stent grafts designed by different manufacturers encompassing diverse diameter, lengths, and deployment strategies. These stents are often coupled together to optimize the desired characteristics and fit the anatomic conditions of the patient. The purpose of this chapter is to describe currently available stents for bridging of target visceral vessels during endovascular aneurysm repair with fenestrated and branched stent grafts (F/BEVAR).

B.C. Mendes • G.S. Oderich (✉)
Division of Vascular and Endovascular Surgery, Mayo Clinic, 200 First Street SW, Rochester, MN 55905, USA
e-mail: mendes.bernardo@mayo.edu; oderich.gustavo@mayo.edu

The Ideal Stent

The ideal stent is currently not available. Therefore, a combination of multiple stents is often needed to meet the desired characteristics of the ideal stent. A limitation of this technique is the added cost and the multiple exchanges that are needed to complete each branch. As a general rule, balloon-expandable covered stents are used for fenestrations and self-expandable stent grafts are selected for branches. With the introduction of the Viabahn Balloon Expandable Covered Stent (VBX), this paradigm is changing because of excellent flexibility that adapts well to tortuous anatomy.

Designing the ideal stent may not even be possible, but endovascular technology and nanotechnology are evolving fast, so it may be possible in the next years. Profile should be small and yet allow it to be introduced using 0.035-in. system, unless 0.014–0.018 guide-wires can be manufactured with similar strength characteristics as 0.035-in. guide-wires. The sheath should be 6Fr or 7Fr. The stent needs to combine multiple characteristics (Fig. 25.1), including high radial force in the proximal segment where it is attached to the fenestration or cuff (Fig. 25.2). The stent would completely flare against the fabric of the aortic graft, creating a watertight seal. The mid-segment would be covered yet highly flexible, except for the distal 5–10 mm where it attaches into the branch. The very distal segment would again be flexible, kink resistant. The bare portion would need a material that is resistant to inducing intimal hyperplasia. And the covered material would also be resistant to thrombus formation by having antiplatelet and antithrombotic effect. Needless to say, we do not have such a stent and therefore combine what is available commercially to achieve the same effect [7].

Balloon-Expandable Stents

There are at least six balloon-expandable covered stents that have been or could be utilized clinically for fenestrations and branches: Abbot Vascular GraftMaster RX stent, Abbot Jotec

© Mayo Foundation for Medical Education and Research 2017

G.S. Oderich (ed.), *Endovascular Aortic Repair*, DOI 10.1007/978-3-319-15192-2_25

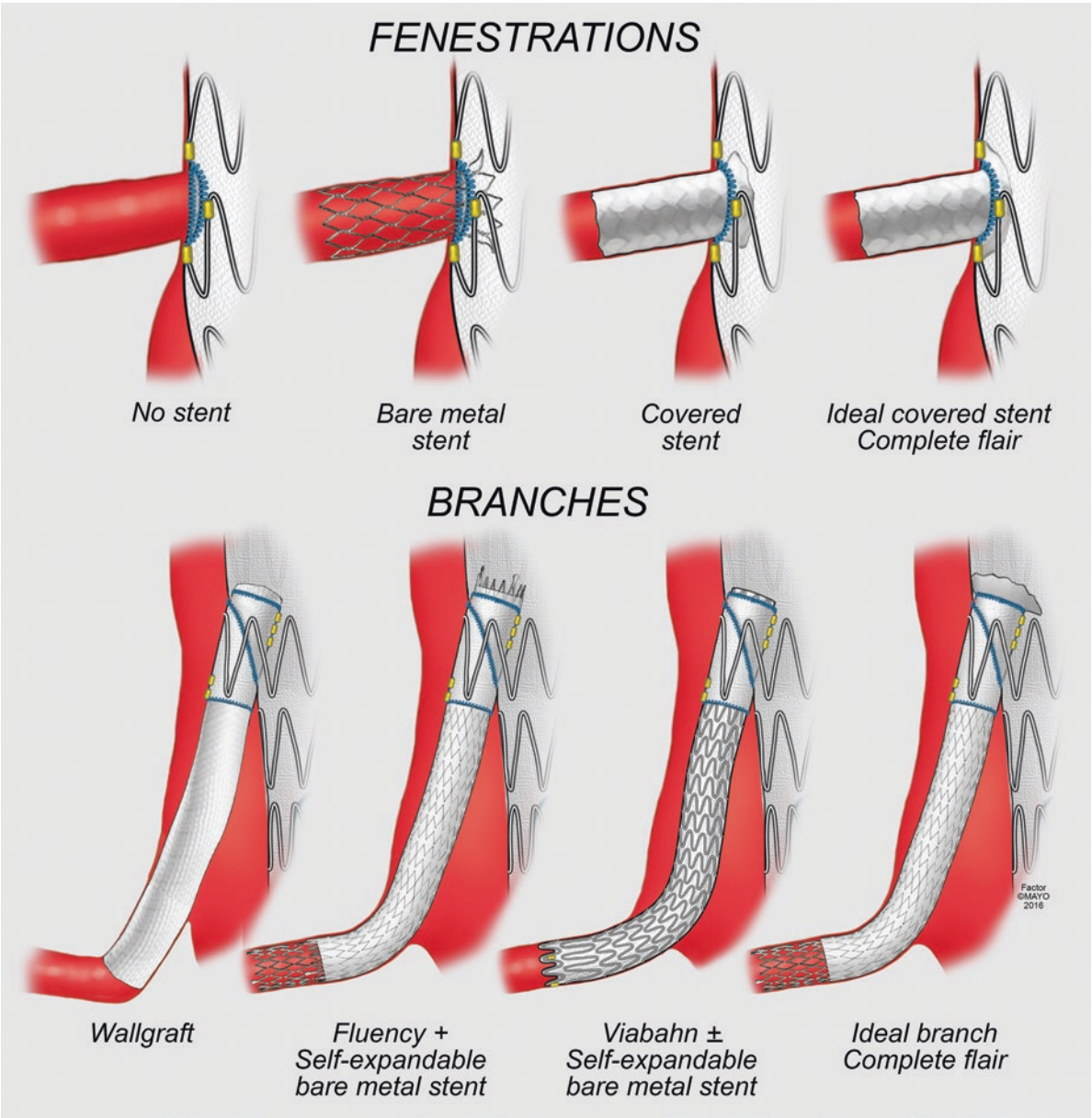


Fig. 25.1 Types of alignment and bridging stents for fenestrations and branches. By permission of Mayo Foundation for Medical Education and Research. All rights reserved

Covered Stent, InSitu Coronary Direct-Stent, Maquet Atrium iCAST or V12 stent, Bentley BeGraft, and Viabahn VBX stents. Of these, the largest worldwide experience has been accumulated using the iCAST or V12 stent, and more recently using the Bentley BeGraft and the Viabahn VBX stents.

Maquet Atrium iCast or V12 Covered Stent

The Maquet Atrium iCast or V12 covered stent (Maquet, Wayne, NJ) is a balloon-expandable covered stent which has been originally approved by the US Food and Drug Administration (FDA) for treatment of tracheobronchial strictures, but has been increasingly used in arterial beds [8, 9]. The stent structure is made of 316L stainless steel, which is encapsulated based on *Atrium's film-cast encapsulation technology* with two layers of polytetrafluoroethylene (PTFE) with a porosity of 100–120 μm (Fig. 25.3). The inner layer prevents the stent struts from contacting the luminal wall. The system is mounted on a noncompliant balloon catheter and has gold markers in the ends of the balloon. Available diameters in the USA range from 5 to 10 mm, with stent lengths of 16–59 mm

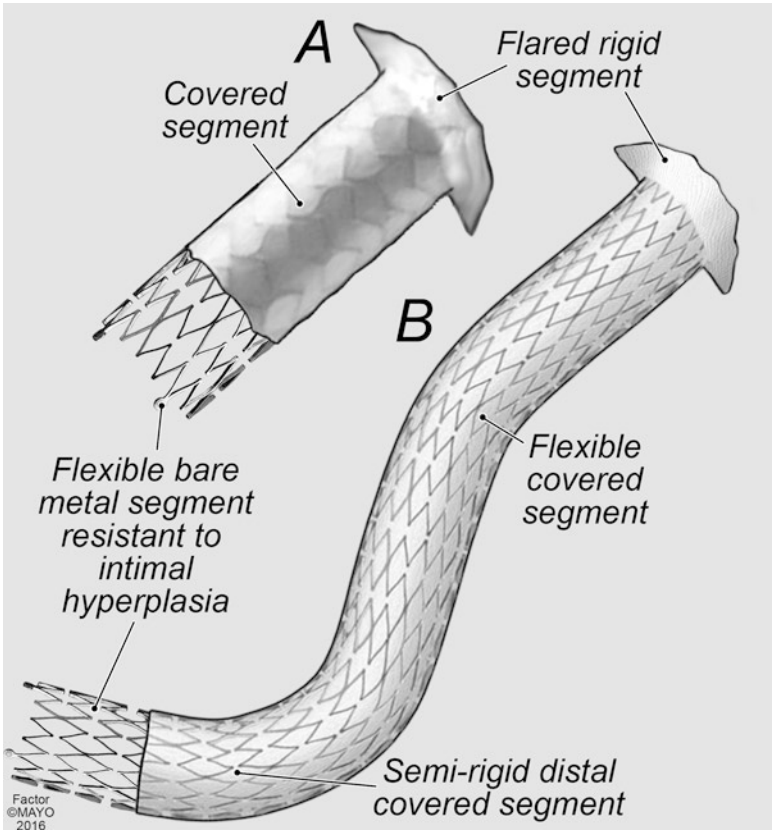


Fig. 25.2 Ideal configuration of alignment stent for fenestrations (**a**) and bridging stent for directional branches (**b**) would combine different radial force, flared and bare metal stents. By permission of Mayo Foundation for Medical Education and Research. All rights reserved

and balloon shafts of 80 and 120 cm, with a 5-French outer diameter. All iCast stents are 0.035″ guide-wire compatible and should be delivered through a 6- or 7-French introducer sheath. In the European market, a 0.018 option is available but this has not been widely used for fenestrations and therefore durability has not been tested for this indication. In addition to its ability to provide a seal as a bridging stent during F/BEVAR, the iCast covered stent has increasingly been used for treatment of atherosclerotic arterial occlusive disease in the mesenteric, brachiocephalic and aortoiliac territories, with encouraging clinical results [8, 9]. The iCast covered stent has the advantages of a precise deployment typical of balloon-expandable stents, excellent radial force and extremely uncommon stent fractures; nevertheless, it lacks flexibility and diameter/length versatility.

WL Gore Balloon-Expandable Viabahn (VBX)

The WL Gore balloon-expandable Viabahn VBX stent graft (WL Gore, Flagstaff, AZ) was designed specifically to be used as the bridging stent for the Gore Thoracoabdominal Branched Endoprosthesis (TAMBE). It has similar characteristics to the standard self-expandable Viabahn stent graft, with a reinforced ePTFE liner attached to an external nitinol stent structure and a heparin-bonded bioactive surface (Fig. 25.4). Information regarding lengths and diameters is still limited due to the investigational nature of this device, however it is known that its profile will be relatively low (7–8 French) compared to currently available self-expandable stent grafts. Based on preliminary clinical experience, the advantages of the VBX are the radial force, precise deployment of a balloon-expandable stent and flexibility comparable to a self-expandable stent. The unique feature of extreme ability to overtake tortuous anatomy is most appealing for use in branches and is likely to be incorporated as a stent of choice for any type of branch endograft (Fig. 25.5). However, long-term durability is not available for the TAMBE nor for other devices, and therefore clinical experience should be carefully analyzed until it is widely utilized.

Bentley BeGraft Stent

The Bentley BeGraft stent (Bentley, Hechingen, Germany) is commercially available in Europe and the UK and has been already used clinically during fenestrated and branched endografts (Fig. 25.6). Clinical data is lacking on specific device durability for this indication. The stent is a 0.035-in. balloon-expandable covered stent with

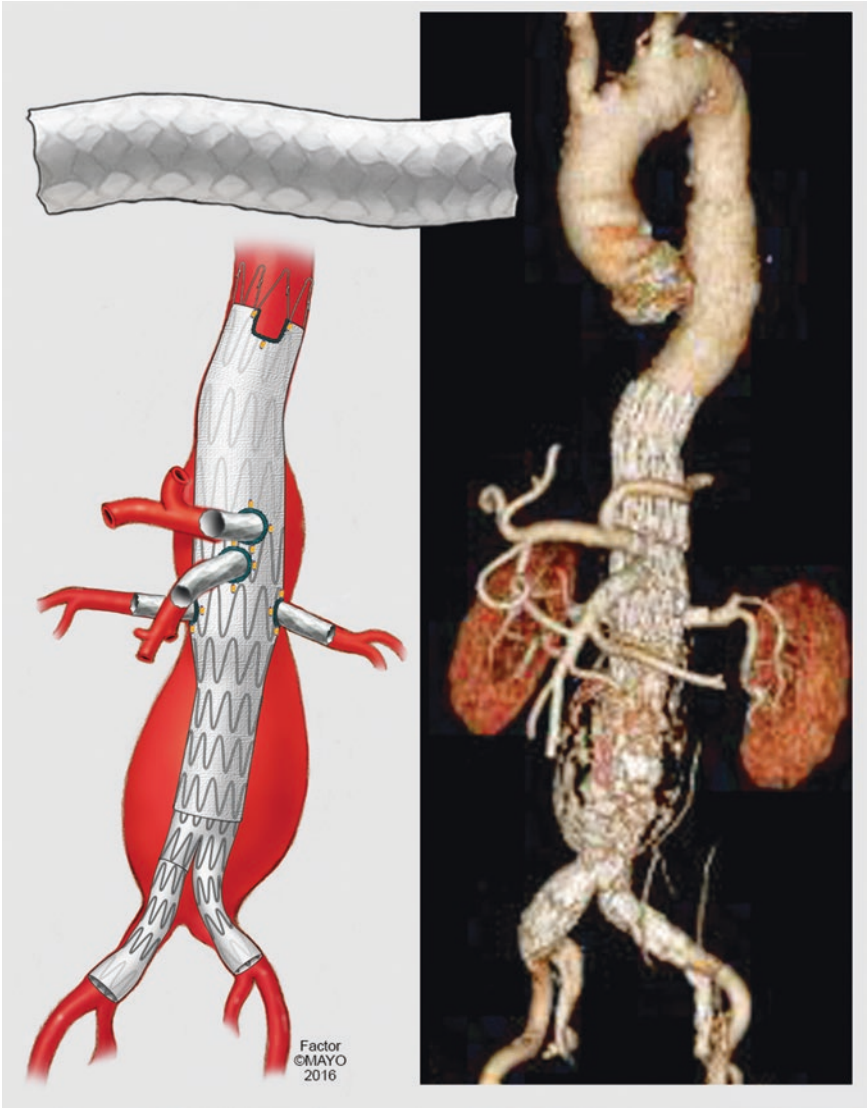


Fig. 25.3 iCAST balloon-expandable covered stent. By permission of Mayo Foundation for Medical Education and Research. All rights reserved

diameters of 5–10 mm and lengths of 18, 22, 28, 38, and 58 mm. The stent is introduced using a 6Fr delivery sheath up to 8 mm diameter, and 7Fr delivery sheath for those that are 9 or 10 mm in diameter. The graft material is a microporous expanded PTFE with 203 μm tubing. The stent has Chromium–Cobalt composition with strut dimensions of 0.135–165 × 0.145 mm. The stent uses a 0.035-in. platform with 5Fr shaft size and working lengths of 70 and 120 cm.

Self-Expandable Stents

There are at least five self-expandable stent grafts that have been used clinically for peripheral vascular procedures: Boston Scientific Wallgraft, WL Gore Viabahn, Bard Fluency, Jotec E-Ventus Stent Graft, and Coronary Prograft Stent Graft. Of these, the Wallgraft, Viabahn, and Fluency have 0.035-in. platform and have been used in larger clinical experiences with branched endografts [5, 10–12].

WL Gore Viabahn Stent Graft

The Gore Viabahn self-expandable stent graft (WL Gore, Flagstaff, AZ) is constructed with an expanded PTFE graft attached to an external nitinol stent structure (Fig. 25.7). It has been known for its flexibility and ability to traverse tortuous areas in the femoropopliteal segment. For this reason, durability has been tested in the most adverse environment across the knee joint [13]. Both 0.035″ and 0.018″ guide-wire compatible systems are available, but for branched endografts the 0.035-in. platform has been used widely. Diameters are 5 to 13 mm with lengths of 25, 50, 75, 100, 150, 250 mm for diame-

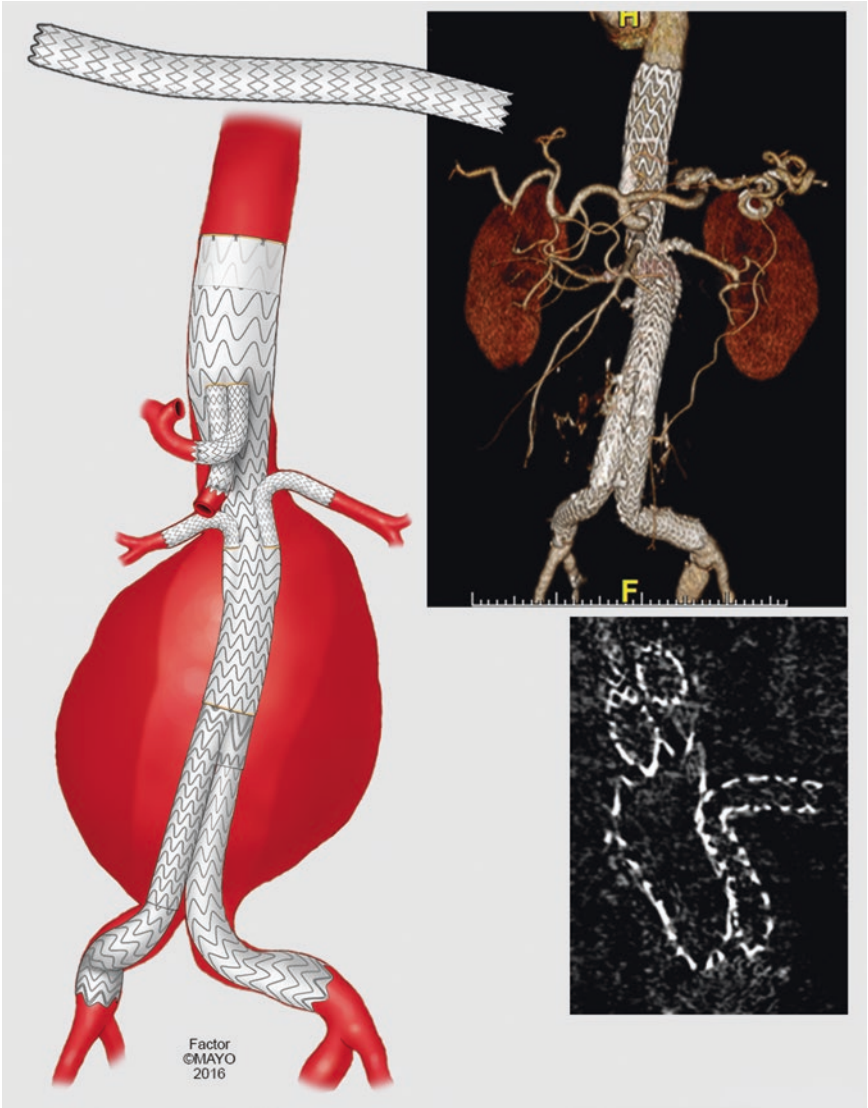


Fig. 25.4 VBX Viabahn balloon-expandable covered stent, which has been used under clinical investigation for the TAMBE device. By permission of Mayo Foundation for Medical Education and Research. All rights reserved

ters of 5–8 mm, 50, 75, 100, and 150 mm for 9 mm stents, 25, 50, 100, and 150 mm for 10 mm stents and 25, 50, and 100 mm for 11 and 13 mm stents. The 75 mm length has been added in 2015 and is likely to become widely available soon. The 0.018″ system comprises 5–8 mm stents only, which are delivered through 6–7 French sheaths, whereas the 0.035″ system comprises diameters or 5–8 mm and the larger stents of 9–13 mm, which are only available with the 0.035″ system. The 0.035″ stents are delivered through 7–12 French sheaths. The main advantage of the Viabahn stent graft over the other stents relies on its superior flexibility, which is ideal for use in tortuous vessels or long branches, particularly renal branches; in contrast, its disadvantage lies on need for larger delivery system (12Fr) for larger stents (≥9 mm).

Bard Fluency Plus

The Bard Fluency Plus (Bard Peripheral Vascular, Tempe, AZ) is self-expanding vascular endoprosthesis with a nitinol stent framework and expanded PTFE fabric (Fig. 25.8). The FDA-approved indication of the Fluency stent graft is treatment of in-stent restenosis in peripheral arterial disease or for outflow stenosis in hemodialysis access arteriovenous fistulae or grafts [14]. The Fluency stent graft has approximately 2 mm of uncovered stent at each end of the device. The inner lumen of the stent graft is carbon impregnated. It is compatible with 0.035″ systems, with working lengths of 80 and 117 cm; available stent lengths are 40, 60, 80, 100, and 120 mm, with lengths of 6, 7, 8, 9, 10, 12, and 13.5 mm. Recommended sheath diameters

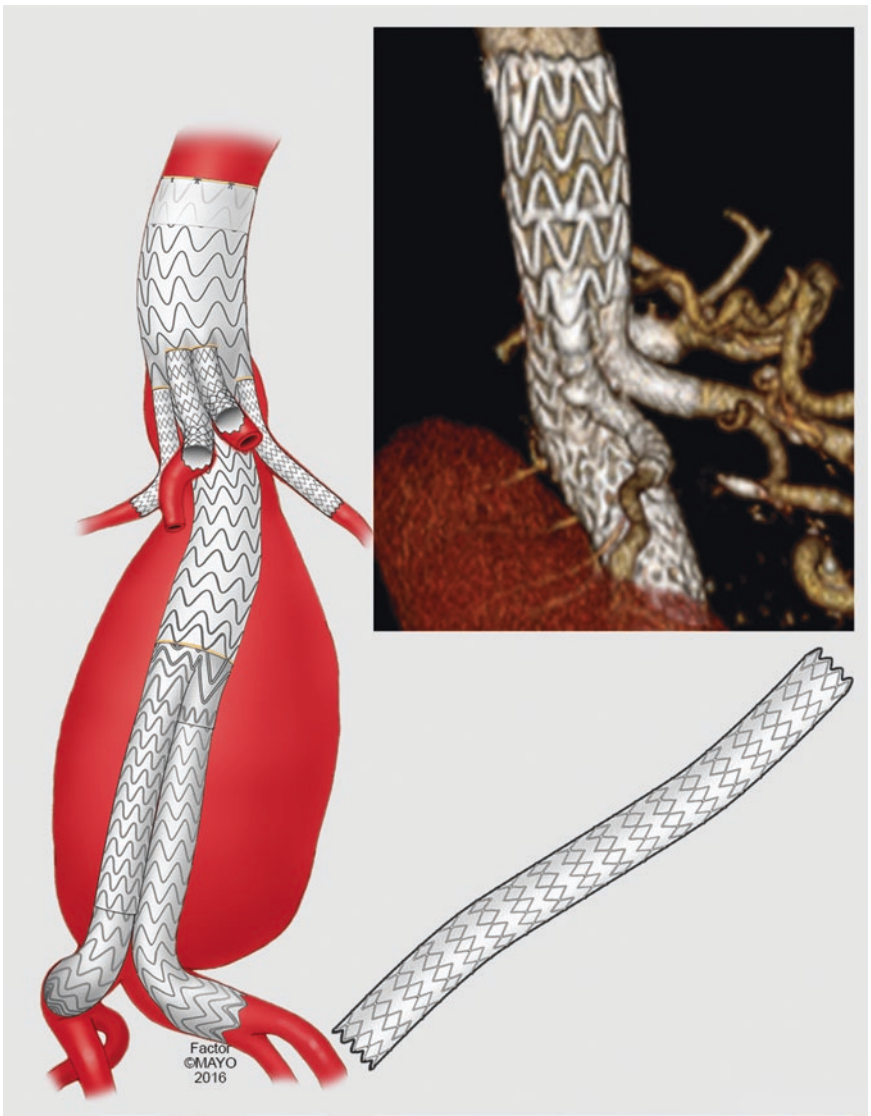


Fig. 25.5 VBX Viabahn balloon-expandable covered stent demonstrating the curved anatomy in a patient with antegrade TAMBE device. By permission of Mayo Foundation for Medical Education and Research. All rights reserved

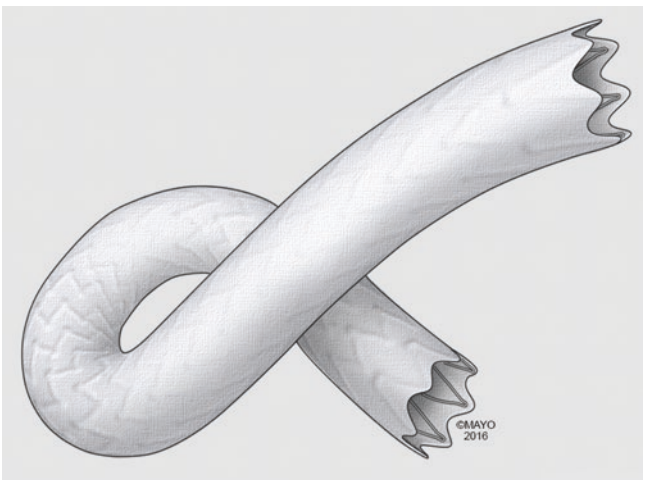


Fig. 25.6 Bentley BeGraft stent. By permission of Mayo Foundation for Medical Education and Research. All rights reserved

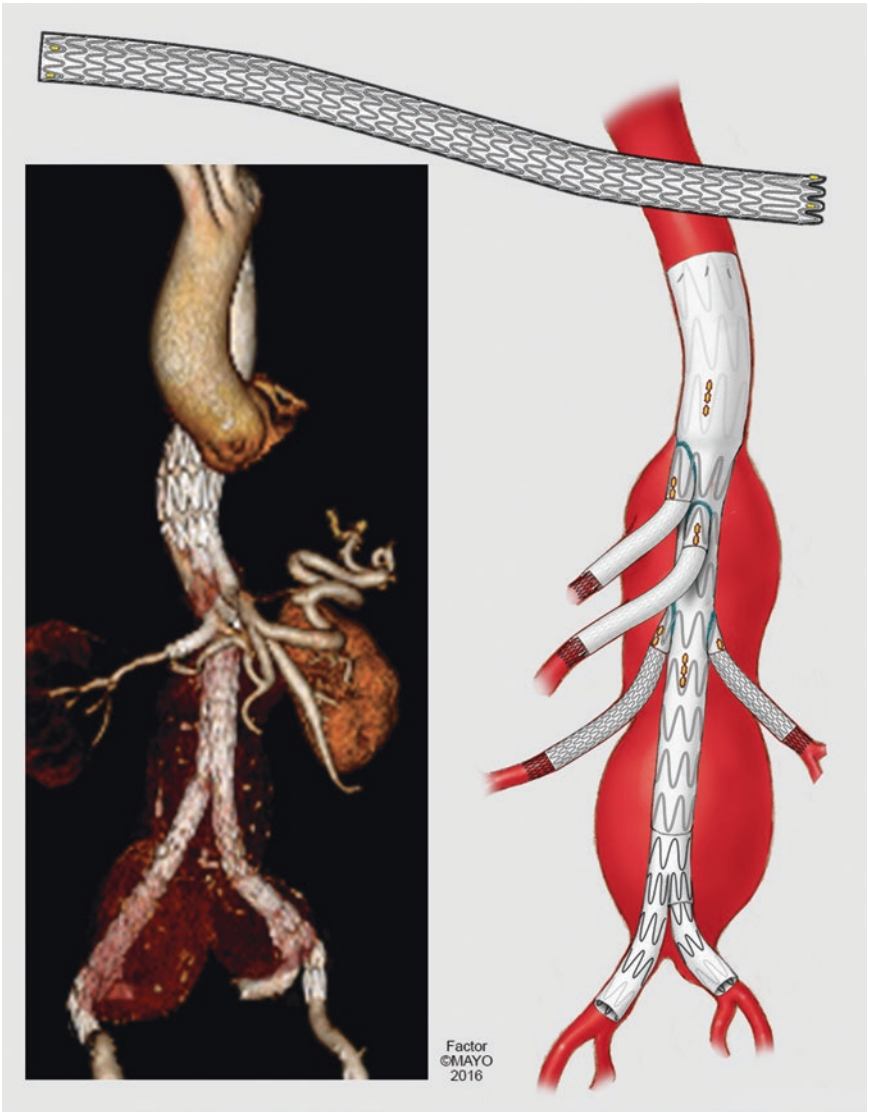


Fig. 25.7 Viabahn self-expandable stent graft. By permission of Mayo Foundation for Medical Education and Research. All rights reserved

are 8- to 10-French depending on the stent diameter and length. The main advantages of the Fluency platform are the multitude of available lengths and diameters and the lower system profile (8–9 French for all stents < 10 mm diameter). The Fluency Flair has a flared outflow configuration, which is potentially suited for bridging ectatic target vessels. However, the flaired segment is short, measuring 1 cm in length and therefore seal may not be achieved in a larger target. The stent comes in 6–9 mm proximally and up to 13 mm distally and is delivered using a 9Fr sheath (Fig. 25.9).

Boston Scientific Wallgraft

The Wallgraft (Boston Scientific, Bloomington MN) was the first commercially available stent graft, which has been used clinically for peripheral indications (Fig. 25.10) [15–17]. This was also the first alignment stent graft used for thoracoabdominal repair until other stents with superior flexibility became commercially available [4]. Currently, the wallgraft has not been used because it is more rigid and not as adaptable to tortuous anatomy. The stent combines ePTFE with a nitinol plantform using 0.035-in. delivery system. The stent is available in 6- to 14-mm diameters with lengths of 20, 30, 50, and 70 mm. Catheter length is 116 cm.

Bare-Metal Stents

A wide variety of balloon expandable and self-expandable bare metal stents is used for alignment of fenestrations and branches [7]. Usually this is not the first option because of the occurrence of neointimal hyperplasia, which may be triggered by the excessive balloon flaring that is done in the fenestration or in the distal edge of a self-expandable

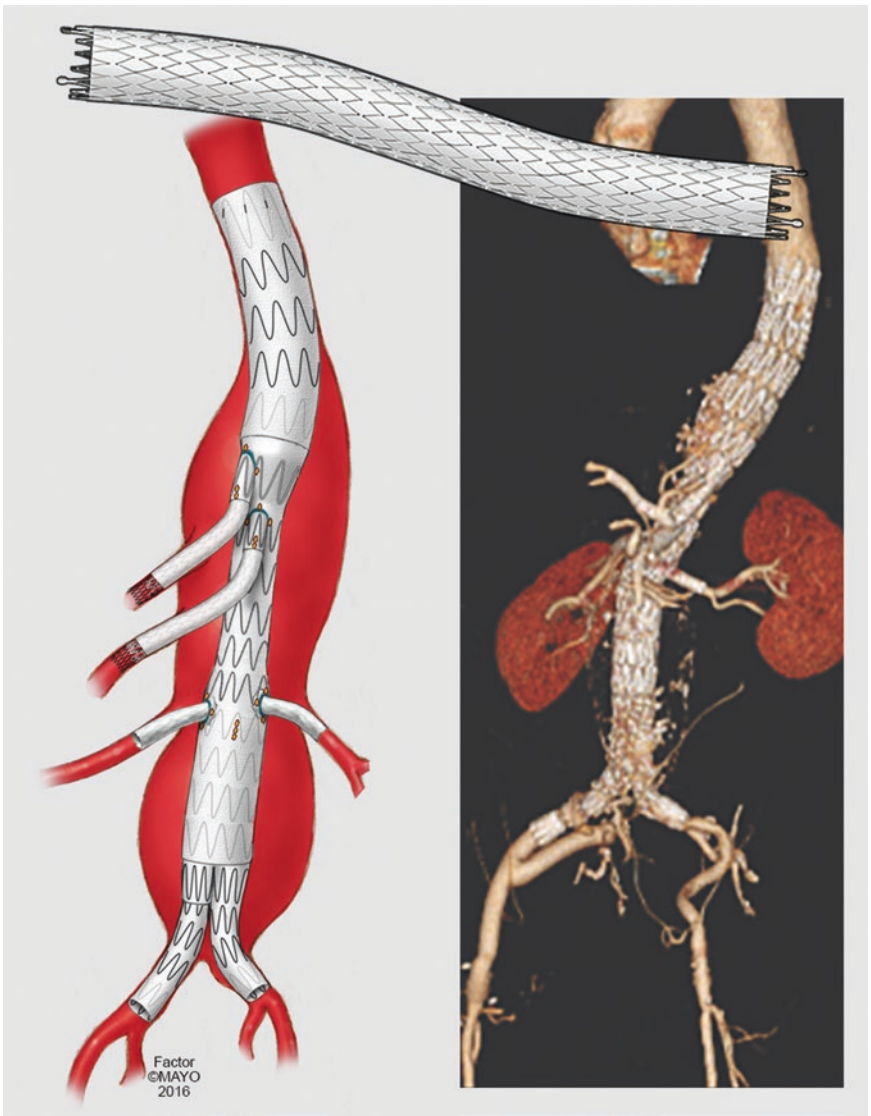


Fig. 25.8 Fluency self-expandable stent graft. By permission of Mayo Foundation for Medical Education and Research. All rights reserved

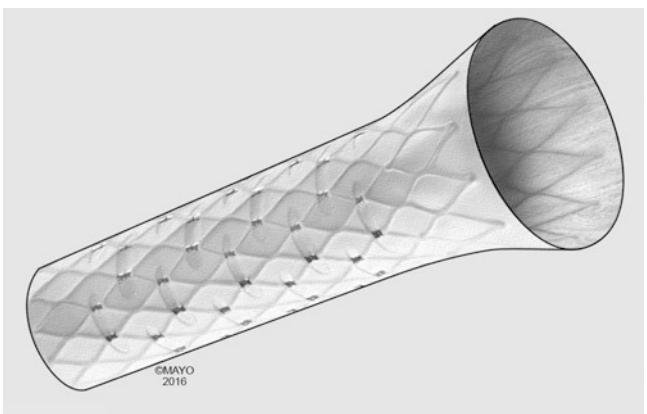


Fig. 25.9 Fluency Flare self-expandable stent graft. By permission of Mayo Foundation for Medical Education and Research. All rights reserved

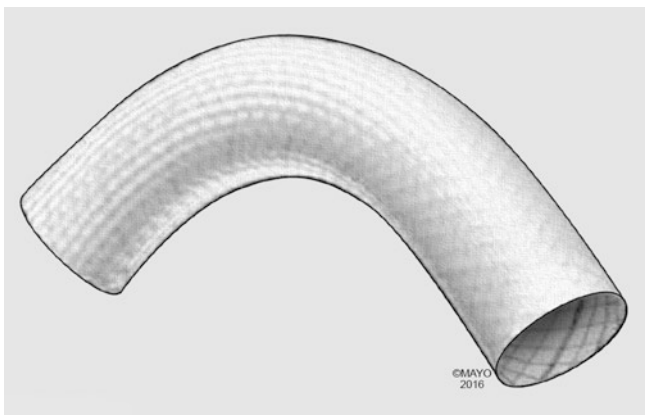


Fig. 25.10 Wall Graft self-expandable stent graft. By permission of Mayo Foundation for Medical Education and Research. All rights reserved

stent (Fig. 25.11). Nonetheless, bare metal stents are most useful for alignment of smaller vessels that are 3 mm or vessels with early bifurcations (Fig. 25.12). Self-expandable bare metal stents have also been used widely at the distal edge of balloon expandable and self-expandable covered stents to prevent kinks (Fig. 25.13).

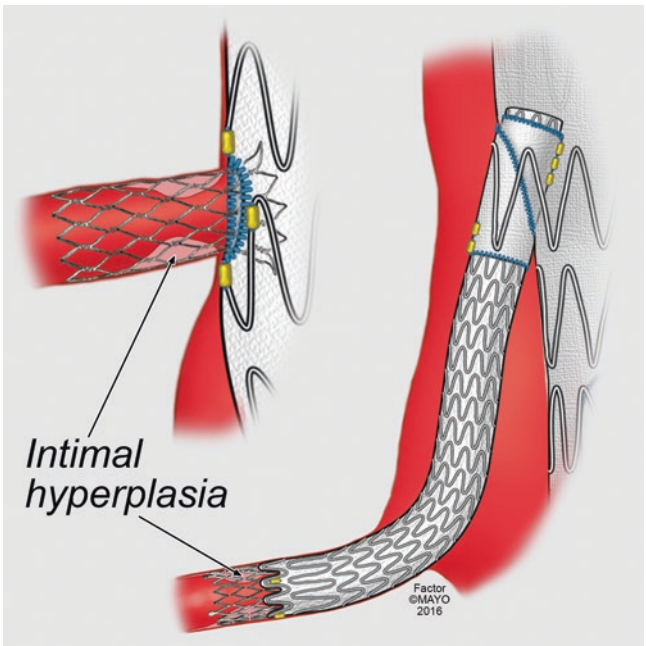


Fig. 25.11 Intimal hyperplasia occurs at the distal edges and in bare-metal stents. By permission of Mayo Foundation for Medical Education and Research. All rights reserved

Planning and Selection of Bridging Stents

Selection of optimal bridging stents during F/BEVAR should be performed carefully and likely has major influence on long-term durability, freedom from branch-related complications and subsequent reinterventions. One should not be bound to a single alignment stent. Instead, the stent or stents need to be tailored to the patient anatomy. This should be performed during preoperative planning using three-dimensional centerline reconstruction of computed tomography images. The stent type, number, diameter, and estimated lengths should be planned prior to starting the procedure and should be immediately available during the procedure to avoid delays.

Fenestrations

Alignment of fenestrations in the author's opinion is best done using the iCast or V12 covered stent. This stent has the largest worldwide experience and has performed well in all respects, with low rates of occlusion, dislodgement, migration, fracture and tears [5]. Characteristics that are beneficial include its precise deployment, diameters of 5–9 mm with post-dilatation up to 12 mm, and lengths of 16, 22, 38, and 59 mm. If the stent is kept in the proximal third of the renal artery, it allows perfect alignment with the target vessel and there is minimal kink, obviating the need for increased stent flexibility. However, if the vessel assumes a posterior course early on or the stent is extended to the middle or distal third of the renal artery, a self-

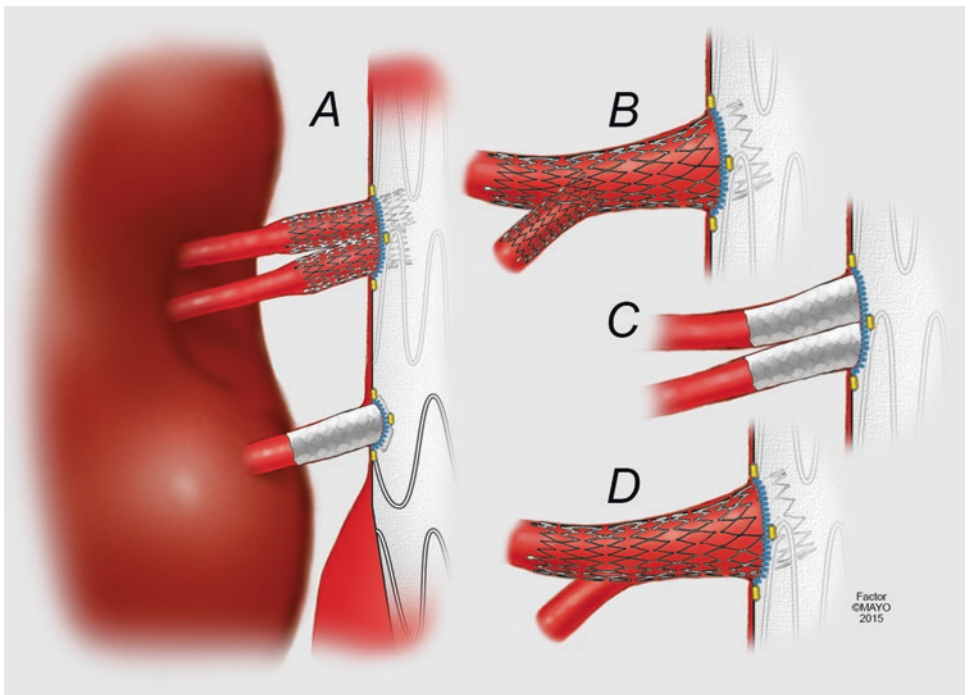


Fig. 25.12 Examples of alignment of fenestrations using bare-metal stents in different configurations (**a**), including bifurcated stent techniques using combination of open cell self-expandable stent with stenting of side branch (**b**), double covered stent placement (**c**) and bare metal stenting across side branches (**d**). By permission of Mayo Foundation for Medical Education and Research. All rights reserved

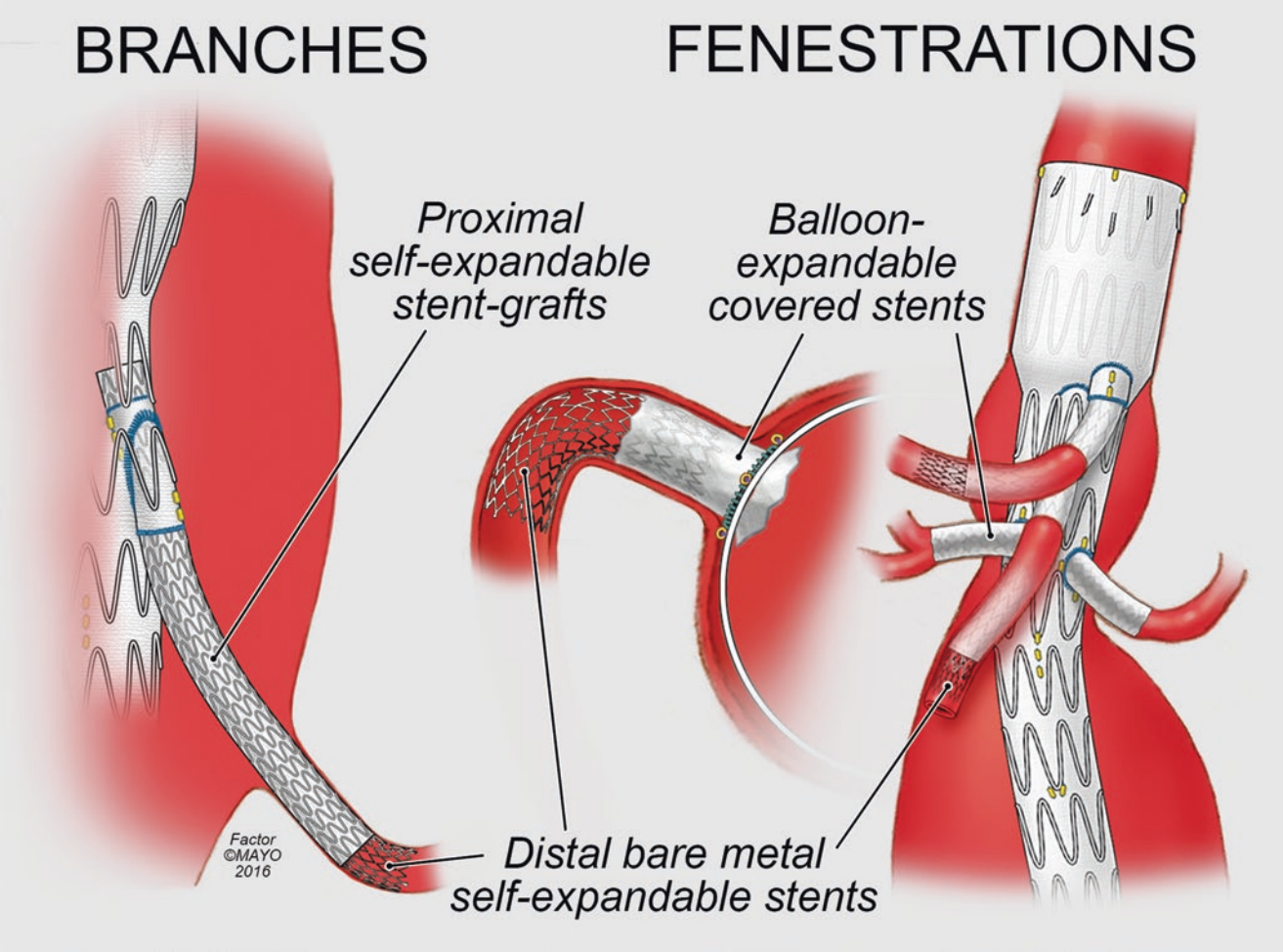


Fig. 25.13 Bare metal self-expandable stents are often used to reinforce distal branches and to prevent kinks after placement of rigid balloon expandable rigid balloon expandable covered stents. By permission of Mayo Foundation for Medical Education and Research. All rights reserved

expandable bare metal stent may be needed to avoid kink at the transition with the native artery. Self-expandable stents are needed more frequently in the right renal artery, which dives posterior to the inferior vena cava (Fig. 25.14).

Directional Branches

Directional branches or cuffs usually require longer bridging stents, which are often delivered through the brachial approach, in which case a lower profile is key. Our choice for celiac artery and superior mesenteric artery branches has been to use the Fluency stent graft because of its profile (9 French), flared configuration, and availability of 60 and 80 mm lengths in the 7–10 mm diameter range. Conversely, renal branches are more prone to late occlusions and have lower freedom from branch-related events compared to mesenteric branches or renal fenestrations in long-term follow-up; it is postulated that the smaller diameter, ostial disease, more tortuous anatomy, and the tendency to form kinks in the mid segment of the renal arteries coupled with respiratory motion influence occlusion rates [5, 10–12, 18]. Therefore, it is not surprising that the more rigid Wallgraft stent fell in disfavor for this indication. For these reasons, our technique evolved to using routinely self-expandable Viabahn stent grafts for bridging renal artery branches. The limited availability of lengths (formerly 50 or 100 mm) and the difficult visualization (lack of markers), have recently improved with the introduction of a 75-mm length stent and placement of radiopaque markers. We often couple more than one stent and use a balloon-expandable covered stent (iCast) proximally at the level of the branch/cuff to provide additional radial force and avoid cuff disconnection and subsequent endoleak (Fig. 25.15). In many cases, both visceral and renal branches might require reinforcement with a self-expandable bare metal stent to avoid kinks. This is particularly important in the presence of tortuous anatomy.

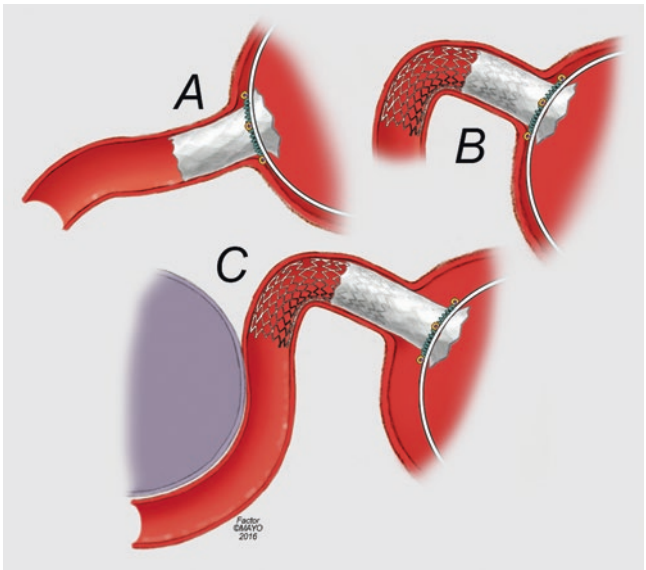


Fig. 25.14 Vessel tortuosity and orientation determines the need of additional self-expandable stent. For vessels with straight orientation no stent is needed (**a**). Stents are needed if the vessel takes a posterior course (**b**), which is more common in the right renal artery (**c**) which is oriented posterior to the inferior vena cava. By permission of Mayo Foundation for Medical Education and Research. All rights reserved

Special Scenarios

Small Renal Branches

Small renal arteries (<4 mm) such as accessory branches or those with early bifurcations pose a major challenge [19, 20]. For fenestrations a coronary bare metal stent may be indicated provided the vessel originates from normal aortic diameter at the sealing zone. If a small renal artery originates from the aneurysm, it may require to be sacrificed. A 3-mm renal artery may still be treated using a 5-mm iCAST with a modified technique for deployment of the stent (Fig. 25.16). The stent is partially expanded, and the balloon is moved proximally within the stent, which is secured by the sheath. The proximal stent is then carefully flared. It is recommended to do this as the last vessel and to have additional stents and coils available in case of a disruption. However, using meticulous technique the authors have been successful even for 3-mm vessels.

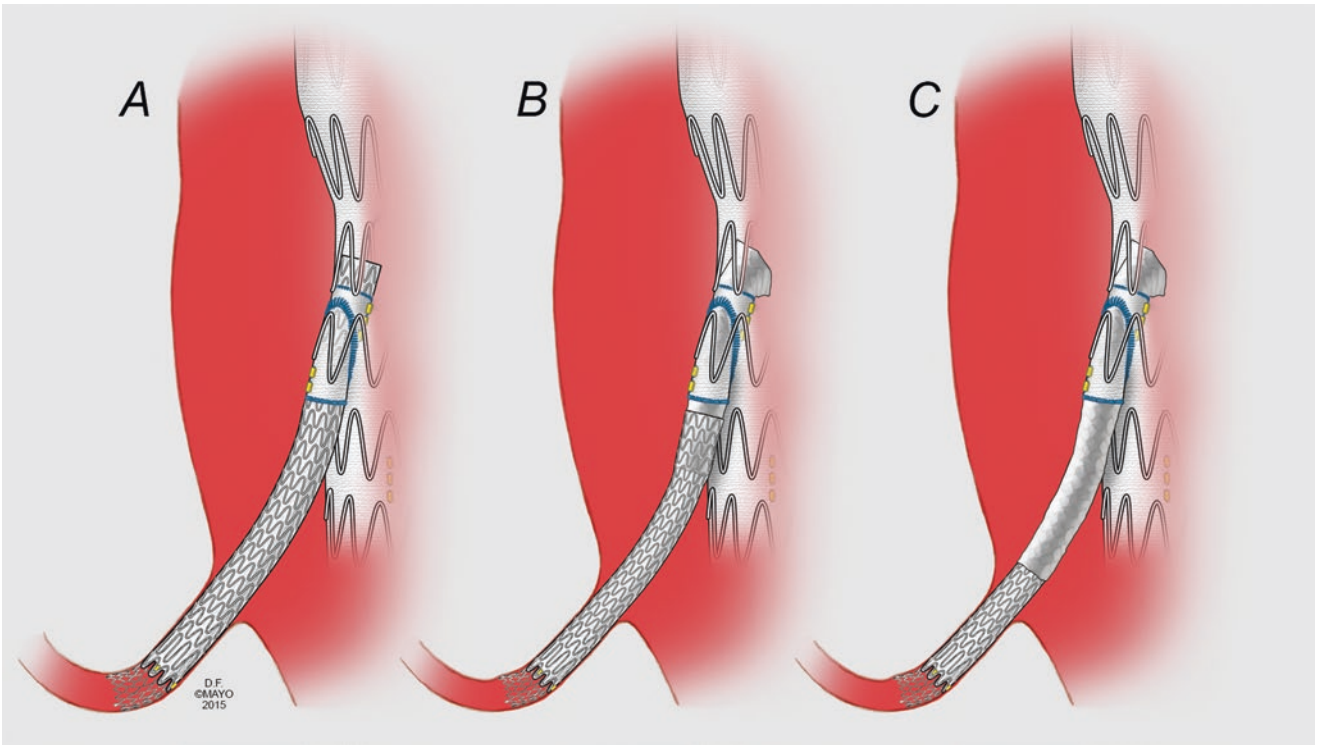


Fig. 25.15 Stenting of renal branches is done preferentially with Viabahn stent graft using reinforcement of the distal end with self-expandable stents (**a**). If the stent is too short, a second balloon expandable stent may be needed (**b**) or the Viabahn can be placed inside the balloon-expandable stent (**c**). By permission of Mayo Foundation for Medical Education and Research. All rights reserved

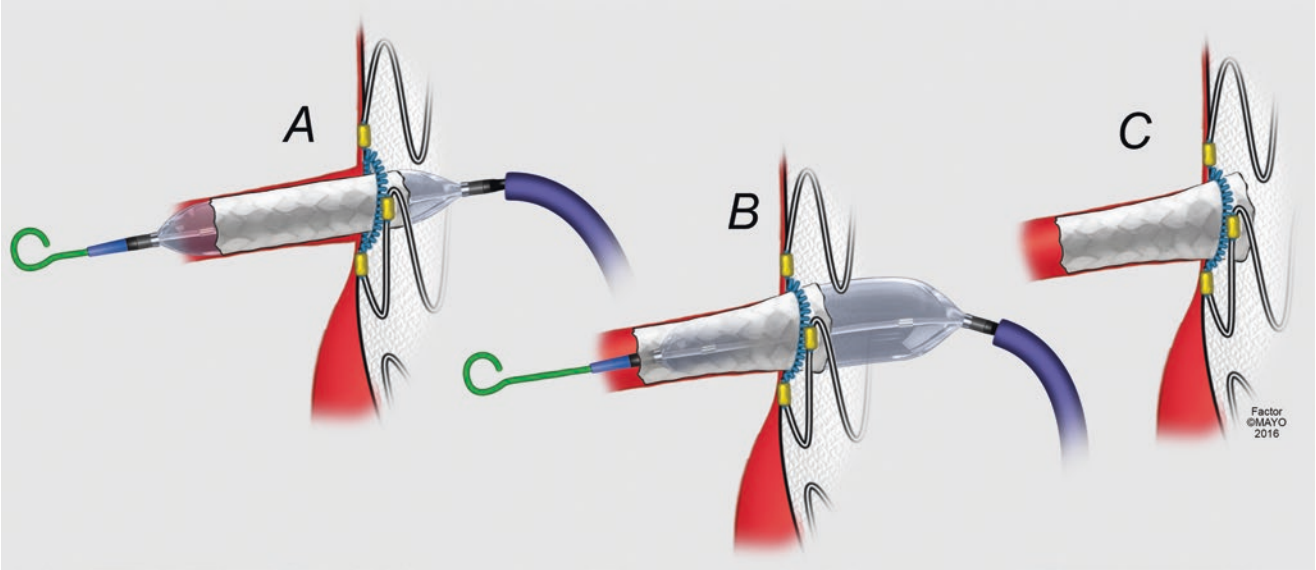


Fig. 25.16 The iCAST covered stent is placed with 3- to 5 mm of stent into the aorta (**a**). This is flared using a 10-mm balloon in the same orientation of the vessel (**b**). Final configuration of the flared stent (**c**). By permission of Mayo Foundation for Medical Education and Research. All rights reserved

Early Bifurcation Lesions

Early bifurcations can occur in the renal arteries or in the celiac axis with premature branching of the hepatic artery and in the superior mesenteric artery with early branching of a replaced hepatic artery. Techniques of bifurcated stents for renal arteries are well described in Fig. 25.12. The author has used a bifurcated stent technique of coupling an open cell self-expandable stent for the main trunk with a balloon-expandable bare metal stent to keep perfusion in a side branch through the cells of the self-expandable stent (Fig. 25.17). This has been used in the SMA for replaced hepatic arteries, for treatment of lesions in the distal common iliac artery involving the internal iliac artery and for stenting of celiac bifurcation lesions [21].

Large Target Vessels

The upper limit for stenting with current available technology is 11 mm. Vessels with diameters of 12 mm or more are likely not ideally suited for current bridging stents. For 11-mm vessels treated by branches, the author started using Fluency Flair stents, but has been disappointed by the occurrence of distal endoleaks, likely due to the relatively short length of the flared segment. This technique has been modified to using a 13-mm Viabahn coupled with an Atrium iCAST stent. The oversized 13-mm Viabahn is deployed in the target vessel and into the 8-mm mesenteric branch. Because of the excessive oversizing, a balloon expandable stent or covered stent is added in the cuff segment to avoid any infolding of the stent (Fig. 25.18).

Two other techniques can be used for large branches. The parallel bridging stent technique has been used in a patient

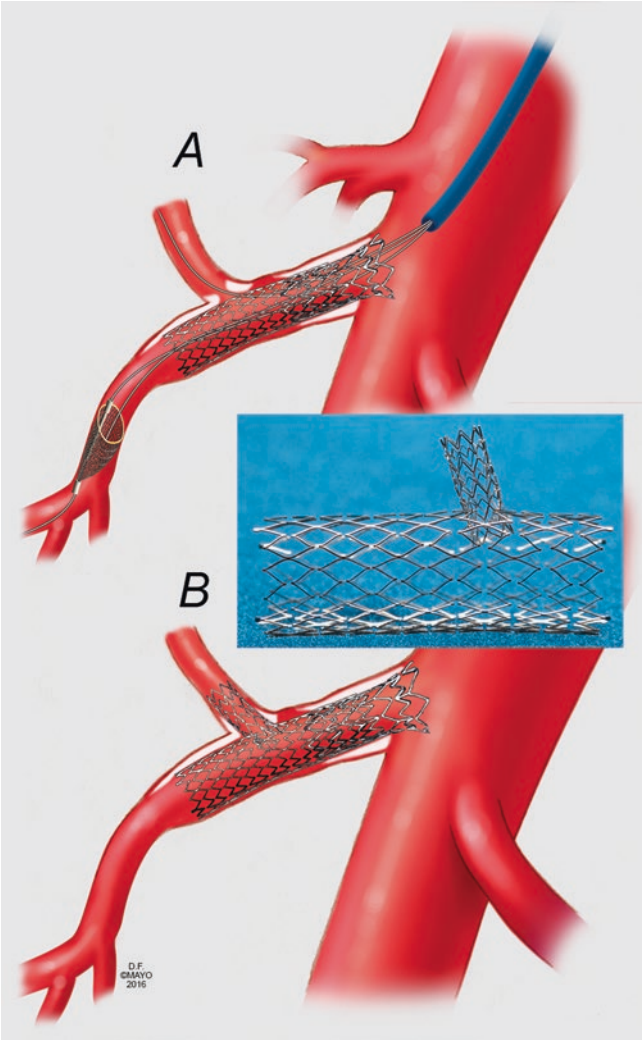


Fig. 25.17 Technique of bifurcated stent is done by placement of an open cell self-expandable bare metal stent (**a**) with selective catheterization of the stent cell and placement of balloon expandable stent (**b**). By permission of Mayo Foundation for Medical Education and Research. All rights reserved

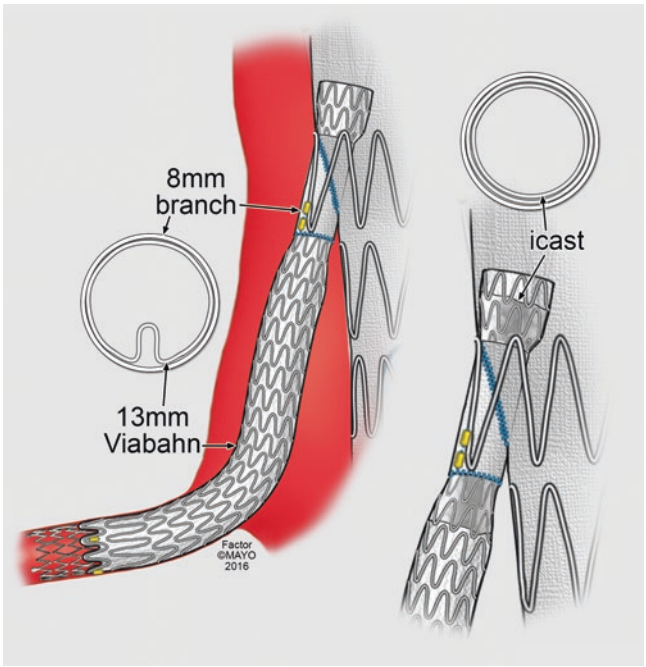


Fig. 25.18 Technique of stent flaring using combination of a 13-mm viabahn stent placed into an 8-mm cuff. Note possible infolding of the stent, which is treated by placement of a balloon expandable covered stent. By permission of Mayo Foundation for Medical Education and Research. All rights reserved

with very large 14-mm SMA and early bifurcation of a replaced hepatic artery. In this case, a Fluency flair was deployed in the proximal SMA and two Viabahn stents to secure seal and flow into the replaced hepatic artery and the SMA distally (Fig. 25.19). Alternatively, the branched endograft can be planned with two cuffs for the same vessel (Fig. 25.20). Finally, if stenting of large vessel is done and the landing zone is relatively short, it is prudent to extend into one of the branches (the most critical branch) with a bare metal self-expandable stent to avoid disconnection or migration into the aneurysm (Fig. 25.21).

Intentional Branch Occlusion

Intentional occlusion of a directional branch can be done by extending the branch with an iCAST covered stent and then occluding the branch with AMPLATZER plugs as depicted in Fig. 25.22.

Conclusion

With the exception of the balloon-expandable Viabahn stent grafts, there are no covered stents developed specifically for the purpose of bridging fenestrations and branches during endovascular repair of complex aortic aneurysms. All of the stents described in this chapter were originally developed to treat peripheral arterial (or tracheobronchial) stenosis, and therefore its indication for use during fenestrated and branched stent graft repair of complex aortic aneurysms should be carefully planned. The ideal stent graft should have a low profile, be flexible, and yet have appropriate radial force allowing precise deployment system. The stent should be available in multiple diameters (4–13 mm) and lengths (20–80 mm) and be compatible with both 0.018″ and 0.035″ guide-wire platforms. As endovascular technology evolves, more bridging stent-specific options should be available in the forthcoming years, optimizing clinical outcomes of fenestrated and branched stent graft repair of complex aortic aneurysms even further.

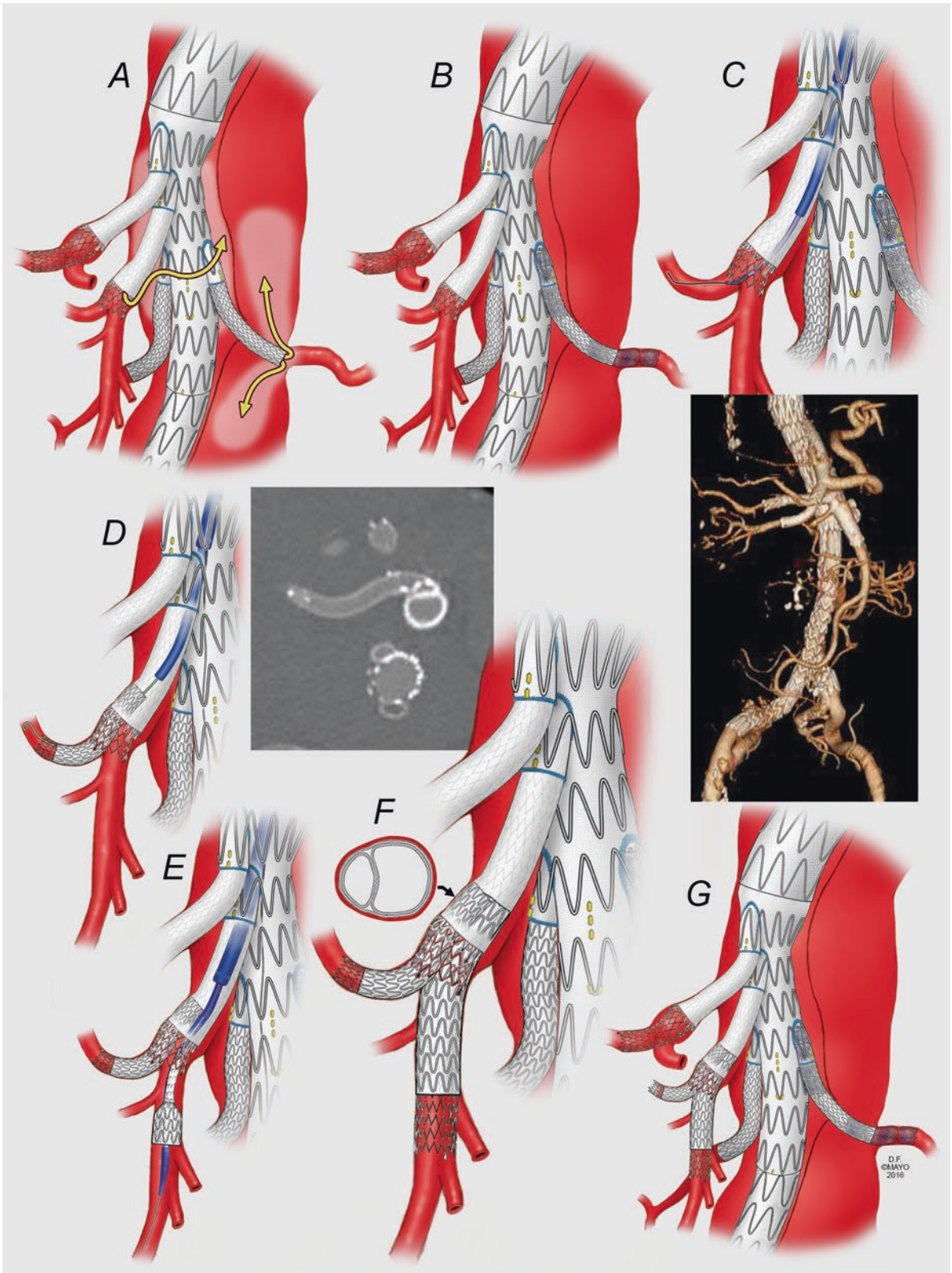


Fig. 25.19 Technique of treatment of multiple endoleaks in a patient on chronic hemodialysis who underwent branched thoracoabdominal repair (**a**). The left renal branch was excluded with AMPLATZER plugs (**b**) and the SMA branch was extended using parallel technique. After catheterization of a large hepatic artery (**c**), the repair was extended distally using a Viabahn into the replaced hepatic artery (**d**) and one into the distal SMA (**e**). Note the parallel stent configuration (**f**) and resolution of the endoleak (**g**). By permission of Mayo Foundation for Medical Education and Research. All rights reserved

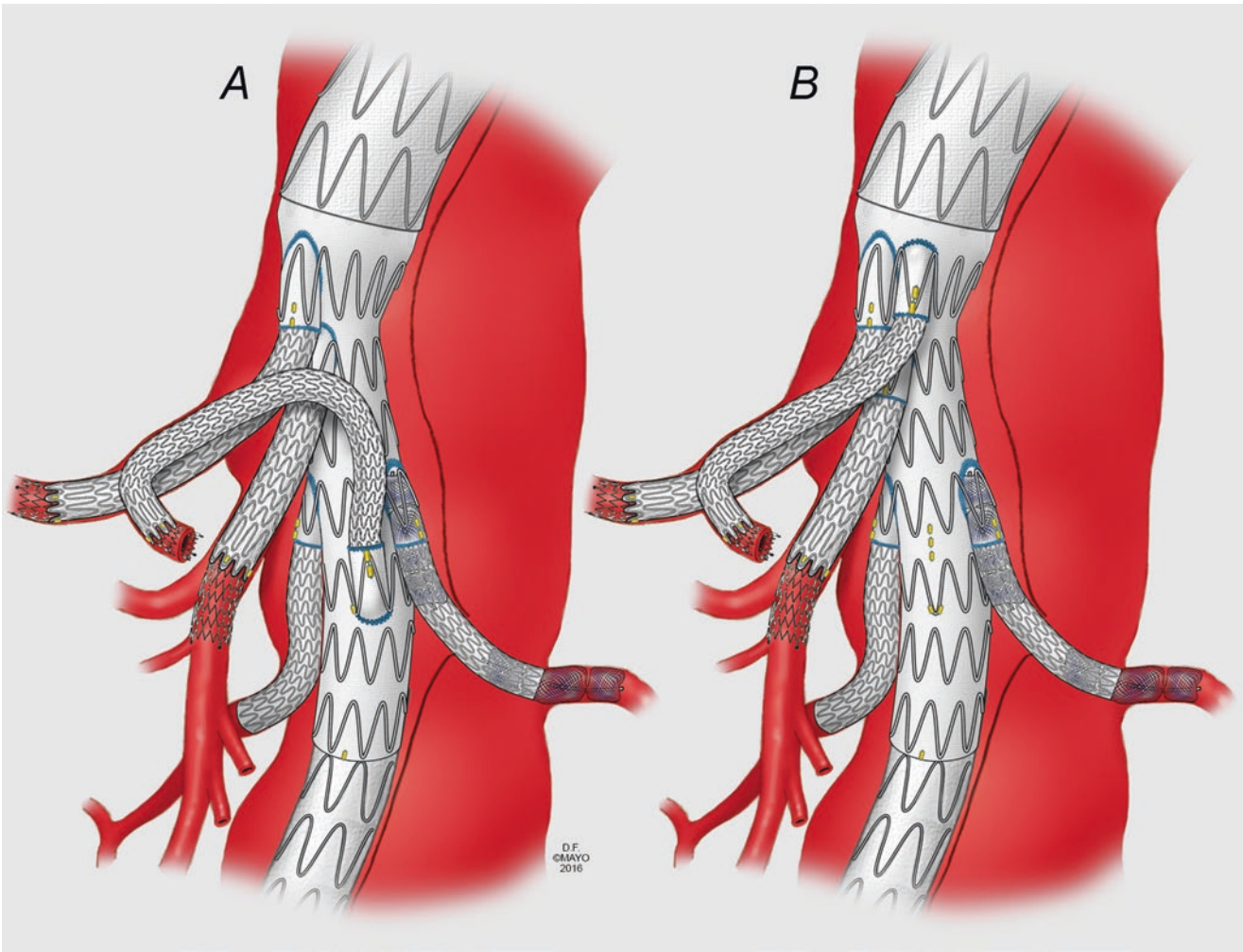


Fig. 25.20 Techniques of dealing with large and short celiac axis include extending the repair into the hepatic branch while excluding the splenic branch, or revascularization of both branches using an additional retrograde (**a**) or antegrade branch (**b**). By permission of Mayo Foundation for Medical Education and Research. All rights reserved

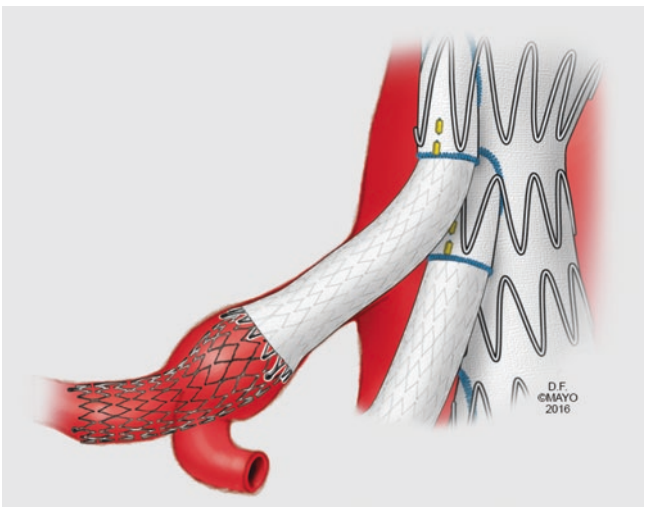


Fig. 25.21 To avoid disconnection of branches into short celiac axis segments an additional self-expandable stent is used to extend into the hepatic artery. By permission of Mayo Foundation for Medical Education and Research. All rights reserved

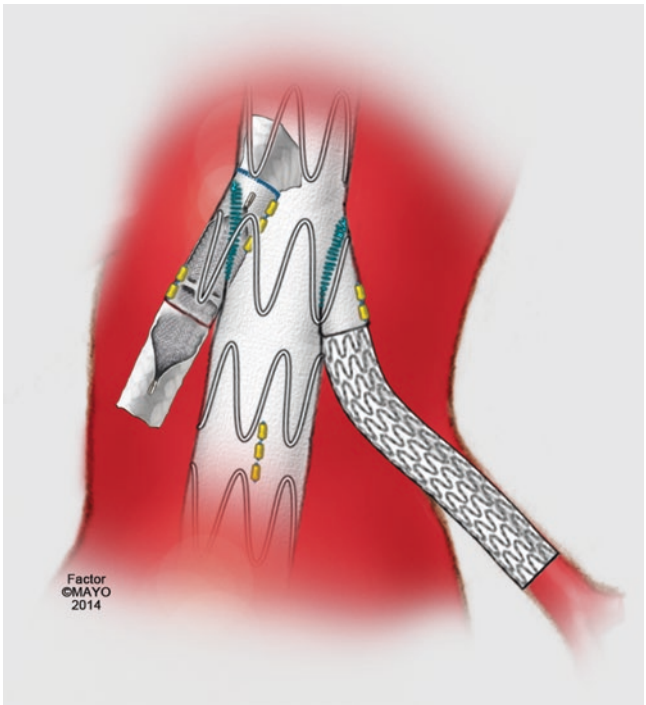


Fig. 25.22 Technique of exclusion of directional branches using stent extension and plug. By permission of Mayo Foundation for Medical Education and Research. All rights reserved

References

1. Anderson JL, Berce M, Hartley DE. Endoluminal aortic grafting with renal and superior mesenteric artery incorporation by graft fenestration. J Endovasc Ther. 2001;8(1):3–15.
2. Faruqi RM, Chuter TAM, Reilly LM, Sawhney R, Wall S, Canto C, et al. Endovascular repair of abdominal aortic aneurysm using a para-renal fenestrated stent-graft. J Endovasc Surg. 1999;6(4):354–8.
3. Chuter TAM, Gordon RL, Reilly LM, Goodman JD, Messina LM. An endovascular system for thoracoabdominal aortic aneurysm repair. J Endovasc Ther. 2001;8(1):25–33.
4. Chuter TAM. Branched and fenestrated stent grafts for endovascular repair of thoracic aortic aneurysms. J Vasc Surg. 2006;43:111A–5.
5. Mastracci TM, Carrell T, Constantinou J, Dias N, Martin-Gonzalez T, Katsargyris A, et al. Editor's choice—effect of branch stent choice on branch-related outcomes in complex aortic repair. Eur J V Endovasc Surg. 2016;51(4):536–42.
6. Mohabbat W, Greenberg RK, Mastracci TM, Cury M, Morales JP, Hernandez AV. Revised duplex criteria and outcomes for renal stents and stent grafts following endovascular repair of juxtarenal and thoracoabdominal aneurysms. J Vasc Surg. 2009;49(4):827–37. discussion 37.
7. Mendes BC, Oderich GS. Endovascular repair of thoracoabdominal aortic aneurysm using the off-the-shelf multibranched t-Branch stent graft. J Vasc Surg. 2016;63(5):1394–1399.e2.
8. Oderich GS, Erdoes LS, LeSar C, Mendes BC, Gloviczki P, Cha S, et al. Comparison of covered stents versus bare metal stents for treatment of chronic atherosclerotic mesenteric arterial disease. J Vasc Surg. 2013;58(5):1316–23.
9. Mwipatayi BP, Thomas S, Wong JK, Temple SEL, Vijayan V, Jackson M, et al. A comparison of covered vs bare expandable stents fbr the treatment of aortoiliac occlusive disease. J Vasc Surg. 2011;54(6):1561–70.
10. Eagleton MJ, Follansbee M, Wolski K, Mastracci T, Kuramochi Y. Fenestrated and branched endovascular aneurysm repair outcomes for type II and III thoracoabdominal aortic aneurysms. J Vasc Surg. 2016;63(4):930–42.
11. Verhoeven ELG, Katsargyris A, Bekkema F, Oikonomou K, Zeebregts CJAM, Ritter W, et al. Editor's choice—ten-year experience with endovascular repair of thoracoabdominal aortic aneurysms: results from 166 consecutive patients. Eur J Vasc Endovasc Surg. 2015;49(5):524–31.
12. Mastracci TM, Greenberg RK, Eagleton MJ, Hernandez AV. Durability of branches in branched and fenestrated endografts. J Vasc Surg. 2013;57(4):926–33.
13. Antonello M, Frigatti P, Battocchio P, Lepidi S, Cognolato D, Dall'Antonia A, et al. Open repair versus endovascular treatment for asymptomatic popliteal artery aneurysm: results of a prospective randomized study. J Vasc Surg. 2005;42(2):185–93.
14. Haskal ZJ, Trerotola S, Dolmatch B, Schuman E, Altman S, Mietling S, et al. Stent graft versus balloon angioplasty for failing dialysis-access grafts. N Engl J Med. 2010;362(6):494–503.
15. Xenos ES, Freeman M, Stevens S, Cassada D, Pacanowski J, Goldman M. Covered stents for injuries of subclavian and axillary arteries. J Vasc Surg. 2003;38(3):451–4.
16. Tielliu IFJ, Verhoeven ELG, Zeebregts CJ, Prins TR, Span MM, van den Dungen J. Endovascular treatment of popliteal artery aneurysms: results of a prospective cohort study. J Vasc Surg. 2005;41(4):561–6.
17. Rzucidlo EM, Powell RJ, Zwolak RM, Fillinger MF, Walsh DB, Schermerhorn ML, et al. Early results of stent-grafting to treat diffuse aortoiliac occlusive disease. J Vasc Surg. 2003;37(6):1175–80.
18. Ullery BW, Suh G-Y, Lee JT, Liu B, Stineman R, Dalman RL, et al. Geometry and respiratory-induced deformation of abdominal branch vessels and stents after complex endovascular aneurysm repair. J Vasc Surg. 2015;61(4):875–84.
19. Mendes BC, Oderich GS, de Souza LR, Banga P, Macedo TA, DeMartino RR, et al. Implications of renal artery anatomy for endovascular repair using fenestrated, branched, or parallel stent graft techniques. J Vasc Surg. 2016;63(5):1163–1169.e1.
20. Spear R, Maurel B, Sobocinski J, Perini R, Guillou M, Midulla M, et al. Technical note and results in the management of anatomical variants of renal vascularisation during endovascular aneurysm repair. Eur J Vasc Endovasc Surg. 2012;43(4):398–403.
21. Manunga JM, Oderich GS. Orbital atherectomy as an adjunct to debulk difficult calcified lesions prior to mesenteric artery stenting. J Endovasc Ther. 2012;19(4):489–94.

Sizing and Planning Fenestrated and Multibranched Endovascular Repair

26

Gustavo S. Oderich and Bernardo C. Mendes

Introduction

Endovascular repair using fenestrated and branched endografts requires meticulous planning. Current techniques rely on measurements of lengths and diameters using computed tomography angiography and centerline of flow (CLF) analysis [1, 2]. Selection of specific stent design (fenestration vs. branch) and the approach (brachial vs. femoral) takes into consideration the extent of aortic disease, location of sealing zones, diameter of the aortic lumen, vessel orientation, atherosclerotic debris and quality of access vessels. As a general rule, branches are preferred or ideally suitable to target vessels originating from a large aortic lumen, whereas fenestrations were initially designed to incorporate vessels that originate from normal aortic segments (Fig. 26.1). Nonetheless, other patient or anatomy related factors influence the specific method of incorporation [3]. This chapter summarizes sizing and planning for complex endovascular aortic repair using fenestrated and branched endografts.

Evidence of Disease Progression

There is evidence that aortic disease is progressive regardless of the type of approach (open or endovascular), stent type (balloon or self-expandable) and manufacturer. Majewski et al. studied prospectively 30 patients treated by open repair for juxtarenal abdominal aortic aneurysms with biopsies of the aortic wall and aneurysm sac. In that study, 19 patients (60 %) had significant enlargement of the aorta immediately above the graft anastomosis, averaging 5 mm after a mean follow-up of 2 years. Among patients with enlargement, biopsies had shown significant degeneration of cellular architecture and altered distensibility, similar to changes in the aneurysm sac [4].

Evidence that aortic disease moves cranially in the aorta also comes from EVAR feasibility studies. Timaran and associates found that 80 % of patients with small abdominal aortic aneurysm met the minimum neck requirement of 15 mm, compared to less than 20 % for those who had aneurysms >7 cm. In that study, patients with favorable necks remained suitable for EVAR during follow-up, but two thirds of the patients with marginal necks lost suitability over time [5]. Therefore, given an infinite lifespan, an infrarenal aneurysm would progress into juxtarenal, pararenal, paravisceral, and thoracoabdominal segments (Fig. 26.2). For those who advocate EVAR in borderline necks or use of parallel grafts, the following assumptions need to be met:

1. Results of EVAR in short, angulated, and hostile necks are as durable as long necks.
2. Neck dimensions (diameter and length) are stable and aortic disease does not progress.
3. Once sac regression occurs, progression of disease ceases and does not lead to failure.
4. Once a repair fails, secondary interventions are as safe and effective as a well done first repair.

Suboptimal Necks Yield Suboptimal Results

The push for EVAR in patients with suboptimal necks (Fig. 26.3) has been fed by interest in expanding indications with minimal increment in technical challenge. This push is largely supported by the fact that EVAR is often associated with acute success in patients with short necks.

G.S. Oderich (✉) • B.C. Mendes
Division of Vascular and Endovascular Surgery, Mayo Clinic,
200 First Street SW, Rochester, MN 55905, USA
e-mail: oderich.gustavo@mayo.edu; mendes.bernardo@mayo.edu

© Mayo Foundation for Medical Education and Research 2017

G.S. Oderich (ed.), *Endovascular Aortic Repair*, DOI 10.1007/978-3-319-15192-2_26

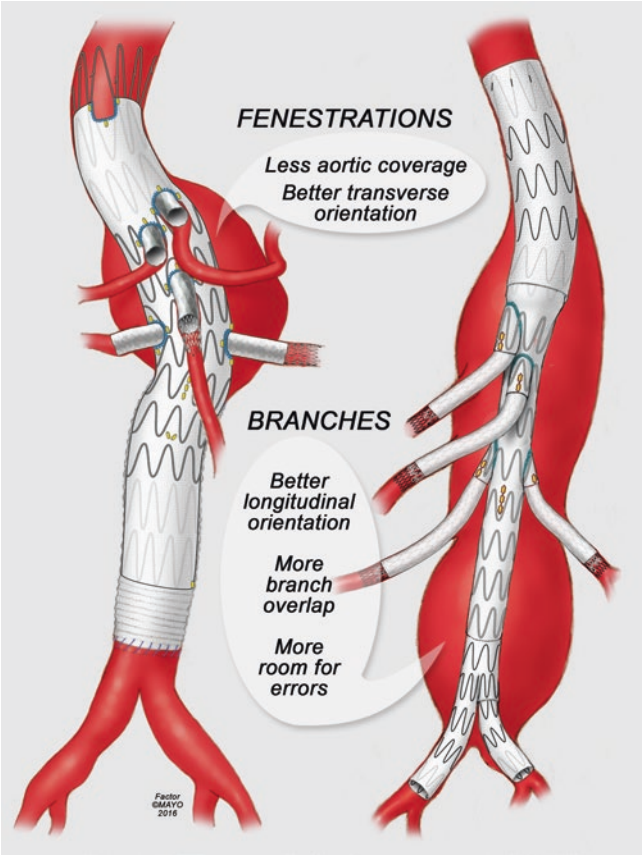


Fig. 26.1 Advantages and disadvantages of fenestrations versus directional branches to treat complex aortic aneurysms. By permission of Mayo Foundation for Medical Education and Research. All rights reserved

Most studies have follow-up limited to less than 1 or 2 years, and none has shown follow-up beyond 5 years or provides anatomical data analyzed by an independent core lab. One of the first studies to raise concern with suboptimal necks comes from the EuroStar registry. Hobo and associates analyzed 5183 patients treated by EVAR, of which 1152 had angulated necks. In that study, patients with >60° neck angulation had more proximal endoleaks (4.9 % vs. 1.9 %) and experienced more device migrations (1.6 % vs. 0.8 %). After a short mean follow-up of 20 months, there were more neck dilatations, more type Ia endoleaks and more secondary interventions, independent of which specific stent was used [6].

Neck length is the most studied anatomical surrogate for neck quality. Buth et al. reported in the EuroStar registry that type Ia endoleaks occurred in 2.4 % of patients with necks >15 mm, 3.2 % in those with necks 10–15 mm and 11 % in those with necks 5–10 mm. There were more systemic complications and deaths in the shorter neck groups. Subsequently, Leurs et al. reported similar findings in a cohort of 3499 EuroStar registry patients [7]. In addition, short necks are often associated with other hostile features such as angulation, thrombus, or calcification. Bisdas et al. reported on 79 patients treated for hostile necks with EVAR, of which 80 % had short, angulated, and thrombus-laden necks [8]. AbuRahma and associates found that these patients had 11 % rate of type Ia endoleak and 35 % rate of reintervention, as compared to 3 and 15 % for patients with optimal necks, respectively [9].

Neck Dimensions Are Not Stable

Evidence that necks are not stable has been widely reported. It occurs with open and endovascular repair and is independent of the type of stent (balloon or self-expandable) and stent manufacturer. Roadway and colleagues reported neck enlargement in participants of the EVAR I prospective trial. In that study, neck dilatation occurred after EVAR and open repair, with the greatest dilatation 15 mm below the renal artery origin [10]. This was also observed by Oberhuber and colleagues in a study of 46 open surgical and 103 EVAR patients followed for over 3 years. Mean neck diameter enlarged 3 mm in both the open and endovascular groups, leading to reinterventions in 11 and 31 %, respectively [11]. Dilatation is more evident in EVARs done for aneurysms with necks >30 mm in diameter. Arthurs and associates followed 31 patients treated by EVAR for necks >30 mm with placement of Palmaz stents. After a mean follow-up of 53 months, 63 % of the patients had >10 % neck enlargement ocurring 15 mm below the renal arteries [12].

There is evidence that neck enlargement continues to progress even in patients who have shrinking aneurysm sac. Kaladji and associates followed 61 patients treated by EVAR and compared neck changes in those who had sac regression and those who had sac enlargement. Rate of neck enlargement was identical in both groups, irrespective of sac regression [13]. In addition, neck enlargement does not stop. Tsilimparis and colleagues reported on a cohort of 756 patients enrolled in the prospective pivotal study that evaluated the Cook Zenith endograft. Rate of neck enlargement continues even beyond 5 years after the repair [14].

Rescue Procedures for Failed Necks Are Morbid and Less Effective

Finally, several studies have shown that open surgical explantations of failed EVAR carry substantial morbidity and mortality, averaging 10 % in most reports [15], and that

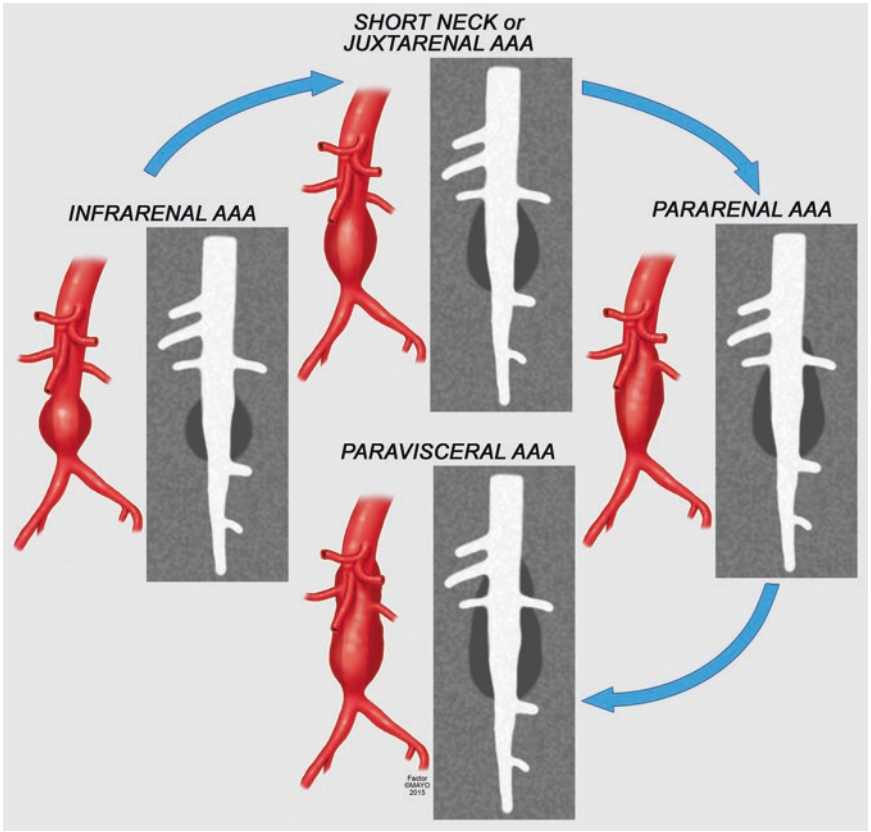


Fig. 26.2 Longitudinal progression of aortic disease cranially into the renal-mesenteric segment of the aorta. By permission of Mayo Foundation for Medical Education and Research. All rights reserved

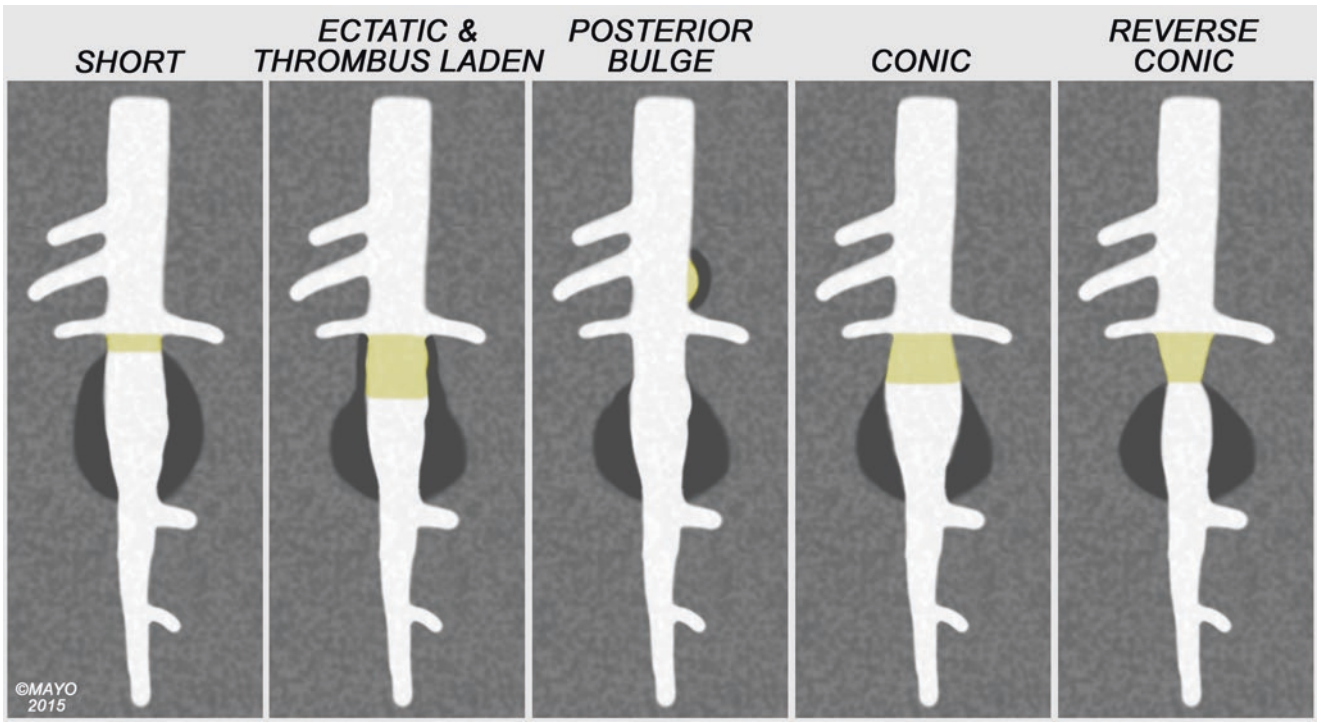


Fig. 26.3 Suboptimal necks for endovascular aortic repair and selection of parallel walled aorta for placement of endograft. By permission of Mayo Foundation for Medical Education and Research. All rights reserved

bail out endovascular procedures such as placement of cuff extensions or chimney grafts are not as effective, potentially leading to more reinterventions, added cost and renal function deterioration. A fenestrated and branched repair after failed EVAR is technically more difficult due to access problems, supra-renal fixation devices and shorter distance between the renal arteries and the neo aortic bifurcation [16]. For these reasons, the first repair needs to be planned with the goal of long-term durability for the lifespan of the patient, well beyond the 5 years mark.

CTA Protocol and Measuring Techniques

Specific protocols of CT scanning and techniques of CLF are discussed in detail in Chap. 11. All patients with aortic pathology need assessment of the entire aorta for preoperative planning, irrespective of the disease extent, or whether the primary problem is an aneurysm, dissection, or other aortic disorder. If a patient had CTA of the abdomen and pelvis, a chest CTA is needed. The importance of a thorough imaging evaluation relies on the incidence of concomitant multi-segment disease and the need to assess the arch for access. If the proximal aorta is not diseased, subsequent CTAs are tailored to image only the relevant anatomy such as the abdomen and pelvis. The non-contrast phase provides valuable information on assessment of calcifications.

The aorta and its branches are evaluated for stenosis or dilatation in the optimal phase of arterial enhancement. This should be done in a systematic manner, usually relying upon the axial images. Scrolling through the axial images, the aorta is inspected first, followed by each of the main aortic branches, including the supra-aortic trunks, the celiac, superior mesenteric artery (SMA), renals, and internal iliac arteries. When pathology is noted and specific measurements are needed, one can rely upon MIP images and the creation of CLF for the assessment of luminal narrowing, and the projection of images perpendicular to the CLF for measurements of the outer wall diameter.

Selecting the Seal Zone

Arteries are cylindrical and have decreasing diameter as they travel distally through the circulation. Disease assessment is performed using surrogates such as changes in diameter or presence of arterial wall abnormalities such as calcium, thrombus, debris or thickening. The vessel wall, in the absence of any pathology, is difficult to accurately quantify on most CT studies. A vessel wall that appears thick or is lined by atherosclerotic debris indicates pathology and should not be selected for sealing zone with few exceptions. Aortic disease moves cranially with progressive involvement of side branches. Therefore, it is common that very large aneurysms have signs of disease affecting the renal and mesenteric arteries, or the aorta in the chest.

CLF studies provide the greatest amount of information when carefully assessing the aorta. The area of aortic dilatation can be readily identified, compared with adjacent segments, and evaluated for specific vessel involvement. Selection of a healthy proximal and distal sealing zone is the single most importance aspect of proper planning to achieve a successful and durable repair. The proximal and distal landing zones must be selected in "normal aortic segments", defined by parallel aortic wall, with minimal or no thrombus or calcification (Fig. 26.3). A minimum length of >2 cm is used, although longer lengths are preferred. Areas that are conic, calcified or thrombus-laden are not considered suitable necks and instead are regarded as part of the aneurysm itself (Fig. 26.4). Longer lengths are needed in tortuous segments, such as in the aortic arch, in patients with familial history of aortic disease, ectasia or thrombus-laden aorta (Fig. 26.5). Because it is critical to assure 360° apposition between the stent graft fabric and aortic wall, the requirement of healthy sealing zone should never be compromised with the idea of planning an "easier" procedure. Of course there are some exceptions, but these should be infrequent, and rarely justified. Acute success, defined by implantation of a graft with no endoleak, is not synonymous of durability; most failures occur between 3 and 5 years after the repair when the neck enlarges.

Supra-celiac sealing zones are preferred whenever possible. Over the last 5 years, most patients with short neck infrarenal or infrarenal aneurysms have been treated by minimum of three fenestrations and a scallop for the celiac axis. For those with paravisceral and type IV TAAAs, four fenestrations have been used. The Cleveland Clinic group has reported extensively on durability of fenestrated grafts, including a higher rate of type Ia endoleak for repairs based on suprarenal sealing zones with renal fenestrations and SMA scallop [17]. For TAAAs, we often select sealing zones of 3 or 4 cm or even longer. In these cases, attention is directed to pairs of intercostal segment arteries. A minimum seal zone of 2.5 cm is selected, but if there are no intercostal arteries immediately above that, the sealing zone is extended proximally until few millimeters below the next pair of intercostal arteries.

Selection of sealing zone is more problematic in the patient who has diffuse aortic ectasia or a thrombus-laden aorta. For example, if a patient has a thoracic aorta that is 4 cm but parallel and the aortic aneurysm enlarges below the level of the renal-mesenteric arteries, treatment of the entire aorta may not be justified given the added risk of spinal cord injury. In these cases, the author's preference is to treat the patient with a 10-cm sealing zone above the celiac axis,

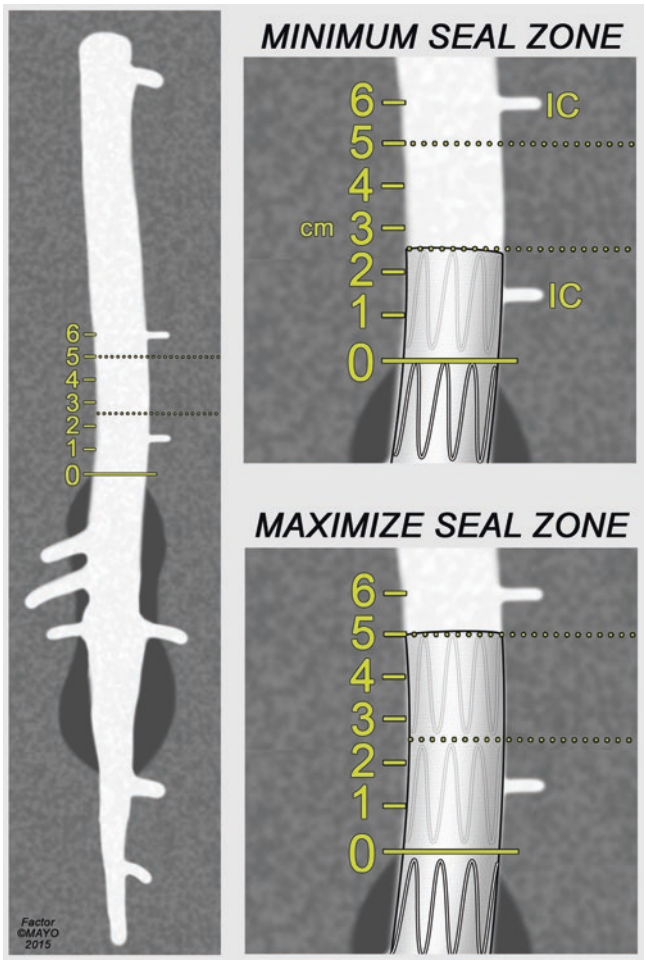


Fig. 26.4 Selection of healthy landing zones. Note that minimum of 2.5 cm is used by the author, ideally in the supra-celiac segment with minimum of double scallop for the celiac axis. Nonetheless, neck is maximized if there are no intercostal pairs in the area. By permission of Mayo Foundation for Medical Education and Research. All rights reserved

allowing enough overlap for future endovascular repair if there is further degeneration. The same approach is adopted for a thrombus-laden aorta. Patients with strong family history of aortic disease (Fig. 26.5) and those with multifocal aortic dilatation and smaller aneurysms in the proximal thoracic aorta also need special attention in selection of sealing zone. In these patients, the author extends the sealing zone above the celiac axis even for short neck or juxtarenal aneurysms, with a minimum of two supra-celiac sealing stents.

Selecting the Access Site

Endovascular repair is most often performed using access via one or both iliofemoral arteries. For complex procedures involving fenestrated and branched endografts, brachial access is needed when directional down-going branches are used. For

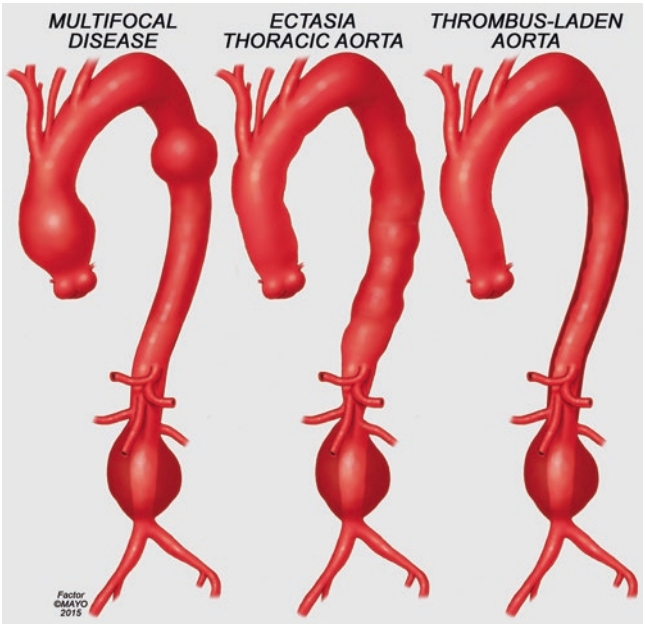


Fig. 26.5 Longer lengths are needed in tortuous segments, such as in the aortic arch, in patients with familial history of aortic disease, ectasia or thrombus-laden aorta. By permission of Mayo Foundation for Medical Education and Research. All rights reserved

four-vessel fenestrated repairs, the author has changed his practice to use brachial access with preloaded catheters that can be accessed from above whenever possible. Difficulties in gaining access can be anticipated based on review of preoperative imaging. An adequate CTA study should image the iliac arteries and the common femoral artery bifurcation. Patients with small iliac artery diameter, severe calcification, stenosis or occlusion, excessive tortuosity or dissection may need iliofemoral conduits. In these patients, the author's preference is to plan a staged conduit whenever possible.

Selection of which side to introduce the main device is dependent on a number of factors including iliac artery diameter, occlusive disease, tortuosity, prior stents or surgical grafts. For most operators who are right handed, the right iliac artery is favored for placement of renal fenestrations, whereas the device is introduced via the left femoral approach. If preloaded renal guides are used, then the device is introduced via the right femoral access. For brachial access, most operators select the left side to avoid the arch, but working from the right brachial access is easier and less cumbersome. Several centers are moving towards routine right brachial artery access.

Selecting the Type of Incorporation

Vessel incorporation can be done with fenestrations and branches (Fig. 26.6). Once the sealing zone has been selected based on normal aorta, the next step in the plan-

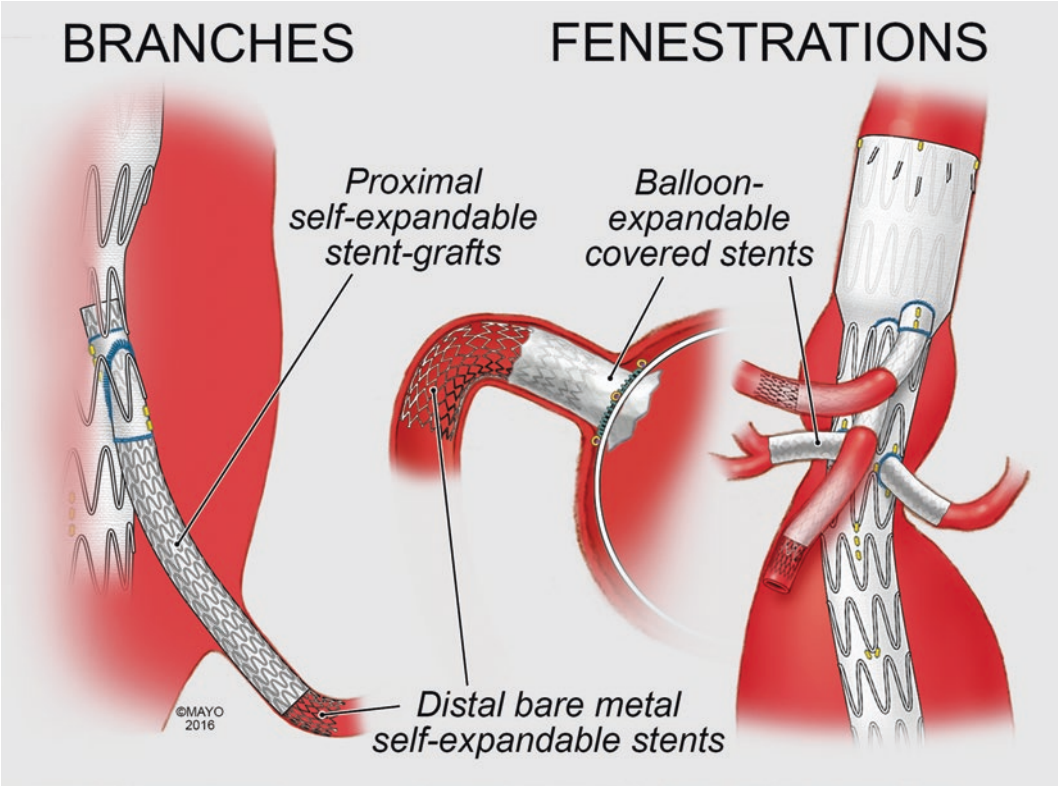


Fig. 26.6 Vessel incorporation using either fenestrations or branches. For directional branches a self-expandable stent is used to bridge the aortic graft to the target, whereas for fenestrations the alignment is done using balloon-expandable stents. By permission of Mayo Foundation for Medical Education and Research. All rights reserved

ning is to identify which vessels need incorporation and which specific type of incorporation will be used. If an off-the-shelf design is contemplated, the anatomy is analyzed for suitability as described in Chap. 27. In nearly all patients treated in our practice, all four vessels are incorporated with a minimum of a double wide scallop for the celiac axis in cases of short neck infrarenal or juxtarenal aneurysms.

There are three types of fenestrations that can be manufactured: small, large, and scallop fenestrations. *Small fenestrations* have dimensions of 6×6 mm or 6×8 mm, do not have struts crossing the middle of the fenestration and are reinforced by a nitinol ring. *Large fenestrations* have dimensions of 8, 10, or 12 mm in diameter and may have stent struts crossing the edge or middle of the fenestration, which limits placement of alignment stents. Large fenestrations of 8×8 mm can be strut free outside the USA or in centers with access to IDE protocols. *Scallops* are openings in the upper edge of the fabric, and are sized as single (10 mm), double (20 mm), or triple (30 mm) wide, with height ranging from 6 to 20 mm in dimension. If a fenestration is selected, the author uses 6×6 mm fenestrations for renal arteries, and 8×8 mm fenestrations for SMA and celiac axis, or double wide 20×20 mm scallops for the celiac axis. In addition, 10×10 mm access scallops may be added for stents designed with preloaded catheters.

Directional branches are either 6 or 8 mm in diameter and 18 or 22 mm in length. Branches can be internal, external, down-going or up-going, and can be coupled with diamond shaped fenestrations to facilitate branch vessel catheterization in narrower aortic segments. As a general rule, if branches are selected, 6 mm branches are used for renal arteries and 8 mm branches for the celiac and SMA.

Selecting Fenestrations Versus Branches

Fenestrations are selected preferentially for vessels that originate from relatively narrow aortic diameters (<30 mm). This is the most frequent type of incorporation used for pararenal and type IV TAAAs (Fig. 26.7), and for more extensive Type I–III TAAAs who have some narrowing at the renal segment (Fig. 26.8). Because patency of renal fenestrations is excellent beyond 5 years with only few occlusions (<3 to 5%), these are particularly

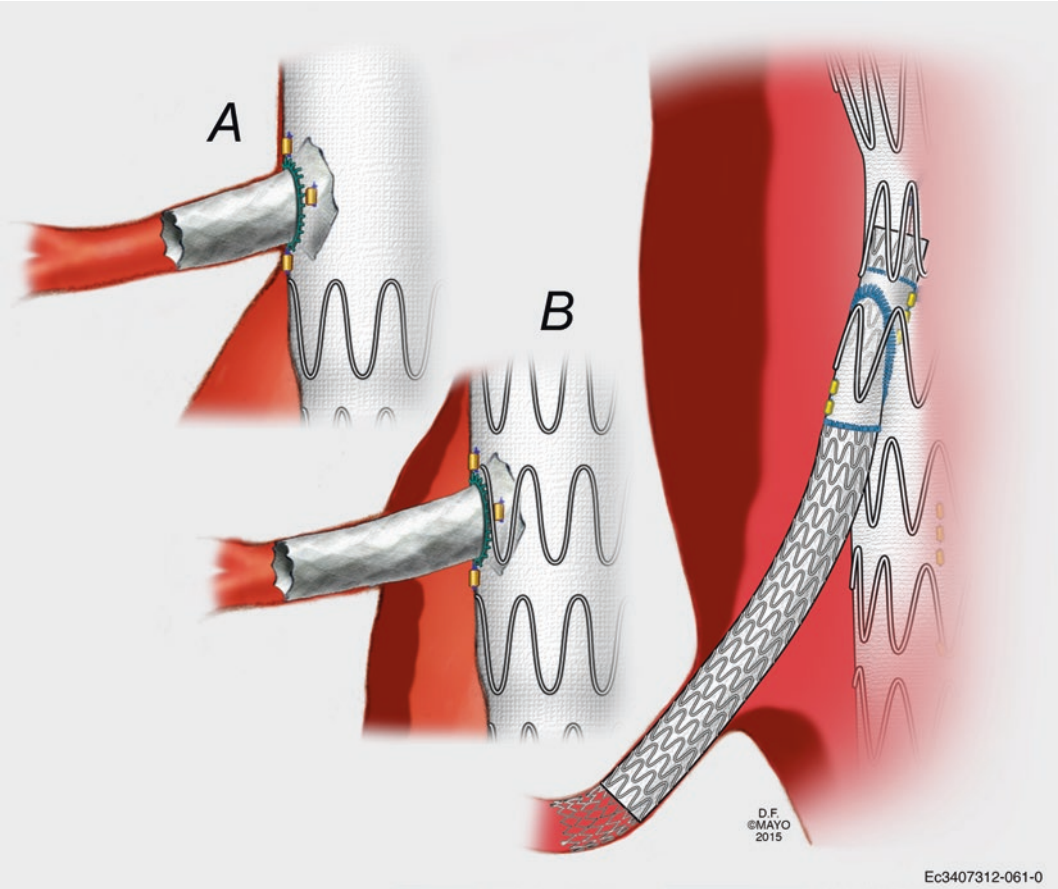


Fig. 26.7 Fenestrations are selected preferentially for vessels that originate from relatively narrow aortic diameters (<30 mm). The term fenestrated repair indicates that the vessel originates from normal aortic diameter (**a**). A fenestrated-branch is needed when there is a gap between the fenestration and target, whereas directional branches use a cuff for attachment (**b**). By permission of Mayo Foundation for Medical Education and Research. All rights reserved

attractive in patients who have significant chronic kidney disease or a single kidney. Fenestrations are ideally suited for transversely oriented vessels like the renal arteries, and for patients who have up-going vessels. This if often the case of patients with type I TAAAs who have predominance of thoracic disease and up-going renal arteries. Fenestrations can also be adapted to smaller vessels such as 3 mm accessory renal arteries, using either bare metal stents or flared covered stents as discussed in Chap. 25. Also, repairs based on fenestrations require less coverage of the thoracic aorta compared to those based on branches.

Branches are used for more extensive TAAAs and are preferred in patients who have larger aortic diameters (>30 mm). These have several advantages over fenestrated grafts, notably easier implantation, better alignment with longitudinally oriented or tortuous vessels (e.g., celiac, SMA, down-going renal arteries). However, because branches originate from a narrow segment of graft (with exception of new internal branches with diamond shaped fenestrations), the repair is extended to the thoracic aorta where the sealing stents are located (Fig. 26.9). Ideally, branches should be positioned with the distal edge 1.5–2 cm above its intended target vessel to facilitate catheterization. If the vessel has particularly difficult anatomy due to occlusive disease, angulation, or tortuosity, longer distances are recommended. Nonetheless, exceedingly long branches (>10 cm) are avoided whenever possible.

Visceral Artery Triangulation

Detailed analysis with centerline of flow and axial measurements is used for accurate sizing and planning of fenestrated grafts. In addition to the vessel location, factors to be considered include presence of occlusive disease, excessive calcification or thrombus, unusual or aberrant anatomy. Small sized, calcified, or multiple renal

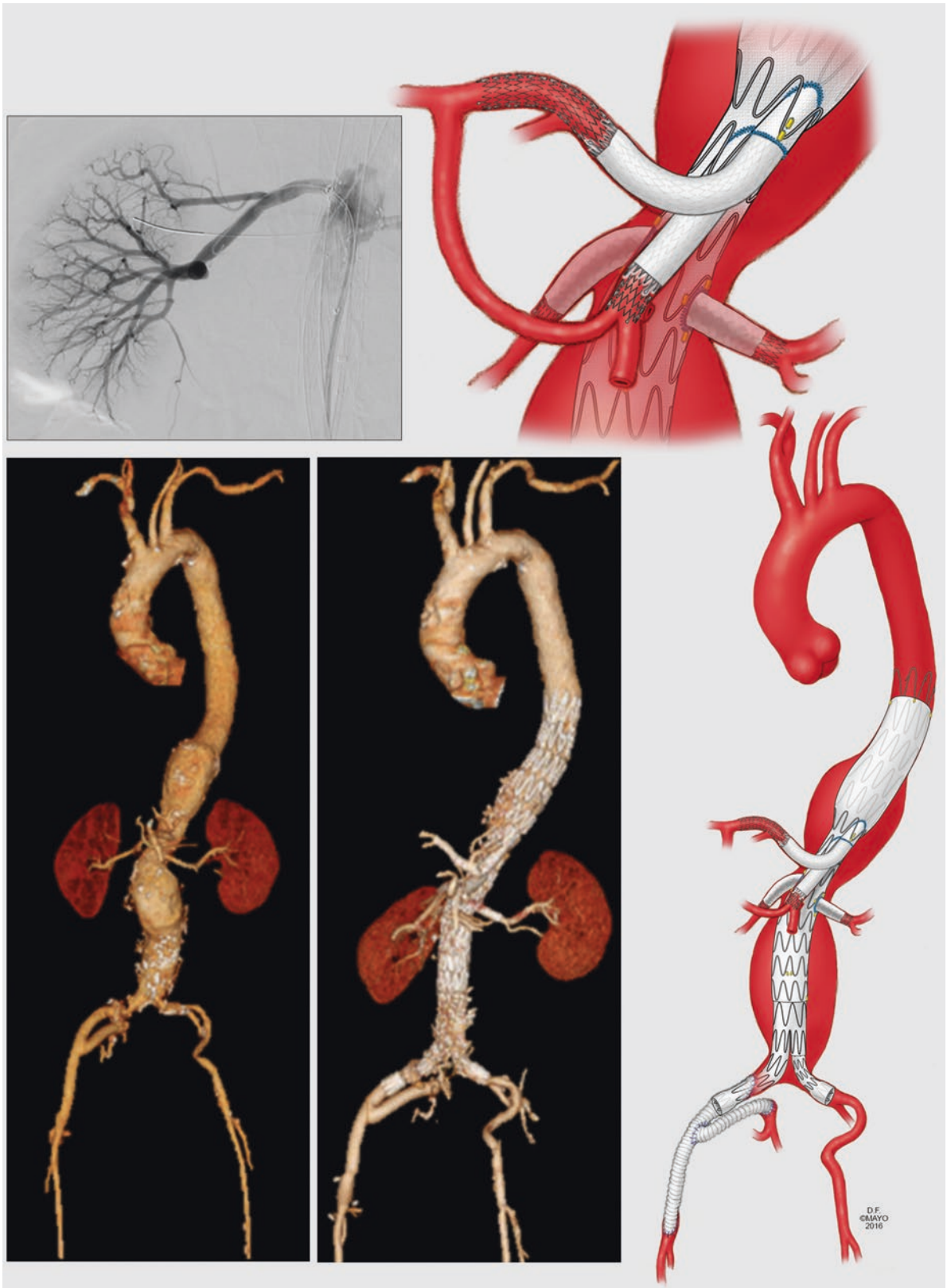


Fig. 26.8 Illustration of a Type III TAAA with narrowing at the renal segment treated with branches for the mesenteric arteries and fenestrations for the renal arteries. By permission of Mayo Foundation for Medical Education and Research. All rights reserved

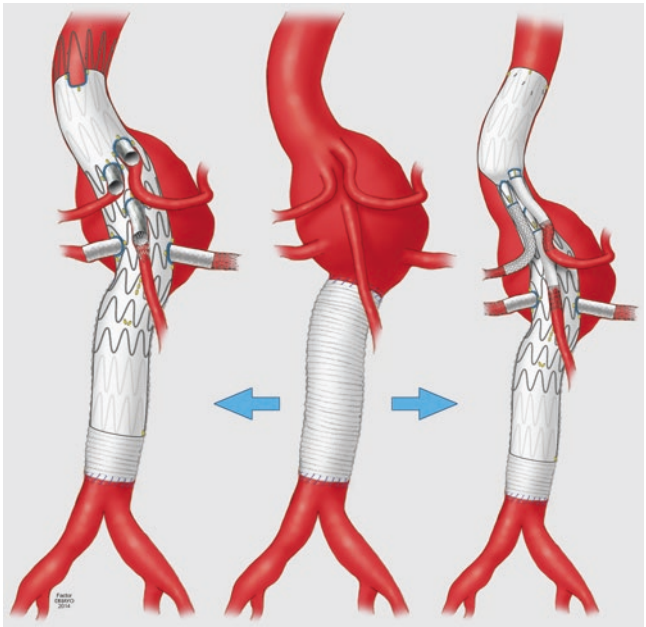


Fig. 26.9 Use of directional branches requires extension of the repair to the thoracic aorta where the sealing stents are located covering more intercostal arteries compared to fenestrations. By permission of Mayo Foundation for Medical Education and Research. All rights reserved

arteries pose a challenge. If an endovascular technique is selected to incorporate a side branch, special attention should be taken to side branch anatomy, vessel tortuosity, adjacent thrombus, or occlusive disease. Independent of which technique is utilized to treat the visceral artery, anatomical factors may significantly impact technical difficulties and method of reconstruction.

Although limited repairs with one or two vessel (e.g., celiac and SMA) can be planned, more often a four-vessel repair is recommended with extension of the landing zone to the supra-celiac segment. Triangulation technique is defined by the relationship of all four renal-mesenteric vessels with respect to length measurements and its axial location in relation to clock position (Fig. 26.10). Each vessel is marked in the middle of the ostia and distances between vessels are measured from center to center. If a vessel is affected by aneurysm at the origin or is very large, the mark is placed 4 mm above the lower edge of the vessel (Fig. 26.11). Distances are obtained from the celiac axis to the SMA and each of the renal arteries. Next, the axial location is identified using clock position and arc lengths (Fig. 26.12). For measurements of arc length, the inner vessel diameter (IVD) and the intended graft diameter at the location of the specific vessel needs to be considered. For example, for a juxtarenal aneurysm where the graft is somewhat oversized in relation to the aorta, the arch length is calculated using the IVD as depicted in Fig. 26.13. However, if a fenestration is planned in a location where the aorta is wider than the diameter of the graft, a corrected IVD of the diameter of the graft minus one is used to calculate the arc length in the graft.

Measuring Location of Fenestrations and Branches

The location of fenestrations and branches is calculated from the top of the fabric. For fenestrations, this distance corresponds to the measurement of the top of the fabric at the anticipated sealing site to the middle of the target vessel (see Fig. 26.13). For branches, the distance corresponds to the top of the fabric to the distal edge of the branch, which is positioned 2 cm above the intended target vessel. Mixed designs with fenestrations and branches may be used. In these cases, the branches often originate from a narrower segment (18, 20 or 22 mm), and the graft flares to a larger diameter in the location of the fenestrations. If the visceral aorta is crowded due to proximity of three or more vessels, combination of branches and fenestrations can be used of offset this limitation and separate the ostia of the vessels (Fig. 26.14). For example, the SMA and celiac may be targeted by branches, leaving the fenestrations for the renal arteries and thereby separating the three vessels.

Graft Tapering

A feature of patient-specific grafts that can be used to facilitate repair is the addition of a tapered diameter to facilitate branch vessel catheterization. This is routinely used with branched grafts and is universally adopted by off-the-shelf designs described in Chap. 27. Traditionally, fenestrations have been based on wider graft diameters to promote apposition between the graft fabric and the aortic wall and the taper is placed below the renal arteries (Fig. 26.15). However, this can cause problems with vessel catheterization and renal ischemia if there is misalignment. It can also result in infolding of the graft if the sealing stent is based on a larger diameter above the celiac axis and the aorta tapers at the level of the renal arteries. To overcome this problem, the author often selects a design with two sealing stents above the middle of the SMA, adding a 20–30 mm tapering of the graft below the SMA, ending the tapered diameter below the renal arteries. Although this tapered configuration may

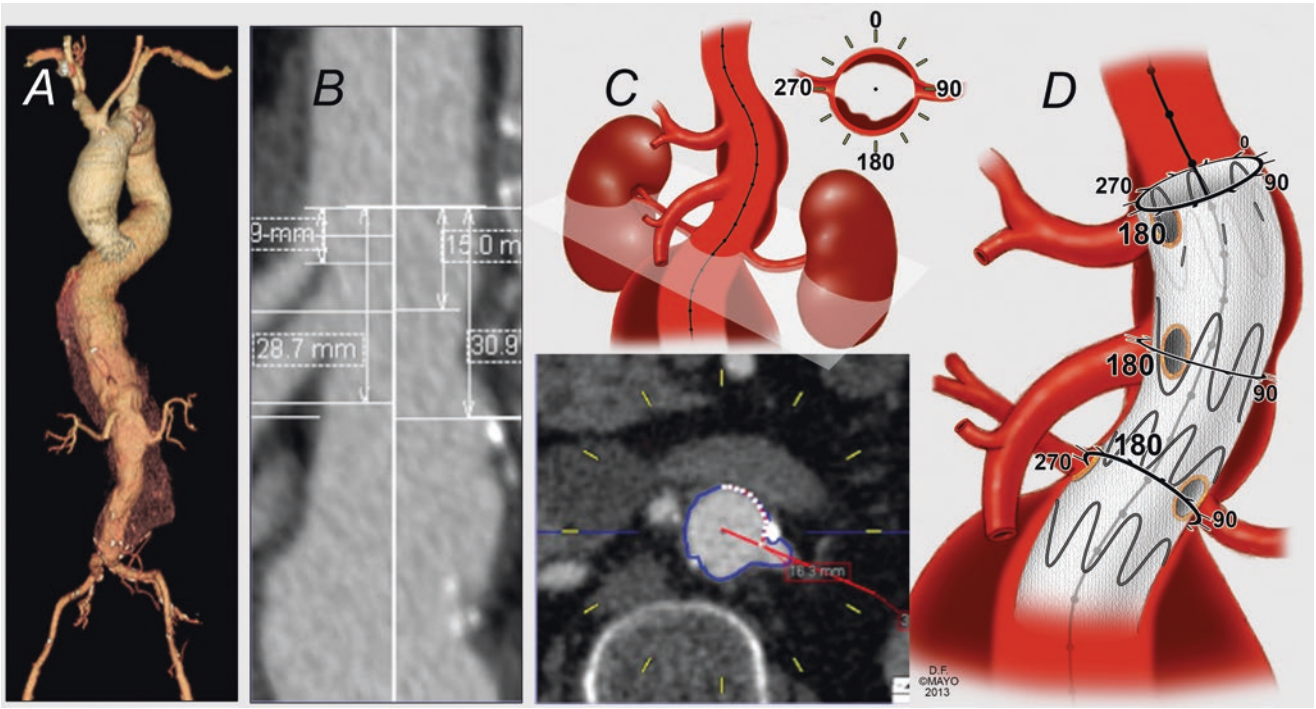


Fig. 26.10 Triangulation technique for measurement of target vessel location. The 3D CTA (**a**) is analyzed using centerline of flow (**b**). Length measurements and analysis of axial cuts (**c**) allow precise location of all four vessels allowing precise design (**d**). By permission of Mayo Foundation for Medical Education and Research. All rights reserved

be associated with type III endoleaks, this has not been observed in the author's experience, and catheterization of the renal arteries is easier with less risk of graft infolding.

Adjuncts to Facilitate Vessel Catheterization

Implantation of fenestrated and branched endografts is a technically demanding procedure with many steps. Therefore limiting the number of steps that are needed to complete placement of a bridging stent is a priority. This can be done by dividing the procedure between femoral and brachial segments, and using preloaded systems for each of these. From the brachial approach, preloaded catheters into the celiac and SMA are added and routed internally to exit via access scallops placed in the top edge of the graft (Fig. 26.16). For the renal arteries, preloaded guide-wire/guide-catheters can be utilized. However, these guide sheaths are 6Fr and measure 90 cm or 110 cm depending on specific design of the delivery system. Although preloaded renal guides eliminate the need to catheterize the renal arteries, the vessel catheterization and exchanges are made more difficult compared to using shorter 7Fr sheaths from the femoral approach. For the novel TAMBE stent and the novel Cook delivery systems, all four vessels can be preloaded with guide-wires that are immediately accessible from the brachial approach.

Special Scenarios

Staged Repairs

Staged repairs are planned for extensive TAAAs, including all type I to II and selective patients with Type III TAAAs. These procedures are typically done at least 1 week before the completion TAAA repair, and usually 4–6 weeks before in patients who have patient-specific devices. As part of the staged repair, any cervical debranching or permanent iliofemoral conduit is done if needed. The proximal sealing zone is selected in the healthy aortic segment in the distal arch (Zones 1–3) or proximal thoracic aorta (Zone 4 or 5). Sealing can also be achieved in a prosthetic graft in patients with prior arch replacement using elephant trunk technique. The graft is tapered to achieve ideally a diameter of 30 mm just above the celiac axis. The distal graft diameter of the proximal thoracic graft should be ideally 30 mm so that the branched graft can be designed with a diameter of 34 mm to sit

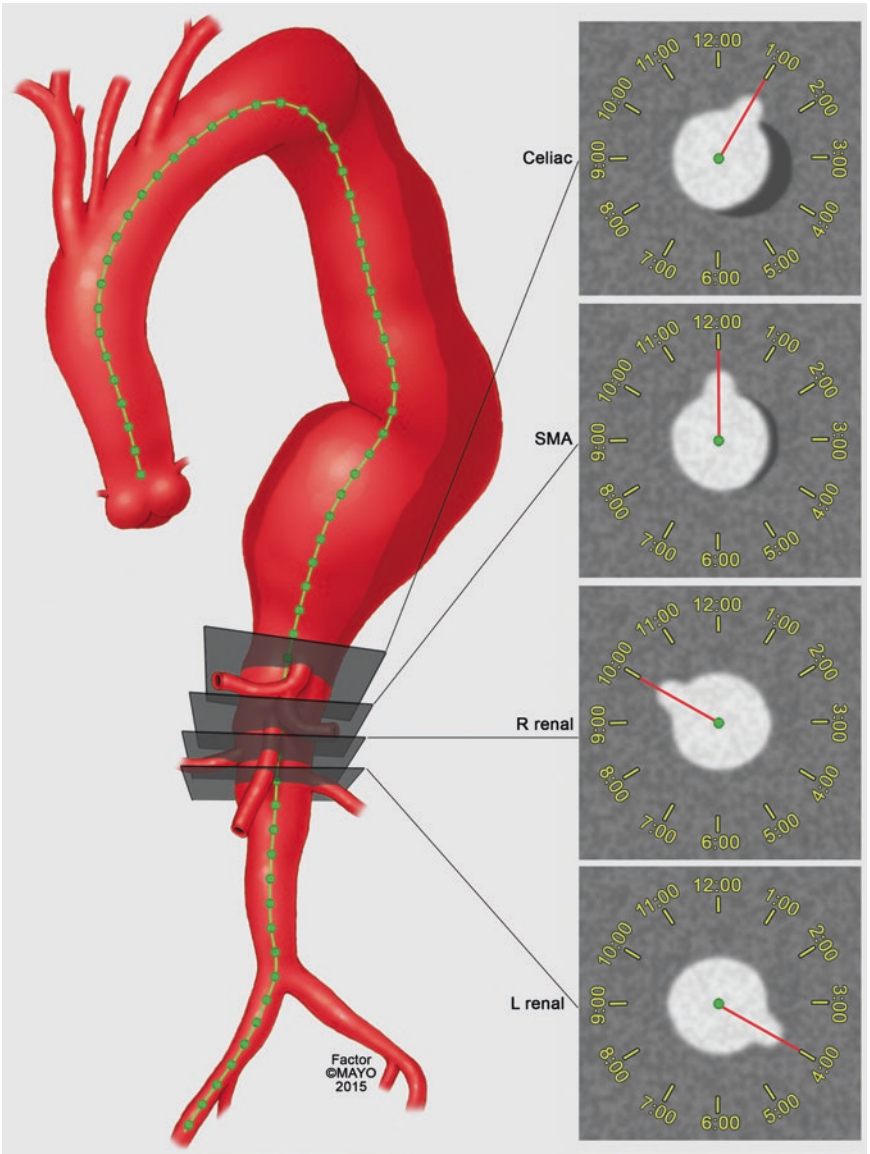


Fig. 26.11 Centerline of flow is used for length measurements, with each vessel marked in the middle of the ostia and analysis of axial location is identified using clock position. By permission of Mayo Foundation for Medical Education and Research. All rights reserved

inside the previously placed graft. Bell-bottom thoracic grafts that flare to 46 or 48 mm have been designed to avoid the distal type Ib endoleak, which is expected and routine with first stage repairs.

Chronic Dissections

Endovascular repair has been increasingly utilized to treat patients with large TAAAs after extensive chronic dissections. In these cases, the location of the target vessel needs to be analyzed with respect to origin from true or false lumen. The other important factor is the diameter of the true lumen in renal-mesenteric segment. In general, any vessel that is perfused primarily by the false lumen has a fenestration in the septum, which corresponds to the origin of the vessel. However, the fenestration may have been sealed by thrombus or can be small, creating an isolated vessel from the false lumen that is perfused by another fenestration located proximally or distally to the vessel. In general, for chronic dissections the authors used a staged approach, first with stenting of the thoracic aorta up to the level of the celiac axis. This allows further expansion of the true lumen and gradual thrombosis of the false lumen in the thoracic aorta. If the true lumen is narrow in the renal-mesenteric segment, the design is based on fenestrations, which originate from an 18 or 20 mm graft (Fig. 26.17), using preloaded catheters or guidewires for access using brachial approach. Branches are selected for cases with large lumen diameter, and are preferred for vessels that are isolated in the false lumen.

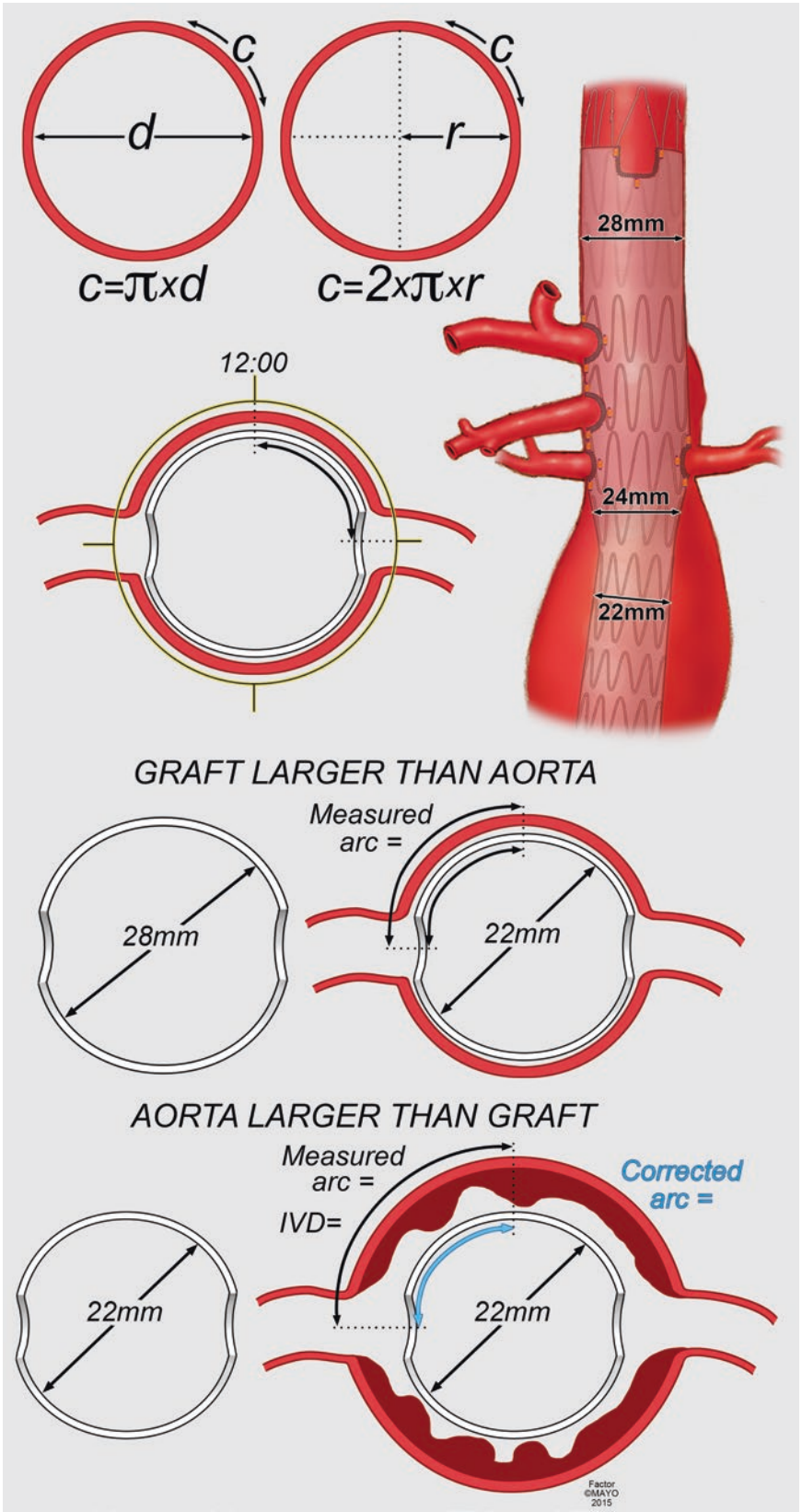


Fig. 26.12 Measurement of arc length is depicted in the illustration. Note that the measurement is made from 12:00' to the center of the vessel origin using an arc. If the graft is larger than the aortic segment, the measurement of the arc in the aorta can be used to create the arc in the stent graft. However, if the aorta is larger, a corrected arc length is needed. In these cases the diameter of the stent minus 1 is used as the inner vessel diameter. By permission of Mayo Foundation for Medical Education and Research. All rights reserved

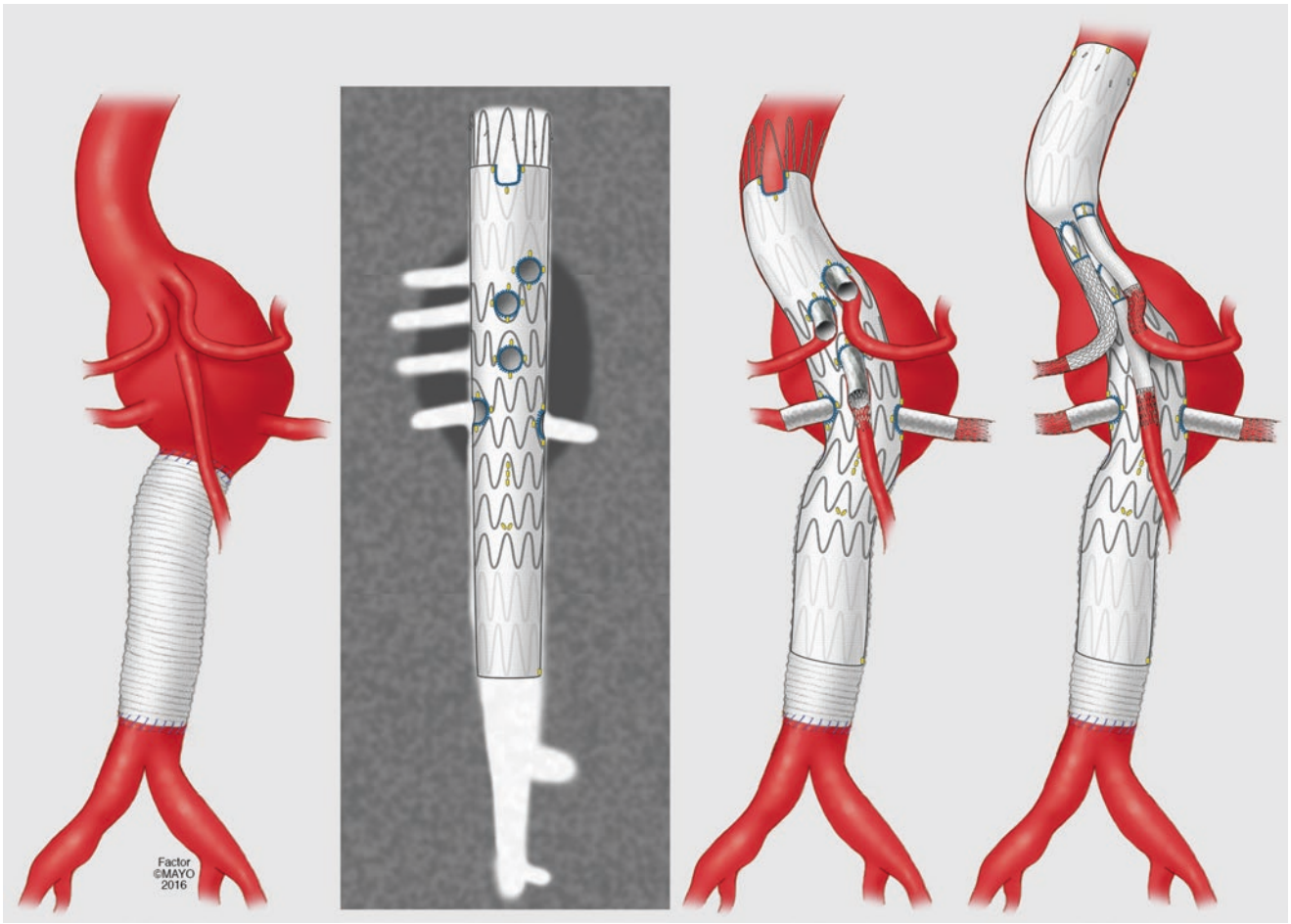


Fig. 26.13 For fenestrations, this distance corresponds to the measurement of the top of the fabric at the anticipated sealing site to the middle of the target vessel. For branches, the distance corresponds to the top of the fabric to the distal edge of the branch, which is positioned 2 cm above the intended target vessel. By permission of Mayo Foundation for Medical Education and Research. All rights reserved

Type I TAAAs

Type I TAAAs have few specific characteristics that need to be considered in the planning, notably the presence of a normal infrarenal aortic segment that is not affected by aneurysm and higher frequency of up-going renal arteries (Fig. 26.18). In these cases, seal is planned with minimum of two sealing stents below the renal arteries, which are targeted preferentially by fenestrations.

Short Distance to Aortic Bifurcation

An increasing number of patients who fail open or endovascular repair need revisions with fenestrated and branch grafts. In these patients, the distance between the renal arteries and the aortic bifurcation is shortened to a few centimeters. If the distance is very short (<3 cm), branches are selected allowing placement of a bifurcated device. Alternatively, a bifurcated device can be designed with an inverted limb, which can be designed with 3, 4 or 5 cm main body.

Conclusion

Design of fenestrated and branched endografts continues to evolve. Repairs changed in the last decade from use of one to two fenestrations to three or four fenestrations (Fig. 26.19). New designs include preloaded catheters and guide-wires to facilitate the procedure. It is critical that physicians performing these procedures have understanding that aortic disease is progressive, and palliative treatment with aortic endografts needs to be planned to minimize late failures from type I endoleak or migration. Repair of a failed fenestrated or branched endograft remains a challenge.

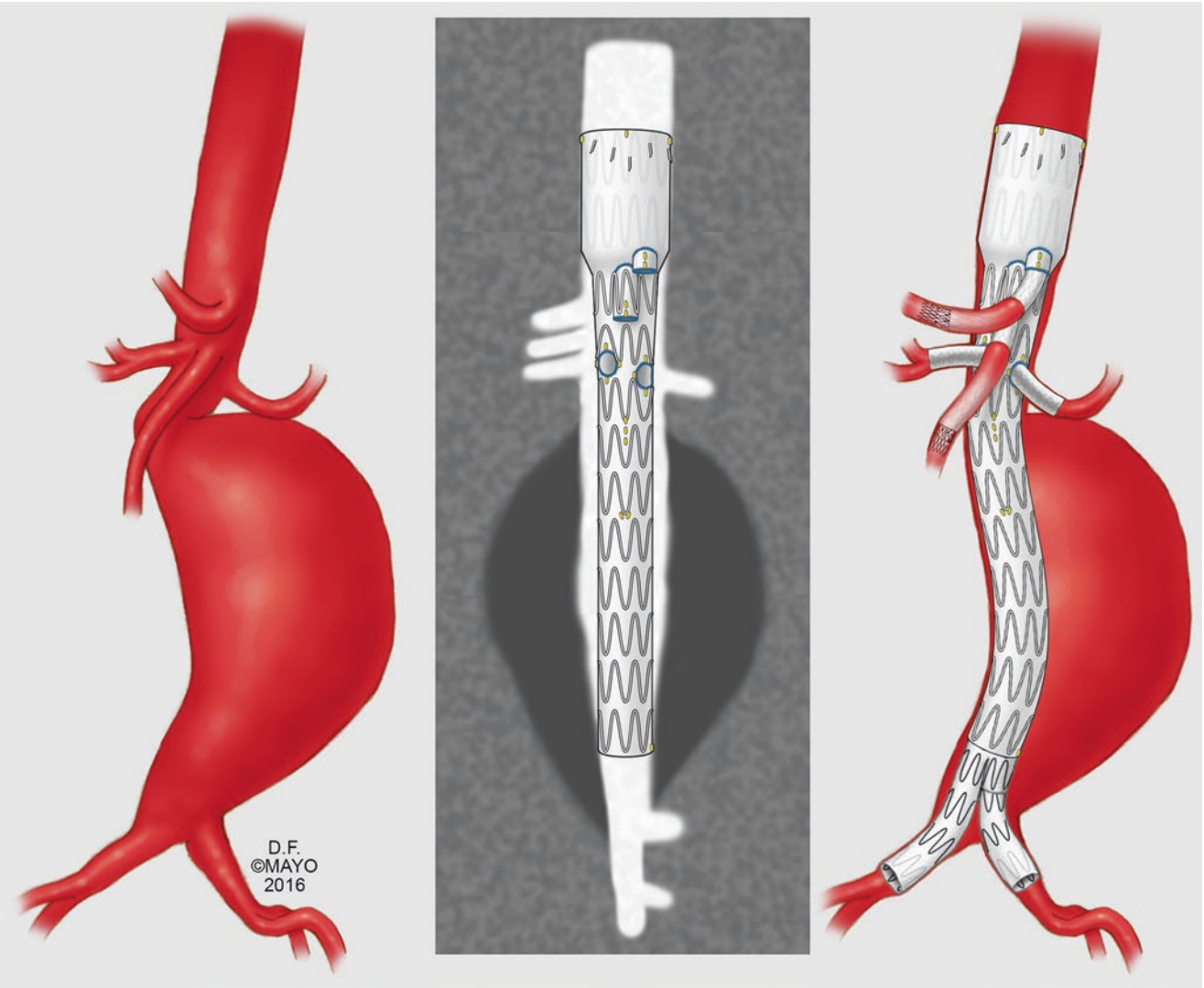


Fig. 26.14 Mixed designs with fenestrations and branches may be used. If the visceral aorta is crowded due to proximity of three or more vessels, combination of branches and fenestrations can be used of offset this limitation and separate the ostia of the vessels. By permission of Mayo Foundation for Medical Education and Research. All rights reserved

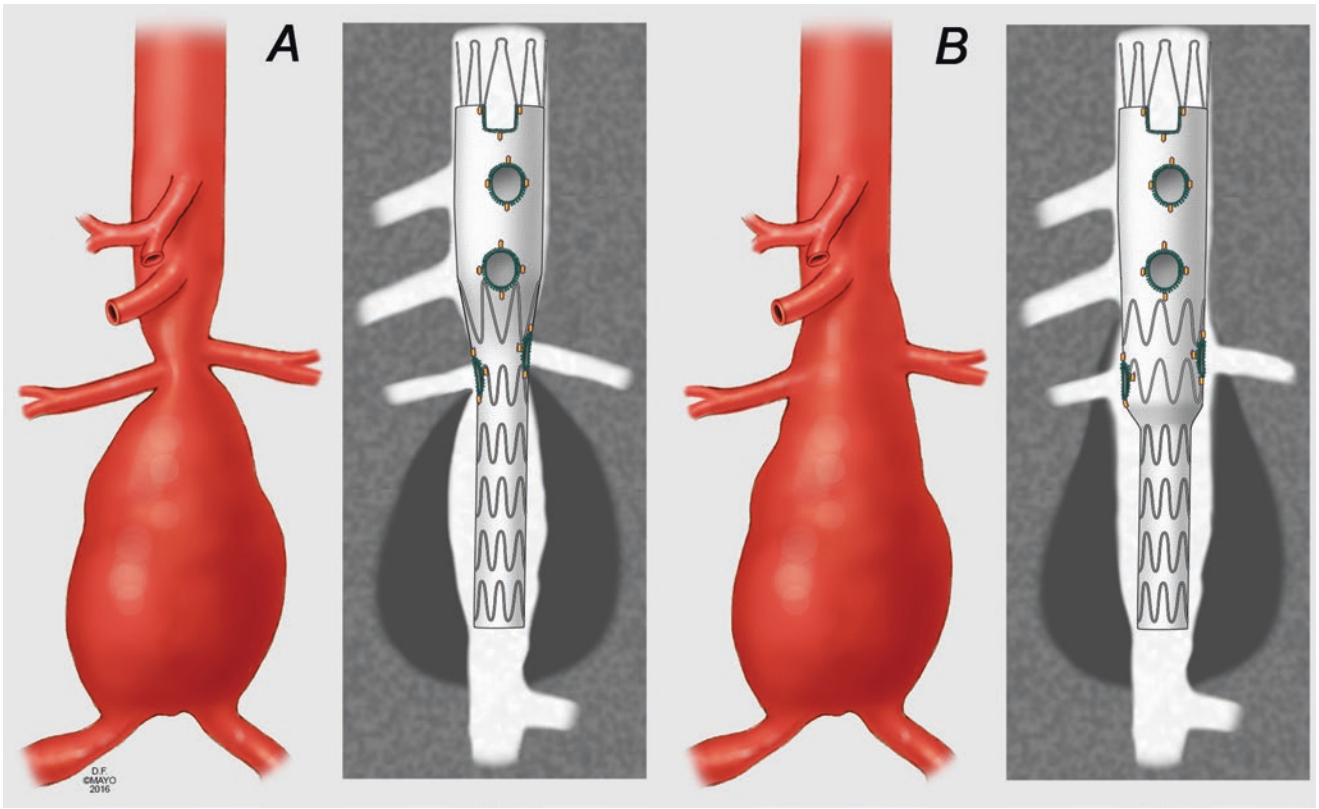


Fig. 26.15 Fenestrations have been based on wider graft diameters to promote apposition between the graft fabric and the aortic wall. Some designs may start the tapered segment in the SMA ending below the renal artevries (**a**) or use the traditional design of rapid tapering below the renals (**b**). By permission of Mayo Foundation for Medical Education and Research. All rights reserved

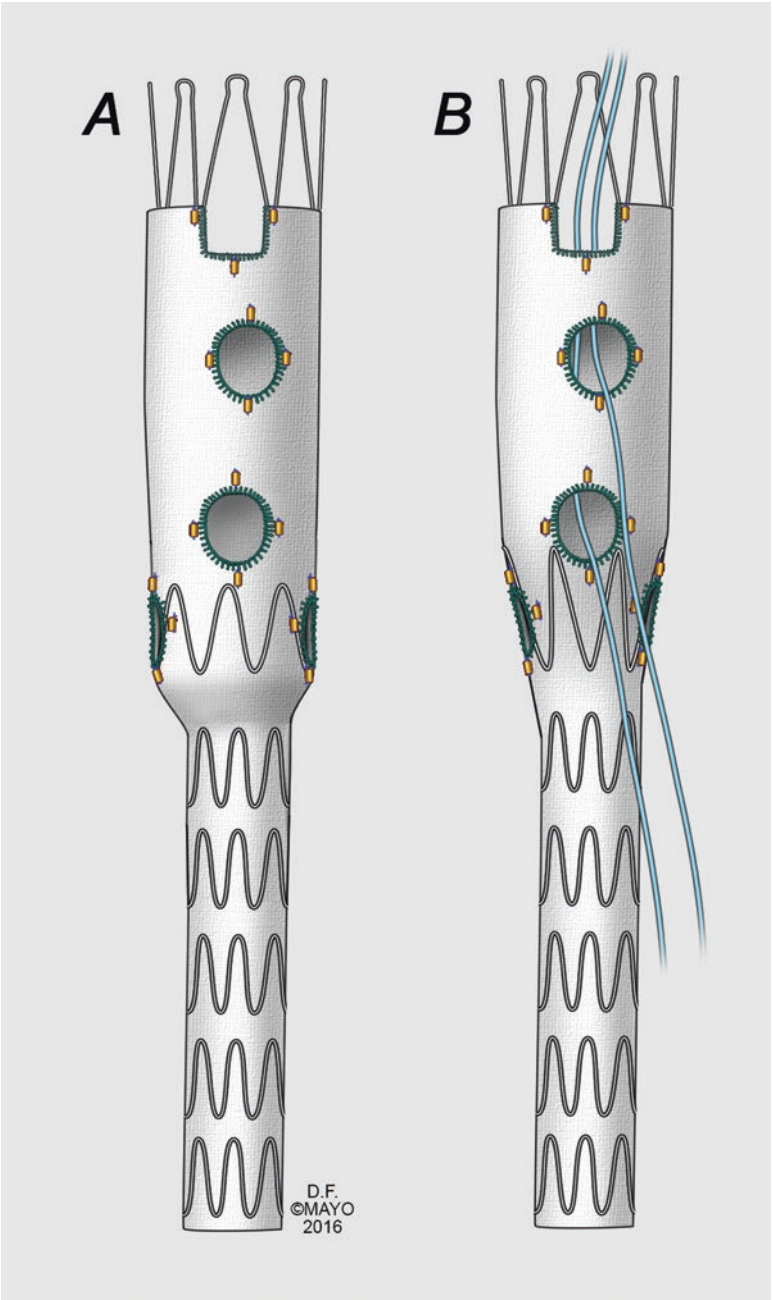


Fig. 26.16 Access scallops can be added in the top of the stent to allow access from brachial approach (**a**). In these cases the operator can advance a catheter from below or preloaded catheters (**b**) can be ordered in the device. By permission of Mayo Foundation for Medical Education and Research. All rights reserved

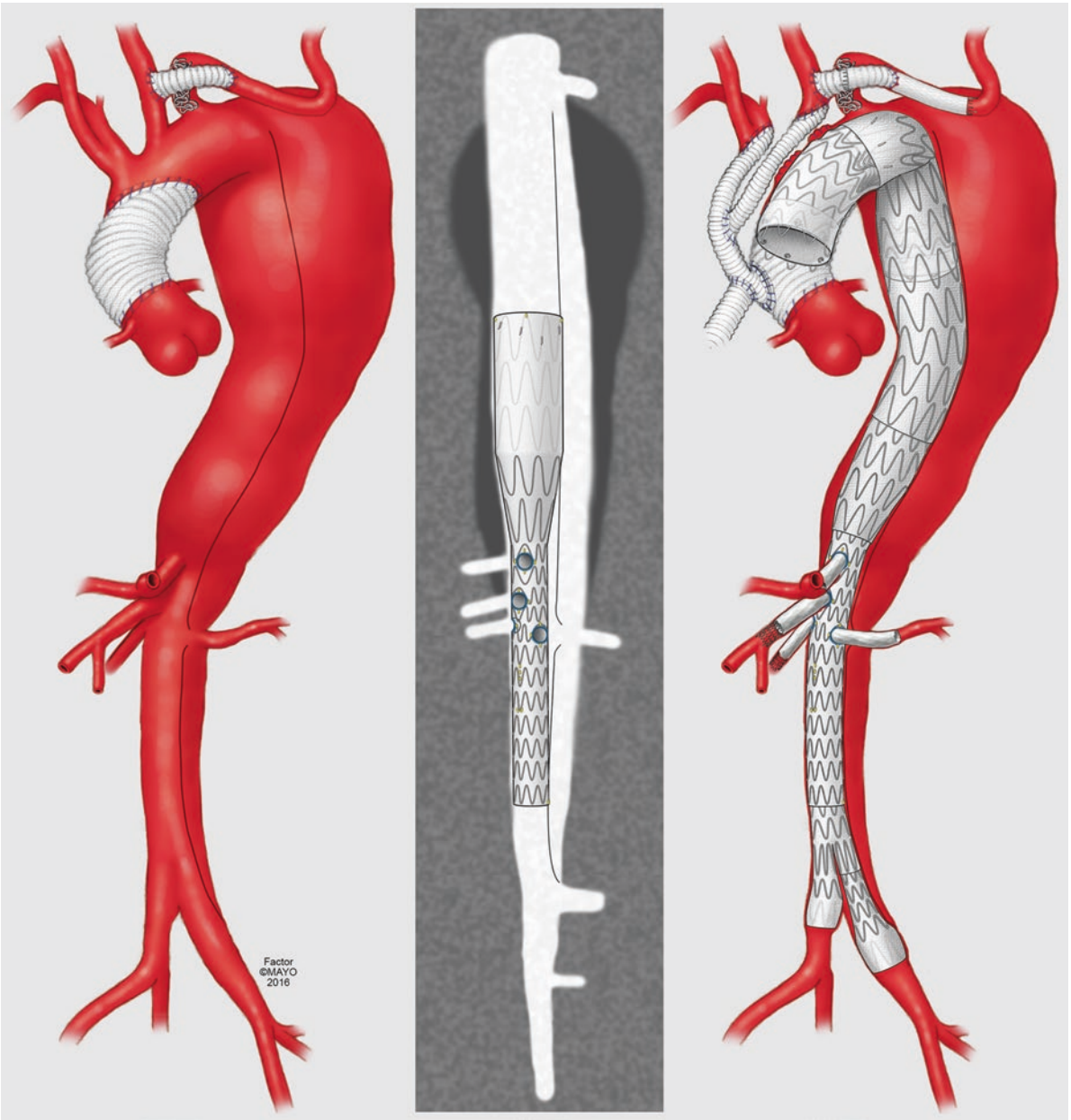


Fig. 26.17 Chronic aortic dissection with compressed true lumen in the renal-mesenteric segment. The graft is designed with fenestrations originating from an 18 or 20 mm graft using preloaded catheters or guide-wires for access using brachial approach. By permission of Mayo Foundation for Medical Education and Research. All rights reserved

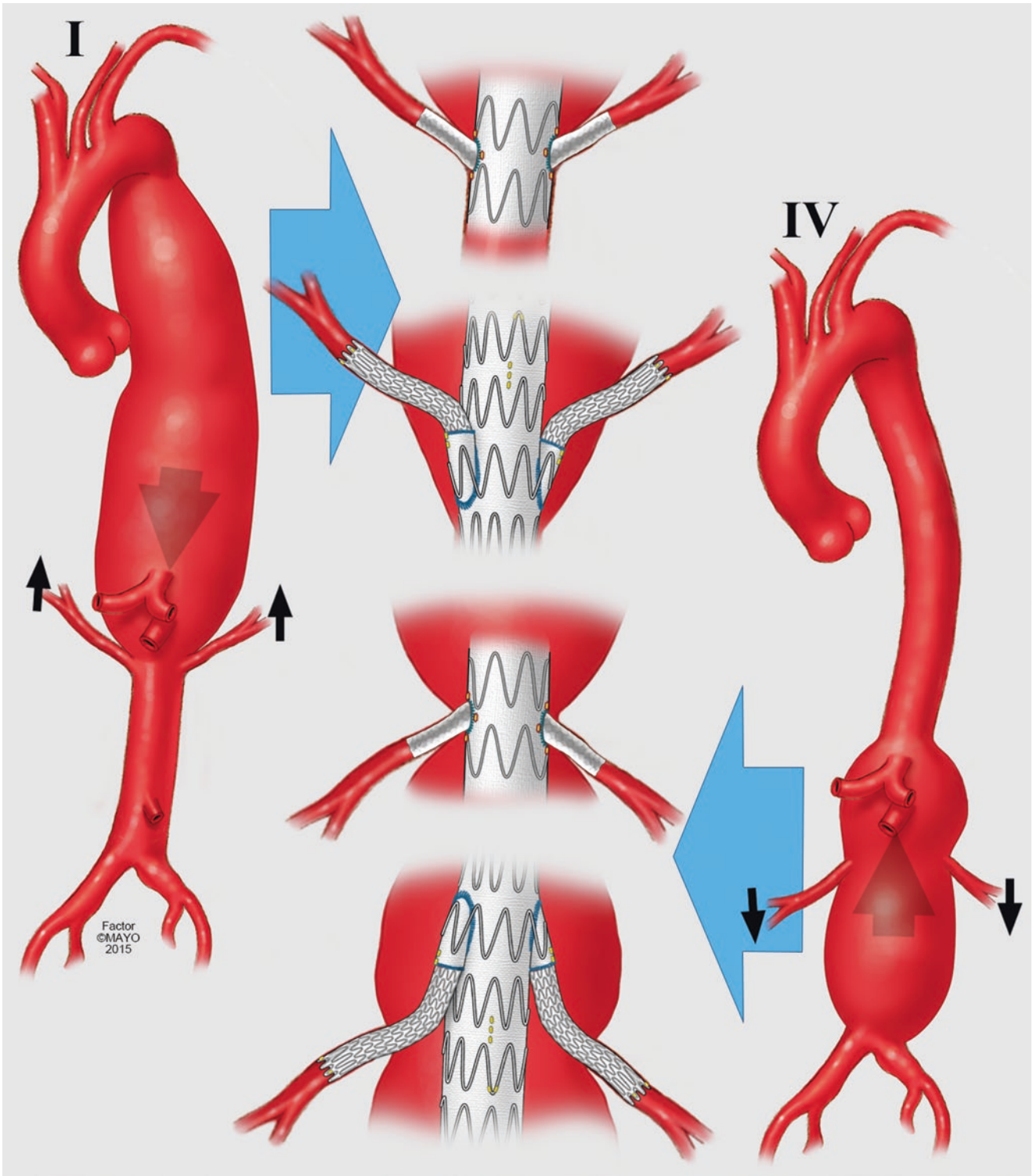


Fig. 26.18 Orientation of the renal arteries and the aortic diameter may dictate choice of fenestrations and branches. In general, fenestrations for the renal arteries are preferred because of superior patency rates. In the example of a type I TAAA the renal arteries are often up-going. The illustration depicts choice of fenestrations for narrow diameter or retrograde branch for wider diameter. By permission of Mayo Foundation for Medical Education and Research. All rights reserved

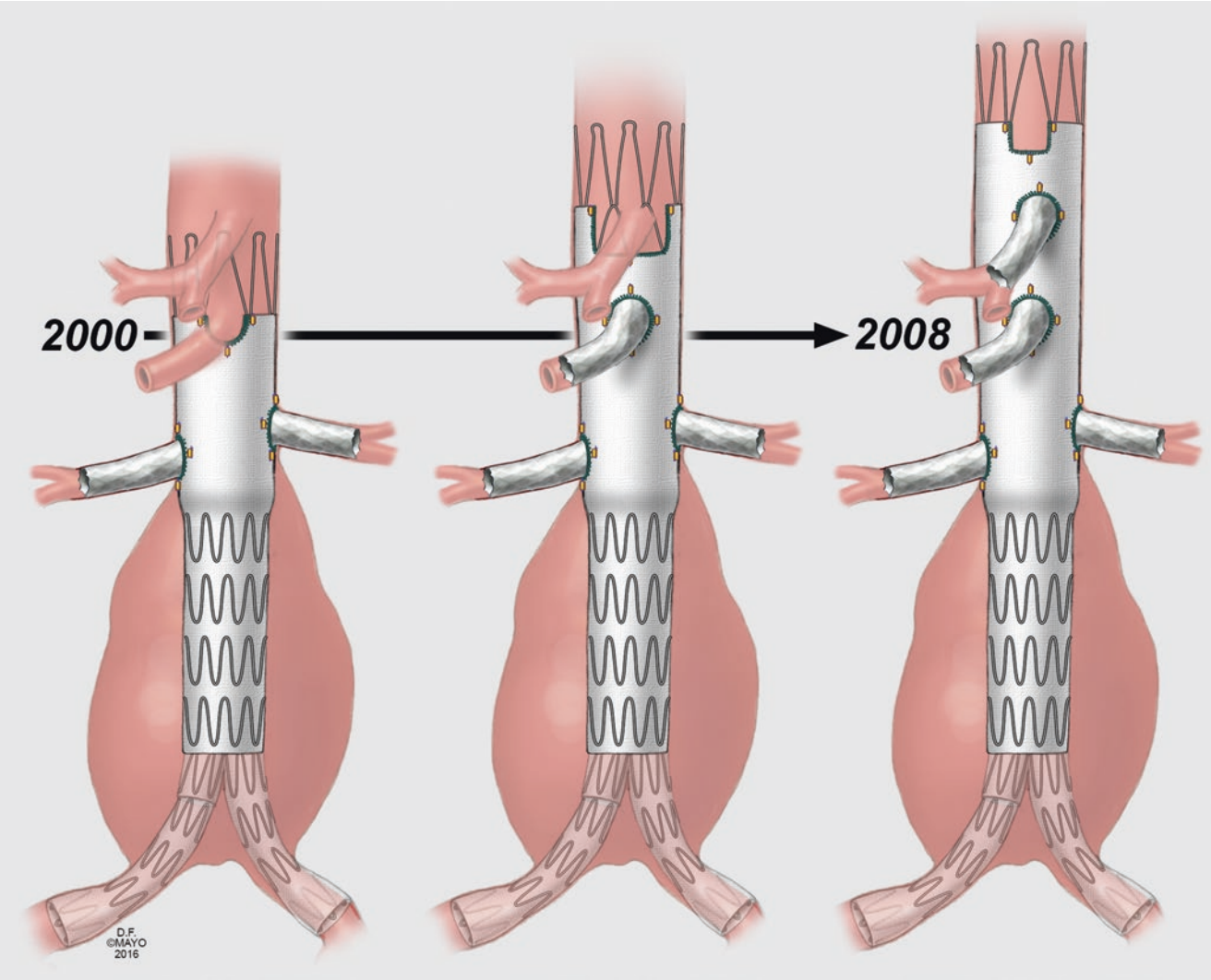


Fig. 26.19 Evolution from two to four vessel designs in the last decade. By permission of Mayo Foundation for Medical Education and Research. All rights reserved

References

1. Oderich GS, Correa MP, Mendes BC. Technical aspects of repair of juxtarenal abdominal aortic aneurysms using the Zenith fenestrated endovascular stent graft. J Vasc Surg. 2014;59(5):1456–61.
2. Oderich GS, Mendes BC, Correa MP. Preloaded guidewires to facilitate endovascular repair of thoracoabdominal aortic aneurysm using a physician-modified branched stent graft. J Vasc Surg. 2014;59(4):1168–73.
3. Verhoeven EL, Katsargyris A, Fernandes e Fernandes R, Bracale UM, Houthoofd S, Maleux G. Practical points of attention beyond instructions for use with the Zenith fenestrated stent graft. J Vasc Surg. 2014;60(1):246–52.
4. Majewski W, Stanisic M, Pawlaczyk K, Marszalek A, Seget M, Biczysko W, et al. Morphological and mechanical changes in juxtarenal aortic segment and aneurysm before and after open surgical repair of abdominal aortic aneurysms. Eur J Vasc Endovasc Surg. 2010;40(2):202–8.
5. Timaran CH, Rosero EB, Smith ST, Modrall JG, Valentine RJ, Clagett GP. Influence of age, aneurysm size, and patient fitness on suitability for endovascular aortic aneurysm repair. Ann Vasc Surg. 2008;22(6):730–5.
6. Hobo R, Kievit J, Leurs LJ, Buth J, Collaborators E. Influence of severe infrarenal aortic neck angulation on complications at the proximal neck following endovascular AAA repair: a EUROSTAR study. J Endovasc Ther. 2007;14(1):1–11.
7. Leurs LJ, Kievit J, Dagnelie PC, Nelemans PJ, Buth J, Collaborators E. Influence of infrarenal neck length on outcome of endovascular abdominal aortic aneurysm repair. J Endovasc Ther. 2006;13(5):640–8.
8. Bisdas T, Weiss K, Eisenack M, Austermann M, Torsello G, Donas KP. Durability of the Endurant stent graft in patients undergoing endovascular abdominal aortic aneurysm repair. J Vasc Surg. 2014;60(5):1125–31.
9. AbuRahma AF, Campbell J, Stone PA, Nanjundappa A, Jain A, Dean LS, et al. The correlation of aortic neck length to early and late outcomes in endovascular aneurysm repair patients. J Vasc Surg. 2009;50(4):738–48.

10. Rodway AD, Powell JT, Brown LC, Greenhalgh RM. Do abdominal aortic aneurysm necks increase in size faster after endovascular than open repair? Eur J Vasc Endovasc Surg. 2008;35(6):685–93.
11. Oberhuber A, Buecken M, Hoffmann M, Orend KH, Muhling BM. Comparison of aortic neck dilatation after open and endovascular repair of abdominal aortic aneurysm. J Vasc Surg. 2012;55(4):929–34.
12. Arthurs ZM, Lyden SP, Rajani RR, Eagleton MJ, Clair DG. Long-term outcomes of Palmaz stent placement for intraoperative type Ia endoleak during endovascular aneurysm repair. Ann Vasc Surg. 2011;25(1):120–6.
13. Kaladji A, Cardon A, Laviolle B, Heautot JF, Pinel G, Lucas A. Evolution of the upper and lower landing site after endovascular aortic aneurysm repair. J Vasc Surg. 2012;55(1):24–32.
14. Tsilimparis N, Dayama A, Ricotta JJ. Remodeling of aortic aneurysm and aortic neck on follow-up after endovascular repair with suprarenal fixation. J Vasc Surg. 2015;61(1):28–34.
15. Turney EJ, Steenberge SP, Lyden SP, Eagleton MJ, Srivastava SD, Sarac TP, et al. Late graft explants in endovascular aneurysm repair. J Vasc Surg. 2014;59(4):886–92.
16. Katsargyris A, Yazar O, Oikonomou K, Bekkema F, Tielliu I, Verhoeven ELG. Fenestrated stent-grafts for salvage of prior endovascular abdominal aortic aneurysm repair. Eur J Vasc Endovasc Surg. 2013;46(1):49–56.
17. Mastracci TM, Eagleton MJ, Kuramochi Y, Bathurst S, Wolski K. Twelve-year results of fenestrated endografts for juxtarenal and group IV thoracoabdominal aneurysms. J Vasc Surg. 2015;61(2):355–64.

Limitations for Branch Incorporation and Implications on Off-the-Shelf Designs

27

Bernardo C. Mendes, Mauricio S. Ribeiro, and Gustavo S. Oderich

Introduction

Endovascular repair with fenestrated and branched stent grafts has been demonstrated to be a safe and feasible treatment for patients with complex abdominal aortic aneurysms (AAAs) and thoracoabdominal aortic aneurysms (TAAAs). Results of multicenter experiences and systematic reviews indicate that these procedures can be performed with high technical success and lower mortality and morbidity compared to open surgical repair [1, 2]. Mid- and long-term follow-ups indicate that the rate of branch-related stenosis, occlusion, disconnection, or endoleak is relatively low, averaging 5–15 % in 5 years [2, 3]. Most of these complications can be treated by secondary interventions using local anesthesia and percutaneous techniques. The majority of the worldwide clinical experience has been with patient-specific fenestrated and branched stent grafts using the Cook Zenith® platform [4]. Other designs have been used clinically or under investigation including the Vascutek Anaconda®, Endologix Ventana®, Gore Excluder® Thoracoabdominal Multi Branch Endoprosthesis (TAMBE), and Jotec® multi-branched stent grafts.

Patient-specific devices have several shortcomings; there is a 6- to 8-week time delay for manufacturing, which exposes patients to risk of interval aneurysm rupture and limits the use of these devices to elective treatment of stable aneurysms. Device planning is complex, requiring advanced training and a steep learning curve. Off-the-shelf devices can potentially eliminate several of these constraints by avoiding treatment delays and allowing standardization of manufacturing, planning and techniques of implantation. However, these devices have anatomical limitations and long-term results are not as well established compared to what has been already reported for patient-specific designs. This chapter summarizes the state of the art on off-the-shelf fenestrated and branched stent grafts, with emphasis in anatomic feasibility, limitations, implications for clinical use, and clinical results.

Factors Affecting Design

The two main variables to be considered on design of off-the-shelf stent grafts are cranial extension of the aneurysm and variability in renal-visceral anatomy. Prior studies have shown that investigational stent grafts, including the Cook p-Branch® and t-Branch® (Cook Medical, Brisbane, Australia) and the Endologix Ventana® (Endologix Inc, Irvine, Calif—currently unavailable for clinical use) were applicable to 50–80 % of patients with complex AAAs or TAAAs [5–7]. While some studies demonstrated feasibility in 80 % of patients, these were limited by the inclusion of patients that already had been treated by patient-specific stent grafts. Therefore, these studies excluded patients who were not considered good candidates for an endovascular approach because of clinical or anatomic reasons and were treated by other methods or observed.

Proximal Extension of Aortic Disease

The ability to provide adequate seal is the single most important criteria of any stent graft. This cannot be compromised, particularly when planning a fenestrated or branched repair, where the implications of inadequate seal or progression of

B.C. Mendes • G.S. Oderich (✉)
Division of Vascular and Endovascular Surgery, Mayo Clinic, 200 First Street SW, Rochester, MN 55905, USA
e-mail: mendes.bernardo@mayo.edu; oderich.gustavo@mayo.edu

M.S. Ribeiro
Department of Surgery and Anatomy, Ribeirão Preto Clinical Hospital, Ribeirão Preto Medical School, University of São Paulo, Campus Universitário s/n, Ribeirão Preto, São Paulo 14048-900, Brazil
e-mail: mribeiro@fmrp.usp.br

© Mayo Foundation for Medical Education and Research 2017

G.S. Oderich (ed.), *Endovascular Aortic Repair*, DOI 10.1007/978-3-319-15192-2_27

aortic disease can jeopardize the entire repair, with few to no options for bail out. Based on prior experiences, most investigators recommend a minimum of 20–25 mm of landing zone, although often necks are much longer than that on contemporary experiences. A 15-mm landing zone can provide acute success, but has already been associated with unacceptable rates of proximal endoleak beyond 5 years of follow up, averaging 10–15 % [8].

Distribution of proximal aneurysm extension has been reported on a review of 520 patients with complex AAAs (Fig. 27.1). In that study the Cook p-branch® (three fenestrations and one celiac scallop) and the Endologix Ventana® (two fenestrations and one SMA scallop) stent grafts were compared. Although the later design is no longer available for investigational use, its concept of two fenestrations based on minimum of 15 mm infra-SMA neck can still be analyzed for future designs. A three-fenestration design allowed adequate seal in all patients with pararenal aneurysms, compared to 61 % if a two-fenestration design is utilized. Because of risk of progression of disease, most large volume users of fenestrated stent grafts are currently planning repairs with four fenestrations in most patients, and a minimum of three fenestrations and a scallop for the celiac axis in patients with short neck or juxta-renal aneurysms. It is logical that a simpler repair (two fenestrations) has shorter operating times and is a simpler procedure, but recent studies indicate that results of 4- versus 2-vessel incorporation are similar in experienced hands, except for more operating time and contrast volume with 4-vessel designs [9, 10].

Renal-Mesenteric Arterial Anatomy

The anatomy of the renal-mesenteric arteries can limit vessel incorporation with any type of endovascular technique. Important variables are vessel location in the axial and longitudinal planes, length, diameter, tortuosity, and presence of occlusive disease. Variations of the 4-vessel anatomy are also important when considering use of an off-the-shelf stent. The renal arteries can be problematic because of multiple accessory anatomy (Fig. 27.2a), early bifurcation (Fig. 27.2b), and small vessel diameter (<4 mm). Catheterization and stenting of renal arteries can be difficult if there is excessive angulation, occlusive disease, or prior renal stents. A recent study demonstrates that nearly 20 % of all patients are not ideal candidates for endovascular repair with fenestrations, branches, or parallel grafts because of these anatomic issues [11]. One-third of the patients also have excessive downward RA angulation, which is optimal for brachial access but can be difficult using femoral approach (Fig. 27.3). Other common limitations are high-grade ostial stenosis or a previously placed renal artery stent. Conway and colleagues evaluated specifically the angles of implantation of the renal arteries according to aneurysm anatomy. In that study, patients with predominance of abdominal disease (e.g., type IV TAAA) more often had a downward orientation of the renal arteries as compared to those with predominance of thoracic disease (e.g., types I TAAA), which had more often a neutral or up-going configuration (Fig. 27.4) [12]. This was corroborated by the Mayo Clinic anatomic analysis. Incorporation of up-going renal

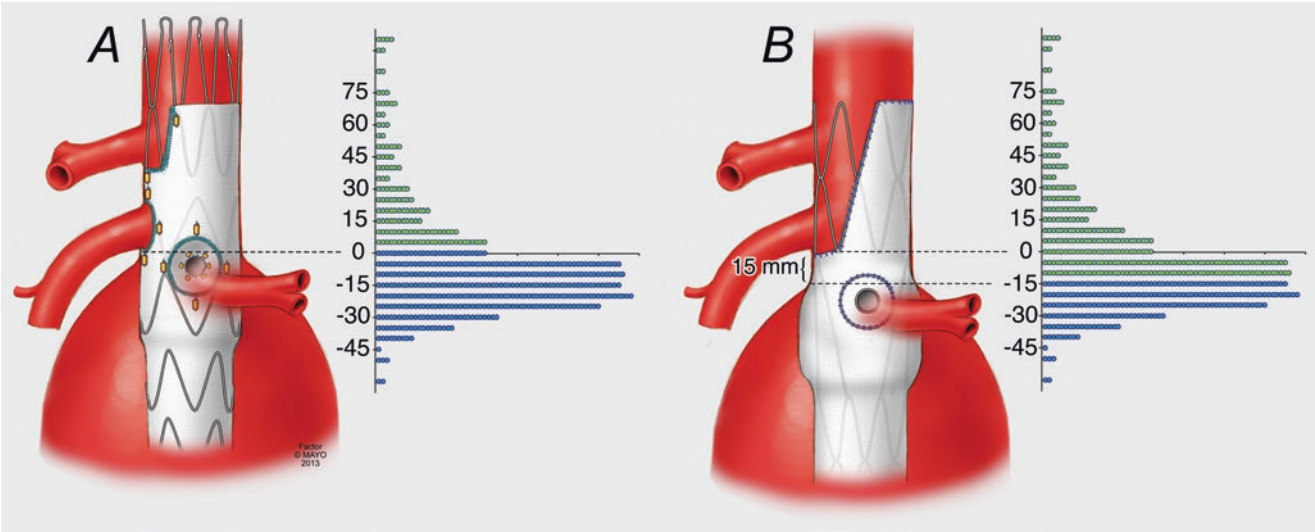


Fig. 27.1 Proximal extension of 520 complex abdominal aortic aneurysms. Each *dot* represents the start of the aneurysm as related to the visceral vessels; *green dots* represent aneurysms which would not be suitable for treatment with the Cook P-Branch (**a**), which requires no neck distal to the superior mesenteric artery (SMA), and the Endologix Ventana (**b**), which requires 15 mm of infra-SMA neck for suitability. Note the large number of patients that would have been excluded with the 15-mm neck requirement. By permission of Mayo Foundation for Medical Education and Research. All rights reserved

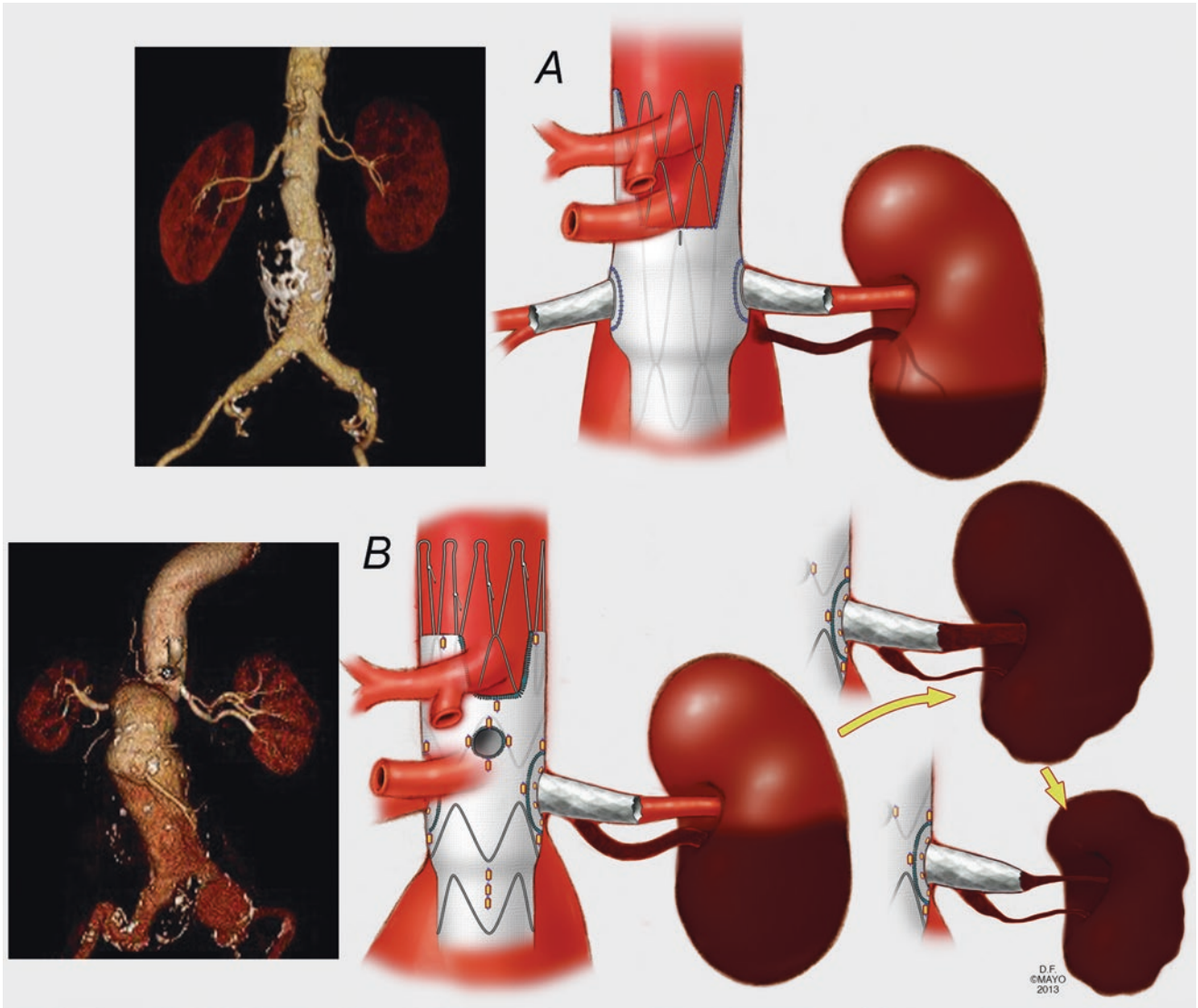


Fig. 27.2 Three-dimensional reconstruction of computed tomography angiography (CTA) on a patient with a pararenal abdominal aortic aneurysm and two left renal arteries of similar caliber. Exclusion of an accessory renal artery can lead to kidney infarction (**a**). Three-dimensional reconstruction of CTA on a patient with early (<13 mm) bifurcation of the left renal artery. Use of a covered stent across the ostium of a large renal arterial branch can also lead to thrombosis and renal infarction; if there is a significant decrease in caliber of the main branch distal to the bifurcation, this branch is in similar manner at higher risk for thrombosis (**b**). By permission of Mayo Foundation for Medical Education and Research. All rights reserved

arteries with down-going branches is not ideal and may lead to kink, stenosis or branch thrombosis. Movement at the distal edge of the stent may lead to development of neo-intimal hyperplasia. Conversely, down-going branches are very well suited for vessels with down-going configuration, which is frequently the case for celiac axis and SMA. Variations in target vessel configuration remain the main limitation to widespread use of off-the-shelf multibranched designs [5].

Variations of 4-vessel anatomy are present in 5–10 % of the patients. These include patients with chronic occluded celiax axis due to median arcuate ligament compression or ostial disease, occluded renal arteries or prior nephrectomy, aberrant hepatic and splenic arteries with origin from the aorta, celio-mesenteric trunks and multiple accessory renal arteries. Some of these variations are flexible to changes in technique, such as coverage of an accessory renal or splenic artery and use of plugs to occlude predesigned branches.

Aortic Angulation

Excessive angulation and tortuosity affects alignment of the sealing stents, fenestrations, and branches. Angulation is

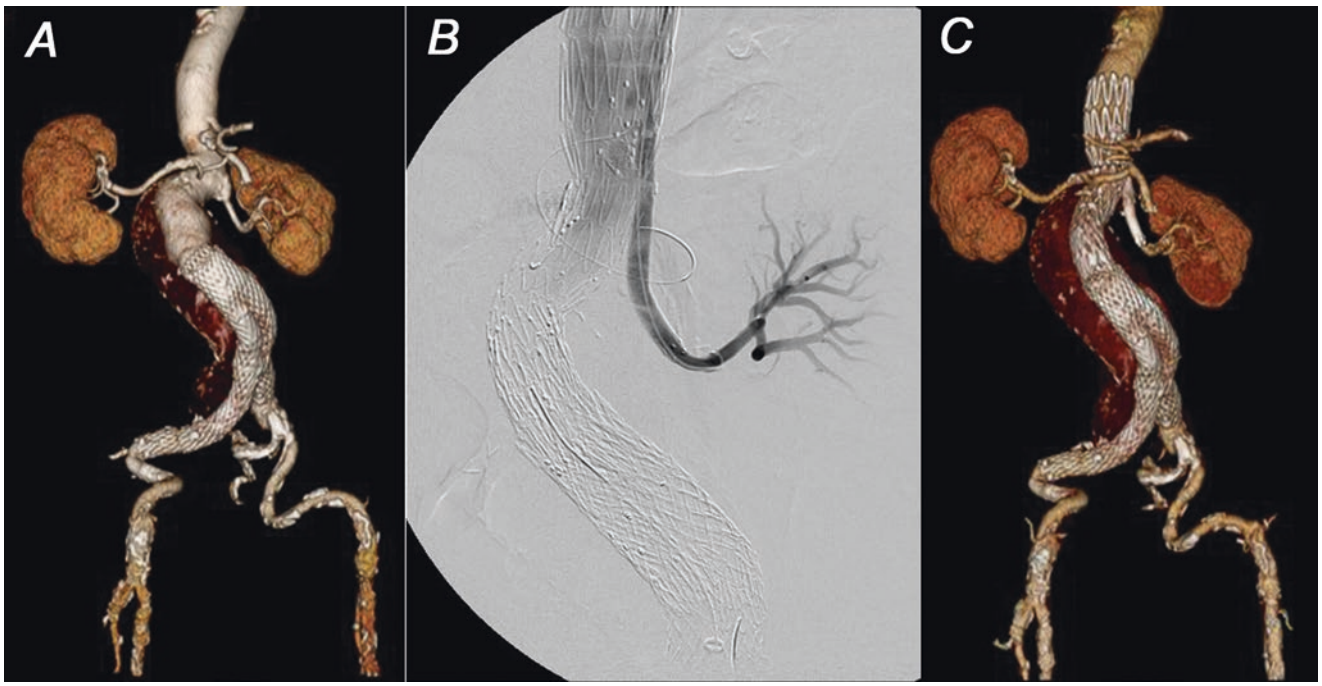


Fig. 27.3 Down-going renal arteries pose significant technical and planning challenges. CTA of a patient with previous infrarenal AAA treatment and type I endoleak demonstrates a down-going left renal artery with its ostium in an angulated portion of the aneurysm neck (**a**). A patient-specific fenestrated-branched stent graft was planned with a down-going internal branch to the left renal artery, which was cannulated via brachial access (**b**). Postoperative CTA demonstrated successful exclusion of the aneurysm and patent left renal branch (**c**). By permission of Mayo Foundation for Medical Education and Research. All rights reserved

often associated with inadequate aortic necks, mural thrombus or calcification that can also compromise seal and pose technical challenges during device implantation. This is particularly important with devices based on fenestrations, because of risk of malrotation and misalignment caused by tortuous anatomy (Fig. 27.5). In the study by Mendes and colleagues, 11% of patients were considered unsuitable because of severe angulation (>60°), according to strict instructions for use (IFU) [5]. Although most patients can still be considered candidates using a liberal IFU, excessive angulation makes implantation more difficult, adds strain into the visceral stents, and may compromise the apposition between the stent graft fabric and the aortic wall. The long-term effect of excessive angulation on patency of visceral branches and endoleak rates has not yet been determined, but prior reports indicate that these patients may be subjected to greater risk of stent fracture, dislodgment, and target vessel loss (Fig. 27.6) [2].

Other Factors

A number of other factors can affect suitability to endovascular repair. These include prior aortic endografts or surgical grafts, short distance between the renal arteries and neoaortic bifurcations, renal and visceral stents, diffuse aortic wall debris ("shaggy aorta," Fig. 27.7), unsuitable iliofemoral access because of narrowing, calcification, tortuosity or prior stents. Several of these factors can be eliminated by adjunctive procedures (iliac conduits, etc.).

Devices

Off-the-shelf stent grafts (Fig. 27.8) can be classified with respect to the intended proximal sealing zone. Stents designed to achieve seal between the celiac axis and renal arteries are intended for aneurysms that abut the renal arteries (e.g., short neck, juxtarenal and pararenal aneurysms), whereas stents designed to achieve seal in the supra-celiac or thoracic aorta are intended for aneurysms involving one or both mesenteric arteries (e.g., paravisceral and TAAAs).

Sealing Between the Celiac and Renal Artery Segment

Two off-the-shelf devices have been investigated for treatment of pararenal aortic aneurysms, the Cook p-Branch® and the Endologix Ventana® stent grafts. Although the Endologix Ventana® stent graft has been discontinued for clinical investigation, we included a limited discussion of its concept which can be applied to future designs.

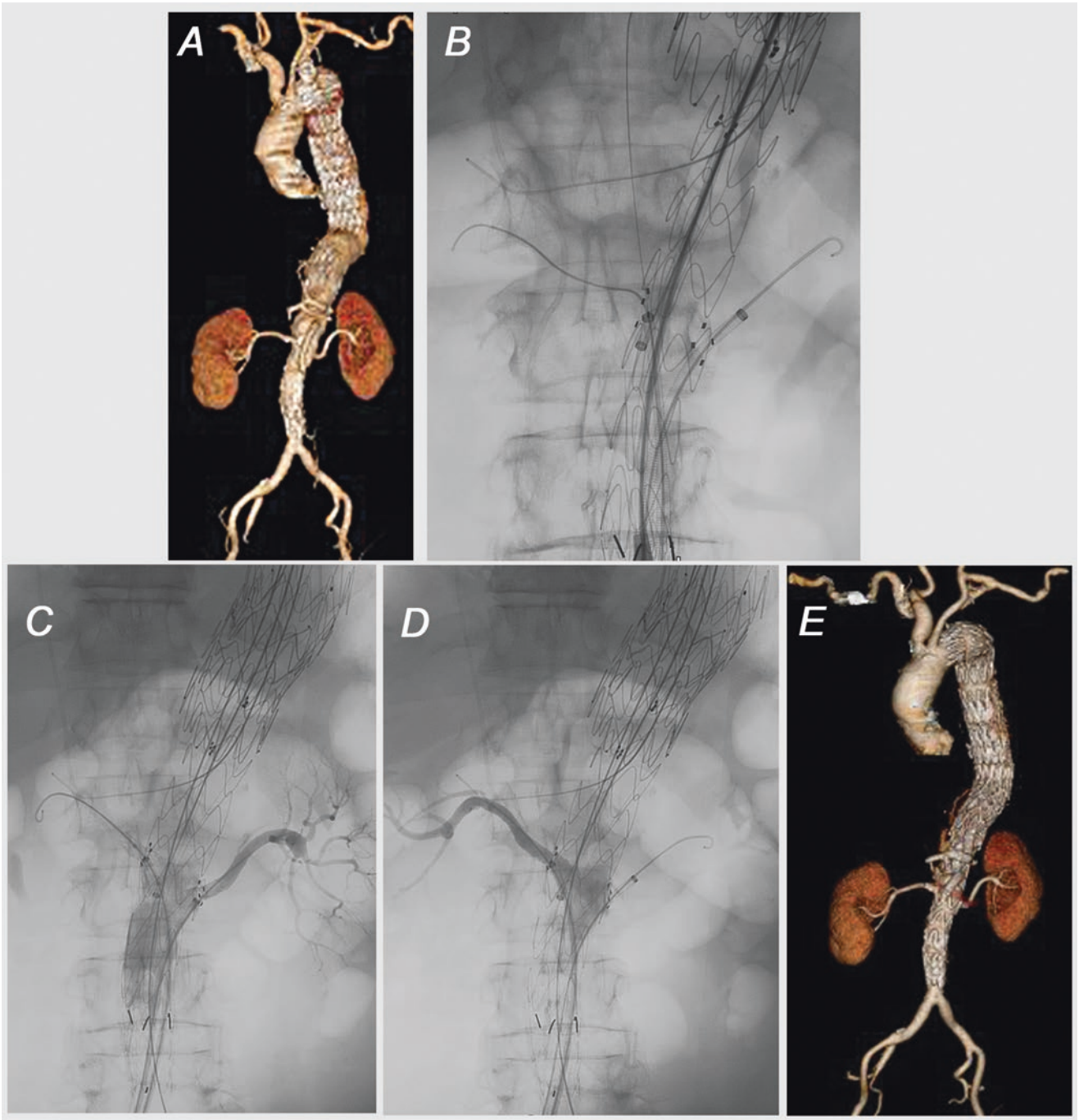


Fig. 27.4 Preoperative CTA of a patient with an extent II thoracoabdominal aortic aneurysm demonstrates up-going configuration of both renal arteries, typically seen in patients with extensive thoracic aortic involvement (**a**). The device was planned with two fenestrations for the renal arteries, which were accessed via femoral approach due to its angulation (**b**). Deployment of bridging stents was performed after confirmation of access in both renal arteries (**c**, **d**). Postoperative CTA demonstrated patent stent graft with no endoleaks and patent stents to celiac, SMA and both renal arteries (**e**). By permission of Mayo Foundation for Medical Education and Research. All rights reserved

Cook p-Branch® Stent-Graft

The Cook p-Branch® stent graft is a modular system with 26–36 mm in diameter. The main component is a tubular device that has a proximal stainless steel uncovered barbed supraceliac stent, followed by nitinol z-stents with one scallop for the celiac axis, one fixed 8-mm strut-free fenestration for the SMA, and two conical renal artery pivot fenestrations. These pivot fenestrations have an outer diameter of 15 mm and inner diameter of 6 mm, and confer the

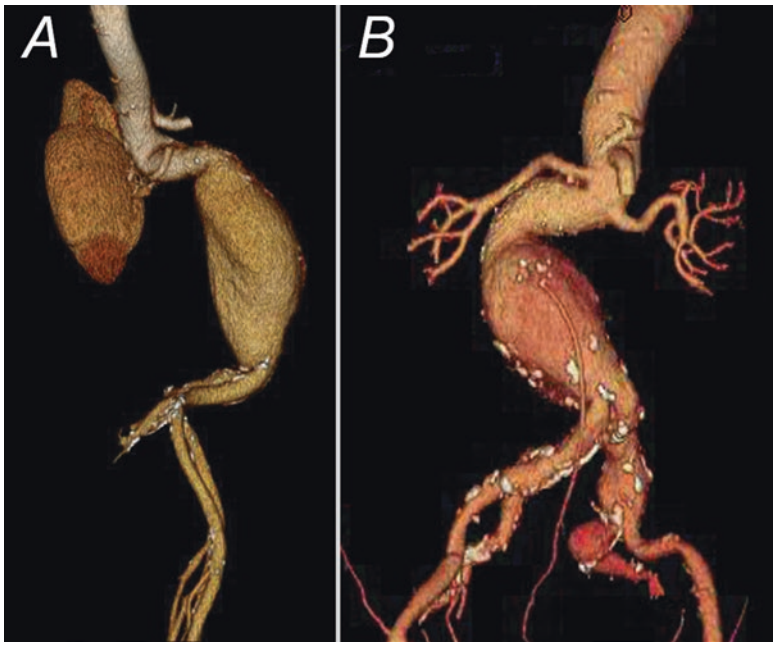


Fig. 27.5 Examples of abdominal aortic aneurysm with anterior (**a**) and lateral (**b**) severe angulation of nearly 90°. By permission of Mayo Foundation for Medical Education and Research. All rights reserved

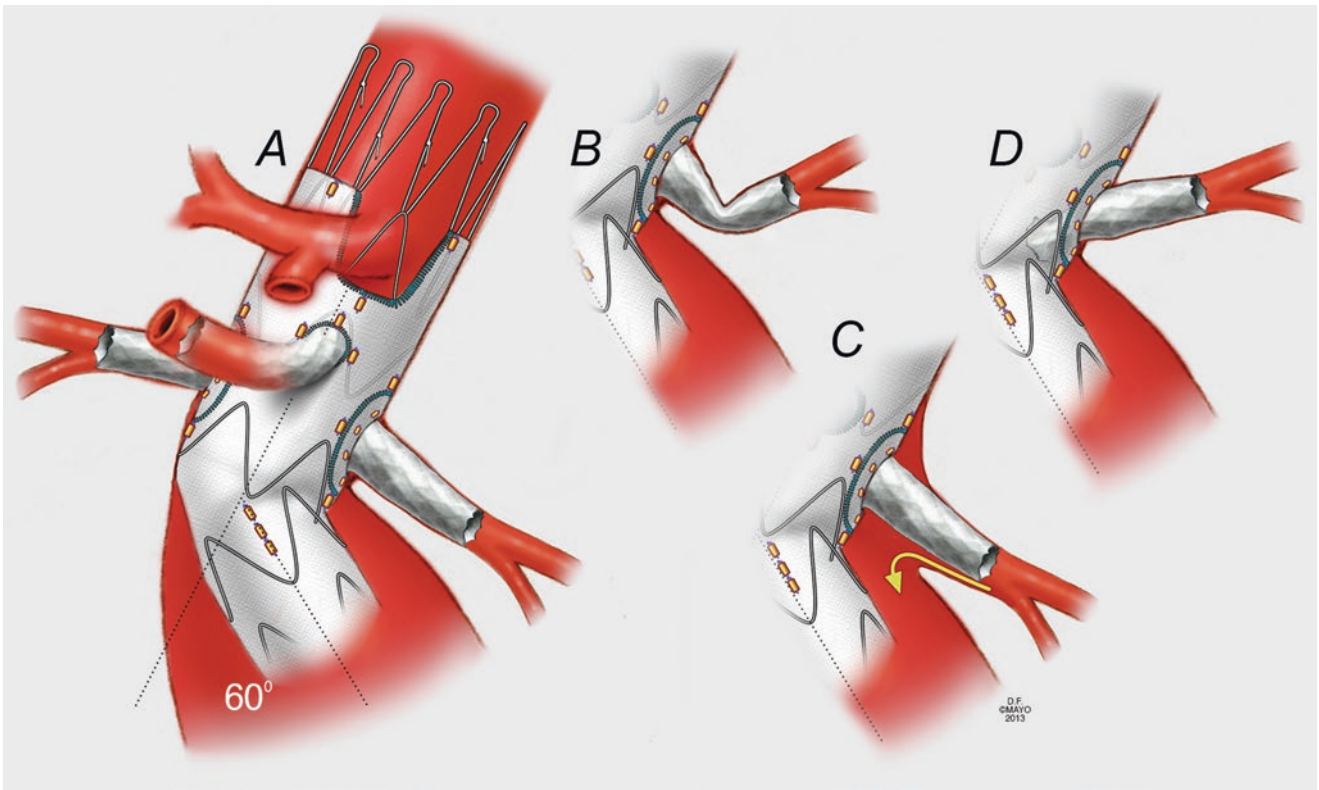


Fig. 27.6 Implantation of fenestrated/branched stent grafts in patients with severely angulated aortic aneurysms (**a**) can potentially cause serious complications, including bridging stent kinks (**b**), endoleak with inappropriate stent apposition (**c**) and encroaching of the bridging stent, which could lead to branch occlusion (**d**). By permission of Mayo Foundation for Medical Education and Research. All rights reserved

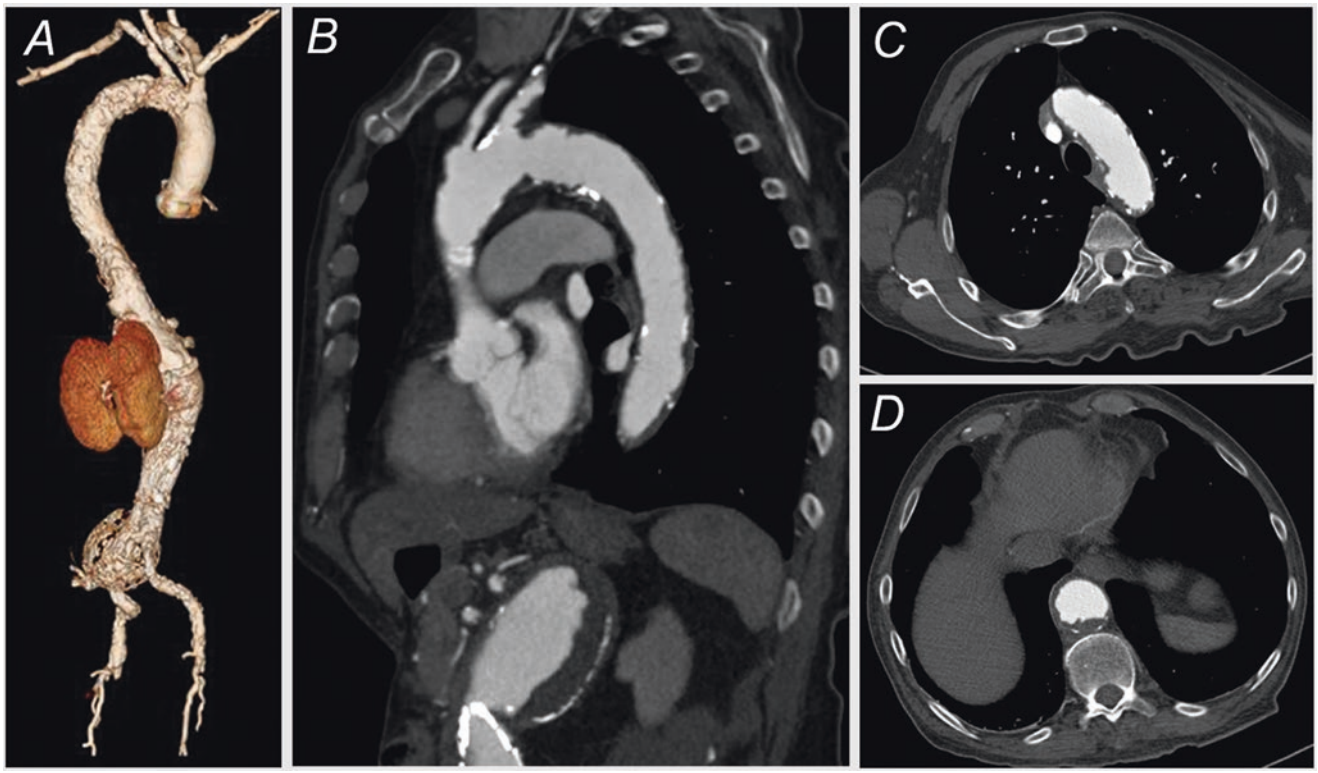


Fig. 27.7 Computed tomography angiogram of a patient with diffuse, severe intramural thrombus (**a**), present in the descending thoracic aorta (**b**), aortic arch (**c**), and abdominal aorta (**d**). By permission of Mayo Foundation for Medical Education and Research. All rights reserved

theoretical ability to catheterize renal arteries within the outer 15 mm diameter while keeping the inner 6 mm fenestration to provide bridging stent seal (Fig. 27.9). Two different renal configurations are available, one with both renals arising at the same longitudinal position (*configuration A*) and one with the left renal artery (LRA) 4 mm caudal to the right renal artery (RRA) (*configuration B*). The device is deployed through a 20-French system. The anatomic feasibility criteria for the p-Branch device, both configurations A and B, are summarized in Table 27.1.

The anatomic feasibility of the Cook p-Branch design has been evaluated by a number of publications. This device is intended to treat aneurysms which originate distal to the SMA origin, with no infra-SMA neck required, given its three-fenestration design. For the US Pivotal p-Branch® study, the neck criteria has been revised to minimum of 15-mm neck below the SMA, which is what was initially applied for the Ventana® trial. The main limitation of this design is renal artery incorporation. Kitagawa and colleagues demonstrated visceral vessel applicability of p-Branch® fenestrations in 75 % of patients treated by custom-made devices [13]. In the analysis by Mendes and associates, a visceral vessel incorporation feasibility of 61 % for the p-Branch® design was demonstrated (Fig. 27.10). The longitudinal distance requirements from the SMA to the right renal (4.5–23.5 mm) and left renal arteries (4.5–27.5 mm) were met by 80 and 86 % of the patients, respectively. These were the two most common factors precluding visceral incorporation with the p-Branch device. When considering all strict IFU criteria for device implantation, that study found that only a third of all patients would be suitable for treatment with the p-Branch stent graft (see Table 27.1); this parcel of patients would increase to nearly half of patients if a more liberal set of criteria was applied, excluding angulation, access related issues and mural aortic thrombus [5].

Endologix Ventana® Stent-Graft

Enrollment in the US Ventana® Pivotal study has been discontinued, but the design concept of two renal fenestrations with one scallop for the SMA can still be analyzed for future considerations (Fig. 27.11). Applicability of steerable fenestrations was 90 % for visceral incorporation, but the ability to provide seal was only 61 % with overall suitability for both in 42 % of the patients.

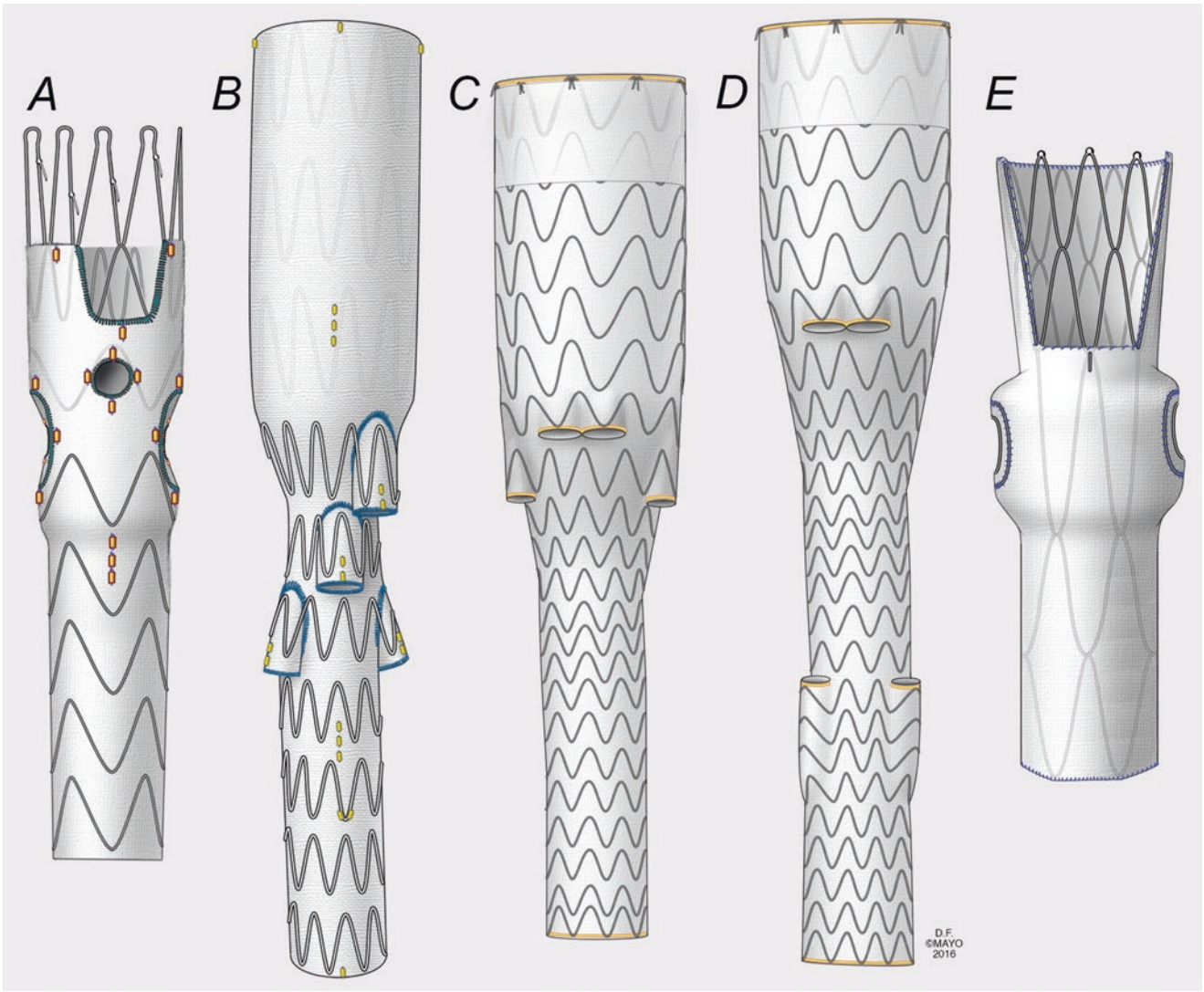


Fig. 27.8 Off-the-shelf fenestrated stent graft designs include the Cook P-Branch, with a scallop for the celiac axis (CA), one fixed fenestration for the superior mesenteric artery (SMA), and two pivotal fenestrations for the left and right renal arteries (**a**); the Cook T-Branch design has four down-going directional cuffs for the CA, SMA and both renal arteries (**b**); the Gore Thoracoabdominal Branch Endoprosthesis (TAMBE) is a modular stent graft with either antegrade (**c**) or retrograde (**d**) renal portals; the Endologix Ventana stent graft is based on a design with a single large cuff to accommodate both CA and SMA, with movable fenestrations to incorporate right and left renal arteries (**e**). By permission of Mayo Foundation for Medical Education and Research. All rights reserved

Sealing in the Supra-Celiac and Thoracic Aortic Segment

Interest in devices with supra-celiac sealing is increasing because of recognition that aortic disease is progressive and that durability beyond 5–10 years needs to take into consideration aortic neck enlargement that follows placement of a stent graft. Adequate balance between extent of repair (e.g. risk of paraplegia and other complications) needs to be weighed against the risks of a less extensive repair (e.g., Type I endoleak, migration and conversion).

Cook T-Branch® Stent-Graft

The Cook t-Branch® stent graft consists of a tapered woven polyester stent graft sutured to a Z-stent stainless steel exoskeleton [14]. The mid-portion of the device contains four short axially-oriented, caudally-directed cuffs for attachment of covered stents which will be the branches for visceral vessel incorporation. The cuffs are situated in the external surface of the stent graft and are based on a relatively predictable location of the visceral vessels as depicted in Fig. 27.12 [6]. The device has a diameter of 34 mm at the top

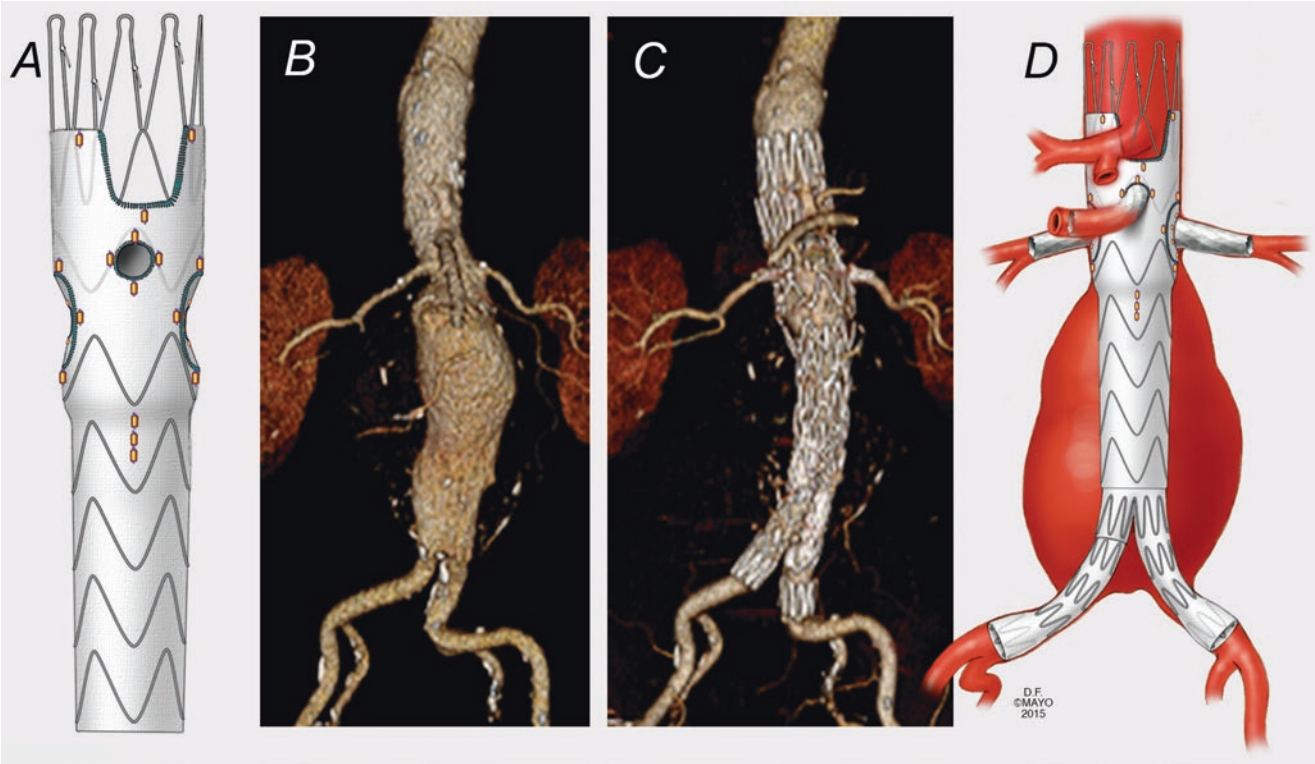


Fig. 27.9 The Cook P-Branch is designed with a scallop for the celiac axis, one fixed central fenestration for the SMA and two conical pivotal fenestrations for the renal arteries (**a**). CTA of a patient with a pararenal abdominal aortic aneurysm (**b**) treated with a P-Branch off-the-shelf stent graft (**c**). Schematic representation demonstrates the final aspect of the repair with bridging stents to the SMA and bilateral renal arteries (**d**). By permission of Mayo Foundation for Medical Education and Research. All rights reserved

and 18 mm at the bottom, with a length of 202-mm. Celiac and superior mesenteric artery cuffs are 8 mm in diameter, 21 and 18 mm in length, and are axially located in the 01:00 and 12:00 positions, respectively. Right and left renal artery cuffs are 6 mm in diameter, 18 mm in length, and located in the 10:00 and 03:00 positions, respectively. The device is delivered through a 22-French system. Anatomic feasibility criteria for the t-Branch stent graft are summarized in Fig. 27.13.

Anatomic feasibility of the t-Branch® stent graft has been assessed by a few studies. Sweet and associates evaluated aortic anatomy in 66 patients treated by multibranched stent grafts [6]. In that study 88 % of patients met all the anatomical criteria proposed in Fig. 27.13, suggesting that a standardized off-the-shelf multibranch stent graft has wide applicability. Park and associates analyzed the shape and length of branches as determinants of suitability for repair. Twenty-three percent of branches had >30° misalignment, suggesting that the design was quite forgiving for errors of implantation or variations in patient anatomy [15]. A follow-up study by Gasper et al. analyzed the applicability of multibranched stent grafts in a broader study population of 201 potential candidates for repair of TAAAs. Anatomic suitability was accessed using a patient-specific or an off-the-shelf version with either standard (22Fr) or lower profile (18Fr) device. Of the 201 patients, 58 % were candidates for repair in a single-stage and another 29 % could be candidates for repair with adjunct procedures to provide suitable landing zone. Women were significantly more likely to require a conduit, which was less frequently needed with lower profile design. Patients with chronic dissections were significantly less likely to qualify for repair because of involvement of iliac arteries, compressed true lumen or aberrant vessel anatomy. Although the off-the-shelf design has the advantages of eliminating the need to wait for customization, only 94 patients (<50 %) qualified for use of this device [16].

Gore Excluder® TAMBE

The GORE® EXCLUDER® Thoracoabdominal Branch Endoprosthesis is an off-the-shelf, modular, multicomponent system composed of a proximal multibranched aortic component, a distal bifurcated component, and iliac limb extensions.

Table 27.1 Proposed anatomical criteria for endovascular repair using the p-Branch™ stent graft

	Juxtarenal and paravisceral	
Criteria	*n*	%
Patients	390	100
Aneurysm origin distal to the SMA origin	390	100
Greater than 10 % increase in diameter over length of proximal seal zone	0	0
Proximal sealing zone angulated > 60° relative to the centerline of the aneurysm or proximal sealing zone angulated >45° relative to the supraceliac aorta	49	13
Proximal sealing zone diameter >31 mm or <21 mm	25	6
Non bifurcated segment of any artery to be stented <15 mm in length if use of covered stent is planned	39	10
Renal artery or SMA stenosis >50 %	37	10
Sacrifice of accessory renal artery, IMA or hypogastric that would significantly compromise physiological function in the opinion of the investigator	48	12
Accessory renal artery that supplies >40 % of one kidney or >25 % of both kidneys	23	6
Previous endograft in the aorta that precludes the deployment of the p-Branch device	2	0.5
Ability to incorporate visceral arteries	239	61
Configuration A	165	42
CA arises from aorta between 11:30 O'clock and 1:30 o'clock (345° and 45°)	387	99
The SMA is ≥11 mm distal to the celiac artery	366	94
Longitudinal position of RRA arise 4.5–19.5 mm distal to the SMA	277	71
Longitudinal position of LRA arise 4.5–19.5 mm distal to the SMA	270	69
Circumferential location of the RRA can range between 8:30 o'clock and 10:30 O'clock (255° and 315°)	364	93
Circumferential location of the LRA can range between 1:30 o'clock and 3:30 O'clock (45° and 105°)	355	91
Configuration B	180	46
The CA arises from the aorta between 11:00 o'clock and 2:00 o'clock (330° and 60°)	390	100
The SMA is ≥9 mm distal to the celiac artery	386	99
Longitudinal position of the RRA arises 8.5–23.5 mm distal to the SMA	263	67
Longitudinal position of the LRA arises 12.5–27.5 mm distal to the SMA	292	75
Circumferential location of the RRA can range between 8:30 O'clock and 10:30 O'clock (255° and 315°)	364	93
Circumferential location of the left renal artery can range between 1:30 O'clock and 3:30 O'clock (45° and 105°)	355	91
Prohibitive occlusive disease, calcification or thrombus of the PLZ	19	5
Distance from the distal-most aspect of the lowest renal artery to the aortic bifurcation that is compatible with the available lengths of the Zenith® Universal Distal Body Endovascular Graft (if used)	383	98
Unsuitable arterial anatomy	13	3
Suitability: strict criteria	128	33
Suitability: liberal criteria	193	49

SMA superior mesenteric artery, *RRA* right renal artery, *LRA* left renal artery, *IMA* inferior mesenteric artery

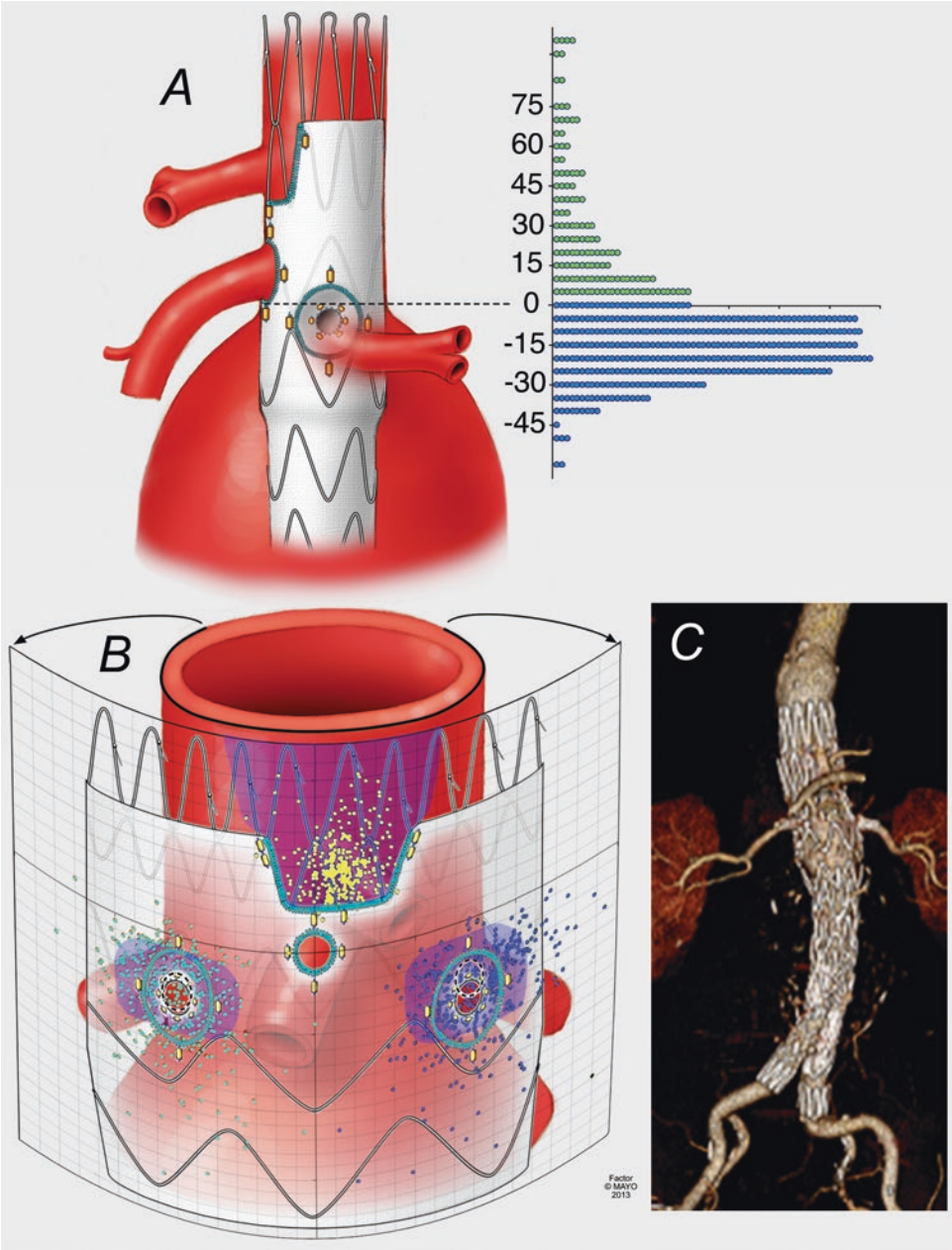


Fig. 27.10 The Cook P-Branch was designed to treat patients with aneurysms originating distal to the ostium of the superior mesenteric artery; in the figure, each dot represents the origin of the aneurysm in each of 520 patients whose anatomy was evaluated for feasibility for the P-Branch stent graft, with the blue dots representing patients that would be suitable for treatment with the device (**a**). Visceral vessel incorporation was evaluated in both configurations A and B of the device; the blue shadow area demonstrates the area of feasibility for the P-Branch design, with each dot representing the origins of the celiac axis (*yellow*), right (*green*) and left (*blue*) renal arteries (**b**). Postoperative three-dimensional reconstruction of a computed tomography angiography of a patient with a pararenal abdominal aortic aneurysm treated with the P-Branch stent graft (**c**). By permission of Mayo Foundation for Medical Education and Research. All rights reserved

The preferred side branch component is a specially designed balloon-expandable covered stent, the GORE® VIABAHN® BX Endoprosthesis. Unique characteristics of the GORE® VIABAHN® BX Endoprosthesis bridging stent couple the radial force, precise deployment, and relative low profile (7–8Fr) of a balloon-expandable stent with flexibility comparable to a self-expandable stent. The side branch components have Heparin Bioactive Surface.

The GORE® EXCLUDER® Thoracoabdominal Branch Endoprosthesis has been designed with either retrograde (Fig. 27.14) or antegrade (Fig. 27.15) renal portals. These designs are currently being investigated as part of an early feasibility study in the USA. The first in man implant of the retrograde design was performed by Dr. Pierre Galvagni Silveira in Brazil. The first US implant of the retrograde design and the first in man implant of the antegrade designs were performed by the author (GSO) in December of 2015 and March 2016, respectively. The first three clinical cases have used retrograde renal portals. Device dimensions include a proximal diameter of 26, 31 and 37 mm, length of

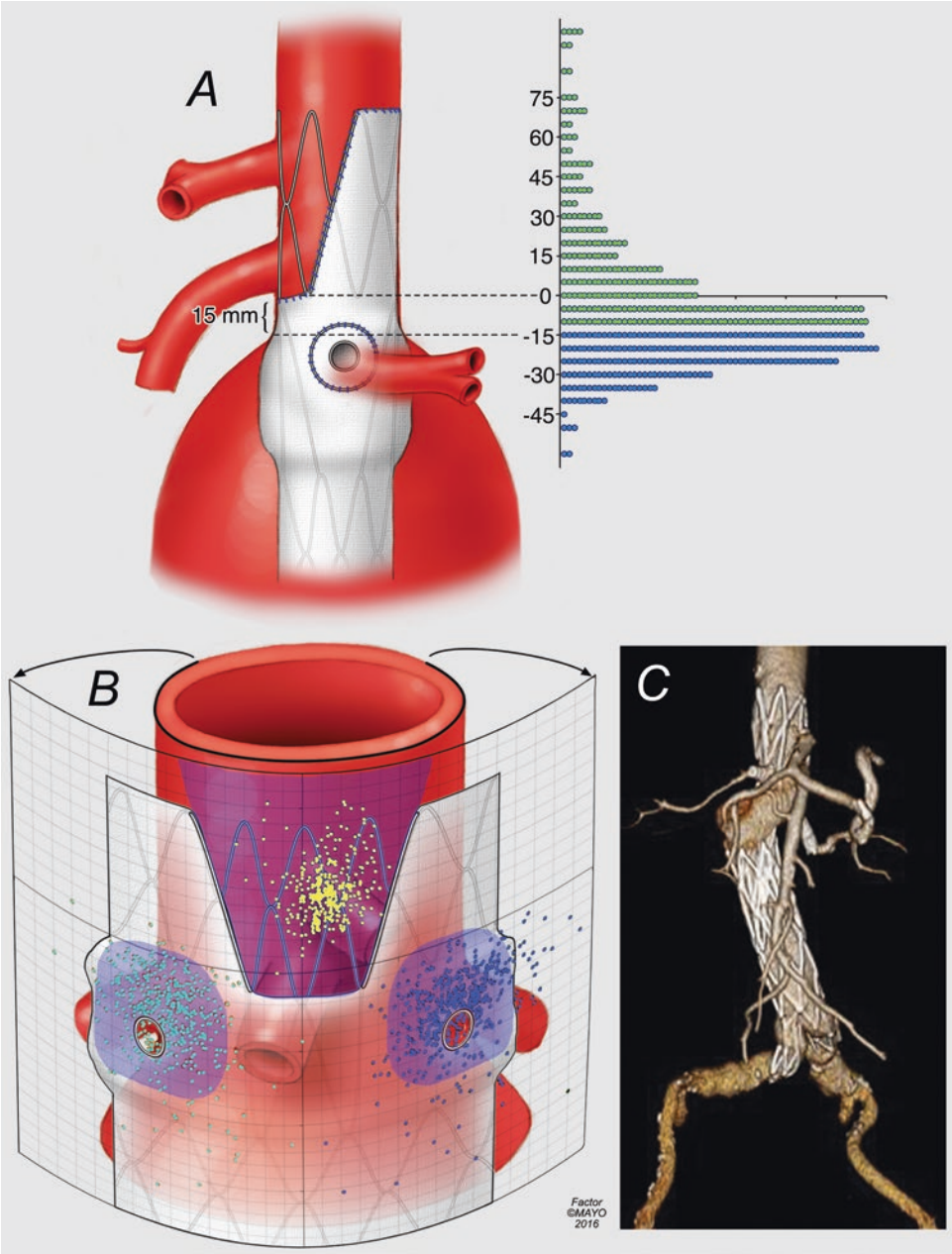


Fig. 27.11 The endologix Ventana requires a 15-mm healthy aortic neck distal to the origin of the superior mesenteric artery for suitability. All patients identified by green dots would not be suitable for repair with the Ventana stent graft (**a**). Visceral vessel incorporation was possible in 90 % of patients due to the concept of moveable fenestrations in the Ventana stent graft, represented by the blue shadow area incorporating the celiac axis (*yellow*), right (*green*) and left (*blue*) renal arteries (**b**). Postoperative three-dimensional reconstruction of a computed tomography angiography of a patient with a juxtarenal abdominal aortic aneurysm treated with the Ventana stent graft (**c**). By permission of Mayo Foundation for Medical Education and Research. All rights reserved

215 mm and distal diameter of 20 mm. An alternative option is also available with four antegrade portals, with proximal diameters of 31 and 37 mm, length of 160 mm, and distal diameter of 20 mm. Both options require a 22 Fr transfemoral introducer for the aortic device (with the exception of the 31 mm antegrade configuration, which is 20 Fr) and a 12 Fr brachial or axillary artery introducer for access into the antegrade portals.

The aortic component allows for placement of through-and-through pre-loaded guide-wires, eliminating the need to catheterize the portal in order to access the target vessel. To facilitate placement of the guide-wires and prevent guide-wire wrapping within the aorta, a specially designed triple-lumen catheter is inserted from the brachial approach and exteriorized via the femoral access.

Results

None of these off-the-shelf stent grafts is currently commercially available in the USA. The p-Branch® feasibility study has already completed enrollment and the US Pivotal phase

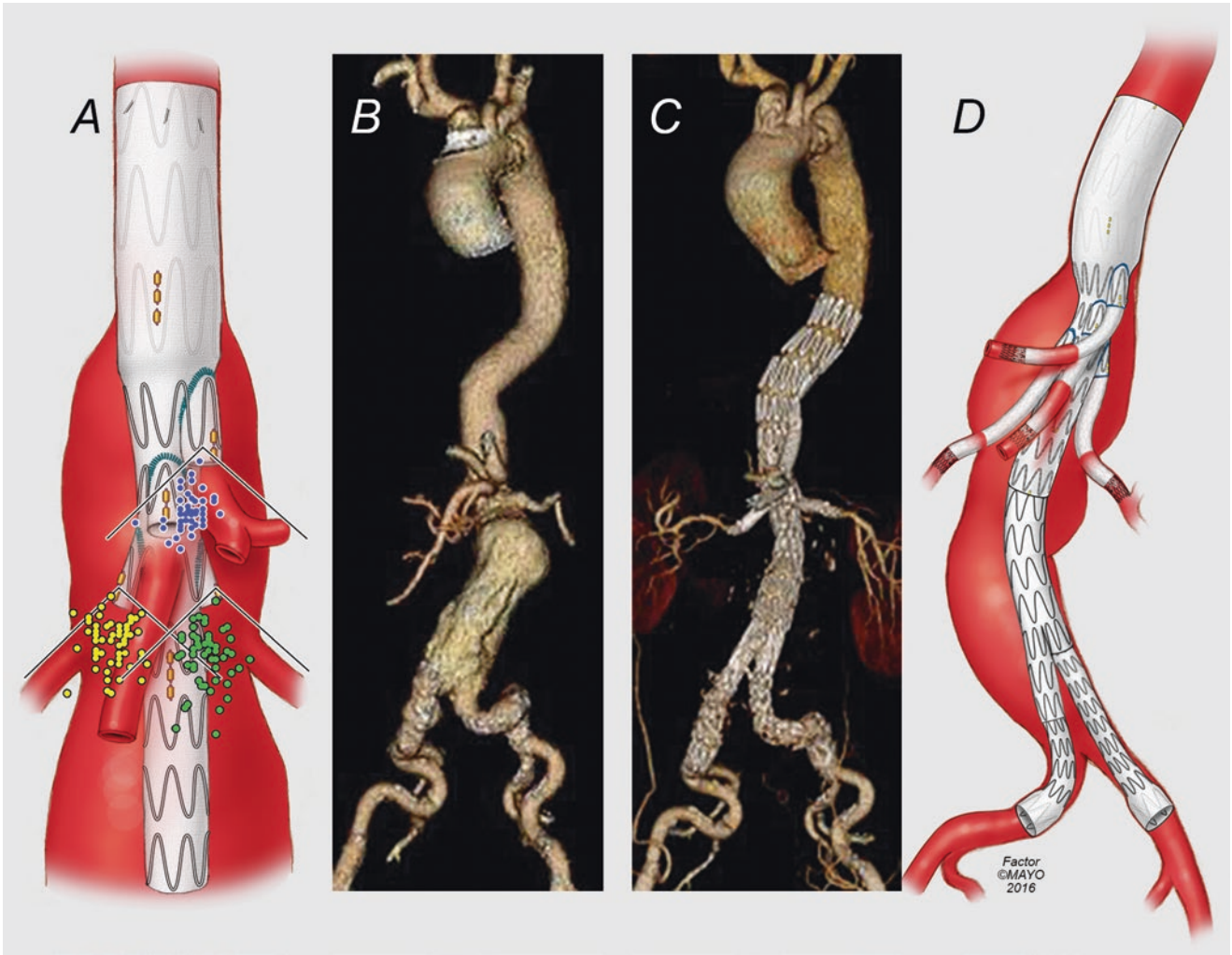


Fig. 27.12 The Cook T-Branch stent graft design includes four cuffs intended to fit a large proportion of visceral anatomies in patients with thoracoabdominal aortic aneurysms (**a**). Pre- (**b**) and post-operative (**c**) three-dimensional reconstruction of a computed tomography angiography of a patient with a type III thoracoabdominal aortic aneurysm treated with a T-Branch stent graft with repair extended to the common iliac arteries bilaterally. All branches are bridged with stent grafts (Viabahn or Fluency) and typically reinforced with a bare-metal stent in its entirety (**d**). By permission of Mayo Foundation for Medical Education and Research. All rights reserved

has started in late 2015. The Gore Excluder® TAMBE early feasibility study has just started enrollment with the first US implant performed at the Mayo Clinic in December 11, 2015. The Cook thoracoabdominal platform includes the options of both patient-specific and off-the-shelf designs, which are likely to start clinical investigation in the USA in the near future.

Cook p-branch® Stent-Graft

Early outcomes were reported for p-Branch® in 2013 after treatment of juxtarenal and suprarenal abdominal aortic aneurysms originating distal to the superior mesenteric artery. Patients were included if anatomic feasibility criteria based on instructions for use were met. Sixteen patients were enrolled, two of which presented with aneurysm rupture. The average infra-SMA neck length was 16 mm. Technical success rate was 100 %, mean procedure time 254 min, mean fluoroscopy time 62 min and contrast utilization was < 70 mL. Median length of stay in the intensive care unit was 2 days and overall length of hospital stay 5 days (range 3–8 days). There were no deaths, ruptures or open surgical conversions after treatment during the median follow up of 4.3 months. No spinal cord ischemia, myocardial infarction, pulmonary or renal failure, and type I/III endoleaks were noted

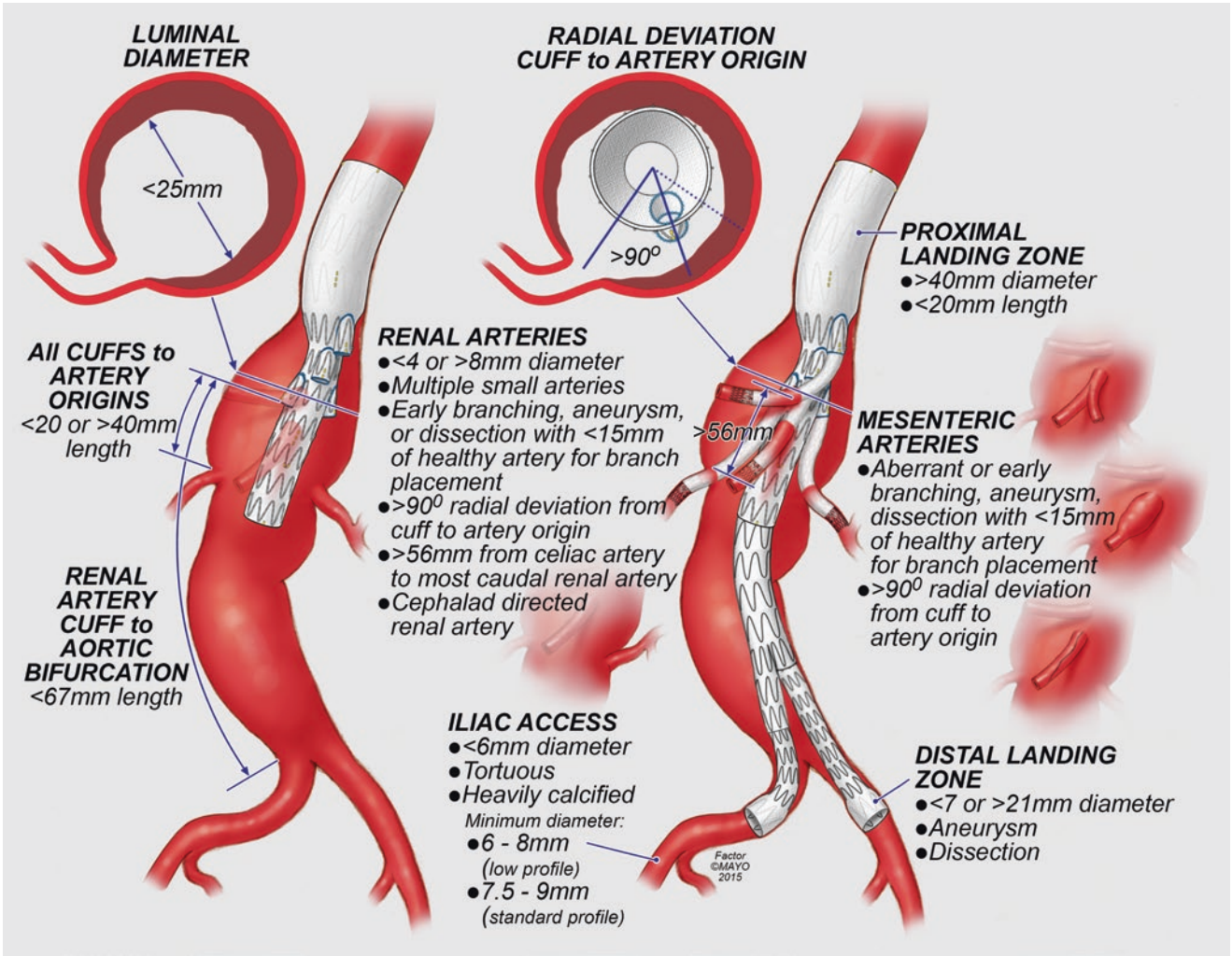


Fig. 27.13 Anatomical criteria for t-Branch stent graft are depicted in the illustration. Important considerations are the minimal luminal diameter of 25 mm, ability to incorporate all vessels within 90° angle to each cuff and target vessel diameter of 4–8 mm for renal arteries. By permission of Mayo Foundation for Medical Education and Research. All rights reserved

for the subjects. One patient required a late reintervention for recanalization of an occluded renal artery stent, with no additional branch-related events reported in the series [13].

Cook t-Branch® Stent-Graft

Clinical outcomes of the t-Branch® stent graft for treatment of thoracoabdominal aortic aneurysms have been published in small retrospective single-center reports. Bisdas and colleagues described outcomes in 46 patients treated with multibranched stent grafts, 22 of which received the t-Branch configuration [17]. Technical success was universal between both groups. Early mortality was zero, spinal cord injury was identified in one patient, and freedom from any reintervention at 6 months was 90 % in the t-Branch group. Three patients developed occlusion of a renal artery bridging stent, as compared to no branch occlusions in the patient-specific group. Importantly, the University of California San Francisco group has used primarily patient-specific or off-the-shelf stent grafts with directional branches. In their most recent report of 81 patients, 31 of which treated with the t-Branch configuration, 30-day mortality was 3.7 % and renal branch occlusion occurred in 9 % [14].

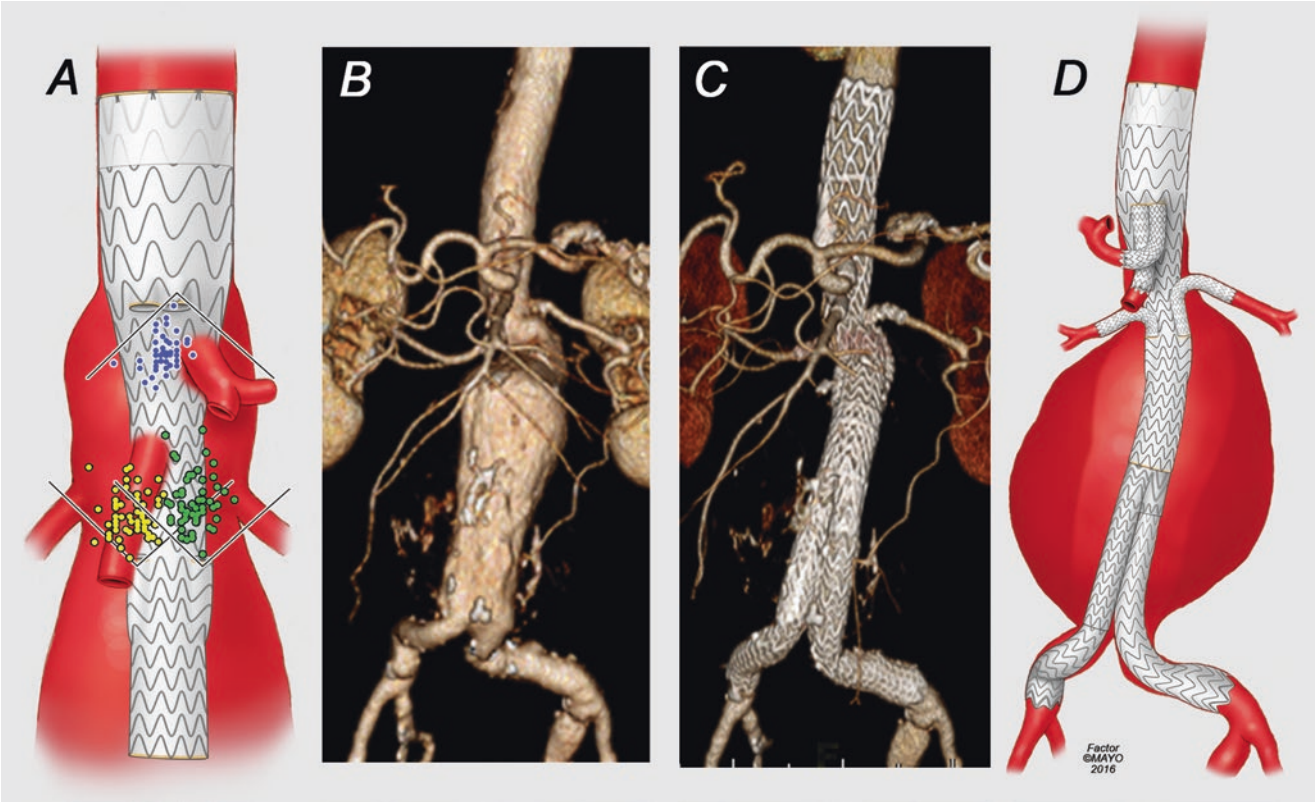


Fig. 27.14 Schematic illustration of the spectrum of anatomies suitable for the Gore Thoracoabdominal Branch Endoprosthesis (TAMBE) in the retrograde approach (**a**). Pre- (**b**) and post-operative (**c**) three-dimensional reconstruction of a computed tomography angiography of a patient with a type IV thoracoabdominal aortic aneurysm treated with the retrograde TAMBE device. Final aspect of the repair with distal extension to the common iliac arteries with the Gore Excluder platform, and bridging to the target visceral vessels with balloon-expandable Viabahn BX endoprosthesis (**d**). By permission of Mayo Foundation for Medical Education and Research. All rights reserved

Future Directions

The ideal off-the-shelf stent graft should combine wide anatomical applicability, ease of implantation from a technical standpoint, and durable and reproducible branch-related outcomes. Although there is controversy with respect to which design is best suited for most patients with TAAAs, experts agree that directional branches are ideal for down-going vessels that originate from large aortic lumens, whereas fenestrations may be preferred for vessels that originate from the sealing zone or narrow aortic segments. The advantage of a multibranched stent graft relies on the ability to implant the device without a high degree of precision, which is needed for fenestrated stent grafts. Nevertheless, feasibility of these designs should not be overstretched to accommodate more extensive aneurysms or anatomies that are beyond the proposed guidelines. From a technical standpoint, implantation of these devices can be more difficult compared with custom-made stent grafts because of mismatch between the aortic anatomy and the intended off-the-shelf configuration. Notably, long-term results remain unknown for off-the-shelf designs, but concern remains with respect to branch durability in the setting of misaligned bridging stents that can be prone to kinks, fracture, or migration. Ultimately, it is critical that the results of off-the-shelf devices be analyzed in contrast to what has already been achieved with custom-made devices. Long-term patency of renal fenestrations has to be determined for off-the-shelf designs before these new concepts are recommended to patients who are good candidates for either open repair or patient-specific stent grafts. Until then, off-the-shelf devices should be investigated under clinical protocols with strict anatomic guidelines. For patients who have urgent indications, more liberal criteria can be applied.

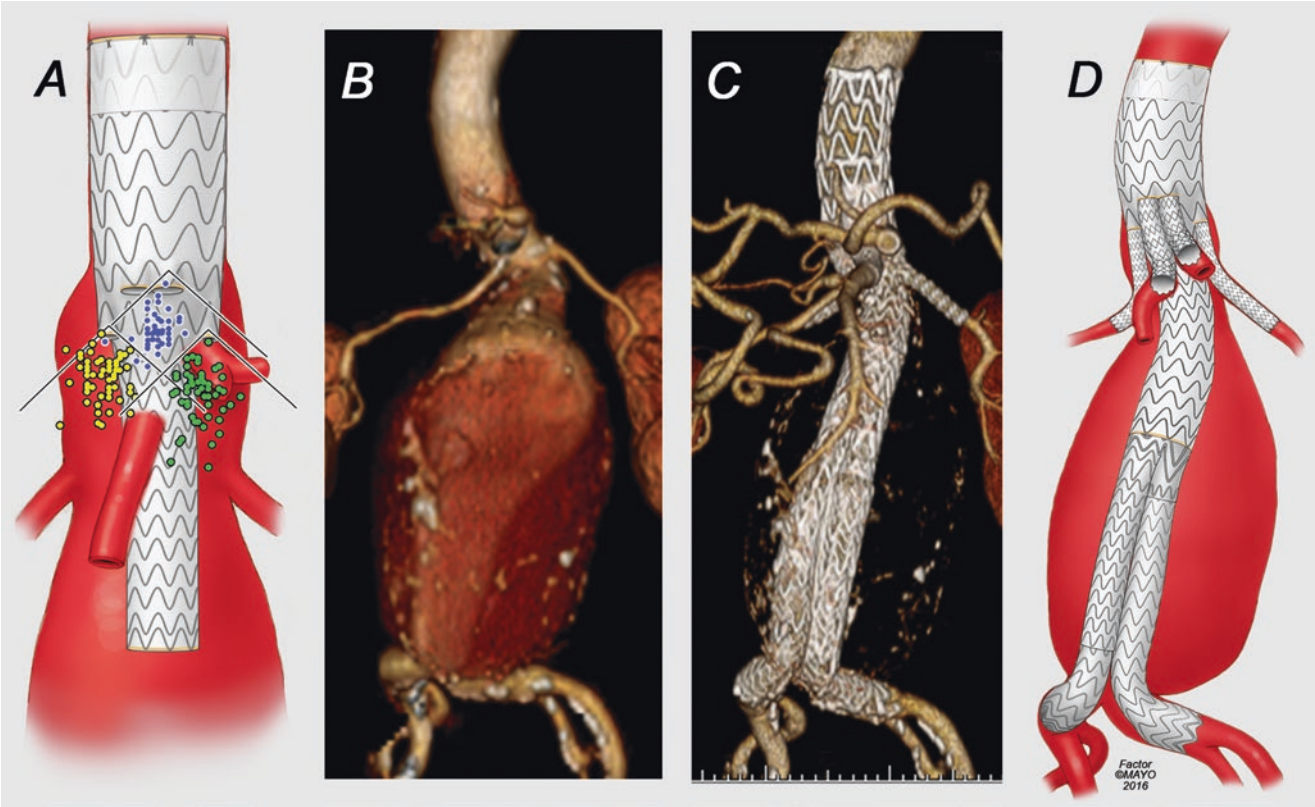


Fig. 27.15 The Gore Thoracoabdominal Branch Endoprosthesis (TAMBE) antegrade approach complements the retrograde version to accommodate additional patient anatomies, including patients with down-going renal arteries (**a**). Preoperative (**b**) and postoperative (**c**) three-dimensional reconstruction of a computed tomography angiography of a patient with a type IV thoracoabdominal aortic aneurysm treated with the antegrade TAMBE device. Final aspect of the antegrade repair with distal extension to the common iliac arteries with the Gore Excluder platform, and bridging to the target visceral vessels with balloon-expandable Viabahn BX endoprosthesis (**d**). By permission of Mayo Foundation for Medical Education and Research. All rights reserved

References

1. Verhoeven EL, Katsargyris A, Bekkema F, Oikonomou K, Zeebregts CJ, Ritter W, et al. Editor's choice—ten-year experience with endovascular repair of thoracoabdominal aortic aneurysms: results from 166 consecutive patients. Eur J Vasc Endovasc Surg. 2015;49(5):524–31.
2. Mastracci TM, Greenberg RK, Eagleton MJ, Hernandez AV. Durability of branches in branched and fenestrated endografts. J Vasc Surg. 2013;57(4):926–33.
3. Martin-Gonzalez T, Pincon C, Maurel B, Hertault A, Sobocinski J, Spear R, et al. Renal outcomes following fenestrated and branched endografting. Eur J Vasc Endovasc Surg. 2015;50(4):420–30.
4. Oderich GS, Greenberg RK, Farber M, Lyden S, Sanchez L, Fairman R, et al. Results of the United States multicenter prospective study evaluating the Zenith fenestrated endovascular graft for treatment of juxtarenal abdominal aortic aneurysms. J Vasc Surg. 2014;60(6):1420.e1–5.
5. Mendes BC, Oderich GS, Macedo TA, Pereira AA, Cha S, Duncan AA, et al. Anatomic feasibility of off-the-shelf fenestrated stent grafts to treat juxtarenal and pararenal abdominal aortic aneurysms. J Vasc Surg. 2014;60(4):839–47. discussion 847-8.
6. Sweet MP, Hiramoto JS, Park KH, Reilly LM, Chuter TA. A standardized multi-branched thoracoabdominal stent-graft for endovascular aneurysm repair. J Endovasc Ther. 2009;16(3):359–64.
7. Kristmundsson T, Sveinsson M, Bjorses K, Törnqvist P, Dias N. Suitability of the Zenith p-Branch standard fenestrated endovascular graft for treatment of ruptured abdominal aortic aneurysms. J Endovasc Ther. 2015;22(5):760–4.
8. O'Callaghan A, Greenberg RK, Eagleton MJ, Bena J, Mastracci TM. Type Ia endoleaks after fenestrated and branched endografts may lead to component instability and increased aortic mortality. J Vasc Surg. 2015;61(4):908–14.
9. Mastracci TM, Eagleton MJ, Kuramochi Y, Bathurst S, Wolski K. Twelve-year results of fenestrated endografts for juxtarenal and group IV thoracoabdominal aneurysms. J Vasc Surg. 2015;61(2):355–64.
10. Banga PV, Oderich GS, Farber M, et al. Impact of number of vessels targeted by fenestrations or branches on outcomes of patients undergoing endovascular repair of complex abdominal aortic aneurysms. Eur J Vasc Endovasc Surg. 2015;50(3):392.
11. Mendes BC, Oderich GS, Macedo TA, et al. Assessment of renal arterial anatomy and implications for endovascular repair with fenestrated, branched, or parallel stent-graft techniques. J Vasc Surg. 2014;59(6):8S–9.

12. Conway BD, Greenberg RK, Mastracci TM, Hernandez AV, Coscas R. Renal artery implantation angles in thoracoabdominal aneurysms and their implications in the era of branched endografts. J Endovasc Ther. 2010;17(3):380–7.
13. Kitagawa A, Greenberg RK, Eagleton MJ, Mastracci TM. Zenith p-branch standard fenestrated endovascular graft for juxtarenal abdominal aortic aneurysms. J Vasc Surg. 2013;58(2):291–300.
14. Reilly LM, Rapp JH, Grenon SM, Hiramoto JS, Sobel J, Chuter TA. Efficacy and durability of endovascular thoracoabdominal aortic aneurysm repair using the caudally directed cuff technique. J Vasc Surg. 2012;56(1):53–63. discussion 63-4.
15. Park KH, Hiramoto JS, Reilly LM, Sweet M, Chuter TA. Variation in the shape and length of the branches of a thoracoabdominal aortic stent graft: implications for the role of standard off-the-shelf components. J Vasc Surg. 2010;51(3):572–6.
16. Gasper WJ, Reilly LM, Rapp JH, Grenon SM, Hiramoto JS, Sobel JD, et al. Assessing the anatomic applicability of the multibranched endovascular repair of thoracoabdominal aortic aneurysm technique. J Vasc Surg. 2013;57(6):1553–8. discussion 1558.
17. Bisdas T, Donas KP, Bosiers MJ, Torsello G, Austermann M. Custom-made versus off-the-shelf multibranched endografts for endovascular repair of thoracoabdominal aortic aneurysms. J Vasc Surg. 2014;60(5):1186–95.

Techniques of Implantation of Fenestrated and Multibranched Stent Grafts for Visceral Artery Incorporation

28

Gustavo S. Oderich and Bernardo C. Mendes

Introduction

Visceral artery incorporation using fenestrations and directional branches has been increasingly utilized to treat complex aortic aneurysms. Ideal visceral branch characteristics include short length, long overlap with attachment site and vector alignment to the target visceral artery. While fenestrations have the advantages of short length and transverse orientation, their attachment is dependent upon radial force between a balloon-expandable stent and a nitinol ring (Fig. 28.1), which makes this configuration ideal for vessels with origin from narrow aortic segments. Conversely, directional branches allow for much longer overlap between the bridging stent and the attachment site. These stents are usually oriented axially and need to conform to the axis of the target vessel, which often requires reinforcement of the side stents by additional self-expandable bare metal stents. Directional branches can be internal, external, and internal/external with diamond shaped fenestrations to facilitate catheterization (Fig. 28.2). Although technical aspects of implantation of fenestrated and branched stent grafts share several similarities, some basic maneuvers differ depending on specific designs. In general, fenestrated stent grafts require very precise deployment to avoid misalignment with the target vessel. Because there is limited space for catheter manipulations, any misalignment can be problematic and result in inability to place the bridging stent. Conversely, directional branches do not require the same level of precision during deployment because there is space to manipulate catheters. Regardless of which technique is used, procedure planning, knowledge of the patient's anatomy, and familiarity with complex endovascular techniques are critical to achieve technical success. This chapter summarizes the basic techniques of implantation of fenestrated and branched stent grafts used to treat pararenal and thoracoabdominal aortic aneurysms (TAAAs).

Definitions

The extent of repair has been extensively discussed in Chap. 5, and details of device design and sizing have been summarized in Chap. 26. The term *fenestrated endovascular repair* is applied when a fenestrated stent graft is used to repair an aneurysm with inadequate or short infrarenal neck, yet the target vessels (e.g., renal arteries) originate from normal aorta. There is no gap between the fenestration and the target vessel (Fig. 28.3). Alignment stents are typically used to prevent vessel occlusion or stenosis from misalignment between the fenestration and the origin of the target vessel. Examples of devices designed for fenestrated repair include the Zenith® fenestrated stent graft (ZFEN®, Cook Medical, Brisbane, Australia) and the Vascutek Anaconda® stent grafts.

A *branched endovascular repair* implies endovascular repair of aneurysms involving side branches. In these cases the target vessel originates from the aneurysm itself, and therefore there is a space gap between the main aortic stent graft and the aortic wall. Visceral branches can be performed using one of two approaches. *Fenestrated-branches* are based on reinforced fenestrations, which are bridged by balloon-expandable covered stents that connect the fenestration to the target vessel. *Directional branches* are based on pre-sewn cuffs, which can assume several configurations depending on physician preference or patient anatomy. The most commonly utilized branch configuration is a straight, short down-going branch intended to be accessed via the brachial approach. However, branches can be helical, up-going, internal or external. In general, directional branches are bridged by self-expandable stent grafts, but several physicians utilized balloon-expandable covered stents depending

G.S. Oderich (✉) • B.C. Mendes
Division of Vascular and Endovascular Surgery, Mayo Clinic,
200 First Street SW, Rochester, MN 55905, USA
e-mail: oderich.gustavo@mayo.edu

© Mayo Foundation for Medical Education and Research 2017

G.S. Oderich (ed.), *Endovascular Aortic Repair*, DOI 10.1007/978-3-319-15192-2_28

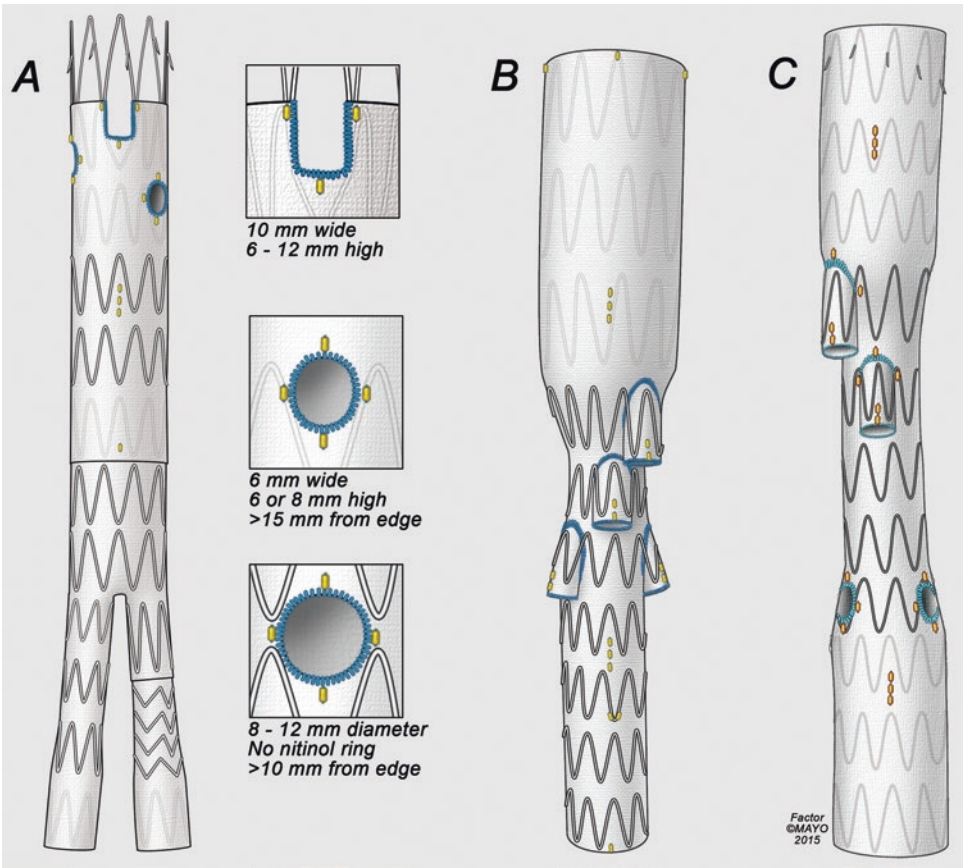


Fig. 28.1 Different configurations of fenestrated and branched stent grafts are depicted in this illustration. Patient specific stent grafts are designed with a proximal fenestrated component and distal universal bifurcated component with iliac limb extensions (**a**). Three types of fenestrations are available including scallops, small fenestrations (6×6 or 6×8 mm), and large fenestrations (8×8). The three most common designs described in this chapter include fenestrated stent grafts (**a**), multibranched stent grafts (**b**), and mixed designs with any combination of fenestrations and branches (**c**). By permission of Mayo Foundation for Medical Education and Research. All rights reserved

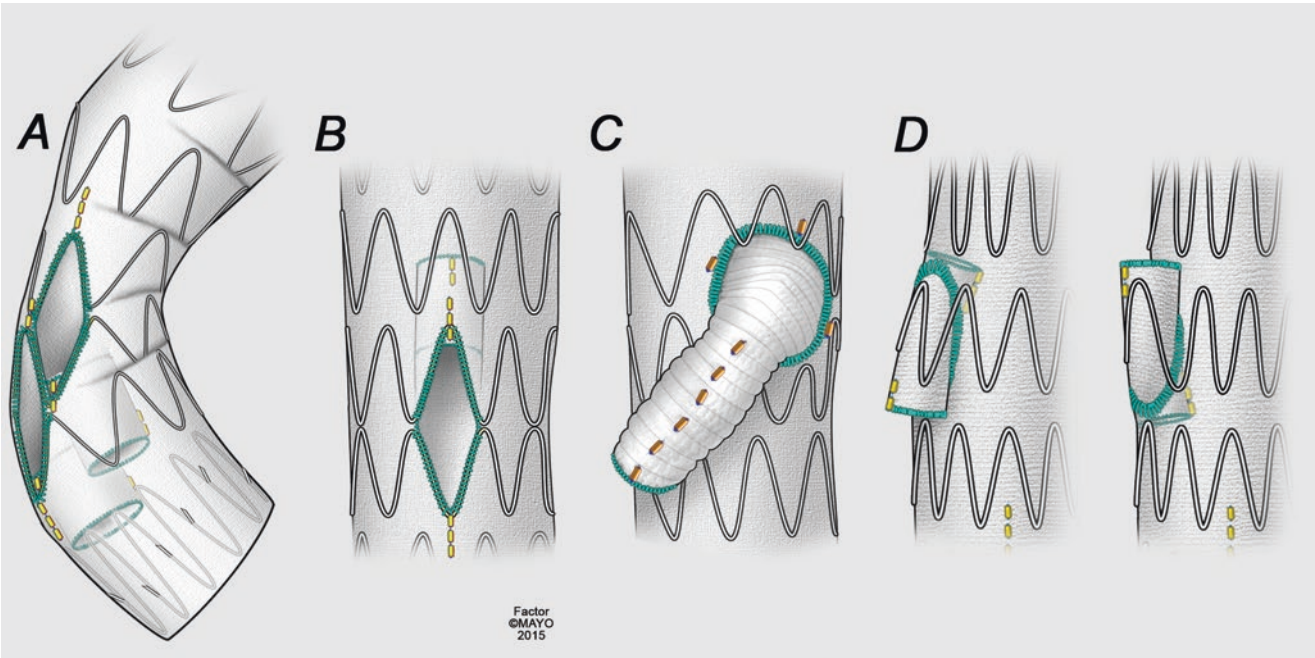


Fig. 28.2 Configurations of directional branches include internal branches with diamond shaped fenestrations (**a**, **b**), helical branches (**c**) and straight internal external branches with down or up going orientation (**d**). By permission of Mayo Foundation for Medical Education and Research. All rights reserved

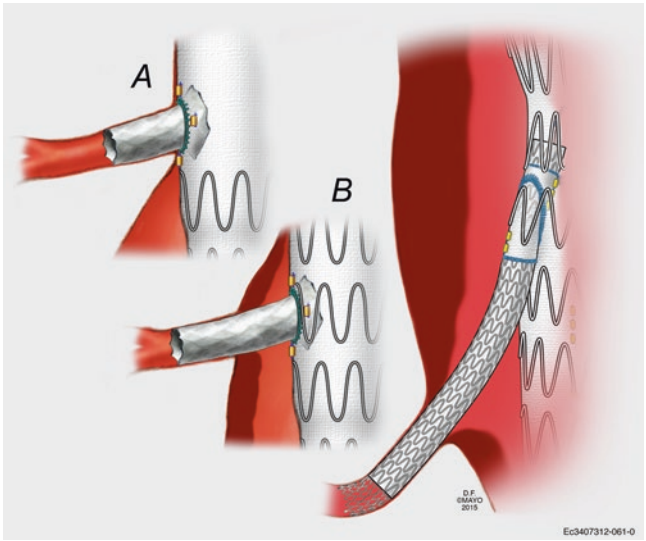


Fig. 28.3 Basic types of endovascular repair of aneurysms involving the visceral arteries include fenestrated repair (**a**) or branched repair (**b**) using fenestrated branches or directional branches. By permission of Mayo Foundation for Medical Education and Research. All rights reserved

on patient anatomy. Examples of thoracoabdominal stent grafts with directional branches include the Cook t-Branch® stent graft, Gore TAMBE® stent graft, Bolton® and Jotec® thoracoabdominal stent grafts.

Anatomical Review

Familiarity with detailed patient anatomy and device planning is critical to perform fenestrated and branched endovascular repair. The patient's computed tomography angiography and procedure plan are reviewed before procedure with special attention to access sites, target vessel characteristics and technical challenges. The intended proximal landing zone should be based on "healthy" aorta, which consists of at least a 2-cm length placed in a segment of "normal," non-calcified, parallel aortic wall. We often use a template of the patient's anatomy with detailed anatomical information, which is placed in several locations within the operating room to facilitate communication between members of the surgical team.

Ancillary Tools

These procedures require advanced endovascular skills and a comprehensive inventory with a wide range of catheters, balloons and stents, as described in Chap. 14. A brief summary of the most commonly utilized inventory is described in Table 28.1. Dedicated training in fenestrated and branched techniques is highly recommended for physicians who are already very experienced with other types of endovascular procedures.

Perioperative Measures

We routinely pre-admit the night prior to the procedure patients with chronic kidney disease and estimated glomerular filtration rate < 60 ml/min or serum creatinine > 1.8 mg/dl and advanced age (>80 years old) for gentle bowel preparation (magnesium citrate) and intravenous hydration with bicarbonate infusion (D5W with sodium bicarbonate 150 mEq/l intravenous at 3.5 ml/kg/h for 1 h prior to procedure and 1.5 ml/kg/h for 6 h after the procedure). Oral acetylcysteine (1200 mg twice a day orally, for 2 days) is administered to minimize risk of renal function deterioration. Acetyl-salicylic acid (325 mg/day) is used routinely, but clopidogrel is discontinued at least 10 days prior to the operation if placement of a cerebrospinal fluid drain is anticipated. Beta-blockers and statins are continued in the day of the operation with sips of clears sips of clear liquids. Vasodilator antihypertensive medications are decreased or discontinued starting the week prior to the operation in order to keep a systolic blood pressure >140 mmHg and <160 mmHg. All patients are instructed to shower with Hibiclens® liquid skin cleanser (chlorhexidine gluconate 4%) the day prior to the procedure to reduce bacterial counts. In the obese patient, the skin over the groin crease needs to be inspected several days prior to the procedure and any fungal infection is treated. Perioperative antibiotics are administrated intravenously prior to incision and redosed up to 24 h after the procedure.

Optimal imaging is recommended using a hybrid endovascular suite with a fixed imaging unit. Most procedures are performed using general endotracheal anesthesia, although select cases can also be done under local or regional anesthesia depending on assessment of airway and the ability of the patient to lay supine for prolonged time. Intra-operative blood salvage ("cell-saver") is recommended at the beginning of one's experience and for difficult cases with prolonged operating time. A useful tip is to create large pockets within the surgical drapes to allow for the blood to be collected with cell saver.

Contrast Use and Radiation Safety

The use of iodinated contrast is minimized throughout all the steps of the procedure. This can be done using several maneuvers but in general conventional contrast angiographies are avoided during implantation of the device and placement of side stents. Aortography is almost never performed for device

Table 28.1 List of ancillary tools recommended for physicians performing fenestrated-branched stent graft procedures

Category	Manufacturer	Application
Sheaths		
20–24 Fr Check-FLO sheath (30 cm)	Cook Medical Inc., Bloomington, IN	Femoral access for multi-vessel catheterization
16–24 Fr DrySeal sheath (28 cm)	WL Gore, Flagstaff, AZ	Femoral access for multi-vessel catheterization
7 Fr Ansel sheath (55 cm, flexible dilator)	Cook Medical Inc., Bloomington, IN	Femoral access for branch artery stenting
7 and 8 Fr Raabe sheath (90-cm long)	Cook Medical Inc., Bloomington, IN	Brachial access for branch artery stenting
12 Fr Ansel sheath (55 cm, flexible dilator)	Cook Medical Inc., Bloomington, IN	Brachial access for tortuous aortic arch to facilitate branch artery stenting
5 Fr Shuttle sheath (90 cm)	Cook Medical Inc., Bloomington, IN	Branch artery access during difficult arch
7 and 8.5 Fr Oscor Destino Twist guiding sheath (110 cm)	Oscor Inc., Palm Harbor, FL	Branch artery access during difficult target vessel catheterization
Catheters		
Kumpe catheter 4 Fr (65 cm)	Multiple	Selective vessel catheterization
Kumpe catheter 5 Fr (65 cm)	Multiple	Selective vessel catheterization
Kumpe catheter 5 Fr (100 cm)	Multiple	Selective vessel catheterization
C1 catheter 5 Fr (100 cm)	Multiple	Selective vessel catheterization
MPA catheter 5 Fr (125 cm)	Multiple	Selective vessel catheterization
MPB catheter 5 Fr (100 cm)	Multiple	Selective vessel catheterization
Van Schie 3 catheter 5 Fr (65 cm)	Cook Medical Inc., Bloomington, IN	Selective vessel catheterization
Vertebral catheter 4 Fr (125 cm)	Multiple	Selective vessel catheterization
VS1 catheter 5 Fr (80 cm)	Multiple	Selective vessel catheterization
Simmons I catheter 5 Fr (100 cm)	Multiple	Selective vessel catheterization
Diagnostic flush catheter 5 Fr (100 cm)	Multiple	Diagnostic angiography
Diagnostic pigtail catheter 5 Fr (100 cm)	Multiple	Diagnostic angiography, selective vessel catheterization
Quick-cross catheter 0.014–0.035 in. (150 cm)	Spectranetics Co., Maple Grove, MN	Selective vessel catheterization
Renegade catheter (150 cm)	Boston scientific, Minneapolis, MN	Selective vessel catheterization
CXI support catheter 4 Fr (135 cm)	Cook Medical Inc., Bloomington, IN	Selective vessel catheterization
Indy OTW vascular retriever snare (100 cm)	Cook Medical Inc., Bloomington, IN	Through-and-through access
Guide catheters		
LIMA guide 7 Fr (55 cm)	Cordis Corporation, Bridgewater, NJ	Pre-catheterization
Internal mammary (IM) guide 7 Fr (100 cm)	Multiple	Selective vessel catheterization
MPA guide 7 Fr (100 cm)	Multiple	Selective vessel catheterization
Balloons		
10 mm × 2 cm angioplasty balloon	Multiple	Proximal stent flare
12 mm × 2 cm angioplasty balloon	Multiple	Proximal stent flare
5 mm × 2 cm angioplasty balloon	Multiple	Advance sheath over balloon
4–6 mm × 4 cm 0.018 Sterling angioplasty balloon	Boston Scientific, Minneapolis, MN	Pre-dilatation using 0.014 or 0.018 systems
Wires		
Bentson wire, 0.035 in. (150 cm)	Multiple	Initial access
Soft glidewire, 0.035 in. (260 cm)	Multiple	Target vessel catheterization
Stiff glidewire, 0.035 in. (260 cm)	Multiple	Target vessel catheterization
Rosen wire, 0.035 in. (260 cm)	Multiple	Branch artery stenting
1 cm tip Amplatzer wire, 0.035 in. (260 cm)	Multiple	Branch artery stenting
Lunderquist wire, 0.035 in. (260-cm)	Multiple	Aortic stent graft
Glidegold wire, 0.018 in. (180 cm)	Multiple	Target vessel catheterization
Tracer Metro Direct wire, 0.025 in. (480 cm)	Cook Medical Inc., Bloomington, IN	Through-and-through access
Steelcore wire, 0.018 in. (300 cm)	Abbott Vascular Inc., Santa Clara, CA	Target vessel catheterization
Spartacore wire, 0.014 in. (300 cm)	Abbott Vascular Inc., Santa Clara, CA	Target vessel catheterization
Stents		

(continued)

Table 28.1 (continued)

Category	Manufacturer	Application
iCAST stent grafts, 5–10 mm	Atrium, Hudson, NH	Branch artery stenting
Viabahn stent grafts, 5–10 mm (5, 7.5, 10 cm)	WL Gore, Flagstaff, AZ	Branch artery stenting
Fluency stent graft, 6–10 mm (4–12 cm)	Bard Peripheral Vascular Inc., Tempe, AZ	Branch artery stenting
Flair stent graft, 6–9 mm (3–7 cm)	Bard Peripheral Vascular Inc., Tempe, AZ	Branch artery stenting
Balloon-expandable stents 0.035 in.	Multiple	Branch artery stenting or reinforcement
Self-expandable stents, 0.035 in.	Multiple	Distal branch artery stenting
Self-expandable stents, 0.014 in.	Multiple	Distal branch artery stenting

deployment. Instead, our preference has been to use small hand injections of 10 ml of diluted 30 % contrast (3 ml of contrast in 7 ml of saline) to locate the side branches. A completion aortography is obtained after all the stents are placed using diluted contrast at 50 %. Pre-catheterization to locate the target vessels is optional. This maneuver can be beneficial, and we continue to perform pre-catheterization of at least one vessel in most cases, which is typically done with minimal catheter manipulation in an expeditious manner. Whenever possible, our preference is to rely on on-lay CT and iGuide markers to locate the target vessels.

Radiation protection is critical when performing these procedures by following "as low as reasonably achievable" (ALARA) principles, which aim the lowest radiation exposure to complete the procedure. To achieve this, frame rates are reduced to the lowest possible (7.5 images/s), fluoroscopic pedal is left at the control of the operating senior surgeon, digital subtraction is avoided whenever possible, and gantry angulations are limited to <30° left or right anterior oblique. Operator shielding is used to minimize scattered radiation, including protective garments, eye protection, lead hats, and protective surgical drapes.

Positioning

Patients are positioned supine (Fig. 28.4) with the imaging unit oriented from the head of the table. Arterial access is obtained using only femoral approach for pararenal aneurysms requiring up to three fenestrations. Brachial and femoral access is preferred for nearly all thoracoabdominal aneurysms or four-vessel designs, unless there is a specific contra-indication to brachial access such as difficult arch with atherosclerotic debris. If brachial access is required, the author's preference is to surgically expose the vessel via small incision and to repair the brachial arteriotomy with interrupted prolene; the author almost never uses a total percutaneous approach for the brachial artery.

The brachial artery is imaged just prior to prepping the patient to select the incision site. If access is needed with a 12 Fr sheath, the author's preference is to expose the brachial artery near the axillary hairline provided that the vessel measures ≥4 mm by duplex ultrasound (Fig. 28.5). If the brachial artery is smaller than 4 mm, arterial exposure is performed using an incision in the delto-pectoral groove or infraclavicular fossa, but this is exceedingly infrequent. If brachial access is needed using a 7–8 Fr sheath for a single vessel, an incision is made just above the elbow crease. The left arm is abducted and prepped in the surgical field up to the axilla for larger sheaths, or tucked to the side and prepped when brachial access is not anticipated. A working side table is oriented in the same axis of the abducted arm for placement of wires and catheters. EKG leads, urinary catheter and other monitoring cables and lines should be taped or secured so that they are not in the path of the X-ray beam of the fluoroscopic unit or do not get caught during movement of the C-arm gantry.

Arterial Access

Percutaneous access is used in all cases whenever possible, including all pararenal and thoracoabdominal aortic aneurysms. Patients with non-calcified or minimally calcified femoral arteries are ideally suited. This technique is not used for patients with high femoral bifurcations, dense calcifications, or anterior plaque (Fig. 28.6). Techniques of iliac access using permanent or temporary iliac conduits are needed in 10–20 % of the patients and have been summarized in Chap. 23.

Percutaneous femoral access is established using ultrasound guidance with a stiff 0.018-in. micro-puncture needle entrance in the anterior common femoral artery wall 1- to 2-cm proximal to the bifurcation (Fig. 28.7). Punctures distal to the femoral bifurcation or in calcified areas were avoided. In the obese patient, large and non-calcified superficial femoral arteries may be accessed to avoid the problem of high punctures into the inguinal ligament. After access is established, the 0.018-in. stiff guide-wire is exchanged for a 0.035-in. guide-wire of choice (e.g., Bentson guide-wire) and a 6 Fr sheath. A small oblique incision is made and the subcutaneous tissue is dilated circumferentially to facilitate placement of the PVCDs. For each femoral puncture, a set of two Perclose® ProGlide closure devices (Abbott Vascular,

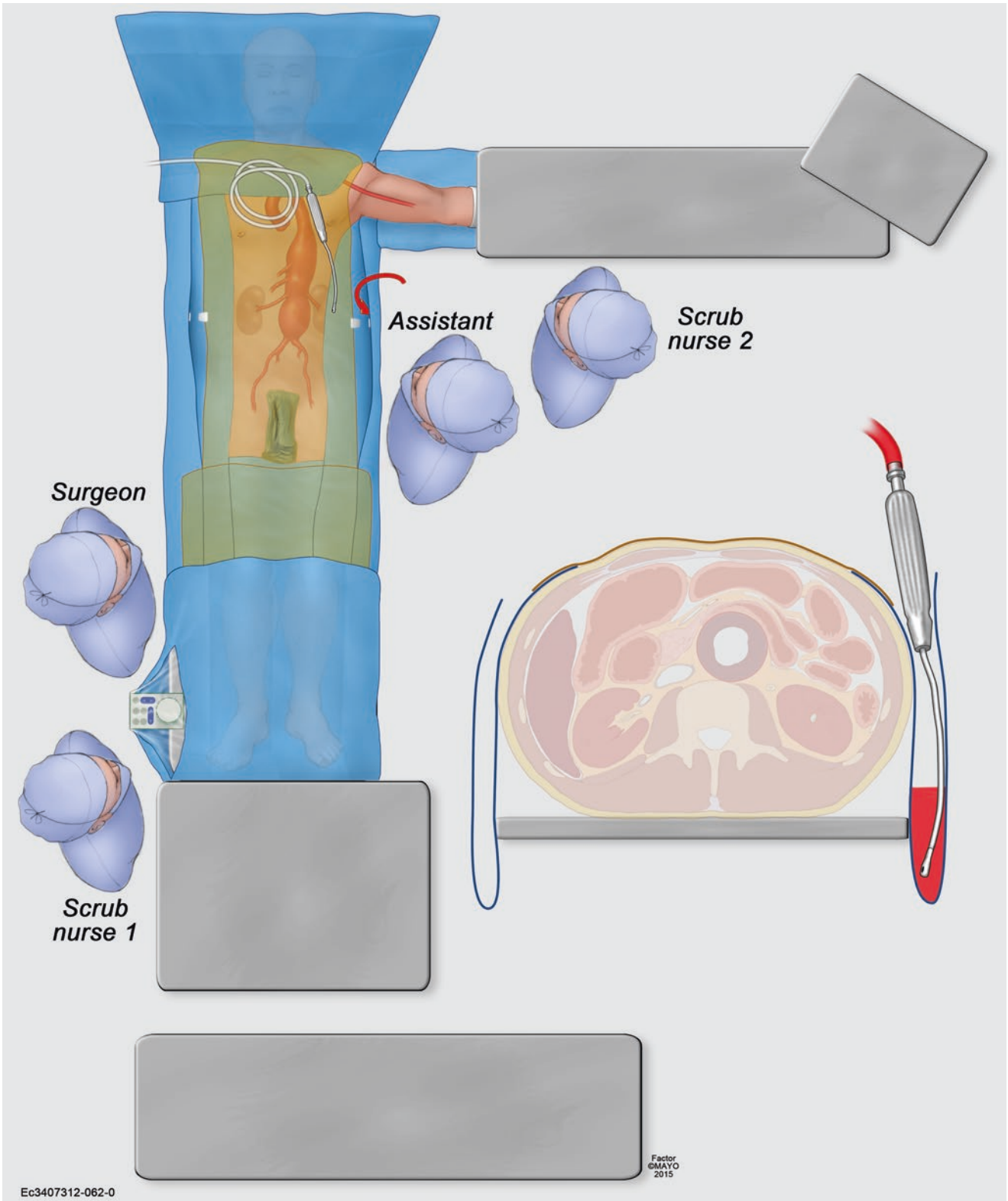


Fig. 28.4 General setup for complex endovascular procedures. The author's preference is to have the left (or right) upper extremity abducted and to access the high brachial artery at the level of the axillary hairline. The arm may be prepped and tucked to the side if lateral views are anticipated. However, lateral views are generally avoided because of higher radiation doses. A useful tip is to create pockets with the surgical drapes for intraoperative blood salvage. By permission of Mayo Foundation for Medical Education and Research. All rights reserved



Fig. 28.5 Standard access sites for brachial artery exposure include small incision close to the axillary hairline for larger diameter sheaths (12 Fr), or a small incision just above the antecubital crease for smaller diameter sheaths (7 or 8 Fr). Occasionally in patients with very small upper brachial arteries (<4 mm), an incision can be done at the delto-pectoral crease or infraclavicular area. By permission of Mayo Foundation for Medical Education and Research. All rights reserved

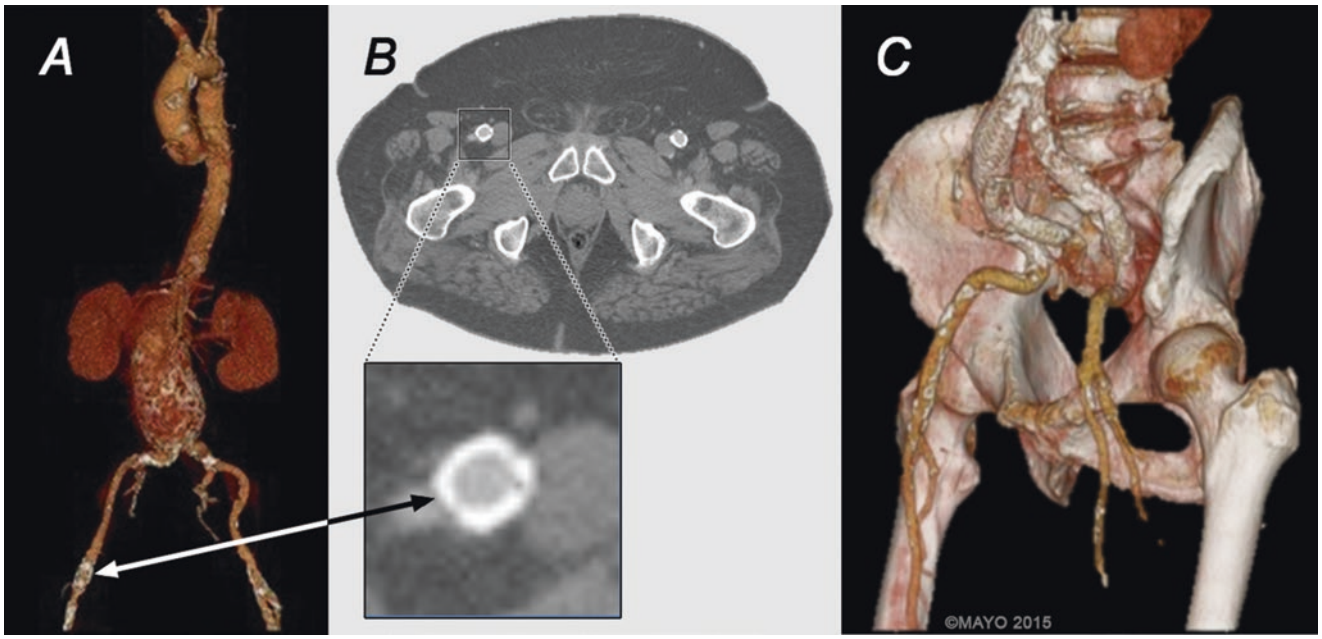


Fig. 28.6 Examples of patients not ideally suited for total percutaneous technique of complex endovascular repair because of excessive femoral artery calcification (**a** and **b**) or high bifurcation of the common femoral artery (**c**). By permission of Mayo Foundation for Medical Education and Research. All rights reserved

Santa Clara, CA) is deployed at 1:30 and 10:30 o'clock position prior to introduction of the larger diameter sheath (Figs. 28.8 and 28.9). At the completion of the procedure, a 0.035-in. non-braided stiff glide-wire is used to maintain access until adequate closure is confirmed (Fig. 28.10). In patients with inadequate hemostasis, an additional PVCD is used. In a small number of patients (<5 %) where closure is not deemed successful using percutaneous technique, a large sheath can be reintroduced or proximal control can be obtained over the guide-wire with balloon occlusion and a small groin incision is performed to expose and repair the common femoral artery. The concept that percutaneous access leads to prolonged lower extremity ischemia time is misleading and erroneous. In fact, the author immediately removes the sheaths and tightens the sutures without tying the knots once all steps are completed via the femoral approach, restoring immediate flow to the lower extremity faster than with primary arterial closure. If access needs to be obtained for any revision, this can be done by reintroduction of the sheath using the guide-wire. Failure of percutaneous closure can occur in <5 % of access sites due to several potential mechanisms, which are usually immediately recognized and suitable to repair with open exposure of the femoral artery (Fig. 28.11). The author has not experienced significant bleeding complications from percutaneous access procedures.

Open surgical exposure of the femoral arteries is performed in patients with small, calcified or who have high bifurcation of the femoral artery at the level of the inguinal ligament. In these cases, the author's preference is for a small

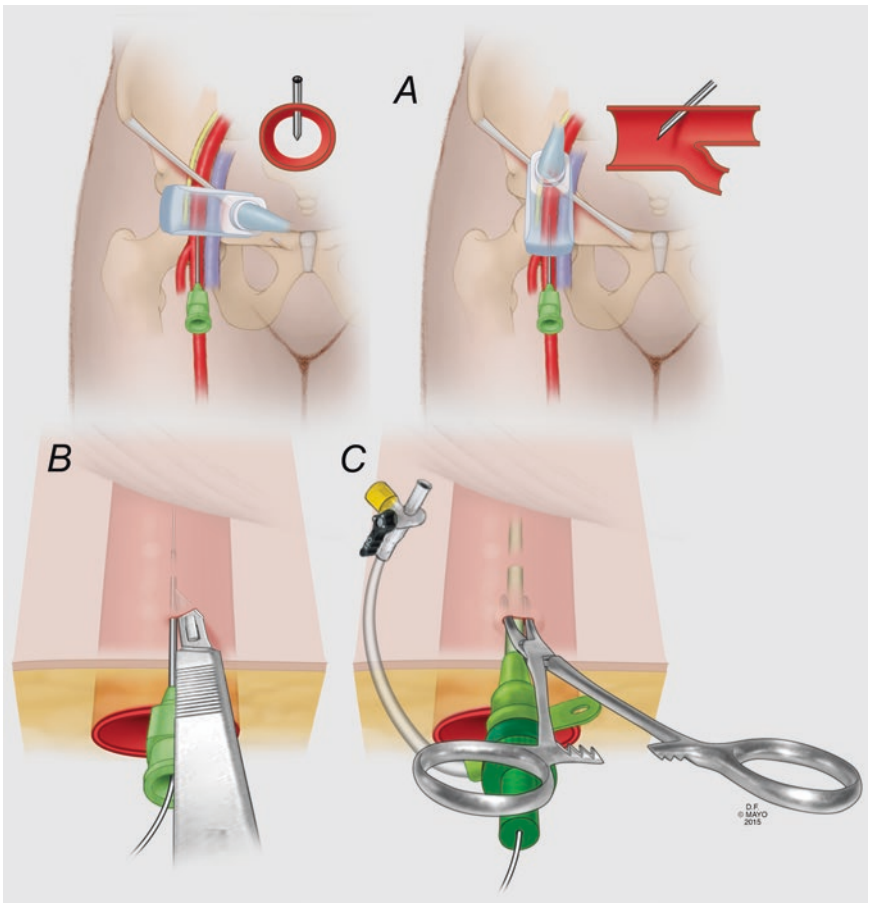


Fig. 28.7 Percutaneous access is established using ultrasound guidance with a micro-puncture set (**a**). Note access is established just proximal to the origin of the profunda femoral artery. Once access is obtained, a small oblique incision is made with careful attention to avoid any dermal tissue within the entrance site (**b**). A 6 Fr sheath is advanced over a 0.035-in. guide-wire and the soft tissue around the sheath is dilated with forceps (**c**). By permission of Mayo Foundation for Medical Education and Research. All rights reserved

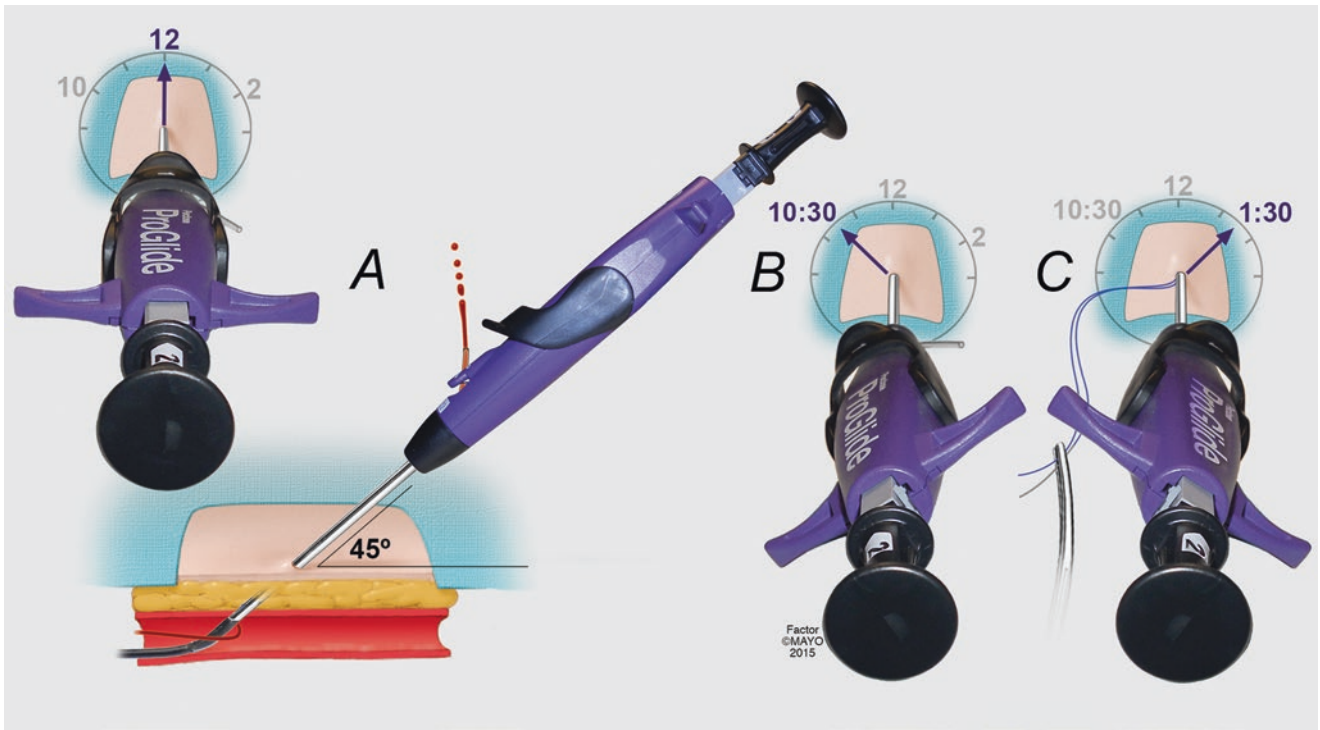


Fig. 28.8 Standard pre-closure technique is performed using the Perclose Proglide® device. The device is introduced with a 45° angle to the skin entrance until there is pulsatile bleeding via the side port (**a**). Each of the percutaneous stitches are deployed at 10:30 (**b**) and 1:30 (**c**) o'clock positions. By permission of Mayo Foundation for Medical Education and Research. All rights reserved

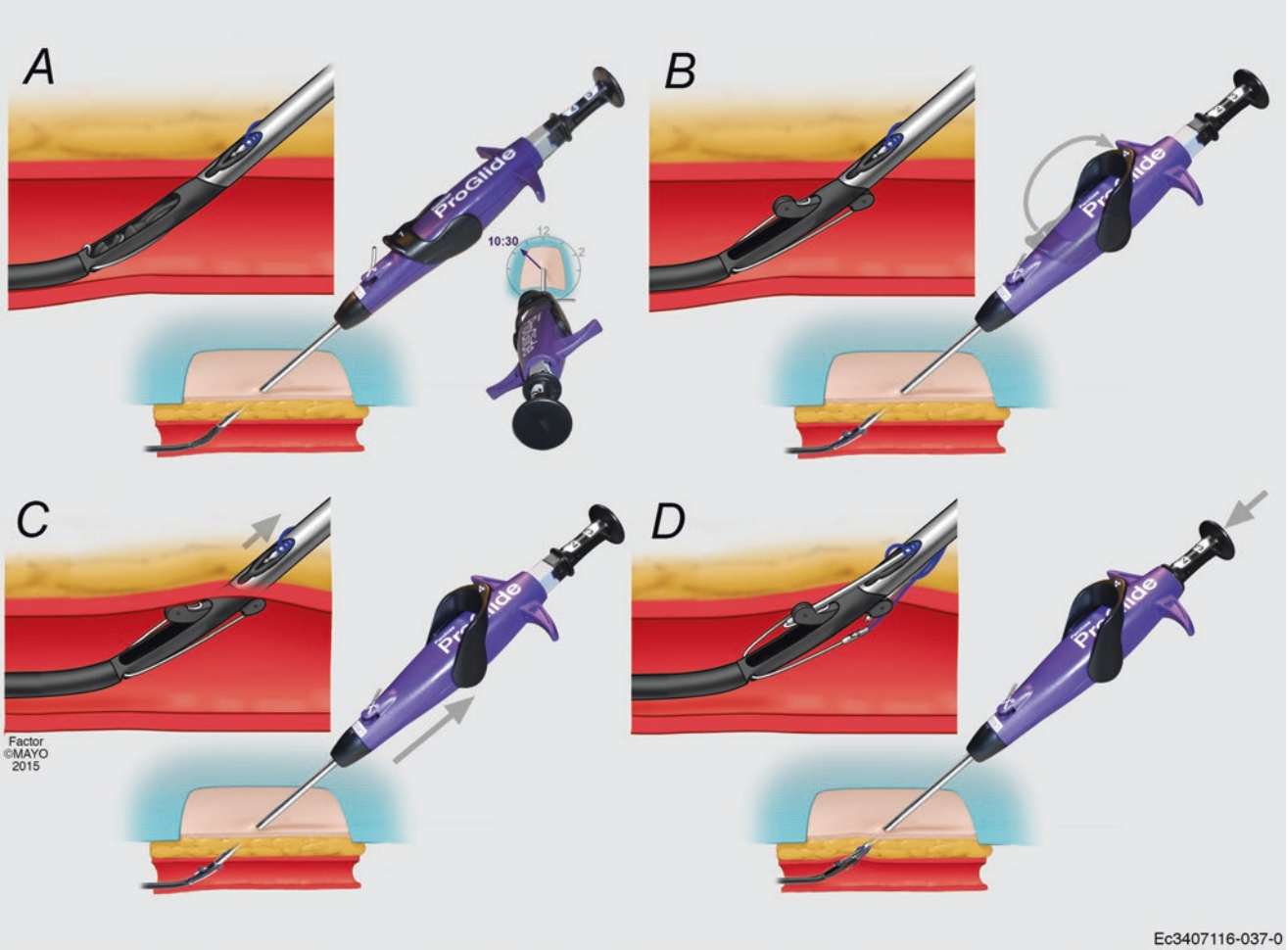


Fig. 28.9 Each Perclose Proglide® suture is sequentially deployed in a series of four steps. After the device is introduced in a 45° angle to the skin (**a**), the lever is pulled up positioning the spatulas (**b**) parallel to the arterial wall. Gentle traction is applied to pull the spatula against the arterial wall (**c**) while the stitch is applied (**d**). The suture string is pulled out (**e**) as indicated by #3 and the white portion of the suture is cut (**f**). The lever is lowered as indicated by #4 (**g**) and both suture strings are secured to the drapes (**h**). By permission of Mayo Foundation for Medical Education and Research. All rights reserved

oblique incision, but a longitudinal incision is used if the femoral artery is heavily diseased and femoral endarterectomy is needed. Proximal and distal control is obtained using vessel loops. Finally, a useful technique in select cases is the anastomosis of a Dacron graft into the common femoral artery. A "temporary femoral conduit" (Fig. 28.12) as outlined in Chap. 20 has been used to immediately restore lower extremity flow during difficult procedures, optimizing flow to the pelvis, leg, and spinal cord.

The patient is systemically heparinized with intravenous bolus of heparin (80–100 units/kg), which is administered immediately after femoral and brachial access is established. It is important to communicate with the anesthesia team so that appropriate heparin dose is administered and redosed multiple times to achieve and maintain an activated clotting time (ACT) >250 s throughout the procedure. The author emphasizes the importance of achieving and maintaining adequate heparinization. The ACTs are rechecked every 30 min, and additional heparin needs to be administered if <250 s. A continuous drip of heparin (500–1000 units/h) is also started and diuresis is induced with intravenous mannitol and/or furosemide.

Techniques

This chapter outlines the most common endovascular techniques, which exemplify variations of stent graft designs to treat complex aortic aneurysms involving the visceral arteries. It is important to emphasize that these techniques as herein described represent preferences of the author and do not follow necessarily the exact sequence of steps proposed by the recommendations for use of these devices. In addi-

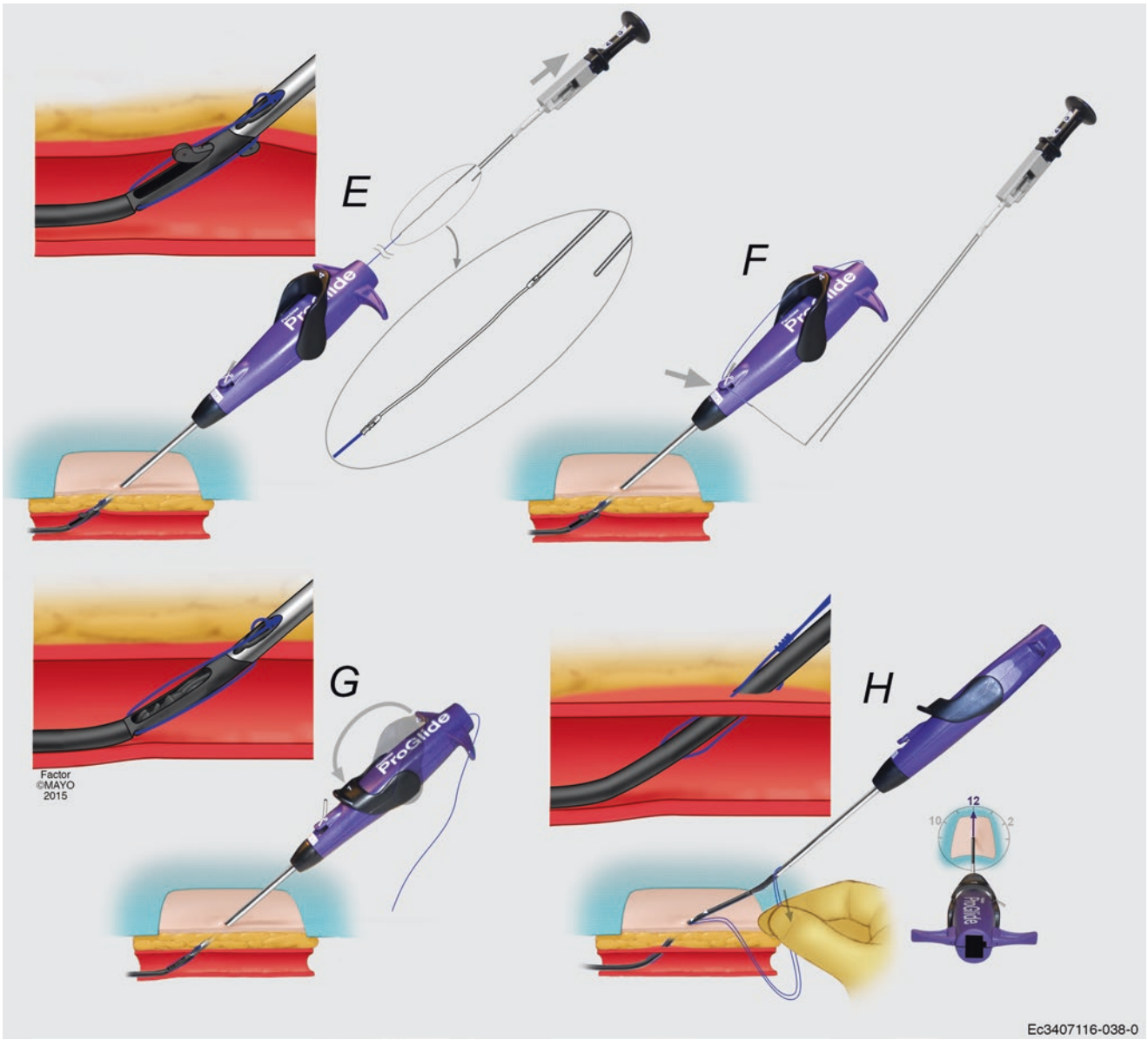


Fig. 28.9 (continued)

tion, for purpose of this chapter the author has described use of the Cook® stent graft platform, which has been implanted in over 15,000 patients. These techniques include the following device configurations:

- Fenestrated stent grafts (Cook Medical, Brisbane, Australia).
- Mixed designs with fenestrated and/or branched stent grafts (Cook Medical, Brisbane, Australia).
- Multibranched stent grafts (Cook Medical, Brisbane, Australia).

Patient-Specific Fenestrated Stent-Grafts

The technique of fenestrated-branched endovascular repair is currently performed using the Cook Zenith® stent graft lineage. Newer designs by Endologix (Ventana®), Terumo (Anaconda®) and Cook Medical (p-Branch®) are also under clinical investigation but are not available in the USA. This technique is most frequently utilized using the Cook ZFEN® stent graft, which was approved for commercial use in April 2012. The Cook Zenith patient-specific fenestrated stent graft consists of a proximal fenestrated tubular component, a

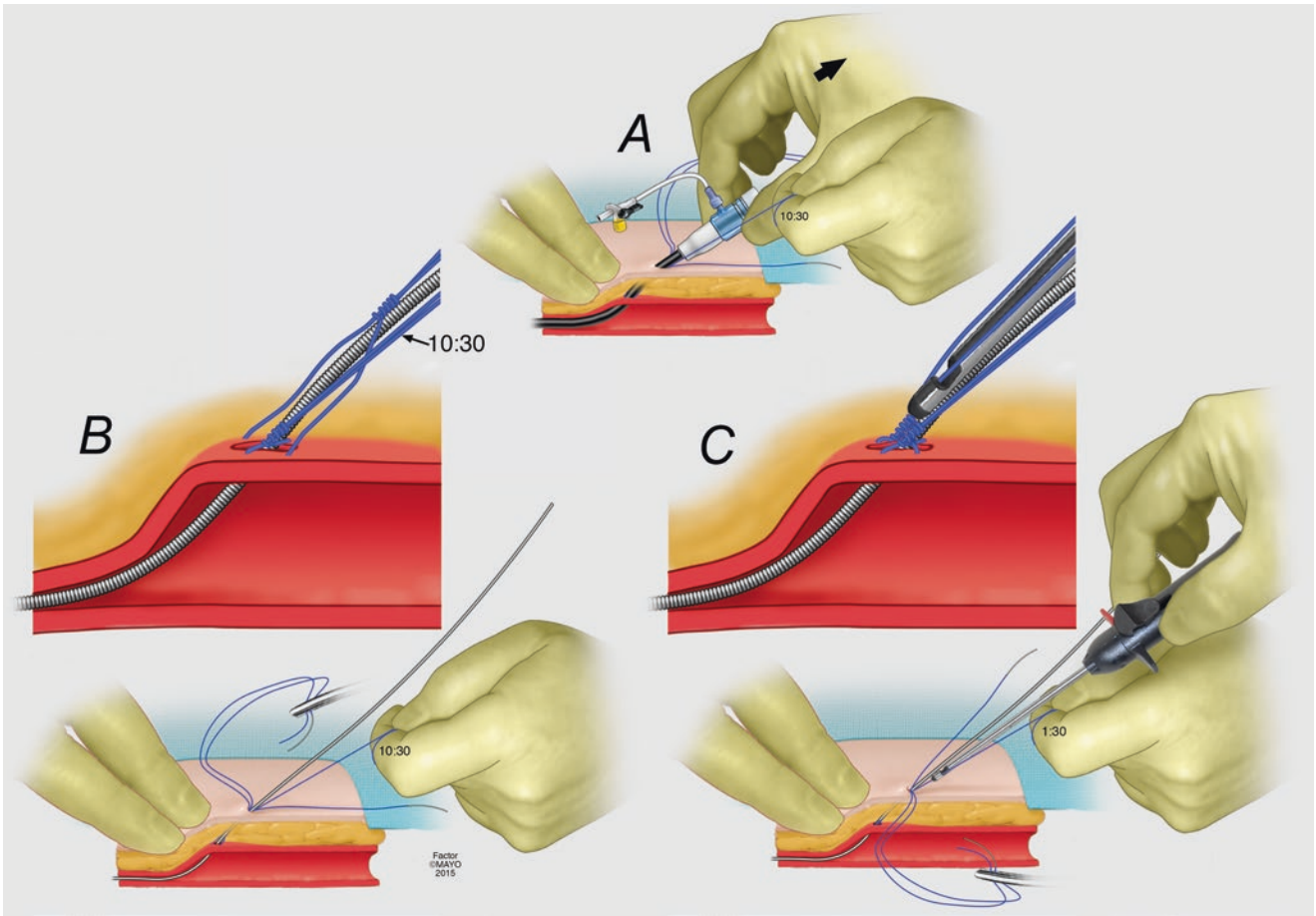


Fig. 28.10 The large diameter sheath is removed over the guide-wire while one of the assistants applies pressure over the puncture site (**a**). Each one of the sutures is pulled sequentially (**b**). Note the suture with the white marker locks the knot. Once both knots are tied the sutures are cut (**c**). By permission of Mayo Foundation for Medical Education and Research. All rights reserved

distal bifurcated universal component, and a contralateral iliac limb extension (see Fig. 28.1). The fenestrated tubular component is custom-made to fit the patient's anatomy, which takes 6–10 weeks for manufacturing. In the current configuration approved by the FDA in the USA, the device can be manufactured with up to three fenestrations, two of which can be of the same type (e.g., two small renal fenestrations and one SMA scallop). However, the device can be manufactured with any combination of fenestrations and/or branches, including double wide scallops (20×20 mm), access scallops, preloaded renal guide catheters, and preloaded catheters.

The procedure starts with bilateral percutaneous femoral access, which is established under ultrasound guidance as previously outlined. After each femoral puncture is preclosed using two Perclose devices, 8 Fr sheaths are introduced into the external iliac arteries over Bentson guide-wires (Cook Medical, Bloomington, IN) to minimize oozing via the fresh puncture sites. The Benson guide-wires are exchanged for 0.035-in. soft glide-wires and Kumpe catheters, which are advanced to the ascending aorta. Once in the ascending aorta, the glide-wires are exchanged for stiff 0.035 Lunderquist guide-wires (Cook Medical, Bloomington, IN).

The choice of access site is dependent upon tortuosity and vessel diameter. However, provided that there are no issues in both iliac arteries, the author's preference is to perform the branch vessel catheterizations via the right femoral approach and to introduce the fenestrated and bifurcated devices via the left femoral approach. Alternatively, if a preloaded renal guide-catheter system is used with the fenestrated component (e.g., p-Branch stent graft), it is introduced via the right femoral approach. Once the stiff guide-wires are positioned, a large Check-Flo sheath (20 Fr for two fenestrations or 22 Fr for three fenestrations) is introduced via the right femoral approach (Fig. 28.13). This sheath is optimal because the valve of the Check-Flo sheath has four leaf-

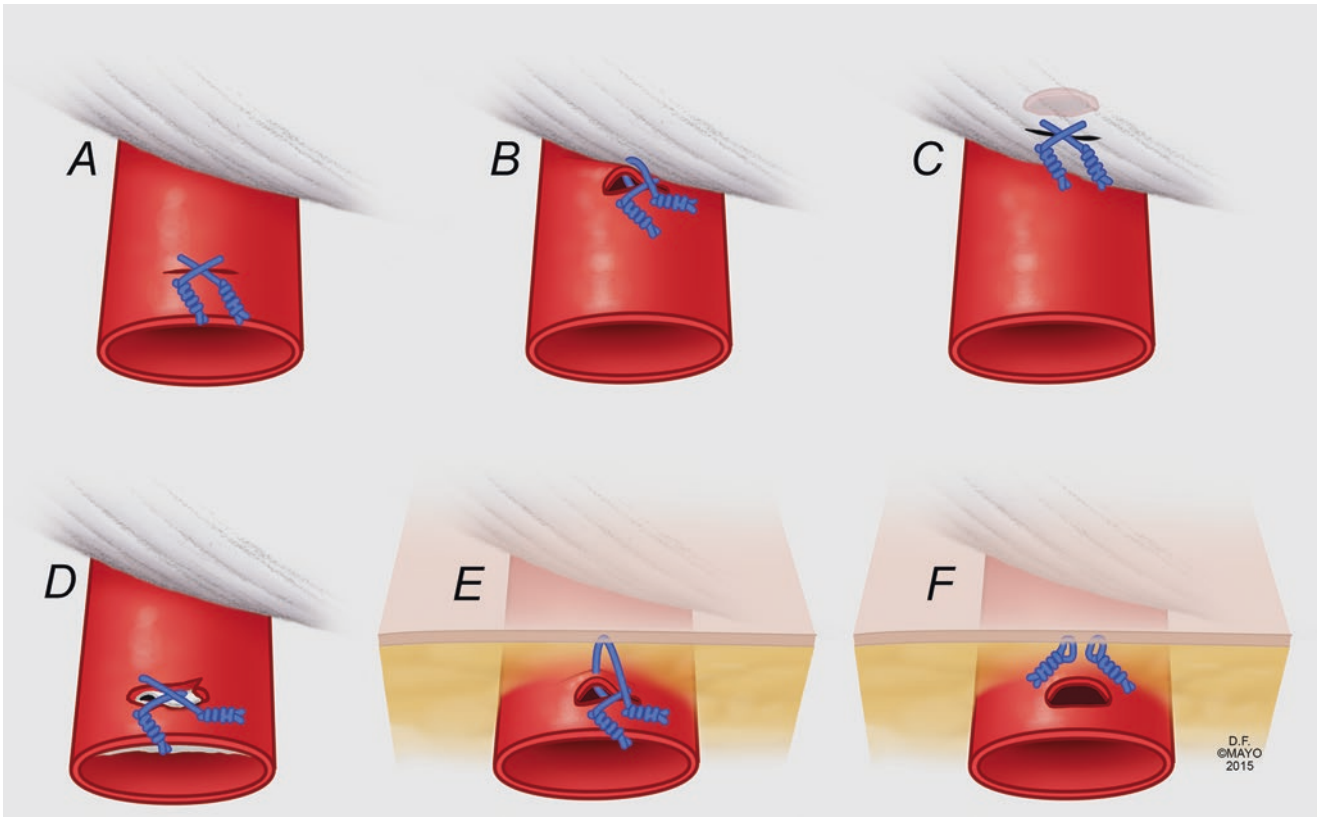


Fig. 28.11 The stitches are deployed at opposite angles creating a figure of eight configuration (**a**). Several failure mechanisms can occur in a small number of patients including stitches placed in the artery and inguinal ligament (**b**), stitches placed solely in the inguinal ligament (**c**), calcified plaque preventing closure (**d**), or stitches partially (**e**), or completely placed in the dermis (**f**). By permission of Mayo Foundation for Medical Education and Research. All rights reserved

lets, which are accessed by two short 7 Fr sheaths at 2 and 7 o'clock position.

Pre-catheterization of the renal arteries is performed in at least one of the vessels to calibrate the on-lay fusion CT. This is done using 0.035-in. soft glide-wire and 5 Fr Kumpe or C1 catheter (Cook Medical, Bloomington, IN), which is supported by 7 Fr LIMA guide-catheters (see Fig. 28.13). Catheterization of both renal arteries as depicted in Fig. 28.13 is optional; in general this is no longer performed if on-lay CT imaging is available. Whatever technique is selected based on physician preference, it is important to be conscious about minimizing use of aortography, which requires larger amount of contrast and often needs to be repeated.

Once the target vessels are located on the basis of pre-catheterization or on-lay imaging, the fenestrated stent graft is oriented extracorporeally (Fig. 28.14), introduced via the contralateral (left) femoral approach, and deployed with perfect apposition between the fenestrations and the target catheters. It is critical to assure proper orientation of the device using the anterior and posterior markers. It is useful to deploy the first two or three stents and then rotate the imaging unit laterally, confirming alignment between the catheter and its respective fenestration. The device should be deployed slightly higher than what is anticipated, with the catheter matching the lowest of the four radiopaque markers in the fenestration (Fig. 28.15). The diameter-reducing wire allows some rotational and cranial–caudal movement of the main stent graft to optimize alignment. After deployment of the fenestrated component, each catheter is removed from its target artery and used to sequentially regain access into the fenestrated component, fenestration and target vessel. The renal arteries are typically catheterized using the same catheter or guide-catheter, which was utilized during pre-catheterization (Figs. 28.16 and 28.17). In most cases the target vessel is accessed without difficulty. Although this technique is used for two or three vessel designs (e.g., ZFEN® stent grafts), our preference is to modify the sequence of catheterization by combining brachial approach in cases with four fenestrations. In these patients the four vessel fenestrated design is ordered with preloaded catheters into the celiac and SMA fenestrations (Fig. 28.18a–d). These catheters exit via an access scallop in the top part of the stent. A 480-cm 0.025-in. Metro guide-wire (Cook Medical, Bloomington, IN) is advanced into each of the two preloaded guide-wires and snared via a 12 Fr left brachial sheath which is positioned in the descend-

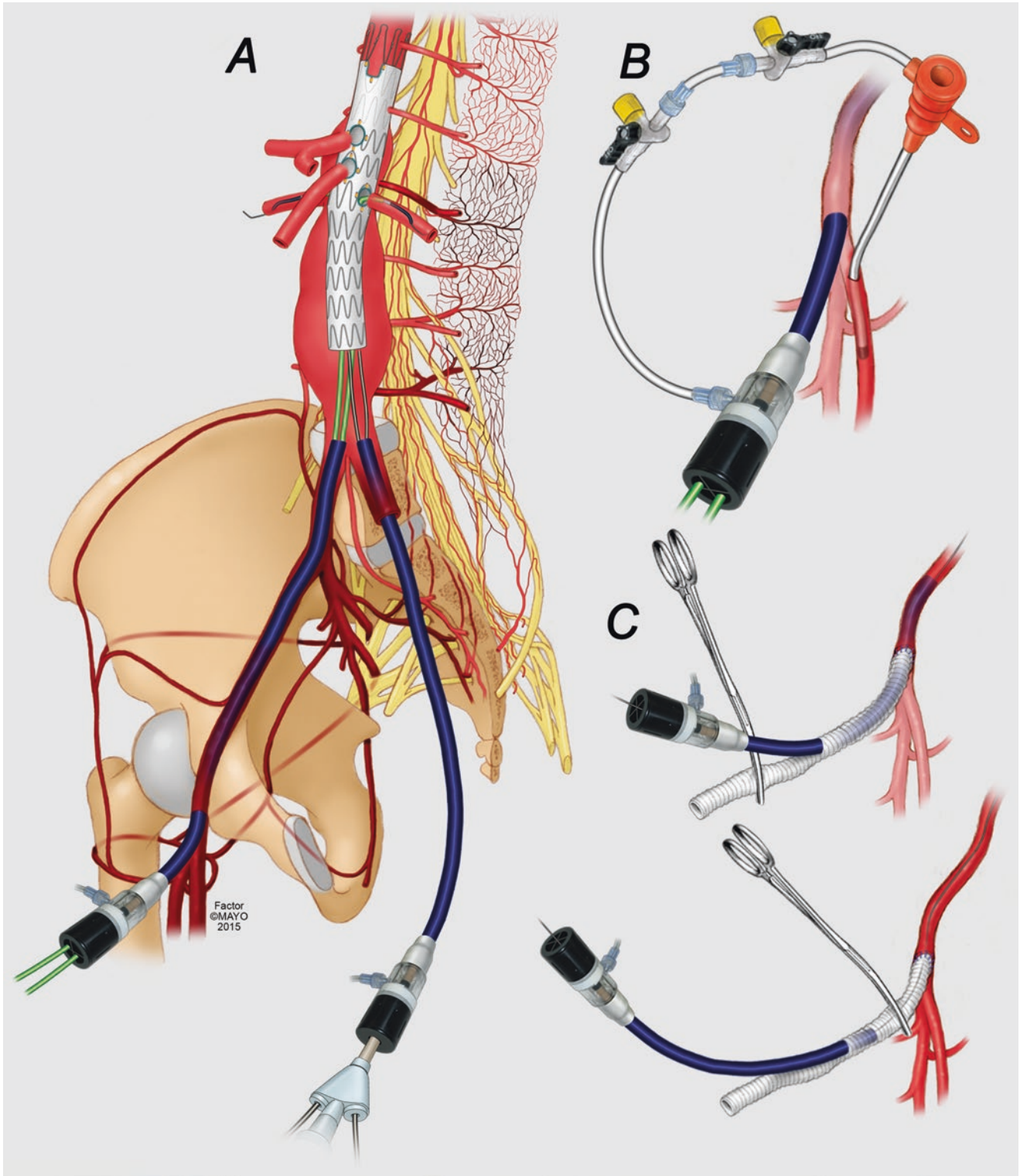


Fig. 28.12 Temporary common femoral artery conduit technique has been used in complex cases to minimize lower extremity ischemia. Note that the iliofemoral sheath is occlusive to the internal iliac artery and profunda femoral artery, which can compromise collateral perfusion into the pelvis and spine (**a**). One option to avoid lower limb ischemia is placement of a small antegrade sheath in the superficial femoral artery (**b**), while connecting both sheath ports with a three-way stopcock. However, this technique does not eliminate ischemia via the profunda or internal iliac arteries. A temporary femoral artery conduit can be anastomosed end-to-side (**c**) for introduction of the sheath. Once the device is deployed the sheath is retracted back restoring flow to the lower extremity (**c**). By permission of Mayo Foundation for Medical Education and Research. All rights reserved

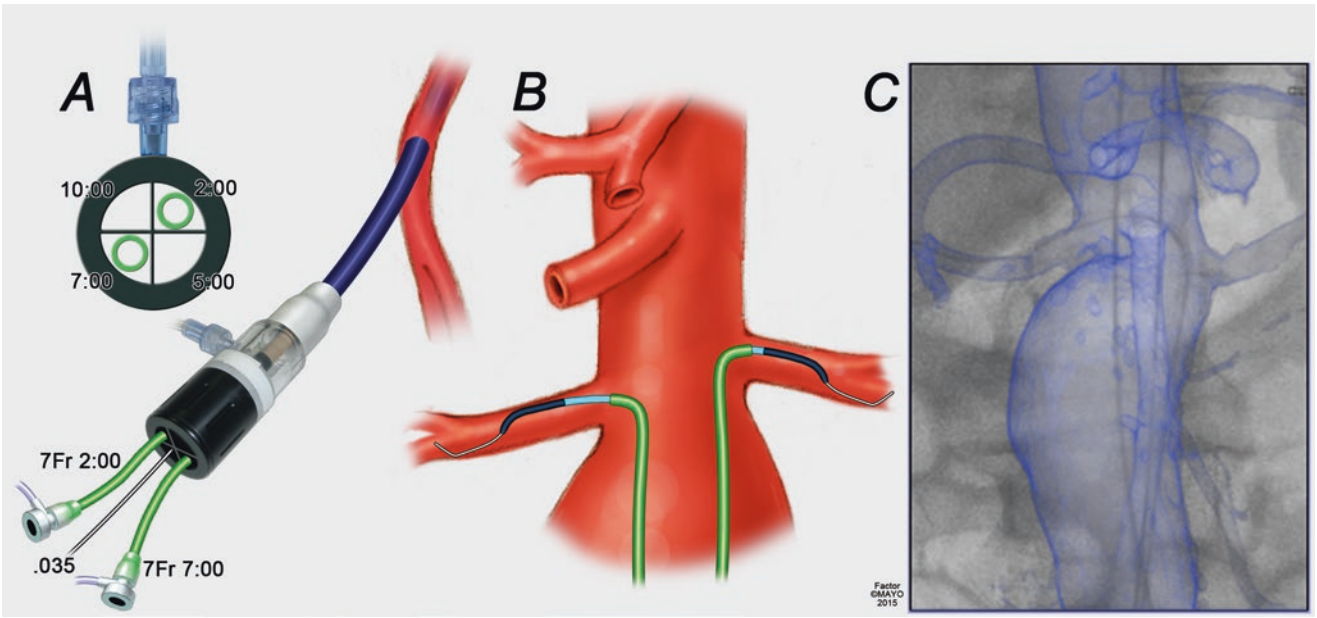


Fig. 28.13 Right femoral multi-sheath access is established using a Check-Flo sheath (**a**). The sheath valve has four leaflets (**a**), which are punctured for placement of two 7 Fr sheaths. Access into one or both renal arteries is obtained using LIMA guide-catheters and catheters (**b**) or alternatively on-lay fusion computed tomography (**c**) is used to locate the target vessels and minimize use of contrast. By permission of Mayo Foundation for Medical Education and Research. All rights reserved

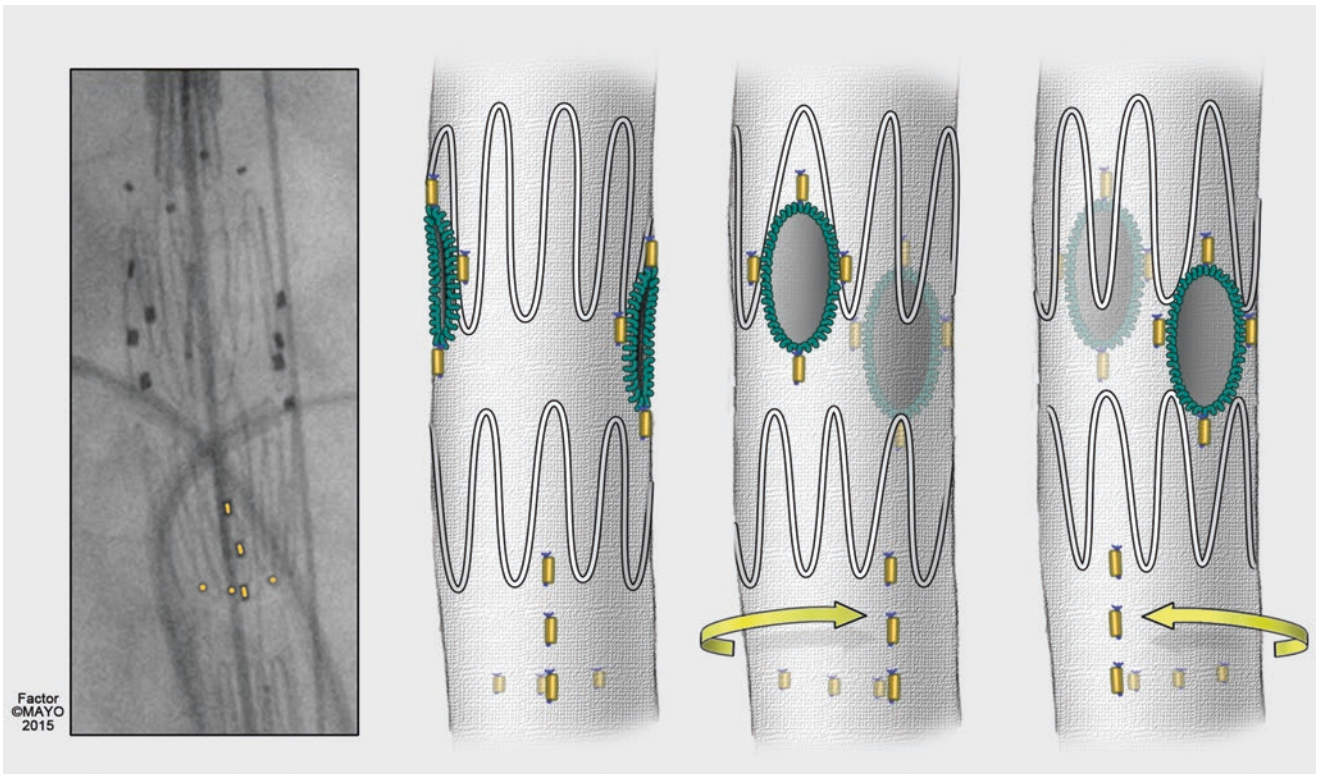


Fig. 28.14 Orientation of the fenestrated and branched stent graft is performed extracorporeally by rotating the device under fluoroscopy while observing the anterior and posterior markers. Clockwise and counterclockwise rotation of the device will move the anterior markers to the left side and right side of the patient, respectively, provided the device is in the correct orientation. Ideally, for fenestrated stent grafts, the anterior and posterior markers should be positioned in a perfect cross configuration. By permission of Mayo Foundation for Medical Education and Research. All rights reserved

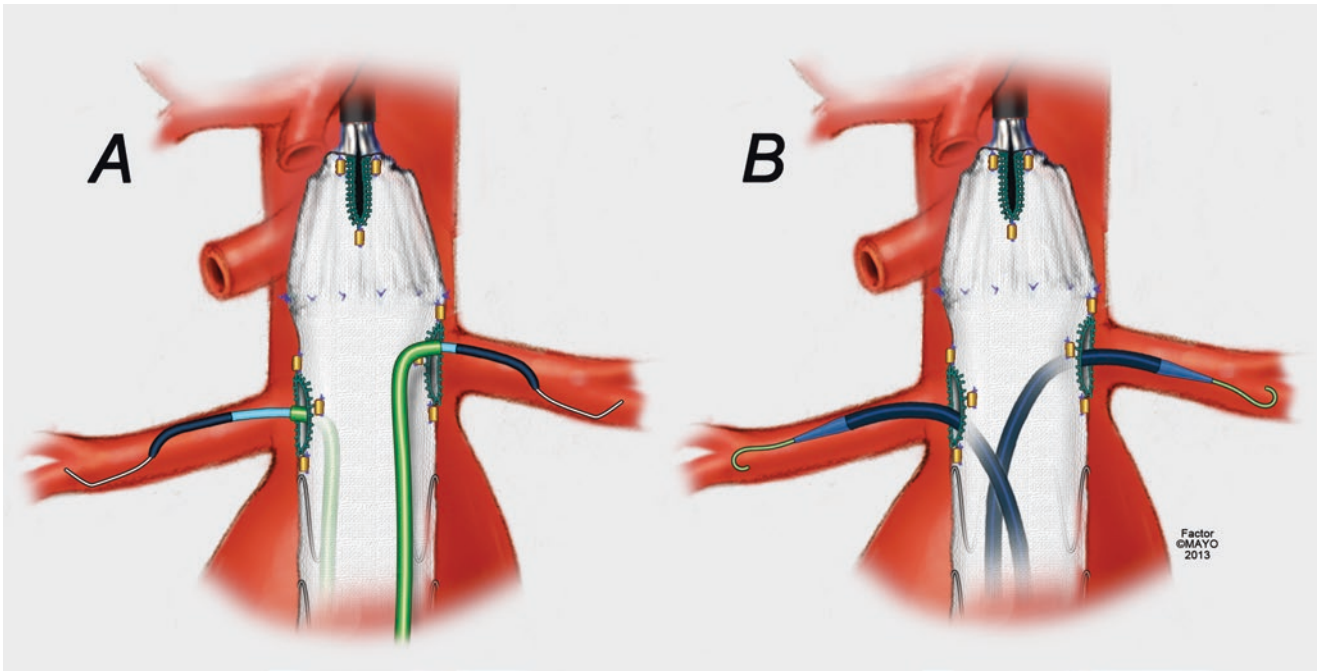


Fig. 28.15 Deployment of a two-vessel fenestrated stent graft is depicted in the illustration. For two or three vessel designs the author's preference is to use only femoral access whenever possible. Note the device is deployed matching the renal catheters or slightly higher (**a**). Excessive device manipulation is not recommended. Each catheter is sequentially removed from the renal artery and used to regain access into the fenestrations and target vessels (**b**), followed by advancement of a hydrophilic sheath over 0.035-in. Rosen guide-wires. By permission of Mayo Foundation for Medical Education and Research. All rights reserved

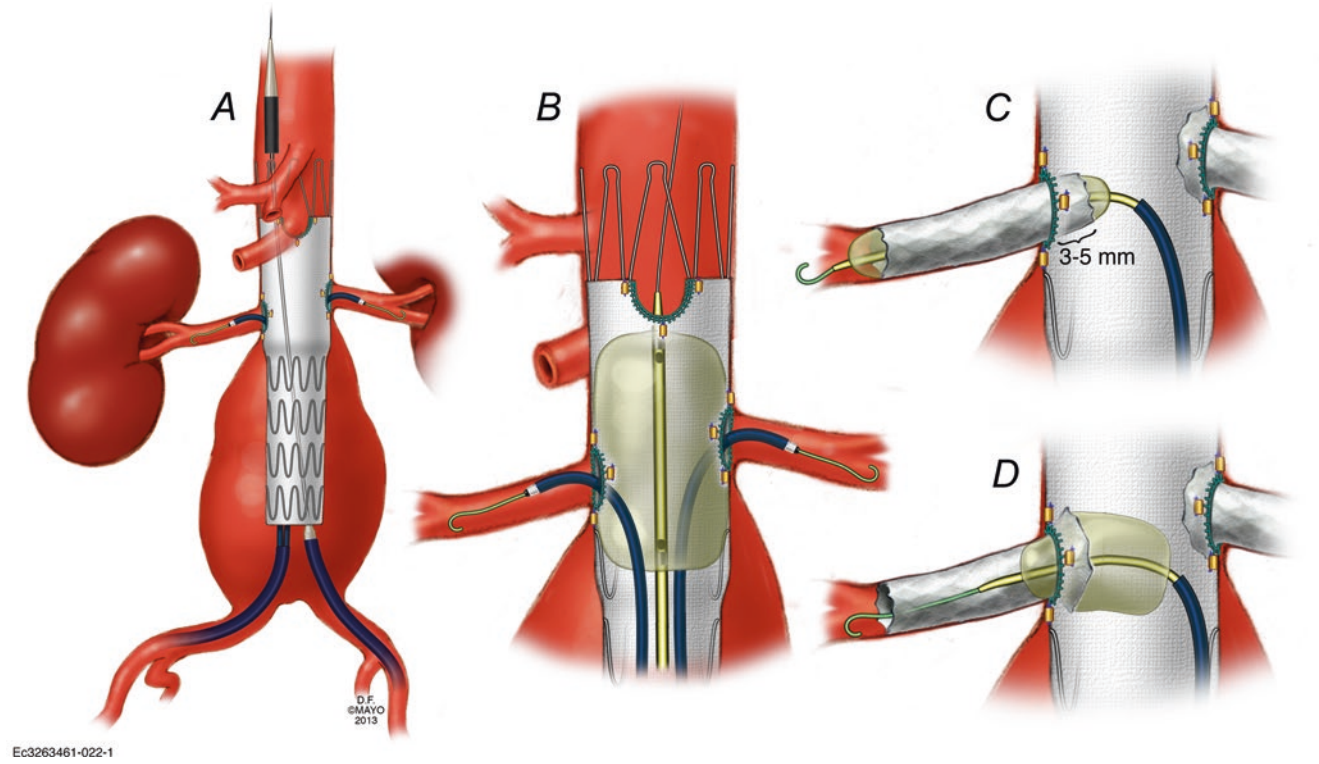


Fig. 28.16 Once the renal sheaths are positioned, the diameter-reducing tie is removed and the top cap is retrieved (**a**). The proximal neck is gently dilated with coda balloon (**b**), followed by placement of alignment stents (**c**). Each of the stents is flared using a 10-mm angioplasty balloon (**d**). By permission of Mayo Foundation for Medical Education and Research. All rights reserved

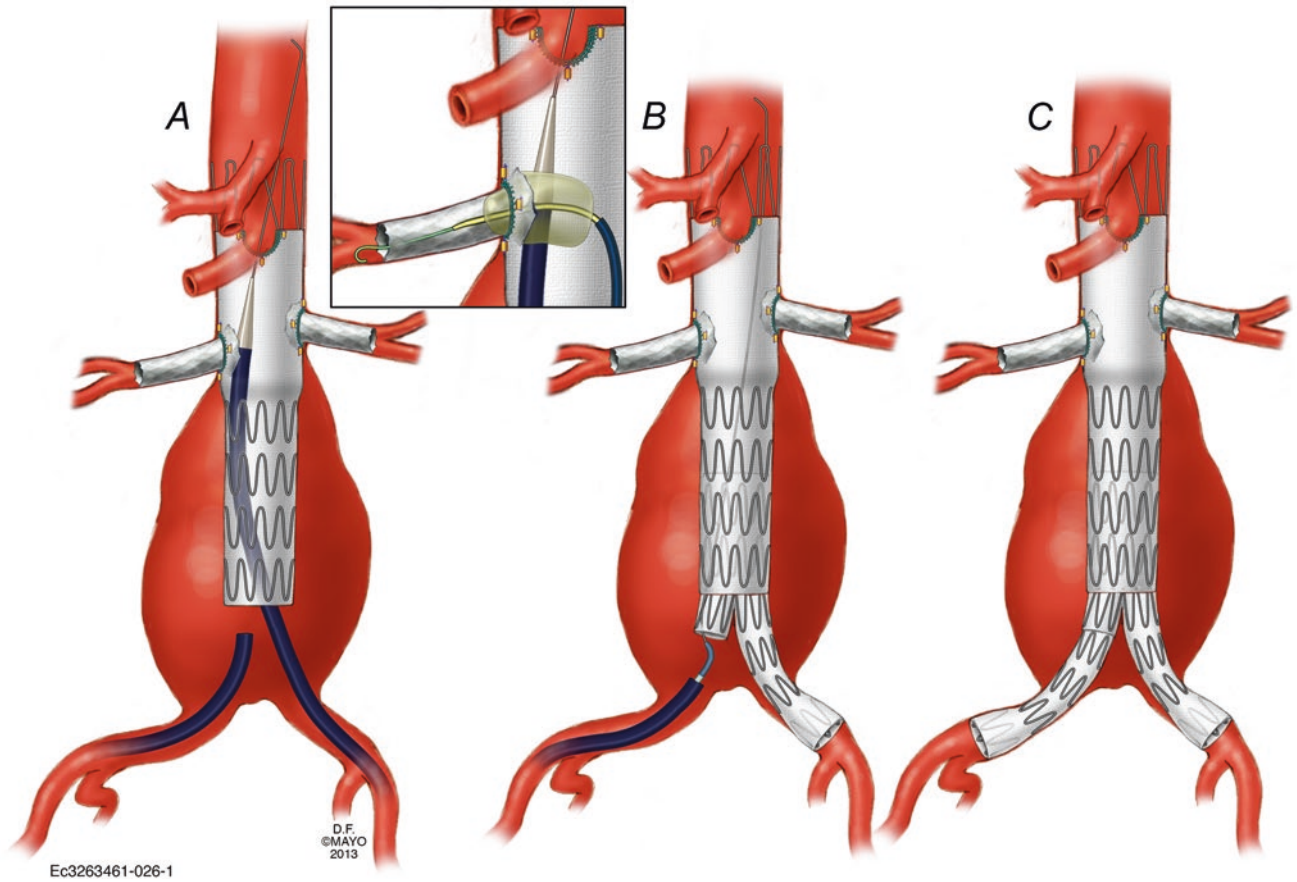


Fig. 28.17 During advancement and deployment of the bifurcated stent graft it is useful to protect the renal stents (**a**) to avoid compression or kink (**b**). The repair is completed by placement of bifurcated stent graft. By permission of Mayo Foundation for Medical Education and Research. All rights reserved

ing thoracic aorta. This allows immediate access into the celiac and SMA fenestration. In these cases the device is deployed only up to the SMA fenestration, thereby allowing room for catheterization of the celiac and SMA from above. After the celiac is catheterized and a 0.035-in. Amplatz guide-wire is positioned, the same steps are performed with the SMA. A 7 Fr hydrophilic sheath is advanced into the SMA and the remaining of the device is deployed.

Catheterization of the renal artery fenestrations is done using the femoral approach with a soft glide-wire and Kumpe catheter once the celiac and SMA are catheterized via the brachial approach (Fig. 28.18e–i), hand injections are used to confirm location prior to introduction of 0.035-in. Rosen guide-wires (Cook Medical Inc, Bloomington, IN) into the renal arteries. The Rosen guide-wire has a J-tip, which is less prone to cause branch perforations. If additional support is needed, the Amplatz guide-wire (Cook Medical Inc. Bloomington, IN) with 1-cm soft tip can be utilized, but this guide-wire has greater potential for trauma, dissections, and perforations. After the Rosen guide-wire or stiff guide-wire of choice is positioned, a 7 Fr Ansel sheath with flexible dilator is advanced into the renal arteries and SMA, if the vessel is intended to be stented via the femoral approach. Alternatively, if the celiac and SMA are performed from the brachial approach, the renal fenestrations are done from below once the device is deployed. If there is difficulty to advance the sheath, an undersized balloon may be used as a dilator to facilitate advancement as depicted in Chap. 19.

The alignment stents are positioned under protection of the sheath with the tip of the stent just beyond the distal edge of the sheath to function as dilators (see Fig. 28.18e–i). This helps prevent inadvertent trauma to the renal arteries with any advancement of the renal sheaths, which can occur during ballooning of the aortic neck. Slight variations of the fenestrated technique are dependent upon number of fenestrations, approach and use of preloaded systems. For repairs performed using two or three vessel fenestrations with the ZFEN® stent graft, the target vessels are accessed sequentially using femoral approach. For those requiring four fenestrations, the celiac axis and the SMA are accessed via brachial approach using a preloaded catheter as previously outlined.

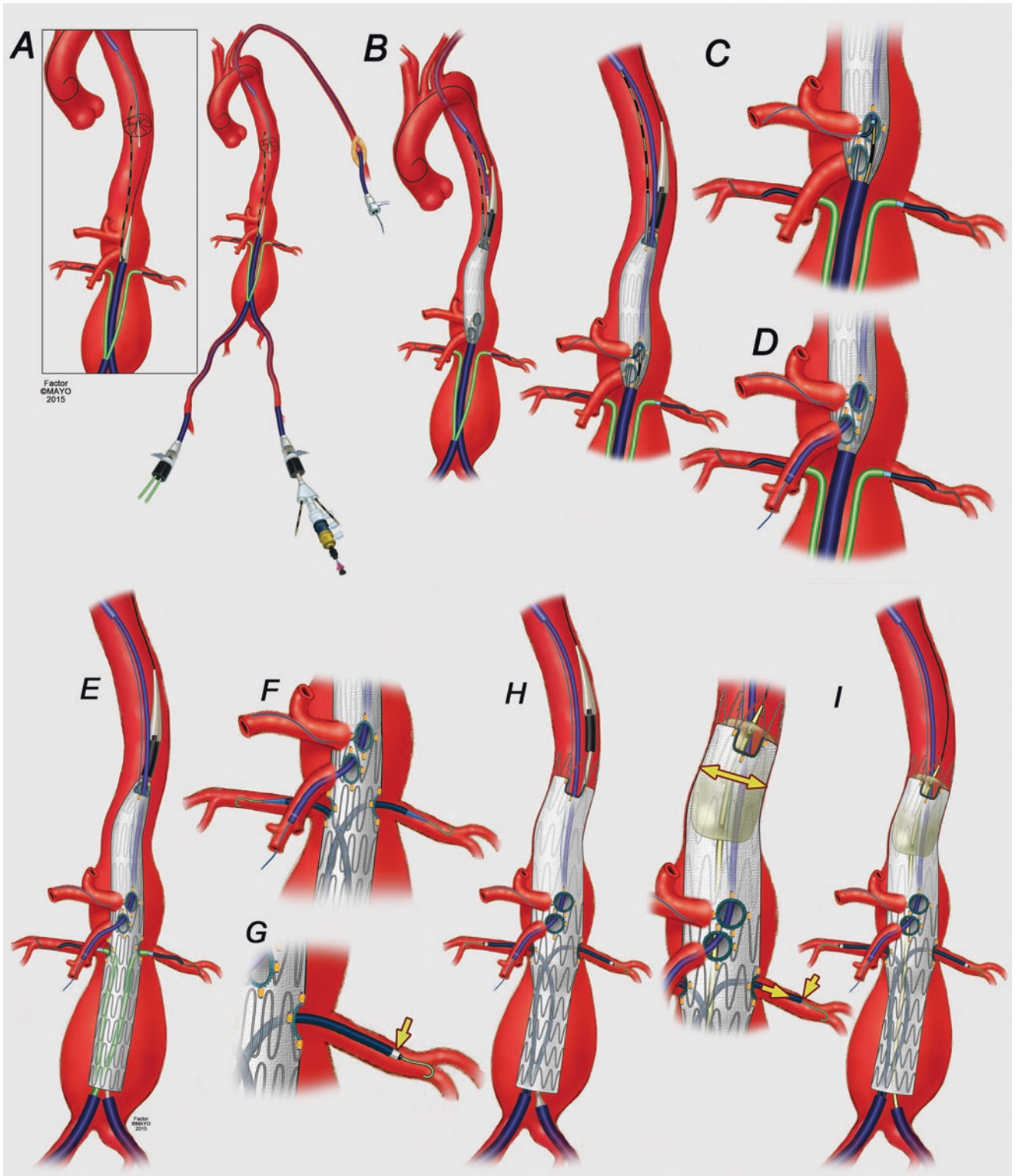


Fig. 28.18 Illustration depicts the technique used for four vessel fenestrations with preloaded catheters into the celiac and SMA fenestration. These catheters exit via an access scallop in the top of the device (**a**). The catheters allow guide-wires to be advanced and snared via the brachial approach using an Indy Snare (Cook Medical). Once both guide-wires are snared, the device is deployed to the level of the SMA fenestration (**b**). First a 7 Fr sheath is advanced over the celiac fenestration (**c**) and a buddy catheter is used for catheterization of the celiac axis. A 0.035-in. Amplatz guide-wire is left in the celiac axis. The sheath is then advanced over the SMA fenestration and the SMA is sequentially catheterized in similar fashion (**d**). The 7 Fr sheath is positioned into the SMA while the celiac is secured only by guide-wire access (**d**). The distal portion of the device is deployed once the celiac and SMA are catheterized by the brachial access (**e**). The guide-catheters

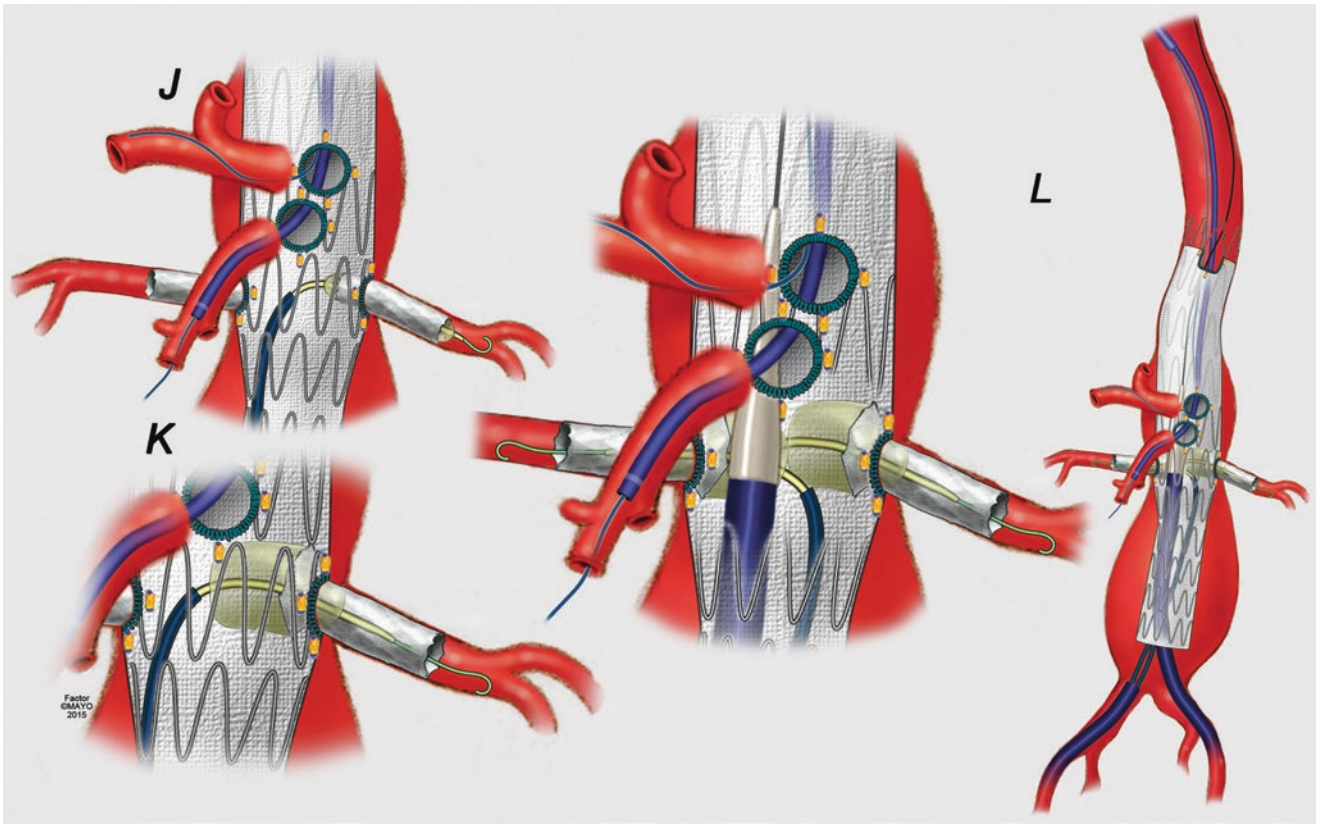


Fig. 28.18 (continued) are sequentially removed from the renal arteries and used to regain access into the renal fenestrations and renal arteries from the femoral approach (**f**). Seven French sheaths are advanced over a Rosen guide-wire into each of the renal arteries (**f**). The renal alignment stents may be positioned inside the sheath with the tip of the stent serving as a dilator (**g**) to protect the vessel from a dissection. Before deployment of the alignment stents (h), the proximal sealing zone is dilated (**i**). The diameter-reducing tie and the uncovered stent of the fenestrated component are deployed once access into all target vessels is obtained. The top cap is removed and the proximal landing zone is dilated using balloon prior to placement of the alignment stents. The renal stents are deployed first starting with the highest renal artery (**j**), followed by the lowest renal artery. Each stent is flared with a 10-mm angioplasty balloon (**k**). The author's preference is to place the bifurcated device prior to the SMA and celiac stent. Note that during introduction of the bifurcated component angioplasty balloons are inflated in the renal stents to prevent compression (**l**). After the bifurcated component is deployed the contralateral gate is catheterized (**m**). The repair is extended into the common iliac artery using an extension (**n**) with careful attention to avoid compression of the renal stents. The SMA and celiac stents are deployed sequentially via the brachial approach (**o**) to complete the repair. By permission of Mayo Foundation for Medical Education and Research. All rights reserved

The diameter-reducing ties are removed after all the target arteries are accessed and secured by placement of 7 Fr hydrophilic sheaths. Most devices are ordered with a single diameter-reducing tie, but two or more ties are also optional. With the four vessel repairs, the only exception is the celiac axis, which is secured by a 0.035-in. Amplatz wire with no sheath; it is important not to loose guide-wire access once the device is completely deployed. The top cap of the device is advanced forward and the uncovered fixation stent is deployed, which fully fixates the aortic component in the aorta (see Fig. 28.18e–i). The top cap is retrieved prior to deployment of the alignment stents. It is important during this segment of the procedure to avoid dislodgement of the sheaths. After the top cap and dilator are removed, the proximal landing zone is gently dilated using a compliable balloon such as the Coda balloon (Cook Medical Inc., Bloomington, IN). It is critical that the balloon dilation is performed prior to placement of alignment stents, or alternatively each stent has to be protected by separate balloons. One caveat is to avoid excessive dilation around the visceral arteries if there is excessive debris in the aorta to prevent embolization of this into the target vessels.

The next step following deployment of the aortic component is placement of the alignment stents. The technique can be slightly changed depending on the specific design. A basic principle is to start with the most cranial stent and work downwards when using the femoral approach. The alignment stents are sequentially deployed after removal of the diameter-reducing tie, retrieval of the top cap and balloon dilatation of the neck. The author's preference when working from the femoral approach is to start by the SMA, followed by the highest renal artery, finishing with the lowest renal

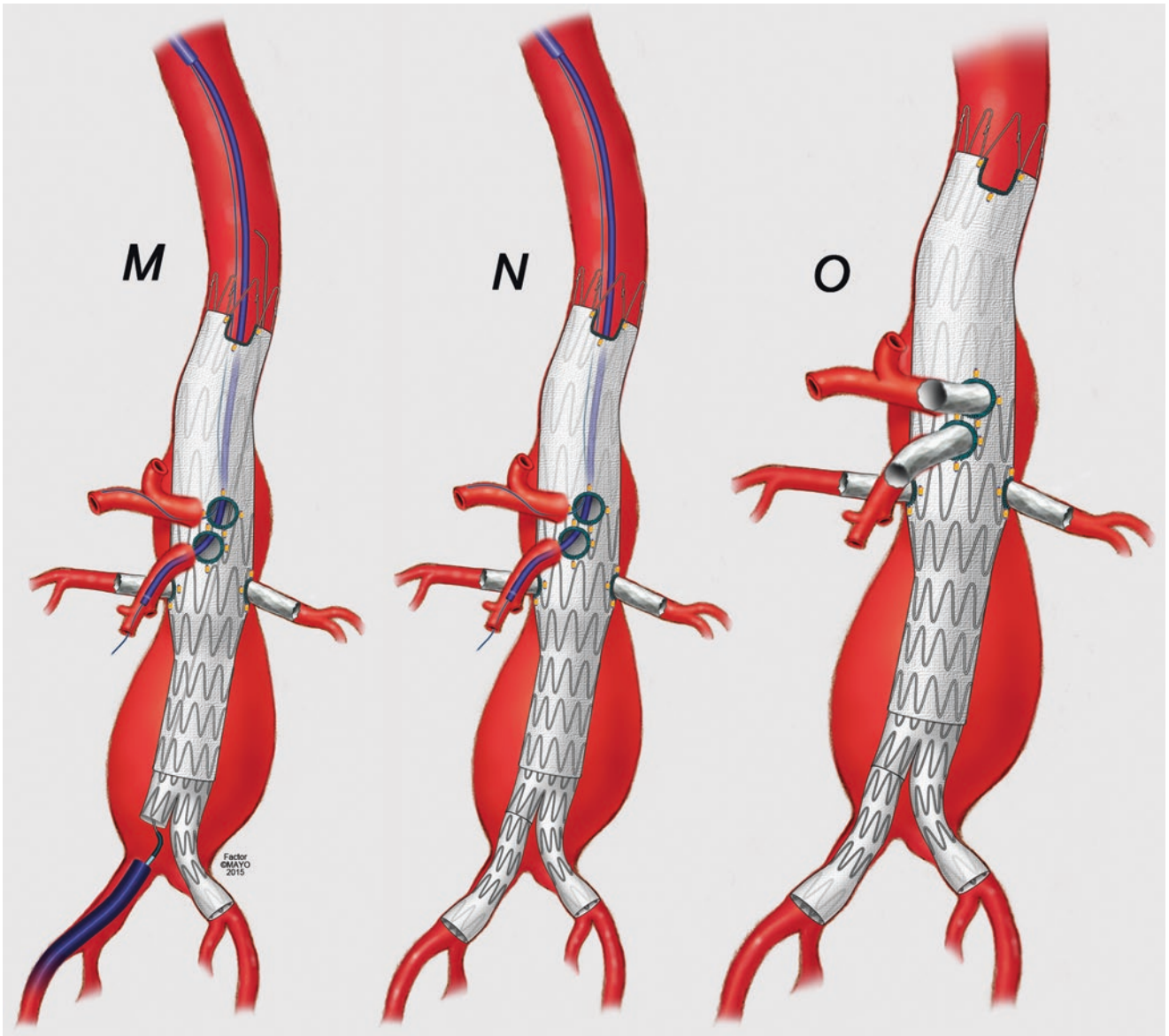


Fig. 28.18 (continued)

artery. For four vessel designs with preloaded catheters, the renals are done first, then bifurcated device, followed by the SMA and celiac axis. Prior to each stent deployment, the position of the stent is confirmed by hand injection. The stent is deployed 3–5 mm into the aorta and flared using a 10 mm × 2 cm balloon (Fig. 28.18j–l). A completion angiography of each branch is performed using hand injection. Occasionally administration of 100–200 μg of nitroglycerin is used to minimize spasm.

Following placement of the renal alignment stents, a distal bifurcated stent graft is oriented, advanced and deployed with preservation of the ipsilateral internal iliac artery. The dilator of the bifurcated device may encroach the contralateral renal stent or the SMA stent if this has already been done via the femoral approach. In these cases it is useful to leave a 10-mm balloon inflated in the renal stent to prevent damage (Fig. 28.18m–o). The minimum overlap between the bifurcated and the fenestrated component is two full-length stents, but ideally three or more full-length stents is recommended to minimize risk of component separation. After deployment of the bifurcated device, the dilator is removed with attention to avoid damage to the renal stents. The sequence is changed for four vessel designs with preloaded catheters from above. The author's preference is to place first the bifurcated device and iliac limbs, restore flow to the lower extremities, and

then finish the case with the SMA and celiac stent (see Fig. 28.18m–o). This optimizes lower extremity flow and avoids issues related to damage of the SMA and celiac stent during introduction of the dilator.

The contralateral gate is catheterized using a soft glide-wire and 5 Fr catheter. Access is confirmed by 360° catheter rotation and often by inflation of a coda balloon in the gate. The glide-wire is exchanged for a 0.035-in. Lunderquist guide-wire. Limited iliac angiography is performed using contralateral oblique views with hand injection. The contralateral limb extension is deployed with preservation of the internal iliac artery. A completion angiography of the aorta and iliac arteries is obtained using power injection to demonstrate patency of the visceral arteries, main body, iliac limbs and iliac arteries.

Patient-Specific Fenestrated and Branched Stent-Grafts

Combinations of fenestrations and branches allow for optimal customized designs that match the patient's anatomy (Fig. 28.19). The rationale for using a patient-specific design as opposed to an off-the-shelf design strategy is to maximize device characteristics to facilitate implantation and improve long-term branch outcomes. A frequently utilized design combines two directional branches for the celiac and SMA with two fenestrations for the renal arteries. This approach has been widely adopted by the Cleveland Clinic group and was initially proposed by Roy Greenberg. A helical branch for the celiac and SMA with 6×8 fenestrations for the renal arteries was the most common thoracoabdominal design

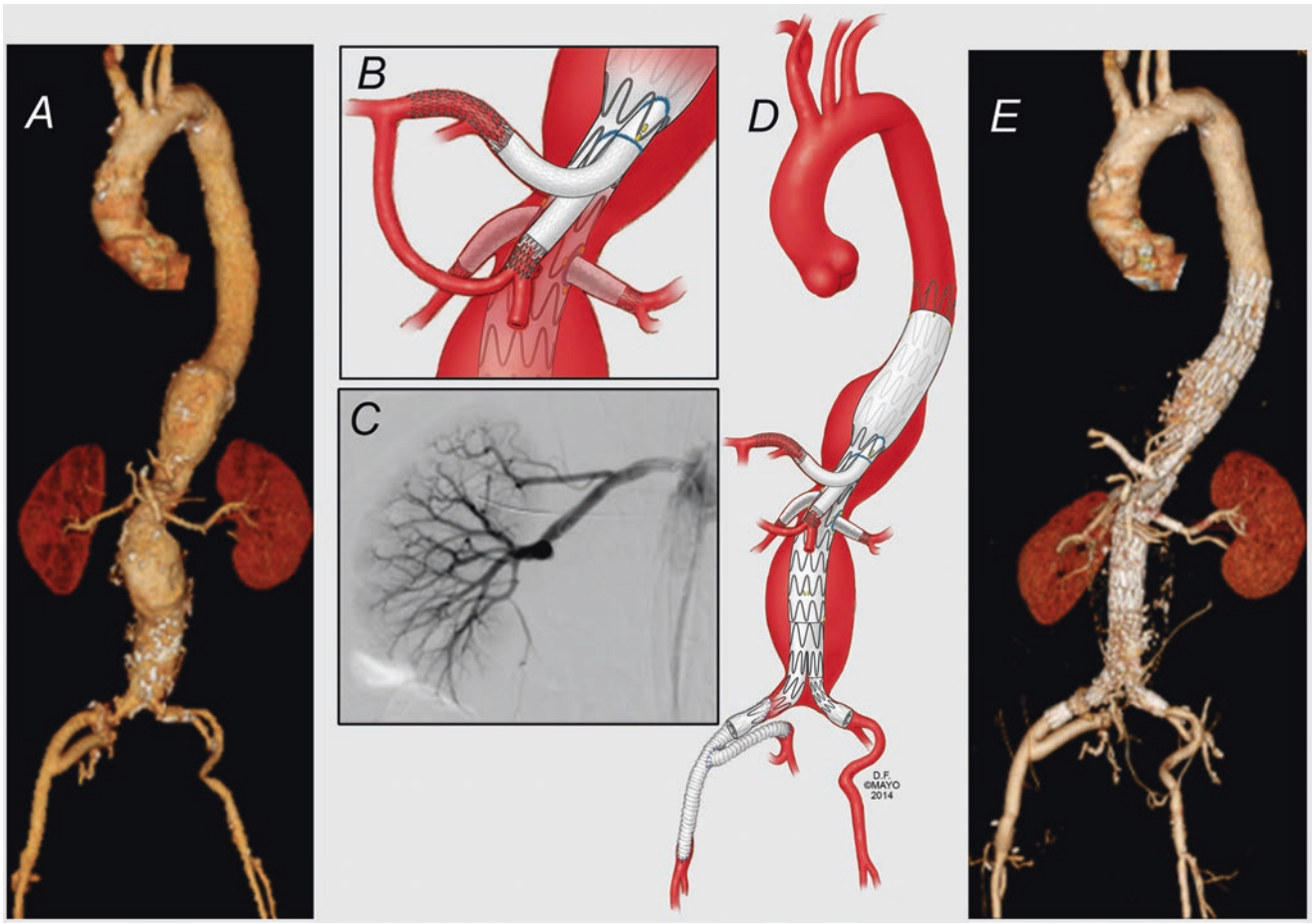


Fig. 28.19 Computed tomography angiography (CTA) of a patient with type III thoracoabdominal aortic aneurysm (**a**). Note the renal arteries originate from narrow aortic segment and are transversely oriented. A design with two directional branches for the celiac and SMA and two renal fenestrations (**b**) allow optimal alignment with the target vessels. Renal angiography (**c**) confirms widely patent renal artery with no endoleak. Illustration depicts the complete repair (**d**) which is demonstrated on follow-up CTA (**e**). By permission of Mayo Foundation for Medical Education and Research. All rights reserved

used in their experience. The author's preference whenever possible is to select two straight down going branches for celiac and SMA with 6×6 renal fenestrations for the renal arteries provided there is relatively narrow aortic diameter at this level. The author preference for 6×6 versus 6×8 renal fenestrations is to optimize a circular configuration of the nitinol ring. However, there is no clinical data demonstrating that one type of fenestration is better than other. This design has the advantage of short, transversely oriented branches for the renal arteries, which have been associated with exceedingly low occlusion rates.

The same principles already described for fenestrated stent grafts are applied with respect to device design, planning and arterial access. In these cases bilateral femoral access and left upper brachial artery access is needed (Fig. 28.20a–e). Similar to what has been described before, the right femoral access is utilized for pre-catheterization of the renal arteries whereas the left brachial access is used for the celiac axis and SMA with assistance of preloaded catheters in many cases.

Most extensive type I or II thoracoabdominal aortic aneurysms are staged. In the first stage, the proximal thoracic aorta is covered to the level of the celiac axis. Cervical debranching and permanent iliac conduits are done as part of the first stage if needed. In the second stage, the procedure is focused only on placement of the fenestrated and branch components to complete the repair. Nevertheless, if additional proximal thoracic stenting is needed, the author's preference is to start first with placement of the proximal thoracic TX2 stent graft (Cook Medical Inc., Bloomington, IN), depending on the need for a proximal extension. After one of the target vessels (renal artery or SMA) is pre-catheterized, the fenestrated-branched stent graft is oriented extracorporeally, introduced via the femoral approach and deployed with perfect apposition to the level of the SMA branch (see Fig. 28.20a–e). At this point the deployment is stopped and the preloaded catheters (if available) are used for advancement of guide-wires (Metro®, Cook Medical, Bloomington, IN), which are snared via the left brachial sheath. After access is obtained into the celiac branch and celiac axis, a 0.018-in. Steelcore guide-wire is positioned into the celiac axis. The same is repeated for the SMA and a 9 Fr sheath is positioned into the SMA over a short tip Amplatz guide-wire. The device is then adjusted so that the renal fenestrations match the target renal arteries. The device is then completed unsheathed and each catheter is sequentially removed from the renal arteries and used to regain access into the fenestrated component, renal fenestration and target renal artery (see Fig. 28.20a–e). Seven French hydrophilic sheaths and alignment renal stents are advanced into the renal arteries as previously described.

Once all four vessels are catheterized and sheaths are positioned into the renal arteries and SMA, the diameter-reducing tie is removed, allowing complete expansion of the fenestrated-branched component (Fig. 28.20f–i). Sequential renal artery stenting is performed using balloon-expandable covered stents for the renal fenestrated-branches, which are flared with 10 mm balloons. Again the sequence of the procedure has been modified to allow immediate restoration of blood flow into the lower limbs. Once the renal fenestrated stents are deployed, our preference at this point is to complete the distal reconstruction with placement of the bifurcated device while protecting both renal stents, followed by placement of iliac limb extensions, ballooning of attachment sides and landing zones and restoration of flow into both lower extremities. The procedure is completed by placement of self-expandable stent grafts for the SMA and celiac axis (see Fig. 28.20f–i). These are often reinforced by placement of a bare metal self-expandable stent into each of these branches. Selective branch angiography is performed after each branch stent is placed.

Multibranched Stent-Grafts

Directional branches designed with pre-sewn cuffs are currently performed using the Cook Zenith® branched stent graft lineage. Other designs including the Gore TAMBE®, Bolton® and Jotec® thoracoabdominal stent grafts apply similar concepts of directional branches and are currently under clinical investigation. The concept of a four-vessel multibranch stent graft design (T-branch®) was pioneered by Tim Chuter at the University of California San Francisco. Currently the device can be ordered as a patient-specific or off-the-shelf configuration.

The extent of repair varies depending on the proximal extension of aneurysm within the thoracic aorta. The procedure is performed using bilateral femoral and upper brachial approach (Fig. 28.20f–i). In general, the repair starts with deployment of a proximal thoracic TX2 stent graft (Cook Medical, Bloomington, IN), followed by deployment of a patient-specific or off-the-shelf T-branch® stent graft (Cook Medical, Brisbane, Australia). One of the advantages of using directional branches is that there is room to use selective catheters between the cuffs and target vessels; therefore implantation does not need to be done with extreme precision, which is needed for fenestrated stent grafts. In these cases the author's preference is to deploy the distal bifurcated component and contralateral limb extension. The self-expandable stents are placed into the four branches after all the aortic components are deployed.

Bilateral femoral and left brachial arterial access is obtained using the techniques already described. If needed, a proximal thoracic stent graft is deployed depending on aneurysm extension (Fig. 28.21). In these cases pre-catheterization of the renal arteries is not required, but it is critical that the distal edge of each of the directional branches is deployed

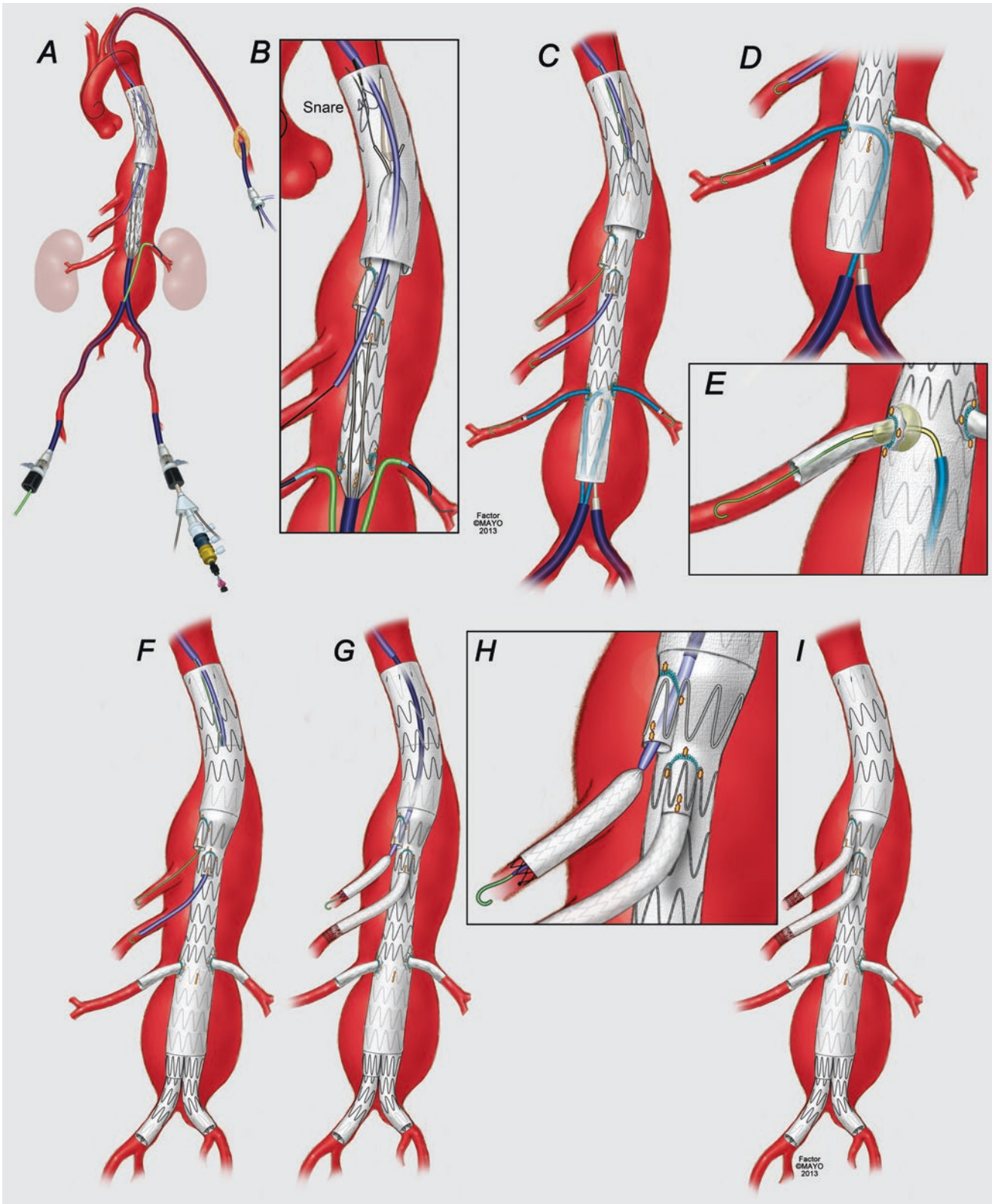


Fig. 28.20 A two branch-two fenestration stent graft design has been used to treat complex thoracoabdominal aortic aneurysms. The procedure is performed usually using bilateral femoral and left brachial approach. A proximal thoracic component is deployed first if needed (**a**). Pre-catheterization of at least one of the renal arteries is used to locate the target vessels using on-lay CT. The branched component is deployed up to the level of the renal fenestrations (**a**). Using preloaded catheters, guide-wires are snared from the brachial approach (**b**), and the celiac axis and SMA are catheterized from above. A sheath is typically placed into the SMA (**c**). The device is unsheathed completely (**c**)

1.5–2.0 cm above its intended target vessels and that there is a minimum internal aortic diameter of 25 mm to allow space for catheter manipulations. To guide deployment of the T-branch component, one of the vessels (e.g., one renal or the SMA) is often pre-catheterized via the brachial or femoral approach. The T-branch® stent graft is oriented extracorporeally, introduced via the femoral approach, and deployed with the directional branches located proximal to its intended target vessel. Deployment of the distal universal bifurcated stent graft and contralateral iliac extension are identical to what was described in the fenestrated technique. However, one important caveat is to avoid aggressive dilatation of the aortic bifurcation in these patients because the aneurysm sac is still perfused and inadvertent rupture of the aortic bifurcation can be a devastating complication.

The femoral arteries are closed at this point, restoring flow into the lower extremities. If the procedure is done percutaneously this can be done in an expeditious manner leaving the wire in place along with a small sheath. It is useful to maintain access into one of the femoral arteries with a 5–8 Fr sheath. This maneuver allows passage of a 0.014-in. guide-wire from the left brachial artery to femoral artery. The guide-wire is clamped in both ends, which locks the 12 Fr sheath in place and provides support for deployment of the side branches (Fig. 28.22a–c).

The 12 Fr Ansel I sheath (Cook Medical, Bloomington, IN) is advanced via the left brachial approach and positioned inside the T-branch® component in the to descending thoracic aorta. At this point a 0.014-in. guide-wire is advanced through-and-through from the left brachial to femoral artery,

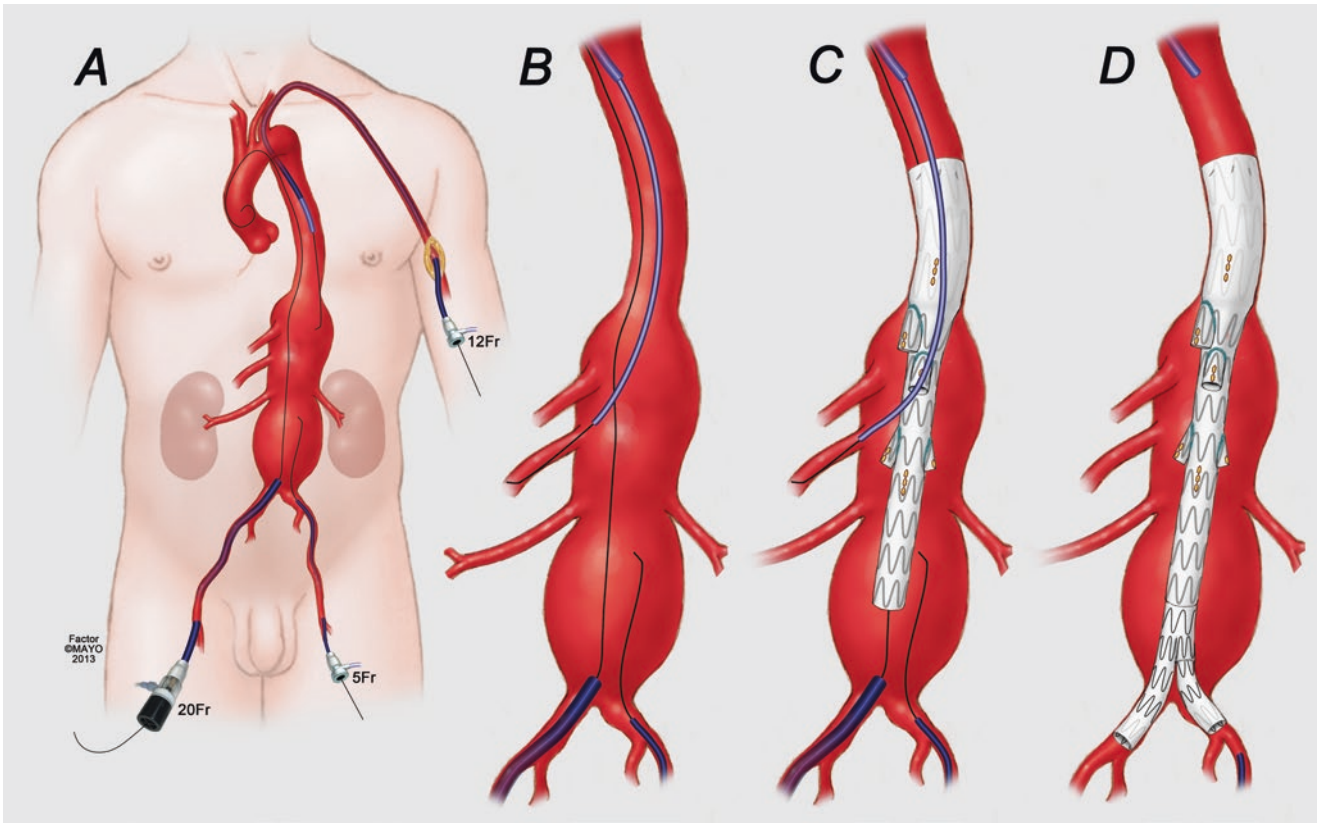


Fig. 28.21 Multibranched stent grafts are designed with four directional branches for the celiac axis, SMA and both renal arteries. The procedure is done using bilateral femoral and left brachial access (**a**). One of the target vessels is catheterized (**b**) to guide deployment of the multibranched stent graft (**c**). The distal bifurcated device and iliac limbs are added and flow is restored to the lower limbs (**d**). By permission of Mayo Foundation for Medical Education and Research. All rights reserved

Fig. 28.20 (continued) and the renal fenestrations and renal arteries are catheterized from the femoral approach. Hydrophilic sheaths are advanced into both renal arteries over 0.035-in. Rosen guide-wires (**c**). Sequential renal artery stenting is performed using balloon-expandable covered stents (**d**), which are flared using a 10-mm angioplasty balloon (**e**). The bifurcated component and iliac limbs are deployed after placement of the renal stents (**f**). Flow is restored into both lower limbs. The procedure is completed by placement of the SMA and celiac self-expandable stents (**g**). Note that each stent is extended distally with a bare metal self-expandable stent (**h**). Final illustration depicts complete repair (**i**). By permission of Mayo Foundation for Medical Education and Research. All rights reserved

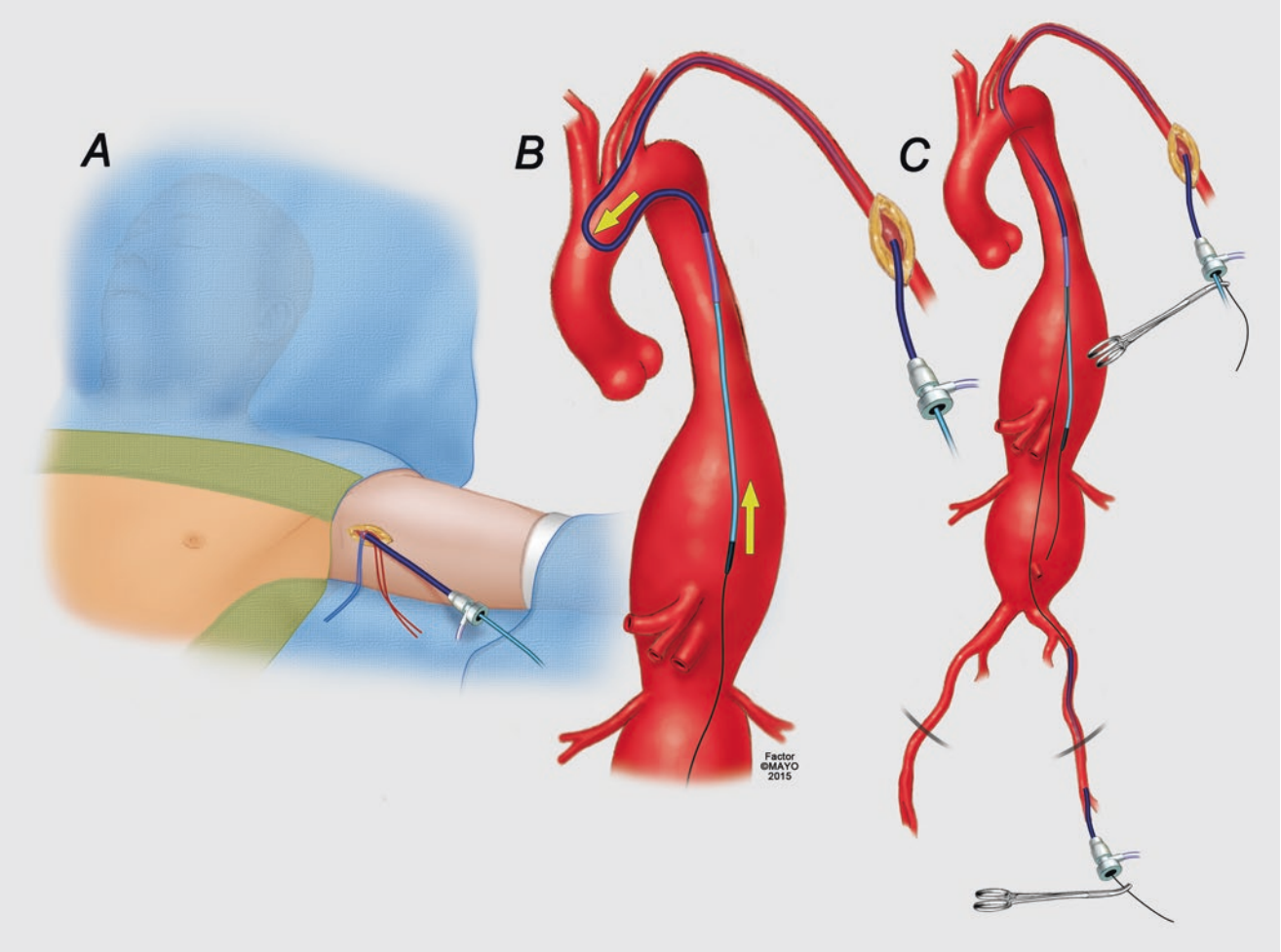


Fig. 28.22 An upper brachial artery exposure is usually adequate for access (**a**). The through-and-through maneuver with placement of a 0.014-in. guide-wire from the 12 Fr brachial artery to the 5–8 Fr femoral artery avoids the problem of the sheath protruding into the ascending aorta and arch (**b**) with each manipulation, securing the sheath in a more stable position (**c**). Once all aortic components are deployed and blood flow is restored to the lower extremities, a small sheath is maintained in one of the femoral arteries for through-and-through access (**d**). Each branch is accessed via the brachial approach followed by placement of bridging stents into the target vessels (**e**), starting by the renal arteries, followed by SMA and celiac axis. A self-expandable bare-metal stent is added to avoid kink at the distal edge (**f**). The repair is completed by placement of all four side-branch stents (**g**). By permission of Mayo Foundation for Medical Education and Research. All rights reserved

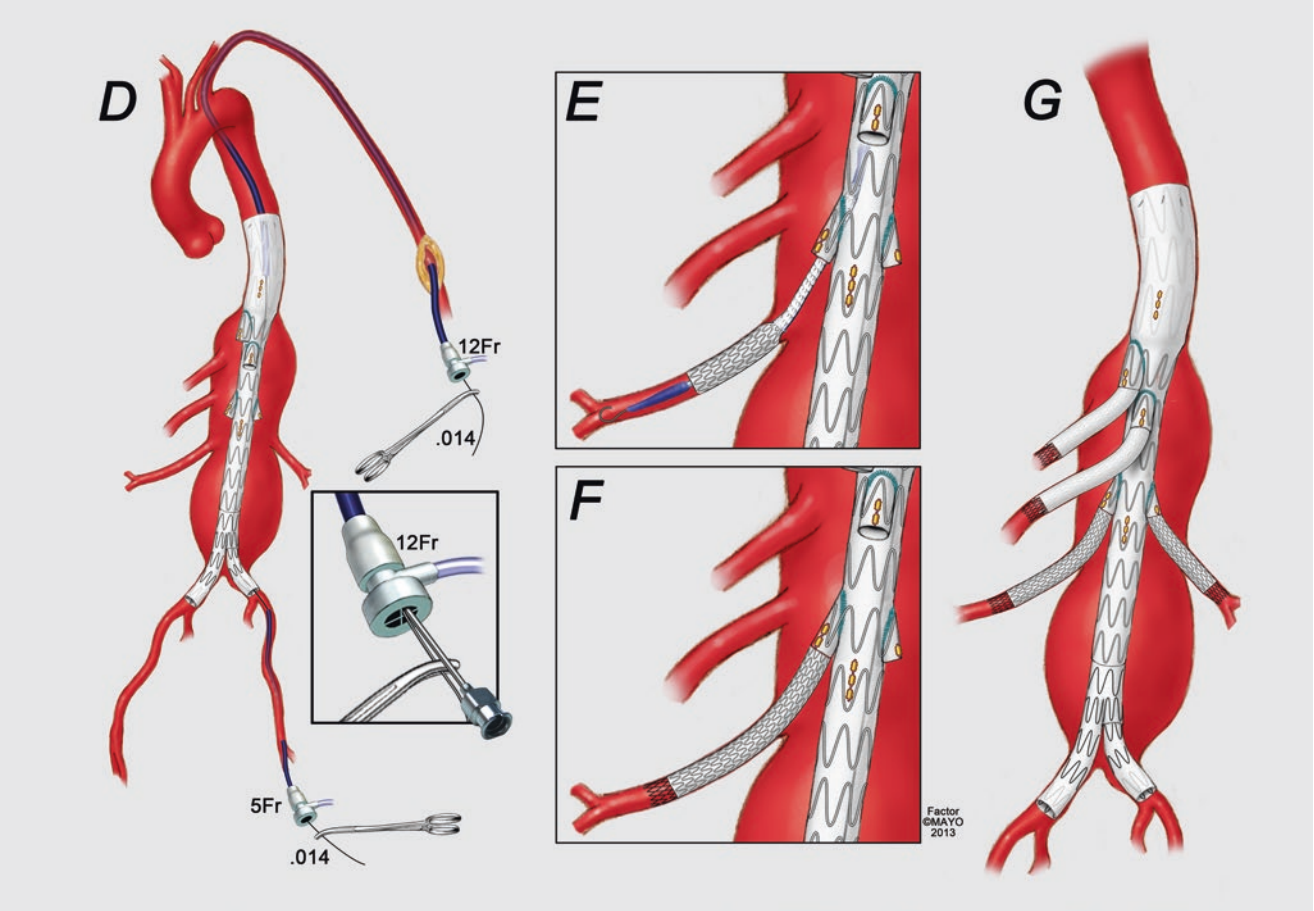


Fig. 28.22 (continued)

preventing movement of the 12 Fr sheath in the aortic arch. Each side branch is individually catheterized in a sequential fashion, starting with the renal arteries (Fig. 28.22d–g), followed by the SMA and celiac axis. A 5 Fr MPA or Kumpe catheter (Cook Medical, Bloomington, IN) is used to access the directional branch and target vessel. Once the vessel is catheterized, the soft glide-wire is exchanged for a stiff guide-wire (Rosen or short tip Amplatz, Cook Medical IN), which is positioned in the target vessel. Before the stent is deployed it is critical that one confirms that the guide-wire is placed into the correct cuff. This requires moving the imaging projection in different oblique views to visualize the guide-wire and the cuff (Fig. 28.23).

The author's preference is to use Viabahn® stent grafts (WL Gore, Flagstaff, AZ) for the renal arteries (Fig. 28.24) because of excellent conformability and possible superior patency rates. A Rosen guide-wire is used for the renal arteries. However, these stents are limited by either short (5 cm) or long length (10 cm) as well as difficult deployment. Therefore, one needs to be careful during deployment not to pull the stent out of the vessel. This can be prevented by slow deployment while leaving the sheath into the proximal half of the stent; then once the stent engages the vessel the sheath is pulled and the deployment is slowly completed. If the stent is too short or a 5-mm diameter is used, the author's preference is to use a proximal balloon-expandable covered stent to tack the Viabahn® into the cuff. The distal edge of the Viabahn® is reinforced by placement of a self-expandable bare metal stent. This is followed by balloon dilatation of all stents to profile and completion angiography.

Catheterization of each cuff can be facilitated by keeping the stiff wire into the branch (Fig. 28.25), while working with a buddy catheter to catheterize the next intended target branch. It is critical to assure that the catheter is in the correct branch before deployment of the bridging stent. One can easily misjudge the SMA for the celiac cuff or other and place the stent into the incorrect branch, compromising the entire repair. For stenting of the celiac and SMA a 9 Fr 70-cm Flexor sheath (Cook Medical, Bloomington, IN) is advanced coaxially within the 12 Fr sheath. Each target vessel is stented with a self-expandable stent graft—Fluency® or Viabahn®. The stent graft should be oversized by 1–2 mm and should provide at least 2-cm of distal landing zone in the target vessel, extending 2–5 mm into the aortic lumen of the T-branch® device. The author's preference is for Fluency® stent grafts (Bard Peripheral Vascular, Temple AZ) for the celiac and SMA

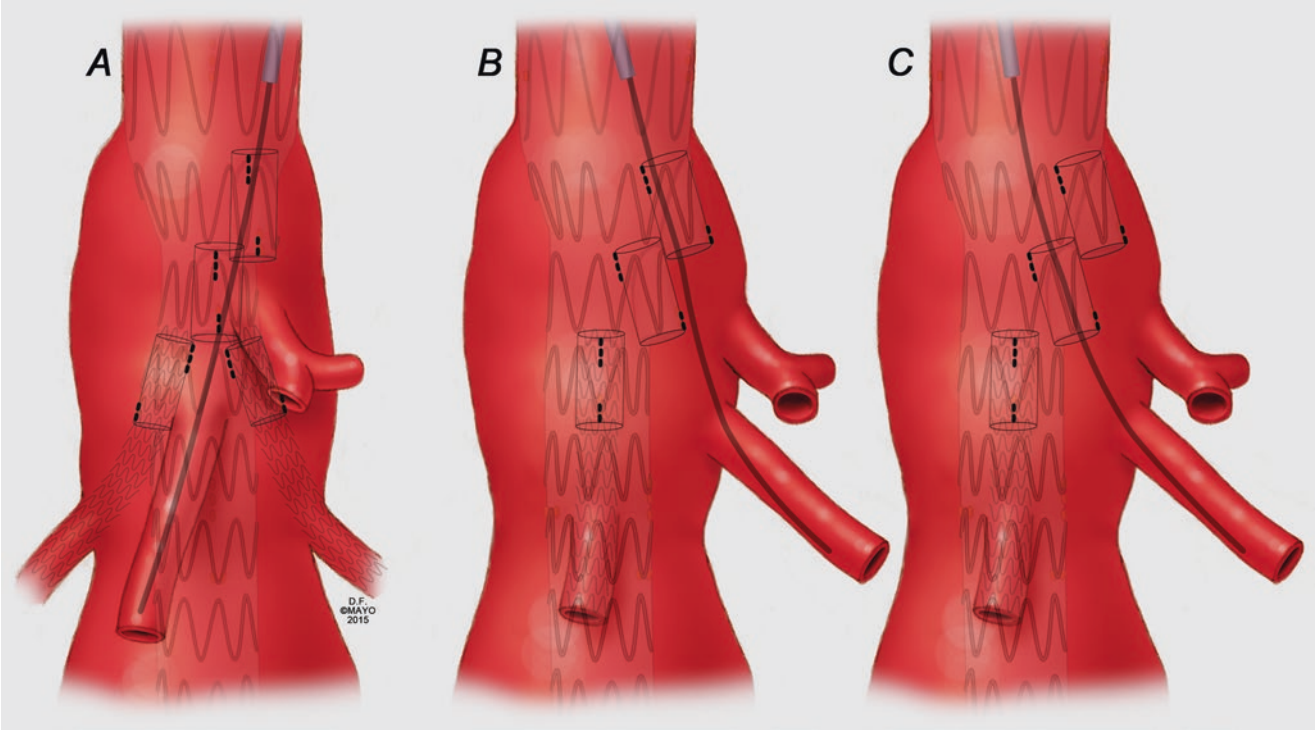


Fig. 28.23 Prior to stent placement it is important to confirm that the guide-wire was positioned in the correct cuff. The illustration depicts a guide-wire that on anterior–posterior view can be located in either the SMA or celiac cuff (**a**). By rotating the imaging in different projection, it is confirmed that the guide-wire is passing via the celiac cuff and not the SMA cuff, which is the intended target vessel (**b**). Stent placement in the celiac cuff would cause inability to complete the repair in the intended celiac axis. By permission of Mayo Foundation for Medical Education and Research. All rights reserved

because of smaller profile sheath with the larger diameter stents and greater availability of lengths. To prevent kinks in the transition of the stent graft to the target artery, each self-expandable stent graft is reinforced by a second self-expandable stent, which is deployed 1 cm beyond the distal edge of the stent graft. Selective completion angiography is obtained for each sequential branch. A completion angiography of the arch and thoracoabdominal aorta is obtained after all matting stent grafts are deployed. Figure 28.26 illustrates a patient treated by multibranched thoracoabdominal stent graft.

Staging

Staging procedures are needed in approximately 20–30 % of patients to overcome issues related to landing zone, access or need to cover extensive segments of the aorta. Approximately 15 % of the patients require an iliac conduit with standard device. The author's preference has been to use a permanent 10-mm common iliac to distal external or common femoral artery bypass. This is often combined with staged coverage of the proximal thoracic aorta for extensive type I and II thoracoabdominal aortic aneurysms (Figs. 28.27 and 28.28). Cervical debranching procedures are performed if needed. These techniques are further described in other chapters devoted to specific topics.

Preloaded Renal Guide Catheters

Preloaded guide-wires and guide-catheters can be used to facilitate the procedure by reducing some of the necessary steps, notably catheterization of each fenestration and/or branch, which is needed with conventional devices. A preloaded renal guide-catheter system is an integral part of the p-Branch® fenestrated stent graft (Fig. 28.29a–d), but can also be added to patient-specific designs. Because the guide catheters are preloaded over a stiff guide-wire into the renal fenestration, there is no need to catheterize the renal fenestration via the contralateral femoral approach (Fig. 28.29e–h). Instead, a 6 Fr 90-cm hydrophilic sheath is advanced using the preloaded system. Once the sheath is positioned outside the fenestration, a 4 Fr "curly" catheter can be shaped in multiple fashions to selectively catheterize the target renal

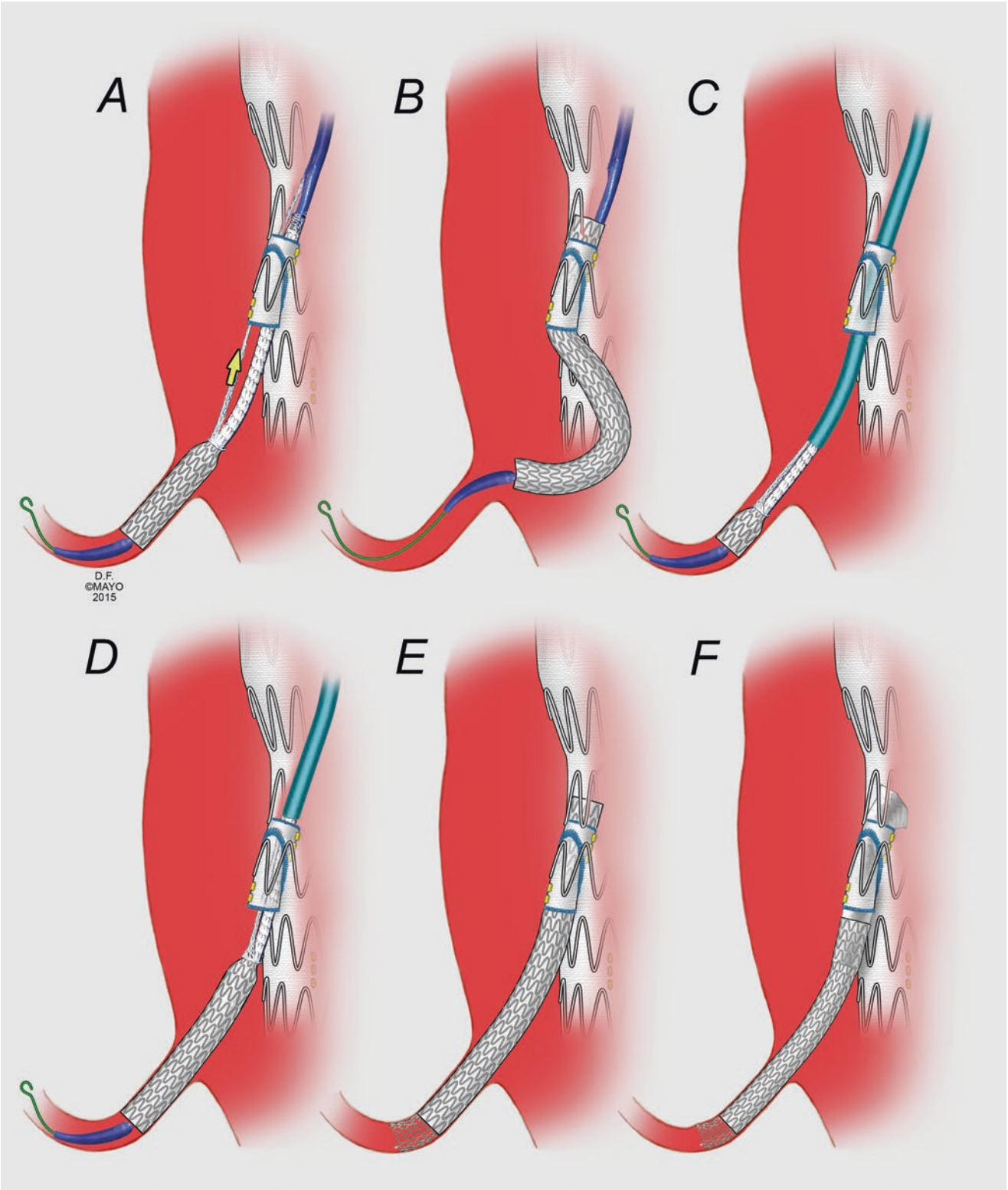


Fig. 28.24 Deployment of Viabahn stent grafts into the branches is done carefully to avoid dislodgement of the stent. Note that the deployment mechanism of the Viabahn is through a suture string (**a**) that when removed opens a sleeve that constrains the stent. The stent can be pulled out of the intended target vessel if this is done rapidly or in uncontrolled fashion (**b**). A useful technique is to keep the sheath in the middle portion of the stent graft (**c**), while the stent graft is deployed slowly to that level. The sheath is then retracted (**d**) and the deployment is completed (**e**). If needed, a proximal balloon-expandable covered stent or additional Viabahn stent graft is deployed to connect to the branch cuff (**f**). By permission of Mayo Foundation for Medical Education and Research. All rights reserved

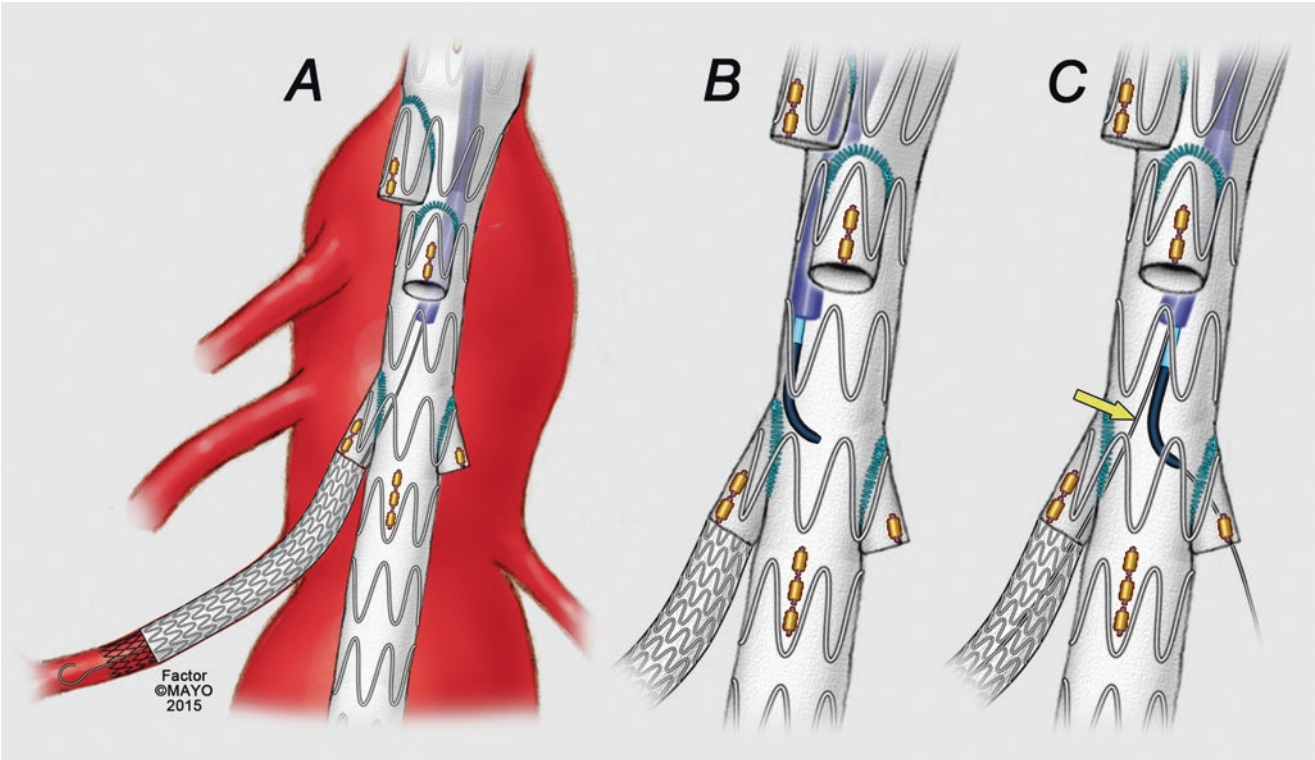


Fig. 28.25 Illustration depicts maneuver to facilitate branch catheterization after one of the branches is completed (**a**). Note that if the guide-wire is removed from the branch, the sheath and the catheter tend to be displaced to the lateral wall of the stent graft, which can make catheterization more difficult (**b**). Instead, keeping the guide-wire in the previous branch while using a "buddy" catheter (**c**, arrow) facilitates catheterization of the next intended branch. By permission of Mayo Foundation for Medical Education and Research. All rights reserved

artery. Although preloaded renal catheters eliminate at least one of the steps of the procedure, they require placement of the renal stent via a long 6 Fr instead of a short 7 Fr sheath. A limited number of catheter shapes are available in 4 Fr diameter and long length (125 cm), which is needed for selective catheterization. Therefore, at least in some cases pre-catheterization can be associated with technical difficulties, which offset the benefits of the system. Once the vessel is catheterized with a floppy glide-wire, the curly catheter is advanced into the vessel. Once both renals are catheterized using the 4 Fr catheter, the through-and-through guide-wire is removed and the 6 Fr hydrophilic sheaths are advanced via the catheters into the target renal arteries. The procedure follows the typical steps already described for fenestrated and mixed fenestrated and branched designs. The sheath diameter for the aortic stent graft delivery system ranges from 20 to 22 Fr depending on the graft diameter.

Preloaded Catheters and Guide-Wire Systems

The use of preloaded catheters or guide-wires serves as an adjunct to facilitate catheterization into fenestrations and branches. Typically the author uses preloaded catheters into the celiac and SMA fenestration and/or branch. These catheters are preloaded into the specific target fenestration or branch and exit via an access scallop, which is located in the top part of the device (see Fig. 28.18); or alternatively if the aortic stent is based on a TX2 stent graft, access scallop is not needed. A useful tip to snare the wires is to keep the catheters just above the level of the renal arteries when advancing the guide-wires. The guide-wire tip should also be gently bent into a 45° angle, so it seeks the outer edge of the aorta instead of the central lumen. To snare the guide-wire, our

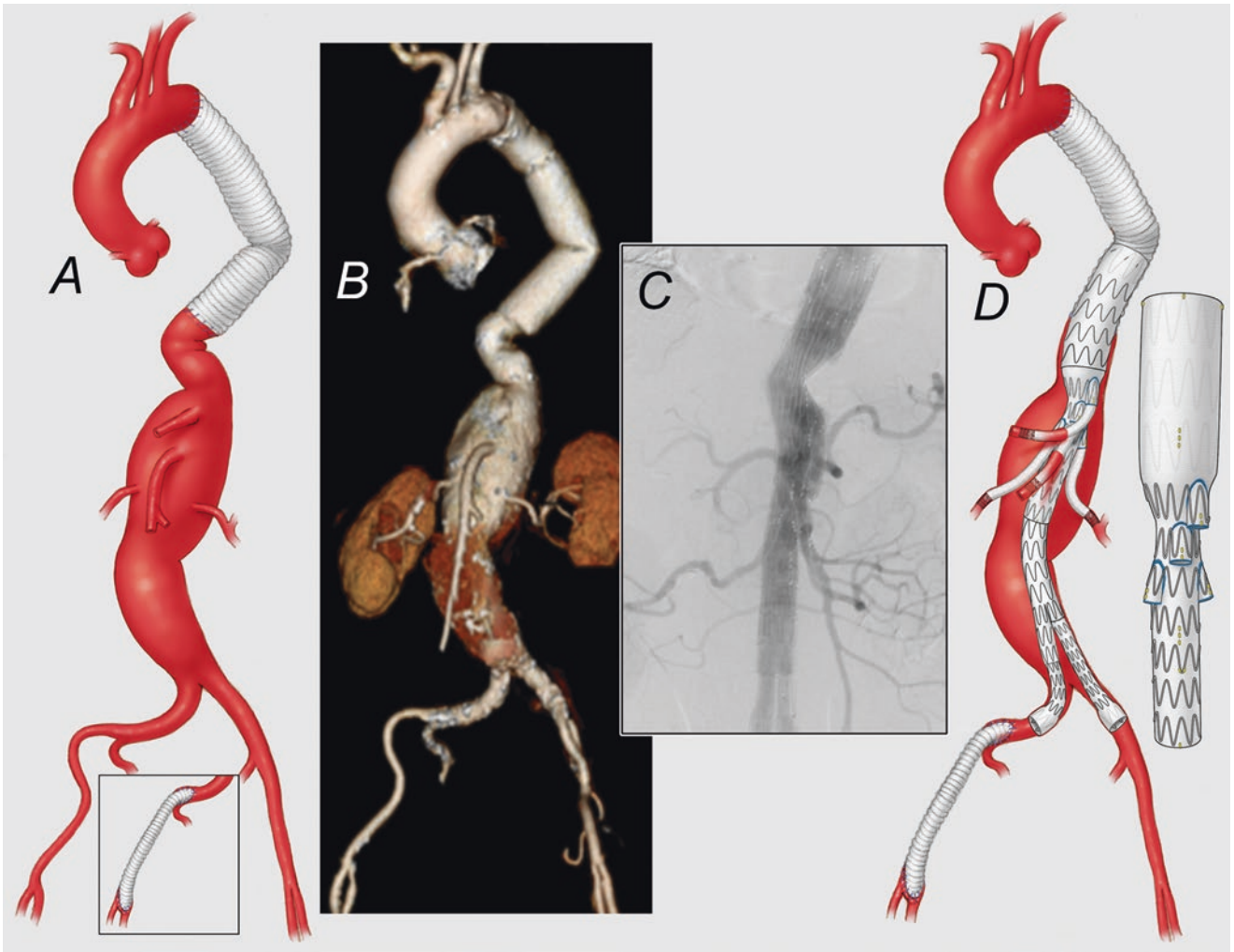


Fig. 28.26 Illustration of a patient with extensive thoracoabdominal aortic aneurysm after prior repair of thoracic aortic aneurysm (**a**) using iliofemoral conduit (**a**, inset). Preoperative computed tomography angiography (CTA) demonstrates large aneurysm with wide aortic lumen (**b**). Completion angiography demonstrates no endoleak after placement of a multibranched stent graft (**c**). Illustration after the repair (**d**) using a four vessel multibranched stent graft. By permission of Mayo Foundation for Medical Education and Research. All rights reserved

preference has been to use an 8 Fr over-the-wire Indy Snare (Cook Medical, Bloomington, IN). The guide-wire of choice for this is a 0.025-in. Metro guide-wire (Cook Medical, Bloomington, IN). Once the guide-wire is snared, the catheter needs to be pulled back out of the fenestration or branch approximately 30 cm before the sheath is advanced. Withdrawal of the catheter can be difficult if the entire device has not been completely deployed because of resistance within the delivery system. In these cases the catheter should not be forced out or it can disrupt. A 7 Fr sheath is advanced sequentially into the fenestration or branch, and a 4 Fr buddy catheter is used to selectively catheterize the vessel. Our preference has been to perform first the celiac axis and leave a 0.035-in. Amplatz guide-wire for fenestrations or a 0.018-in. Steelcore guide-wire for branches. Next the same steps are repeated for the SMA and a 0.035-in. Amplatz guide-wire and sheath are positioned within the vessel. The next steps of the procedure have been already described in the previous sections.

Inverted Limb

Patient-specific bifurcated stent grafts with an inverted iliac stent graft limb (Fig. 28.30) are useful adjuncts in patients with prior open or endovascular aortic repair who have a short distance between the lowest renal artery and the bifurcation of the prior stent graft or surgical graft. Some technical tips help prevent issues related to inaccurate deployment of the aortic stent graft or damage of the renal

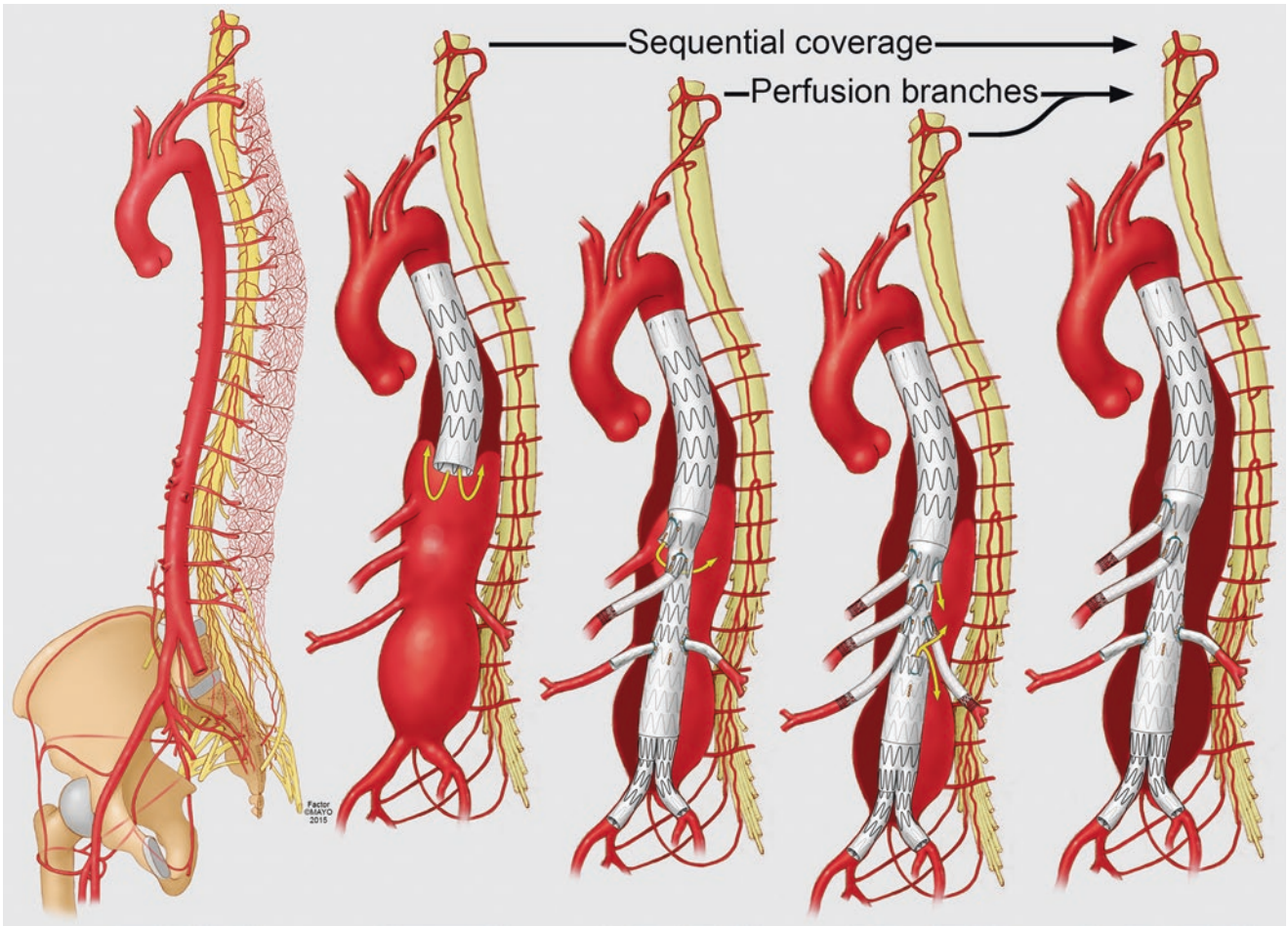


Fig. 28.27 Rationale of staged thoracoabdominal repair is based on the concept of extensive collateral network to the spine circulation as depicted in the illustration. The staged procedure can be done with sequential coverage or replacement of the aorta, or with perfusion branches. The later option can be done with specially designed branches or simply by using incomplete repair by not stenting the celiac branch or the contralateral gate of an iliac limb. Note sac thrombosis is completed days or weeks after the first procedure by placement of all stent components. By permission of Mayo Foundation for Medical Education and Research. All rights reserved

side stents. For these cases, preloaded catheters for the celiac and SMA are very useful because the device can be partially released to the level of the celiac and SMA, and the renals can be left sheathed until the two vessels are secured. The aortic stent graft is then deployed with careful attention to avoid encroaching the bifurcation of the previous graft while maintaining alignment between the fenestrations and renal arteries. The renal arteries are sequentially catheterized and/or preloaded renal guide catheters are used if available. Once the renal arteries are sequentially catheterized from below, 7 Fr hydrophilic sheaths are advanced over Rosen guide-wires as previously described. The device is completely deployed and the proximal and distal landing zones are dilated with a Coda balloon. Sequential renal artery stenting is performed starting by the highest stent first. The author's preference at this point is not to stent the SMA. Instead, once the renals are stented both vessels are protected by placement of 10-mm angioplasty balloons, while the inverted limb device is advanced and deployed immediately below the renal arteries. Balloon protection of the renal stents avoids risk of compression of the stent during advance of the delivery system. The contralateral gate of the inverted limb device is marked with three longitudinal radiopaque markers at the distal edge. Once the gate is catheterized, the device is completely deployed, the delivery system is removed, and the renal protection balloons are deflated. The repair is completed by adding an iliac extension limb into the side of the inverted limb, which requires removal of the renal sheaths. Therefore for this step of the procedures the renal arteries are not protected by balloon and one should be careful to prevent stent compression. Finally, once the distal stents are all deployed including the iliac limbs, the SMA and the celiac arteries are stented using the brachial approach.

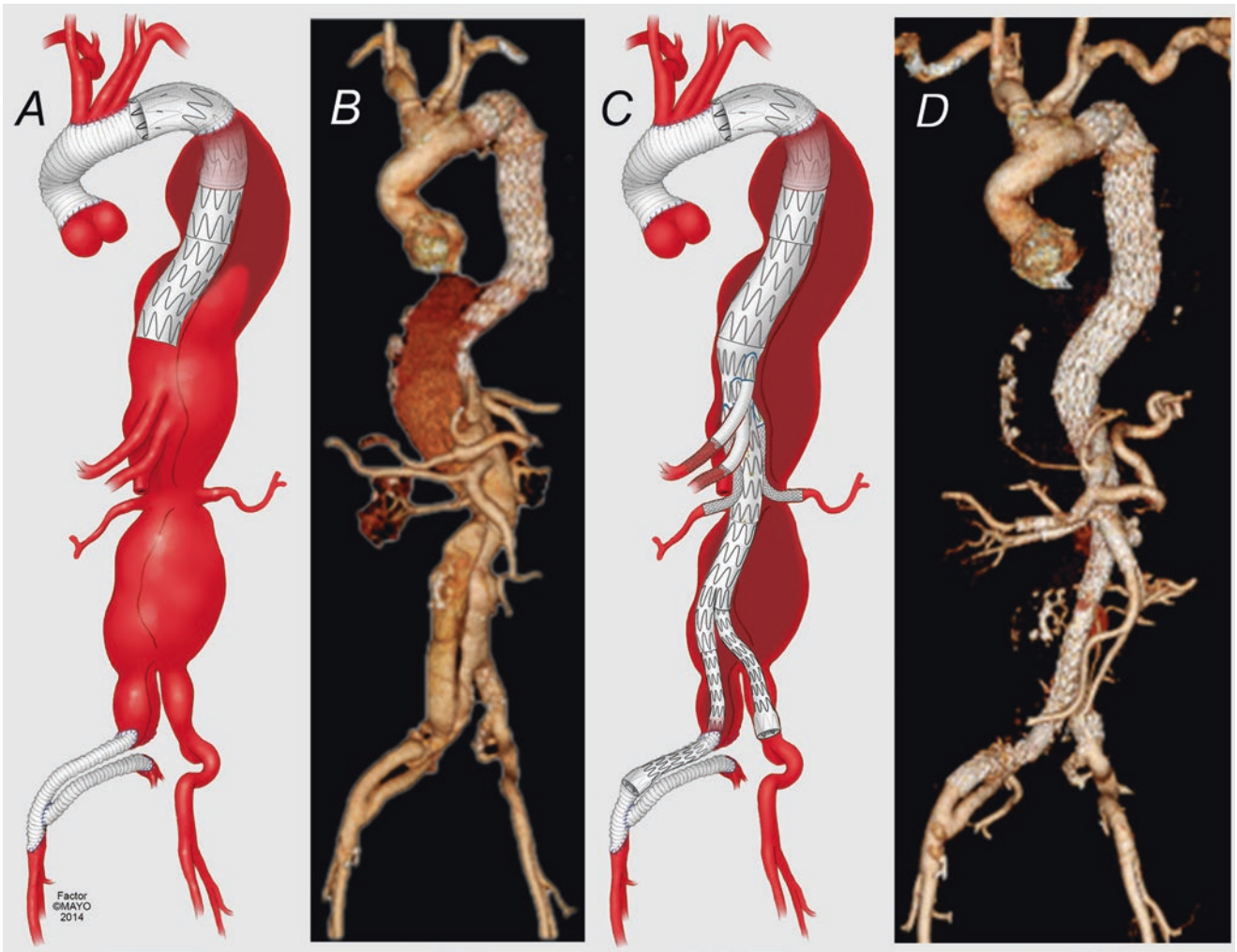


Fig. 28.28 Extensive aortic aneurysm with chronic dissection treated in multiple staged procedures. First the ascending aorta and arch were replaced by elephant trunk repair (**a**). The patient underwent a first-stage thoracic endovascular repair by placement of stent grafts to the level of the celiac axis (**b**). Note that the false lumen is excluded in the proximal thoracic aorta. The patient also had revascularization of the internal iliac artery using bypass. Illustration depicts the completed repair with placement of a multibranch stent graft (**c**). Follow-up computed tomography angiography (**d**) demonstrates widely patent stent graft with no attachment endoleak. By permission of Mayo Foundation for Medical Education and Research. All rights reserved

Conclusion

Fenestrated and branched stent graft techniques continue to evolve and differ according to physician preference. The key technical point is extensive physician planning to make these procedures technically easier whenever possible. Important contributions from large clinical series are staging of extensive thoracoabdominal aortic aneurysms and early restoration of lower extremity perfusion whenever possible. To this end, the author often uses preloaded catheters to target the celiac and SMA from above, restoring flow to the lower extremities prior to completing the mesenteric arteries.

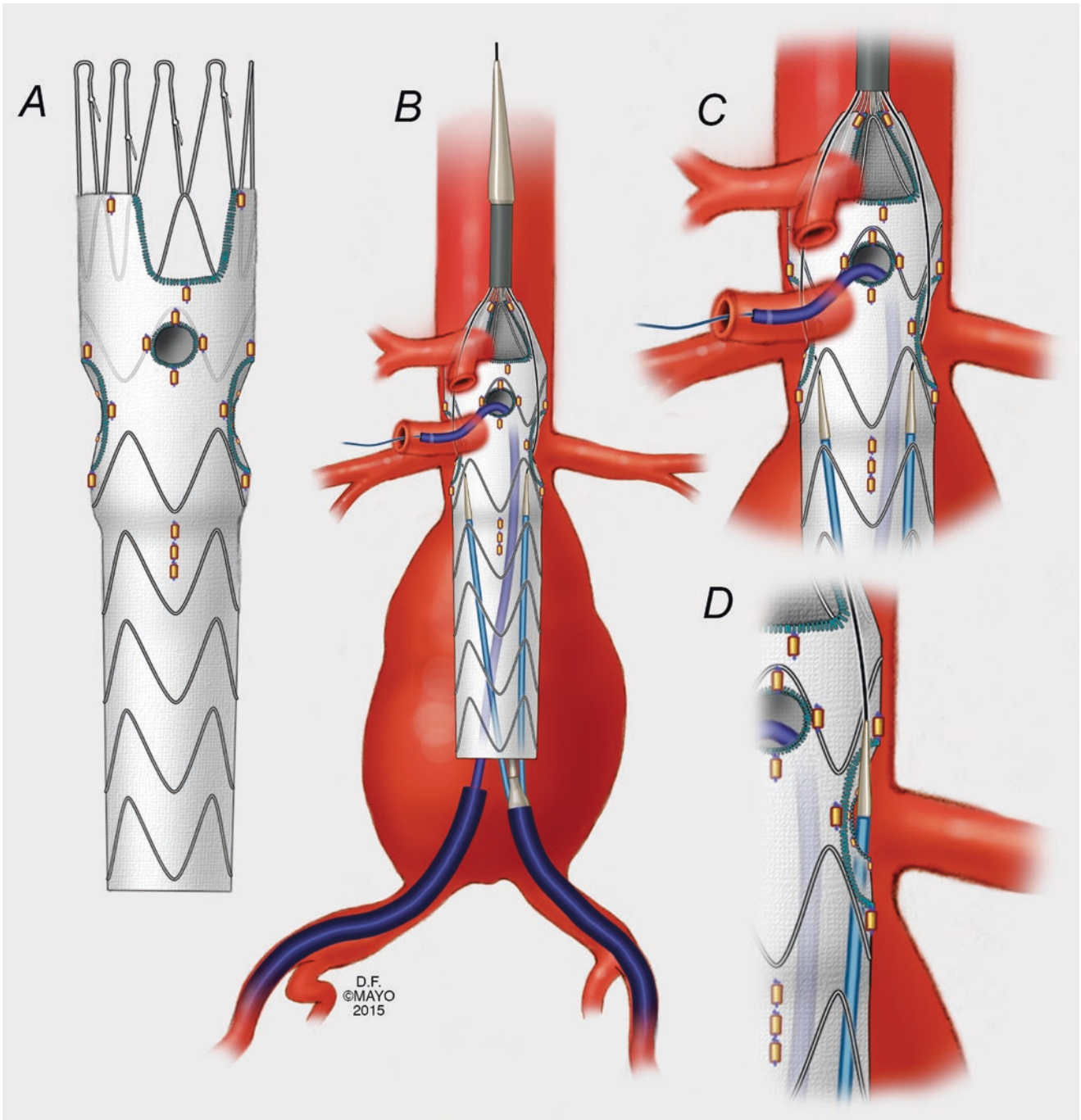


Fig. 28.29 A preloaded renal guide-wire/guide-catheter system is available in the p-Branch® stent graft (**a**) or can be requested in patient-specific designs. The delivery system has two portals for introduction of 6 Fr 90-cm or 110-cm hydrophilic sheaths, which are used for placement of the renal stents. The system consists of a nitinol guide-wire that goes through-and-though each of the renal fenestrations and exits via the portals. Once the device is deployed with apposition between fenestrations (**b**) and the target renal arteries the SMA fenestration is catheterized via the contralateral femoral approach (**c**). A The renal sheaths are advanced via both preloaded renal guide-wires (**d**).

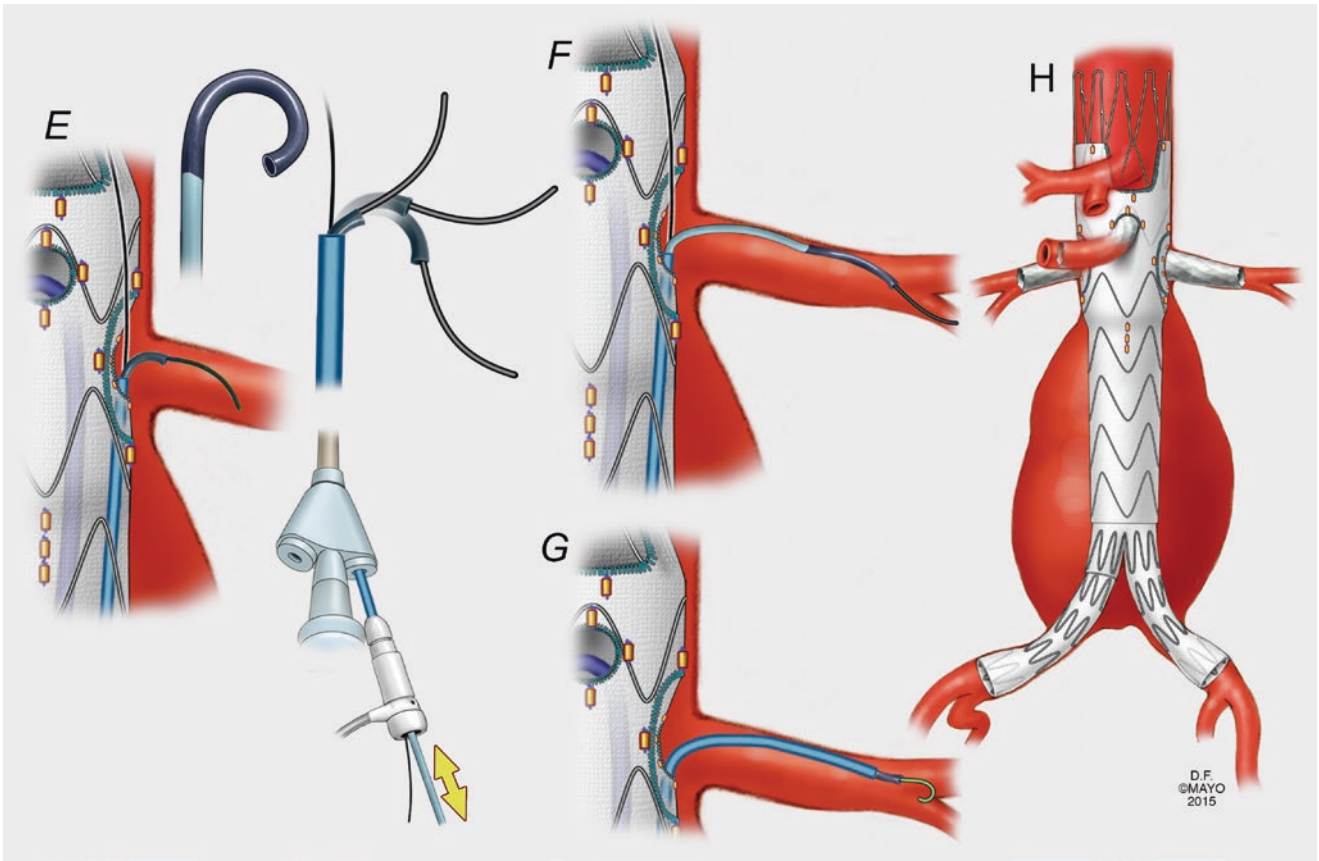


Fig. 28.29 (continued)A curly catheter can be manipulated in the renal sheaths to selectively catheterize each of the renal arteries (**e**). Once the catheter and glidewire are advanced into both of the renal arteries (**f**), the through-and-through preloaded renal guide-wire is removed and the 6 Fr sheaths are advanced into the renal arteries (**g**). Following placement of the renal and SMA stents, a distal bifurcated stent graft is placed (**h**). By permission of Mayo Foundation for Medical Education and Research. All rights reserved

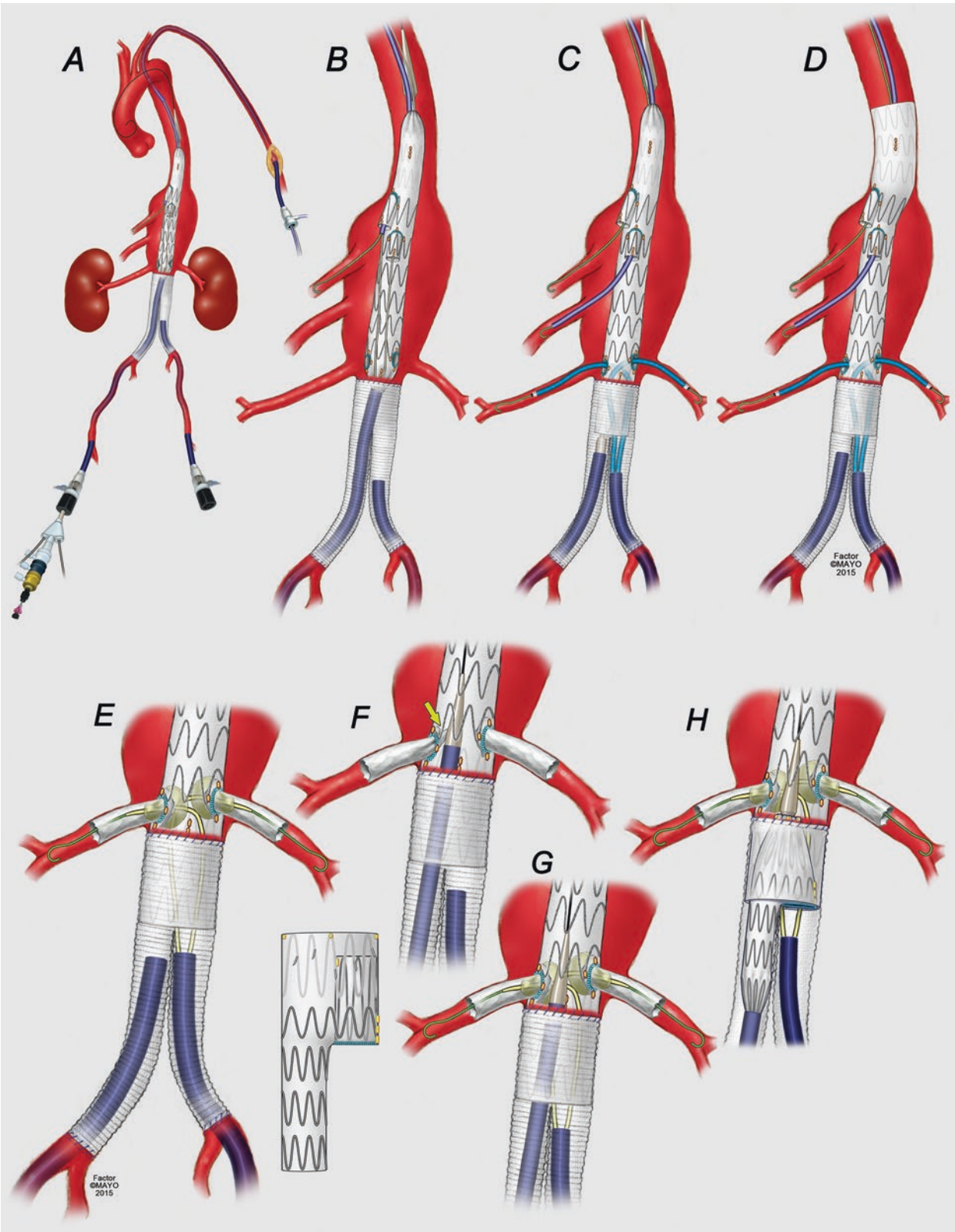


Fig. 28.30 Illustration of a fenestrated stent graft with two preloaded catheters in a patient with short distance between the renal arteries and the bifurcation of an aortic graft (**a**). Guide-wires are advanced via the preloaded catheters and snared from the brachial approach (**b**). After both guide-wires are snared, the aortic fenestrated stent graft is deployed to the level of the renal fenestrations (**b**). This allows for space for catheter manipulations from above. A sheath is advanced first into the celiac fenestration, while a "buddy" catheter is used for selective catheterization of the celiac axis. Once the celiac axis Amplatz guide-wire is positioned, the same steps are repeated for the SMA and a 7 Fr sheath is positioned into the SMA. The device is deployed with careful attention to the bifurcation of the aortic graft (**c**). The renal arteries are catheterized from the femoral

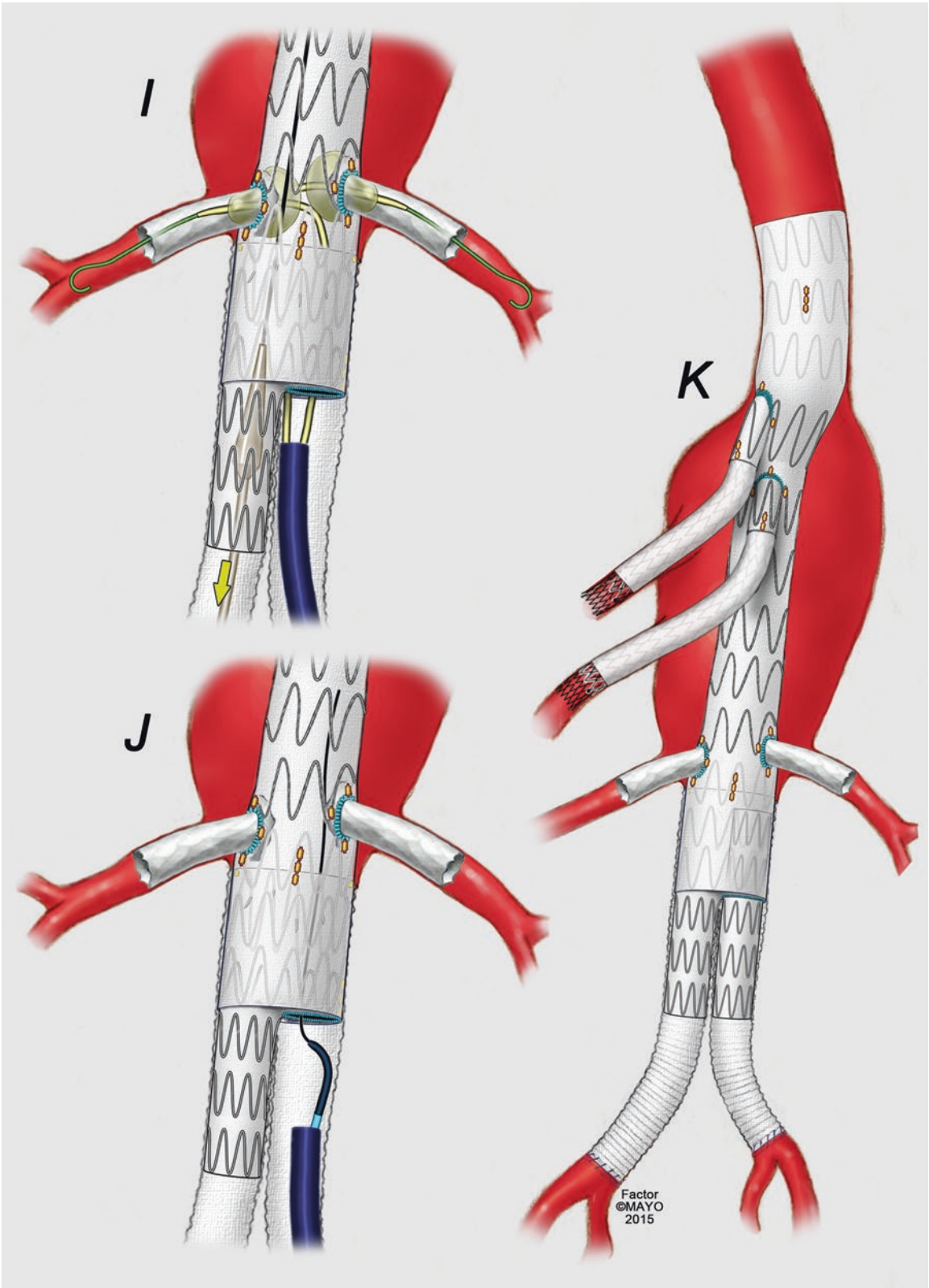


Fig. 28.30 (continued) approach. Once all vessels are catheterized the diameter-reducing tie is removed (**d**). Renal alignment stents are sequentially deployed (**e**). Note that introduction of the inverted limb bifurcated stent graft without renal protection risks compression of the renal alignment stents (**f**, *arrow*). Instead, angioplasty balloons are inflated into both renal stents (**g**) while the bifurcated device is deployed just below the renal stents (**h**). After deployment of the bifurcated device (**i**), the inverted limb is catheterized (**j**), and the repair is extended into the contralateral limb of the aorto-iliac graft. The procedure is completed by placement of the SMA and celiac self-expandable stent grafts (**k**). By permission of Mayo Foundation for Medical Education and Research. All rights reserved

Suggested Reading

1. Oderich GS, Correa MP, Mendes BC. Technical aspects of repair of juxtarenal abdominal aortic aneurysms using the Zenith fenestrated endovascular stent graft. J Vasc Surg. 2014;59(5):1456–61.
2. Oderich GS, Mendes BC, Kanamori KS. Technique of implantation and bail-out maneuvers for endovascular fenestrated repair of juxtarenal aortic aneurysms. Perspect Vasc Surg Endovasc Ther. 2013;25(1–2):28–37.
3. Oderich GS, Mendes BC, Correa MP. Preloaded guidewires to facilitate endovascular repair of thoracoabdominal aortic aneurysm using a physician-modified branched stent graft. J Vasc Surg. 2014;59(4):1168–73.
4. Manning BJ, Harris PL, Hartley DE, Ivancev K. Preloaded fenestrated stent-grafts for the treatment of juxtarenal aortic aneurysms. J Endovasc Ther. 2010;17(4):449–55.
5. Verhoeven ELG. The first phase of another exciting chapter in the development of fenestrated stent-grafts: preloaded devices. J Endovasc Ther. 2010;17(4):456–7.
6. Verhoeven EL, Katsargyris A, Fernandes e Fernandes R, Bracale UM, Houthoofd S, Maleux G. Practical points of attention beyond instructions for use with the Zenith fenestrated stent graft. J Vasc Surg. 2014;60(1):246–52.
7. Moore R, Hinojosa CA, O'Neill S, Mastracci TM, Cina CS. Fenestrated endovascullar grafts for juxtarenal aortic aneurysms: a step by step technical approach. Catheter Cardiovasc Interv. 2007;69(4):554–71.

Results of Fenestrated, Branched, and Parallel Stent Grafts for Pararenal and Thoracoabdominal Aortic Aneurysms

29

Gustavo S. Oderich and Bernardo C. Mendes

Introduction

Complex aortic aneurysms are defined by involvement of side branches and include aneurysms of the aortic arch, thoracoabdominal and iliac bifurcation. During the last decade, significant improvements in endovascular technology have allowed total endovascular repair using one of three methods of vessel incorporation: fenestrations, branches and parallel grafts. It is critical that future developments are compared to benchmark results of conventional open surgical repair, which remains the gold standard treatment for most of these aneurysms. This chapter summarizes the state of the art and results of fenestrated, branched, and parallel grafts to treat pararenal and thoracoabdominal aortic aneurysms (TAAAs).

Open Conventional Repair

Open surgical repair has been considered the gold standard for repair of aortic aneurysms against which novel technology should be compared [2]. The simplest form of aortic aneurysm affects the infrarenal aorta, where the operation is performed using midline transperitoneal or a left retroperitoneal incision. The operation does not require opening the chest cavity, and aortic cross clamping is typically located below the renal arteries, allowing the reconstruction to be performed with no visceral ischemia. The technical difficulty of the operation increases with aortic aneurysms that involve the visceral segment. The degree of complexity in these cases correlates with the need to expose and dissect more proximal aorta above the renal or mesenteric arteries, the more cranial position the aortic clamp and consequently longer visceral ischemia time, which is required to reconstruct the visceral arteries. Therefore, it is logical that patients with more complex abdominal aortic aneurysm have higher mortality and morbidity rates as compared to patients undergoing repair of infrarenal abdominal aortic aneurysms.

Open repair of TAAAs has been associated with high mortality and morbidity in most centers (Tables 29.1 and 29.2) [6–18]. Type IV thoracoabdominal aortic aneurysm represents the simplest and less extensive form, with outcomes similar to suprarenal aortic aneurysms, yet with higher mortality rates in most centers. Only a few aortic centers have shown that these operations can also be performed with satisfactory results. Coselli and associates [6] reported 2286 patients treated by open TAAA repair, with an operative mortality of 7 %. Other aortic centers have shown mortality rates in the range of 5–15 %. "Real world" data using national and regional datasets have demonstrated more ominous results. In the study by Rigberg and associates [19] on 797 Medicare beneficiaries who underwent elective open TAAA repair in the State of California the mortality was 19 % at 30 days and 31 % in 1 year. Most importantly, not only are mortality and morbidity high but a large number of patients require prolonged hospitalization and additional rehabilitation. Oderich and associates reported the outcomes in 5776 Medicare beneficiaries treated by open repair for TAAAs. In that study, only 31 % of the patients were dismissed home from the hospital, whereas 16 % died from complications and 53 % required to be transferred to another hospital or to assisted care or rehabilitation centers [20].

Endovascular Repair

Endovascular aortic aneurysm repair (EVAR) has gained widespread acceptance and is currently considered the first treatment option for most patients with abdominal aortic aneurysms. Prospective randomized trials [21–23] have demonstrated several short-term advantages over open

G.S. Oderich (✉) • B.C. Mendes
Division of Vascular and Endovascular Surgery, Mayo Clinic, 200 First Street SW, Rochester, MN 55905, USA
e-mail: oderich.gustavo@mayo.edu

© Mayo Foundation for Medical Education and Research 2017

G.S. Oderich (ed.), *Endovascular Aortic Repair*, DOI 10.1007/978-3-319-15192-2_29

Table 29.1 Results of open surgical reports dealing with Type IV thoracoabdominal aortic aneurysms

Author, year	*N*	30-day Mortality (%)
Coselli et al., 2003	225	5.3
Kiefer et al., 2006	171	13.4
Richards et al., 2010	53	6
Ockert et al., 2009	63	7.9
Oderich et al., 2011	51	7.8
Patel et al., 2011	179	2.8

Table 29.2 Results of open surgical reports dealing with types I–IV thoracoabdominal aortic aneurysms

Author, year	*N*	30-day Mortality (%)
Coselli et al., 2007	2286	6.6
Schepens et al., 2007	500	12.4
Etz et al., 2007	858	9.7
Achneck et al., 2007	130	12
Conrad/Cambria, 2007	455	8.6
Jacobs et al., 2004	279	8.6
Safi et al., 2005	1106	14.6
Grabitz et al., 1996	260	14.2
Svensson et al., 1993	1509	8.2

conventional repair, including less blood loss, operative time, hospital stay, mortality, and morbidity. Several anatomical constraints limit the use of endovascular stent grafts in patients with complex aortic aneurysms. The presence of short infrarenal aortic neck, severe angulation or involvement of the visceral arteries continues to limit the application of endovascular approaches. In these patients, open conventional repair remains the standard treatment, but technical complexity increases with more extensive dissection, higher clamp site, prolonged visceral ischemia, and more extensive reconstruction. It is logical to speculate that the advantages achieved with endovascular repair of infrarenal aneurysms will pale in comparison to the potential for reduction in morbidity and mortality for treatment of more complex aneurysms that involve the visceral and thoracoabdominal aortic segment.

Fenestrated and Branched Stent Grafts

Fenestrated and branched stent grafts were introduced as a minimally invasive alternative to treat complex aneurysms in higher risk patients using total endovascular techniques [31, 32]. The use of fenestrated and branched stent graft designs has increased worldwide with several reports from Australia, Asia, Europe, Canada, South America and from select centers in the USA [33–47]. Their clinical application has been well described in patients with complex aortic anatomy, as well as for salvage of anastomotic aneurysms or failed endovascular procedures. In the USA, access to fenestrated and branched stent grafts has been limited to centers participating in investigational trials or to patients who are prospectively enrolled in physician-initiated investigational device exemption (IDE) protocols. The custom-made Zenith® Fenestrated AAA Endovascular Graft was the first fenestrated stent graft to become commercially approved in the USA in April 2012. Nonetheless, this design is adequate for only a minority of patients due to its limitation of maximum of three fenestrations, two of the same type. Therefore, most patients with suprarenal aneurysms and all of those with thoracoabdominal aortic aneurysms are not candidates for the device [10]. In addition, device customization requires a 6- to 8-week time period, which limits the use of these devices in patients with unstable aneurysms.

Pararenal Aneurysms

The first report of a fenestrated aortic stent graft was by Park and associates [31] in 1996, who described the use of a fenestration to incorporate an indispensable inferior mesenteric artery. This initial report was followed by the development of a more versatile fenestrated device using the Cook Zenith® platform by Anderson, Lawrence-Brown, and Hartley, as exposed in Chap. 1. The initial experience with fenestrated endografts to treat pararenal aortic aneurysms has shown that the procedure could be performed with low morbidity and mortality rates. During the last decade, several centers have accumulated a large experience with these types of repairs.

The Cleveland Clinic reported a prospective study of 119 patients treated by fenestrated endografts between 2001 and 2005 with a mean aneurysm size of 6.5 cm [41]. Procedural success was 100 % and there was no acute visceral artery loss. There were no ruptures or conversions to open surgery. The 30-day operative mortality was 0.8 %, and survival at 12, 24, and 36 months was 92 %, 83 %, and 79 %, respectively, with mean follow-up period of 19 months. Aneurysm sac shrinkage of greater than 5 mm was noted in 79 % of the patients at 12 months and 77 % of patients at 24 months, and mean aneurysm size decreased from 6.5 cm postoperatively to 5.0 cm at 3 years, demonstrating efficacy of the fenestrated device. Endoleaks were uncommon and were noted in 10 % of the patients at 30 days (all were type II endoleaks) and 4 %, 6 %, and 3 % at 12, 24, and 36 months, respectively. Thirty patients (25 %) developed at least a transient increase in serum creatinine of >30 %. Five patients (4 %) required transient or permanent dialysis. In this study, a total of 302 visceral vessels were treated. In-stent stenosis occurred in 12 renal arteries and 1 superior mesenteric artery. Six of these renal arteries and the superior mesenteric artery were successfully treated by endovascular approach. Additionally, 10 of the 231 renal arteries that were treated subsequently occluded. One of these was re-stented. Based on this data, one can conclude that the cumulative target vessel patency was excellent at 97 %.

The group from Western Australia reported a series of 58 patients from 7 centers in Perth and Adelaide treated for pararenal aortic aneurysms using fenestrated endografts between 1997 and 2004 [43]. Technical success was achieved in 91 %. There were no ruptures or open surgical conversions. The 30-day mortality was 3.4 %. Overall patient survival was 90 % after a mean follow-up period of 18 months. Total endoleak rate was similar to the Cleveland Clinic report at 10 %, with 7 % type I and 3 % type II endoleak rates, respectively. One patient had persistent endoleak (1.7 %). Only four patients (6.9 %) developed renal impairment, and none required dialysis. Target vessel patency was 91 %. Factors associated with target vessel loss were absence of a stent to align the fenestration, >60° neck angulation, multiple renal vessels, and vessel diameter ≤4 mm. For this reason, the authors recommend routine stenting for all fenestrations including scallops, and that fenestrations should be performed only for vessels greater than 4 mm in diameter that can also accommodate placement of a stent. This practice of stenting all fenestrations for vessel alignment has been widely accepted as standard practice since this initial report.

Eric Verhoeven and colleagues reported their results with endovascular aneurysm repair using fenestrated endografts. In their initial report, 38 patients were prospectively enrolled in a single institution investigational device protocol database between 2001 and 2005 [48]. Overall technical success was achieved in 37/38 patients (97 %). There were no aneurysm ruptures, conversions to open surgery, or intra-operative deaths. Perioperative (30 day) mortality was 2.6 %. Mean follow-up was 26 months and there were no patients lost to follow-up. All-cause mortality was 13 % (5/38 patients), with all deaths occurring within the first postoperative year, however, aneurysm-related mortality was 0 %. Seven patients (18 %) experienced a type II endoleak and a persistent type I endoleak was observed in one patient (2.5 %), resulting in an overall endoleak rate of 20.5 %. Analyzed on an intention-to-treat basis, cumulative target visceral branch vessel patency was 92 % at 46 months. Only three target vessels (4 %) were lost postoperatively. All postoperative stent occlusions occurred during the first year in un-stented fenestrations or scallops. No occlusions occurred in stented vessels. As a result, the authors currently recommend stenting of all renal fenestrations or scallops, similar to the group from Perth. Freedom from secondary interventions in this patient cohort was 90 %. All secondary interventions were needed within the first postoperative year, but no further interventions were required in subsequent years. Renal function remained unchanged during the follow-up period. No patient required dialysis. Limb perfusion as assessed by the ankle/brachial index was not affected postoperatively in any patients, and mean aneurysm sac size decreased from 6.3 to 5.0 cm at 36 months. More recently, Verhoeven and associates reported their updated clinical experience with 100 patients treated for short-neck and juxtarenal aortic aneurysms [46]. The 30-day mortality was 1 %, with one conversion to open repair. Operative visceral artery perfusion was achieved in 99 % of the 275 target renal and mesenteric arteries. There were no late aneurysm related deaths or ruptures. Cumulative primary visceral artery patency was 93 % at 5 years.

In 2007, Ziegler et al. [47] reported a 7-year single-center experience with fenestrated endografts in 63 patients that reinforced the mid-term results of the aforementioned other large center series. Technical success was achieved in 87 % of patients and in 97 % of target vessels. Treatment success was 94 %. No intra-operative deaths occurred. Mean follow-up was 23 months. One rupture (1.6 %) occurred at 10 months and there was one (1.6 %) patient who was converted to open surgery at 9 months. There was one (1.6 %) perioperative death as a result of ischemic colitis and gangrene of the colon following endograft implantation. Overall mortality was 24 % during follow-up of 23 months, and aneurysm-related deaths occurred in three patients (4.8 %). The total endoleak rate was 19 %, with 8 % being primary endoleaks and 11 % secondary endoleaks. Overall, nine (7.4 %) visceral branches were lost; four intraoperatively, two perioperatively, and three in late follow-up. Analyzed on an intention-to-treat basis, the cumulative target visceral branch patency rate was 92.2 % at 77 months. As in previous reports, all stent occlusions occurred within the first postop-

erative year. Overall, 13 (20.6%) patients required a secondary intervention which was successfully completed in 12, while one patient required open surgical conversion. All secondary interventions were carried out within the first 14 months. On intention-to-treat analysis, freedom from secondary intervention was 75% at 77 months. Fourteen cases (22%) of renal impairment were observed. Of these, 6 were permanent and 8 were transient, with only 1 patient (1.5%) requiring dialysis.

Based on the contemporary results from high-volume aortic centers, endovascular repair of complex abdominal aortic aneurysms can be safely and effectively carried out in the hands of an experienced endovascular team (Table 29.3) [33–47]. Early postoperative mortality was exceptionally low as was aneurysm-related mortality, the incidence of aneurysm rupture and conversion to open surgery. Type I and III endoleaks are infrequent and mid-term target visceral branch vessel patency is exceptionally high. However, close surveillance is mandatory for early identification of visceral or branched vessel stenosis or pre-occlusion. Failures appear to occur within the first postoperative year and then plateau in subsequent follow-up. Secondary intervention rates range between 10 and 20%. Postoperative renal failure is not uncommon (up to 25%), however incidence of dialysis requirement is exceedingly low (0–3%) [33–47]. The results of these large series are in agreement with previously published series of conventional endovascular repair of infrarenal abdominal aortic aneurysms. As the fenestrated and branched endografting procedure matures and evolves, long-term results and randomized trials will ultimately be required to determine the safety, efficacy, and durability of endovascular repair of pararenal and juxtarenal aortic aneurysms.

Type IV Thoracoabdominal Aortic Aneurysms

The complexity of an endovascular repair using fenestrated and branched endografts has been assessed primarily with the extent of aortic coverage, the number of vessels requiring incorporation into the repair, and to difficulties imposed by inability to access to the aorta and target visceral arteries. The increasing number of vessels requiring incorporation by fenestrations and branches correlates with longer operative times, higher radiation doses, and may be associated with increased morbidity rates at least in the beginning of the experience. Manning and associates [49] reported procedural data and clinical outcomes on 20 patients treated by single-, double- or triple fenestrated endografts. In that study, procedure time and length of stay in the intensive care unit was significantly longer with more complex repairs, which required three fenestrations.

A recent clinical update from the Cleveland Clinic group led by Roy Greenberg [50] and colleagues indicates that type IV TAAAs and pararenal aneurysms can be treated with similar outcomes and significantly lower mortality rates as compared to more extensive types I–III TAAAs, which require more extensive aortic coverage. In that study, clinical outcomes were reported in 406 patients treated for thoracoabdominal aortic aneurysms and 227 patients treated for juxtarenal or suprarenal aortic aneurysms. The 30-day mortality and 2-year survival were nearly identical for juxtarenal/suprarenal aneurysms (1.8 and 78%) and type IV thoracoabdominal aortic aneurysms (2.3 and 82%), and markedly different than outcomes obtained with more extensive thoracoabdominal aortic aneurysms. Operative mortality was 5.2% for types II and III thoracoabdominal aortic aneurysms.

Table 29.3 Results of clinical reports of endovascular repair of complex abdominal aortic aneurysms with fenestrated and branched endografts

Author	Year	Aneurysm type	*N*	Vessels	Technical success (%)	30-day mortality (%)	Dialysis (%)	Endoleaks (%)	Branch patency (%)	Follow-up (months)
Greenberg et al.	2004	JRA	32	83	100	3.1	3.1	6.50	98	9.2
Greenberg et al.	2004	JRA	22	58	100	0.0	4.5	9		6
O'Neil et al.	2006	JRA	119	302	100	0.8	3.4	25	92	19
Semmens et al.	2006	JRA, SRA	58	116	91	3.4	0.0	7	95	24
Muhs et al.	2006	JRA, SRA	38	87	94	2.6	0.0	24	92	25
Ziegler et al.	2007	JRA, SRA	63	122	97	1.5	1.5	19	92	23
Scurr et al.	2008	JRA	45	117	–	2.0	0.0	0	97	24
Beck et al.	2009	JRA	18	56	100	0.0	–	–	95	23
Greenberg et al.	2009	JRA	30	54	100	0.0	–	60	94	24
Kristmundsson et al.	2009	JRA	54	134	98	3.7	0.0	31	96	25
Amiot et al.	2010	JRA, SRA	134	403	99	2.0	4.5	18	97	15
Haulon et al.	2010	JRA, SRA	80	237	99	2.5	4.0	11	95	10
Verhoeven et al.	2010	JRA	100	275	99	1.0	2.0	–	94	24
Tambyraja et al.	2011	JRA	29	79	–	0.0	0.0	21	–	20
GLOBALSTAR Collaborators	2012	JRA, SRA	318	889	75	3.5	–	16	99	21
Starnes et al.	2012	JRA	47	82	98	2.0	–	13	–	20

Type I to III Thoracoabdominal Aortic Aneurysms

Endovascular approaches to TAAAs have varied depending on stent graft design. A critical analysis of outcomes should include morbidity, mortality, patient survival, and rates of renal function deterioration (dialysis), spinal cord injury, neurological events, reinterventions, and visceral artery patency rates. Timothy Chuter from the University of California San Francisco has introduced the concept of a multibranched stent graft in 2001 [51]. The most recent clinical update from the UCFS group was reported by Reilly and colleagues in 2012 [51]. The study included 81 patients with mean age of 73 years old treated by multibranch stent grafts (t-branch stent graft) for TAAAs. Aneurysm extent was type II–III in 48 % of patients, and type IV in 52 %. A total of 306 visceral arteries were incorporated. Operative mortality was 6 %, including three perioperative deaths (4 %) and two late treatment-related deaths. Spinal cord injury occurred in 24 % of patients, including 5 % paraplegia and 19 % transient paraparesis. Four patients (5 %) required dialysis, which was permanent in three. After a mean follow-up of 21 months, there were no aneurysm ruptures and only 5 % had enlarged. Of the 306 branches, 16 developed occlusion or stenosis requiring re-stenting. Primary visceral artery patency was 94 % and secondary patency was 95 %. Thirty-two patients (40 %) required secondary interventions to treat endoleak or branch complications. The authors concluded that endovascular repair using directional branches with a multibranched device was safe, effective, and durable in the intermediate-term.

Technological improvements with lower profile technology, better bridging stents, and innovative stent graft designs are likely to bring further progress to treatment of TAAAs. A limitation of current available technology is the need for customization. Sweet and associates [52] evaluated aortic anatomy in 66 patients treated by multibranched stent grafts with the t-branch design. In that study the anatomic criteria for branch insertion was analyzed, including presence of up to four indispensable visceral arteries, diameter of celiac and SMA of 6–10 mm, diameter of renal arteries of 4–8 mm, arterial access via brachial approach, distance from each cuff to target vessel <50 mm, angle between cuff and origin of vessel <45°. In that study 88 % of patients met all anatomical criteria, suggesting that a standardized multibranch stent graft has wide applicability. Park and associates [53] analyzed the shape and length of branches as determinants of suitability for repair. In that study, there were no instances of migration, kinks or disconnections in 136 visceral branches. Twenty-three percent of branches had >30° misalignment, suggesting that the design was quite forgiven for errors of implantation or variations in patient anatomy.

A follow up study by Gasper et al. [54] analyzed the applicability of multibranched stent grafts in a broader study population of 201 potential candidates for repair of TAAAs. In that study anatomic suitability was accessed using CTA measurements according to the recommended criteria for treatment using a custom-made multibranched stent graft or an off-the-shelf version with standard profile (22 Fr) or lower profile (18 Fr). Of the 201 potential candidates for TAAA repair, 109 (58 %) were candidates for repair in a single-stage using custom-made low profile stent graft. Another 58 patients (29 %) could be candidates for repair with adjunct procedures in a two stages to revascularize the subclavian or iliac arteries to provide a suitable landing zone. Women were significantly more likely to require a conduit for introduction of the stent graft, which was less frequently needed with lower profile design. Patients with chronic dissections were significantly less likely to qualify for repair because of involvement of iliac arteries, compressed true lumen, or aberrant vessel anatomy. Although the off-the-shelf design has the advantage of eliminating the need to wait for customization, only 94 patients (<50 %) qualified for use of this device.

One of the main limitations of the universal use of an off-the-shelf device is vessel configuration, particularly with respect to the renal arteries. Conway et al. [55] evaluated the angles of implantation of the renal arteries according to aneurysm anatomy. In that study CTA measurements of 147 patients with TAAAs were analyzed in two groups of patients, including those with predominance of thoracic disease (types II and III) versus abdominal disease (type IV). The authors noted that patients with predominance of abdominal disease (type IV) more often had a downward orientation for the renal arteries as compared to those with predominance of thoracic disease (types II and III), which had more often a neutral or up-going configuration. Incorporation of up-going renal arteries with down-going branches, as proposed using a multibranch t-branch device, is not ideal and leads to kinks, stenosis and ultimately branch vessel loss from thrombosis. Conversely, down-going branches are very well suited for vessels with down-going configuration, which is frequently the case for celiac axis and SMA, and less frequently for renal arteries. Differences in angulation along with branch stent length have direct impact on branch durability. In the study of Reilly et al. [51] (using down-going branches with self-expandable stents) occlusion rate was 9.5 % for renal and 2 % for mesenteric arteries. Mastracci et al. [56] reported a large experience with 650 patients treated by fenestrated–branched stent grafts for TAAAs. In that study, 1679 visceral branches were evaluated. The most common stent graft design consisted of two down-going branches for the celiac and SMA, and two fenestrations for the renal arteries. Whereas fenestrations rely on a nitinol ring and may be more prone to type III endoleak with large TAAAs, these allow a very short branch

configuration, which is specially suited for renal arteries that have a neutral or up-going configuration. The renal artery occlusion rate was significantly lower at 1.7 % as compared to the rate reported by Reilly et al. [51] with no difference for mesenteric arteries. These two large single-center experiences demonstrate that there is not a single design, which can be applied to all patients. Instead, individually adapting the best design to the patient's anatomy, with directional branches and/or fenestrations, using custom-made or off-the-shelf designs, is likely the best strategy.

Spinal Cord Injury

The most feared and vexing complication of TAAA repair is spinal cord injury. Regardless of the type of approach utilized, open or endovascular, paraplegia is a devastating complication for the patient, the family and the medical team caring for these patients. Several factors have been demonstrated to affect rates of spinal cord injury. The single most important is the extent of aortic disease, with the highest rates observed for type II TAAAs.

Greenberg et al. [57] compared rates of spinal cord injury among 724 patients treated by open or endovascular approach. An open approach has the advantage of allowing reimplantation of intercostal arteries into the repair, which is not possible with endovascular technique. In that study, there was a nonsignificant trend towards lower rates of spinal cord injury with endovascular (4.3 %) as compared to open repair (7.8 %). Extent of aneurysm was the most important independent predictor of spinal cord injury (Type II > I > III > IV) as was presence of prior aortic repair. For type II TAAAs, both open (22 %) and endovascular (19 %) were associated with high rates of spinal cord injury. Eagleton et al. [58] presented the results of 1251 patients enrolled in a physician-sponsored IDE protocol over the last 10 years, with an overall rate of spinal cord injury of 2.9 %. Rates were 0.3 % for abdominal, 0.5 % for pararenal, 5.2 % for thoracic, and 5 % for TAAAs. The authors found that presence of a single collateral bed occlusion (e.g., subclavian or iliac artery) predicted immediate onset of paraplegia and the lack of recovery. A reason for improved results may be the more frequent use of a staged approach to cover the intercostal arteries, along with better techniques of implantation.

The rationale for a staged coverage of the intercostal arteries has been supported by the concept that an extensive collateral network can be progressively recruited over a period of days to a few weeks [59]. In a chronic porcine model, staged segmental ligation of the intercostal arteries over a period of 1 week was associated with no occurrence of paraplegia [60–62]. Bischoff et al. reported a prospective, randomized study comparing single stage versus two-stage coverage or ligation of segmental intercostal arteries in a porcine model. In that study, 20 pigs had coverage of all thoracic intercostal arteries in one or two stages with monitoring of collateral network perfusion pressures. In the group treated in a single stage, collateral network pressure decreased to 34 % of baseline values as compared to 55 % in the two-stage group. There was no paraplegia in the staged group, compared to 50 % paraplegia rate in the single stage group [59]. Staged approaches to endovascular TAAA repair include use of staged coverage of the thoracoabdominal aorta in two or more procedures, use of perfusion branches and use of one of the visceral branches to perfuse the aneurysm sac. The Cleveland Clinic group has reported on the use of staged coverage of the thoracoabdominal aorta. The first stage includes placement of proximal stent grafts from the subclavian to the celiac axis, depending on extent of the aneurysm. After a period of 4–6 weeks, which is typically required for manufacturing of a custom-made device, the second stage is performed with placement of a fenestrated–branched stent graft and distal bifurcated device. Using this technique, Eagleton et al. reported a remarkably low spinal cord injury rate of 5 % for TAAAs [58].

Perfusion branches imply use of additional directional branches directed to perfuse the aneurysm sac. Typically these devices include at least two branches positioned in the thoracic or abdominal component. The branches are left patent for 2–3 weeks, after which endovascular plugs are placed under local anesthesia to occlude the perfusion branch [63]. Based on current experience (Table 29.4), endovascular repair of thoracoabdominal aortic aneurysms carries operative mortality in the range of 0–18 % and results in spinal cord injury in 0–17 % of patients [50, 64–73].

Bridging Stent Characteristics

It has become evident from initial reports of fenestrated and branched endografts that all fenestrations need to be aligned by stent placement to minimize risk of target vessel occlusion [50]. The ideal stent has not been determined or standardized. In general, fenestrations are aligned by a balloon expandable stent, bare metal or covered. The use of a covered stent has the advantages of optimal seal, minimizing risk of endoleak, and improved patency rates, likely due to occurrence of neointimal hyperplasia in the proximal aspect of bare metal stents [70]. The two most widely used stents are the iCAST covered stent (Atrium Medical) and the JoMed stent (Abbott). More recently, the Viabahn balloon-expandable stent (VBX) has been investigated in patients treated by Gore Excluder Thoracoabdominal Multibranched Endoprosthesis (TAMBE). The iCAST covered stent has been widely used and reported in the literature, and was the most frequently used stent in the recent GLOBALSTAR registry, with only 5 of 889 visceral arteries lost during follow up [35]. The JoMed stent has been also widely used at the Cleveland Clinic group, with recent report of >95 % 5-year visceral artery patency among 632

Table 29.4 Clinical results of endovascular repair of TAAAs using fenestrated and branched stent grafts

Author	Year	Aneurysm type	*N*	Target vessel	Technical success (%)	30-day mortality (%)	30-day morbidity (%)	Spinal cord injury (%)	Dialysis (%)
Anderson et al.	2005	TAAA	4	13	92	25	25	0	0
Roselli et al.	2007	TAAA	73	–	93	5.5	14	2.7	1.4
Chuter et al.	2008	TAAA	22	81	100	9	41	–	–
Gilling-Smith et al.	2008	TAAA	6	–	100	0	16.7	0	0
Ferreira et al.	2008	TAAA	11	43	100	18	45	27	0
Bicknell et al.	2009	JRA, TAAA	15	40	98	0	33.4	6.7	6.7
Mohabbat et al.	2009	JRA, TAAA	287	518	98	4.2	–	–	3
Verhoeven et al.	2009	TAAA	30	97	93	6.7	43	16.7	3.3
Amiot et al.	2010	JRA, SRA, TAAA	134	403	99	2	12	0.7	4.5
Haulon et al.	2010	JRA, SRA, TAAA	80	237	99	2.5	11	1.3	4
Haulon et al.	2010	TAAA	33	116	98	9	–	12	9
Greenberg et al.	2010	JRA, TAAA	633	–	–	5.7	–	4.3	0.3
Metcalfe et al.	2012	JRA, SRA, TAAA	42	95	98	7	–	2	2
Guillou et al.	2012	TAAA	89	292	98	8.9	–	7.8	6.7
Ferreira et al.	2012	TAAA	48	–	–	–		2	8.5

patients treated by fenestrated endografts [50]. This has been substituted by the iCAST in their recent experience. The long-term risks of stent fracture and dislodgment have not been systematically reported but seem to be exceptionally low with adequate selection of proximal landing zone. The Fluency stent (Bard Peripheral Vascular, Tempe, AZ) has been used by Timothy Chuter from the University of California, San Francisco, with excellent patency rates and low risk of kinking or stent fracture [67].

In select patients a variety of other self-expandable or balloon-expandable stents may be indicated to treat unanticipated complications or issues related to branch stent configuration. Patients who have a kink or dissection distal to the stent edge are often treated by a self-expandable uncovered stent. A vessel perforation may require placement of stent graft (e.g., Fluency or Viabahn). If a balloon-expandable stent has a proximal kink at the level of the reinforced fenestration, placement of a second balloon-expandable stent may provide more radial force to prevent future loss of target vessel patency.

Late Results

Recent reports have demonstrated that fenestrated and branched endografts are durable beyond 5–10 years of follow up. The overall patient survival for patients with complex aortic aneurysms has been reported in numerous publications, averaging approximately 60 % in 5 years and only 20 % in 10 years (Figs. 29.1 and 29.2). Nearly all deaths are due to non-aneurysm related causes, mostly cardiac, pulmonary, renal, or malignancies. It is important to put this into perspective when selecting open versus endovascular repair. Patients with complex aneurysms have significantly reduced life expectancy compared to the general population, and most are on their 70s or 80s when aortic repair is needed. Perhaps the one exception is younger patients with genetically triggered aortic diseases and those with aneurysms associated with aortic dissections.

The best data on durability of branches comes from the Cleveland Clinic experience. Mastracci and colleagues reported late branch-related stability using a composite end-point which included any potential branch-related event, intervention or death: endoleak, stenosis, occlusion, disconnection, rupture. In that study, freedom from any branch-related event was 89 % in 5 years and 70 % in 10 years (Fig. 29.3). Notably, freedom of events was high in the first 2 years, emphasizing the importance of planning durable repairs beyond acute success. This was possible with increasing utilization of three to four-vessel repairs over two-vessel repairs, which were commonplace prior to 2005 (Figs. 29.4 and 29.5). In a subsequent publication, the Cleveland Clinic group analyzed late failures after fenestrated endografts. O'Callaghan and associates reported that most type I endoleaks after fenestrated endografts became evident after 2–5 years of follow up

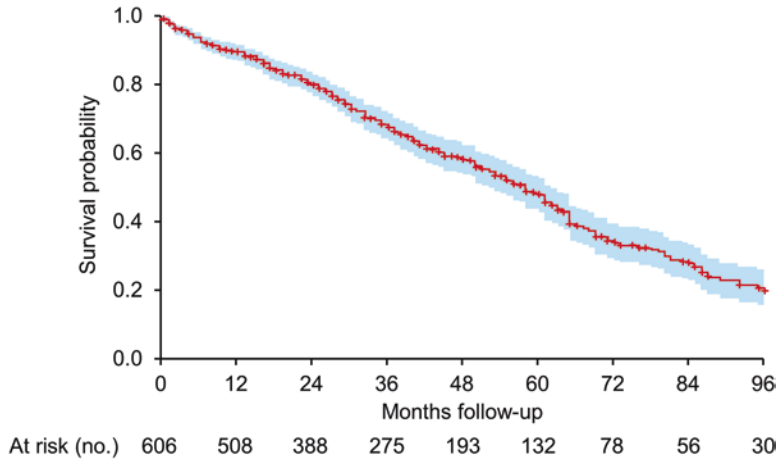


Fig. 29.1 Kaplan–Meier estimates of patient survival in 606 patients treated by fenestrated and branched endografts at the Cleveland Clinic. Courtesy of Matt Eagleton

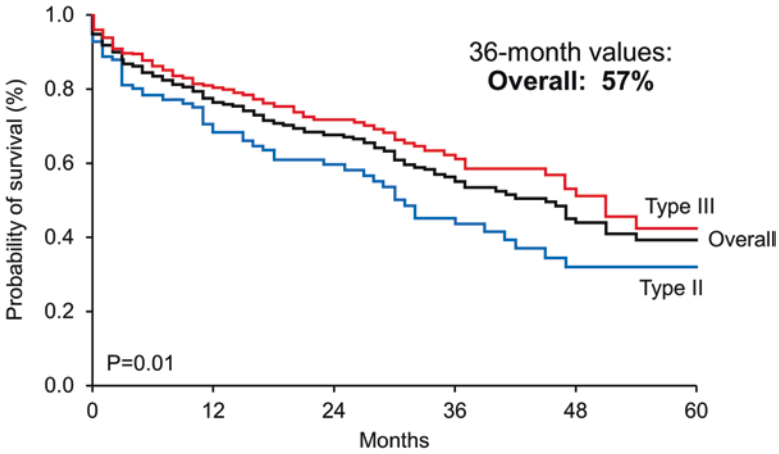


Fig. 29.2 Kaplan–Meier estimates of patient survival in patients treated for Type II and III TAAAs by fenestrated and branched endografts at the Cleveland Clinic. Courtesy of Matt Eagleton

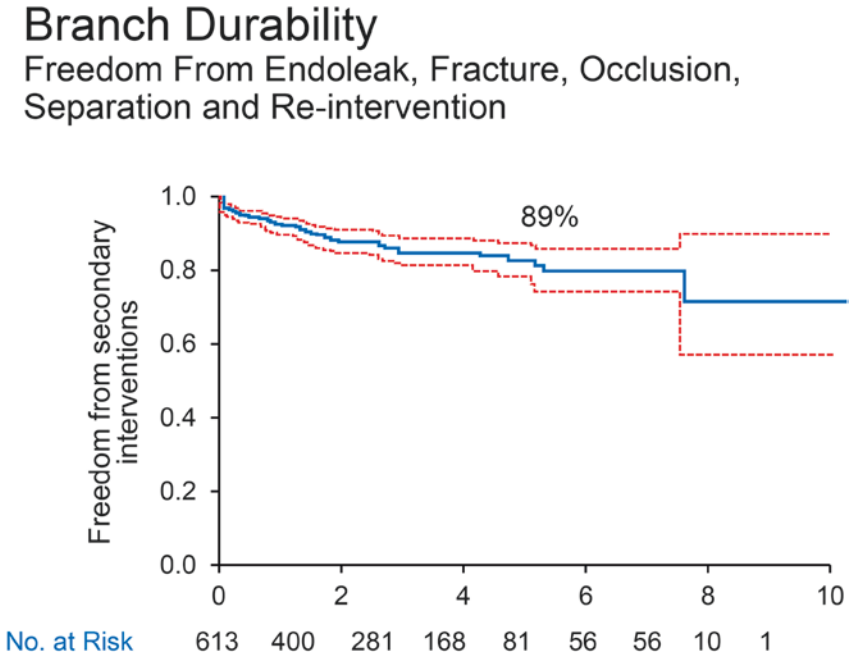


Fig. 29.3 Kaplan–Meier estimates of survival free of branch related events. Adapted from [56]. By permission of Mayo Foundation for Medical Education and Research. All rights reserved

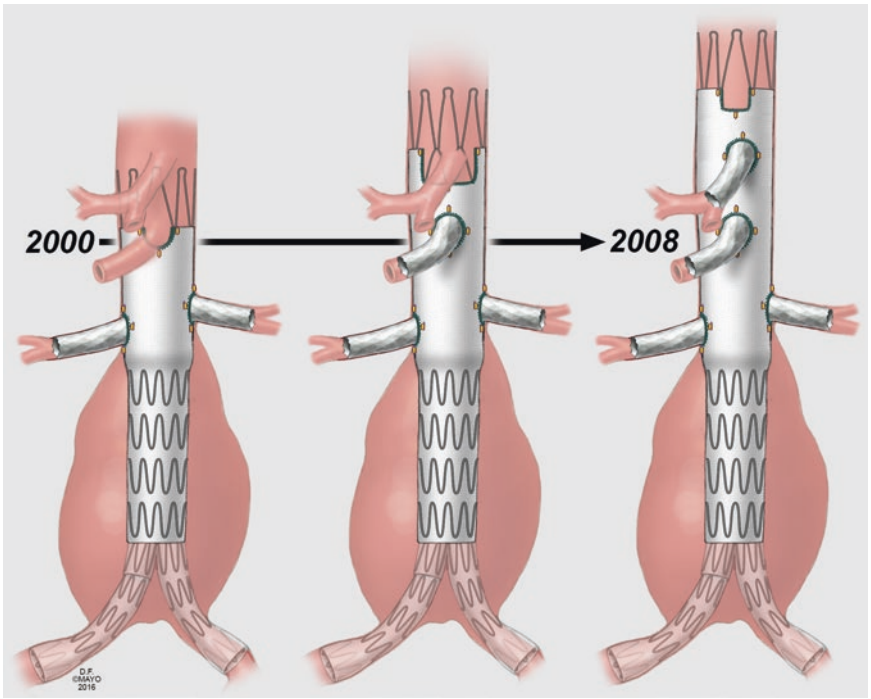


Fig. 29.4 Increasing stent design complexity. By permission of Mayo Foundation for Medical Education and Research. All rights reserved

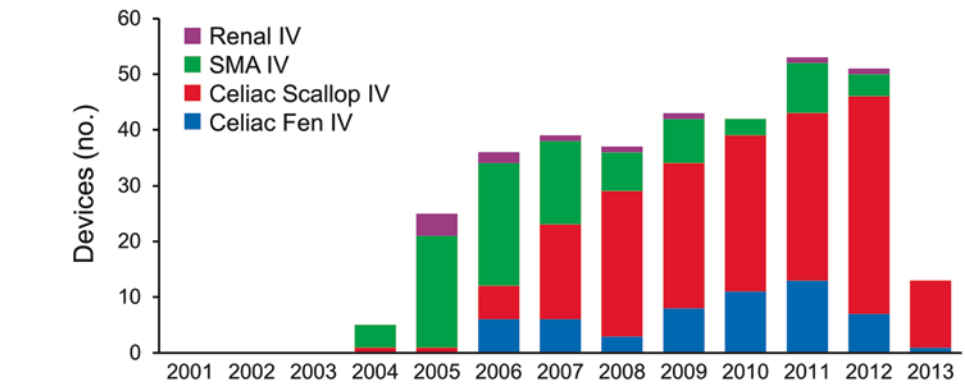


Fig. 29.5 Increasing complexity in device design at the Cleveland Clinic. Courtesy of Matt Eagleton

(Fig. 29.6). In that study, patient survival was decreased among patients who developed a type I endoleak (Fig. 29.7). In addition, the authors noted a significant decline in endoleak rates in their late experience, which was attributed to the use of more complex designs with supra-celiac sealing zones (Fig. 29.8). European experiences reported by Verhoeven, Haulon and Resch also demonstrate similar trends and durable results of fenestrated and branched endografts.

Mayo Clinic Experience

The Mayo Clinic advanced endovascular aortic program started in 2007. The initial experience was with physician-modified endovascular grafts, which were gradually replaced by manufactured devices under industry and physician-sponsored investigational device exemption protocols. A total of 320 patients were treated between

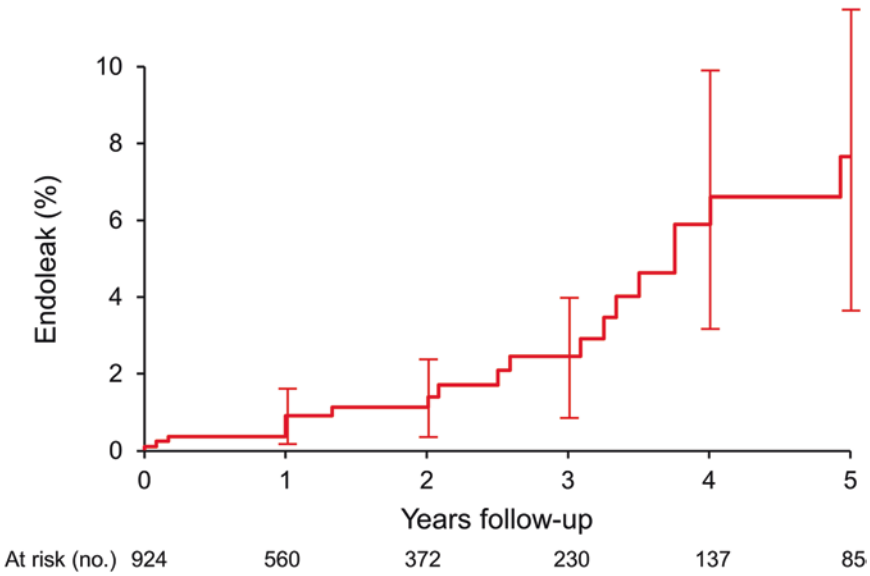


Fig. 29.6 Cumulative incidence of type Ia endoleak after fenestrated and branched repair. Adapted from [76]. By permission of Mayo Foundation for Medical Education and Research. All rights reserved

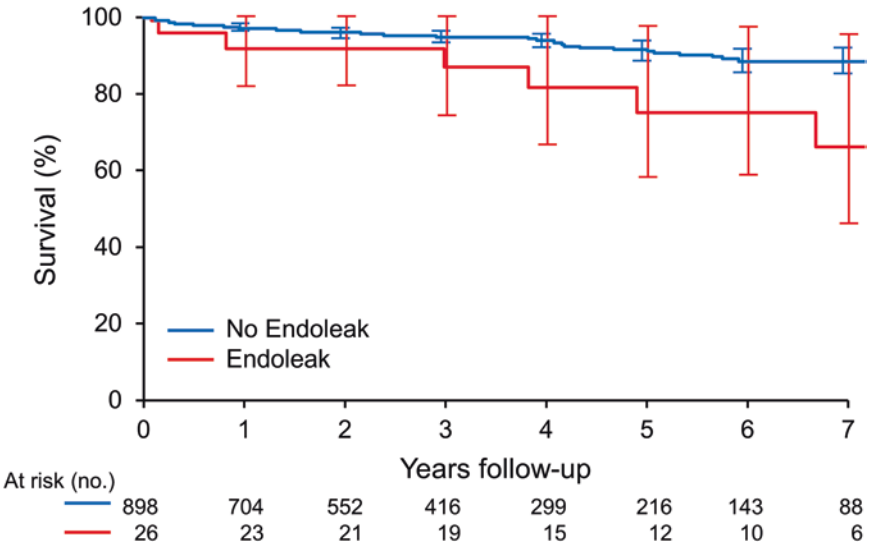


Fig. 29.7 Survival in patients with and without type Ia endoleak. Adapted from [76]. By permission of Mayo Foundation for Medical Education and Research. All rights reserved

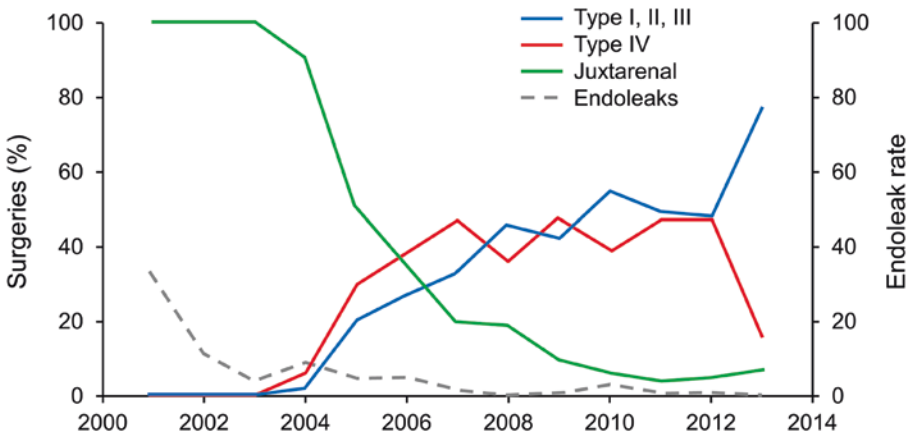


Fig. 29.8 Decreasing rates of endoleak with increasing complexity of stent design. Adapted from [76]. By permission of Mayo Foundation for Medical Education and Research. All rights reserved

Table 29.5 Results of a prospective, non-randomized study to evaluate endovascular repair of pararenal and thoracoabdominal aortic aneurysms using 4-vessel fenestrated and branched endografts

	PRAs $N=37$		TAAAs $N=63$		P value
30-day outcomes	No. of events and %				
Any MAE	7	19 %	7	19 %	0.99
Any cause mortality	0	0	0	0	–
Myocardial infarction	3	8 %	3	5 %	0.7
Acute kidney injury	2	5 %	2	3 %	0.58
Respiratory failure	2	0 %	2	3 %	0.27
Spinal cord injury	1	3 %	2	2 %	0.13
Blood loss >1 l	1	3 %	7	11 %	0.13
1-year outcomes	No. of events and % ± Standard Deviation				
Patient survival	4	93 ± 6 %	0	100 %	0.86
Freedom from reintervention	5	89 ± 6 %	8	83 ± 7 %	0.87
Freedom from type Ia/III endoleak	2	97 ± 2 %	3	98 ± 2 %	0.86
Freedom from branch occlusion	3	99 ± 2 %	1	99 ± 2 %	0.99
Freedom from sac growth	1	99 ± 2 %	1	99 ± 2 %	0.99

2007 and 2015. Thirty-day or in-hospital mortality was 2.1 %, with 7 deaths among the 320 patients. There were 167 patients treated for TAAAs and 153 for pararenal aneurysms. Mortality was 0.6 % for pararenal aneurysms and 3.5 % for TAAAs. The results of the first 100 patients enrolled in a prospective, non-randomized study were recently presented at the 2016 Vascular Annual Meeting in Washington, DC. In that study, all patients had endografts based on supra-celiac sealing zones with minimum of four fenestrations. There were 75 male and 25 female patients with mean age of 78 ± 7 years old. Follow up include clinical examination, laboratory studies, duplex ultrasound and computed tomography imaging at hospital discharge, 1-month, 6-months and yearly. End-points were adjudicated by independent clinical event committee included mortality, major adverse events (MAEs), freedom from reintervention, branch vessel occlusion, type Ia/III endoleak, sac aneurysm enlargement, and aneurysm rupture. Risk factors included smoking (87 %), hypertension (87 %), hyperlipidemia (81 %), coronary artery disease (54 %), stage III–V chronic kidney disease (45 %), chronic pulmonary disease (33 %), prior aortic repair (27 %) and congestive heart failure (17 %). There were 37 PRAs, 35 type IV and 28 type I–III TAAAs with mean diameter of 65 ± 8 mm. A total of 387 visceral arteries were incorporated by 276 fenestrations, 98 branches, and 13 scallops (mean 3.9 ± 0.6 vessels/patient). Technical success was 100 %. There were no 30-day or in-hospital deaths, nor new dialysis requirement. MAEs occurred in 19 patients (Table 29.5). Follow up was >30 days in all, > 6-months in 75 and >12-months in 51 patients (mean, 9 ± 4 months). There were 13 patient reinterventions, five for type Ia/III endoleaks, four for renal stent occlusions, four late unrelated deaths, two patients with aneurysm sac enlargement and no ruptures or conversion to open repair.

Parallel Stent Grafts

Parallel stent graft techniques were initially described as a "bail out" in patients with short landing zones or inadvertent coverage of side branches. The technique has been increasingly utilized in some centers as the primary treatment method for complex aneurysms including arch, thoracoabdominal, pararenal, and iliac bifurcation aneurysms. Potential advantages of parallel grafts include immediate availability and ability to access the target vessels prior to placement of the aortic endograft, eliminating issues of device misalignment that can occur with fenestrated grafts. These procedures can also be performed with smaller profile devices, which may be an advantage in the patient with difficult iliac access. However, there has been skepticism in the adoption of parallel grafts for elective procedures in good anatomical candidates for fenestrated or branched endografts. Potential complications, which occur at higher rates with parallel grafts, include stroke from multiple sheaths via arm access and gutter endoleaks. Vessel occlusion can occur, but reported rates are low (<5 %). Donas, Lee and associates presented the largest report of the collected worldwide experience in several centers. The study was a retrospective review of self-reported outcomes and there was no adjudication of events or independent review of imaging in a core

lab. A total of 517 patients with 898 chimney grafts (1.7 vessel per patient) were analyzed. A difference from fenestrated techniques is the lower number of vessels per patient, indicating that these procedures were performed likely for less extensive aneurysms, or that less optimal sealing zones were accepted for the repair. The 30-day mortality was 3.7 % with stroke in 1.7 % of patients. Early type Ia endoleak was noted in only 3.7 %, and persisted in only two patients. After a mean follow-up of 17 months, primary patency was 94 %.

Limitations of the parallel graft literature include retrospective design in all studies, small single-center experiences in most, use of 1–2 vessel incorporation with lack of 3–4 vessel data, and limited follow up interval of less than 2 years. There is also no uniform technique on how to perform the procedure in terms of selection of which aortic and side branch component are used, sequence of deployment or minimum neck requirements. A review of the available literature showed an average of 1.7 vessels per patient. Studies included from 14 to 128 patients treated for pararenal aneurysms. Technical success was high, ranging from 94 to 100 % in all studies. Thirty day mortality ranged from 0 to 10 %, and stroke rates from 1.6 to 10 %. Type Ia endoleak occurred on average in 10 % of the patients, ranging from 1.6 to 31 %. Branch occlusion rates ranged from 3.6 to 15 %.

Conclusion

Total endovascular repair is unquestionably replacing open surgical repair for most indications. Exceptions are patients with aortic infections and genetically triggered aortic diseases, where open surgery remains the first option. In the last decade, several reports have shown that fenestrated and branched endografts can be performed with high technical success and low morbidity and mortality compared to open surgical results. It is likely that these results will continue to improve with increasing experience and refinements in stent design and endovascular technology.

References

1. Clouse WD, Cambria RP. Complex aortic aneurysm: pararenal, suprarenal, and thoracoabdominal. In: Hallett Jr JW, Mills JL, Earnshaw J, Reekers JA, Rooke T, editors. Comprehensive vascular and endovascular surgery: expert consult. 2nd ed. Philadelphia: Mosby; 2009.
2. Crawford ES, Crawford JL, Safi HJ, Coselli JS, Hess KR, Brooks B, et al. Thoracoabdominal aortic aneurysms: preoperative and intraoperative factors determining immediate and long-term results of operations in 605 patients. J Vasc Surg. 1986;3(3):389–404.
3. Coselli JS, Bozinovski J, LeMaire SA. Open surgical repair of 2286 thoracoabdominal aortic aneurysms. Ann Thorac Surg. 2007;83(2):S862–4. discussion S90–2.
4. Kieffer E, Chiche L, Godet G, Koskas F, Bahnini A, Bertrand M, et al. Type IV thoracoabdominal aneurysm repair: predictors of postoperative mortality, spinal cord injury, and acute intestinal ischemia. Ann Vasc Surg. 2008;22(6):822–8.
5. Richards JM, Nimmo AF, Moores CR, Hansen PA, Murie JA, Chalmers RT. Contemporary results for open repair of suprarenal and type IV thoracoabdominal aortic aneurysms. Br J Surg. 2010;97(1):45–9.
6. Ockert S, Riemensperger M, von Tengg-Kobligk H, Schumacher H, Eckstein HH, Bockler D. Complex abdominal aortic pathologies: operative and midterm results after pararenal aortic aneurysm and type IV thoracoabdominal aneurysm repair. Vascular. 2009;17(3):121–8.
7. Oderich GS, Tallarita T, Kalra M, Duncan AA, Gloviczki P, Vrtiska T, et al. SS23. Contemporary results of open complex abdominal aortic aneurysm repair using a standardized classification for comparison with fenestrated endografts. J Vasc Surg. 2011;53(6 Suppl):27S–8S.
8. Patel VI, Ergul E, Conrad MF, Cambria M, LaMuraglia GM, Kwolek CJ, et al. Continued favorable results with open surgical repair of type IV thoracoabdominal aortic aneurysms. J Vasc Surg. 2011;53(6):1492–8.
9. Schepens MA, Kelder JC, Morshuis WJ, Heijmen RH, van Dongen EP, ter Beek HT. Long-term follow-up after thoracoabdominal aortic aneurysm repair. Ann Thorac Surg. 2007;83(2):S851–5. discussion S90–2.
10. Achneck HE, Rizzo JA, Tranquilli M, Elefteriades JA. Safety of thoracic aortic surgery in the present era. Ann Thorac Surg. 2007;84(4):1180–5. discussion 5.
11. Conrad MF, Crawford RS, Davison JK, Cambria RP. Thoracoabdominal aneurysm repair: a 20-year perspective. Ann Thorac Surg. 2007;83(2):S856–61. discussion S90–2.
12. Jacobs MJ, van Eps RG, de Jong DS, Schurink GW, Mochtar B. Prevention of renal failure in patients undergoing thoracoabdominal aortic aneurysm repair. J Vasc Surg. 2004;40(6):1067–73. discussion 73.
13. Safi HJ, Estrera AL, Miller CC, Huynh TT, Porat EE, Azizzadeh A, et al. Evolution of risk for neurologic deficit after descending and thoracoabdominal aortic repair. Ann Thorac Surg. 2005;80(6):2173–9. discussion 9.
14. Grabitz K, Sandmann W, Stuhmeier K, Mainzer B, Godehardt E, Ohle B, et al. The risk of ischemic spinal cord injury in patients undergoing graft replacement for thoracoabdominal aortic aneurysms. J Vasc Surg. 1996;23(2):230–40.
15. Svensson LG, Crawford ES, Hess KR, Coselli JS, Safi HJ. Experience with 1509 patients undergoing thoracoabdominal aortic operations. J Vasc Surg. 1993;17(2):357–68. discussion 68–70.
16. Rigberg DA, McGory ML, Zingmond DS, Maggard MA, Agustin M, Lawrence PF, et al. Thirty-day mortality statistics underestimate the risk of repair of thoracoabdominal aortic aneurysms: a statewide experience. J Vasc Surg. 2006;43(2):217–22. discussion 23.
17. Oderich GS, Rosero EB, Ricotta II JJ, Gloviczki P, Bower TC, Duncan AA, et al. In-hospital mortality of open thoracoabdominal aortic aneurysm repair in the United States prior to widespread use of hybrid and endovascular branched techniques. J Vasc Surg. 2009;49(5S):55S.
18. De Bruin JL, Baas AF, Buth J, Prinssen M, Verhoeven EL, Cuypers PW, et al. Long-term outcome of open or endovascular repair of abdominal aortic aneurysm. N Engl J Med. 2010;362(20):1881–9.
19. Greenhalgh RM, Brown LC, Powell JT, Thompson SG, Epstein D, Sculpher MJ. Endovascular versus open repair of abdominal aortic aneurysm. N Engl J Med. 2010;362(20):1863–71.
20. Schermerhorn ML, O'Malley AJ, Jhaveri A, Cotterill P, Pomposelli F, Landon BE. Endovascular vs. open repair of abdominal aortic

aneurysms in the Medicare population. N Engl J Med. 2008;358(5):464–74.
21. Park JH, Chung JW, Choo IW, Kim SJ, Lee JY, Han MC. Fenestrated stent-grafts for preserving visceral arterial branches in the treatment of abdominal aortic aneurysms: preliminary experience. J Vasc Interv Radiol. 1996;7(6):819–23.
22. Uflacker R, Robison JD, Schonholz C, Ivancev K. Clinical experience with a customized fenestrated endograft for juxtarenal abdominal aortic aneurysm repair. J Vasc Interv Radiol. 2006;17(12):1935–42.
23. Amiot S, Haulon S, Becquemin JP, Magnan PE, Lermusiaux P, Goueffic Y, et al. Fenestrated endovascular grafting: the French multicentre experience. Eur J Vasc Endovasc Surg. 2010;39(5):537–44.
24. Beck AW, Bos WT, Vourliotakis G, Zeebregts CJ, Tielliu IF, Verhoeven EL. Fenestrated and branched endograft repair of juxtarenal aneurysms after previous open aortic reconstruction. J Vasc Surg. 2009;49(6):1387–94.
25. GLOBALSTAR Collaborators. Early results of fenestrated endovascular repair of juxtarenal aortic aneurysms in the United Kingdom. Circulation. 2012;125(22):2707–15.
26. Greenberg RK, Haulon S, O'Neill S, Lyden S, Ouriel K. Primary endovascular repair of juxtarenal aneurysms with fenestrated endovascular grafting. Eur J Vasc Endovasc Surg. 2004;27(5):484–91.
27. Greenberg RK, Sternbergh III WC, Makaroun M, Ohki T, Chuter T, Bharadwaj P, et al. Intermediate results of a United States multicenter trial of fenestrated endograft repair for juxtarenal abdominal aortic aneurysms. J Vasc Surg. 2009;50(4):730–7. e1.
28. Haulon S, Amiot S, Magnan PE, Becquemin JP, Lermusiaux P, Koussa M, et al. An analysis of the French multicentre experience of fenestrated aortic endografts: medium-term outcomes. Ann Surg. 2010;251(2):357–62.
29. Kristmundsson T, Sonesson B, Malina M, Bjorses K, Dias N, Resch T. Fenestrated endovascular repair for juxtarenal aortic pathology. J Vasc Surg. 2009;49(3):568–74. discussion 74–5.
30. Muhs BE, Verhoeven EL, Zeebregts CJ, Tielliu IF, Prins TR, Verhagen HJ, et al. Mid-term results of endovascular aneurysm repair with branched and fenestrated endografts. J Vasc Surg. 2006;44(1):9–15.
31. O'Neill S, Greenberg RK, Haddad F, Resch T, Sereika J, Katz E. A prospective analysis of fenestrated endovascular grafting: intermediate-term outcomes. Eur J Vasc Endovasc Surg. 2006;32(2):115–23.
32. Scurr JR, Brennan JA, Gilling-Smith GL, Harris PL, Vallabhaneni SR, McWilliams RG. Fenestrated endovascular repair for juxtarenal aortic aneurysm. Br J Surg. 2008;95(3):326–32.
33. Semmens JB, Lawrence-Brown MM, Hartley DE, Allen YB, Green R, Nadkarni S. Outcomes of fenestrated endografts in the treatment of abdominal aortic aneurysm in Western Australia (1997–2004). J Endovasc Ther. 2006;13(3):320–9.
34. Starnes BW. Physician-modified endovascular grafts for the treatment of elective, symptomatic, or ruptured juxtarenal aortic aneurysms. J Vasc Surg. 2012;56(3):601–7.
35. Tambyraja AL, Fishwick NG, Bown MJ, Nasim A, McCarthy MJ, Sayers RD. Fenestrated aortic endografts for juxtarenal aortic aneurysm: medium term outcomes. Eur J Vasc Endovasc Surg. 2011;42(1):54–8.
36. Verhoeven EL, Vourliotakis G, Bos WT, Tielliu IF, Zeebregts CJ, Prins TR, et al. Fenestrated stent grafting for short-necked and juxtarenal abdominal aortic aneurysm: an 8-year single-centre experience. Eur J Vasc Endovasc Surg. 2010;39(5):529–36.
37. Ziegler P, Avgerinos ED, Umscheid T, Perdikides T, Stelter WJ. Fenestrated endografting for aortic aneurysm repair: a 7-year experience. J Endovasc Ther. 2007;14(5):609–18.
38. Verhoeven EL, Tielliu IF, Muhs BE, Bos WT, Zeebregts CJ, Prins TR, et al. Fenestrated and branched stent-grafting: a 5-years experience. Acta Chir Belg. 2006;106(3):317–22.
39. Manning BJ, Agu O, Richards T, Ivancev K, Harris PL. Early outcome following endovascular repair of pararenal aortic aneurysms: triple- versus double- or single-fenestrated stent-grafts. J Endovasc Ther. 2011;18(1):98–105.
40. Greenberg R, Eagleton M, Mastracci T. Branched endografts for thoracoabdominal aneurysms. J Thorac Cardiovasc Surg. 2010;140(6 Suppl):S171–8.
41. Reilly LM, Rapp JH, Grenon SM, Hiramoto JS, Sobel J, Chuter TA. Efficacy and durability of endovascular thoracoabdominal aortic aneurysm repair using the caudally directed cuff technique. J Vasc Surg. 2012;56(1):53–63. discussion 63–4.
42. Sweet MP, Hiramoto JS, Park KH, Reilly LM, Chuter TA. A standardized multi-branched thoracoabdominal stent-graft for endovascular aneurysm repair. J Endovasc Ther. 2009;16(3):359–64.
43. Park KH, Hiramoto JS, Reilly LM, Sweet M, Chuter TA. Variation in the shape and length of the branches of a thoracoabdominal aortic stent graft: implications for the role of standard off-the-shelf components. J Vasc Surg. 2010;51(3):572–6.
44. Gasper WJ, Reilly LM, Rapp JH, Marlene Grenon S, Hiramoto JS, Sobel JD, et al. Assessing the anatomic applicability of the multibranched endovascular repair of thoracoabdominal aortic aneurysm technique. J Vasc Surg. 2013;57(6):1553–8. discussion 1558.
45. Conway BD, Greenberg RK, Mastracci TM, Hernandez AV, Coscas R. Renal artery implantation angles in thoracoabdominal aneurysms and their implications in the era of branched endografts. J Endovasc Ther. 2010;17(3):380–7.
46. Mastracci TM, Greenberg RK, Eagleton MJ, Hernandez AV. Durability of branches in branched and fenestrated endografts. J Vasc Surg. 2013;57(4):926–33. discussion 933.
47. Greenberg RK, Lu Q, Roselli EE, Svensson LG, Moon MC, Hernandez AV, et al. Contemporary analysis of descending thoracic and thoracoabdominal aneurysm repair: a comparison of endovascular and open techniques. Circulation. 2008;118(8):808–17.
48. Eagleton MJ, Shah SK, Petkovsek D, Mastracci T, Greenberg RK. Collateral bed patency affects outcomes of spinal cord ischemia (SCI) following aortic endografting. J Vasc Surg. 2013;57(5):28S–9.
49. Bischoff MS, Scheumann J, Brenner RM, Ladage D, Bodian CA, Kleinman G, et al. Staged approach prevents spinal cord injury in hybrid surgical-endovascular thoracoabdominal aortic aneurysm repair: an experimental model. Ann Thorac Surg. 2011;92(1):138–46. discussion 46.
50. Etz CD, Zoli S, Bischoff MS, Bodian C, Di Luozzo G, Griepp RB. Measuring the collateral network pressure to minimize paraplegia risk in thoracoabdominal aneurysm resection. J Thorac Cardiovasc Surg. 2010;140(6 Suppl):S125–30. discussion S42–46.
51. Etz CD, Zoli S, Mueller CS, Bodian CA, Di Luozzo G, Lazala R, et al. Staged repair significantly reduces paraplegia rate after extensive thoracoabdominal aortic aneurysm repair. J Thorac Cardiovasc Surg. 2010;139(6):1464–72.
52. Zoli S, Etz CD, Roder F, Brenner RM, Bodian CA, Kleinman G, et al. Experimental two-stage simulated repair of extensive thoracoabdominal aneurysms reduces paraplegia risk. Ann Thorac Surg. 2010;90(3):722–9.
53. Lioupis C, Corriveau MM, Mackenzie KS, Obrand DI, Steinmetz OK, Ivancev K, et al. Paraplegia prevention branches: a new adjunct for preventing or treating spinal cord injury after endovascular repair of thoracoabdominal aneurysms. J Vasc Surg. 2011;54(1):252–7.
54. Anderson JL, Adam DJ, Berce M, Hartley DE. Repair of thoracoabdominal aortic aneurysms with fenestrated and branched endovascular stent grafts. J Vasc Surg. 2005;42(4):600–7.
55. Roselli EE, Greenberg RK, Pfaff K, Francis C, Svensson LG, Lytle BW. Endovascular treatment of thoracoabdominal aortic aneurysms. J Thorac Cardiovasc Surg. 2007;133(6):1474–82.

56. Bicknell CD, Cheshire NJ, Riga CV, Bourke P, Wolfe JH, Gibbs RG, et al. Treatment of complex aneurysmal disease with fenestrated and branched stent grafts. Eur J Vasc Endovasc Surg. 2009;37(2):175–81.
57. Chuter TA, Rapp JH, Hiramoto JS, Schneider DB, Howell B, Reilly LM. Endovascular treatment of thoracoabdominal aortic aneurysms. J Vasc Surg. 2008;47(1):6–16.
58. Ferreira M, Lanziotti L, Monteiro M. Branched devices for thoracoabdominal aneurysm repair: early experience. J Vasc Surg. 2008;48(6 Suppl):30S–6. discussion 6S.
59. Gilling-Smith GL, McWilliams RG, Scurr JR, Brennan JA, Fisher RK, Harris PL, et al. Wholly endovascular repair of thoracoabdominal aneurysm. Br J Surg. 2008;95(6):703–8.
60. Mohabbat W, Greenberg RK, Mastracci TM, Cury M, Morales JP, Hernandez AV. Revised duplex criteria and outcomes for renal stents and stent grafts following endovascular repair of juxtarenal and thoracoabdominal aneurysms. J Vasc Surg. 2009;49(4):827–37. discussion 37.
61. Verhoeven EL, Tielliu IF, Bos WT, Zeebregts CJ. Present and future of branched stent grafts in thoraco-abdominal aortic aneurysm repair: a single-centre experience. Eur J Vasc Endovasc Surg. 2009;38(2):155–61.
62. Guillou M, Bianchini A, Sobocinski J, Maurel B, D'Elia P, Tyrrell M, et al. Endovascular treatment of thoracoabdominal aortic aneurysms. J Vasc Surg. 2012;56(1):65–73.
63. Metcalfe MJ, Holt PJ, Hinchliffe RJ, Morgan R, Loftus IM, Thompson MM. Fenestrated endovascular aneurysm repair: graft complexity does not predict outcome. J Endovasc Ther. 2012;19(4):528–35.
64. O'Callaghan A, Greenberg RK, Eagleton MJ, Bena J, Mastracci TM. Type Ia endoleaks after fenestrated and branched endografts may lead to component instability and increased aortic mortality. J Vasc Surg. 2015;61(4):908–14.

Parallel Graft Techniques to Treat Complex Aortic Aneurysms Involving the Renal and Mesenteric Arteries

30

Jason T. Lee

Introduction

There is little debate that routine endovascular aneurysm repair (EVAR) has gained widespread acceptance as the procedure of choice for patients with suitable aortic neck anatomy. However, the optimal approach to the more complicated aneurysm, namely juxtarenal aortic aneurysm (JAA) remains controversial [1]. These JAAs in the endovascular literature are often lumped together as short-neck infrarenal aneurysms, suprarenal aneurysms, type IV thoracoabdominal aneurysms (TAAA), and distal thoracic aneurysms. While open repair is an effective and durable option for patients with JAA, particularly in centers of excellence and for low physiologic risk patients [2], endovascular techniques including fenestrated and branched EVAR (F-BEVAR) have emerged as effective, potentially less invasive alternatives [3].

In the USA, however, lack of widespread availability of F-BEVAR has allowed other techniques to emerge, and in this chapter we describe the increasingly popular "snorkel" or "chimney" techniques (ch-EVAR), defined as a parallel stent graft adjacent to the endograft main body to maintain perfusion to renal and visceral branches during EVAR and placed from a cranial direction, and the "periscope" technique, where the parallel stent graft is placed from the caudal direction. Further iterations of this approach that are discussed in this chapter include the "octopus" approach mixing branched and parallel graft strategies with off the shelf devices.

First described by Greenberg et al. [4], ch-EVAR can be employed either as a bailout from accidental coverage of vital side branches during deployments requiring close approximation of the main body to the branch artery in question, or the intentional cranial relocation of the EVAR seal zone for JAAs [5–8]. More recent literature and international registries have established the merits and positive outcomes of ch-EVAR as compared to FBE, and acceptable outcomes for both these strategies make it likely that moving forward the techniques will be seen as complementary [9, 10].

Preoperative Imaging

High-quality computed tomography angiography (CTA) of the chest/abdomen/pelvis on a modern 64-slice scanner able to produce at least 2-mm thin cuts is a requirement for treatment using parallel graft techniques. These imaging algorithms allow the creation of virtual models of the aneurysm to better appreciate the relationship of branches and potential areas of technical challenge. With most of these strategies relying upon upper arm brachial access, understanding arch anatomy becomes paramount to assure safe passage of sheaths and wires without increasing risk of cerebrovascular events. The presence of a challenging type 3 arch (Fig. 30.1) where the subclavian inserts below the inner curve of the aortic arch makes the procedure more challenging and many times prohibitive due to concerns about arch manipulation, cerebral emboli, and deliverability of stent grafts.

Patients with compromised kidney function that cannot receive contrast media are poor candidates for parallel grafts procedures, as non-contrast scans fail to elucidate thrombus, patency, and accurate diameters of branch vessels. Additionally, and perhaps most important of all, access to a three-dimensional workstation/program and familiarity with reconstruction software by the implanting surgeon for manipulation of the images and creating centerline pathways should be mandatory to most accurately plan out device orientation, selection, and sizing. For patients with chronic kidney disease, high grade renal stenosis, atretic kidneys, or multiple visceral and renal vessels involved in the endo-

J.T. Lee (✉)
Division of Vascular Surgery, Stanford University Medical Center, 300 Pasteur Drive, Suite H3600, Stanford, CA 94025, USA
e-mail: jtlee@stanford.edu

© Mayo Foundation for Medical Education and Research 2017

G.S. Oderich (ed.), *Endovascular Aortic Repair*, DOI 10.1007/978-3-319-15192-2_30



Fig. 30.1 Type 3 aortic arch with origin of subclavian artery being lower than inner curve of aortic arch. The ability to advance a snorkel sheath from the left arm is severely compromised in this configuration. By permission of Mayo Foundation for Medical Education and Research. All rights reserved

vascular plan, nuclear medicine split renal function tests can help determine if it is reasonable to potentially sacrifice one of the renal arteries. This can be done in order to simplify the ch-EVAR strategy and keep the number of cranially oriented stent grafts to two, which may have an influence on overall morbidity and mortality from the procedure [1, 7, 8, 10]

Surgical Management

Preoperative Planning

All patients considered for parallel graft techniques should undergo an extensive informed consent discussion related to off-label use of endograft components for treatment of their complex aneurysm. At our institution, we have them sign an IRB-approved research consent form. Alternatives often discussed include open surgery with suprarenal clamping, hybrid debranching, referral to a center with IDE access to fenestrated or branched or custom devices, or no surgery at all. Once the decision is made to proceed with the ch-EVAR strategy, we recommend a two-surgeon approach with one performing the femoral access portion, and one the arm or brachial access portion (Fig. 30.2). Both surgeons should have reviewed on the 3D workstation the anatomy and endovascular plan and sequence for deployment.

Access to a hybrid endovascular suite is highly recommended, as fixed imaging units provide improved accuracy, reliability, and reproducibility of the visible anatomy throughout the sequence of the procedure. Knowledgeable operating room and cath-angio staff should be assigned to these cases, and available endografts and wires/catheters as well as backups should all be arranged ahead of time to provide an efficient working environment. Choosing the main body endograft and its configuration and size has been described by numerous authors who all report excellent results overall with a wide variety of devices and formulas [10, 11]. In general, we often "oversize" to about 25–30 % instead of the typical 15–20 % for standard EVAR to account for the additional fabric infolding to accommodate the parallel stent graft(s).

Given the amount of dye often used as well as renal artery manipulation during most parallel graft cases, we prefer to admit the patient the evening before or several hours prior to surgery for additional intravenous hydration. General anesthesia is utilized, with consideration for preoperative lumbar drainage based on risk of spinal cord ischemia particularly during periscope or octopus cases when the distal thoracic aorta is involved, and arterial monitoring is necessary via the right arm. Adequate venous access can consist of either large bore peripheral IVs, or a central line. There is usually not a need for auto-transfusion or cell-saver setups unless an iliac or axillary conduit is planned where there is more potential for early blood loss during the procedure.

Positioning

The hybrid room can be set up as either "Head" position if the left arm is tucked and an infraclavicular incision is planned, or more commonly "Right-Side, Table Rotated" when a high brachial incision is used for ch-EVAR (see Fig. 30.2). With the right arm tucked, the left arm is prepped circumferentially and placed on an armboard at about 75°–90°, while the chest and abdomen down to the groins are prepped. Surgeon A stands at the patient's right hip, has control of the C-arm and imaging functions, and is in charge of obtaining femoral access and delivery of devices from the groins. Surgeon B stands above the outstretched left arm and has an additional sterile table extending off the left hand to allow for wires and catheters to be laid down during the procedure. The monitor is placed at a slight angle towards the foot of the bed to allow both surgeons to visualize, and a slave monitor should be employed.

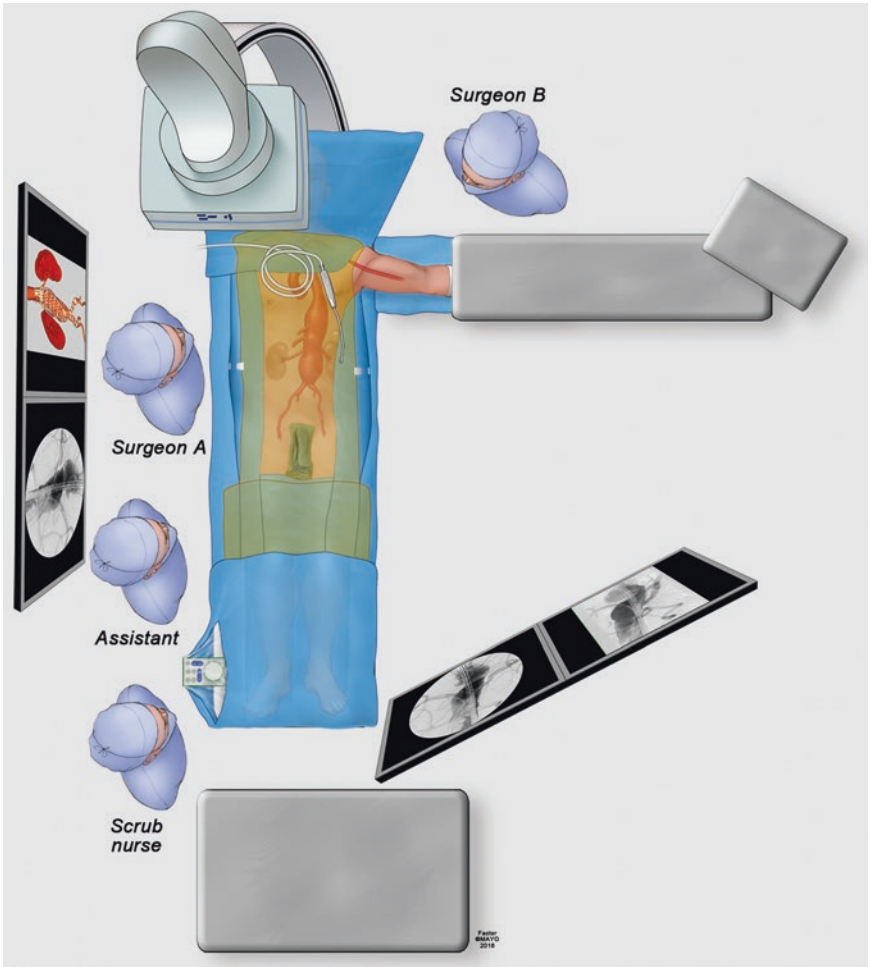


Fig. 30.2 Endovascular suite setup for snorkel/chimney EVAR with left arm prepped and outstretched, C-arm at head position to allow for lateral imaging, monitors at foot of bed. Surgeon A stands at patient's right hip and controls C-arm. Surgeon B stands above patients left arm to delivery wires and catheters from side table. By permission of Mayo Foundation for Medical Education and Research. All rights reserved

Arm Access

A 4 cm transverse incision slightly below the left axilla over the palpable brachial pulse affords several centimeters of longitudinal exposure of the high brachial artery (Fig. 30.3a, b). Staying proximal to the deep brachial artery takeoff allows the larger portion of the brachial artery to be exposed for typical delivery of two 7 F sheaths for a double renal chimney procedure. About 6–7 cm of healthy brachial artery should be dissected free and slung with vessel loops, and the two punctures should be placed at least 2-cm apart and not next to each other to facilitate individual primary closure at the conclusion of the arm access.

For cases when larger delivery sheaths need to be inserted due to needing larger chimney or branch stents (i.e., when a 12 F Ansel sheath is needed for a 10-mm or larger Viabahn), or in cases where potentially up to three or four chimney stents (each needing 6 or 7 F sheaths) are used such as in the case of the octopus configuration described below, then an infraclavicular incision and exposure of the axillary artery for creation of a 10-mm Dacron conduit is recommended (Fig. 30.3c). Finally, in the simplest of all chimney cases when just a single renal artery needs stenting, a lower longitudinal brachial incision can be made near the antecubital crease to allow insertion of a single 7 F sheath (see Fig. 30.3a).

Single or Double Chimney Procedure

Renal/Visceral Cannulation and Sheath Advancement

Access is obtained with 5 F micropuncture kit under direct visualization into the brachial artery. A Bentson wire is advanced under fluoroscopic guidance most often into the ascending aorta. A short 5 or 6 F sheath can then be inserted.

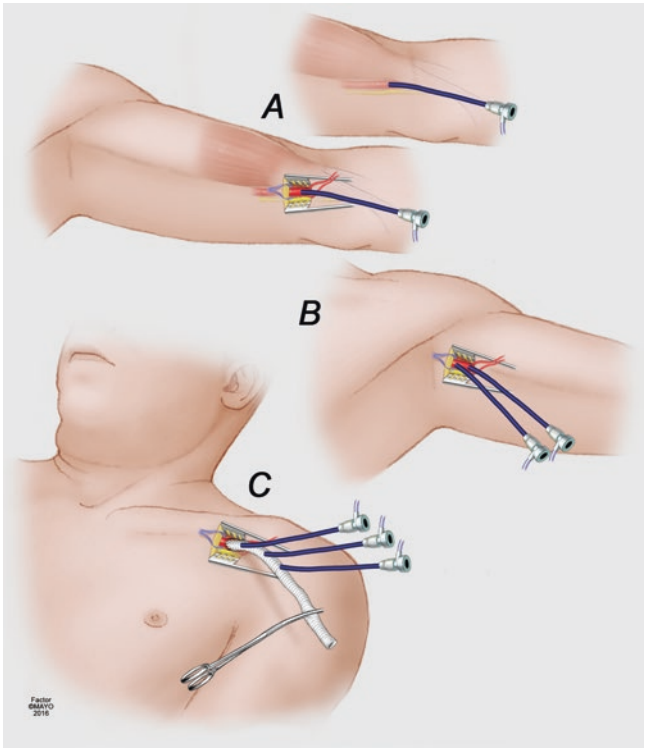


Fig. 30.3 (**a**) Small incision over palpable brachial artery near antecubital crease can be used when only single snorkel/chimney sheath necessary. (**b**) Skin incision via a high brachial incision near the axilla exposes the proximal brachial artery often giving adequate size for double puncture. (**c**) Infraclavicular incision to expose the axillary artery necessary when three or four snorkel/chimney sheaths needed. A 10-mm or 12-mm Dacron conduit can be sewn into the axillary artery in this position. By permission of Mayo Foundation for Medical Education and Research. All rights reserved

The use of a 65-cm omniflush catheter and glide wire to direct the wire towards the descending thoracic aorta then affords a wire exchange for a stiffer platform, either a 260-cm Rosen or Amplatz (Cook Medical, Bloomington, IN). Over this stiffer platform, a 7 sheath (70 cm Ansel 1 [Cook Medical] or 90-cm Pinnacle Destination [Terumo Medical, Somerset, NJ]) is positioned near the visceral target branches ready for cannulation attempts (Fig. 30.4a).

Through the 7 Fr sheaths, the targeted renal and visceral branches are cannulated using 260 cm length hydrophilic guidewires and a 125 cm JB1 catheter or Vert catheter (Cook Medical). An angiographic run can be performed from a flush catheter placed from the femoral approach to visualize the renal or visceral origins to aid in cannulation (Fig. 30.4b). Thorough knowledge of the preoperative anatomy and study on the 3D workstation facilitates this portion of the procedure and allows for optimal angulation of the C-arm.

Once the targets are cannulated, exchange for a j-tip Rosen wire provides a stiffer platform and minimizes potential damage to the distal renal bifurcations. The 7 Fr sheaths are then advanced coaxially into the target artery orifice over the JB1 catheter or after exchanging back for the obturator. When necessary or in cases where there is more angulation to the branch or if the Rosen is not stiff enough, one can exchange for a 260-cm Amplatz Superstiff (1-cm tip) to facilitate sheath advancement into the target renal artery (Fig. 30.4c). Deflectable sheaths can also facilitate this maneuver (Tourguide sheath (Medtronic Vascular, Santa Rosa, CA) or Destino sheath (Oscor Inc., Palm Harbor FL)). Confirmation angiography is then performed through the sheath to assure patency of the renal, correct cannulation of a main renal artery, and no early side branches.

Positioning of Main Body Endograft and Chimney Stent Grafts

Standard femoral access for EVAR is employed in these chimney techniques and described in other chapters. Briefly, a small transverse incision below the inguinal ligament can be used to expose the common femoral artery to the bifurcation for delivery of endograft components. The percutaneous approach involves the "Preclose" technique and employs two Perclose Proglide devices (Abbott Vascular, Santa Clara, CA) oriented at 10:00 and 2:00 [12].

The main body endograft can then be delivered up the chosen femoral side to the para-visceral aorta at the same time the iCAST (Atrium Medical, Hudson, NJ) stents are introduced through the brachial access 7 F sheaths to the target renal arteries (see Fig. 30.4c). The typical length of the iCAST is 59 mm, with the diameter sized appropriately to seal in the target renal artery, most often 5, 6, or 7 mm. The positioning of the chimney stent requires that at least 10 mm of fixation into the renal artery be present, and that the proximal extent of the graft is above the fabric of the main body endograft.

In a lateral projection angiogram, the superior mesenteric artery is visualized (when performing the typical double renal ch-EVAR), and the main body fabric edge placed immediately below the origin of the SMA (Fig. 30.4c, d). At this point, final small adjustments can be made as well as further angiography to assure that the chimney stents are in good position. To avoid the issue of the iCAST stent being unstable on its wire platform, we often leave the 7 Fr sheaths in place to protect them until final deployment.

Sequence of Stent Graft Deployment and Balloon Molding

The main body endograft is deployed at the target location with its fabric edge being immediately below the SMA edge (Fig. 30.4e). Depending on the endograft system used, unsheathing proceeds down to the contralateral gate opening and then release of the suprarenal bare fixation stents. From

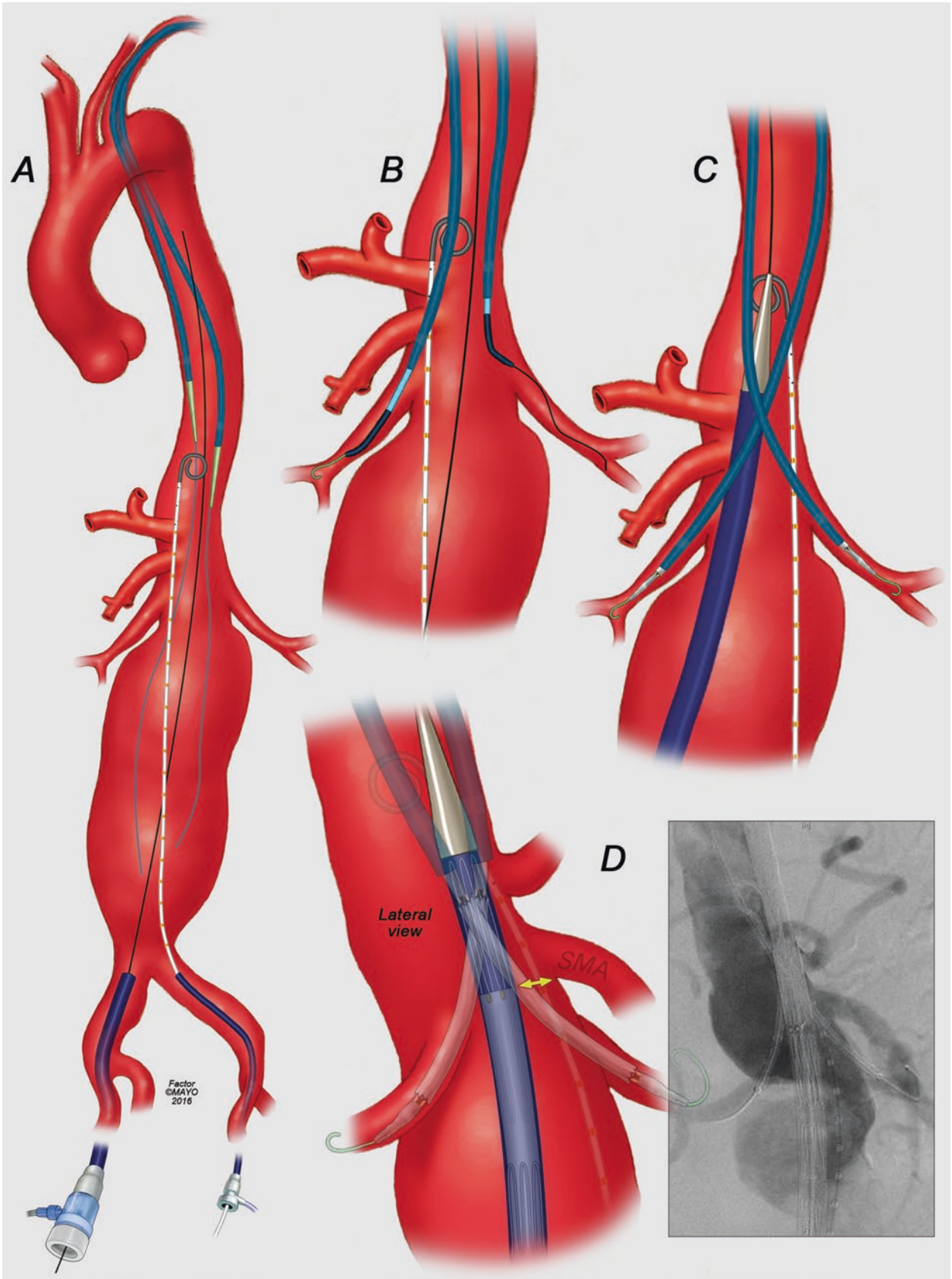


Fig. 30.4 Technique of single- or double-snorkel grafts for treatment of juxta-renal abdominal aortic aneurysms (**a**–**k**). (**a**) Two 7 F Terumo sheaths placed from arm access down descending thoracic aorta ready to be positioned near visceral aortic region. (**b**) Right renal artery cannulated with glide wire and JB1 catheter. Omniflush catheter from below reveals in an angiogram the position of the left renal artery to be cannulated next. (**c**) Both snorkel iCAST stents in position from arm approach along with main body endograft being put into position. (**d**) Lateral view angiogram shows takeoff of SMA (*yellow arrow*) and positioning of the main body endograft fabric edge (*yellow arrow*) immediately below SMA. (**e**) Main body endograft deployed in AP view with snorkel stents in position. (**f**) After cannulation of contralateral gate and advancement

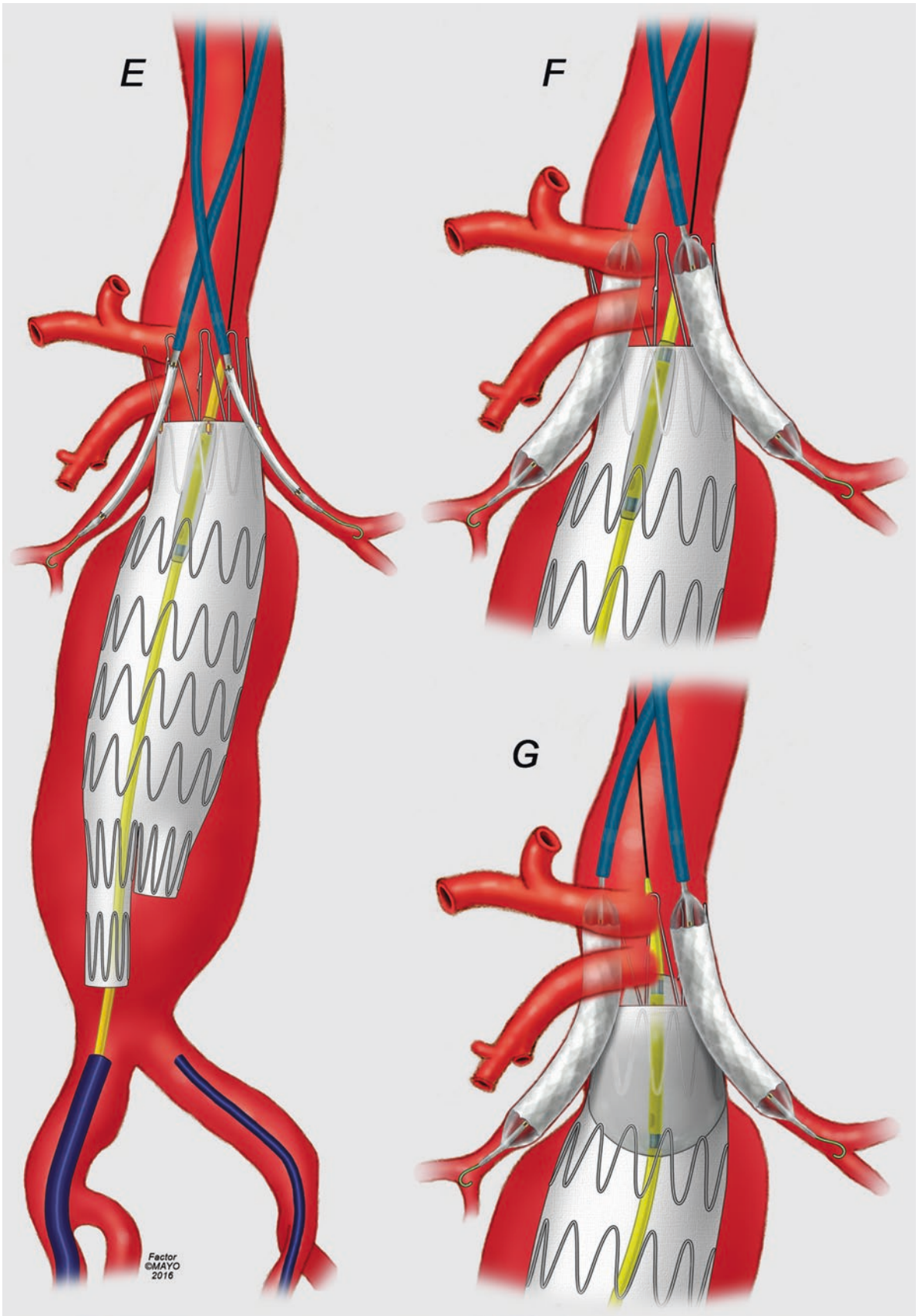


Fig. 30.4 (continued) of proximal molding balloon into aortic stent, the two snorkel stents are fully inflated. (**g**) The molding balloon is then maximally inflated to profile and to minimize gutters. (**h**) The modling balloon is completely deflated prior to snorkel stent balloon deflation. (**i**) Final aspect of the repair with two snorkel stents and aortic stent completely deployed. (**j**) Postoperative CT-A axial view showing molding of main body endograft around two widely patent snorkel stents. (**k**) 3D reconstruction demonstrating excellent perfusion of both kidneys and no evidence of endoleak. By permission of Mayo Foundation for Medical Education and Research. All rights reserved

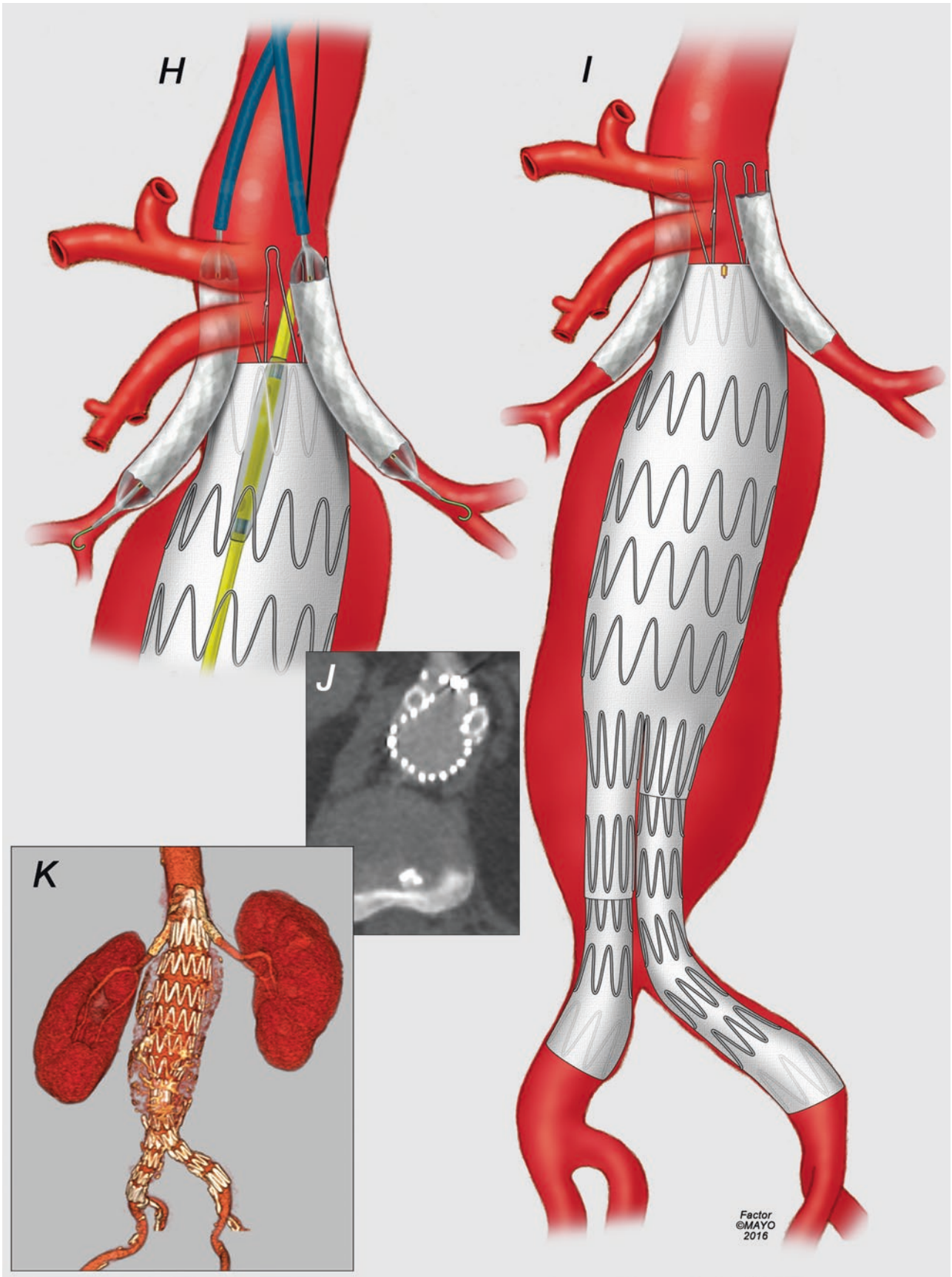


Fig. 30.4 (continued)

the contralateral femoral access, cannulation of the gate is confirmed, and a compliant molding balloon (32- or 40-mm Coda balloon [Cook Medical]), is placed up to the level of the renal vessels.

The 7 Fr sheaths are slowly withdrawn from the brachial approach so the tip is just proximal to the edge of the renal chimney stents, and deployment of the iCAST occurs, most often simultaneously and to a nominal pressure of eight atmospheres (Fig. 30.4f). At the same time that the iCAST stents are being deployed by balloon inflation, slower inflation of the CODA occurs to slowly mold the main body fabric around the chimney stents to minimize gutter formation. Only when the renal chimney stents are maximally inflated can the CODA balloon go up to full main body endograft diameter (Fig. 30.4g). This step cannot be overemphasized, as deflation of the chimney stents while the CODA is inflated is likely to crush the balloon-expandable covered stents. There are techniques described in other chapters, however, to create more of an oval shaped parallel stent that does require crushing the iCAST.

With the renal snorkel stents still maximally inflated, the CODA balloon can finally be let down after a few seconds of balloon molding to complete the sequence (Fig. 30.4h). After the proximal molding balloon is completely deflated, the renal chimney balloons are deflated to allow perfusion of the kidneys (Fig. 30.4i).

Completion of Distal Components

Prior to losing wire access to the renal vessels, a proximal aortogram is performed to look for a large type I endoleak or poor perfusion of either targeted kidney. If this is satisfactory, the distal components of the endograft can be advanced and deployed in the usual fashion. Repair of the access sites, particularly the brachial site, requires careful interrupted 6-0 or 7-0 prolene sutures, and adequate hand and foot perfusion is verified prior to completion of the case.

Postoperative CTA demonstrates the typical appearance of the snorkel stents adjacent to the main body endograft with minimal gutters (Fig. 30.4j), and the 3D reconstruction shows excellent alignment and configuration of the snorkel EVAR components (Fig. 30.4k).

Periscope EVAR/TEVAR

Femoral Access for Introduction of Main Body Endograft

Periscope EVAR/TEVAR builds on the concept above of parallel endografts but places the visceral stents from a femoral approach, requiring blood flow to go through the main body stent graft, then turn around and return cranially to the visceral or renal vessel [13].

The femoral access for periscope cases in contradistinction to snorkel/chimney strategies often involves the use of larger caliber thoracic or fenestrated main body components (often 22–26 F) leading to a slightly higher utilization of open or endovascular iliac conduits. A useful modification to an iliac conduit that can be helpful in delivering and torqueing large caliber main body components or sheaths during periscope EVAR/TEVAR involves creating a patch at the distal end of the dacron conduit. This patch region is created by cutting a 10- or 12-mm dacron graft along its long access, creating an oval sewing patch that enlarges the transition from graft to vessel, and not limiting the flexibility of the branch to the initial angle it is sewn into.

Contralateral Access and Cannulation of Target Visceral Branch(es)

After the femoral access side has been chosen and prepared for main body endograft delivery, the contralateral femoral site is used to cannulate the planned visceral or renal branches from the bottom. In the periscope configuration, the parallel stent graft is often required to make a U-turn, so a more flexible covered stent, the self-expanding Viabahn (Gore Medical, Flagstaff, AZ) is preferred. This often requires larger sheath access (up to 12 F) than the iCAST described above, so for a double periscope configuration a larger 20 or 22 F (white arrow) sheath is usually necessary to place multiple longer sheaths into (Fig. 30.5a). We caution against the use of 0.018″ Viabahn stents, as the delivery system becomes too flimsy on a 0.018″ wire to safely deploy the periscope stents in the u-turn fashion.

The typical periscope EVAR/TEVAR case as depicted in our case involves the need for a longer distal landing zone of a distal TAA (see Fig. 30.5a). In this particular case, the celiac and one renal artery are already occluded, so the periscope technique is utilized to revascularize the SMA and remaining renal artery and obtain improved distal seal in the infrarenal aorta, with an 11-mm Viabahn in the SMA requiring a 12 F sheath, and an 8-mm Viabahn as the renal periscope requiring an 8 F sheath (Fig. 30.5b).

Sheath Advancement and Periscope Stent Graft Positioning

Similar to the single/double chimney EVAR procedure above, the general principles of advancing the sheath into the target visceral vessel are repeated, but in periscope EVAR/TEVAR, all is performed from the femoral approach. The

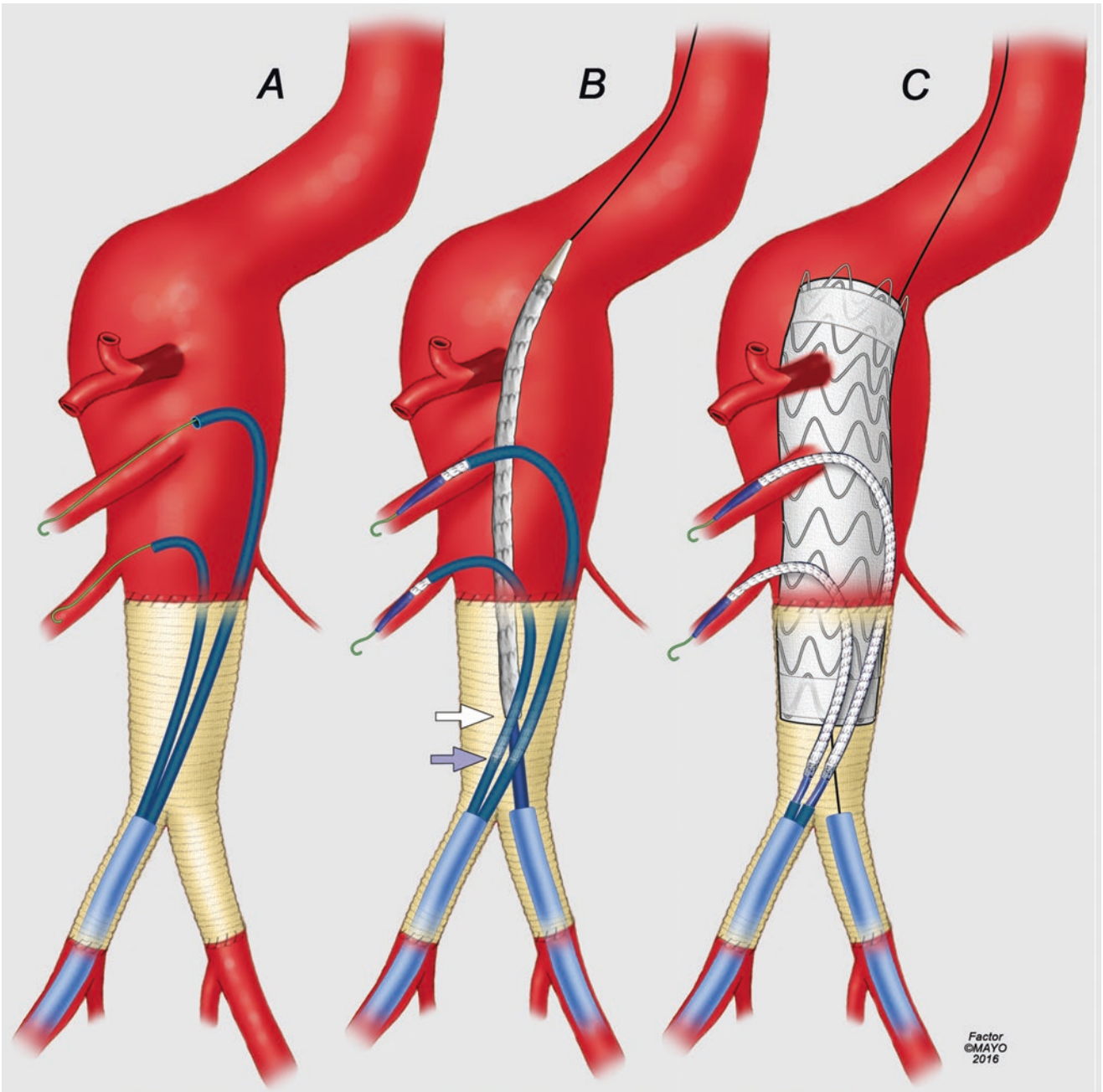


Fig. 30.5 Technique of periscope grafts for treatment of complex abdominal and thoracoabdominal aortic aneurysms. Thoracoabdominal aneurysm formed above prior open repair with occluded left renal and celiac (**a**). Periscope configuration to keep superior mesenteric artery and right renal perfused (**b**). 22 F sheath houses 12 F periscope sheath into SMA as well as 8 F sheath positioned to try to cannulate renal artery. (**b**) Bottom of both periscope stents (SMA and right renal) are at *blue arrow position*, and therefore lower than bottom of planned distal component of main body endograft (*white arrow*). (**c**) The aortic stent graft is deployed first. (**d**) After withdrawal of sheaths, periscope stents (Viabahn) deployed. (**e**) Balloon molding of main body endograft with compliant aortic balloon against balloon expandable bare stents placed within periscope stents at level of contact and distal seal. (**f**) Final appearance of the periscope grafts which extend 1-cm distal to the edge of the aortic stent. (**g**) Proximal angiography shows region of proximal aneurysm to treat and the proximal main body endograft is delivered. (**h**) The stent graft is deployed and overlap is molded with compliant aortic balloon. (**i**) Final configuration of the periscope graft. By permission of Mayo Foundation for Medical Education and Research. All rights reserved

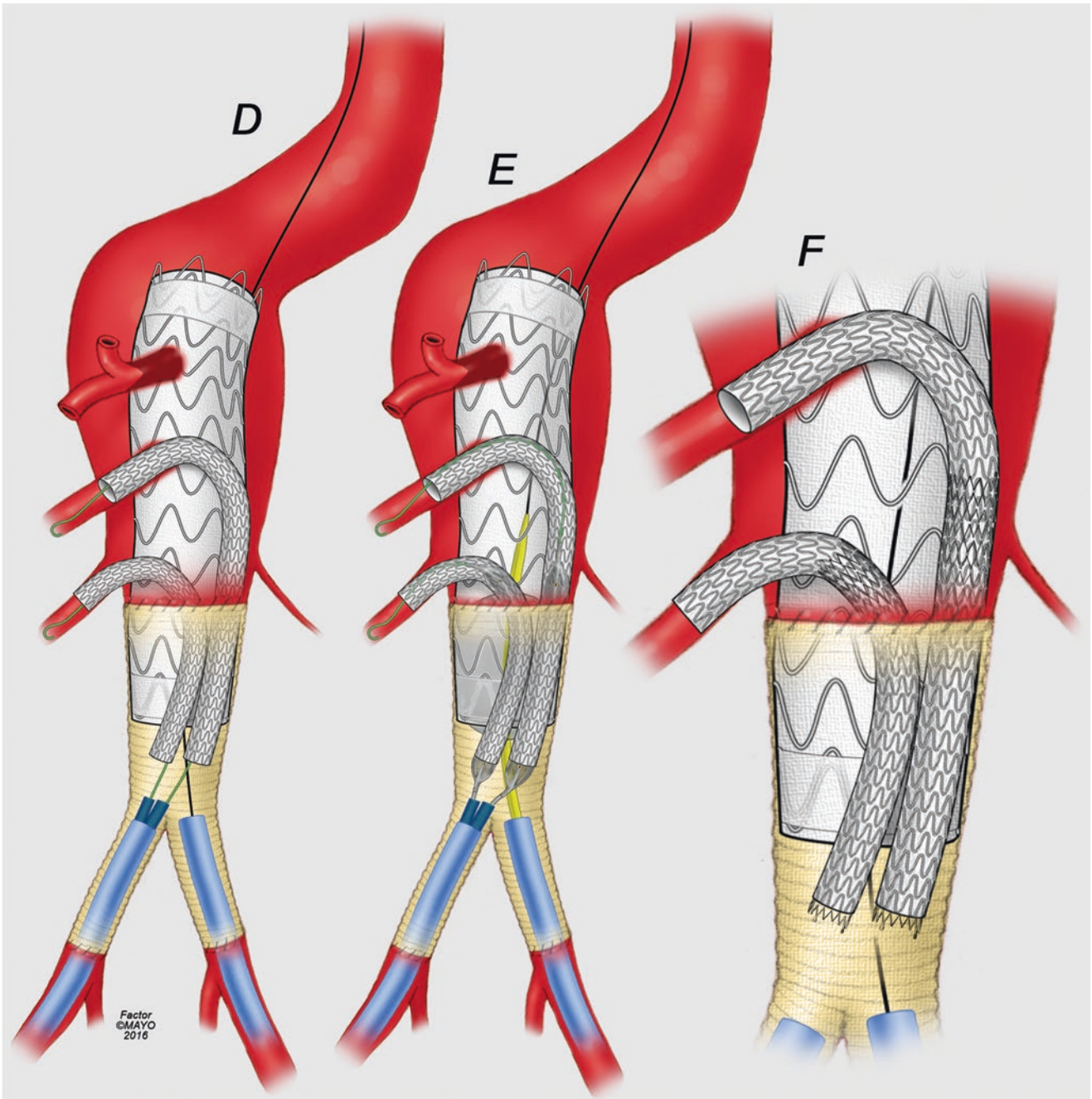


Fig. 30.5 (continued)

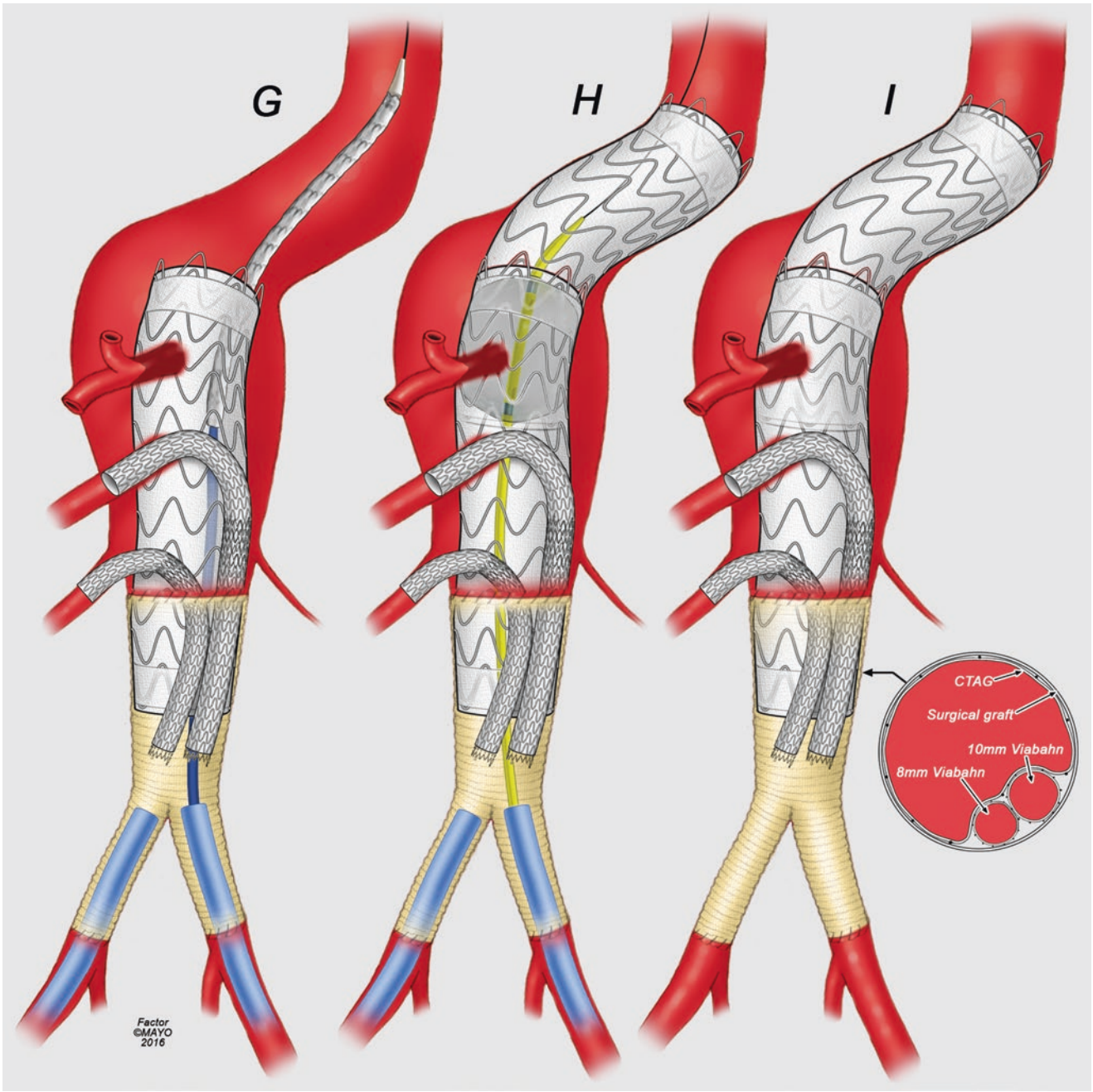


Fig. 30.5 (continued)

SMA and renal periscopes are positioned several centimeters into the target vessel origin, with the distal end (blue arrow) below the bottom end of the main body stent graft (white arrow) (Fig. 30.5b).

Sequence of Deployment and Balloon Molding

The main body endograft is deployed with the periscope sheaths still in position (see Fig. 30.5c). A key component to delivering Viabahn as chimneys or periscopes involves withdrawing the sheath slowly a few centimeters at a time, then deploying some of the Viabahn, then slowly withdrawing more sheath, and repeating these maneuvers (Fig. 30.5d). This important step protects the Viabahn from bowing out and pulling out of the target visceral branch artery and requires coordinated effort of experienced surgeons. Because there is often some compression of the self-expanding periscope stents, an additional balloon expandable bare stent can be placed along where there is contact with the main body endograft, and a similar sequence as above of balloon molding is performed to minimize gutter formation (Fig. 30.5e, f).

The remainder of the proximal aspect of the thoracic aneurysm is visualized and appropriately stent grafted with proximal extensions and ballooned (Fig. 30.5g,h), and postoperative CTA confirms aneurysm exclusion with wide patency of the periscope stent grafts and normal target vessel perfusion (Fig. 30.5i).

Octopus Off-the-Shelf Branch Repair

The so-called "octopus" repair has several iterations as an off-the-shelf solution using commercially approved devices that combines concepts of parallel graft and branched graft techniques. Very few case series or even case reports are currently published, and lack of standardization makes interpretation and recommendations challenging. Our description below has already undergone several modifications and serves as our template while we await clinical trial devices of purpose-specific endovascular solutions for TAAAs.

Chimney Stage

In a TAAA when four branches need revascularization (Fig. 30.6a), our current strategy utilizes a single chimney to the celiac (Fig. 30.6b). As described in the section above, an axillary conduit is created to allow for multiple sheath access from above. An 8 Fr Ansel 1 sheath is useful for delivering either a 7- or 8-mm by 15- or 25-cm Viabahn and be assured it reaches near the proximal edge of the main body endograft (either an abdominal EVAR device, or a cuff/TEVAR component). After catheterization of the celiac is performed using techniques described above (see Fig. 30.6b), the sheath is inserted into the celiac. The main body endograft is positioned based on where the distal limbs need to point to and then deployed. Withdrawing the long chimney sheath centimeters at a time, the long Viabahn chimney is deployed in stepwise fashion, and while maintaining wire access, we will extend the celiac chimney proximally with an iCAST so that it can be crushed later with a molding balloon should a proximal gutter leak persist. Molding of the celiac snorkel and the proximal main body stent graft can be performed at this point to assure a reasonable proximal seal.

SMA Revascularization

The SMA is the key visceral branch vessel in the octopus strategy because if acute occlusion occurs postoperatively it often leads to severe morbidity or death. For this reason, the main body bifurcated graft is positioned in the mid-descending thoracic aorta so that the ipsilateral limb is 1–3 cm above the origin of the SMA and becomes the source branch (Fig. 30.6c). After the main body endograft is deployed fully and the celiac chimney stage completed as described above, an extension cuff (10 mm × 7 cm) is placed within the ipsilateral limb to convert the end to 10 mm. This allows a seal if a 10-mm Viabahn is used to extend into the SMA. If a smaller Viabahn is required to seal the SMA, then an additional iCAST is used to seal the smaller Viabahn into the 10 mm extension cuff (see Fig. 30.6c). To facilitate the delivery sheath that will come down from the axillary conduit through the ipsilateral limb and out to the SMA, a 12 × 20 tri-lobe snare can be used to pull the wire from above into the SMA limb. With the through and through wire facilitating the SMA sheath (often 8 F to 10 F) to be inserted and positioned just outside the SMA limb, a 125-cm Vert catheter and glide wire is often most useful to cannulate the SMA. The most common length of Viabahn utilized is 10 cm, and is deployed in step-wise fashion as described in prior sections (Fig. 30.6c, d). Note that after the SMA sheath is through the ipsilateral limb and while attempting to cannulate the SMA, the femoral wire access is given up.

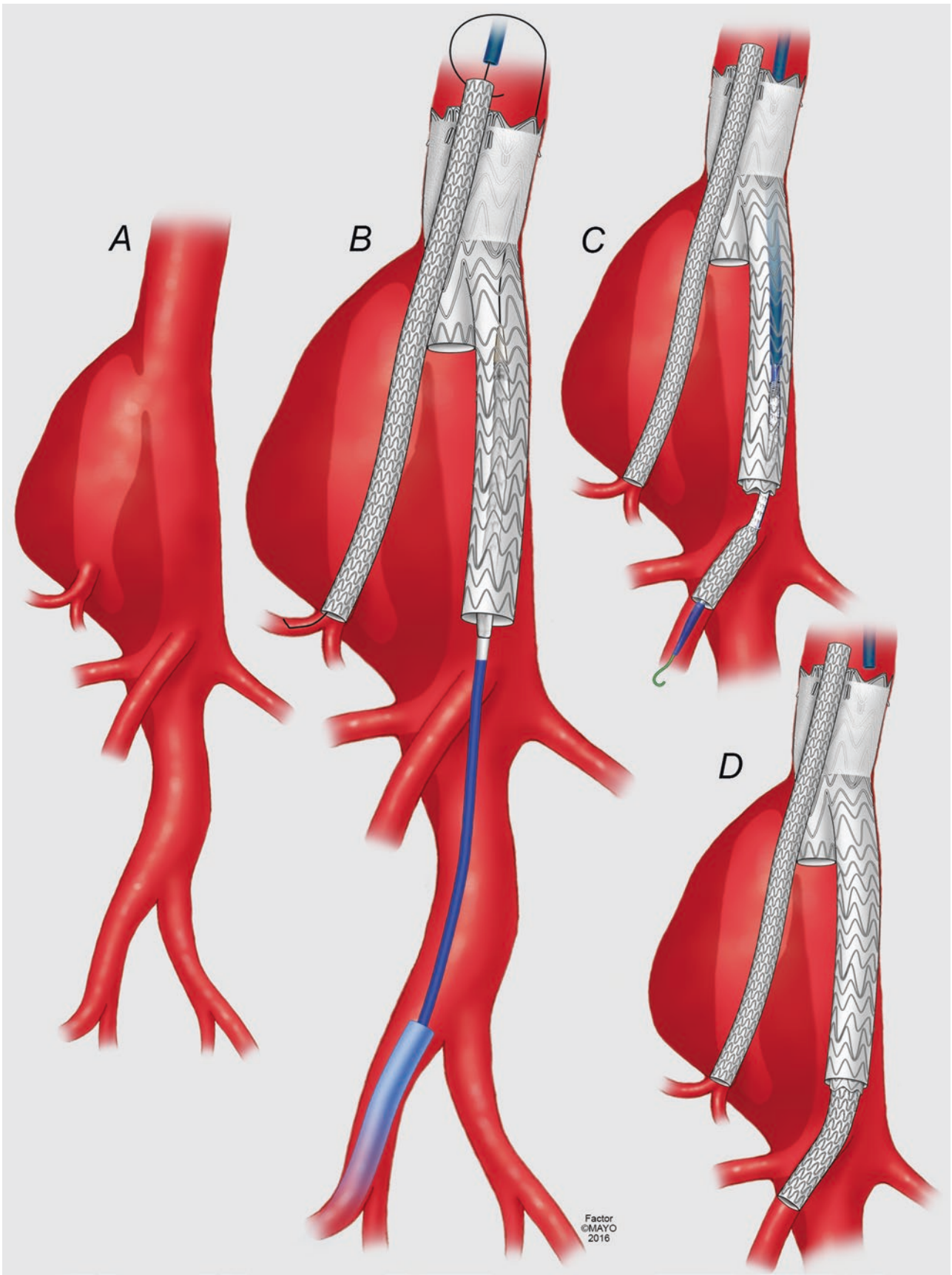


Fig. 30.6 (**a**) Thoracoabdominal aneurysm with chronic dissection. (**b**) Chimney graft to the celiac axis with placement of bifurcated stent graft in the thoracic aorta. (**c**) extension of the ipsilateral iliac limb. (**d**) Deployment of the SMA stent graft. (**e**) Distal extension of the contralateral iliac limb. (**f**) Positioning of bilateral renal sheaths and iliac limb extension. (**g**) Placement of bell bottom stent into the infrarenal aorta. (**h**) Deployment of bilateral renal stents. By permission of Mayo Foundation for Medical Education and Research. All rights reserved

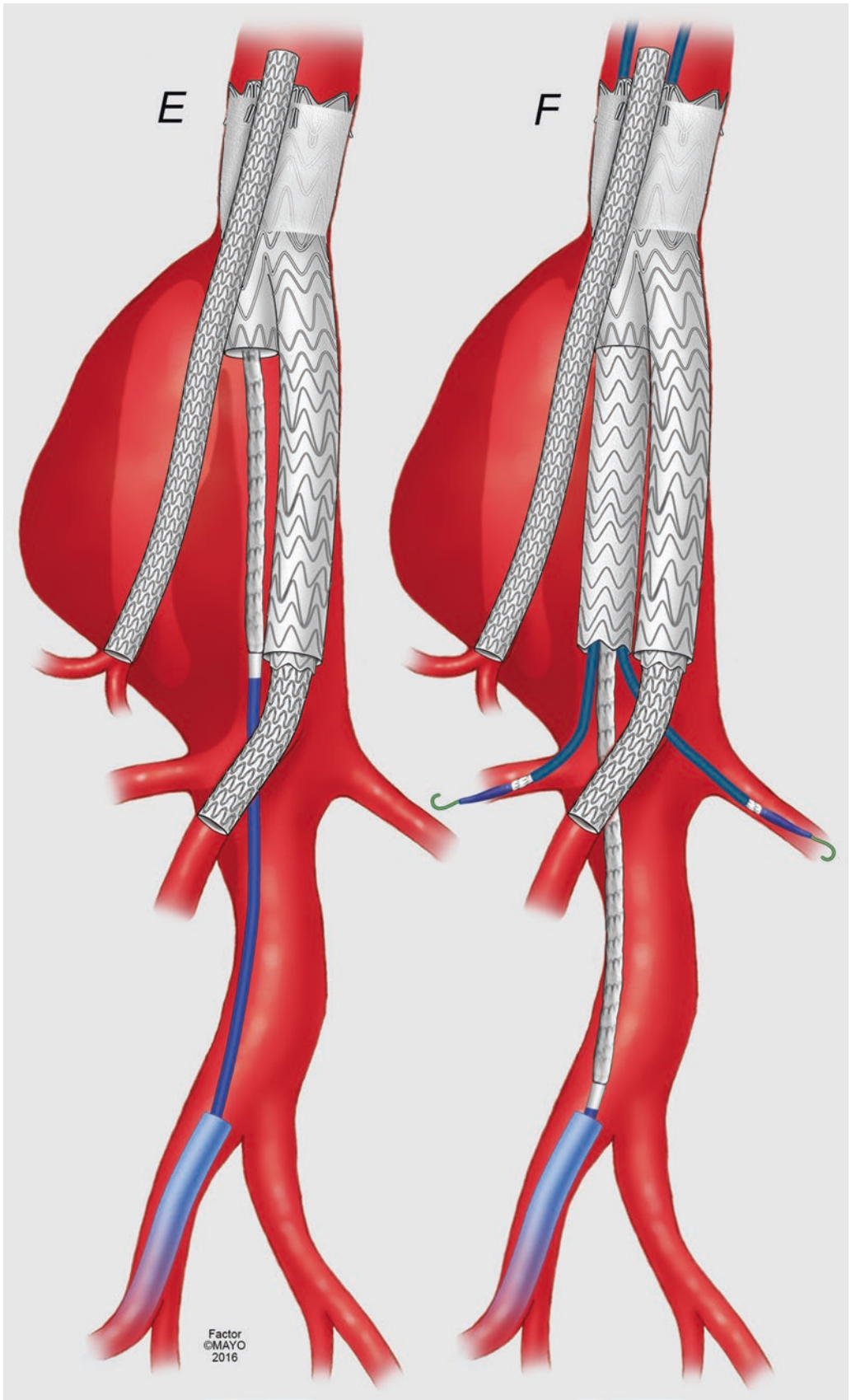


Fig. 30.6 (continued)

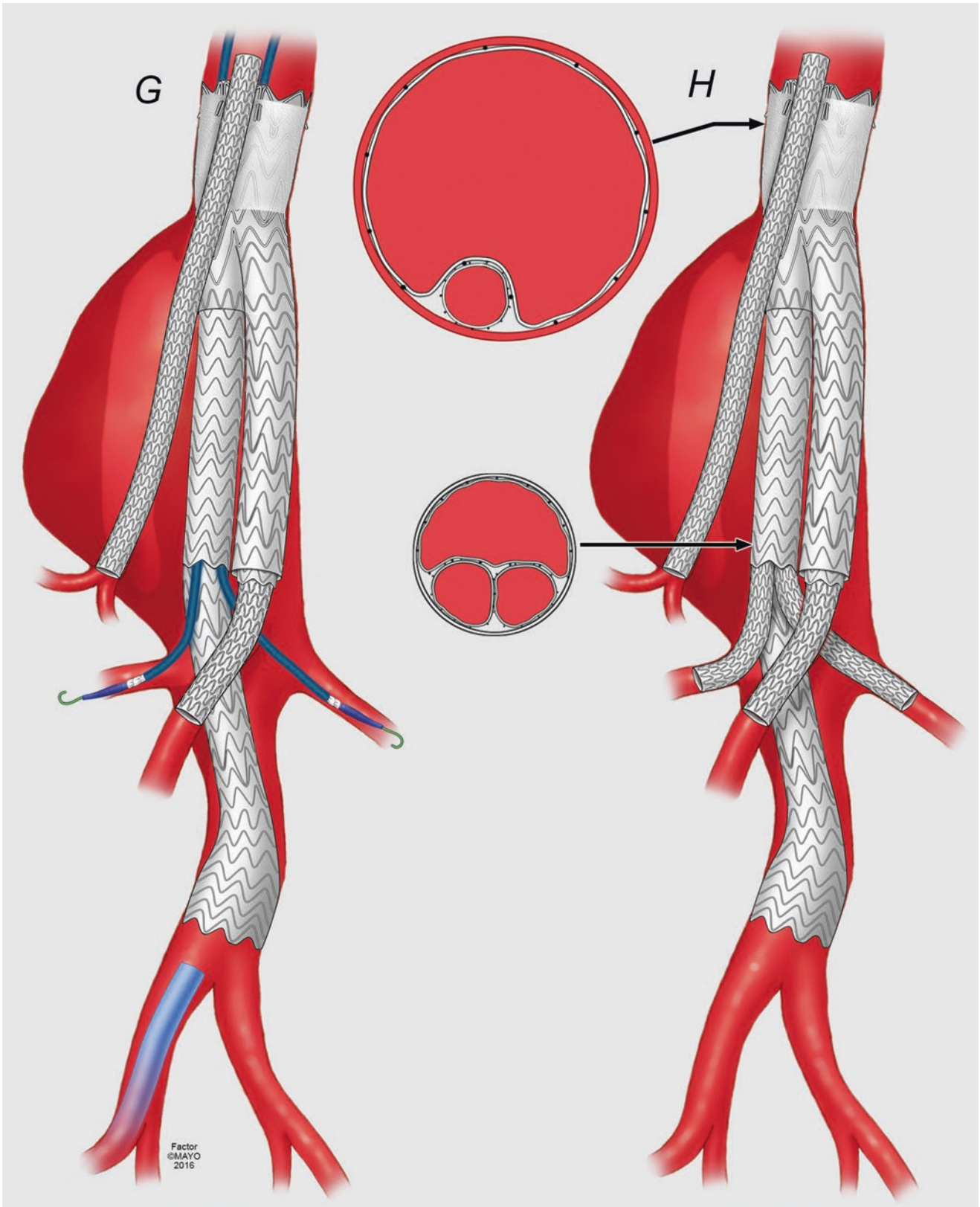


Fig. 30.6 (continued)

Contralateral Gate Positioning and Renal Cannulation

From the femoral sheath (most likely 18–24 F) we now cannulate the contralateral gate of the bifurcated main body in the mid-descending thoracic aorta and place short extension cuff (14.5 mm by 10 cm) so that it sits at about the level of the ipsilateral limb (Fig. 30.6e). A 12 F 80-cm sheath is placed into the limb and three separate wires are run up through the contralateral gate extension cuff so that two of them can be snared from sheaths from the axillary conduit. This allows two 7 Fr sheaths to then be advanced from the axillary conduit through the contralateral extension to be positioned for renal cannulation (Fig. 30.6f).

Again using JB1 or Vert catheters through each axillary sheath both renal arteries are wired and the 7 F sheaths advanced into the renal artery origins (Fig. 30.6g). 6 or 7 mm by 15 cm Viabahn stents are most often needed in this stage and positioned so they are at the same proximal level within the contralateral limb extension. On the third wire from the femoral access that has not been snared, one now advances a 20 mm × 10 or 12 cm bell-bottom limb to create an "elephant trunk" into the infrarenal aorta. Essentially in this 14.5-mm contralateral gate extension sits two renal chimney stents (6 or 7 mm) and a 16-mm elephant trunk extension to create a triple parallel graft configuration to provide flow to both renal arteries and the infrarenal aorta (Fig. 30.6h). The elephant trunk extension is deployed first, then the renal Viabahn stents deployed to minimize gutter formation. A completion angio through this triple chimney limb confirms patency and if there is a large gutter leak triple balloon molding can be performed. If satisfactory, at this point the axillary conduit sheaths and renal wires can be withdrawn.

Infrarenal Completion

The elephant trunk bell-bottom piece can be sized distally up to 27 mm to obtain adequate seal if there is no infrarenal component to the TAAA. If extension to both iliac bifurcations is necessary to adequately exclude the aneurysm, then a 20-mm bell-bottom is chosen so that an additional 23-mm main body bifurcated graft can be placed and appropriate iliac limbs inserted. When there is concern about potential spinal cord ischemia, we will stage this portion of the procedure to this final bifurcated device and leaving the contra limb to be cannulated and completed from a contralateral puncture at a future date. Note that in this example described above that only one femoral access site was necessary for the entire case.

"Sandwich" Grafts

The "sandwich" graft technique was pioneered by Armando Lobato from Sao Paulo for treatment of thoracoabdominal aortic aneurysms using the same principles described above (Fig. 30.7). In this technique, the parallel stent graft is deployed between two aortic stent graft components, ideally with >5-cm overlap to minimize risk of gutter endoleaks. In the example herein illustrated preoperative CTA demonstrates (Fig. 30.7a) a patient with ruptured TAAA following TEVAR for type B aortic dissection (Fig. 30.7b), likely due to tear of the dissection membrane with pressurization of the false lumen (see Fig. 30.7c) complicated by contained rupture (Fig. 30.7c–e). Using the principles of parallel grafts described above, the patient was treated with a "sandwich" graft for the SMA and two periscope grafts for the renal arteries (Fig. 30.7f, g). Repeat CTA a few months after the procedure revealed complete remodeling of the ruptured type B aortic dissection and aneurysm (Fig. 30.7h).

The "sandwich" technique has also been used as a "bail out" to treat difficult complications of fenestrated and branched endografts. In the example illustrated in Fig. 30.8 a patient treated by 4-vessel fenestrated endograft developed an endoleak likely due to a fabric tear in the location of the diameter-reducing ties, posterior to the celiac and SMA branches (Fig. 30.8a). The patient was treated by extension of the stent graft to the level of the celiac branch (Fig. 30.8b), followed by double "sandwich" parallel grafts to the celiac and SMA (Fig. 30.8c) using an aortic stent graft to cover the segment affected by the tear (Fig. 30.8d). Note in this example there is perfect fabric apposition in the posterior aspect of the stent graft.

Postoperative Care and Outcomes

At the conclusion of the procedure, patients are usually extubated, observed for 2–3 days in a monitored setting (in the intensive care unit overnight if lumbar drain present), and discharged home when ambulating, tolerating a normal diet, and with stable renal function. Additional spinal cord protection maneuvers include holding blood pressure lowering agents or even using pressors to keep the mean arterial pressure adequate. Clopidogrel and aspirin are given if the patients are not already taking these medications for at least 6 weeks postoperatively.

Multiple reviews of the worldwide experience with snorkel/chimney and periscope techniques continue to find it to be technically successful with target revascularization rates in the 95–100 %, mortality in the 2–5 % range, morbidity up to 10 %, and mid-term renal and branch patency rates of

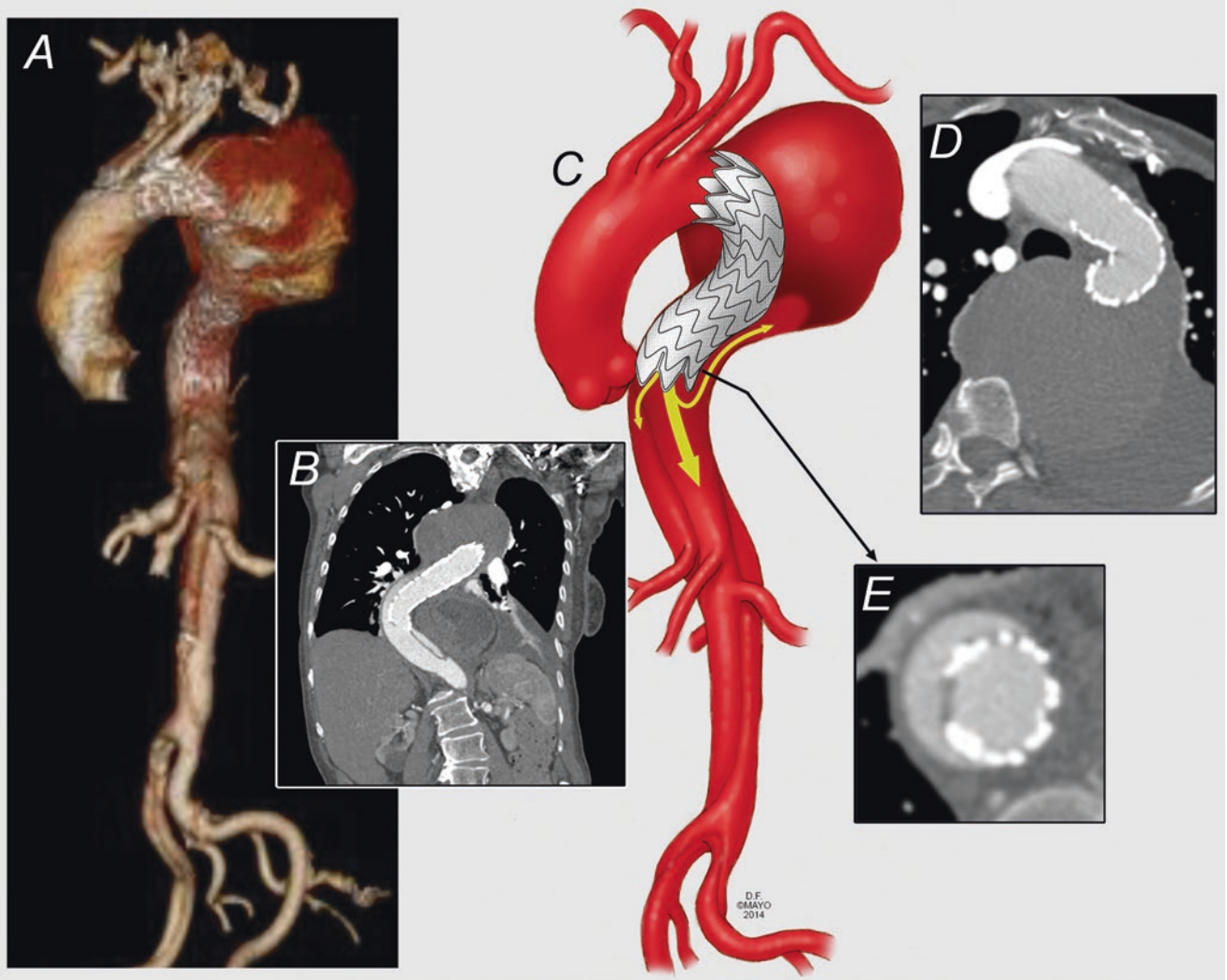


Fig. 30.7 Illustration of patient with complicated dissection following TEVAR (**a**–**e**). (**f**–**h**) Illustration of patient with complicated dissection following TEVAR treated by sandwich stent graft and periscope. By permission of Mayo Foundation for Medical Education and Research. All rights reserved

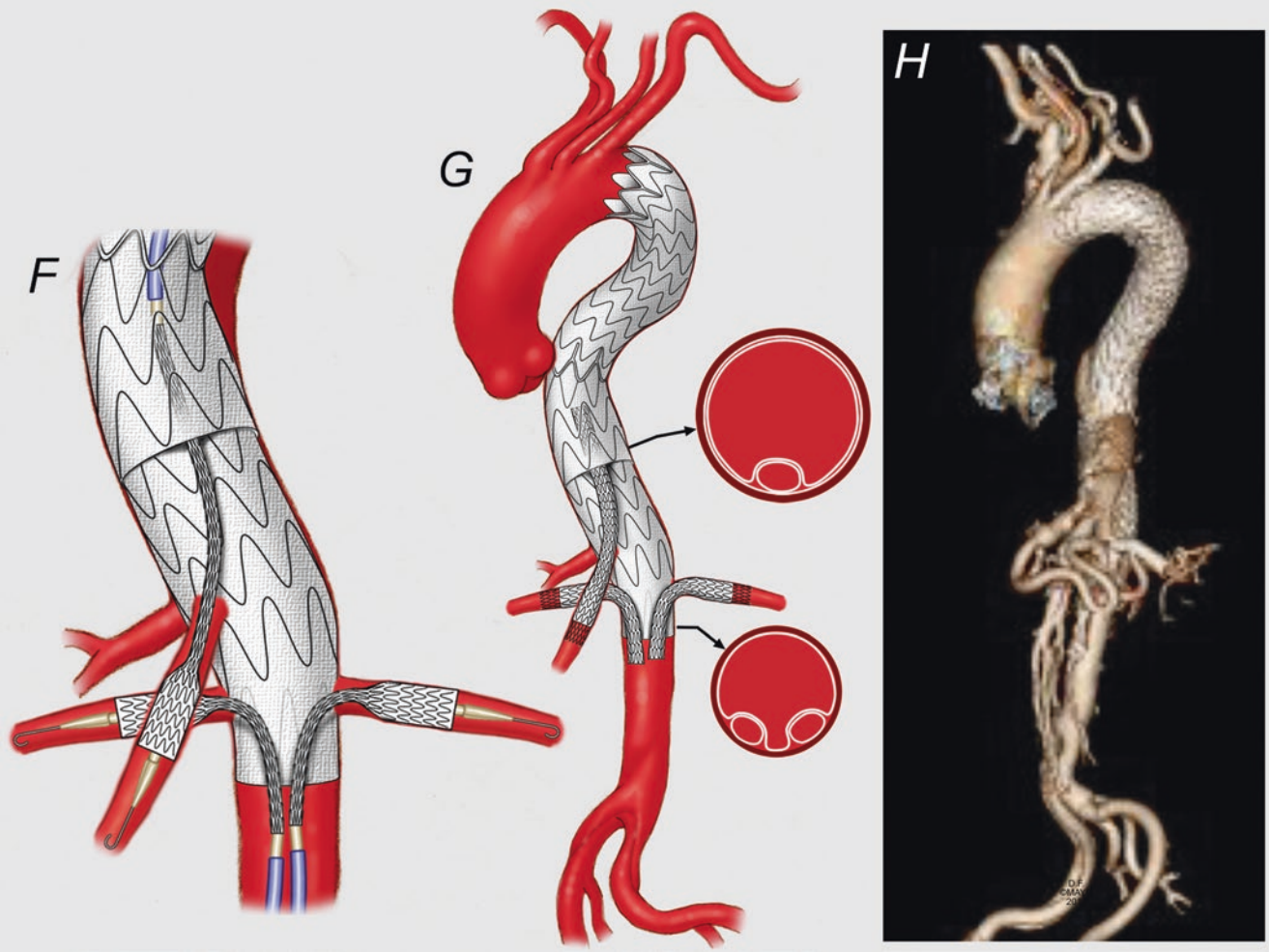


Fig. 30.7 (continued)

92–96 % [10, 14, 15]. Rupture-free survival after snorkel/chimney or periscope EVAR is excellent in the small amount of literature published on this new approach, but will be important to observe in the mid- and long-term to assure that this technique is durable as a strategy for endovascular repair of complex aneurysms.

Complications

Perioperative complications related to complex EVAR in general include cardiac ischemia, arrhythmias or exacerbation of heart failure, groin wound seroma and infection, early thrombosis of endograft components, and bleeding issues related to access site. Reported rates of these issues are not particularly different than the wealth of literature for routine EVAR.

Particular to parallel graft techniques involve the use of the arm access, which has the potential of leading to arm ischemia, nerve injury/irritation of the brachial plexus, and axillary seromas. Wire and catheter manipulation and poor wire hygiene can lead to inadvertent renal parenchymal injury which can lead to hematomas and excessive bleeding requiring transfusion. The rate of renal function decline is certainly more than in standard EVAR, although we do not believe it to be significantly worse than open suprarenal surgery, fenestrated, or branched devices [16, 17].

Right arm access for multiple snorkel/chimney stents has been reported to lead to higher rates of cerebrovascular complications [1, 8]. This is likely due to moderate amounts of time that sheaths are across the aortic arch and the possibility of thrombus formation that can lead to cerebral emboli. Like many complications, this risk is optimally minimized by proper patient selection.

Finally, gutter leaks are a unique consequence of the parallel stent graft strategy, and are poorly understood. Some general guidelines involve placing as long of stents as possible in parallel configuration to force gutter leaks to thrombose, and careful long-term imaging follow-up to assure that the aneurysm is excluded. More accurate reporting

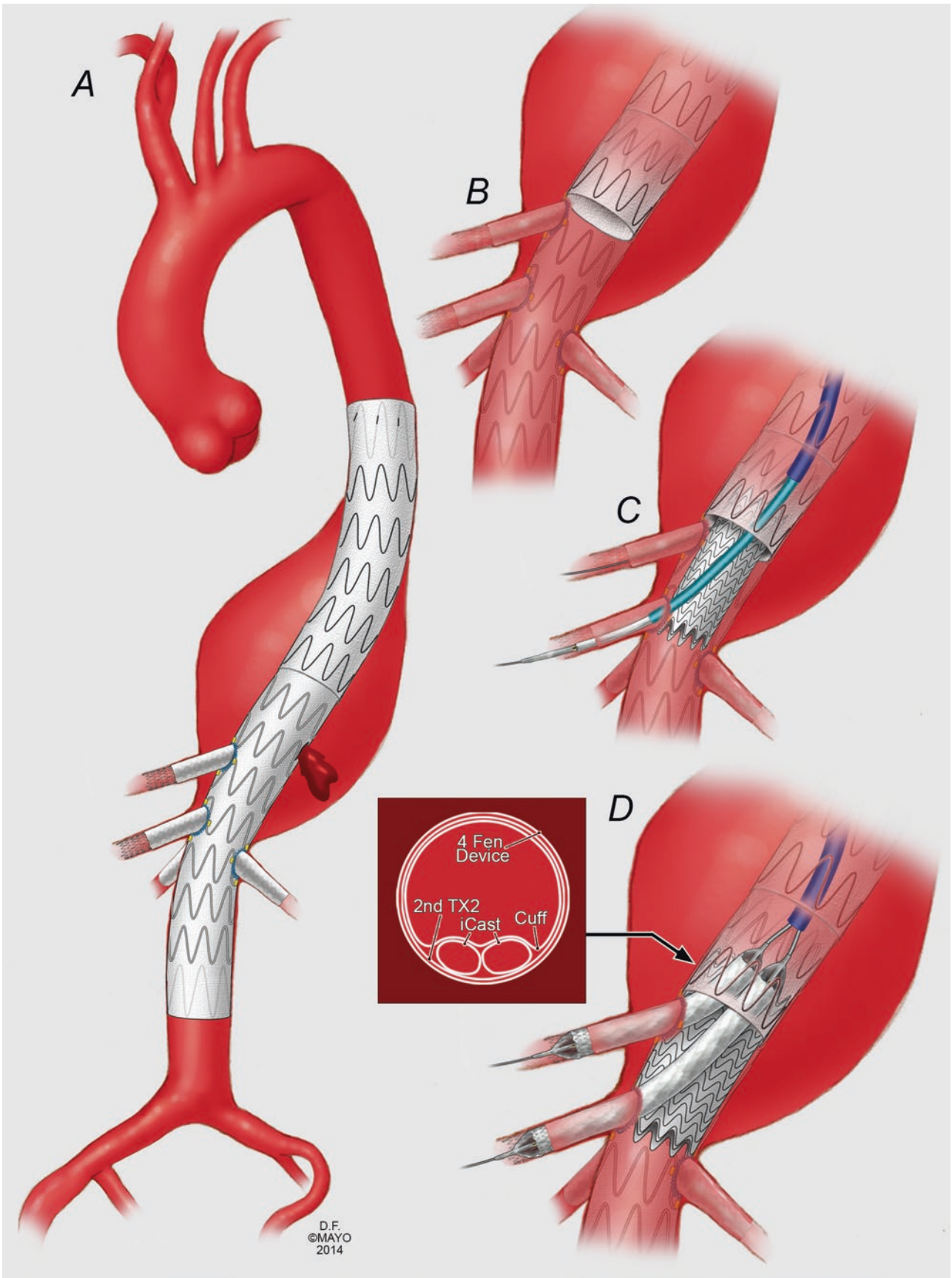


Fig. 30.8 A patient treated by a four-vessel fenestrated stent graft developed an endoleak likely due to a fabric tear in the location of the diameter-reducing ties, at the level of the celiac and SMA branches (**a**). The patient was treated by extension of the stent graft to the level of the celiac branch (**b**), followed by double "sandwich" parallel grafts to the celiac and SMA (**c**) using an aortic stent graft to cover the segment affected by the tear (**d**). Note in this example there is perfect fabric apposition in the posterior aspect of the stent graft (*inset*). By permission of Mayo Foundation for Medical Education and Research. All rights reserved

and longer-term data coming out of registries will likely provide better information as to best practices strategies to optimize outcomes.

References

1. Lee JT, Greenberg JI, Dalman RL. Early experience with the snorkel technique for juxtarenal aneurysms. J Vasc Surg. 2012;55:935–46.
2. Knott AW, Kalra M, Duncan AA, Reed NR, Bower TC, Hoskin L, et al. Open repair of juxtarenal aortic aneurysms (JAA) remains a safe option in the era of fenestrated endografts. J Vasc Surg. 2008;47:695–701.
3. Greenberg RK, Sternbergh III WC, Makaroun M, Ohki T, Chuter T, Bharadwaj P, et al. Intermediate results of a United States multicenter trial of fenestrated endograft repair for juxtarenal abdominal aortic aneurysms. J Vasc Surg. 2009;50:730–7.
4. Greenberg RK, Clair D, Srivastava S, Bhandari G, Ture A, Hampton J, et al. Should patients with challenging anatomy be offered endovascular aneurysm repair? J Vasc Surg. 2003;38:990–6.
5. Ohrlander T, Sonesson B, Ivancev K, Resch T, Dias N, Malina M. The chimney graft: a technique for preserving or rescuing aortic branch vessels in stent graft sealing zones. J Endovasc Ther. 2008;15:427–32.
6. Donas KP, Torsello G, Austermann M, Schwindt A, Troisi N, Pitoulias GA. Use of abdominal chimney grafts is feasible and safe: short-term results. J Endovasc Ther. 2010;17:589–93.
7. Bruen KJ, Feezor RJ, Daniels MJ, Beck AW, Lee WA. Endovascular chimney technique versus open repair of juxtarenal and suprarenal aneurysms. J Vasc Surg. 2011;53:895–905.
8. Coscas R, Kobeiter H, Desgranges P, Becquemin JP. Technical aspects, current indications, and results of chimney graft for juxtarenal aortic aneurysms. J Vasc Surg. 2011;53:1520–7.
9. Hertault A, Haulon S, Lee JT. Debate: whether branched/fenestrated EVAR procedures are better than snorkels, chimneys, or periscopes in the treatment of most thoracoabdominal and juxtarenal aneurysms. J Vasc Surg. 2015;62:1357–65.
10. Donas KP, Lee JT, Lachat M, Torsello G, Veith FJ. Collected world experience about the performance of the snorkel/chimney endovascular technique in the treatment of complex aortic pathologies: the PERICLES registry. Ann Surg. 2015;262:546–53.
11. Moulakakis KG, Mylonas SN, Avgerinos E, Papaetrou A, Kakisis JD, Brountzos EN, et al. The chimney graft technique for preserving visceral vessels during endovascular treatment of aortic pathologies. J Vasc Surg. 2012;55:1497–503.
12. Al-Khatib WK, Dua MM, Zayed MA, Harris EJ, Dalman RL, Lee JT. Percutaneous EVAR in females leads to fewer wound complications. Ann Vasc Surg. 2012;26:476–82.
13. Rancic Z, Pfammatter T, Lachat M, Hechelhammer L, Frauenfelder T, Veith FJ, et al. Periscope graft to extend distal landing zone in ruptured thoracoabdominal aneurysms with short distal necks. J Vasc Surg. 2010;51:1293–6.
14. Katsargyris A, Oikonomou K, Klonaris C, Töpel I, Verhoeven EL. Comparison of outcomes with open, fenestrated, and chimney graft repair of juxtarenal aneurysms: are we ready for a paradigm shift? J Endovasc Ther. 2013;20:159–69.
15. Donas KP, Pecoraro F, Bisdas T, Lachat M, Torsello G, Rancic Z, et al. CT angiography at 24 months demonstrates durability of EVAR with the use of chimney grafts for pararenal aortic pathologies. J Endovasc Ther. 2013;20:1–6.
16. Lee JT, Varu V, Tran K, Dalman RL. Renal function changes following snorkel/chimney repair of juxtarenal aneurysms. J Vasc Surg. 2014;60:563–70.
17. Tran K, Fajardo A, Ullery BW, Goltz, C, Lee JT. Renal function changes following fenestrated endovascular aneurysm repair. J Vasc Surg. 2016; epub ahead of print May 27, 2016.

Hybrid Repair Using Visceral Debranching and Aortic Stent Grafts to Treat Complex Aortic Aneurysms

31

Gustavo S. Oderich, Guillermo A. Escobar, Peter Gloviczki, Thomas C. Bower, and Bernardo C. Mendes

Introduction

Hybrid repair has been introduced in 1999 as an alternative to extend the indications of endovascular aortic aneurysm repair (EVAR) to those patients with short necks or aneurysms involving the visceral arteries [1–2]. In these patients, open conventional repair remains the standard treatment, but technical complexity increases with more extensive dissection, higher clamp site, prolonged visceral ischemia, and more extensive reconstruction [3–7]. It is logical to speculate that the advantages achieved with endovascular repair of infrarenal aneurysms will pale in comparison to the potential for reduction in morbidity and mortality for treatment of more complex aneurysms that involve the visceral segment [8–12]. This chapter summarizes some of the surgical techniques for visceral reconstruction combined with aortic stent-graft placement, results, and future directions.

Rationale

Hybrid procedures have been introduced as a less invasive alternative to open conventional repair, avoiding the need for a thoracotomy and in many patients aortic cross clamping. The first report was by Quinones-Baldrich (Fig. 31.1) and associates from UCLA in 1999 [13]. The operation aimed to reduce the anatomic and physiologic stress to the patient by avoiding several shortcomings of open surgery: thoracotomy, single-lung ventilation, aortic cross clamping, and prolonged end-organ ischemia.

Since its introduction, hybrid procedures have been widely adopted as an alternative to open surgery. Its current role in the treatment of patients with complex aortic aneurysms has evolved. Most centers with access to fenestrated and branched endografts have relegated hybrid procedures to a subset of patients who are neither candidates for total endovascular repair or open surgery. It is likely that hybrid repair will continue to be replaced by total endovascular techniques in most centers. However, because branch vessel stenting is difficult or may be contraindicated in patients with small vessels, early branch bifurcation, diffuse atherosclerotic debris, and in those who already failed a fenestrated or parallel stent graft, hybrid repair remains an important technique that should be in the armamentarium of surgeons treating complex aortic aneurysms. Its future application is likely to be one of the main alternatives in patients who fail total endovascular repair or in centers without access or experience with fenestrated and branched endografts. Patient selection, case planning, and technical aspects of the procedure are key for successful outcomes.

Preoperative Evaluation

Clinical Risk Assessment

Clinical evaluation of patients with complex aortic disease is discussed in Chap. 10. A comprehensive evaluation of cardiac, pulmonary, and renal performance is crucial to optimize patient selection. These operations are often directed toward the sickest patient, but clinical data suggests that prohibitively high-risk patients and those with limited life expectancy are not ideal candidates for hybrid procedures either. Their evaluation should include noninvasive cardiac stress test (DSE or sestamibi study), pulmonary function tests, and carotid ultrasound. The Society for

G.S. Oderich (✉)
Division of Vascular and Endovascular Surgery,
Department of Surgery, Mayo Clinic,
200 First Street SW, Rochester, MN 55905, USA
e-mail: oderich.gustavo@mayo.edu

P. Gloviczki • B.C. Mendes • T.C. Bower
Division of Vascular and Endovascular Surgery, Mayo Clinic,
200 First Street SW, Rochester, MN 55905, USA

G.A. Escobar
Division of Vascular and Endovascular Surgery,
University of Arkansas for Medical Sciences,
4301 W Markham St. #520-2, Little Rock, AR 72205-7199, USA

© Mayo Foundation for Medical Education and Research 2017

G.S. Oderich (ed.), *Endovascular Aortic Repair*, DOI 10.1007/978-3-319-15192-2_31

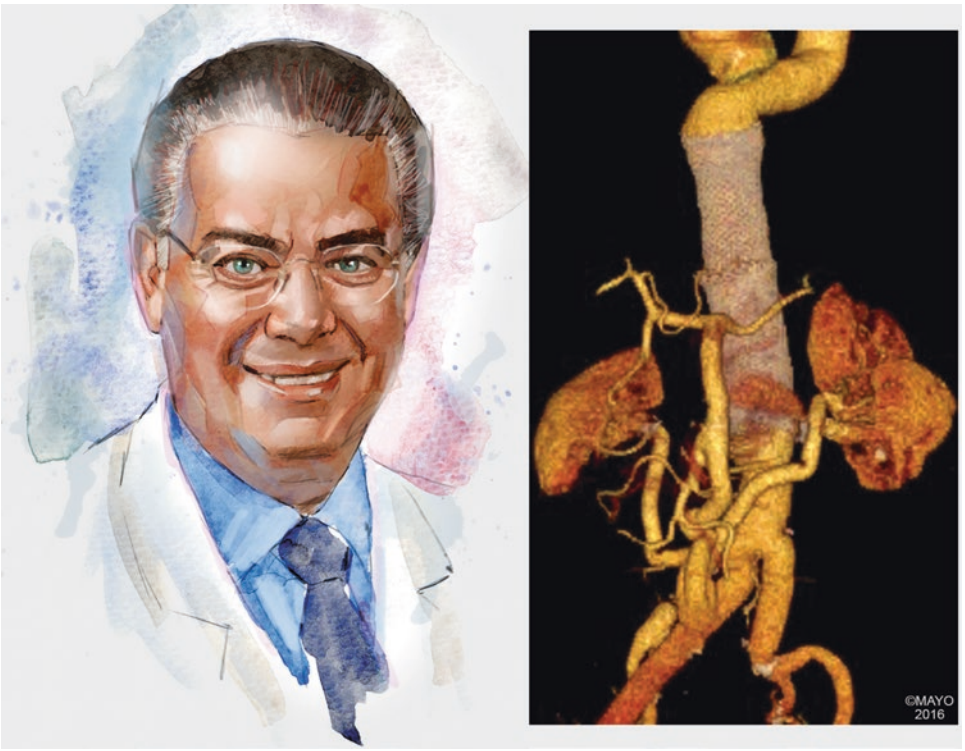


Fig. 31.1 Dr. William Quinones-Baldrich from the University of California Los Angeles described the first use of hybrid visceral debranching procedure in 1999. By permission of Mayo Foundation for Medical Education and Research. All rights reserved

Vascular Surgery (SVS) clinical comorbidity score system can be used to stratify operative risk, but the criteria has not been validated prospectively in patients undergoing complex aortic surgery [14]. Nonetheless, most agree that factors associated with increased risk include unstable angina, symptomatic or poorly controlled ectopy, recurrent CHF, ejection fraction <25 %, myocardial infarction <6 months, vital capacity <1.8 l, FEV1 < 800 ml, DLCO < 30 %, resting pO2 < 60 mmHg and pCO2 > 50 mmHg, and serum creatinine > 2.5 mg/dl.

Aortic Imaging and Planning

A basic tenet of endovascular repair is the presence of normal sealing zones. A hybrid procedure should only be considered if it can be performed with adequate proximal and/or distal sealing zones. In most centers, computed tomography angiography (CTA) is the preferred imaging modality to plan the operation; less frequently, magnetic resonance angiography (MRA) can also be used. The presence of a conic calcified and angulated neck compromises seal. A minimum length of 2 cm of parallel aortic wall without excessive calcification or thrombus is required in the thoracic aorta, and longer seal zones may be needed in the aortic arch. Distal attachment is equally important and most often can be achieved in the common iliac arteries, infrarenal aorta, or prior aortic graft. If the common iliac arteries are aneurysmal, preservation of pelvic flow is critical to minimize risk of spinal cord injury [15]. Similarly, proximal debranching of the subclavi an artery may reduce rates of paraplegia in patients who need extensive coverage of the thoracic aorta.

Aortic side branches requiring incorporation should also be analyzed for the presence of occlusive disease, for the presence of excessive calcification or thrombus, and for the presence of unusual or aberrant anatomy. Small-sized, calcified, or multiple renal arteries pose a challenge and may require complex reconstruction. The quality of the inflow site, which is typically located in the distal common and proximal external iliac artery, should be reviewed for the presence of occlusive disease. In cases where the aorta has already been replaced, then the aortic graft may allow for excellent inflow and avoid the use of the iliac arteries. It is critical to assure optimal inflow to the visceral grafts and enough residual length within the common iliac artery to seal the distal portion of the endograft. The presence of any abnormal venous anatomy (e.g., left-sided vena cava, retroaortic renal vein, etc.) should be noted to avoid inadvertent injury. Finally, it is critical to assure adequate iliac access, which ideally should be planned in the opposite side. Failure to later be able to advance the endograft through complex iliac anatomy after debranching can be avoided by creating a conduit before closing. The latter is ligated and buried within the retroperitoneum where it can be retrieved for the endovascular stage of the procedure.

Techniques

The debranching procedure can be done using midline transperitoneal or retroperitoneal incision, either in one or two separate stages, followed by aortic stent-graft coverage. The two-stage approach has been widely advocated in recent reports to minimize morbidity and mortality rates and to decrease rates of spinal cord injury. Staging is particularly important in the higher-risk patient or in those who require difficult open surgical reconstructions and have extent I or II TAAAs. However, single-stage procedures are advantageous by avoiding the risk of aneurysm rupture between stages, and should be considered in those patients who have ruptures, uneventful debranching, and excessively large aneurysms, and require more limited extent of aortic coverage. The source of inflow for extra-anatomic reconstruction is usually the distal common iliac artery extending into the proximal external iliac artery. Other alternative sites are the infrarenal aorta, previous aortic grafts, or the hepatic and splenic arteries. A variety of graft configurations have been described (Fig. 31.2). Our preference is to use a trifurcated graft from one of the common iliac arteries whenever possible, with an added limb depending on the patient anatomy. Alternatively, a bifurcated graft can be anastomosed with a short main body and graft limbs to the right renal and superior mesenteric arteries. Separate graft limbs can be added for the celiac axis and left renal artery, allowing selection of the ideal position for the graft limb and avoiding kinking which can occur with prefashioned trifurcated grafts. More recently, Dr. Peter Gloviczki designed a prefabricated polyester graft with four limbs that eliminate the need to construct grafts on table (Fig. 31.3).

Exposure

Transperitoneal approach using a long midline incision is used in most patients. The incision is extended alongside the

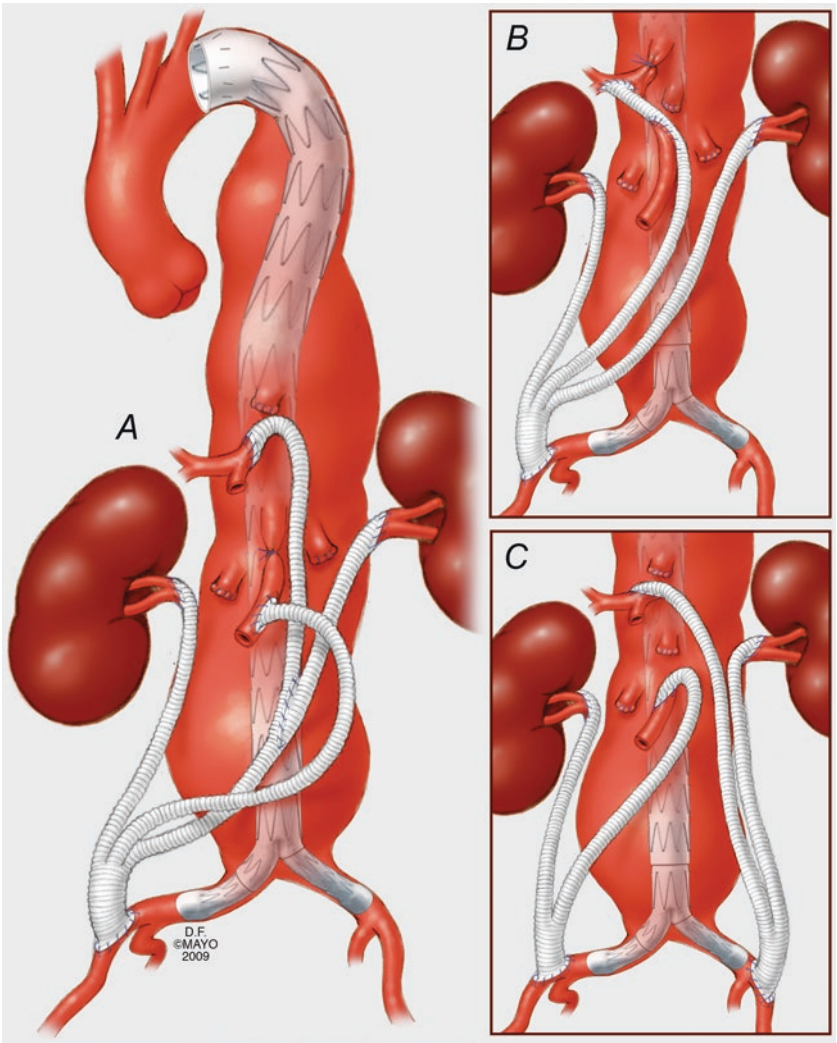


Fig. 31.2 Graft configurations of hybrid debranching including trifurcated graft from the right iliac artery with separate graft limb to left renal artery (**a**) or end-to-side anastomosis to the SMA (**b**) and the use of both common iliac arteries For inflow inflow (**c**). By permission of Mayo Foundation for Medical Education and Research. All rights reserved

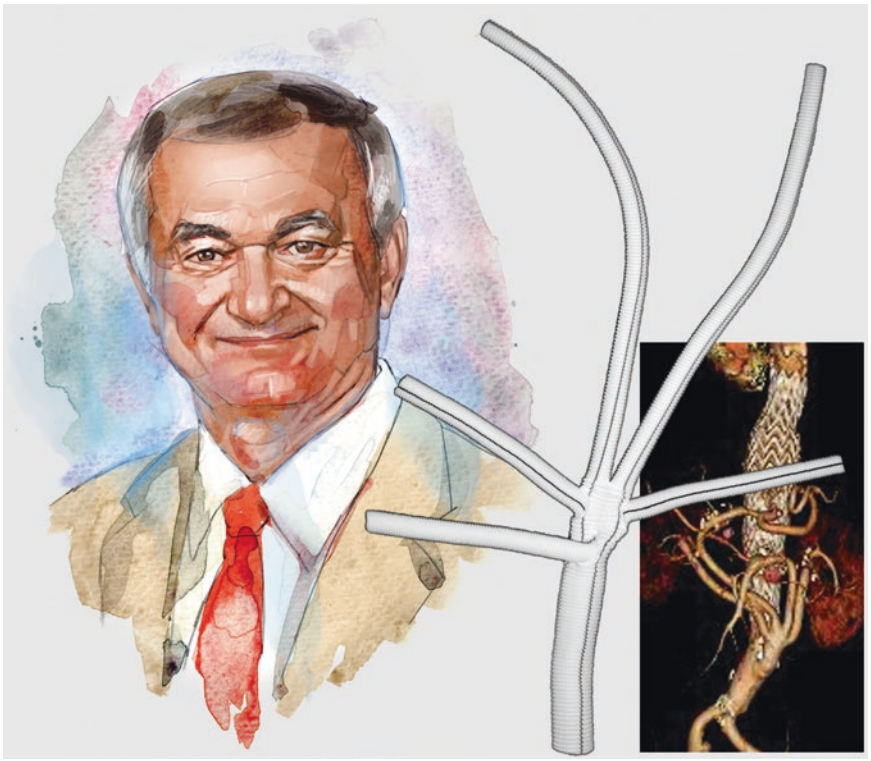


Fig. 31.3 Dr. Peter Gloviczki design of a four-vessel visceral debranching graft. By permission of Mayo Foundation for Medical Education and Research. All rights reserved

xiphoid process, which releases five aponeuroses and ligaments and allows upward retraction of the costal edges (Fig. 31.4). Patients with wide costal flare may benefit from retroperitoneal approach, but exposure of the right renal artery and iliac bifurcation can be difficult. After abdominal exploration is performed, a self-retaining retractor is placed in a standard fashion as depicted in Fig. 31.5. The mesocolon is retracted cephalad and the mesentery to the right side of the abdomen. The inferior mesenteric vein is ligated and divided. The left renal vein and branches are mobilized (Fig. 31.6). It is useful to ligate and divide the renal vein branches to avoid risk of tearing the branch points with excessive retraction. The adrenal, gonadal, and lumbo-renal vein branches are ligated and divided. If the aorta is relatively narrow at the level of the renal arteries, the proximal third of both renal arteries is dissected free and prepared for clamping. The right and left diaphragmatic crura can be transected adjacent to the aorta to allow more space for the anastomosis (Fig. 31.7). However, if the aneurysm is large and wide at the level of the renal arteries, the mid or distal segments of the renal arteries need to be dissected. This may require medial visceral rotation (Fig. 31.8) in the left side or extended Kocher maneuver in the right side. The renal arteries need to be handled carefully without excessive retraction. It is critical that enough length of the renal artery is dissected to allow proper ligation of the vessel proximally and distal anastomosis. The superior mesenteric artery (SMA) is exposed also using similar approach in the base of the mesentery where it is just anterior to the left renal vein. Dissection of the mid segment of the SMA (Fig. 31.9a) is also recommended and can be done by relaxing the mesentery, which is incised just to the right of the proximal jejunum. The mesocolon is relaxed and the lesser sac is entered. It is important to have a nasogastric tube in the stomach, which can be palpated at the gastroesophagel junction. The triangular ligament of the liver is taken and retracted to the right side of the abdomen, while the esophagus is retracted to the left side. The right diaphragmatic crura is opened longitudinally (Fig. 31.9b), similar to what is done to expose the supraceliac aorta. The proximal celiac axis is dissected circumferentially and prepared to be ligated. The common hepatic artery is dissected and prepared for clamping and for the anastomosis. In these cases, the graft limb can be tunneled through the mesocolon into the lesser sac.

Inflow for the extra-anatomic bypasses is most commonly done at the iliac arteries, but it can also come from the aorta, an aortic graft, or one of the visceral arteries. Our preference is to provide inflow from one of the iliac arteries by anastomosing the graft from the distal common to the proximal external iliac arteries (Figs. 31.2 and 31.10). However, inflow can also come from both iliac arteries. In patients who have inadequate iliac access for introduction

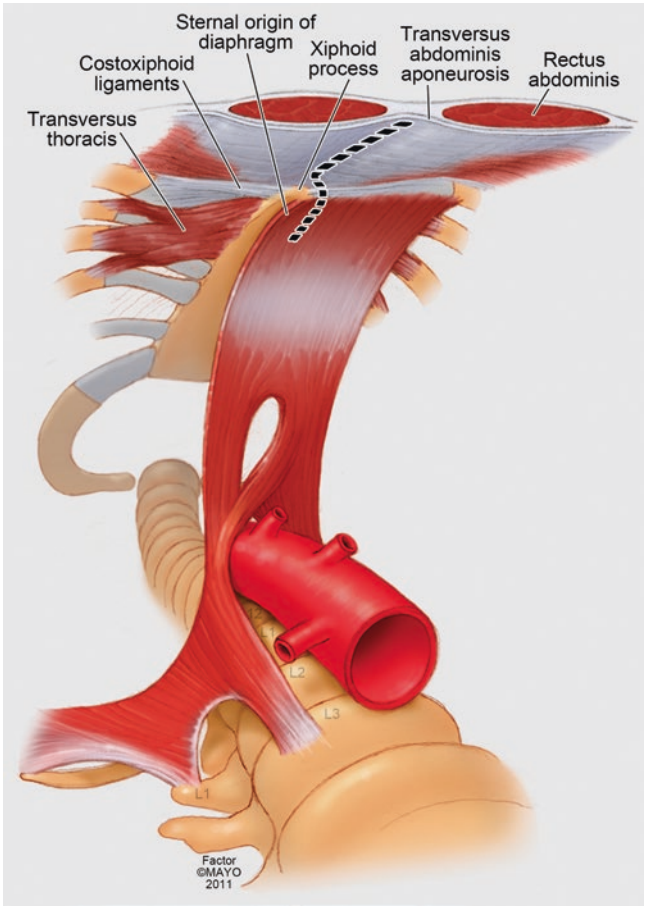


Fig. 31.4 Incision alongside the xiphoid process releases five aponeuroses or ligaments including the transversus thoracis, costoxiphoid ligament, transverse abdominis aponeurosis, and rectus abdominis aponeurosis. By permission of Mayo Foundation for Medical Education and Research. All rights reserved

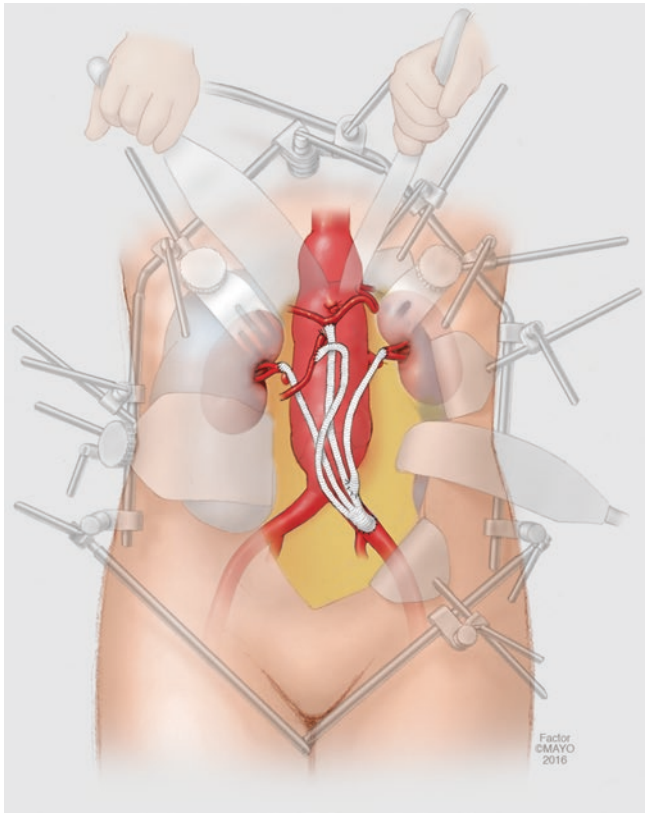


Fig. 31.5 Standard placement of self-retaining retractors using midline incision to expose the aorta and its branches. By permission of Mayo Foundation for Medical Education and Research. All rights reserved

of thoracic stent grafts, a conduit is planned either by replacement of the external iliac artery using a 10-mm graft or alternatively by anastomosing a graft to the hood of the proximal renal-mesenteric graft.

Graft Selection and Preparation

Our preference has been to use polyester grafts instead of PTFE because of handling and needle hole bleedings. We avoid using 6-mm grafts with the exception of very small renal arteries. Instead our preference has been to use either a 14×7- or 16×8-mm bifurcated polyester graft and anastomose a 7- or 8-mm graft limb to fashion a trifurcated or quadri-furcated graft. In these cases, selection of the 16×8-mm bifurcated graft is ideal, and additional 7-mm graft limbs can be anastomosed for the renal arteries. The exact configuration of the graft varies widely and is essentially done to fit the patient anatomy. However, the author's preference is to use one limb for the right renal artery (Fig. 31.11) and the other limb for the SMA (side to side) and celiac axis (end to side, Fig. 31.12). For the left renal artery, a separate 7-mm graft can be anastomosed either to the hood of the bifurcated graft or to the SMA graft limb (Fig. 31.13a). Other option is to bring a separate graft from the left common iliac artery to the left renal artery, which is tunneled in the retroperitoneum (Fig. 31.13b).

Proximal Anastomosis

The patient is systemically heparinized. The proximal common iliac artery and the internal iliac and external iliac arteries are clamped sequentially. A 3-cm longitudinal arteriotomy is made extending from the distal common to the external iliac artery. A 16×8 -bifurcated polyester graft is cut to length and spatulated. The graft is anastomosed end to side to the iliac arteries using running 4-0 Prolene suture. After the anastomosis is tested, flow is restored to the lower extremities, and the graft is clamped close to the anastomosis. Blood should be aspirated from the graft limbs.

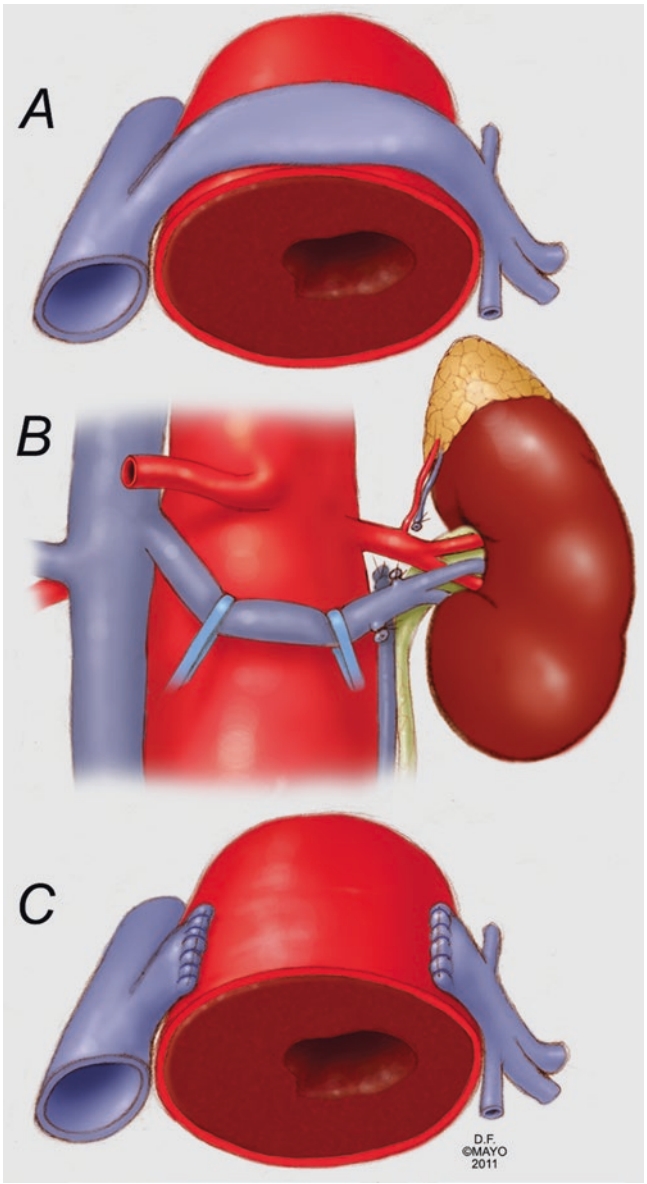


Fig. 31.6 The left renal vein is often splayed on top of the enlarged aorta in patients with thoracoabdominal aneurysms (**a**). Full mobilization requires ligation of the adrenal, gonadal, and lumbo-renal branches (**b**). Rarely the left renal vein is transected to facilitate exposure (**c**). It is critical to preserve the venous branches in patients who need ligation. By permission of Mayo Foundation for Medical Education and Research. All rights reserved

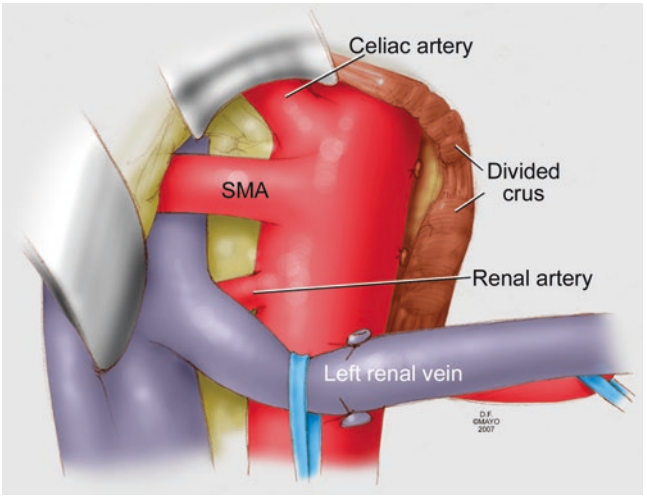


Fig. 31.7 Exposure of the renal arteries and the SMA with transection of the diaphragmatic crura. By permission of Mayo Foundation for Medical Education and Research. All rights reserved

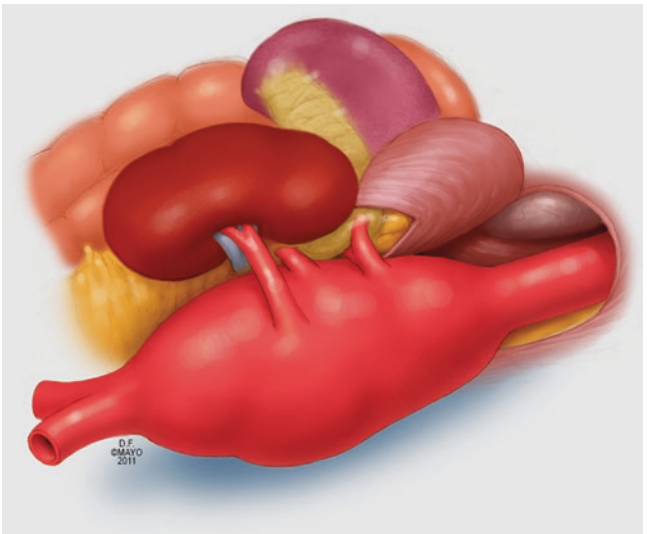


Fig. 31.8 Medial visceral rotation to expose the aorta and its branches. By permission of Mayo Foundation for Medical Education and Research. All rights reserved

Distal Renal and Mesenteric Anastomosis

The right renal artery is exposed using a Cattell and extended Kocher maneuver. One of the 7- or 8-mm graft limbs is tunneled toward the right renal artery (Fig. 31.11). The proximal renal artery is double clipped using large clips, while the distal renal artery is controlled using bulldog clamps. The artery is carefully transected and the proximal stump is closed with running 5-0 Prolene sutures. The distal renal artery is spatulated and beveled for the anastomosis. The renal artery anastomoses can be undoubtedly the most difficult part of the operation, particularly if the aneurysm is large and the patient is obese. In these cases using a parachute technique with triangulation of the anastomosis is useful. After the graft limb is cut to length and spatulated, the toe and heel of the anastomosis are tagged using 5-0 or 6-0 Prolenes (Fig. 31.14). A few stitches are placed in the heel of the anastomosis, which is then approximated. For the toe of the anastomosis, the author

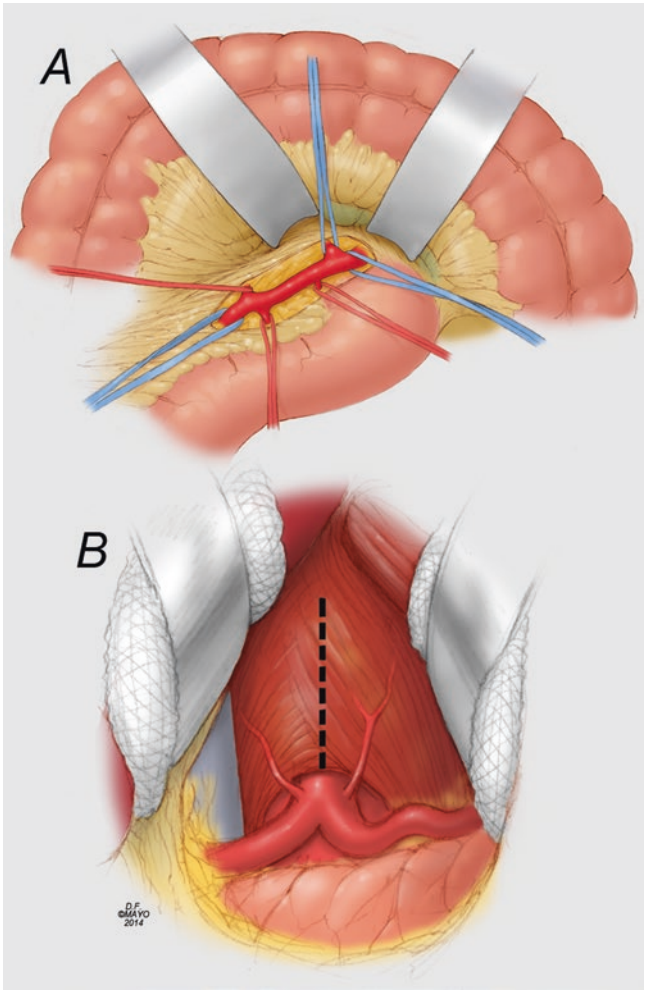


Fig. 31.9 (**a**, **b**) Exposure of the SMA and the celiac axis. By permission of Mayo Foundation for Medical Education and Research. All rights reserved

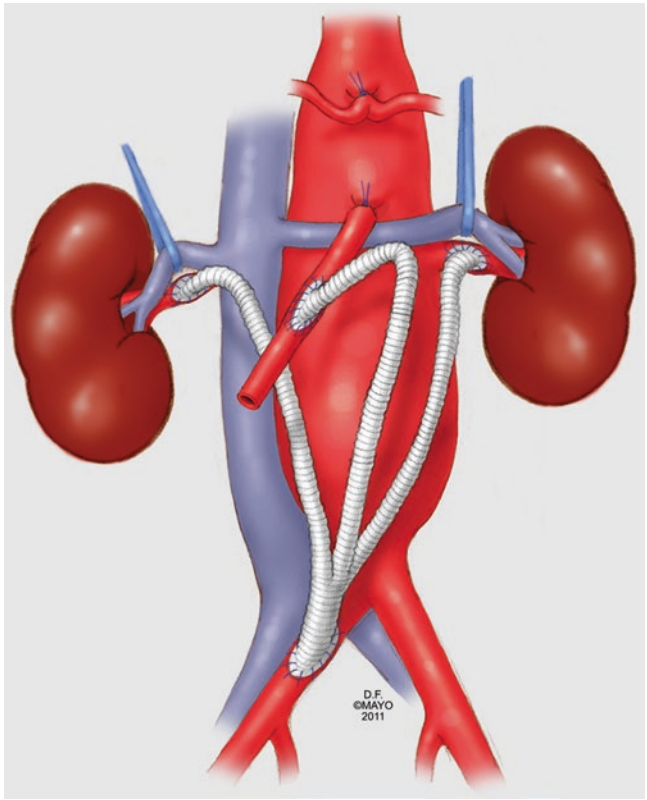


Fig. 31.10 The use of a trifurcated graft anastomosed to the right common iliac artery with limbs to both renal arteries and the SMA. The celiac axis is ligated. By permission of Mayo Foundation for Medical Education and Research. All rights reserved

often uses three interrupted sutures to facilitate visualization and avoid purse string. Flow is restored to the renal artery after a clamp time that averages 10–20 min. Next, attention is directed to the mesenteric arteries. The second graft limb can be tunneled via the mesocolon anterior to the pancreas the pancreas through the lesser sac (see Fig. 31.12), or tunneled posterior to the pancreas the pancreas, parallel to the aorta. The common hepatic artery is ideally suited for the anastomosis. The artery is controlled proximally and distally, a small 10-mm arteriotomy is made, and the graft limb is anastomosed end to side using running 5-0 Prolene sutures. Flow is restored into the hepatic artery. The proximal celiac axis is double ligated with Ethibond sutures, but it is not transected. It is important to ligate the celiac axis close to its origin to preserve retrograde flow into the splenic artery (see Fig. 31.12). Next, the SMA anastomosis is done either in a side-to-side fashion or using a short separate graft limb, which is anastomosed to the celiac graft. The final step of reconstruction is the anastomosis to the left renal artery. This is fashioned using either a separate graft from the contralateral iliac artery (see Fig. 31.13) or alternatively a short graft limb anastomosed end-to-side to the celiac-SMA graft. The VORTEC technique (Fig. 31.15) is a modification described by Lachat and associates that allows a sutureless anastomosis using Viabahn or hybrid stent grafts (WL Gore, Flagstaff, AZ). The target vessel is accessed first using a micropuncture wire under direct vision. The arteriotomy is gently dilated with a 6-Fr dilator, followed by introduction of a Viabahn into the vessel. The stent is deployed and secured into the vessel using a few Prolene stitches. The stent is then cut to length and anastomosed to the polyester graft using running 5-0 Prolene sutures. This technique has been widely used particularly for the renal anastomosis, but also in the arch and for the internal iliac arteries. The newer Gore hybrid vascular graft (Gore, Flagstaff, AZ), which is fashioned with a Viabahn distally and a PTFE graft proximally, is ideally suited for this technique.

A conduit may be needed in patients with small iliac arteries. This can be anastomosed either to the hood of the graft

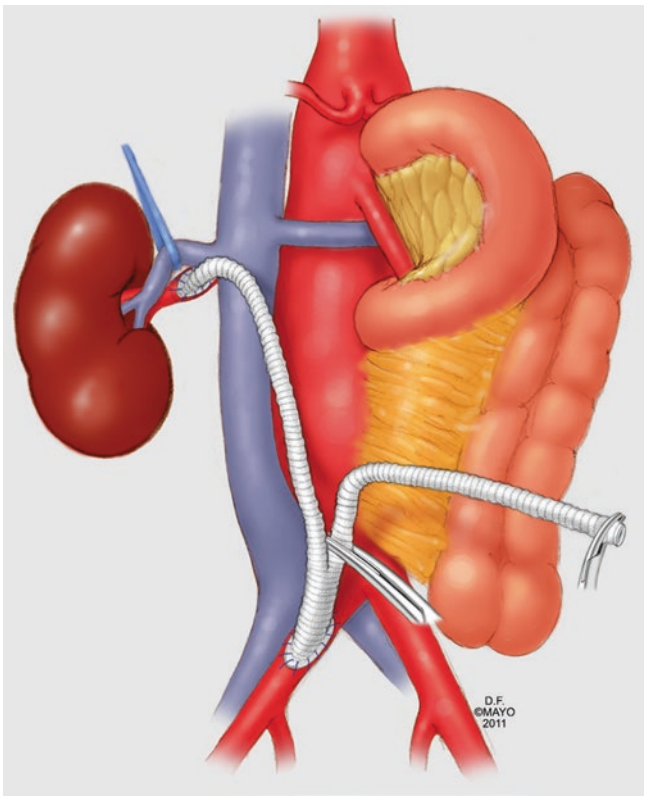


Fig. 31.11 The use of a bifurcated graft anastomosed to the right common iliac artery with one limb anastomosed to the right renal artery. By permission of Mayo Foundation for Medical Education and Research. All rights reserved

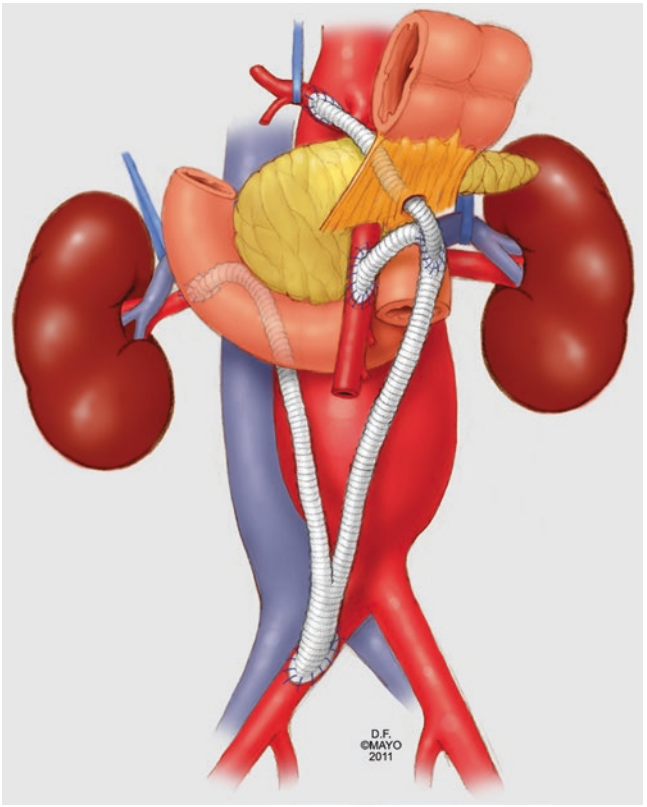


Fig. 31.12 Anastomosis of the second limb to the SMA. A separate graft limb is anastomosed to the hepatic artery tunneled via the mesocolon. By permission of Mayo Foundation for Medical Education and Research. All rights reserved

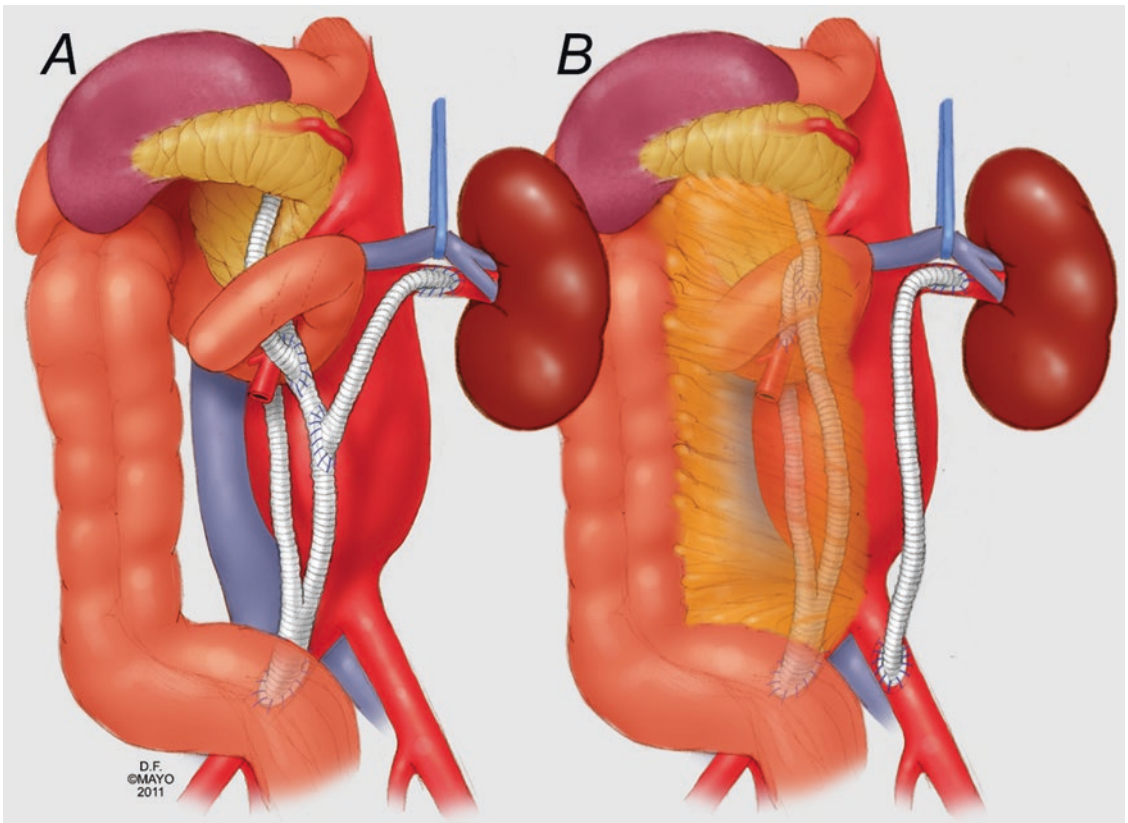


Fig. 31.13 Using medial visceral rotation, a separate limb is added to the left renal artery (**a**). Alternatively the left common iliac artery is used for a left renal artery bypass (**b**). By permission of Mayo Foundation for Medical Education and Research. All rights reserved

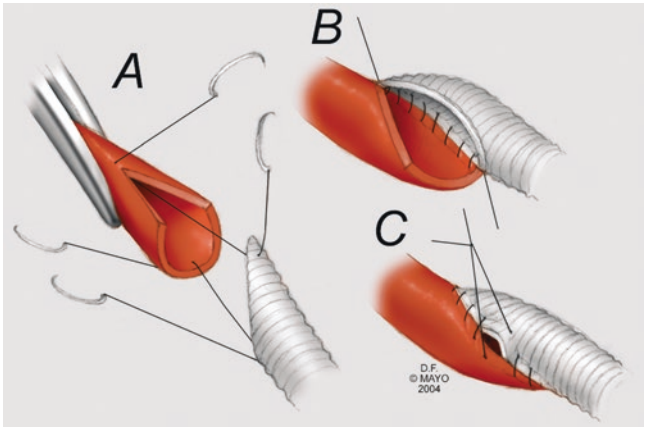


Fig. 31.14 Triangulation technique for anastomosis to the renal arteries. The renal artery and the graft are beveled (**a**) with anchor 5-0 or 6-0 Prolene sutures which are tied (**b**). Each suture line is run to complete the anastomosis (**c**). By permission of Mayo Foundation for Medical Education and Research. All rights reserved

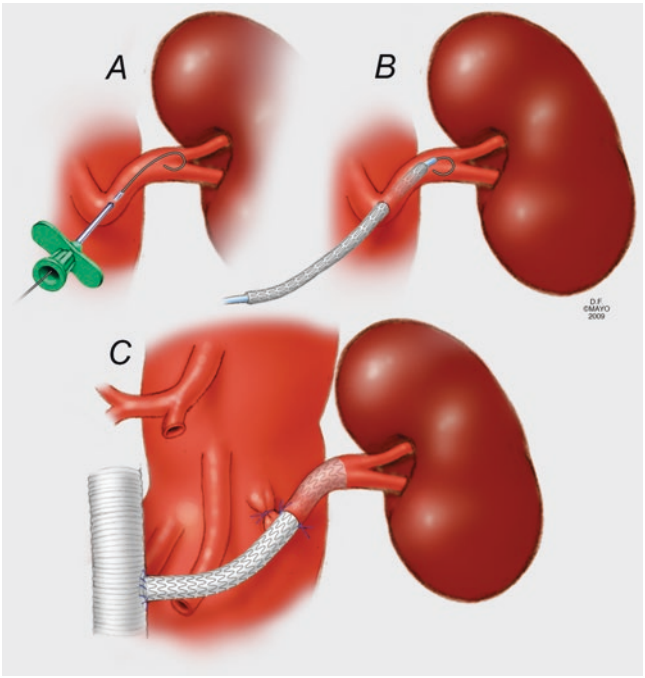


Fig. 31.15 VORTEC technique described by Mario Lachat uses direct access of the renal artery with guidewire (**a**) and gentle dilation of the puncture using dilator. This is followed by introduction of a Viabahn stent graft (**b**) which is deployed and secured with few 6-0 Prolene sutures. The Viabahn is anastomosed to one of the polyester graft limbs (**c**). By permission of Mayo Foundation for Medical Education and Research. All rights reserved

or directly into the iliac artery (Fig. 31.16). Ideally, the conduit should be anastomosed in the contralateral side to avoid ischemia of the grafts and risk of occlusion because of the large-diameter sheath. If the procedure is staged, the conduit can be constructed, ligated distally, and buried under the inguinal ligament. In the second-stage procedure, the conduit is exteriorized via a small groin incision. Thrombectomy is done using Fogarty balloon while the femoral artery is clamped to prevent distal embolization. Several examples illustrate the variations in graft configuration depending on aneurysm and visceral artery anatomy, including hybrid repair of a supra-graft type IV TAAA (Fig. 31.17) and extent type II TAAA (Figs. 31.18 and 31.19).

Results

Single-Center Experiences

Despite logical advantages over open repair and early successes, results of hybrid procedures have been tempered by high morbidity and mortality rates in several centers [13, 15–25]. The UCLA and University of Michigan groups have reported two of the largest experiences with remarkably low mortality rates of 0 and 3.4 %, respectively [17, 18]. Others (Cleveland Clinic, Mayo Clinic, Mass General Hospital, Methodist Hospital Houston) have shown higher mortality rates in the range of 10–25 %. Lin and associates reported high mortality rates for hybrid repair of TAAAs using single- or two-stage approaches in a center with large referral of open TAAAs. Spinal cord injury occurs in 2–25 % and correlates with extent of aortic coverage, preservation of flow into the subclavian and hypogastric arteries, and periprocedural hypotension [13, 15–25]. Rates of type I and II endoleaks have been reported in the range of 3–15 % and 5–25 %, respectively.

Systematic Reviews

Two systematic reviews of the available literature have been published on hybrid repair of TAAAs [26, 27]. Bakoyiannis and associates reviewed the outcomes of 108 patients from 15 reports between 1999 and 2008. Technical success was 92 % and 30-day mortality 10 % [26]. In this report, 19 patients (17 %) had primary endoleaks and other three (3 %) developed secondary endoleaks. Spinal cord injury occurred in three patients (3 %) and renal insufficiency in 12 (11 %). After a mean follow-up of 10 months, 97 % of the visceral grafts remained patent and 24 % of patients died of unrelated causes.

A more recent review by Moulakakis and associates included 507 patients and 19 reports published since 1999. There were 319 male (64 %) and 188 female patients with mean age of 70 years old. Aneurysm extent was classified as type I in 14 %, type II in 27 %, type III in 34 %, type IV in 14 %, and type V in 11 %. A single-stage procedure was used in 55 % and two-stage procedure in 45 %, with mean period of 28 days between the two stages. Thirty-day or in-hospital mortality was 13 %, and

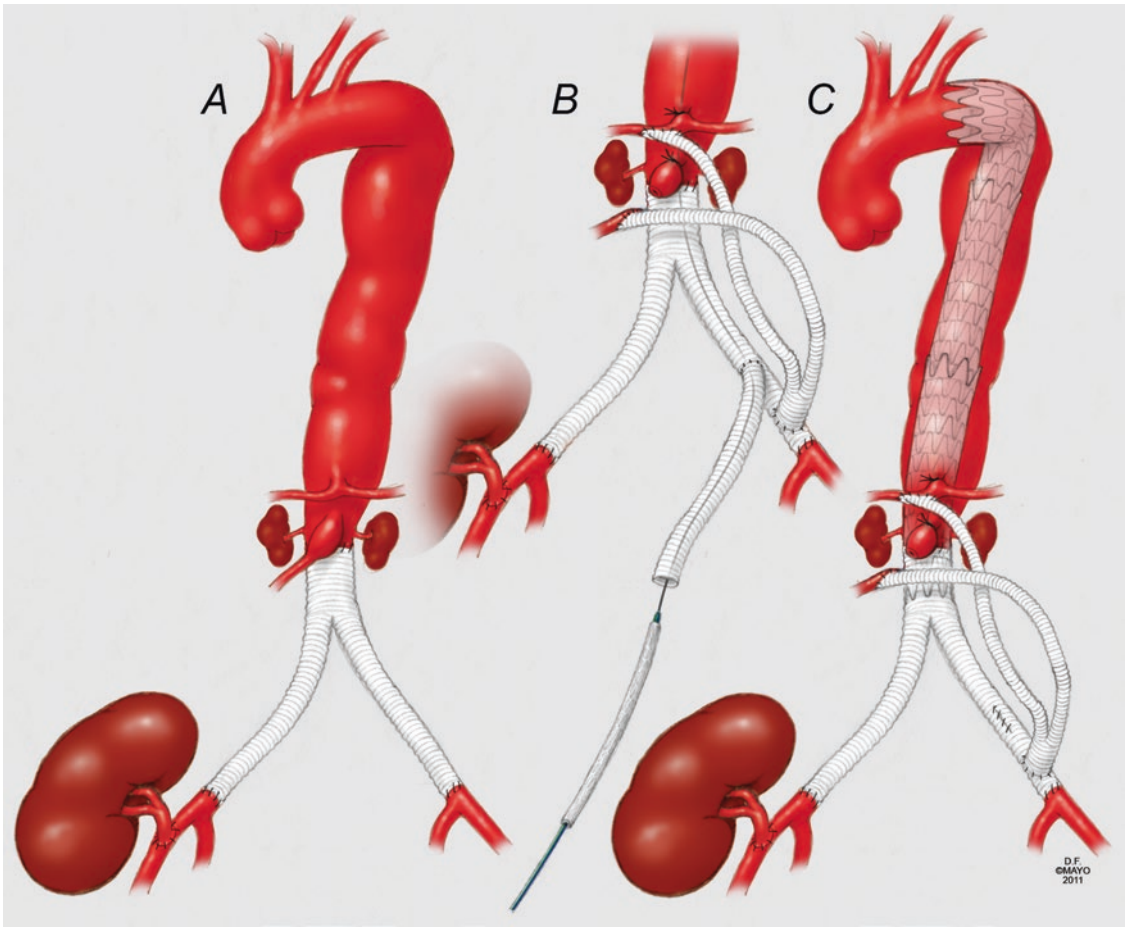


Fig. 31.16 Patient with supra-graft TAAA after prior abdominal aneurysm repair (**a**). The bifurcated abdominal graft is used for source of inflow of the visceral debranching in addition to a conduit (**b**). The conduit is excised after placement of the aortic stent grafts (**c**). By permission of Mayo Foundation for Medical Education and Research. All rights reserved

the most common causes of death were multisystem organ failure, ischemic colitis, respiratory failure, and aneurysm rupture prior to a second-stage procedure. Pooled rates of spinal cord injury were 7.5 %, with irreversible paraplegia in 4.5 %. After a mean follow-up of 35 months, a total of 111 patients (22 %) had endoleaks and visceral graft patency was 96 %.

North American Complex Abdominal Aortic Debranching (NACAAD) Registry

The preliminary results of the NACAAD registry were presented at the 2011 Vascular Annual Meeting [28]. This study included 208 patients treated for complex abdominal aortic aneurysms in 14 academic centers of North America. There were 118 male (57 %) and 90 female patients with mean age of 71 years old. Cardiovascular risk factors included hypertension in 86 %, cigarette smoking in 78 %, hyperlipidemia in 60 %, coronary artery disease in 58 %, chronic pulmonary disease in 43 %, prior aortic repair in 42 %, and chronic kidney disease stage >3 (eGFR < 60 ml/h/1.73 m^2) in 28 %. Aneurysm diameter averaged 6.6 ± 1.3 cm, and aneurysm extent included 163 TAAAs (type I in 6 %, type II in 25 %, type III in 31 %, and type IV) and 45 pararenal aneurysms. A total of 659 visceral arteries were reconstructed using single-stage debranching in 92 patients (44 %) or two-stage approach in 116 (56 %). Arch debranching was needed in 22 patients (11 %) to provide adequate proximal landing zone. The inflow for visceral reconstruction was based on the iliac arteries in 63 %, aorta or aortic graft in 29 %, or a hepatic/splenic artery in 8 %. Extent of visceral reconstruction includes one or two vessels in 58 patients (28 %) and three or four vessels in 150 (72 %).

Thirty-day or in-hospital mortality was 14 % for all patients, 16 % for TAAAs, and 9 % for pararenal aneurysms. Mortality rates ranged from 0 to 21 % in centers with >10 cases. In this study, mortality was associated with severity of

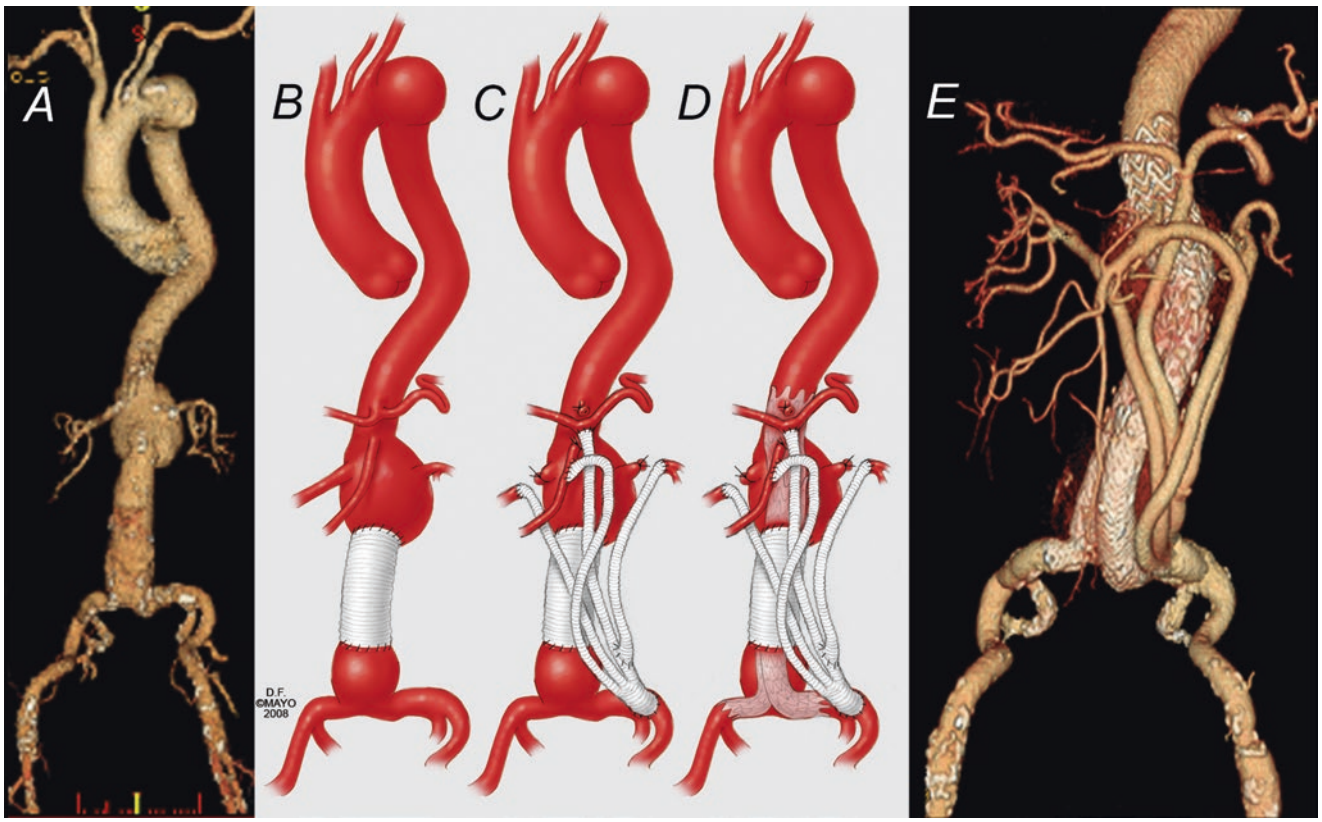


Fig. 31.17 Patient with large supra-graft Extent IV TAAA after prior open abdominal repair (**a** and **b**). The patient was treated in a staged fashion using four-vessel visceral debranching (**c**) followed by placement of the aortic stent grafts (**d** and **e**). By permission of Mayo Foundation for Medical Education and Research. All rights reserved

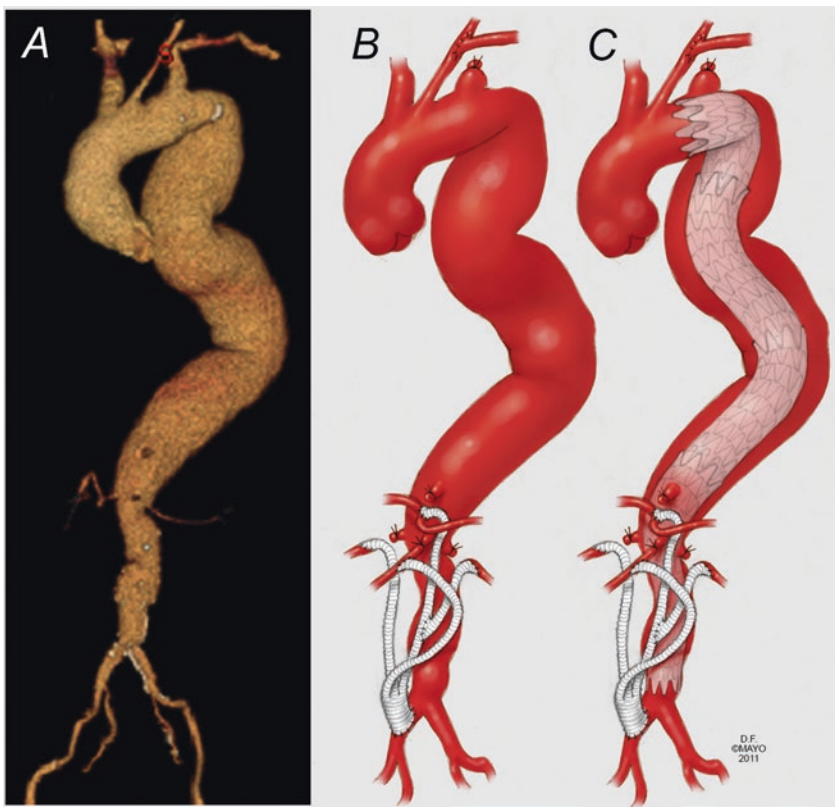


Fig. 31.18 Preoperative CTA of a patient with large extent II TAAA (**a**). The patient was treated by four-vessel visceral debranching (**b**), followed by aortic stent grafts (**c**). By permission of Mayo Foundation for Medical Education and Research. All rights reserved

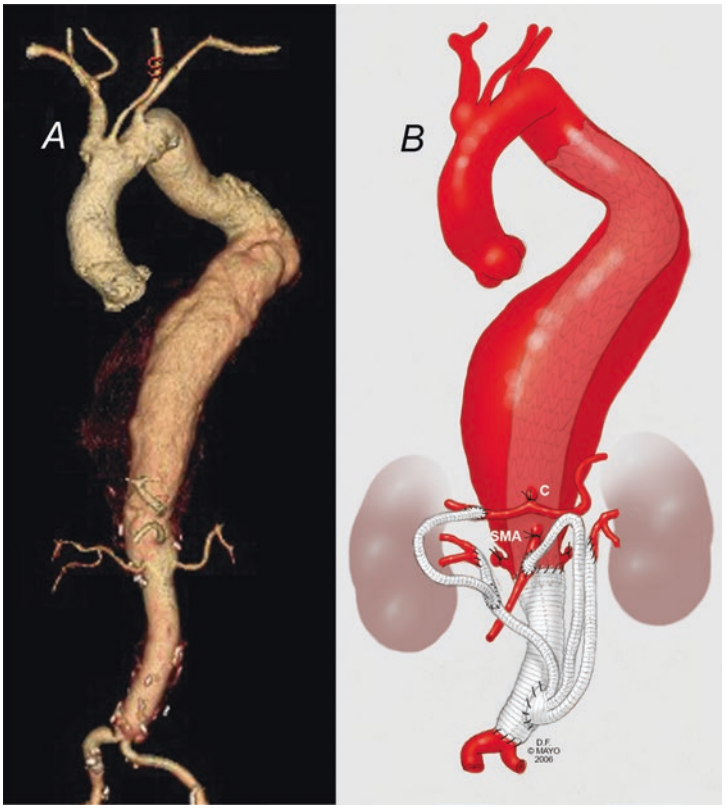


Fig. 31.19 Preoperative CTA of a patient with large extent II TAAA (**a**). The patient was treated by four-vessel visceral debranching and aortic stent grafts (**b**). By permission of Mayo Foundation for Medical Education and Research. All rights reserved

comorbidities as determined by SVS clinical scores (Fig. 31.20): 3% for low-risk patients (SVS score <9) and 17% for high-risk patients (score >9). Independent predictors of early mortality included >3 vessel reconstruction, coronary artery disease, CHF, high SVS scores, and chronic kidney disease stage >3. Any morbidity occurred in 73% of the patients, most commonly pulmonary (22%), renal (19%), and gastrointestinal complications (14%). Spinal cord injury occurred in 21 patients (10%) and ischemic colitis in 13 (6%). The mean length of hospital stay was 21 days. Patient survival at 1 and 5 years were 77±3% and 61±5% (Fig. 31.21), and predictors of late mortality included chronic kidney disease (stage >3), high SVS scores, and >3 vessel reconstruction. After a median follow-up of 21 months, 70% of the patients had repeat aortic imaging. Endoleaks occurred in 23 patients (13%) and were classified as type I in 3%, type II in 8%, and type III in 1%. Primary visceral graft patency (Fig. 31.22) and freedom from re-interventions (Fig. 31.23) were 90±2% and 85±3% at 1 year, respectively.

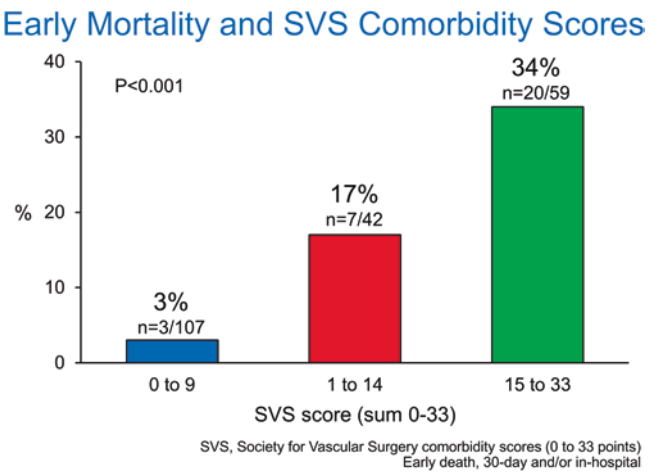
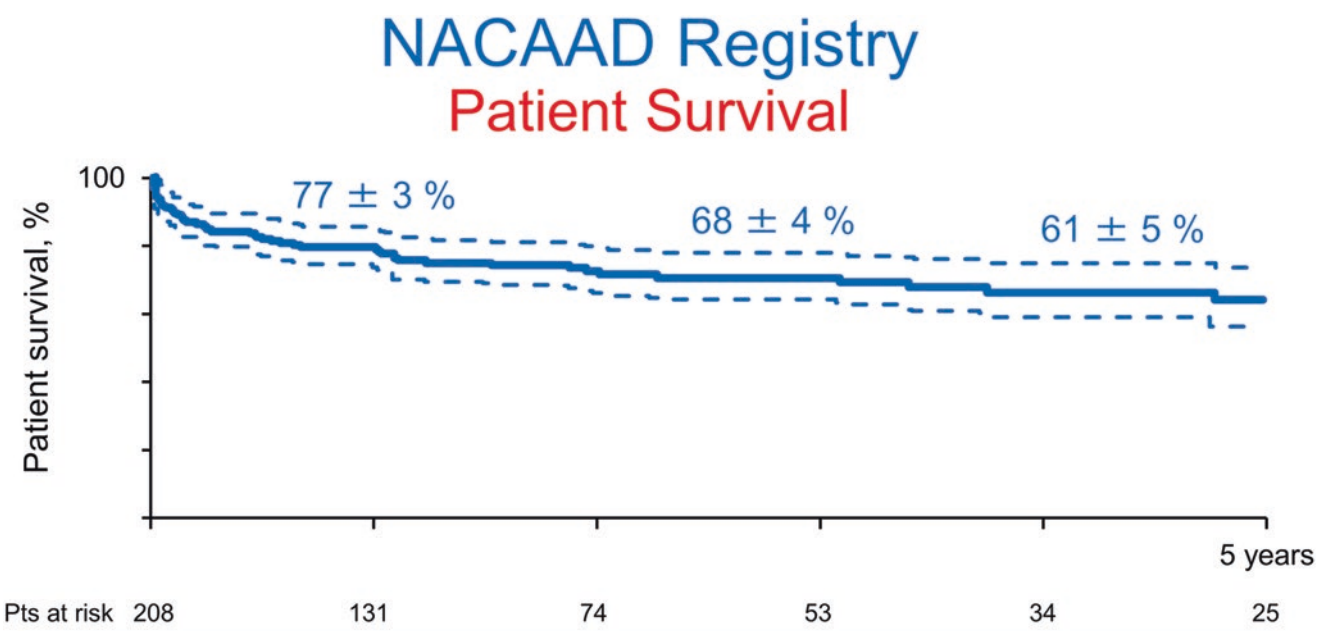


Fig. 31.20 Thirty-day mortality in the North American Abdominal Debranching Registry study was associated with clinical risk defined by Society for Vascular Surgery comorbidity scores. By permission of Mayo Foundation for Medical Education and Research. All rights reserved



Predictors of Late Mortality

P	Odds ratio	95% Confidence Interval	
Renal insufficiency	27	5.97-128.38	<0.0001
3-4 vessel reconstruction	3.45	1.63-7.27	0.0012
Diabetes mellitus	2.15	1.12-4.12	0.021
Chronic pulmonary disease	2.05	1.21-3.47	0.0074
SVS total score >15	1.97	1.15-3.36	<0.013

Fig. 31.21 Kaplan-Meier survival estimates of patient survival in the North American Abdominal Debranching Registry study. By permission of Mayo Foundation for Medical Education and Research. All rights reserved

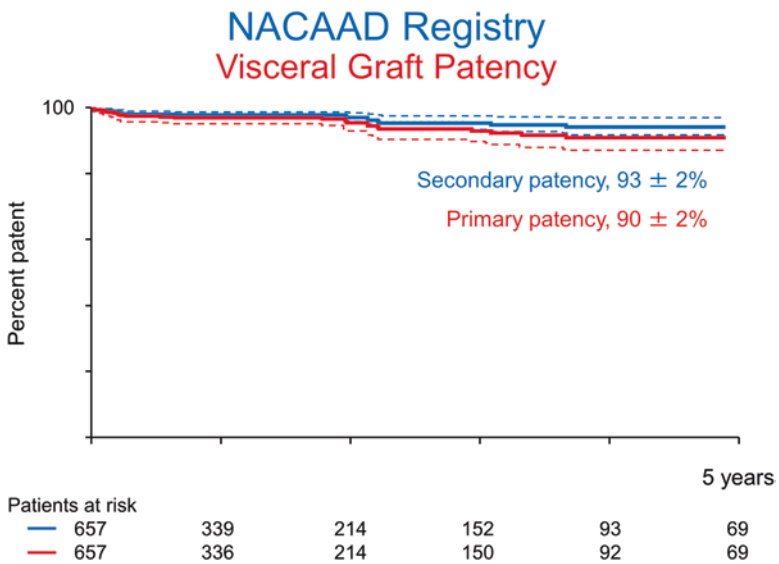


Fig. 31.22 Kaplan-Meier survival estimates of graft patency in the North American Abdominal Debranching Registry study. By permission of Mayo Foundation for Medical Education and Research. All rights reserved

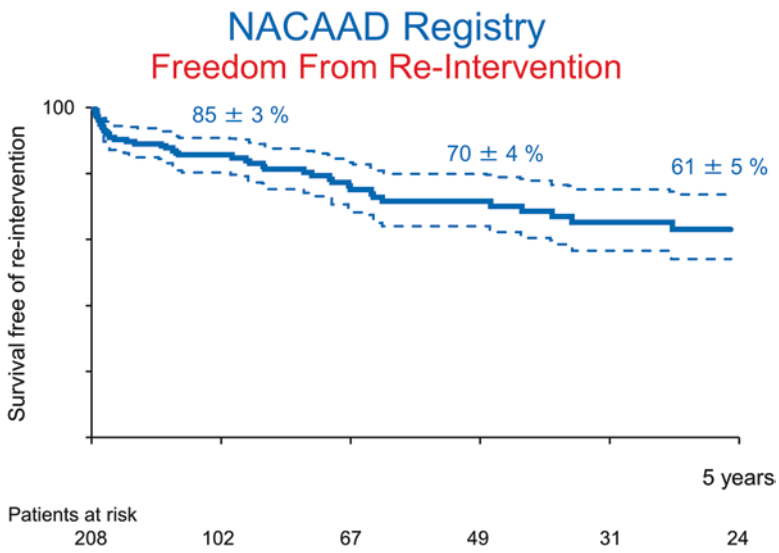


Fig. 31.23 Kaplan-Meier survival estimates of freedom from re-interventions in the North American Abdominal Debranching Registry study. By permission of Mayo Foundation for Medical Education and Research. All rights reserved

Conclusion

Hybrid procedures have several advantages over conventional open repair including avoiding thoracotomy, single-lung ventilation, aortic cross clamping, and minimizing end-organ ischemia. Shortcomings are the need for extensive dissection in multiple abdominal areas and prolonged operative time. Patient selection is key for optimal results. A few centers have adopted hybrid procedures as their primary treatment option in intermediate- and high-risk patients with good results. However, several centers with large complex aortic volume, systematic reviews, and a national registry have shown that these hybrid procedures can carry high mortality rates.

References

1. Endovascular aneurysm repair versus open repair in patients with abdominal aortic aneurysms (EVAR Trial 1): randomized controlled trial. Lancet. 2005;365:2179–86.
2. Prinssen M, Verhoeven EL, Buth J, Cuypers PW, van Sambeek MR, Balm R, et al. A randomized trial comparing conventional and endovascular repair of abdominal aortic aneurysms. N Engl J Med. 2004;351:1607–18.
3. Coselli JS, Bozinovski J, LeMaire SA. Open surgical repair of 2286 thoracoabdominal aortic aneurysms. Ann Thorac Surg. 2007;83:S862–4.
4. Conrad MF, Crawford RS, Davison JK, Cambria RP. Thoracoabdominal aneurysm repair: a 20-year experience. Ann Thorac Surg. 2007;83:S856–61.
5. Jacobs MJ, van Eps RG, de Jong DS, Schurink GW, Mochtar B. Prevention of renal failure in patients undergoing thoracoabdominal aortic aneurysm repair. J Vasc Surg. 2004;40:1067–73.
6. Safi HJ, Estrera AL, Miller CC, Huynh TT, Porat EE, Azizzadeh A, et al. Evolution of risk for neurologic deficit after descending and thoracoabdominal aortic repair. Ann Thorac Surg. 2005;80:2173–9.
7. Rigberg DA, McGory ML, Zingmond DS, Maggard MA, Agustin M, Lawrence PF, et al. Thirty-day mortality statistics underestimate the risk of repair of thoracoabdominal aortic aneurysms: a statewide experience. J Vasc Surg. 2006;43:217–22.
8. Greenberg RK, Eagleton M, Mastracci T. Branched endografts for thoracoabdominal aneurysms. J Thorac Cardiovasc Surg. 2010;140:S171–8.
9. Rodd CD, Desigan S, Chesire NJ, Jenkins MP, Hamady M. The suitability of thoracoabdominal aortic aneurysms for branched and fenestrated stent grafts—and the development of a new scoring method to aid case assessment. Eur J Vasc Endovasc Surg. 2011;41:175–85.
10. Sweet MP, Hiramoto JS, Park KH, Reilly LM, Chuter TM. A standard multi-branched thoracoabdominal stent-graft for endovascular aneurysm repair. J Endovasc Ther. 2009;16:359–64.
11. Ohrlander T, Sonesson B, Ivancev K, Resch T, Dias N, Malina M. The chimney graft: a technique for preserving or rescuing aortic branch vessels in stent-graft sealing zones. J Endovasc Ther. 2008;15(4):427–32.
12. Oderich GS, Fatima J, Gloviczki P. Stent graft modification with mini-cuff reinforced fenestrations for urgent repair of thoracoabdominal aortic aneurysms. J Vasc Surg. 2011 Nov;54(5):1522–6.
13. Quinones-Baldrich WJ, Panetta TF, Vescera CL, Kashyap VS. Repair of type IV thoracoabdominal aneurysm with a combined endovascular and surgical approach. J Vasc Surg. 1999;30(3):555–60.
14. Chaikof EL, Fillinger MF, Matsumura JS, Rutherford RB, White GH, Blakensteijn JD, et al. Identifying and grading factors that modify the outcome of endovascular aortic aneurysm repair. J Vasc Surg. 2002;35:1061–6.
15. Drinkwater SL, Goebells A, Haydar A, Bourke P, Brown L, Hamady M, et al. The incidence of spinal cord ischemia following thoracic and thoracoabdominal endovascular intervention. Eur J Vasc Endovasc Surg. 2010;40:729–35.
16. Lachat M, Mayer D, Criado FJ, Pfammatter T, Rancic Z, Genoni M, et al. New technique to facilitate renal revascularization with use of telescoping self-expanding stent grafts: VORTEC. Vascular. 2008;16(2):69–72.

17. Quinones-Baldrich W, Jimenez JC, DeRubertis B, Moore WS. Combined endovascular and surgical approach (CESA) to thoracoabdominal aortic pathology: a 10-year experience. J Vasc Surg. 2009;49:1125–34.
18. Patel HJ, Upchurch GR, Eliason JL, Criado E, Rectenwald J, Williams DM, et al. Hybrid debranching with endovascular repair for thoracoabdominal aneurysms: a comparison with open repair. Ann Thorac Surg. 2010;89:1475–81.
19. Resch TA, Greenberg R, Lyden SP, Clair DG, Krajewski L, Kashyap VS, et al. Combined staged procedures for the treatment of thoracoabdominal aneurysms. J Endovasc Ther. 2006; 13:481–9.
20. Black SA, Wolfe JHN, Clark M, Harmady M, Cheshire NJW, Jenkins MP. Complex thoracoabdominal aortic aneurysms: endovascular exclusion with visceral revascularization. J Vasc Surg. 2006;43:1081-9.E HE.
21. Patel R, Conrad MF, Paruchuri V, Kwolek CJ, Chung TK, Cambria RP. Thoracoabdominal aneurysm repair: hybrid versus open repair. J Vasc Surg. 2009;50(1):15–22.
22. Chiesa R, Tshomba Y, Melissano G, Marone EM, Bertoglio L, Setacci F, et al. Hybrid approach to thoracoabdominal aortic aneurysms in patients with prior aortic surgery. J Vasc Surg. 2007;45(6):1128–35.
23. Drinkwater SL, Bockler D, Eckstein H, Cheshire NJ, Kotelis D, Wolf O, et al. The visceral hybrid repair of thoraco-abdominal aortic aneurysms—a collaborative approach. Eur J Vasc Endovasc Surg. 2009;38(5):578–85.
24. Lee WA, Brown MP, Martin TD, Seeger JM, Huber TS. Early results after staged hybrid repair of thoracoabdominal aortic aneurysms. J Am Coll Surg. 2007;205(3):420–31.
25. Lin PH, Kougias P, Bechara CF, Weakley SM, Bakaeen FG, LeMaire SA, Coselli JS. Clinical outcome of staged versus combined treatment approach of hybrid repair of thoracoabdominal aortic aneurysm with visceral debranching and aortic endograft. Perspect Vasc Surg Endovasc Ther. 2012;24(1):5–13.
26. Bakoyiannis C, Kalles V, Economopoulos K, Georgopoulos S, Tsigris C, Papalambros E. Hybrid techniques in the treatment of thoracoabdominal aortic aneurysms: systematic review. J Endovasc Ther. 2009;16:443.
27. Moulakakis KG, Mylonas SN, Avgerinos E, Kakisis J, Liapis CD. Hybrid open endovascular technique for aortic thoracoabdominal pathology. Circulation. 2011;124:2670.
28. Oderich GS, Farber M, Quinones-Baldrich W, Greenberg R, Upchurch G, Timaran C, et al. Preliminary results of the North American Complex Abdominal Debranching registry. Presented at the 2011 Vascular Annual Meeting, Chicago IL, June 18 2011.

Part V

Arch Branch Incorporation

Current Device Designs to Incorporate Supra-aortic Arch Trunks for Endovascular Repair

32

Muhammad Ali Rana and Gustavo S. Oderich

Introduction

Aortic arch aneurysms may represent distal extension of ascending aortic aneurysms or proximal extension of descending thoracic aortic aneurysms, or occur as isolated aneurysms. Open surgical repair remains the gold standard against which results of novel techniques need to be compared. During the last decade, significant progress has been made in technical refinements and case selection for both hybrid and total endovascular techniques of aortic arch repair. These techniques include open surgical debranching, parallel stent grafting, creation of in situ fenestrations, and the use of manufactured fenestrated and branched stent grafts. Current designs of arch fenestrated and branched stent grafts have changed over the last year with better understanding of the anatomical requirements, risk of embolic stroke, and late branch failure. Most of recent efforts have been devoted to branched stent grafts intended for deployment into zone 0 and zone 2. This chapter summarizes current device designs for total endovascular arch repair.

Arch Anatomy Requirements

There are many technical challenges specific to the aortic arch and supra-aortic trunks. The arch is naturally curved and angulated; it has variable origin of the supra-aortic trunks, and relative short distance to the coronary ostia and aortic valve. Other factors such as coronary grafts, atherosclerotic debris, mechanical aortic valves, and lack of suitable landing zone may prohibit treatment by endovascular techniques. The natural angulation of the arch curvature may render stents difficult to maneuver, making alignment of branches and fenestrations impossible. Because of hostile hemodynamic forces and respiratory motion, long-term durability requires special stent designs resistant to fatigue, fracture, migration, and kinks. During the last decade, lessons learned with fenestrated arch devices led to the preferential use of branches to overcome the challenging arch anatomy.

Historical Perspective

The first use of branched endografts for arch vessel incorporation was reported by Inoue in 1996 (Fig. 32.1b) [1]. The device was a custom-made polyester unibody stent graft with 1–3 side limbs. The proximal fixation was placed in the ascending aorta, and each of the side limbs was snared and pulled into corresponding arch vessel. In a follow-up report, aneurysm exclusion was successfully achieved in 73 % of 15 patients, and failures were attributed to endoleaks and access problems. One patient had an embolic stroke from the operation, and another had spinal cord injury. One-year patient survival was 87 % [2].

In the Western world, Dr. Timothy Chuter and colleagues from the University of California San Francisco performed the first arch repair using a branched endograft in 2003. This was the first modular arch device, which was designed with a branched stent graft to incorporate the innominate artery combined with cervical debranching of the left carotid and subclavian arteries [3]. The stent graft consisted of a proximal bifurcated component with a wide proximal main trunk and two asymmetric distal limbs; a long and narrow limb for the innominate artery and other short and wide limb serve as the overlap zone for the distal aortic component. The bifurcated component was delivered via the right carotid artery, followed by transfemoral cannulation of the aortic limb and delivery of the distal tubular aortic component via femoral approach. The drawback was the need to access the right

M.A. Rana
Division of Vascular Surgery, University of New Mexico, MSC 10 5610, Albuquerque, NM 87131, USA
e-mail: mrana@salud.unm.edu

G.S. Oderich (✉)
Division of Vascular and Endovascular Surgery, Mayo Clinic, 200 First Street SW, Rochester, MN 55905, USA
e-mail: oderich.gustavo@mayo.edu

© Mayo Foundation for Medical Education and Research 2017

G.S. Oderich (ed.), *Endovascular Aortic Repair*, DOI 10.1007/978-3-319-15192-2_32

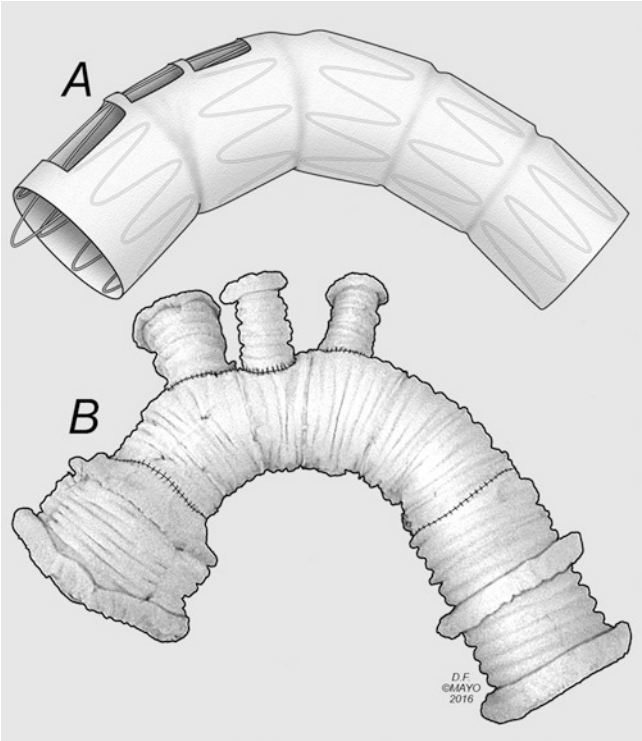


Fig. 32.1 Asian experience with arch devices include pioneering work using the Najuta (**a**) and Inoue arch devices (**b**). By permission of Mayo Foundation for Medical Education and Research. All rights reserved

carotid artery with a large sheath, which often required a conduit. The design was eventually abandoned in favor of newer designs introduced via the femoral approach. Concurrent to the development of arch branch design, Roy Greenberg, Tilo Koebel, and others gained large experience with patient-specific fenestrated arch repair. A major disadvantage of fenestrated approach was the difficulty to orient the device in the aortic arch, which often required more manipulations and resulted in higher risk of stroke.

The design developed by Chuter became the platform for the subsequent generations of specific arch designs by Cook Medical (Bloomington, IN, USA, and Brisbane, Australia). Cherry Abraham and colleagues in 2009 performed the first customized arch multi-branched graft completely delivered via femoral approach. The initial design had external funnel-shaped cuffs, which were then redesigned to completely internal branches. The graft had stainless steel Z stents to seal at both ends with nitinol endoskeleton for the rest of it with polyester graft. The internal branches had internal reinforcing stents. Initial experience reported included seven successful repairs by Abraham et al. and other implants by groups from Cleveland Clinic, UCSF, and London [4].

The currently available and investigational devices for arch vessel incorporation can be broadly divided into those intended for proximal arch (zone 0) or distal arch (zone 2 and less frequently zone 1). Devices are described according to manufacturer.

Kawasumi Najuta Fenestrated Endograft

Najuta endograft (Fig. 32.1a, Kawasumi Laboratories Inc., Tokyo, Japan) is a custom arch fenestrated device and is commercially available in Japan. The design is comprised of longitudinally connected stainless steel Z stent endoskeleton with expanded polytetrafluoroethylene fabric that is sutured only to the ends of the stent framework. The device is designed for zone 0 to 2 deployments and is highly customizable with 21 patterns of fenestration configurations and 64 available patterns of stent frame configuration. The delivery system is also available with three different degrees of precurvature to facilitate delivery and positioning. The device is designed to place large fenestrations across the origins of great vessels without placement of bare metal or covered branch stents. The struts may cross fenestrations, which makes it difficult to place branch stents if intended. This gives rise to the major limitation of the device, which is the inability to treat aneurysms involving the origins of supra-aortic trunks or involving the greater curvature of the arch.

The Najuta endograft was based on initial Japanese experience with mostly surgeon-made stent grafts [5]. Iwakoshi et al. recently reported the initial experience with the current generation Najuta graft [6]. A total of 32 patients were treated at three centers in Japan. Technical success was 91 % with failures attributed to endoleaks. Operative complications included retrograde type A dissections in two patients, stroke in one patient, spinal cord injury in one patient, and celiac ischemia in one patient. There were two branch occlusions (left common carotid in one and left subclavian in other) noticed at 2 weeks postoperative due to endograft infolding. No device migration was seen. Overall patency of supra-aortic trunks was 97 % at 3 years. Freedom from aneurysm growth and freedom from re-intervention at 3 years was 85 % and 84 %, respectively.

Cook Medical

The Cook Medical arch platform has evolved since the first clinical experience with the arch device to patient-specific designs using fenestrations and scallops or inner branches (Fig. 32.2). Helical branches may also prove to be beneficial in the aortic arch, particularly for retrograde incorporation of the left subclavian artery.

Fenestrated Stent Grafts

Patient-specific arch devices can be manufactured with combinations of fenestrations and scallops, and preloaded catheters to facilitate alignment with supra-aortic trunks. The largest experience has been with zone 1 and zone 2 deployments and incorporation of the left common carotid and left subclavian arteries, respectively. The devices are designed using polyester grafts with stainless steel Z stents.

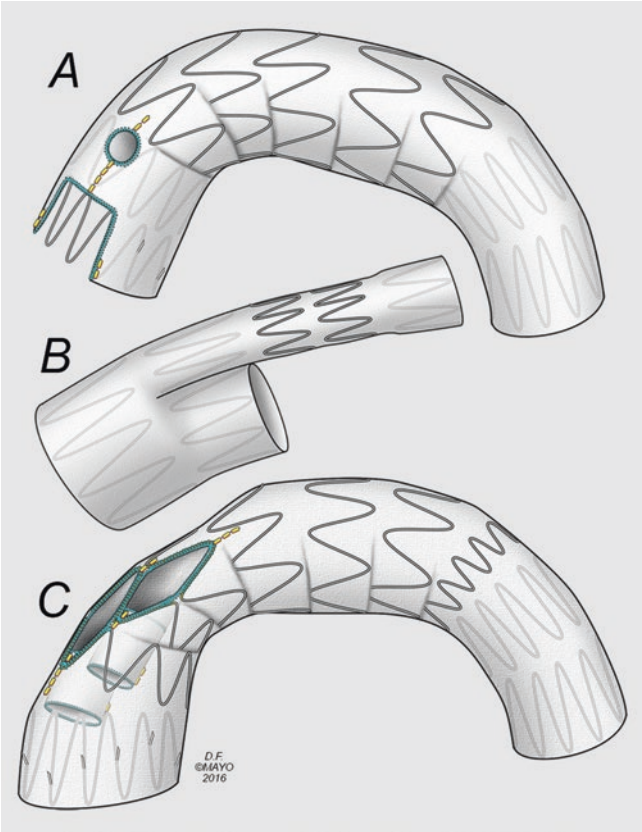


Fig. 32.2 Cook Medical platform includes patient-specific fenestrated devices (**a**), the first branch device performed by Chuter in 2003 (**b**), and the novel inner branch device (**c**). By permission of Mayo Foundation for Medical Education and Research. All rights reserved

Inner Branches

Since the first description of branch device by Chuter and the first multi-branch device placed by Abraham, significant improvements have been made based on clinical experience. The Cook A-branched arch endograft is the third-generation arch design developed by Cook Medical (Brisbane, Australia, and Bloomington, IN, USA). The device is available in select centers under clinical investigation. It is a custom-made design for zone 0 deployment with one or two proximal and two distal sealing stents. There are two internal branches with large diamond-shaped external openings that occupy the central narrower portion of the graft. The delivery system is equipped with pre-curved cannula with a nitinol wire securing the outer curve of the stent graft with the inner cannula to facilitate alignment.

The device is constructed using low-profile fabric. The fabric is polyester similar to the standard TX2 and Zenith AAA devices; however the weave is thinner and altered such that it is of higher density. This fabric is identical to Alpha Thoracic low profile (LP) endograft. The stents are similarly redesigned. Although the proximal and/or distal stent(s) may be stainless steel coupled with (or without) barbs, the stents in the body are constructed of nitinol in a manner similar to that in the abdominal and thoracic low profile devices. This enables them to accommodate the marked tortuosity associated with standard arch anatomy. The supra-aortic trunk branches are also constructed of the LP graft material and attached to the aortic device internally using polyester suture. Nitinol rings are used within the branches to provide radial support and to help stabilize the joint with mating devices in a manner analogous to those used for branches employed in the thoracoabdominal and iliac vasculatures.

Preloaded catheters and wires are optionally included with this device and are loaded in a fashion similar to the helical and iliac branches. However, the exit point of the preloaded wire may be placed in a variable location depending upon the individual patient anatomy. The catheter/wire combination may arise from either the first or second internal side-branch opening or just distal to the second side-branch opening. Such an approach may be necessary in the setting of marked tortuosity of the innominate, subclavian, or carotid arteries and in aortic dissections.

The arch branch device has trigger wires attaching the proximal and distal ends of the device to the delivery system. In addition to the optional use of diameter-reducing ties, cannula wires are used to help with orientation along the greater curvature of the arch and to aid with the sequence of stent deployment proximally for alignment in the proximal thoracic aorta. The ascending thoracic devices may be coupled with the arch branch device whereby it would be deployed proximally, prior to, or following the arch branch device if deemed necessary. The mating distal devices may be standard TX2 or Alpha devices or ancillary components that will be used depending upon the requisite anatomy.

WL Gore Thoracic Branch Endoprosthesis (TBE)

The Gore TAG Thoracic Branch Endoprosthesis (Fig. 32.3, WL Gore, Flagstaff, AZ) is an off-the-shelf stent graft designed with an inner portal to incorporate a single arch vessel, either the innominate artery (zone 0) or the left subclavian artery (zone 2) and less frequently the left common carotid artery (zone 1). The device is currently undergoing clinical investigation in the United States. The aortic component is based on the Gore C-TAG platform (expanded polytetrafluoroethylene supported with self-expanding nitinol stents) with diameters ranging from 21 to 53 mm. It is built with a precannulated internal retrograde branch, which is either 8 mm (zone 2) or 12 mm (zone 0). There are sealing cuffs on both ends with a partially uncovered stent proximally for wall apposition. The separate side branch is available in 8–20 mm diameters and is heparin bonded to improve patency. The overlapping segment of the side branch has retrograde anchors to prevent migration with a tapered more flexible segment in the middle to accommodate arch movement. The distal segment has reenforced sealing cuffs for durable distal seal.

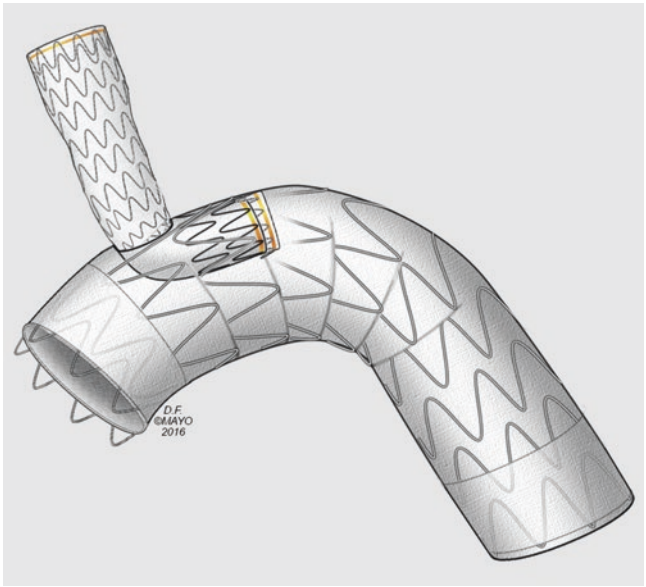


Fig. 32.3 WL Gore Thoracic Branch Endoprosthesis. By permission of Mayo Foundation for Medical Education and Research. All rights reserved

The main device is delivered over two wires, one in the aorta and the other in the arch branch to be incorporated. The wire for the side branch can be snared for a through and through access to help with alignment in hostile anatomy. There is also optional aortic extender to extend proximally if needed.

Medtronic Mona LSA

The Valiant Mona LSA stent graft (Fig. 32.4, Medtronic, Inc., Minneapolis, MN) is a modular system modified from Valiant Captivia. The design is currently undergoing second-phase multicenter investigational feasibility study in the United States. The aortic component has low-profile polyester sewn to nitinol exoskeleton with a proximal bare stent. It has a single "volcano"-type pre-cannulated flexible externally oriented cuff. The cuff itself is composed of high-density polyester fabric with a mobile external connector stent and two platinum-iridium markers. It is designed to pivot to allow 20–30° of misalignment. The separate side-branch component is conformed with a proximal flare with an intended 1 cm overlap to enhance proximal seal. The aortic component diameter ranges from 30 to 46 mm, and the branch stent has available diameters of 10, 12, and 14 mm.

The IFU for the investigational Mona LSA device mandates through and through brachial-femoral access. The device is delivered over the aortic wire. Prior to deployment, a separate wire is advanced via the pre-cannulated branch lumen and is snared along the outer curvature via brachial access. The device is then aligned and deployed with simultaneous traction on the brachial-femoral wire to position the branch at the subclavian orifice. The branch graft is then advanced and deployed over the subclavian wire.

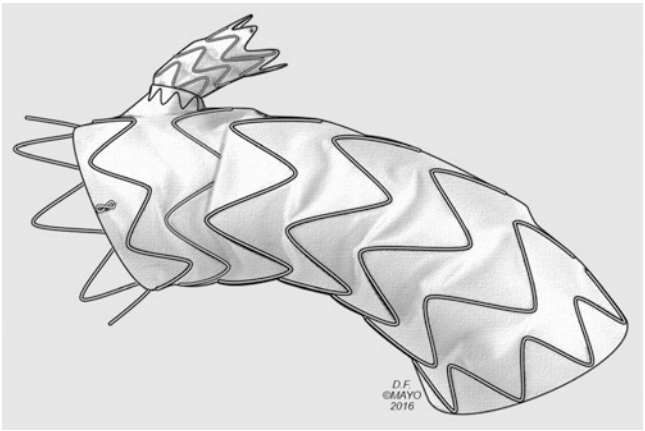


Fig. 32.4 Medtronic Mona LSA. By permission of Mayo Foundation for Medical Education and Research. All rights reserved

Bolton Relay Plus Thoracic Arch System

The Bolton Medical arch branch device (Fig. 32.5, Bolton Medical, Barcelona, Spain, and Sunrise, FL, USA) is a custom-made branched design based on the Relay NBS Plus platform. The device is currently available in European Union but is not yet being studied in the United States. The stent graft is comprised of nitinol exoskeleton sutured to polyester fabric. It is intended for zone 0 deployment with options of 1 or 2 antegrade internal branches. The device is equipped with a dual sheath design along with a pre-curved cannula and a proximal capture mechanism to facilitate alignment. The internal branches have anchors for a locking mechanism to prevent branch migration. The device comes in diameters ranging from 22 to 46 mm. It is oriented and advanced on an aortic wire and branches are cannulated from retrograde access via cervical carotid and/or brachial access.

The initial experience with the device was presented at the ICI meeting in 2015 but has not been published (http://2015.icimeeting.com/wp-content/uploads/2016/01/0843-Riambau-Hall-A-tue.pdf). Single branch device was successfully implanted in eight patients with 25 % perioperative mortality and 87.5 % freedom from endoleak. The dual-branch stent graft was used in 26 patients with 100 % operative success, 11.5 % perioperative mortality, and 92 % freedom from endoleak. One patient each in single- and dual-branch groups had a stroke.

Frozen Elephant Trunk Devices

There are two hybrid prosthesis commercially available in Europe specific for frozen elephant trunks, the JOTEC E-vita Open Plus prosthesis (Fig. 32.6a, JOTEC GmbH, Hechingen, Germany) and Terumo Thoraflex Hybrid graft (Fig. 32.6b, Terumo Corporation, Tokyo, Japan, and Somerset, NJ, USA).



Fig. 32.5 Bolton arch device with double branches. By permission of Mayo Foundation for Medical Education and Research. All rights reserved

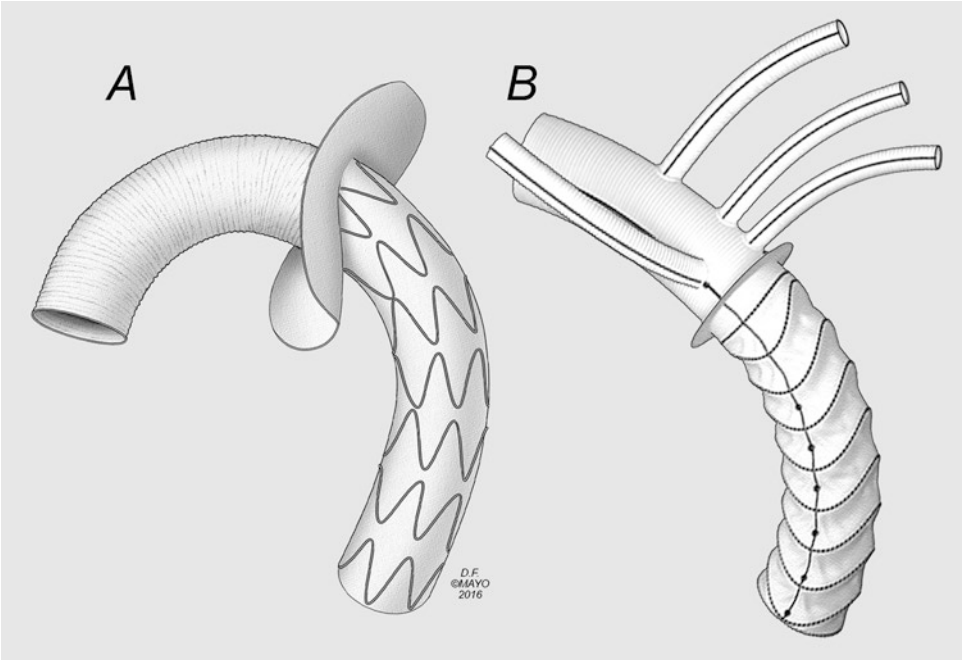


Fig. 32.6 JOTEC E-vita Open Plus prosthesis (**a**) and Terumo Thoraflex Hybrid arch graft (**b**). By permission of Mayo Foundation for Medical Education and Research. All rights reserved

The E-vita Open Plus hybrid prosthesis has a woven polyester graft attached to the stent graft based on JOTEC E-vita thoracic endograft. The Terumo Thoraflex Hybrid graft combines the Gelweave Siena woven polyester multi-branched graft pre-sewn to a distal stent graft. Both devices are equipped with suture collars for native aorta to graft anastomosis. None of these grafts are currently available in the United States, and the frozen elephant trunks are performed with available thoracic stent grafts with techniques detailed in Chaps. 36 and 37.

References

1. Inoue K, Sato M, Iwase T, Yoshida Y, Tanaka T, Tamaki S, et al. Clinical endovascular placement of branched graft for type B aortic dissection. J Thorac Cardiovasc Surg. 1996;112(4):1111–3.
2. Inoue K, Hosokawa H, Iwase T, Sato M, Yoshida Y, Ueno K, et al. Aortic arch reconstruction by transluminally placed endovascular branched stent graft. Circulation. 1999;100(19 Suppl):II316–21.
3. Chuter TA, Schneider DB, Reilly LM, Lobo EP, Messina LM. Modular branched stent graft for endovascular repair of aortic arch aneurysm and dissection. J Vasc Surg. 2003;38(4):859–63.

4. Lioupis C, Abraham CZ. Results and challenges for the endovascular repair of arch aneurysms. Perspect Vasc Surg Endovasc Ther. 2011;23(3):202–13.
5. Azuma T, Yokoi Y, Yamazaki K. The next generation of fenestrated endografts: results of a clinical trial to support an expanded indication for aortic arch aneurysm treatment. Eur J Cardiothorac Surg. 2013;44(2):e156-63; discussion e63.
6. Iwakoshi S, Ichihashi S, Itoh H, Tabayashi N, Sakaguchi S, Yoshida T, et al. Clinical outcomes of thoracic endovascular aneurysm repair using commercially available fenestrated stent-graft (Najuta endograft). J Vasc Surg. 2015;62(6):1473–8.

Technical Aspects and Results of Branched Endografts for Repair of Aortic Arch Aneurysms

33

Charles P.E. Milne, Stéphan Haulon, and Gustavo S. Oderich

Introduction

Open conventional repair of aortic arch aneurysms remains the gold standard to which novel endovascular techniques need to be compared. This option is primarily reserved for good-risk patients, but the need for median sternotomy, cardiopulmonary bypass, and deep hypothermic circulatory arrest limit its use in the elderly or high-risk patient. Endovascular techniques have evolved to allow less invasive treatment options, potentially decreasing the mortality and morbidity of these procedures. Endovascular techniques include hybrid procedures, "chimney" or parallel stent-grafts, in situ fenestrations, and fenestrated and branched stent-grafts [1]. In recent years, the successful application of fenestrated and branched endograft technology in the visceral aortic segment has been expanded to include the aortic arch. The largest experience in the western hemisphere has been reported using a third-generation arch branch stent-graft developed by Cook Medical. Other companies have also developed novel designs with more limited clinical experience. This chapter focuses on patient selection, techniques of implantation, and results with aortic arch fenestrated and branched endografts.

C.P.E. Milne
Department of Surgery, The Alfred Hospital, Monash University, Melbourne, VIC 3004, Australia

Aortic Centre, Hôpital Cardiologique, Centre Hospitalier Régional Universitaire de Lille (CHRU), Lille 59000, France

S. Haulon (✉)
Aortic Centre, Hôpital Cardiologique, Centre Hospitalier Régional Universitaire de Lille (CHRU), Lille 59000, France
e-mail: stephan.haulon@chru-lille.fr

G.S. Oderich
Division of Vascular and Endovascular Surgery, Department of Surgery Mayo Clinic, 200 First Street SW, Rochester, MN 55905, USA
e-mail: oderich.gustavo@mayo.edu

Important Considerations for Endovascular Arch Repair

A number of challenges exist specific to endovascular procedures in the aortic arch, including seal zone, device durability, the aortic valve, device alignment, stroke, and mortality [2].

Seal Zone

Adequate endograft seal zones are vital to ensure long-term success [3]. Being strict with seal zone criteria is mandatory to achieve technical success and long-term durability. In the aortic arch, the proximal seal zone should consist of parallel walls in relatively "healthy" aorta, with a diameter <38 mm. The proximal neck should be at least 25 mm in length and free from excessive thrombus or calcification. Aortic angulation should be <60° [2]. For cases involving an a-branch stent endograft (Cook Medical), with proximal seal in the ascending aorta, we recommend a seal zone of at least 40 mm in length.

Device Durability

Long-term durability data is available for standard thoracic and abdominal, and for fenestrated and branched endografts in the visceral aortic segment, showing that these devices are a durable option [4]. Clinical data for aortic arch devices, however, is limited to a few centers in Europe, the USA and Japan, with early to midterm results. Indeed the arch represents a new horizon in terms of physiologic loads that will challenge endograft design. Increased aortic pulsatility along with significant motion of the supra-aortic vessels during respiration may increase complications related to graft wear and fatigue, including stent fracture and kinking [2].

© Mayo Foundation for Medical Education and Research 2017

G.S. Oderich (ed.), *Endovascular Aortic Repair*, DOI 10.1007/978-3-319-15192-2_33

Aortic Valve

Endovascular arch repair may require passage of guidewires, catheters, and the tip of the delivery system through the aortic valve, adding the potential risk of damage to the aortic valve or left ventricle. Graft design features must incorporate shorter, lower-profile, more flexible nose cones on the delivery system, which will be better tolerated by the aortic valve. Until recently, previous aortic valve replacement (especially mechanical) was considered a contraindication to such procedures [5].

Device Alignment

Device positioning and alignment in the aortic arch is vital to ensure that the coronary arteries and supra-aortic trunks are preserved during deployment. As the arch is remote from femoral access, precise control of the device is limited. Therefore, arch endografts should be designed with specific "auto-alignment" features.

Stroke

Stroke rates of >6 % have been reported for endovascular repair of the descending thoracic aorta [6]. Major contributing factors include manipulation of guidewires, catheters, and the device itself in the aortic arch; air emboli released from the delivery system; and coverage of branch vessels [2]. Evolution of techniques and devices should include strict efforts to minimize the risk of stroke.

Mortality

The rate of perioperative and 30-day device-related mortality remains significant for endovascular aortic arch repair, although results are improving with increasing clinical experience and better patient selection in high-volume centers [7]. It is important to consider that these procedures are currently performed primarily in patients considered unfit for open surgery. To minimize the perioperative complications and mortality, these procedures should be performed in high-volume, specialized centers, where complex open and endovascular aortic procedures are performed routinely.

Endograft Design

Scalloped and Fenestrated Endografts

Scalloped and fenestrated endografts can be used to extend a seal zone from the descending thoracic aorta into the aortic arch. These devices are ideally suited to aneurysms involving the descending thoracic aorta, which arise close to the left subclavian artery (LSA). The use of a scallop or fenestration proximally allows for a single supra-aortic trunk (e.g., LSA) to continue to be perfused while extending the seal zone more proximally. Concerns remain over the use of scallops in a seal zone, given that a large portion of the proximal sealing stent remains uncovered [2]. Proximal seal can be improved by implanting a covered balloon-expandable bridging stent through a fenestration.

The technical demands of the procedure increase significantly when multiple fenestrations are used. Meticulous preoperative planning is needed to ensure that fenestrations line up with the supra-aortic trunks. Because the arch is curved, it is difficult to predict exactly how the device will be positioned and thus the location of fenestrations when the endograft is deployed. Also, as devices are delivered from a femoral approach with a long delivery system, they are difficult to maneuver precisely when in the arch [2]. For these reasons, arch devices with multiple fenestrations are relatively unforgiving if problems arise with misalignment of target vessels. To overcome this issue, a guidewire advanced in a preloaded catheter positioned through a fenestration can be snared from a supra-aortic trunk. Tension on this through-and-through wire while deploying the fenestrated endograft will ensure adequate positioning of the fenestration. Endovascular maneuvers in the arch to snare the wire, which can wrap around the nose cone of the delivery system, and tension on the wire increase the stroke risk.

Branched Endografts

Branched endografts have emerged in recent years offering advantages over arch devices with multiple fenestrations. Modern arch endografts have branches located in a tapered, narrow segment of the endograft body. This ensures that the branches are positioned away from the origin of target vessels, simplifying the cannulation and allowing for misalignment with the target vessels.

The first series describing the use of branched endograft repair for treatment of arch aneurysms was reported by Inoue et al. in 1999 [8]. This demonstrated the technical feasibility of the procedure, but high procedure-related mortality (23 %) and severe complication rate (17 %) include stroke, dissection, and persistent endoleak [2]. The device itself had limitations, most importantly *externally* located side branches, which complicated cannulation and placement of covered stents.

Several models of arch branched endografts have been trialed since (Fig. 33.1). In recent years, the a-branch stent-graft from Cook Medical (Bloomington, IN) has been used in select high-volume centers in Europe, the USA, and Canada (Fig. 33.2). This is a third-generation device, which was designed to address specific challenges encountered with endovascular procedures in the aortic arch and lessons learned from earlier devices.

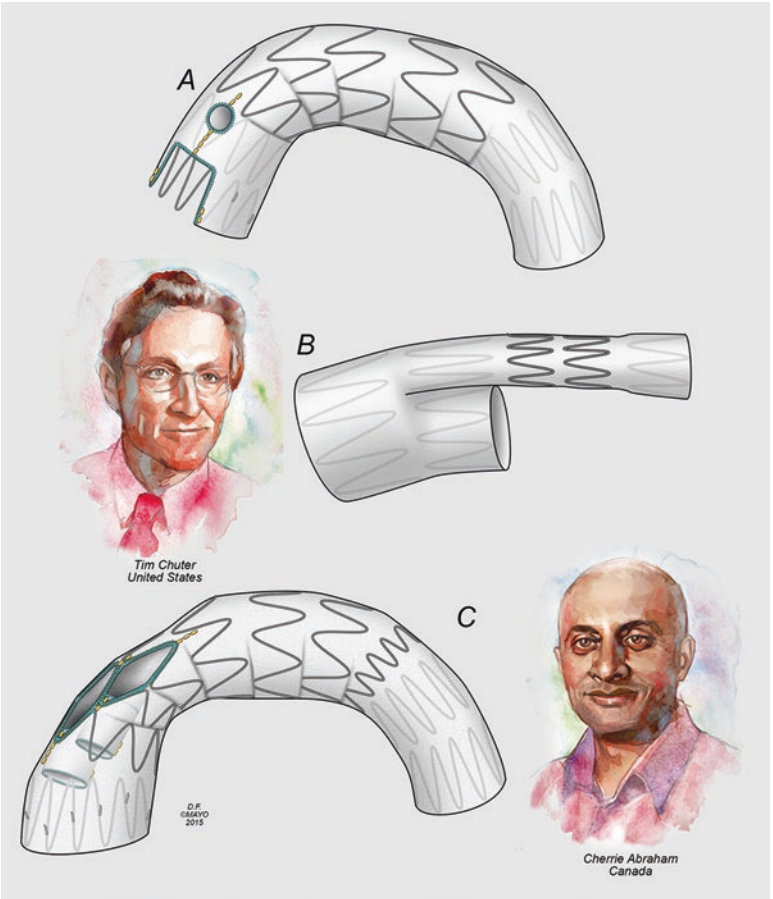


Fig. 33.1 Evolution of fenestrated and branched stent-grafts using the Cook Zenith stent-graft platform. Scalloped and fenestrated stent-grafts (**a**) and the first-generation arch branch stent graft (**b**) have led to the development of the a-branch stent graft (**c**), with inner branches with diamond-shaped fenestrations to facilitate catheterization. By permission of Mayo Foundation for Medical Education and Research. All rights reserved

A-Branch Stent-Graft (Cook Medical)

The device design varies significantly from early arch branched endografts. It is designed to seal in the ascending aorta, with one or two proximal sealing stents and active fixation with circumferential barbs (Fig. 33.2). There are two distal sealing stents, but often the main body requires a distal extension to completely exclude an extensive aneurysm. The delivery system is pre-curved with a hydrophilic sheath. The nose cone is short, flexible, and tapered, which allows for it to be advanced into the left ventricle.

The device uses two *internalized* ("inner") side branches, which are flush with the wall of the endograft, creating a smooth external contour. The branches have large diamond-shaped openings at their distal end to facilitate cannulation and to better adapt to misalignment. The number of inner branches is limited to two in order to simplify the procedure and allow for more flexibility of device alignment. The diameter is normally 12 mm for the first branch, which is intended for the innominate artery, and 8 mm for the second branch, which is intended for the left common carotid artery (CCA). In normal aortic arch anatomy, the presence of only two branches necessitates a left common carotid artery (CCA)-LSA transposition or bypass prior to deployment of the graft.

The proximal and distal ends of the device are wide and flexible, while the middle section of the graft (housing the branches) is narrow. This ensures that the distal ends of the side branches are separated from the origins of the supra-aortic trunks, allowing for easier cannulation of the branches, but also ongoing perigraft flow (and perfusion of the supra-aortic trunks) during the procedure.

The inner branches are located on the outer curvature of the graft, which is attached to the inner cannula of the delivery system with a nitinol wire. This acts as a rotational "auto-alignment" feature of the device, which greatly facilitates alignment of the branches with the outer curvature of the arch. Markers are placed on the proximal and distal ends of

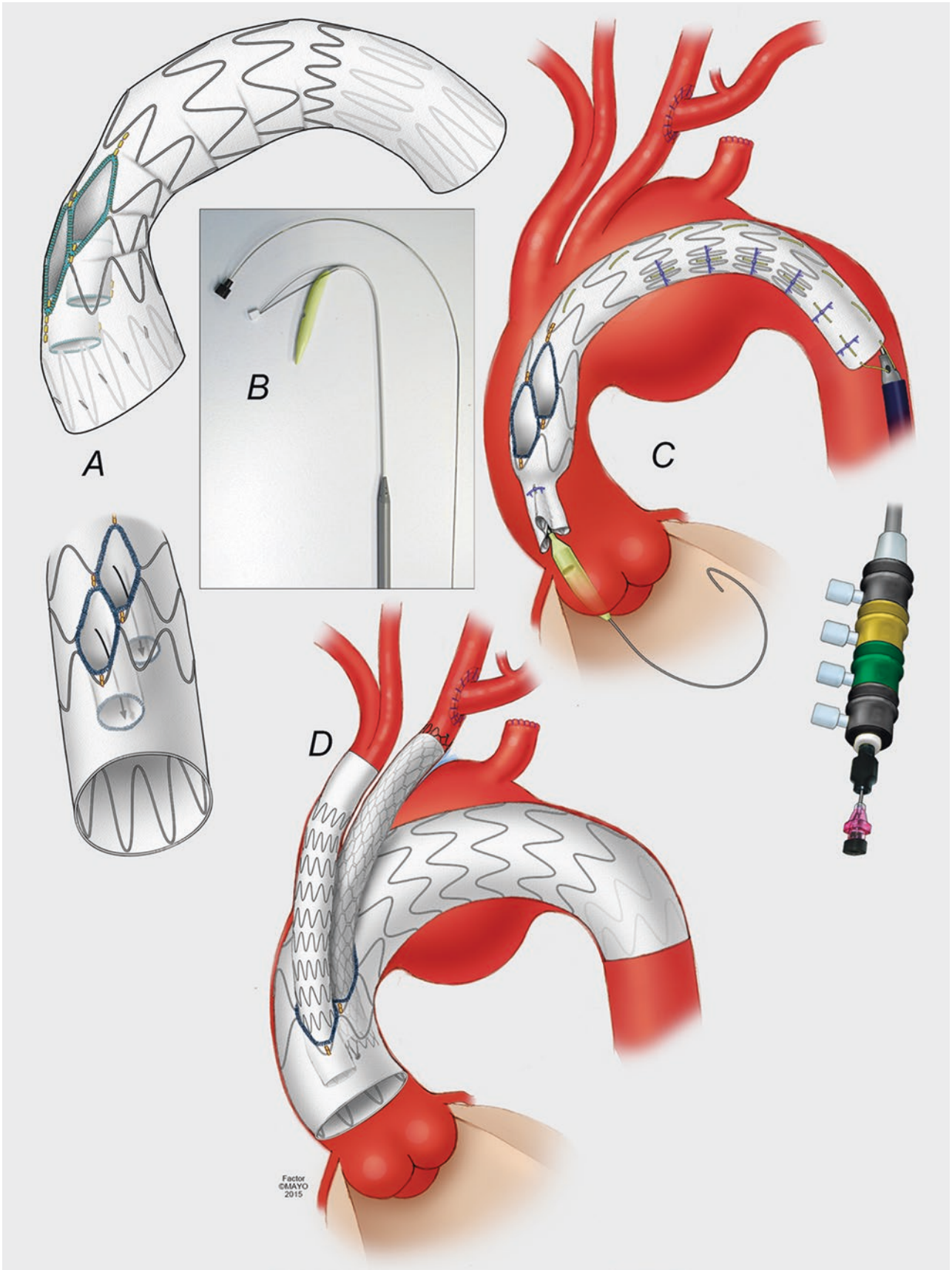


Fig. 33.2 Third-generation branched device with two inner branches, tapered component, and diamond-shaped fenestrations (**a**). The prebent delivery system with a notch in the outer curvature (**b**) to facilitate orientation in the aortic arch. A stepwise trigger wire mechanism allows controlled, precise deployment and self-orientation of the device with the diamonds facing the outer curvature of the aorta (**c**). The inner branches are bridged to the innominate and left common carotid arteries with self-expandable stents (**d**). By permission of Mayo Foundation for Medical Education and Research. All rights reserved

Table 33.1 Anatomic and physiologic criteria for selection of patients undergoing inner-branched aortic arch endograft repair [7]

Anatomic criteria	Physiologic criteria[a]
Arch aneurysm or chronic dissection	Minimum 2-year life expectancy
Suitable iliac access to accommodate 22–24-Fr sheaths	Negative cardiac stress test
	If positive, cardiology consult and clearance required
No prior aortic valve replacement (biological or mechanical)	
	No stroke or myocardial infarction within 12 months
Ascending aorta:	
≥50-mm length (sinotubular junction to origin of innominate artery)	No class III or IV congestive cardiac failure (NYHA criteria)
≥40-mm sealing zone length	
≤38-mm diameter	No significant carotid bifurcation disease (<70 %, NASCET criteria)
Innominate artery:	eGFR ≥45 ml/min/1.73 m^2
≤20-mm diameter	
≥20-mm sealing zone length	

[a]Exceptions to some physiologic criteria may occur based on surgeon discretion and anesthetic review

the branches to further aid positioning under fluoroscopy and subsequent cannulation.

A total of four nitinol wires attach to the graft and delivery system, which are removed using four handles located in sequence on the delivery system handle. In addition to the "greater curvature" wire, the other wires provide proximal and distal attachment of the endograft to the delivery system, a "pro-form" shape to adapt to the arch curvature, and release of the diameter-reducing ties.

Stenting of the innominate artery is done using a modified Zenith iliac limb component (Cook Medical), which is delivered with a 14F delivery system via the right common carotid or axillary artery. For the LCCA, a self-expanding Fluency covered stent (BARD Inc., Tempe, AZ) is used to bridge the distal inner branch.

Patient Selection

Patients diagnosed with an aortic arch aneurysm with a minimum diameter of 5.5 cm who are deemed unfit for surgery and have appropriate anatomy to accommodate a custom-designed a-branch stent-graft are considered potential candidates for total endovascular repair of the aortic arch. Important considerations are to avoid excessive aortic debris and to limit repair to patients with aortic diameter <38 mm, potentially decreasing issues related to retrograde aortic dissection or late progression of aortic disease with ectatic necks. Table 33.1 summarizes the anatomic and physiologic criterion used in the global review of branched endograft experience [7].

Technique

Preparation and Setup

Our center performs all complex aortic procedures in a hybrid operating suite with the assistance of fusion imaging. Fusion is set by acquiring AP and lateral fluoroscopic images of osseous landmarks, which are registered to the preoperative CT angiogram [9].

The patient is positioned supine with both upper extremities tucked by the side. The anesthetic team ideally achieves central venous access in the left upper internal jugular or right subclavian vein. Blood pressure is monitored using a right and/or left radial arterial line.

A diagram of the aortic arch anatomy and endoprosthesis is affixed to the LED screen adjacent to the operating table to allow easy reference throughout the procedure. The graft component sizes and optimal angles for visualization of the proximal landing zones for the IA and left CCA are labeled, which are established preoperatively using 3D workstation analysis. Throughout the procedure, meticulous and thorough flushing of the endovascular equipment is performed to ensure that no air bubbles are introduced into the aortic arch.

Subclavian Artery Revascularization

A left CCA-LSA transposition or bypass is performed prior to the arch branched endograft repair. Techniques of subclavian revascularization have been described in detail in Chap.

36. The revascularization can be done at the same time as the arch repair, or in a staged fashion, which is our preferred option. If a bypass is performed, the most proximal aspect of the LSA should be occluded proximal to the vertebral artery origin (coils or Amplatzer plug) at the completion of the endovascular repair, avoiding type II endoleak and the risk of occlusion of the bypass by competitive flow if a staged approach is planned. If the procedure is done in a single stage, our preference is to leave the proximal subclavian artery open in case access to the internal branch from the left CCA is not possible, in which case we would switch to LSA access. This has not yet been required in our experience.

Arterial Access

Arterial access is obtained in three locations. Our preference is to surgically expose the femoral arteries for delivery of the main device to the aortic arch. The side is selected based on which is best to accommodate a 22–24-Fr delivery sheath. For the innominate artery, our preference is to expose the right CCA. This allows delivery of the modified iliac limb component between the proximal (first) inner side branch and the IA, while the CCA is clamped to avoid embolization of air or debris.

Alternatively, an axillary approach can be used if the carotid territory is hostile because of occlusive disease, previous carotid surgery, or radiotherapy, but angles are less favorable for delivery of the bridging stent. Finally, a left open axillary approach is used to deliver the covered bridging stent between the distal (second) internal side branch and the left CCA. In this case, the bridging stent must be delivered via the LSA-left CCA transposition or bypass. If the transposition or bypass is performed at the same time as the arch branched stent-graft, direct open left CCA access can instead be used.

A method of cardiac-output reduction is required for the procedure. Our preference is to use rapid cardiac pacing to achieve this (Fig. 33.3). Open common femoral vein access is gained on the same side as the open femoral artery exposure. Right internal jugular vein access can also be easily gained through the right cervicotomy. A transvenous pacing probe is introduced and positioned in the apex of the right ventricle, and a test run of rapid pacing is performed.

Establishing the Delivery Platform

Systemic heparin is administered at a dose of 100 IU/kg. The target ACT throughout the procedure is >300 s. Right CCA access is obtained using a short 5-Fr sheath. A soft, angled hydrophilic guidewire is advanced into the ascending aorta to allow delivery of a pigtail side-hole catheter. This is advanced to make contact with the aortic valve and connected to the contrast power injector. The line is checked to ensure absence of air bubbles.

Left axillary artery access is obtained using a short 10-Fr sheath. The hydrophilic guidewire is navigated through the LSA-left CCA transposition or bypass and advanced into the ascending aorta. Femoral access is obtained using a short sheath. A long 260-cm hydrophilic guidewire and 5F 100-cm vertebral catheter are advanced into the ascending aorta. The guidewire is used to gently navigate through the aortic valve and into the left ventricle. The catheter is advanced into the left ventricle, and the wire is exchanged for a curly stiff Lunderquist (Cook Medical) wire, which acts as the platform for delivery of the branched device. The floppy tip of this wire should sit in the apex of the left ventricle. The position of the tip must be visualized during every step of the procedure so that inadvertent left ventricular perforation does not occur.

The gantry is positioned at the predetermined optimal viewing angle for deployment of the endoprosthesis, and an angiogram performed (25 ml at 10 ml/s). The fusion mask is adjusted to correspond to the angiogram.

Delivery and Deployment of the Branched Stent-Graft

The delivery system for the endoprosthesis is prepared by flushing the delivery sheath and inner lumen of the inner cannula. We use at least 120 ml (six 20-ml syringes) of heparin/saline solution to flush the delivery sheath to ensure the absence of air bubbles. Under fluoroscopy, the radiopaque markers on the endoprosthesis are checked outside the patient. The short femoral sheath is removed, and the device is inserted over the Lunderquist wire and positioned in the ascending aorta. In order to position the proximal sealing stent at the level of the origin of the ascending aorta, the tapered short tip of the delivery system must be advanced through the aortic valve and into the left ventricle.

A second angiogram is performed to check the position of the coronary arteries and supra-aortic trunks relative to the markers on the endoprosthesis. The markers for the inner branches are positioned upstream of the IA and left CCA.

Deployment of the graft is performed next under rapid pacing. The graft is unsheathed in its entirety and the first three trigger wires are pulled from the delivery device (Fig. 33.4a). This must be performed quickly so that normal cardiac output can be resumed. The stiff guidewire and tapered delivery tip are then withdrawn from the left ventricle and positioned within the distal end of the endograft. The fourth trigger wire is intentionally left in place as it is attached to the distal end of the endoprosthesis. In cases of difficulty with cannulation of the inner branches, it can be

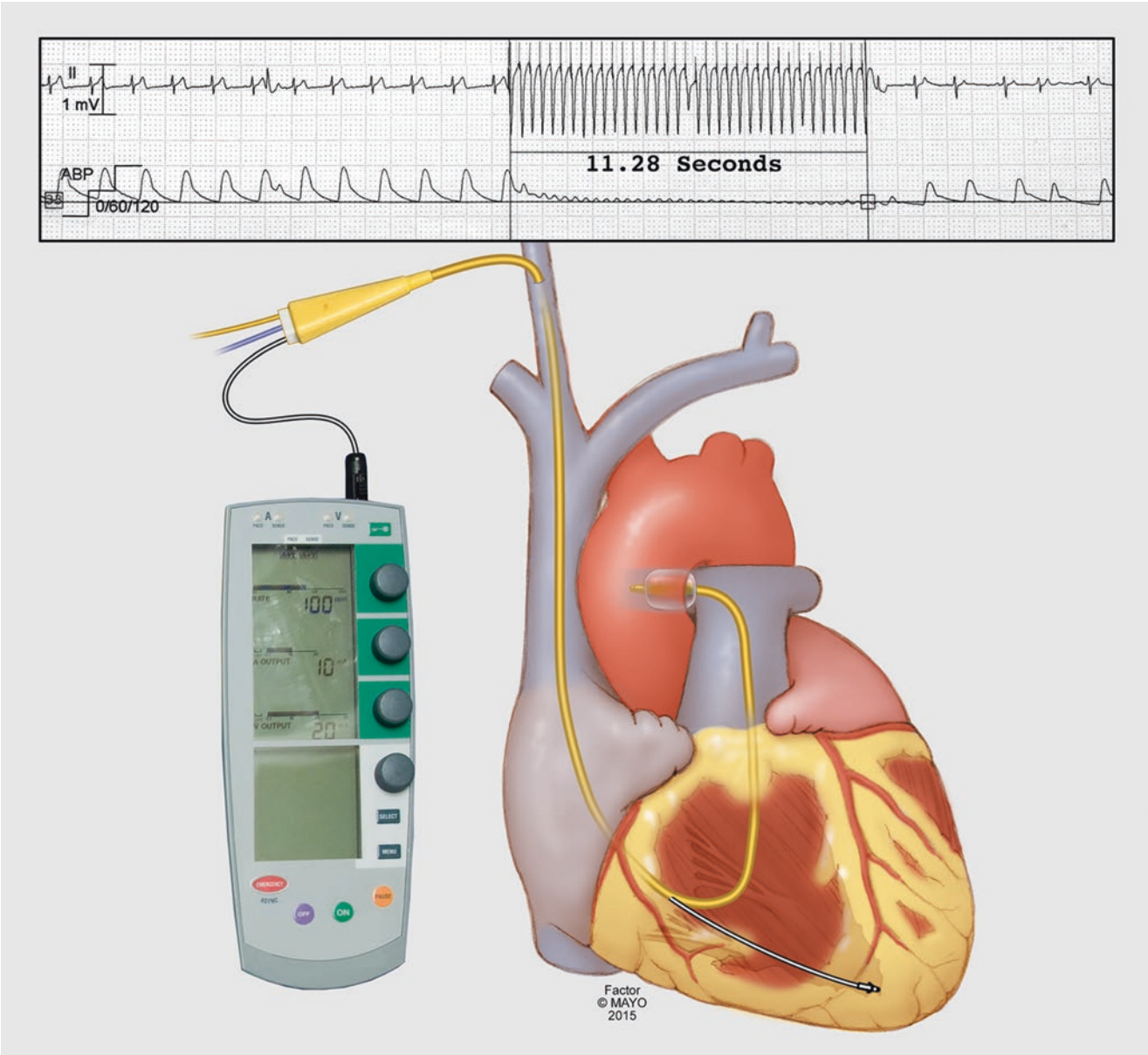


Fig. 33.3 Rapid ventricular pacing is used for deployment of the aortic arch device into Zone 0. Note the short interval of 11 s with target heart rate of 160 beats per minute and rapid control of mean arterial pressure.

By permission of Mayo Foundation for Medical Education and Research. All rights reserved

used to provide traction on the endoprosthesis and move it away from the greater curvature of the arch to provide more working space.

Innominate Artery Bridging Stent

After removal of the pigtail catheter, the first inner branch is cannulated from the right CCA access using a 180-cm 0.035 soft, angled hydrophilic guidewire and 5F 65-cm KMP catheter (Fig. 33.4b). The right common carotid artery may be clamped during this portion of the procedure. The guidewire and catheter are positioned in the left ventricle. The soft, angled hydrophilic guidewire is replaced by a 180-cm 0.035 J-tipped Rosen wire. The catheter is then exchanged for a 12×40-mm noncompliant balloon, which is inflated in the first inner branch (Fig. 33.4c). Multiple fluoroscopic views are obtained to ensure the guidewire is correctly positioned inside the branch, and not between the walls of the aorta and the endograft. A retrograde angiogram is performed

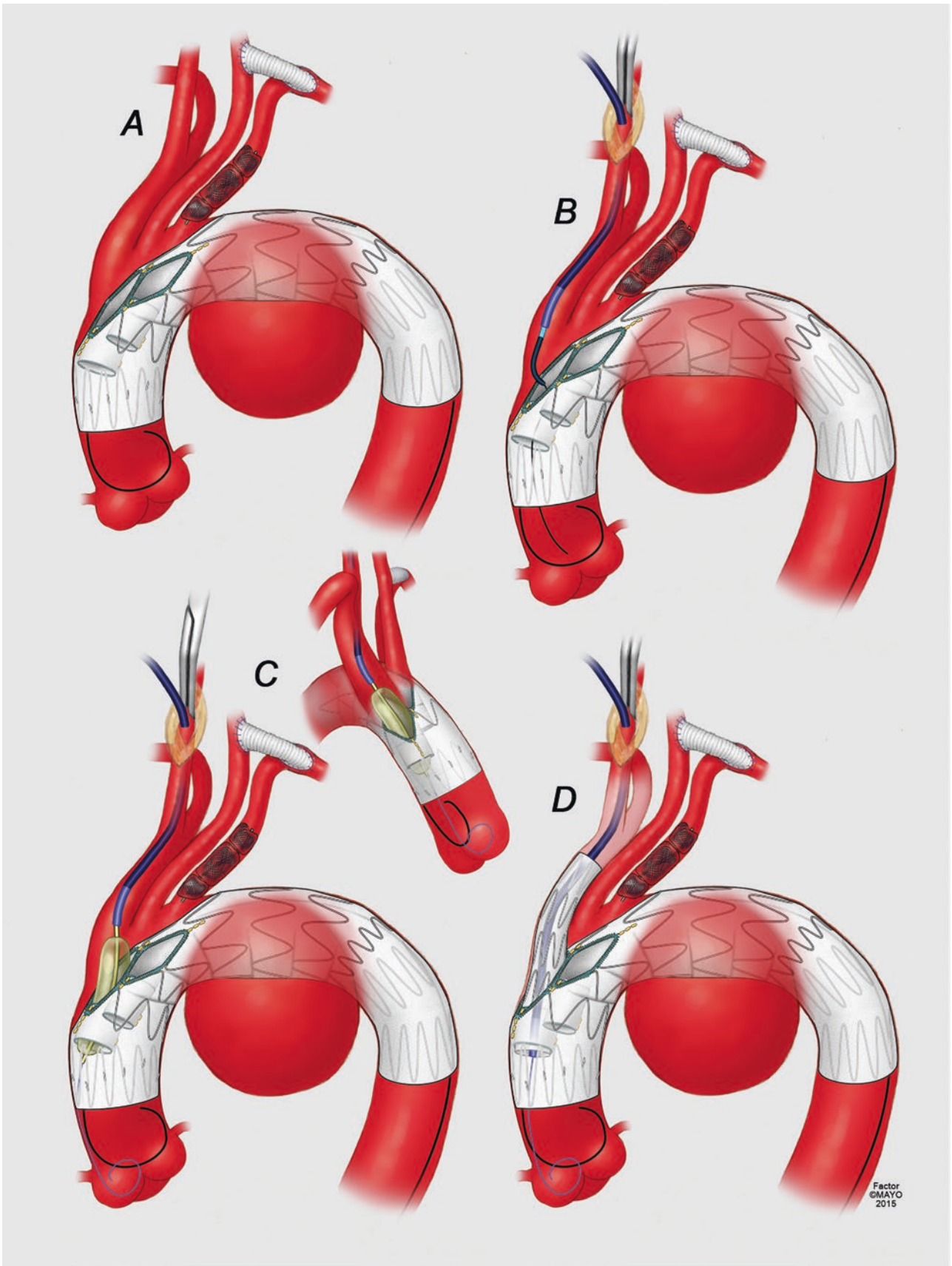


Fig. 33.4 Deployment of the a-branch stent graft (**a**), followed by retrograde access of the right common carotid artery (CCA) via direct puncture (**b**). The innominate artery is catheterized using a soft, angled guidewire, which is exchanged for a Rosen wire. A balloon is inflated and the gantry is moved to the right anterior oblique position to confirm that the correct inner branch has been cannulated (**c**). Stenting of the innominate artery is done using a modified iliac limb (**d**), noting that the right CCA is clamped during this portion of the procedure to avoid

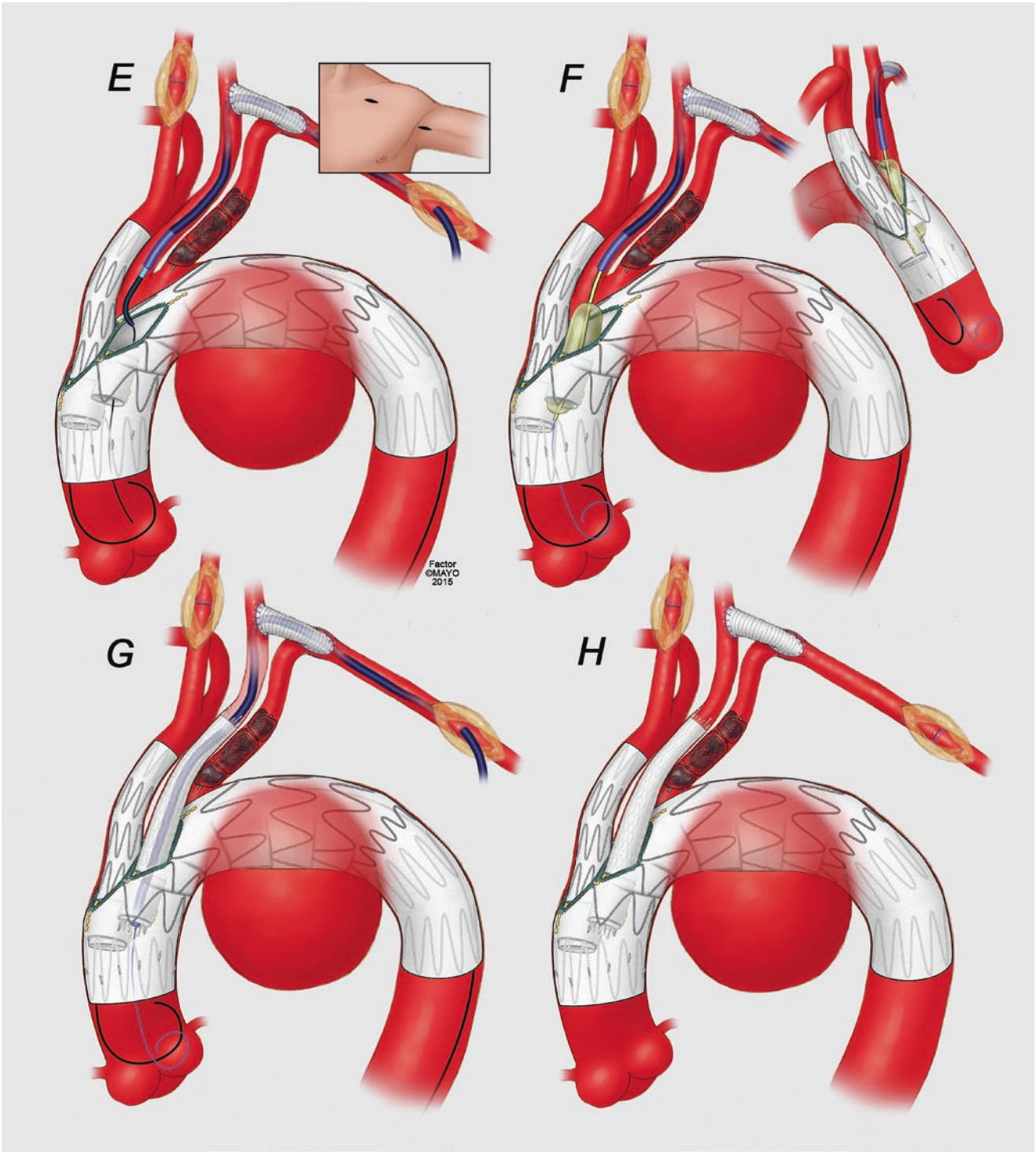


Fig. 33.4 (continued) embolization. A completion angiography is done to document patency, the sheath is removed, and flow is restored to the right CCA. Access is established in the left axillary artery using either an infraclavicular or high upper brachial incision (**E**). A soft, angled Glidewire is used to catheterize the distal inner branch. The guidewire is exchanged for a Rosen wire, and an 8-mm balloon is inflated into the branch to confirm correct position in the left anterior oblique position (**f**). A 10-Fr flexor sheath is advanced into the left common carotid artery and inner branch, followed by deployment of a self-expandable Fluency stent-graft, which is reinforced by self-expandable bare-metal stent (**g**). If needed, the repair is extended into the thoracic aorta, followed by completion angiography (**h**). By permission of Mayo Foundation for Medical Education and Research. All rights reserved

through the CCA sheath to identify the bifurcation of the IA. The angulation of the C-arm is determined preoperatively by analysis of the CT scan on the 3D workstation. The distal CCA is clamped for cerebral protection, the short sheath is removed, and the modified Zenith iliac limb is advanced over the Rosen wire. The proximal edge of the limb is aligned with the proximal inner branch markers and the distal edge positioned proximal to the bifurcation of the IA. The limb is deployed and the sealing zone between the inner branch and limb is ballooned using the 12×40-mm balloon, and a completion angiogram is performed through the delivery sheath to confirm good seal of the bridging limb and to exclude technical issues such as kinking of the stent and target vessel dissection (Fig. 33.4d). The sheath is then removed, the CCA flushed, and the arteriotomy closed using interrupted Prolene sutures. Right CCA perfusion is then restored.

Left Common Carotid Artery Bridging Stent

The distal inner branch is next cannulated from the left axillary artery access using the same guidewire and catheter combination as previously described (Fig. 33.4e). If the carotid-subclavian bypass is done in the same stage, the left common carotid artery may be clamped, similar to what was previously described for the right CCA. Balloon-inflation maneuver is used to confirm correct cannulation using an 8×40-mm balloon (Fig. 33.4f). A 45-cm 10-Fr sheath is advanced over the Rosen wire into the inner branch to facilitate the positioning of the bridging stent delivery system. An angiogram can be performed through the long sheath to identify the origin of the LSA-left CCA transposition or bypass. A self-expanding covered stent (Fluency, Bard Inc.) is advanced over the Rosen wire and the long sheath withdrawn to allow deployment of the stent. The proximal edge of the Fluency stent is aligned with the proximal inner branch markers and the distal edge positioned proximal to the origin of the LSA-left CCA transposition or bypass (Fig. 33.4g). We routinely reline the bridging stent with a self-expandable bare-metal nitinol stent. A completion angiogram is performed through the delivery sheath. The sheath is then removed and the axillary artery repaired in the same manner as the right CCA (Fig. 33.4h).

Distal Thoracic Extension

The distal end of the main body of the a-branch stent-graft may need to be extended into the descending thoracic aorta depending on the seal zone distal to the left CCA. In the setting of challenging tortuous arch and descending thoracic aorta anatomy, it is recommended to insert the delivery system of the distal thoracic extension from the contralateral groin. The trigger wire holding the distal aspect of the branched endograft is not removed until the extension has been advanced into position.

The last trigger wire is removed once the distal thoracic device is positioned inside the a-branch stent-graft. The pigtail catheter is advanced over the Lunderquist wire, into the ascending aorta, and then connected to the power injector. Completion angiography is performed to confirm proximal and distal seal of the main body of the graft, as well as seal of the bridging stents between the inner branches and their corresponding target vessels. The supra-aortic trunks are again examined to ensure patency and exclude issues such as kinking and dissection.

Special Situations

Through-and-Through Wire Technique

In some situations, despite a stiff wire platform positioned in the apex of the left ventricle, an endograft is unable to traverse the arch due to hostile anatomy. One example is a large distal arch aneurysm in a "gothic" arch, which promotes "bowing" of the delivery system into the sac of the aneurysm as it engages with the curve of the arch. Rheaume et al. describe a solution to this problem by using a through-and-through wire platform with an externalized transseptal guidewire technique [10]. The authors describe using a right common femoral vein access to establish a long sheath platform in the right atrium (Fig. 33.5). Under transesophageal echocardiography guidance, the foramen ovale was punctured using a transseptal needle to access the left atrium. A steerable introducer and a 400-cm long guidewire was then used to navigate through the mitral valve, left ventricle, aortic valve, and into the aorta. The wire was snared from a left common femoral access to establish a stable through-and-through wire platform. The graft was successfully advanced and deployed using this system.

Other authors have described using a left ventricular trans-apical through-and-through wire [11]. With this technique, needle access is obtained through the apex of the left ventricle, and the guidewire passed through the aortic valve and into the aorta. The wire is then snared from the femoral access. Access to the left ventricle can be obtained via a mini-thoracotomy or even using percutaneous techniques.

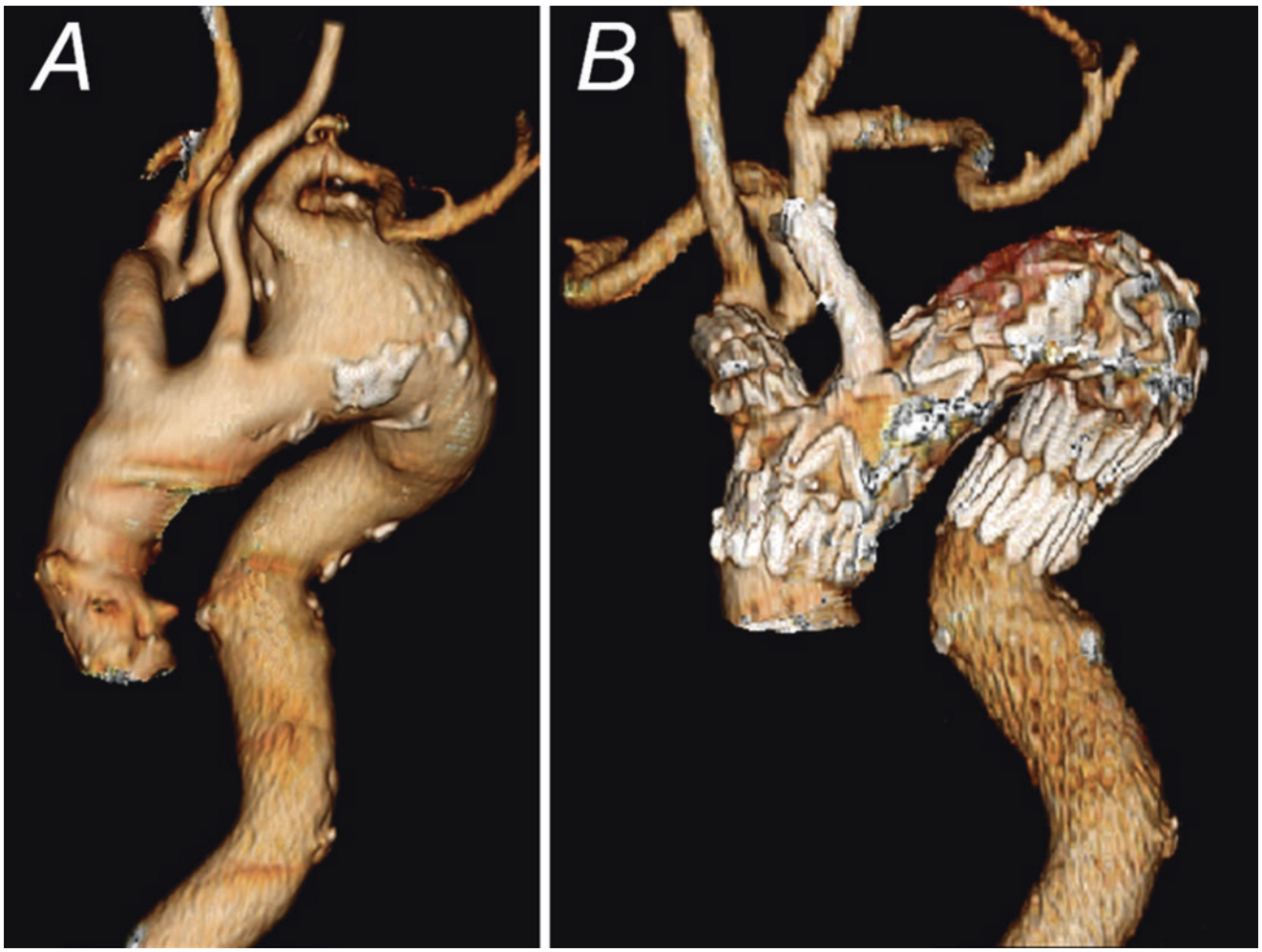


Fig. 33.5 Challenging arch anatomy with significant tortuosity of the descending thoracic aorta and angulated aortic arch (**a**) treated with doubled inner-branched stent-graft using transseptal guidewire technique (**b**). By permission of Mayo Foundation for Medical Education and Research. All rights reserved

Modified "Bullet" Nose Tip

As previously discussed, previous aortic prosthetic valve replacement was considered a contraindication to arch branched endograft repair. This is due to the inability to cross the valve with the tip of the delivery system.

Spear et al describe a solution to this problem by using a modified endograft delivery system with a short bullet nose tip [5]. The authors describe positioning a long 24-Fr sheath just above the level of the aortic valve (Fig. 33.6). The dilator of the sheath was withdrawn in order to advance the sheath to this level. The modified delivery system is loaded into a cartridge that is inserted and advanced through the long sheath. The modified short bullet nose tip is positioned against the aortic valve. The graft was successfully deployed 10 mm distal to the coronary ostia.

Thoracic Branch Endoprosthesis® (WL Gore, Flagstaff, AZ)

The WL Gore Thoracic Branch Endoprosthesis (TBE) has been designed using the C-TAG platform with a specially designed side branch stent intended for the left subclavian (Zone 2) or innominate artery (Zone 0). The device has been used in select patients under clinical investigation as part of a feasibility study in the USA. A brief description of the steps of the procedure for Zone 2 and Zone 0 deployment is described below.

Zone 2 TBE® Implantation Steps

Arterial access is established using bilateral femoral and left trans-brachial approach. The author preference (GSO) is to



Fig. 33.6 Mechanical aortic valve represents a relative contraindication as depicted in the computed tomography angiography (**a**). The patient was treated using a modification of the technique with a bullet point dilator (**b**). Deployment of the arch device with the dilator abutting the aortic valve (**c**), followed by placement of the innominate artery stent (**d**). By permission of Mayo Foundation for Medical Education and Research. All rights reserved

perform the procedure using through-and-through femoral to brachial access to improve support and avoid issues of side branch instability during delivery and deployment; in addition, placement of a small sheath in the target LSA minimizes the use of contrast dye and allows for precise deployment.

Access in the femoral arteries is typically done percutaneously whenever possible. Open exposure is used if there is any calcification or high bifurcation. A 22–24-Fr DrySeal sheath (WL Gore, Flagstaff, AZ) is used for delivery of the TBE®, and a contralateral 6-Fr femoral sheath is placed for diagnostic angiography. A curly Lunderquist wire is positioned in the ascending aorta using the technique previously described. The left brachial artery is surgically exposed just proximal to the antecubital crease (Fig. 33.7a). Access is established using a micropuncture kit, which is exchanged for 5-Fr sheath (Fig. 33.7b). A soft, angled Glidewire and C2 catheter are used to catheterized the descending thoracic aorta from the left brachial approach. The Glidewire is snared via the large femoral artery sheath in the descending thoracic aorta or in the common iliac artery (Fig. 33.7c, d) to establish left brachial-femoral access and exchanged for a 0.035-in Nitrex guidewire. We often establish access by cannulating a small 8-Fr sheath inside the larger transfemoral sheath (Fig. 33.7e).

The left brachial sheath is retracted to the LSA and can be used for small volume angiographies for deployment of the device (Fig. 33.7f). The TBE® is advanced using the Lunderquist guidewire for the aortic device and the preloaded Nitrex guidewire for the side port (Fig. 33.7g). It is critical to avoid guidewire wrapping, which is usually achieved by careful rotation of the device during advancement in the iliac arteries and abdominal or distal thoracic aorta. Once the device reaches position in the distal aortic arch, confirmation of guidewire position with no wrapping is needed prior to deployment (Fig. 33.7h). The device is positioned for deployment with small injections performed using the left brachial sheath. The assistant advances the device toward the aortic arch curvature, thereby "hugging" the arch curvature, while the through-and-through wire is left under

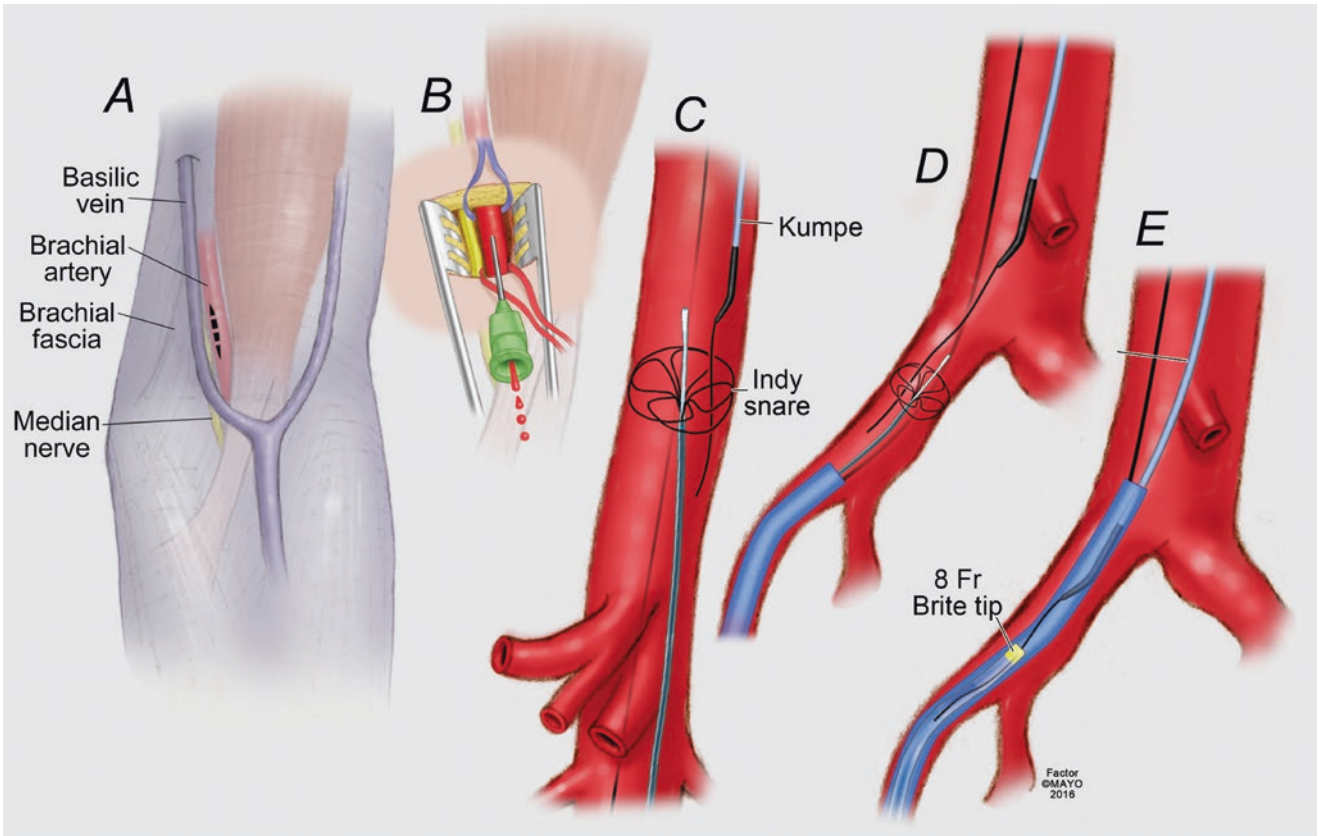


Fig. 33.7 Establishment of bilateral femoral access and left brachial access (**a**–**e**) for delivery of the Thoracic Branch Endoprosthesis® (TBE, WL Gore). The device is loaded and advanced into position (**f**–**g**), followed by deployment (**h**–**k**), advancement of the left subclavian sheath (**l**–**p**), and placement of the bridging stent (**q**–**s**). Pre- and postoperative computed tomography angiography (**t**–**u**). By permission of Mayo Foundation for Medical Education and Research. All rights reserved

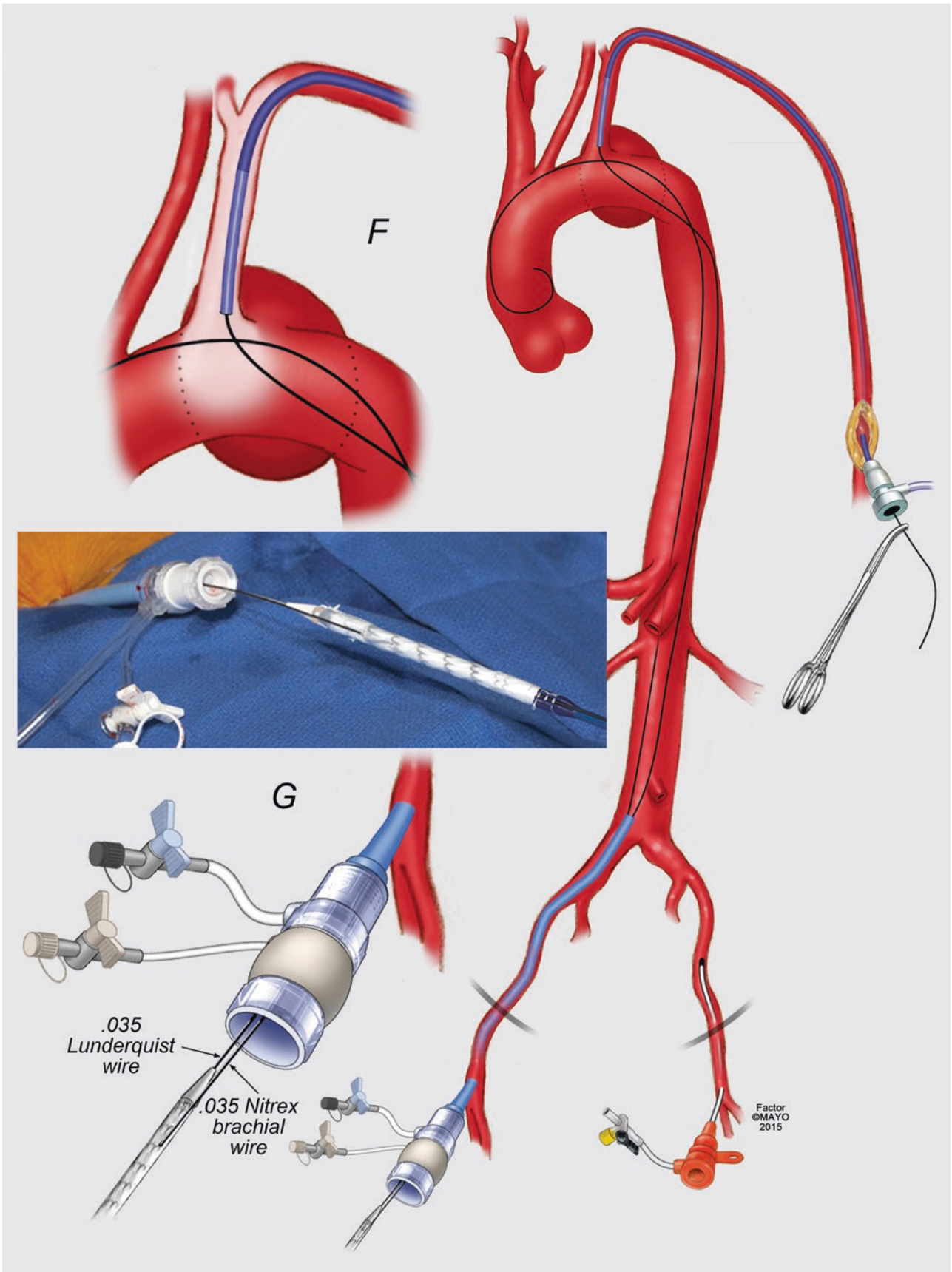


Fig. 33.7 (continued)

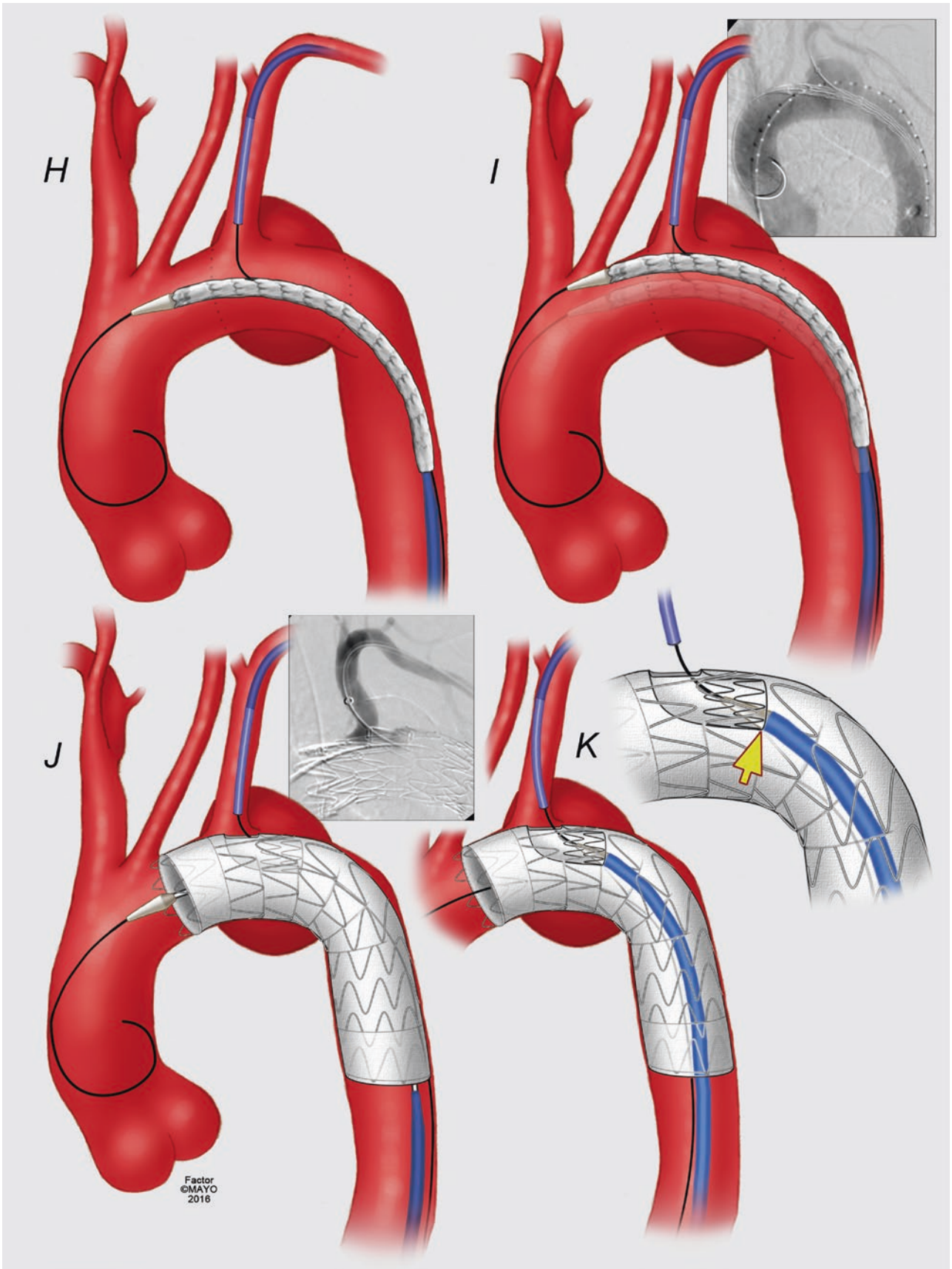


Fig. 33.7 (continued)

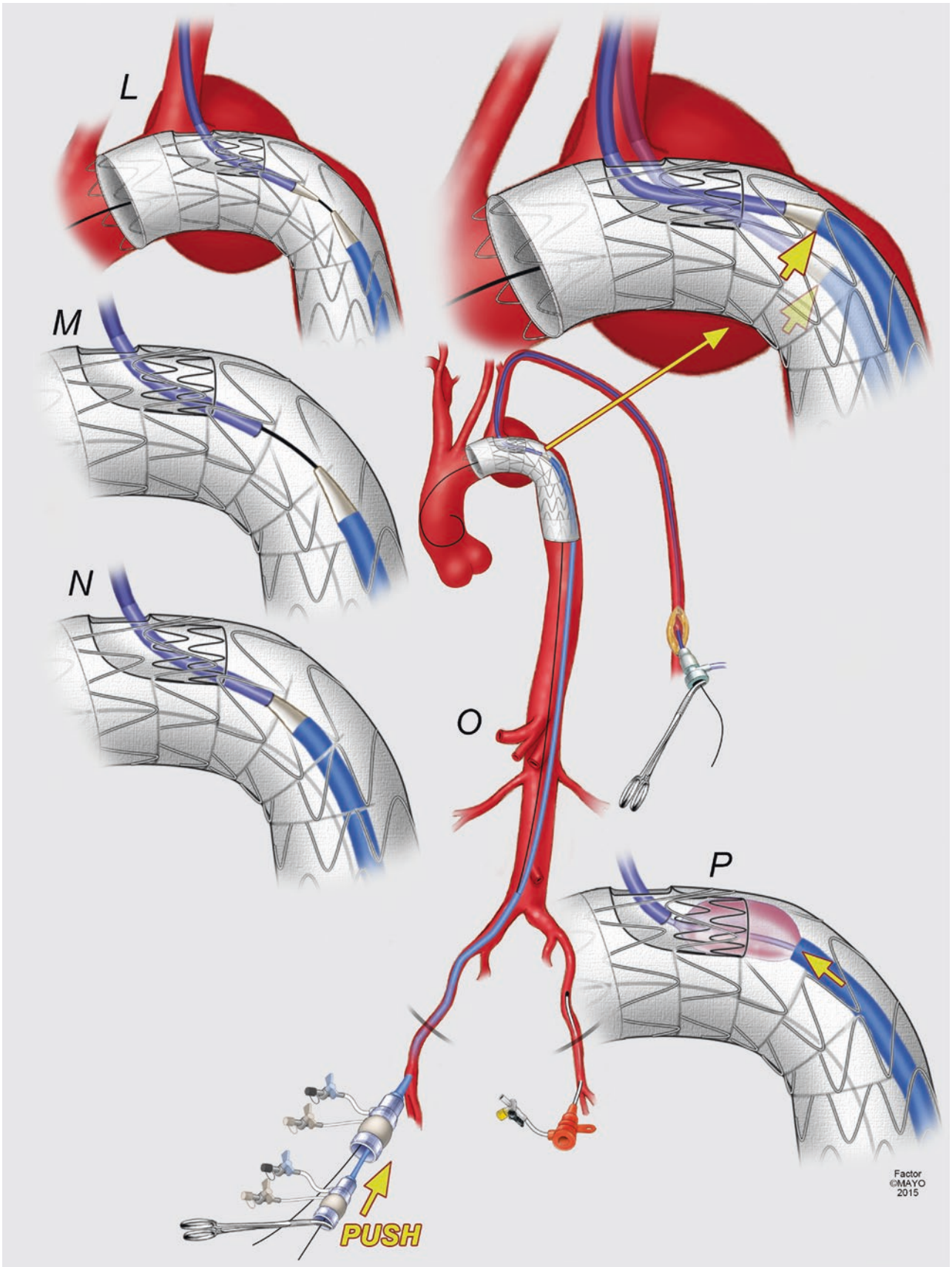


Fig. 33.7 (continued)

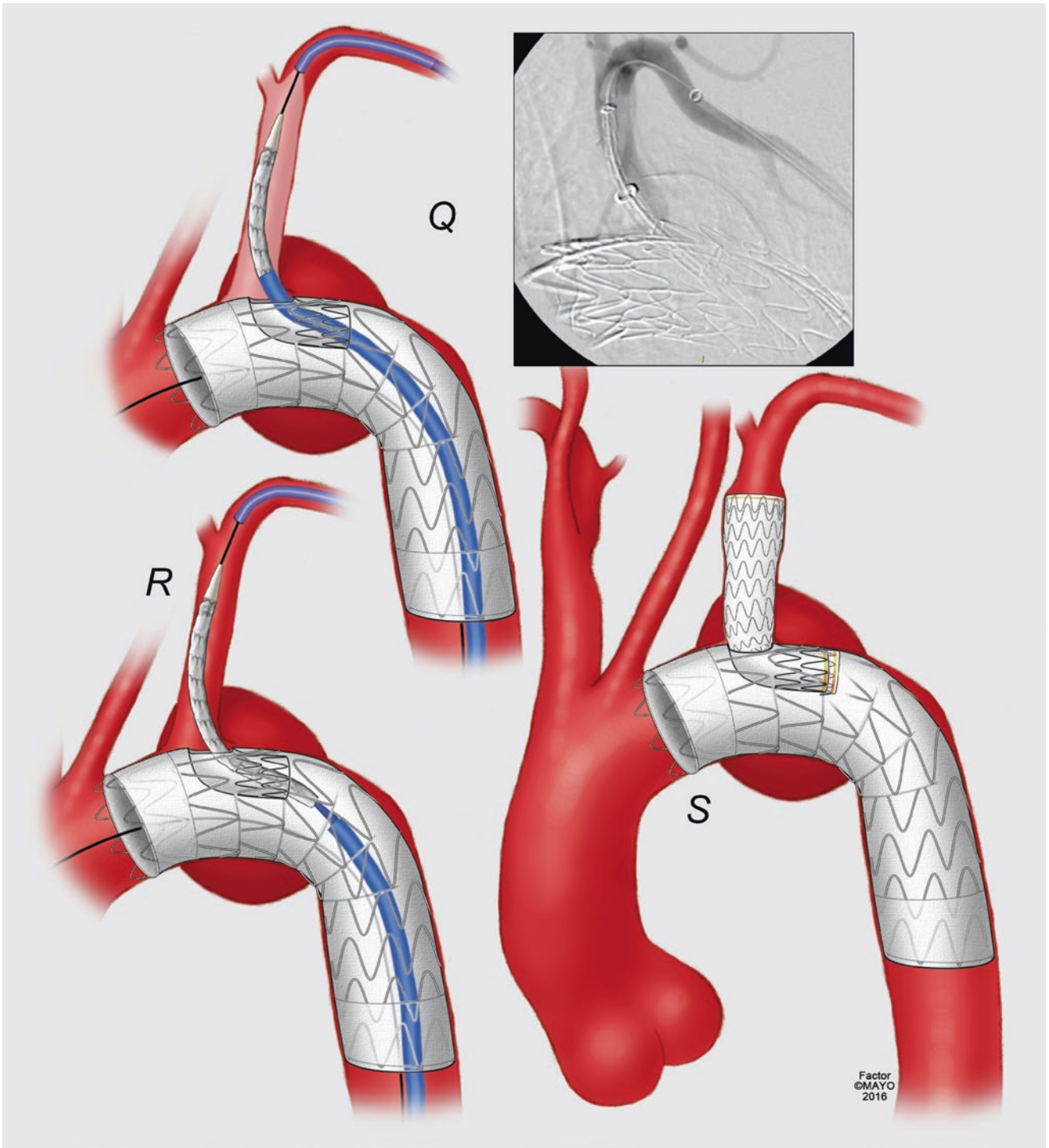


Fig. 33.7 (continued)

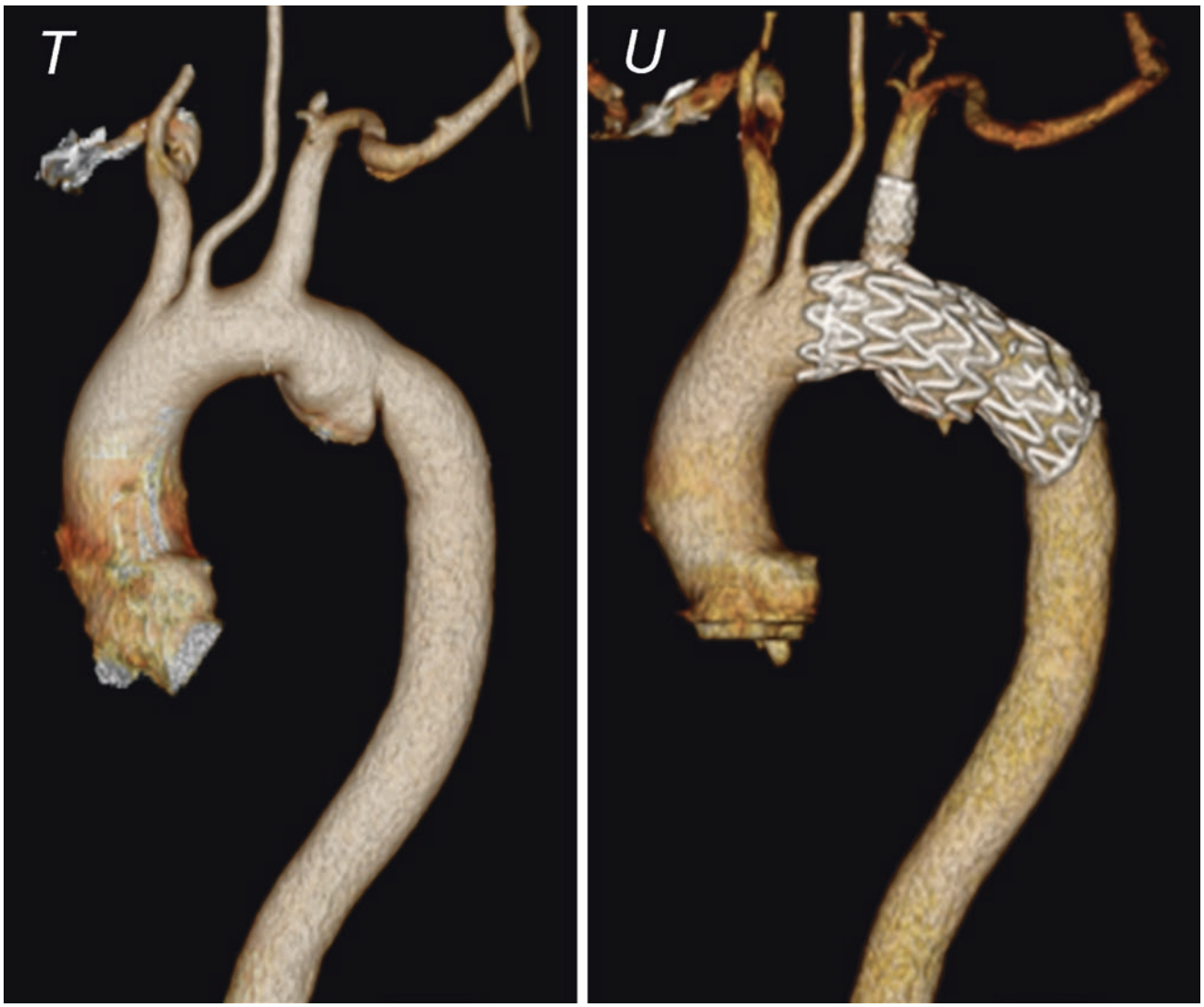


Fig. 33.7 (continued)

some tension (Fig. 33.7i). This allows for very precise deployment of the inner side portal (Fig. 33.7j).

The TBE® delivery system is removed over the Lunderquist wire, allowing room in the femoral sheath for advancement of a 14-Fr DrySeal sheath (WL Gore, Flagstaff, AZ), which is needed for delivery of the side branch component (Fig. 33.7k). Advancement of the sheath via the internal portal can be challenged by resistance between the transition points at the sheath dilator into the flexible portal (see Fig. 33.7k, yellow arrow). During this step of the procedure, the use of through-and-through access is important and several maneuvers can be useful. Exchanging the Nitrex wire for a Rosen wire, which is more flexible and helps avoid the lower edge of the portal, is usually sufficient. The author often advances the 7-Fr brachial sheath into the portal and aortic graft with no difficulty (Fig. 33.7l). The 7-Fr dilator is removed (Fig. 33.7m), and the tip of the 14-Fr dilator is docked inside the 7-Fr Ansel sheath (Fig. 33.7n). Surgical clamps are placed into both ends of the wires with tension, and a movement of "push-and-pull" is performed allowing control of the sheath and dilator during advancement across the portal (Fig. 33.7o). Note that the sheath can be bowed to the outer curvature by advancing the sheath against resistance (Fig. 33.7o, yellow arrow). Alternatively a balloon can be used instead of the dilator, but this is usually not necessary (Fig. 33.7p).

After the 14-Fr sheath is advanced across the portal, the bridging stent is positioned, and contrast is injected via the left brachial sheath to demonstrate the origin of the left vertebral artery (Fig. 33.7q). Once the sheath is retracted into the aortic stent (Fig. 33.7r), the bridging stent is deployed (Fig. 33.7s), and the portal is carefully dilated, followed by contrast angiography (Fig. 33.7t, u).

Zone 0 TBE® Implantation Steps

The Zone 0 TBE® requires a staged cervical debranching procedure to revascularize the left CCA and LSA. The author preference is to perform this portion of the procedure a few days before, using right cervical oblique and left supraclavicular incision. The graft is fashioned with three anastomoses, including a proximal end-to-side anastomosis to the right CCA with distal end-to-side anastomosis to the left SCA. The left CCA is reimplanted into the graft, while the proximal CCA stump is oversewn in two layers. The proximal subclavian artery is occluded using an Amplatzer plug to avoid competitive flow. The following steps are nearly identical to what was described above for Zone 2, but it is imperative with Zone 0 for the use of through-and-through access and avoidance of any device manipulation within the aortic arch. A small right lower arm incision is made (Fig. 33.8a) to expose the right distal brachial artery (Fig. 33.8b). Retrograde access is established with a micropuncture set. A C2 catheter is advanced across the arch (Fig. 33.8c, d) into the descending thoracic aorta. Establishment of brachial-femoral access is done using snare in the iliac artery (Fig. 33.8e) or via the sheath (Fig. 33.8f). The snare can also be used in the descending thoracic aorta, but one should not manipulate the snare in the aortic arch (Fig. 33.8g). Guidewire wrapping needs to be avoided prior to device deployment, which can be achieved with manipulation of the device within the iliac arteries and abdominal or distal thoracic aorta. Once the guidewire is deemed in good position, the device is advanced into the aortic arch (Fig. 33.8h). If the guidewire remains wrapped in the delivery system, the device needs to be withdrawn to the thoracic aorta while rotation is done to undo the wrapping. The device is deployed with the portal under the origin of the innominate artery (Fig. 33.8i). Advancement of the sheath is done using similar technique as described for Zone 2. Small volume angiography is done to demonstrate the bifurcation of the innominate artery, and the side branch stent is deployed (Fig. 33.8j–l).

Early Results

Clinical experience in the Western world has been limited for the most part to a few centers with access to Cook arch branched devices. The first clinical experience with the Cook a-branch stent-graft was reported by Lioupis et al. in 2012 [12]. This was a small series of six patients, where 11 out of 12 branches were successfully cannulated and preserved. This study demonstrated the technical feasibility of the device. Recently, a retrospective, multicenter analysis of the first 38 patients treated with the Cook a-branch stent-graft was published by Haulon and colleagues [7]. This series included the patients from the Lioupis et al. series. Technical success was achieved in 32 of 38 patients (84 %). Five patients (13 %) died within 30 days of the procedure, and six (16 %) had cerebrovascular complications, which included four TIAs, one stroke, and one subarachnoid hemorrhage. The median follow-up was 12 months. During this time, no aneurysm-related mortality was reported. When an analysis of the first ten patients was compared with the latter 28 patients, early mortality appeared higher in the first ten patients (30 % vs. 7 %), though the difference was not statistically significant ($p = 0.066$). Interestingly, when early mortality was combined with neurologic complications, the difference between the two groups became significant ($p = 0.019$). This likely represents the learning curve associated with the first patients treated with the graft. The combined endpoint of early mortality and neurologic complications was also significantly higher in those with ascending aortic diameters >38 mm ($p = 0.026$). The authors concluded that the study confirms the feasibility and safety of the endovascular repair of arch aneurysms in selected patients who may not have other conventional options.

The preliminary results of the US feasibility TBE multicenter clinical trial were recently reported in the first 22 patients (mean age 74.1 ± 10.5 years, 54.5 % male) undergoing branched thoracic endovascular aortic repair (B-TEVAR) in Ishimaru Zone 2. Pathology treated included fusiform ($n = 10$) or saccular ($n = 12$) aneurysm, with a mean aortic diameter of 5.7 ± 1.1 cm. Mean preoperative left-right brachial index (BI) was 1.0 ± 0.1. Mean total treatment length was 17.6 ± 8.9 cm, with eight patients treated with a single 10-cm graft for isolated arch pathology. The primary endpoint of device delivery and branch vessel patency was achieved in 100 % of patients, without 30-day mortality, stroke, or permanent paraplegia. Median duration of hospitalization was 4.0 days. Type I endoleaks at completion angiography were observed in four patients, all resolving by 1 month without re-intervention. All side branches were patent at 1 month. Kaplan-Meier survival at 6 months was 94.7 %. The authors concluded that endovascular repair of distal Zone 2 arch aortic aneurysms can be safely achieved with the TBE. Future studies will evaluate feasibility of this approach for aneurysms encompassing the brachiocephalic trunk and left carotid artery.

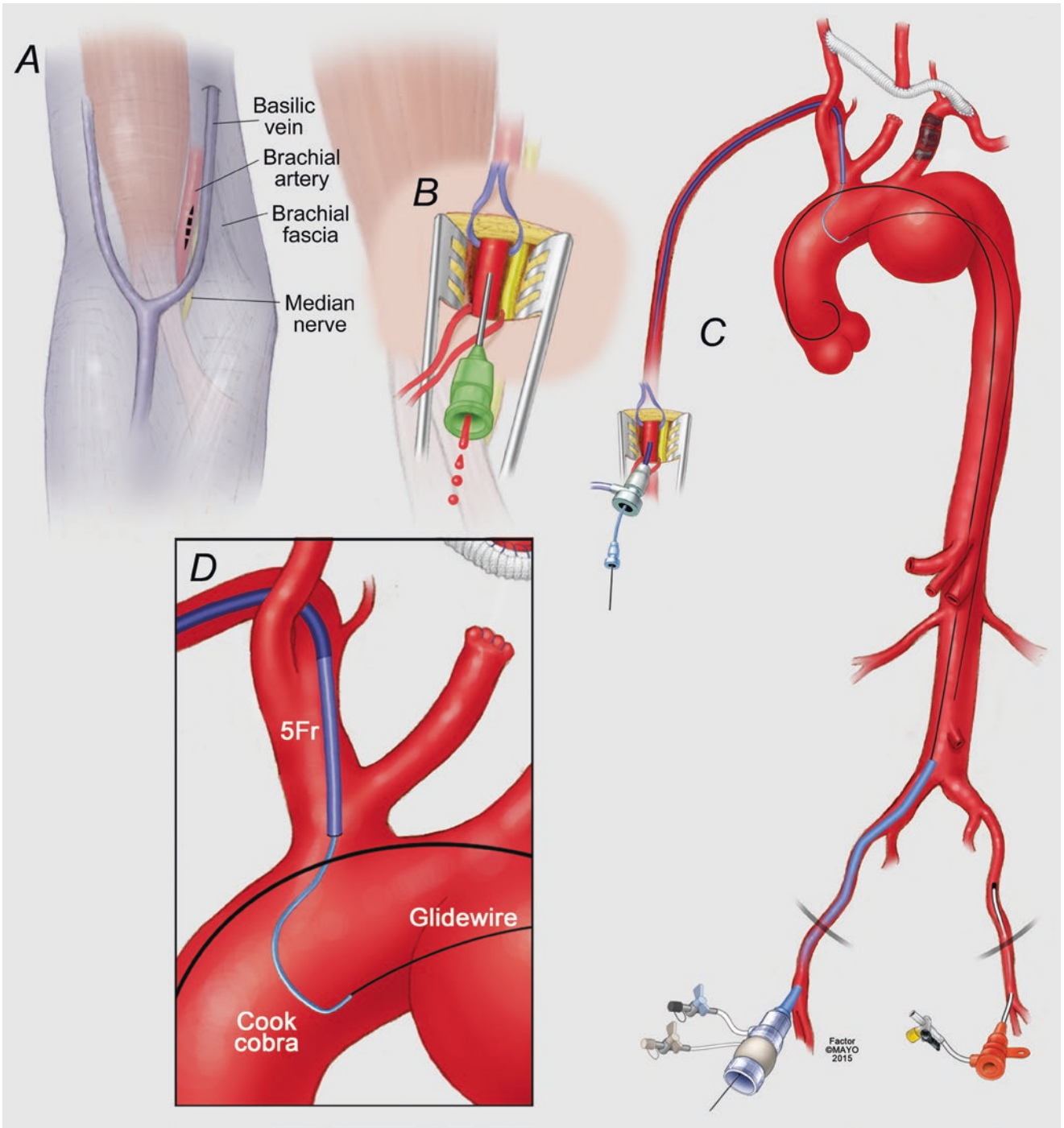


Fig. 33.8 Technique of establishment of brachial-femoral access (**a**–**g**) for Zone 0 deployment, device advancement, deployment, and placement of bridging stent (**h**–**j**). Pre- and postoperative computed tomography angiography (**k**–**l**). By permission of Mayo Foundation for Medical Education and Research. All rights reserved

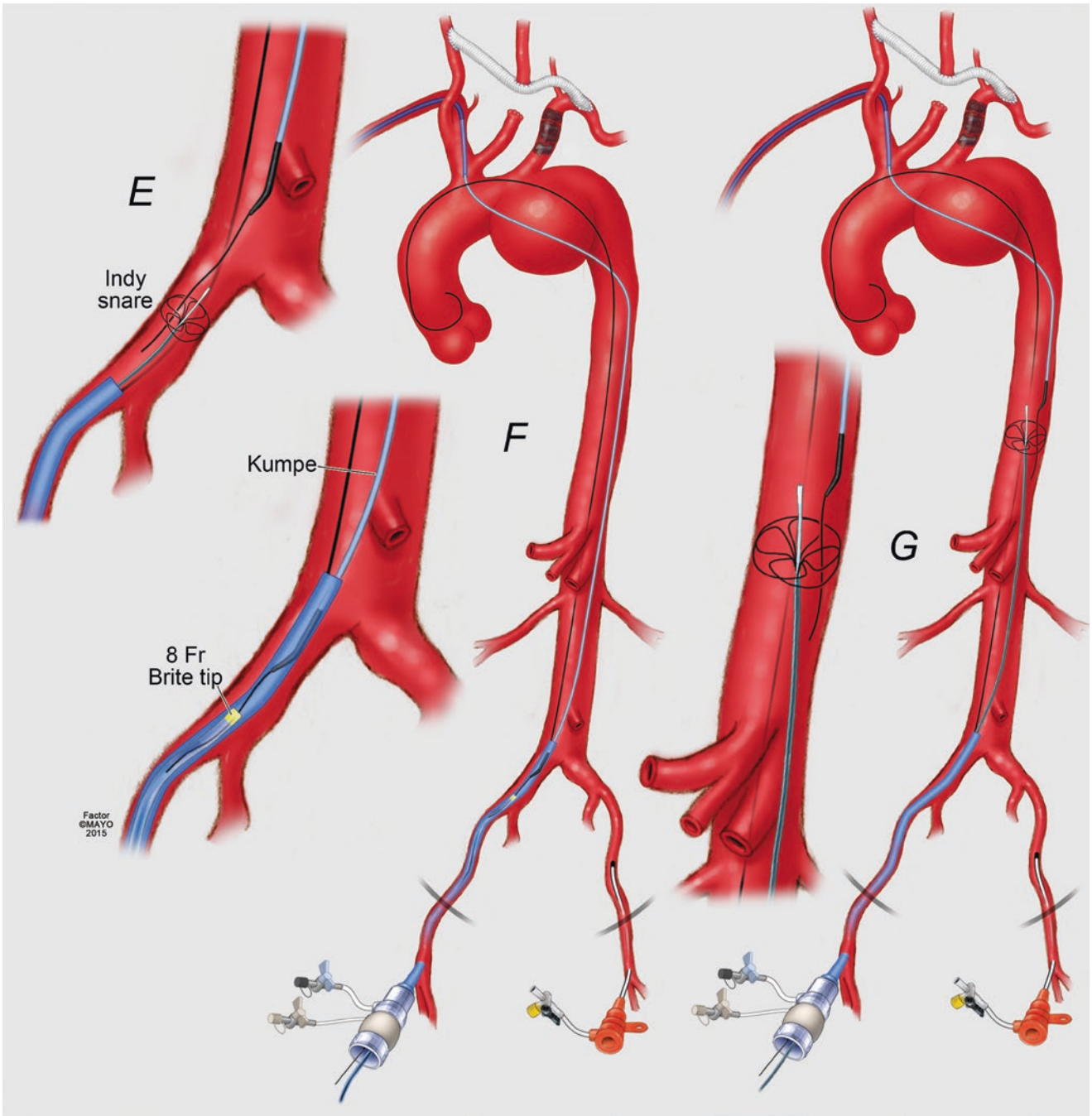


Fig. 33.8 (continued)

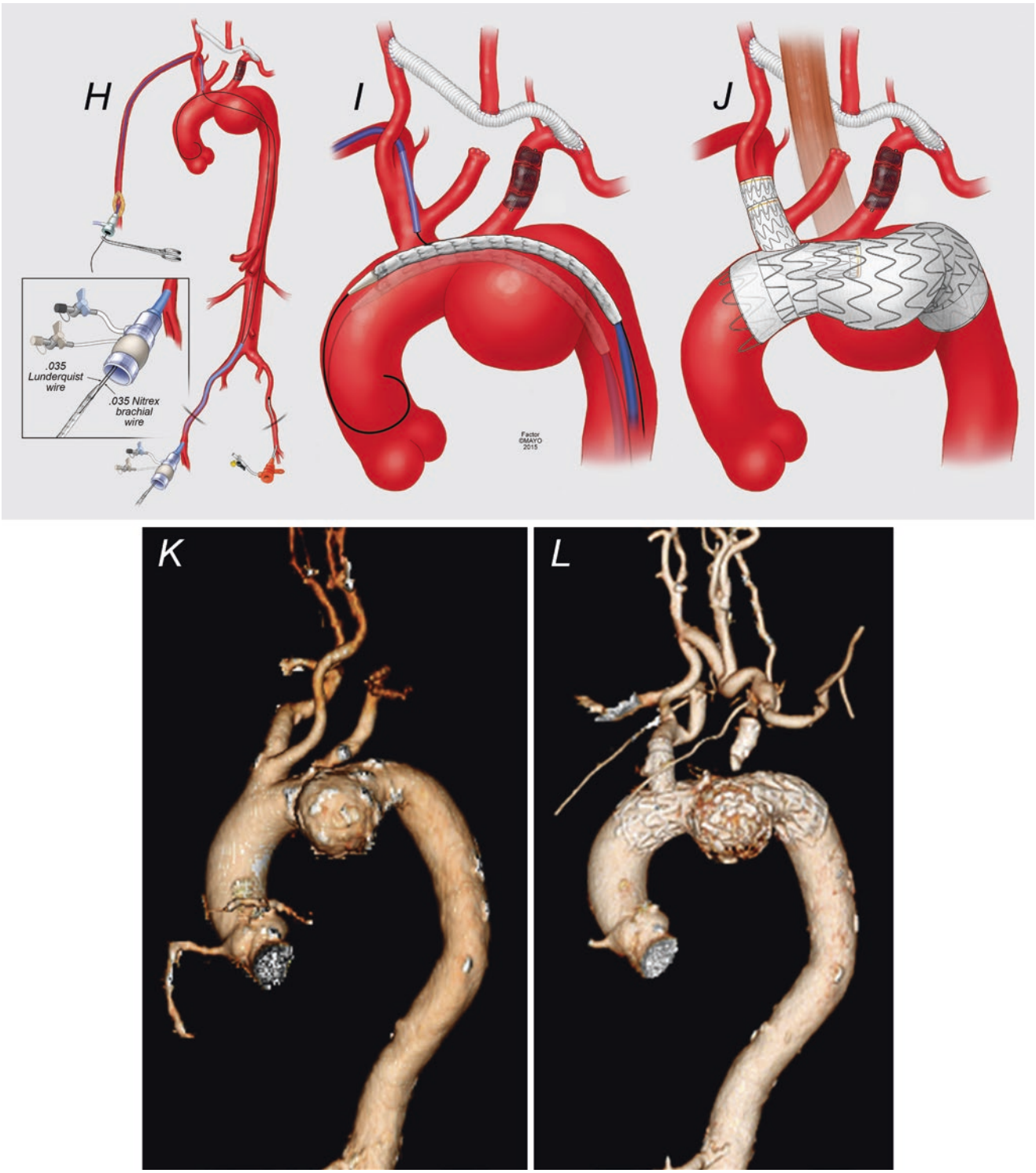


Fig. 33.8 (continued)

References

1. Benedetto U, Melina G, Angeloni E, Codispoti M, Sinatra R. Current results of open total arch replacement versus hybrid thoracic endovascular aortic repair for aortic arch aneurysm: a meta-analysis of comparative studies. J Thorac Cardiovasc Surg. 2013;145:305–6.
2. Haulon S, Sobocinski J, Spear R, Katzberg J, Roeder B, Azzaoui R, Maurel B. Total endovascular repair of the aortic arch. Endovasc Today. 2014;November:67–73.
3. Abu Rahma AF, Campbell J, Stone PA, Nanjundappa A, Jain A, Dean LS, et al. The correlation of aortic neck length to early and late outcomes in endovascular aneurysm repair patients. J Vasc Surg. 2009;50(4):738–48.
4. Mastracci TM, Greenberg RK, Eagleton MJ, Hernandez AV. Durability of branches in branched and fenestrated endografts. J Vasc Surg. 2013;57(4):926–33. discussion 33.
5. Spear R, Azzaoui R, Maurel B, Sobocinski J, Roeder B, Haulon S. Total endovascular treatment of an aortic arch aneurysm in a patient with a mechanical aortic valve. Eur J Vasc Endovasc Surg. 2014;48(2):144–6.
6. Fairman RM, Tuchek JM, Lee WA, Kasirajan K, White R, Mehta M, et al. Pivotal results for the Medtronic Valiant Thoracic Stent Graft System in the VALOR II trial. J Vasc Surg. 2012;56(5):1222–31 e1.
7. Haulon S, Greenberg RK, Spear R, Eagleton M, Abraham C, Lioupis C, et al. Global experience with an inner branched arch endograft. J Thorac Cardiovasc Surg. 2014;148(4):1709–16.
8. Inoue K, Hosokawa H, Iwase T, Sato M, Yoshida Y, Ueno K, et al. Aortic arch reconstruction by transluminally placed endovascular branched stent graft. Circulation. 1999;100(19 Suppl): II316–21.
9. Hertault A, Maurel B, Sobocinski J, Martin Gonzalez T, Le Roux M, Azzaoui R, et al. Impact of hybrid rooms with image fusion on radiation exposure during endovascular aortic repair. Eur J Vasc Endovasc Surg. 2014;48(4):382–90.
10. Rheaume P, Perini P, Daligault M, Maurel B, Sobocinski J, Azzaoui R, et al. Total endovascular repair of an aortic arch aneurysm using an externalized transseptal guidewire technique. Ann Thorac Surg. 2012;93(5):1710–3.
11. Ye J, Cheung A, Lichtenstein SV, Carere RG, Thompson CR, Pasupati S, et al. Transapical aortic valve implantation in humans. J Thorac Cardiovasc Surg. 2006;131(5):1194–6.
12. Lioupis C, Corriveau MM, MacKenzie KS, Obrand DI, Steinmetz OK, Abraham CZ. Treatment of aortic arch aneurysms with a modular transfemoral multibranched stent graft: initial experience. Eur J Vasc Endovasc Surg. 2012;43(5):525–32.

Techniques and Results of Endovascular In Situ Arch Fenestrations

34

Joseph C. Wuamett, S. Sadie Ahanchi, and Jean M. Panneton

Introduction

Thoracic endovascular aortic repair (TEVAR) has gained widespread use in the treatment of acute and chronic pathologies of the thoracic aorta. Optimal outcomes in TEVAR are dependent upon obtaining adequate proximal and distal apposition of stent graft against a healthy aortic wall. In the proximal thoracic aorta, this may require coverage of one or more of the supra-aortic trunks. The most common vessel requiring coverage to obtain an adequate proximal seal during TEVAR is the left subclavian artery (LSA). Coverage of the LSA during TEVAR has been recognized in the literature as an important modifiable risk factor for stroke, spinal cord ischemia, and upper extremity ischemia [1, 2].

Accordingly, multiple methods for LSA revascularization have been used in conjunction with TEVAR.

Open revascularization of the left subclavian artery is the most frequently used method for extending the proximal landing zone. Multiple large series have demonstrated the feasibility of combining open revascularization with TEVAR in patients with a variety of thoracic aortic pathologies, with stroke and death rates of 8.8 and 7.1 %, respectively [3, 4]. In addition to open revascularization, novel endovascular technologies, such as branched or scalloped endografts, chimneys, snorkels, and in situ fenestrations, have been developed for revascularization of aortic arch vessels during TEVAR. This chapter focuses on the technique of in situ arch fenestration.

J.C. Wuamett • S.S. Ahanchi • J.M. Panneton (✉)
Division of Vascular Surgery, Eastern Virginia Medical School, Sentara Heart Hospital, 600 Gresham Drive Suite 8620, Norfolk, VA 23517, USA
e-mail: pannetjm@evms.edu

Development of In Situ Arch Fenestrations in TEVAR

In 2004, McWilliams et al. reported the use of a retrograde in situ stent graft fenestration technique to preserve the LSA during endograft repair of a saccular thoracic aortic aneurysm [5]. The technique required direct 6-Fr sheath access in the LSA, utilizing the stiff end of an 0.018-in guidewire to penetrate the graft material, needle puncture to cut threads of the graft material, and serial cutting balloons for dilation of the graft before deployment of a covered stent into the LSA. Manning et al. later modified this technique in 2010. The authors used a semirigid pre-curved sheath and a pre-curved 22-gauge spinal needle to facilitate in situ fenestration of more difficult arch anatomy limited by an acute takeoff of the LSA [6].

Due to concern for tearing of the aortic stent graft fabric and reducing the long-term structural integrity of the device, additional tools for creating an in situ fenestration, including laser and radiofrequency, have been investigated. Laser-assisted in situ fenestration of a stent graft covering the LSA during endovascular repair of a traumatic thoracic aortic transection was reported by Murphy et al. in 2009 [7]. This approach allowed for laser fenestration to be performed through a 7-Fr sheath placed in the left brachial artery. Wire passage was accomplished after the laser fenestration of the stent graft and followed by balloon dilation of the graft in preparation for placement of a covered stent across the endograft into the LSA. Our group has since used this method to facilitate aortic arch vessel revascularization across a wide spectrum of acute aortic pathologies [8, 9].

Pathology

Numerous types of acute and chronic aortic pathologies have been treated with in situ aortic arch fenestration techniques and reported in the literature. At our institution, while open surgical LSA revascularization and aortic arch debranching

© Mayo Foundation for Medical Education and Research 2017

G.S. Oderich (ed.), *Endovascular Aortic Repair*, DOI 10.1007/978-3-319-15192-2_34

are frequently employed in the elective setting for revascularization, utilization of in situ aortic arch fenestration is reserved for urgent and emergent acute thoracic aortic pathologies, such as acute complicated type B dissection, symptomatic penetrating atherosclerotic ulcer (PAU), symptomatic intramural hematoma (IMH), and ruptured or symptomatic aneurysms of the thoracic aorta.

Anatomic Limitations and Patient Selection

Anatomy dictates the technical success of in situ aortic arch fenestration during TEVAR, most notably aortic arch type and branch vessel anatomy characteristics, which include angulation, location of distal branches, dissection, and size. The arch can be classified into three types (Fig. 34.1) based on the geometric relationship of the supra-aortic trunks to horizontal lines drawn parallel to the outer and inner curves of the aortic arch. The arch vessels arise in the same plane as the upper outer curve line in a type I arch, between the parallel lines of the outer and inner curve in a type II arch, and proximal to or below the lower inner curve line in a type III arch. The complexity of in situ arch fenestration increases from type I to type III arch.

Similarly, the angle with which the arch vessel comes off the aortic arch also affects the feasibility of in situ fenestration. The optimal angle of target vessel takeoff from the aorta is 90°. The technical difficulty rises exponentially in angles <30° and in situ fenestration should be avoided in these circumstances. The combination of arch type and arch vessel angulation impacts the ability of the operator to create a clean fenestration perpendicular to the aortic stent graft fabric. Flow dynamics from the aortic stent graft to the covered stent in the revascularized vessel may also be altered leading to stenosis or thrombosis of the covered stent. Similar problems are associated with arch vessels that have an offset anterior or posterior takeoff from the arch. Examples of acute angulation and anteriorly offset aortic arch branches are seen in Fig. 34.2.

The anatomic characteristics of the target vessel for revascularization can also limit the success of an in situ arch fenestration. These factors include a low vessel branching, dissection into the branch vessel, and large arch vessel diameter. A low vertebral artery or short innominate artery limits the distal seal zone for placement of a covered stent. Avoidance of vertebral artery coverage is critical to avoid neurologic complications in patients with dominant left vertebral artery circulation or discontinuity of the circle of Willis [10, 11].

In patients with dissection extending into the arch vessel, in situ arch fenestration and subsequent stenting can result in antegrade and/or retrograde propagation of the dissection into the arch or arch branch vessels. Lastly, the size of the target vessel is also of critical importance. A covered stent of adequate length and diameter is required to create not only a seal at the fenestration but also a seal along the distal aspect of the target vessel. Currently, the largest diameter for a balloon expandable covered stent is 10 mm. In situ fenestration and stenting of an arch vessel without adequate seal zone in the target vessel may lead to an increased risk for a type Ic endoleak.

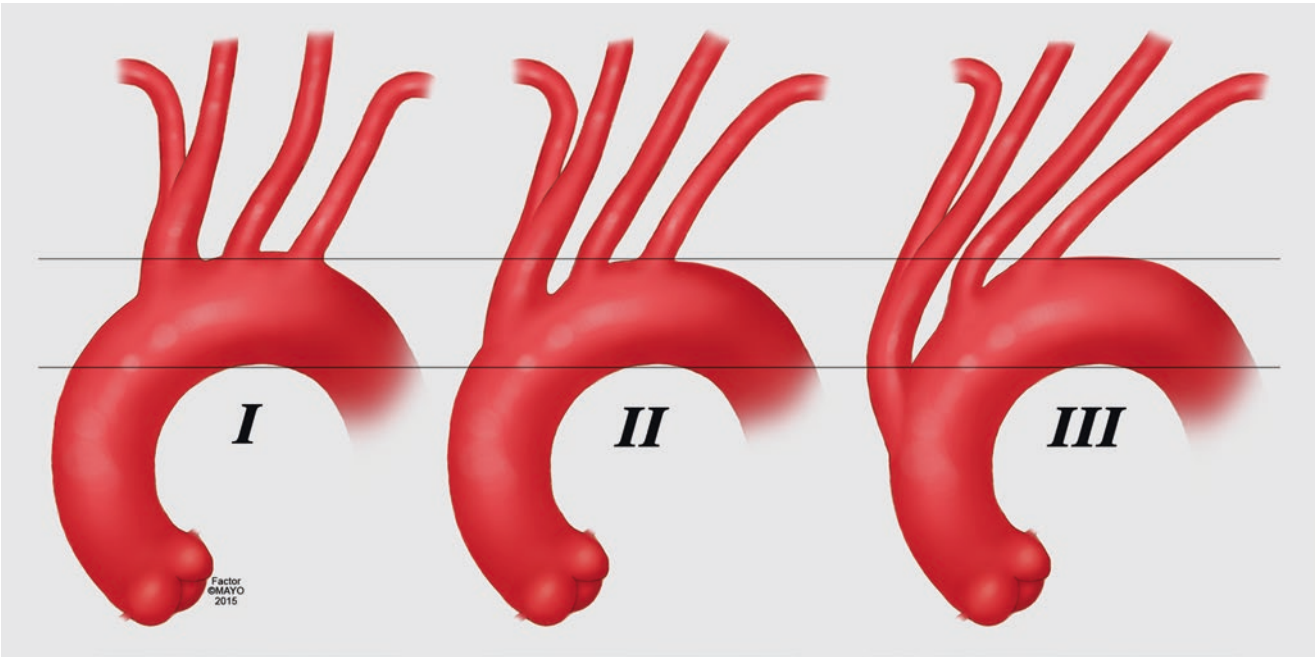


Fig. 34.1 Aortic arch types I, II and III. The difficulty of in situ aortic arch fenestration increases dramatically from a type I to type III aortic arch. By permission of Mayo Foundation for Medical Education and Research. All rights reserved

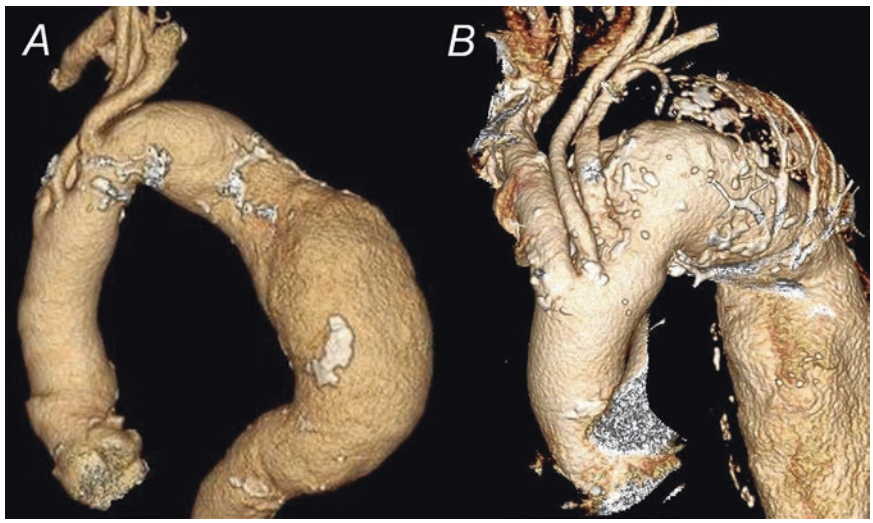


Fig. 34.2 (**a**) Acute takeoff of the arch vessels in a type III arch. (**b**) Type III arch demonstrating arch vessels that are both angulated and anteriorly offset. By permission of Mayo Foundation for Medical Education and Research. All rights reserved

In summary, the ideal candidate for in situ arch fenestration during TEVAR is a patient that requires arch vessel revascularization in an urgent or emergent setting and does not have complicated aortic arch or target vessel anatomy. Patients with a type III aortic arch, target vessel takeoff angle <30°, target vessel diameter >10–12 mm, a low vertebral takeoff, or innominate bifurcation should not be treated with in situ aortic arch fenestration and are at higher risk for failure. Revascularization should be done by other means in these patients.

Needle Versus Laser In Situ Arch Fenestration

There is no direct comparison of needle and laser puncture for endograft fenestration in the literature. Riga et al. examined the structural consequences of needle puncture methods for in situ fenestration using an in vitro model [12]. The structural quality of the fenestration was affected by the angle of puncture, graft material, and type of balloon, which was used to enlarge the fenestration. EndoFit thin-walled expanded polytetrafluoroethylene (ePTFE; LeMaitre Vascular, Inc., Burlington, MA, USA) grafts were easier to puncture and dilate than the polyester grafts, but resulted in elliptical or slit-like fenestrations oriented transversely along the endograft. In comparison, polyester graft fenestrations were mostly squared or elliptical. Notably, the ideal circular fenestration was only achieved in the monofilament twill woven polyester Medtronic Talent endograft (0.09-mm-thick polyester; Medtronic Vascular, Santa Rosa, CA, USA) at a 90° puncture angle and not in the multifilament tubular woven polyester Cook Zenith endograft (0.15-mm-thick polyester; Cook Inc., Bloomington, IN, USA and Brisbane, Australia). Furthermore, the quality of fenestrations decreased with the angle of puncture in all graft materials. There was also a tendency for cutting balloons to create more tears in the graft material than a standard angioplasty balloon.

In our own in vitro experiments, it was shown that the dispersion of the area and length of fenestration was more predictable after angioplasty with the 8-mm balloon compared to fenestrations dilated with 10- and 12-mm balloons [13]. A subsequent in vitro experiment conducted by our group compared the effect of needle and laser puncture on quality of fenestration. It was demonstrated that laser fenestration creates less tearing of the endograft material and is superior to needle puncture. Furthermore, it is our opinion that the more controlled self-sealing heat fenestration made by the laser limits the potential for type III endoleaks in comparison to needle puncture. However, laser use to create fenestrations is not without limitations. It is known that when PTFE is heated or burned at high temperatures, hydrogen chloride, trifluoroacetate, and other toxic substances are released [14]. We have limited our in vitro and in vivo experience with laser fenestration to polyester grafts only.

In summary, while laser fenestration appears to be a more attractive modality than needle puncture, a durable result is affected by numerous variables including graft material, arch vessel angulation, type of balloon, and size of balloon. Nonetheless, alternative methods for in situ arch fenestrations are being investigated. Of note, early clinical results with radiofrequency ablation (RFA) suggest technical feasibility and acceptable early outcomes [15].

Technique

Performing in situ laser fenestration of the LSA during TEVAR requires the following instruments: a Spectranetics Turbo Elite 2.3–2.5 Laser (Spectranetics, Colorado

Springs, CO, USA); a 7 or 8-Fr sheath, 0.018-in Platinum Plus wire (Boston Scientific, Natick, MA, USA); a 0.035-in stiff guidewire; a 6 × 40-mm balloon; an 8–10 × 38-mm iCAST covered stent (Atrium Maquet, Hudson, NH, USA); and a 14 × 20-mm balloon. Newer endovascular tools that can facilitate this procedure are discussed later in the chapter.

Establishing Access

The sheath in the left brachial artery is upsized to a long 8-Fr LAMP (St. Jude Medical, St. Paul, MN, USA) or 7-Fr Ansel 1 (Cook Inc., Bloomington, IN, USA and Brisbane, Australia) sheath with a preformed angle at the tip. The tip of the sheath is delivered to the ostium of the LSA using standard endovascular techniques. The wire within the sheath is exchanged for an 0.018-in wire, and the laser is advanced to the tip of the sheath. The sheath and laser are positioned at the orifice of the LSA with the wire pulled back 1–2 cm into the laser device (Fig. 34.3a). TEVAR is performed as described elsewhere with the proximal stent graft positioned as close to the takeoff of the left common carotid artery as possible (Fig. 34.3b).

Creating the In Situ Fenestration

Once the endograft for TEVAR is deployed, the laser is advanced to make contact with the endograft fabric. A left anterior oblique (LAO) view is useful for delivering the laser to the endograft; however, this view does not ensure the laser is perfectly centered for optimal contact with the endograft (Fig. 34.4a). A right anterior oblique (RAO) view offers a "barrel view" of the endograft and confirms biplane perpendicular positioning (Fig. 34.4b). Laser energy (45 mJ/mm^2 fluence at a rate of 25 pulses per second) is applied for 3–5 s as gentle forward pressure is applied until tactile feedback indicates passage through the endograft material in LAO deployment view (Fig. 34.4c).

Passage of Guidewire

Once the laser has penetrated the graft material and is within the endograft lumen, the 0.018-in wire is advanced through the laser catheter and fenestration into the lumen of the endograft. A 0.035-in compatible Quick-Cross catheter (Spectranetics, Colorado Springs, CO, USA) is used to exchange for a stiff 0.035-in wire (Fig. 34.5).

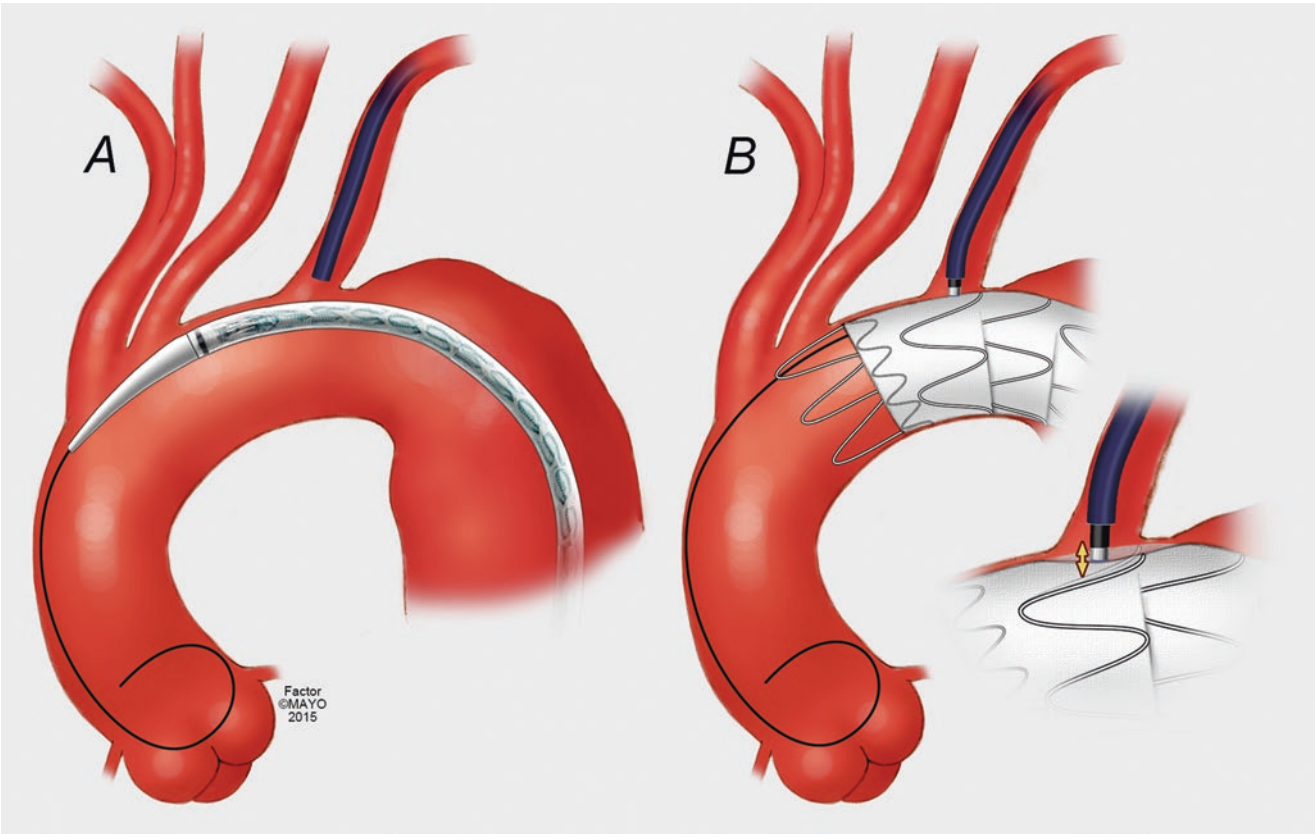


Fig. 34.3 (**a**) Sheath and laser positioned near the ostium of the LSA. (**b**) TEVAR performed with laser and sheath positioned for creation of fenestration. By permission of Mayo Foundation for Medical Education and Research. All rights reserved

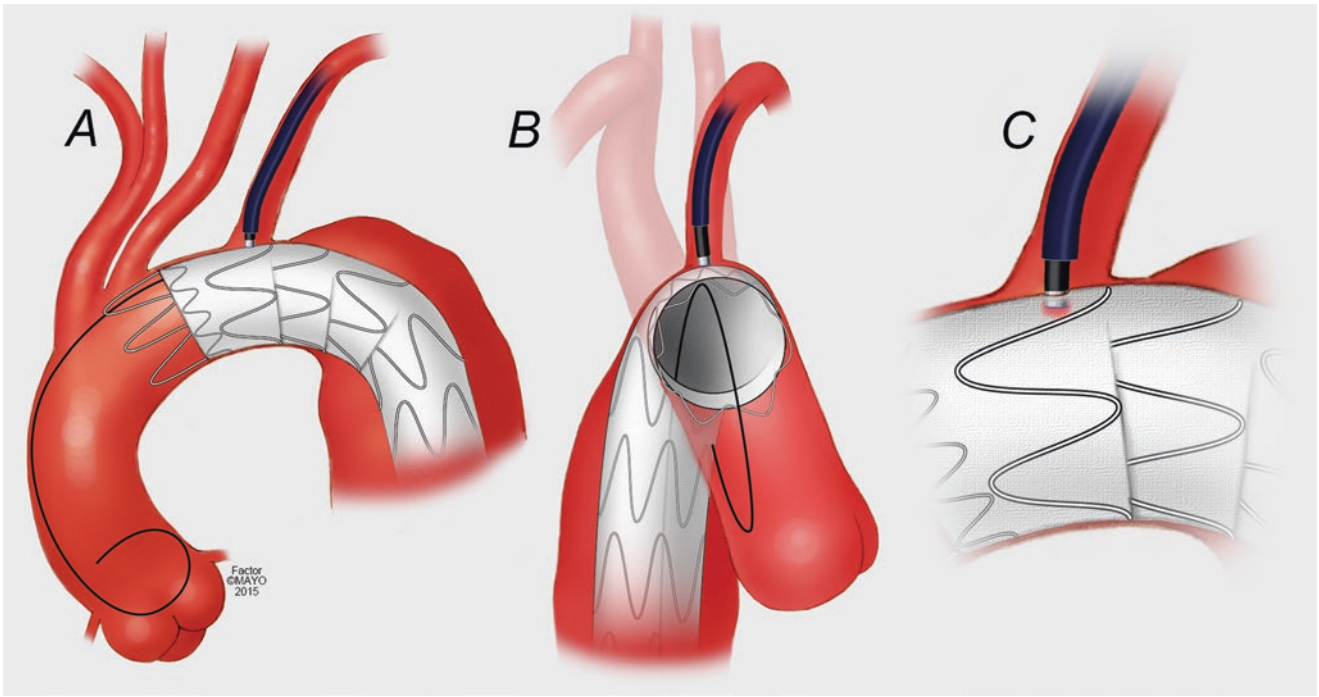


Fig. 34.4 (**a**) LAO deployment view for delivery of the laser. (**b**) RAO view to ensure flush perpendicular, centered contact between the laser and endograft. (**c**) Laser energy applied while applying gentle forward pressure. By permission of Mayo Foundation for Medical Education and Research. All rights reserved

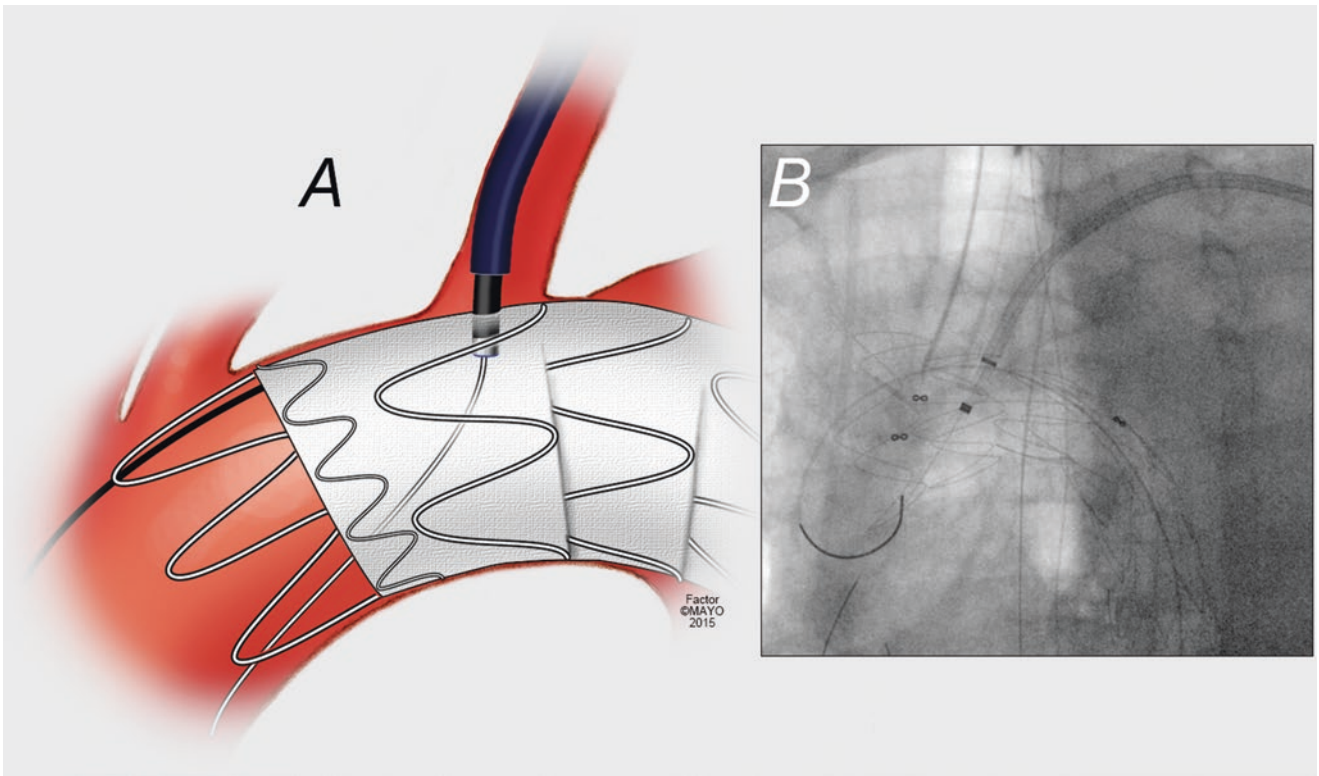


Fig. 34.5 (**a**) Laser fenestration created with gentle forward pressure and application of laser energy. A 0.018 inch wire passed through the fenestration. (**b**) Fluoroscopic view post laser fenestration and wire passage. By permission of Mayo Foundation for Medical Education and Research. All rights reserved

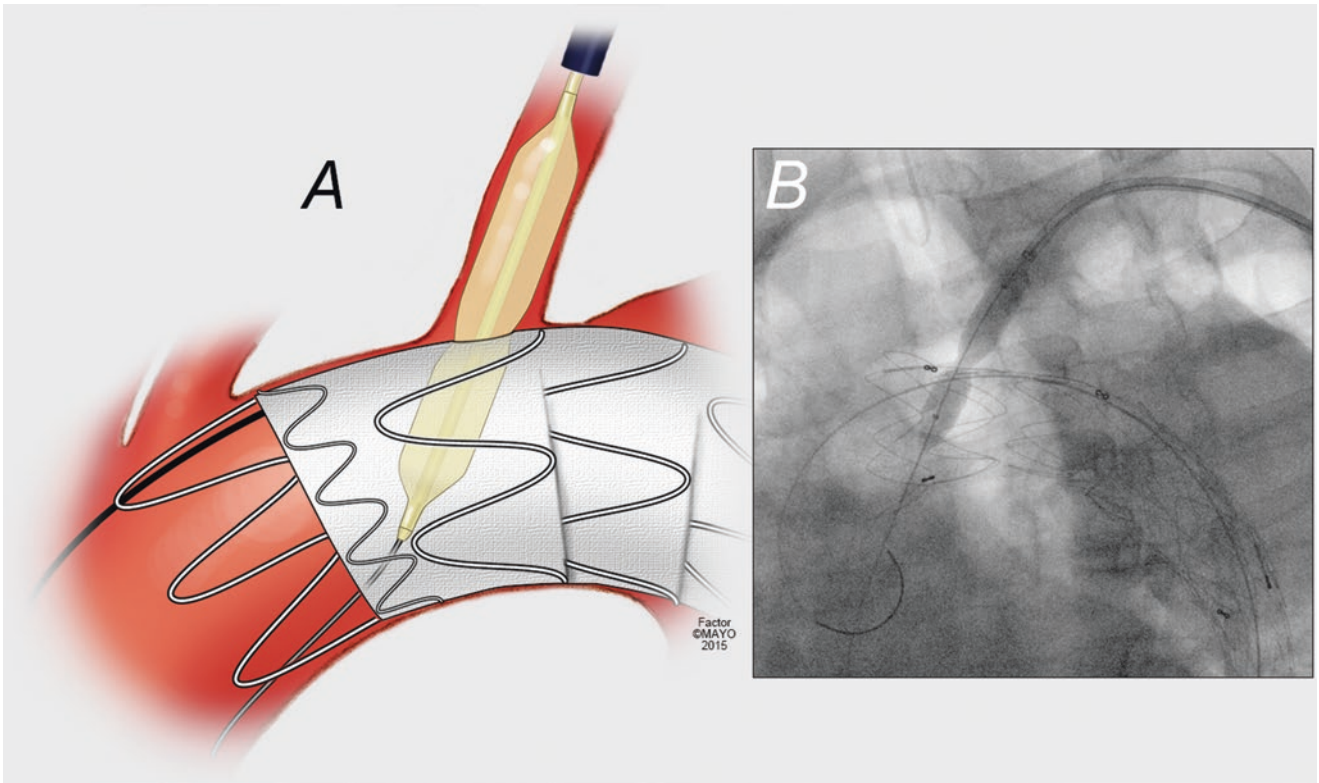


Fig. 34.6 (**a**) Dilation of laser fenestration with 6mm-balloon. (**b**) Flouroscopic view of 6-mm balloon inflated to profile. By permission of Mayo Foundation for Medical Education and Research. All rights reserved

Angioplasty and Stenting

A 6-mm non-cutting balloon is used to pre-dilate the endograft fenestration. A cutting balloon will create unwanted tears in the endograft material (Fig. 34.6). An 8–10-mm iCAST balloon expandable covered stent is positioned partially within the endograft and the LSA. A retrograde arteriogram is performed through the sheath to determine the position of the left vertebral artery (Fig. 34.7). The 8–10-mm iCAST balloon expandable covered stent is deployed with approximately one-quarter of the stent into the endograft lumen and three-quarters into the target vessel proximal to the left vertebral artery (Fig. 34.8a). The intragraft portion of the stent graft is flared using a 14 × 20-mm balloon delivered through the brachial sheath (Fig. 34.8b). It is critical not to dilate the section of stent graft crossing endograft as this will create tears in the thoracic endograft fabric.

Completion Angiogram

A completion aortogram is performed to confirm patency and absence of endoleak (Fig. 34.9).

Complex In Situ Arch Fenestration of the Left Common Carotid

In our experience, laser in situ arch fenestration has proven to be a useful adjunct in expanding the proximal extent of TEVAR in order to obtain adequate seal. One example is a patient that was electively treated for a type II thoracoabdominal aortic aneurysm using a staged approach with LSA to left common carotid artery (LCCA) transposition followed by TEVAR and four-vessel fenestrated endovascular aneurysm repair (FEVAR). A type Ia endoleak was detected during admission for chest pain 1 year later. A redo TEVAR extending the proximal extent to the innominate artery and covering the left common carotid artery was required to seal the type Ia endoleak. Options to expand the proximal seal zone included right common carotid artery to left common carotid artery bypass, a chimney or snorkel graft into the left common carotid artery, or in situ fenestration from the left brachial artery access. The urgency, anatomy, frailty of the patient, and prior neck surgery made in situ fenestration of the LCCA the most logical option.

First, access was gained at the left brachial artery. A catheter and wire were used to cross the left subclavian artery-

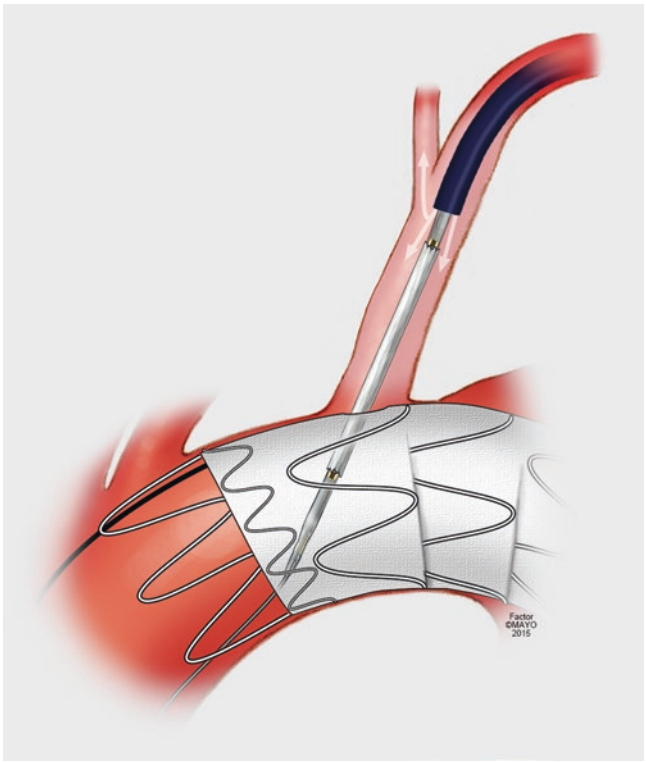


Fig. 34.7 A retrograde arteriogram performed through the brachial artery sheath allows for visualization of the left vertebral artery takeoff. By permission of Mayo Foundation for Medical Education and Research. All rights reserved

left common carotid artery anastomosis. The wire was placed across the left common carotid artery ostium and into the aorta. A 7-Fr sheath was positioned over the wire and parked distal at the LCCA ostium (Fig. 34.10a). The wire was exchanged for an 0.018-in wire and the laser fiber was advanced through the sheath also to the LCCA orifice. The redo TEVAR was performed and the endograft was deployed immediately distal to the innominate artery with the endograft covering the LCCA.

Multiple imaging angles were obtained to ensure adequate perpendicular apposition of the laser fiber to the endograft. A short burst of energy, at 45 mJ/mm^2 fluence and a rate of 25 pulses per second, was applied with gentle forward pressure on the laser catheter to create the fenestration. The 0.018-in wire was then advanced into the endograft and exchanged through a Quick-Cross catheter for a 0.035-in stiff wire. The fenestration was dilated with a 6-mm balloon, and this was followed by deployment of an iCAST 10×38-mm covered stent across the fenestration (Fig. 34.10b). This achieved LCCA revascularization within 3 min. A 14-mm balloon was used to flare the intragraft portion of the iCAST stent. A small type Ia endoleak was present on completion aortogram (Fig. 34.10c). This resolved after EndoAnchor application at the inner curve of the landing zone to reinforce the endograft to aortic wall apposition (Fig. 34.10d). A completion aortogram was performed without evidence of endoleak (Fig. 34.10e).

Fig. 34.8 (**a**) Balloon expandable covered stent deployed across the TEVAR into the LSA. (**b**) Only the intragraft portion of the stent is angioplastied to allow it to flare. By permission of Mayo Foundation for Medical Education and Research. All rights reserved

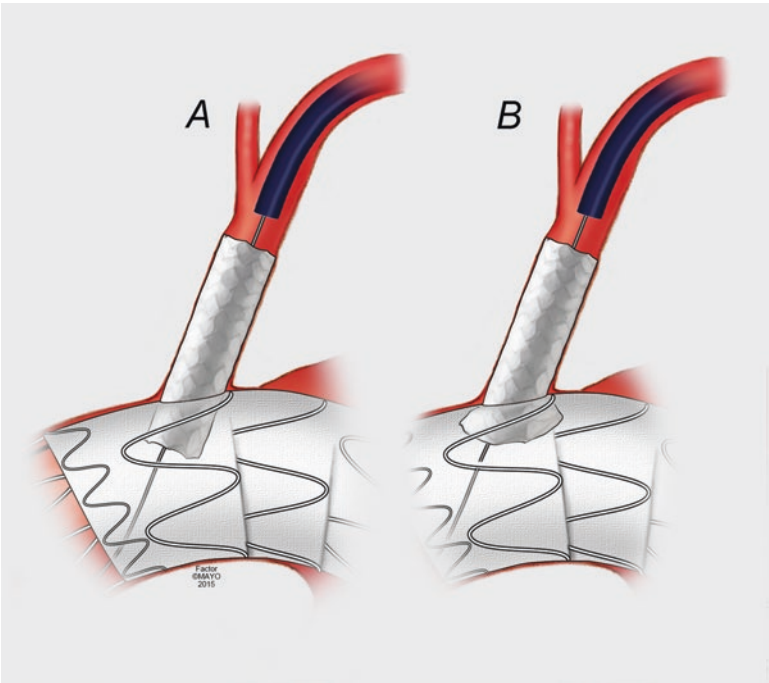




Fig. 34.9 Completion aortogram after laser in situ arch fenestration and covered stent placement into the LSA. By permission of Mayo Foundation for Medical Education and Research. All rights reserved

Application of New Technologies

The in situ fenestration limitations from arch and target vessel anatomy are influenced by the versatility of the tools available to perform the procedure. The development of steerable endovascular sheaths, changes in guidewire and laser compatibility, and the emergence of radiofrequency technology have the potential to push the current anatomic limitations of in situ aortic arch fenestration, increase operative efficiency, and affect long-term durability. In our practice we have begun to use steerable sheaths, such as the TourGuide Steerable sheath (Medtronic Vascular, Santa Rosa, CA, USA), to facilitate accurate positioning of the laser for fenestration in patients with acute target vessel takeoffs. The 180-degree steerable function of the sheath tip optimizes the operator's ability to create perpendicular contact between the fenestration device and the endograft that would not be possible using non-steerable sheath technology (Fig. 34.11). The current drawback of the steerable sheaths is the large French size requiring open axillary or brachial artery exposure.

In addition to steerable sheaths, alterations in the Spectranetics 2.3–2.5 laser have negated the need for wire exchange before balloon dilation of the endograft fenestration. Now, a 0.018-in guidewire is no longer needed for the passage of the laser. A 0.035-in guidewire can be used to deliver the laser to the endograft and pass through the fenestration immediately after its creation. Fewer wire and catheter exchanges decrease procedural time but also simplify the technique and reduce the opportunity for error.

Lastly, radiofrequency ablation (RFA) has shown promising results as an effective energy source for creating in situ aortic arch fenestrations. Eadie et al. studied the effect of RFA on Dacron and ePTFE graft durability and fatigue in an ex vivo model utilizing advanced materials testing [16]. The group found no increase in fenestration size in the Cook Zenith, Medtronic Valiant, and ePTFE grafts after fatigue testing. However, they did note the size of the fenestrations in the Medtronic Talent to be enlarged after accelerated fatigue testing.

Tse et al. followed this initial report with a small series of patients requiring TEVAR with in situ arch fenestration using an 0.035-in PowerWire radiofrequency guidewire (Baylis Medical Company, Mississauga, ON, Canada) [13]. The wire is delivered to the thoracic endograft through a brachial artery 7-Fr sheath. A guiding catheter is sometimes used to provide additional support. The fenestration is created by using a 2-s duty cycle on the high setting of the radiofrequency puncture generator (Baylis Medical Company, Mississauga, ON, Canada) before serial balloon dilation of the fenestration and covered stent deployment. Technical success was achieved in six out of ten planned fenestration cases. The thoracic endograft was landed in zone 3 in two of the patients without need for fenestration. One patient had the LSA covered, but fenestration was not performed due to excellent retrograde filling of the LSA from the left vertebral artery. In the last case, puncture was unsuccessful in a double-layered graft. Five patients received Medtronic Valiant endografts and the other five were Cook Zenith TX2 endografts. The advantages of radiofrequency in comparison to the laser include cost, familiarity of use, and no need for additional safety equipment. Long-term outcomes are not available and no direct comparisons to laser fenestration exist.

Outcomes of In Situ Laser Fenestration

Our group has reported on the use of in situ laser fenestration as a method for arch vessel revascularization during urgent and emergent TEVAR for thoracic aneurysm, acute complicated type B dissection, IMH, and PAU [8, 9]. Including unreported patients treated since publication, a total of 36 patients have undergone attempted revascularization using laser in situ fenestration with a technical success of 97.2 % (35/36). In our very early experience, one patient with a difficult type III arch and sharp target vessel angulation was converted to a snorkel graft technique. Revascularization was limited to the LSA in 33 out of the 35 patients that had successful in situ laser arch vessel fenestration. One patient underwent a total arch debranching with staged TEVAR and innominate fenestration. The other had the LCCA fenestration that was previ-

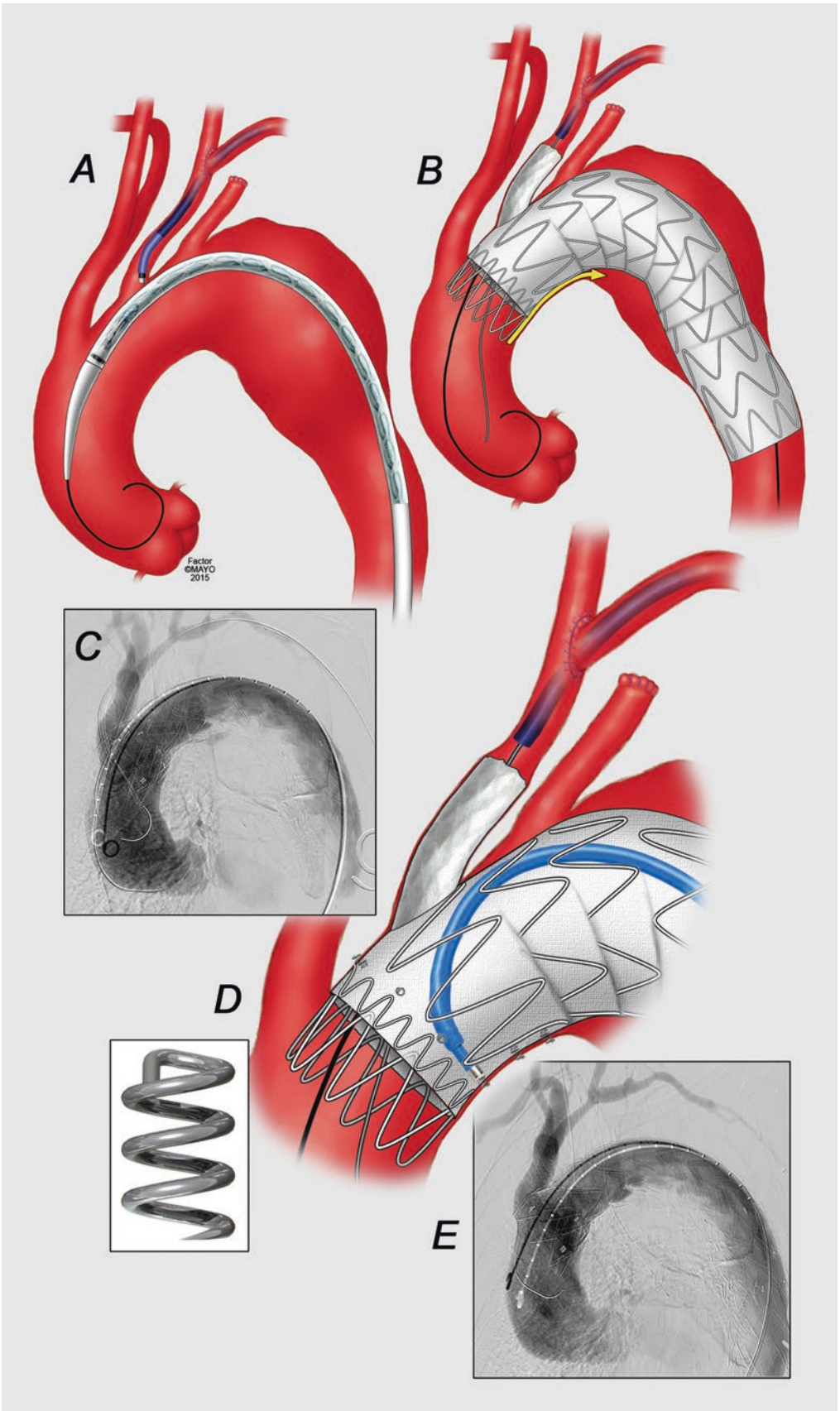


Fig. 34.10 (**a**) 7-Fr sheath and laser parked at the LCCA ostium. (**b**) TEVAR deployed and iCAST stent positioned across the endograft and into the LCCA. (**c**) Aortogram with persistent type Ia endoleak. (**d**) EndoAnchors deployed circumferentially to create proximal seal. (**e**) Completion aortogram demonstrating patent LCCA and no evidence of endoleak. By permission of Mayo Foundation for Medical Education and Research. All rights reserved

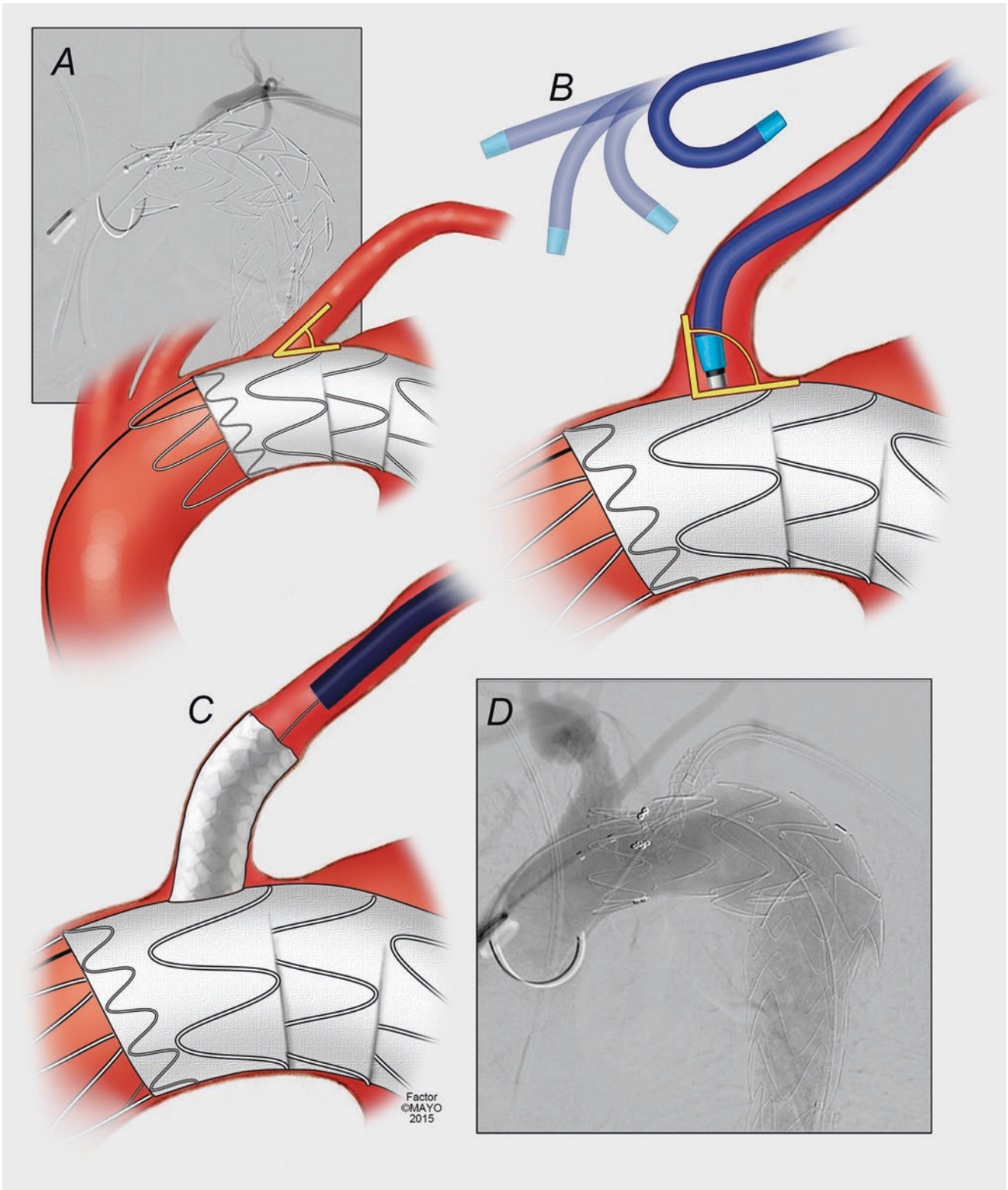


Fig. 34.11 (**a**) Arteriogram demonstrating acute takeoff of the LSA. (**b**) The steerable catheter is used to create perpendicular contact between the laser and endograft. (**c**) A covered stent is deployed across the fenestration. (**d**) Completion aortogram with stent fully deployed. By permission of Mayo Foundation for Medical Education and Research. All rights reserved

ously illustrated by Fig. 34.10a–e. Altogether, no major fenestration-related complications occurred. The minor fenestration-related complication rate was 5.7 % and limited to two arm hematomas requiring operative evacuation. Operative mortality and stroke rates were 5.7 % and 2.9 %, respectively. Paraplegia rate was 2.9 % and occurred in one patient with a ruptured type B dissection. These results suggest this method is a feasible and effective option for a wide spectrum of acute thoracic aortic pathologies.

Conclusion

In conclusion, there are many options for revascularization of aortic arch vessels when treating thoracic aortic pathology with TEVAR. The choice of technique is highly dependent on the severity and acuity of the pathology, arch and target vessel anatomy, availability of various endograft technologies, and local expertise. In situ arch fenestration is an attractive method for arch vessel revascularization in the urgent or emergent setting for thoracic aortic pathologies. It avoids many of the potential risks of open revascularization and can be done in a single operation with shorter procedure times. Additionally, in properly selected patients, the technical challenge of the procedure is often less than deploying chimneys and does not jeopardize the proximal seal zone. Furthermore, it does not require access to custom-made devices that may not be available to surgeons based on geography or the acute nature of the patient's presentation. In situ arch fenestration is a viable technique that can be performed quickly and with good results when treating acute thoracic aortic disease requiring endograft coverage of the arch vessels.

References

1. Patterson BO, Holt PJ, Nienaber C, Fairman RM, Heijmen RH, Thompson MM. Management of the left subclavian artery and neurologic complications after thoracic endovascular aortic repair. J Vasc Surg. 2014;60(6):1491–7.
2. Zamor KC, Eskandari MK, Rodriguez HE, Ho KJ, Morasch MD, Hoel AW. Outcomes of thoracic endovascular aortic repair and subclavian revascularization techniques. J Am Coll Surg. 2015;221(1):93–100.
3. Scali ST, Chang CK, Pape SG, Feezor RJ, Berceli SA, Huber TS, et al. Subclavian revascularization in the age of thoracic endovascular aortic repair and comparison of outcomes in patients with occlusive disease. J Vasc Surg. 2013;58(4):901–9.
4. Bünger CM, Kische S, Liebold A, Leibner M, Glass A, Schareck W, et al. Hybrid aortic arch repair for complicated type B aortic dissection. J Vasc Surg. 2013;58(6):1490–6.
5. McWilliams RG, Murphy M, Hartley D, Lawrence-Brown MM, Harris PL. In situ stent-graft fenestration to preserve the left subclavian artery. J Endovasc Ther. 2004;11(2):170–4.
6. Manning BJ, Ivancev K, Harris PL. In situ fenestration in the aortic arch. J Vasc Surg. 2010;52(2):491–4.
7. Murphy EH, Dimaio JM, Dean W, Jessen ME, Arko FR. Endovascular repair of acute traumatic thoracic aortic transection with laser-assisted in-situ fenestration of a stent-graft covering the left subclavian artery. J Endovasc Ther. 2009;16(4):457–63.
8. Ahanchi SS, Almaroof B, Stout CL, Panneton JM. In situ laser fenestration for revascularization of the left subclavian artery during emergent thoracic endovascular aortic repair. J Endovasc Ther. 2012;19(2):226–30.
9. Redlinger Jr RE, Ahanchi SS, Panneton JM. In situ laser fenestration during emergent thoracic endovascular aortic repair is an effective method for left subclavian artery revascularization. J Vasc Surg. 2013;58(5):1171–7.
10. Rizvi AZ, Murad MH, Fairman RM, Erwin PJ, Montori VM. The effect of left subclavian artery coverage on morbidity and mortality in patients undergoing endovascular thoracic aortic interventions: a systematic review and meta-analysis. J Vasc Surg. 2009;50:1159–69.
11. Chung J, Kasirajan K, Veeraswamy RK, Dodson TF, Salam AA, Chaikof EL, et al. Left subclavian artery coverage during thoracic endovascular aortic repair and risk of perioperative stroke or death. J Vasc Surg. 2011;54:979–84.
12. Riga CV, Bicknell CD, Basra M, Hamady M, Cheshire NJ. In vitro fenestration of aortic stent-grafts: implications of puncture methods for in situ fenestration durability. J Endovasc Ther. 2013;20(4):536–43.
13. Udgiri N, Lin J, Guidoin R, Zhang Z, Dexter D, et al. Scanning electron microscope analysis of ex-vivo laser fenestration of thoracic endografts: variables for optimal fenestrations? Society for clinical vascular surgery 42nd annual symposium, Carlsbad, CA, 19 Mar 2014.
14. Longo GM, Pipinos II. Endovascular techniques for arch vessel reconstruction. J Vasc Surg. 2010;52:77S–81S.
15. Tse LW, Lindsay TF, Roche-Nagle G, Oreopoulos GD, Ouzounian M, Tan KT. Radiofrequency in situ fenestration for aortic arch vessels during thoracic endovascular repair. J Endovasc Ther. 2015;22(1):116–21.
16. Eadie LA, Soulez G, King MW, Tse LW. Graft durability and fatigue after in situ fenestration of endovascular stent grafts using radiofrequency puncture and balloon dilatation. Eur J Vasc Endovasc Surg. 2014;47(5):501–8.

Parallel Stent Graft Techniques to Facilitate Endovascular Repair in the Aortic Arch

35

Frank J. Criado

Introduction

Whether using a traditional open-chest approach or endovascular techniques, the arch remains a big challenge in thoracic aortic surgery, and this is mostly related to the presence of critical branches—*the supra-aortic trunks*. The need to preserve flow into these branches represents a notorious potential impediment to endografting [1]. Historically, the so-called chimney grafts emerged as "bailout" and rescue technique in the effort to preserve or revascularize branches that were inadvertently covered by the endograft [2, 3]. This was certainly true in the author's first arch chimney case, performed in April 2003, when a left common carotid artery (LCCA) chimney stent was deployed via retrograde cervical puncture in the course of endovascular repair of a dissecting thoracic aneurysm that resulted in unintentional coverage of the left carotid artery [4–6].

Chimney graft techniques have evolved significantly over the past 15 years, alongside developments with fenestrated and branched endograft devices that are meant to address some of the same issues [7]. Other terms in use to characterize chimney techniques include *snorkels*, *periscopes*, and *sandwich grafts*. I believe the best all-encompassing term is *parallel stent grafts* (PGs) [8, 9].

Almost immediately after the initial reports, chimneys and PGs were recognized as clearly useful bailout resources, but not without significant downsides and possible complications—mainly those related to the breakage of the seal at the fixation zone and the creation of gutters at the interface between the PG conduit and the intra-aortic endograft leading (potentially) to development of a type 1 endoleak. Published reports have substantiated these fears [10], but showing also wide variability in the rates of gutter-related endoleaks [11, 12]. The aortic segment involved, the number of chimney grafts in the same segment, and the type of PG conduit and aortic endograft used have all been identified as influential factors. This realization and the paucity of data containing high-level evidence have combined to relegate chimneys and PG techniques to a place of inferiority in the minds of some experts who continue to feel their use can be justified only in the context of branch vessel rescue or urgent cases, but refuse to consider their use reasonably in elective situations where other more traditional and accepted forms of arch management strategies are available [10].

This picture is beginning to change, though, as additional recent publications have shown increasingly the undeniable utility of PGs and a lower-than-expected complication rate—especially type I endoleak that would appear to be less common than once feared [12]. The techniques have thus been proclaimed to be "viable" or "acceptable" treatment options—in the aortic arch, pararenal, and iliac segments—by many respected authors and experts in the aortic endografting field around the world [13]. Moreover, their off-the-shelf availability makes them particularly attractive to operators and centers without experience with or access to fenestrated and branched stent graft technologies that are arguably more resource intensive.

The techniques described in this chapter reflect the author's personal experience and lessons learned from others. It is meant to offer readers a relatively simple *how-to* guide on the fundamental technical principles and procedural steps leading to successful execution. However, caution must be exercised at the time of choosing one of these PG techniques versus a more traditional approach to arch branch management for a given patient—and especially so in the context of an elective procedure.

F.J. Criado (✉)
Department of Vascular Surgery, MedStar Union Memorial Hospital, 3333 N. Calvert St., Suite 560, Baltimore, MD 21218, USA
e-mail: frankjcriado@gmail.com

© Mayo Foundation for Medical Education and Research 2017

G.S. Oderich (ed.), *Endovascular Aortic Repair*, DOI 10.1007/978-3-319-15192-2_35

Basic Principles

Not unexpectedly, there is wide variability in the choice of PG conduit and other technical aspects. But the following guidelines should prove useful:

- While bare-metal stents have worked well in our hands for some simple cases, there is now near consensus that in most situations a covered stent (*stent graft*) device should be used.
- Balloon-expandable chimneys (i.e., iCAST) are preferred where a short PG conduit will suffice (i.e., in the LCCA) and, especially, in areas exposed to severe compressive forces and possible crushing (i.e., the origin of the LSA).
- Self-expanding conduits (i.e., the Viabahn device) are widely used where a long PG conduit is needed.
- The greatest disadvantage of the chimney/PG technique relates to the breakage of the seal zone and creation of gutters. The problem can be mitigated or avoided altogether by placing the chimney across a long (2 cm or more) seal zone or by avoiding crossing such area altogether (see description of the LSA periscope technique).

Techniques

Techniques of parallel stent grafts can be used as a primary method to extend the proximal landing zone in patients with thoracic or distal arch aneurysms or as a "bailout" maneuver if there is inadvertent coverage of one of the supra-aortic trunks. These techniques are summarized below according to the Zones of Ishimura and which of the supra-aortic trunks is targeted by the parallel stent.

Zone 2 Deployment

Zone 2 arch deployment is needed in patients undergoing thoracic endovascular aortic repair (TEVAR) for thoracic aortic aneurysms and dissections that extend into the distal arch and require coverage of the left subclavian artery. In these cases, access is established into the left upper extremity using either a trans-brachial percutaneous approach (Fig. 35.1a, inset) or, occasionally, via surgical cutdown exposure. A Glidewire and 5Fr catheter are advanced into the ascending aorta via the brachial approach, while transfemoral access is established into the aortic arch. The Glidewire is exchanged for a stiff 0.035-in. wire for advancement of the thoracic stent graft (Fig. 35.1b). The thoracic endograft is advanced into position in the aortic arch, while a hydrophilic sheath and a chimney stent are delivered to the target position in the LSA (Fig. 35.1c). The thoracic device is deployed just distal to the origin of the left common carotid artery, covering the origin of the LSA (Fig. 35.1d).

The LSA sheath is withdrawn to expose the stent (Fig. 35.1e–g). Selective angiography can be performed via the sheath to demonstrate the origin of the left vertebral artery prior to stent deployment. The LSA chimney-covered stent is deployed fully (Fig. 35.1h). A short balloon-expandable covered stent (e.g., iCAST, Atrium Maquet, Hudson NH) is preferred for short segments. It is critical that the proximal intra-aortic end of the chimney stent be positioned >10 mm proximal to the proximal-most fabric edge of the aortic stent graft to ensure optimal intake of blood flow into the LSA branch. While balloon-expandable stents are preferred for the LSA, a self-expanding device may at times need to be used—mainly for large-diameter LSA vessels or when the chimney is designed to traverse several cm within the aorta (Fig. 35.1i). In such case, it is advisable to add implantation of a short balloon-expandable bare-metal stent within the conduit, placed across the origin of the LSA to protect it and prevent collapse of the crushing-prone self-expanding device (Fig. 35.1j).

Parallel grafts can also be deployed in a retrograde or periscope configuration (Fig. 35.2). The LSA periscope is a relatively new and appealing addition to our armamentarium as it avoids interfering with the proximal seal zone altogether. For these cases, a Viabahn stent graft (Gore, Flagstaff, AZ) is preferred because of its flexibility and wide range of diameters and lengths. Transfemoral access with delivery of long sheath into LSA is depicted in Fig. 35.2a, while the thoracic aortic stent-graft is positioned for deployment in zone 2. A long Viabahn device is delivered through the sheath, which is then retracted, allowing deployment of the covered conduit (Fig. 35.2c). Deploying the Viabahn (tip to hub) has to be done slowly and carefully to avoid pulling the stent out of the target vessel, which can happen with forceful and fast deployment. Note in the illustration that more than one stent may be needed to allow adequate length to reach the distal end of the thoracic endograft. In these cases, deployment is started proximally at the LSA and then carried distally to the end of the thoracic stent. Implantation of a second Viabahn device (Fig. 35.2d), overlapping with the first, is often needed to encompass the full extent of the thoracic stent graft in the descending thoracic aorta and to emerge below some 10–20 mm beyond the distal edge of the fabric (Fig. 35.2e). This technique has also been applied using the transfemoral LSA periscope to revascularize the aberrant RSA (aRSA) (Fig. 35.2f). It is quite appealing given the suitable anatomical course of the proximal portion of the aRSA for targeting from a transfemoral approach.

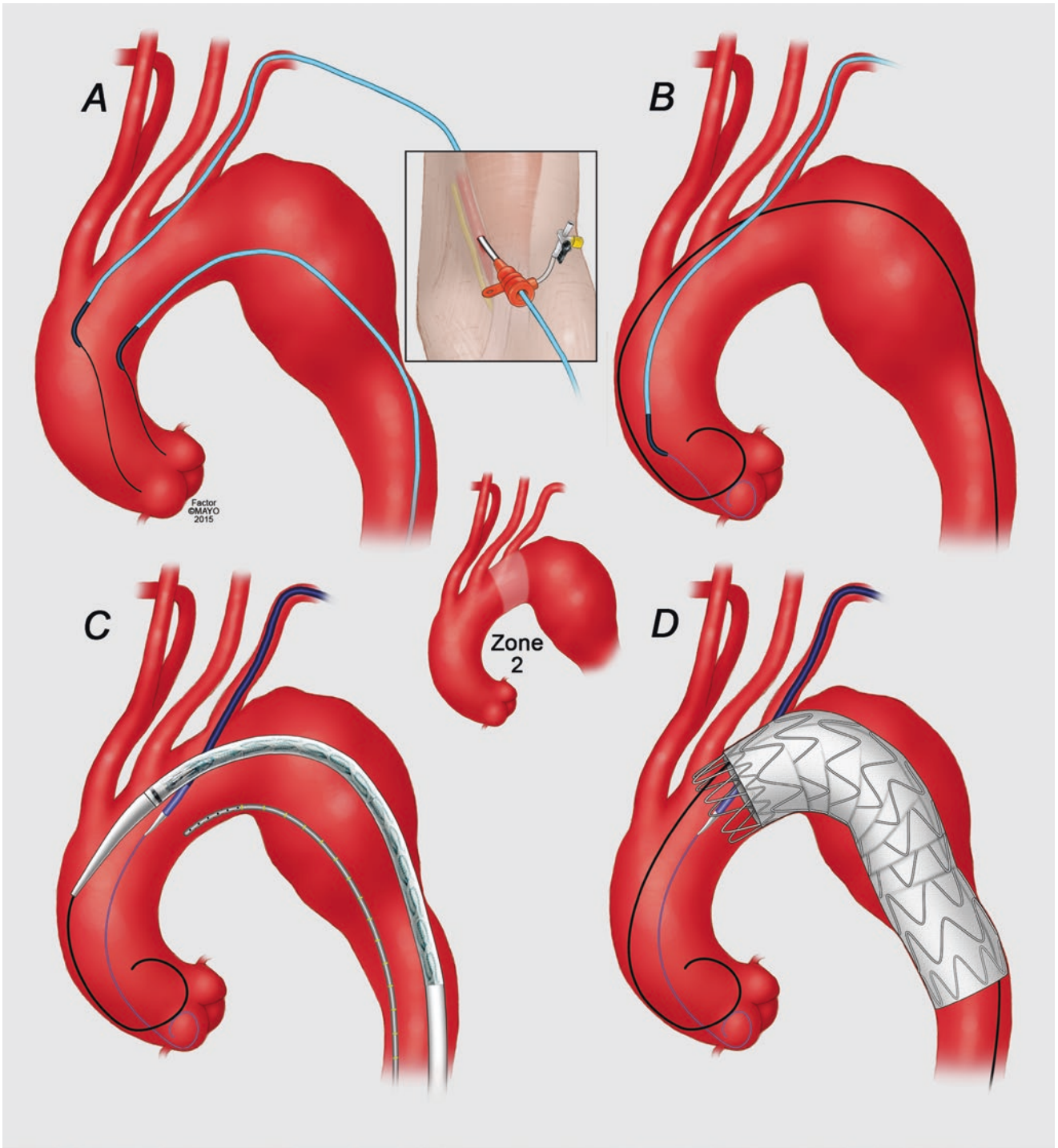


Fig. 35.1 Technique of parallel stent graft for Zone 2 thoracic endovascular aortic repair. (**a**) Access is established using trans-brachial percutaneous (inset) or surgical cutdown exposure. (**b**) Glidewire is exchanged for a 0.035-in. stiff wire for advancement of a thoracic stent graft. (**c**) The thoracic endograft and LSA chimney stent have been delivered to the target position, and (**d**) the thoracic device has been deployed. Deployment of LSA chimney-covered stent (**e**–**h**). Self-expanding stent is used for larger vessels (**i**) and should be reinforced with balloon expandable bare metal stent (**j**). By permission of Mayo Foundation for Medical Education and Research. All rights reserved

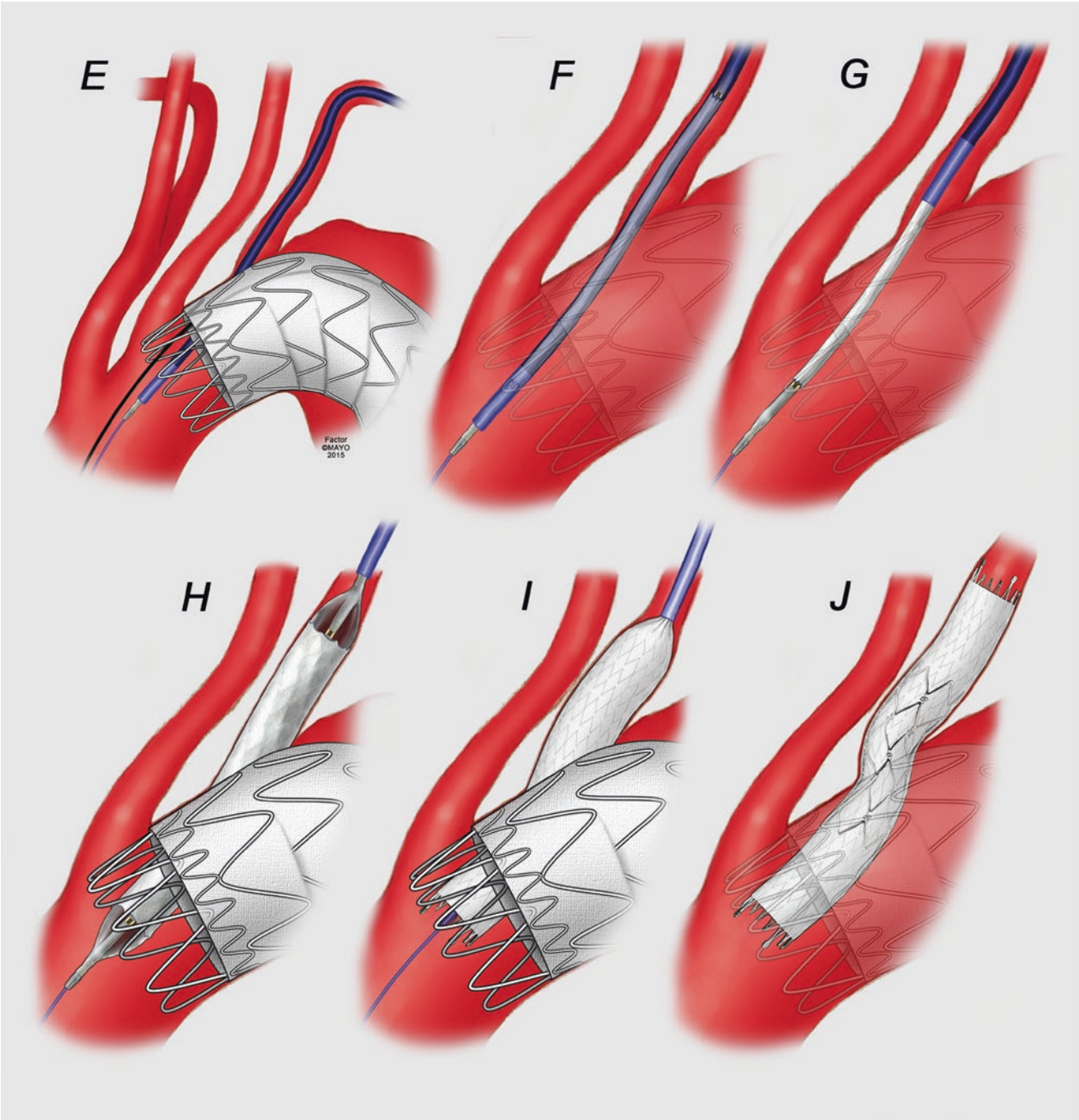


Fig. 35.1 (continued)

Zone 1 Deployment

Proximal landing in arch zone 1 implies coverage of the LSA and LCCA (Fig. 35.3a, inset). The latter must be preserved or revascularized in most if not all such cases. While I have personally most often accessed the left carotid via (retrograde) percutaneous puncture in the left neck, many would prefer to do so using a small-incision cutdown operative technique, in which case preliminary placement of a purse-string suture in its anterior wall would make sense for easy tying and hemostasis after sheath removal. Others might prefer to simply clamp or "finger-pinch" the vessel for a short time while suturing the hole shut.

Access is established both in the LCCA and LSA, which are to be preserved with chimney conduits (Fig. 35.3b). For the LSA, a similar setup is used which has been described

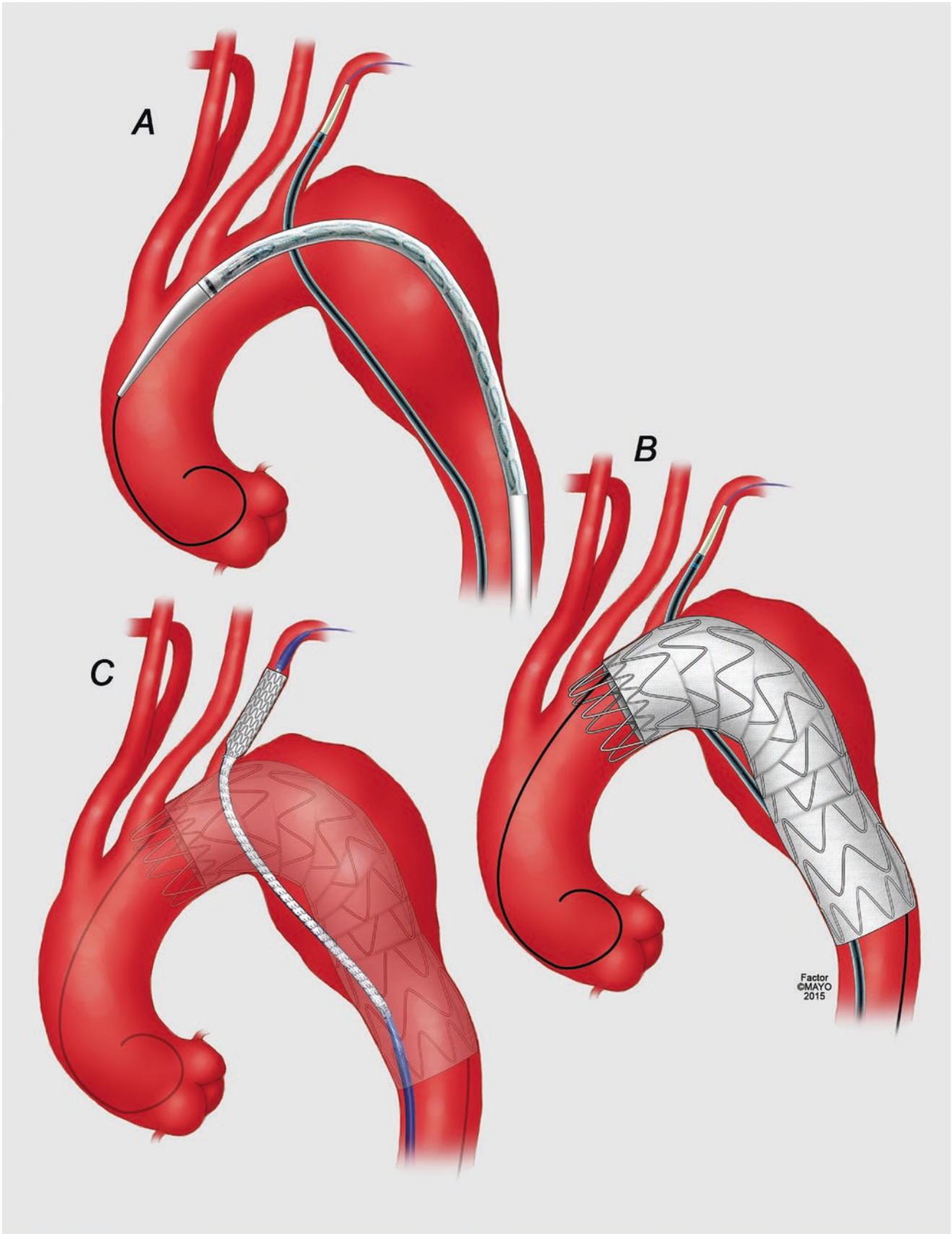


Fig. 35.2 (**a**) The LSA periscope is performed using transfemoral access with delivery of long sheath into LSA. (**b**) After deployment of the thoracic stent, (**c**) a Viabahn is deployed. (**d**) Implantation of a second Viabahn device is often needed to encompass the full extent of the thoracic stent graft. (**e**) The stent 10–20 mm beyond the distal edge of the fabric. (**f**) Transfemoral LSA periscope technique to revascularize the aberrant RSA (aRSA). By permission of Mayo Foundation for Medical Education and Research. All rights reserved

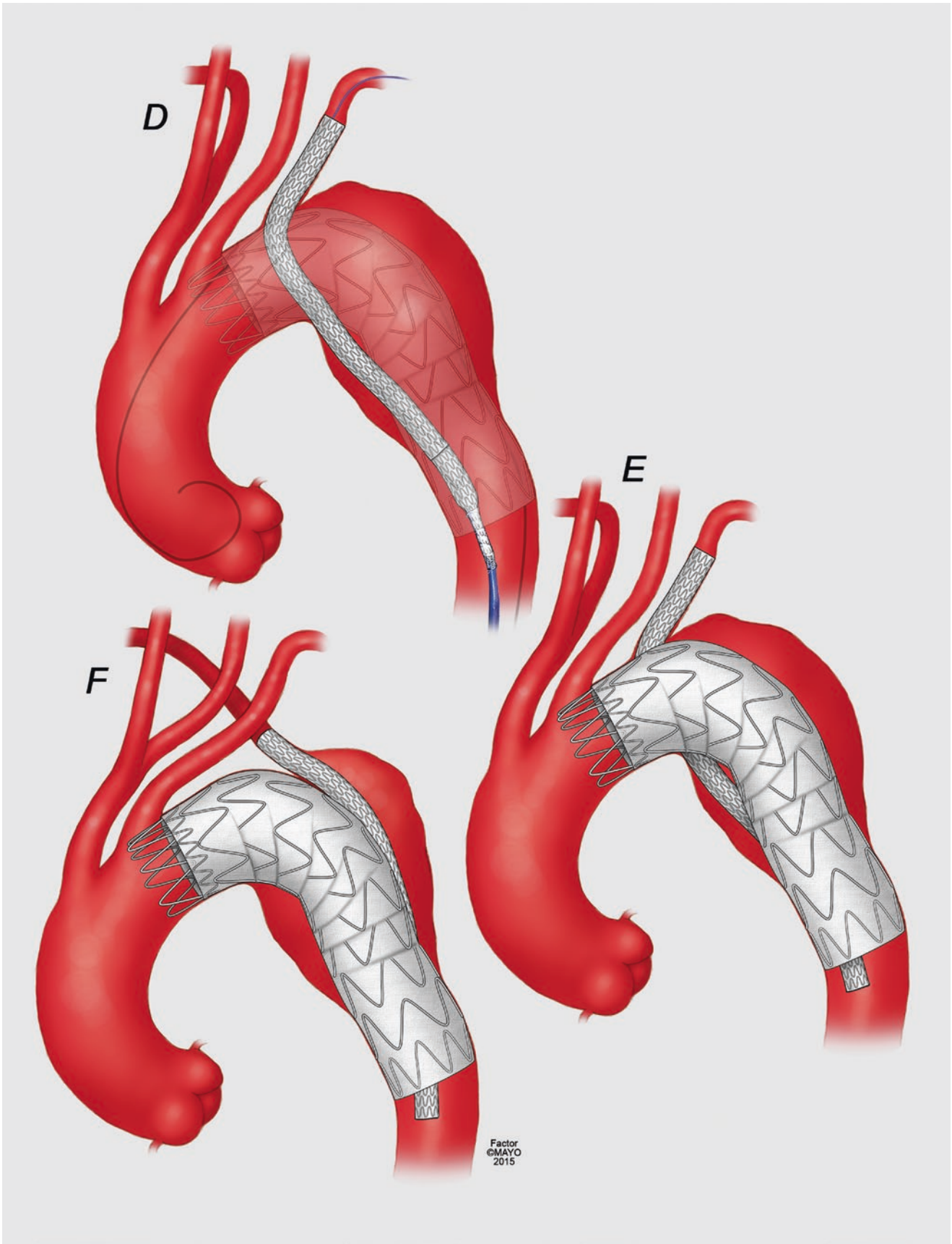


Fig. 35.2 (continued)

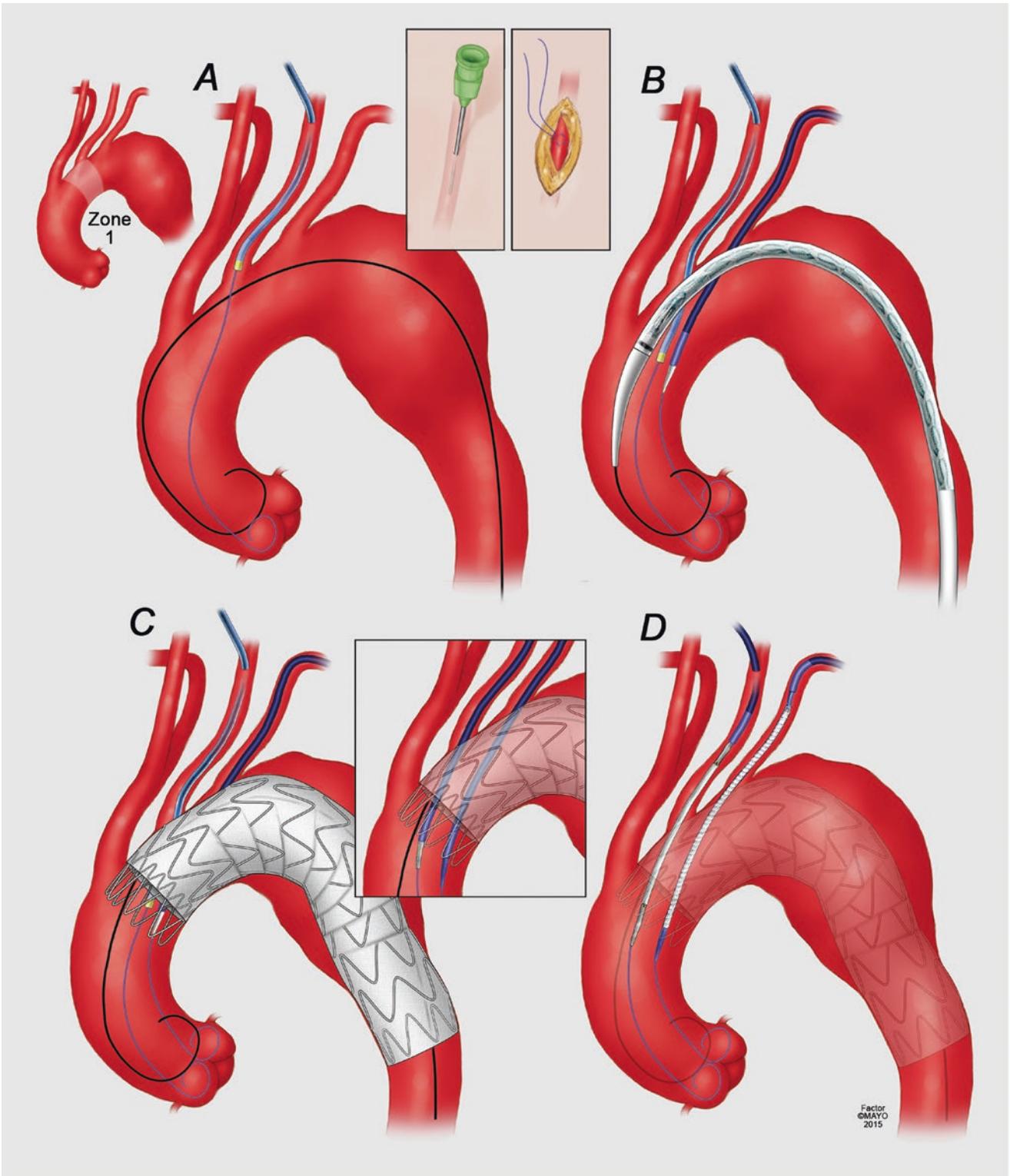


Fig. 35.3 (**a**) Access via left carotid artery (retrograde) using percutaneous puncture or small incision. (**b**) Thoracic stent and sheaths in both LCCA and LSA. (**c**) Thoracic stent is deployed in Zone 1. (**d**) The LCCA and LSA stents are exposed for deployment. (**e**) Preservation of the LCCA with placement of a transcervical iCAST conduit, vascular plug closure of the proximal LSA, and a surgical left carotid-subclavian bypass. (**f**) LSA is not revascularized, and vessel closure is deemed unnecessary because the aortic endograft occludes its origin from within the aorta. (**g**) Cervical bypass revascularization of the LSA using carotid-axillary bypass. By permission of Mayo Foundation for Medical Education and Research. All rights reserved

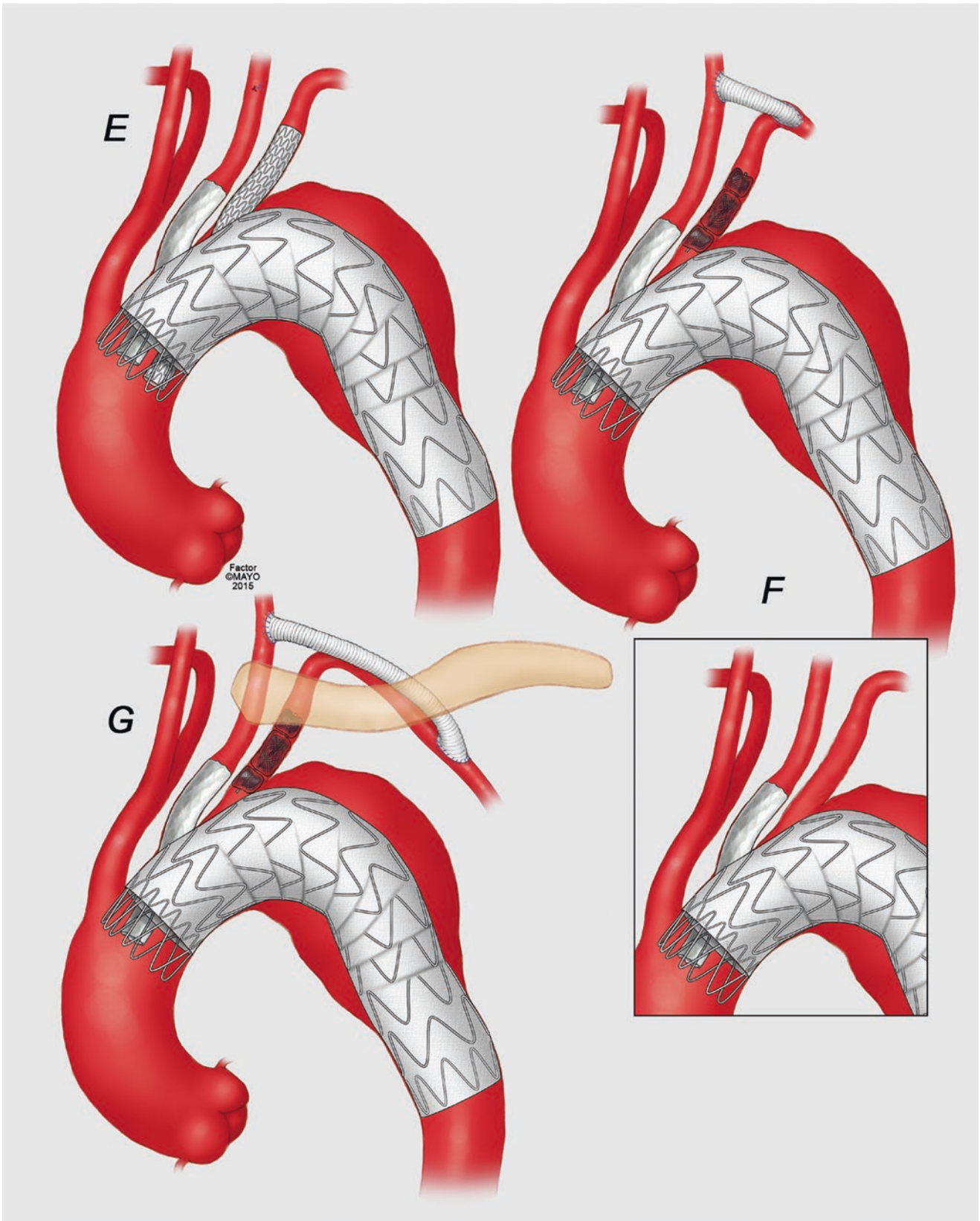


Fig. 35.3 (continued)

in Fig. 35.1 for chimney technique in Zone 2 with the addition of a stiff guidewire and sheath introduced in the LCCA and positioned within the distal ascending aorta. The thoracic endograft is delivered to the arch for deployment in Zone 1. The thoracic stent graft is deployed first, covering the origins of both vessels (Fig. 35.3c). Note technical steps followed for deployment of chimney conduits into both the LSA and LCCA. The sheaths are carefully retracted exposing the chimney stents in both vessels. A Viabahn device is chosen for the longer LSA conduit, and an iCAST balloon-expandable covered stent for the LCCA (Fig. 35.3d). Worth noting are the intra-aortic proximal ends both lying several mm proximal to the proximal edge of the main endograft.

Variations of this technique can be used to decrease the number of chimney grafts and potentially the risk of gutter endoleaks associated with double chimney grafts (Fig. 35.3e). A slightly different strategy consists of preserving the LCCA with placement of a transcervical iCAST conduit, while the proximal LSA is excluded using a vascular plug closure, and a surgical left carotid-subclavian bypass is performed to preserve flow (Fig. 35.3e). The inset shows yet another variation where the covered LSA is not revascularized and vessel closure deemed unnecessary because the aortic endograft is expected to completely occlude its origin from within the aorta.

The author's choice for cervical bypass revascularization of the LSA is illustrated in Fig. 35.3g. In these cases, a left carotid-axillary bypass is performed using two incisions to expose the LCCA in the left neck and the axillary artery via small infraclavicular incision. An 8-mm ringed vascular graft is tunneled under the clavicle and anastomosed end to side to the axillary artery. Axillary-artery exposure, instead of the subclavian artery, is felt to be technically easier and essentially free of potential nerve and lymphatic complications. In suitable anatomies, a right trans-brachial or trans-axillary approach may be considered for deployment of the LCCA chimney (Fig. 35.4).

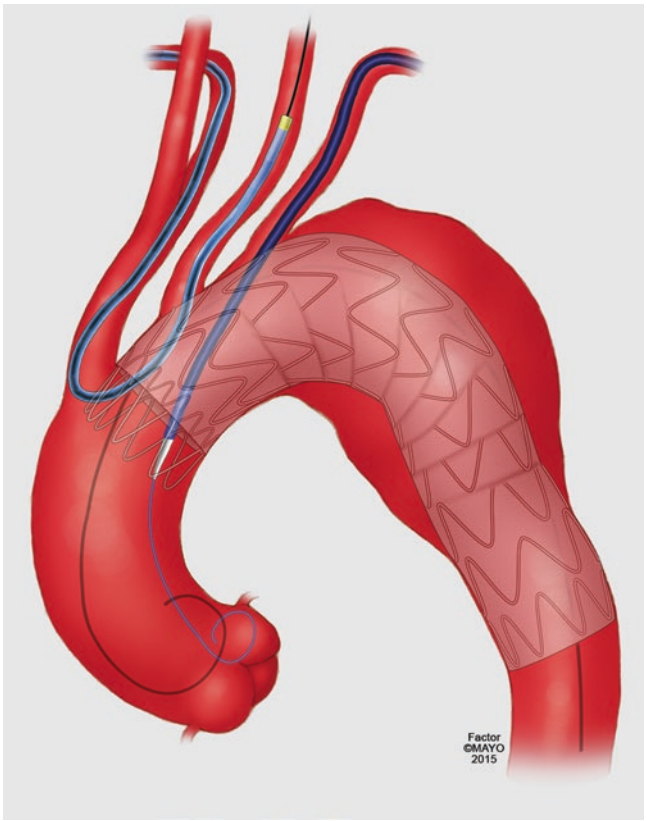


Fig. 35.4 A right trans-brachial or trans-axillary approach may be considered for deployment of the LCCA chimney. By permission of Mayo Foundation for Medical Education and Research. All rights reserved

Zone 0 Deployment

Even more controversial than the rest are chimney solutions for extra-thoracic total arch debranching through a hybrid combination of surgical maneuvers in the neck and placement of a PG conduit into the innominate artery (IA, brachiocephalic trunk). The technical strategy is largely based on the use of the RCCA as access site for IA chimney delivery and deployment and as the origin for a surgical crossover bypass to the LCCA—and to the LSA (if desired). Care must be exercised to sequence the various steps in the best possible way to minimize or avoid cerebral ischemia.

First, construction of the crossover carotid-carotid bypass, plus a left carotid-subclavian (or carotid-axillary) bypass, is performed as discussed in Chap. 36 (Fig. 35.5a). Retrograde access into the IA is established using a puncture of the surgically exposed RCCA at a point below the graft anastomosis, followed by advancement of guidewire into the ascending aorta and insertion of a suitable (14–16F) introducer sheath through which one can deliver the PG conduit. In these cases, the IA may be of larger diameter (14–18 mm), which often requires the use of an iliac limb of an EVAR graft system. The thoracic stent graft is positioned for deployment in Zone 0. After the thoracic stent is deployed (Fig. 35.5b), it is probably best to complete deployment of the IA device and to surgically repair the arteriotomy site in the RCCA to reestablish normal antegrade flow (Fig. 35.5c), followed by a separate needle puncture to regain guidewire access into the conduit which will be necessary for subsequent post-ballooning to be done after deployment of the aortic endograft.

It is wise to position precisely the constrained aortic endograft in the target Zone 0 for landing and in its relation to the IA chimney in its sheath *before* deploying the chimney device to ensure optimal final placement of the two as shown in Fig. 35.5c. Alternatively, one could choose to deploy the

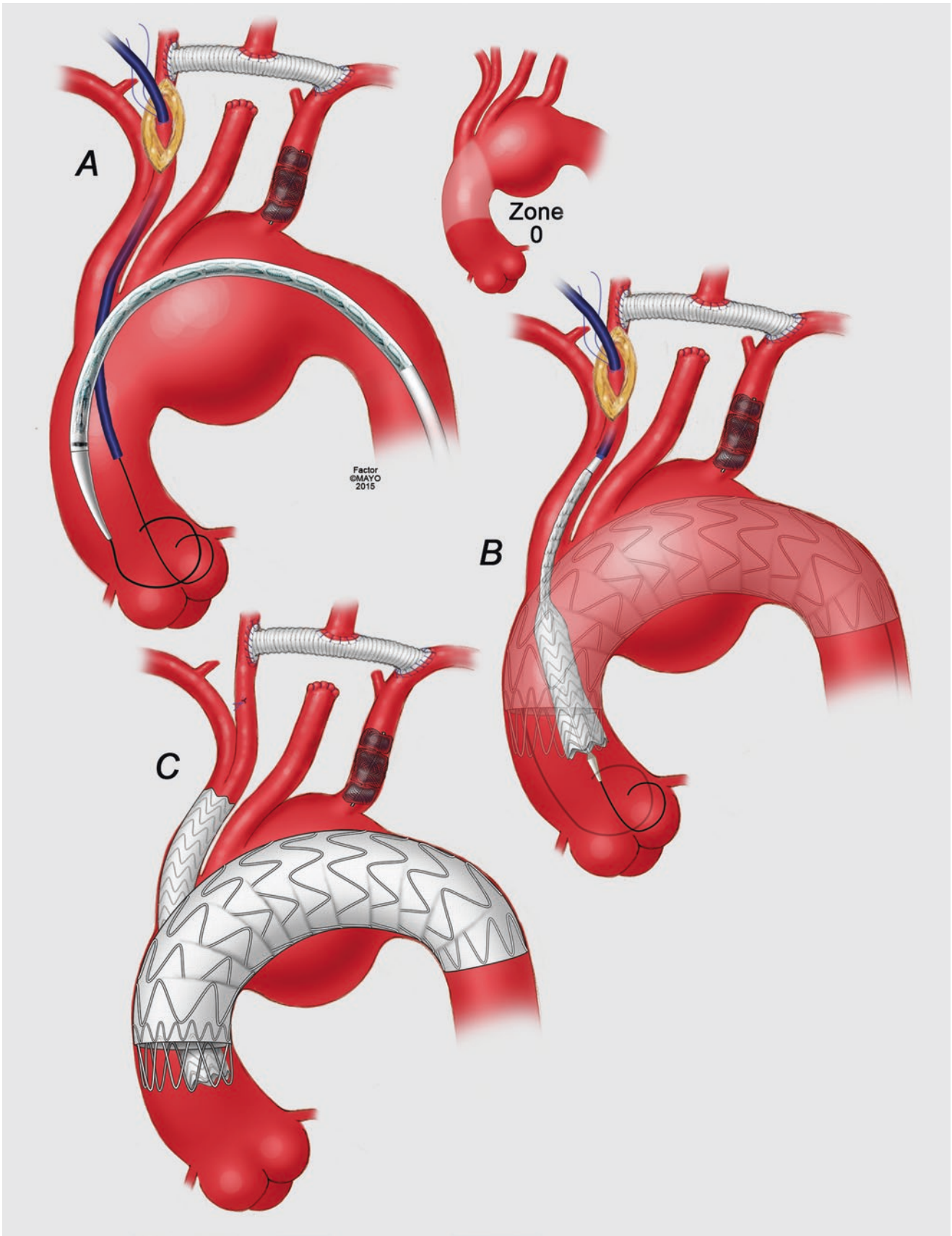


Fig. 35.5 (**a**) Surgical crossover bypass to the LCCA and to the LSA. (**b**) Deployment of the IA stent is completed. (**c**) The RCCA puncture is surgically repaired to reestablish normal antegrade flow immediately.

By permission of Mayo Foundation for Medical Education and Research. All rights reserved

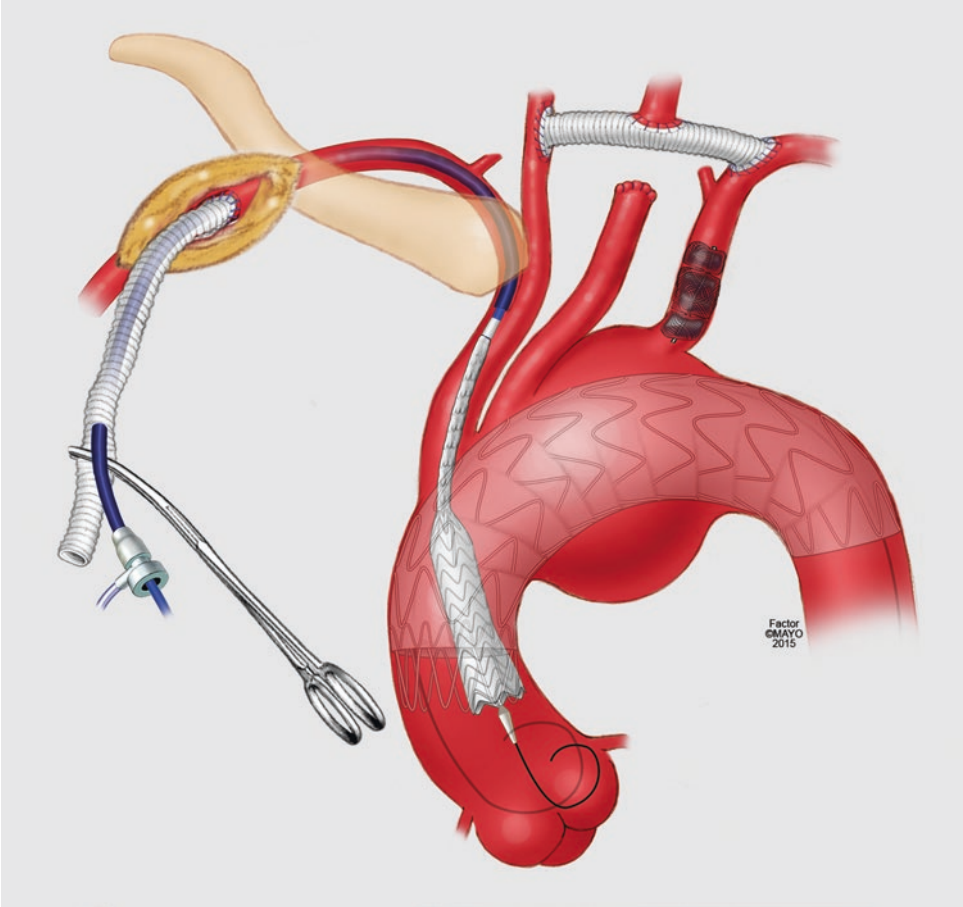


Fig. 35.6 A right axillary artery access conduit can also be used for delivery and deployment of the IA chimney. By permission of Mayo Foundation for Medical Education and Research. All rights reserved

aortic endograft first and then quickly proceed to IA chimney deployment and reestablishment of normal blood flow in the RCCA—using a small partial occlusion clamp to control the arteriotomy site if necessary. But such strategy is definitely more risky and haste inducing because of the danger of prolonged cerebral ischemia. Lastly, the proximal LSA can be closed (if deemed necessary) with a vascular plug delivered through a left trans-brachial approach. A modification of this technique is depicted in Fig. 35.6. A right axillary artery access conduit can also be used for delivery and deployment of the IA chimney.

Conclusion

Parallel stent graft techniques have emerged as a reasonable alternative in patients with complex aneurysms who need extension of proximal landing zones across critical aortic branches. The technique has been widely applied in the aortic arch, pararenal, and iliac arteries.

References

1. Greenberg RK, Clair D, Srivastava S, Bhandari G, Turc A, Hampton J, et al. Should patients with challenging anatomy be offered endovascular aneurysm repair? J Vasc Surg. 2003;38:990–6.
2. Criado FJ, Barnatan MF, Rizk Y, Clark NS, Wang CF. Technical strategies to expand stent-graft applicability in the aortic arch and proximal descending thoracic aorta. J Endovasc Ther. 2002;9(suppl II):II-32–II-38.
3. Ohrlander T, Sonesson B, Ivancev K, Resch T, Dias N, Malina M. The chimney graft: a technique for preserving or rescuing aortic arch branch vessels in stent-graft sealing zones. J Endovasc Ther. 2008;15:427–32.
4. Mangialardi N, Serrao E, Kasemi H, Alberti V, Fazzini S, Ronchey S. Chimney technique for aortic arch pathologies: an 11-year single-center experience. J Endovasc Ther. 2014;21:312–23.
5. Criado FJ. A percutaneous technique for preservation of arch branch patency during thoracic endovascular aortic repair (TEVAR): retrograde catheterization and stenting. J Endovasc Ther. 2007;14:54–8.
6. Criado FJ. Chimney grafts and bare stents: aortic branch preservation revisited. J Endovasc Ther. 2007;14:823–4.
7. Donas KP, Torsello G, Bisdas T, Osada N, Schönefeld E, Pitoulias GA. Early outcomes for fenestrated and chimney endografts in the

treatment of pararenal aortic pathologies are not significantly different: a systematic review with pooled data analysis. J Endovasc Ther. 2012;19:723–8.
8. Criado FJ, Duson S. Parallel grafts in perspective: definitions and a new classification. Vasc Dis Manag. 2013;10:16–9.
9. Lachat M, Veith FJ, Pecoraro F, Glenck M, Bettex D, Mayer D, et al. Chimney and periscope grafts observed over 2 years after their use to revascularize 169 renovisceral branches in 77 patients with complex aortic aneurysms. J Endovasc Ther. 2013; 20:597–605.
10. Scali S, Feezor RJ, Chang CK, Waterman AL, Berceli SA, Huber TS, et al. Critical analysis of results after chimney endovascular aortic aneurysm repair raises cause for concern. J Vasc Surg. 2014;60:865–73.
11. Hogendoorn W, Schlosser FJV, Moll FL, Sumpio BE, Muhs BE. Thoracic endovascular aortic repair with the chimney graft technique. J Vasc Surg. 2013;58:502–11.
12. Gehringhoff B, Torsello G, Pitoulias GA, Austermann M, Donas KP. Use of chimney grafts in aortic arch pathologies involving the supra-aortic branches. J Endovasc Ther. 2011;18:650–5.
13. Donas KP, Lee JT, Lachat M, Torsello G, Veith FJ, PERICLES investigators. Collected world experience about the performance of the snorkel/chimney endovascular technique in the treatment of complex aortic pathologies. Ann Surg. 2015;262:546–53.

Techniques and Results of Aortic Arch Hybrid Repair

36

Muhammad Ali Rana, Gustavo S. Oderich, and Alberto Pochettino

Introduction

Aneurysms involving the supra-aortic arch vessels have been traditionally treated by total or partial arch replacement. Open repair remains the gold standard in low- and intermediate-risk patients. However, the need for cardiopulmonary bypass and circulatory arrest with deep hypothermia increases risk and complexity of reconstruction in patients who are elderly, are frail, and have multiple comorbidities [1–5]. Endovascular repair of the arch is an area of much interest and ongoing innovation; however, there are significant technical obstacles. The arch has natural angulation, variable origins of the supra-aortic trunks, the presence of atherosclerotic debris, proximity to coronary arteries and aortic valve, the presence of coronary bypass grafts, and the hemodynamic and respiratory forces that are unique compared to other aortic segments. Combining open revascularization of the supra-aortic trunks with endovascular exclusion provides a way to limit the extent of open surgery, while simplifying the endovascular portion in order to potentially reduce the incidence of neurological, cardiovascular, and respiratory complications. Such hybrid techniques have emerged as an attractive option in the higher-risk patients who are considered poor candidates for open repair because of severe pulmonary dysfunction, heart failure, or multiple prior sternotomies. Although some centers can achieve excellent results with open arch repair on almost every patient, outcomes in the community are more ominous. Hybrid approaches include supra-aortic trunk debranching as well as the endovascular extension of a surgical aortic arch replacement using frozen elephant trunk or elephant trunk with endovascular completion techniques. This chapter describes the concepts and techniques as well as contemporary results with hybrid arch repairs using arch debranching and also some of the technical aspects of frozen elephant trunk techniques.

Anatomy and Patient Selection

The goal of arch debranching is to secure a suitable proximal seal zone within the native aorta or in a surgically replaced ascending aorta in patients with proximal dissections. Proximal landing zones should be at least 20 mm in length and ideally less than 38 mm in diameter (although devices of 45 mm accept larger landing zones), without excessive thrombus or atherosclerosis. In the proximal arch, a landing landing zone length of 30–40 mm is better and 20 mm is probably too short. 20 mm is probably too short. Selection of the landing zone requires careful review and consideration of patient's anatomy, including the identification and quality of the arch and its relation to the origins of the supra-aortic trunks. Consideration is also given to the inner curve angulation of the potential proximal landing zone in order to avoid "bird beak" of the proximal stent graft. The location of the proximal seal zone has been classified by Ishimaru [6] (Fig. 36.1). This classification determines the approach and extent of debranching. Similarly, the distal landing zone is determined by the distal extent of the aneurysm and may also require consideration of visceral segment coverage or reconstruction. The arch debranching operations are classified into proximal and distal debranching based on the need to revascularize the innominate artery via a median sternotomy.

M.A. Rana
Division of Vascular Surgery, University of New Mexico, MSC 10 5610, Albuquerque, NM 87131, USA

G.S. Oderich (✉)
Division of Vascular and Endovascular Surgery, Mayo Clinic, 200 First Street SW, Rochester, MN 55905, USA
e-mail: oderich.gustavo@mayo.edu

A. Pochettino
Division of Cardiovascular Surgery, Mayo Clinic, 200 First Street SW, Rochester, MN 55905, USA

© Mayo Foundation for Medical Education and Research 2017

G.S. Oderich (ed.), *Endovascular Aortic Repair*, DOI 10.1007/978-3-319-15192-2_36

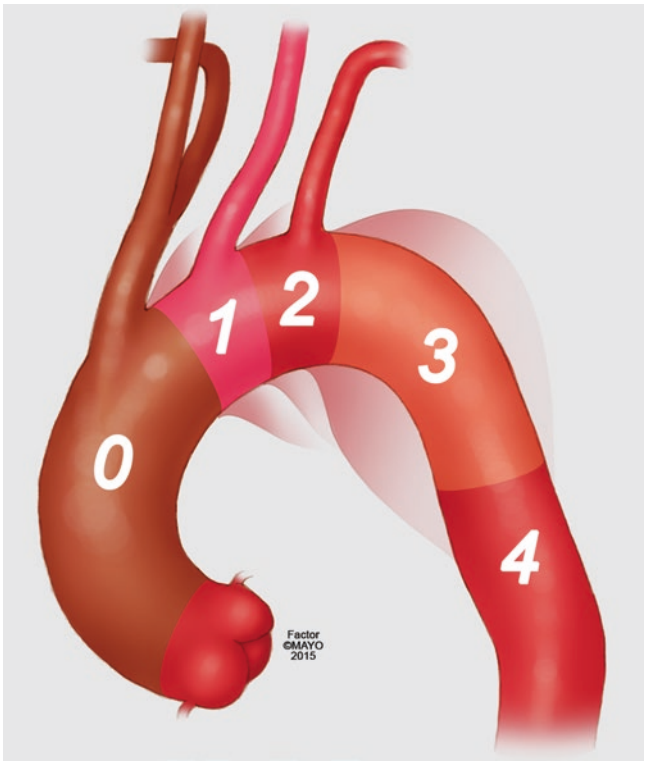


Fig. 36.1 The arch zones of implantation as described by Ishimaru. By permission of Mayo Foundation for Medical Education and Research. All rights reserved

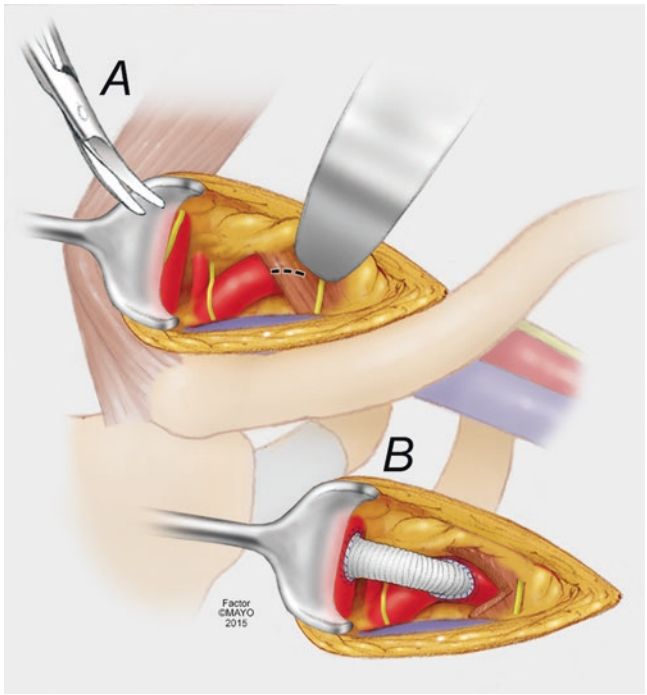


Fig. 36.2 Left subclavian artery revascularization is done via supraclavicular incision. After the anterior scalene fat pad is retracted cephalad, the phrenic nerve is identified on top of the anterior scalene muscle (**a**), and the muscle is transected. The subclavian artery is exposed for the distal anastomosis. Bypass is done using a short 7- or 8-mm polyester graft (**b**). By permission of Mayo Foundation for Medical Education and Research. All rights reserved

Distal Arch Debranching

Distal arch debranching is done using a cervical based extra-anatomical bypass. These patients typically have 2–3 cm landing zone distal to the origin of innominate artery in zones 1 and 2. There is no need for sternotomy, although translocation of the left common carotid to the innominate artery can be done using a mini-sternotomy. The location of the landing zone determines the extent of reconstruction (e.g., carotid-carotid, carotid-subclavian).

Left Subclavian Artery Revascularization

Coverage of the left subclavian artery (LSA) origin may be indicated in patients with aneurysms involving the distal arch or in patients with dissections or traumatic aortic injuries in proximity to the subclavian origin (Zone 2). Although routine revascularization of the LSA remains controversial, most agree that it can be performed with relatively low morbidity and may decrease neurological complications in patients with extensive aortic involvement. A recent systematic review indicated that subclavian artery coverage without revascularization was associated with threefold increase in paraplegia, 2.5-fold increase in anterior circulation strokes, 48-fold increase in arm ischemia, and 11-fold increase in vertebrobasilar ischemia. There is a 4.4 % incidence of phrenic nerve palsy in patients who underwent surgical subclavian revascularization [7]. Recent guidelines of the Society for Vascular Surgery, therefore, recommend preoperative subclavian revascularization in patients undergoing elective TEVAR requiring coverage of the left subclavian artery for adequate stent graft seal and in patients with patent left internal mammary to coronary artery graft, termination of the left vertebral artery into the posterior inferior cerebellar artery, absent or atretic right vertebral artery, patent left arm arteriovenous fistula or graft, prior infrarenal aortic repair, planned extensive coverage (>20 cm) of the descending thoracic aorta, and occlusion of the internal iliac arteries [8].

Revascularization of LSA can be performed with either a left carotid-subclavian bypass or subclavian to carotid transposition. Arteries are exposed with a supraclavicular incision and division of the clavicular head of sternocleidomastoid (Fig. 36.2). The same incision can be used to access both the left carotid and LSAs. The pre-scalene fat pad is raised cranially, while the phrenic nerve is identified and protected on top of the anterior scalene muscle. The muscle is transected with scissors and cautery exposing the subclavian artery, which lies under the muscle. This portion of the procedure is done with careful preservation of the phrenic nerve. The subclavian artery is dissected free from just distal to the verte-

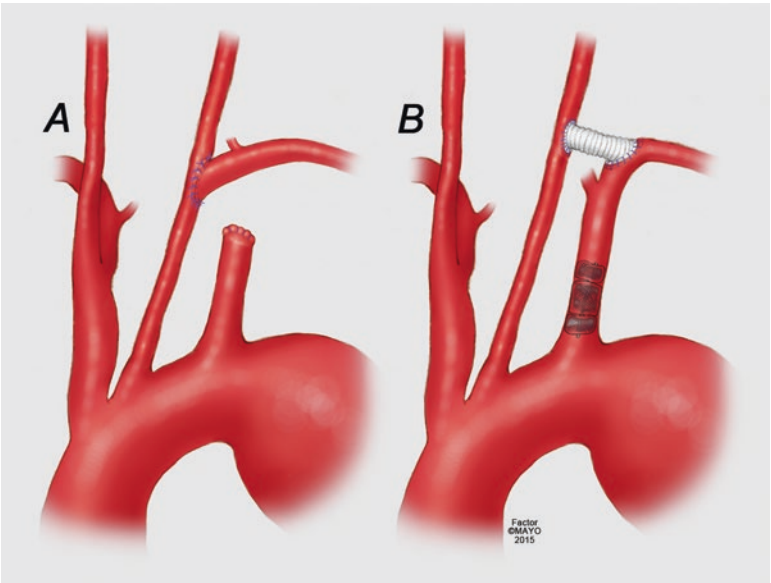


Fig. 36.3 Left subclavian artery revascularization done with transposition technique (**a**). Note in these cases the proximal subclavian artery is transected and closed with running Prolene suture. Anastomosis to the left common carotid artery is done with a running posterior suture and interrupted sutures in the anterior wall to avoid narrowing. Our preference is to perform a prosthetic carotid-subclavian bypass (**b**). In these cases, the proximal subclavian artery is occluded using an Amplatzer plug. By permission of Mayo Foundation for Medical Education and Research. All rights reserved

bral and internal mammary arteries to under the clavicle. Side branches are controlled with vessel loops. The left carotid artery is dissected free by mobilizing the sternocleidomastoid muscle anteriorly. Once the left carotid artery is mobilized, a tunnel is created behind the internal jugular vein and in front of the vagus nerve. Transposition (Fig. 36.3a) offers the advantage of a single anastomosis without the need of prosthetic graft conduit; however, it requires more extensive dissection proximally beyond the origin of the left vertebral artery. Clamping is also done proximal to the vertebral and internal mammary artery, which poses some disadvantage in the patient with LIMA coronary grafts. In general, the author's preference is to do a bypass (Fig. 36.3b), which greatly simplifies the operation and is associated with excellent patency rates of well beyond 95 % over 5 years.

The patient is systemically heparinized with 80 units/kg of intravenous heparin. The distal and proximal left subclavian arteries are clamped and the side branches are controlled with loops. A longitudinal arteriotomy is made in the anterior wall of the subclavian artery. Our preference is to use polyester graft as opposed to PTFE, and ringed grafts are not needed even for carotid crossover bypass. A 7- or 8-mm graft is ideal, and we avoid 6-mm grafts which may have higher failure rates, even in those patients with smaller subclavian arteries. The graft is beveled and anastomosed end to side using 6-0 Prolene suture. The subclavian artery is one of the most fragile vessels, so relatively larger bites are taken. We start the anastomosis at the heel and work toward the middle. Three interrupted sutures are used at the toe of the anastomosis. These are then approximated and the sutures are run toward the middle to complete the anastomosis, which is tested by flushing the graft with heparinized saline. Back-bleeding and fore-bleeding are allowed through the graft and the clamps are released, restoring flow into the left upper extremity. The clamp is applied into the graft, adjacent to the anastomosis, and the blood is aspirated from the graft, which is tunneled behind the internal jugular vein. The graft should not be under tension. The location of the arteriotomy is marked in the lateral wall of the left common carotid artery. The proximal and distal carotid artery is clamped and an arteriotomy is made. The graft is cut to length, gently beveled, and anastomosed end to side using running 5-0 Prolene. Our preference is to start the anastomosis in the middle of the posterior wall and run the suture toward the corners. Each corner is interrupted to avoid purse-string effect in the anastomosis. Adequate back-bleeding and fore-bleeding are allowed, the anastomosis is completed, and the flow is restored first toward the left subclavian artery and then into the left common carotid artery.

Left subclavian revascularization is done nearly always as a single stage procedure in conjunction with TEVAR. In these cases, the proximal subclavian artery is occluded using an Amplatzer plug, which is introduced via small incision and puncture in the distal left brachial artery. Introduction of the sheath and catheter can also be done at the distal anastomosis of the carotid-subclavian graft, but this is more cumbersome and risky damaging the fragile anastomosis to the subclavian artery.

Left Common Carotid Artery Revascularization

In patients with aneurysms requiring coverage of the left carotid artery with landing zone in Zone 1 or 0, revascularization of both the left carotid and subclavian arteries is needed. If a total endovascular approach is used with the Cook Arch device, one of the internal branches of the device

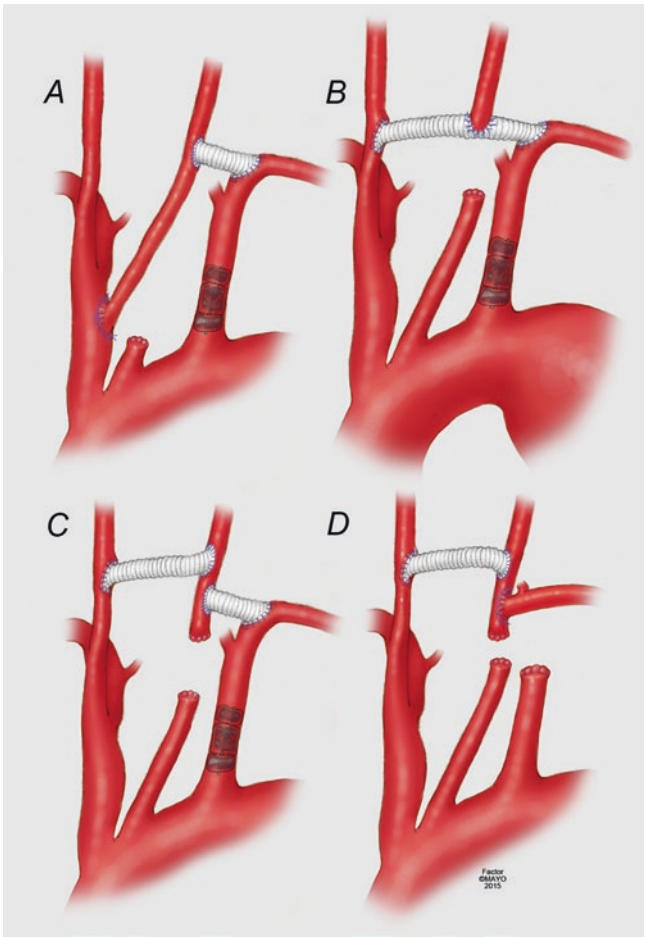


Fig. 36.4 Several configurations of cervical debranching for proximal arch procedures: small median sternotomy may be used for transposition of the left common carotid artery into the innominate artery, combined with carotid-subclavian bypass (**a**); carotid to left subclavian bypass with reimplantation of the left common carotid artery (**b**); carotid-carotid and carotid-subclavian grafts (**c**); and carotid-carotid graft with translocation of the left subclavian artery (**d**). By permission of Mayo Foundation for Medical Education and Research. All rights reserved

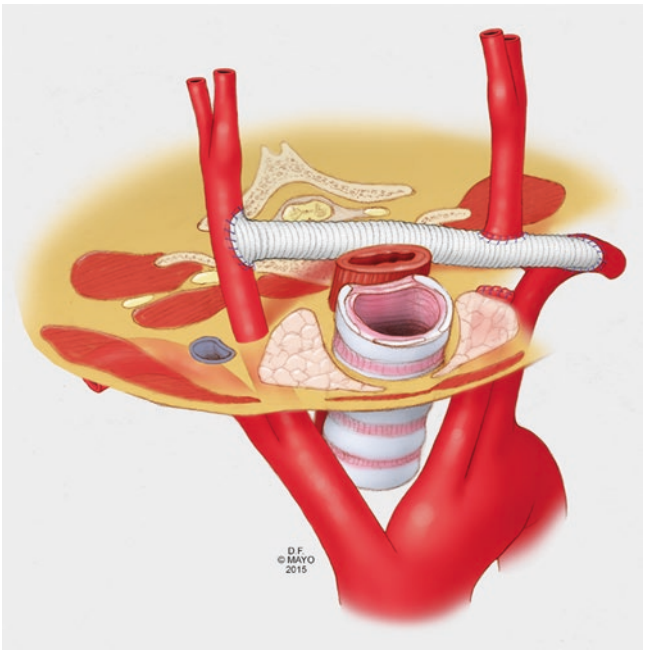


Fig. 36.5 Our preferred technique is a retropharyngeal tunnel using right common carotid to left subclavian bypass and reimplantation of the left common carotid artery. By permission of Mayo Foundation for Medical Education and Research. All rights reserved

is intended for the left common carotid artery. However, for the Gore TBE device, there is a single retrograde portal designed for the innominate artery.

Left carotid reconstruction can be performed using several potential graft configurations as illustrated in Fig. 36.4. A mini-sternotomy can be used to expose the proximal carotid and innominate arteries for translocation of the left common carotid artery into the right common carotid or innominate artery (Fig. 36.4a). A crossover graft from the right common carotid to the left subclavian artery with reimplantation of the left common carotid artery into the graft (Fig. 36.4c) is the most frequently used configuration at our center. Alternatively, two separate grafts for carotid-carotid and left carotid-subclavian bypass (Fig. 36.4c) or a carotid-carotid graft with transposition of the left subclavian artery (Fig. 36.4d) may be performed.

A right oblique cervical incision is needed to expose the right common carotid artery. The left common carotid and left subclavian arteries are exposed via a single left supraclavicular incision as previously described. The graft can be tunneled anterior to the trachea or behind the esophagus. Each of these options has limitations. In a patient with severe pulmonary dysfunction and who may need tracheostomy, pre-tracheal tunnel is a major limitation. Retropharyngeal tunnel may be associated with dysphagia or erosion into the esophagus, although this has not occurred in our experience (Fig. 36.5). We have routinely used retropharyngeal tunnel for hybrid repair in the last decade. The tunnel needs to be carefully created staying close to the vertebral ligaments and away from the esophagus, which can be identified by placement of a pediatric esophageal probe. The tunnel is created before intravenous heparin is administered.

Once both carotid arteries and the left subclavian artery are dissected free, the left subclavian artery is clamped and the graft is anastomosed as previously described (Fig. 36.6a). An 8-mm polyester graft is used. There is no need to use reinforced, externally supported grafts. Flow is restored into the left subclavian artery and the graft is clamped and tunneled behind the internal jugular vein and the esophagus. The left common carotid artery is test clamped. Although we use EEG monitoring, we have not experienced any changes in patients with patent bilateral carotid arteries when clamping is done proximal to the carotid bifurcation. The proximal

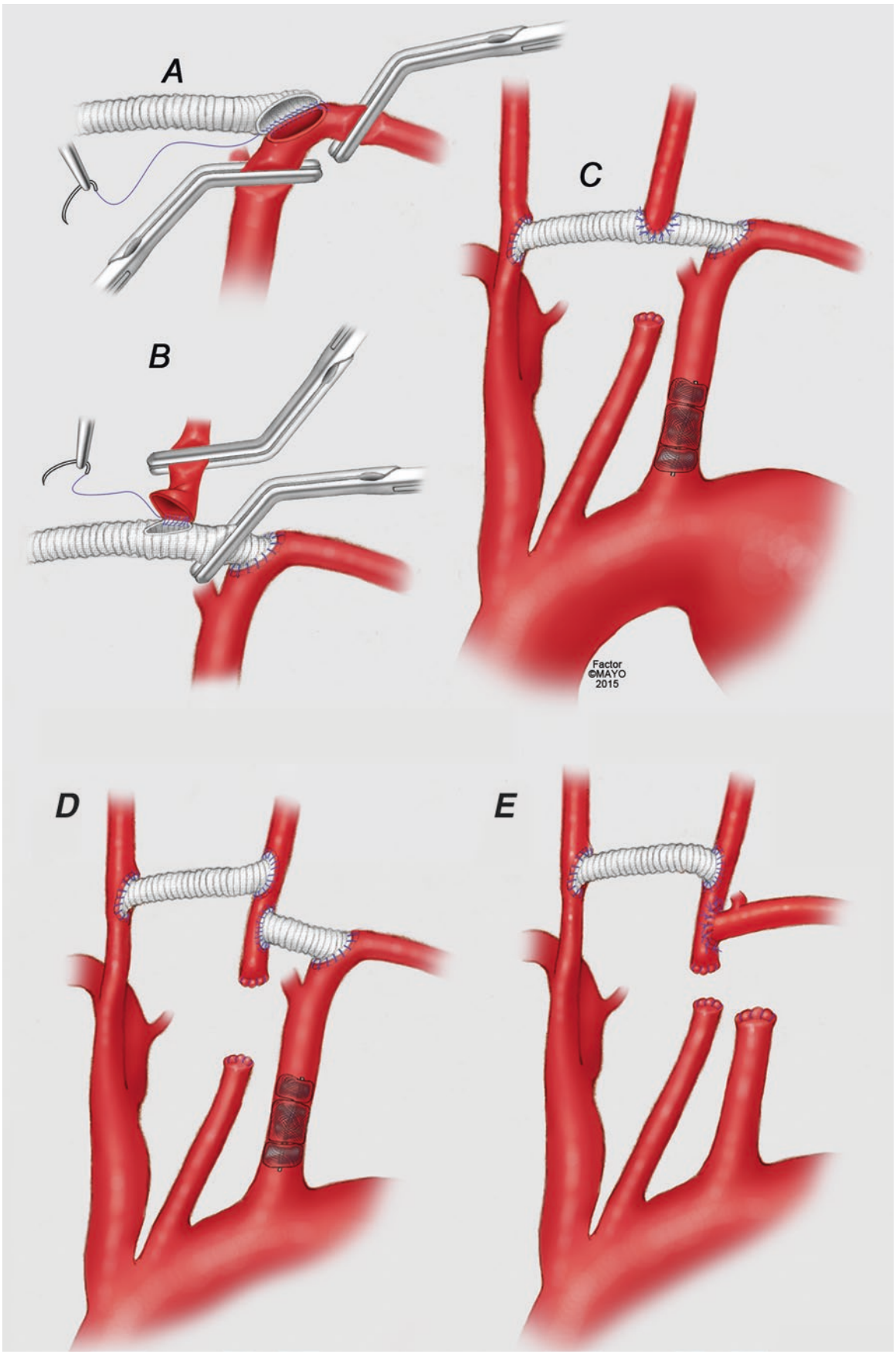


Fig. 36.6 Technical aspects of proximal cervical arch debranching. The distal anastomosis to the left subclavian artery is done first (**a**), followed by reimplantation of the left common carotid artery into the graft (**b**) and proximal anastomosis to the right common carotid artery (**c**). Alternative techniques using carotid-carotid and carotid-subclavian graft (**d**), carotid-carotid graft with transposition (**e**). By permission of Mayo Foundation for Medical Education and Research. All rights reserved

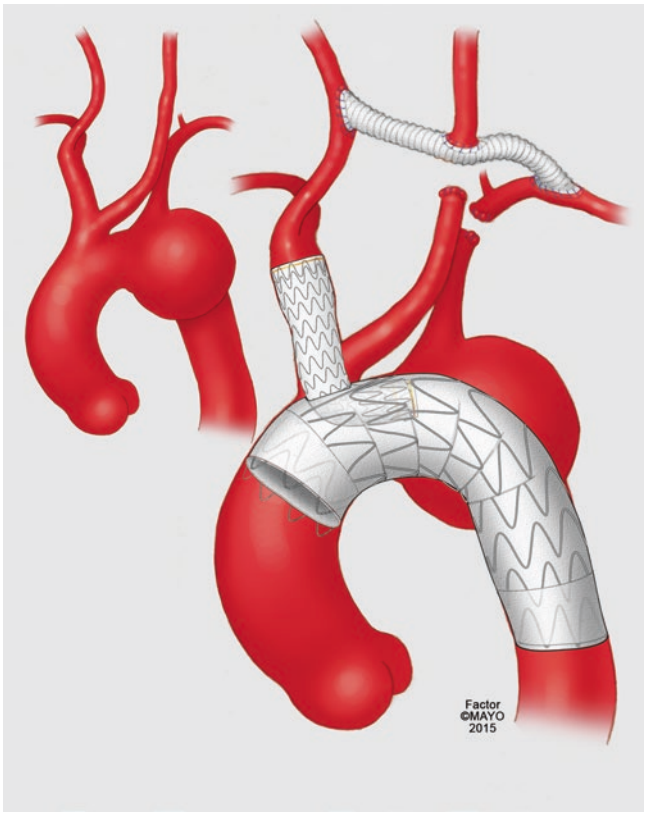


Fig. 36.7 Patient treated with the WL Gore Thoracic Branch Endoprosthesis deployed in Zone 0 with portal branch into the innominate artery. Complete cervical debranching is needed. By permission of Mayo Foundation for Medical Education and Research. All rights reserved

left common carotid artery is transected and closed in two layers using mattress and running 4-0 Prolene suture. A small graftotomy is made in the upper portion of the graft. The carotid artery is gently beveled and anastomosed end to side using running 5-0 Prolene for the posterior layer and interrupted 5-0 Prolene for the anterior layer (Fig. 36.6b). After back-bleeding and fore-bleeding are allowed, flow is restored to the left common carotid artery and the clamp is transferred to the graft just beyond the carotid anastomosis. The last anastomosis is performed end to side to the right common carotid artery using running 5-0 Prolene suture (Fig. 36.6c). Once flow is restored, the proximal left subclavian artery is occluded using an Amplatzer plug.

Distal arch debranching can be used in conjunction with an arch branched endograft. The WL Gore thoracic branch endoprosthesis has a single 12-mm retrograde portal to preserve flow into the innominate artery. This is currently under clinical investigation in the United States (Fig. 36.7). This approach avoids the need for a median sternotomy in patients with aortic arch aneurysms who need placement of the endograft into Zone 0.

Proximal Arch Debranching

Proximal arch debranching is needed in patients with aneurysms that encroach the left common carotid or innominate artery and require placement of the endograft into Zone 0. This is done using an aortic-based extra-anatomic reconstruction via full or partial median sternotomy, with or without extension of the incision into the neck (Fig. 36.8). The pericardial sac is opened below the left innominate vein to expose the ascending aorta, followed by mobilization of the innominate vein to access the innominate and left common carotid arteries. Our preference in these cases has been to revascularize the left subclavian artery via left supraclavicular incision, usually staged a few days prior to the ascending aortic debranching procedure (Fig. 36.9).

The proximal ascending aorta is generally spared of atherosclerotic debris, and side-biting clamp can be used to fashion the inflow for the graft. We use a 12-mm prosthetic graft for the aorta to innominate revascularization, with a separate 8-mm graft for the left common carotid artery. A bifurcated graft is avoided due to risk of compression upon sternotomy closure and also because management of a proximal type Ia endoleak is more difficult if there are two grafts originating from the ascending aorta. The mean arterial pressure is decreased to allow side-biting clamp placement. The proximal aortic anastomosis is done in the medial wall using 3-0 or 4-0 Prolene. The anastomosis should not be done in the anterior aortic wall (which is easier), because of risk of graft compression by the sternum. The graft is tunneled behind the innominate vein, and the distal anastomosis to the innominate artery is done using running 4-0 or 5-0 Prolene. It is useful to pre-sew the 8-mm graft prior to anastomosis to the innominate artery. The anastomosis to the left common carotid artery is done last using running 5-0 Prolene.

In these patients our preference is to proceed with TEVAR in the same setting. A useful maneuver is to mark the proximal anastomosis of the aortic graft with clips, a wire, or snare, to facilitate identification during deployment of the aortic stent graft. Placement of the aortic stent graft can be done using an antegrade approach with a conduit pre-sewn to the proximal anastomosis of the aortic graft (Fig. 36.10). This is useful in patients with small iliac arteries or excessive tortuosity in the thoracic aorta. However, the graft remains in reverse position, and the proximal landing zone cannot be encroached into the anastomosis of the aortic graft, which may lead to bird beak. Alternatively, retrograde femoral access is used to deliver the stent graft (Fig. 36.11). In these cases, the guidewire should be carefully placed in the left ventricle to allow the tip of the delivery system to cross the aortic valve with precise deployment in the ascending aorta, very close to the anastomosis of the ascending aortic graft (Fig. 36.12). Rapid ventricular pacing is used to induce hypotension for stent deployment.

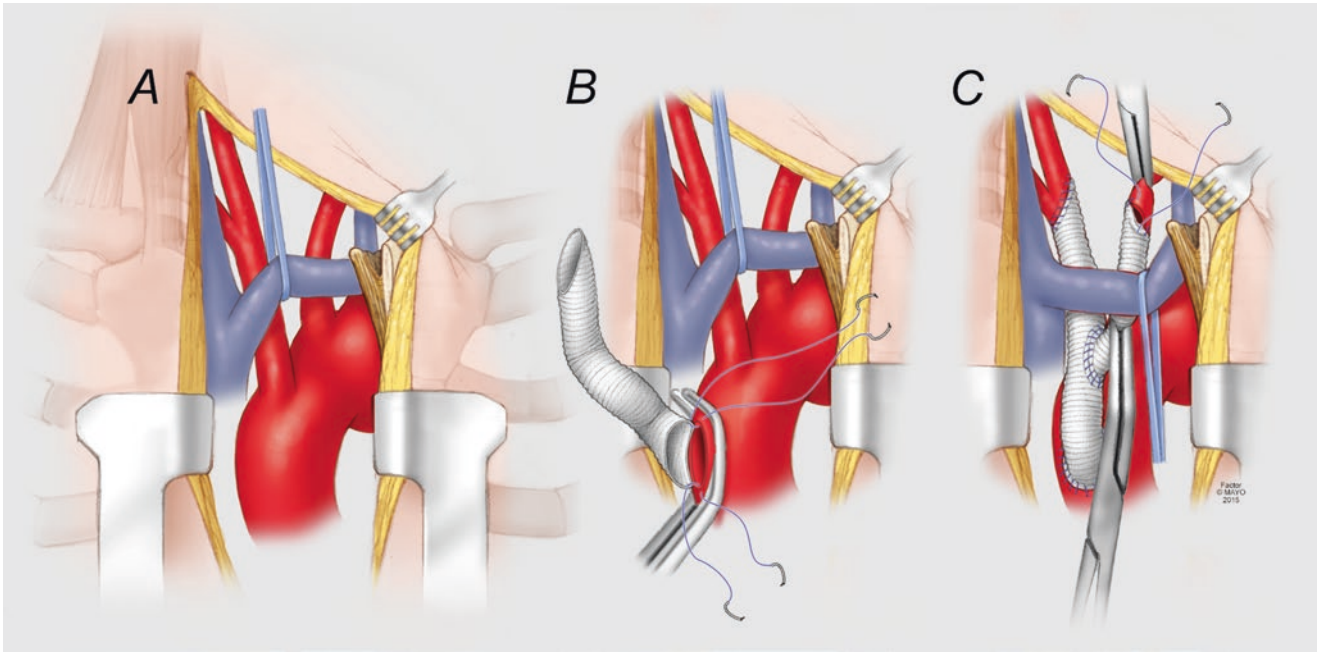


Fig. 36.8 Technique of aortic to innominate and left common carotid bypass using median sternotomy (**a**). A 12-mm polyester graft is anastomosed end to side to the ascending aorta (**b**), with distal anastomosis to the innominate artery and a separate 8-mm graft to the left common carotid artery (**c**). By permission of Mayo Foundation for Medical Education and Research. All rights reserved

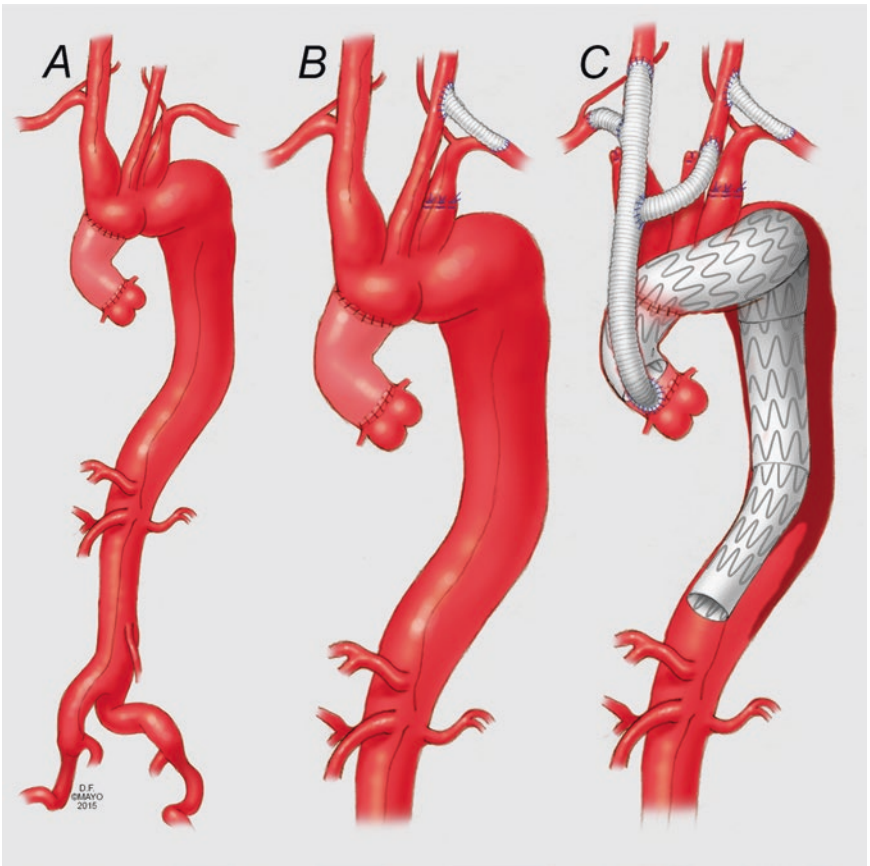


Fig. 36.9 Patient treated for complex thoracoabdominal aortic dissection (**a**) with arch debranching. The procedure was done in two stages, first with carotid to left subclavian artery bypass (**b**) and then with ascending aortic to innominate, right subclavian, and left common carotid bypass. The stent graft was deployed in Zone 0 and into the true lumen of the dissection (**c**). By permission of Mayo Foundation for Medical Education and Research. All rights reserved

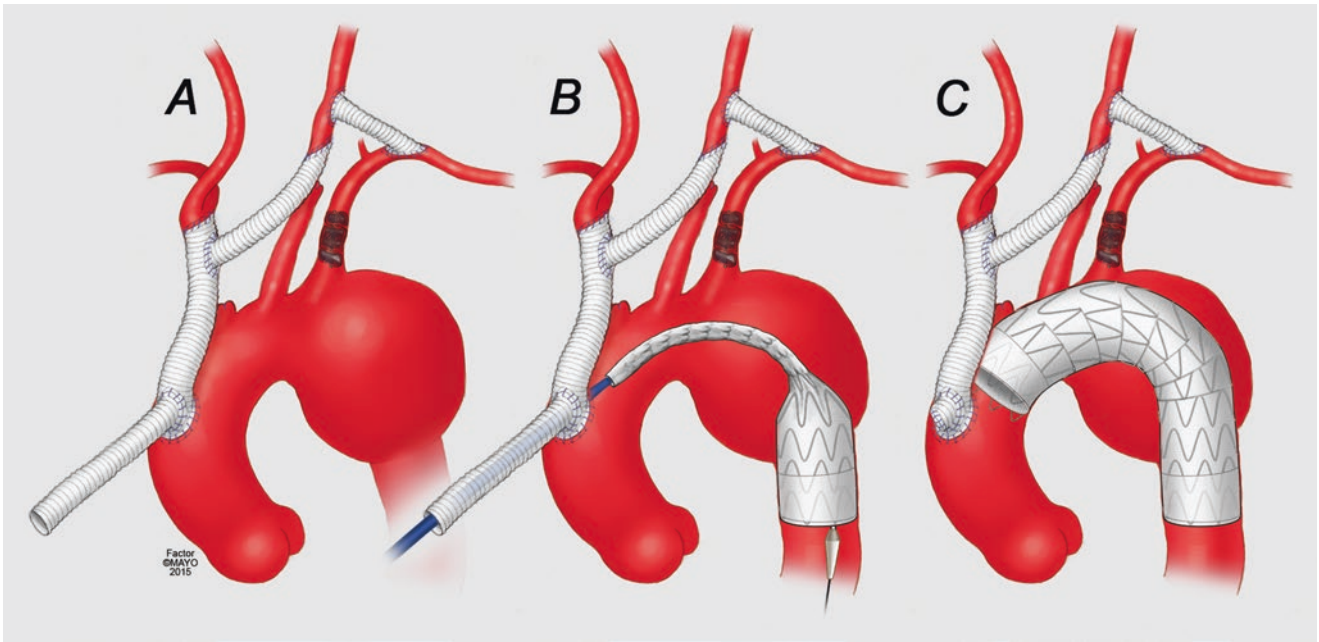


Fig. 36.10 Arch debranching done with ascending aortic to innominate and left common carotid graft using a conduit anastomosed end to side to the proximal graft anastomosis (**a**). Antegrade deployment of a Gore stent graft introduced via the conduit (**b**). The conduit is excised leaving a small patch of graft at the proximal anastomosis (**c**). By permission of Mayo Foundation for Medical Education and Research. All rights reserved

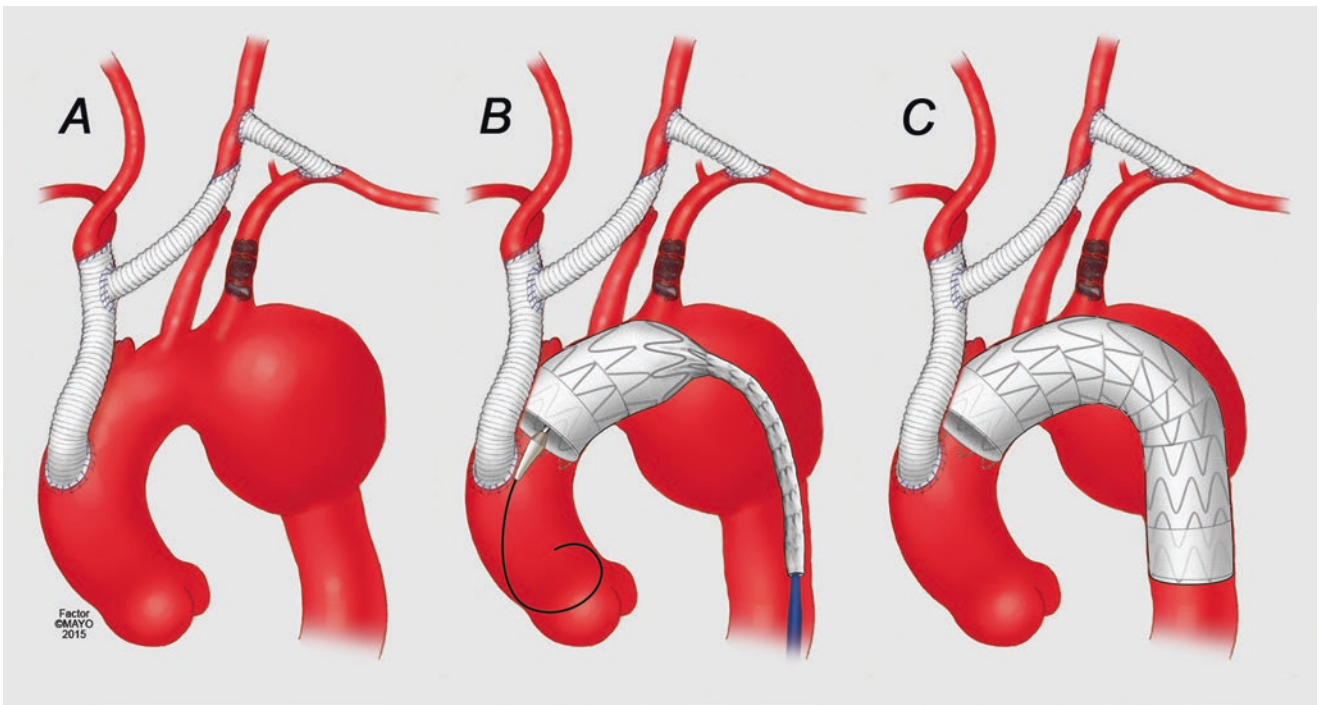


Fig. 36.11 Arch debranching done with ascending aortic to innominate and left common carotid graft (**a**). Retrograde deployment of a Gore stent graft introduced via trans-femoral approach (**b** and **c**). By permission of Mayo Foundation for Medical Education and Research. All rights reserved

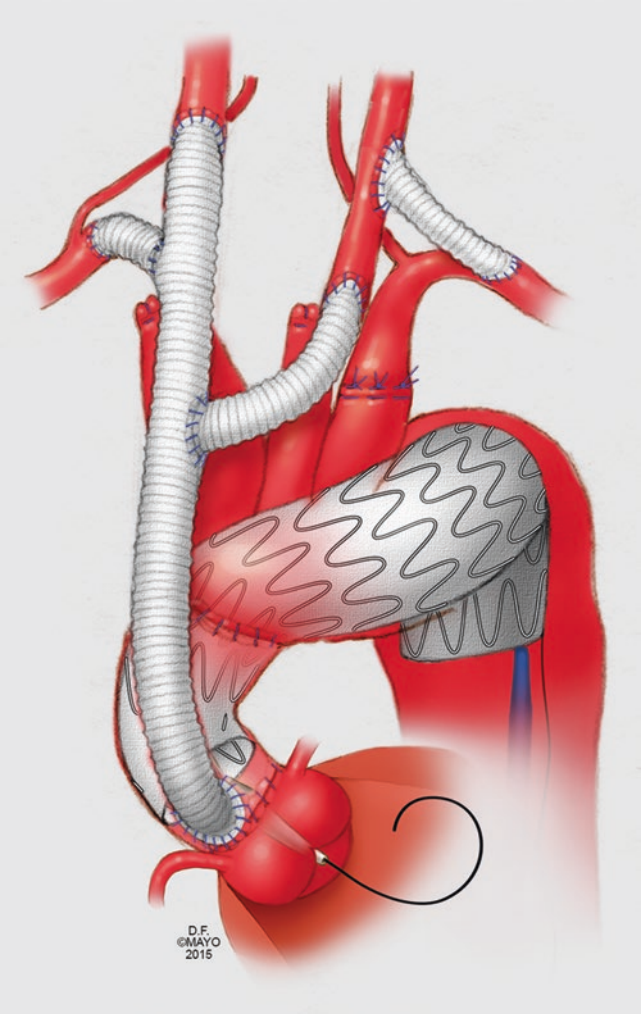


Fig. 36.12 Final configuration of the patient treated in Fig. 36.9. Note the retrograde stent deployment allows introduction of the delivery system into the left ventricle reaching the proximal ascending aorta to maximize landing zone. By permission of Mayo Foundation for Medical Education and Research. All rights reserved

Frozen Elephant Trunk

Total arch repair using frozen elephant trunk is discussed in detail in Chap. 37. Our preference has been to revascularize each of the supra-aortic trunks with separate grafts rather than an island patch (Fig. 36.13). Our technique has evolved and differs somewhat than the one described in Chap. 37.

A median sternotomy is performed in standard fashion. Percutaneous femoral access is obtained with a 6Fr sheath. A stiff Glidewire and Kumpe catheter are advanced into the aorta and positioned into the distal arch. The imaging unit is retracted away of the field at this point. The innominate vein is dissected and mobilized away from the posteriorly located aortic arch. The individual arch vessels are dissected and encircled with vessel loops to be used during the arch reconstruction as snares to secure the selective antegrade perfusion cannulae. The left subclavian artery may be incorporated into the repair or revascularized via separate supraclavicular incision either as a staged procedure or in the same operation (Fig. 36.14a). If the proximal/intrathoracic subclavian artery is dilated or dissected, it may be preferable to do the revascularization as a separate staged procedure. The pericardium is opened. The patient is systemically heparinized. The distal ascending aorta and the superior vena cava/right atrium are cannulated. Arterial cannula can also be placed in the brachiocephalic trunk or using a right axillary artery conduit via a separate right subclavian incision. Once on cardiopulmonary bypass with a left ventricular vent inserted via the left superior pulmonary vein, core cooling is begun to achieve flat EEG, which usually requires approximately 45 min. After documented flat EEG, the ascending aorta is cross clamped, and antegrade cardioplegia is instilled to achieve a myocardial temperature of 10 °C. Throughout the cardiac ischemic portion of the operation, intermitted antegrade and retrograde cold blood cardioplegia is utilized to maintain myocardial temperature between 10 and 15 °C. The ascending aorta is then transected and amputated proximal to the aortic cross clamp, and the proximal ascending aorta is mobilized away from the aortic arch. Antegrade cardiopulmonary bypass is interrupted and retrograde cerebral perfusion is begun via the snared SVC cannula. The patient is positioned in slight Trendelenburg, and the remaining of the ascending aorta and arch aneurysm are excised to the area of anastomosis just distal to the left common carotid or the left subclavian artery. The left carotid artery and the innominate artery are dissected free, mobilized away from the arch, and cannulated. Retrograde cerebral perfusion is interrupted, and antegrade cerebral perfusion is initiated in the innominate and left carotid arteries (Fig. 36.14b). The left subclavian artery can also be cannulated with a selective antegrade perfusion cannula if suitable. Via the open aneurysm, the origin of the left subclavian artery is identified and either dissected free or ligated, depending on whether revascularization was done via supraclavicular incision. Ligation of the subclavian artery is usually done from inside the aorta with pledgeted 3-0 Prolene sutures. At this point, the location of the graft anastomosis is prepared. The catheter and guidewire inserted at the beginning of the surgery are visualized and retrieved manually. A C-TAG stent graft of choice is loaded onto the stiff Glidewire with clamps in each end. The stent is advanced into position and deployed under direct vision with the stent edge just at the level of the intended anastomotic site. The stent graft can be gently dilated using either a Foley catheter or a Coda Balloon. It is important not to overdilate the stent, which can cause aortic disruption. Our preference is to use a Siena graft (Fig. 36.14b), which has pre-sewn graft limbs for antegrade perfusion and supra-aortic trunks, as well as radiopaque markers and a skirt which can be trimmed for the

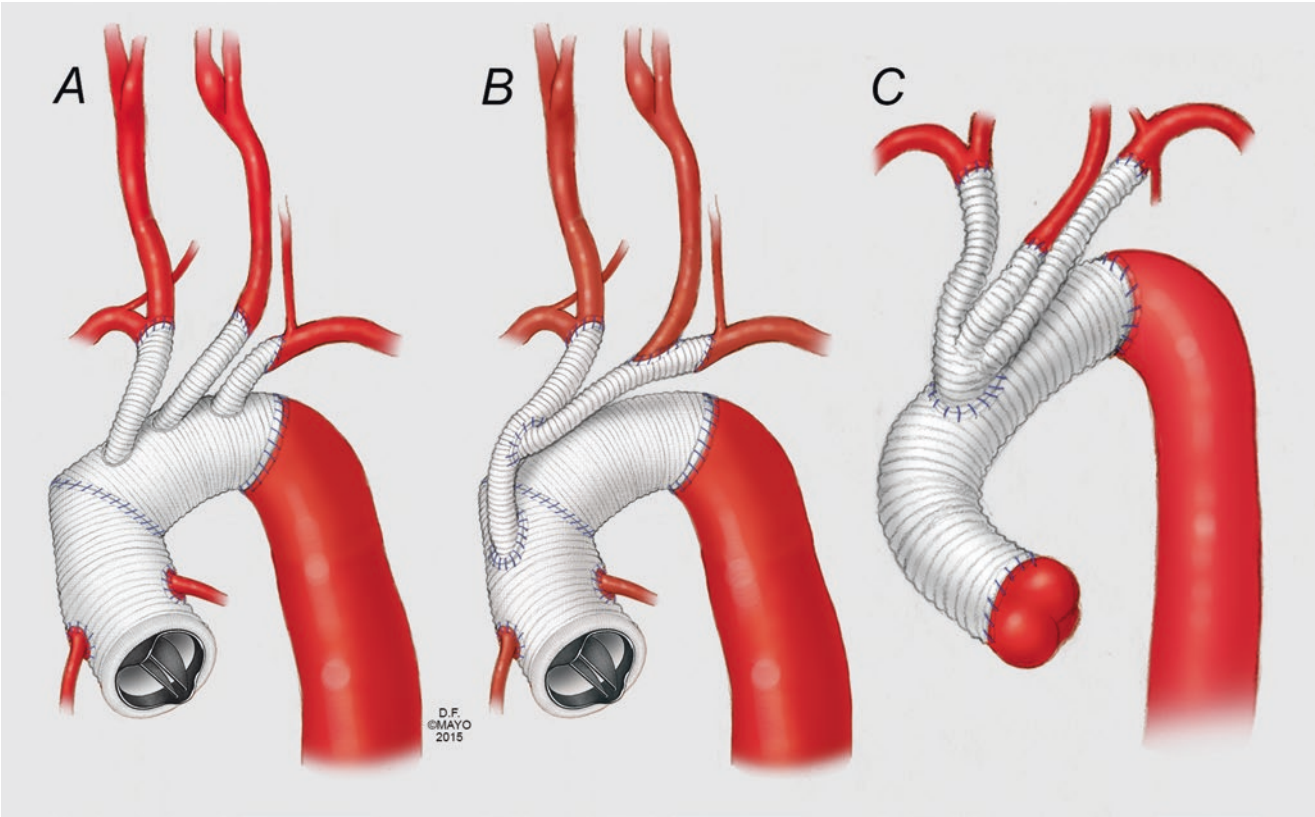


Fig. 36.13 In patient with extensive arch and ascending aortic disease, total arch replacement is needed using elephant trunk technique. Graft configuration in a patient who need aortic valve replacement and separate grafts into all three supra-aortic trunks (**a**) or use of a bifurcated graft (**b**). A trifurcated graft is less favored due to risk of compression (**c**). By permission of Mayo Foundation for Medical Education and Research. All rights reserved

anastomosis. Currently we transect the graft leaving a 5-cm elephant trunk inside the stent graft and perform the anastomosis incorporating aortic wall, stent graft, and the polyester graft with running 3-0 Prolene sutures. The small elephant trunk inside the Gore device allows an alternative in case of endoleak associated with small tears in the fabric of the stent at the anastomosis. Once the anastomosis is completed and tested, antegrade perfusion is restored into the lower body and the graft is clamped just proximal to the cannula (Fig. 36.14c). If the left subclavian is not revascularized within the chest, the first 8-mm limb of the Sienna graft is oversewn at its origin. The second pre-sewn 8-mm limb of the Sienna graft is beveled and anastomosed end to end to the proximal left common carotid artery. The clamp is transferred proximal to the carotid limb to allow antegrade perfusion (Fig. 36.14d). Next, the last pre-sewn 10 mm limb of the Sienna graft is beveled and anastomosed end to end to the innominate artery. The clamp is transferred proximal to the limb to restore antegrade perfusion to the innominate artery (Fig. 36.14e). Once the arch reconstruction is completed, full rewarming is begun and attention is directed to the ascending aorta. The ascending aorta is excised close to the sinotubular junction. Three pledged 4-0 Prolene sutures are placed in the three commissures. A Dacron graft is sized to be about 2 mm larger than the patient's annular diameter. The chosen graft is intussuscepted inside the root and anastomosed to the sinotubular junction with running 4-0 Prolene suture. The proximal aortic reconstruction is then tested by injecting cold blood cardioplegia in the ascending graft under physiologic pressures. The aortic valve is examined for competence, and the sinotubular junction is examined for hemostasis. The ascending graft is then matched to the arch graft, and a graft-to-graft anastomosis is performed using running 3-0 Prolene sutures (Fig. 36.14f). After appropriate de-airing maneuvers, the clamp is removed. Once rewarming is completed, the left ventricular vent is removed and the vent site is oversewn.

Results

There is growing literature on the use of hybrid approaches to extend the indications of endovascular repair in patients with arch or proximal thoracic aneurysms. Most studies are retrospective reviews of single center experiences and small prospectively maintained databases. Limitations of these reports include a tendency to combine patients with proximal and

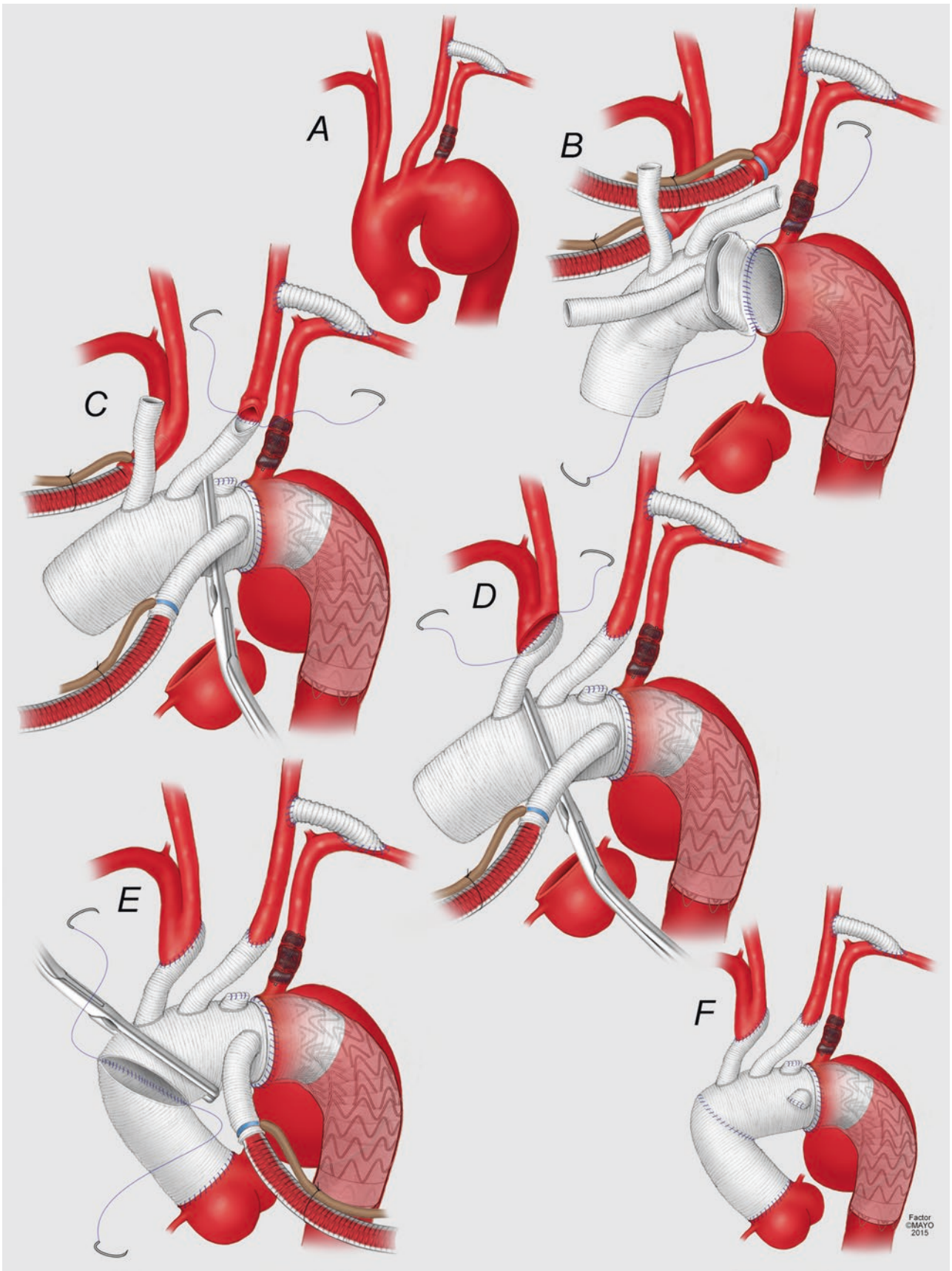


Fig. 36.14 Evolution of the frozen elephant trunk technique using the Sienna graft and C-TAG combination for a large distal arch aneurysm (**a**). A left carotid-subclavian bypass was done. The distal anastomosis is done incorporating graft, aorta, and stent with a 5-cm elephant trunk (**b**). Antegrade perfusion is restored to the lower body, and the left common carotid artery is reconstructed (**c**), followed by the innominate artery (**d**). The ascending aorta is reconstructed using a separate graft (**e**). Final configuration of the frozen elephant trunk repair (**f**). By permission of Mayo Foundation for Medical Education and Research. All rights reserved

distal debranching and total arch replacement with elephant trunk reconstructions. In our opinion, results of distal debranching are not comparable to elephant trunk procedures, nor the procedures should be used for the same indication.

Antoniou et al. reported a systematic review in 2010, which included 195 patients treated by arch debranching of at least one carotid artery. Technical success was of 86 % and 30-day mortality was 9 %. Stroke and spinal cord injury occurred in 7 % and 0.5 % of the patients, respectively. Nine percent of the patients had endoleak of any type [9]. Our group reported pooled results of the literature up to 2012, which included seven studies and 255 patients. Technical success was 97 % and 30-day mortality was 6 %. Stroke and spinal cord injury were reported in 2 % and 1.5 % of the patients, respectively. The total endoleak frequency was of 6 % [10].

Czerny et al. published midterm results of a prospectively maintained registry of patients undergoing proximal arch debranching. Sixty-six patients were treated with ascending aorta to innominate and left carotid bypass, followed by endovascular repair of the arch with stent grafts placed in Zone 0. In-hospital mortality was 9 %. Spinal cord ischemia occurred in 3 % and stroke in 5 %, with two retrograde aortic dissections. Five-year survival was 72 % [11].

In 2013, Moulakakis et al. reviewed 46 studies including 2272 patients treated by hybrid aortic arch reconstructions. The study included patients who had arch debranching, elephant trunk with endovascular completion, and frozen elephant trunk. Of these, 26 studies reported a total of 956 patients who had arch debranching done in Zone 0 in 42 %, Zone 1 in 29 %, and Zone 2 in 29 %. Overall technical success was 93 %. Retrograde dissections were noted in 4.5 %. Pooled perioperative mortality was 12 %. Perioperative cerebrovascular event and irreversible paraplegia occurred in 7.6 % and 3.6 %, respectively. After a mean follow-up of 22 months, 17 % of the patients had endoleaks (106 type 1, 51 type 2, and 8 type 3). The authors noted that despite the difference in risk stratification between patients treated by debranching or elephant trunk procedure, the outcomes were comparable [12]. A meta-analysis of comparative studies of open arch replacement versus hybrid repair revealed no significantly difference in operative mortality (6 % vs 9 %, odds ratio 0.67, $P=0.66$) and neurological events (12 % vs 6 %, odds ratio 1.93, $P=1$) between the two approaches in 378 patients [13].

In conclusion, arch debranching with endovascular exclusion is an alternative to total endovascular and open reconstructions. Despite the operative advantages, debranching carries a persistent high risk of perioperative mortality and neurological complications. The interpretation of results is limited by small numbers and retrospective nature of the data along with inconsistency in graft configuration and heterogeneity in pathology.

References

1. Safi H, Miller C, Take-Youn L. Repair of ascending and transverse aortic arch. J Thorac Cardiovasc Surg. 2011;142:630–3.
2. Etz C, Konstadinos P, Kari F. Staged repair of thoracic and thoracoabdominal aortic aneurysms using the elephant trunk technique: a consecutive series of 215 first stage and 120 complete repairs. Eur J Cardiothorac Surg. 2008;34:605–15.
3. LeMaire S, Carter S, Coselli J. The elephant trunk technique for staged repair of complex aneurysms of the entire thoracic aorta. Ann Thorac Surg. 2006;81:1561–9.
4. Sundt T, Orszulak T, Cook D. Improving results of open arch replacement. Ann Thorac Surg. 2008;86:787–96.
5. Svensson L, Kim K, Blackstone E. Elephant trunk procedure: newer indications and uses. Ann Thorac Surg. 2004;78:109–16.
6. Mitchell RS, Ishimaru S, Ehrlich MP, Iwase T, Lauterjung L, Shimono T, et al. First international summit on thoracic aortic endografting: round table on thoracic aortic dissection as an indication for endografting. J Endovasc Ther. 2002;9 Suppl 2:II98–105.
7. Rizvi AZ, Murad MH, Fairman RM, Erwin PJ, Montori VM. The effect of left subclavian artery coverage on morbidity and mortality in patients undergoing endovascular thoracic aortic interventions: a systematic review and meta-analysis. J Vasc Surg. 2009;50:1159–69.
8. Matsumura JS, Lee WA, Mitchell RS, Farber MA, Murad MH, Lumsden AB, et al. The Society for Vascular Surgery Practice Guidelines: management of the left subclavian artery with thoracic endovascular aortic repair. J Vasc Surg. 2009;50(5):1155–8.
9. Antoniou GA, El Sakka K, Hamady M, Wolfe JH. Hybrid treatment of complex aortic arch disease with supra-aortic debranching and endovascular stent graft repair. Eur J Vasc Endovasc Surg. 2010;39(6):683–90.
10. Rana MA, Gloviczki P, Oderich GS. Endovascular stenting with open surgery for reconstruction of the ascending aorta and the aortic arch: a review of indications and results of hybrid techniques. Perspect Vasc Surg Endovasc Ther. 2012;24:184–92.
11. Czerny M, Weigang E, Sodeck G. Targeting landing zone 0 by total arch rerouting and TEVAR: midterm results of a transcontinental registry. Ann Thorac Surg. 2012;94(1):84–9.
12. Moulakakis K, Mylonas S, Markatis F, Kotsis T, Kakisis J, Liapis C. A systemic review and meta-analysis of hybrid aortic arch replacement. Ann Cardiothorac Surg. 2013;2(3):247–60.
13. Benedetto U, Melina G, Angeloni E, Codispoti M, Sinatra R. Current results of open total arch replacement versus hybrid thoracic endovascular aortic repair for aortic arch aneurysm: a meta-analysis of comparative studies. J Thorac Cardiovasc Surg. 2013;145:305–6.

Techniques and Results of Hybrid Arch Replacement with Elephant Trunk

37

Ourania Preventza and Joseph S. Coselli

Introduction

Hybrid procedures of the aortic arch that include elephant trunk (ET) repair have been developed to treat patients with complex arch and descending and thoracoabdominal aortic pathology. Although a hybrid arch operation does not necessarily require circulatory arrest and cardiopulmonary bypass (CPB), an ET repair—whether "stented," "non-stented," or "frozen" (FET)—is a total aortic arch operation that requires a period of circulatory arrest and is designed to treat pathology that includes the aortic arch and extends into the descending thoracic or thoracoabdominal aorta. Although in the literature the definition of a FET procedure can be unclear and surgical methods are not uniform, our FET approach is a hybrid Type III approach [1].

To date, no "hybrid stented graft" has been approved in the USA for treating the extent of the previously described aortic pathology. Two prostheses are commercially available in Europe: the E-vita® OPEN PLUS stent graft (Jotec GmbH, Hechingen, Germany) [2] and the Thoraflex® 4-branched hybrid graft (Vascutek Terumo, Renfrewshire, Scotland) [3]. The arch vessels are reimplanted as an island with the E-vita prosthesis or reimplanted separately as branch grafts with the Thoraflex system. In 2003, Haverich's group [4] reported using a custom-made, prototype Chavan-Haverich stent graft (Curative Medical Devices Gmbh, Dresden, Germany).

O. Preventza (✉)
Division of Cardiothoracic Surgery, Michael E. DeBakey Department of Surgery, Baylor College of Medicine, Texas Heart Institute, 6770 Bertner Avenue C-330, Houston, TX 77030, USA

Department of Surgery, CHI St Luke's Health-Baylor St. Luke's Medical Center, Texas Heart Institute,
6770 Bertner Avenue C-330, Houston, TX 77030, USA
e-mail: preventz@bcm.edu

J.S. Coselli
Department of Surgery, CHI St Luke's Health-Baylor St. Luke's Medical Center, Texas Heart Institute,
6770 Bertner Avenue C-330, Houston, TX 77030, USA

Division of Cardiothoracic Surgery, Michael E. DeBakey Department of Surgery, Baylor College of Medicine, Texas Heart Institute, 6770 Bertner Avenue C-330, Houston, TX 77030, USA

Technique

The following are some of the technical aspects associated with performing FET for patients who need replacement of their total arch and endovascular repair of their proximal descending thoracic aorta, or open total arch repair and FET to facilitate future endovascular repair of the remaining thoracic aorta. Arterial inflow for CPB is established mainly via the innominate artery (Fig. 37.1a), the right axillary artery (Fig. 37.1b), or, in some cases, the femoral artery. After CPB is initiated, the target nasopharyngeal temperature is set between 21 and 25 °C, depending on the expected duration of the repair (colder temperatures are used in more complex cases). The near-infrared spectroscopy signals are monitored during the period of circulatory arrest. The arch is reconstructed in an island patch configuration with either two or all three head vessels implanted (Fig. 37.2a), or by placing a prefabricated or custom-made bifurcated (Y) or trifurcated (double-Y) graft (Vascutek Terumo, Fig. 37.2b). With the Y-graft technique, part of the head vessel reconstruction (left subclavian artery and left common carotid artery anastomosis) is performed during cooling and not during circulatory arrest. When the target nasopharyngeal temperature is reached, the circulatory arrest period is initiated with the adjunct of antegrade cerebral perfusion, first via the right common carotid artery and later via the (Fig. 37.3). We use a skirted ET graft with a side arm (Vascutek Terumo) for the open arch replacement because the skirt of the graft has a sewing collar, which facilitates anastomosis, and the side arm is used to perfuse the body distally with full flow during the aortic reconstruction. The skirted ET graft also facilitates the initiation of the rewarming process. The trunk of the ET is cut so that approximately 10 cm of the graft will extend into the descending thoracic aorta (Fig. 37.4).

© Mayo Foundation for Medical Education and Research 2017

G.S. Oderich (ed.), *Endovascular Aortic Repair*, DOI 10.1007/978-3-319-15192-2_37

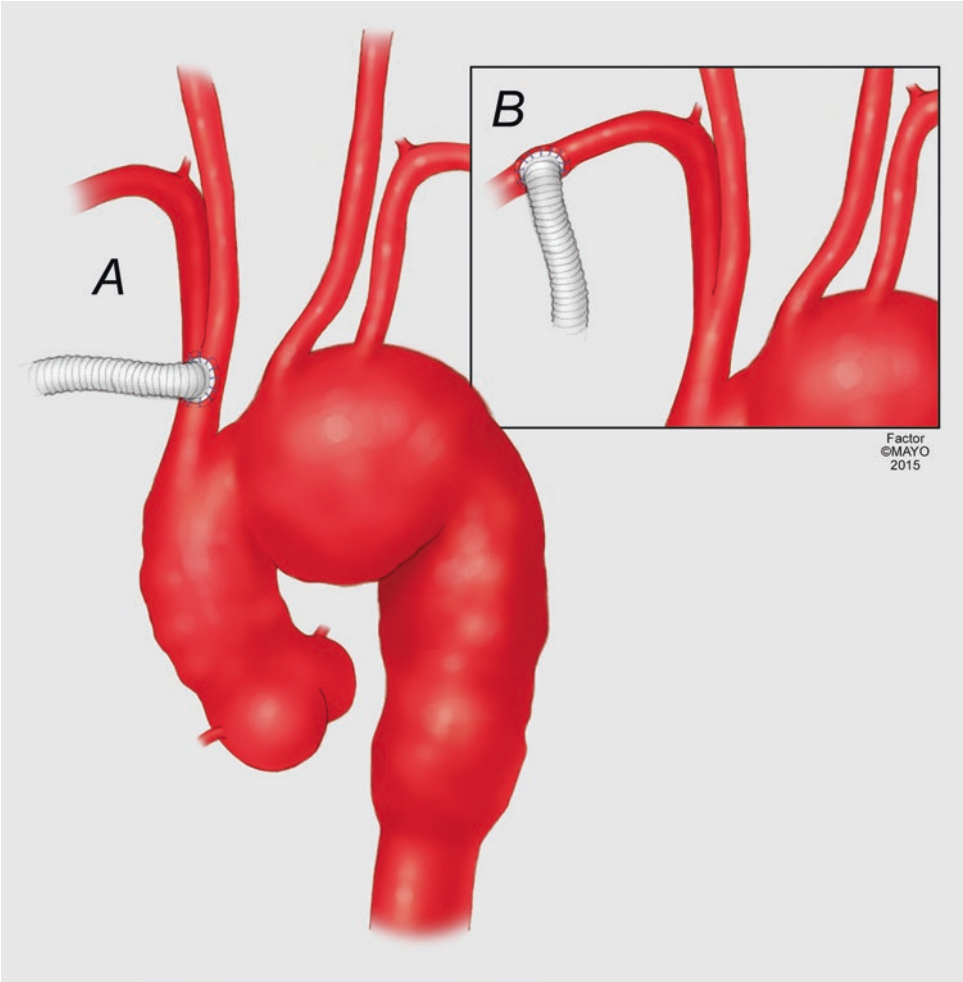


Fig. 37.1 Antegrade cerebral perfusion, first via the right common carotid artery and later via the left common carotid artery. (**a**) or right axillary artery conduit (**b**). By permission of Mayo Foundation for Medical Education and Research. All rights reserved

After the distal aortic stump is prepared, we perform the distal anastomosis with a running 2-0 or 3-0 Prolene suture, reinforced with 3-0 pledgeted sutures as necessary. The level of the distal anastomosis, depending on the patient's anatomy, is distal or proximal to the left subclavian artery.

The FET is created after completion of the distal anastomosis. Under direct vision, we deliver the C-TAG Gore thoracic endograft antegrade through the trunk of the ET [5]. In this part of the procedure, a soft glide wire is inserted under direct vision into the trunk of the ET and is exchanged for a stiff Amplatz wire via a catheter. The endograft is advanced antegrade over the stiff wire and under direct vision. When the end of the stent is parked distally to the distal aortic anastomosis, the endograft is deployed (Fig. 37.5). Warm saline is used to enhance the expansion of the nitinol frame of the stent because the deployment is performed at a body temperature of 21–25 °C. We use the C-TAG endograft almost exclusively (instead of other commercially available thoracic stent grafts) because the device allows visual confirmation of accurate positioning in the distal arch. In addition, the stent is used bare, without a sheath, so we do not need to unsheathe the stent graft for deployment. The head vessels are then anastomosed to the main graft of the ET (i.e., the graft that is used for the ascending aortic repair), either as a Y- or double Y-graft (Fig. 37.6) or as an island (Fig. 37.7a, b).

Results

Most of the available data regarding the results of FET procedures comes from the E-Vita registry [2] and the experience of high-volume single centers [6, 7]. Among the 509 patients listed in the E-Vita registry at the time Leontyev et al. [2] accessed it, 350 had acute or chronic dissections, and 159 had atherosclerotic aneurysms. The overall in-hospital mortality was 15.9 % (17.1 % for patients with dissec-

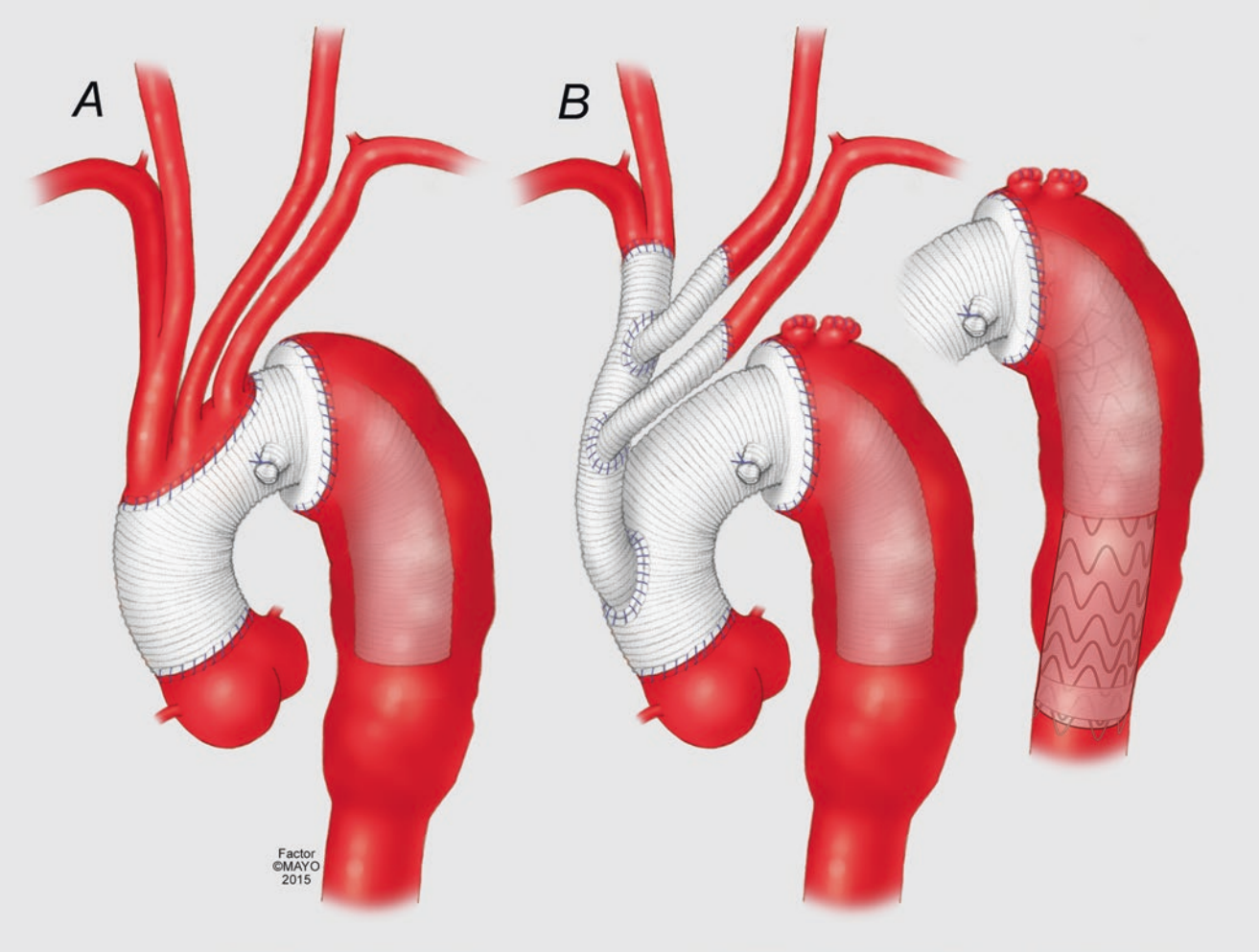


Fig. 37.2 Arch reconstruction using island patch (**a**) or custom bifurcated or trifurcated graft (**b**). By permission of Mayo Foundation for Medical Education and Research. All rights reserved

tions vs 13.2 % for patients with aneurysms). Hemodynamic instability, peripheral vascular disease, diabetes, and selective cerebral perfusion time greater than 60 min were independent predictors of early mortality in this study. In contrast, age less than 60 years and the use of guide wire during FET implantation were predictors of early survival [2]. Ius et al. [6] reported the results of using, in 131 patients, all of the abovementioned available hybrid prostheses: the custom-made Chavan-Haverich stent graft ($n=66$), the Jotec E-vita graft ($n=30$), and the 4-branched Thoraflex graft ($n=35$). Their in-hospital mortality was 15 %, which is similar to the rate observed in the E-vita registry patients. The stroke rate in these studies was 7.7 % [2] and 11 % [6], whereas the paraplegia rate was 7.5 % [2] and 1 % [6]. Leontyev et al. [7] reported in-hospital mortality of 8.7 % and a stroke rate of 13 %; Type A dissection was an independent predictor of both. Spinal cord ischemia is the Achilles heel of the FET procedure, and the incidence of new spinal cord injuries ranged from 1 to 21.7 % in the abovementioned studies [2, 6, 7]. Body core temperature greater than 28 °C in combination with a circulatory arrest time of more than 40 min was found to be an independent predictor of paraplegia [7], as was a distal landing zone lower than T10 [2]. In our own unpublished experience, the FET repair is associated with a greater total number of neurologic events than the conventional elephant trunk procedure when used for total arch replacement.

The Vascular Domain of the European Association for Cardio-Thoracic Surgery, together with surgeons with particular expertise in aortic surgery, recently published a position paper describing their recommendations regarding the use of the FET procedure to treat aortic arch pathology [8]. These are level II A and II B class recommendations with level C evidence.

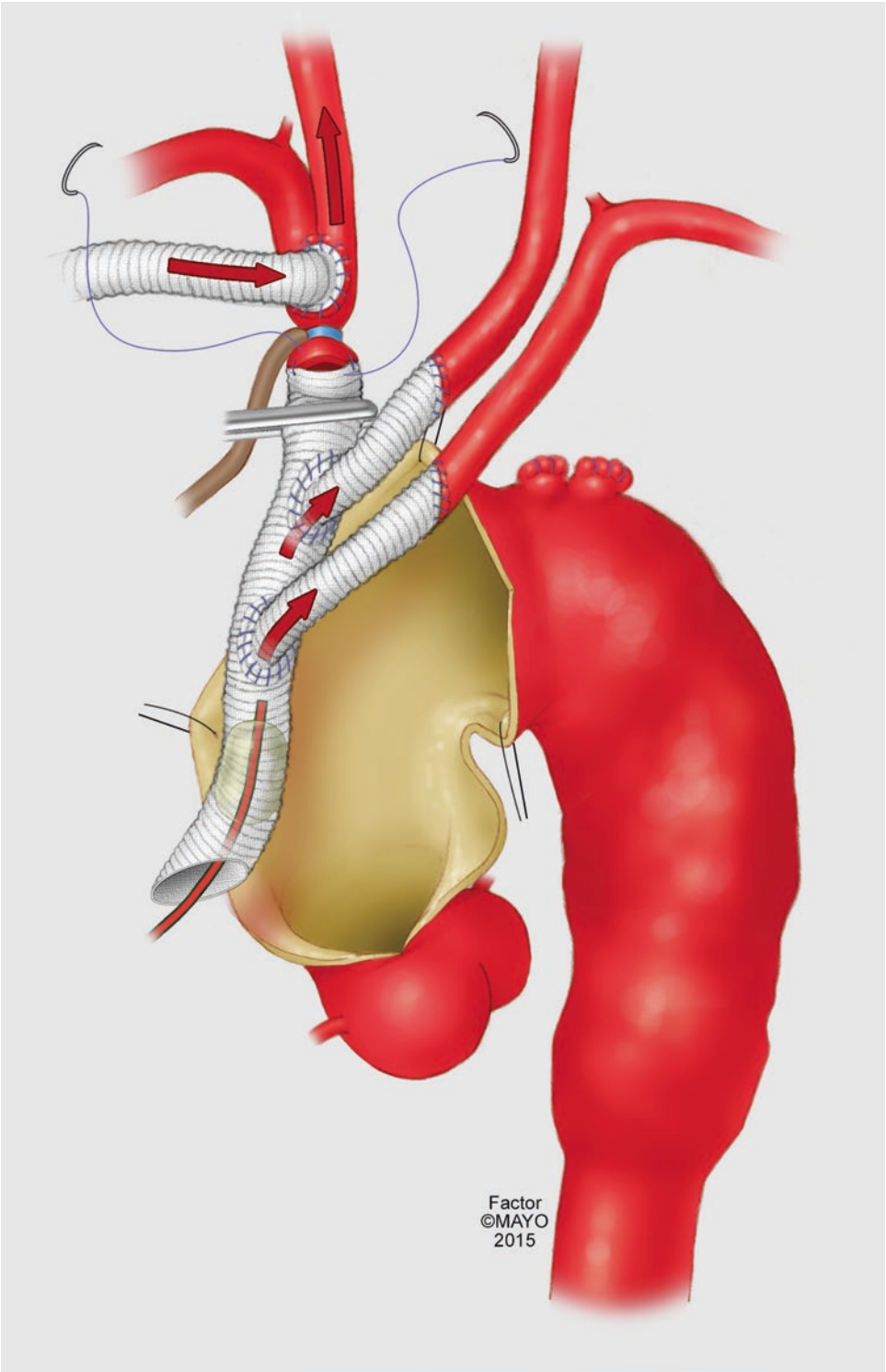


Fig. 37.3 Antegrade cerebral perfusion, first via the right common carotid artery and later via the left common carotid artery. By permission of Mayo Foundation for Medical Education and Research. All rights reserved

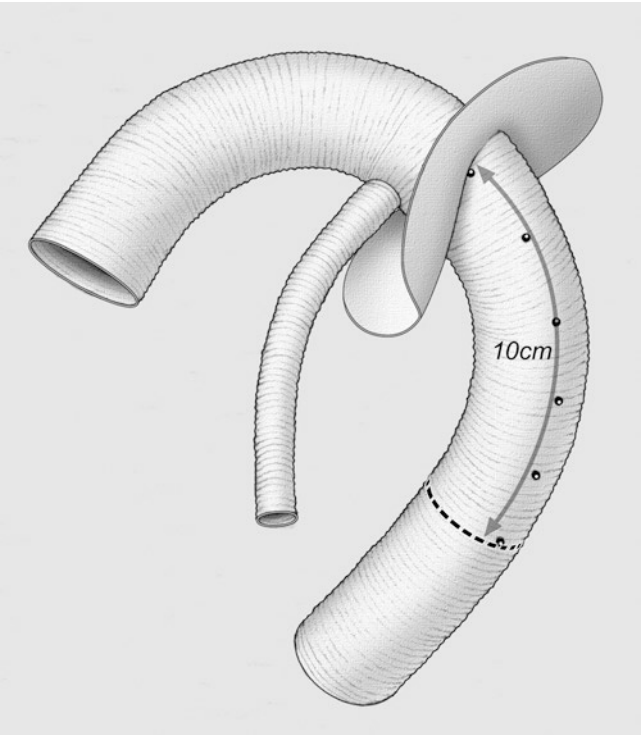


Fig. 37.4 Elephant trunk graft is cut approximately 10 cm long. By permission of Mayo Foundation for Medical Education and Research. All rights reserved

Modification for Acute Type I Aortic Dissection

Because of the lack of uniform surgical methods for the FET procedure, we want to touch briefly on another hybrid arch approach that includes proximal arch replacement with antegrade stent delivery. This approach has been used in patients with acute Type I aortic dissection [9, 10] and has been shown to benefit patients who present with malperfusion [9]. In addition, the approach has been used in other patients whose aortic arch is mildly dilated and does not warrant surgical replacement but whose ascending and descending aorta are diseased and needed to be replaced.

Technical aspects of this approach are as follows: After CPB is established, the target nasopharyngeal temperature is achieved, and circulatory arrest is induced—but before the distal anastomosis is reconstructed—a soft glide wire is exchanged over a catheter for a stiff Amplatz wire. The stent graft is inserted under direct vision into the descending thoracic aorta. Interrupted 3-0 pledgeted sutures are used in the lesser and outer curvature of the aortic arch to secure the stent in place and to decrease the risk of a proximal endoleak (Fig. 37.8). Other centers have also implemented this technique [8, 9]. The main advantages of this method are resolution of malperfusion, distal aortic remodeling, and a decreased incidence of late distal reoperation in patients with Type I aortic dissection [8, 9]. More long-term data are needed to validate these results.

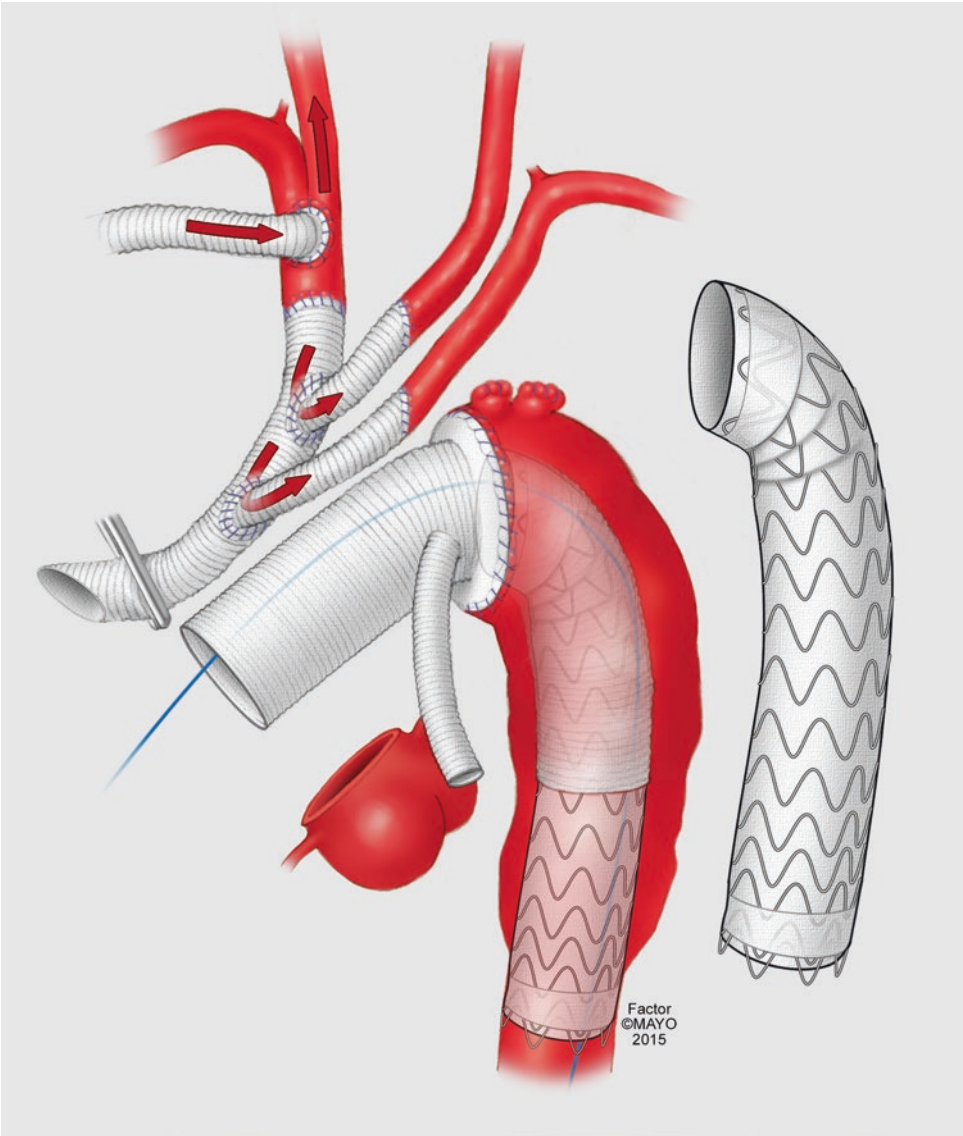


Fig. 37.5 Endograft deployment inside the elephant trunk graft. By permission of Mayo Foundation for Medical Education and Research. All rights reserved

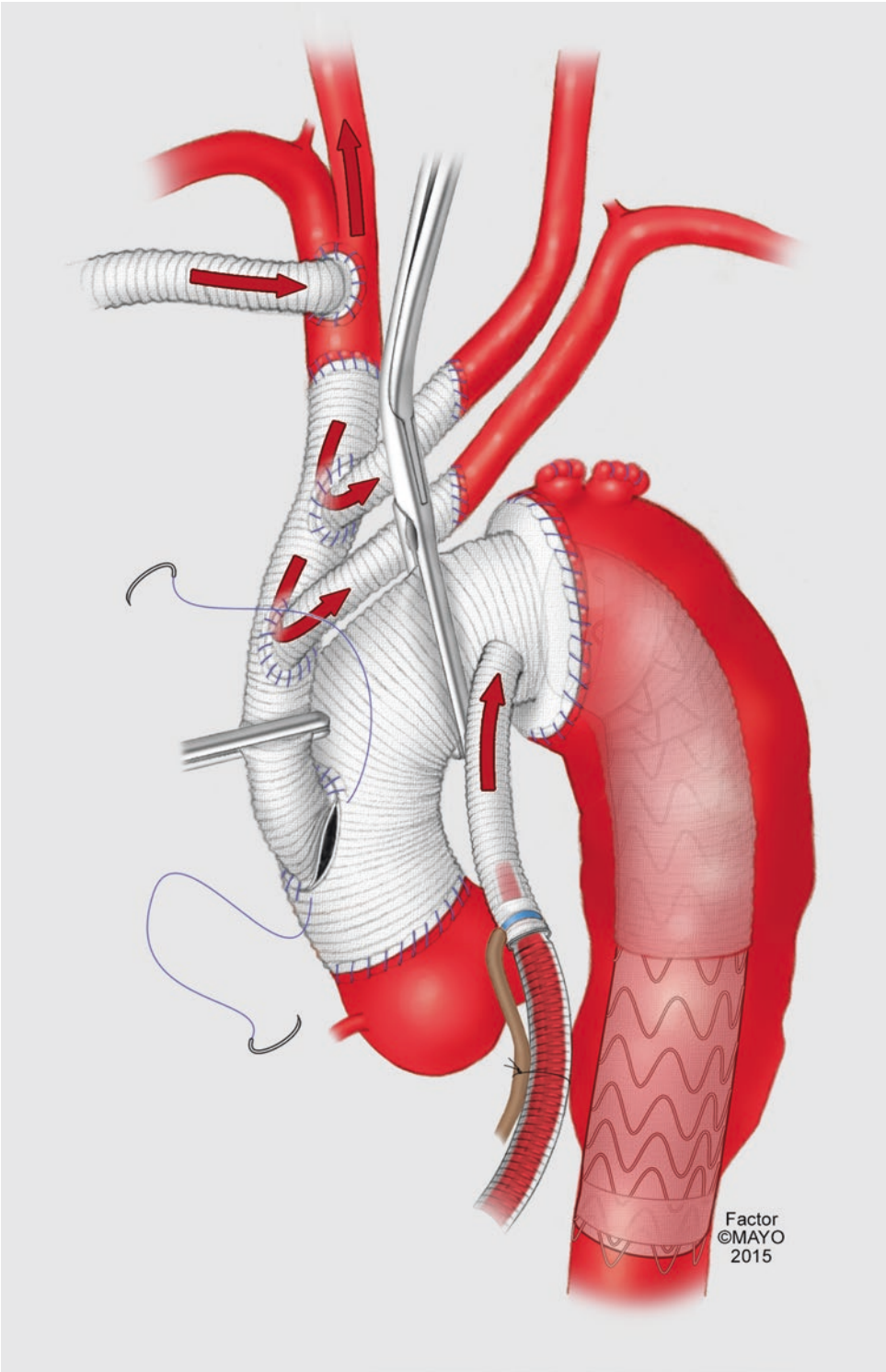


Fig. 37.6 Completion of the anastomosis using bifurcated or trifurcated graft. By permission of Mayo Foundation for Medical Education and Research. All rights reserved

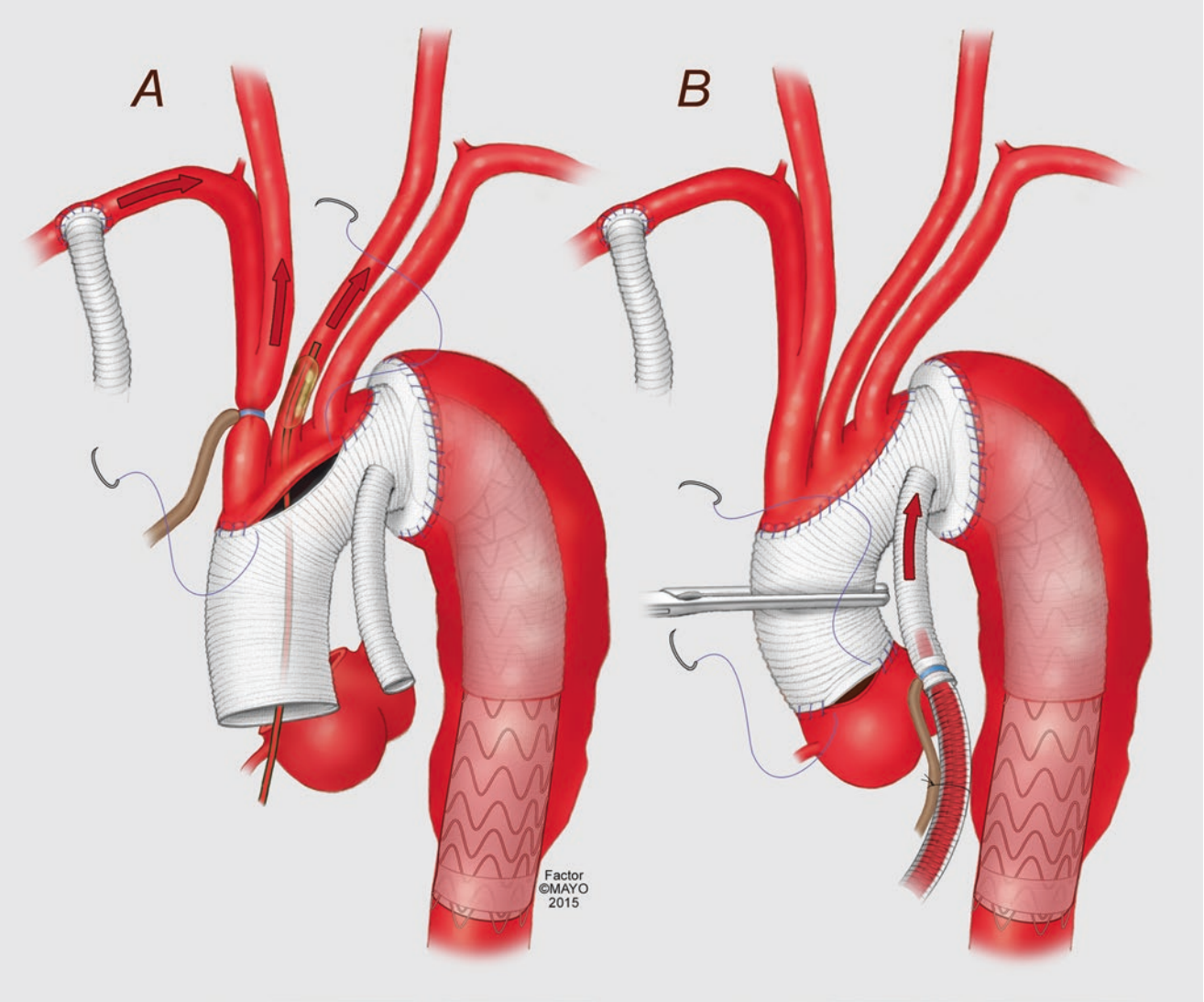


Fig. 37.7 Completion of the anastomosis using island patch (**a** and **b**). By permission of Mayo Foundation for Medical Education and Research. All rights reserved

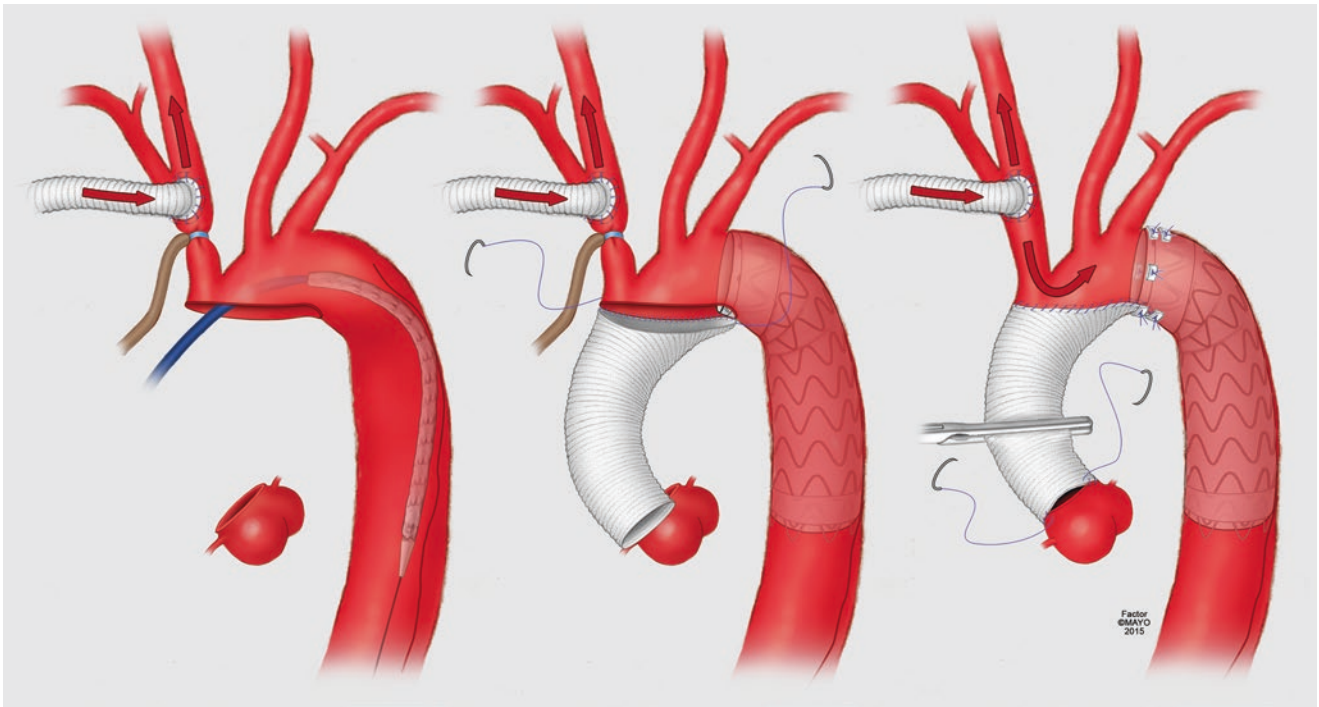


Fig. 37.8 Technique used for acute Type I aortic dissections with graft replacement of the ascending aorta and hemiarch with stent-graft placement in the proximal descending thoracic aorta. Note the interrupted 3-0 pledgeted sutures in the lesser curvature and outer curvature. By permission of Mayo Foundation for Medical Education and Research. All rights reserved

References

1. Bavaria J, Vallabhajosyula P, Moeller P, Szeto W, Desai N, Pochettino A. Hybrid approaches in the treatment of aortic arch aneurysms: postoperative and midterm outcomes. J Thorac Cardiovasc Surg. 2013;145 Suppl 3:S85–90.
2. Leontyev S, Tsagakis K, Pacini D, Di Bartolomeo R, Mohr FW, Weiss G, et al. Impact of clinical factors and surgical techniques on early outcome of patients treated with frozen elephant trunk technique by using EVITA open stent-graft: results of a multicentre study. Eur J Cardiothorac Surg. 2016;49(2):660–6.
3. Shrestha M, Pichlmaier M, Martens A, Hagl C, Khaladj N, Haverich A. Total aortic arch replacement with a novel four-branched frozen elephant trunk graft: first-in-man results. Eur J Cardiothorac Surg. 2013;43(2):406–10.
4. Karck M, Chavan A, Hagl C, Friedrich H, Galanski M, Haverich A. The frozen elephant trunk technique: a new treatment for thoracic aortic aneurysms. J Thorac Cardiovasc Surg. 2003;125(6):1550–3.
5. Preventza O, Al-Najjar R, LeMaire SA, Weldon S, Coselli JS. Total arch replacement with frozen elephant trunk technique. Ann Cardiothorac Surg. 2013;2(5):649–52.
6. Ius F, Fleissner F, Pichlmaier M, Karck M, Martens A, Haverich A, et al. Total aortic arch replacement with the frozen elephant trunk technique: 10-year follow-up single-centre experience. Eur J Cardiothorac Surg. 2013;44(5):949–57.
7. Leontyev S, Borger MA, Etz CD, Moz M, Seeburger J, Bakhtiary F, et al. Experience with the conventional and frozen elephant trunk techniques: a single-centre study. Eur J Cardiothorac Surg. 2013;44(6):1076–82. discussion 83.
8. Shrestha M, Bachet J, Bavaria J, Carrel TP, De Paulis R, Di Bartolomeo R, et al. Current status and recommendations for use of the frozen elephant trunk technique: a position paper by the vascular domain of EACTS. Eur J Cardiothorac Surg. 2015;47(5):759–69.
9. Preventza O, Cervera R, Cooley DA, Bakaeen FG, Mohamed AS, Cheong BY, et al. Acute type I aortic dissection: traditional versus hybrid repair with antegrade stent delivery to the descending thoracic aorta. J Thorac Cardiovasc Surg. 2014;148(1):119–25.
10. Vallabhajosyula P, Szeto WY, Pulsipher A, Desai N, Menon R, Moeller P, et al. Antegrade thoracic stent grafting during repair of acute Debakey type I dissection promotes distal aortic remodeling and reduces late open distal reoperation rate. J Thorac Cardiovasc Surg. 2014;147(3):942–8.

Part VI

Internal Iliac Artery Branch Stent-Grafts

Iliac Branch Device Designs

38

Javariah Fatima and Gustavo S. Oderich

Introduction

Endovascular aneurysm repair has revolutionized the treatment of abdominal aortic aneurysms. However, its applicability is challenged in patients with unfavorable anatomy. Patients with common iliac artery ectasia or aneurysm often have unsuitable landing zones at the iliac bifurcation. This has been overcome by exclusion of one or both internal iliac arteries with extension of the stent graft into the external iliac artery. However, up to 80% of the patients develop complications of pelvic flow interruption, including buttock or thigh claudication or erectile dysfunction with bilateral interruption. Less frequently, more severe complications such as gluteal or perineal necrosis, ischemic colitis, and spinal cord injury can also occur. Hybrid approaches coupling EVAR with internal iliac artery bypass or transposition and use of "bell-bottom" grafts with a flared cuffs for distal common iliac artery, snorkels, and sandwich techniques have facilitated preservation of pelvic flow. Advances in endovascular techniques have materialized the development of iliac branch devices (IBDs). This was first pioneered using the Cook Zenith platform, and more recently also by WL Gore and Jotec. This chapter summarizes the device designs from each manufacturer.

Device Designs

Cook Medical

The Zenith endovascular iliac branch device is a bifurcated branch vessel graft with openings to connect the common iliac to the side branch and external iliac segments. This device is available in three configurations: straight branch or Z-BIS (S-IBD), helical iliac branch (H-IBD), and bifurcated–bifurcated design (BIF-IBD).

The three designs are constructed with a full thickness woven (light-weight shrink-resistant) polyester fabric which is sewn to self-expanding stainless steel and nitinol Cook Z-stents with braided polyester and polypropylene monofilament suture. The graft is fully stented to provide stability and expansile force necessary to maintain the lumen of the graft during deployment. Nitinol rings positioned at the proximal end of the graft and within the side branch help maintain lumen patency during access and secure bridging stent seal. Additionally, the Z-stents provide the necessary seal of the graft to the vessel wall. Gold markers on the internal iliac branch ensure precise positioning of the components.

The Zenith branch devices are preloaded with a curly catheter onto the introduction system. The catheter and guide wire pass along the external aspect of distal device, and then into the helical branch ostium after passing through the common iliac segment, and exiting the sheath along a grooved pusher device. It has a sequential deployment method with built-in features to provide continuous control of the vascular graft throughout the deployment procedure. The proximal end of the graft is attached to the delivery system by two nitinol trigger wires. The distal end of the graft is also attached to the delivery system and held by an independent stainless steel trigger wire. The introduction system enables precise positioning and allows the readjustment of the final graft position before full deployment.

The delivery system uses a 20 French (6.7-mm inner diameter) introduction system that includes the preloaded catheter and the guide wire. All systems are compatible with a 0.035-in. wire guide. This delivery system introducer sheath (Flexor) is kink-resistant with a hydrophilic coating.

Zenith iliac limb extensions such as the ZSLE or TFLE (polyester tubular grafts with self-expanding nitinol and stainless steel stents) are used in construction of the bifurcation. Balloon-expandable or self-expandable covered

J. Fatima
Division of Vascular and Endovascular Surgery,
University of Florida, 1600 SW Archer Rd., NG-45,
P.O. Box 100128, Gainesville, FL 32610, USA

G.S. Oderich (✉)
Division of Vascular and Endovascular Surgery,
Department of Surgery Mayo Clinic,
200 First Street SW, Rochester, MN 55905, USA
e-mail: oderich.gustavo@mayo.edu

© Mayo Foundation for Medical Education and Research 2017

G.S. Oderich (ed.), *Endovascular Aortic Repair*, DOI 10.1007/978-3-319-15192-2_38

peripheral stent is deployed within the side branch segment extended into their internal iliac artery.

Straight and Helical Branch Devices

The straight iliac branch (Fig. 38.1a) has a relatively short overlap and therefore is preferentially used with a balloon-expandable stent. This device currently has a second generation that is available which is a modular two-component device compared to the first generation which was a unibody graft. The helical iliac branch has an internal iliac artery limb that courses around the external posterior portion of the iliac leg and has a twofold benefit: it orients the terminal branch ostium in line with natural IIA flow direction allowing for accommodation of the inherent angulation between the IIA and CIA, and secondly, supports extensive overlap with the mating device (Fig. 38.1b). Right and left oriented devices are manufactured. The total length of the helical device is 98 mm and length to internal iliac branch exit of 52 mm or 63 mm. Side branch length is 27 mm to maximize the overlap of peripheral covered stent. Side-branch diameter of 8 mm is anastomosed 22 mm or 31 mm distal to its proximal edge in an end-to-side fashion. The newer generation helical branch has reinforcing rings to facilitate catheterization (Fig. 38.1c). A Zenith crimped limb extension (ZCLE) connects the helical branch device with the main body of the Zenith device. This limb has distal 17 mm crimped segment that locks with the sealing zone of the helical branch device. It is available in 59 and 76 mm lengths on a 16Fr delivery catheter.

Bi-Branch Bifurcated-Bifurcated Device

While the S-IBD and H-IBD are suited for concomitant aorto-iliac aneurysms as well as for isolated common iliac artery aneurysms, they are limited to common iliac arteries longer than 5.5 cm. If the common iliac artery is short, the device is extended into the aortic sac compromising the durability of the proximal repair. Given this shortcoming of the straight and helical branch device, the bi-Branch device (Fig. 38.2) was designed to accommodate common iliac arteries that were shorter than 5.5 cm. This bifurcated–bifurcated device is a polyester graft with nitinol Z stents throughout its length for stability and expansile force to maintain graft patency, in addition to providing seal. It essentially incorporates a coil reinforced helical side arm into the distal bifurcated component of a branched fenestrated device. Access is obtained from the contralateral side into the side arm is via a fenestration cranial to the branch ostium, which is later sealed via a self-sealing valve. Gold markers are posi-

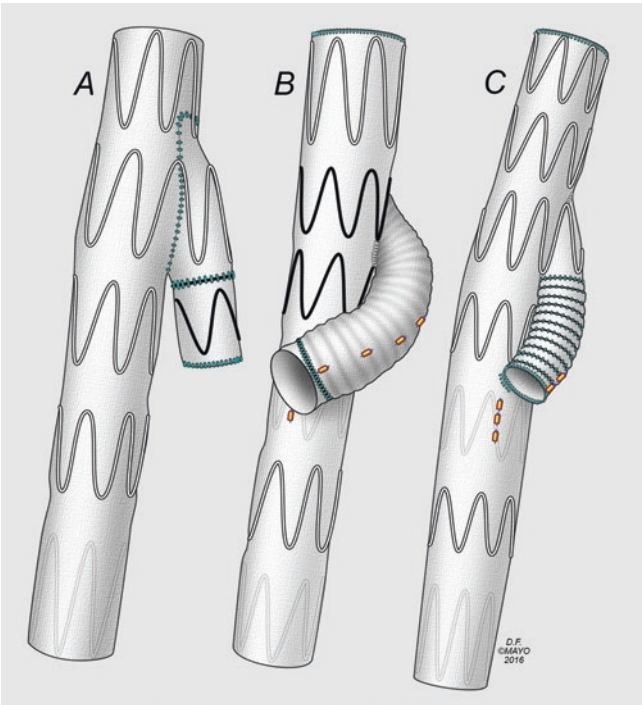


Fig. 38.1 Cook Zenith straight (**a**) and helical (**b** and **c**) iliac branch devices. By permission of Mayo Foundation for Medical Education and Research. All rights reserved

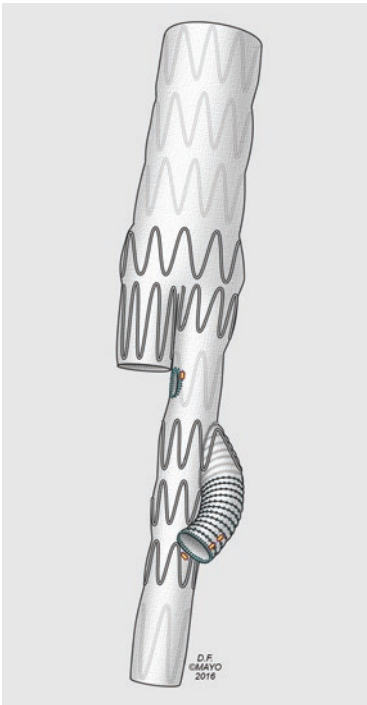


Fig. 38.2 Cook Zenith bifurcated-bifurcated iliac branch device. By permission of Mayo Foundation for Medical Education and Research. All rights reserved

tioned strategically lateral to the valve, at the bifurcation flow divider, two at the outer edge of the side branch, and there are three posterior orientation markers below the distal outer opening of the side branch. This design obviates the need for leg extensions, and therefore, has two modular joints with the aortic body.

Gore Excluder Iliac Branch Endoprosthesis (IBE)

The Gore Excluder IBE (Fig. 38.3) has two primary components including the bifurcated iliac branch component (with an external iliac leg and an internal iliac artery gate on the contralateral side) and the internal iliac component (that extends into the internal iliac artery). This device is used in conjunction with the Gore Excluder AAA Endoprosthesis.

Expanded polytetrafluoroethylene (ePTFE) and fluorinated ethylene propylene (FEP) constitute the graft material of this device with external support of Nitinol wires. The endoprosthesis is constrained with an ePTFE/FEP sleeve and preloaded on a delivery catheter.

The delivery system uses a 16 French introduction system that includes the preloaded catheter and the guide wire, and a 12 French flexible 45-cm long sheath for the contralateral internal iliac branch delivery system. All systems are compatible with a 0.035 in. wire guide. The iliac branch component has two short markers at the proximal end. There are two markers at the bifurcation as well; the long one is intended for orientation of the internal iliac limb, and the short marker denotes the proximal end of the external iliac limb. A marker ring is present at the internal iliac gate and positioned proximal to the internal iliac artery origin to facilitate cannulation during the deployment process.

There are two deployment knobs on this device, an outer white knob and an inner gray knob. The outer white knob is pulled with a steady continuous pull to release the proximal endoprosthesis past the internal iliac gate (marked by the radio-opaque ring). The device may be repositioned to tweak its position for maximal precision at this time. The internal iliac limb is cannulated from the contralateral side via the up and over approach and the internal iliac component is deployed with a 2.5-cm overlap with the internal iliac gate of the branch component (as marked by the proximal internal iliac component and the radiopaque ring of the branch component's internal iliac gate). The inner gray knob is then turned in a counter-clockwise direction to deploy the external iliac limb and complete release of the endoprosthesis. Once the gray knob is deployed, no further repositioning is permissible.

Jotec E-liac Stent Graft System

The Jotec E-liac stent graft system (Fig. 38.4) consists of a bifurcated graft including a main iliac limb with an additional reinforced stump for the internal iliac artery side branch. The stent design incorporates a polyester fabric over an asymmetric nitinol stent framework sutured in with braided polyester.

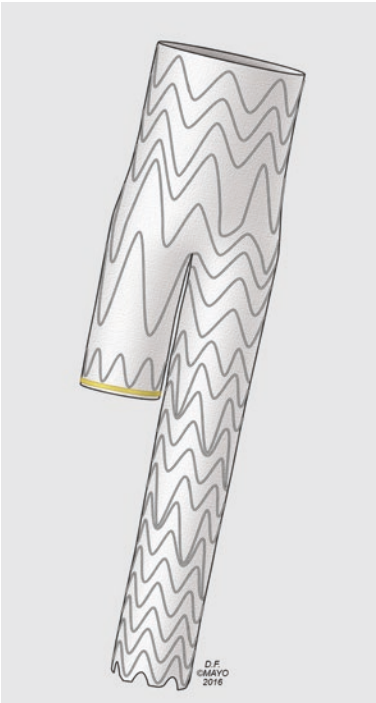


Fig. 38.3 WL Gore Excluder iliac branch endoprosthesis. By permission of Mayo Foundation for Medical Education and Research. All rights reserved

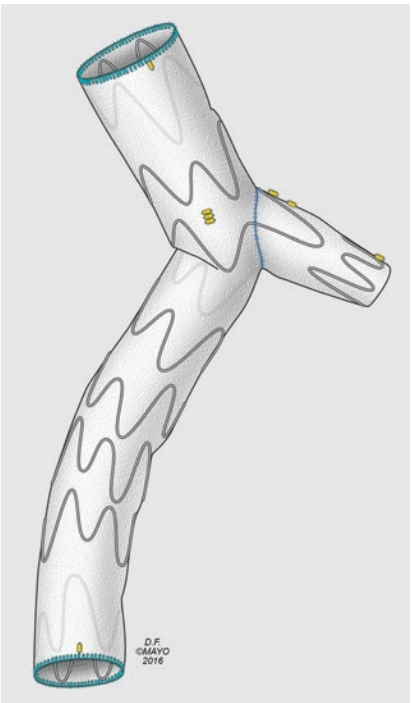


Fig. 38.4 Jotec E-liac Stent Graft System. By permission of Mayo Foundation for Medical Education and Research. All rights reserved

The asymmetry of the stents provides flexibility of the graft as well as improved visibility during the deployment process. Compression springs in the side branch ensure mating and sealing of the bridging stent to the side branch.

The E-liac graft system is sheathed in a coiled 18Fr hydrophilic sheath system with an atraumatic tip and two guidewire lumens is positioned with E-marker and ton markers located to allow for medial orientation while deploying the device. A hydrophilic crossover wire is loaded to the device through a lateral wire lumen on the device. The device has a squeeze-to-release mechanism for stepwise release of the stent graft until the side branch opens. A crossover maneuver from contralateral side is used to snare to guide an 8Fr sheath through the main device and exiting through the side branch into the internal iliac artery, which is then stented with a covered stent.

This device is available in several configurations with proximal diameter ranging from 14 to 18 mm and the distal diameter between 10 and 14 mm. The common iliac artery lengths available are 41, 53, and 6 5 mm, while the external iliac artery lengths are 44 and 56 mm. The internal iliac artery branch diameter is 8 mm.

Preoperative Planning and Sizing for Iliac Branch Devices

39

Javariah Fatima and Gustavo S. Oderich

Introduction

Preoperative planning and sizing is of paramount importance to achieve technical success with stent implantation and a durable long-term result after endovascular repair of aortoiliac aneurysms using iliac branch devices and parallel stent-grafts. Computed tomographic angiography with three-dimensional reformatting is the most important preoperative study to define the patient anatomy and the morphologic conditions that affect selection of a specific design, bridging stent, or approach. This chapter summarizes some of the pitfalls for preoperative sizing and planning complex endovascular repair using iliac branch devices.

CTA Imaging

Details of specific protocols of CTA are discussed in Chap. 11. The first study should ideally include imaging of the chest, abdomen, and pelvis to evaluate presence of concomitant disease in chest and quality of the arch vessels if access is needed. Detailed morphologic analysis is done using a variety of software, which allows measurements using centerline of flow (CLF). In addition to the measurements pertinent to the aortic repair which were already discussed in other chapters, the iliac arteries and the internal iliac artery target should be evaluated in detail (Fig. 39.1). These measurements include distance and diameters within the common, internal, and external iliac arteries, presence of angulation or excessive tortuosity, prior stents, diameter of the lumen or excessive narrowing and calcification.

J. Fatima
Division of Vascular and Endovascular Surgery,
University of Florida, 1600 SW Archer Rd., NG-45,
P.O. Box 100128, Gainesville, FL 32610, USA

G.S. Oderich (✉)
Division of Vascular and Endovascular Surgery,
Department of Surgery Mayo Clinic, 200 First Street SW,
Rochester, MN 55905, USA
e-mail: oderich.gustavo@mayo.edu

Anatomic Considerations

For the most part, anatomic limitations are almost universal for any technique that is utilized. The challenges imposed with placement of a bridging stent in the internal iliac artery are the same for any specific iliac branch device and also for parallel stent-grafts. The most common limitation is inadequacy of the internal iliac artery because of aneurysm involving branches without a suitable landing zone. Although this represents a violation of the recommendations for use of these devices, it is not an absolute contra-indication. Repair can still be done to one of the internal iliac branches, usually the posterior branch. Other limitation is an excessively short distance between the aortic and iliac bifurcation. This is a limitation that is more important for iliac branch devices as compared to parallel grafts. Finally, a very narrow common iliac artery at the origin of the internal iliac artery may be a relative contra-indication with any approach.

Cook Iliac Branched Devices

Iliac branch devices are indicated in patients with common iliac artery aneurysms with size greater than 20–24 mm. The common iliac artery should have a minimum length of 50 mm. A shorter iliac segment causes the IBD device to extend higher up into the abdominal aorta, creating challenge to advance a sheath up and over the aortic bifurcation and potentially destabilizing the proximal repair. The sizing guidelines for use of iliac branch devices are noted in Tables 39.1 and 39.2. Additionally, the following criteria should be met for optimal results:

1. Adequate iliac and femoral access compatible with the 20 French 7.7 mm outer diameter introduction system, without excessive tortuosity or calcifications.
2. Nonaneurysmal external iliac artery fixation segment distal to the aneurysm with the length of at least 20 mm and an outer wall to outer wall diameter of no greater than 11 mm and no less than 8 mm.

© Mayo Foundation for Medical Education and Research 2017

G.S. Oderich (ed.), *Endovascular Aortic Repair*, DOI 10.1007/978-3-319-15192-2_39

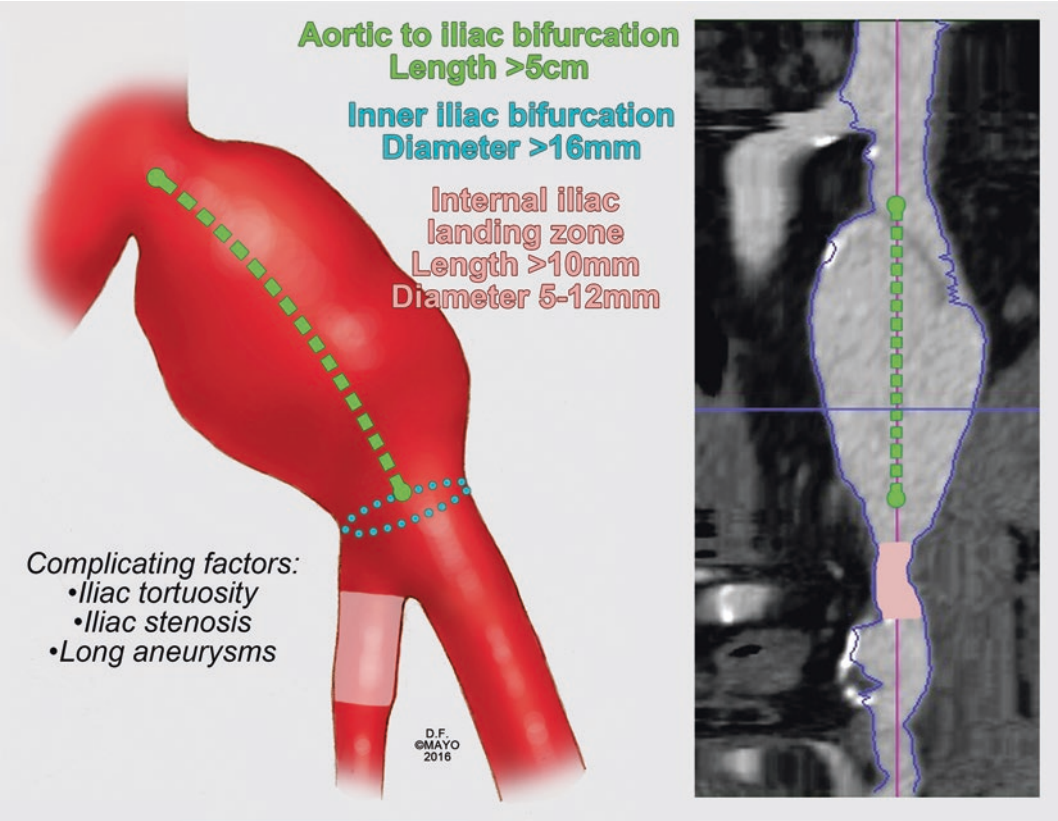


Fig. 39.1 Sizing of iliac artery aneurysms for endovascular repair using iliac branch devices requires centerline of flow analysis of length and diameter. By permission of Mayo Foundation for Medical Education and Research. All rights reserved

Table 39.1 Sizing guidelines for Cook Iliac branch device

Proximal diameter (mm)	Distal diameter (mm)	Side-branch diameter (mm)	Sheath size (Fr)	Common iliac segment length (mm)	External iliac segment length (mm)	Total graft length (mm)
12	10	8	20	45	41	86
12	10	8	20	61	41	102
12	10	8	20	45	58	103
12	10	8	20	61	58	119
12	12	8	20	45	41	86
12	12	8	20	61	41	102
12	12	8	20	45	58	103
12	12	8	20	61	58	119

Table 39.2 Sizing guidelines for Cook bifurcated–bifurcated device

Intended aortic vessel diameter (mm)	Distal diameter (mm)	Ipsilateral length (mm)	Contralateral length (mm)	Configuration	Sheath size (Fr)
8–11	12	39	78, 95	Left/right	20

Table 39.3 Sizing guidelines for WL Gore iliac branch endoprosthesis

Intended external iliac vessel diameter (mm)	Diameter iliac end (mm)	Iliac branch component (mm)	Recommended sheath size (Fr)
Iliac branch endoprosthesis component			
6.5–9	10	10	16
10–11	12	10	16
12–13.5	14.5	10	16
Bridging stent component			
6.5–9	10	7	12
10–11	12	7	12
12–13.5	14.5	7	12

3. Nonaneurysmal internal artery segment distilled to the aneurysm with a length of at least 10 mm (preferably 20–30 mm) with an inner wall diameter of 6–10 mm.

If the common iliac artery is less than 50 mm, a bifurcated–bifurcated (Bi-Branch) device should be considered or one case use brachial approach. It is also possible to access the iliac branch up and over the bifurcation of a previous endograft.

Gore Excluder Iliac Branch Endoprosthesis

The Gore Excluder Iliac branch endoprosthesis was the first to become commercially available in the USA. The device can be used for aortoiliac aneurysms and for isolated iliac aneurysms. The anatomic criteria and sizing guidelines proposed in the information for use of the device are listed in Table 39.3. These include:

1. Adequate iliac and femoral access compatible with the 16 French outer diameter introduction system, without excessive tortuosity or calcifications
2. Minimum proximal common iliac artery diameter of 17 mm
3. External iliac artery with diameter range between 6.5 and 25 mm and at least 30 mm length with a nonaneurysmal seal zone of at least 10 mm
4. Internal iliac artery with diameter should range between 6.5 and 13.5 mm and at least 30 mm of length with a nonaneurysmal seal zone of at least 10 mm

Jotec E-liac Branch Stent Graft

The E-liac stent graft system may be used in patients with aortoiliac artery aneurysms and isolated iliac artery aneurysms. The sizing guidelines are shown in Table 39.4 and include:

1. A patent common iliac artery at least 18 mm in diameter and 40 mm in length, with a distal landing zone of at least 10 mm length on the internal iliac artery.
2. At least 15 mm of distal landing zone on the external iliac artery, with a diameter of at least 8 mm or greater.

Pitfalls and Anatomical Challenges

Suitability for iliac branch devices has been studied widely using the Cook platform, which has been available for over 10 years worldwide with greater than 6000 implants. Karthikesalingam and associates studied 51 patients and 66 internal iliac targets with CTA for anatomical suitability. Overall 62 % of the internal iliac artery targets had at least one anatomical limitation by IFU. The most common limitations did not represent absolute contra-indications and could still be treated by adjuvant techniques. These include unsuitable landing zone in the main trunk of the internal iliac artery, which can be treated by extending the stent to the posterior branch; or a short common iliac artery, which can be treated by placement of the iliac branch in the aorta, use of arm access or a bifurcated–bifurcated device; and narrow common iliac artery lumen, which may still be amenable to placement of internal iliac artery bridging stent. Inadequate diameter in the main trunk of the internal iliac artery (<4 or >11 mm) was present in 40 % of patients and one third of the patients had common iliac arteries shorter than 50 mm in length. Subsequently, two reports by the Muenster and Cleveland Clinic groups demonstrated the technical success and long-term durability is also achieved in patients with unsuitable internal iliac diameter or a short and narrow common iliac artery.

Ostial Disease

Presence of calcification or thrombus in the origin of the internal iliac artery can make catheterization more challenge or impossible (Fig. 39.2). After deployment of the iliac branch device, the internal iliac artery may need to be predilated and a kissing balloon technique is done once the bridging stent is deployed.

Table 39.4 Sizing guidelines for Jotec E-liac branch device

Proximal length (mm)	Distal length (mm)	Proximal diameter (mm)	Distal diameter (mm)	Total length (mm)
Isolated iliac aneurysms				
65	56	16	12	121
65	56	16	14	121
65	56	18	12	121
Aortoiliac aneurysms				
53	44	14	10	97
53	44	14	12	97
53	56	14	12	109
53	44	14	14	97
53	56	14	14	109
41	44	14	10	85
41	44	14	12	85
41	56	14	12	97
41	56	14	14	97

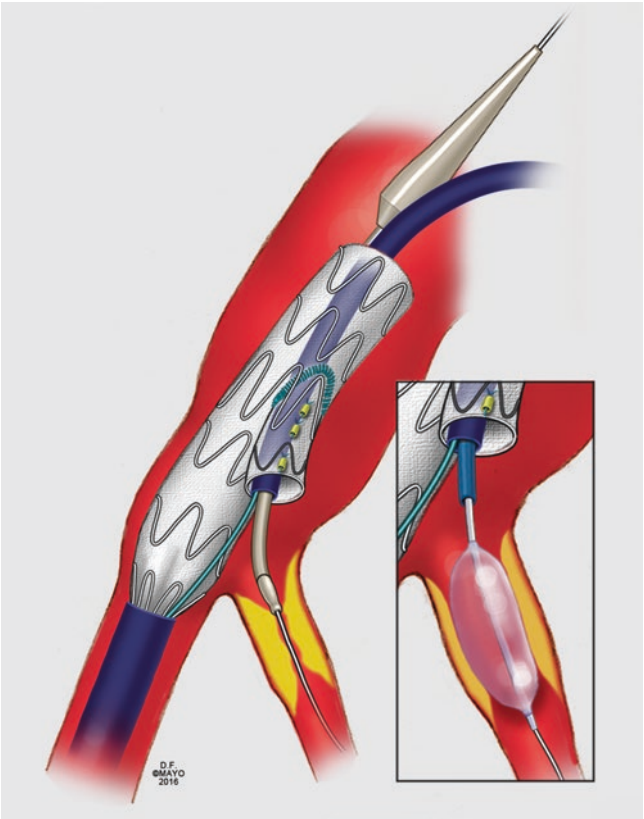


Fig. 39.2 Ostial disease can be treated by balloon angioplasty before or after deployment of the iliac branch device. By permission of Mayo Foundation for Medical Education and Research. All rights reserved

Short Length

Iliac branch devices are not recommended with excessively short common iliac arteries (<4 cm), unless a bifurcated–bifurcated device is selected or the repair is extended into the infrarenal aorta. In these cases, a parallel stent-graft can still be performed (Fig. 39.3) or alternatively, a hybrid approach.

Narrow Diameter

The inner diameter of the common iliac artery should be ideally 16 mm at the bifurcation. However, technical success can be achieved with narrower diameters of 12–14 mm. If the internal iliac artery originates from a normal diameter artery or there is a shelf between the origin of the vessel and the common iliac artery aneurysm, the anatomy is not ideal for an iliac branch device and alternative technique should be selected (Fig. 39.4).

Internal Iliac Artery Aneurysm

Presence of an internal iliac artery aneurysm does not contraindicate the use of an iliac branch device. The anterior branches may be coiled or excluded with plugs to allow extension of the seal zone to the posterior branch. The techniques of internal iliac artery embolization and stenting are described in Chap. 40. Use of superior gluteal artery as distal

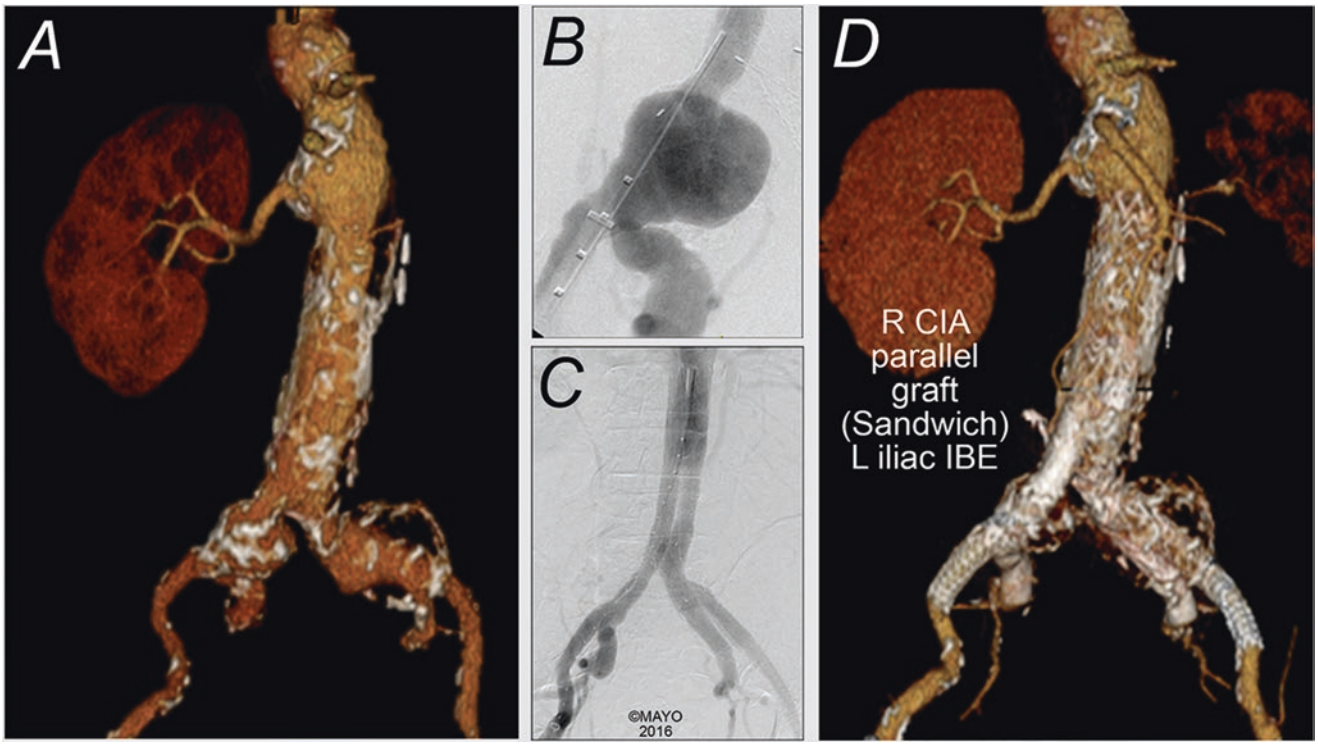


Fig. 39.3 Patient with bilateral common iliac artery aneurysms (**a**) and relative short right common iliac artery, which also has saccular configuration with narrow diameter at the bifurcation (**b**). The patient was treated by right parallel graft and left iliac branch device (**c**). Follow-up computed tomography angiography shows widely patent grafts and no endoleak (**d**). By permission of Mayo Foundation for Medical Education and Research. All rights reserved

landing zone has been reported in patients with aneurysmal internal iliac arteries. However, if there is a short or narrow common iliac artery that cannot accommodate the iliac branch device, alternative techniques should be selected (Fig. 39.5).

Dissections

Extensive dissections to the iliac arteries with flow in the true and false lumen pose a significant challenge. Patient specific devices with fenestrations for the internal iliac artery have been used in select patients. Iliac branch devices can be utilized provided there is sufficient seal zone in the internal iliac or posterior branch, and in the external iliac arteries (Fig. 39.6).

Saccular Aneurysms

A saccular aneurysm in the common iliac artery can be challenging because it may be associated with a normal segment at the level of the iliac bifurcation where the internal iliac artery originates. Also if the internal iliac artery originates from the saccular aneurysm one needs to assure access to the neck of the aneurysm for placement of the iliac branch device (Fig. 39.7).

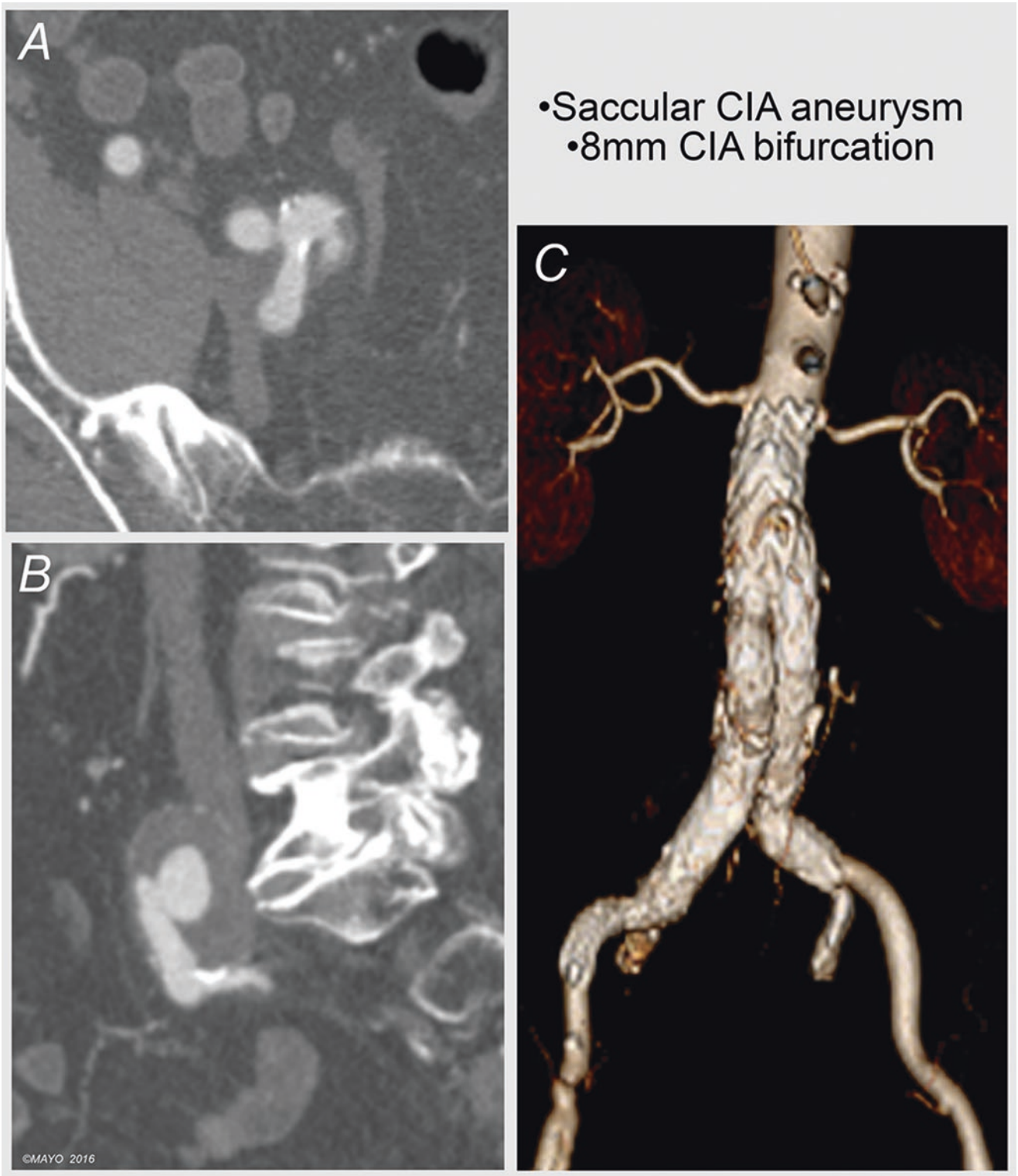


Fig. 39.4 A saccular aneurysm with very narrow right iliac bifurcation (8 mm) was considered not ideally suited for iliac branch device (**a** and **b**). Treatment was done using coverage of the internal iliac artery (**c**). By permission of Mayo Foundation for Medical Education and Research. All rights reserved

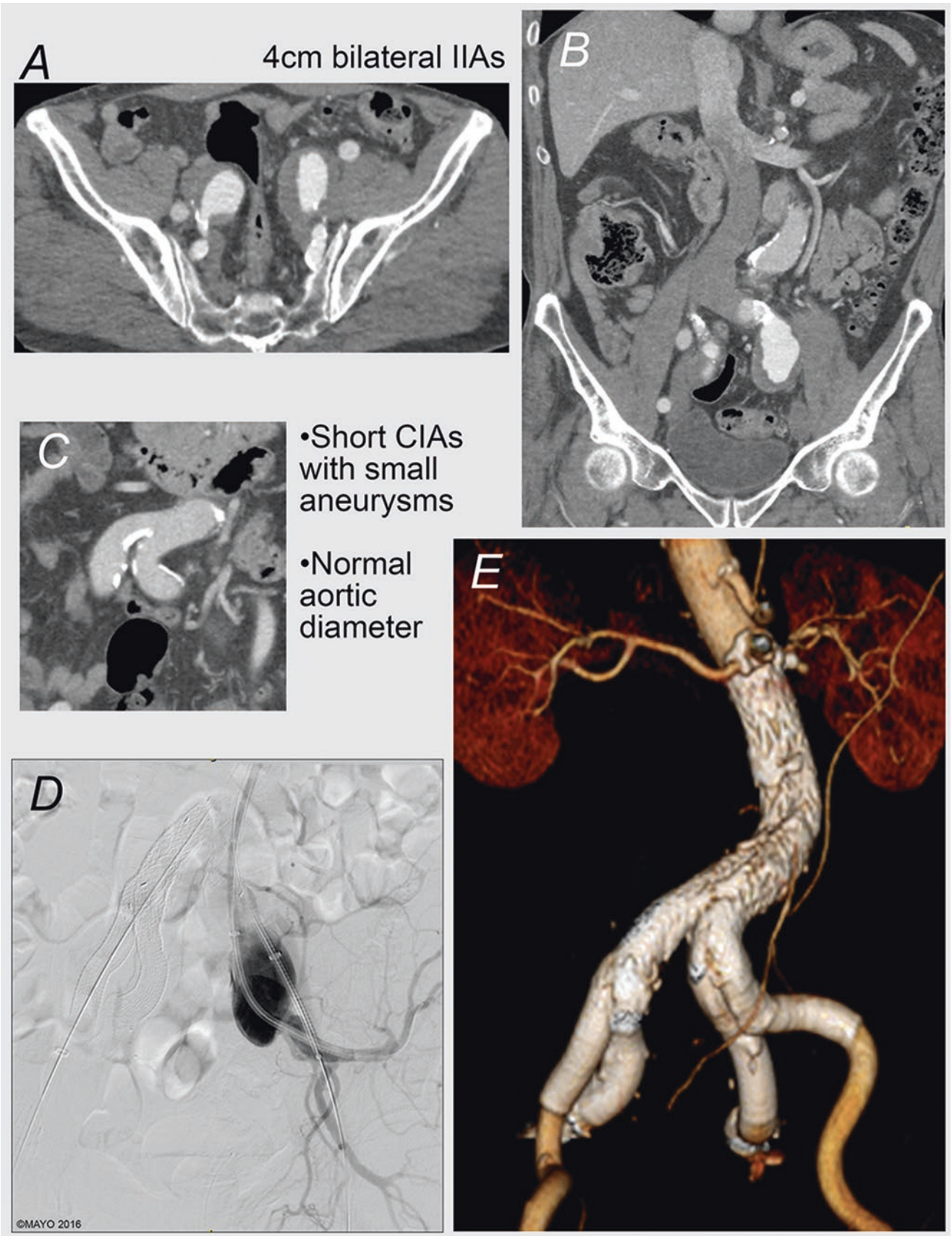


Fig. 39.5 Large bilateral internal iliac artery aneurysms (**a**) with mildly ectatic and short length common iliac arteries (**b** and **c**). The patient was treated by bilateral parallel grafts (**d**) with widely patent stents and no endoleak (**e**). By permission of Mayo Foundation for Medical Education and Research. All rights reserved

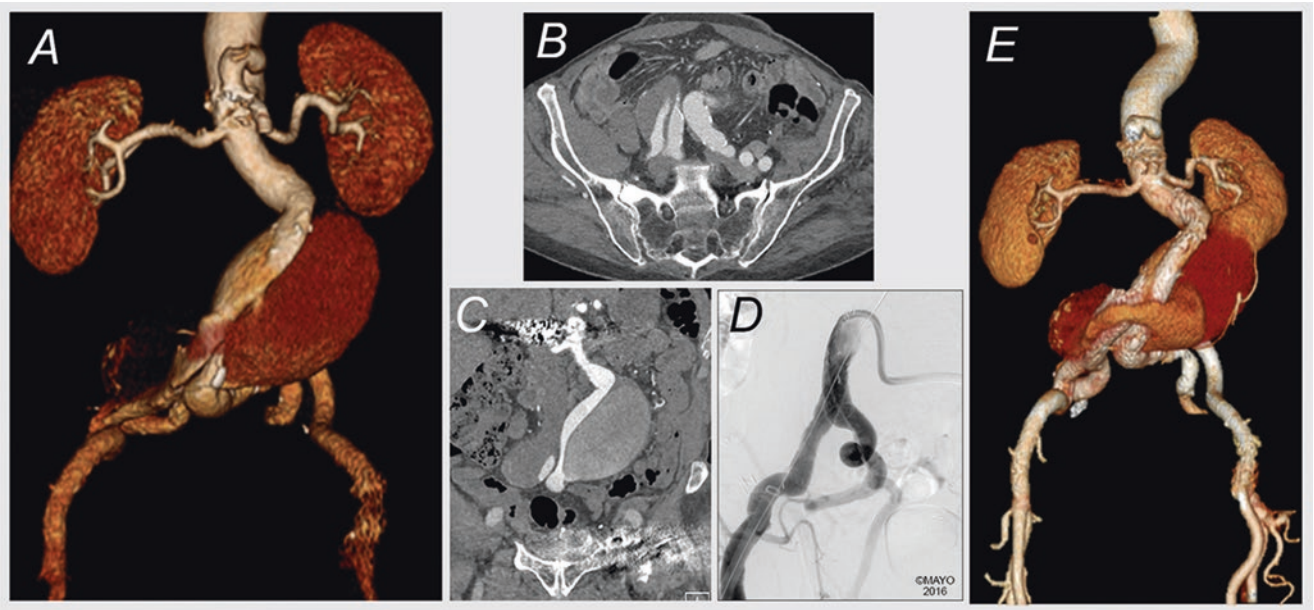


Fig. 39.6 Complex infrarenal aortic dissection (**a**) with bilateral aortoiliac aneurysms (**b** and **c**). The patient was treated by bilateral iliac branch devices (**d**). Computed tomography angiography reveals widely patent stents and endoleak originating from large IMA and lumbar arteries (**e**). By permission of Mayo Foundation for Medical Education and Research. All rights reserved

Bilateral Aneurysms

In the presence of bilateral iliac artery aneurysms can still be treated using either unilateral embolization or bilateral iliac branch devices. If the aneurysm is complex involving the renal-mesenteric arteries our preference is to salvage both internal iliac arteries whenever possible (Fig. 39.8). A BIF-IBD may be used on one of the sides, with an S-IBD or H-IBD on the contralateral side.

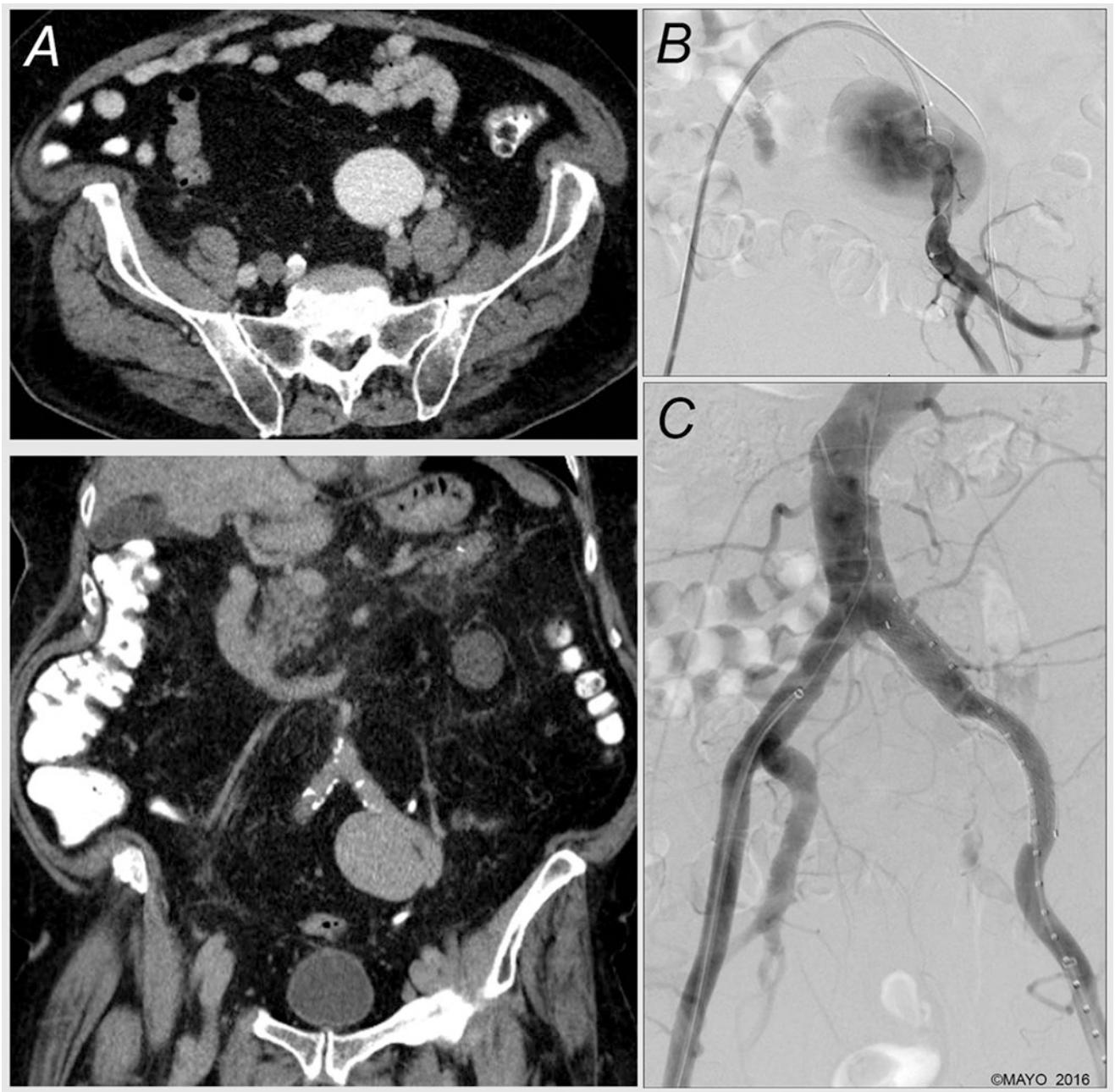


Fig. 39.7 Saccular aneurysm of the left common iliac artery (**a**). Note the origin of the internal iliac artery is from the aneurysm (**b**). Embolization was performed with coverage of the origin of the aneurysm by stent-graft (**c**). By permission of Mayo Foundation for Medical Education and Research. All rights reserved

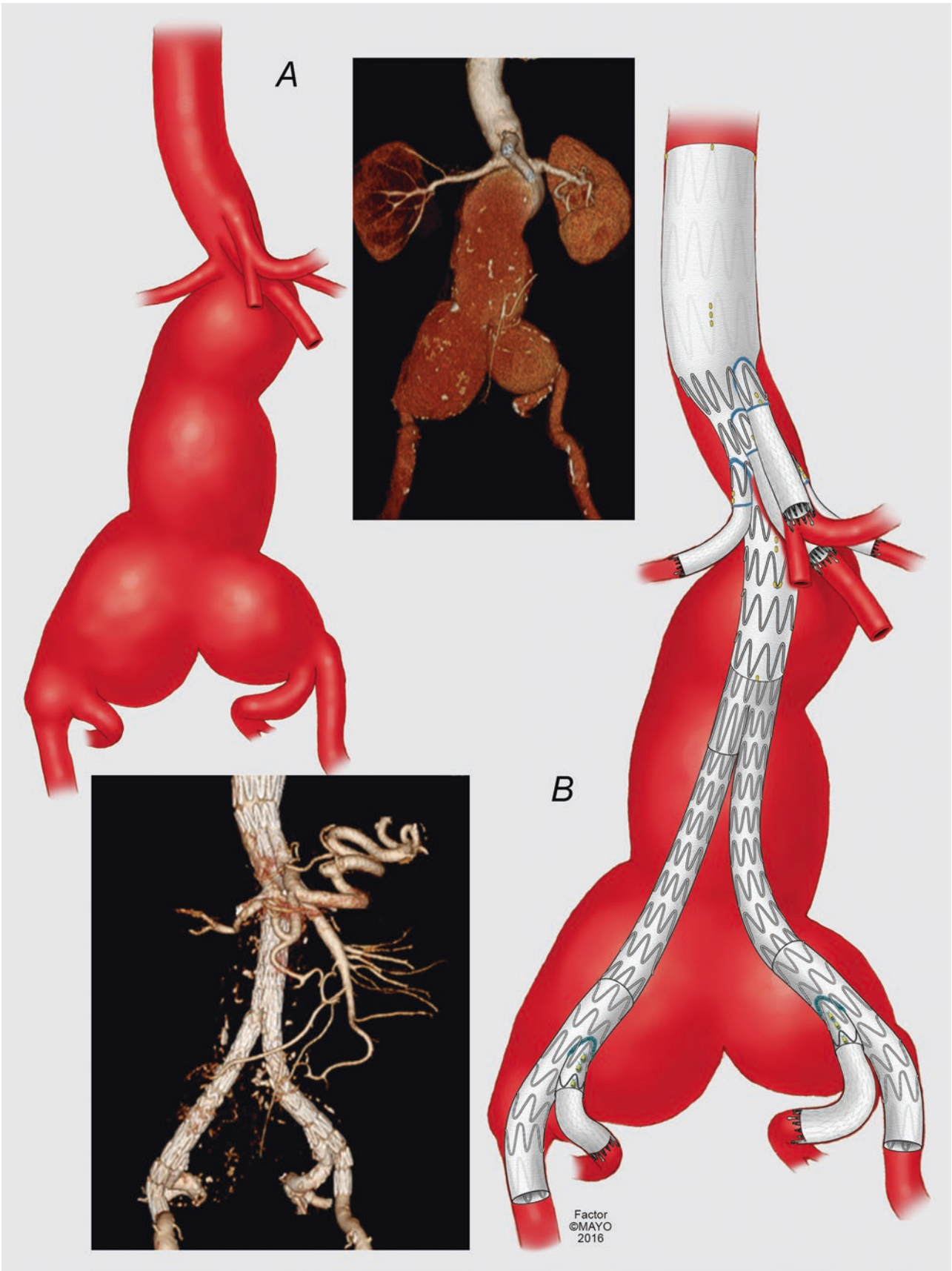


Fig. 39.8 Complex type IV thoracoabdominal aneurysms with large bilateral iliac aneurysms (**a**) treated by multibranched TAAA device with bilateral iliac branch devices (**b**). By permission of Mayo Foundation for Medical Education and Research. All rights reserved

Suggested Reading

1. Oderich GS, Greenberg RK. Endovascular iliac branch devices for iliac aneurysms. Perspect Vasc Surg Endovasc Ther. 2011;23(3):166–72.
2. Karthikesalingam A, Hinchliffe RJ, Malkawi AH, Holt PJ, Loftus IM, Thompson MM. Morphological suitability of patients with aortoiliac aneurysms for endovascular preservation of the internal iliac artery using commercially available iliac branch graft devices. J Endovasc Ther. 2010;17(2):163–71.
3. Bisdas T, Weiss K, Donas KP, Schwindt A, Torsello G, Austermann M. Use of iliac branch devices for endovascular repair of aneurysmal distal seal zones after EVAR. J Endovasc Ther. 2014;21(4):579–86.
4. Wong S, Greenberg RK, Brown CR, Mastracci TM, Bena J, Eagleton MJ. Endovascular repair of aortoiliac aneurysmal disease with the helical iliac bifurcation device and the bifurcated-bifurcated iliac bifurcation device. J Vasc Surg. 2013;58(4):861–9.

Techniques of Endovascular Repair of Aorto-Iliac Aneurysms Using Iliac Branch Devices

40

Gustavo S. Oderich and Javariah Fatima

Introduction

Endovascular aortic aneurysm repair (EVAR) has revolutionized treatment of abdominal aortic aneurysms. Prospective comparative studies have shown that EVAR significantly decreases blood loss, operative time, hospital stay, morbidity and mortality rates compared to open surgical repair [1–3]. However, the applicability of EVAR has been challenged in patients with unfavorable anatomy because of short or angulated proximal neck, aneurysm involvement of the visceral arteries, or distal extension to the iliac arteries. Approximately 40 % of the patients have inadequate distal landing zones because of aneurysmal involvement of the common iliac artery. Exclusion of one or both internal iliac arteries and extension of the stent graft to the external iliac artery have been applied frequently to extend the indications of EVAR, accepting the risks of buttock or thigh claudication, erectile dysfunction, ischemic colitis, gluteal or perineal necrosis, spinal cord injury, and acute limb ischemia.

The development of iliac branch devices (IBDs) has allowed incorporation of one or both internal iliac arteries using a total endovascular approach with modular stent grafts. There are currently five IBD configurations by three manufacturers (Fig. 40.1). The early and mid-term outcomes of IBDs have shown excellent technical success and patency rates, without increase in mortality or stent-graft related complications. In this article, we summarize techniques of implantation of IBDs and bail out maneuvers for the most common intra-procedural complications.

Rationale

Few would argue that one of the basic tenets of vascular surgical reconstructions is vessel preservation whenever possible. Claudication is not a life-threatening issue, and much like with superficial femoral artery disease, patients learn to live their limitations and modify their lifestyle by limiting their mobility. Sexual dysfunction is not well reported in most series. Complications such as claudication or sexual dysfunction may affect up to 50 % of patients treated with unilateral internal iliac artery occlusion, and up to 80 % of those who require treatment of both iliacs. The risk of serious complications is greater in patients with thoracoabdominal aneurysms (TAAA), where compromise of the IIA circulation has been shown to increase the risk of paraplegia in experimental models and clinical reports. Thus the ability to maintain antegrade perfusion of the pelvic circulation using IBD grafts is potentially useful in patients with limited disease, but critical in patients with more extensive disease.

Design Options

Design options by three manufacturers are extensively discussed in Chap. 38. For the purposes of this chapter, we discuss the techniques of implantation with three designs manufactured by Cook Medical (Bloomington, IN) and with the newly approved Gore Excluder Iliac Branch Endoprosthesis (Gore, Flagstaff, AZ). Cook Medical has pioneered the use of IBDs and most of the worldwide clinical experience. There are currently three available designs by Cook

G.S. Oderich (✉)
Division of Vascular and Endovascular Surgery,
Department of Surgery Mayo Clinic, 200 First Street SW,
Rochester, MN 55905, USA
e-mail: oderich.gustavo@mayo.edu

J. Fatima
Division of Vascular and Endovascular Surgery,
University of Florida, 1600 SW Archer Rd., NG-45,
P.O. Box 100128, Gainesville, FL 32610, USA

© Mayo Foundation for Medical Education and Research 2017

G.S. Oderich (ed.), *Endovascular Aortic Repair*, DOI 10.1007/978-3-319-15192-2_40

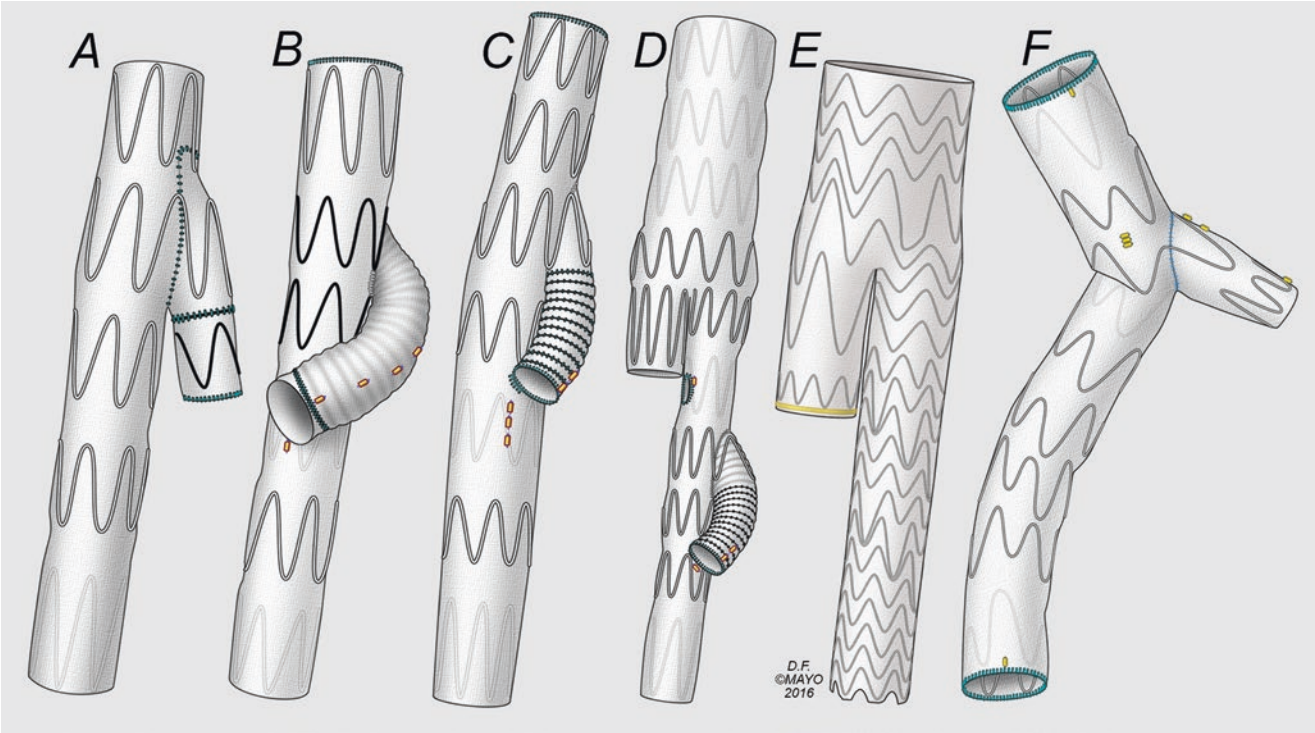


Fig. 40.1 Current designs of iliac branch devices, which were pioneered by Cook Medical, including the straight (**a**), helical (**b** and **c**) and bifurcated–bifurcated iliac branch devices (**d**). More recently, the WL Gore Excluder Iliac Branch Endoprosthesis (**e**) and the Jotec (**f**) iliac branch devices have also been used clinically. By permission of Mayo Foundation for Medical Education and Research. All rights reserved

including the straight IBD or Z-BIS (straight IBD or S-IBD), a helical IBD with a longer branch component (helical or H-IBD) and a bifurcated, bifurcated device which incorporates a helical branch into one of the iliac limbs (bifurcated–bifurcated or B-B-IBD).

Ancillary Tools

Techniques of IBD require advanced endovascular skills and a comprehensive inventory with wide variety of balloons, stents, stent-grafts catheters, guide-wires, and sheaths. Although many of the tools are variable depending on physician preference, a few are essential to the success of the technique. Our preference is to use a 45-cm 12Fr Ansel hydrophilic sheath with flexible dilator (Fig. 40.2), which can easily be advanced up and over the aortic bifurcation and is kink resistant. The new 12Fr DrySeal sheath with flexible dilator was designed specially for the IBE procedure, and should soon be available for commercial use in the USA. For through-and-through femoral access, we use the 0.25-in. Metro guide-wire (Cook Medical Inc., Bloomington, IN), which is 480-cm long and has enough length for exchanges while allowing continuous traction from the foot of the table. In addition, the over-the-wire Indy Snare (Cook Medical Inc., Bloomington, IN) is optimal for advanced aortic procedures. A wide range of balloon-expandable covered stents (iCAST Atrium Maquet, Hudson, NJ) and stent-grafts is recommended.

Technique

Access

Percutaneous technique or open surgical exposure of both femoral arteries is needed for EVAR using IBDs. Our preference is to use percutaneous approach with two Perclose devices as previously discussed in other chapters, unless the common femoral arteries are calcified or there is a high bifurcation. After obtaining access, the patient is systematically heparinized and an activated clotting time (ACT) >225 s is maintained throughout the case. On-lay fusion technology is used to locate the ostia of the internal iliac arteries whenever possible. If this is not available, selective angiographies can usually be performed using the contra-lateral 12 Fr sheath and/or the ipsi-lateral femoral sheath. Most of the guide-wire and catheter manipulations are done using a Kumpe catheter (Cook Medical Inc., Bloomington, IN) and a floppy 0.035-in. glide-wire and the catheter of choice. In the ipsi-lateral side, a catheter and glide-wire is advanced into the descending thoracic aorta and exchanged for a 0.035-in.

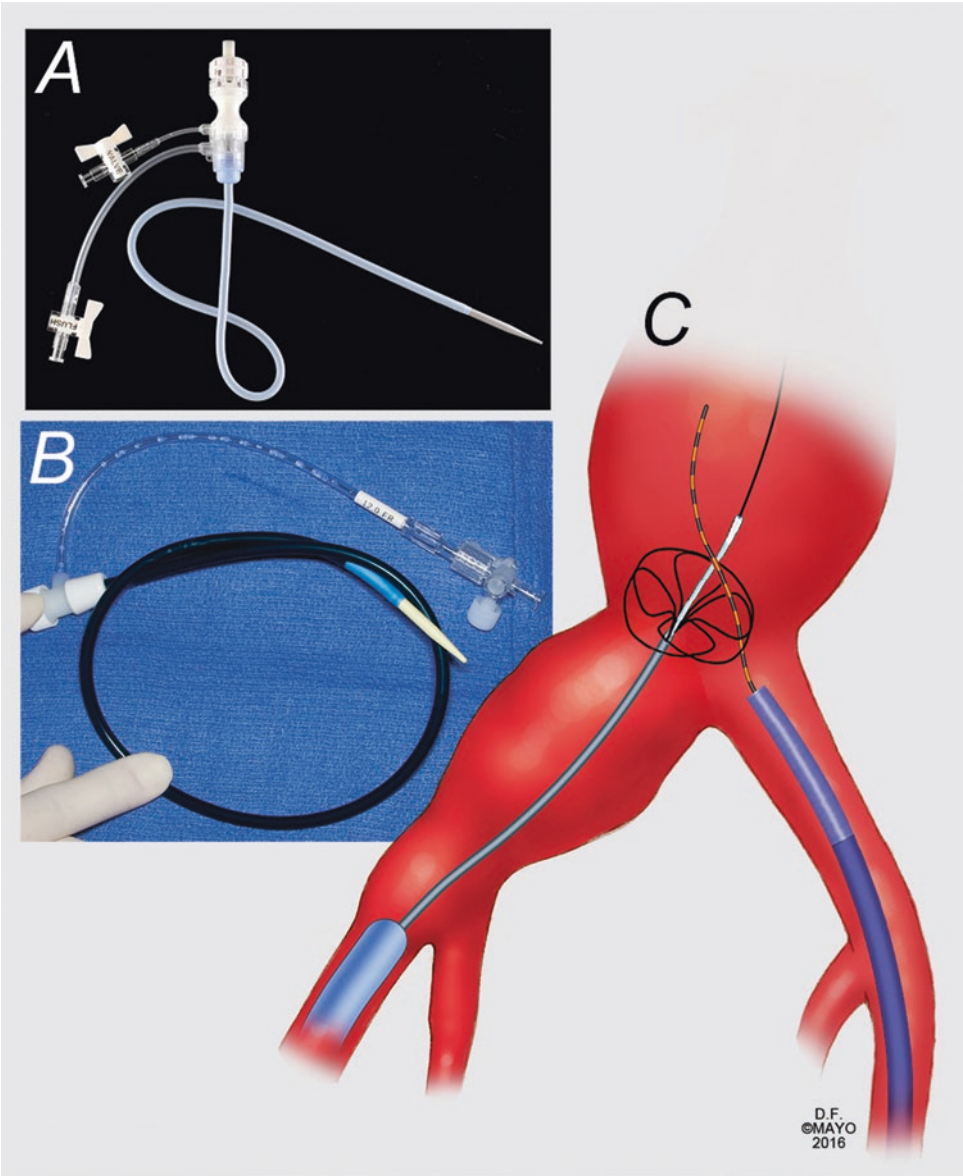


Fig. 40.2 Ancillary tools that are used for iliac branch procedures include the use of flexible 12Fr sheaths such as the new Gore DrySeal (**a**) or the Cook Ansel flexor sheaths (**b**). Typically, the Cook Indy Snare, which is advanced over the wire, is most useful to snare the 480-cm Cook Metro wire (**c**). By permission of Mayo Foundation for Medical Education and Research. All rights reserved

Lunderquist wire (Cook Medical Inc., Bloomington, IN). In the contra-lateral side, a catheter and glide-wire are advanced into the lower thoracic aorta, and exchanged for a Lunderquist wire. The dilator of the 12Fr sheath is removed over the wire, and an Indy Snare (Cook Medical) is advanced and positioned at the level of the aortic bifurcation.

Straight and Helical IBDs

All Cook IBDs are loaded into a 20F delivery system that contains a pre-loaded curly tip catheter, which is pointing towards the side of the branch. The catheter resides just proximal to the proximal aspect of the device for the S-IBD and H-IBD. The B-B-IBD allows the pre-loaded wire to exit the limb using a fenestration that is created opposite to the branch ostium. This fenestration seals automatically when the wires and catheters are removed by a flap of fabric that is attached to a stent above the fenestration that falls over the opening (self-sealing fenestration).

The device is oriented extra-corporeally with the branch pointing medially and slightly posteriorly. It is useful to obtain an angiography of the target iliac bifurcation prior to introduction of the stiff delivery system. If on-lay fusion imaging is used, this needs to be adjusted to match the selective view obtained with contrast angiography. The IBD is introduced

over the Lunderquist wire. Following insertion of the IBD over a stiff wire, the device is oriented such that the three markers immediately distal to the branch ostium in order to align with the internal iliac ostium clock position on an axial image (usually 5:00 for a right internal iliac orifice, and 7:00 for the left). This should result in the pre-loaded catheter oriented at the 3:00 position for right-sided devices, and 9:00 for left-sided devices. Proper orientation does facilitate snaring of the pre-loaded wire. The 12 Fr sheath (Cook Medical Inc., Bloomington, IN) is inserted in the contra-lateral femoral artery and placed at the origin of the common iliac artery (Fig. 40.3). An over-the-wire Indy snare (Cook Medical Inc., Bloomington, IN) is introduced over the contra-lateral Lunderquist wire and 12Fr sheath used A 0.025-in. Metro guide-wire is advanced via the pre-loaded catheter, which is allowed to form into a curly curve by slightly deploying the sheath to expose only the tip of the catheter. The guide-wire is snared using the Indy snare. Occasionally, snaring is more difficult in the aortic bifurcation if the aortic diameter is very large. Advancing the device into the aortic neck may facilitate the snare process.

The H-IBD or S-IBD is advanced to the desired location with the branch terminus 1–1.5 cm above the target internal iliac artery, and the sheath is withdrawn to expose the branch. At this point, the contra-lateral Lunderquist is removed, leaving only the through and through Metro wire. The dilator is introduced in the 12Fr sheath, which is advanced against the pre-loaded catheter. Both are kept under tension with surgical clamps applied on each end to maintain the tip of the catheter and the dilator close to each other. The 12Fr sheath is then advanced from the contra-lateral side up and over the aortic bifurcation in a movement of push and pull done by the main operator. The sheath is advanced into the target branch using the pre-loaded wire. This maneuver of withdrawing the pre-loaded catheter and 12Fr sheath as a unit is critically important and avoids any strain to be placed in the proximal edge of the IBD (Fig. 40.4). Once the 12Fr is in position, a second puncture is then made in the valve of the 12F sheath (optional), and a 5F sheath is placed, followed by a steerable guidewire-catheter combination (Kumpe catheter, Cook Medical Inc., Bloomington, IN), which is advanced along side the through-and-through wire within the 12F sheath. This "buddy" catheter and wire are used to catheterize the internal iliac artery. Preferably, the catheter is advanced into the posterior (gluteal) branch of the target vessel. A short 1-cm tip Amplatz guide-wire (Cook Medical Inc., Bloomington, IN) is then placed through the catheter and the catheter removed. A marker catheter can be introduced over the wire to allow measurement of the side branch stent length. During this portion of the procedure, an assistant maintain continuous gentle traction in the metro wire. The internal iliac artery is imaged in a manner that will demonstrate the branch terminus as well as the sealing zone in the internal iliac artery. An appropriate length matting self-expandable stent graft (Fluency stent graft, Bard Peripheral Vascular Inc., Tempe, AZ, or Viabahn, Gore, Flagstaff, AZ) for H-IBDs or balloon-expandable stent graft (iCAST, Atrium Maquet Medical, Hudson, NH) for S-IBDs is inserted over the stiff wire and deployed. For self-expandable stents, the through-and-through wire can be maintained; for the balloon-expandable stent, it is recommended to remove the through-and-through wire prior to deployment. Caution must be taken when advancing balloon-expandable stent-grafts beyond the protecting sheath, and sometimes an 8 or 9F sheath will be needed to gain purchase to the desired level of sealing within the internal iliac circulation. During this process, traction on the through-and-through wire stabilizes the 12F sheath, such that the delivery of mating devices is not treacherous. For helical branches, the self-expandable stent graft is deployed with at least 2 cm overlap with the helical branch and 2 cm seal within the internal iliac artery. Additional radial force may be required in some cases where there is marked tortuosity or minimal luminal size within the common iliac artery. In these cases the matting stent graft is reinforced with a second self-expanding stent or a balloon-expandable stent, but removal of the through-and-through wire should precede this step. Once the IBD and matting stent graft are fully deployed, the remainder of the branch is deployed by sheath withdrawal, the trigger wires are then deployed, leaving the internal iliac wire over which the matting stent graft was deployed in place, with an 8 mm balloon transcending the internal iliac and external iliac junction. The 8-mm balloon is then inflated, protecting the branch, and the delivery system is removed (Fig. 40.5). A 12-mm balloon can then be inflated at the junction of the two iliac arteries in a kissing balloon fashion to ensure patency of the internal and external iliac arteries. The repair is then imaged by injecting through the 12F sheath while aspirating blood through the 20Fr sheath. The remainder of the repair is carried out using a standard bifurcated modular component, which is introduced via the contra-lateral side (Fig. 40.6). If there is a kink at the distal edge of the external iliac artery stent-graft limb, a self-expandable bare metal stent is added to prevent occlusion (Fig. 40.7). The IBD is mated to the remainder of the Zenith stent graft (Cook Medical Inc., Bloomington, IN) with a short iliac extension.

BB-IBD

The BB-IBD devices are oriented such that the pre-loaded fenestrations are above the aortic bifurcation. Typically, the device is placed inside a proximal component, which is either a tubular stent for infra-renal aneurysms or a fenestrated device (Fig. 40.8). Care must be taken with a BB-IBD in the setting of very short common iliac artery that the three markers distal to the branch exit are above the origin of the target internal iliac artery. The BB-IBD carries certain advantages

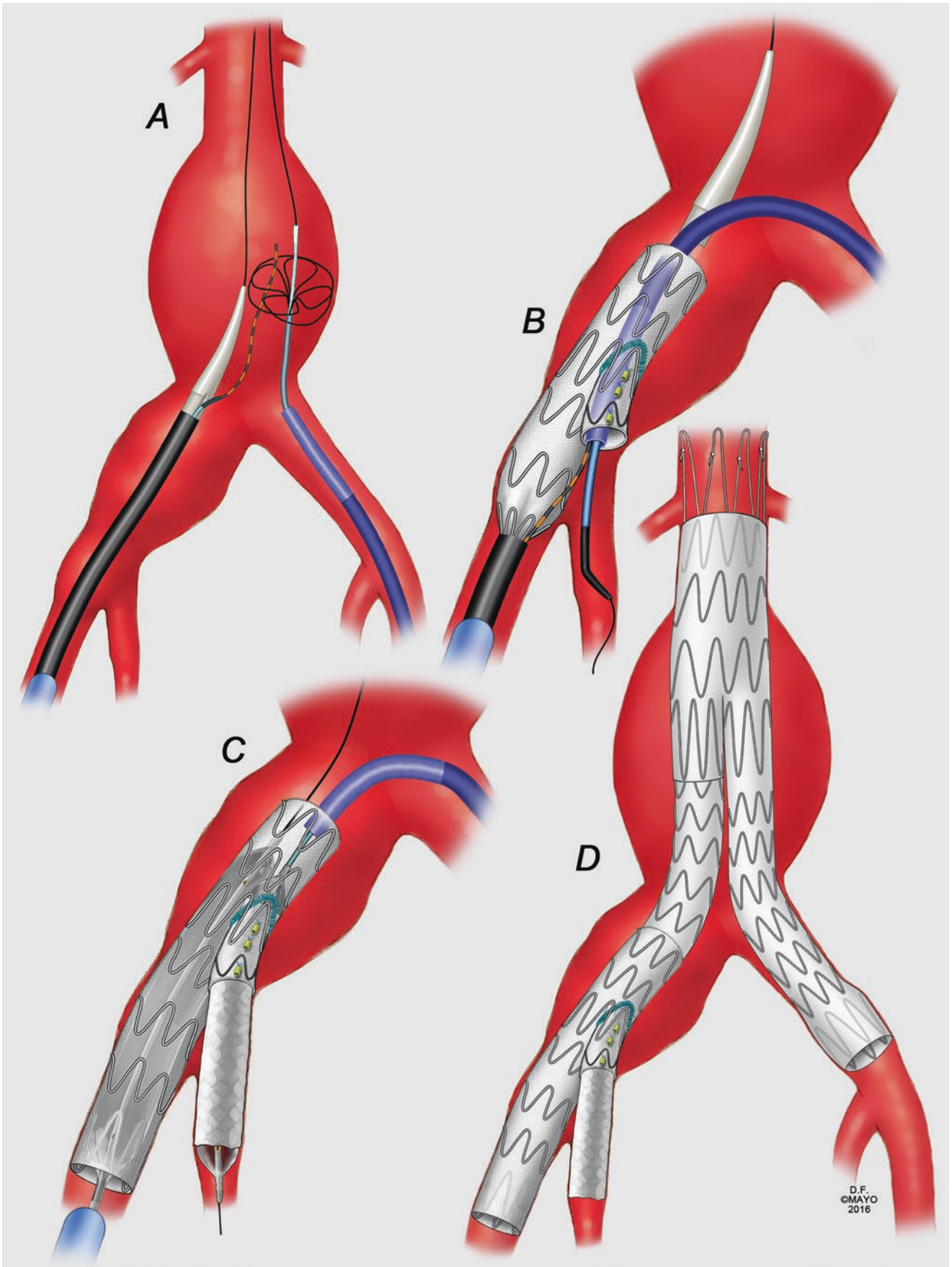


Fig. 40.3 Technique of endovascular repair using the Cook Iliac branch device includes advancement of the iliac branch after proper orientation with snaring of the wire using a pre-loaded catheter (**a**), followed by deployment of the proximal portion of the iliac branch with advancement of the 12Fr contra-lateral sheath (**b**), placement of a balloon-expandable stent into the internal iliac artery (**c**) and completion of the endovascular aortic repair in standard fashion (**d**). By permission of Mayo Foundation for Medical Education and Research. All rights reserved

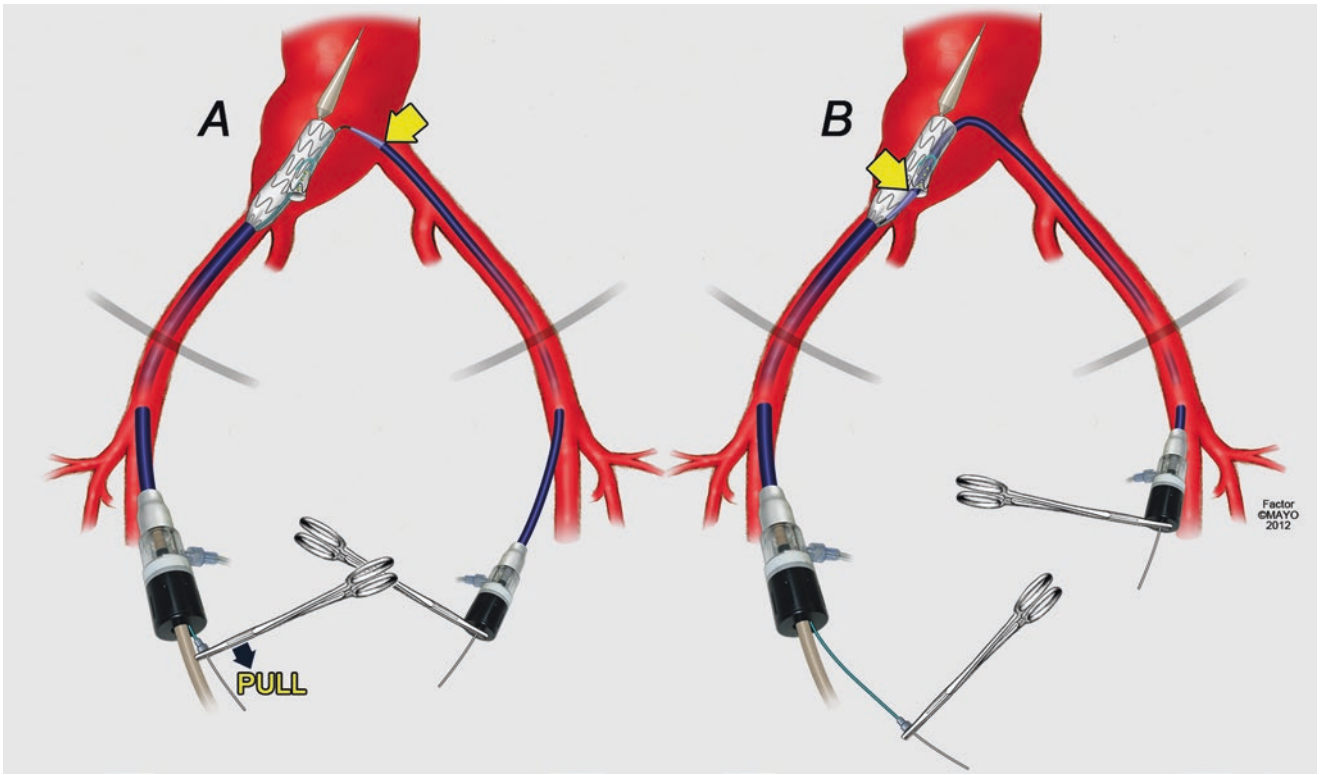


Fig. 40.4 The push and pull maneuver is most useful for advancing the contra-lateral sheath without damaging the tip of the sheath (**a**) or the iliac branch device. The sheath is positioned at the terminus of the branch (**b**). By permission of Mayo Foundation for Medical Education and Research. All rights reserved

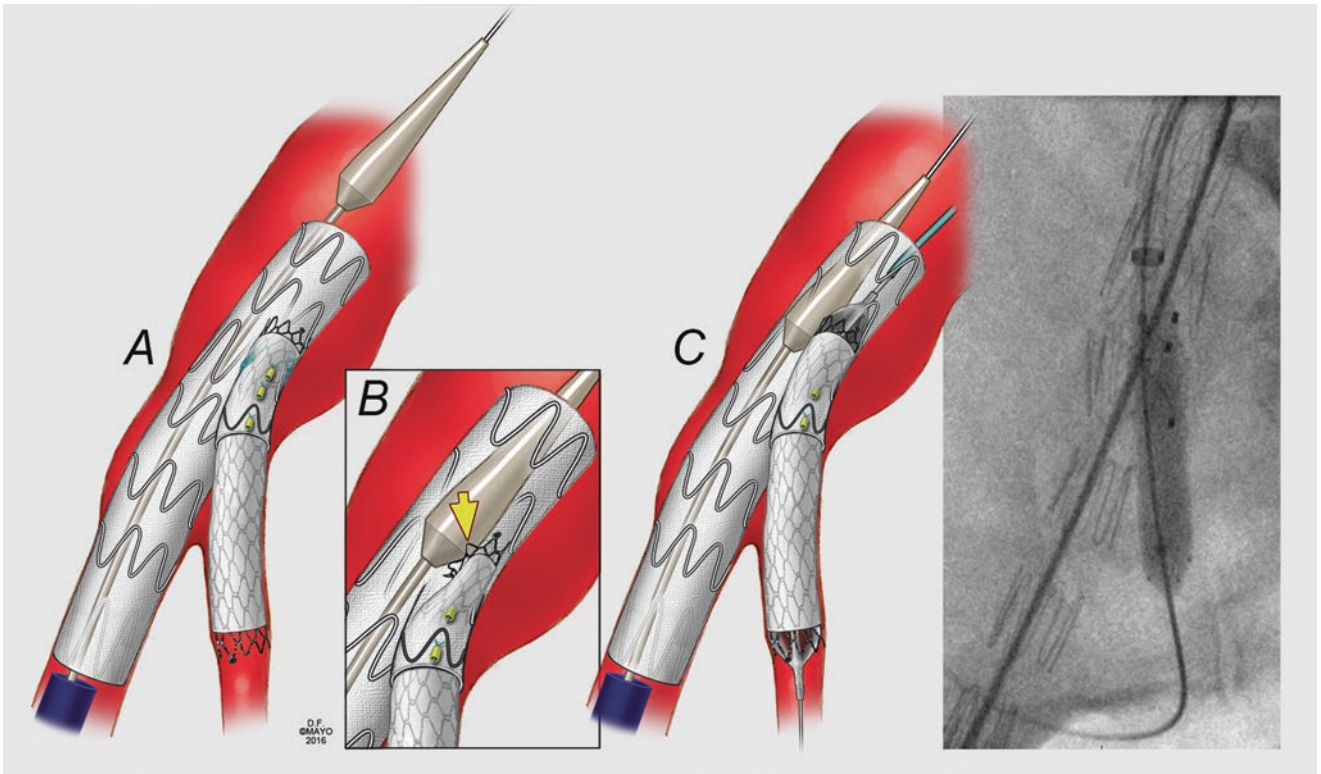


Fig. 40.5 Removal of the branch delivery system should be done carefully (**a**). If the sheath and balloon are removed prematurely from the iliac branch bridging stent, the tip of the dilator can compress the stent or dislodge it (**b**). Instead, it is recommended to protect the bridging stent by balloon inflation (**c**) during removal of the sheath. By permission of Mayo Foundation for Medical Education and Research. All rights reserved

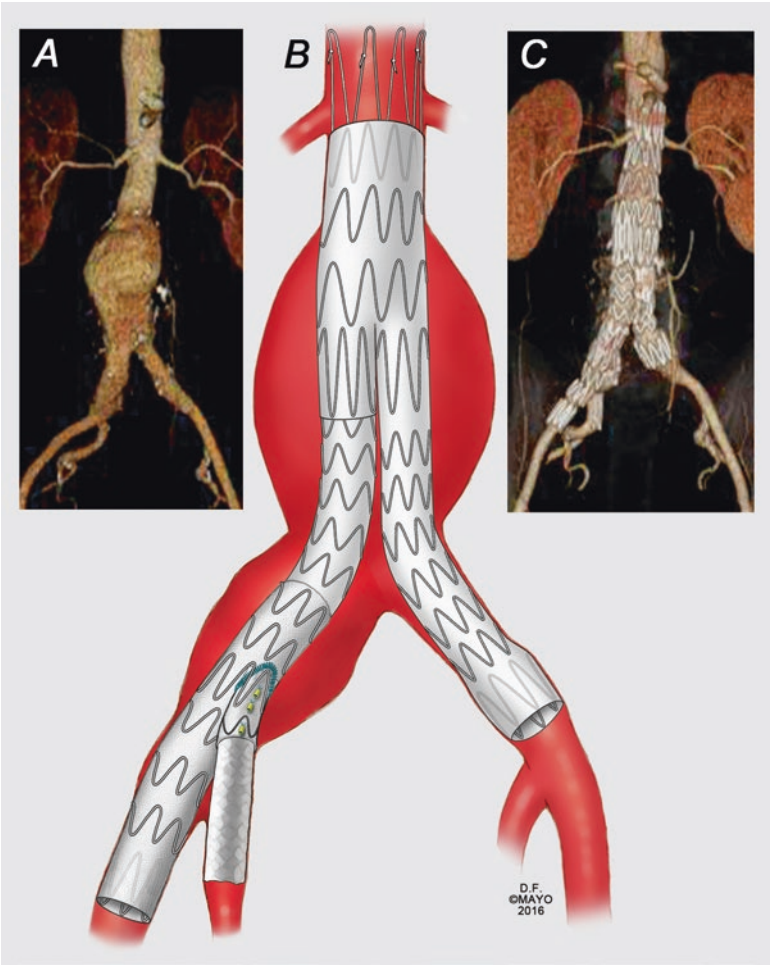


Fig. 40.6 Patient with large aorto-iliac aneurysm (**a**) treated by Cook iliac branch device (**b**). Follow-up computed tomography angiography revealed widely patent stent and no endoleak (**c**). By permission of Mayo Foundation for Medical Education and Research. All rights reserved

over the earlier designs. Primarily the modular connection to the AAA repair is moved proximally, allowing extensive overlap between the IBD device and aortic repair device, eliminating the two joints that are created when the H-IBD or S-IBD is mated to the AAA repair. Additionally, the length of required common iliac artery (CIA) to safely perform the procedure is reduced. With both the H-IBD and S-IBD a reasonably long CIA is required (>5 cm) to prevent the IBD device from extending into the aortic aneurysm proper. The BB-IBD device can be used in the setting of shorter (>2.5 cm) CIA, allowing for treatment of significantly more patients, particularly women and Asian patients.

Similar to the S- and H-IBDs, the BB-IBD has a pre-loaded curly catheter that can be exposed by withdrawing the sheath. A Metro guide-wire is snared via the contra-lateral side using the Indy Snare. During deployment of the BB-IBD, the assistant needs to maintain the pre-loaded catheter and guide-wire taught under tension, to avoid entrapment of the catheter or guide-wire in the top portion of the device, which can occur and requires re-snaring. The device is slowly withdrawn to expose the self-sealing fenestration, which should be located medially and above the aortic bifurcation. The



Fig. 40.7 Presence of a kink distal to the external iliac limb extension should be recognized and treated by self-expandable bare metal stent. By permission of Mayo Foundation for Medical Education and Research. All rights reserved

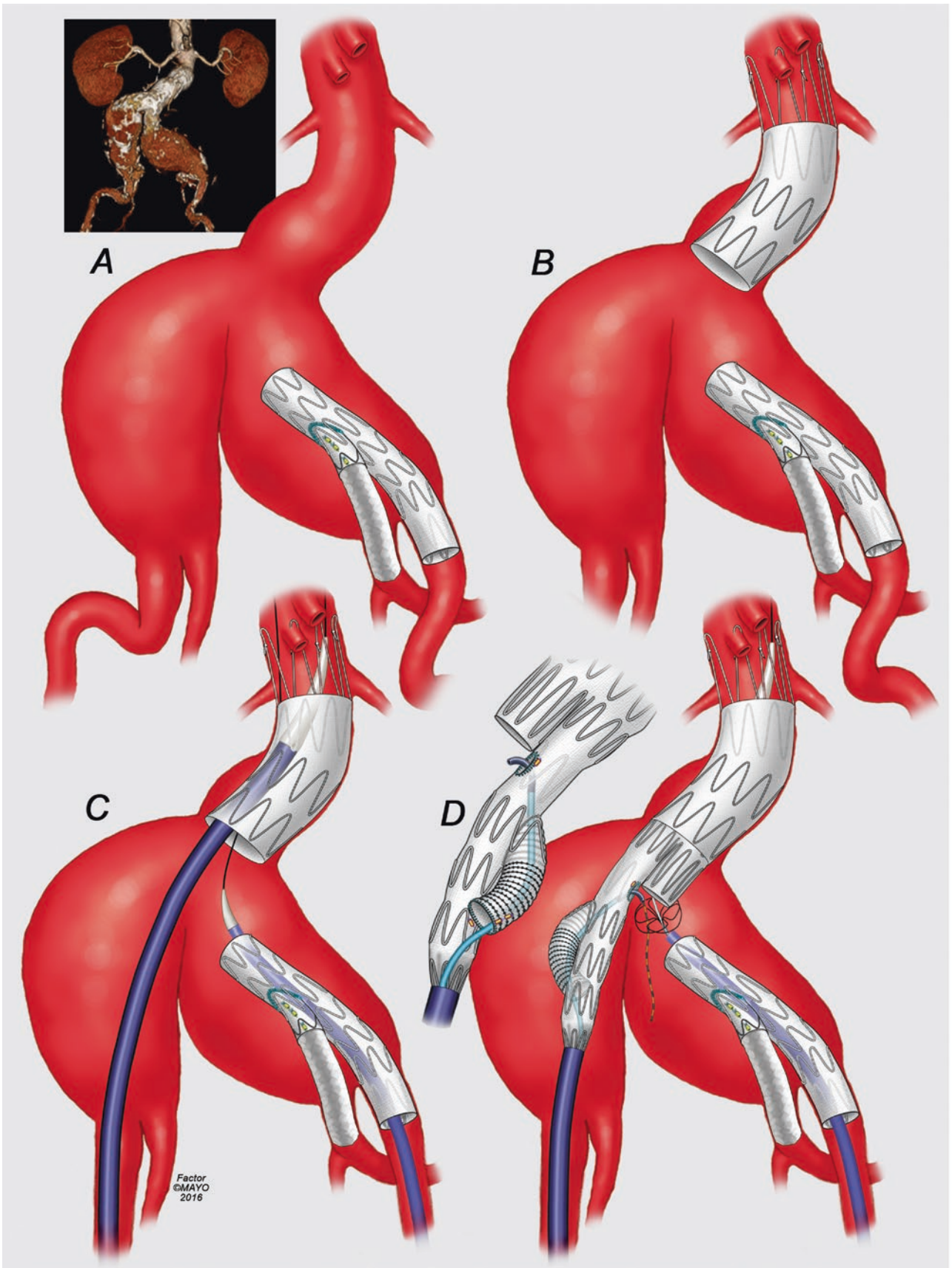


Fig. 40.8 Patient with large bilateral common iliac artery aneurysms and unusually short distance between the renal arteries and the aortic bifurcation (**a**) was treated by placement of a left-side straight iliac branch device and right-side bifurcated–bifurcated iliac branch device. First, a tubular component is deployed below the renal arteries (**b**). The bifurcated–bifurcated device is advanced via the right femoral approach (**c**), and deployed releasing the helical branch (**d**). A wire is snared using the pre-loaded catheter which exits via a self-sealing fenestration. A 12Fr Ansel sheath is advanced up and over the aortic bifurcation and through the self-sealing fenestration into the terminus of the helical branch

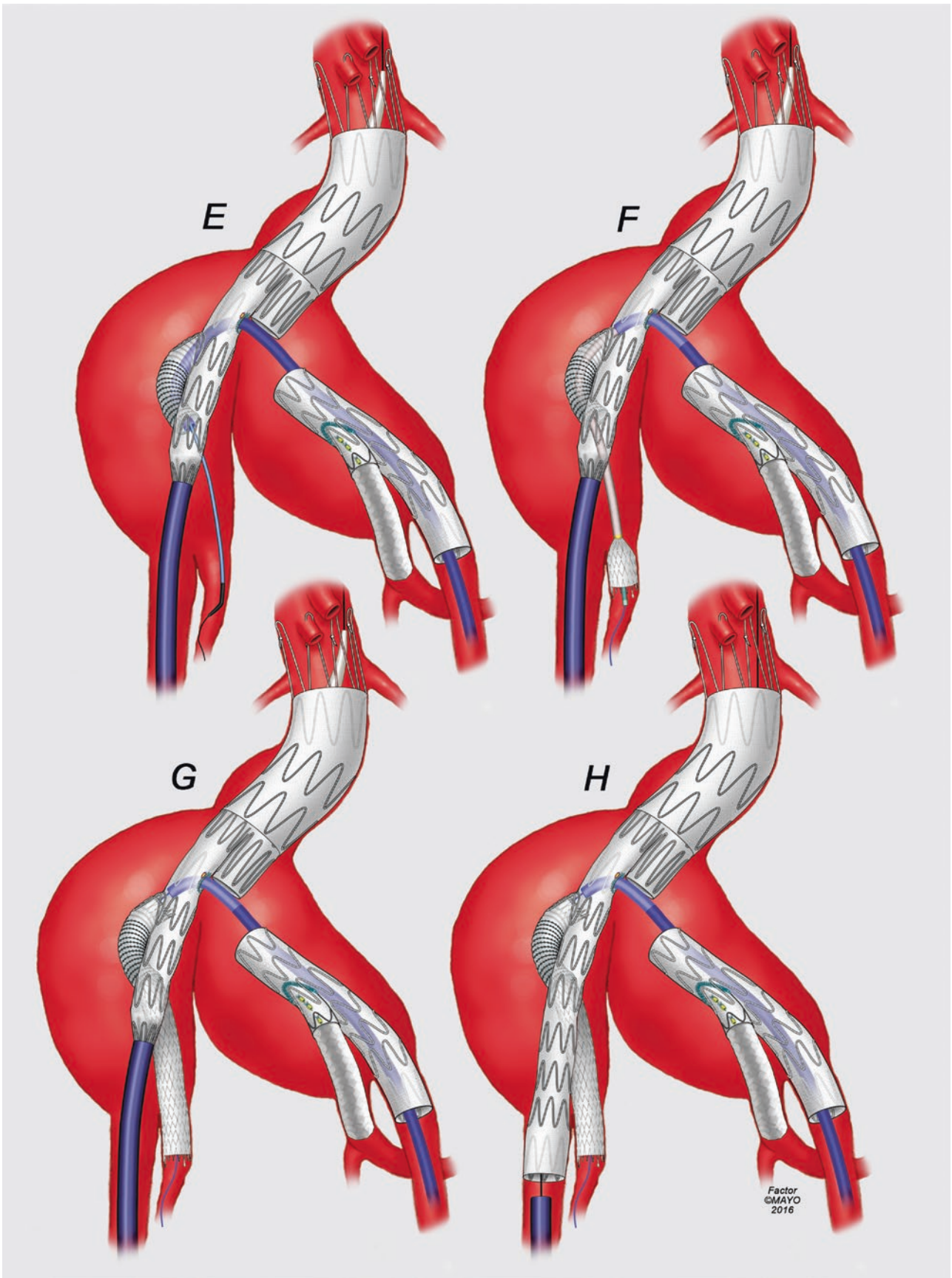


Fig. 40.8 (continued) (**e**). The internal iliac artery is catheterized and the repair is extended into the internal iliac artery using a self-expandable Fluency stent-graft (**f**). The stent graft is ballooned (**g**), and the remaining external iliac limb is deployed (**h**). The delivery system is retroacted while protecting the internal iliac branch by balloon inflation. Kissing balloon angioplasty is performed in the overlapping segment of the iliac bridging stent and iliac branch device (**i**). Final appearance of the repair is documented by computed tomography angiography (**j**). By permission of Mayo Foundation for Medical Education and Research. All rights reserved

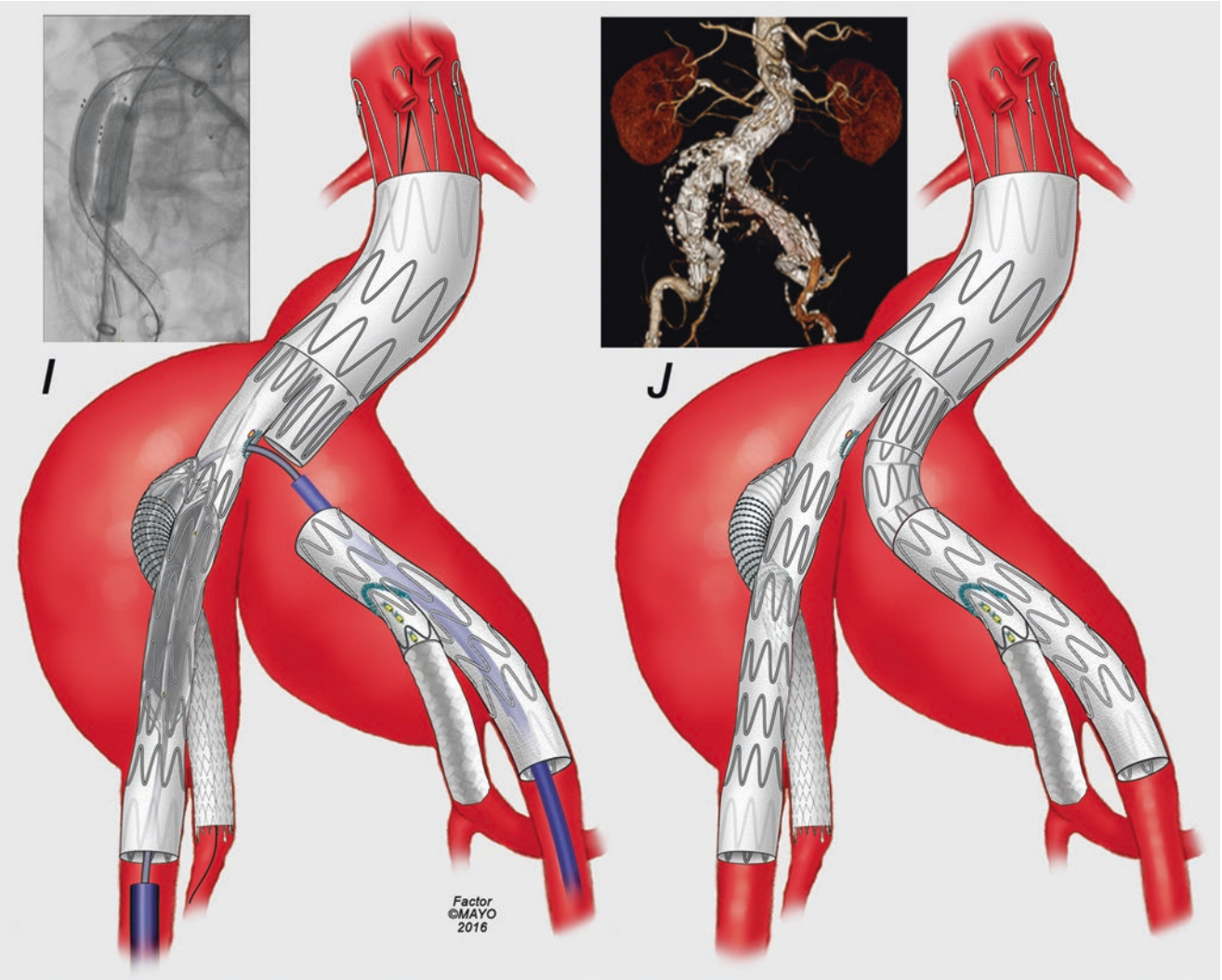


Fig. 40.8 (continued)

12Fr sheath and dilator are then advanced to the tip of the pre-loaded catheter. Surgical clamps are applied into each end, and the BB-IBD is further deployed to expose the helical branch, which should be 1–1.5 cm above the iliac bifurcation. The 12Fr is advanced across the self-sealing fenestration and helical branch using the technique already described. Selective cannulation of the internal iliac artery is then accomplished in a similar fashion and a stiff wire is placed into the posterior trunk of the IIA. The internal iliac artery matting stent is performed using a self-expandable stent-graft. The steps are then identical to what was already described for the S- or H-IBD.

Gore Excluder IBE

The Gore Excluder IBE is introduced over a 16Fr sheath and has a pre-loaded guide-wire system and a repositionable, two-step deployment mechanism. Similar to the Cook IBDs, the bridging stent is also introduced via a 12Fr sheath from the contra-lateral femoral approach.

Bilateral femoral access is established in standard fashion as previously described (Fig. 40.9). A 16Fr DrySeal sheath is advanced over a Lunderquist guide-wire in the ipsi-lateral side, and a 12Fr Ansel or Flexible DrySeal Ansel sheath advanced over a Lunderquist guide-wire in the contra-lateral side. A buddy catheter is introduced via the 16Fr sheath and an Indy Snare in the contra-lateral 12Fr sheath. The Metro guide-wire is snared establishing the through-and-through femoral access. The IBE is prepped with normal saline flushes. It has a stainless steel packing mandrel, which is introduced to allow pre-loading of the guide-wire. This mandrel should not be removed at this point. Instead, the through-and-through guide-wire is loaded through the mandrel and green cannula, while the IBE is loaded into the Lunderquist wire. The green cannula is then removed and

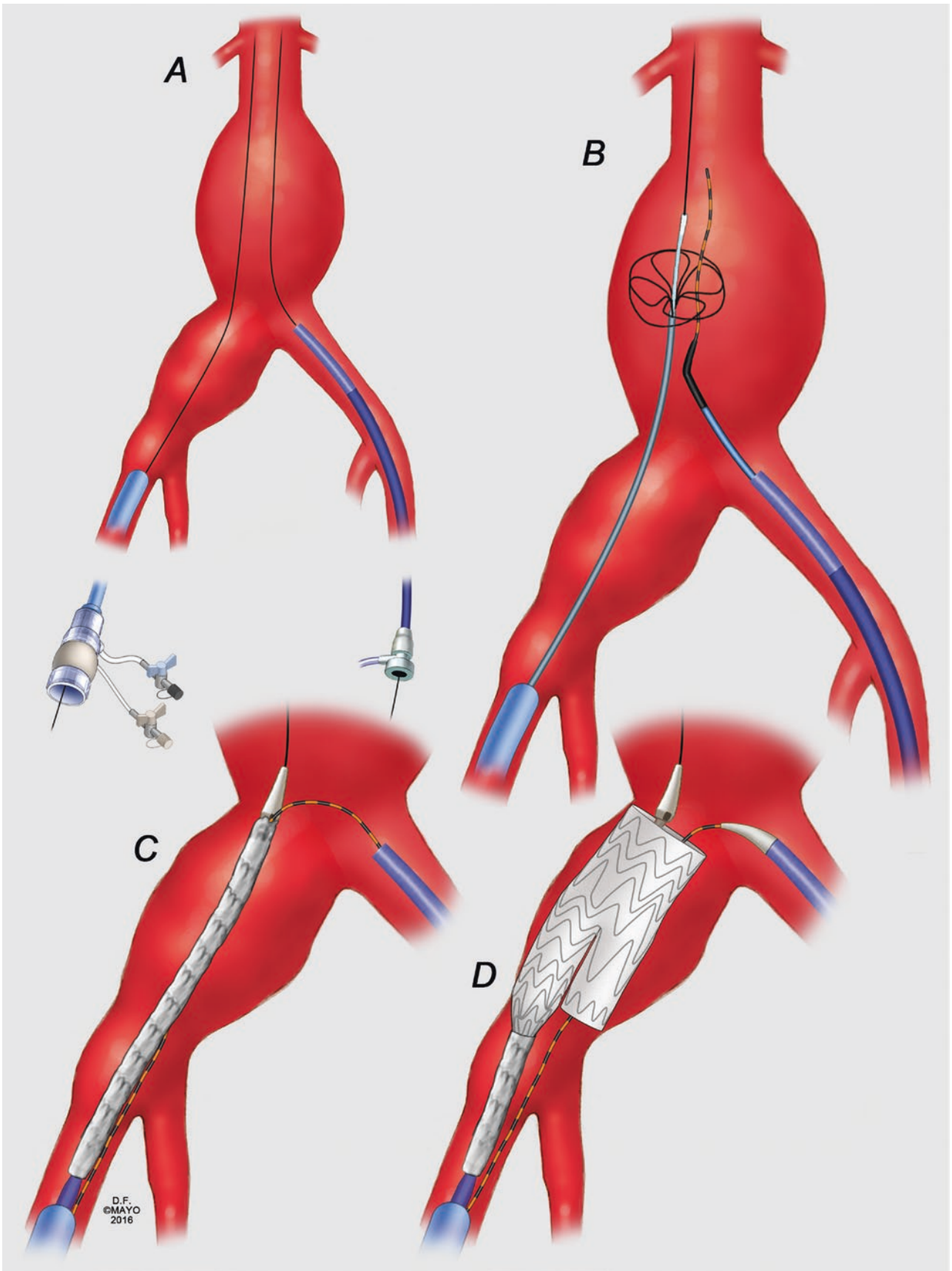


Fig. 40.9 Technique of endovascular repair using WL Gore Excluder Iliac branch endoprosthesis. Bilateral femoral access is established (**a**), and a guide-wire is snared to establish femoral–femoral access (**b**). The device is loaded into the aortic wire and the pre-loaded wire and advanced into position (**c**). It is important to document that there is no wire wrapping. The device is deployed releasing the iliac branch (**d**). A 12Fr sheath is advanced up and over the aortic bifurcation into the iliac branch (**e**). A buddy catheter is used to selectively catheterize the internal iliac artery

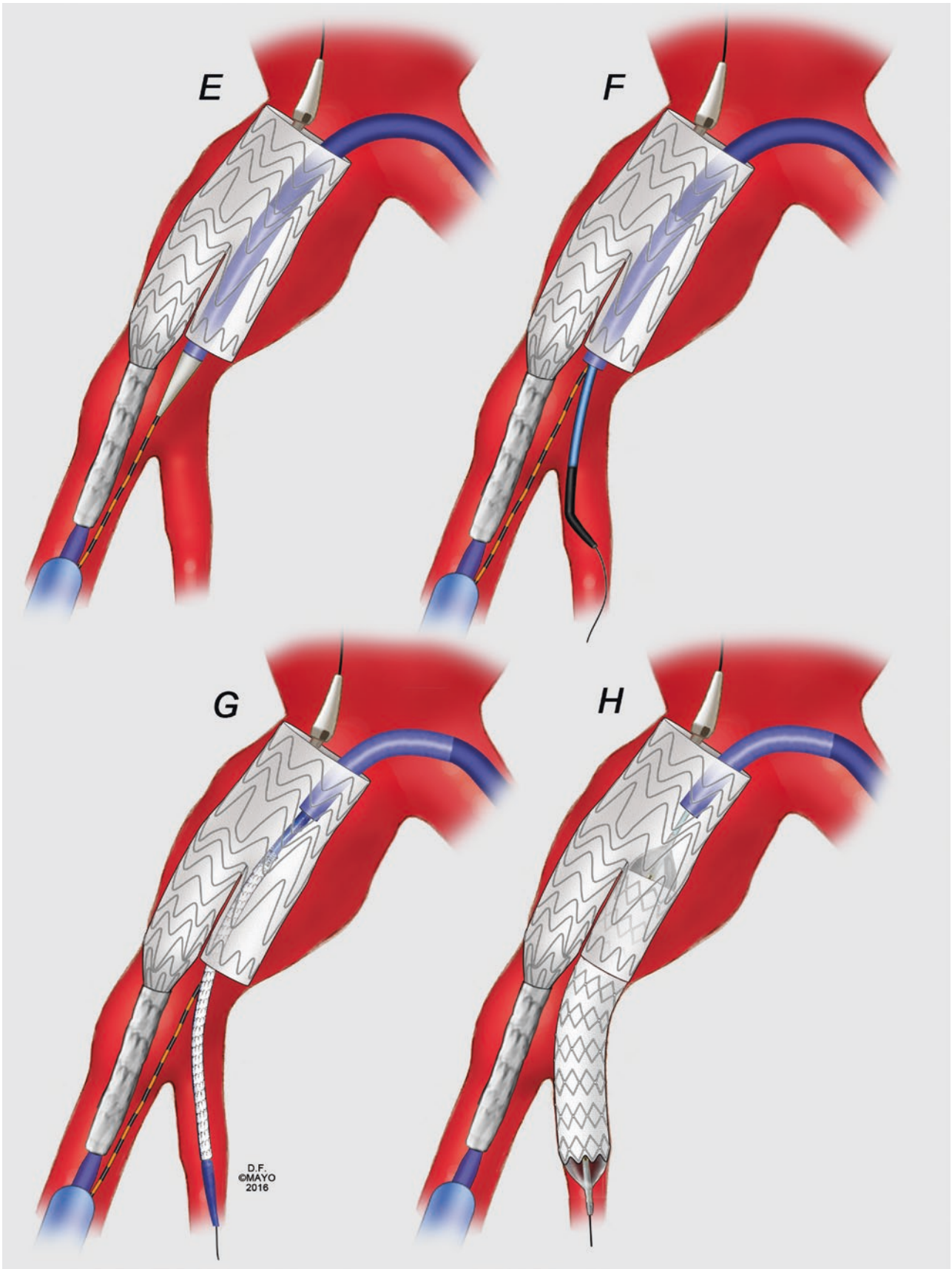


Fig. 40.9 (continued) (**f**). The bridging stent is advanced into the internal iliac artery (**g**) and deployed (**h**). The stent is ballooned and the remaining external iliac limb is deployed. The delivery system is removed. Kissing balloon angioplasty is performed in the transition of the iliac branch (**i**). The remaining of the repair includes deployment of a WL Gore Excluder device via the contra-lateral femoral approach (**j**), followed by a 27-mm iliac extension from the contra-lateral gate to the IBE device (**k**). By permission of Mayo Foundation for Medical Education and Research. All rights reserved

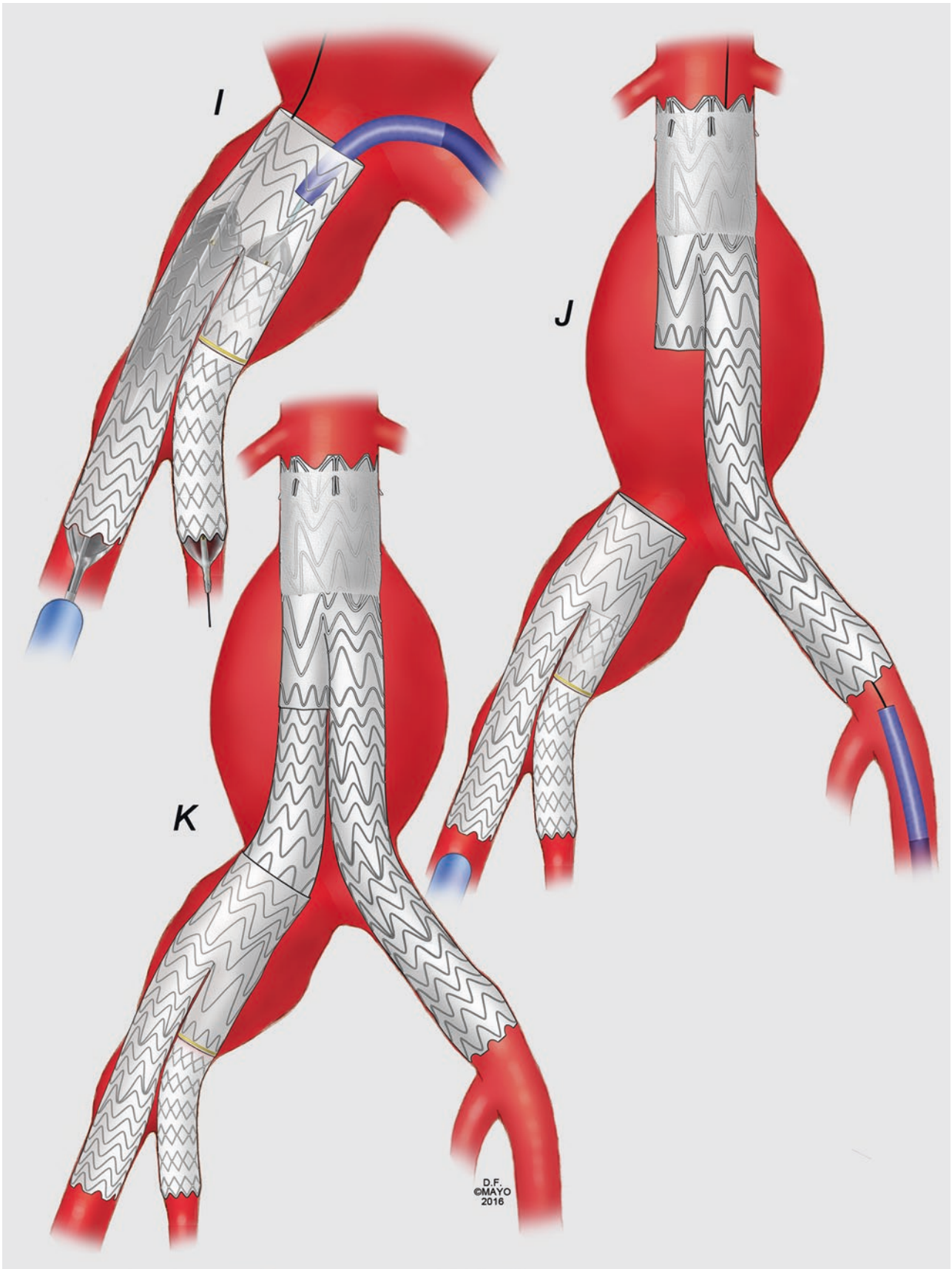


Fig. 40.9 (continued)

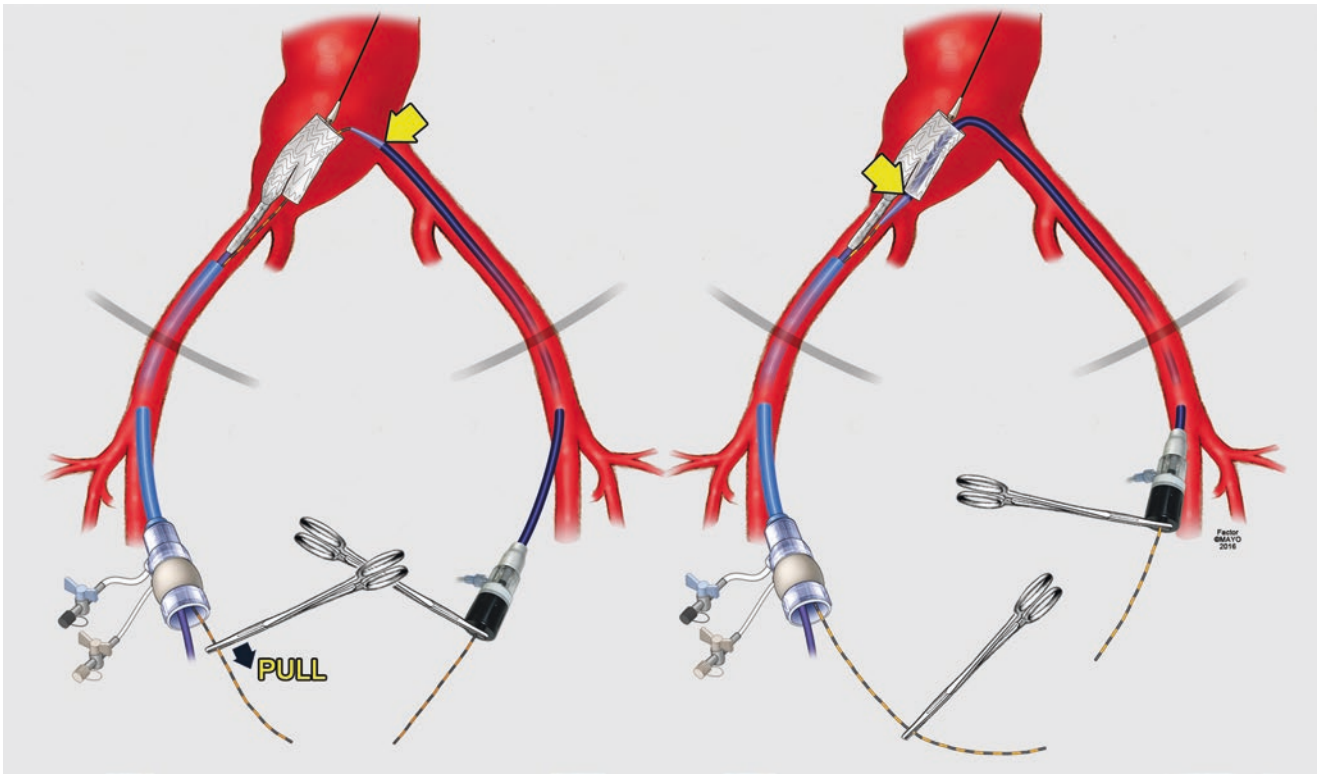


Fig. 40.10 Through and through advancement of the 12Fr sheath with the Gore TBE device is also done using the push and pull technique. By permission of Mayo Foundation for Medical Education and Research. All rights reserved

the IBE is advanced into position. Contrast angiography can be obtained either through the 16Fr ipsi-lateral sheath or contra-lateral side. One of the first and most important steps is to determine that there is no wire wrapping involving the pre-loaded guide-wire and the device cannula. If wire wrapping is noted, the device should be rotated to unwrap the wire. The first step deployment is done, releasing the iliac branch, which should be deployed 1–1.5 cm above the iliac bifurcation. Using a similar maneuver with two clamps on each end, the 12Fr sheath is advanced up and over the aortic bifurcation using the movement of "push-and-pull" (Fig. 40.10). The sheath is positioned at the distal end of the iliac branch. If a 0.035-in. wire is used for snaring, it needs to be exchanged for a smaller profile wire. However, if the 0.025-in. Metro wire is used, there is no need for wire exchange. The next steps are similar to the Cook IBDs. A buddy catheter and guide-wire are used to catheterize the internal iliac artery and posterior branch. The glide-wire is exchanged for a 1-cm short tip Amplatz wire. A marker catheter is introduced and contrast angiography is obtained for measurements and to determine the distal landing zone. The Gore iliac branch stent is introduced over the Amplatz wire and deployed into the internal iliac artery. The iliac branch is dilated using a 12-mm angioplasty balloon, while the external iliac stent portion of the device is deployed and the delivery cannula is removed. Kissing balloon angioplasty is performed using a Coda balloon for the external iliac artery. Completion angiography of the iliac branch is performed with injection via the 12Fr sheath, while the 16Fr sheath is aspirated. The remaining of the procedure is a standard EVAR, with introduction of the Gore Excluder aortic device using the contra-lateral femoral approach. The device main body is deployed below the lowest renal artery while the ipsi-lateral iliac limb remains constrained. The contra-lateral gate is cannulated via the side of the IBE. The repair is extended from the contra-lateral gate to the main body of the IBE using a flared 27-mm iliac limb extension. At this point the ipsi-lateral limb of the Excluder device is deployed and attachments are dilated with Coda balloon (Fig. 40.11).

Bilateral Aneurysms

The indications of IBDs have been expanded to patients with bilateral iliac aneurysms (Fig. 40.12). A recent study from the Cleveland Clinic group indicated that >60 % of the patients had repair performed outside the strict IFU that are used under clinical trials. In the Gore Pivotal study, bilateral aneurysms were allowed to be repaired using IBEs, with no detrimental effect on clinical outcomes. The BB-IBD is particularly useful for bilateral aneurysms because it eliminates

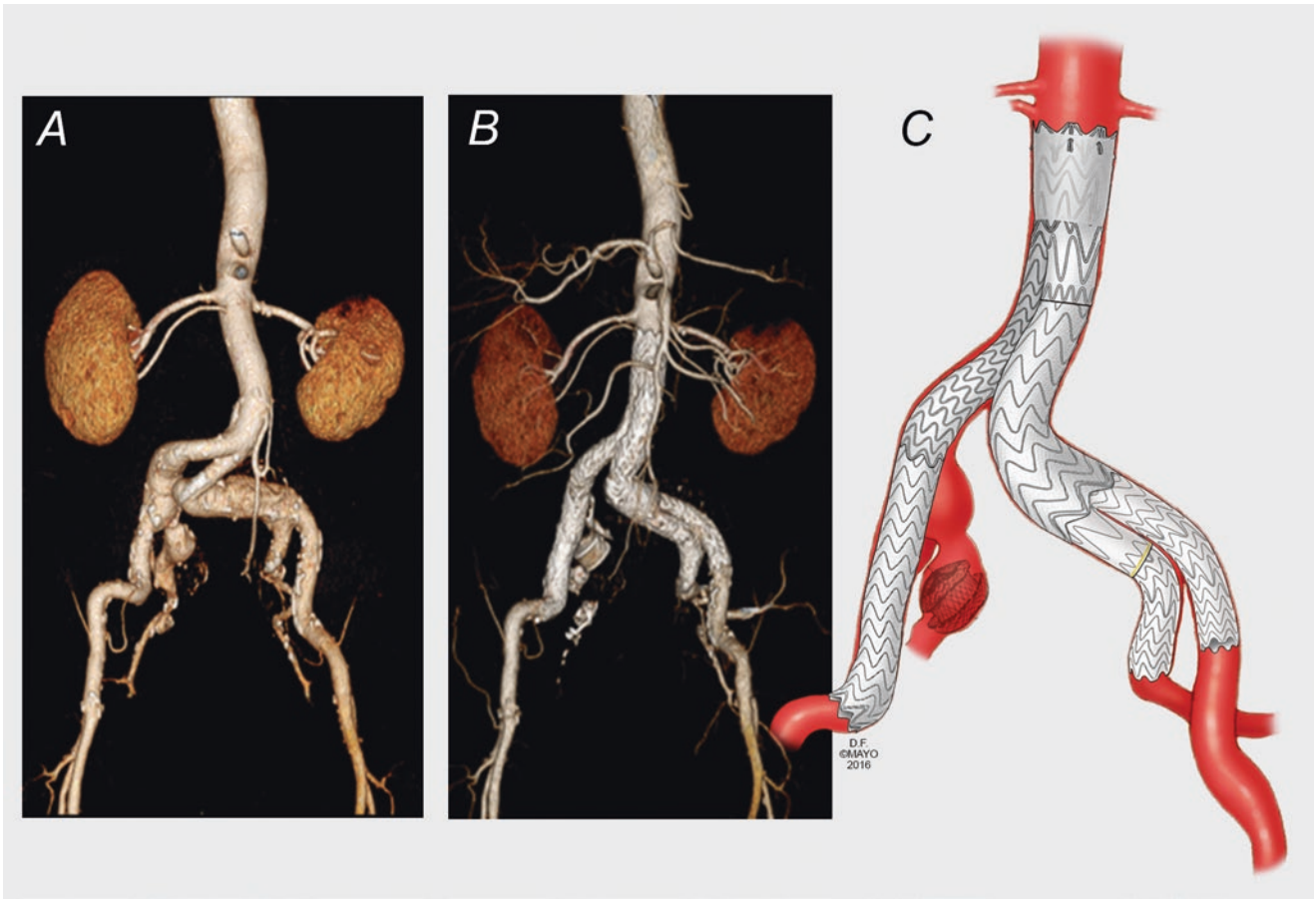


Fig. 40.11 Patient with bilateral common iliac and right internal iliac aneurysm (**a**) was treated by right internal iliac artery exclusion and left iliac branch endoprosthesis (**b**) using the WL Gore Excluder device (**c**). By permission of Mayo Foundation for Medical Education and Research. All rights reserved

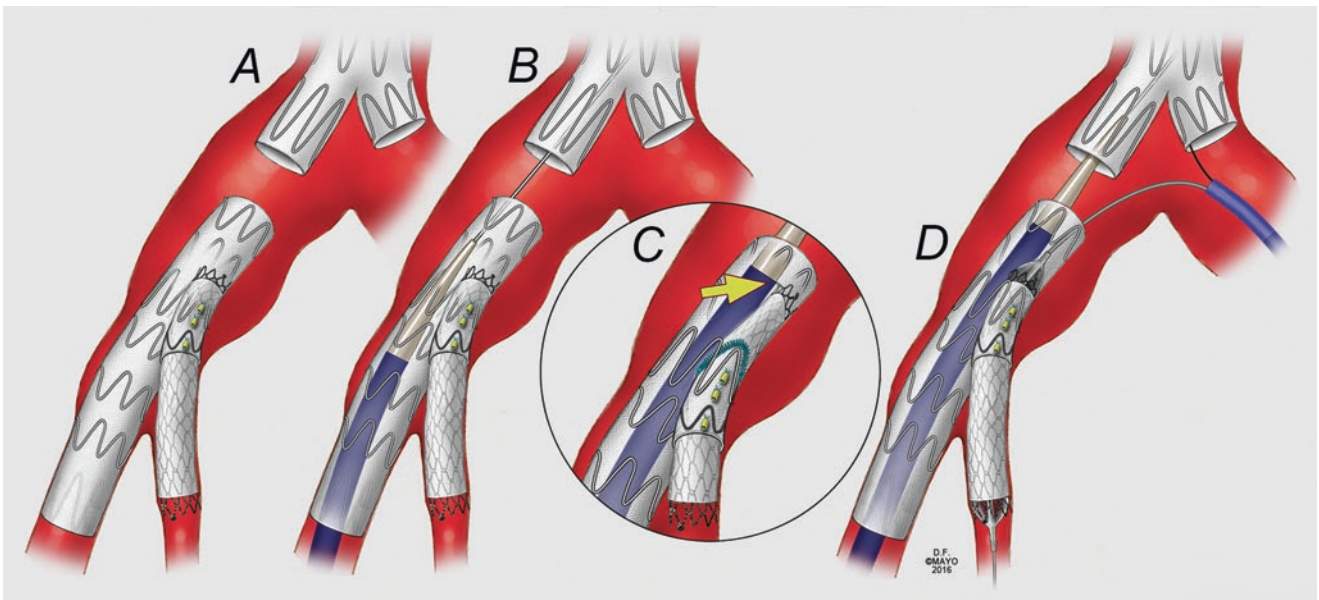


Fig. 40.12 In patients with bilateral iliac aneurysms, the aortic device component may need to be advanced via the iliac branch, which has potential risk of stent dislodgement. One alternative technique involves finishing first the aortic repair while leaving both limbs above the aortic bifurcation (**a**). Both iliac branch devices are completed (**b**), allowing protection of the iliac branch during advancement of large sheath to avoid stent compression (**c** and **d**). By permission of Mayo Foundation for Medical Education and Research. All rights reserved

one of the joints, and also avoids crossing the IBD with the aortic component, which can subject the IBD to movement or dislodgement of the side stent. Conversely, if bilateral repair is to be done using S-IBD or H-IBD, our preference is to perform one side at a time and then to introduce the aortic stent-graft via the side with the better anatomical conditions in terms of iliac diameter and less tortuosity. However, upon advancement of the aortic stent-graft delivery system, it is critical to avoid dislodgement of the iliac branch component. This can be done by maintaining the balloon inflated in the iliac branch and side stent while the aortic device is advanced via the Lunderquist wire. When using the Gore IBE device, it is important to assure that there is enough length to add the connecting 27-mm iliac limb extensions without compromising the iliac branch.

Internal Iliac Aneurysms

The presence of aneurysmal internal iliac arteries with inadequate landing zone for placement of the bridging stent represents the main reason for anatomical unsuitability to IBDs. Increasing clinical experience has been reported with extension of the repair to the posterior division branch of the internal iliac artery, while using coils or plugs to exclude the anterior branch or other smaller side branches. In these cases, the IBD or IBE is deployed using the techniques already described. The internal iliac artery is catheterized and a 7 or 8Fr Raabe sheath is advanced into the aneurysmal iliac artery (Fig. 40.13). The anterior division branch is excluded using Amplatzer plugs or coils, although plugs are ideal because of lack of metallic artifact on surveillance CT studies. If the branch is excluded, it is useful to leave the plug connected and to use a "buddy" catheter to go the next branch or the posterior branch. This maneuver keeps the sheath in close proximity to the next branch, minimizing manipulations. The target posterior branch is catheterized and an Amplatz wire is positioned. The repair is extended into the posterior branch using one of the two techniques. A safe option is to extend the branch into the internal iliac artery using an ICAST or a self-expandable stent first, and then to further extend the branch into the posterior gluteal artery using a self-expandable stent-graft. This is beneficial to avoid losing guide-wire access into the branch. Alternatively, one can deploy first a long self-expandable stent starting distal in the gluteal branch, and then add proximal stents if needed (Fig. 40.14). Deployment of the viabahn has to be done slowly to avoid dislodgement of the stent. Finally, the internal iliac aneurysm may be large and may have numerous side branches. It is important to exclude all side branches to avoid retrograde type II endoleak (Fig. 40.15). The technique of going from one side branch to the other using a buddy catheter is very useful to help minimize catheter manipulations.

Concomitant Fenestrated and Branched Stent-Graft Repair

Preservation of internal iliac artery perfusion is important to minimize risk of spinal cord injury. Among patients who have extensive aortic coverage during repair of thoracoabdominal aortic aneurysms, occlusion of a collateral network has been associated with higher rates of immediate paraplegia and lack of recovery. Therefore, every attempt should be done to preserve the internal iliac artery using IBD or alternative techniques. In these cases, it is important to minimize lower extremity ischemia, which can be done by expeditious technique, use of femoral conduits or preferential use of branches for the visceral arteries, which can be performed via the brachial approach. In the case herein illustrated a type IV thoracoabdominal aneurysm with large bilateral common iliac aneurysms was treated using bilateral S-IBDs and a t-Branch TAAA stent-graft (Fig. 40.16). Technical details of these procedures have been discussed in Chap. 28.

Prior Bifurcated Aortic Stents

Failure of a distal landing zone after prior EVAR may necessitate distal extension using an IBD. In these cases, it can be challenging to use the contra-lateral femoral access and brachial access may be needed to place the bridging stents into the internal iliac artery (Fig. 40.17). The technique is identical to what has been described for standard IBD procedures, except that access is established high in one of the brachial arteries using a 12Fr sheath. The case herein illustrated demonstrates a large left common iliac artery aneurysm after prior repair using a Gore Excluder device, which was treated by Gore IBE with left brachial access for placement of the internal iliac artery stent.

Common Problems and "Bail Out" Maneuvers

Similar to fenestrated and branch grafts done for aneurysms involving the renal-mesenteric arteries, iliac branch devices require familiarity with advanced endovascular techniques and the availability of a comprehensive inventory with wide range of guide-wires, balloons, catheters, sheaths, and stents. Some of the most common intra-procedural problems are described below.

Pseudo-Occlusion of the Internal Iliac Artery

Patients with exceedingly tortuous and non-calcified iliac arteries may have the uncommon occurrence of a pseudo-obstruction of the origin of the internal iliac artery after

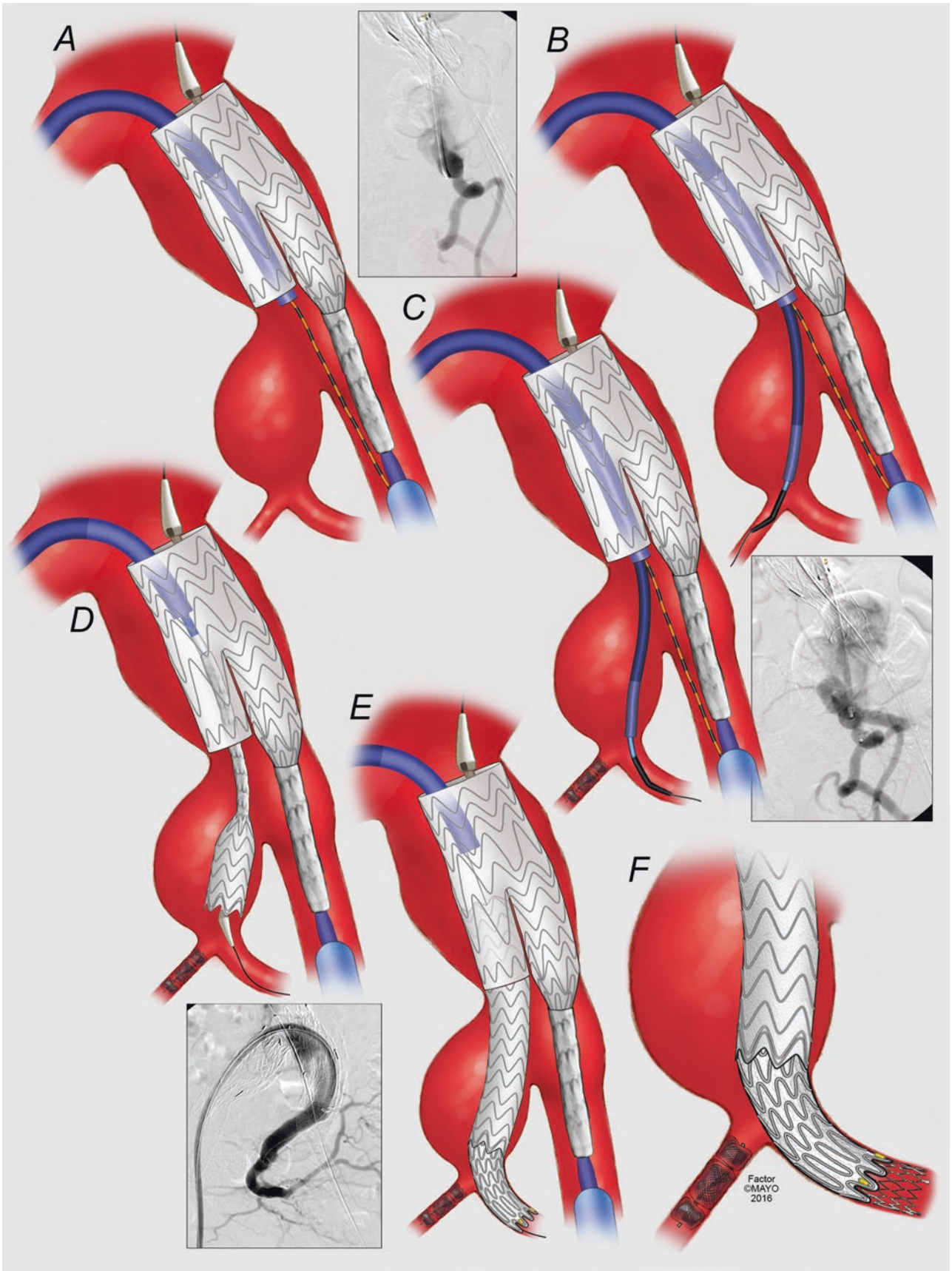


Fig. 40.13 Patient with large internal iliac artery aneurysms needs a modification of the technique. After deployment of the iliac branch device (**a**), the 12 Fr sheath is advanced and the anterior division branches are catheterized (**b**) and excluded using Amplatzer plugs or coils (**c**). The posterior division branch is then catheterized. The safest maneuver is to place first the proximal stent into the aneurysm sac (**d**), and then extend the repair into the posterior branch by placement of additional self-expandable stent-graft (**e**). Note the distal edge of the internal iliac branch may need reinforcement with a self-expandable bare metal stent (**f**). By permission of Mayo Foundation for Medical Education and Research. All rights reserved

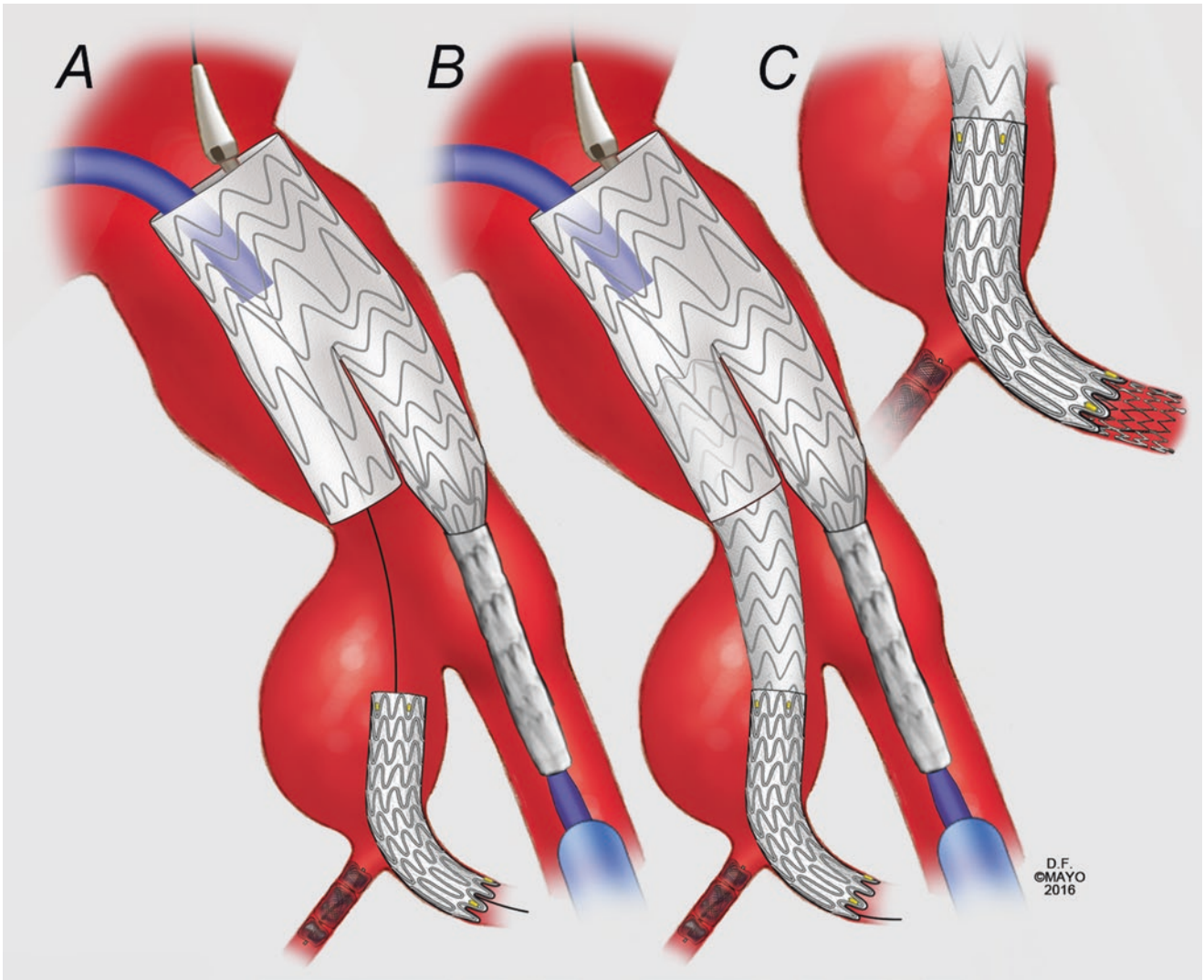


Fig. 40.14 The technique can also be done by placing first the distal stent (**a**), and then completing the repair with placement of the proximal bridging stent (**b**). Note again the distal edge of the internal iliac branch may need reinforcement with a self-expandable bare metal stent (**c**). By permission of Mayo Foundation for Medical Education and Research. All rights reserved

placement of a stiff guide-wire system as depicted in Fig. 40.18. Prior to introduction of the iliac branch device and its deployment, it is prudent to document patency of the internal iliac artery. If occlusion is documented, the delivery system should be removed and repeat angiography would reveal a widely patent origin of the internal iliac artery. Some of the techniques to solve the problem include placement of a short balloon-expandable iCAST stent at the origin of the vessel with careful attention to avoid stent into the common iliac artery, or a double contra-lateral puncture to introduce a separate sheath, with stenting only if absolutely needed because of inability to catheterize the vessel via the 12 Fr contra-lateral sheath.

Difficult Catheterization of the Internal Iliac Artery

Catheterization of the internal iliac artery may be difficult or impossible because of misalignment of the branch, presence of a shelf precluding enough space for the delivery system and causing occlusion of the origin of the internal iliac artery, or ostial occlusive disease (Fig. 40.19). With deployment of the iliac branch that is not well aligned, the device can be gently rotated so that catheterization is easier. The presence of occlusive ostial disease can be dealt by pre-emptive angioplasty (Fig. 40.20). However, the most difficult scenario is when there is not enough space for the delivery system.

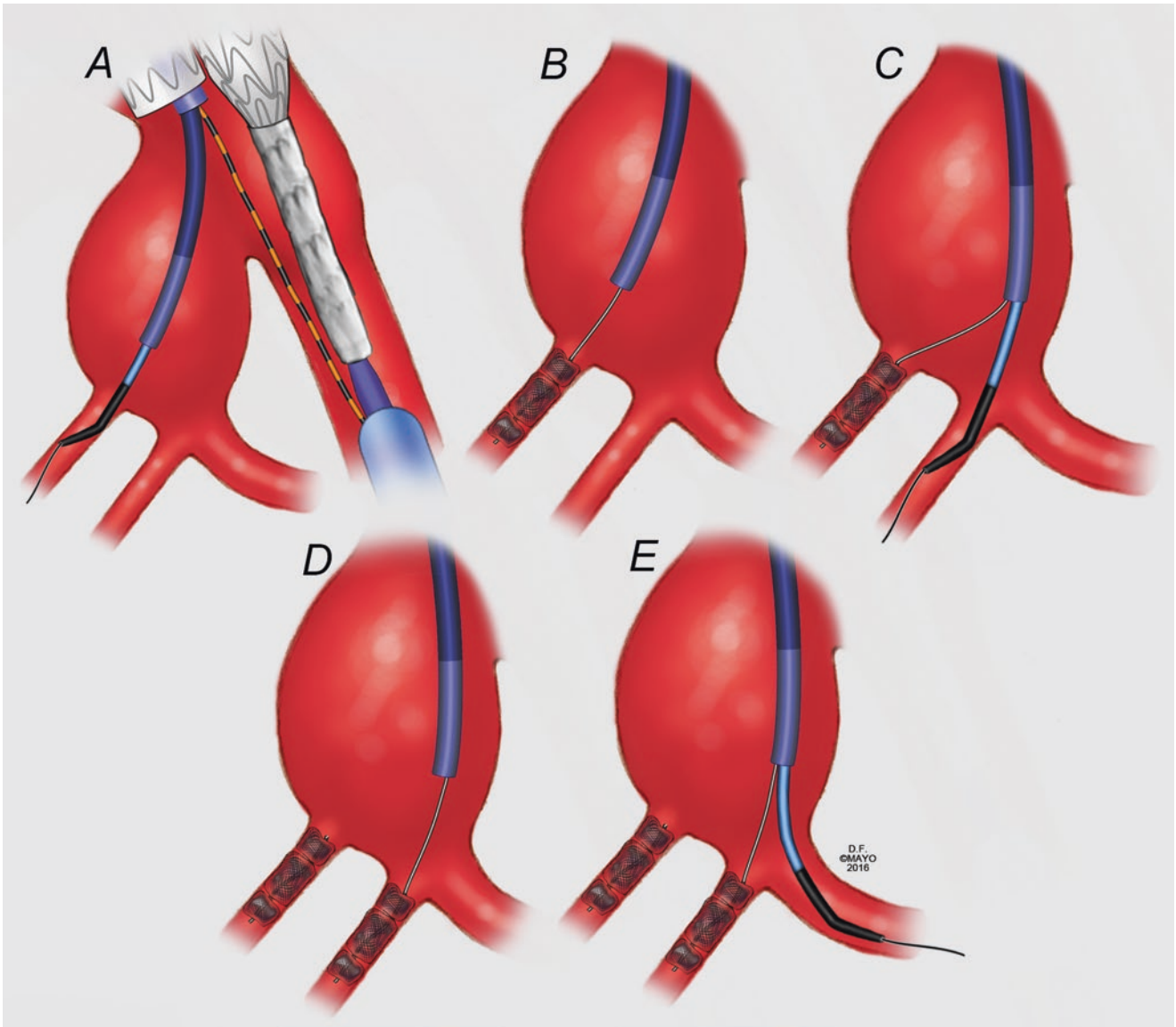


Fig. 40.15 When multiple branches need to be excluded, this is done by selective catheterization of each branch (**a**) and placement of Amplatzer plugs or coils (**b**). It is most useful to keep the plug connected to secure the sheath either with the connecting plug wire or a separate buddy wire, while a catheter is used to catheterize the next adjacent branch (**c**). This maneuver is repeated (**d**) and the posterior branch is used as a target for the iliac branch device (**e**). By permission of Mayo Foundation for Medical Education and Research. All rights reserved

Currently recommendation is a minimum diameter of 16 mm in the iliac bifurcation, but this can be decreased to 12–14 mm in experience hands with high technical success (Fig. 40.21).

Kinks

One of the most frequent failure mechanisms are kinks which can occur in almost any of the joints involving the iliac branch, the bridging stent or the iliac limb extension (Fig. 40.22). Of these, by far the most common failure mechanism is a kink either beyond the external iliac limb stent or within the distal stent in cases of iliac branch using the Cook platform. This needs to be immediately recognized intra-operatively and treated by placement of additional stent as depicted in Fig. 40.23.

Branch Occlusion

Branch occlusion is rare intra-operatively and uncommon in the first 30 days. However, early occlusion of an iliac branch is usually technical or patient selection-related and typically has a culprit lesion or cause. Some of the most common causes are depicted in Fig. 40.24, and include kinks in the bridging

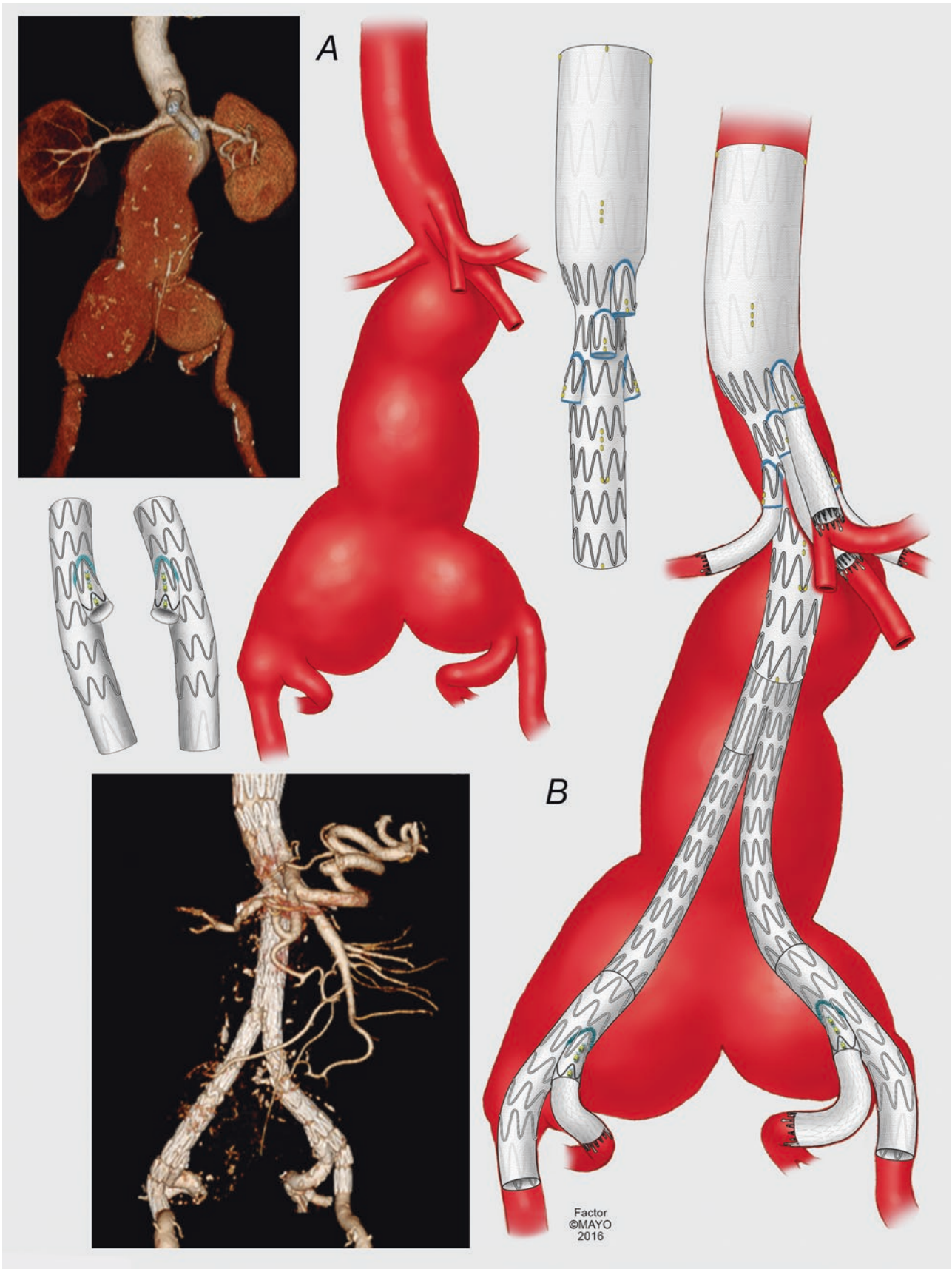


Fig. 40.16 Patient with extensive type IV thoracoabdominal aortic aneurysm (**a**) treated by t-Branch multibranch stent-graft and bilateral iliac branch devices (**b**). By permission of Mayo Foundation for Medical Education and Research. All rights reserved

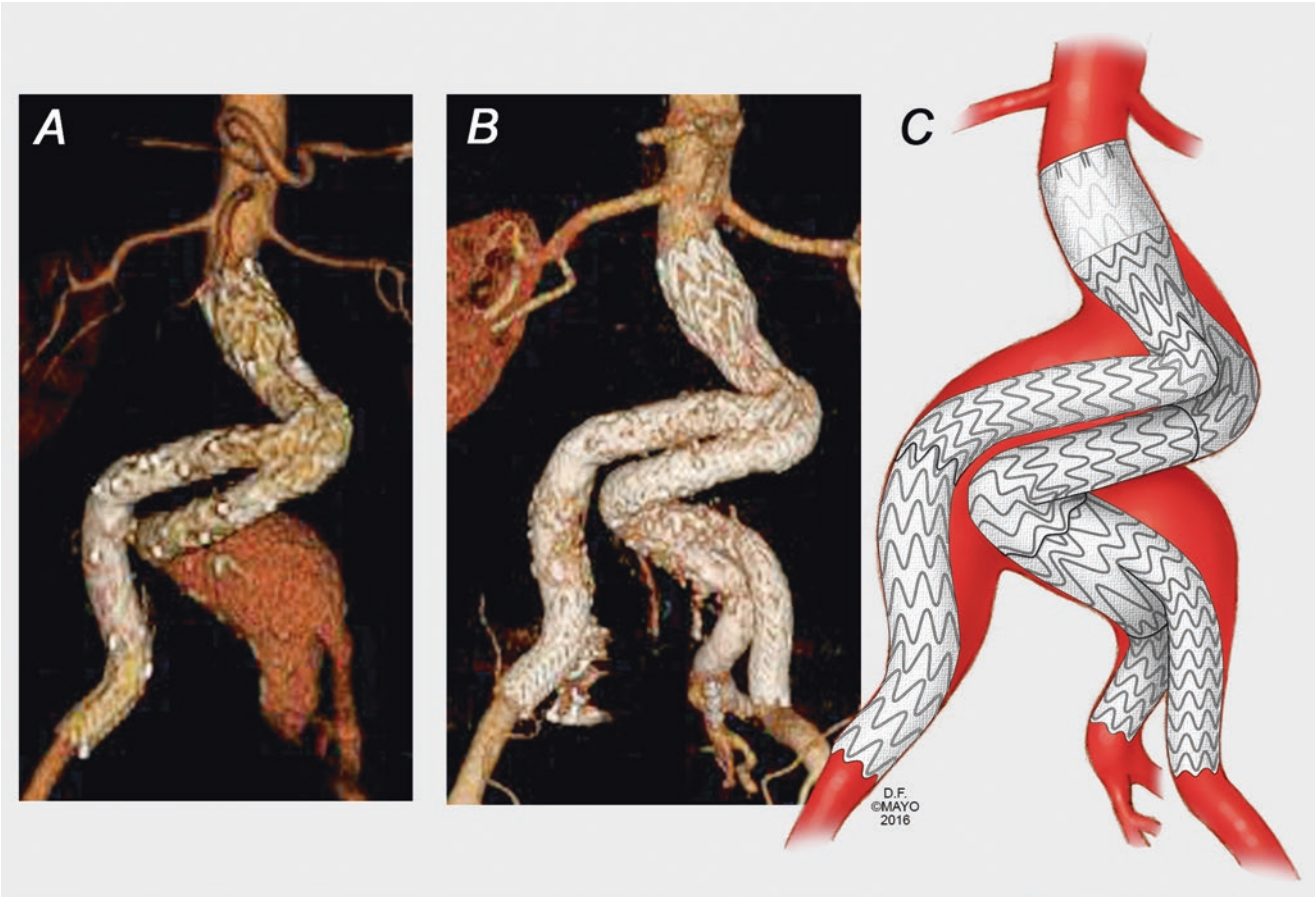
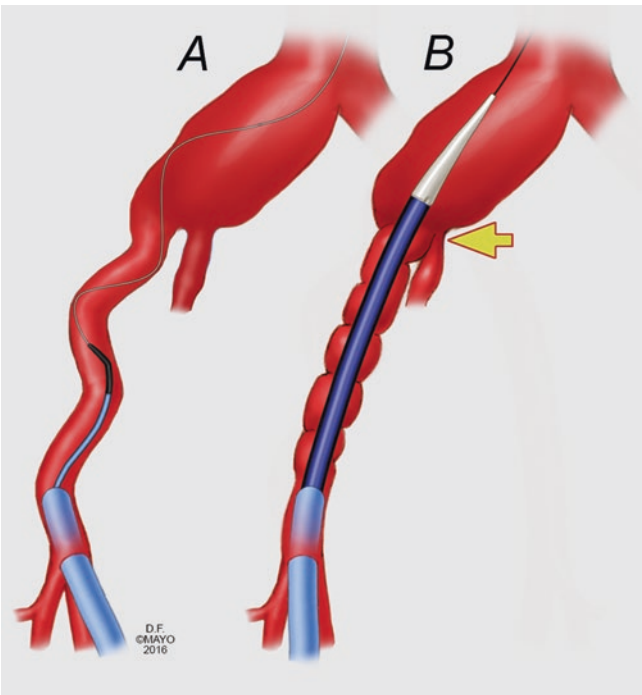


Fig. 40.17 Patient who survived emergency EVAR for rupture aortic aneurysm developed a large left common iliac artery aneurysm (**a**), which was treated using a WL Gore Excluder Iliac Branch Endoprosthesis (**b** and **c**). By permission of Mayo Foundation for Medical Education and Research. All rights reserved



stent, placement of long stents into divisional branches, history of prior branch occlusions, disease outflow branches of the internal iliac artery, and vessel dissection with flow compromise. In patients with these complications or predisposing factors, all measures to improve flow should be done and long-term double anti-platelet therapy with or without anti-coagulation is recommended.

Perforations and Dissections

Branch stenting requires advancement of stiff guide-wires and delivery sheaths. Preferentially the guide-wire should be positioned in the larger segment of the posterior division

Fig. 40.18 Pseudo-occlusion of the internal iliac artery occurs in patients with very tortuous, non-calcified external iliac arteries (**a**), who develop occlusion from kinks after placement of stiff guide-wire system (**b**). By permission of Mayo Foundation for Medical Education and Research. All rights reserved

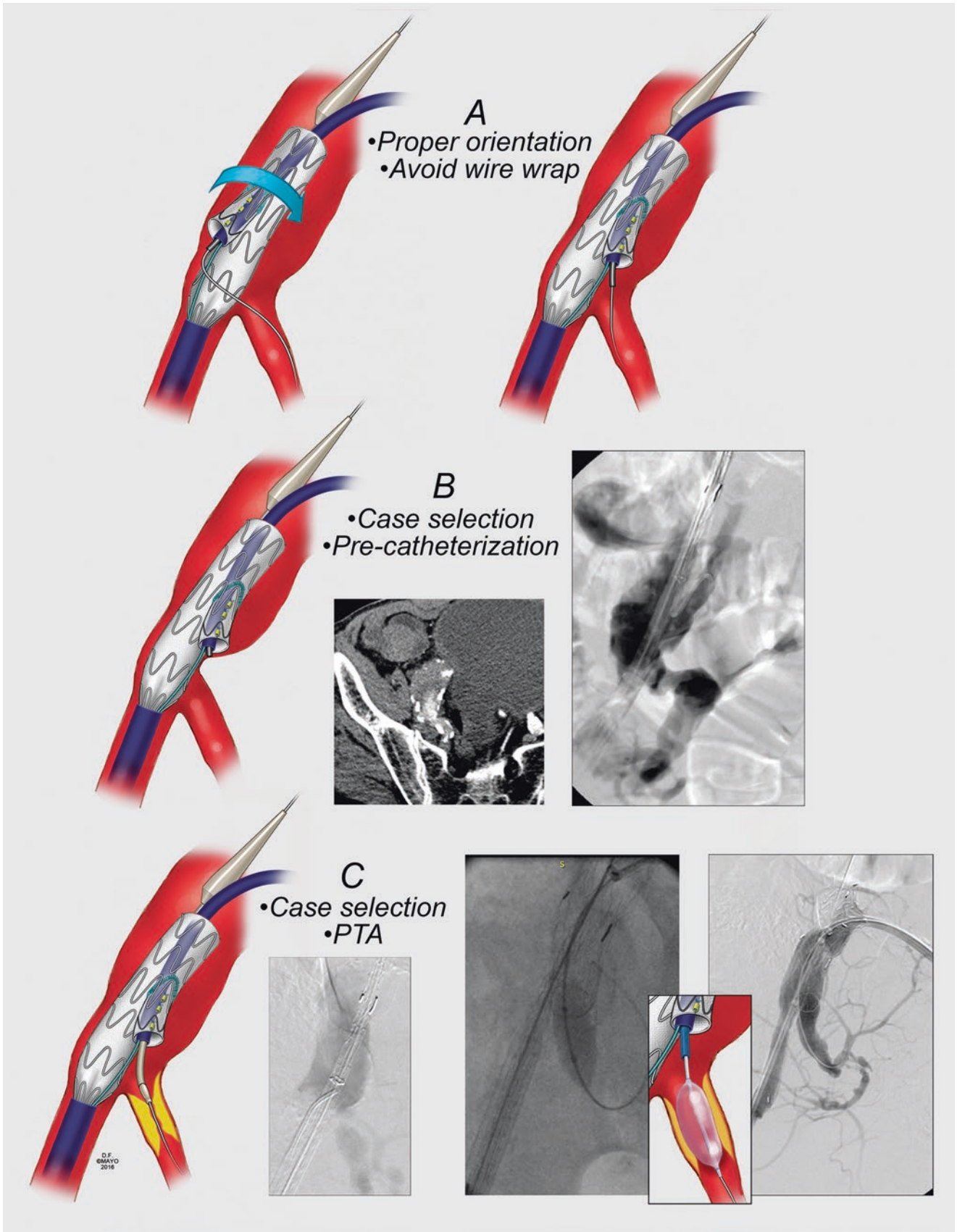


Fig. 40.19 Common bail out maneuvers for difficult catheterization from improper orientation (**a**), lack of enough space in the common iliac artery (**b**) or ostial stenosis (**c**). By permission of Mayo Foundation for Medical Education and Research. All rights reserved

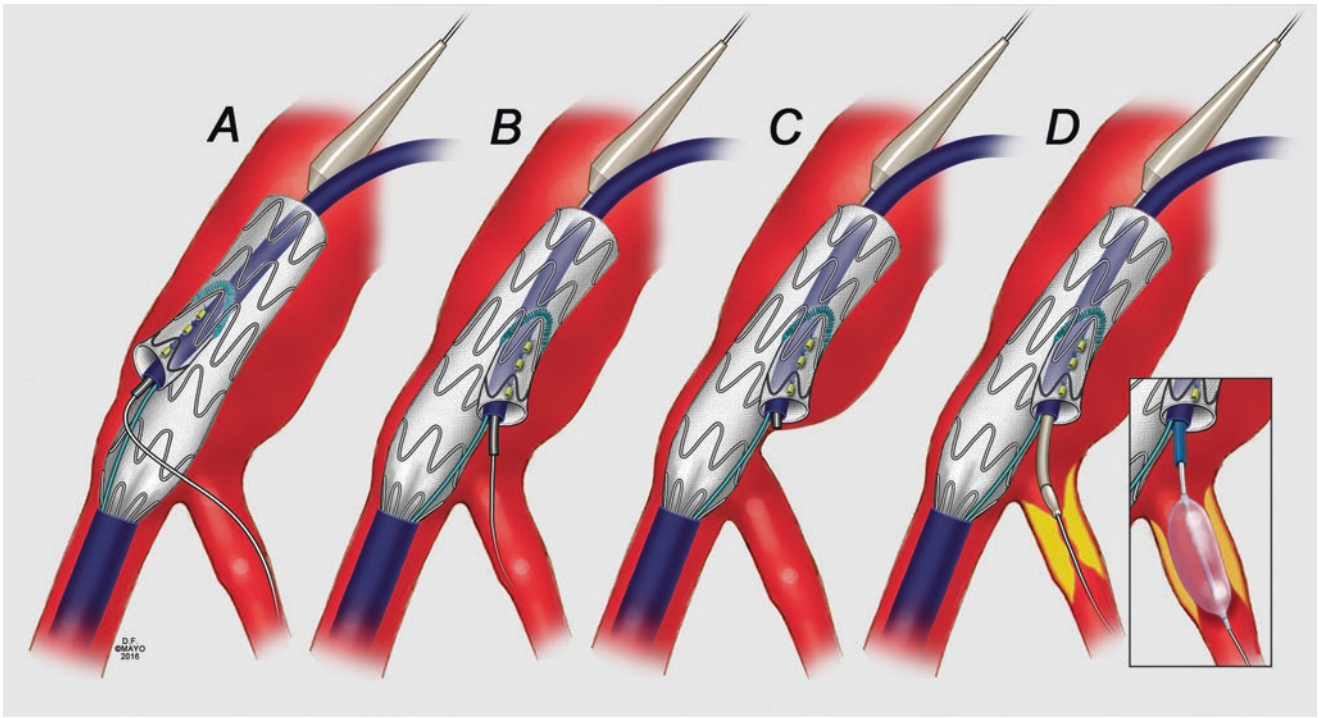


Fig. 40.20 A device is deployed with improper orientation (**a**), which may be solved by modest rotation of the device (**b**). The most difficult problem is lack of space in the common iliac artery (**c**), which should contra-indicate the procedure. Ostial stenosis (**d**) can be treated by balloon angioplasty. By permission of Mayo Foundation for Medical Education and Research. All rights reserved

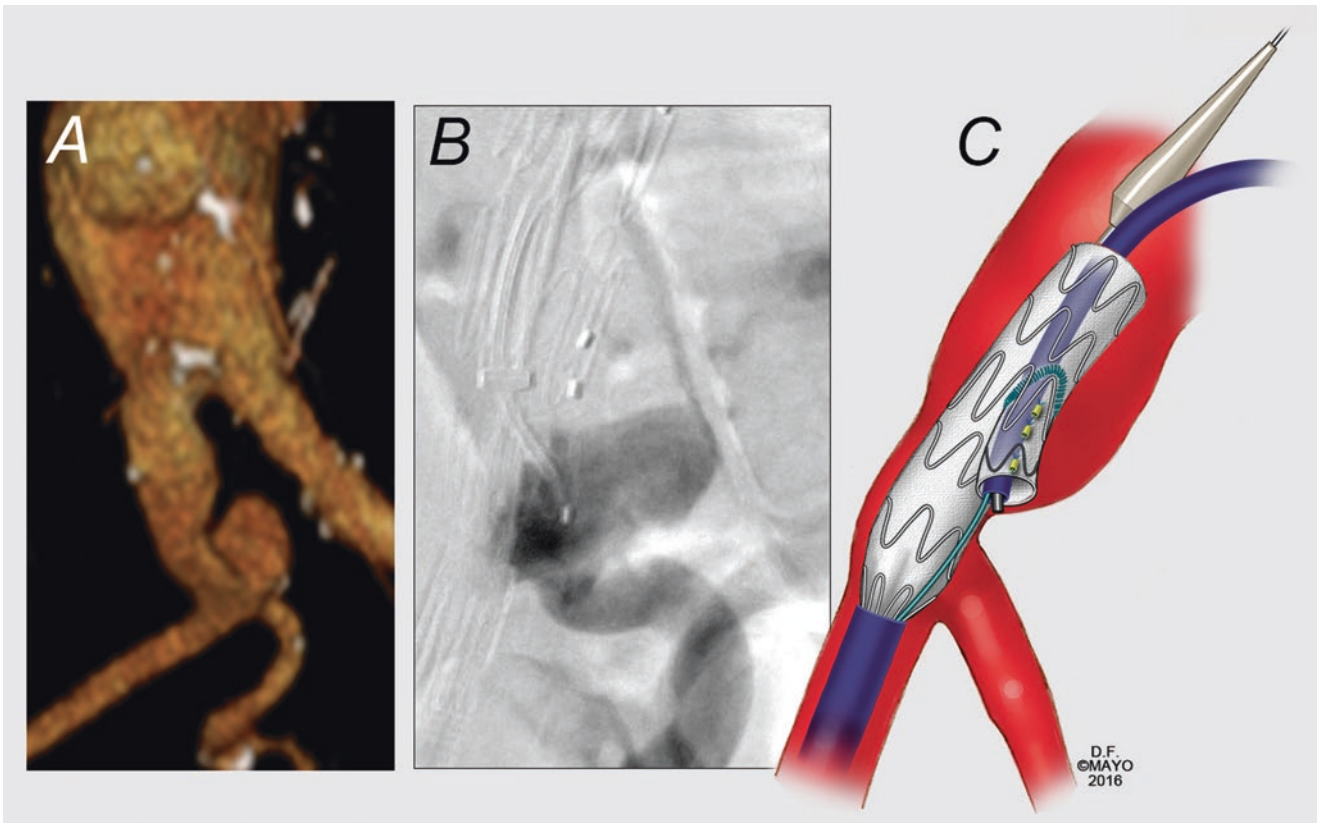


Fig. 40.21 Patient with limited space in the common iliac artery (**a**) is treated by precise deployment (**b**). For internal iliac arteries that have origin from a normal segment measuring <12 mm, catheterization may be impossible (**c**). By permission of Mayo Foundation for Medical Education and Research. All rights reserved

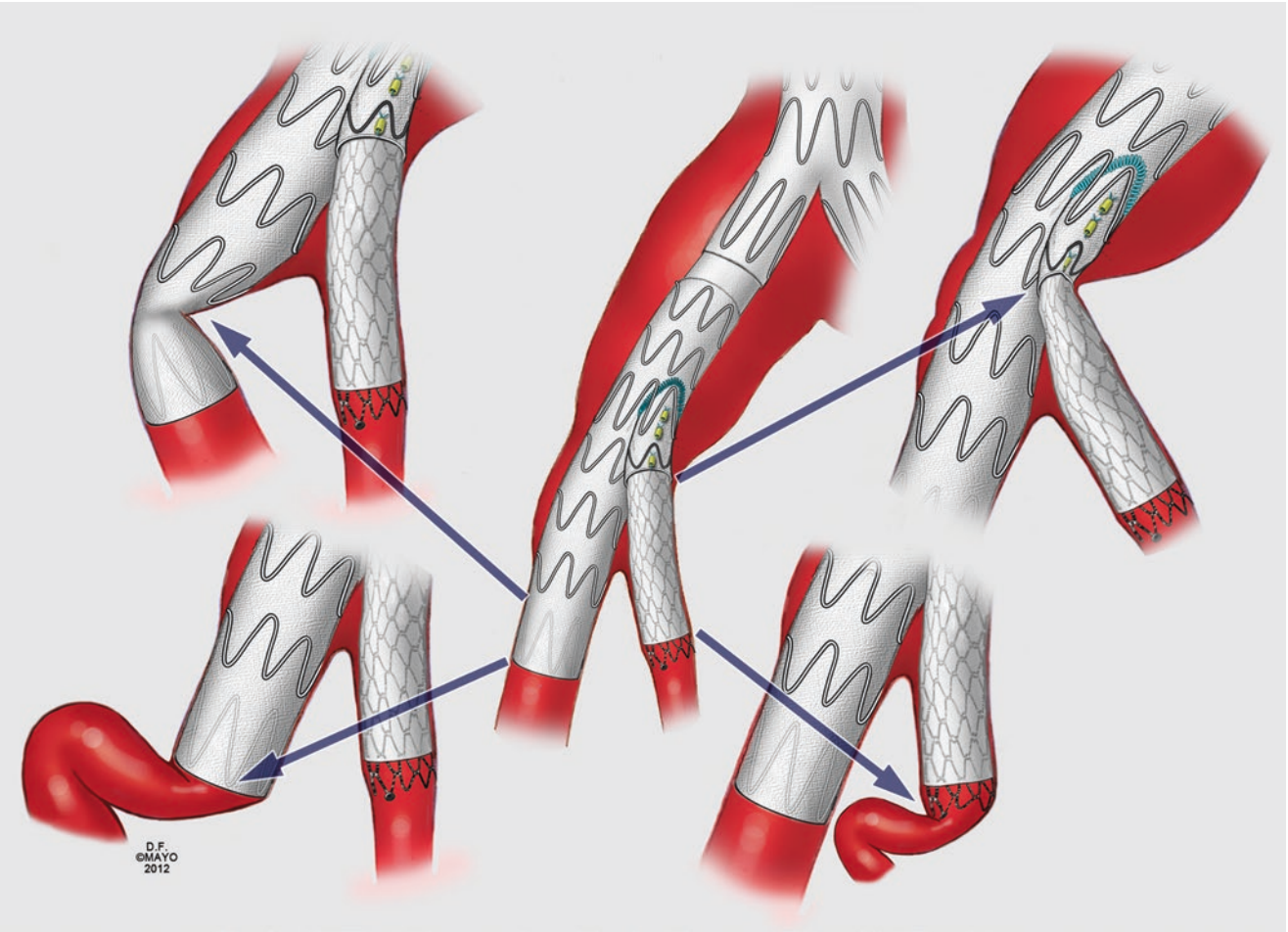


Fig. 40.22 Iliac branch device kinks are a source of occlusion and should be recognized. By permission of Mayo Foundation for Medical Education and Research. All rights reserved

branch, avoiding positioning the tip within a small branch, which is more prone to perforation (Fig. 40.25). In addition, any manipulation should be done with a floppy glide-wire with careful attention to avoid inducing a dissection of the branch.

Integrity Issues

Integrity issues are usually infrequent and occur long-term. Extensive worldwide experience with the Atrium iCAST, Fluency, and Viabahn indicates excellent interaction with the available iliac branch designs with low rate of disconnection, tear, fractures, or migration (Fig. 40.26). Nonetheless, follow-up surveillance is recommended to detect and treat these complications if they occur.

Results

Although over 1000 IBDs have been implanted worldwide, yet such numbers are not represented in the published literature. The first reported series by Greenberg and associates in 2006 included 21 patients with three technical failures (14 %), all related to the inability to visualize the origin of the internal iliac artery due to significant stenosis [4]. Ziegler and associates analyzed 46 patients treated with S-IBDs, the first 26 patients were treated using an early generation unibody configuration, and the last 20 utilized the S-IBD system [5]. Technical success improved from 58 % with the early generation device to 85 % with the current S-IBD. There were no perioperative deaths, and of the 35 IBDs successfully implanted, none developed endoleak, component separations

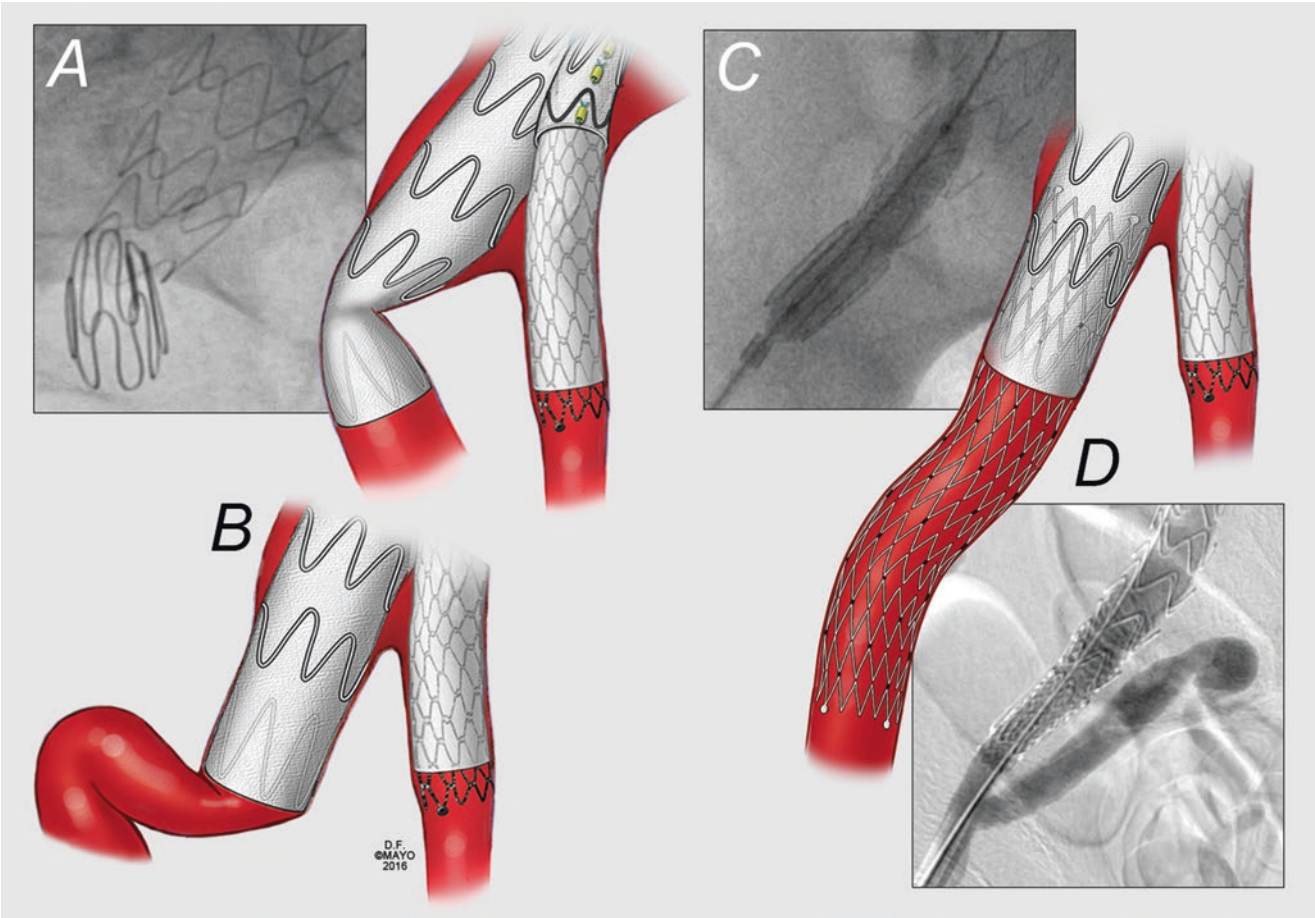


Fig. 40.23 The most common location for kink is in the distal stent of the Cook external iliac limb (**a**). If this is noted or anticipated by review of imaging (**b**), a self-expandable stent (in the native artery) with or without a balloon-expandable stent (in the iliac limb) may be needed to prevent occlusion (**c**). Note the patent external iliac limb proximal to an internal iliac bypass (**d**). By permission of Mayo Foundation for Medical Education and Research. All rights reserved

or migration. There were four branch occlusions after a mean follow-up of 26 months. Haulon reported on 52 patients treated in Lille France or at the Cleveland Clinic [6]. Technical success occurred 94 % of the time, and during the mean follow-up of 14 months there were no conversions, ruptures, or aneurysm-related deaths. Verzini and associates from Perugia, Italy reported the only comparative analysis of IBDs versus hypogastric exclusion in 74 patients [7]. In this study, there were no differences in procedure time, contrast use, and technical success, and no early deaths. However, there was a trend towards more endoleaks (19 % vs. 4 %) and pelvic ischemic symptoms (22 % vs. 4 %) among patients treated with coil embolization when compared with patients treated with iliac branch devices. Karthikesalingam and associates published a conglomerate analysis of nine studies involving 196 patients treated with IBDs [8]. Technical success ranged from 85 to 100 %. There were no aneurysm-related deaths. Only one patient with patent IBD complained of buttock claudication. However, late thrombosis of the IBD occurred in 24 patients (12 %) and resulted in buttock claudication in 12 (50 %). Endoleak rates were exceedingly low, with only one type I (0.5 %) and two type III endoleaks (1 %). Type II endoleaks were treated conservatively and were not associated with sac expansion. Re-interventions were required in 12 patients (6 %), including five with occlusion stent graft limbs to the external iliac artery. The anatomical suitability for IBD was not detailed in most studies, but in one study (Tielliu et al.) the applicability of the repair was criticized for being acceptable in only 52 % of their potential IBD candidates [9]. An update from Cao's group reported 100 patients treated with 95 % technical success and 81 % patency at 5 years. Growth was noted in only 4 % of the patients and there were three device related endoleaks (one type III and two distal type I) that required treatment [10]. The latest report from the Cleveland Clinic included 138 devices in 130 patients [11]. Technical success was 95 % and patency at 5 years was 82 %. There were no patients with aneurysmal growth following IBD placement in this series.

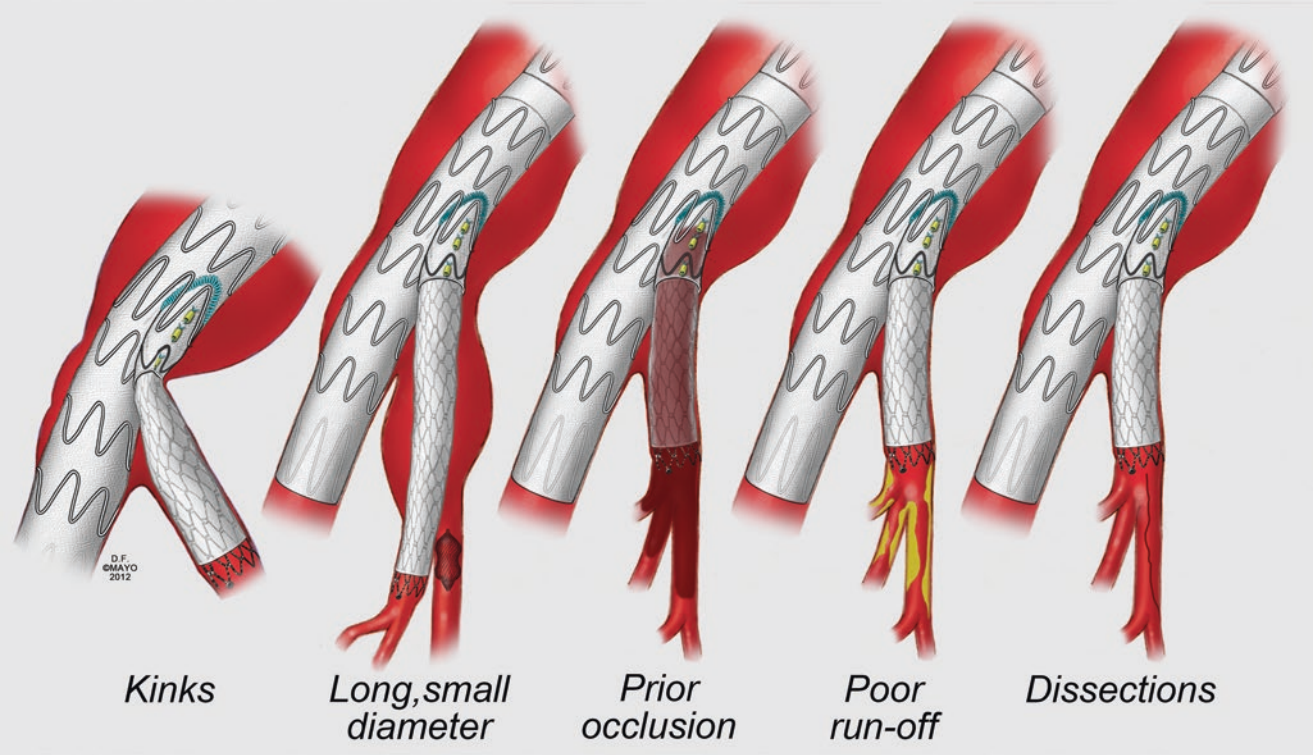


Fig. 40.24 Common mechanism of occlusion of iliac branch bridging stents. By permission of Mayo Foundation for Medical Education and Research. All rights reserved

In this paper anatomical challenges were stratified such that separate analyses were conducted for small CIA, the presence of an IIA aneurysm mandating seal within one of the IIA trunks, and tight ostial stenosis of the IIA. None of these factors had any affect on patency or endoleaks, and only the latter category was associated with a lower technical success rate than experienced in patients without concomitant IIA occlusive disease.

Lessons Learned

The most common cause of technical failures resulted from an inability to visualize the target IIA following introduction of the IBD delivery system. This occurs in the setting of small external iliac arteries and diseased internal iliac artery origins, and results from compression of the IIA origin by the IBD delivery system. The initial technical failures were potentially avoidable be using a modified delivery technique. Following IBD sheath introduction, if the IIA origin is not visualized, the pre-loaded wire is snared, and the constrained IBD device (still entirely within the delivery sheath) is withdrawn into the external iliac artery. The contralateral sheath is advanced "up and over" and the target IIA is cannulated while the IBD delivery system remains distal to the IIA origin. A balloon (4–6 mm) is placed into the IIA and inflated. The IBD is advanced while the IIA balloon remains inflated, akin to a kissing balloon technique. When this technique is used, the IIA can be visualized and accessed more readily following IBD deployment. Additional causes of technical failure resulted from the iatrogenic dissections that occurred during implantation. The distal IIA bed is always tortuous and often fragile. We now obtain access into a distal gluteal branch with a gentle steerable catheter and wire system, and then place a stiff wire through the catheter. The self-expanding stentgraft generally passes easily and the likelihood of iatrogenic injury is minimized when the wire is placed into the distal circulation rather than into the common trunk or proximal divisions. Caution must be taken when advancing large sheaths through an implanted IBD. Dislodgement of the IBD can occur and is preventable by stabilization of the IIA branch with a balloon from the contralateral side, or using an alternative access to introduce sheaths that are larger than 20F.

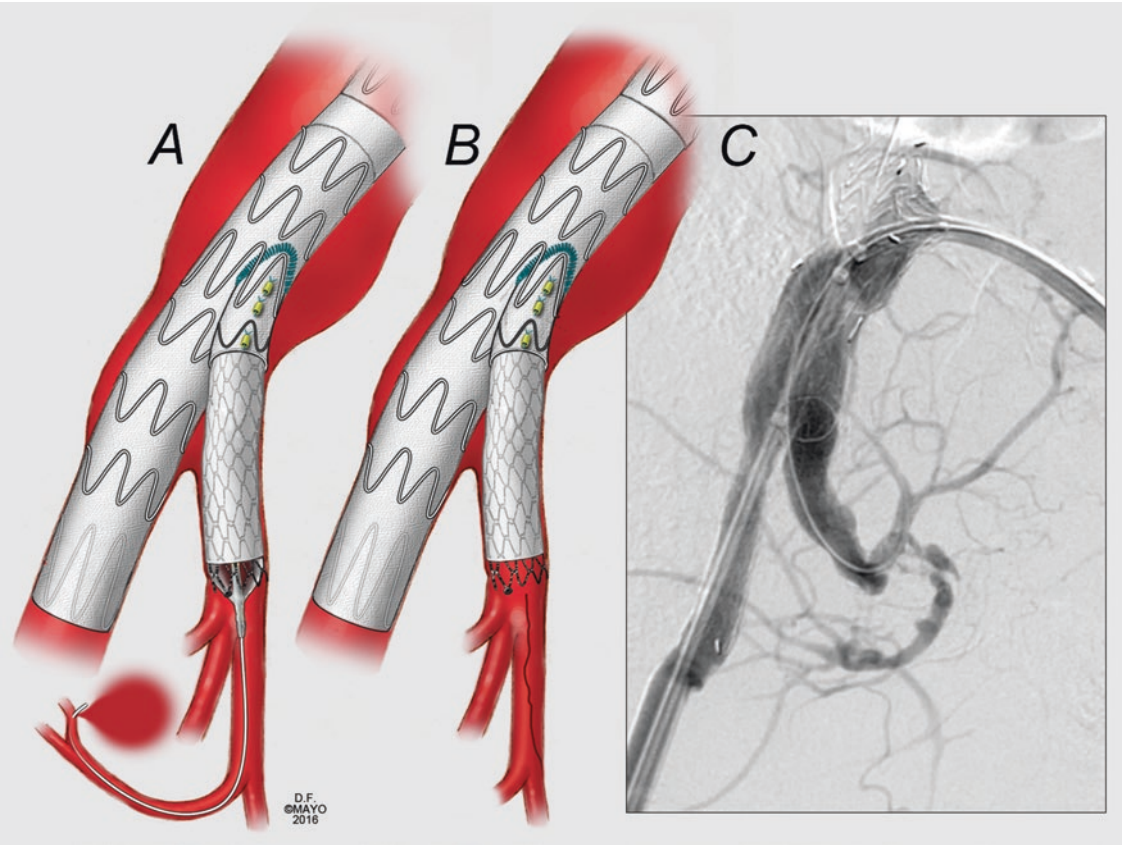


Fig. 40.25 Intra-procedural complications include vessel perforation (**a**) and dissections (**b** and **c**). By permission of Mayo Foundation for Medical Education and Research. All rights reserved

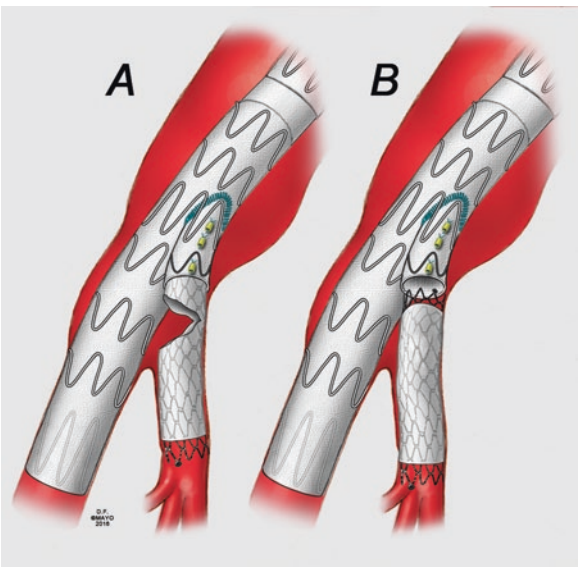


Fig. 40.26 Integrity issues are uncommon and include fractures (**a**) and disconnections (**b**). By permission of Mayo Foundation for Medical Education and Research. All rights reserved

There is also a learning curve associated with procedure planning. Prior to the development of the B-IBD device, many patients were excluded as a result of CIA length. The advent of a device that simplifies the use of IBDs in patients with CIA of 6 cm or less, the need for H-IBD or S-IBD devices has declined, and these devices have been modified to mitigate some of the theoretical complications that may occur as a result of limited overlap between the limb bridging the IBD repair with the AAA repair. An additional stent has been placed proximal to the branch, providing a longer segment of overlap, resulting in the need for a longer CIA. Thus, currently patients with CIA>6 cm are treated with and H-IBD or S-IBD and all others with the B-IBD.

Future Considerations

Iliac branch technology represents one of the methods by which complex anatomy can be treated with an endovascular approach in a manner analogous to open repair. The princi-

ples of antegrade pelvic blood flow are maintained and patients are encouraged to exercise following their repair. The techniques required for implantation of IBDs are similar to techniques required to do other complex procedures, such as thoracoabdominal branches and supra-aortic trunk branch repairs. The iliac bed is an appealing region to perfect such techniques, as a technical failure in the setting of an iliac aneurysm most frequently results in an occluded IIA, which is how most aneurysms are managed today. The use of such devices does require longer procedure times and potentially more contrast and radiation, and thus must be employed judiciously in the context of a risk and benefit to such patients. In our practice this translates into the reservation of IBD for patients that ambulate enough to be effected by claudication, and all patients considered to be at risk for spinal cord ischemia as a result of more proximal aortic disease.

Conclusion

The option for unilateral or bilateral internal iliac artery preservation with IBDs further advances the potential advantages of endovascular repairs. The procedure can be performed with high technical success rates, acceptable long-term patency results, without any considerable increase to the risks of the standard endovascular aneurysm repair. The use of these devices in difficult anatomies must be carefully considered. Short IIA appears to be well managed by the development of the B-IBD, yet extreme calcification and ostial disease of the IIA remain a challenge. However, widespread utilization of IBD still faces several challenges including regulatory approval, physician training, and an evaluation of the late results of IBDs including device integrity, re-interventions, and occlusion rates.

References

1. Schanzer A, Greenberg RK, Hevelone N, Robinson WP, Eslami MH, Goldberg RJ, Messina L. Predictors of abdominal aortic aneurysm sac enlargement after endovascular repair. Circulation. 2011;123:2848–55.
2. Oderich GS, Greenberg RK. Endovascular iliac branch devices for iliac aneurysms. Perspect Vasc Surg Endovasc Ther. 2011;23:166–72.
3. Greenberg RK, Lu Q, Roselli EE, Svensson LG, Moon MC, Hernandez AV, Dowdall J, et al. Contemporary analysis of descending thoracic and thoracoabdominal aneurysm repair: a comparison of endovascular and open techniques. Circulation. 2008;118:808–17.
4. Greenberg RK, West K, Pfaff K, Foster J, Skender D, Haulon S, Sereika J, et al. Beyond the aortic bifurcation: branched endovascular grafts for thoracoabdominal and aortoiliac aneurysms. J Vasc Surg. 2006;43:879–86. discussion 886–7.
5. Ziegler P, Avgerinos ED, Umscheid T, Perdikides T, Erz K, Stelter WJ. Branched iliac bifurcation: 6 years experience with endovascular preservation of internal iliac artery flow. J Vasc Surg. 2007;46:204–10.
6. Haulon S, Greenberg RK, Pfaff K, Francis C, Koussa M, West K. Branched grafting for aortoiliac aneurysms. Eur J Vasc Endovasc Surg. 2007;33:567–74.
7. Verzini F, Parlani G, Romano L, De Rango P, Panuccio G, Cao P. Endovascular treatment of iliac aneurysm: concurrent comparison of side branch endograft versus hypogastric exclusion. J Vasc Surg. 2009;49:1154–61.
8. Karthikesalingam A, Hinchliffe RJ, Holt PJ, Boyle JR, Loftus IM, Thompson MM. Endovascular aneurysm repair with preservation of the internal iliac artery using the iliac branch graft device. Eur J Vasc Endovasc Surg. 2010;39:285–94.
9. Tielliu IF, Bos WT, Zeebregts CJ, Prins TR, Van Den Dungen JJ, Verhoeven EL. The role of branched endografts in preserving internal iliac arteries. J Cardiovasc Surg. 2009;50:213–8.
10. Parlani G, Verzini F, De Rango P, Brambilla D, Coscarella C, Ferrer C, Cao P. Long-term results of iliac aneurysm repair with iliac branched endograft: a 5-year experience on 100 consecutive cases. Eur J Vasc Endovasc Surg. 2012;43:287–92.
11. Wong S, Greenberg R, Eagleton M, Mastracci T, Melgard C, Sylver Y. Endovascular repair of aortoiliac aneurymal disease with the helical iliac branch device and the bifurcated-bifurcated branch device. J Vasc Surg. 2013;58(4):861–9.

Results of Iliac Branch Stent-Grafts

41

Fabio Verzini, Gianbattista Parlani, Paola De Rango*,
Luca Farchioni, Gioele Simonte, and Piergiorgio Cao

Introduction

Iliac branch grafts (IBGs) have emerged in the last decade as a method to preserve internal iliac artery (IIA) flow during endovascular aneurysm repair (EVAR) in patients with inadequate sealing zones in the common iliac artery. These devices provide a novel iliac extension limb with a side branch for cannulation and stent implantation into the IIA. The IBG is indicated in patients with aneurysms of common iliac artery (CIA), allowing extension of the repair into the external iliac artery (EIA) for effective distal fixation while flow is maintained in the IIA.

Preservation of pelvic perfusion during EVAR is advocated whenever possible to minimize the risk of ischemic pelvic complications, which occur in up to 45% of patients who undergo unilateral IIA occlusion with higher rates in those who have bilateral IIA occlusion [1–11]. The clinical sequelae of interruption of IIA flow may vary and range from relatively benign hip and buttock claudication (in most of the cases) to severe and life-threatening colonic infarction, paraplegia, vasculogenic impotence, or sacral necrosis. These symptoms are frequently irreversible as the thrombosis of IIA commonly involves its distal branches and is not easily accessible to allow successful direct revascularization [3]. Although IIA occlusions can be often asymptomatic, it is not possible to predict those who will develop ischemic symptoms or those who develop colon or spinal cord ischemia [10].

IBGs have been used for more than a decade with commercially available devices. Nevertheless, studies detailing the use of IBGs and their late complications remain limited due to the lack of widespread device availability. Furthermore, most published data are largely confined to single non-US centers [11–13]. Two prospective multicenter pivotal trials are investigating the Cook IBD (Iliac Branch Device) (Cook Medical, Inc., Bloomington, IN) and the Gore Excluder IBE (Iliac Branch Endoprosthesis) (W.L. Gore &Associates, Flagstaff, AZ) in the USA. The increasing clinical experience and available data supports a better understanding of the feasibility, anatomical requirements, and outcomes of IBGs, including its use outside instructions for use and for bilateral iliac aneurysms. This chapter summarizes the current evidence regarding the use of IBGs

Anatomical Feasibility

One of the main reasons precluding widespread application and in-depth understanding of IBGs is related to the technical complexity of the procedure, which requires more rigorous anatomical constraints than simple aortic stent-grafts. It is well recognized that implantation of IBGs necessitates additional training. Operators can effectively and safely perform the technique, but a higher level of expertise is needed compared to infra-renal EVAR. IBG technology has evolved over the last decade with the evolution from a single body [14] to a modular configuration [13, 15–18]. New designs have allowed for additional flexibility and accommodated for a broader range of iliac anatomies. Yet, several anatomical restrictions continue to limit the wide applicability of these devices. Recent evidence is consistent with existing findings suggesting low anatomical applicability rate of IBG in patients undergoing EVAR for aortoiliac or solitary iliac aneurysms. The majority of patients who should be treated are not fully compliant with selection criteria for IBG according to the device manufacturers or expert vascular surgeons [19]. Since the initiation of two US pivotal trials on iliac branch devices, Pearce et al. analyzed the anatomical feasibility in 99 patients with CIAs. The authors measured centerline diameters and lengths of aortoiliac morphology using

* Deceased

F. Verzini (✉) • G. Parlani • L. Farchioni • G. Simonte
Unit of Vascular Surgery, Santa Maria della Misericordia Hospital, University of Perugia, Perugia, Italy
e-mail: fabio.verzini@unipg.it

P. Cao
Gruppo Villa Maria GVM, Rome, Italy

© Mayo Foundation for Medical Education and Research 2017

G.S. Oderich (ed.), *Endovascular Aortic Repair*, DOI 10.1007/978-3-319-15192-2_41

three-dimensional (3D) workstation and compared with the inclusion/exclusion criteria for both the Cook and Gore pivotal IBG trials [18]. They found that only 35 % of the patients with CIAs would have been candidates for one of the two IBG designs using the proposed trial criteria. The main reason for exclusion for both devices was an inadequate IIA landing zone [18]. Similarly, Gray et al. in 2015 analyzed the applicability of the Cook IBD in 66 patients with 88 CIAs [20]. In that study, the authors analyzed the manufacturers Instructions For Use (IFU), the criteria published by experts, and a more liberal institutional criteria [20]. Nearly 60 % of CIAs could have been treated with an iliac side branch device based on the current experience. Suitability was 41 % according to IFUs, 40 % using published criteria, and 58 % with the institutional criteria. The most common morphological exclusion criterion was an aneurysmal IIA [20].

Results of anatomical feasibility using contemporary data are similar to what has been previously reported by others: 46 % by Tielliu et al. in 2009 and 38 % by Karthikesalingam et al. in 2010 [21, 22]. These findings highlight the need to modify future generation of iliac branch technology to specifically address the need to improve seal in the distal IIA. Extension of the internal iliac branch component into the superior gluteal artery (SGA) has been recently applied with 100 % patency rate at a mean of 18 months. However, there is limited data [23] to assess the expanded feasibility and long-term durability of IBGs in patients with IIA aneurysms.

Results of Commercially Available IBGs

In 2010 Karthikesalingam et al. [22] reported a systematic review of seven published series including 196 patients treated by commercially available IBDs [21, 24–29]. Since this initial report, at least 12 series have been published, with 462 patients [10–13, 17, 23, 30–35]. After excluding duplicated reports from one of the largest series, a total of 410 patients were analyzed. Follow-up ranged in these studies from 20 months up to 32 months [11, 13, 17, 33]. Clinical outcomes are summarized in Tables 41.1 and 41.2.

Although most of these new series employed the last generation modular IBG platform from Cook, some included several types of devices. As discussed in prior chapters, three types of Cook IBDs have been used clinically: straight-branch (Z-BIS, Zenith Bifurcated Iliac Stentgraft, or Australian version), helical branch (H-IBD, or Greenberg version), and bifurcated–bifurcated branch (BIF-IBD) [3, 13, 28]. The last was developed to handle short CIAs by incorporating a helical IBD into the ipsilateral leg of an aortic bifurcated graft [13]. Technical differences between Z-IBD and H-IBD include the length of overlap with the mating IIA stent-graft (longer with H-IBD) and the mechanism of directing flow into the branch. Only one small series published on the most recently available Gore IBE device [31].

Indications

A wide range of morphological and clinical indications has been applied in these studies, including unilateral, bilateral, or isolated CIAs. In most patients, CIAs were associated with EVAR for infra-renal AAAs. IBGs have also been used in conjunction with fenestrated and branched endografts to treat thoracoabdominal aneurysms [13, 34]. In one series [23] extension to the superior gluteal artery (SGA) was employed to expand the anatomical application of IBGs to patients with IIA aneurysms.

Technical Success

The rate of technical success with IBGs is high, averaging 86–100 % (see Table 41.2). This demonstrates the feasibility of IBGs when applied in selected patients by experienced operators. The main reason for technical failures is complex anatomy, which suggests the need for careful preoperative assessment. Patient selection is of paramount importance to preclude technical failure, independent of which generation IBG device is used. A narrow lumen of the CIA or thrombus, severe kinking (tortuosity) of the external iliac artery, narrow or stenotic internal iliac ostium, and wide angle (>50) of the IIA branches are found as common sources of technical failure [27]. It has been also reported that difficulty in advancing a sheath up and over the aortic bifurcation can lead to technical failure, particularly in patients undergoing IBGs after prior EVAR. In these cases, use of brachial or axillary approach may be needed for IIA cannulation. Although there is potential risk of stroke with trans-brachial access [22, 27], this has not been reported [27]. Cases of post-operative IBG occlusion were managed with a range of techniques. Most IBG occlusions were managed conservatively, and sometimes spontaneously recanalization was found [22, 27].

Early Outcomes

Studies have shown that IBGs are safe and can be performed with low perioperative mortality, similar to what has been reported for standard EVAR. Most studies have 30-day mortality rates of 0 or 1 %. Mortality occurred more likely with complex aortic repairs in association with thoracoabdominal aneurysms or in high-risk patients who were poor candidates for open surgery. Most of the perioperative major

Table 41.1 Studies on commercially available IBG: early results

Authors	Years	Study	*N* (IBG)	Settings	Device	Stent	Immediate success	Peri-operative death	Peri-operative morbidity	Mean follow-up (months)
Perugia (2015) (unpublished)[a] see Verzini (2009) and Parlani (2012)	2006–2015	Single center Italy retrospective	136	AAA	Z-BIS Cook Gore IBE	Fluency Advanta	95.6 %	0	Fem pseudoaneur. femhemorrhage, AF, renal failure, PE, CHF	42 ± 30
Loth (2015)	2004–2014	Single center Germany retrospective	45 41 pts	30 AAA 15 CIA	Z-BIS Cook 2 generation		87 % (39/45)	0	1 subarachnoid hemorrhage full recovery	32 ± 27 22 median (0–109)
Noel-Lamy (2015)	2009–2014	Single center Canada retrospective	20 15 pts	Aneurysm IIA	IBD- Cook + extension to superior gluteal. artery (SGA)	Viabahn Fluency iCast	100 %	1 (5 %)	2 lower limb paresis 2 MI 3 arrhythmia 1 pneumonia	Clinical 19.7 ± 18 Imaging 18.3 ± 15
Chowdhury (2015)	2007–2010	2 center UK retrospective	28 27 pts		Z-BIS H-IBD		100 %	1 (3.7 %)		11.3 ± 5.3
Ferrer (2014)	2013–2014	Single center retrospective	7 5 pts	6 AAA 1 CIA	Gore IBE		100 %	0		1
Fernandez-Alonso (2013)	2009–2010	Single center Spain retrospective	9	7 AAA 2 CIA	Z-BIS Cook	Advanta	100 %	0		14.4
Pratesi (2013)	2007–2012	2 center Italy retrospective	85 81 pts	AAA	71 Z-BIS 11 H-IBD 3 BB-IBD Cook	Advanta	98.7 %	0		20.4 ± 15
Wong, Greenberg (2013)[a] (see Haulon 2007)	2003–2012	Single center U.S. retrospective	138 130 pts	AAA or TAAA	98 H-IBD/ H-IBD2 40 BB-IBD Cook	Fluency Viabahn	94 % 129/138	1 (0.8 %)	1 fatal MI	20.3
Maurel (2013)	2009–2010	Multicenter France prospect	39	24 AAA 15 CIA	39 Z-BIS Cook	Advanta Fluency	95 % (37/39)	0	1 iliac dissection 1 renal failure coverage renal ostium	1
Parlani 2012[a] (see Verzini 2009)	2006–2011	2- center Italy retrospective	100	68 AAA 33 CIA	Z-BIS Cook 2 generation	Fluency Advanta	95 %	0	1 fem pseudoaneur 1 fem hemorrhage 1 AF 1 renal failure, 1PE 1CHF	21
Pua (2011)	2007–2009	Single center Canada retrospective	14	11 AAA 3 CIA	Z-BIS Cook 2 generation	Viabahn iCast Fluency	86 % (12/14)	0	1 psoas abscess 1 hypotension 1 lymphatic leak	18.7
Donas (2011)[a] (see Bisdas 2014)	2004–2010	2-center Germany-Greece retrospective	64	EVAR vs open	Z-IBS Cook	Advanta	Not Available	0	1 fem rupture 1 IBD occlusion 1 non vascular	30.5 ± 20.0
Bisdas (2014)[a] (see Donas 2011)	2005–2014	Single center Germany retrospective	18	Post EVAR reint	Z-IBS Cook	Advanta Viabahn BeGraft	100 %	0		15
Ferreira (2010)	2006–2008	Single center Brazil retrospective	47 37 pts	45 AAA 2 CIA	36 BB-IBD 11 H-IBD Cook		97.3 (46/47)	0	1 minor stroke 1 lymphocele 1 EIA occlusion (thrombolysis)	Up to 22

(continued)

Table 41.1 (continued)

Authors	Years	Study	*N* (IBD)	Settings	Device	Stent	Immediate success	Peri-operative death	Peri-operative morbidity	Mean follow-up (months)
Karthikesalingam review (2010)		Seven series	*N* = 196				85–100 %			
Verzini (2009)[a] (see Parlani 2012)	2000–2008	Single center Italy retrospective	32	25 AAA 7 CIA	Z-BIS Cook	Advanta Fluency	94 % (30/32)	0	1 pseudo 1 fem hemorrh 1 AF 1 renal failure, 1PE	9.8
Karthikesalingam (2009)	2006–2008	Single center UK retrospective	8	6 AAA 2 CIA	Z-BIS Cook	Advanta	75 % (6/8)	0		11.3
Tielliu (2009)	Since 2004	Single center The Netherlands retrospective	30 27 pts	23 AAA 7 CIA	30 IBD Cook	Advanta Jostent	96.3 % (29/30)	0	1 EIA rupture 1 pneumonia	16 ± 14
Serracino-Inglott (2007)	2005–2006	Single center UK retrospective	8	5 AAA 3 CIA	8 Z-BIS Cook	Advanta	100 %		2 lymphocele	6
Ziegler (2007)	2001–2006	Single center Germany retrospective	51 46 pts	34 AAA 17 CIA or other	26, 1 gen IBD 20, 2 gen IBD		69 %(35/51) 85% 2 gen 62% 1 gen	0	1 subarachnoid hemorrhage	26 ± 17
Haulon/Greenberg 2007[a] (see Wong 2013)	2003–2006	Multicent U.S.-Europe Canada	53 52 pts	48 AAA 5 CIA	H–IBD Cook	Advanta Fluency	94 % (50/53)	7/52 (13 %) 0.aneurysm related		14.2
Dias/Malina (2006)	2002–2007	Single center Sweden retrospective	22		2 custom 18 Z-IB Cook 3 H-IBD Cook	Advanta Fluency Jomed	91 % (21/23)	2/22 (9 %) 0.aneurysm related	1 TIA	20

[a]For duplicated series from same centers/authors

IBG iliac branch graft, *Z-BIS* zenith bifurcated iliac sidebranched, *AF* atrial fibrillation, *PE* pulmonary embolisms, *CHF* congestive heart failure, *H-IBD* helical iliac bifurcation device, *BB-IBD* bifurcated–bifurcated iliac bifurcation device, *TIA* transient ischemic attack, *MI* myocardial infarction

Table 41.2 Studies on commercially available IBG: mid-term and late results

Authors (year)	*N*	Mean follow-up (months)	Buttock claudication	IBG Patency	EIA occlusion	IIA occlusion	Leak	Other	Reinterv
Perugia (2015) (unpublished)[a] see Verzini (2009) Parlani (2012)	136 132 pts	42±30		91 % at 5 years	*N*=3	*N*=10	*N*=30		*N*=21
Loth (2015)	45 41 pts	32±27	*N*=1 (2.4 %) at 18 months (recovered)	3 asymptomatic occlusions within 23 m 81 % patency at 109 m		81 % patency at 109 m	*N*=7 83 % leak freedom at 109 m	*N*=2 growth	*N*=7 83 % freedom most first 18 m
Noel-Lamy (2015)	20 15 pts	Clinical 19.7±18 Imaging 18.3±15	0	100 %	*N*=1 kink revised at 6 days	*N*=1 partial thrombosis solved with coumadin	*N*=1		*N*=1 at 6 day EIA kink asymptomatic
Chowdhury (2015)	28 27 pts	11.3±5.3	–	94 % patency 24 m			*N*=1		
Ferrer (2014)	7 5 pts	1	0	100 % patency	–	–	–		
Fernandez-Alonso (2013)		14.4	0	100 % patency			*N*=3 periop		*N*=1 at 22 days
Pratesi (2013)	85 81 pts	20.4±15	*N*=7 (8.6 %)	*N*=1 occlusion at 30 days 98 % patency at 48 months		*N*=1	*N*=3 at 30-day 88.3 % leak free at 48 m		*N*=3 88.3 % reintervention free at 48 m
Wong (2013)[a] (see Haulon 2007)	138 130 pts	20.3	*N*=5 (3.8 %) of 7 late occlusion	*N*=18 occlusions: 11 early, 7 late first 26 m occlusion 82 % patency at 5 years	*N*=4	*N*=4	*N*=4 96 % leak free at 5-year		*N*=12
Maurel, Haulon (2013)	39	1	*N*=2 (5.1 %)	*N*=3 occlusions at 30 days	–	*N*=1	*N*=10		*N*=1
Parlani 2012[a] (see Verzini 2009)	100	21	*N*=4 (2 %)	*N*=7 91.4 % patency at 5 years	*N*=3	*N*=7	*N*=3 All solved 100 % leak free 5-year		*N*=9
Pua (2011)	14	18.7	0	100 % patency	0	0	*N*=2		*N*=1
Donas (2011)[a] (see Bisdas 2014)	64	30.5±20.0	*N*=2 (3.2 %) restenosis IIA	*N*=1 occlusion postop 98.4 % patency		*N*=2 restenosis	*N*=8 12.5 % Leak Kaplan-Meier rate	*N*=1 rupture IIA aneurysm for stent dislocation	*N*=4
Bisdas (2014)[a] (see Donas 2011)	18	15		100 % at 15 months	*N*=1	0	0		*N*=2
Ferreira (2010)	47 37 pts	Up to 22	*N*=3 (8.1 %)	*N*=5 occlusions 87 % patency at 22 months	*N*=1 at 16 days treated by thrombolysis		0	0	

(continued)

Table 41.2 (continued)

Authors	*N*	Follow-up	Buttock Claudic	IBG occlusion	EIA occlusion	IIA occlusion	Leak	Other	Reinterv
Karthikesalingam review (2010)	196		12/24 occlusion	24/196 occlusion (88 %)					
Verzini (2009)[a] (see Parlani 2012)	32	9.8	*N* = 1	*N* = 2	*N* = 2	No late	1/32 (4 %) at 1 year		5/32 at 1 year
Karthikesalingam (2009)	9 8 pts	11.3	*N* = 1	*N* = 2	–	–	1/8		–
Tielliu (2009)	30 27 pts	16 ± 14	*N* = 1	*N* = 3	–	–	0		–
Serracino-Inglott (2007)	8	6	*N* = 0	*N* = 1 within 30 days	–	–	0		–
Ziegler (2007)	46 36 pts	26 ± 17	*N* = 1	*N* = 4 within 12 m 87 % patency at 5 years	–	–	0 late		–
Haulon/Greenberg (2007)[a] (see Wong 2013)	52	14.2	*N* = 6	*N* = 6 within 30 days			*N* = 6		*N* = 3
Dias/Malina (2006)	23 22 pts	20	*N* = 3	*N* = 6 occlusions (2 intraop, 4 late) 74 % patency			*N* = 4		*N* = 4

[a]For duplicated series from same centers/authors
IBG iliac branch graft, *IIA* internal iliac artery, *EIA* external iliac artery, *m* months

complications were local and related to access vessel rupture or iliac vessel occlusion leading to technical failure. Nevertheless, a few medical complications were also reported, including cardiac [13, 23, 24], renal failure [12], lower limb paresis [23], cerebral hemorrhage [17, 28, 29], and stroke [35].

Mid-Term and Late Outcomes

Failure mechanisms have been well described given the increasing number of IBG implants and longer follow-up availability. A wide range of complications with associated pelvic ischemic symptoms (buttock claudication, colonic ischemia) or morphological asymptomatic findings have been reported, including external and IIA stent occlusions, endoleak, disconnection, migration, fractures, loss of integrity. Occlusions of iliac vessels may involve the entire IBG and iliac limb, the external iliac stent segment (Fig. 41.1) or the IIA bridging stent (Fig. 41.2). The latter may occur from presence of ostial IIA stenosis, EIA narrowing or angulation of the IIA bridging stent with a kink. Some authors postulated an increased risk of limb thrombosis in cases where seal is established within the external iliac vessel after IIA occlusion, a hypothesis that was not confirmed by others. The possibility that increased flow within the iliac limb in the presence of a patent internal iliac branch may be protective of limb thrombosis cannot be substantiated by solid evidence [28]. Most of the occlusions seem to occur early, within the first 30 days, but rare instances have been observed up to 26 months. Predisposing errors during patient selection include high-grade ostial stenosis, excessive tortuosity and diffuse distal internal iliac disease. Other problems during original proceduresthat may increase the risks of late failure are coverage of IIA, angulation, inappropriate landing, IIA embolization, thrombus or dissections from catheter manipulations. If the device is satisfactorily deployed and IIA is well preserved without graft kinks, long-term patency may be achieved and the related buttock claudication averted. Finally, occlusion of the entire iliac limb, IBG, and bridging stent can also occur (Fig. 41.3).

Progression of aortic and iliac disease occurs also at the distal landing zone of the IIA bridging stent (Fig. 41.4). Placement of IIA bridging stents into aneurysmal or diseased IIA segments is associated with risk of future aneurysmal enlargement with loss of seal and fixation. Endoleak occurring after IBG is frequently of type II, but loss of distal fixation and distal iliac reperfusion from IIA may also occur leading to distal type I endoleak in the side branch component (Fig. 41.5). The lack of IBG fixation, with or without evidence of device migration or disconnection, may allow for the risk of aneurysm reperfusion (Fig. 41.6). Loss of device integrity (Fig. 41.7) may be a consequence or cause of stent disconnection with late failure. It has been suggested that new generations IBGs with higher flexibility and longer overlapping zones between the branch device and the mating self-expanding stent in the IIA result in minimized angulation between the IBG components. This allows for improved resistance to the potential conformational changes that may occur over time following endovascular aortoiliac repair [28]. There are five published reports with more than 40 IBGs, with mean follow up intervals of 20 months [11, 13, 17, 33, 36]. The study with the longest follow up (mean 32 + 27 months) from Frankfurt included 45 IBGs (all second generation straight Z-BIS). The IIA patency rate was 81 %, the freedom from iliac-related endoleak rate was 83 % and freedom from any endoleak rate was 76 % at 109 months [17]. Most reinterventions occurred within the first 18 months with an overall freedom rate of 83 %. Nevertheless only a few patients reached the longer time follow-up. No patients reported symptoms of pelvic ischemia and permanent buttock claudication [17]. The largest series available from Cleveland Clinic with 138 IBGs (H-IBD or BB-IBD) in 130 patents had a median follow-up of 20.3 months (ranging 1–72 months). The estimated patency at 5 years of 81.8 % [13]. Of the 18 occlusions, 11 occurred within 30 days of implantation and seven between 1 and 26 months: 71 % of these developed persistent hip claudication. Freedom from IBD-related endoleak was 96 % at 5 years and all were due to loss of distal sealing in IIA. The authors performed 12 reinterventions to correct endoleak and occluded vessels. No stent fractures or component separations of IBGs or mating stents were noted on follow-up. No aneurysm growth was also found, and all the aneurysms remained stable or shrunk [13]. Pratesi et al., reported on 88 patients treated for CIAs using different types of devices (Z-BIS, H-IBD, BB-IBD). The estimated 48 month freedom from branch occlusion and reintervention were 98 % and 88.3 % respectively (mean follow-up of 20.4 months) [33]. Seven patients (8.6 %) suffered from buttock claudication, which occurred mostly in patients treated for bilateral CIA and unilateral IBG and did not improve during follow-up. All three endoleaks recorded were distal type I endoleaks and occurred early, within the first 30 days. No other late events occurred with an estimated freedom from endoleak at 48 months of 88.3 % [33].

Predictors of failure after IBG implantation have been searched to help select the patient pre-operatively. Parlani et al. analyzed the results on the first 100 consecutive patients treated with IBGs. Only the presence of an internal iliac aneurysm predicted the need for reintervention after 5 years, with a hazard ratio (HR) of 5.9; 95 % confidence interval (CI) 1.57–22.08, $p = 0.008$ [36]. Internal iliac aneurysm was indeed recognized as an adverse feature for IBG repair also in the Munster experience [11]. Austermann et al. suggested therefore a technical modification of the IBG procedure to treat those patients with IIA aneurysms.

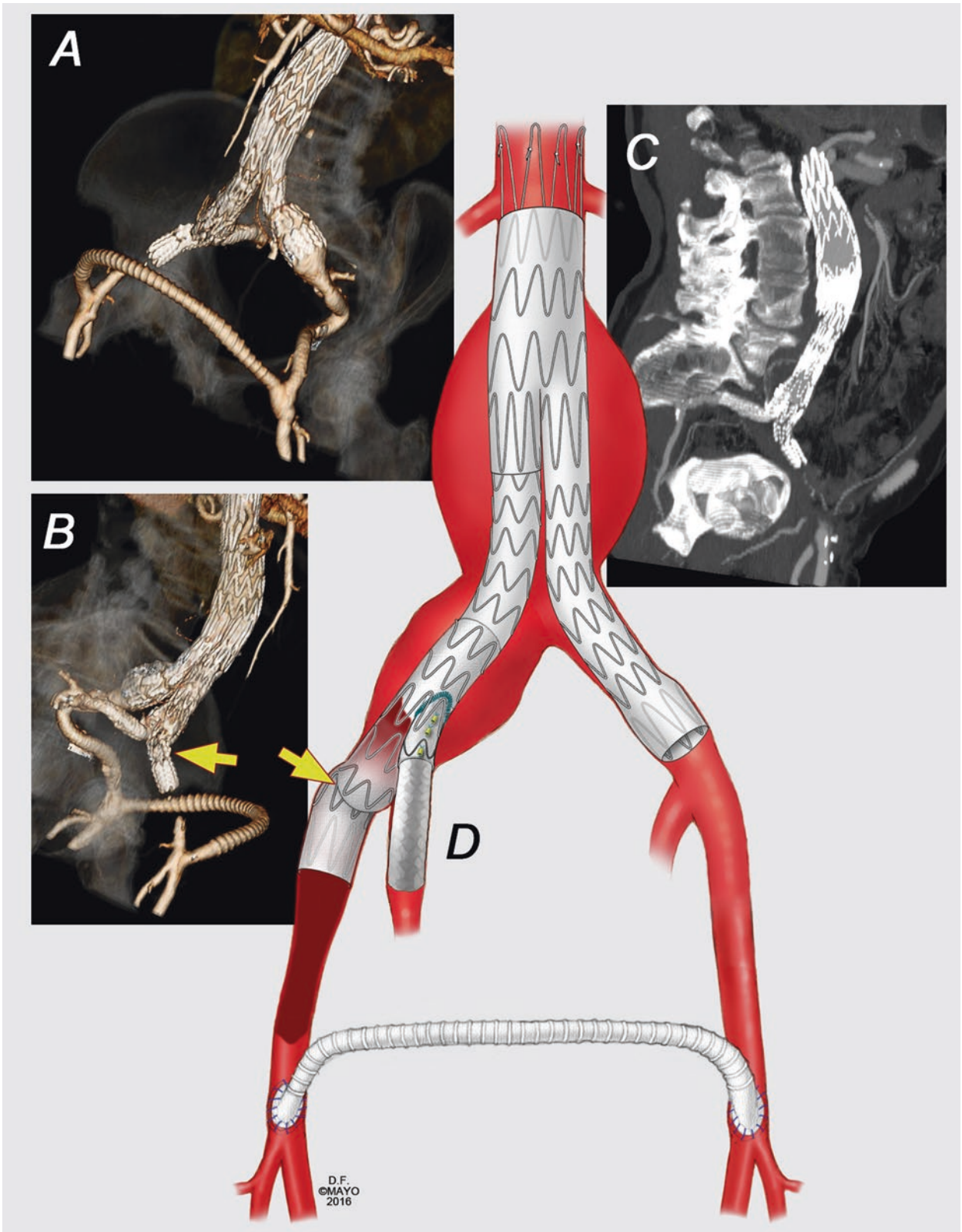


Fig. 41.1 Computed tomography angiography with left anterior view demonstrates right internal iliac side branch with late external iliac stent occlusion and a patent femoral crossover bypass graft (**a**). Note on the posterior right oblique view (**b**) a slight kink in the proximal external iliac stent which is depicted in the Maximum Intensity Projection reconstruction (**c**) and in the artist illustration (**d**, *yellow arrow*). By permission of Mayo Foundation for Medical Education and Research. All rights reserved

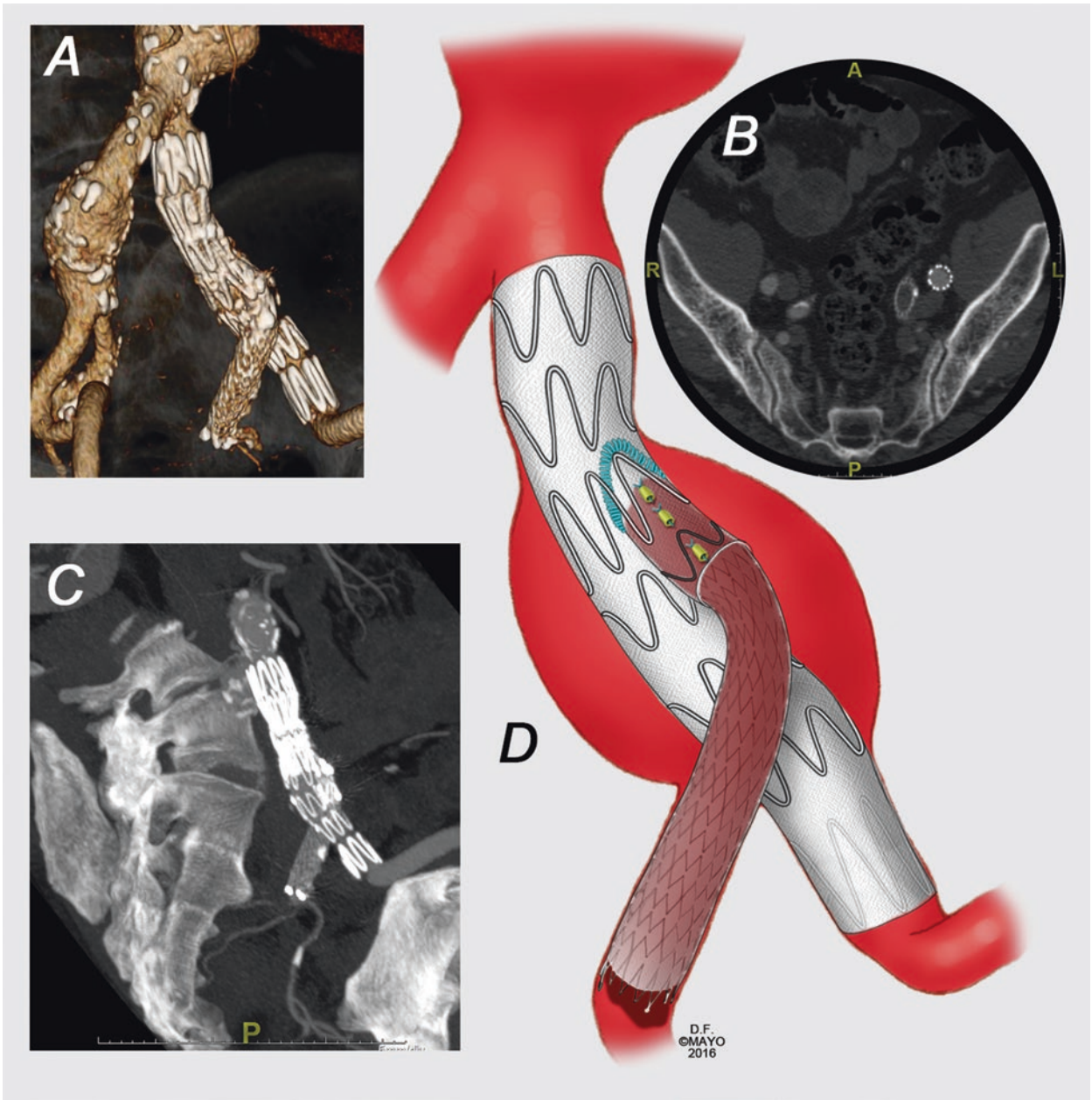


Fig. 41.2 Computed tomography angiography with right anterior view demonstrates occlusion of the left internal iliac side branch (**a**), which is confirmed by review of axial section (**b**), and Maximum Intensity Projections (**c**). Artist depiction of the occluded iliac branch with potential mechanism due to misalignment of the straight branch in relation to axis of the internal iliac artery (**d**). By permission of Mayo Foundation for Medical Education and Research. All rights reserved

The modification included the use of a balloon expandable stent-graft as a proximal segment to be deployed inside the IIA limb of the Z-BIS Cook device, followed by a distal self-expanding stent-graft (internally reinforced by a self-expanding bare stent) to seal into the parietal division branch of the IIA, with previous eventual embolization of the visceral branch. They reported favorable results in 16 patients, with promising primary patency of 95.6 % and assisted primary patency rate of 100 % [37].

Other smaller series with limited follow-up showed comparable rates of clinical and anatomical mid-term complications after implantation of commercially available IBGs as summarized in Table 41.2. These more recent findings are comparable to those summarized in the pooled review of the literature by Karthikesalingam et al. [22]: occlusion rates (12.2 %, 24/196) 50 % symptomatic for buttock claudication. Nevertheless, there are still few data with appropriate length of follow-up to draw conclusive information on late

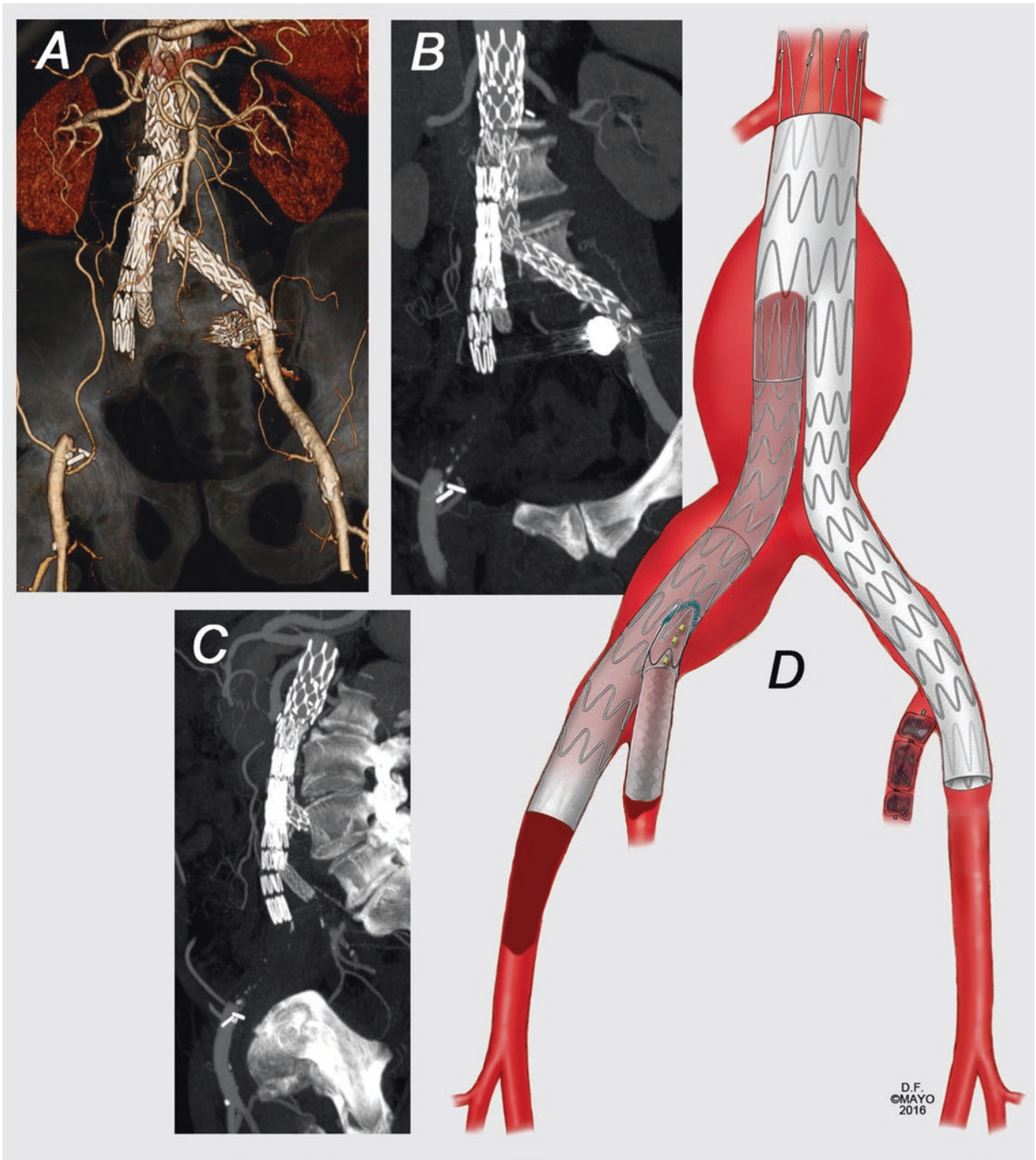


Fig. 41.3 Total occlusion of the right iliac stent extension and right internal iliac side branch is demonstrated on computed tomography angiography with three-dimensional (3D) reconstruction in anterior view (**a**), Maximum Intensity Projection reconstruction with anterior-left view (**b**) and lateral view (**c**). Artist representation of the occluded stent (**d**). By permission of Mayo Foundation for Medical Education and Research. All rights reserved

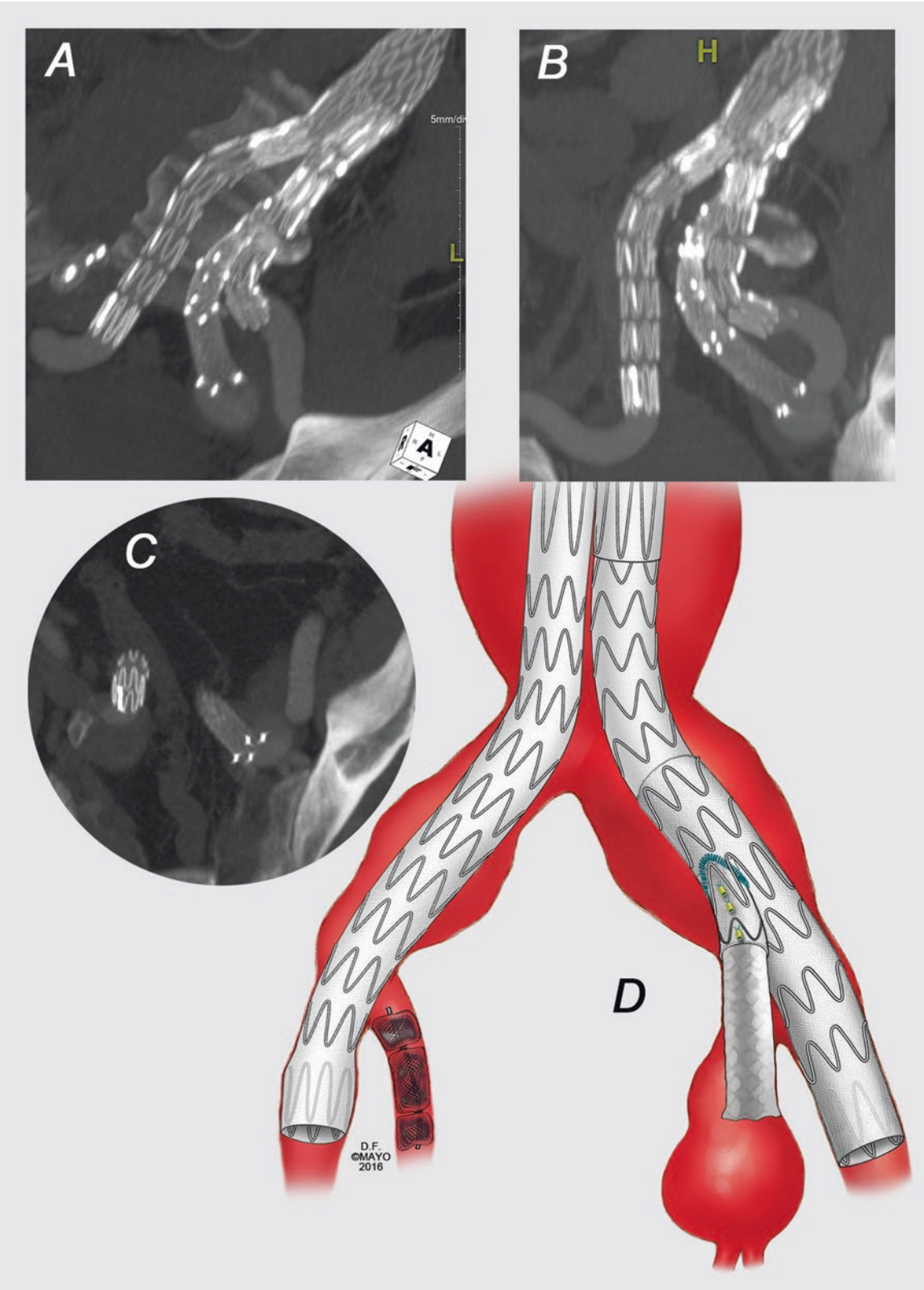


Fig. 41.4 Progressive enlargement of the distal left internal iliac artery is depicted on the computed tomography angiography and Maximum Intensity Projections in anterior-right (**a**), anterior-left (**b**), and anterior views (**c**). Artist representation demonstrates loss of distal seal zone in the internal iliac artery from progressive enlargement (**d**). By permission of Mayo Foundation for Medical Education and Research. All rights reserved

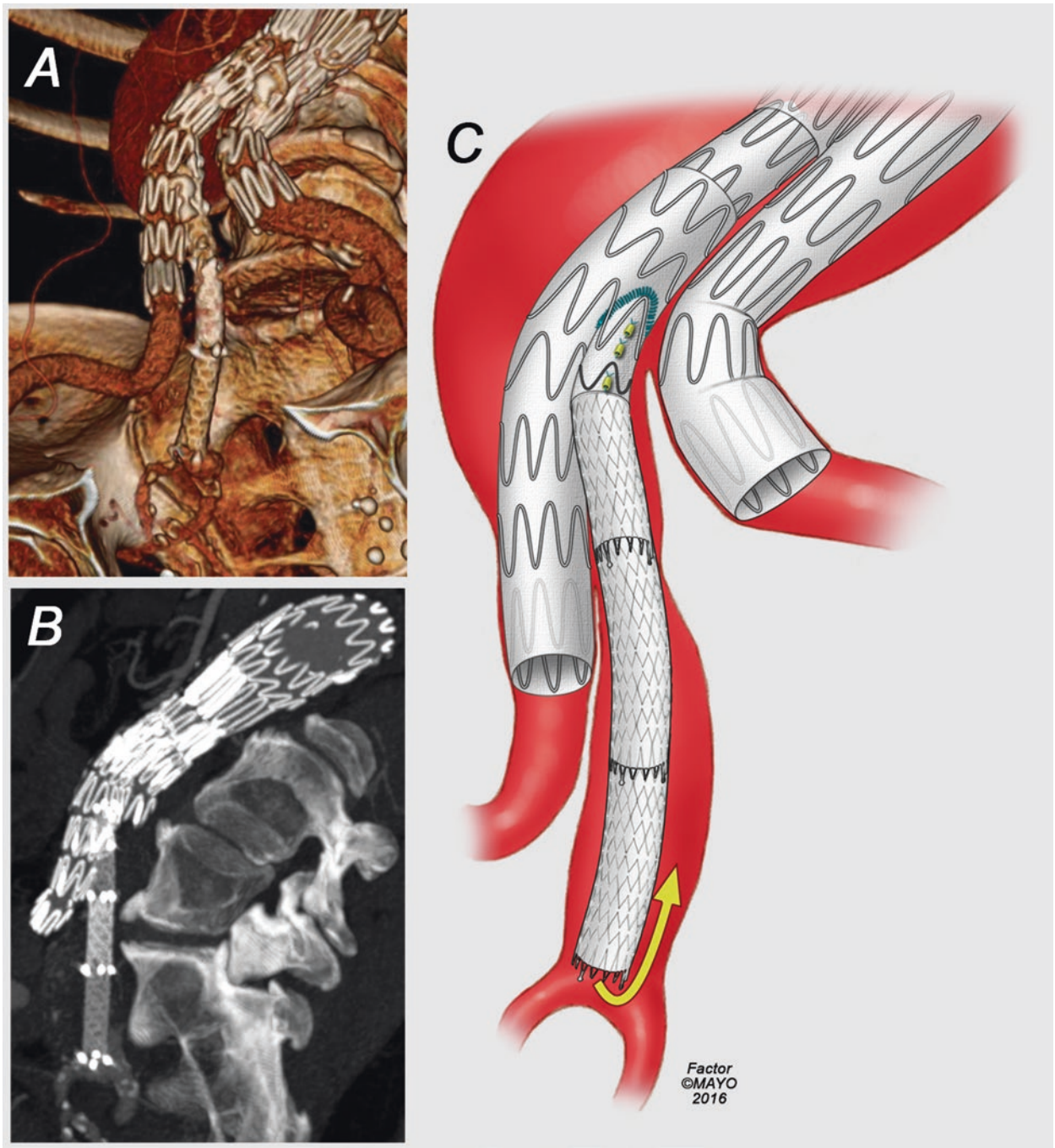


Fig. 41.5 Computed tomography angiography demonstrates a right internal iliac side branch with late distal internal iliac type 1 endoleak (**a**), which is well visualized on Maximum Intensity Projection reconstruction (**b**) and in the artist representation (**c**). By permission of Mayo Foundation for Medical Education and Research. All rights reserved

performance of such devices, but results of the few comparative studies on endovascular iliac preservation, opposed to the results of open surgery, or IIA occlusion, seem to favor endovascular repair using IBGs.

In the two-center German-Greek experience comparing 64 endovascular with 54 open surgical repairs for aneurysms involving the iliac bifurcation, results from IBG (straight Z-BIS) were provided after a mean follow-up of 30.5 + 20.0 months. The reported 30-day mortality and major morbidity rates favored the endovascular treatment vs open repair, with rates of 0 % vs 5.5 %, and 4.6 % vs 9.3 %, respectively ($p < 0.001$). Buttock claudication and colonic ischemia resulted in 3.1 % ($N = 2$) and 0 % of endovascular IBG repairs vs. 5.9 % ($N = 3$) and 2 % ($N = 1$), respectively, in the open

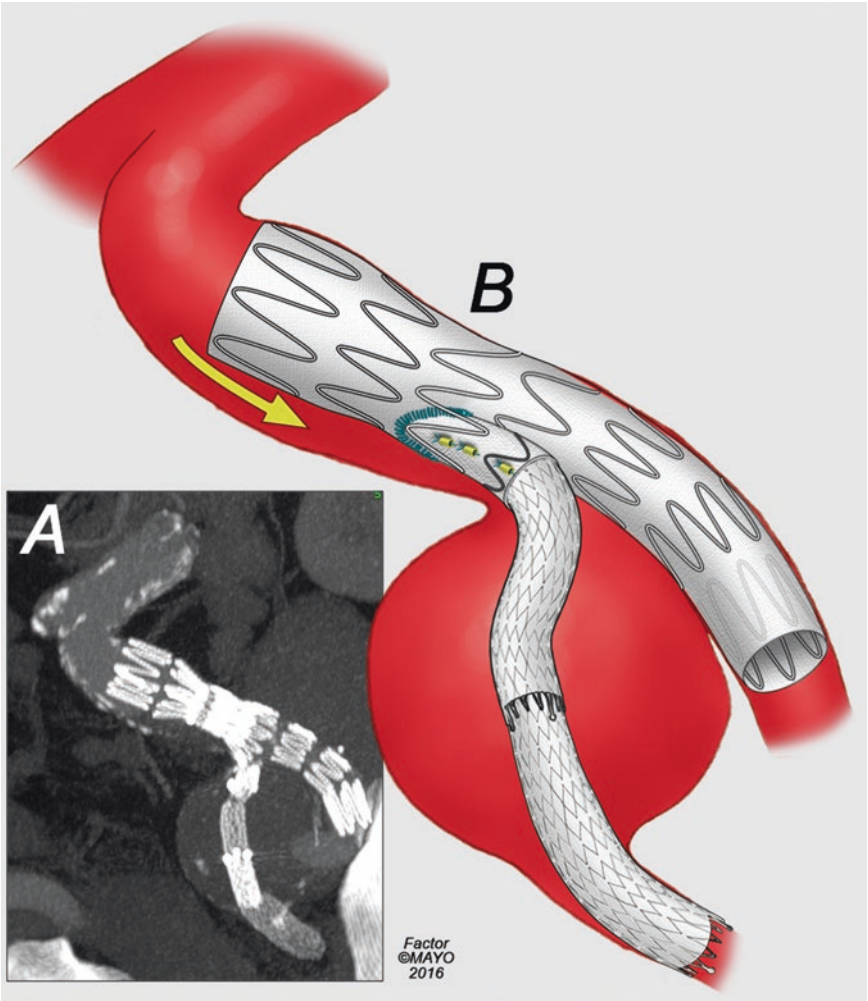


Fig. 41.6 Left internal iliac side branch with late migration and proximal type 1 endoleak is evident on the Maximum Intensity Projection reconstruction in anterior-left view (**a**) and depicted in the artist representation (**b**). By permission of Mayo Foundation for Medical Education and Research. All rights reserved

surgical group [11]. Primary patency rates after IBGs was 98.4 % (100 % after open surgery) and primary and secondary endoleak rates 12.5 % and 6.3 %. One case of dislodged covered IIA stent with persistence of IIA perfusion and rupture was reported 23 months after IBG deployment [11].

In our early experience published in 2009, comparing IBD with IIA occlusion, results on 32 patients with IBD were compared to 42 patients treated by IIA occlusion and simple EVAR. The risk of iliac graft occlusion was similar in the two groups, (6 % vs 5 %), while buttock claudication and iliac endoleak were both more frequent after IIA embolization (4 % vs 22 %, and 4 % vs 19 %, $p = 0.1$) [24].

The Perugia Experience

Between 2006 and 2015 a total of 136 iliac aneurysms were repaired in 132 patients (94.1 % males) with a mean age of 74.3 ± 7.2 years using iliac branched devices, including 119 Cook Zenith and 17 Gore Excluder IBGs. Procedural success was achieved in 96 % (126/132) of patients and 96 % (130/136) of vessels with no intraoperative deaths. Of the six technical failures, three occurred because of endoleaks at the end of the procedure, two due to intraoperative hypogastric stent thrombosis, and one from hypogastric dissec-

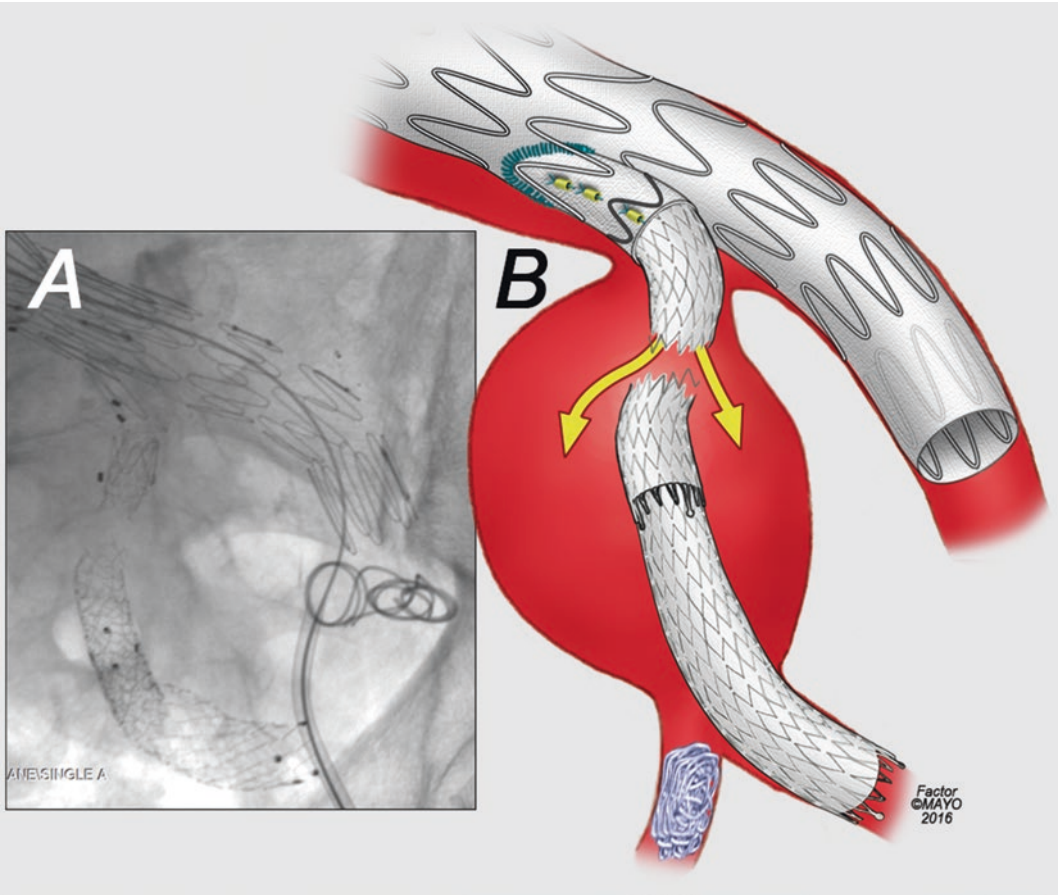


Fig. 41.7 Left internal iliac side branch with late internal iliac stent fracture (**a**) also depicted in the illustration (**b**). By permission of Mayo Foundation for Medical Education and Research. All rights reserved

tion at the origin, which resulted in inability to deploy the covered stent. The mean follow-up was 42 ± 31 months (range, 1–109 months). The IIA patency rate was 91 % at 60 months (Fig. 41.8). Freedom from reintervention per patient was 80.1 % at 60 months (Fig. 41.9). Endoleak detection anytime was reported in 30 patients (22.7 %); in the majority of these (76.7 %) was type II.

Physician-Modified IBGs

The limited access to commercial devices and regulatory constraints led to a number of creative solutions to maintain IIA perfusion, including the use of physician-modified IBGs, parallel stent-grafts, and off-label use of aortic devices [38–41]. In 2010 Oderich et al. reported surgeon-modified hypogastric branched stent-graft created using a 73-mm iliac stent-graft limb with a pre-sewn 6–8 mm polyester side graft re-sheathed into a 20F sheath and preloaded with a wire and catheter. This was indicated as "compassionate use" on three high-risk patients with large aortoliac aneurysm [38]. The technical success was 100 % with no intraoperative deaths or complications. All the branched hypogastric arteries remained patent without endoleak, migration, or loss of device integrity [38]. Additional experiences were published more recently especially in Asian countries where commercial availability of devices remains limited. Park et al. in 2014 reported on four patients from Korea successfully treated with a surgeon custom-made iliac branch device: technical success was achieved in 100 %, all the aneurysms were excluded and during a follow-up of 3 months all IBGs were patent without clinical complications [39]. A larger Chinese experience by Zhang et al. reported on 11 male patients who underwent endovascular repair with 15 "novel-designed" off-the shelf iliac branch stent-graft [40]. The stent-graft deployment was technically successful in all cases. In seven patients procedure was totally uneventful; in four minor complications (fever, groin hematoma, and renal insufficiency) were recorded. There was no perioperative mortality but one patient died after 14 months for unrelated cause. At a median follow-up of 12 months, two endoleaks occurred and were both successfully treated with IIA extensions. The overall primary patency was 86.7 % and all the aneurysm shrunk during follow-up according to computed tomography assessment [40]. Similarly, Wu et al. from

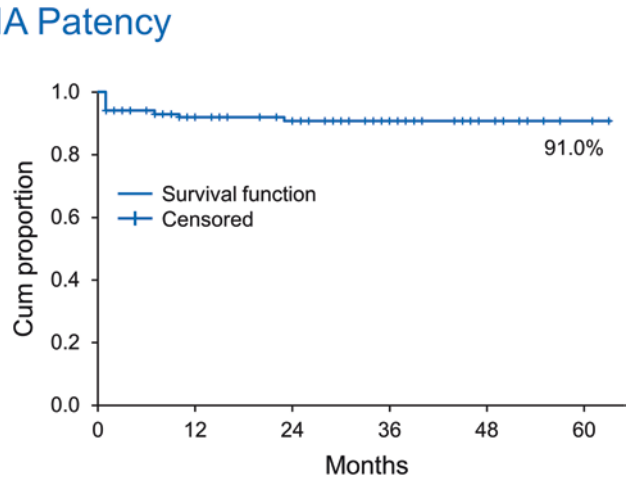


Fig. 41.8 Primary internal iliac artery patency at 60 months after iliac branch grafts. By permission of Mayo Foundation for Medical Education and Research. All rights reserved

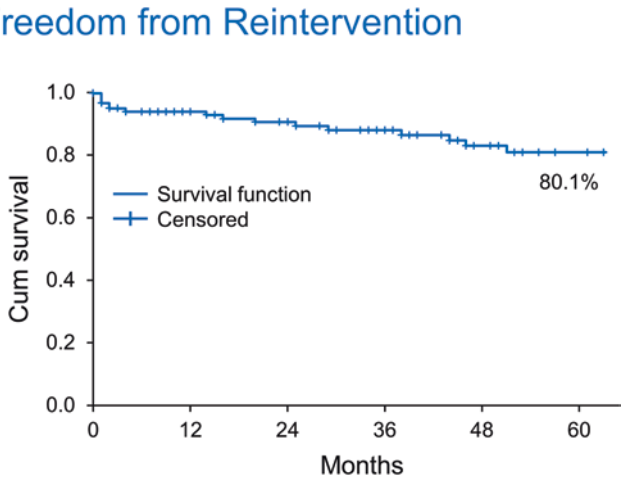


Fig. 41.9 Freedom from reintervention at 60 months after iliac branch grafts. By permission of Mayo Foundation for Medical Education and Research. All rights reserved

China published on five patients treated between 2011 and 2013 using a surgeon-modified off-the shelf iliac branch device and followed for a mean follow-up of 24 months: technical success was achieved in all cases and there was no aneurysm rupture, deaths, or other complications. All grafts remained patent without endoleak [41]. Results are summarized in Table 41.3.

Results for Bilateral Iliac Aneurysms

With increasing experience and developments in technology, applications of IBG have expanded to more challenging conditions such as bilateral iliac arteries aneurysms. Patients with extensive aortoiliac aneurysms and bilateral CIA and IIA involvement offer particular technical issues during endovascular repair because of the lack of secure distal landing zone. Most of the times the endovascular repair is accomplished with the sacrifice of one IIA and revascularization of the other side: IBG may be used for this purpose [42, 43]. Unno et al. reported on six bilateral CIA treated with one side IIA embolization and contralateral IBG using Cook Z-BIS. No patients complained of buttock claudication or ischemic colitis. At a mean follow-up of 14 months all the Z-BIS were patent and one type II endoleak was overall recorded. The presence of bilateral aneurysm of IIA raises further challenges [42]. Riesenman et al. performed a successful repair of a 7.4 cm AAA with bilateral common and internal iliac involvement using selective coil embolization of the distal right IIA followed two weeks later by EVAR with full antegrade flow preservation of left IIA and EIA using an off-the-shelf iliac branched stent-graft configured with available stent-graft components [43]. Hybrid approaches with standard EVAR with distal landing into one EIA with ipsilateral IIA embolization, plus contralateral IIA iliac endograft landing via a brachial approach and femorofemoral crossover bypass have been also applied, but these procedures may increase the risk of buttock claudication [44]. Bilateral application of IBD, in synchronous or staged approaches, has been more recently reported. Although sporadically described within series encompassing a larger number of unilateral IBG application, a number of reports focused specifically on bilateral IBG. Successful results without sexual dysfunction, buttock claudication and with optimal device patency were achieved with either commercially available or homemade devices [45, 46].

Conclusion

IBG can be performed today with high rate of technical success: this was favored by the versatility of current devices that allowed the application also for most complex aneurysmal cases in selected experienced centers. Mid-term and late patency rates are encouraging but risk of reintervention, mostly to deal with secondary endoleaks, is still present in 1/5 of the cases after 5 years. These findings also suggest that the need for careful pre-implant assessment and patient selection remain paramount to preclude technical failure even with more advanced and flexible IBG devices. The feasibility rates as per the instructions for use provided by the manufacturers remain sub-optimal, while expanded indications with most recent devices and technical modifications may help in broadening the spectrum of use in patients at high risk for open surgery or IIA occlusion. Finally, cost-effectiveness appraisals remain as a major issue further limiting the generalization of the technique.

Table 41.3 Results of studies using homemade IBG

Authors	Country	*N* (IBG)	Settings	Device technique	Imm success	Peri-op morbidity	Follow-up	Late outcome
Oderich (2009)	US	3 high-risk	Aortoiliac aneurysm + inadequate CIA landing zone	73 mm iliac stentgraft limb with a pre-sewn 6–8 mm polyester sidegraft, re-sheathed into 20F sheath. Sidegraft preloaded with wire and catheter. Fluency reinforced with Wallstent for bridging IBD and target hypogastric	100 %	0	9 ± 3 months	100 % patency no leak, migration fractures or buttock claudication
Park (2014)	Korea	4	Aortoiliac aneurysm + bilateral CIA	IBD created in back table before EVAR operation using TFLE Zenith iliac limb stentgraft. Advanta V12 or Viabahn for bridging IBD and target hypogastric	100 %	0	3 months	100 % patency, no complications No buttock claudication
Wu (2014)	China	5	Aortoiliac aneurysm; bilateral or unilateral CIA	On-table IBG modification prepared with a 16 × 12 × 120 mm MicroPort iliac stentgraft limb (MicroPort, Shanghai, China) deployed in vitro and anastomosed with vascular PTFE graft. The modified IBG reloaded into a larger sheath, with or without guidewire, and then placed in the iliac artery, with a covered stent bridging (Fluency or Jostent)	100 %	0	24 months	100 % patency no leak, rupture, buttock claudication
Zhang (2015)	China	11	Aortoiliac aneurysm + bilateral/ unilateral CIA	Novel-designed IBG of woven polyester supported by Z-stent exoskeleton stainless steel. Different lengths for CIA; side branch 8 mm × 10 mm supported with Z nitinol stent. Jostent for bridging internal iliac artery and the branch	100 %	*N* = 4: renal failure, fever, 2 hematoma	12 months	87 % patency 1 unrelated death at 14-month 2 leak with reintervention. No buttock claudication

IBD iliac bifurcation device, *EVAR* endovascular aortic aneurysm repair, *CIA* common iliac aneurysm

References

1. Lee WA, Nelson PR, Berceli SA, Seeger JM, Huber TS. Outcome after hypogastric artery bypass and embolization during endovascular aneurysm repair. J Vasc Surg. 2006;44:1162–8.
2. Oderich GS, Greenberg RK. Endovascular iliac branch devices for iliac aneurysms. Perspect Vasc Surg Endovasc Ther. 2011;23:166–72.
3. Lee WA. Branched endograft for aortoiliac artery aneurysms. Vascular. 2009;17 Suppl 3:S111–8.
4. Razavi MK, DeGroot M, Olcott 3rd C, Sze D, Kee S, Semba CP, Dake MD. Internal iliac artery embolization in the stent-graft treatment of aortoiliac aneurysms: analysis of outcomes and complications. J Vasc Interv Radiol. 2000;11:561–6.
5. Karch LA, Hodgson KJ, Mattos MA, Bohannon WT, Ramsey DE, McLafferty RB. Adverse consequences of internal iliac artery occlusion during endovascular repair of abdominal aortic aneurysms. J Vasc Surg. 2000;32:676–83.
6. Yano OJ, Morrissey N, Eisen L, Faries PL, Soundararajan K, Wan S, Teodorescu V, Kerstein M, Hollier LH, Marin ML. Intentional internal iliac artery occlusion to facilitate endovascular repair of aortoiliac aneurysms. J Vasc Surg. 2001;34:204–11.
7. Mehta M, Veith FJ, Darling RC, Roddy SP, Ohki T, Lipsitz EC, Paty PS, Kreienberg PB, Ozsvath KJ, Chang BB, Shah DM. Effects

of bilateral hypogastric artery interruption during endovascular and open aortoiliac aneurysm repair. J Vasc Surg. 2004;40:698–702.
8. Bratby MJ, Munneke GM, Belli AM, Loosemore TM, Loftus I, Thompson MM, Morgan RA. How safe is bilateral internal iliac artery embolization prior to EVAR? Cardiovasc Intervent Radiol. 2008;31:246–53.
9. Cochennec F, Marzelle J, Allaire E, Desgranges P, Becquemin JP. Open vs endovascular repair of abdominal aortic aneurysm involving the iliac bifurcation. J Vasc Surg. 2010;51:1360–6.
10. Pua U, Tan K, Rubin BB, Sniderman KW, Rajan DK, Oreopoulos GD, Lindsey TF. Iliac branch graft in the treatment of complex aortoiliac aneurysms: early results from a North American institution. J Vasc Interv Radiol. 2011;22:542–9.
11. Donas KP, Torsello G, Pitoulias GA, Austermann M, Papadimitriou DK. Surgical versus endovascular repair by iliac branch device of aneurysms involving the iliac bifurcation. J Vasc Surg. 2011;53:1223–9.
12. Maurel B, Bartoli MA, Jean-Baptiste E, Reix T, Cardon A, Goueffic Y, Martinez R, Cochennec F, Albertini JN, Chauffour X, Steinmetz E, Haulon S, Association Universitaire de Recherche en Chirurgie Vasculaire, France. Perioperative evaluation of iliac ZBIS branch devices: a French multicenter study. Ann Vasc Surg. 2013;27:131–8.
13. Wong S, Greenberg RK, Brown CR, Mastracci TM, Bena J, Eagleton MJ. Endovascular repair of aortoiliac aneurysmal disease with the helical iliac bifurcation device and the bifurcated-bifurcated iliac bifurcation device. J Vasc Surg. 2013;58:861–9.
14. Inoue K, Iwase T, Soto M, Yoshida Y, Ueno K, Tamaki S, Yamazato A. Transluminal endovascular branched graft placement for a pseudoaneurysm: reconstruction of the descending thoracic aorta including the celiac axis. J Thorac Cardiovasc Surg. 1997;114:859–61.
15. Brener BJ, Faries P, Connelly T, Sefranek V, Hertz S, Kirksey L, Hollier L, Marin ML. An in situ adjustable endovascular graft for the treatment of abdominal aortic aneurysms. J Vasc Surg. 2002;35:114–9.
16. Abraham CZ, Reilly LM, Schneider DB, Dwyer S, Sawhney R, Messina LM, Chuter TA. A modular multi-branched system for endovascular repair of bilateral common iliac artery aneurysms. J Endovasc Ther. 2003;10:203–7.
17. Loth AG, Rouhani G, Gafoor SA, Sievert H, Stelter WJ. Treatment of iliac artery bifurcation aneurysms with the second-generation straight iliac bifurcated device. J Vasc Surg. 2015;pii: S0741-5214(15)01380-4. doi:10.1016/j.jvs.2015.06.135.
18. Pearce BJ, Varu VN, Glocker R, Novak Z, Jordan WD, Lee JT. Anatomic suitability of aortoiliac aneurysms for next generation branched systems. Ann Vasc Surg. 2015;29:69–75.
19. Karthikesalingam A, Hinchliffe RJ, Malkawi AH, Holt PJ, Loftus IM, Thompson MM. Morphological suitability of patients with aortoiliac aneurysms for endovascular preservation of the internal iliac artery using commercially available iliac branch graft devices. J Endovasc Ther. 2010;17:163–71.
20. Gray D, Shahverdyan R, Jakobs C, Brunkwall J, Gawenda M. Endovascular aneurysm repair of aortoiliac aneurysms with an iliac side-branched stent graft: studying the morphological applicability of the Cook device. Eur J Vasc Endovasc Surg. 2015;49:283–8.
21. Tielliu IF, Bos WT, Zeebregts CJ, Prins TR, Van Den Dungen JJ, Verhoeven EL. The role of branched endografts in preserving internal iliac arteries. J Cardiovasc Surg (Torino). 2009;50:213–8.
22. Karthikesalingam A, Hinchliffe RJ, Holt PJ, Boyle JR, Loftus IM, Thompson MM. Endovascular aneurysm repair with preservation of the internal iliac artery using the iliac branch graft device. Eur J Vasc Endovasc Surg. 2010;39:285–94.
23. Noel-Lamy M, Jaskolka J, Lindsay TF, Oreopoulos GD, Tan KT. Internal iliac aneurysm repair outcomes using a modification of the iliac branch graft. Eur J Vasc Endovasc Surg. 2015;pii: S1078-5884(15)00399-8. doi:10.1016/j.ejvs.2015.05.021.
24. Verzini F, Parlani G, Romano L, De Rango P, Panuccio G, Cao P. Endovascular treatment of iliac aneurysm: concurrent comparison of side branch endograft versus hypogastric exclusion. J Vasc Surg. 2009;49:1154–61.
25. Karthikesalingam A, Parmar J, Cousins C, Hayes PD, Varty K, Boyle JR. Midterm results from internal iliac artery branched endovascular stent grafts. Vasc Endovascular Surg. 2010;44:179–83.
26. Serracino-Inglott F, Bray AE, Myers P. Endovascular abdominal aortic aneurysm repair in patients with common iliac artery aneurysms. Initial experience with the Zenith bifurcated iliac side branch device. J Vasc Surg. 2007;46:211–7.
27. Ziegler P, Avgerinos ED, Umscheid T, Perdikides T, Erz K, Stelter WJ. Branched iliac bifurcation: 6 years experience with endovascular preservation of internal iliac artery flow. J Vasc Surg. 2007;46:204–10.
28. Haulon S, Greenberg RK, Pfaff K, Francis C, Koussa M, West K. Branched grafting for aortoiliac aneurysms. Eur J Vasc Endovasc Surg. 2007;33:567–74.
29. Dias NV, Resch TA, Sonesson B, Ivancev K, Malina M. EVAR of aortoiliac aneurysms with branched stent-grafts. Eur J Vasc Endovasc Surg. 2008;35:677–84.
30. Chowdhury MM, Schiro A, Farquharson F, Smyth JV, Serracino-Inglott F, Murray D. Treatment of aortoiliac aneurysms with the iliac bifurcated device for preservation of internal iliac artery flow. Vasc Endovascular Surg. 2014;48:153–8.
31. Ferrer C, De Crescenzo F, Coscarella C, Cao P. Early experience with the Excluder® iliac branch endoprosthesis. J Cardiovasc Surg (Torino). 2014;55:679–83.
32. Fernández-Alonso L, Fernández-Alonso S, Grijalba FU, Fariña ES, Aguilar EM, Alegret Solé JF, Pascual MA, Centeno R. Endovascular treatment of abdominal aortic aneurysms involving iliac bifurcation: role of iliac branch graft device in prevention of buttock claudication. Ann Vasc Surg. 2013;27:851–5.
33. Pratesi G, Fargion A, Pulli R, Barbante M, Dorigo W, Ippoliti A, Pratesi C. Endovascular treatment of aorto-iliac aneurysms: four-year results of iliac branch endograft. Eur J Vasc Endovasc Surg. 2013;45:607–9.
34. Bisdas T, Weiss K, Donas KP, Schwindt A, Torsello G, Austermann M. Use of iliac branch devices for endovascular repair of aneurysmal distal seal zones after EVAR. J Endovasc Ther. 2014;21:579–86.
35. Ferreira M, Monteiro M, Lanziotti L. Technical aspects and mid-term patency of iliac branched devices. J Vasc Surg. 2010;51:545–50.
36. Parlani G, Verzini F, De Rango P, Brambilla D, Coscarella C, Ferrer C, Cao P. Long-term results of iliac aneurysm repair with iliac branched endograft: a 5-year experience on 100 consecutive cases. Eur J Vasc Endovasc Surg. 2012;43:287–92.
37. Austermann M, Bisdas T, Torsello G, Bosiers MJ, Lazaridis K, Donas KP. Outcomes of a novel technique of endovascular repair of aneurysmal internal iliac arteries using iliac branch devices. J Vasc Surg. 2013;58:1186–91.
38. Oderich GS, Ricotta 2nd JJ. Novel surgeon-modified hypogastric branch stent graft to preserve pelvic perfusion. Ann Vasc Surg. 2010;24:278–86.
39. Park YE, Lee JH, Yun WS, Park KH. Surgeon custom-made iliac branch device to salvage hypogastric artery during endovascular aneurysm repair. J Korean Med Sci. 2014;29:1678–83.
40. Zhang T, Guo W, Ma X, Jia X, Liu X, Dong Y, Xiong J, Jia S. Novel-designed iliac branch stent graft for internal iliac artery reconstruction during aneurysm repair. Ann Vasc Surg. 2015;29:189–96.
41. Wu WW, Lin C, Liu B, Liu CW. Using a surgeon-modified iliac branch device to preserve the internal iliac artery during

endovascular aneurysm repair: single-center experiences and early results. Chin Med J (Engl). 2015;128:674–9
42. Unno N, Inuzuka K, Yamamoto N, Sagara D, Suzuki M, Konno H. Preservation of pelvic circulation with hypogastric artery bypass in endovascular repair of abdominal aortic aneurysm with bilateral iliac artery aneurysms. J Vasc Surg. 2006;44: 1170–5.
43. Riesenman PJ, Ricotta JJ 2nd, Veeraswamy RK. Preservation of hypogastric artery blood flow during endovascular aneurysm repair of an abdominal aortic aneurysm with bilateral common and internal iliac artery involvement: utilization of off-the-shelf stent-graft components. Ann Vasc Surg. 2012;26:109.e1–5.
44. Mertens RA, Bergoeing MP, Mariné LA, Valdés F, Krämer AH. Antegrade hypogastric revascularization during endovascular aortoiliac aneurysm repair: an alternative to bilateral embolization. Ann Vasc Surg. 2010;24:255.e9–12.
45. Cuff R, Banegas S, Mansour A, Chambers C, Wong P, Slaikeu J. Endovascular repair of bilateral common iliac artery aneurysms following open abdominal aortic aneurysm repair with preservation of both hypogastric arteries using commercially available stent grafts. J Vasc Surg. 2014;59:516–9.
46. You JH, Park HK, Park CB. Endovascular repair of bilateral iliac artery aneurysm with branched iliac stents: case report and review of the current literature. J Korean Surg Soc. 2013;85:145–8.

Technical Aspects and Results of Hybrid Iliac Revascularization

42

Javairiah Fatima and Gustavo S. Oderich

Introduction

Open surgical revascularization of the internal iliac artery is uncommonly needed but is an alternative to coil embolization in order to preserve pelvic flow and avoid the associated ischemic complications. This technique was initially described by Parodi and Ferreira [1] in 1999 and since then has been widely employed in select cases. The procedure combines an extra-anatomic reconstruction of the internal iliac artery using a flank retroperitoneal approach with endovascular aneurysm exclusion and placement of the iliac limb extension into the internal iliac artery. Recent developments on iliac branch technology diminished or nearly eliminated the need for open iliac revascularization, but its use continues to be indicated in select cases. This chapter summarizes the indications, techniques, and results of hybrid iliac revascularization combined with EVAR.

Indications

The need for a flank retroperitoneal incision offsets some of the benefits of total endovascular aortic repair done using trans-femoral exposure or percutaneous technique. Indications for hybrid iliac reconstructions include those patients who are not ideal candidates for iliac branch devices or who need concomitant replacement of the external iliac artery because of narrow diameter not suitable for minimum of 16–20Fr sheath profile, which is needed for current iterations of iliac branch devices. Hybrid reconstructions are also useful for physicians and centers that currently don't have access to iliac branch technology due to regulatory or financial issues. Patients with small external iliac vessels (<5 mm) and who need preservation of at least one of the internal iliac arteries may benefit from a hybrid reconstruction that combines replacement of the external iliac artery as a permanent conduit with revascularization of the internal iliac artery (Fig. 42.1). Another potential indication is the patient with complex dissections where the common and internal iliac arteries are heavily involved by dissection flaps, and a total endovascularization solution is not available or possible (Fig. 42.2). The need for hybrid reconstruction requires at a minimum a common iliac artery aneurysm with unacceptable distal landing zone and/or an internal iliac artery aneurysm not amenable to endovascular therapy or with compressive symptoms. Anatomic characteristics such as extreme tortuosity or calcification precluding use of endovascular devices like iliac branch devices or unavailability of such devices may also require familiarity with hybrid internal iliac artery reconstructions.

Technique

The flank retroperitoneal approach is used for hybrid reconstruction. Selection of which side is based on optimal anatomy, but our preference is to select the right side whenever possible if there is a choice. It is critical that the surgeon assures that the arteries are suitable for clamping. Presence of dense circumferential calcification or a large aneurysm involving the common and iliac internal iliac arteries may preclude safe placement of a clamp. In patients with partially calcified vessels, control can be obtained using balloon occlusion.

A curvilinear flank incision is created in the upper part of the mid third between the umbilicus and the anterior superior iliac spine (Fig. 42.3). A common mistake is to make the incision too low. It is better to error on an incision that is a bit higher than to have to deal with low incisions where exposure of the common and internal iliac artery is not possible or

J. Fatima
Division of Vascular and Endovascular Surgery,
University of Florida, 1600 SW Archer Rd., NG-45,
P.O. Box 100128, Gainesville, FL 32610, USA

G.S. Oderich (✉)
Division of Vascular and Endovascular Surgery,
Department of Surgery Mayo Clinic,
200 First Street SW, Rochester, MN 55905, USA
e-mail: oderich.gustavo@mayo.edu

© Mayo Foundation for Medical Education and Research 2017

G.S. Oderich (ed.), *Endovascular Aortic Repair*, DOI 10.1007/978-3-319-15192-2_42

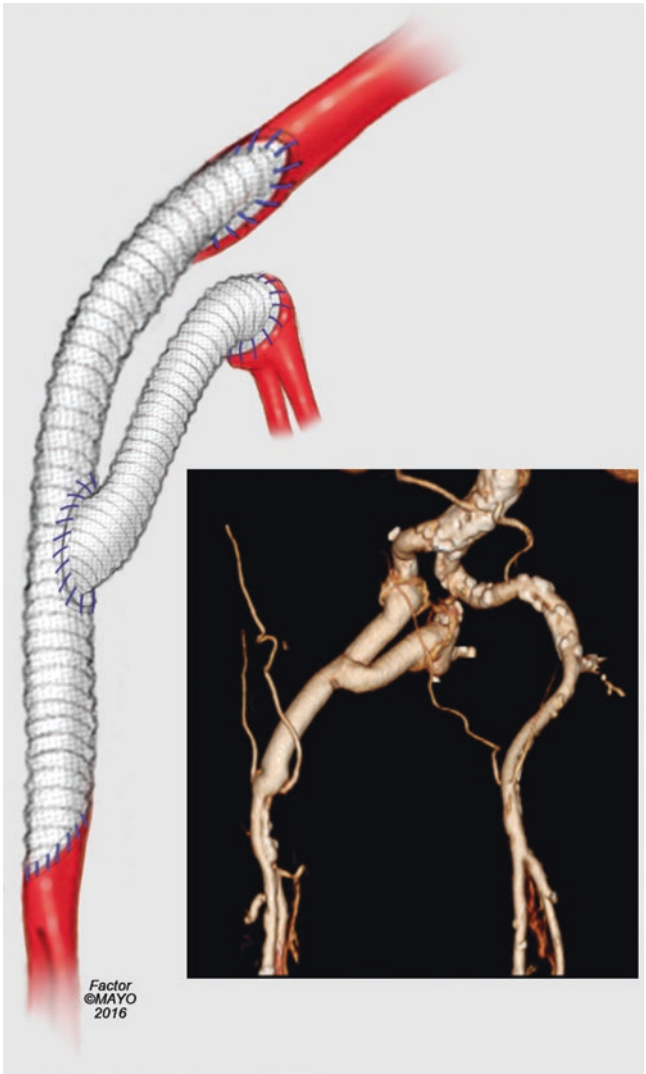


Fig. 42.1 Technique of permanent iliac conduit using iliofemoral bypass with concomitant internal iliac bypass to preserve internal iliac flow in a patient with complex thoracoabdominal aortic aneurysm. By permission of Mayo Foundation for Medical Education and Research. All rights reserved

suboptimal. The aortic bifurcation is usually at the umbilicus, and the iliac bifurcation is 3–5 cm below. Dissection is carried through the subcutaneous tissue. The external oblique, internal oblique, and transversus abdominis muscles and the transversalis fascia are entered using muscle splitting technique for the external oblique and transection of the other muscles. The rectus abdominis muscle can usually be retracted medially with minimal splitting of lateral muscle fibers. The inferior epigastric vessels may need to be ligated and transected but if possible are preserved.

The retroperitoneal space is entered with careful attention to avoid the peritoneum. This is best done by starting the dissection as lateral as possible where there is more preperitoneal fat. Starting in the anterior part of the incision is often leads to opening the intraperitoneal cavity. Using blunt dissection, the viscera are reflected medially. Blunt dissection can be done using a finger, the back part of a forceps, a sponge on a stick, or a Kittner. The distal common iliac artery, the external iliac artery, and internal iliac artery are dissected free and controlled with vessel loops. It is important to identify and protect the ureter as it crosses anterior to the iliac artery bifurcation. The ureter can be retracted cranially and medially. It may need to be mobilized. It is important to keep the fat tissues around the ureter to avoid devascularization, which may lead to stricture or even late perforations. An Omni self-retaining retractor is ideal in the patient who is deep or obese or when the anatomy is difficult such as in the patient with iliac calcifications or a larger aneurysm needing more extensive dissection.

Configuration of the reconstruction is variable (Fig. 42.4). The two most common techniques are to use a bypass to the internal iliac artery or a transposition. The latter option avoids a graft but usually is not possible because there is not enough length in the internal iliac artery to allow sufficient mobilization for an anastomosis in the distal part of the external iliac artery. If a bypass is selected, our preference is to use a 7–10 mm polyester graft, which can be anastomosed end to end or end to side to the internal iliac artery (Fig. 42.5). The location of the proximal graft anastomosis can also be at the distal external iliac artery using the same flank incision (Fig. 42.6) or preferably at the proximal common femoral artery using a separate groin incision. In case the anastomosis is selected in the common femoral artery, our preference is to use a higher access puncture in the common femoral artery, which is placed more medially in the intended location of the anastomotic site. The typical sequence is to perform first the distal internal iliac artery anastomosis, then the EVAR, and finally the proximal internal iliac bypass anastomosis to the common femoral artery once all sheaths and wires are removed.

The patient is systematically heparinized with 80 units/kg of intravenous heparin. The proximal internal iliac artery is ligated with a 1-0 silk or Ethibond suture. The distal internal iliac artery is then clamped and transected. The proximal stump may be reinforced with running a 4-0 prolene suture. If the internal iliac artery is of normal size, a 7 or 8 mm polyester graft is gently beveled and anastomosed end-to-end to the internal iliac artery using 4-0 or 5-0 prolene with parachute technique. The anastomosis is tested using a syringe with heparinized saline. The clamp is transferred to the graft in close proximity to the anastomosis, and blood is aspirated from the polyester graft. At this point access is obtained in the common femoral artery by using a bit higher and medial puncture just beneath the inguinal ligament. This puncture site will be the intended location of the proximal graft anastomosis once the EVAR is completed.

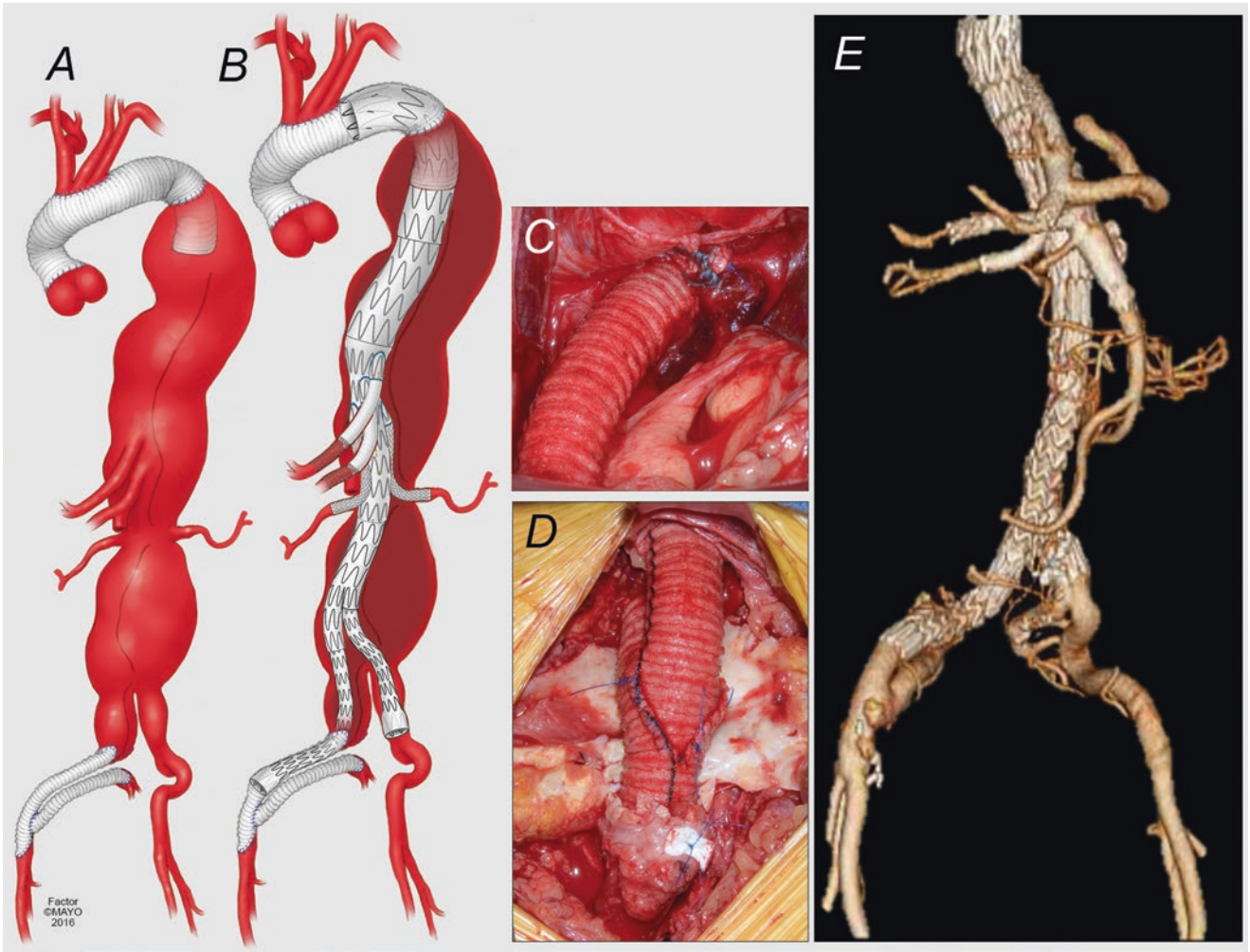


Fig. 42.2 Patient with extensive chronic dissection and a thoracoabdominal aneurysm after prior arch repair. The patient was treated in a staged fashion using first right iliofemoral conduit and internal iliac bypass (**a**), followed by extensive branched stent grafts (**b**). Note the internal iliac bypass graft is anastomosed from end to end to the internal iliac artery (**c**), whereas the proximal anastomosis is done to the iliofemoral graft (**d**). Computed tomography angiography was performed for surveillance after extensive repair (**e**). By permission of Mayo Foundation for Medical Education and Research. All rights reserved

The EVAR is done in standard fashion. Once all stents are deployed and completion angiography shows a satisfactory result, all sheaths and wires are removed. The distal external and common femoral arteries are clamped. The femoral puncture site is examined for any dissection or dislodged plaque, and the arteriotomy is increased longitudinally. The iliac graft is cut to length, spatulated, and anastomosed from end to side using a running 4-0 or 5-0 prolene. Alternatively, the iliac graft can be anastomosed in the external iliac artery using the same flank incision. This is the case in some patients who have staged procedures or total percutaneous EVAR where a groin incision is not planned or wants to be avoided. However, the anastomosis of the graft in the external iliac is more difficult and cumbersome than when this is done to the common femoral artery.

Aneurysmal Internal Iliac Artery

If the internal iliac artery is aneurysmal, control of the vessel may not be possible using traditional clamps or even balloon occlusion. In these cases it is possible to expose the iliac vessels from the retroperitoneal space and to perform the EVAR first using trans-femoral access with placement of the iliac limb into the external iliac artery. It is critical to document by angiography the total absence of type I or type III endoleak prior to entering the iliac aneurysm. The distal internal iliac branches are dissected and controlled with vessel loops if possible. If the patient has a deep pelvis or a very large aneurysm, this may not be possible. In these cases we have entered the aneurysm and used Fogarty balloon occlusion from inside the aneurysm sac, but the surgeon needs to be

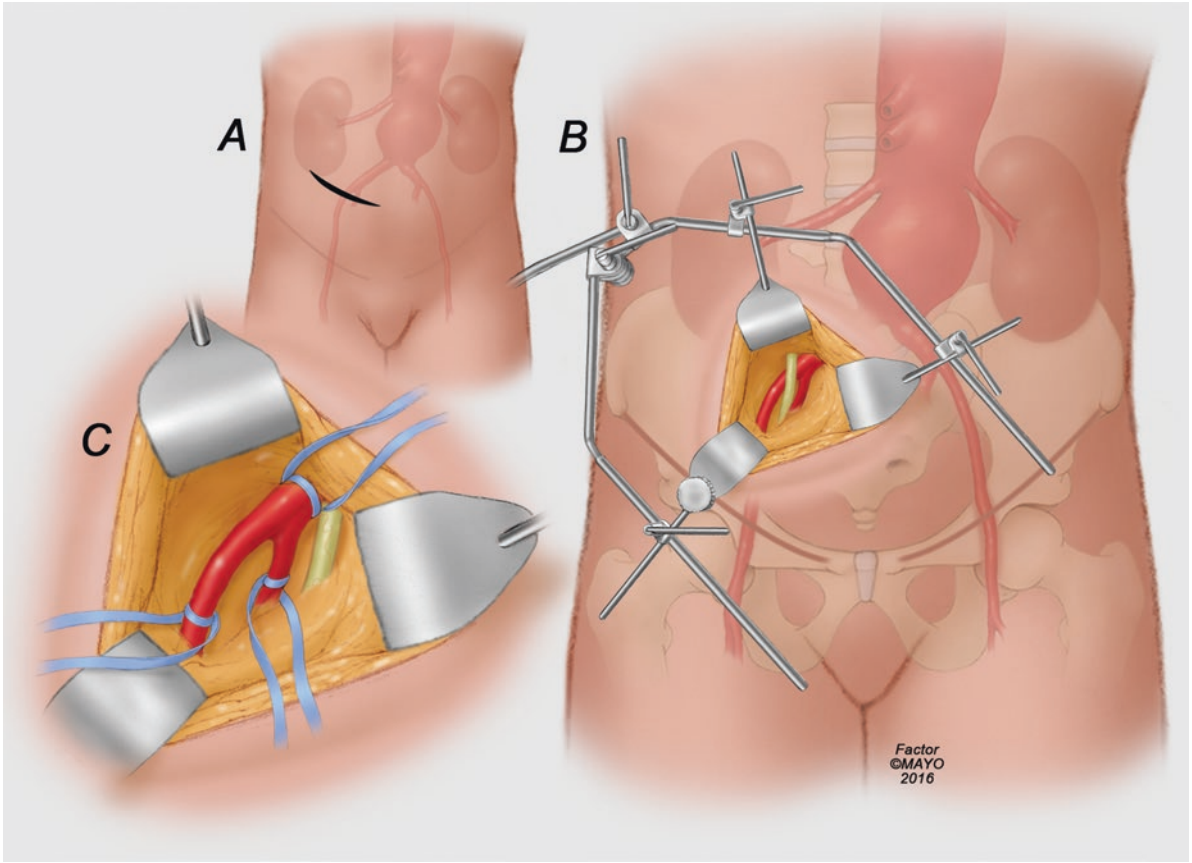


Fig. 42.3 Standard retroperitoneal flank incision is used for exposure of the iliac arteries (**a**) with self-retaining retractor (**b**). The ureter is identified and protected while the iliac vessels are controlled with vessel loops (**c**). By permission of Mayo Foundation for Medical Education and Research. All rights reserved

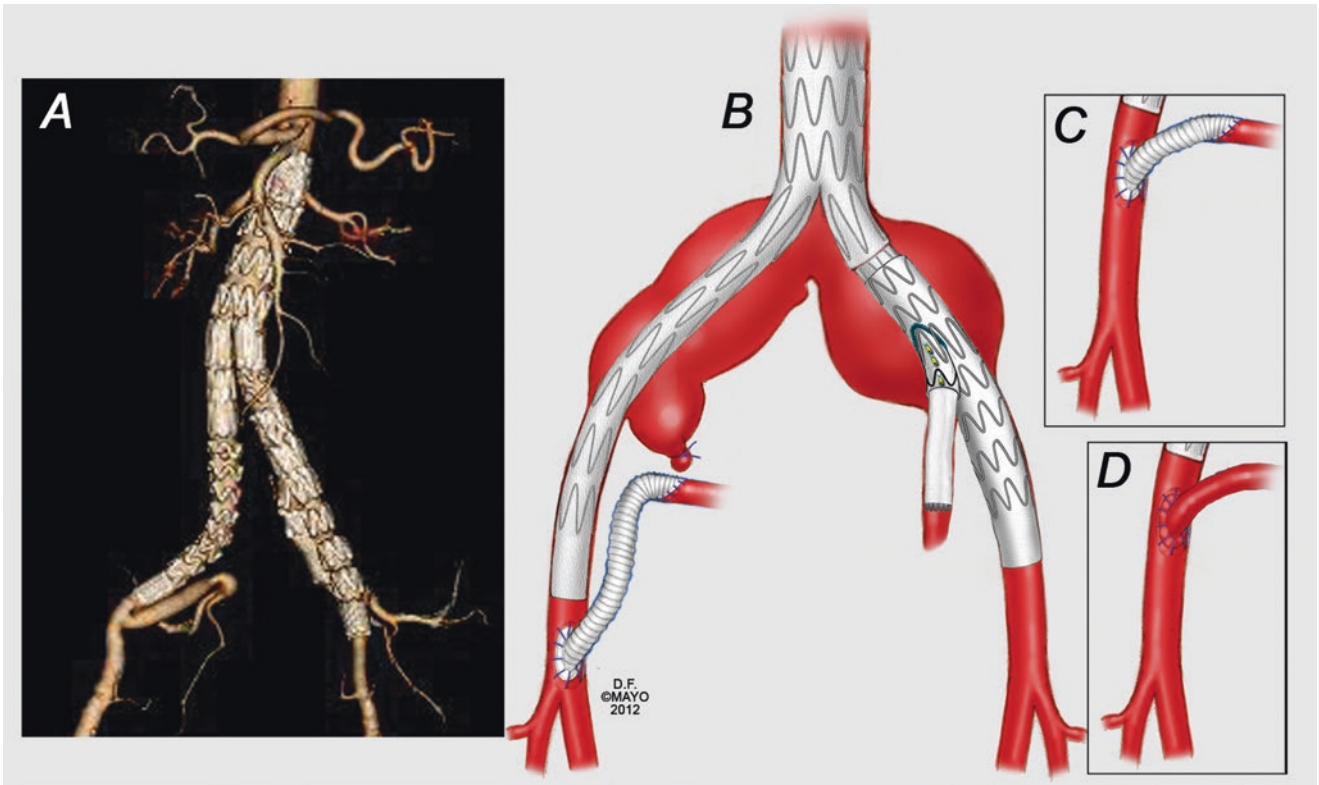


Fig. 42.4 Patient treated by endovascular aortic repair using bifurcated Cook Zenith stent graft with left iliac branch device and right internal iliac artery bypass (**a**). The most common configuration of the internal iliac bypass involves an end-to-end anastomosis to the internal iliac artery with proximal anastomosis to the common femoral artery (**b**). Alternatively, the proximal anastomosis can be done to the distal external iliac artery (**c**), or a transposition can be done (**d**). By permission of Mayo Foundation for Medical Education and Research. All rights reserved

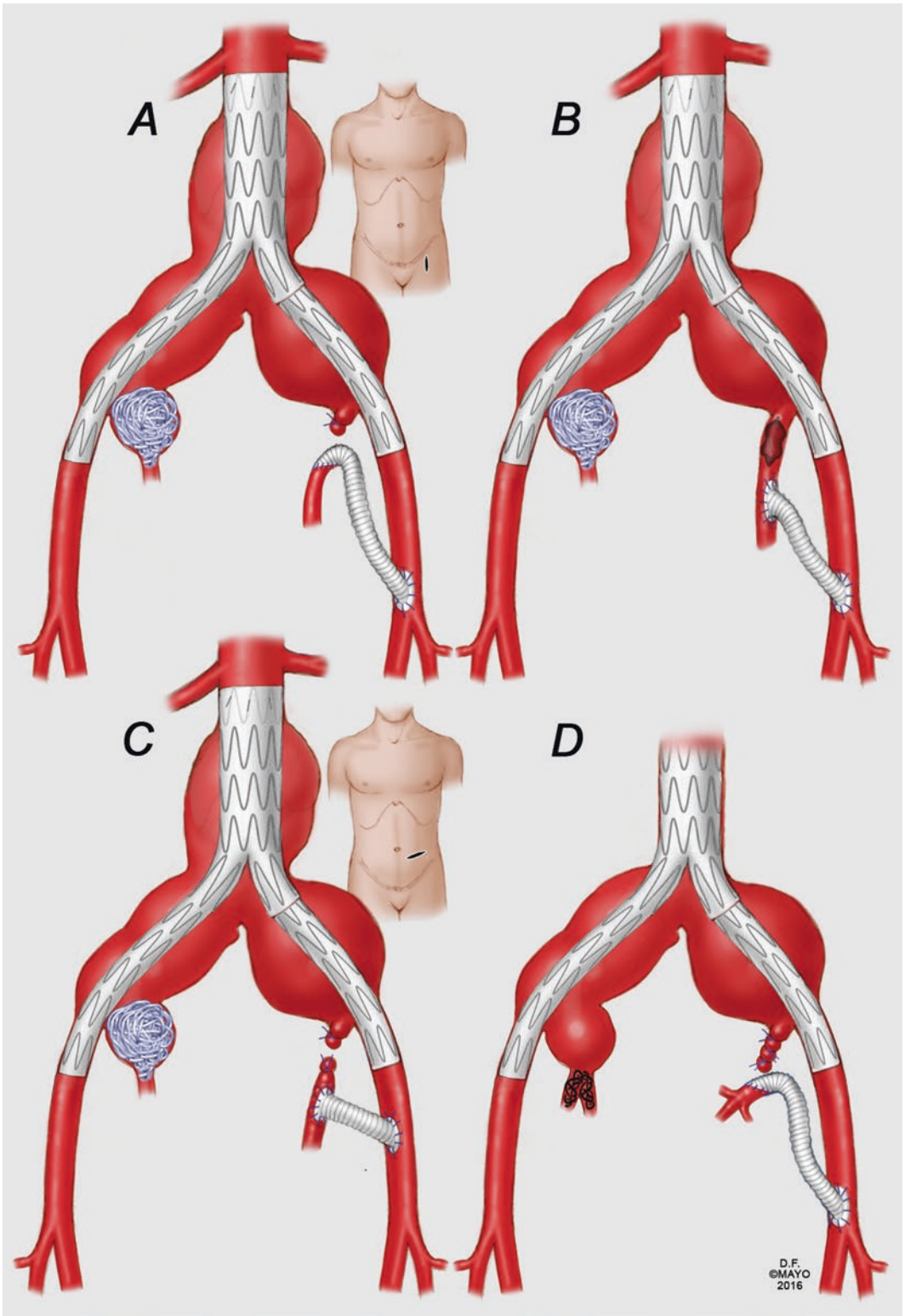


Fig. 42.5 Various graft configurations for hybrid iliac reconstruction including bypass with anastomosis in the common femoral artery with end-to-end (**a**) or end-to-side anastomosis to the internal iliac artery (**b**) or anastomosis of the graft based on the external iliac artery (**c**). In general, exclusion of the internal iliac artery is done with plugs as opposed to coils whenever possible to minimize metallic artifact (**d**). By permission of Mayo Foundation for Medical Education and Research. All rights reserved

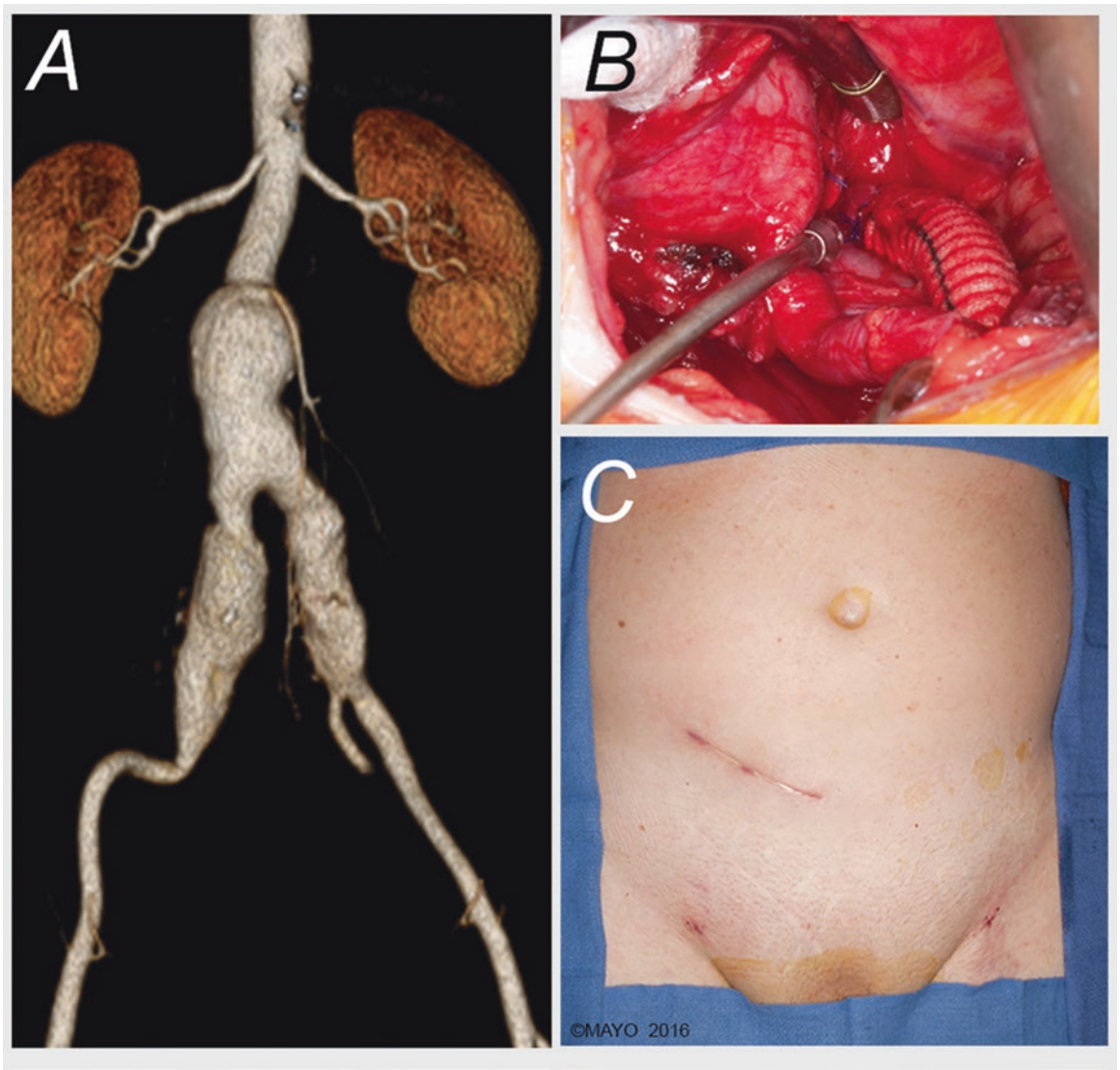


Fig. 42.6 Patient with bilateral iliac aneurysms (**a**) treated by right internal iliac bypass (**b**) done using small flank incision (**c**). By permission of Mayo Foundation for Medical Education and Research. All rights reserved

very familiar with this technique to avoid excessive retrograde bleeding from the internal iliac branches. Once the aneurysm is entered, distal control is obtained. Any oozing from the proximal internal iliac artery is controlled with a running 3-0 or 4-0 prolene suture. A polyester graft (usually 10 mm) is then anastomosed to the distal internal iliac artery incorporating as many or all branches as a single anastomosis. This is best done using the parachute technique, ideally with the graft loaded into the Fogarty balloon occlusion catheter. When this anastomosis is satisfactory for hemostasis, the polyester graft is cut to length, spatulated, and anastomosed to the common femoral artery as described above.

Iliofemoral Conduit with Internal Iliac Reconstruction

This technique is described in detail in Chap. 23 and is depicted in Fig. 42.1. It is indicated in patients with heavily diseased or small external iliac vessels who already have a primary indication for iliac conduit and necessitate a complex endovascular repair. Our preference on cases of thoracoabdominal aneurysms is to stage this procedure together with coverage of the proximal thoracic aorta by stent. The visceral portion of the repair is completed weeks later. A problem on performing the flank incision and internal iliac bypass in conjunction with the

entire TAAA repair is that there is potential risk for excessive blood loss, hypotension, and added ischemia to the pelvis. In addition, the coagulopathy that follows the first 24–48 h after extensive aortic repair may result in bleeding complications from the fresh retroperitoneal exposure.

Retroperitoneal approach is performed as previously described, but a femoral incision is also added. The proximal external iliac artery is ligated. The common iliac and internal iliac arteries are controlled. A 10 mm polyester graft is spatulated and anastomosed end to end to the distal common iliac artery extending to the proximal external iliac artery past the origin of the internal iliac artery. The graft is clamped proximally and tunneled under the inguinal ligament. The common femoral artery is clamped. The graft is cut to length and anastomosed to the common femoral artery as high as possible using either end-to-end or end-to-side anastomosis. A portion of the 10 mm graft is then used to fashion the internal iliac artery bypass which is done using the technique already described.

External to Internal Iliac Stents with Femoral Crossover Graft

A variation of the technique has been used selectively in patients who develop aneurysms in the stump of the common iliac artery after aortoiliac or aortofemoral graft reconstruction (Fig. 42.7). In these cases an external to internal iliac

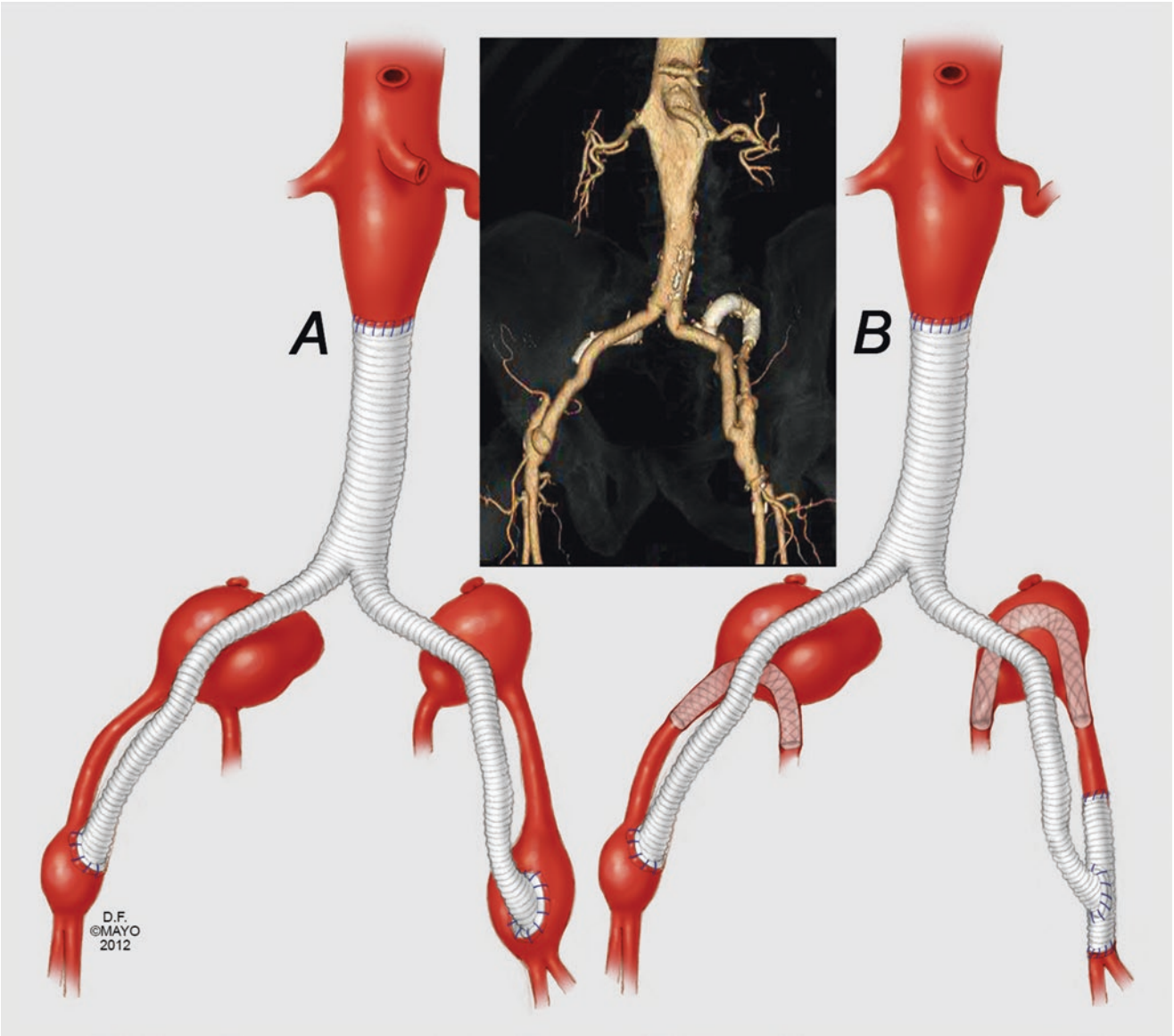


Fig. 42.7 Patient treated by aortofemoral reconstruction developed large common iliac artery aneurysms in the stump of the common iliac arteries (**a**). The patient was treated by external iliac to internal iliac stent graft placement (**b**). Note occlusion of the right iliac stent on late follow-up. By permission of Mayo Foundation for Medical Education and Research. All rights reserved

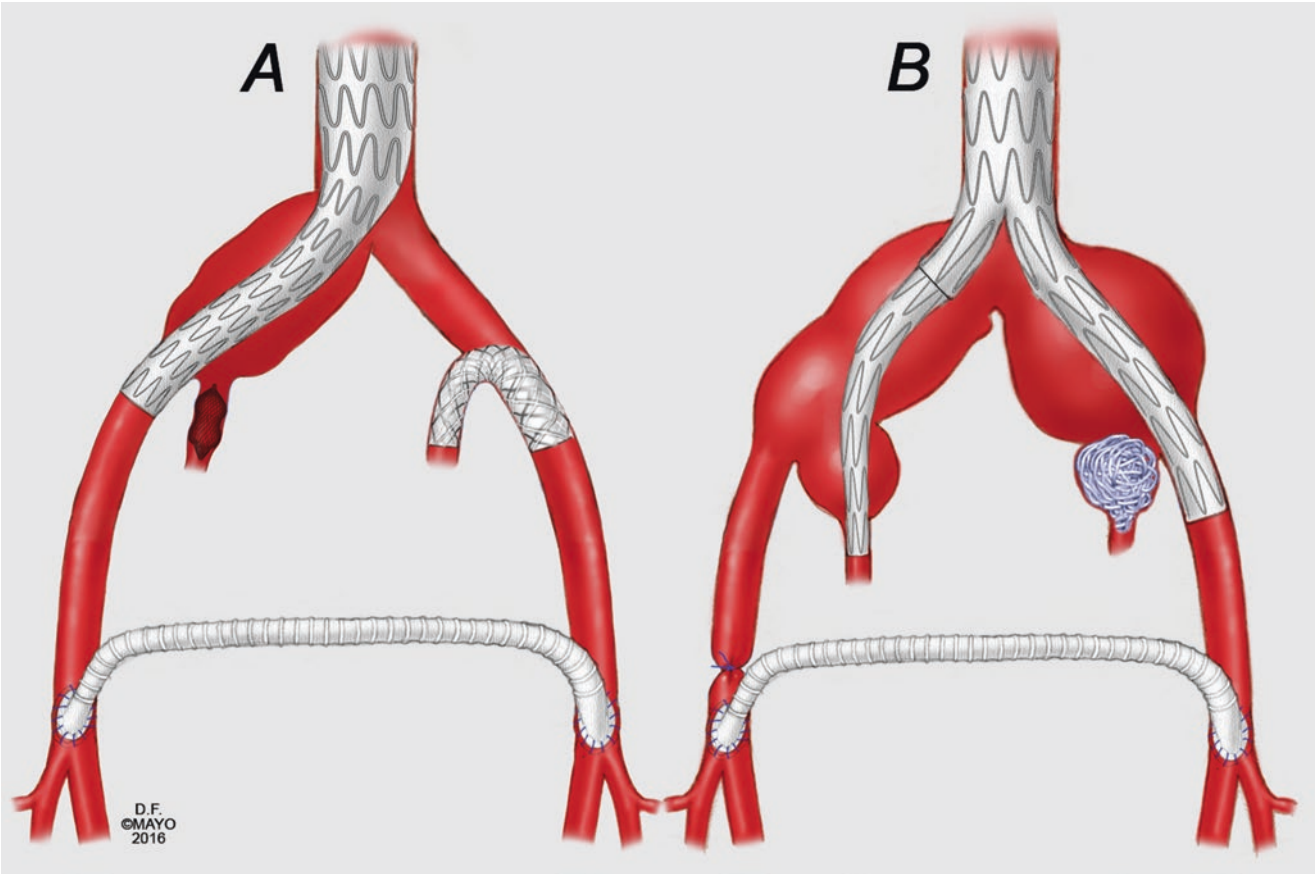


Fig. 42.8 Variations of hybrid techniques using femoral crossover bypass with external to internal iliac stent (**a**) or a stent from the contralateral gate to the internal iliac artery done using brachial access (**b**). By permission of Mayo Foundation for Medical Education and Research. All rights reserved

stent can be placed to exclude the common iliac artery. This technique can also be used primarily to revascularize the internal iliac artery using a femoral crossover bypass to keep lower extremity flow (Fig. 42.8). Another variation of this technique is to place a self-expandable stent from the contralateral gate of the bifurcated device to the internal iliac artery, with exclusion of the external iliac artery in the same side [5].

Results

Embolization of the internal iliac artery has been widely used in patients with aneurysms encroaching the iliac bifurcation. This technique is usually well tolerated in patients with unilateral aneurysms, but there is a predictable rate of buttock claudication in at least one third of the patients and potential risk of serious ischemic complications in a minority of patients [6–8]. In a systematic review of 605 cases reported in the literature, Rayt et al. [2] found buttock claudication in 27 % and sexual dysfunction in 14 % of patients (Fig. 42.9). The rate of ischemic complications was highly variable in the reports, ranging from 16 to 50 % and 16 to 80 % for buttock claudication with unilateral and bilateral embolization, respectively.

Results of hybrid repair are lacking in the literature, with a paucity of larger clinical series. Lee et al. [3] reported one of the largest series comparing standard EVAR with EVAR done with coil embolization or iliac preservation using hybrid repair (Fig. 42.10). In that report, standard EVAR was associated with ischemic complications in 6 %, claudication in 3 %, and any postoperative complications in 26 % of patients. Rates of these complications were significantly higher for patients who had embolization or a bypass. However, compared to embolization, bypass was associated with less ischemic complications (27 % vs 55 %), claudication (27 % vs 39 %), and postoperative complications (54 % vs 69 %). Kobayashi et al. [4] reported a small series of six Japanese patients. There were no complications, and all bypass grafts were patent after a mean follow-up of 18 months. For external to internal iliac stenting, data is also scarce. Massière et al. [5] reported on 12 patients treated by external to internal iliac stents with femoral crossover grafts. None of the patients had stent occlusion or claudication.

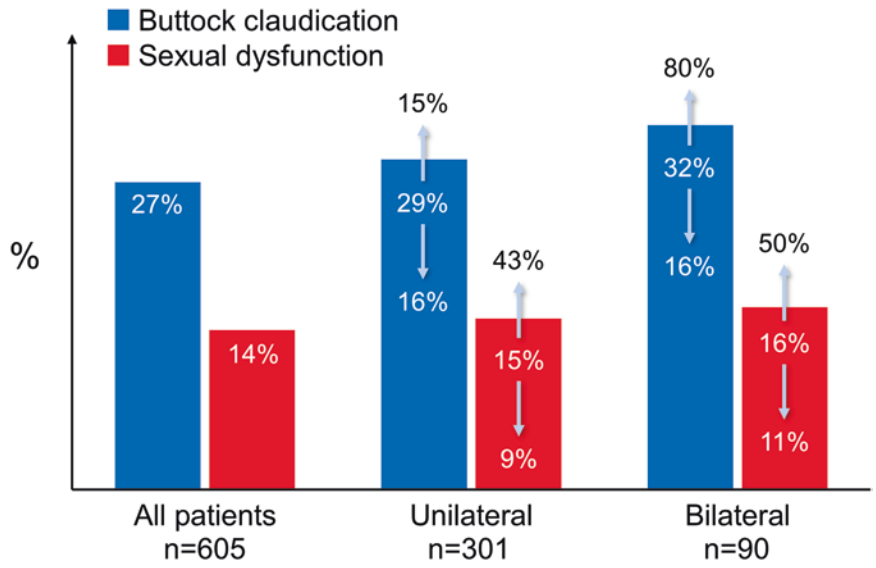


Fig. 42.9 Incidence of buttock claudication and sexual dysfunction with unilateral and bilateral internal iliac embolization in a large systematic review of 605 patients. Created based on [2]. By permission of Mayo Foundation for Medical Education and Research. All rights reserved

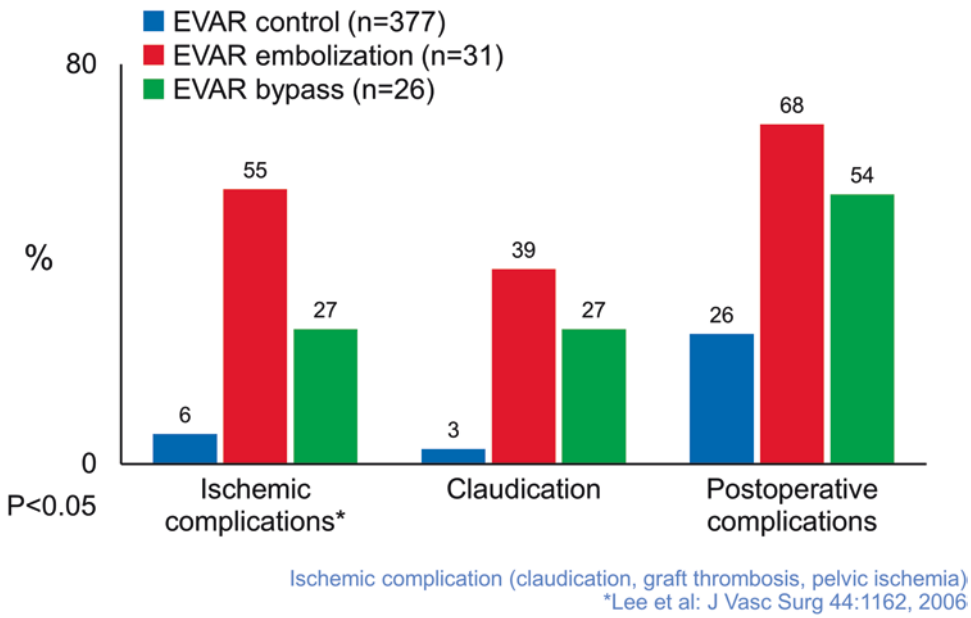


Fig. 42.10 Incidence of ischemic complications, claudication, and postoperative complications with standard EVAR, embolization, or bypass. Created based on [3]. By permission of Mayo Foundation for Medical Education and Research. All rights reserved

References

1. Parodi JC, Ferreira M. Relocation of the iliac artery bifurcation to facilitate endoluminal treatment of abdominal aortic aneurysms. J Endovasc Surg. 1999;6(4):342–7.
2. Rayt HS, Bown MJ, Lambert KV, Fishwick NG, McCarthy MJ, London NJ, Sayers RD. Buttock claudication and erectile dysfunction after internal iliac artery embolization in patients prior to endovascular aortic aneurysm repair. Cardiovasc Intervent Radiol. 2008;31(4):728–34.
3. Lee WA, Nelson PR, Berceli SA, Seeger JM, Huber TS. Outcome after hypogastric artery bypass and embolization during endovascular aneurysm repair. J Vasc Surg. 2006;44(6):1162–8. discussion 1168–9.
4. Kobayashi Y, Sakaki M, Yasuoka T, Iida O, Dohi T, Uematsu M. Endovascular repair with contralateral external-to-internal iliac artery bypass grafting: a case series. BMC Res Notes. 2015;8:183.
5. Massière B, von Ristow A, Vescovi A, Pedron C, Fonseca LM. Management of aortoiliac aneurysms by retrograde endovascular hypogastric artery preservation. Vascular. 2014;22(2):116–20.
6. Rana MA, Kalra M, Oderich GS, de Grandis E, Gloviczki P, Duncan AA, Cha SS, Bower TC. Outcomes of open and endovascular repair for ruptured and nonruptured internal iliac artery aneurysms. J Vasc Surg. 2014;59(3):634–44.
7. Fatima J, Correa MP, Mendes BC, Oderich GS. Pelvic revascularization during endovascular aortic aneurysm repair. Perspect Vasc Surg Endovasc Ther. 2012;2:55–62.
8. Oderich GS, Picada-Correa M, Pereira AA. Open surgical and endovascular conduits for difficult access during endovascular aortic aneurysm repair. Ann Vasc Surg. 2012;26(7):1022–9.

Off-Label Use of Aortic Devices and Parallel Stent Grafts for Iliac Revascularization

43

David J. Minion

Introduction

The off-label use of aortic devices and parallel stent grafts for iliac preservation is commonly referred to as the sandwich technique. The term was coined by Armando Lobato who initially described its use to treat thoraco-abdominal and aortoiliac aneurysms. The name derives from external and internal iliac extensions being "sandwiched" together inside of the common iliac limb of the aortic device [1]. The external iliac extension is usually placed retrograde from the ipsilateral femoral access, while the internal iliac limb is usually advanced antegrade from either the contralateral femoral access or axillo-brachial access. The main challenges encountered with this technique relate to delivery of the internal iliac device into its target vessel and achieving seal with the parallel configuration.

Although the delivery of the internal iliac device into its target vessel represents a challenge for any method of hypogastric preservation, the actual cannulation of the hypogastric artery is often simplified in the sandwich technique compared to other options. As dedicated iliac branch devices (IBDs) become more widely available, this simplification may ultimately prove to be the utility of parallel endografts. The reason for this is because with dedicated iliac branch grafts, the branch of the graft must be cannulated prior to the hypogastric artery, which can lead to difficulties if the branch is not aligned with the orifice of the hypogastric artery. In contrast, with the sandwich technique, the hypogastric artery is cannulated directly from the common iliac limb. To take full benefit of this advantage, one of the first key points of the successful use of this technique is to extend the common iliac limb of the aortic device as close as possible to the bifurcation of the external and internal iliac arteries. This maneuver not only maximizes the overlap of parallel extensions but also forces any subsequent catheters and wires toward the iliac bifurcation rather than the aneurysm sac. Therefore, the task of cannulating the hypogastric artery is now comparable to that in non-aneurysmal anatomy. If there is still any difficulty, then a balloon can be inflated from the ipsilateral femoral access to block the origin of the external iliac artery (Fig. 43.1). However, we have rarely found this maneuver necessary. Once the main hypogastric artery has been cannulated, the wire is advanced into a distal pelvic branch vessel and exchanged for a stiffer wire to allow for tracking of the stent graft used for the sandwich.

The bigger challenge with this technique relates to achieving seal where the two parallel stents interface within the common iliac stent. This challenge is more mathematical than technical. Therefore, an understanding of the mathematics and geometry of the parallel endograft configuration is paramount for success with this technique. Our approach is based on six key principles, the *Minion's Maxims for Parallel Endografts:*

1. Sizing should be based on perimeters (i.e., native circumference).
2. The minimum combined length of the perimeters of the parallel extensions is the sum of the perimeter of the parent lumen (i.e., the common iliac stent) plus twice the length of the segment where the two parallel extensions appose each other.
3. The length of the segment where the two parallel extensions appose each other is dependent on its shape.
4. The segment where the two parallel extensions appose each other must, by default, form at least two acute angles or four right angles at its points of contact with the parent lumen perimeter for complete apposition to occur.
5. Round self-expanding stents resist any shape with acute angles.
6. The effect of standard balloon angioplasty is to make a stent more round.

D.J. Minion (✉)
Division of Vascular Surgery, University of Kentucky Medical Center, 800 Rose Street, Room C217, Lexington, KY 40536, USA
e-mail: djmini@email.uky.edu

© Mayo Foundation for Medical Education and Research 2017

G.S. Oderich (ed.), *Endovascular Aortic Repair*, DOI 10.1007/978-3-319-15192-2_43

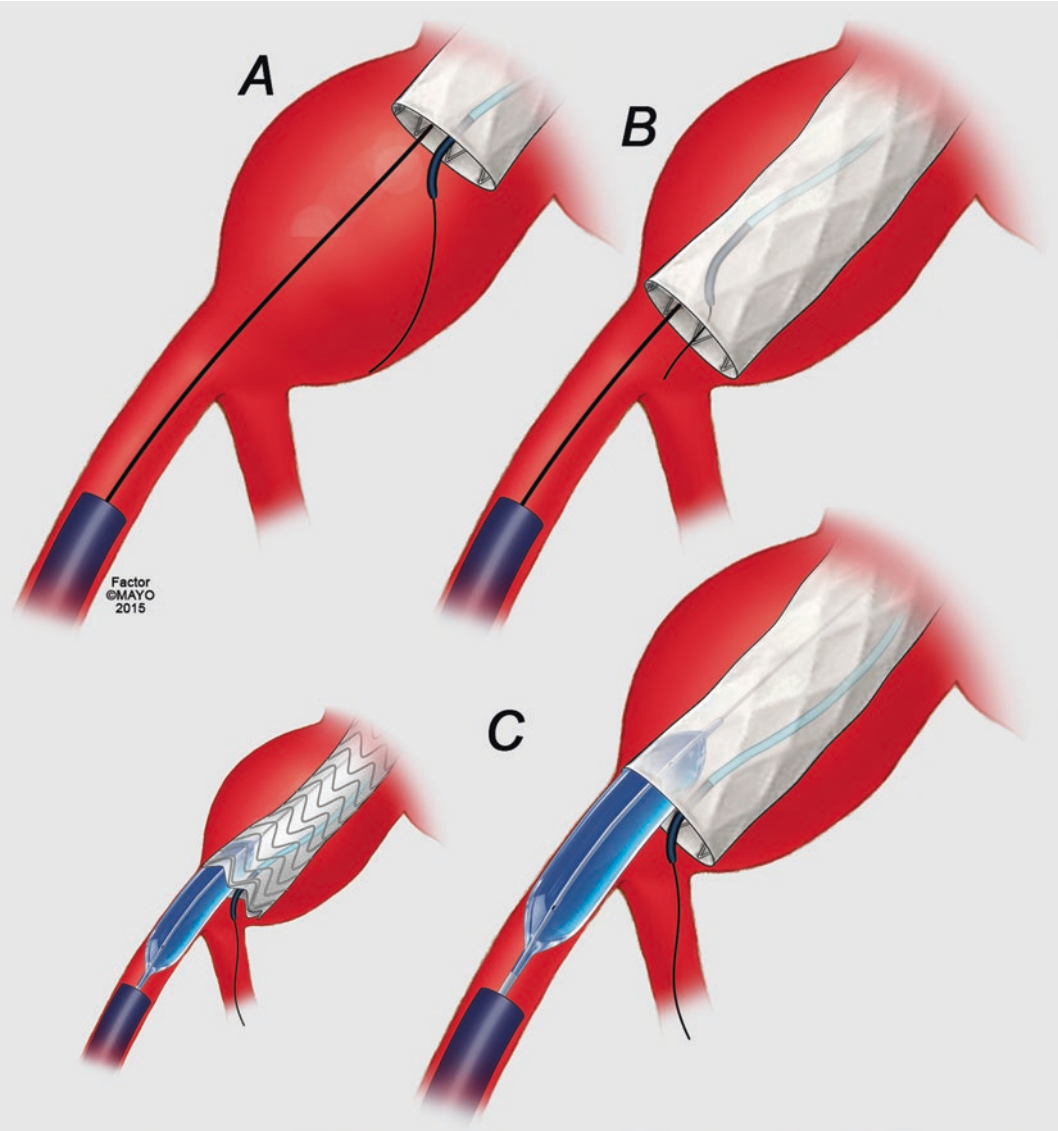


Fig. 43.1 "Principle of exclusion" as applied to cannulation of the internal iliac artery. (**a**) If the common iliac limb is relatively short, then the guide wire has the option of traversing nearly anywhere in the aneurysm sac instead of the hypogastric target. (**b**) In contrast, if the common iliac limb is extended very close to the bifurcation of the common iliac artery, then the majority of the space of the aneurysm sac is excluded as a possible trajectory for the path of the guide wire, essentially forcing the guide wire toward the origins of the external and internal iliac arteries. (**c**) Inflation of a balloon in the external iliac artery will further restrict the possible trajectory of the guide wire toward the origin of the internal iliac artery. By permission of Mayo Foundation for Medical Education and Research. All rights reserved

The Perimeter Method for Sizing

For most endovascular interventions, sizing is based on diameters. At first glance, then, it may seem that placing two 8 mm iliac extensions side by side in a 16 mm common iliac limb would be appropriate. However, the diameters of the two 8 mm extensions add up to 16 mm in only a single cross-sectional plane, leaving significant portions of the cross-section without apposition (Fig. 43.2). These areas of poor apposition are commonly referred to as gutters. Gutters are the inherent weakness of parallel endografting and can lead to continued pressurization of the aneurysm sac.

Since a diameter-based approach will result in undersizing and significant cross-sectional area without apposition, one might conclude that sizing should therefore be based on cross-sectional area. In other words, if a 16 mm common iliac limb (with an 8 mm radius) has a cross-sectional area of $\pi(8^2)$ or approximately 201 mm^2, then apposition should occur if the two parallel extensions had a combined cross-sectional area of at least 201 mm^2. In this sense, it seems that seal should be achieved by using a 12 mm external iliac extension with a native cross-sectional area of $\pi(6^2)$ and an 11 mm internal iliac extension with a native cross-sectional area of $\pi(5.5^2)$, since these two devices add up to a combined native cross-sectional area of approximately 208 mm^2. However, it

is important to realize that the cross-sectional area is highly dependent on the actual final shape of the extensions (Fig. 43.3). For any given perimeter, a circular shape achieves the maximum cross-sectional area. Flattening along any portion of the circumference will result in loss of cross-sectional area, similar to flattening a tire or an inflatable ball. In the most extreme case, a completely flattened limb will occupy almost no cross-sectional area. Since the final shape of a deployed parallel stent is unpredictable, a cross-sectional area approach to sizing is impractical, if not impossible.

The correct sizing method therefore should be based on perimeters. The principle of this method is that the outer perimeters of the two parallel endografts must be in contact with either each other or the inner perimeter of the parent lumen for complete seal to occur. As such, appropriate sizing is still dependent on the shape assumed by the two parallel endografts. However, the perimeter of each parallel endograft is maintained regardless of shape and equals π times its native diameter.

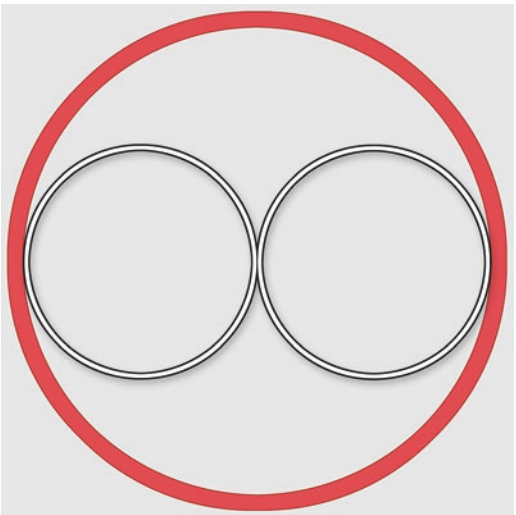


Fig. 43.2 Diameter method of sizing parallel extensions: if the diameter of the parallel extensions are each half of the diameter of the common iliac artery, then the extensions will appose the wall of the parent lumen in only one plane, leaving significant cross-sectional area with the potential for endoleak and continued pressurization of the aneurysm sac. By permission of Mayo Foundation for Medical Education and Research. All rights reserved

The Minimum Combined Length of the Perimeters of the Parallel Extensions

To determine sizing based on perimeters, the geometry of two parallel endografts should be conceptualized in terms of a bisected circle, with the parent lumen representing the circle and the interface of the two parallel extensions with each other representing the plane of bisection. This plane of bisection is "two-ply." In other words, both parallel extensions contribute a portion of their perimeter for the apposition that occurs in this segment. Therefore, the minimum combined length of the perimeters of the parallel extensions is the sum of the perimeter of the parent lumen plus twice the length of the segment where the two parallel extensions appose each other (i.e., the conceptualized plane of bisection, Fig. 43.4).

The Length of the Segment of Apposition Between the Parallel Extensions

Since the segment of apposition of the parallel extensions is "two-ply" and counts double for the minimum combined length of the perimeter, its length is critical in determining sizing requirements. The length of any segment is dependent on its shape, with the shortest length being that of a straight line. For two equally sized parallel iliac extensions, the ideal shape of this segment is a straight line through the center of the parent circle, in other words, a diameter. In this configura-

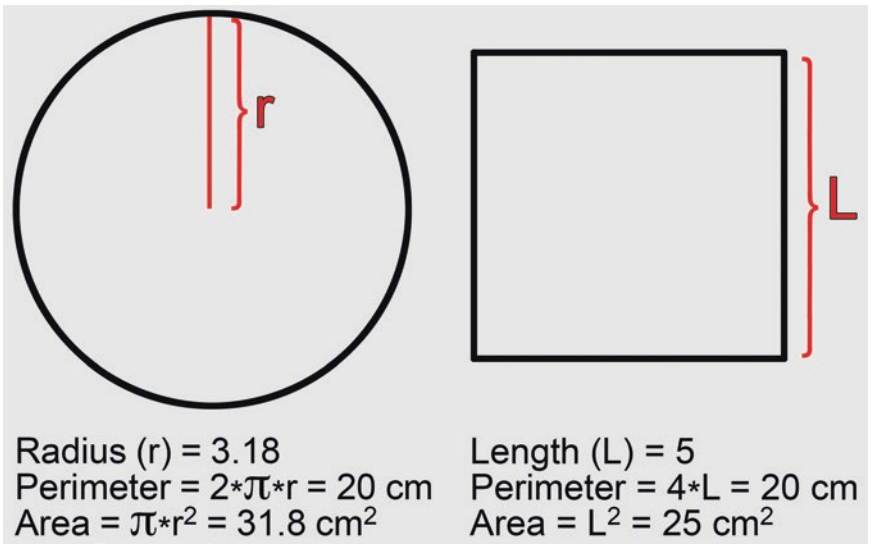


Fig. 43.3 Perimeter versus cross-sectional area: if a perimeter of 20 cm is configured to the shape of a circle with a radius of approximately 3.18 cm, then it will occupy a cross-sectional area of approximately 31.8 cm^2. In contrast, if the perimeter is configured to the shape of a square with 5 cm sides, then it will occupy a cross-sectional area of only 25 cm^2. By permission of Mayo Foundation for Medical Education and Research. All rights reserved

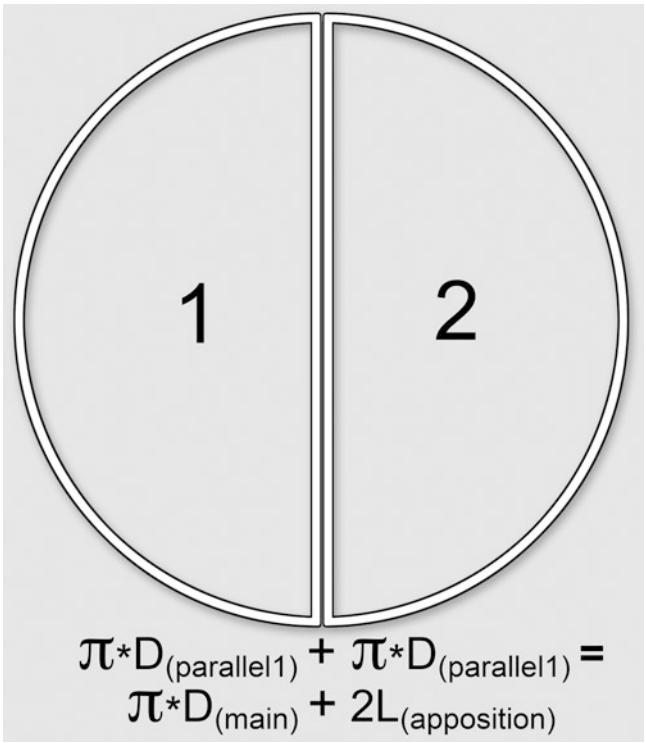


Fig. 43.4 Outer perimeter of the parallel extensions must appose the inner perimeter of the main lumen or each other. Therefore, the minimum combined perimeter of the two parallel extensions equals the perimeter of the main lumen plus twice the length of the segment of apposition, or $L_{(apposition)}$, of the parallel extensions, since it is "two-ply". For two equal-sized parallel extensions, the two-ply segment of apposition equals one diameter of the main lumen or $D_{(main)}$. Therefore, the minimum combined perimeter of the two parallel extensions equals $\pi^*D_{(main)}$ plus $2^*D_{(main)}$. By permission of Mayo Foundation for Medical Education and Research. All rights reserved

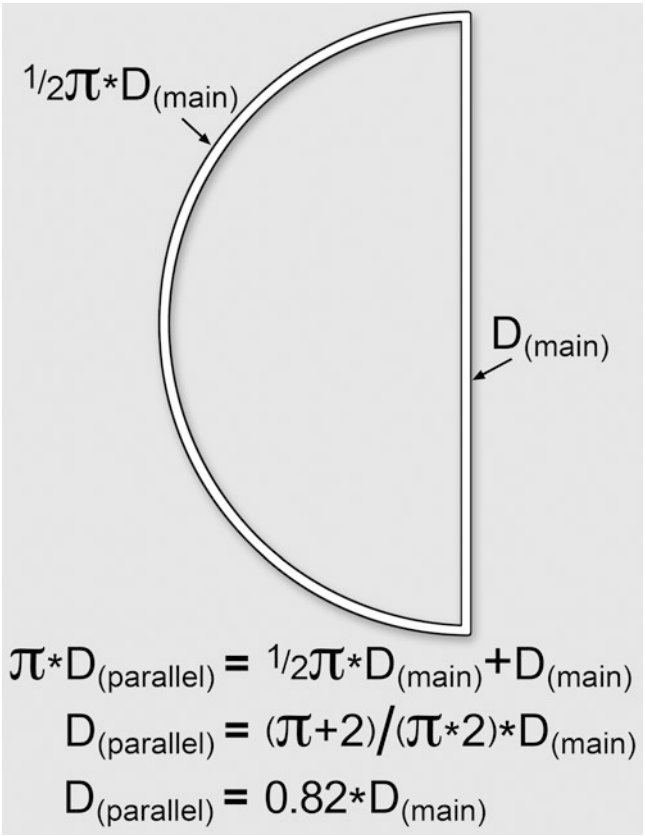


Fig. 43.5 Perimeter of a semicircle equals half the circumference of its parent lumen plus one diameter of the parent lumen. Consequently, the perimeter of a semicircle is approximately 82 % of the perimeter (i.e., circumference) of its parent lumen. By permission of Mayo Foundation for Medical Education and Research. All rights reserved

tion, often referred to as the "double D" configuration, the two parallel extensions assume the shape of back-to-back semicircles. Since the "two-ply" segment is equivalent to a diameter, the combined perimeters (or native circumference) of the parallel extensions must equal the sum of the circumference of the parent lumen plus two times the diameter of the parent lumen. Being of equal size, each parallel extension must equal at least one half the circumference of the parent lumen plus the diameter of the parent lumen. By no coincidence, this is in fact the formula for the perimeter of a semicircle. Mathematically, this means that the diameter of each of the parallel endografts must be a minimum of approximately 82 % of the diameter of the parent lumen (Fig. 43.5) [2].

Returning to our example of a 16 mm common iliac limb, the parallel extensions actually must each have a native diameter of at least 13.1 mm for their perimeters to form an adequately sized semicircle. It should be emphasized that this is the mathematical minimum sizing necessary to achieve full perimeter apposition. Even for a straightforward round shape, most self-expanding stents are designed to be oversized, an additional 10–20 % more than their intended target landing vessel for optimal results.

These sizing requirements can have repercussions. While external iliac extensions are commonly of significant diameter proximally and easily placed, tracking a large stent from a brachial or contralateral approach into the hypogastric can be both difficult and lead to infolding in the target vessel if the hypogastric artery is of normal size. In most cases then, unless the hypogastric artery is ectatic, one probably should not use equally sized parallel extensions.

This asymmetry obviously changes the sizing considerations for the parallel extensions. The parent lumen perimeter is unchanged, but the segment of back-to-back perimeter apposition of the parallel extensions can no longer be a geometric diameter. The effect on sizing depends on the shape of this segment. If this segment remains a straight line that is simply offset from the center, it is referred to geometrically as a chord. A circle's diameter is in fact a chord that passes through its center. All other chords will be shorter than the diameter (Fig. 43.6). Therefore, the minimum com-

bined perimeters necessary for apposition with unequally sized parallel extensions conforming to a chord shape is actually less than that required for equally sized parallel extensions (Figs. 43.7 and 43.8).

Possible Shapes

Of course, a chord is only one possible shape for the segment of apposition of the two parallel extensions. In fact, there are an infinite number of possible shapes that this segment can assume. Since a chord is a straight line, it is the most efficient shape in terms of minimizing sizing requirements, theoretically allowing each of the parallel extensions to be smaller than the parent lumen (see Fig. 43.8). For many of the other possible shapes, at least one of the extensions must be at least as large as the parent lumen. For brevity, we will consider two of these other shapes: rounded and lens shaped.



Fig. 43.6 If the "two-ply" segment of apposition between two parallel extensions is a straight line, then it is referred to as a chord. A diameter, passing through the center of the circle, has a greater length than all other chords. By permission of Mayo Foundation for Medical Education and Research. All rights reserved

The inherent shape of all currently available stent grafts is cylindrical or round. Without any further manipulation, these devices will assume this shape or slightly compressed. At first glance, it may seem easier to simply keep the smaller parallel extension round, since a chord shape requires the graft to fold over on itself (i.e., "out-fold"), forming two acute angles at its "corners." Self-expanding stents are engineered to resist "out-folding" and for all practicality require a chronic overpowering crushing force to maintain them in the folded-over position. To maintain them in a partially folded-over position requires a very delicate balance of complex force vectors that is very difficult to achieve even in vitro. Unfortunately, there is no way to bisect a circle without introducing two acute angles (or four right angles in the case of back-to-back semicircles). Consequently, if the smaller extension is left round, then the bisection plane will need to take the shape of the portion of that stent residing within the interior of the parent lumen, that is, the portion of the perimeter that is not apposing the parent lumen. In this configuration, the two acute angles must now be formed by the external iliac extension, which must also simultaneously wrap around the internal iliac extension (Fig. 43.9). This is an exceptionally complex shape for the external iliac extension to assume, one requiring "out-folding" immediately adjacent to "infolding."

In addition, the round shape of the smaller extension is one of the least efficient in terms of sizing requirements. The "two-ply" bisection plane is now "C"-shaped rather than straight. Consequently, the perimeter of the external iliac extension will now have to be greater than that of the parent lumen. How much greater depends on how much of the internal iliac extension's circumference it must wrap around. If the

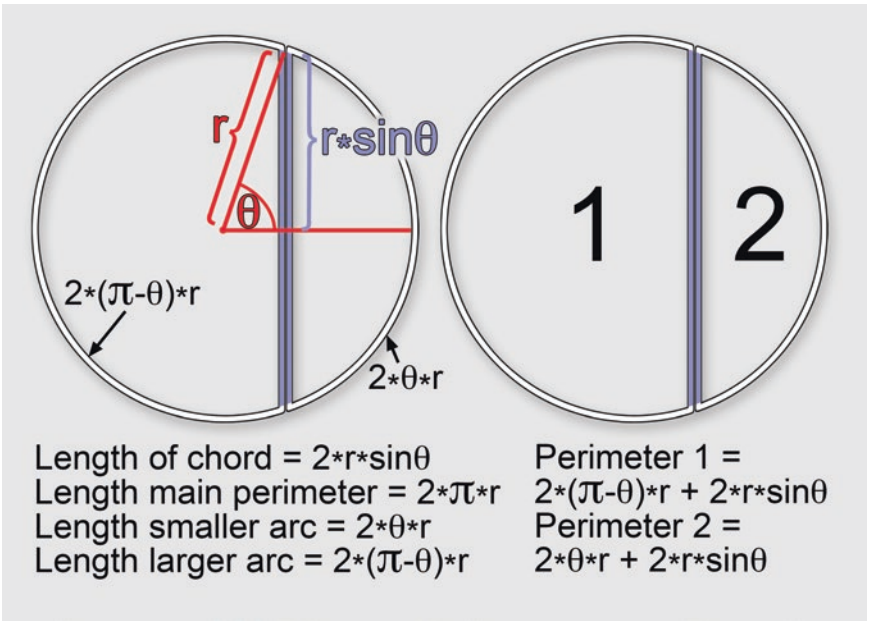


Fig. 43.7 Mathematical formulas for calculating the perimeter of two parallel extensions when the segment of apposition between the two parallel extensions is the shape of a chord. By permission of Mayo Foundation for Medical Education and Research. All rights reserved

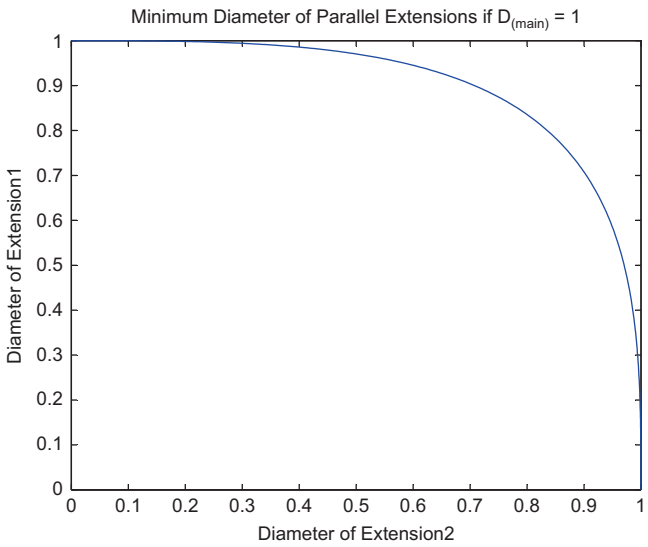


Fig. 43.8 Relationship of the perimeters of parallel extensions to the perimeter of the parent lumen when the segment of apposition between the two parallel extensions is the shape of a chord, based on the formulas from Fig. 43.7. Note that as the asymmetry between the parallel extensions increases, the amount of required combined perimeter decreases. By permission of Mayo Foundation for Medical Education and Research. All rights reserved

internal iliac extension were to remain perfectly round, it would only come into contact with the parent lumen at one point, and the external iliac extension would have to nearly completely envelope the internal iliac stent for seal. Realistically, though, the internal iliac extension will mold enough that the external iliac extension will need to wrap around 65–75 % of the internal iliac extension's circumference. While mathematically this usually corresponds to only an additional few millimeters of oversizing compared to the parent lumen, the complexity of the geometry increases the sizing requirements well beyond the mathematical minimums. Additional oversizing is required because the mathematical minimums assume that the external iliac extension will deploy in such a manner that all of its excess perimeter will be utilized to wrap around the internal iliac extension and fold over on itself to fill in the gaps in apposition between the internal iliac extension and the parent lumen. However, as alluded to above, this scenario is unrealistic and this complex shape may not even be possible. In fact, benchtop studies show that even with 40 % oversizing compared to the parent lumen, the external iliac limb will not fully wrap around its smaller counterpart, leaving gutters, and begin to exaggerate the infolding [3].

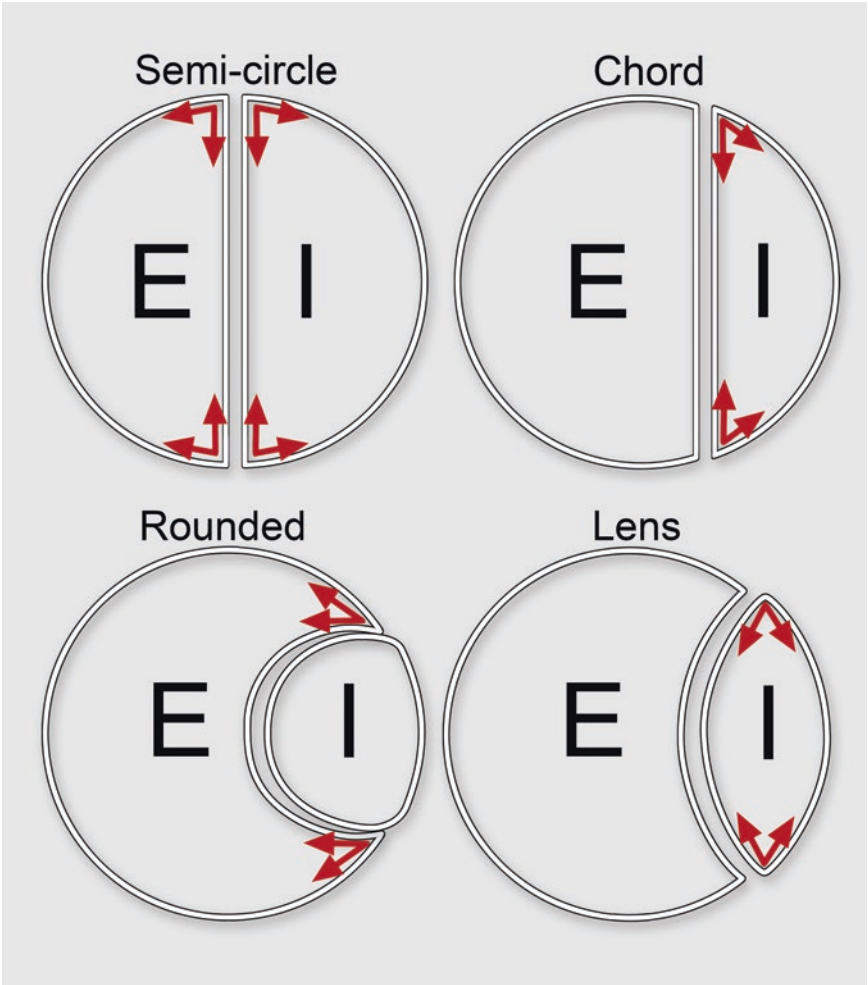


Fig. 43.9 Bisecting a circle into two shapes must introduce at least two acute angles or four right angles. Note that a rounded shape for the internal iliac extension will require that the external iliac extension assume an exceptionally complex shape with increased perimeter requirements. By permission of Mayo Foundation for Medical Education and Research. All rights reserved

The Effect of Angioplasty

A common misconception is that the gutters can be overcome by standard balloon angioplasty. Since the basic effect of balloon angioplasty is to expand the stent outward, one might incorrectly conclude that balloons can force portions of stents to expand into the crevices of the gutters. However, the outward forces of the balloon are symmetrical and will instead act to eliminate any folds or irregularities. In fact, most balloons come packaged with folds to minimize crossing profile, but become round at minimal inflation pressures. Granted, if inflated in an irregular lumen, a balloon will initially conform to that lumen until its inflation pressure overcomes the rigidity of the lumen. Further, a compliant balloon has less ability to overcome this rigidity and is therefore more likely to maintain conformation to an irregular lumen. However, for parallel endografts, the balloons are not inflated directly inside the parent lumen, but rather inside the inherently round extensions. This distinction causes any balloon used for seating of the extensions to perform like an ultra noncompliant balloon wrapped by the graft material of the extensions, similar to the effect of wrapping the balloon with a Kevlar coating. Accordingly, the parallel extension containing the inflated balloon will behave similar to a Kevlar coating and become more round with increasing inflation pressures. As such, it is not clear whether standard post-deployment ballooning after parallel endografting using two self-expanding stent grafts is helpful or harmful.

Despite all of these limitations, one should not necessarily conclude that gutters are an inescapable consequence of parallel endografts. Consider the alternate scenario of a lens-shaped internal iliac extension. In geometry, a lens is the shape formed by two arcs joined at their endpoints. This shape might also be described as football or eye shaped. If the lens is symmetric, then the two arcs will have equal lengths (Fig. 43.10). The "two-ply" bisection plane will be along the interior arc and will also have this same length. Therefore, the total combined perimeter of the two parallel stents will equal the perimeter of the parent lumen plus two times the length of the arc segment forming the lens shape. Subtracting out the perimeter of the lens (i.e., two times the length of the arc segment) means the perimeter of the external iliac extension must equal the perimeter of the parent lumen. In other words, since the "two-ply" bisection plane has the same total length as the lens-shaped internal iliac extension, the external iliac extension should be sized as though there were no internal iliac extension. In addition, the external iliac extension does not have to form any acute angles to conform to its counterpart.

The internal iliac extension, on the other hand, will need to form acute angles at each of its apices. While this is unlikely with self-expanding stents and standard angioplasty, it is fairly easily achieved with balloon-expandable stents and more sophisticated angioplasty.

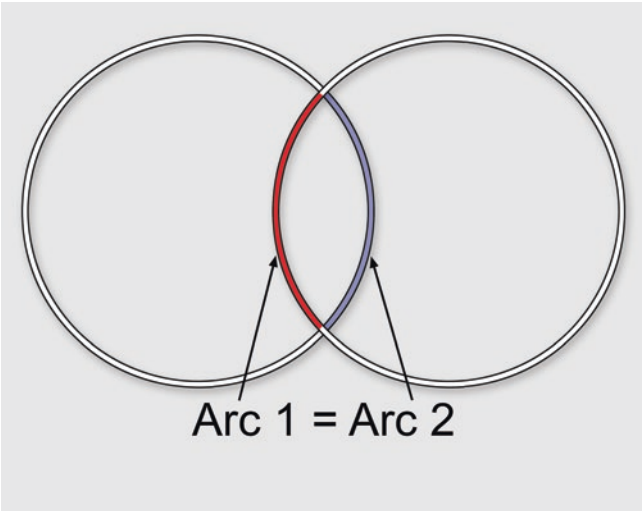


Fig. 43.10 Symmetrical lens is comprised of two arcs of the same length. The net effect is that arcs will subtract out and the perimeter sizing requirements of the counterpart parallel graft will be the same as if the lens-shaped extension were absent. In other words, it will need only to be at least as big as the parent lumen. By permission of Mayo Foundation for Medical Education and Research. All rights reserved

Specifically, the "eye of the tiger" technique can be used to mold a balloon-expandable stent graft to a desired shape that will facilitate seal without compromising lumen [4]. In this technique, post-dilation of the deployed stent provides the internal force to temporarily increase the diameter in all axes of the stent. Dilation of the other parallel endograft then provides the external force to crush the target stent. Reinflation of the original sized balloon (or smaller) in the crushed stent provides the internal force specifically to the central portion of the stent to create a short axis and the eye shape for which the technique is named (Fig. 43.11).

The maneuver of temporarily crushing the stent achieves three objectives. First, it establishes complete apposition of all perimeters. Second, it creates a single long axis in the stent. Third, it places two folds in the stent that will provide the basis for acute angles to fill in any potential gutters. The end result is a lens-shaped internal iliac extension with a long axis equal to the diameter of the balloon used to overdilate and a short axis equal to the diameter of the balloon used for the final inflation. We generally aim to keep the ratio of the short axis to the long axis at approximately 1.6 (φ).

To better illustrate the specifics of this technique, consider again our example a 16 mm common iliac extension and 8 mm external and internal iliac arteries. An 8 mm balloon-expandable covered stent is advanced antegrade into the internal iliac, and standard iliac extension is advanced retrograde partially into the common iliac stent (Fig. 43.12). Currently, the only available balloon-expandable option in the USA is the Maquet iCast. We would use the 8 × 59 mm option. There are more available options for the external iliac extension, but its proximal diameter must be at least as big as

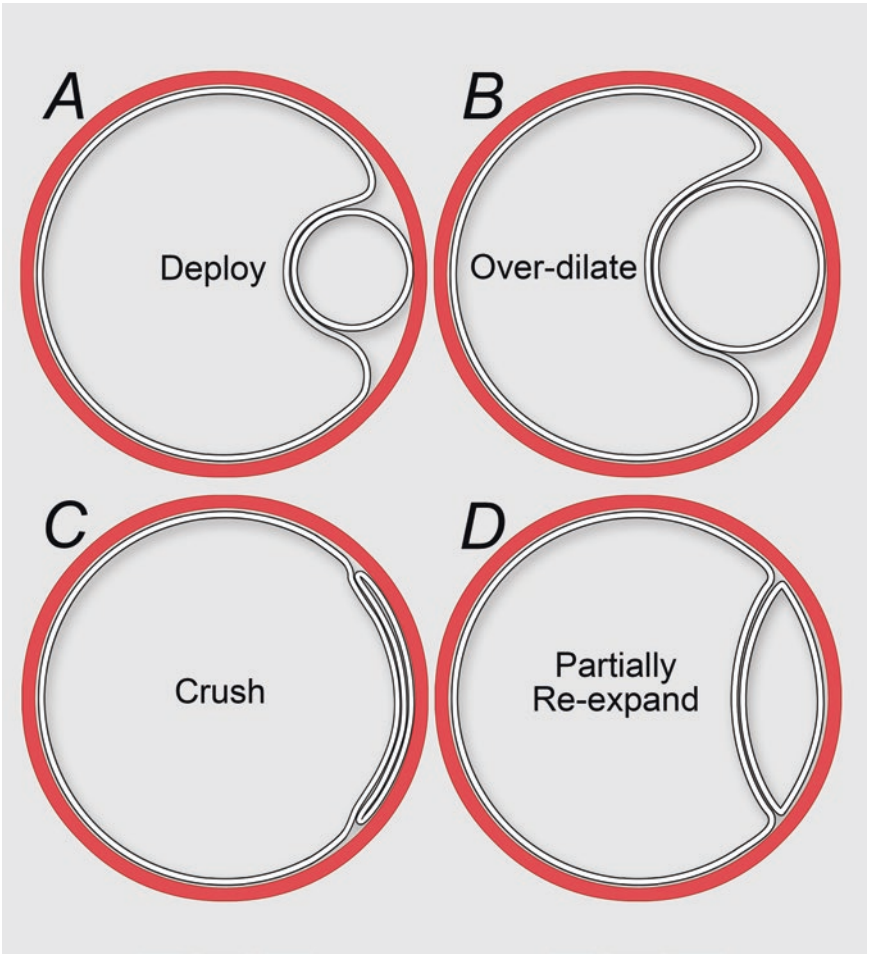


Fig. 43.11 Molding a lens-shaped stent. (**a**) Begin with balloon-expandable parallel stent. (**b**) Overdilate to the desired length of the final long axis. (**c**) Crush the stent by dilating the counterpart stent. (**d**) Re-expand the central portion with the original balloon (or smaller). By permission of Mayo Foundation for Medical Education and Research. All rights reserved

the common iliac extension (in this example, 16 mm.) A good option is the AFX 20-13-80 for many reasons. First, its proximal diameter is 20 mm, providing some slight oversizing. Second is that it exerts a low radial force, minimizing the chances of late compression on the internal iliac stent. Finally, the "active seal" technology may provide at least a theoretical advantage in terms of conforming to any luminal irregularities and sealing off potential gutters. We aim for a standard overlap of 3 cm between the external iliac extension and the common iliac limb. The internal iliac extension should be deployed with 2–3 additional millimeters of overlap to ensure that its proximal end does not get covered by the external iliac extension. The parallel portion of the internal iliac extension is then post-dilated to 10 mm and the balloon exchanged for a 6 mm balloon. The external iliac limb is then aggressively seated with a large balloon to crush the internal iliac stent. The 6 mm balloon is then inflated to create the lens shape. Low-pressure kissing angioplasty (~2 ATM) is then performed for the final seating. If there is a leak on interim angiography, then we would exchange for a smaller internal iliac balloon (e.g., 5 mm) and repeat the kissing angioplasty. This maneuver will decrease the short axis of the lens shape making it closer to a chord shape, decreasing the sizing requirement for the external iliac extension (Fig. 43.13). If there is still a leak, then we would increase the overlap of the stents.

Finally, any time one extends into the external iliac artery, it is important to ensure that the distal end of the stent graft does not terminate in an area of significant tortuosity, which could result in a reverse "bird-beaking" effect and compromise the outflow of the stent. In these scenarios, the vector of flow of the stent can end up being nearly perpendicular to the vector of flow in the artery, leading to obstruction of flow similar to the mechanism in a ball valve. This situation is often masked by the intraoperative straightening effect of large sheaths and stiff wires. Therefore, a final confirmatory angiogram should be performed with only a floppy wire or catheter in place using an oblique view. If there is any concern, then the external iliac limb should be extended through the tortuosity with a bare stent (Fig. 43.14).

Conclusion

Parallel stent-graft techniques have broadened the indications of EVAR and should be in the armamentarium of physicians performing complex endovascular repairs. The "eye of

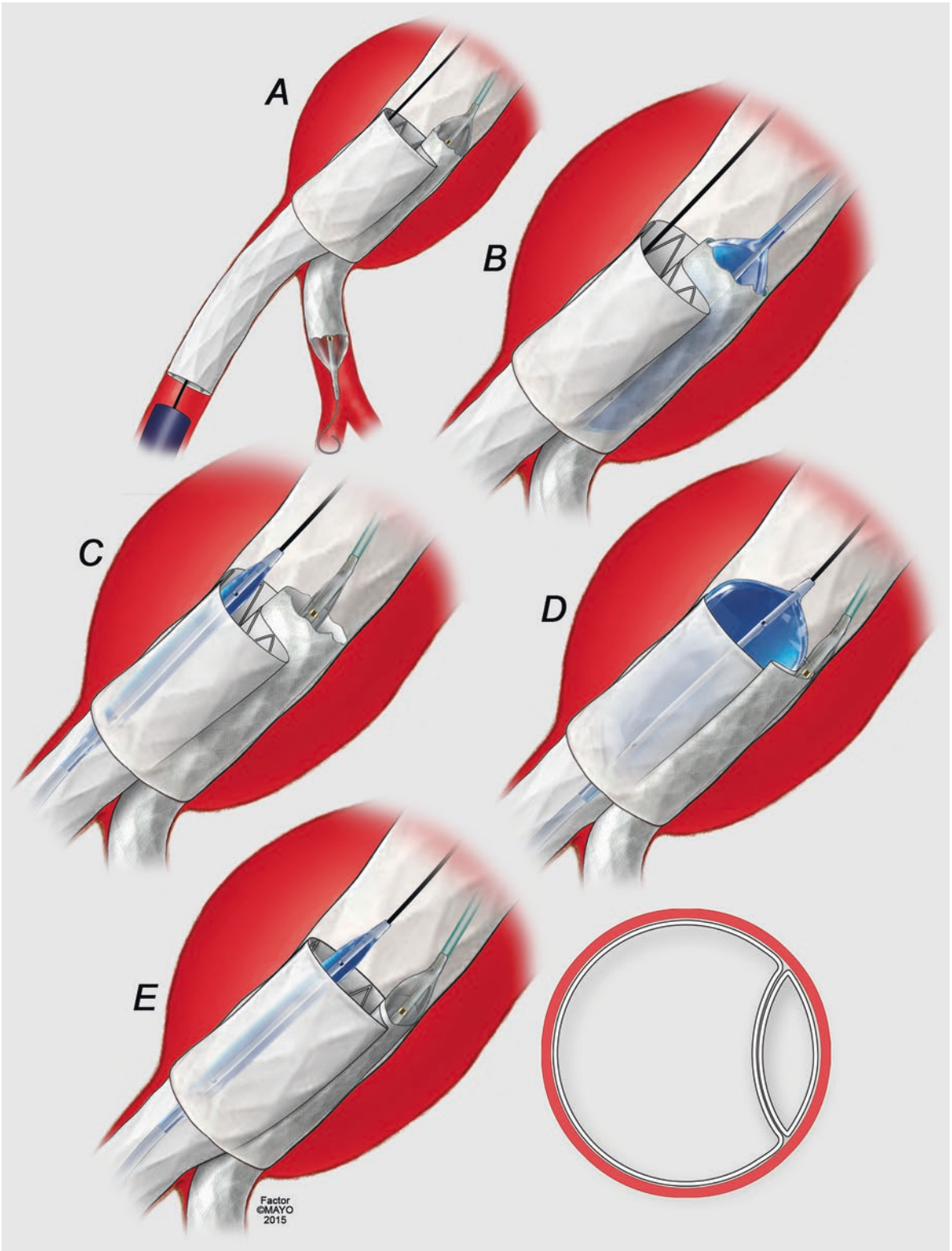


Fig. 43.12 Employing the "eye of the tiger" technique for hypogastric preservation. (**a**) A balloon-expandable stent graft is deployed extending antegrade into the internal iliac an in parallel to a standard external iliac extension. The internal extension should be sized to the diameter of the internal iliac artery and deployed 2–3 mm more proximal to the external iliac extension. The diameter of the proximal portion of the external iliac extension should be at least that of the parent common iliac limb. (**b**) The parallel (proximal) portion of the internal iliac limb is overdilated to the desired length of the long axis of the lens shape. (**c**) In preparation for the next step, the original (or smaller) balloon is reinserted in the internal iliac extension while a large seating balloon is advanced into the external iliac extension from the ipsilateral femoral access. (**d**) The external iliac balloon is then inflated to temporarily crush the internal iliac limb, creating full apposition of all perimeters and eliminating any gutters. (**e**) The internal iliac balloon is then inflated to re-expand the central portion of its stent and create the lens shape, and the two stents are seated with kissing angioplasty. If a leak is identified on interim angiography, then steps C through E can be repeated using a slightly smaller internal iliac balloon to create more of a chord shape. By permission of Mayo Foundation for Medical Education and Research. All rights reserved

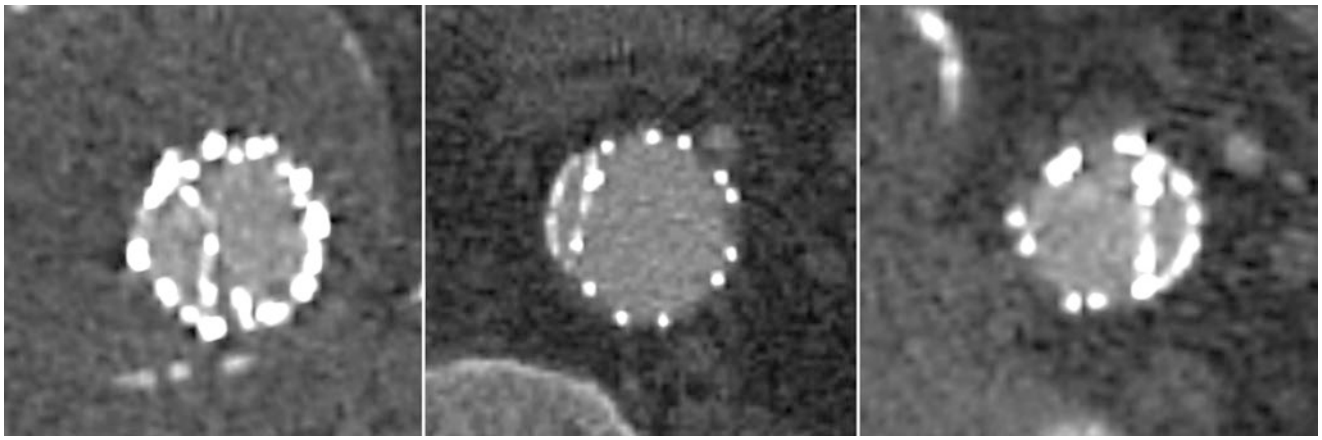


Fig. 43.13 Examples of parallel endografts using various lens and chord shapes to eliminate any gutters and potential for endoleak

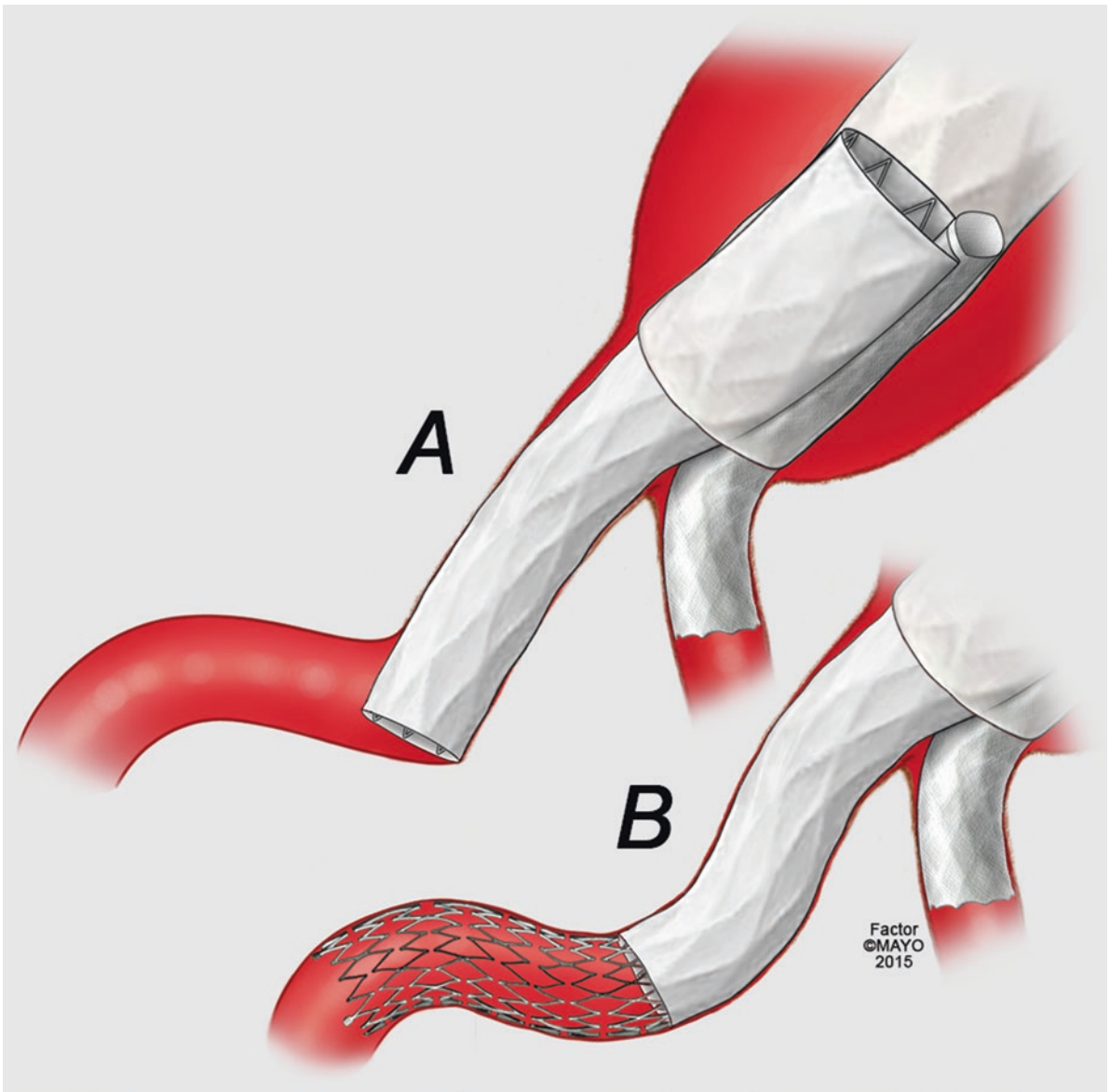


Fig. 43.14 (**a**) Patency of any external iliac extension can be compromised if tortuosity results in malalignment of the extension to the vector of flow in the native artery. This situation is often only apparent after the stiff guide wires are removed. (**b**) Correction is achieved by extending with a bare metal stent, preferably beyond the angulated segment. By permission of Mayo Foundation for Medical Education and Research. All rights reserved

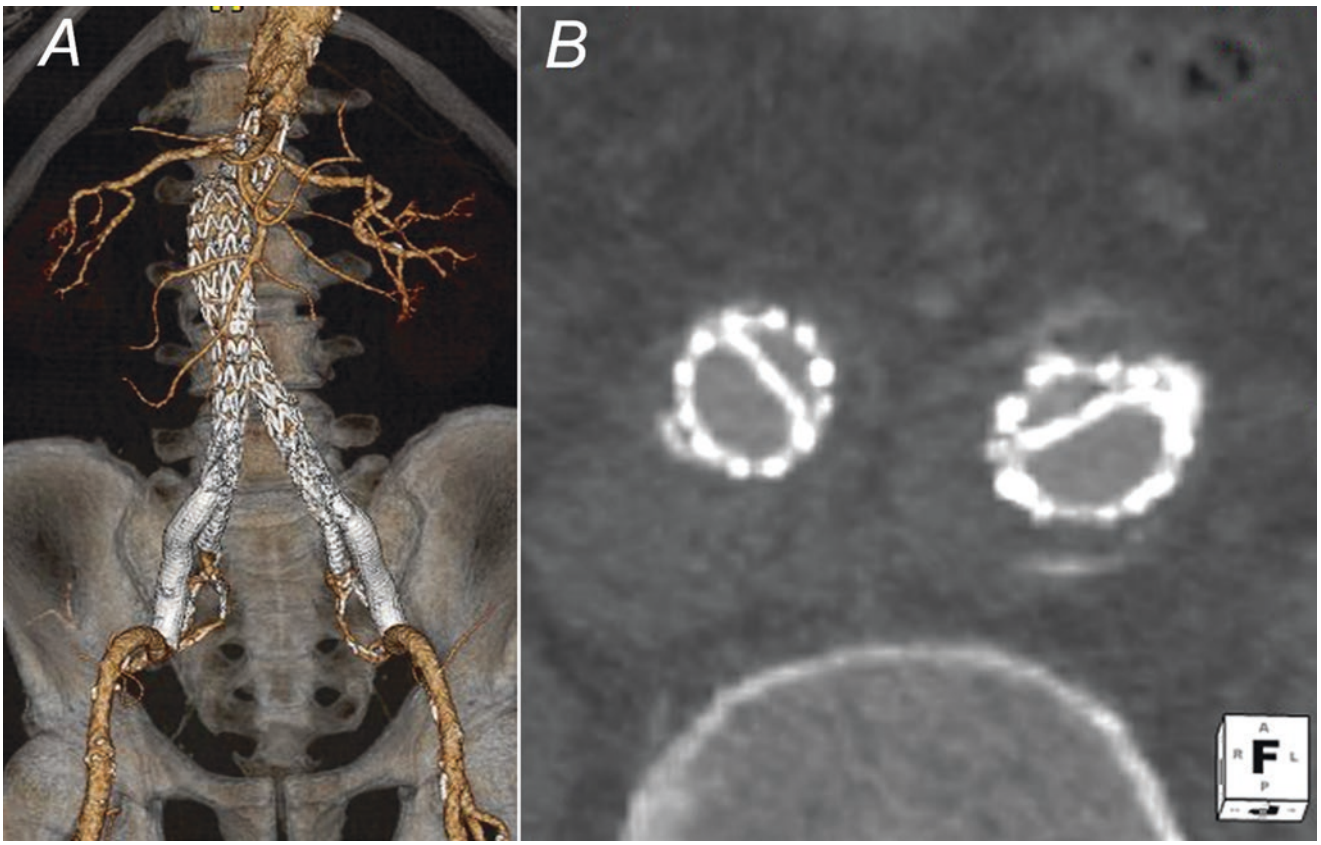


Fig. 43.15 Computed tomography angiography of a patient treated with bilateral parallel stent grafts (**a**) using the "eye of the tiger" technique (**b**). By permission of Mayo Foundation for Medical Education and Research. All rights reserved

the tiger" technique as herein illustrated (Fig. 43.15) allows optimal apposition of the parallel stents and may decrease rates of gutter endoleaks.

References

1. Lobato AC. Sandwich technique for aortoiliac aneurysms extending to the internal iliac artery or isolated common/internal iliac artery aneurysms: a new endovascular approach to preserve pelvic circulation. J Endovasc Ther. 2011;18(1):106–11.
2. Reijnen MM, Minion DJ, Lardenoye JW. Treatment of a type IIIb endoleak in a talent endograft using telescoping cuffs and two parallel upside-down excluder contralateral legs. J Vasc Surg. 2012;56(2):538–41.
3. Mestres G, Uribe JP, García-Madrid C, Miret E, Alomar X, Burrell M, Riambau V. The best conditions for parallel stenting during EVAR: an in vitro study. Eur J Vasc Endovasc Surg. 2012;44(5):468–73.
4. Minion DJ. Molded parallel endografts for branch vessel preservation during endovascular aneurysm repair in challenging anatomy. Int J Angiol. 2012;21(2):81–4.

Part VII

Physician-Modified Endovascular Stent-Grafts

44 Clinical Applications and Regulatory Issues for Physician-Modified Endovascular Grafts (PMEGs)

Jessica P. Simons and Andres Schanzer

Introduction

In response to the early recognition of inadequate proximal neck length as a major limitation for endovascular aneurysm repair, several design modifications were made by manufacturers. The most radical of these modifications was the inclusion of fenestrations for preservation of renal and mesenteric vessel perfusion in order to increase proximal seal zone length (Fig. 44.1) with the first such case reported in 2001 by John Anderson [1]. Soon thereafter, in 2006, Uflacker et al. described the back-table modification of commercially available devices to treat pararenal aneurysms (Fig. 44.2). In this report, the authors noted that physician-modified endovascular grafts (PMEGs) filled an unmet need because commercially manufactured custom-made device alternatives were in short supply and often required many weeks for delivery [2]. With promising early results, the authors suggested that PMEG complements commercially made devices "when the interventionalist does not have access to the commercially available devices or the waiting time is too prolonged to accommodate the patient's clinical situation" [2]. While the exact role for PMEG remains incompletely defined, it is clear that this is a high-risk intervention. The Society for Vascular Surgery (SVS) issued an advisory statement in 2013, noting that both institutional review board (IRB) and investigational device exemption (IDE) approvals are required for the use of PMEG [3].

The statement from SVS also acknowledges that PMEG may be used in an emergency without these additional requirements. And, in fact, several reports of PMEG have been published, without formal approval or oversight, such as an IDE, from a governmental agency [2, 4, 5]. Despite the seeming contradiction, the rationale for involvement of the US Food and Drug Administration (FDA) was clarified in the same journal issue by Abel and Farb [6]. The FDA requires conduct of studies of significant risk devices (such as PMEG) under the IDE mechanism in order to accurately capture and report data and outcomes to ensure safety and effectiveness. According to the FDA, the amount of oversight required (an IDE rather than just local IRB approval) is a function of the degree of risk imposed by the intervention. Aortic endografts are considered "significant risk" devices, since they "present the potential for serious risk to the health, safety, or welfare of a patient" [6]. PMEG treatment is both an off-label use and a significant risk device and therefore requires FDA approval in the form of an IDE, in addition to institutional IRB approval.

Obtaining an IDE

The decision to pursue an application for an IDE through the FDA entails a significant commitment not only to the treatment of patients with complex aortic disease but also to the rigorous study and reporting of outcomes of these interventions. The FDA website provides several important resources: http://www.fda.gov/MedicalDevices/DeviceRegulationandGuidance/HowtoMarketYourDevice/InvestigationalDeviceExemptionIDE/default.htm

In an invited review published by the Journal of Vascular Surgery in 1999, Pritchard et al. from the FDA described the process for obtaining an IDE [7]. They credit the parent legislation, the Federal Food, Drug, and Cosmetic Act, for recognizing the need to exempt certain devices and techniques from standard requirements in order "to encourage, to the extent consistent with the protection of public health and safety and with ethical standards, the discovery and development of useful devices intended for human use, and to that end to maintain optimum freedom for scientific investigators in their pursuit of this purpose" [8]. Rather than limiting physicians in their ability to innovate new methods for treating patients, the FDA seeks to provide a framework to support such innovation and augment it with rigorous clinical

J.P. Simons • A. Schanzer (✉)
Division of Vascular and Endovascular Surgery, University of Massachusetts Medical School,
55 Lake Ave North, S3-824, Worcester, MA 01655, USA
e-mail: Andres.Schanzer@umassmemorial.org

© Mayo Foundation for Medical Education and Research 2017

G.S. Oderich (ed.), *Endovascular Aortic Repair*, DOI 10.1007/978-3-319-15192-2_44

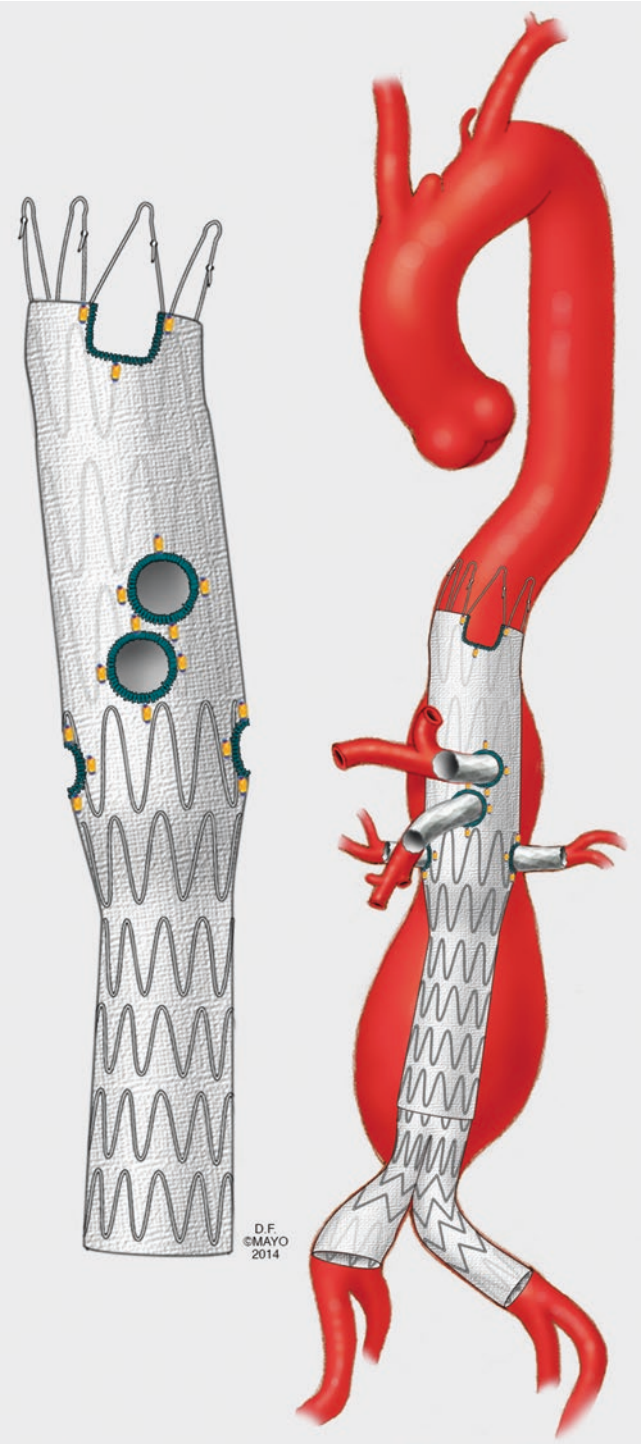


Fig. 44.1 Fenestrated endograft with branches for the celiac, superior mesenteric artery, left and right renal arteries. By permission of Mayo Foundation for Medical Education and Research. All rights reserved

investigation and informed consent to maximize the derived benefit to the public.

The first step in the process of successfully obtaining an IDE is proactively identifying those aspects of the device investigation that the FDA will specifically want addressed in the IDE. This pre-IDE process is somewhat more informal than the IDE application itself, but is no less well recognized by the FDA as a routine and valuable interaction with the sponsor of the device investigation. The pre-IDE process was well described by Pritchard et al. [7]. In brief, the pre-IDE submission should define the device under study, its intended use, the intended patient population, the testing plan including potential safety and effectiveness issues, the testing methodologies, and all reports (supportive and adverse) of prior investigations. The resultant investigational plan contains a detailed rationale, protocol, risk analysis, and intended duration of study. A thorough pre-IDE preparation can simplify the IDE application process to a great extent. It was our group's experience that early and frequent interactions with the FDA were invaluable for the successful design, preparation, and ultimate approval of an IDE application. The FDA is committed to helping investigators navigate the IDE process, and this is made completely evident through their willingness to engage in the pre-IDE process. For complete information on the elements required for an IDE application, the reader is referred to the FDA website: http://www.fda.gov/MedicalDevices/DeviceRegulationandGuidance/HowtoMarketYourDevice/InvestigationalDeviceExemptionIDE/ucm046706.htm. An additional useful resource is the published description, by Dr Starnes et al., on the steps required to obtain an IDE for PMEG at his institution (Table 44.1).

Conducting an IDE Clinical Trial

The commitment required to gain approval for an IDE clinical trial corresponds well to the commitment required to subsequently administer and treat patients within the IDE clinical trial. The IDE application requires careful delineation of the treatment protocol and the necessary infrastructure to rigorously monitor and implement that treatment protocol. While precise details vary according to the specific IDE plan, in general, certain internal and external resources will be required.

A clinical research coordinator and/or research assistants are critical to provide the necessary infrastructure to successfully implement the IDE clinical trial. The required logistics include, and are not limited to, obtaining informed consent, coordinating required follow-up studies and visits, data collection, record keeping, tracking of all devices used, and frequent interactions with the FDA. For our group's physician-sponsored IDE clinical trial evaluating the safety and efficacy of utilizing branched and fenestrated PMEG and custom-made commercial devices for the treatment of complex aortic aneurysms, we employ a research coordinator (nurse practitioner), a program coordinator (nurse practitioner), and a research assistant. Every patient's data are captured on 42 pages of scannable data forms that automatically input into a secure database (Fig. 44.3).

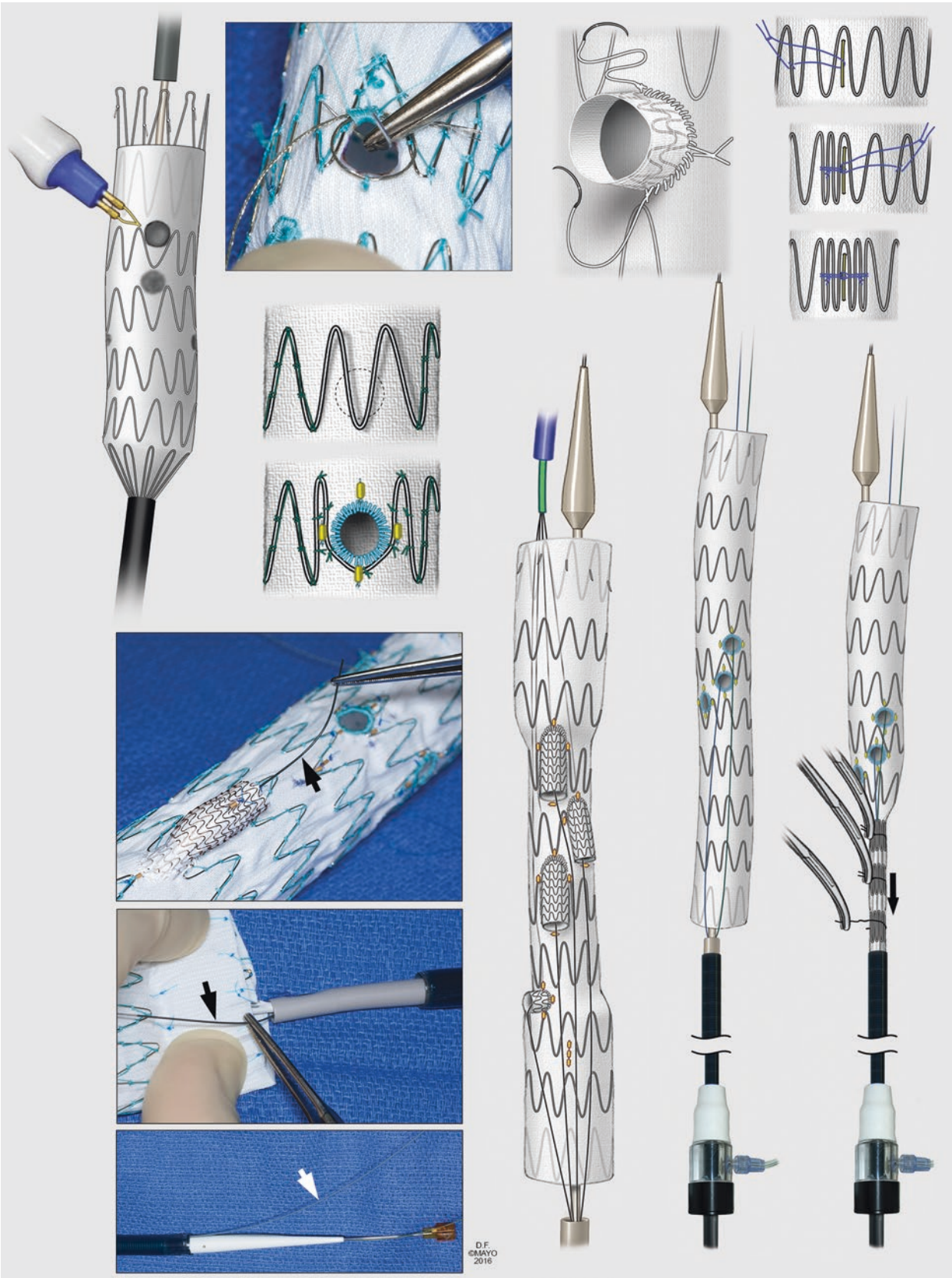


Fig. 44.2 Pre-procedure back-table modification including fenestration and re-sheathing of device. By permission of Mayo Foundation for Medical Education and Research. All rights reserved

Table 44.1 Steps for obtaining an IDE at the University of Washington

Steps for obtaining an IDE
1. Review FDA website for the appropriate submission format to use http://www.fda.gov/MedicalDevices/default.htm
2. Write protocol and obtain references and justification for why this study is being proposed
3. Request trusted colleagues to review the protocol for accuracy and readability
4. After protocol is written, write case report forms (CRFs)
5. Submit protocol to the IRB, and at the same time, request in-person meeting to present directly to them. With non-sponsored studies, the IRB may have questions and it is easier to answer them in person rather than to have to delay the approval due to additional queries. This may not be possible with all IRBs, but it does help pave the way to approval
6. Obtain conditional approval from the IRB meaning that the study cannot begin until FDA approval is obtained, and the FDA amended protocol is resubmitted to the IRB
7. Submit an IRB conditional approval letter and pre-IDE application to the FDA. Follow guidelines on the FDA.gov website
8. Once comments and suggestions are received back from the FDA, submit full IDE application to the FDA. One must follow new IDE submission requirements or one will have a delay in getting approval
9. The budget can be done at any time. If one needs buy-in from the institution, start this process after the protocol and case report forms are written (the coordinator/budget personnel will have a better idea of the time involved if they have two sets of documents)
10. Once FDA approval is received, submit the approval letter to the IRB for their final approval. One may get approval to start the study, but there may be requested changes or corrections to make to the protocol
11. Once the IRB approval is received, submit this document back to the FDA. The initial FDA approval letter will state that the investigator can begin the study after the FDA has received the final approval from the host institution IRB and the FDA has acknowledged receipt of this approval
12. Submit CMS part A and part B. Currently, part A can be submitted electronically, but part B needs to be sent in paper form. Part B will not be approved until part A approval is received. We recommend simultaneous submitting, part A electronically and part B in paper form. Once part A approval is received, part A approval letter can be sent to part B personnel.

Reprinted from Journal of Vascular Surgery, 57(3), Benjamin W. Starnes, A surgeon's perspective regarding the regulatory, compliance, and legal issues involved with physician-modified devices, 829–831, Copyright 2015, with permission from Elsevier



Fig. 44.3 Example of regulatory binder with IDE and scannable case report forms for data capture on enrolled patients

A study monitor is required as part of written standard operating procedures within an IDE clinical trial. Monitoring includes, but is not limited to, the review of informed consent documents, patient records to verify all data are collected according to the protocol, and adverse event data. The study monitor ensures that all clinical research is conducted in compliance with federal regulations and institutional IRB policies. The monitoring group may also coordinate activities for adjudication of major and/or serious adverse events and endpoints in the IDE design (clinical events committee (CEC)). Also, an independent centralized image analysis core laboratory is customary to ensure third party, impartial, evaluation of relevant imaging studies obtained as part of the study protocol.

As part of conducting an IDE clinical trial, the investigators are required to provide periodic reports to the governing IRB and to the FDA on an annual basis. In addition to the required annual reporting, interim progress reports to the FDA may be required, potentially as frequently as after each fifth patient completes the 30-day post-procedural follow-up ("FDA-enhanced reporting"). These interim reports provide a comprehensive picture of the IDE's progress, including information on the number of patients enrolled and treated, information on observed adverse events for each patient, and documentation of "lessons learned" by the investigator that might influence future conduct of the study.

While the conduct of an IDE study requires significant time and resources, it does allow for the potential for reimbursement for the device implantation. A PMEG procedure conducted without an IDE would not be considered for reimbursement according to the Health Care Financing Administration (HCFA). However, once an IDE has been obtained, the FDA will designate the proposed device as either an experimental or nonexperimental investigational device [7]. In the past, PMEG within an IDE setting has been classified as nonexperimental and, thus, is eligible for coverage by Medicare.

Patient Selection for PMEG

The decision to treat a patient with complex aortic disease with a PMEG will always remain at the discretion of the treating provider. While outcomes published to date have been initially favorable, longer-term follow-up is required, as are larger series with prospective data collection. Oderich and Ricotta reported their experience at the Mayo Clinic with PMEG in 2009 [9]. In their series of 30 patients, 47 % with thoracoabdominal aneurysms, for a total of 85 fenestrations, branch stenting success was 98 %, with one perioperative death and a complication rate (not further specified) of 37 %. In this study, median follow-up was 14 months, with 1-year branch patency of 97 % and freedom from endoleak of 88 %.

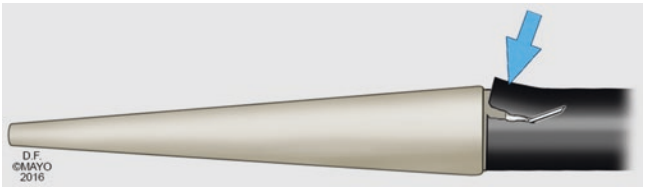


Fig. 44.4 Stent-barb-induced damage to the device delivery sheath. By permission of Mayo Foundation for Medical Education and Research. All rights reserved

In 2012, Starnes et al. described their outcomes on a retrospective series of 47 consecutive patients with juxtarenal aneurysms treated with PMEG [10]. Technical success was 98 %, with a total of 82 fenestrations, and a perioperative mortality of 2 %. There was a 13 % complication rate including one stroke and one permanent renal failure. Median follow-up was 607 days, with three deaths occurred during the first 2 years of follow-up. In 2013, Starnes [11] published a prospective series of 26 patients with juxtarenal aneurysms treated with PMEG within the University of Washington IDE [12]. For a total of 63 fenestrations, one renal artery was not able to be stented, and there was one perioperative death (3.8 %). Major complications occurred in 11.3 %, including respiratory failure leading to death in one patient. Among eight patients with 1-year follow-up, seven had aneurysm sac shrinkage (87.5 %).

Ricotta and Tsilimparis reported their experience in 2012 with PMEG in 12 patients (67 % thoracoabdominal aneurysms) [13]. Of 33 fenestrations and 2 scallops, technical success with target vessel revascularization was 97 %, and the perioperative mortality was 8 %. Complications occurred in 42 %, including three early reinterventions. At mean follow-up of 9 months, there were two non-aneurysm-related deaths.

Despite these promising early results, some points of caution should be noted. First, none of these series compares outcomes between commercially manufactured custom-made devices with PMEG. There are some notable limitations to PMEG compared with custom-made devices. First, there is a potential decrease in quality control that can be achieved with physician modification compared to commercially manufactured devices. Despite refinements in technique, re-sheathing the device can be difficult, resulting in device flaws such as stent-barb-induced damage to the delivery sheath (Fig. 44.4).

There is also a limited capacity for device customization since the inventory is limited to commercially available devices intended for other applications. For example, off-the-shelf devices have a limitation on the amount of tapering that occurs over the length of the device; this can lead to compromises when choosing devices. In the example shown in Fig. 44.5, the smallest diameter tubular stent-graft available was used to seal into a previously placed, significantly smaller diameter, surgical graft. This resulted in significant infolding of the implanted device and subsequent endoleak.

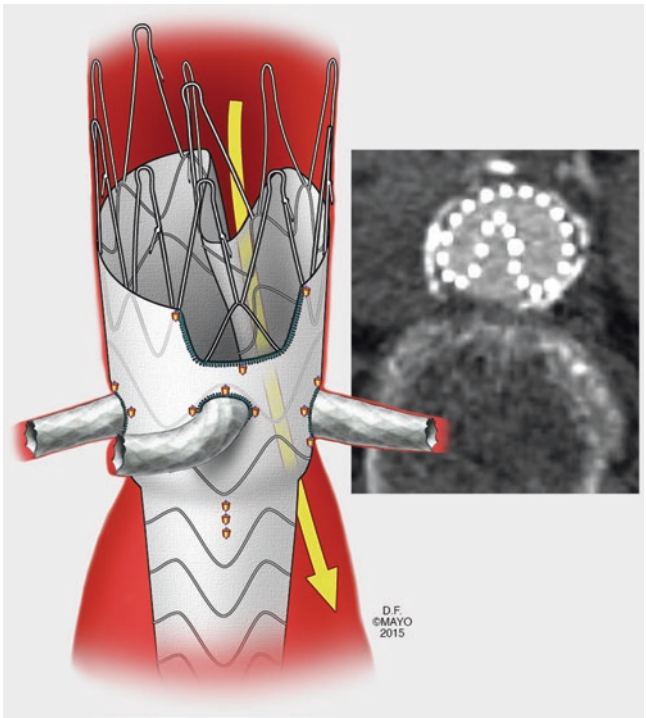


Fig. 44.5 Infolding of endograft due to size mismatch with previously placed surgical graft. By permission of Mayo Foundation for Medical Education and Research. All rights reserved

Given these considerations, the clinical application for PMEG will likely remain for those patients in need of urgent or emergent treatment for complex aortic disease, who are not otherwise candidates for open repair [10, 12–14].

Conclusion

In conclusion, PMEG represents an important innovation, with favorable initial results, in the treatment of patients with complex aortic disease who may not otherwise be a candidate for open repair. In addition, it remains a promising option for high-risk patients in need of urgent repair, who cannot wait for a commercially manufactured custom-made device. While the use of a high-risk commercially available device for off-label use, such as PMEG, ultimately remains at the discretion of the provider, the routine application of such techniques is discouraged outside of an FDA-approved IDE. The decision to apply for an IDE requires sincere dedication not only to these complex patients but also to the rigorous scientific process associated with such clinical investigation. Ultimately, data obtained from well-constructed IDE trials will facilitate evidence-based treatment to maximize the benefit to the public.

References

1. Anderson JL, Berce M, Hartley DE. Endoluminal aortic grafting with renal and superior mesenteric artery incorporation by graft fenestration. J Endovasc Ther. 2001;8(1):3–15.
2. Uflacker R, Robison JD, Schonholz C, Ivancev K. Clinical experience with a customized fenestrated endograft for juxtarenal abdominal aortic aneurysm repair. J Vasc Interv Radiol. 2006;17(12):1935–42.
3. White RA. Advisory statement on clinical use of modified aortic endografts from the Society for Vascular Surgery(R). J Vasc Surg. 2013;57(3):832–3.
4. Park JH, Chung JW, Choo IW, Kim SJ, Lee JY, Han MC. Fenestrated stent-grafts for preserving visceral arterial branches in the treatment of abdominal aortic aneurysms: preliminary experience. J Vasc Interv Radiol. 1996;7(6):819–23.
5. Faruqi RM, Chuter TA, Reilly LM, Sawhney R, Wall S, Canto C, et al. Endovascular repair of abdominal aortic aneurysm using a pararenal fenestrated stent-graft. J Endovasc Surg. 1999;6(4):354–8.
6. Abel D, Farb A. Application of investigational device exemptions regulations to endograft modification. J Vasc Surg. 2013;57(3):823–5.
7. Pritchard Jr WF, Abel DB, Karanian JW. The US Food and Drug Administration investigational device exemptions (IDE) and clinical investigation of cardiovascular devices: information for the investigator. J Vasc Surg. 1999;29(3):566–74.
8. Federal Food Drug and Cosmetic Act Sg. Accessed online, September 28, 2016. http://www.fda.gov/regulatoryinformation/legislation/federalfooddrugandcosmeticactfdcact/
9. Oderich GS, Ricotta 2nd JJ. Modified fenestrated stent grafts: device design, modifications, implantation, and current applications. Perspect Vasc Surg Endovasc Ther. 2009;21(3):157–67.
10. Starnes BW. Physician-modified endovascular grafts for the treatment of elective, symptomatic, or ruptured juxtarenal aortic aneurysms. J Vasc Surg. 2012;56(3):601–7.
11. Starnes BW. A surgeon's perspective regarding the regulatory, compliance, and legal issues involved with physician-modified devices. J Vasc Surg. 2013;57(3):829–31.
12. Starnes BW, Tatum B. Early report from an investigator-initiated Investigational device exemption clinical trial on physician-modified endovascular grafts. J Vasc Surg. 2013;58(2):311–7.
13. Ricotta 2nd JJ, Tsilimparis N. Surgeon-modified fenestrated-branched stent grafts to treat emergently ruptured and symptomatic complex aortic aneurysms in high-risk patients. J Vasc Surg. 2012;56(6):1535–42.
14. Oderich GS, Farber MA, Sanchez LA. Urgent endovascular treatment of symptomatic or contained ruptured aneurysms with modified stent grafts. Perspect Vasc Surg Endovasc Ther. 2011;23(3):186–94.

Techniques of Physician-Modified Endovascular Grafts (PMEGs) for Incorporation of Renal Mesenteric Arteries

45

Gustavo S. Oderich and Mauricio S. Ribeiro

Introduction

Fenestrated and branched stent grafts have been widely applied to treat complex aneurysms involving the arch, thoracoabdominal and pararenal aorta. These stent grafts have reinforced fenestrations or directional branches, which permit incorporation of the visceral arteries enabling an adequate proximal sealing zone without compromising successful aneurysm exclusion. Physician-modified fenestrated and branched stent grafts have been utilized to treat high-risk patients who otherwise would not have access to a manufactured stent grafts or those who cannot await the time period required for device customization because of impending or contained ruptured and rapidly expanding or excessively large aneurysm. This chapter summarizes current techniques of endovascular repair of thoracoabdominal aortic aneurysms (TAAAs) using physician-modified fenestrated and branched stent grafts.

Indications

The use of device modifications should be strictly limited to patients who meet the following criteria:

1. High risk of morbidity and mortality with alternative treatment (e.g., open or hybrid repair)
2. Large aneurysm (>6.5 cm), symptoms, or contained rupture precluding customization of a manufactured fenestrated-branched stent graft
3. Enrollment in a physician-sponsored investigational device exemption (IDE) protocol with institutional review board approval

It is of paramount importance that physicians involved with these techniques have dedicated training and are familiar with advanced concepts of device design using manufactured stent grafts, as well as techniques of device modifications, implantation, and "bail-out" maneuvers.

Ancillary Tools

A comprehensive endovascular inventory is needed to perform these procedures including a wide range of introducer sheaths, catheters, guide catheters, balloons, and stents as described in Chap. 14 (Table 45.1).

Preoperative Planning

Preoperative planning is the most critical step. Measurements are based on careful analysis of aneurysm morphology using high-resolution computed tomography angiography (CTA) datasets. CTA with small (1–3 mm) cuts is recommended, allowing review of three-dimensional reformatting techniques, maximum intensity projection, and volume rendering. The device design is based on analysis of centerline of flow measurements to determine accurate estimates of lengths, axial clock position, and arc lengths and angles (Fig. 45.1).

Stent Graft Design

A >20 mm proximal landing zone is selected within normal aorta. Visceral artery incorporation is done using one of the three types of modifications: reinforced fenestrations, mini-cuff fenestrations, and directional branches.

G.S. Oderich (✉)
Division of Vascular and Endovascular Surgery, Mayo Clinic, 200 First Street SW, Rochester, MN 55905, USA
e-mail: oderich.gustavo@mayo.edu

M.S. Ribeiro
Department of Surgery and Anatomy, Ribeirão Preto Medical School, Ribeirão Preto Clinical Hospital, University of São Paulo, Campus Universitário s/n, Ribeirão Preto, São Paulo 14048-900, Brazil

© Mayo Foundation for Medical Education and Research 2017

G.S. Oderich (ed.), *Endovascular Aortic Repair*, DOI 10.1007/978-3-319-15192-2_45

Table 45.1 List of ancillary tools recommended for physicians performing fenestrated stent graft procedures

Category	Manufacturer	Application
Sheaths		
20–24Fr Check-FLO sheath (30 cm)	Cook Medical Inc., Bloomington, IN	Femoral access for multivessel catheterization
7Fr Ansel sheath (55 cm, flexible dilator)	Cook Medical Inc., Bloomington, IN	Femoral access for branch artery stenting
7 or 8Fr Raabe sheath (90 cm long)	Cook Medical Inc., Bloomington, IN	Brachial access for branch artery stenting
12Fr Ansel sheath (55 cm, flexible dilator)	Cook Medical Inc., Bloomington, IN	Brachial access for tortuous aortic arch to facilitate branch artery stenting
5Fr Shuttle sheath (90 cm)	Cook Medical Inc., Bloomington, IN	Branch artery access during difficult arch
Catheters		
Kumpe catheter 5Fr (65 cm)	Multiple	Selective vessel catheterization
Kumpe catheter 5Fr (100 cm)	Multiple	Selective vessel catheterization
C1 catheter 5Fr (100 cm)	Multiple	Selective vessel catheterization
MPA catheter 5Fr (125 cm)	Multiple	Selective vessel catheterization
MPB catheter 5Fr (100 cm)	Multiple	Selective vessel catheterization
Van Schie 3 catheter 5Fr (65 cm)	Cook Medical Inc., Bloomington, IN	Selective vessel catheterization
Vertebral catheter 4Fr (125 cm)	Multiple	Selective vessel catheterization
VS1 catheter 5Fr (80 cm)	Multiple	Selective vessel catheterization
Simmons I catheter 5Fr (100 cm)	Multiple	Selective vessel catheterization
Diagnostic flush catheter 5Fr (100 cm)	Multiple	Diagnostic angiography
Diagnostic pigtail catheter 5Fr (100 cm)	Multiple	Diagnostic angiography, selective vessel catheterization
Quick-Cross catheter 0.014–0.035 in. (150 cm)	SpectraMedics	Selective vessel catheterization
Renegade catheter (150 cm)	Boston Scientific, Minneapolis, MN	Selective vessel catheterization
Guide catheters		
LIMA guide 7Fr (55 cm)	Cordis Corporation, Bridgewater, NJ	Pre-catheterization
Internal mammary (IM) guide 7Fr (100 cm)	Multiple	Selective vessel catheterization
MPA guide 7Fr (100 cm)	Multiple	Selective vessel catheterization
Balloons		
10 mm × 2 cm angioplasty balloon	Multiple	Proximal stent flare
12 mm × 2 cm angioplasty balloon	Multiple	Proximal stent flare
5 mm × 2 cm angioplasty balloon	Multiple	Advance sheath over balloon
Wires		
Benson wire 0.035 in. (150 cm)	Multiple	Initial access
Soft glidewire 0.035 in. (260 cm)	Multiple	Target vessel catheterization
Stiff glidewire 0.035 in. (260 cm)	Multiple	Target vessel catheterization
Rosen wire 0.035 in. (260 cm)	Multiple	Branch artery stenting
1 cm tip Amplatzer wire 0.035 in. (260 cm)	Multiple	Branch artery stenting
Lunderquist wire 0.035 in. (260 cm)	Multiple	Aortic stent graft
Glidegold wire 0.018 in. (180 cm)	Multiple	Target vessel catheterization
Stents		
iCAST stent grafts 5–10 mm	Atrium, Hudson, NH	Branch artery stenting
Balloon-expandable stents 0.035 in.	Multiple	Branch artery stenting or reinforcement
Self-expandable stents 0.035 in.	Multiple	Distal branch artery stenting
Self-expandable stents 0.014 in.	Multiple	Distal branch artery stenting

Stent Graft Modifications

Device modifications are based on the Cook Zenith platform (Cook Medical Inc., Bloomington, IN). A TX2 thoracic stent graft (Cook Medical Inc., Bloomington, IN) is modified with fenestrations and/or directional branches to accommodate the visceral arteries, and a Zenith abdominal stent graft (Cook Medical Inc., Bloomington, IN) is modified by removing the uncovered stent to be used as distal bifurcated device.

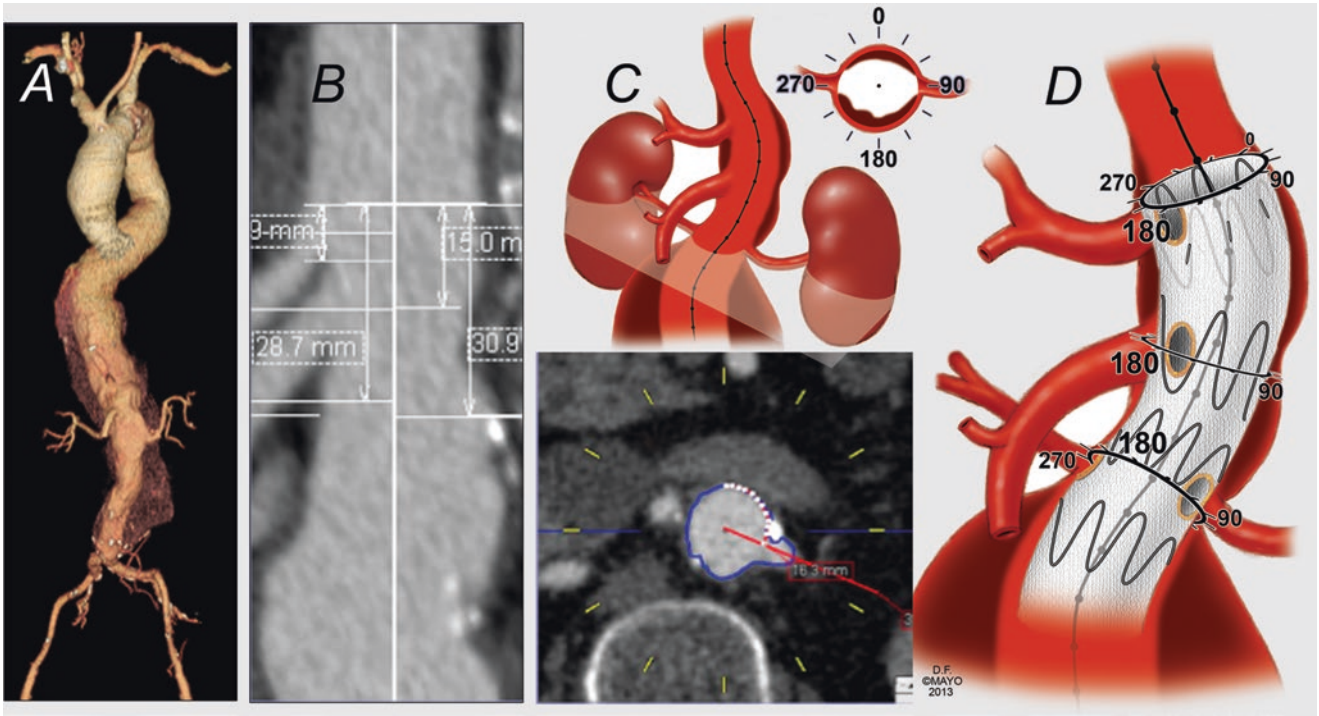


Fig. 45.1 Computed tomography angiography datasets (**a**) are analyzed to determine vessel triangulation. Centerline of flow analysis (**b**) accurately estimates the lengths between each side branch origin. The location of the side branch in the axial plane (**c**) takes into consideration the "clock position" of the vessel, as well as the arc length in relation to the 12:00 o'clock position. At least 20 mm of normal aorta is selected for proximal landing zone; stent graft design (**d**) is based on the extent of aneurysm and number of vessels requiring incorporation in order to obtain at least 20 mm of proximal seal. By permission of Mayo Foundation for Medical Education and Research. All rights reserved

Reinforced Fenestrations

Reinforced fenestrations are utilized for target vessel originating from narrow aortic diameter (<5 mm larger than the TX2 stent graft) or within the sealing zone (Fig. 45.2). Fenestrations are stented using balloon-expandable iCAST covered stents (Atrium, Hudson, NH).

Mini-Cuff Reinforced Fenestration

Mini-cuff reinforced fenestrations provide 3–5 mm overlap, optimizing seal at the attachment site; these are selected if the aortic lumen at the origin of the target vessel is 5–10 mm larger than the diameter of the TX2 stent graft (Fig. 45.3). Mini-cuff fenestrations are bridged to target vessels by balloon-expandable iCAST covered stents.

Directional Branches

Directional branches are selected if the aortic lumen is >10 mm larger than the diameter of the TX2 aortic stent graft (Fig. 45.4). Permanent diameter-reducing ties may be added to reduce the diameter of the TX2 stent graft to 18–20 mm in the location of the directional branch, which is stented to target vessels by self-expandable stent grafts.

Diameter-Reducing Wire

A diameter-reducing wire is added to facilitate vessel catheterization (Fig. 45.5).

Preloaded Guidewires

Preloaded guidewires (0.014 or 0.018 in.) are used through fenestrations or branches to facilitate catheterization via the brachial approach (Fig. 45.6).

Re-sheathing

The modified TX2 stent graft is re-sheathed into its original sheath by using 1-0 silk ties to sequentially collapse the Z stents (Fig. 45.7). A large Silastic vessel loop can be utilized to re-sheath branches and the proximal sealing stent, which contains barbs. The original sheath can accommodate four fenestrations or three fenestrations and one

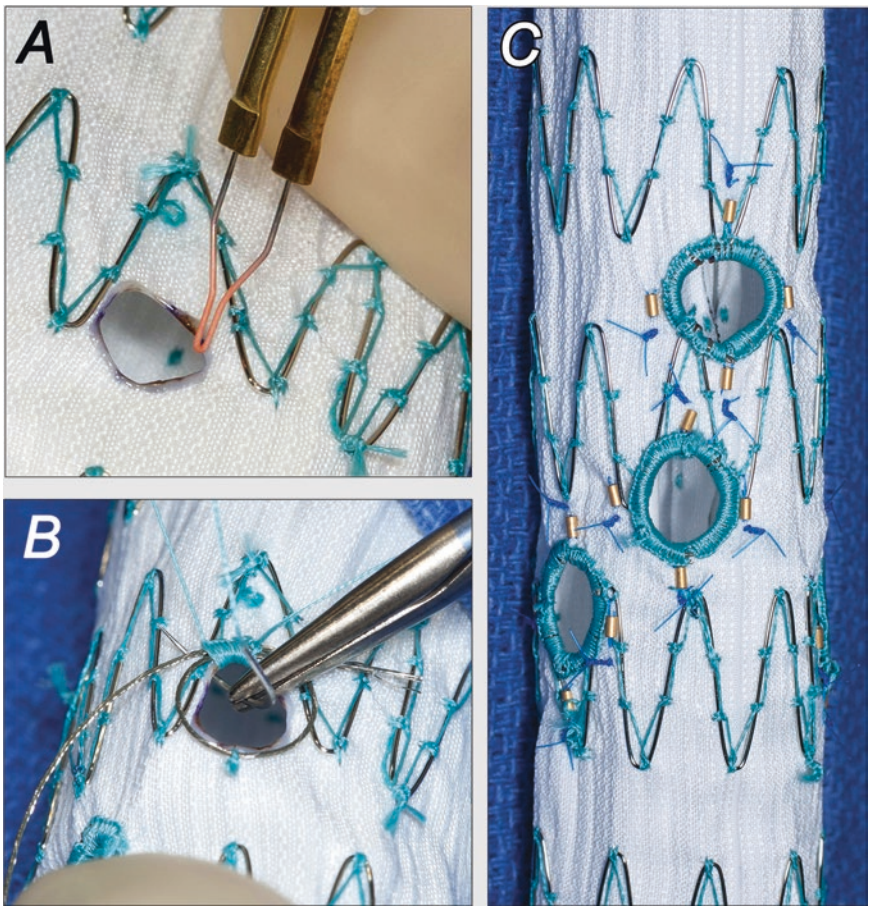


Fig. 45.2 The TX2 stent graft is unsheathed in the usual manner and the pro-form sutures are cut and removed. The location of fenestrations and branches is marked on the fabric. The distal Prolene suture, which holds the device, is positioned posteriorly at 6:00. Reinforced fenestrations are created using ophthalmologic catheter in the exact location of the target vessel (**a**). It is critical to avoid struts within the fenestration. Fenestration size is 6×6 mm for renal arteries and slightly larger for the celiac axis and SMA. Each fenestration is tightly reinforced by a double nitinol loop (**b**), which is obtained from a snare. The nitinol wire is sutured using locking 5-0 Ethibond sutures. Each fenestration is marked by four radiopaque markers (**c**). By permission of Mayo Foundation for Medical Education and Research. All rights reserved

branch. If >two branches are used, the stent graft is reloaded into a 65-cm 24Fr Check-Flo sheath (Cook Medical Inc. Bloomington, IN).

Orientation Markers

Gold beads (Accellent, Wilmington, MA) are utilized for orientation (B). Three gold beads are sutured with 5-0 Prolene in longitudinal configuration at 12:00 position and three gold beads in transverse configuration at 6:00 position. Gold markers are also used in fenestrations and branches.

Modified Bifurcated Stent Graft

The distal bifurcated device is done using a Zenith abdominal stent graft (Cook Medical Inc., Bloomington, IN), which is modified by removing the top uncovered stent (Fig. 45.8). The Zenith stent graft is oversized by 2 mm in relation to the TX2 stent graft.

Perioperative Measures

Patients are pre-admitted for bowel preparation and intravenous hydration with bicarbonate infusion. Oral acetylcysteine is administered to minimize risk of renal function deterioration. Antihypertensive medications (except for beta-blockers) are withheld prior to the procedure. Cerebrospinal fluid drainage and neurologic monitoring (motor and somatosensory-evoked potential) are used for spinal cord protection. Intraoperative blood salvage is highly recommended. The use of iodinated contrast is minimized during all steps of the procedure by avoiding conventional angiographies and instead using selective hand injections and diluted contrast agent in the power injector. Iliac conduits are recommended in patients with difficult iliac access. Intravenous heparinization is administered to achieve a target-activated clotting time >300 s. Diuresis is induced prior to deployment of the fenestrated component with mannitol and/or furosemide.

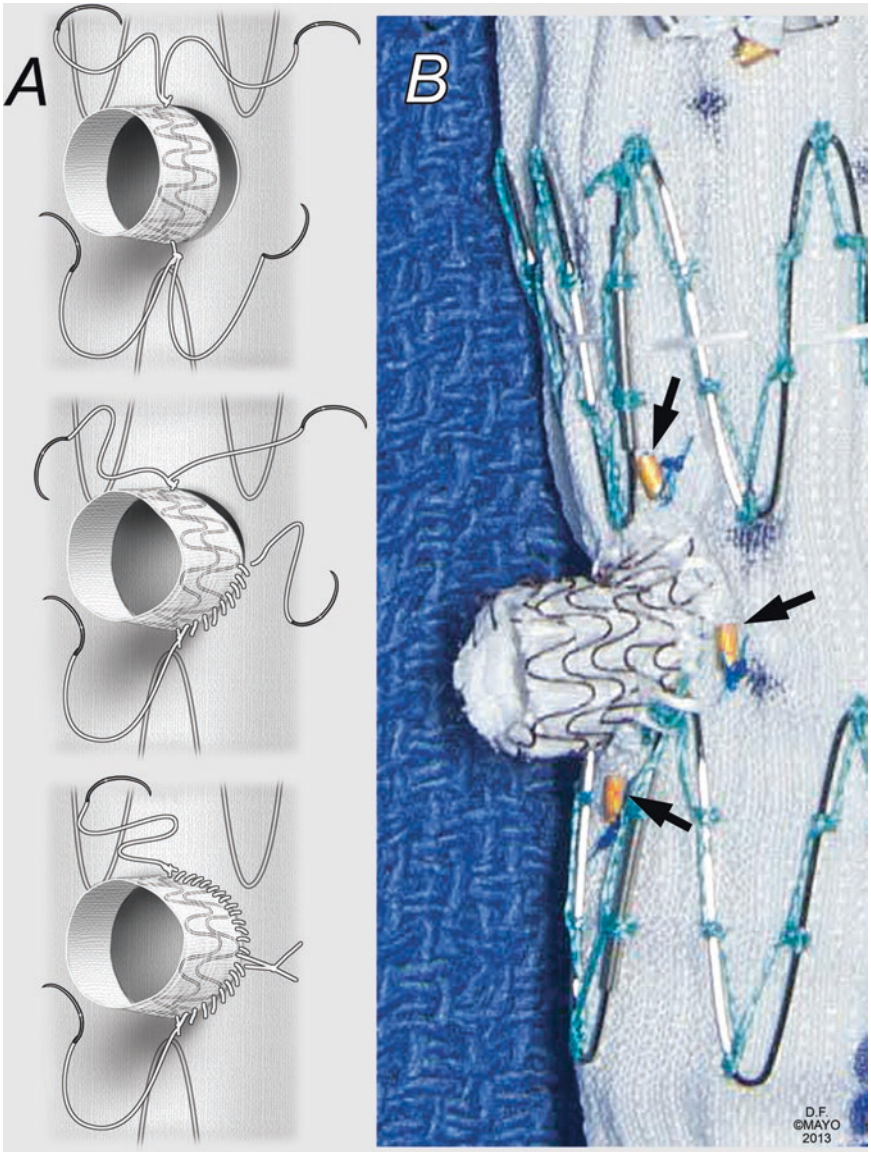


Fig. 45.3 Mini-cuffs are fashioned using 3–5 mm Viabahn stent grafts (WL Gore, Flagstaff AZ), which are cut using scissors in a straight, up-going or down-going fashion (**a**). The mini-cuff is anastomosed end-to-side using 5-0 Gore sutures (WL Gore, Flagstaff, AZ) into the fenestration. Four radiopaque markers are added (**b**, *black arrows*). By permission of Mayo Foundation for Medical Education and Research. All rights reserved

Techniques of Implantation

The procedure is performed in a hybrid operating room with fixed imaging. Using general endotracheal anesthesia and supine position (Fig. 45.9), the left upper extremity, chest, abdomen, and thighs are prepped and draped in sterile fashion. The proximal left brachial artery is surgically exposed via longitudinal incision. Bilateral percutaneous femoral access is established under ultrasound guidance. The patient is systemically heparinized to achieve a target ACT of >300 s. Each femoral puncture is pre-closed using two Perclose devices (Abbott Vascular, Abbott Park, IL), unless there is excessive calcification requiring surgical exposure. Bilateral 8Fr sheaths are introduced to the external iliac arteries over Benson guidewires (Cook Medical Inc., Bloomington, IN). The guidewires are exchanged to 0.035-in. soft glidewires and Kumpe catheters, which are advanced to the ascending aorta and exchanged for stiff 0.035 Lunderquist guidewires (Cook Medical Inc., Bloomington, IN). The repair is started by deployment of proximal TX2 components depending on the proximal extension of the aneurysm. Left brachial access is obtained using a 12Fr Ansel sheath (Cook Medical Inc., Bloomington, IN), which is advanced into the descending thoracic aorta over an Amplatz wire. Down-going directional branches and celiac or SMA fenestrations are preferentially accessed and stented via brachial approach. Renal fenestrations are accessed and stented via femoral approach, unless there is excessive angulation favoring brachial access. Ideally all fenestrations should be strut free (Fig. 45.10).

Four-Vessel Fenestrated Stent Graft

Branches artery stenting is performed via the right femoral approach, provided there are no issues related to iliac access.

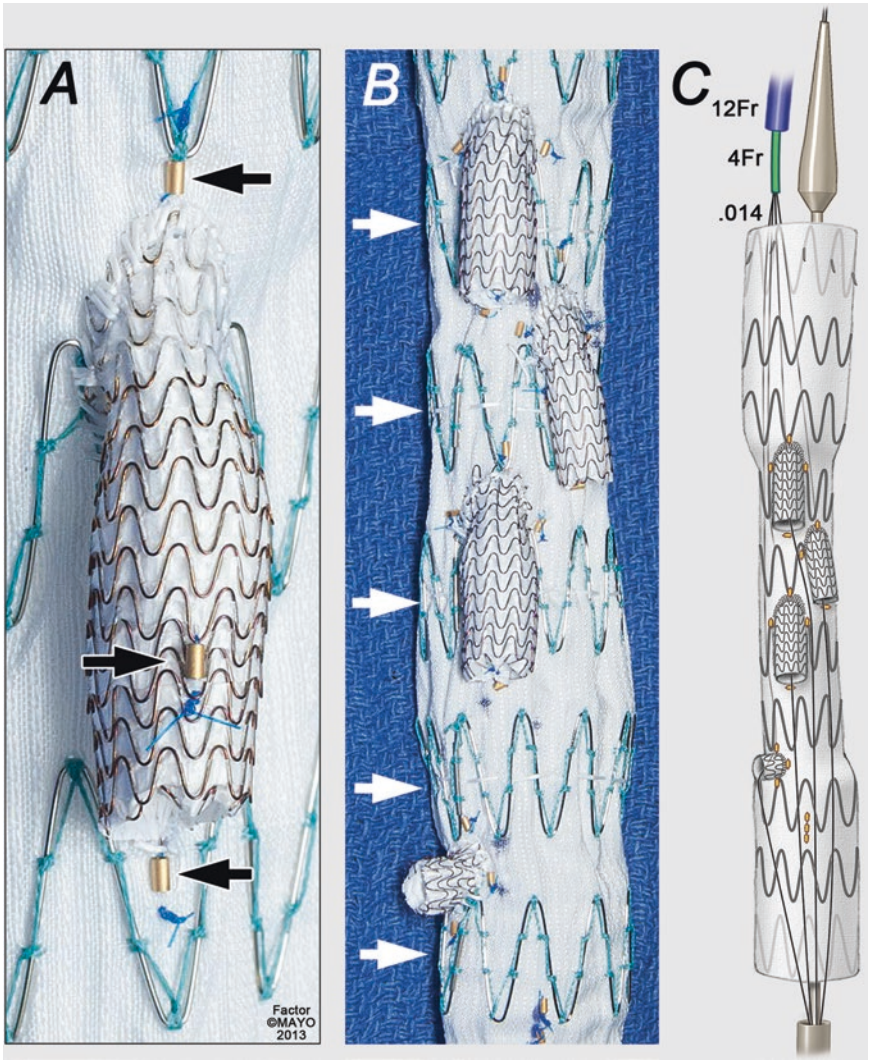


Fig. 45.4 Directional branches are fashioned using 2-cm long Viabahn stent grafts (WL Gore, Flagstaff, AZ). The distal edge of the branch is positioned approximately 2 cm above the intended location of the target vessel within the same clock position. A Viabahn stent graft (**a**) is anastomosed end to side to the fenestration using running 5–0 Gore sutures (WL Gore, Flagstaff, AZ). The distal edge of the Viabahn branch is stitched to the fabric of the TX2 stent graft to prevent movement during re-sheathing and deployment. Radiopaque markers are placed at the proximal and distal edge of the fenestration and at the distal edge of the branch (**a**, *black arrows*). Permanent diameter-reducing ties (**b**, *small black arrows*) may be added to reduce the diameter of the TX2 stent graft to approximately 18–20 mm. Illustration depicted a branched stent graft with preloaded guidewires (**c**). By permission of Mayo Foundation for Medical Education and Research. All rights reserved

A 20–22Fr Check-Flo sheath (Cook Medical Inc., Bloomington, IN) is introduced via the right femoral approach (Fig. 45.11). The sheath valve is accessed with two short 7Fr sheaths, which are used for pre-catheterization of the renal arteries to minimize contrast use during deployment. Once the target vessels are catheterized, the fenestrated stent graft is oriented extracorporeally (Fig. 45.12), introduced via the left femoral approach, and deployed with perfect apposition between the fenestrations and the target catheters. After deployment of the fenestrated component, each catheter is removed from its target artery and used to sequentially regain access into the fenestrated component, fenestration, and target vessel. After the target vessel is catheterized, the soft glidewire is removed and exchanged for a 0.035-in. Rosen guidewire (Cook Medical Inc, Bloomington, IN), followed by placement of hydrophilic sheaths. Once the renal and SMA sheaths are positioned, the diameter-reducing tie is removed and the proximal landing zone or attachment site is dilated using a Coda balloon (Cook Medical Inc., Bloomington, IN). Alignment stents are sequentially deployed starting with the renal arteries, followed by SMA and celiac axis. Prior to each stent deployment, the position of the stent is confirmed by hand injection. The stent is deployed 3–5 mm into the aorta and flared using a 10 mm × 2 cm balloon. A completion angiography of each branch is performed. Following the placement of the alignment stents, a modified distal bifurcated stent graft is oriented, advanced, and deployed with preservation of the ipsilateral internal iliac artery (Fig. 45.13). A completion angiography of the aorta and iliac arteries is obtained and CTA is recommended prior to dismissal.

Combination of Directional Branches and Fenestrations

The most commonly utilized stent graft design includes one or two directional branches (celiac axis and/or SMA) combined with two or three fenestrations (Fig. 45.14). The same steps described above are used for pre-catheterization

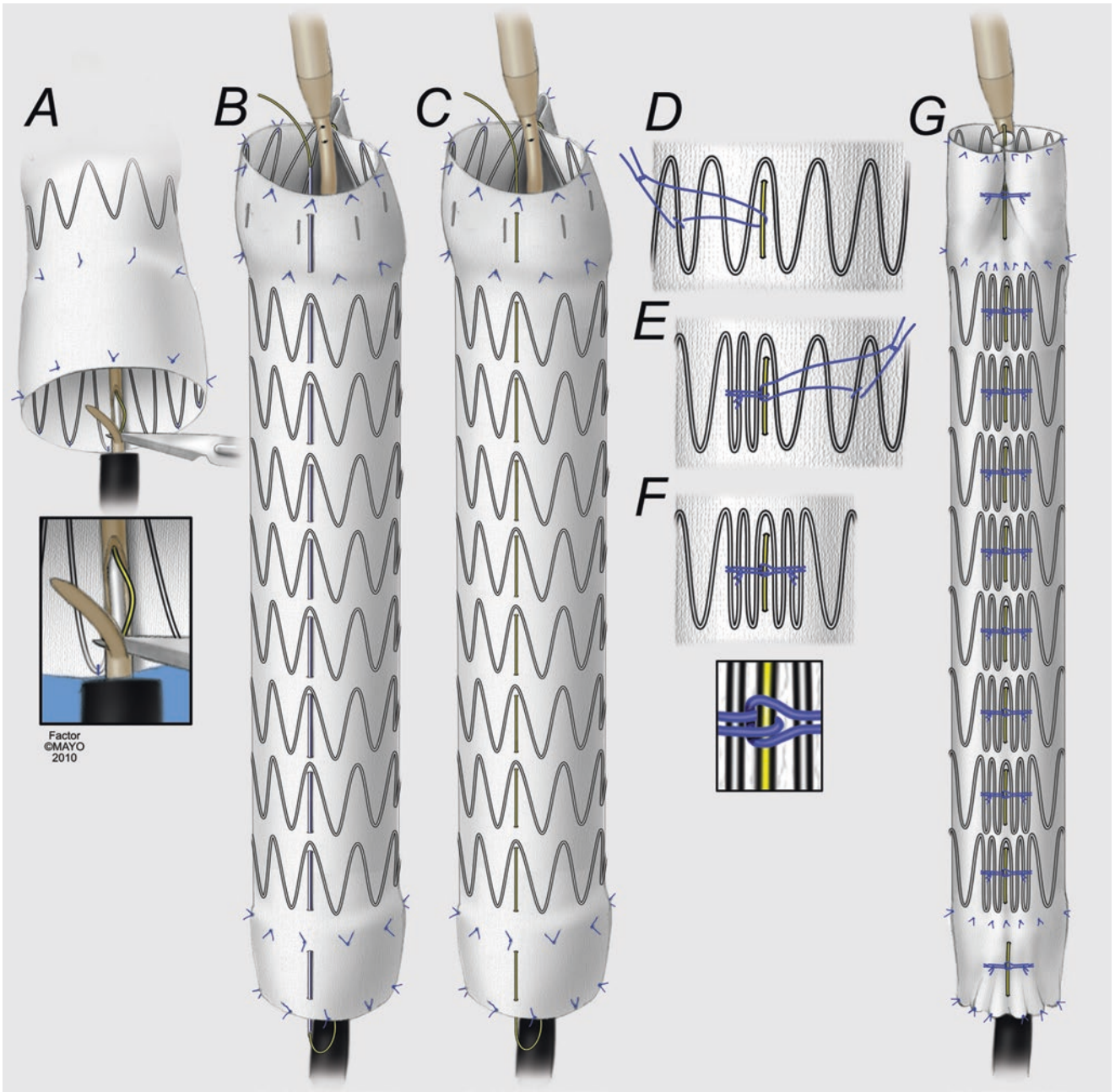


Fig. 45.5 Diameter-reducing wires facilitate implantation by allowing space for catheter manipulations and movement of the TX2 stent graft to adjust for any misalignment of fenestrations. The nitinol wire is retrieved from the inner cannula, which is opened with scalpel (**a**, *inset*). One of the three nitinol wires is retrieved and rerouted posteriorly at 6:00 position through and through the fabric of the stent graft using a long 22-gauge spinal needle (**b**). Once the wire is in place (**c**), the Z stents are constrained using loops of Prolene. The first loop is stitched forehand around fabric and stent strut and then placed around the nitinol wire (**d**). The second loop is stitched backhand into fabric and Z stent and then routed around the first Prolene loop (**e**), with careful attention not to place the suture through the first Prolene loop (**f**, *inset*). The top part of the TX2 is left open to facilitate catheterization from above (**g**). By permission of Mayo Foundation for Medical Education and Research. All rights reserved

(Fig. 45.15). The modified multibranch stent graft is oriented extracorporeally, introduced via the femoral approach, and deployed with the SMA branch located approximately 2 cm proximal to its target vessel. The SMA and celiac branch are catheterized, and Amplatz guidewires are placed to provide support for a 70-cm 9Fr Flexor sheath (Cook Medical Inc., Bloomington, IN) into the SMA branch, which will be needed for placement of bridging stent grafts. Once access is established into the SMA, the distal portion of the device is deployed, and the renal fenestrations are accessed via femoral approach, followed by introduction of 7Fr hydrophilic sheaths over Rosen wires

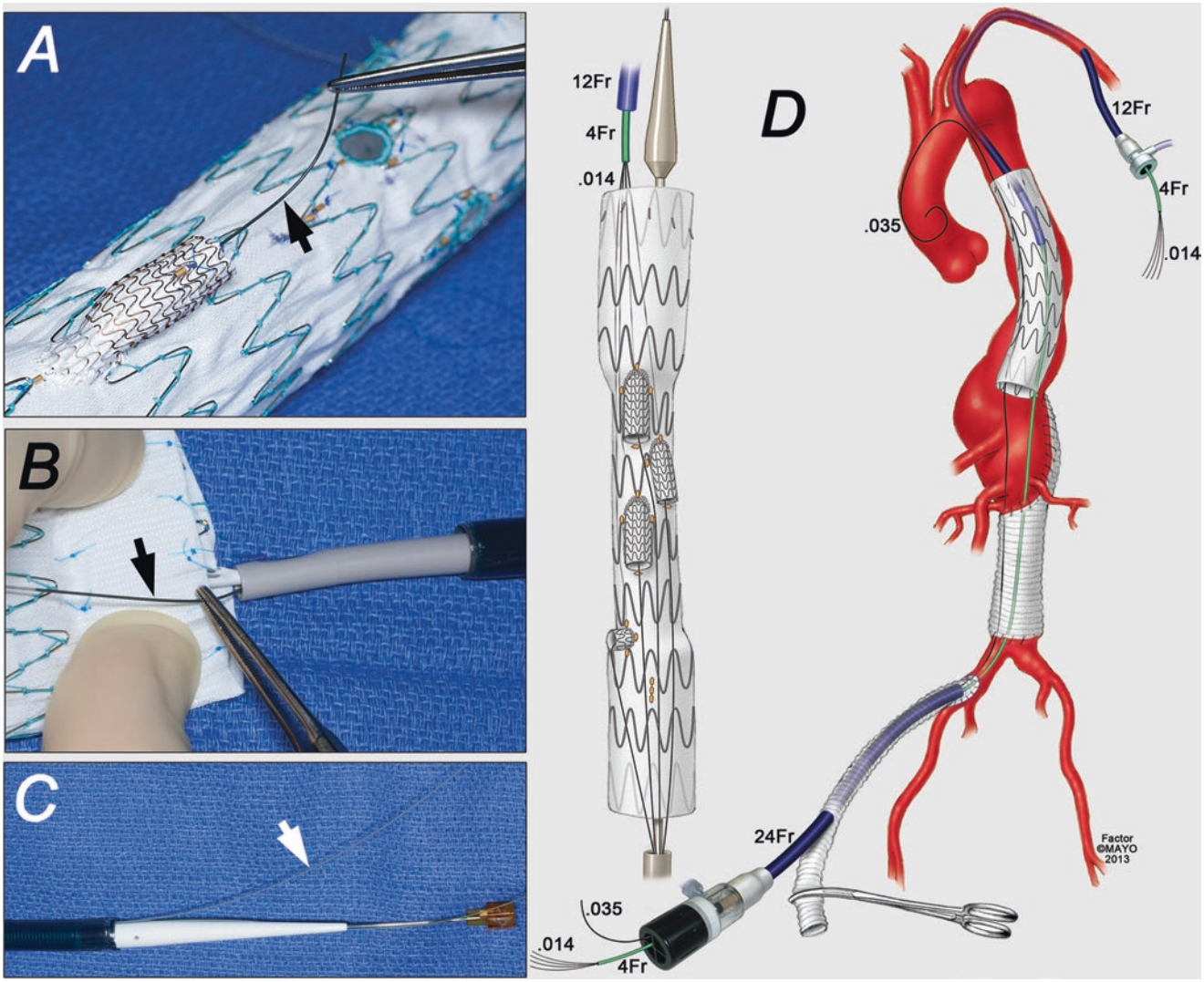


Fig. 45.6 Preloaded guidewires (0.014 or 0.018 in.) facilitate catheterization of fenestrations and branches. These are introduced via the fenestration or branch (**a**, *black arrow*) and into the distal shaft of the TX2 stent graft cannula (**b**, *black arrow*). After the device is reintroduced into its original sheath, the preloaded guidewires are exit from the top portion of the sheath (**c**, *white arrow*). A 110-cm 4Fr sheath is introduced from brachial access and exteriorized via the femoral artery (**d**). While the modified TX2 stent graft is loaded into a 0.035-in. stiff guidewire, the preloaded guidewires are loaded into the 4Fr sheath. These guidewires now exit through the brachial sheath (**d**) and can be accessed after deployment of the TX2 stent graft to sequentially catheterize each fenestration or branch. By permission of Mayo Foundation for Medical Education and Research. All rights reserved

(Fig. 45.16). Each directional branch is stented using self-expandable Fluency stent grafts (Bard Peripheral Vascular, Tempe, AZ), which are reinforced by self-expandable bare metal stents (Fig. 45.17).

Mini-Cuffs

Technique of implantation of device with mini-cuffs is identical to what has been described for fenestrations. When using this design, it is possible that the cuff abuts the aortic wall, which can make catheterization more difficult. Therefore, deployment should be offset as such that the mini-cuff is slightly above or below the target vessel (Fig. 45.18). Its application is ideally suited for aneurysms with a larger luminal diameter when a fenestration is intended (Fig. 45.19).

Preloaded System

Preloaded guidewires are preferentially used in all cases requiring brachial approach and facilitate catheterization in patients with difficult anatomy. This is exemplified in a patient with large type III thoracoabdominal aortic aneurysm (Fig. 45.20) who had significant luminal thrombus. All branches and fenestrations (Fig. 45.21) are loaded with 0.014

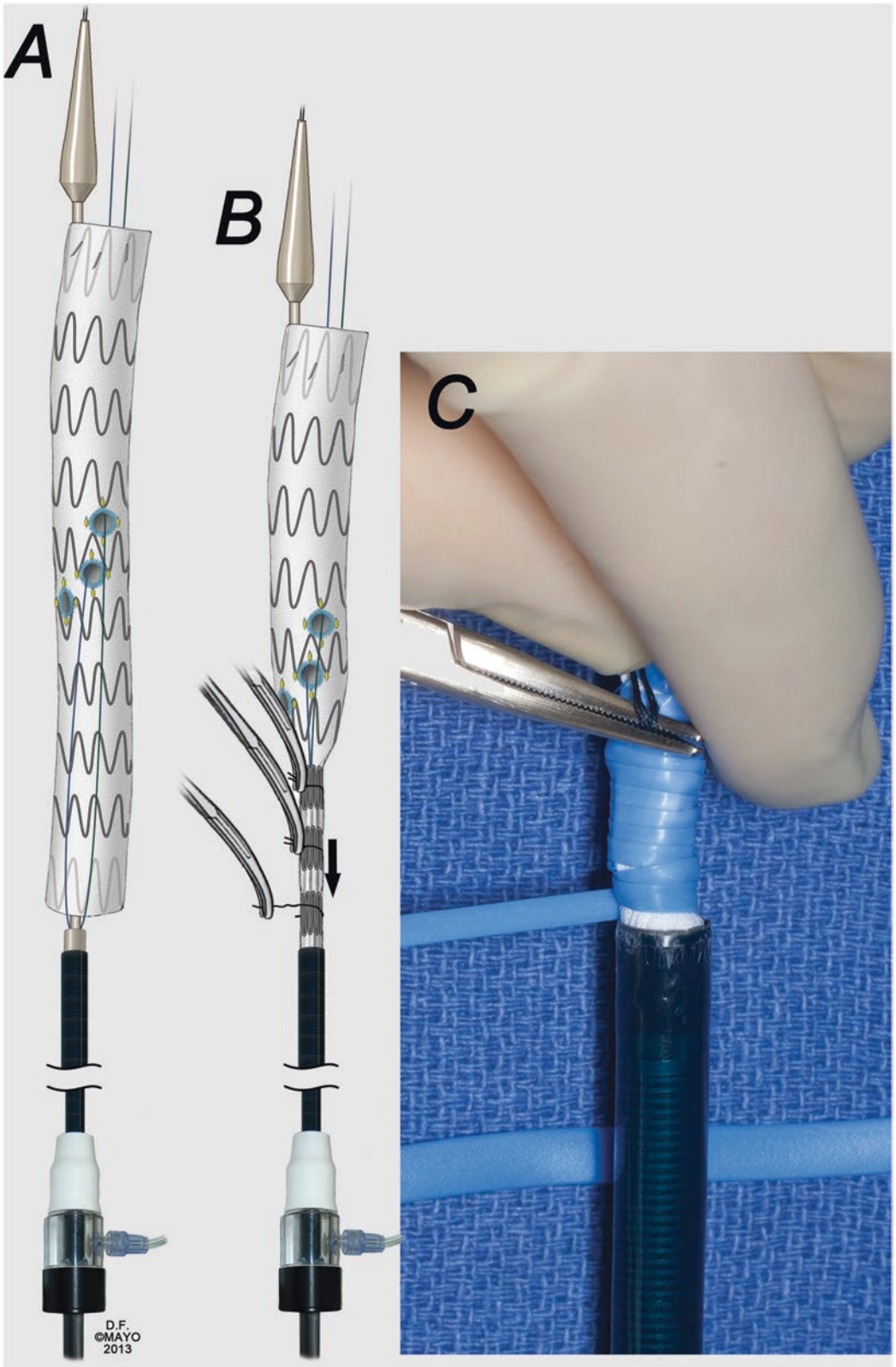


Fig. 45.7 Re-sheathing into the original sheath (**a**) is done using 1-0 silk sutures to collapse each one of the Z stents (**b**). The silk sutures are held by hemostatic clamps and sequentially removed as the device is re-sheathed. For the proximal sealing stent or branches, a large Silastic vessel loop is utilized (**c**). If the TX2 stent graft modifications include more than one branch, the device is loaded into a 24Fr Check-Flo sheath (Cook Medical Inc., Bloomington, IN) using a 26Fr and 24Fr Peel-Away sheath. By permission of Mayo Foundation for Medical Education and Research. All rights reserved

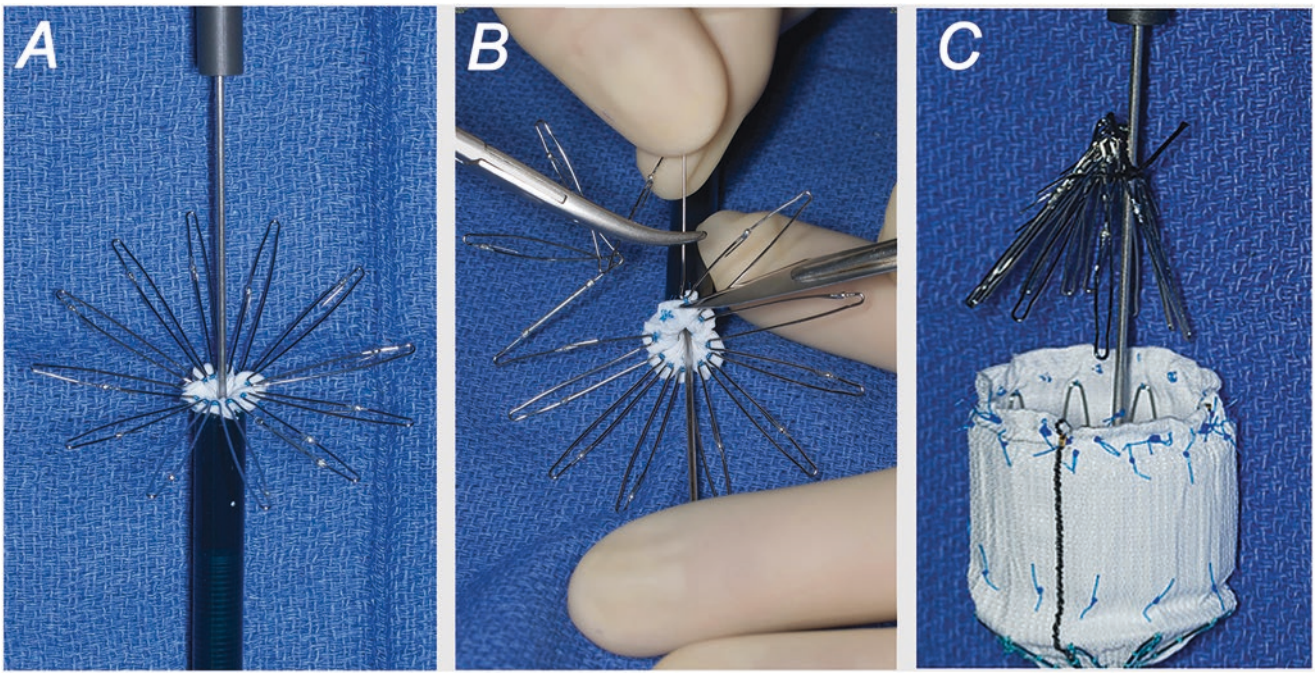


Fig. 45.8 A bifurcated Zenith stent graft is partially deployed releasing only the top uncovered stent (**a**). The stent is excised (**b**) and the endograft is reintroduced into the original sheath (**c**). By permission of Mayo Foundation for Medical Education and Research. All rights reserved

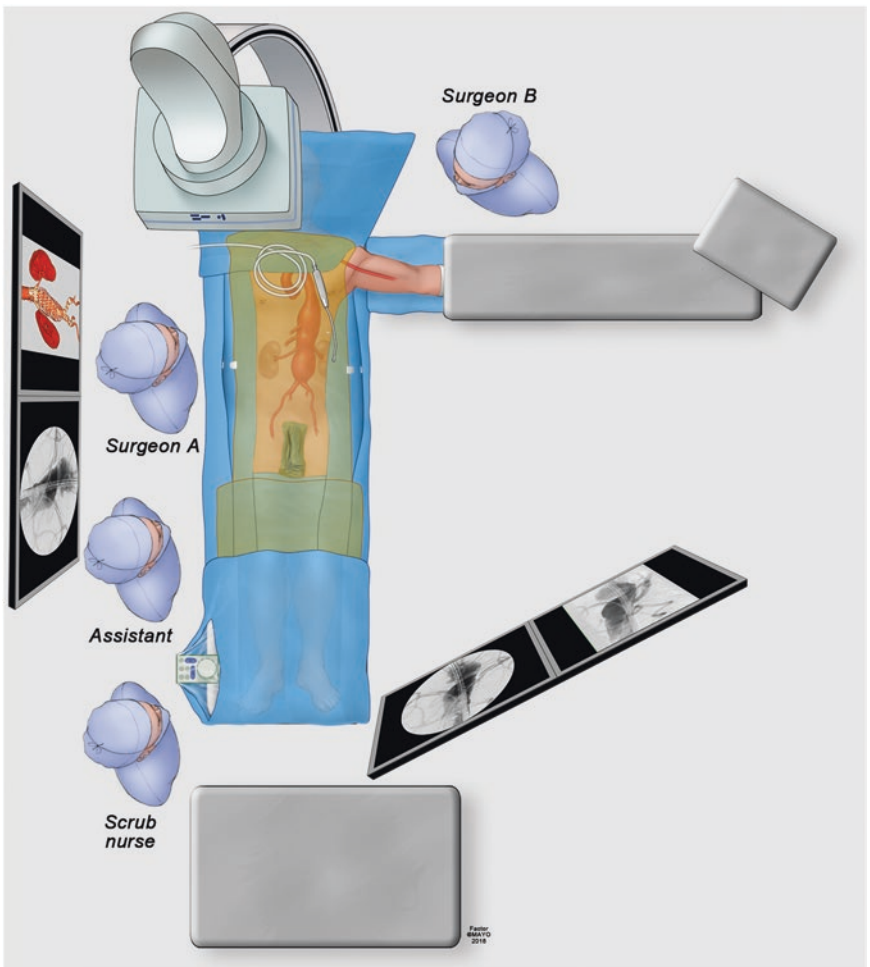


Fig. 45.9 The patient is positioned supine with the left upper extremity, chest, abdomen, and both thighs are prepped and draped in sterile fashion. The fixed imaging unit is best oriented from cranial position, and working side tables are used in the foot of the bed and in the left side for brachial access. By permission of Mayo Foundation for Medical Education and Research. All rights reserved

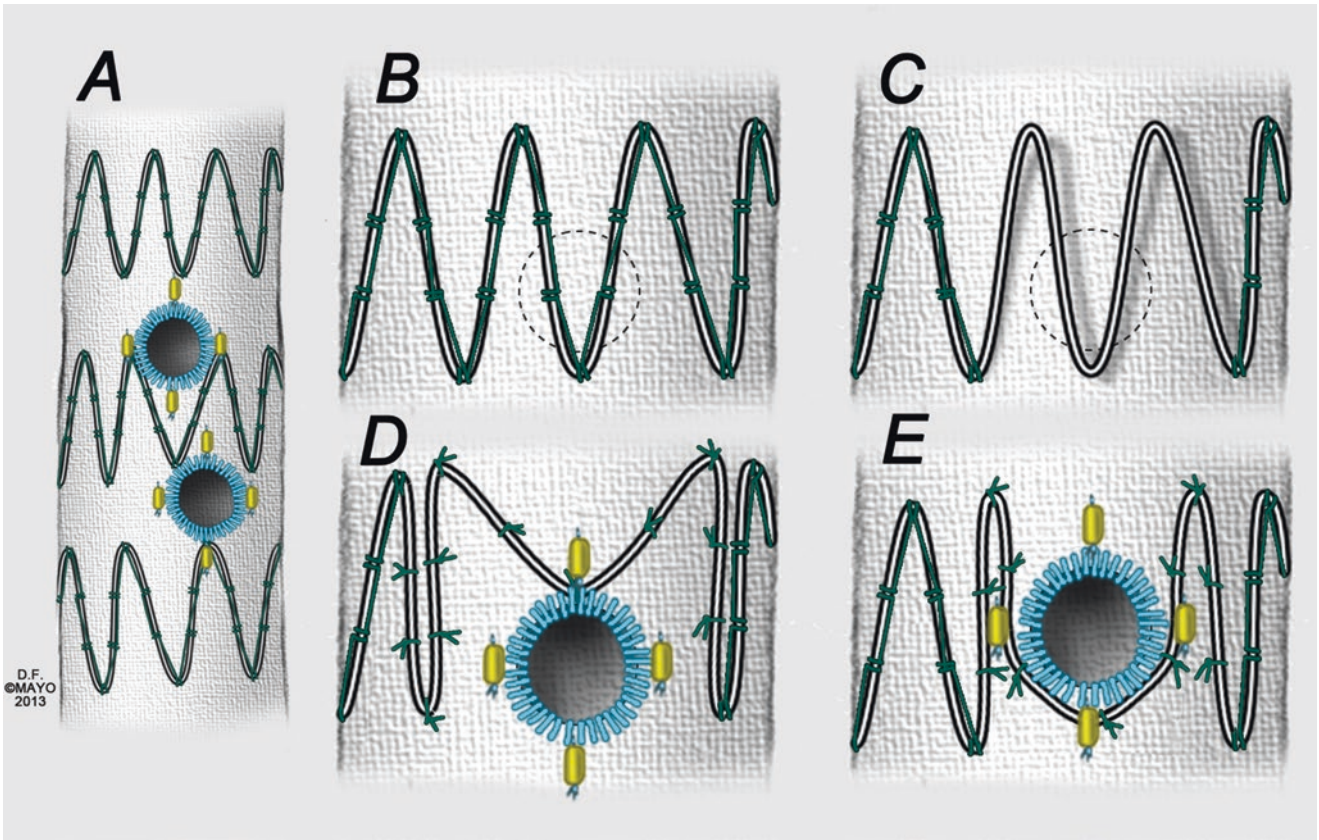


Fig. 45.10 Fenestrations are aligned by balloon-expandable stents. As such, it is ideal that fenestrations are strut free (**a**). Occasionally the position of a fenestration is located between struts (**b**). In these cases the sutures can be excised releasing the Z stent (**c**), which can be relocated by widening the stent in an "M" fashion (**d**) or by bending the stent (**e**). By permission of Mayo Foundation for Medical Education and Research. All rights reserved

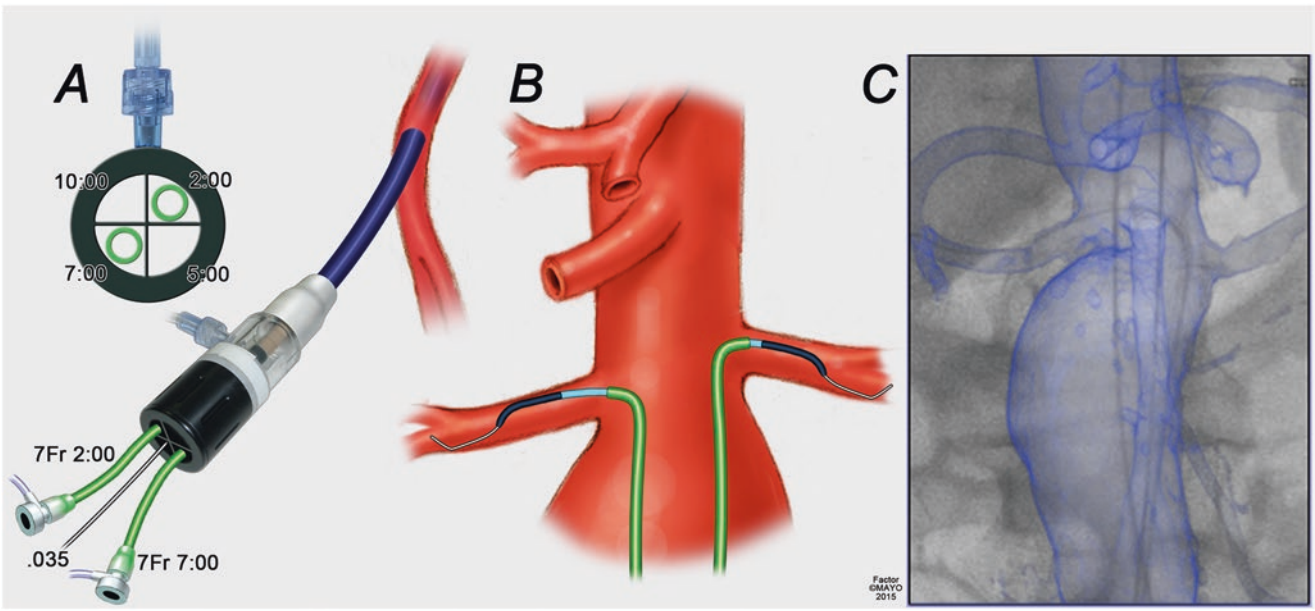


Fig. 45.11 A 20Fr Check-Flo sheath (Cook Medical Inc., Bloomington, IN) is introduced via the right femoral approach (**a**). The valve of the Check-Flo sheath has four leaflets, which are accessed by two short 7Fr sheaths at 2:00 and 7:00 position (**a**). Pre-catheterization of the renal arteries is performed using 0.035-in. soft glidewires and 5Fr catheters supported by 7Fr LIMA guide catheters (**b**). Alternatively, onlay fusion CTA is recommended to minimize contrast use (**c**). By permission of Mayo Foundation for Medical Education and Research. All rights reserved

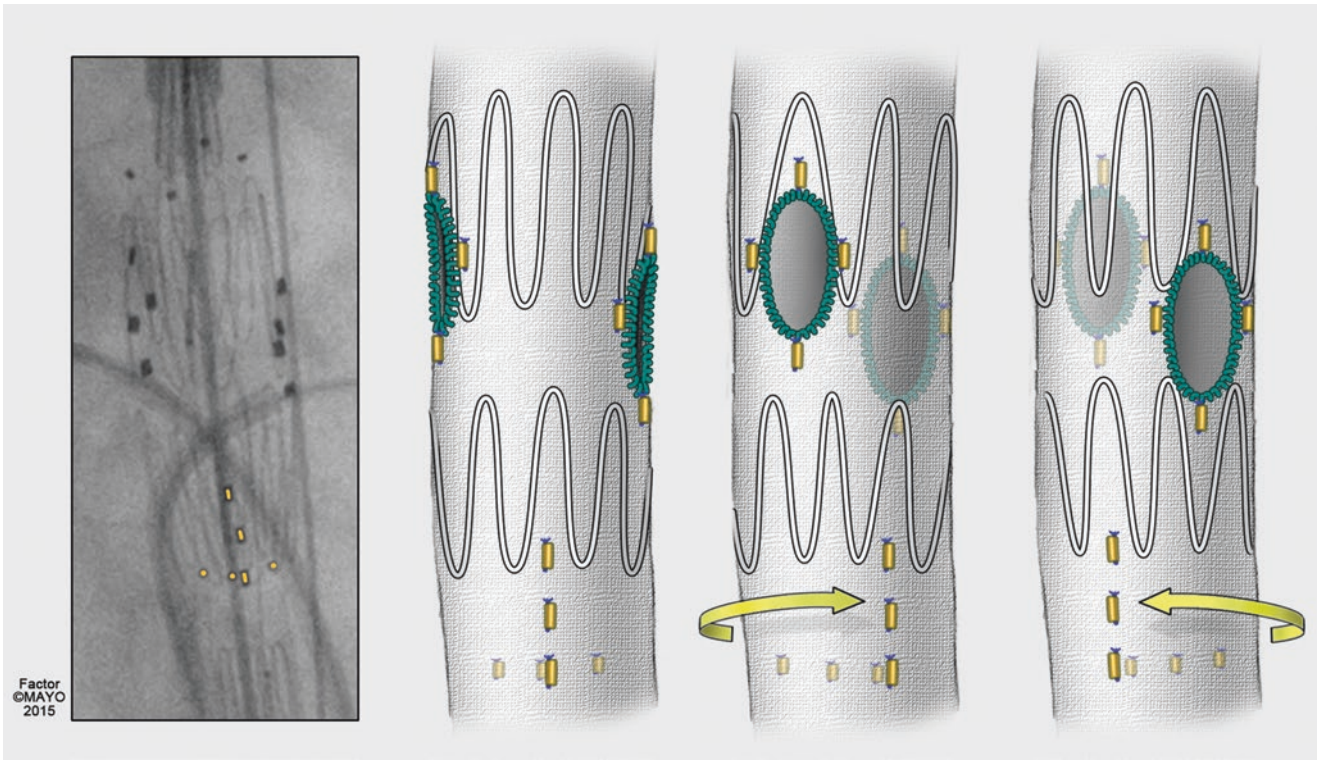


Fig. 45.12 Once the target vessels are catheterized, the fenestrated stent graft is oriented and deployed with perfect apposition between the fenestrations and the target catheters. By permission of Mayo Foundation for Medical Education and Research. All rights reserved

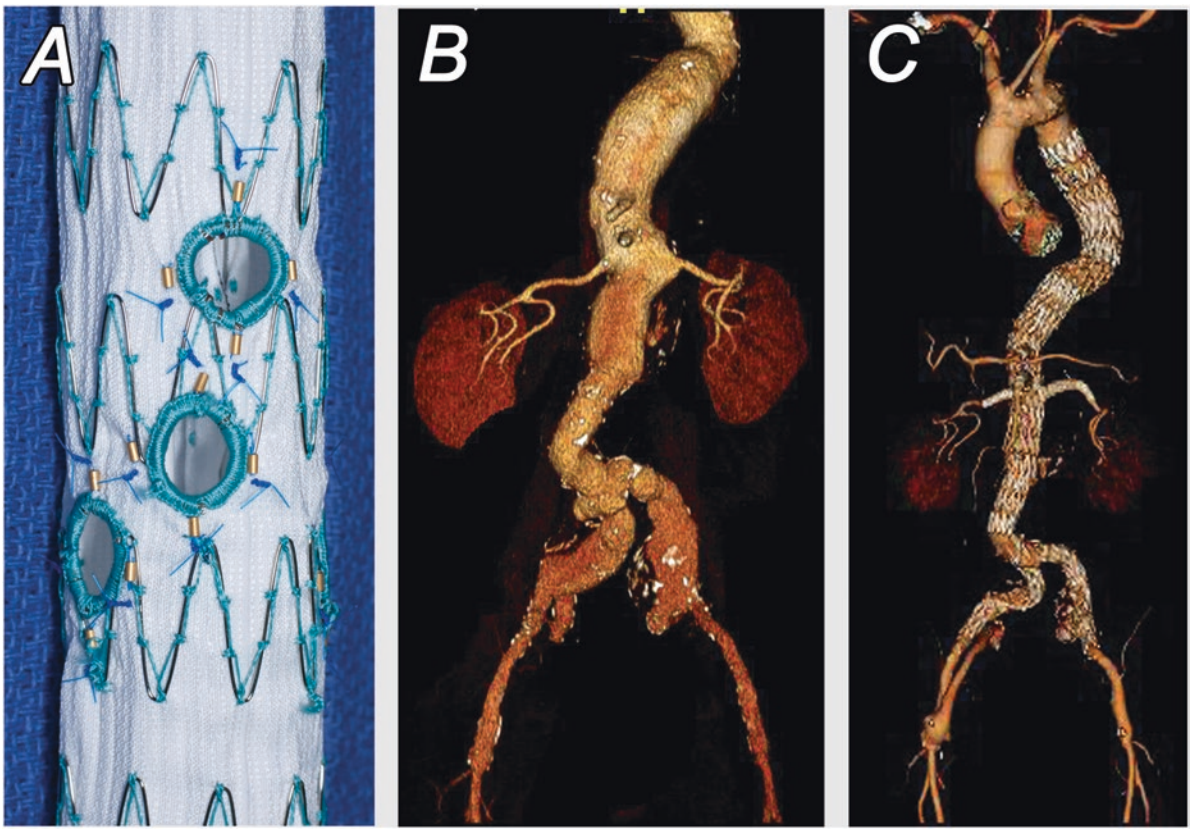


Fig. 45.13 Type II thoracoabdominal aortic aneurysm repaired using four-vessel modified fenestrated stent graft (**a**). Preoperative (**b**) and postoperative (**c**) computed tomography angiography. By permission of Mayo Foundation for Medical Education and Research. All rights reserved

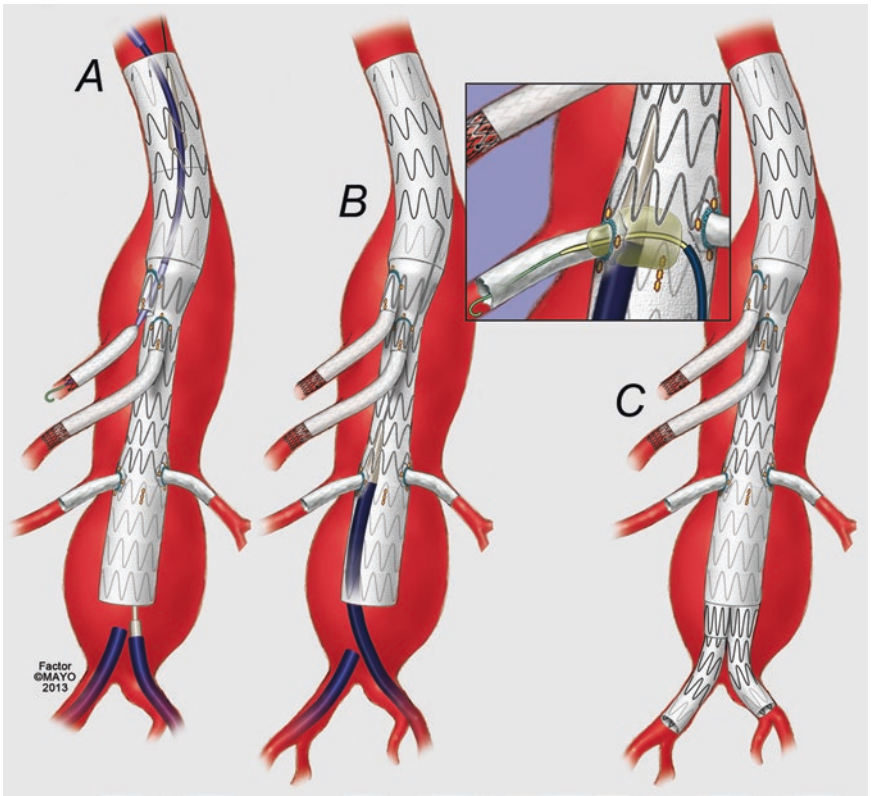


Fig. 45.14 Technique of endovascular repair using two branches and two fenestrations. The renal arteries are stented via femoral approach (**a**) and the SMA and celiac via the left brachial access (**b**). A distal bifurcated stent graft is used to complete the repair (**c**). By permission of Mayo Foundation for Medical Education and Research. All rights reserved

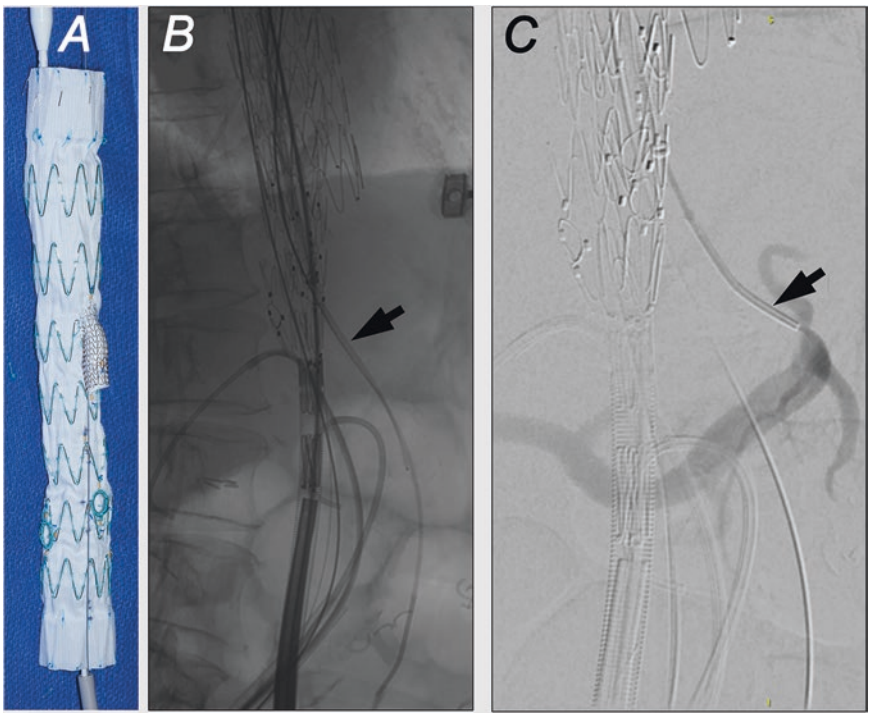


Fig. 45.15 Endovascular thoracoabdominal aortic repair using modified stent graft with one branch for celiac axis and three fenestrations (**a**). Note the main fenestrated stent graft is deployed to the level of the renal arteries (**b**), and the SMA is catheterized (**b**, *black arrow*) with assistance of preloaded guidewire. The celiac is also catheterized with assistance of preloaded guidewire (**c**, *black arrow*). By permission of Mayo Foundation for Medical Education and Research. All rights reserved

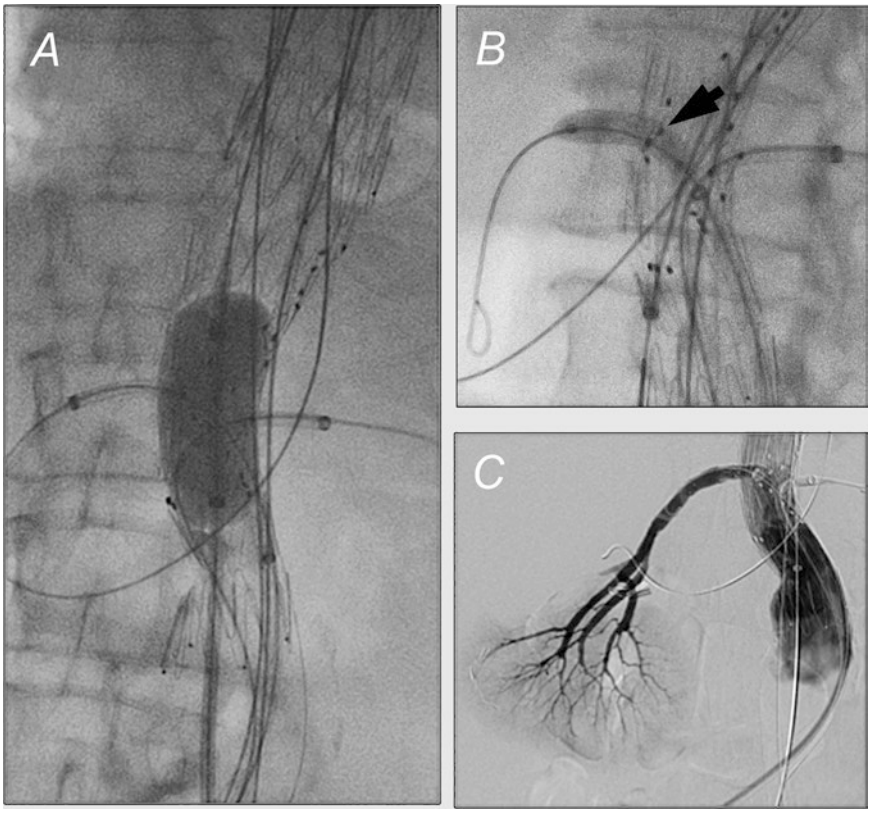


Fig. 45.16 The hydrophilic sheaths with flexible dilators are placed into the renal arteries and SMA (**a**). After removal of the diameter-reducing tie, alignment stents are sequentially deployed (**b**) starting with the renal arteries, followed by SMA and celiac axis. Completion angiography demonstrates patent right renal artery fenestrated-branch (**c**). By permission of Mayo Foundation for Medical Education and Research. All rights reserved

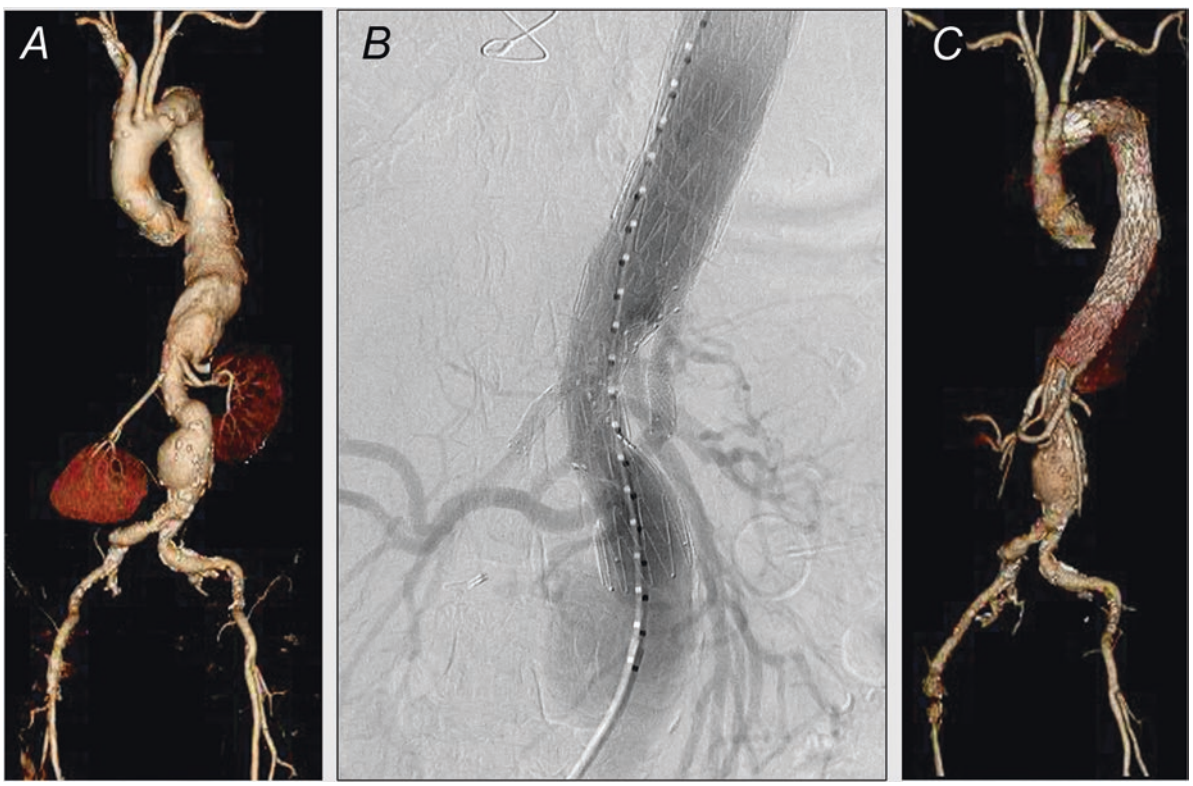


Fig. 45.17 Preoperative computed tomography angiography (CTA) in a patient with type II thoracoabdominal aortic aneurysm (**a**). Completion angiography demonstrates patency of visceral branches (**b**), which is confirmed by postoperative CTA (**c**). By permission of Mayo Foundation for Medical Education and Research. All rights reserved

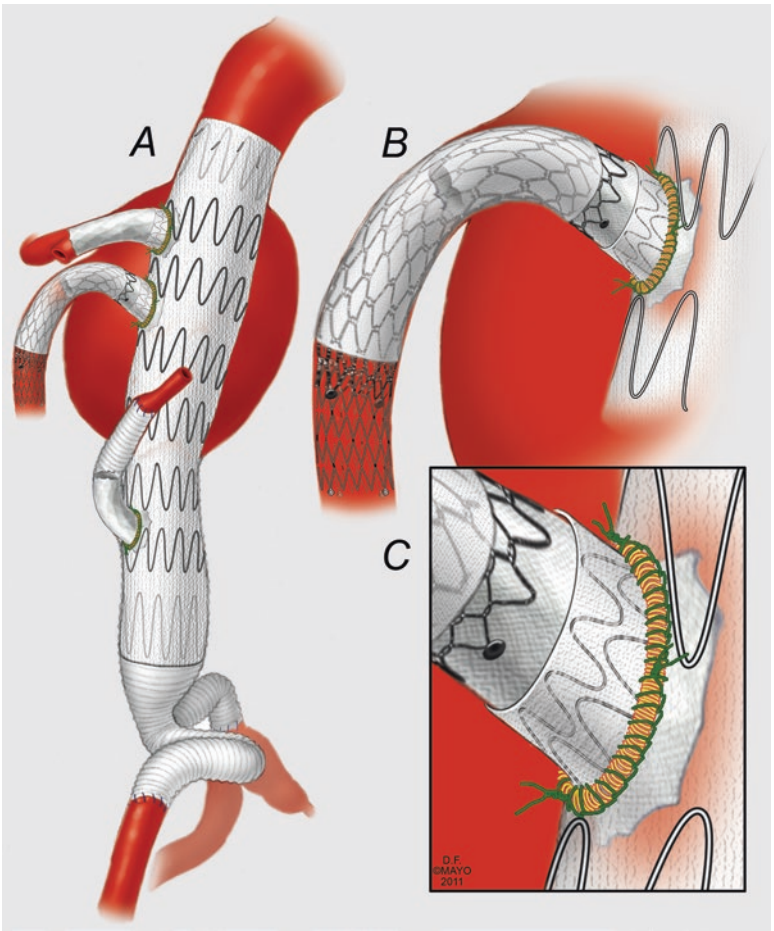


Fig. 45.18 Illustration of the modified fenestrated stent graft (**a**) with two mini-cuff reinforced fenestrations and a standard fenestration. Note that the SMA required a combination of self-expandable stent distally and a balloon-expandable stent proximally because of significant angulation (**b**). The mini-cuff reinforced fenestration was bridged with a balloon-expandable stent graft, which was flared to optimize seal, similar to what is performed using standard fenestrations (**c**). By permission of Mayo Foundation for Medical Education and Research. All rights reserved

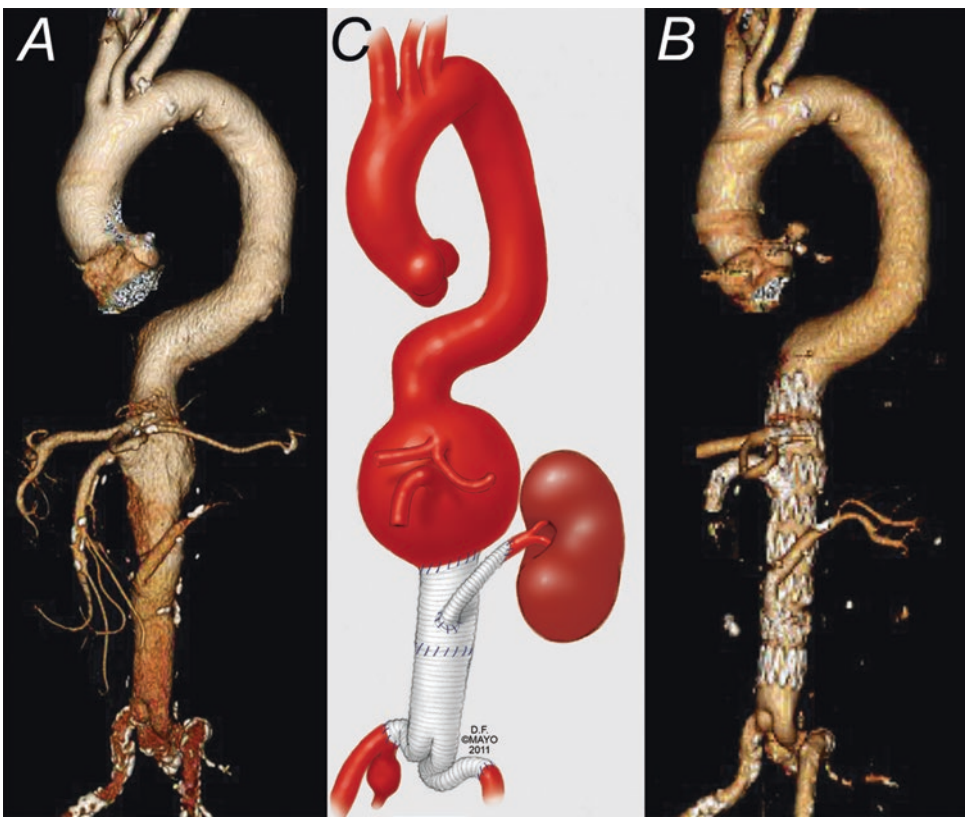


Fig. 45.19 Preoperative computed tomography angiography (CTA) of a supra-graft type IV thoracoabdominal aortic aneurysms (**a**) after prior pararenal aneurysm repair (**b**). The patient was repaired with mini-cuff fenestrations as depicted in Fig. 45.19. Postoperative CTA revealed no endoleak and widely patent branches (**c**). By permission of Mayo Foundation for Medical Education and Research. All rights reserved

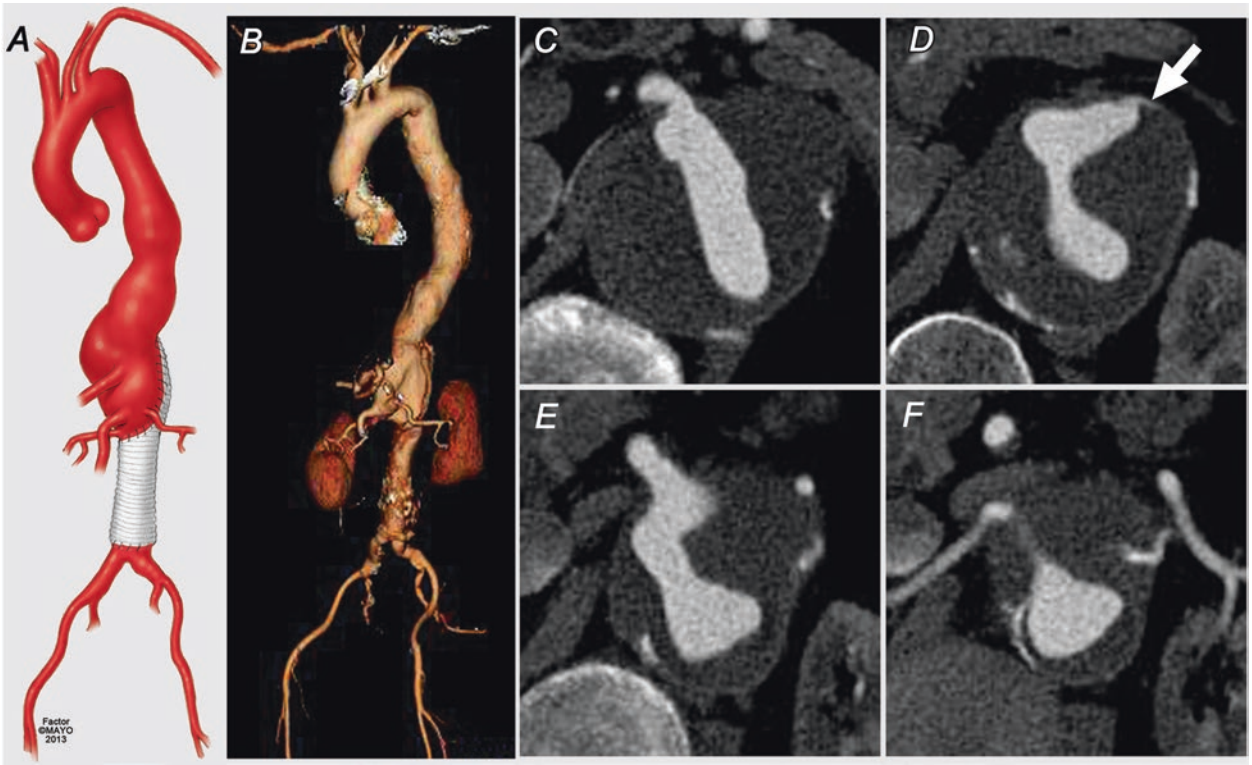


Fig. 45.20 Patient with supra-graft type III thoracoabdominal aortic aneurysm (**a** and **b**). Note the large amount of aortic intraluminal thrombus affecting the visceral segment of the aorta, including the celiac (**c**), stenosed left renal artery (**d**), SMA (**e**), and right renal artery (**f**). By permission of Mayo Foundation for Medical Education and Research. All rights reserved

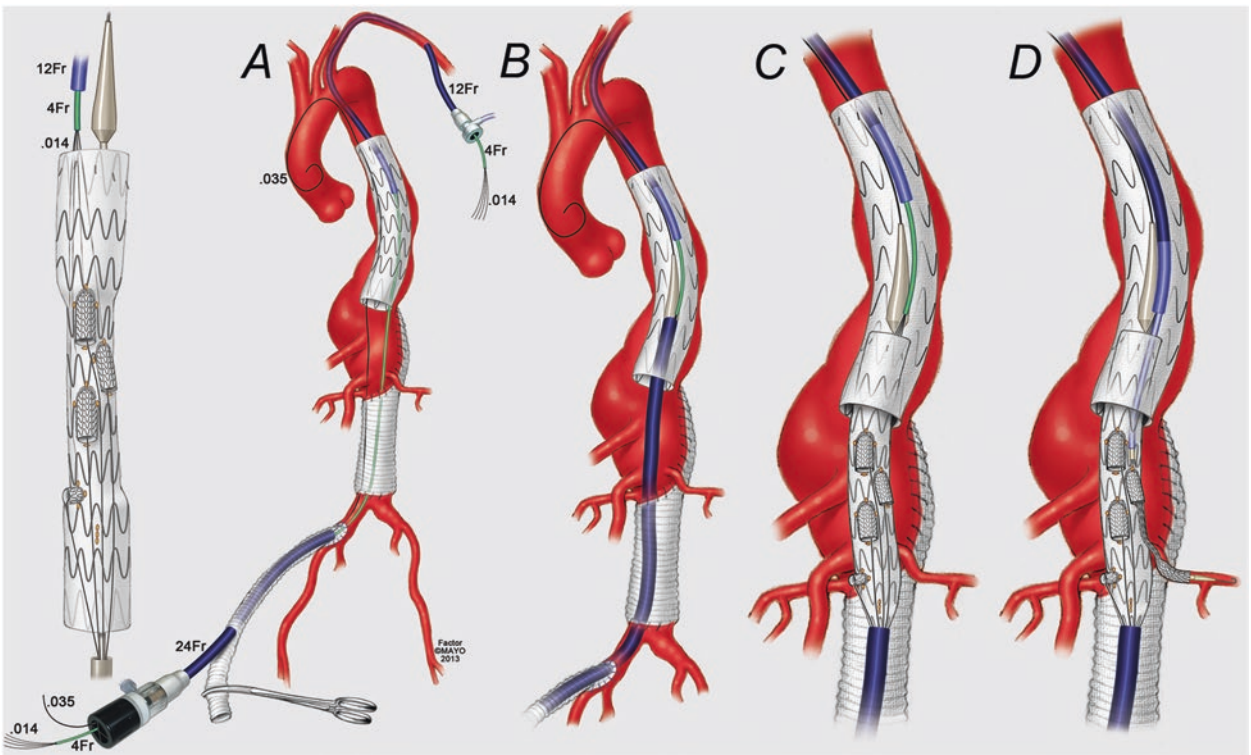


Fig. 45.21 Endovascular repair of thoracoabdominal aortic aneurysm using directional branches with preloaded guidewires. A 36×32×157 mm TX2 stent graft was deployed 6 cm proximal to the origin of the celiac axis (**a**). A 4Fr 110-cm sheath (Cook Medical Inc., Bloomington, IN) was introduced via the left brachial sheath and exteriorized via right iliac conduit (**a**). The branched TX2 stent graft component was loaded over the Lunderquist wires, while the four preloaded 0.014-in. guidewires were loaded into the 4Fr sheath (**b**). The TX2 stent graft and the 4Fr sheath were advanced to the visceral segment, and the stent graft was deployed with the branches positioned 2 cm above each target vessel (**c**). The 4Fr sheath was removed, and celiac axis, left renal artery, and SMA were sequentially catheterized using the preloaded guidewires (**d**). Each catheterization was facilitated by the advancement of a 5Fr shuttle sheath (Cook Medical Inc., Bloomington, IN) with a 0.018-in. dilator. By permission of Mayo Foundation for Medical Education and Research. All rights reserved

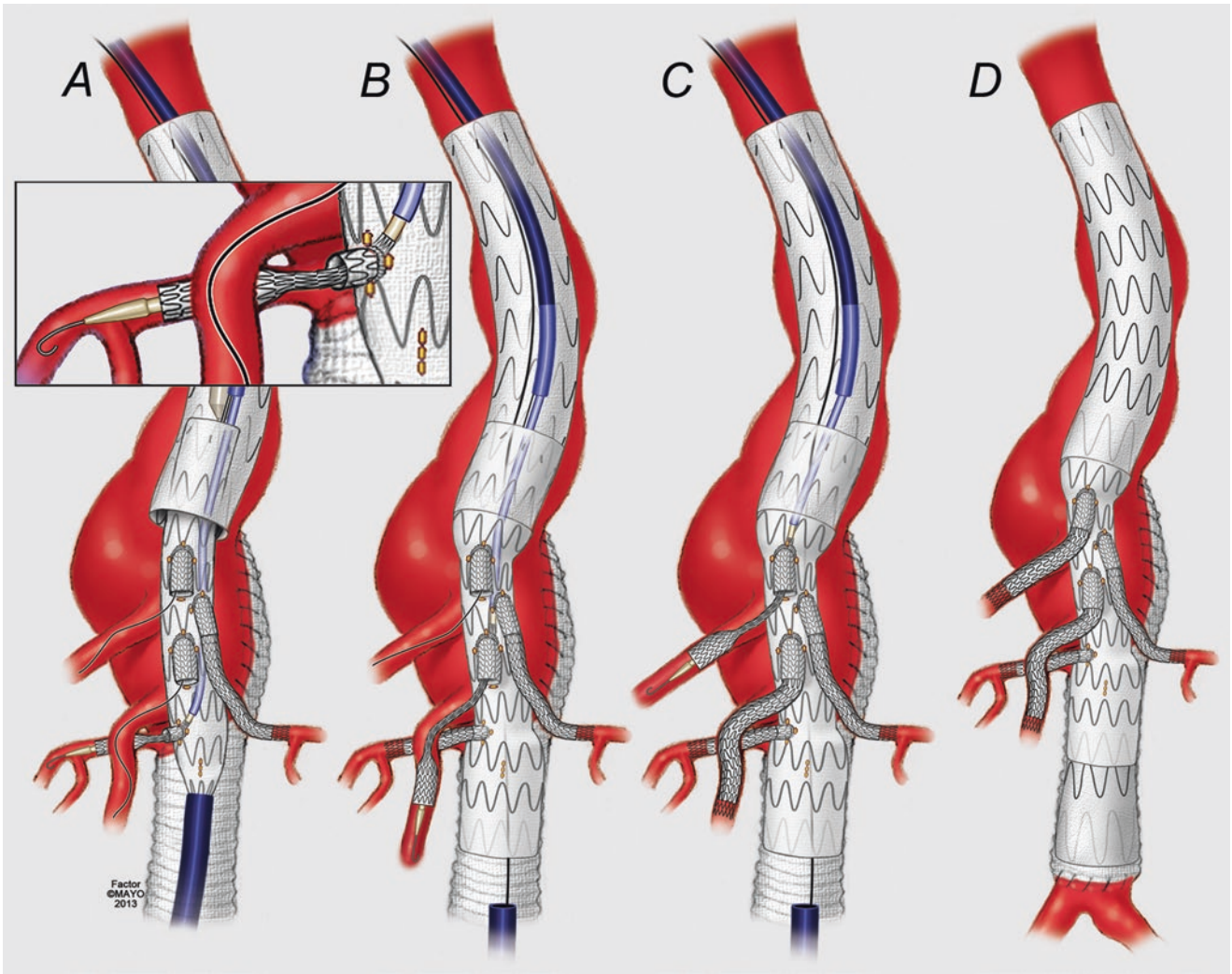


Fig. 45.22 Once the 5Fr was advanced through the branch, the preloaded guidewire was exchanged for a Kumpe catheter, which was used for target vessel catheterization. A 0.035-in. Amplatz guidewire (Cook Medical Inc., Bloomington, IN) was placed in the left renal artery, while V-18 guidewires (Boston Scientific, Bloomington, MN) were positioned into the celiac and SMA. The left renal artery was stented first using a 6×100-mm Viabahn stent graft, reinforced by 6×120-mm Protégé self-expandable stent (Covidien, Plymouth, MN) and introduced via a 7Fr Raabe sheath (Cook Medical Inc., Bloomington IN). Access was then established into the right renal artery (**a**) using the preloaded wire, which was exchanged for a 0.035-in. Rosen guidewire (Cook Medical Inc., Bloomington, IN). The diameter-reducing tie was removed, and the right renal artery was stented using 6×60-mm Fluency stent graft (Bard, Tempe, AZ), 6×60-mm Protégé self-expandable stent (Covidien, Plymouth, MN), and 7×22-mm iCAST covered stent (Atrium, Hudson, NH) introduced via 7Fr sheath. The celiac axis and SMA were sequentially stented by exchanging the 0.018-in. V-18 guidewires (Boston Scientific, Bloomington, MN) for 0.035-in. Rosen guidewires (**b**–**d**). The proximal and distal landing zones and attachment sites were dilated using Coda balloon (Cook Medical Inc., Bloomington, IN). By permission of Mayo Foundation for Medical Education and Research. All rights reserved

guidewires which exit from the top of the device. A 4Fr tibial sheath is passed from the left brachial approach to the femoral access site. The modified device is loaded onto the Lunderquist wire, while all four preloaded wires are loaded into the 4Fr sheath. The patient's branches are sequentially accessed and stented from the brachial access (Figs. 45.22 and 45.23).

Postoperative Management

The length of stay averages 4–6 days. Cerebrospinal fluid drainage is discontinued 48 h after the procedure after a 6-h clamp trial. Oral diet is resumed on postoperative day 2–3. Baseline CTA and baseline duplex ultrasound of the visceral



Fig. 45.23 Note the modified fenestrated-branched stent graft is deployed to just below the level of the right renal fenestration (**a**). The celiac axis (**a**, *double arrow*), SMA (**a**, *arrowhead*), and left renal artery (**a**, *white arrow*) are accessed using the preloaded guidewires as depicted in Fig. 45.23. The left renal stent was done first because of technical difficulty (**b**). Completion angiography revealed no endoleak, dissection or embolization (**c**). Follow-up CTA (**d**) demonstrated widely patent branch stent grafts with no endoleak. By permission of Mayo Foundation for Medical Education and Research. All rights reserved

branches are obtained prior to dismissal. Patients are started on aspirin indefinitely; clopidogrel is avoided early after extensive TAAA repair because of the risk of deployed spinal cord injury, which may necessitate placement of spinal drainage. Follow-up includes clinical examination and imaging (CTA and ultrasound) in 6–8 weeks, every 6 months during the first year and yearly thereafter.

Suggested Reading

1. Greenberg R, Eagleton M, Mastracci T. Branched endografts for thoracoabdominal aneurysms. J Thorac Cardiovasc Surg. 2010;140(6):S171–8.
2. Haulon S, D'Elia P, O'Brien N, Sobocinski J, Perrot C, Lerussi G, et al. Endovascular repair of thoracoabdominal aortic aneurysms. Eur J Vasc Endovasc Surg. 2010;39(2):171–8.
3. Mastracci TM, Greenberg RK, Eagleton MJ, Hernandez AV. Durability of branches in branched and fenestrated endografts. J Vasc Surg. 2013;57(4):926–33.
4. Oderich GS, Ricotta J. Modified fenestrated stent-grafts: device design, modifications, implantation, and current applications. Perspect Vasc Surg Endovasc Ther. 2009;21(3):170–2.
5. Oderich GS, Farber MA, Sanchez LA. Urgent endovascular treatment of symptomatic or contained ruptured aneurysms with modified stent grafts. Perspect Vasc Surg Endovasc Ther. 2011;23(3):186–94.
6. Oderich GS, Fatima J, Gloviczki P. Stent graft modification with mini-cuff reinforced fenestrations for urgent repair of thoracoabdominal aortic aneurysms. J Vasc Surg. 2011;54(5):1522–6.
7. Oderich GS. Technique of adding a diameter-reducing wire to the modified TX2 fenestrated stent graft. Vascular. 2010;18(6):350–5.
8. Oderich GS, Mendes BC, Correa MP. Preloaded guidewires to facilitate endovascular repair of thoracoabdominal aortic aneurysm using a physician-modified branched stent graft. J Vasc Surg. 2014;59(4):1168–73.

Part VIII

Complications of Complex Endovascular Aortic Repair

Thromboembolic Complications During Endovascular Repair of Complex Aortic Aneurysms

46

Mauricio S. Ribeiro, Leonardo Reis de Souza, and Gustavo S. Oderich

Introduction

Embolization of atheromatous debris is a known cause of major morbidity and mortality during complex endovascular procedures. Microembolizations of cholesterol fragments or macroscopic particles of thrombus and plaque can result in end-organ damage and loss of renal function, bowel infarction, spinal cord injury, or stroke [1–7]. Patel et al. reported the association of increased thrombus burden in the aorta as a predictor of mesenteric and renal ischemia in patients treated by fenestrated endografts [8]. In the thoracic and abdominal aorta, severe and irregular thrombus or debris has been identified as a predictor of renal deterioration, and embolic events were associated with floating thrombus [9–11]. Although assessment of aortic thrombus is done routinely as part of preoperative planning, few studies have correlated the severity of aortic wall thrombus (AWT) with specific events using a standardized classification system. This chapter summarizes current results of fenestrated and branched endovascular aortic repair (F-BEVAR) and parallel stent-grafts and presents a novel classification system to evaluate aortic wall thrombus.

M.S. Ribeiro
Department of Surgery and Anatomy, Ribeirão Preto Medical School, Ribeirão Preto Clinical Hospital, University of São Paulo, Campus Universitário s/n, Ribeirão Preto, São Paulo 14048-900, Brazil

L.R. de Souza
Postgraduate Program in Surgery, School of Medicine, Universidade Federal do Rio Grande do Sul, 2400 Ramiro Barcelos St, 2nd Floor, Porto Alegre 90035-003, Brazil

G.S. Oderich (✉)
Division of Vascular and Endovascular Surgery, Mayo Clinic, 200 First Street SW, Rochester, MN 55905, USA
e-mail: oderich.gustavo@mayo.edu

Clinical Implications

Few studies have reported specific embolic events following endovascular treatment of complex aortic aneurysms. Although most published series have included high-risk patients with multiple comorbidities, specific embolic complications are poorly reported. Acute kidney injury is the most common complication occurring in up to 40 % of the patients, depending on which criteria are used to define renal dysfunction. Postoperative dialysis has been reported in 1–10 % of the patients. Spinal cord injury, with transient or persistent symptoms, has been reported in up to 30 % of patients with thoracoabdominal aortic aneurysms. Strokes or transient ischemic attacks are less frequent. Regarding gastrointestinal complications, the most common complication is prolonged ileus. Bowel ischemia occurs in up to 9 % of the patients, whereas pancreatitis is infrequent (Table 46.1) [12–57].

Risk Stratification

None of the prior reports has described a standardized method to quantify aortic wall thrombus. We have recently analyzed 212 patients entered in a prospective database from 2007 to 2015. The study included patients treated for pararenal (PRA) or type IV thoracoabdominal aortic aneurysms (TAAAs) with F-BEVAR who had normal or relatively normal aortic segments in the arch, thoracic aorta, and above the renal arteries.

Aortic Wall Thrombus Assessment

Volumetric measurement of aortic wall thrombus (AWT) was performed using computed tomography angiography (CTA) and Terarecon Software (Fig. 46.1) in non-aneurysmal aortic segments (≤4 cm) of the ascending aorta and arch

© Mayo Foundation for Medical Education and Research 2017

G.S. Oderich (ed.), *Endovascular Aortic Repair*, DOI 10.1007/978-3-319-15192-2_46

Table 46.1 Operative variables and early complications of studies reporting data on fenestrated/branched endografts

First author (year)	*n*	Operative variables			30-day mortality, *n* (%)	Postoperative events, *n* (%)						
		V/P (mean)	Operative time (min)	Contrast load (ml)		AKI	Dialysis	Bowel ischemia	Ileus	Pancreat	Stroke/TIA	SCI
Eagleton (2016) [12]	354	3.7	m 360 ± 108	m 144 ± 78	17 (15)	18 (15)	8 (2)	2 (1)	6 (2)	1 (1)	8 (2)	31 (9)
Ferrer (2016) [13]	65	NR	NR	NR	5 (8)	NR	6 (9)	2 (3)	NR	NR	2 (3)	8 (12)
Hu (2016) [14]	15	1.9	m 238 ± 55	m 303 ± 56	0	2 (13)	0	0	NR	NR	0	0
Banno (2015)	80	2.4	m 191 ± 99	m 136 ± 84	8 (10)	10 (8)	2 (1)	7 (9)	1 (1)	0	1 (1)	3 (4)
Martin-Gonzalez (2015) [16]	225	1.9	NR	NR	14 (6)	64 (29)	1 (1)	NR	NR	NR	NR	NR
Marzelle (2015) [17]	268	3	M 197 (*r*, 150–260)	M 146 (*r*, 100–195)	26 (10)	48 (18)	15 (6)	3 (1)	NR	0	5 (2)	11 (4)
Sailer (2015)	157	NR	m 220 ± 110	m 162 ± 77	10 (6)	43 (28)	NR	NR	NR	NR	NR	NR
Shahverdyan (2015) [19]	35	2.4	M 188 (*r*, 111–465)	M 159 (*r*, 80–350)	1 (3)	4 (11)	0	2 (6)	NR	0	0	0
Sveinsson (2015) [23]	288	2.3	NR	NR	6 (2)	NR	NR	NR	NR	NR	NR	NR
Glebova (2015) [22]	458	NR	M 156 (IQR, 104–227)	NR	11 (2)	9 (2)	7 (2)	NR	NR	NR	4 (1)	NR
Verhoeven (2015) [24]	166	3.6	NR	M 210 (*r*, 80–500)	15 (9)	9 (5)	1 (1)	2 (1)	NR	NR	2 (1)	15 (9)
Cochennec (2015) [20]	11	3.2	NR	NR	1 (9)	NR	0	1 (9)	NR	NR	0	1 (9)
Gallito (2015) [21]	20	2.4										
Grimme (2014) [25]	138	1.8	NR	M 195 (*r*, 80–350)	2 (1)	57 (41)	2 (1)	2 (1)	NR	NR	2 (1)	0
Kristmundsson (2014, 2009) [27]	54	1.7	M 250 (*r*, 120–333)	M 270	2 (4)	19 (35)	0	1 (1)	NR	NR	0	0
Oderich (2014)	67	1.9	m 236 ± 81	NR	1 (2)	0	0	3 (4)	1 (1)	0	1 (1)	0
Lee (2014)	15	1.7	m 282	m 123	0	NR	NR	0	NR	NR	1 (6)	0
Liao (2014) [31]	8	1.5	NR	m 90	0	NR	NR	0	NR	NR	0	0
Dijkstra (2014) [28]	25	2.2	M 240 (IQR, 190–365)	M 194 (IQR, 103–320)	1 (4)	NR	NR	1 (4)	NR	NR	0	0
Vemuri (2014) [33]	57	2	m 250 ± 15	m 109 ± 6	1 (2)	4 (7)	1 (2)	0	NR	NR	1 (2)	1 (2)
Kasprzak (2014) [29]	83	3.6	NR	NR	6 (7)	NR	3 (4)	3 (4)	NR	NR	3 (4)	9 (11)
Canavati (2013) [34]	53	2.1	M 300 (*r*, 210–600)	NR	2 (4)	8 (15)	0	1 (1)	0	0	1 (1)	0
Kitagawa (2013) [35]	16	2.9	M 254 (*r*, 175–503)	M 69 (*r*, 31–121)	0	0	0	0	NR	NR	0	0
Perot (2013) [36]	115	NR	NR	NR	5 (4)	22 (19)	1 (1)	NR	NR	NR	NR	NR
Suominen (2013) [37]	21	2.1	NR	NR	2 (10)	1 (5)	0	NR	NR	NR	NR	NR
Tsilimparis (2013) [38]	264	NR	m 176 ± 102	NR	2 (1)	4 (2)	NR	NR	NR	NR	1 (1)	NR
Donas (2012) [39]	29	1.5	m 290 ± 122	m 156 ± 56	0	NR	0	NR	NR	NR	0	0
GLOBALSTAR (2012) [40]	318	2.3	M 240 (80–720)	NR	13 (4)	11 (3)	0	5 (2)	1 (1)	0	5 (2)	3 (1)
Metcalfe (2012) [43]	42	2.3	NR	NR	3 (7)	NR	1 (2)	0	NR	NR	0	1 (1)

(continued)

Table 46.1 (continued)

First author (year)	*n*	Operative variables			30-day mortality, *n* (%)	Postoperative events, *n* (%)						
		V/P (mean)	Operative time (min)	Contrast load (ml)		AKI	Dialysis	Bowel ischemia	Ileus	Pancreat	Stroke/TIA	SCI
Ferreira (2012) [41]	48	3.8	m 498 (*r*, 180–900)	m 160 (*r*, 48–295)	10 (21)	8 (17)	4 (8)	0	NR	0	3 (6)	3 (6)
Reilly (2012) [44]	81	3.8	m 370 ± 122	m 137 ± 82	3 (4)	21 (26)	4 (5)	NR	NR	NR	4 (5)	19 (23)
Manning (2011) [42]	20	NR	NR	NR	2 (10)	NR	1 (5)	0	NR	NR	1 (1)	0
Tambyraja (2011) [45]	29	1.7	NR	NR	0	NR	0	NR	NR	NR	NR	NR
Troisi (2011) [46]	107				2 (2)							
Amiot (2010) [47]	134	NR	M 180 (*r*, 85–720)	M 160 (*r*, 65–280)	3 (2)	13 (10)	2 (2)	0	NR	0	3 (2)	1 (1)
Verhoeven (2010) [48]	100	1.7	M 180 (*r*, 110–540)	m 193 ± 50	1 (1)	NR	NR	1 (1)	NR	NR	0	0
Greenberg (2009) [49]	30	1.7	M 234 (*r*, 170–554)	NR	0	NR	0	0	1 (3)	0	0	0
Scurr (2008) [50]	45	1.7	M 350 (*r*, 240–600)	NR	2 (4)	1 (2)	0	0	NR	NR	1 (2)	0
Ziegler (2007) [51]	63	2.2	m 204 ± 93	m 96 ± 46	3 (5)	14 (22)	1 (2)	1 (2)	NR	NR	0	0
Roselli (2007) [52]	73	NR	m 320 ± 106	m 210 ± 99	4 (6)	6 (11)	1 (1)	1 (1)	NR	NR	1 (1)	2 (3)
Halak (2006) [53]	17	1.2	NR	NR	0	NR	1 (6)	NR	NR	NR	NR	NR
Muhs (2006) [54]	38	NR	m 192 ± 65	m 182 ± 62	1 (3)	NR	0	1 (3)	NR	NR	0	0
O'Neill (2006) [55]	119	NR	m 227 ± 76	m 179 ± 53	1 (1)	30 (25)	3 (2)	NR	NR	NR	NR	NR
Semmens (2006) [56]	58	2	NR	NR	2 (3)	4 (7)	0	0	NR	NR	0	1 (1)
Anderson (2001) [57]	13	2.5	NR	NR	0	NR	0	0	NR	NR	0	0

n number of patients, *V/P* number of fenestrations or branches per patient, *AKI* acute kidney injury, *Pancreat* pancreatitis, *TIA* transient ischemic attack, *SCI* spinal cord injury, *m*, mean ± standard deviation, *M* median; *r* range; *IQR* interquartile range, *NR* not reported

(Segment A), descending thoracic aorta (Segment B), and renal-mesenteric aorta (Segment C). An index was calculated using the Terarecon software volumetric tool to measure AWT burden in the three segments and in the entire length of aorta starting at the aortic annulus and extending 1-cm below the renal arteries. The infra-renal aorta, which was typically affected by large aneurysm and extensive laminated thrombus, was not measured. Because it is not possible to measure the volume of the thin walled intima, media, and adventitia, an AWT index was calculated by subtracting the volume of the aortic lumen from the total aortic volume, which includes the aortic lumen, any AWT, and the intima, media, and adventitia. Therefore, the AWT index was representative of the solid portion of the aortic wall. The AWT index was presented as a percent value (AWT Index = [Total Aortic Volume − Aortic Lumen Volume/Total Aortic Volume] × 100, Fig. 46.2).

In order to facilitate assessment of AWT in clinical practice, a novel classification was proposed using a 0–10 score system to quantify thrombus type, thickness, area of involvement, circumference, and number of affected segments. The patients were classified as mild (score 0–3), moderate (score 4–8), and severe AWT (score 9 and 10, Fig. 46.3). For purposes of this classification, we analyzed the most severely affected segment of the aorta using axial cuts. The area was selected after examination of the entire length of the aorta. The final score was correlated with the AWT volume index measured in the three aortic segments and in the entire aorta to validate the proposed classification.

From the 212 patients, 98 (46 %) had minimal AWT, 75 (35 %) had moderate AWT, and 39 (18 %) had severe AWT (Table 46.2). The proposed classification correlated with objective assessment of AWT volume using the index in all

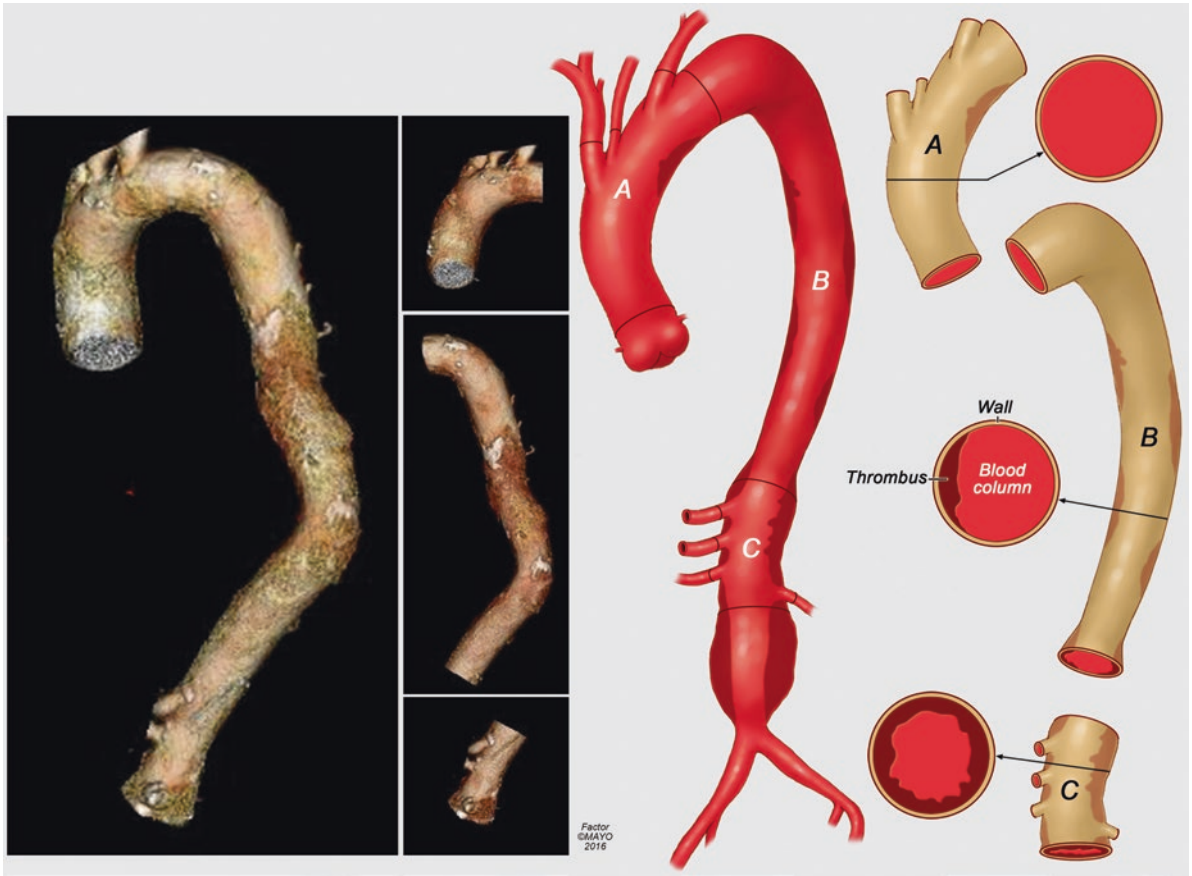


Fig. 46.1 Segmental aortic volumetric evaluation depicted as ascending and arch aorta (segment A), descending thoracic aorta (segment B) and renal-mesenteric aorta (segment C). By permission of Mayo Foundation for Medical Education and Research. All rights reserved

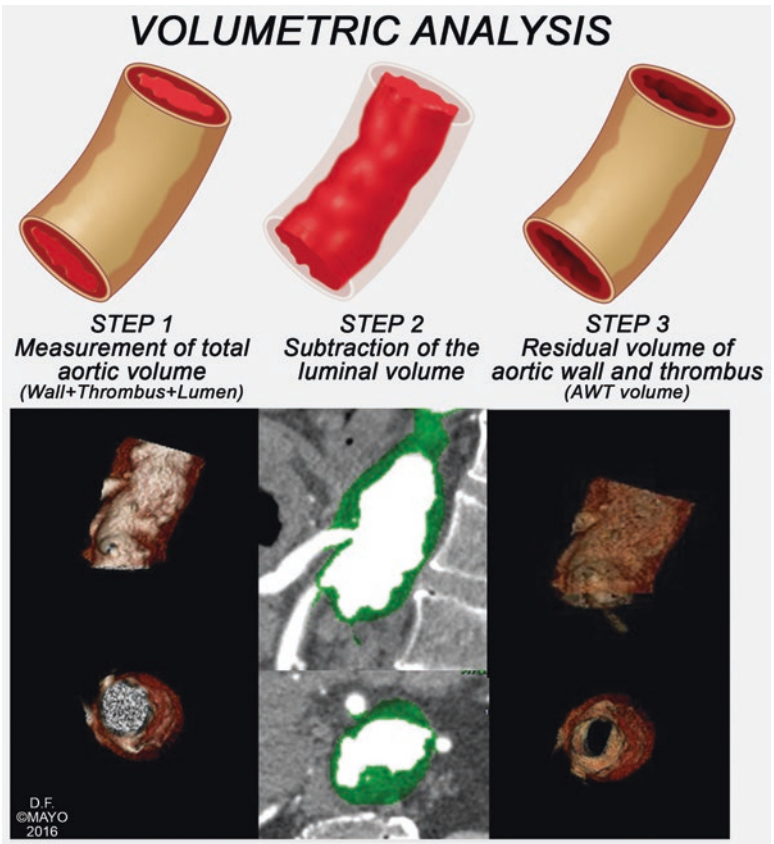


Fig. 46.2 Aortic wall thrombus volume measurement sequence. Total segmental volume measurement (step 1). Luminal volume subtraction (step 2). Remaining residual volume corresponding to the aortic wall and thrombus volume (step 3). By permission of Mayo Foundation for Medical Education and Research. All rights reserved

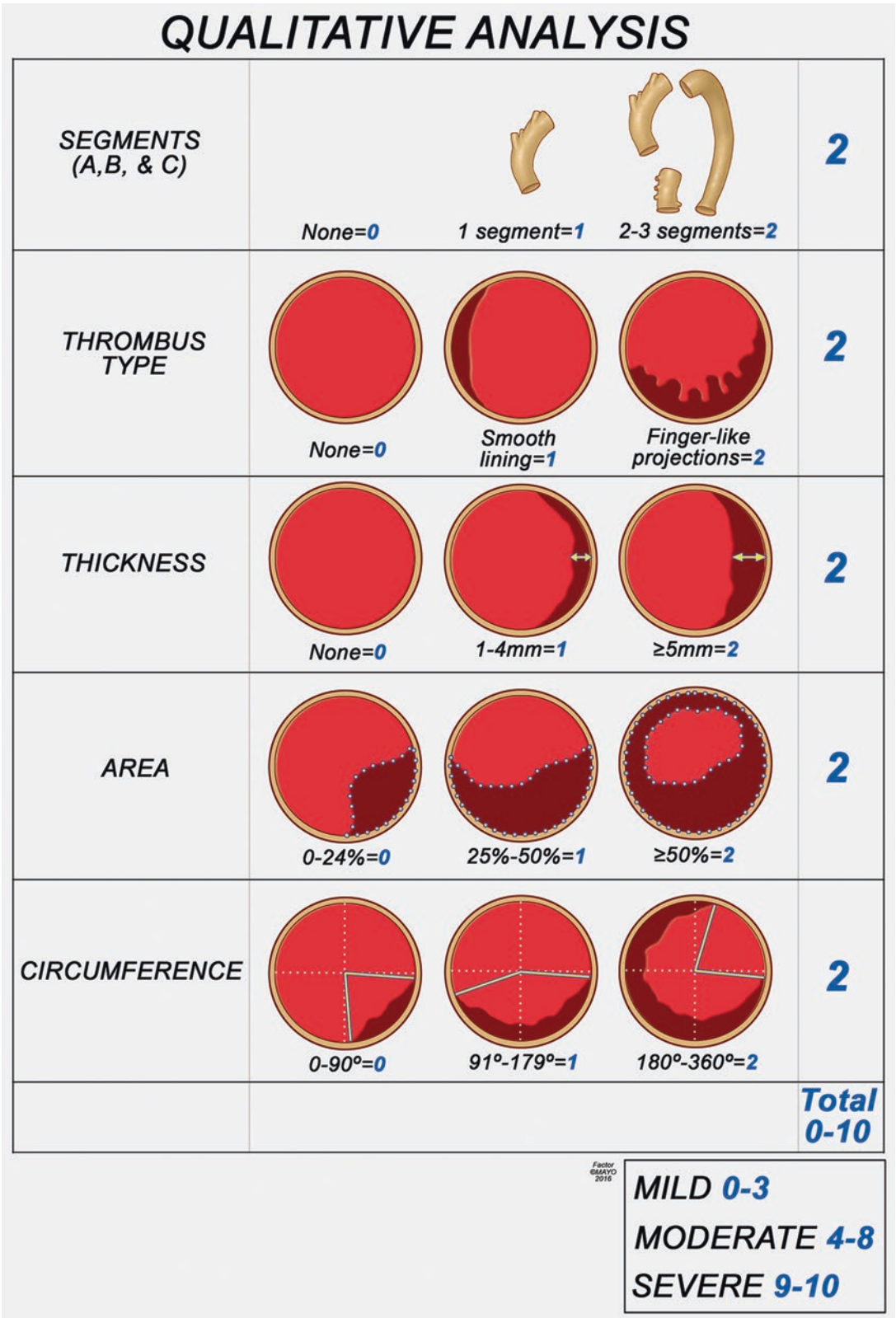


Fig. 46.3 Qualitative score-based classification. The most severely affected aortic area in CTA cross-section is classified for thrombus type (none, smooth lining or finger-like projections), thickness (none, 1–4 mm or ≥5 mm), area (0–24 %, 25–50 % or ≥50 %), and circumference (0–90°, 91–179° or ≥180°). Number of affected segments is also contemplated. Individual items are graded from 0 to 2. Mild AWT range from 0 to 4, moderate AWT from 4 to 8, and severe AWT scores 9 and 10. By permission of Mayo Foundation for Medical Education and Research. All rights reserved

Table 46.2 Clinical postoperative events in 212 patients treated by fenestrated and branched endovascular aortic repair (F-BEVAR) for pararenal and type IV thoracoabdominal aortic aneurysms (TAAA) according to the atherosclerotic aortic wall thrombus (AWT) classification

	All ($n=212$)	Mild ($n=98$)	Moderate ($n=75$)	Severe ($n=39$)	
Variable	*N* and (percent) or mean ± standard deviation				*P* value
Mortality ($n=1$)	1 (0.5)	0	1 (1.3)	0	0.71
Stroke ($n=4$)	4 (1.9)	1 (1)	2 (2.7)	1 (2.6)	0.46
Spinal cord injury ($n=3$)	3 (1.4)	0	2 (2.7)	1 (2.6)	0.16
Liver ($n=3$)	3 (1.4)	0 (0)	2 (2.7)	1 (2.6)	0.16
Spleen ($n=25$)	25 (12)	6 (6)	14 (19)	5 (13)	0.098
Kidney ($n=35$)	35 (17)	11 (11)	12 (16)	12 (31)	*0.009*
Liver-Kidney- Spleen ($n=50$)	50 (24)	16 (16)	20 (27)	14 (36)	*0.01*
Time to resume regular diet	2.9 ± 1.7	2.5 ± 1.4	3.1 ± 1.8	3.4 ± 2	*0.0115*
Pancreatitis ($n=2$)	2 (0.9)	2 (2)	0	0	0.17
Bowel ischemia ($n=5$)	5 (2.4)	2 (2)	2 (2.7)	1 (2.6)	0.81
RIFLE ($n=45$)	45 (21)	16 (16)	16 (21)	13 (33)	*0.034*
AKIN ($n=48$)	48 (23)	17 (17)	17 (23)	14 (36)	*0.024*
All combined ($n=94$)	94 (44)	34 (35)	39 (52)	21 (54)	*0.016*

three segments. Aortic wall thrombus index averaged 15 ± 4 % for segment A, 22 ± 5 % for segment B, 26 ± 7 % for segment C, and 20 ± 4 % for the three segments. Thirteen patients (6 %) had AWT index <15 %.

Study Patients

From the 212 patients included in the study, there were 169 male (80 %) and 43 female (20 %), with mean age of 76 ± 7 years old. Aneurysm extent was PRA in 157 patients (74 %) and type IV TAAA in 55 patients (26 %). The maximum aneurysm diameter average was 63 ± 15 mm (Table 46.3). All procedures were performed in a hybrid endovascular room with fixed imaging unit using general endotracheal anesthesia in 210 patients (99 %). Cerebrospinal fluid drainage was used in 67 patients (32 %) and neuromonitoring in 55 patients (26 %). Ninety-six patients (46 %) had percutaneous trans-femoral approach and 29 required iliac conduits (14 %). There were 700 renal-mesenteric arteries incorporated by 609 fenestrations, 66 scallops, and 25 branches, with a mean of 3.1 ± 1 stented vessels per patient. Total volume of contrast and fluoroscopy time averaged 158 ± 63 ml and 88 ± 42 min, respectively. Technical success, defined by placement of the aortic stent and all intended side branches, was achieved in 207 patients (98 %). Estimated blood loss was 757 ± 859 ml. Seventy-two patients (34 %) received transfusion of packed red blood cells during the procedure (see Table 46.3). All risk factors, stent design, and procedure variables were similar in the mild, moderate, and severe AWT patients.

Clinical Events

Clinical outcomes included 30-day mortality, neurological complications (stroke and spinal cord injury), gastrointestinal (bowel ischemia, pancreatitis and time to resume regular diet) and renal injury by RIFLE and AKIN classification and decline in the estimated glomerular filtration rate (eGFR). Evidence of solid organ infarction was also reviewed in the postoperative CTA. Renal infarctions due to inadvertent occlusion of a main or accessory renal artery were excluded from analysis.

The was one 30-day mortality (0.5 %) for the entire cohort, which included a patient treated for suprarenal aortic aneurysm who died from complications of a type B dissection 8 days following the initial procedure (Table 46.4). The patient had AWT index of 17 % and was classified as moderate AWT. Four patients (1.9 %) had strokes, which occurred in the absence of significant AWT on Segment A, although three patients had moderate to severe AWT in the thoracic or renal-mesenteric segments and one had thrombus within the innominate artery origin (Table 46.5).

Three patients (1.4 %) developed SCI, including two with PRA and one with type IV TAAA. Of these, one had permanent paraplegia and two had improvements, being able to recover the ambulatory status. Patients with any SCI had higher AWT index in segment B (28 ± 3 % versus 22 ± 5 %) and C (30 ± 11 % versus 26 ± 7 %). Although there was no association of AWT index for any neurological events, six of the seven patients (86 %) who developed either stroke or SCI had moderate to severe AWT scores (see Tables 46.4 and 46.5).

Table 46.3 Clinical characteristics and procedural variables in 212 patients treated by fenestrated and branched endovascular aortic repair (F-BEVAR) for pararenal and type IV thoracoabdominal aortic aneurysms (TAAA) according to atherosclerotic aortic wall thrombus (AWT) classification

Variable	All ($n=212$)	Mild ($n=98$)	Moderate ($n=75$)	Severe ($n=39$)	P value
	N and (percent) or mean ± standard deviation				
AWT index (Segment A)	15 ± 4	13 ± 4	14 ± 4	17 ± 4	<0.001
AWT index (Segment B)	22 ± 5	20 ± 4	22 ± 3	27 ± 5	<0.001
AWT index (Segment C)	26 ± 7	23 ± 7	26 ± 6	32 ± 8	<0.001
AWT index (Segments A, B and C)	20 ± 4	18 ± 4	21 ± 4	24 ± 5	<0.001
Demographics					
Age	76 ± 7	75 ± 7	76 ± 7	76 ± 6	0.62
Male	169 (80)	79 (81)	62 (83)	28 (72)	0.37
Cardiovascular risk factors					
Hypertension	188 (89)	90 (93)	64 (90)	34 (89)	0.76
Cigarette smoking	184 (87)	88 (91)	63 (89)	33 (87)	0.79
Hypercholesterolemia	171 (81)	85 (88)	56 (79)	30 (79)	0.25
Coronary Artery Disease	136 (64)	71 (73)	43 (61)	22 (58)	0.12
Chronic Obstructive Pulmonary Disease	110 (52)	55 (57)	34 (48)	21 (55)	0.51
Prior myocardial Infarction	90 (42)	44 (45)	30 (42)	16 (42)	0.9
Active Smoking	51 (24)	20 (21)	21 (30)	10 (26)	0.40
Atrial Fibrillation	45 (21)	25 (26)	14 (20)	6 (16)	0.39
Diabetes Mellitus	41 (19)	18 (19)	15 (21)	8 (21)	0.90
Arrhythmia	36 (17)	18 (19)	13 (18)	5 (13)	0.74
Congestive Heart Failure (CHF)	34 (16)	20 (21)	9 (13)	5 (13)	0.32
Stroke/TIA	33 (16)	21 (22)	10 (14)	2 (5)	0.06
Oxygen dependent	8 (4)	5 (5)	2 (3)	1 (3)	0.67
Unstable Angina	2 (1)	2 (2)	0	0	0.32
Preoperative evaluation and comorbidity scores					
Positive	51 (24)	26 (29)	18 (29)	7 (19)	0.67
Baseline Creatinine (mg/dl)	1 ± 0.8	1 ± 0.8	1 ± 1	1 ± 0.3	0.22
Baseline GFR (mL/min/1.73 m2)	60 ± 20	61 ± 20	58 ± 21	59 ± 15	0.51
CKD Stage III–V	82 (39)	36 (37)	32 (43)	14 (36)	0.14
III	69 (33)	31 (32)	24 (32)	14 (36)	
IV	9 (4)	4 (4)	5 (7)	0	
V	4 (2)	1 (1)	3 (4)	0	
ASA Clinical Score					0.86
I	16 (8)	7 (7)	5 (7)	4 (10)	
II	94 (44)	44 (45)	33 (44)	17 (44)	
III	86 (41)	37 (38)	33 (44)	16 (41)	
IV	16 (8)	10 (10)	4 (5)	2 (5)	
SVS total score	1 ± 0.5	1 ± 0.5	1 ± 0.5	1 ± 0.5	0.60
Body Mass Index (kg/m(2))	29 ± 6	29 ± 6.2	28 ± 5	28 ± 6	0.48
Peripheral Arterial Disease	75 (35)	37 (38)	27 (38)	11 (29)	0.57
Procedure details					
Anesthesia General	210 (99)	96 (98)	75 (100)	39 (100)	0.55
Cerebrospinal Fluid Drainage	67 (32)	25 (26)	27 (36)	15 (38)	0.2
Somatosensory evoked potential (SSP)/Motor evoked potentials (MEP)	55 (26)	20 (20)	20 (27)	15 (38)	0.09
Percutaneous	96 (46)	45 (46)	28 (38)	23 (59)	0.11
Conduit	29 (14)	11 (11)	15 (21)	3 (8)	0.09
Amount of contrast used (cc)	158 ± 63	154 ± 67	167 ± 62	151 ± 55	0.34
Total fluoroscopy time (min)	88 ± 42	87 ± 47	91 ± 40	86 ± 32	0.74
Estimated blood loss (cc)	757 ± 859	750 ± 790	867 ± 866	565 ± 989	0.2
Transfusion blood products					

(continued)

Table 46.3 (continued)

Variable	All ($n=212$)	Mild ($n=98$)	Moderate ($n=75$)	Severe ($n=39$)	P value
	N and (percent) or mean ± standard deviation				
PRBC	72 (34)	34 (35)	26 (35)	12 (31)	0.9
FFP	14 (7)	6 (6)	6 (8)	2 (5)	0.81
Platelets	17 (8)	8 (8)	8 (11)	1 (3)	0.31
Cryoprecipitate	2 (1)	2 (2)	0	0	0.31
Hypogastric branches (unilateral or bilateral)	4 (2)	4 (4)	0	0	0.12
Number of vessels stented per patient (mean)	3.1 ± 1	2.9 ± 1	3.1 ± 1	3.2 ± 0.9	0.25

Table 46.4 Correlation of atherosclerotic aortic wall thrombus (AWT) index values (% ± SD) and clinical events in 212 patients treated by fenestrated-branched endovascular aortic repair (F-BEVAR)

Variable (N)	Segment	AWT index (% ± SD)		P value
		Yes (event)	No	
Mortality ($n=1$)	A	14	15 ± 4	0.78
	B	18	22 ± 5	0.39
	C	23	26 ± 7	0.66
Neurologic				
Stroke ($n=4$)	A	15 ± 3	15 ± 4	0.85
Spinal cord injury ($n=3$)	A	16 ± 5	15 ± 4	0.7
	B	28 ± 3	22 ± 5	0.11
	C	30 ± 11	26 ± 7	0.37
Solid organ infarction				
Liver ($n=3$)	A	17 ± 4	15 ± 4	0.24
	B	25 ± 7	22 ± 5	0.45
	C	37 ± 15	26 ± 7	*0.043*
Spleen ($n=25$)	A	16 ± 4	14 ± 4	0.2
	B	25 ± 5	22 ± 5	*0.011*
	C	29 ± 7	26 ± 7	*0.033*
Kidney ($n=35$)	A	16 ± 3	14 ± 4	*0.039*
	B	24 ± 6	22 ± 5	*0.025*
	C	29 ± 8	26 ± 7	*0.031*
Any infarction ($n=50$)	A	16 ± 4	14 ± 4	*0.016*
	B	24 ± 5	22 ± 5	*0.005*
	C	28 ± 8	25 ± 7	*0.029*
Gastrointestinal events				
Pancreatitis ($n=2$)	A	19	15 ± 4	0.29
	B	24	22 ± 5	0.71
	C	18 ± 6	26 ± 7	0.13
Bowel ischemia ($n=5$)	A	15 ± 4	15 ± 4	0.98
	B	19 ± 5	23 ± 5	0.11
	C	21 ± 3	26 ± 7	0.16
Acute renal deterioration				
RIFLE ($n=45$)	A	15 ± 3	14 ± 4	0.17
	B	25 ± 6	22 ± 4	*0.002*
	C	27 ± 8	26 ± 7	0.46
AKIN ($n=48$)	A	15 ± 3	15 ± 4	0.95
	B	24 ± 6	22 ± 4	*0.038*
	C	27 ± 8	26 ± 7	0.64
All combined ($n=94$)	A	15 ± 4	14 ± 4	0.07
	B	23 ± 6	22 ± 4	0.12
	C	27 ± 8	26 ± 7	0.25

Table 46.5 Renal function deterioration using the RIFLE (Risk, Injury, Failure, Loss, End Stage) and AKIN (Acute Kidney Injury) criteria in 212 patients treated by fenestrated-branched endovascular aortic repair (F-BEVAR)

AWT index (%)		Any stage	*R* (*n*=32)	*I* (*n*=8)	*F* (*n*=4)	*L* (*n*=1)	No	*P* value
		Mean ± standard deviation						
		Mean ± standard deviation						
RIFLE (*n*=45)	A	15±3	15±3	15±3	17±4	17	14±4	0.17
	B	25±6	25±5	21±6	27±7	23	22±4	0.002
	C	27±8	27±8	26±8	26±7	25	26±7	0.46

		Any stage	1 (*n*=39)	2 (*n*=7)	3 (*n*=2)		No	*P* value
		Mean ± standard deviation						
		Mean ± standard deviation						
AKIN (*n*=48)	A	14±3	14±4	15±4	17±0.6		15±4	0.95
	B	24±6	24±6	20±6	25±4		22±4	0.038
	C	26±8	27±8	25±8	27±4		26±7	0.64

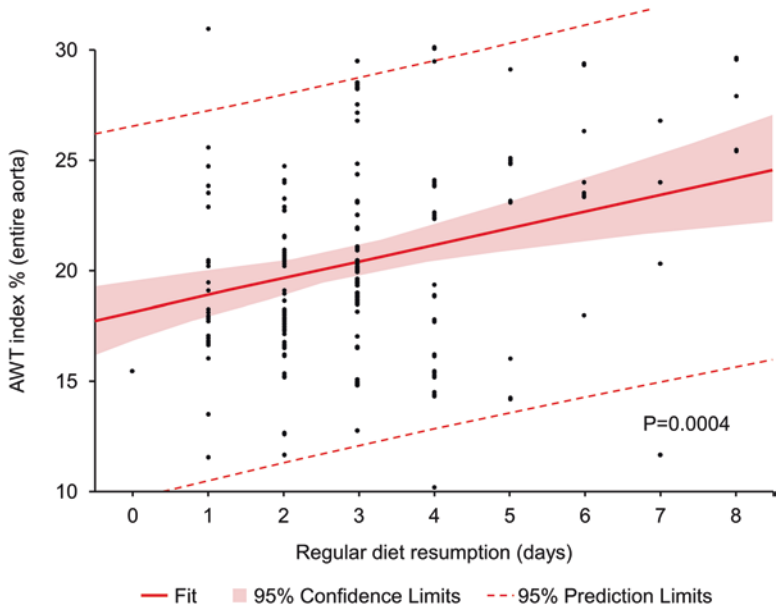


Fig. 46.4 Linear regression analysis curve showing the association between AWT index and postoperative diet resumption. All segments were analyzed as a whole. As higher is the AWT index depicted in the *y* axis as longer is the time to resume the regular diet depicted in the *x* axis. By permission of Mayo Foundation for Medical Education and Research. All rights reserved

The mean time to resume a regular diet was 2.9±1.7 days and was significantly longer in patients with higher AWT volume index in segment B (P=0.018), segment C (P=0.0001) and in the three segments using linear regression analysis (P=0.0004, Fig. 46.4). There was also longer time to resume regular diet for patients with severe and moderate thrombus burden (3.4±2 and 3.1±2 days versus 2.9±1.7 days, P=0.0115). Gastrointestinal complications included ischemic colitis in four patients (1.8%) and pancreatitis in two patients (1%). There was no association between these two complications and AWT index.

Forty-five patients (21%) had acute kidney injury (AKI) using the definitions proposed by RIFLE criteria (see Table 46.4). Thirty-two patients (15%) reached the "Risk" stage, eight (4%) the "Injury" stage, four (2%) the "Failure" stage, and one (0.5%) the "Loss" stage, requiring temporary hemodialysis. None of the patients require permanent hemodialysis. Among patients who developed acute kidney injury, AWT index was higher in segment B (25±6% versus 22±4%, p=0.002), with the highest AWT index observed for those patients who had "failure" (27±7%). Results were similar using the definitions proposed by the AKIN classification, including 48 patients (23%) who had any AKI. Thirty-nine patients (18%) reached stage one, seven (3%) stage two, and two (0.9%) stage three. Segment B had the highest AWT index for patients who developed AKI (24±6% versus 22±4%, p=0.04, see Table 46.4).

There was also direct association between decline in postoperative eGFR and AWT index in segments A and B and for entire evaluated aorta (Fig. 46.5, P=0.023) using

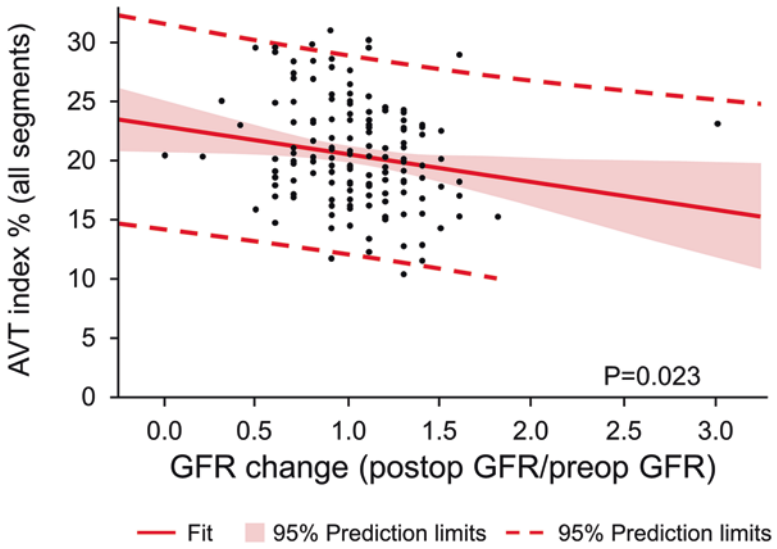


Fig. 46.5 Linear regression analysis curve showing the association between AWT index and early postoperative decline in eGFR. All segments were analyzed as a whole. To evaluate the changes in the renal function, postoperative eGFR was divided by its preoperative value. By deduction, as lower is this ratio as greater is the eGFR decline. The graph depicts an inverse correlation i.e., as higher is the AWT index, as lower is the ratio and, therefore, more severe is the eGFR decline. By permission of Mayo Foundation for Medical Education and Research. All rights reserved

the linear regression analysis. Using multivariate analysis, AWT index in segment B was associated with AKI using both the RIFLE ($P=0.02$) and AKIN criteria ($P=0.0128$ and $P=0.0007$, respectively). Other independent risk factors for AKI were pre-existing CKD stage III–V and volume of contrast. AKI for was significantly more frequent in patients with moderate to severe AWT scores using either RIFLE or AKIN criteria ($P=0.034$ and $P=0.024$, respectively).

Solid organ infarctions (Fig. 46.6) were observed in 50 patients (24%). Three patients had hepatic infarction with significantly higher AWT index scores in segment C (37±15% versus 26±7%, $P=0.043$) compared to patients with no hepatic infarction (see Tables 46.4 and 46.5). Twenty-five patients (12%) had splenic infarctions with higher scores in segments B (25±5% versus 22±5%, $P=0.011$) and C (29±7% versus 26±7, $P=0.033$) compared to patients with no splenic infarcts. Thirty-five patients (17%) had renal infarctions with higher scores in segment A (16±3 versus 14±4, $P=0.039$), B (versus 24±6% versus 22±5, $P=0.025$), and C (29±8% versus 26±7, $P=0.031$) compared to patients with no renal infarcts. The composite of any solid organ infarction was associated with higher AWT index scores for segments A (16±4% versus 14±4%, $P=0.016$), B (24±5% versus 22±5%, $p=0.005$) and C (28±8% versus 25±7%, $P=0.029$). Using multivariate analysis, AWT index in segment B was associated with solid organ embolization in all three organs ($P=0.0028$). Kidney infarctions and any solid organ infarction were more frequent in the severe group ($P=0.009$ and $P=0.01$, respectively).

Cases Examples

Case 1

An 81-year-old male patient presented with asymptomatic type IV thoracoabdominal aneurysm with maximum diameter of 60 mm. His medical comorbidities were hypertension, congestive heart failure, hypercholesterolemia, active smoking, previous myocardial infarction and CABG, peripheral arterial disease and chronic kidney disease stage III with a baseline estimated glomerular filtration rate of 46 ml/min/1.73 m^2 (serum creatinine: 1.4 mg/dl). Using the preoperative risk scales, he was scored as ASA II and 17 by the SVS total score. Preoperative cardiac stress test was positive for myocardial ischemia with an ejection fraction of 43%. He had no prior aortic surgeries or other relevant surgical history.

There was significant aortic wall thrombus in the descending thoracic and renal-mesenteric aorta with a total AWT index of 29% including 31% for segment B and 47% for segment C (both in the highest quartile). Using the score-based classification he had a score of 9 (severe AWT) achieving two points for number of segments, thrombus type, thickness, circumference and 1 point for area (Fig. 46.7). He underwent a

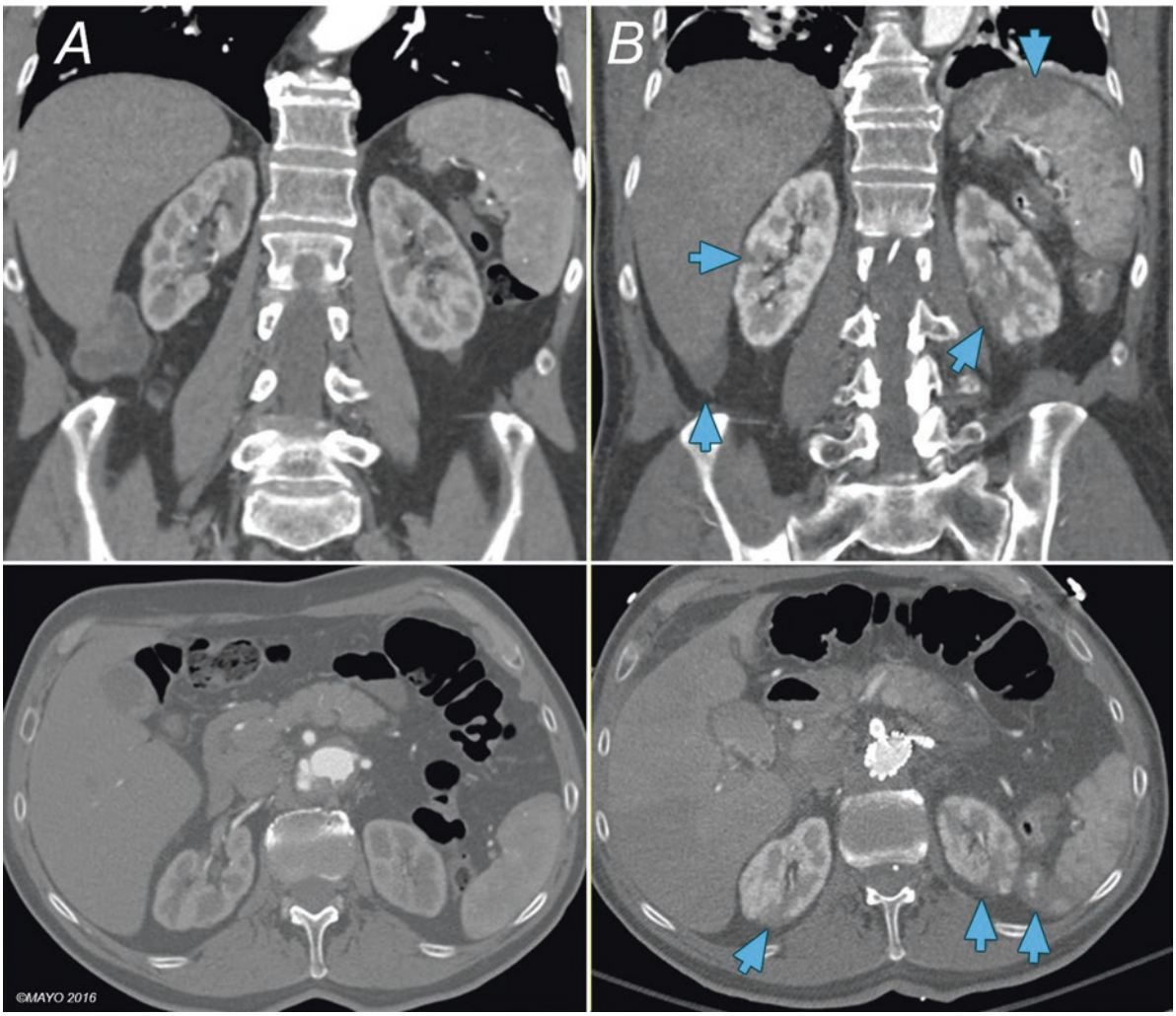


Fig. 46.6 Coronal and axial images of the preoperative (**a**) and early postoperative CTAs (**b**). *Arrows* depict infarction areas in liver, kidney (bilateral), and spleen. By permission of Mayo Foundation for Medical Education and Research. All rights reserved

fenestrated endovascular repair with four-vessel incorporation by fenestrations with a customized non-standard device. There were no intercurrences during the procedure with a total time of 186 min and 180 ml of contrast used.

In the postoperative time, the patient presented abdominal pain and acute renal injury (AKI) with a decline in the eGFR to 20 ml/min/1.73 m^2, classified as "Injury" by RIFLE criteria. Postoperative CTA showed kidney, spleen, and liver infarctions (see Fig. 46.6). In the postoperative day 3, patient had troponin elevations due to a non-Q-wave myocardial infarction. He also had transitory lower limb weakness with complete recovery before discharge. ICU length of stay was 6-day long with progressive improvement of the abdominal pain and clinical condition. He had his regular diet resumed in the postoperative day 5 which was significantly longer than the average time of 2.9 days. Total length of stay was 9 days being discharge in good conditions and with partial recovery of the renal function presenting at the dismissal a serum creatinine of 1.9 mg/dl and an eGFR of 32 ml/min/1.73 m^2.

Case 2

A 58-year-old male presented with an asymptomatic type IV thoracoabdominal aneurysm with maximum diameter of 57 mm. He was an active smoker and his preoperative cardiac stress test was negative with ejection fraction of 65 % and normal baseline renal function. He had a history of resected prostate and testicular cancer without other prior

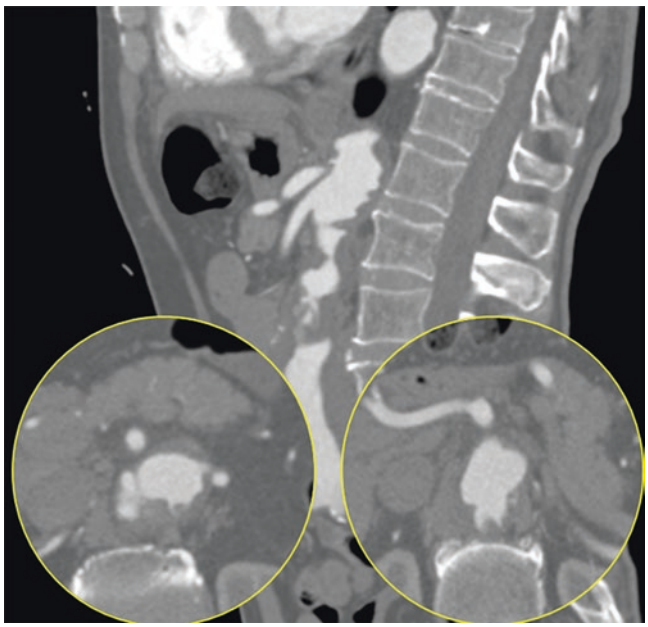


Fig. 46.7 Preoperative CTA of a patient with severe aortic wall thrombus in renal-mesenteric aorta. Thrombus severity details are depicted in the inserted images. By permission of Mayo Foundation for Medical Education and Research. All rights reserved

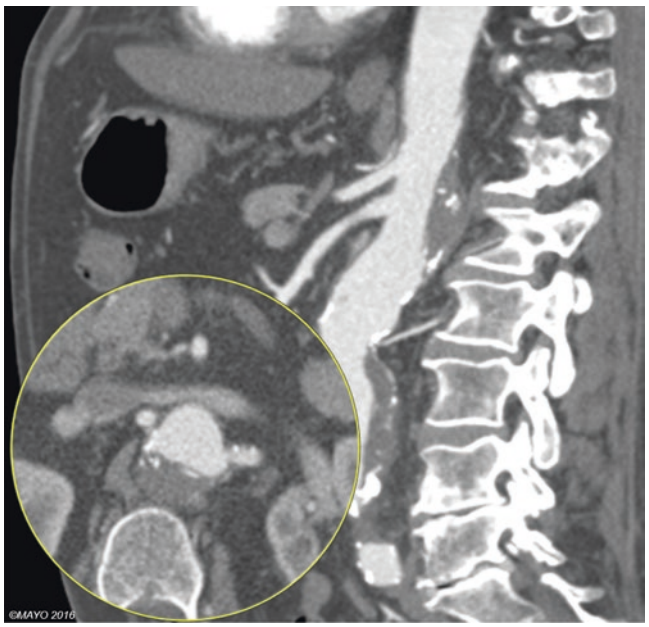


Fig. 46.8 Preoperative CTA showing significant aortic thrombus in the posterior aortic wall in the renal-mesenteric segment. Note its regular characteristic even though was classified as moderate due its expressive volume. By permission of Mayo Foundation for Medical Education and Research. All rights reserved

surgeries. He was classified as ASA II and SVS score three. There was regular aortic wall thrombus mainly in renal-mesenteric aorta with a total AWT index of 23 % including 25 % for segment B and 41 % for segment C, within the fourth quartile. Using the score-based classification he had a score of 7 (moderate AWT) achieving two points for number of segments and thickness and one point for thrombus type, circumference, and area (Fig. 46.8).

He underwent a fenestrated endovascular repair with four-vessel fenestrated component using a customized non-standard device. The length of surgery was 176 min with a total contrast volume of 170 ml without any major technical issue. Postoperative CTA showed mild spleen and left kidney infarctions (Fig. 46.9). However, there was no change in the renal function, being discharged 3 days after the procedure.

Case 3

An 84-year-old male presented with an asymptomatic par-visceral abdominal aneurysm with 59 mm in the maximum diameter. He had hypercholesterolemia and moderate pulmonary dysfunction due to asbestosis. He did not have renal dysfunction with a baseline creatinine of 0.8 mg/dl and an eGFR of 92 ml/min/1.73 m^2. His SVS score was 12 mostly due to his pulmonary disease and age. No previous aortic surgeries.

There was mild to moderate aortic wall thrombus mostly in segment C with a total AWT index of 20 % and an index of 26 % for segment C which matches the third quartile. Using the score-based classification he had a score of 8 (moderate AWT) achieving two points for thrombus type, thickness, circumference and one point for area and number of segments (Fig. 46.10).

He underwent an endovascular repair of his aneurysm with a five-vessel fenestrated endograft with one double-scallop for celiac axis and fenestrations for superior mesenteric artery, right renal artery, and two left-sided renal arteries. Length of surgery was 300 min long (endovascular time of 251 min) with 190 ml of contrast used. The procedure did not have complications.

Postoperatively he presented mild renal deterioration reaching the stage "Risk" by RIFLE criteria with a decrease in eGFR to 55 ml/min/1.73 m^2. He returned to his baseline renal function before discharge. Postoperative CTA showed significant bilateral kidney infarctions mainly in the right side (Fig. 46.11). Overall he recovered well from the surgery with rapid resume of his regular diet, being discharged at postoperative day 5.

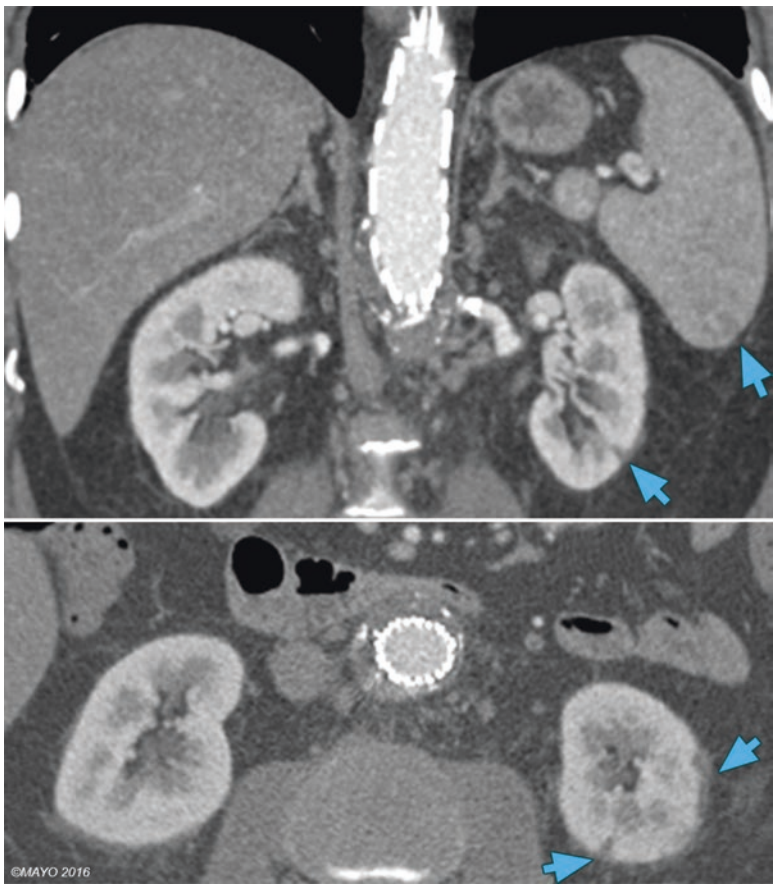


Fig. 46.9 Coronal and axial incidences of the early postoperative CTA showing wedge-shaped infarcted areas in left kidney and spleen (*arrows*). By permission of Mayo Foundation for Medical Education and Research. All rights reserved

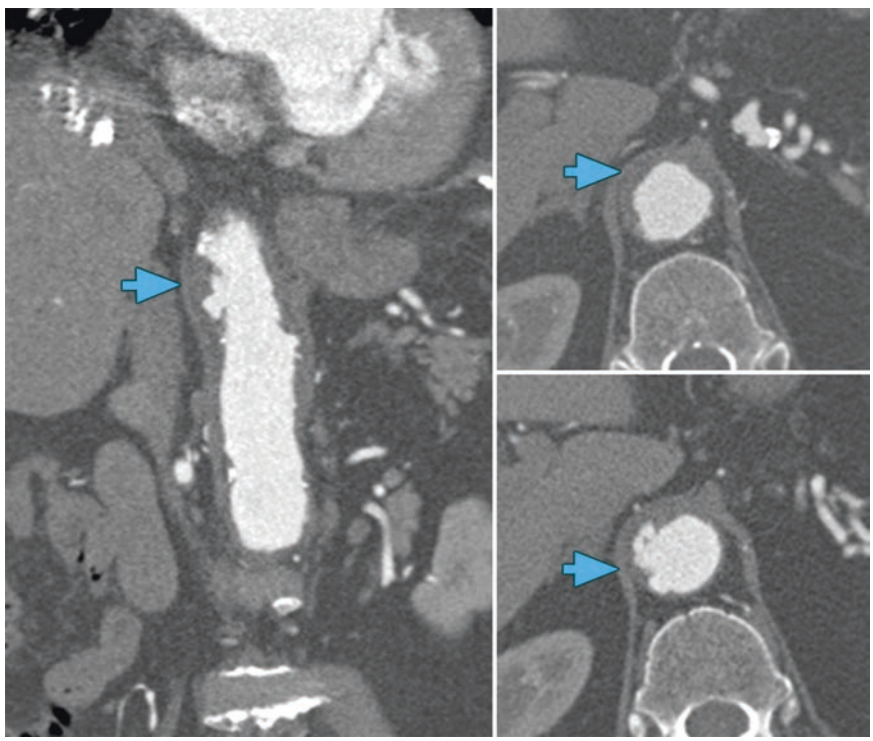


Fig. 46.10 Coronal and axial preoperative CTA images showing irregular thrombus in the renal-mesenteric aortic segment (*arrows*) that had a score eight (moderate AWT). By permission of Mayo Foundation for Medical Education and Research. All rights reserved

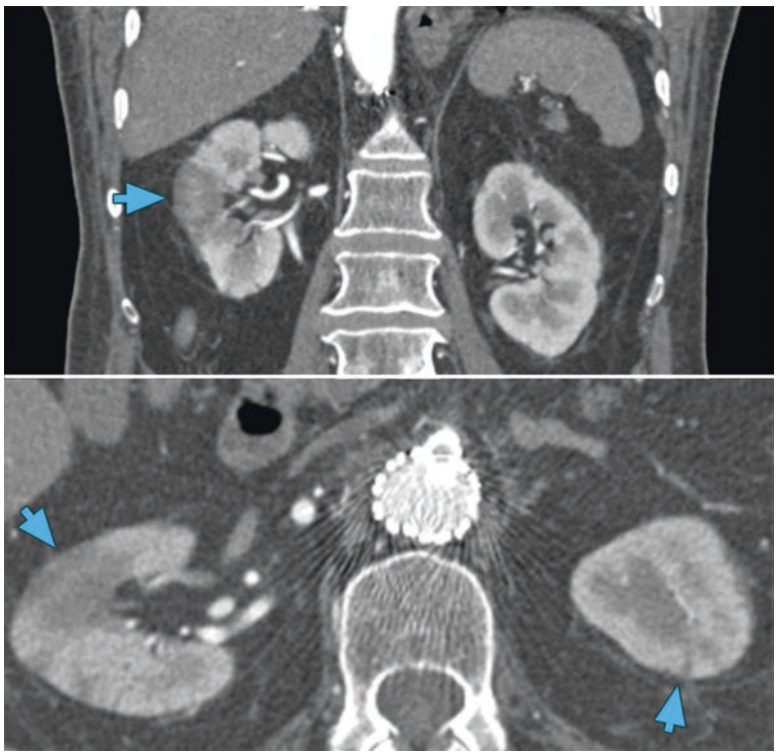


Fig. 46.11 Coronal and axial postoperative CTA images of bilateral kidney infarcts, mainly in the right side (*arrows*). Note the significant hypotenuse area in middle third of the right kidney which affected up to 30 % of the kidney volume. By permission of Mayo Foundation for Medical Education and Research. All rights reserved

Case 4

A 78-year-old female patient was evaluated for a 7.2-cm type IV TAAA. Medical comorbidities included current smoking, hypertension, stage IV chronic kidney disease, and severe ischemic cardiomyopathy. She was denied treatment of her aneurysm due to extensive atherosclerotic debris in the thoracoabdominal aorta as depicted in Fig. 46.12.

Conclusion

Atherosclerotic aortic wall thrombus is a common finding in the preoperative evaluation of F-BEVAR candidates and 54 % of the patients were classified as moderate and severe AWT in this study. A simple classification is proposed to stratify risk according to the amount of atherosclerotic debris in the aorta (Fig. 46.13). Management of embolization is difficult. For small debris prevention is the only effective treatment. Larger particles may be treated by catheter aspiration devices (Fig. 46.14) with careful attention to avoid vessel perforation (Fig. 46.15) which can further result in end-organ ischemia. Volumetric AWT evaluation is a reliable measurement and correlates with adverse events after F-BEVAR and has excellent correlation with the proposed classification. Therefore, AWT burden correlates with renal function deterioration, longer time to resume enteral diet, and more solid organ infarcts. Assessment of AWT should be part of preoperative planning and therapeutic decision-making in patients with complex aortic aneurysms.



Fig. 46.12 Sagittal CTA section depicting extremely severe debris in arch, and descending aorta which carries prohibitive risk for endovascular procedures. By permission of Mayo Foundation for Medical Education and Research. All rights reserved

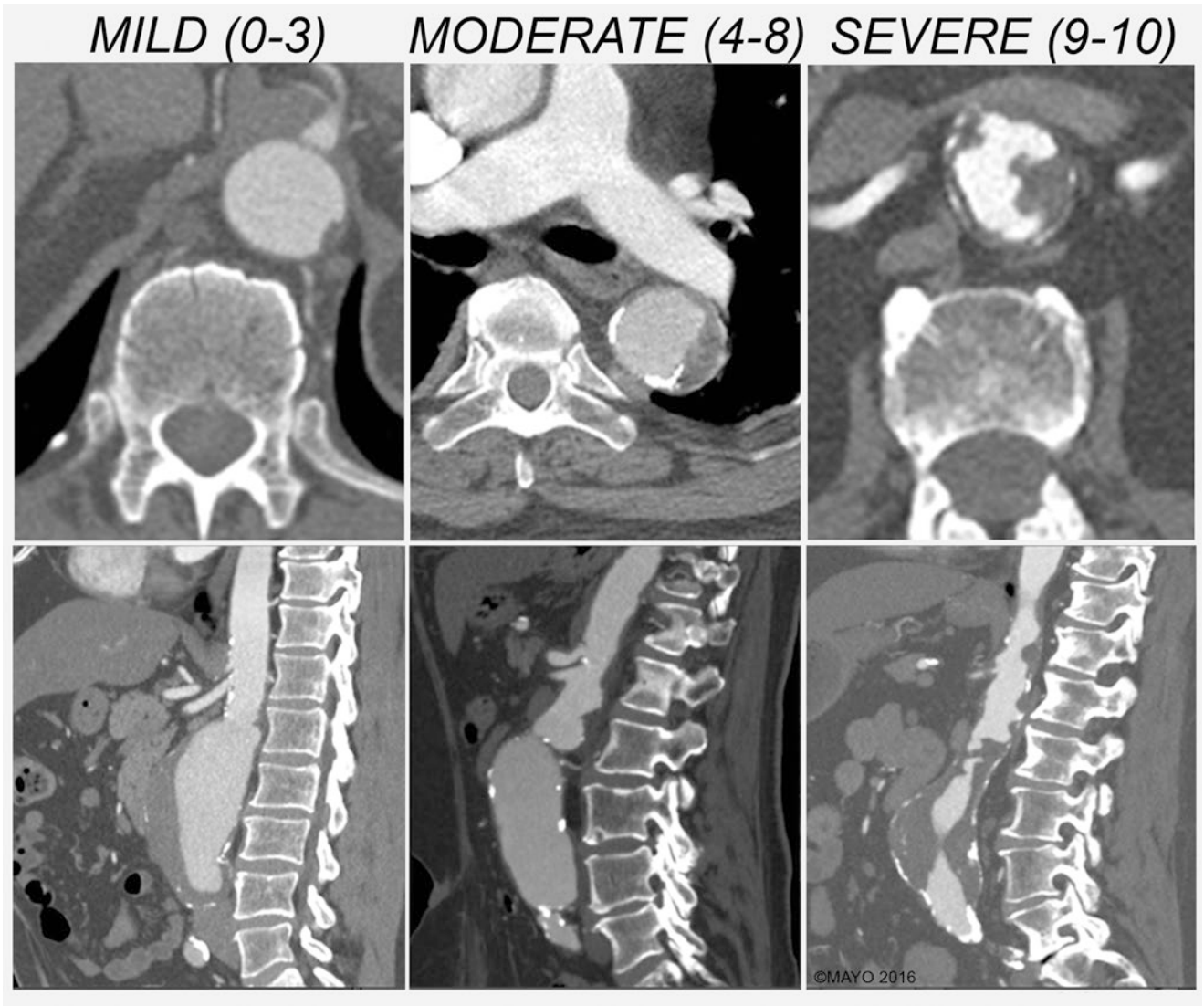


Fig. 46.13 Axial and sagittal CTA sections exemplifying all three aortic wall thrombus graduations by the proposed classification. Mild AWT patients have very slight and regular atheroma plaques without diffuse disease. Moderate AWT patients usually have higher amount of debris with or without finger-like thrombus, whereas severe ones have extremely irregular, large, and diffuse thrombus. By permission of Mayo Foundation for Medical Education and Research. All rights reserved

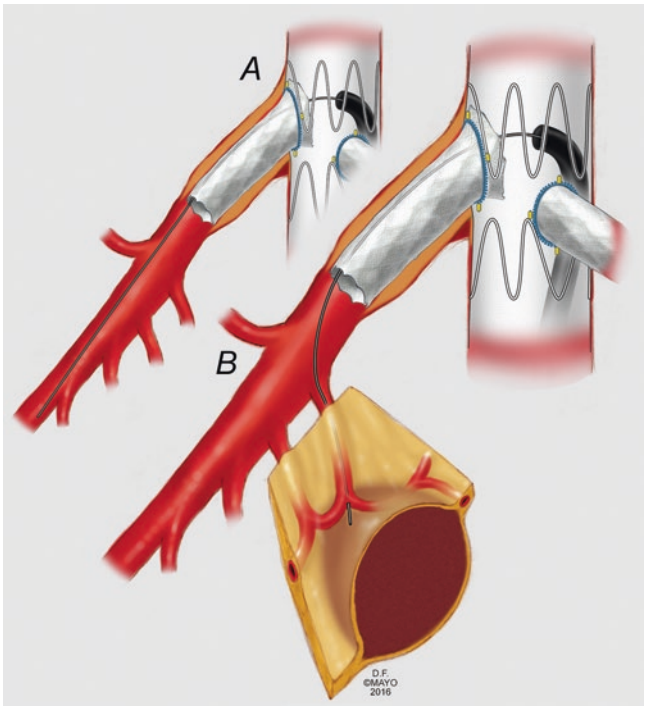


Fig. 46.15 Side-branch catheterization (**a**) depicting a branch mesenteric artery perforation by the guidewire tip resulting in mesenteric hematoma (**b**). By permission of Mayo Foundation for Medical Education and Research. All rights reserved

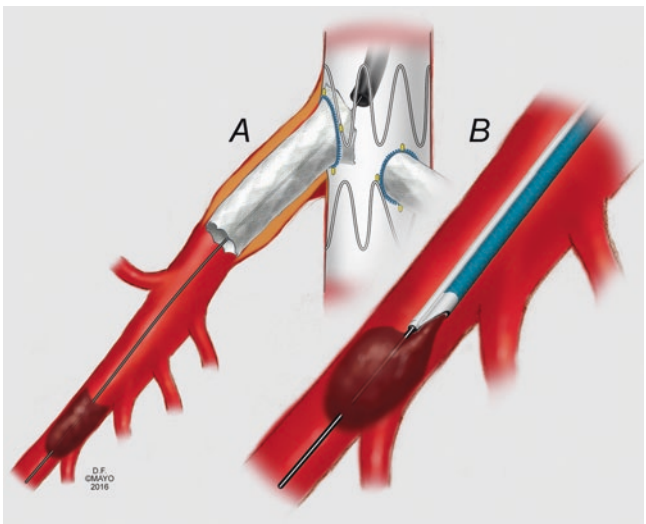


Fig. 46.14 Side-branch macroembolizations may be treated intraoperatively by suction catheters as depicted here. First, the partially or totally occluded segment has to be crossed by the guidewire (**a**). Sequentially, using specific catheter aspiration devices, the fresh thrombus can be aspirated as demonstrated (**b**). By permission of Mayo Foundation for Medical Education and Research. All rights reserved

References

1. Hayashida N, Murayama H, Pearce Y, Asano S, Ohashi Y, Kohno H, et al. Shaggy aorta syndrome after acute arterial macroembolism: report of a case. Surg Today. 2004;34(4):354–6.
2. Barbut D, Hinton RB, Szatrowski TP, Hartman GS, Bruefach M, Williams-Russo P, et al. Cerebral emboli detected during bypass surgery are associated with clamp removal. Stroke. 1994;25(12): 2398–402.
3. Fukumoto Y, Tsutsui H, Tsuchihashi M, Masumoto A, Takeshita A. The incidence and risk factors of cholesterol embolization syndrome, a complication of cardiac catheterization: a prospective study. J Am Coll Cardiol. 2003;42(2):211–6.
4. Dadian N, Ohki T, Veith FJ, Edelman M, Mehta M, Lipsitz EC, et al. Overt colon ischemia after endovascular aneurysm repair: the importance of microembolization as an etiology. J Vasc Surg. 2001;34(6):986–96.
5. Hoshina K, Hosaka A, Takayama T, Kato M, Ohkubo N, Okamoto H, et al. Outcomes after open surgery and endovascular aneurysm repair for abdominal aortic aneurysm in patients with massive neck atheroma. Eur J Vasc Endovasc Surg. 2012;43(3):257–61.
6. Mariscalco G, Piffaretti G, Tozzi M, Bacuzzi A, Carrafiello G, Sala A, et al. Predictive factors for cerebrovascular accidents after thoracic endovascular aortic repair. Ann Thorac Surg. 2009;88(6):1877–81.
7. Van Mieghem NM, El Faquir N, Rahhab Z, Rodríguez-Olivares R, Wilschut J, Ouhlous M, et al. Incidence and predictors of debris embolizing to the brain during transcatheter aortic valve implantation. JACC Cardiovasc Interv. 2015;8(5):718–24.
8. Patel SD, Constantinou J, Hamilton H, Davis M, Ivancev K. Editor's choice—a shaggy aorta is associated with mesenteric embolisation in patients undergoing fenestrated endografts to treat paravisceral aortic aneurysms. Eur J Vasc Endovasc Surg. 2014;47(4):374–9.
9. Abissegue YG, Lyazidi Y, Chtata H, Bakkali T, Taberkant M. Acute systemic embolism due to an idiopathic floating thrombus of the thoracic aorta: success of medical management: a case report. BMC Res Notes. 2015;8:181.
10. Boufi M, Mameli A, Compes P, Hartung O, Alimi YS. Elective stent-graft treatment for the management of thoracic aorta mural thrombus. Eur J Vasc Endovasc Surg. 2014;47(4):335–41.
11. Verma H, Meda N, Vora S, George RK, Tripathi RK. Contemporary management of symptomatic primary aortic mural thrombus. J Vasc Surg. 2014;60(6):1524–34.
12. Eagleton MJ, Follansbee M, Wolski K, Mastracci T, Kuramochi Y. Fenestrated and branched endovascular aneurysm repair outcomes for type II and III thoracoabdominal aortic aneurysms. J Vasc Surg. 2016;63(4):930–42.
13. Ferrer C, Cao P, De Rango P, Tshomba Y, Verzini F, Melissano G, et al. A propensity-matched comparison for endovascular and open repair of thoracoabdominal aortic aneurysms. J Vasc Surg. 2016;63(5):1201–7.
14. Hu Z, Li Y, Peng R, Liu J, Zhang T, Guo W. Experience with fenestrated endovascular repair of juxtarenal abdominal aortic aneurysms at a single center. Medicine. 2016;95(10), e2683.
15. Banno H, Cochennec F, Marzelle J, Becquemin JP. Comparison of fenestrated endovascular aneurysm repair and chimney graft techniques for pararenal aortic aneurysm. J Vasc Surg. 2014;60(1):31–9.
16. Martin-Gonzalez T, Pincon C, Maurel B, Hertault A, Sobocinski J, Spear R, et al. Renal outcomes following fenestrated and branched endografting. Eur J Vasc Endovasc Surg. 2015;50(4):420–30.

17. Marzelle J, Presles E, Becquemin JP, WINDOWS trial participants. Results and factors affecting early outcome of fenestrated and/or branched stent grafts for aortic aneurysms: a multicenter prospective study. Ann Surg. 2015;261(1):197–206.
18. Sailer AM, Nelemans PJ, van Berlo C, Yazar O, de Haan MW, Fleischmann D, et al. Endovascular treatment of complex aortic aneurysms: prevalence of acute kidney injury and effect on long-term renal function. Eur Radiol. 2016;26(6):1613–9.
19. Shahverdyan R, Majd MP, Thul R, Braun N, Gawenda M, Brunkwall J. F-EVAR does not impair renal function more than open surgery for juxtarenal aortic aneurysms: single centre results. Eur J Vasc Endovasc Surg. 2015;50(4):432–41.
20. Cochennec F, Kobeiter H, Gohel M, Leopardi M, Raux M, Majewski M, et al. Early results of physician modified fenestrated stent grafts for the treatment of thoraco-abdominal aortic aneurysms. Eur J Vasc Endovasc Surg. 2015;50(5):583–92.
21. Gallitto E, Gargiulo M, Freyrie A, Mascoli C, Massoni Bianchini C, Ancetti S, et al. The endovascular treatment of juxta-renal abdominal aortic aneurysm using fenestrated endograft: early and mid-term results. J Cardiovasc Surg (Torino). 2015. [Epub ahead of print].
22. Glebova NO, Selvarajah S, Orion KC, Black 3rd JH, Malas MB, Perler BA, et al. Fenestrated endovascular repair of abdominal aortic aneurysms is associated with increased morbidity but comparable mortality with infrarenal endovascular aneurysm repair. J Vasc Surg. 2015;61(3):604–10.
23. Sveinsson M, Sobocinski J, Resch T, Sonesson B, Dias N, Haulon S, et al. Early versus late experience in fenestrated endovascular repair for abdominal aortic aneurysm. J Vasc Surg. 2015;61(4):895–901.
24. Verhoeven EL, Katsargyris A, Bekkema F, Oikonomou K, Zeebregts CJ, Ritter W, et al. Editor's choice—ten-year experience with endovascular repair of thoracoabdominal aortic aneurysms: results from 166 consecutive patients. Eur J Vasc Endovasc Surg. 2015;49(5):524–31.
25. Grimme FA, Zeebregts CJ, Verhoeven EL, Bekkema F, Reijnen MM, Tielliu IF. Visceral stent patency in fenestrated stent grafting for abdominal aortic aneurysm repair. J Vasc Surg. 2014;59(2):298–306.
26. Chisci E, Kristmundsson T, de Donato G, Resch T, Setacci F, Sonesson B, et al. The AAA with a challenging neck: outcome of open versus endovascular repair with standard and fenestrated stent-grafts. J Endovasc Ther. 2009;16(2):137–46.
27. Kristmundsson T, Sonesson B, Dias N, Tornqvist P, Malina M, Resch T. Outcomes of fenestrated endovascular repair of juxtarenal aortic aneurysm. J Vasc Surg. 2014;59(1):115–20.
28. Dijkstra ML, Tielliu IF, Meerwaldt R, Pierie M, van Brussel J, Schurink GW, et al. Dutch experience with the fenestrated Anaconda endograft for short-neck infrarenal and juxtarenal abdominal aortic aneurysm repair. J Vasc Surg. 2014;60(2):301–7.
29. Kasprzak PM, Gallis K, Cucuruz B, Pfister K, Janotta M, Kopp R. Editor's choice—temporary aneurysm sac perfusion as an adjunct for prevention of spinal cord ischemia after branched endovascular repair of thoracoabdominal aneurysms. Eur J Vasc Endovasc Surg. 2014;48(3):258–65.
30. Lee JT, Lee GK, Chandra V, Dalman RL. Comparison of fenestrated endografts and the snorkel/chimney technique. J Vasc Surg. 2014;60(4):849–56. discussion 56–7.
31. Liao TH, Watson JJ, Mansour MA, Cuff RF, Banegas SL, Chambers CM, et al. Preliminary results of Zenith fenestrated abdominal aortic aneurysm endovascular grafts. Am J Surg. 2014;207(3):417–21. discussion 21.
32. Oderich GS. Commentary: physician-modified vs off-the-shelf fenestrated and branched endografts: is this a fair comparison? J Endovasc Ther. 2016;23(1):110–4.
33. Vemuri C, Oderich GS, Lee JT, Farber MA, Fajardo A, Woo EY, et al. Postapproval outcomes of juxtarenal aortic aneurysms treated with the Zenith fenestrated endovascular graft. J Vasc Surg. 2014;60(2):295–300.
34. Canavati R, Millen A, Brennan J, Fisher RK, McWilliams RG, Naik JB, et al. Comparison of fenestrated endovascular and open repair of abdominal aortic aneurysms not suitable for standard endovascular repair. J Vasc Surg. 2013;57(2):362–7.
35. Kitagawa A, Greenberg RK, Eagleton MJ, Mastracci TM. Zenith p-branch standard fenestrated endovascular graft for juxtarenal abdominal aortic aneurysms. J Vasc Surg. 2013;58(2):291–300.
36. Perot C, Sobocinski J, Maurel B, Millet G, Guillou M, D'Elia P, et al. Comparison of short- and mid-term follow-up between standard and fenestrated endografts. Ann Vasc Surg. 2013;27(5):562–70.
37. Suominen V, Pimenoff G, Salenius J. Fenestrated and chimney endografts for juxtarenal aneurysms: early and midterm results. Scand J Surg. 2013;102(3):182–8.
38. Tsilimparis N, Perez S, Dayama A, Ricotta 2nd JJ. Endovascular repair with fenestrated-branched stent grafts improves 30-day outcomes for complex aortic aneurysms compared with open repair. Ann Vasc Surg. 2013;27(3):267–73.
39. Donas KP, Eisenack M, Panuccio G, Austermann M, Osada N, Torsello G. The role of open and endovascular treatment with fenestrated and chimney endografts for patients with juxtarenal aortic aneurysms. J Vasc Surg. 2012;56(2):285–90.
40. British Society for Endovascular Therapy and the Global Collaborators on Advanced Stent-Graft Techniques for Aneurysm Repair (GLOBALSTAR) Registry. Early results of fenestrated endovascular repair of juxtarenal aortic aneurysms in the United Kingdom. Circulation. 2012;125(22):2707–15.
41. Ferreira M, Lanziotti L, Cunha R, D'Utra G. Endovascular repair of thoracoabdominal aneurysms: results of the first 48 cases. Ann Cardiothorac Surg. 2012;1(3):304–10.
42. Manning BJ, Agu O, Richards T, Ivancev K, Harris PL. Early outcome following endovascular repair of pararenal aortic aneurysms: triple- versus double- or single-fenestrated stent-grafts. J Endovasc Ther. 2011;18(1):98–105.
43. Metcalfe MJ, Holt PJ, Hinchliffe RJ, Morgan R, Loftus IM, Thompson MM. Fenestrated endovascular aneurysm repair: graft complexity does not predict outcome. J Endovasc Ther. 2012;19(4):528–35.
44. Reilly LM, Rapp JH, Grenon SM, Hiramoto JS, Sobel J, Chuter TA. Efficacy and durability of endovascular thoracoabdominal aortic aneurysm repair using the caudally directed cuff technique. J Vasc Surg. 2012;56(1):53–63.
45. Tambyraja AL, Fishwick NG, Bown MJ, Nasim A, McCarthy MJ, Sayers RD. Fenestrated aortic endografts for juxtarenal aortic aneurysm: medium term outcomes. Eur J Vasc Endovasc Surg. 2011;42(1):54–8.
46. Troisi N, Donas KP, Austermann M, Tessarek J, Umscheid T, Torsello G. Secondary procedures after aortic aneurysm repair with fenestrated and branched endografts. J Endovasc Ther. 2011;18(2):146–53.
47. Amiot S, Haulon S, Becquemin JP, Magnan PE, Lermusiaux P, Goueffic Y, et al. Fenestrated endovascular grafting: the French multicentre experience. Eur J Vasc Endovasc Surg. 2010;39(5):537–44.
48. Verhoeven EL, Vourliotakis G, Bos WT, Tielliu IF, Zeebregts CJ, Prins TR, et al. Fenestrated stent grafting for short-necked and juxtarenal abdominal aortic aneurysm: an 8-year single-centre experience. Eur J Vasc Endovasc Surg. 2010;39(5):529–36.
49. Greenberg RK, Sternbergh 3rd WC, Makaroun M, Ohki T, Chuter T, Bharadwaj P, et al. Intermediate results of a United States multicenter trial of fenestrated endograft repair for juxtarenal abdominal aortic aneurysms. J Vasc Surg. 2009;50(4):730–7. e1.
50. Scurr JR, Brennan JA, Gilling-Smith GL, Harris PL, Vallabhaneni SR, McWilliams RG. Fenestrated endovascular repair for juxtarenal aortic aneurysm. Br J Surg. 2008;95(3):326–32.
51. Ziegler P, Avgerinos ED, Umscheid T, Perdikides T, Stelter WJ. Fenestrated endografting for aortic aneurysm repair: a 7-year experience. J Endovasc Ther. 2007;14(5):609–18.

52. Roselli EE, Greenberg RK, Pfaff K, Francis C, Svensson LG, Lytle BW. Endovascular treatment of thoracoabdominal aortic aneurysms. J Thorac Cardiovasc Surg. 2007;133(6):1474–82.
53. Halak M, Goodman MA, Baker SR. The fate of target visceral vessels after fenestrated endovascular aortic repair—general considerations and mid-term results. Eur J Vasc Endovasc Surg. 2006;32(2):124–8.
54. Muhs BE, Verhoeven EL, Zeebregts CJ, Tielliu IF, Prins TR, Verhagen HJ, et al. Mid-term results of endovascular aneurysm repair with branched and fenestrated endografts. J Vasc Surg. 2006;44(1):9–15.
55. O'Neill S, Greenberg RK, Haddad F, Resch T, Sereika J, Katz E. A prospective analysis of fenestrated endovascular grafting: intermediate-term outcomes. Eur J Vasc Endovasc Surg. 2006;32(2):115–23.
56. Semmens JB, Lawrence-Brown MM, Hartley DE, Allen YB, Green R, Nadkarni S. Outcomes of fenestrated endografts in the treatment of abdominal aortic aneurysm in Western Australia (1997–2004). J Endovasc Ther. 2006;13(3):320–9.
57. Anderson JL, Berce M, Hartley DE. Endoluminal aortic grafting with renal and superior mesenteric artery incorporation by graft fenestration. J Endovasc Ther. 2001;8(1):3–15.

Spinal Cord Injury Prevention and Management

47

Matthew J. Eagleton

Introduction

Spinal cord ischemia (SCI) is a devastating complication after aortic surgery. This is true regardless of whether an open surgical or endovascular approach is chosen. Much effort has been directed toward understanding the pathophysiology of post-aneurysm repair SCI, and further efforts have been directed toward developing treatment strategies to prevent and treat this problem. These efforts, however, have predominantly been directed toward patients undergoing open surgical repair of thoracoabdominal aortic aneurysms (TAAA). Open surgical repair of TAAA has been associated with variable rates of SCI. Factors affecting the rates of SCI include the extent of aneurysm repaired, renal dysfunction, the ability to maintain direct or indirect perfusion of the spinal cord, and meticulous perioperative patient management. Symptoms of SCI in high-risk patients have been reported to occur at rates as high as 20 % following open surgical repair. High-volume centers, however, that utilize multiple modalities to prevent SCI report more contemporary rates of paraplegia as low as 5 %, if not lower, for the most extensive aneurysms [1–3].

Endovascular therapy is a relatively new approach to treat this complex disease process. Direct comparison of outcomes between open and endovascular therapies for TAAA is sparse, but in one limited study, outcomes for SCI were similar between the two approaches [4]. Many approaches to limit the effects of SCI, however, are not applicable to endovascular patient. Because of this, there is a new interest directed toward the development of treatment paradigms for patients undergoing endovascular therapy in order to help mitigate this untoward event. Despite efforts to prevent SCI, it still occurs and is devastating when it does. The aim of this current chapter is to describe the incidence, presentation, and mechanisms of SCI in the endovascular era and to discuss treatment strategies in the unfortunate scenario in which lower extremity weakness ensues.

SCI Following Endovascular Aortic Repair

The incidence of spinal cord ischemia after endovascular repair is directly related to the extent of the aorta that is excluded with the repair [4, 5]. Rates of SCI after open repair of abdominal aortic aneurysms (AAA) and endovascular repair of AAA (EVAR) are very low with reported rates between 0.2 and 0.3 % [6, 7]. Factors that affect the development of SCI after EVAR include long procedure times, extensive intra-aortic graft manipulation resulting in peripheral embolization, coil embolization of the hypogastric artery, and treatment of ruptured AAA [6, 8]. The development of SCI following endovascular repair of thoracic aortic aneurysms (TEVAR) is more frequent occurring with rates ranging from 2 to 10 %. The majority of symptoms present in a delayed fashion, and only 1–5 % of patients develop permanent deficits [5, 9–14].

The development of SCI symptoms after endovascular repair of thoracoabdominal aortic aneurysms (TAAA) treated with fenestrated or branched endografts (F/B-EVAR) is less well documented. Sobel et al. report 20.6 % of patients develop lower extremity weakness following F/B-EVAR for extensive aneurysmal disease, with 7.7 % of patients having persistent weakness [15]. Only 21 % of patients awoke from anesthesia with leg weakness, while the majority of patients developed symptoms within the first 72 h after surgery. Independent risk factors for the development of SCI were renal insufficiency, prolonged fluoroscopy time, and sustained hypotension. Eagleton et al. similarly documented the development of SCI after endovascular repair of TAAA. Rates varied based on the extent of coverage (as low as 2 % for type IV TAAA and as high as 9 % for type II TAAA) [7]. Few

M.J. Eagleton (✉)
Department of Vascular Surgery, Cleveland Clinic Lerner College of Medicine-CWRU, H32, 9500 Euclid Avenue, Cleveland, OH 44195, USA
e-mail: eagletm@ccf.org

© Mayo Foundation for Medical Education and Research 2017

G.S. Oderich (ed.), *Endovascular Aortic Repair*, DOI 10.1007/978-3-319-15192-2_47

patients (9 %) presented with isolated sensory deficits, while the remaining presented with isolated motor or a combination of motor and sensory deficits. Symptoms were present at the conclusion of the procedure in 42 % of the patients presented, and the rest developed symptoms over a period of 1–10 days postoperatively. In both series, all patients that developed symptoms of SCI in a delayed fashion after surgery had an episode of hypotension that preceded the onset of symptoms. While intercostal preservation was not possible due to the endovascular nature of the repair in either series, the additional occlusion of a single hypogastric or subclavian artery was associated with higher rates of immediate onset of symptoms and lower recovery rates [7]. Overall 30-day and 36-month survivals in those developing SCI were 92 % and 45 %, respectively. In those patients that did not have resolution of their symptoms, 3-month survival was reduced from 92 to 36 %. This highlights the devastating long-term outcomes of patients suffering from profound SCI with paraplegia.

Spinal Perfusion

The concept of spinal collateral network and some of the preventive strategies have been discussed in detail in Chaps. 7 and 20. It is likely that some of the mechanisms for SCI development associated with open surgery differ from endovascular surgery. During open surgery aortic cross-clamping is employed. This decreases the blood supply to the spinal cord, increases central venous pressure and increases spinal fluid pressure (SFP), all of which result in inadequate tissue oxygen delivery and ischemia [16, 17]. Ischemia neurons release free radicals and other neurotoxic agents which further induce neuronal injury [16]. Reperfusion of the spinal cord leads to further exacerbation of the acute injury with a reperfusion injury which incites re-oxygenation, hyperemia, and an inflammatory response [18–20]. It is unlikely that this mechanism plays the same role during endovascular repair, which has no aortic cross-clamping. Endovascular repair, however, does mandate the exclusion of segmental vessels, such as intercostal and lumbar arteries, but currently provides no mechanisms for revascularization of these vessels. The simple occlusion of the segmental vessels, however, likely plays a significant role in developing cord ischemia.

The blood supply to the spinal cord is the main determinant of oxygen delivery. It arises through several direct and indirect routes. The vertebral arteries, which arise from the subclavian arteries, join to form the anterior spinal artery (Fig. 47.1). This route supplies the motor region of the spinal cord, while the proprioceptive and sensory regions of the spinal cord are supplied by the two posterior spinal arteries that also originate from the subclavian arteries. Some of the intercostal arteries, which frequently are occluded during aneurysm repair, contribute to radicular arteries that supplement the anterior spinal artery [16]. The largest intercostal artery, also known as the artery of Adamkiewicz, gives rise to the greater radicular artery—which is a major collateral network to the anterior spinal artery.

Surrounding the perichord region is an even more complex network of collateral flow. This axial network is composed of small arteries in the spinal canal, perivertebral tissues, and paraspinous muscles that connect with each other and the anterior and posterior spinal arteries [21–23]. The thoracic and lumbar segmental vessels contribute to both the anterior spinal artery and an extensive paraspinous network feeding the paraspinous muscles. The anterior spinal artery is connected in multiple locations to epidural arteries, and there are extensive connections between the intraspinous and paraspinous networks. This collateral network can increase cord blood flow from one source when another is reduced. In addition, steal can occur if an alternate low-resistance system is induced into the network.

In the immediate postoperative period, optimizing physiologic factors that determine tissue oxygen delivery are important in reducing the incidence and potentially improving recovery from spinal cord injury. Improvements in oxygen delivery can be manifested through improvements in oxygen saturation, hemoglobin concentration, and cardiac index and by reducing spinal cord oxygen demand.

Risk Reduction and SCI Management Strategies

Methods to reduce SCI following TAAA repair can be categorized into one of two general approaches: neuroprotective measures and attempts to maintain/improve spinal cord perfusion. Frequently these modalities are employed perioperatively in order to prevent the development of SCI, but in some situations they have been used once the symptoms of poor spinal cord perfusion have developed. Neuroprotective measures are important to reduce spinal cord metabolic activity, neural cell apoptosis, and spinal cord inflammation and swelling. Several modalities have been described to limit the neurologic insult of spinal cord hypoperfusion. Many of these, however, have yet to be studied in endovascular surgery and have mainly been applied to open surgical reconstruction. Regional hypothermia with the use of epidural cooling has been demonstrated both in experimental models and clinically to reduce the untoward effects of SCI [16]. The use of hypothermia in the regional setting limits the systemic complications of whole-body hypothermia while allowing for reduction in spinal cord oxygen requirements in the central nervous system tissue.

Other neuroprotective modalities include the use of pharmacologic agents. Lima et al. demonstrated that the use of

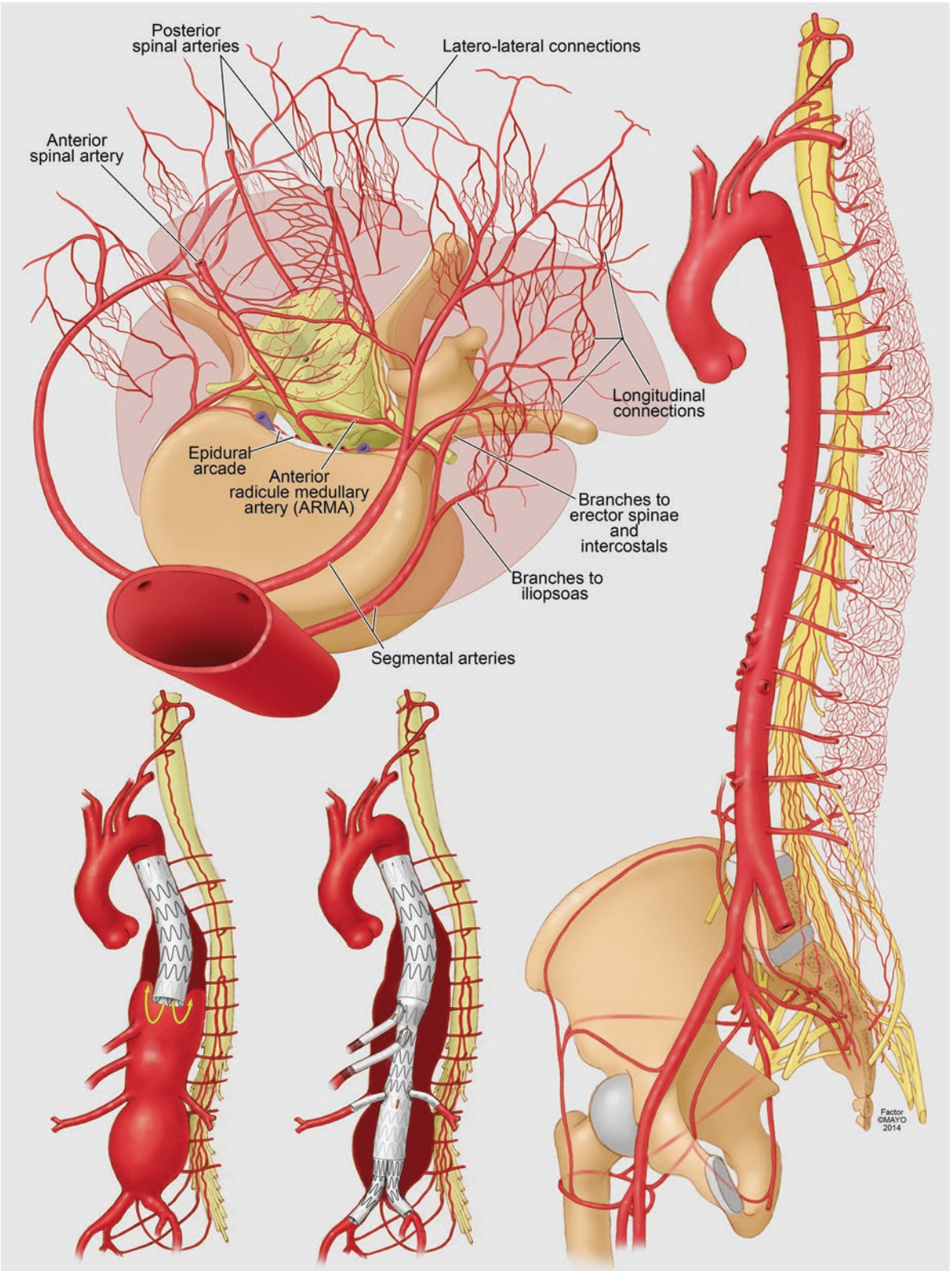


Fig. 47.1 Illustration of the spinal cord collateral network and example of a staged TEVAR with completion repair using fenestrated-branched stent graft. By permission of Mayo Foundation for Medical Education and Research. All rights reserved

Table 47.1 Pharmacologic agents for SCI prevention/treatment

Mechanism of cord protection	Pharmacologic agent
Reduce oxygen demand [24–27]	Barbiturates
Decrease inflammation and stabilize neuronal membranes [28, 29]	Corticosteroids
Reduce excitatory amino acids release in ischemia [30–32]	Naloxone
Scavenge free radicals [33, 34]	Mannitol
Reduce intracellular edema [35]	Mannitol

intrathecal papaverine reduced SCI after open TAAA repair from 7.5 to 3.6% [3]. Intrathecal papaverine is known to induce vasodilation, which may increase peri-spinal blood flow and promote preservation of myelin integrity. Other agents that are under evaluation include the use of systemic and intrathecal propofol, naloxone, and a variety of anti-inflammatory agents. However, the majority of these agents have not been evaluated in the endovascular setting (Table 47.1) [16].

In addition to neuroprotective measures, the other general category for limiting SCI is to maintain or augment spinal cord perfusion. Maintenance of direct spinal cord perfusion during open TAAA can be achieved through reimplantation of intercostal arteries [36]. The routine reimplantation of these arteries, however [37], has been called into question, and perhaps the better approach is to use selective reimplantation driven by the use of neuromonitoring protocols [38]. With current branch technology, however, preservation of these arteries in endovascular therapy is not yet possible. Thus, spinal cord perfusion augmentation strategies may be of particular importance in endovascular therapies in which occlusion of intercostal and lumbar arteries is mandatory, and the spinal cord thus remains dependent on significant collateral routes. For all aneurysm types and in the majority of these series, the importance of the collateral network flow to the spinal cord has become increasingly apparent [22, 23]. Loss of patency of the hypogastric or subclavian artery is associated with increased risk for development and severity of SCI, and significant efforts should be driven toward preserving patency of these vessels during extensive TAAA repair [39]. Additional methods during open surgery have included the use of left heart bypass to provide continued lower extremity and visceral flow during aortic clamping [40]. This is not necessary in endovascular repair, however, as aortic occlusion does not occur, and there is continued flow to the visceral vessels during placement of the stent grafts. Diminished flow to the pelvis and lower extremities can occur, in particular with devices that require larger-size delivery sheaths, but this can be overcome with the use of large iliofemoral conduits or the development of low-profile delivery systems. Early restoration of lower extremity and pelvic flow has been associated with lower rates of SCI and improved overall outcomes [41]. One method to achieve this, when low-profile systems are not available, is the use of a femoral conduit (Fig. 47.2). This allows access of the conduit, maintenance of wire access into the aorta, and continued pelvic and lower extremity perfusion once the large sheath is removed (with continued guide wire access).

One generally universally applied adjunct to limit the rate and severity of SCI is the use of cerebrospinal fluid (CSF) drainage. This approach originally was developed for application to conventional open surgery. Early animal studies demonstrated that when central venous pressure (CVP) increases, spinal fluid pressure (SFP) also increases [42]. Occlusion of the proximal aorta increased upper extremity blood flow and increased CVP and also leads to increased SFP, which was thought to further decrease perfusion of the spinal cord contributing to ongoing ischemia [43, 44]. Investigators hypothesized that lowering SFP may lower the rates of SCI [45]. This is accomplished through the placement of a subarachnoid drain (Fig. 47.3). The initial analysis of the use of CSF drainage to prevent SCI was unsuccessful. Crawford et al. failed to demonstrate any advantage to CSF drainage [25]. This prospective, randomized study was limited, however, given that a maximum of 50 ml of CSF fluid was drained. Both Coselli and Svensson, however, in two separate randomized, prospective evaluations, demonstrated an advantage to the use of CSF drainage during open repair of TAAA [1, 2]. Coselli et al. demonstrated an 80% reduction in the relative risk of developing postoperative neurologic deficits with the use of CSF drainage. Different than Crawford's original work, Coselli drained CSF fluid to a target pressure of less than 10 mmHg or less, and this was continued through the operation and for 48 h postoperatively. In Svensson's evaluation, patients were randomized to a control group or the use of intrathecal papaverine and CSF drainage. CSF fluid was drained freely during aortic cross-clamping and then allowed to drain to keep a CSF pressure below 7–10 cm H_2O. The study was terminated early as on interim analysis there was a clear advantage to the use of intrathecal papaverine and CSF drainage. Given these findings, CSF drainage is widely used on extensive TAAA repairs and is used more selectively during more limited aortic aneurysm repairs with few complications [46, 47].

Protection of the spinal cord is dependent upon the array of collateral flow as outlined above. This is particularly true following endovascular repair during which the segmental arteries are occluded. Highly detailed anatomic studies dem-

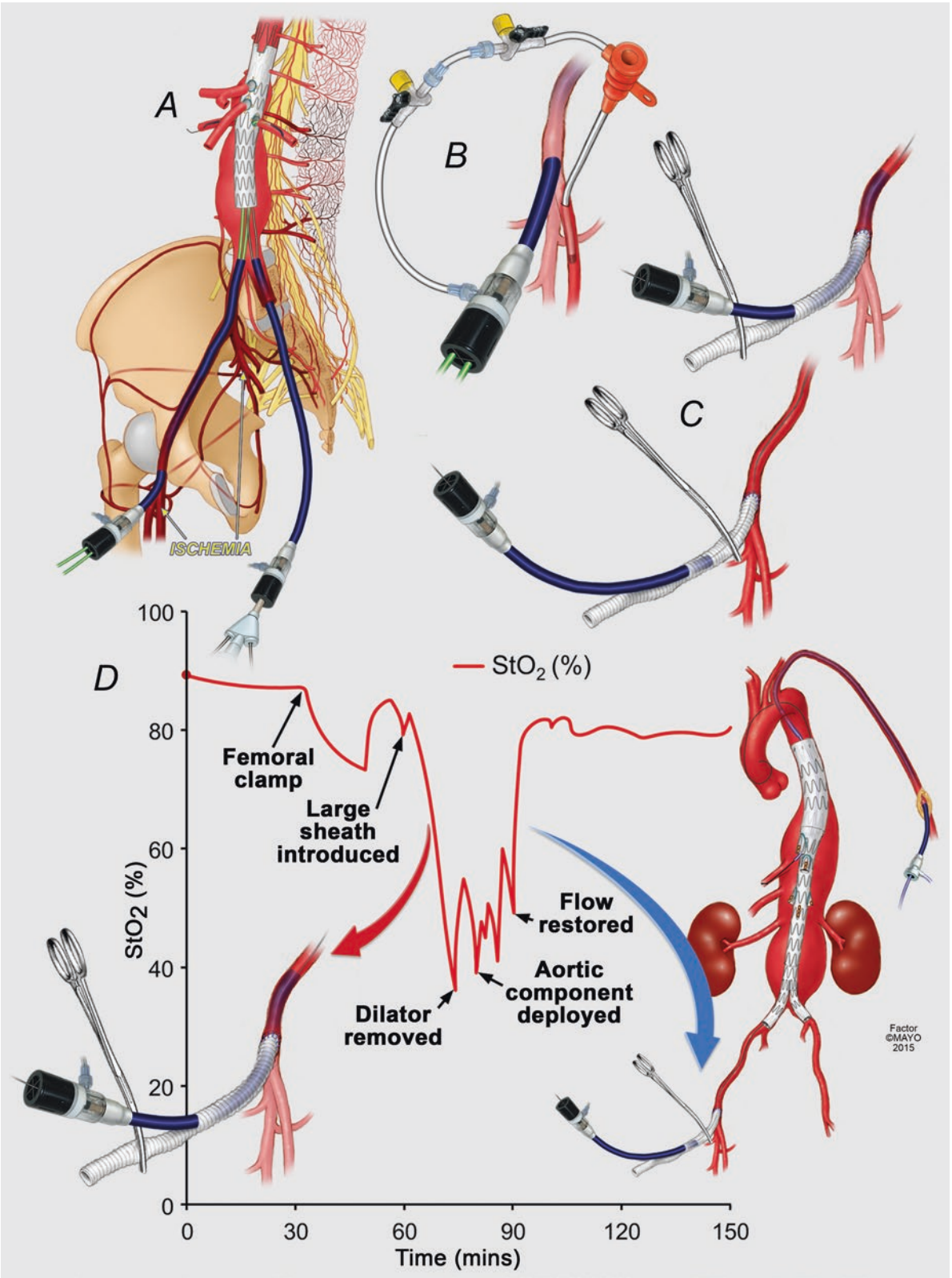


Fig. 47.2 Large profile femoral sheaths are associated with pelvic and lower extremity ischemia (**a**). Technique of antegrade femoral sheath does not relieve the ischemia caused by occlusion of the internal iliac and profunda femoris artery (**b**). The use of femoral conduits (**c**) for sheath access allow early restoration of perfusion to the pelvis and lower extremity, as depicted in the graph (**d**). By permission of Mayo Foundation for Medical Education and Research. All rights reserved

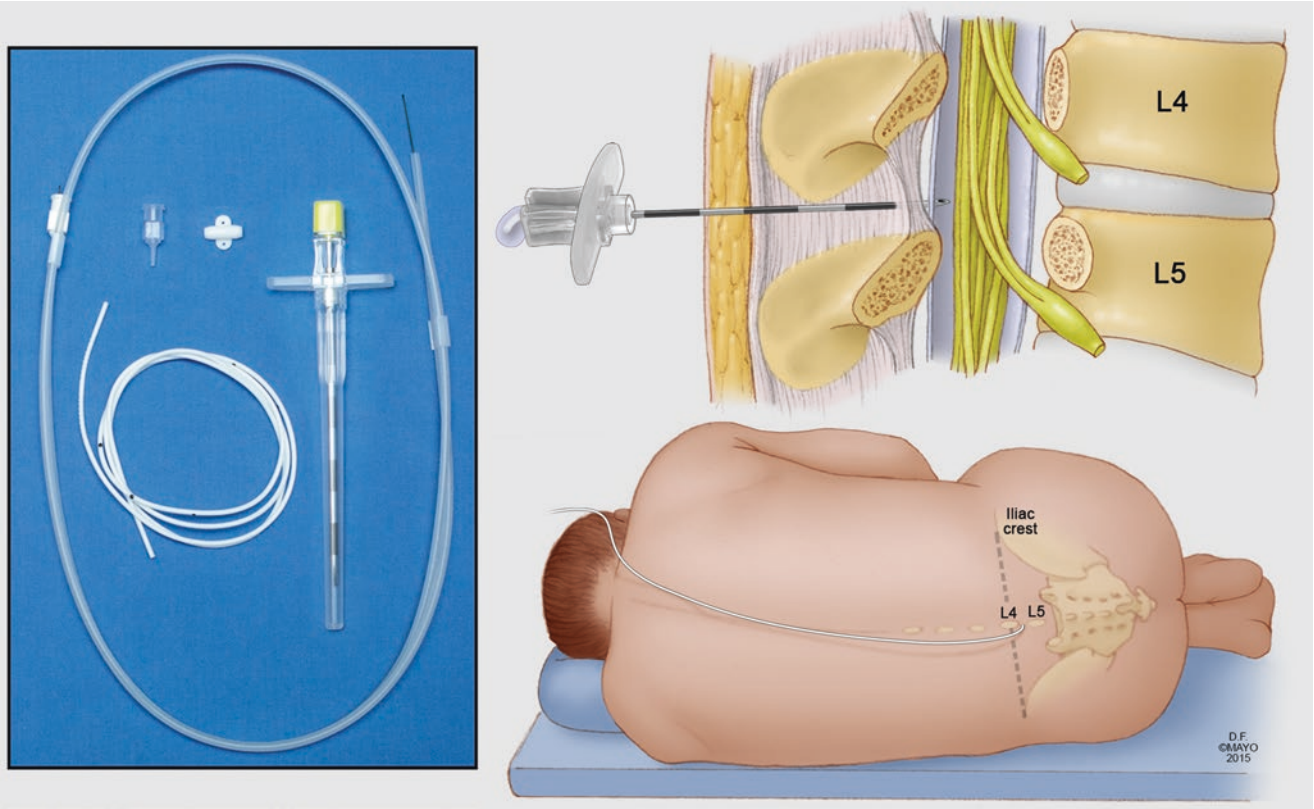


Fig. 47.3 Placement of a subarachnoid drain for extraction of cerebrospinal fluid (CSF). By permission of Mayo Foundation for Medical Education and Research. All rights reserved

onstrate that the anterior spinal artery is connected with the vascular supply of the adjacent musculature of the back (see Fig. 47.1) [23]. The multilevel intraspinal vascular network is also connected to the subclavian and hypogastric arteries and through the intercostal arteries to the intercostal vessels. This extensive collateral network is able to accommodate to alterations in flow that occur when arterial inflow into the spinal cord becomes compromised. Etz et al. have demonstrated that within 24 h of spinal artery ligation, the diameter of the anterior spinal artery had increased dramatically [22]. In addition, within 5 days the anterior spinal artery and the epidural arterial network had both increased by 80–100 % in diameter, with a shift in size (from small to larger arterioles) and an increase in density of the intramuscular paraspinous vasculature. The arterioles became realigned so that they were parallel to the spinal cord. All of these changes demonstrate that the collateral network substrate has altered its morphology to provide improved flow to the spinal cord. Taking advantage of the ability of the spinal vasculature to remodel, several experimental evaluations have been performed to determine whether staging aortic repair could be protective of SCI. Zoli et al. demonstrated that a two-stage procedure was associated with only a mild drop in spinal cord perfusion pressure and an increase in vascular remodeling [48]. In a porcine model, animals were assigned to either extensive spinal artery sacrifice in a single operation or a staged sacrifice with thoracic artery sacrifice occurring 7 days after lumbar artery ligation. Forty percent of those undergoing a single-stage approach developed permanent paraplegia, while all animals in the stage group fully recovered. Bischoff et al. demonstrated similar results utilizing a hybrid endovascular approach in which the thoracic aorta was excluded with a thoracic endograft as opposed to intercostal artery ligation [49]. Spinal cord perfusion pressure was lower after single-stage spinal artery occlusion compared to those at any point after a staged approach. In addition, 50 % of the animals in the single-stage group developed paraplegia, while none in the staged group developed it. Similar results were demonstrated when 2–4 spinal arteries in the T11-L3 region were embolized 10 days prior to extensive hybrid TAAA repair simulation [30].

These experimental models have paved the way for similar evaluations for patients undergoing repair of TAAA. It has been observed that SCI occurs at higher rates in patients who underwent open single-stage extensive TAAA repair compared to those in which repair was performed in a staged fashion [50]. In this retrospective analysis, 15 % of the patients in the single-stage approach developed permanent SCI, while none in the staged approach did. Staging in this series was not planned but was based on the development of

subsequent contiguous aneurysmal degeneration of the aorta requiring more extensive repair.

Staging for endovascular TAAA repair has been favored by several experts, and it has been performed via two different methods. The first is the incorporation of perfusion branches into the endovascular device that allow for continued sac perfusion after initial aneurysm repair (Fig. 47.4) [51, 52]. In the first stage of the procedure, the branched stent graft is placed with branches and bridging stent placed to incorporate the requisite number of visceral vessels involved in the repair. The perfusion branches, allowing for continued sac flow, are left open at this time in order to perfuse segmental arteries. Five to 10 days postoperatively, the perfusion branches are closed with the use of endovascular coils or plugs placed with the patient under local anesthesia. Harrison et al. describe the use of this technique in ten patients undergoing repair of type II TAAA. Three patients developed symptoms of SCI postoperatively. One patient developed monoparesis after myocardial infarction; one patient developed paraplegia after perfusion branch occlusion, but recovered after a carotid-subclavian bypass was performed to revascularize an occluded subclavian artery. Alternately, fenestrations can be left un-stented, and then in a similar time frame, the bridging stent to the target artery is placed. In this technique, the surgeon must be assured that the fenestration is easily accessible from the fenestration at a later time point or there is the increased risk of sacrificing the target vessel. Given this, the most frequently chose fenestration to be left open is the one supplying the celiac artery.

Another approach can be taken that more closely mimics that outlined in the animal experimental models in which a proximal TEVAR is placed in one surgical setting, and then at a later time point the aneurysm repair is completed with the placement of a fenestrated or branched aortic endograft (see Fig. 47.1). Outcomes have been assessed using this method to treat patients with type II TAAA [53]. During the first stage, patients underwent placement of the thoracic endograft. This was placed at the safest proximal seal/fixation zone and extended distally a distance that would not interfere with the subsequent branched endograft repair. A total of 95 patients underwent type II TAAA repair from 2008 to 2013. Patients were divided into three groups: those that were repaired in a single stage ($N=32$), those that were repaired in a planned staged approach ($N=27$), and those that had an unplanned staged approach owing to a prior aortic repair remote from their current evaluation ($N=28$). In those patients undergoing a single-stage approach, 38 % developed symptoms of SCI with nearly 40 % of these developing permanent symptoms. In contrast, only 11 % of patients undergoing planned staged approach developed symptoms, all of which resolved prior to discharge from the hospital. A similar protective effect was seen in the patient group that had an unplanned staged approach. Only 14 % developed symptoms attributable to SCI. In this subgroup, however, only half recovered from symptom development. In addition, those patients undergoing staged approach had symptoms that were less severe in nature, with no patient in the planned staged approach developing paraplegia, while 22 % of those performed in a single stage developed paraplegia. Intentional staging also appears to provide a survival advantage. The 30-day mortality for those patients undergoing a planned staged approach was 0 %, while those undergoing a single-stage procedure had a 30-day mortality of 19 %—likely representative of the devastating effects of SCI development on recovery and survival.

Current Strategies

A number of different strategies can be applied and will vary from institution to institution. It is likely that some of the specific approaches to preventing and treating SCI are less important than having a well-defined overall strategy with treatment options in place prior to surgery. When planning endovascular repair of patients at risk for spinal cord ischemia, surgeons should consider the following prevention/treatment strategies:

Preoperative

- Medically optimize the patient's cardiovascular status.
- Consider decreasing doses of antihypertensives perioperatively.
- Assess the collateral beds (i.e., hypogastric and subclavian arteries) and consider revascularization if possible.

Intraoperatively

- Exclude only the minimum number of intercostal arteries required for a durable repair.
- Avoid inadvertent coverage of the subclavian and/or hypogastric arteries.
- For extensive aneurysms, consider treating in staged fashion.
- Avoid extensive intra-aortic graft manipulation.
- Avoid prolonged iliac artery occlusion and consider the use of iliac or femoral conduits if low-profile devices are not available.
- Consider the use of subarachnoid drains to lower CSF pressure. If these are not placed preoperatively, have a plan in place for expeditious placement postoperatively if the patient develops symptoms.
- Close hemodynamic monitoring and avoidance of hypotension.



Fig. 47.4 (**a**–**d**) Illustration depicts the temporary aneurysm sac perfusion (TASP) branches and subsequent occlusion with coil embolization. By permission of Mayo Foundation for Medical Education and Research. All rights reserved

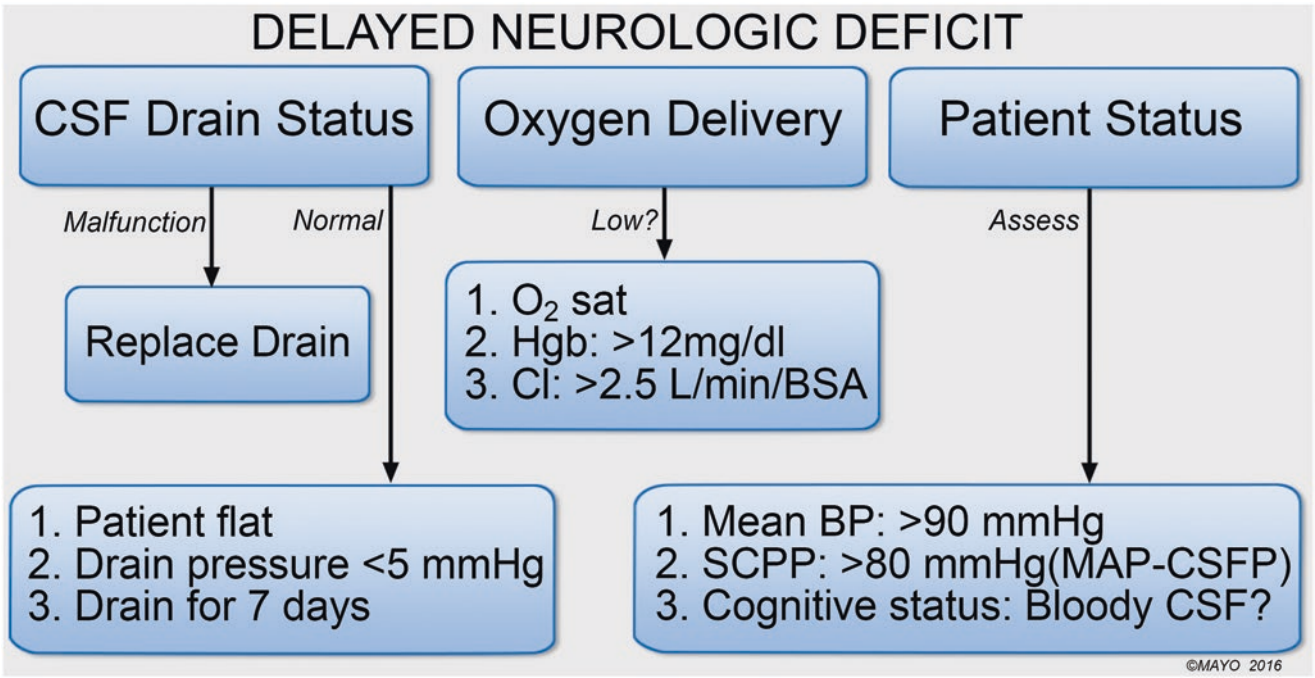


Fig. 47.5 Protocol for management of spinal cord injury. By permission of Mayo Foundation for Medical Education and Research. All rights reserved

Postoperatively

- Consider continued SA drain utilization for 48–72 h. Morphologic changes were observed in the collateral bed for up to 5 days in experimental models.
- Close hemodynamic monitoring with avoidance of hypotension and avoidance of elevated CVP.
- Graded/slow resumption of antihypertensives when appropriate.
- If SCI is detected (Fig. 47.5):
  - Initiate spinal drainage if it is not in place.
  - If it is in place, consider lowering the drainage threshold.
  - Consider transfusion to improve the oxygen carrying capacity with a potential goal of at least 10 g/dL.
  - Balance cardiac output, blood pressure, and CVP aiming for a mean arterial pressure of greater than 90 mmHg. This may require a combination of pressor agents, inotropic agents, and fluid resuscitation.
  - Oxygen supplementation as necessary.
  - Consider pharmacologic adjuncts such as corticosteroids, mannitol, or naloxone.
  - In rare instances, revascularizing the aneurysm bed by stenting alongside the aortic endograft has been utilized to rescue.
  - Assess for other underlying contributing causes such as gastrointestinal bleeding, infection, cardiac dysrhythmia.

Conclusion

Spinal cord ischemia is a devastating complication of aortic surgery and remains so in the endovascular era. Many approaches have been described to help mitigate these risks, some of which are applicable to endovascular surgeries. In both experimental models and in clinical scenarios, staging of repairs of TAAA repair appears to provide a protective advantage against the development of SCI. In addition, meticulous attention to the perioperative management of these patients may help prevent this complication or at least limit the severity with which it occurs. Additional investigations are necessary in order to augment current treatment plans in order to further limit the development of SCI. Future endeavors will likely involve advancements in pharmacologic therapies that either limit the damage that occurs to the spinal cord in the ischemic environment or that allow the injured neurons to more readily heal. Regardless, additional help is necessary in order to make thoracoabdominal aortic aneurysm repair safer and more effective.

References

1. Svensson LG, Hess KR, D'Agostino RS, Entrup MH, Hreib K, Kimmel WA, et al. Reduction of neurologic injury after high-risk thoracoabdominal aortic operation. Ann Thorac Surg. 1998;66(1):132–8.
2. Coselli JS, LeMaire SA, Koksoy C, Schmittling ZC, Curling PE. Cerebrospinal fluid drainage reduces paraplegia after thoracoabdominal

aortic aneurysm repair: results of a randomized clinical trial. J Vasc Surg. 2002;35(4):631–9.
3. Lima B, Nowicki ER, Blackstone EH, Williams SJ, Roselli EE, Sabik III JF, et al. Spinal cord protective strategies during descending and thoracoabdominal aortic aneurysm repair in the modern era: the role of intrathecal papaverine. J Thorac Cardiovasc Surg. 2012;143(4):945–52.
4. Greenberg RK, Lu Q, Roselli EE, Svensson LG, Moon MC, Hernandez AV, et al. Contemporary analysis of descending thoracic and thoracoabdominal aneurysm repair: a comparison of endovascular and open techniques. Circulation. 2008;118(8):808–17.
5. Feezor RJ, Martin TD, Hess Jr PJ, Daniels MJ, Beaver TM, Klodell CT, et al. Extent of aortic coverage and incidence of spinal cord ischemia after thoracic endovascular aneurysm repair. Ann Thorac Surg. 2008;86(6):1809–14. discussion 14.
6. Berg P, Kaufmann D, van Marrewijk CJ, Buth J. Spinal cord ischemia after stent-graft treatment for infra-renal abdominal aortic aneurysms. Analysis of the Eurostar database. Eur J Vasc Endovasc Surg. 2001;22:342–7.
7. Eagleton MJ, Shah S, Petkosevek D, Mastracci TM, Greenberg RK. Hypogastric and subclavian artery patency affects onset and recovery of spinal cord ischemia associated with aortic endografting. J Vasc Surg. 2014;59(1):89–94.
8. Peppelenbosch N, Cuypers PW, Vahl AC, Vermassen F, Buth J. Emergency endovascular treatment for ruptured abdominal aortic aneurysm and the risk of spinal cord ischemia. J Vasc Surg. 2005;42:608–14.
9. Ullery BW, Cheung AT, Fairman RM, Jackson BM, Woo EY, Bavaria J, et al. Risk factors, outcomes, and clinical manifestations of spinal cord ischemia following thoracic endovascular aortic repair. J Vasc Surg. 2011;54(3):677–84.
10. Lee WA, Daniels MJ, Beaver TM, Klodell CT, Raghinaru DE, Hess Jr PJ. Late outcomes of a single-center experience of 400 consecutive thoracic endovascular aortic repairs. Circulation. 2011;123(25):2938–45.
11. Fairman RM, Criado F, Farber M, Kwolek C, Mehta M, White R, et al. Pivotal results of the Medtronic Vascular Talent Thoracic Stent Graft System: the VALOR trial. J Vasc Surg. 2008;48(3):546–54.
12. Matsumura JS, Cambria RP, Dake MD, Moore RD, Svensson LG, Snyder S, et al. International controlled clinical trial of thoracic endovascular aneurysm repair with the Zenith TX2 endovascular graft: 1-year results. J Vasc Surg. 2008;47(2):247–57. discussion 57.
13. Morales JP, Greenberg RK, Morales CA, Cury M, Hernandez AV, Lyden SP, et al. Thoracic aortic lesions treated with the Zenith TX1 and TX2 thoracic devices: intermediate—and long-term outcomes. J Vasc Surg. 2008;48(1):54–63.
14. Buth J, Harris PL, Hobo R, van Eps R, Cuypers P, Duijm L, et al. Neurologic complications associated with endovascular repair of thoracic aortic pathology: incidence and risk factors. A study from the European Collaborators on Stent/Graft Techniques for Aortic Aneurysm Repair (EUROSTAR) registry. J Vasc Surg. 2007;46(6):1103–10. discussion 10–1.
15. Sobel JD, Vartanian SM, Gasper WJ, Hiromoto JS, Chuter TA, Reilly LM. Lower extremity weakness after endovascular aneurysm repair with multibranched thoracoabdominal stent grafts. J Vasc Surg. 2015 Mar;61(3):623–8.
16. Wynn MM, Acher CW. A modern theory of spinal cord ischemia/injury in thoracoabdominal aortic surgery and its implications for prevention of paralysis. J Cardiothorac Vasc Anesth. 2014;28:1088–99.
17. Marini CP, Levison J, Caliendo F, Nathan IM, Cohen JR. Control of proximal hypertension during aortic cross-clamping: its effect on cerebrospinal fluid dynamics and spinal cord perfusion pressure. Semin Thorac Cardiovasc Surg. 1998;10(1):51–6.
18. Reece TB, Okonkwo DO, Ellman PI, Warren PS, Smith RL, Hawkins AS, et al. The evolution of ischemic spinal cord injury in function, cytoarchitecture, and inflammation and the effects of adenosine A2A receptor activation. J Thorac Cardiovasc Surg. 2004;128(6):925–32.
19. Savas S, Delibas N, Savas C, Sutcu R, Cindas A. Pentoxifylline reduces biochemical markers of ischemia-reperfusion induced spinal cord injury in rabbits. Spinal Cord. 2002;40(5):224–9.
20. Oz Oyar E, Korkmaz A, Kardess O, Omeroglu S. Aortic cross-clamping-induced spinal cord oxidative stress in rabbits: the role of a novel antioxidant adrenomedullin. J Surg Res. 2008;147(1):143–7.
21. Etz CD, Homann TM, Luehr M, Kari FA, Weisz DJ, Kleinman G, et al. Spinal cord blood flow and ischemic injury after experimental sacrifice of thoracic and abdominal segmental arteries. Eur J Vasc Endovasc Surg. 2008;33(6):1030–8.
22. Etz CD, Kari FA, Mueller CS, Brenner RM, Lin HM, Griepp RB. The collateral network concept: remodeling of the arterial collateral network after experimental segmental artery sacrifice. J Thorac Cardiovasc Surg. 2011;141:1029–36.
23. Etz CD, Kari FA, Mueller CS, Silovitz D, Brenner RM, Lin HM, et al. The collateral network concept: a reassessment of the anatomy of spinal cord perfusion. J Thorac Cardiovasc Surg. 2011;141(4):1020–8.
24. Naslund TC, Hollier LH, Money SR, Facundus EC, Skenderis II BS. Protecting the ischemic spinal cord during aortic clamping. The influence of anesthetics and hypothermia. Ann Surg. 1992;215(5):409–15. discussion 15–6.
25. Nylander Jr WA, Plunkett RJ, Hammon Jr JW, Oldfield EH, Meacham WF. Thiopental modification of ischemic spinal cord injury in the dog. Ann Thorac Surg. 1982;33(1):64–8.
26. Kirshner DL, Kirshner RL, Heggeness LM, DeWeese JA. Spinal cord ischemia: an evaluation of pharmacologic agents in minimizing paraplegia after aortic occlusion. J Vasc Surg. 1989;9(2):305–8.
27. Tetik O, Islamoglu F, Goncu T, Cekirdekci A, Buket S. Reduction of spinal cord injury with pentobarbital and hypothermia in a rabbit model. Eur J Vasc Endovasc Surg. 2002;24(6):540–4.
28. Laschinger JC, Cunningham Jr JN, Cooper MM, Krieger K, Nathan IM, Spencer FC. Prevention of ischemic spinal cord injury following aortic cross-clamping: use of corticosteroids. Ann Thorac Surg. 1984;38(5):500–7.
29. Bartholdi D, Schwab ME. Methylprednisolone inhibits early inflammatory processes but not ischemic cell death after experimental spinal cord lesion in the rat. Brain Res. 1995;672(1–2):177–86.
30. Faden AI, Jacobs TP, Smith MT, Zivin JA. Naloxone in experimental spinal cord ischemia: dose-response studies. Eur J Pharmacol. 1984;103(1–2):115–20.
31. Kakinohana M, Marsala M, Carter C, Davison JK, Yaksh TL. Neuraxial morphine may trigger transient motor dysfunction after a noninjurious interval of spinal cord ischemia: a clinical and experimental study. Anesthesiology. 2003;98(4):862–70.
32. Kunihara T, Matsuzaki K, Shiiya N, Saijo Y, Yasuda K. Naloxone lowers cerebrospinal fluid levels of excitatory amino acids after thoracoabdominal aortic surgery. J Vasc Surg. 2004;40(4):681–90.
33. Francel PC, Long BA, Malik JM, Tribble C, Jane JA, Kron IL. Limiting ischemic spinal cord injury using a free radical scavenger 21-aminosteroid and/or cerebrospinal fluid drainage. J Neurosurg. 1993;79(5):742–51.
34. Herlambang B, Orihashi K, Mizukami T, Takahashi S, Uchida N, Hiyama E, et al. New method for absolute spinal cord ischemia protection in rabbits. J Vasc Surg. 2011;54(4):1109–16.
35. Mutch WA, Thiessen DB, Girling LG, et al. Neuroanesthesia adjunct therapy (mannitol and hyperventilation) is as effective as cerebrospinal drainage for prevention of paraplegia after descending thoracic aortic cross-clamping in the dog. Anesth Analg. 1995;81:800–5.
36. Safi HJ, Miller III CC. Spinal cord protection in descending thoracic and thoracoabdominal aortic repair. Ann Thorac Surg. 1999;67(6):1937–9. discussion 53–8.
37. Etz CD, Halstead JC, Spielvogel D, Shahani R, Lazala R, Homann TM, et al. Thoracic and thoracoabdominal aneurysm repair: is

reimplantation of spinal cord arteries a waste of time? Ann Thorac Surg. 2006;82(5):1670–7.
38. Estrera AL, Sheinbaum R, Miller III CC, Harrison R, Safi HJ. Neuromonitor-guided repair of thoracoabdominal aortic aneurysms. J Thorac Cardiovasc Surg. 2010;140(6):S131–5. discussion S42–6.
39. Matsumura JS, Lee WA, Mitchell RS, Farber MA, Murad MH, Lumsden AB, et al. The Society for Vascular Surgery Practice Guidelines: management of the left subclavian artery with thoracic endovascular aortic repair. J Vasc Surg. 2009;50:1155–8.
40. Coselli JS, LeMaire SA. Left heart bypass reduces paraplegia rates after thoracoabdominal aortic aneurysm repair. Ann Thorac Surg. 1999;67(6):1931–4. discussion 53–8.
41. Maurel B, Delclaux N, Sobocinski J, Hertault A, Martin-Gonzalez T, Moussa M, et al. Editor's choice—the impact of early pelvic and lower limb reperfusion an attentive peri-operative management of the incidence of spinal cord ischemia during throacoabdomoinal aortic aneurysm repair. Eur J Vasc Endovasc Surg. 2015;49:248–54.
42. Wagner FC, Green BA, Bucy PC. Spinal cord edema associated with paraplegia. Proc Veterans Adm Spinal Cord Inj Conf. 1971;18:9–10.
43. Stokland OMM, Hebekk A, et al. Mechanisms of hemodynamic responses to occlusion of the thoracic aorta. Am J Physiol. 1980;238:H423–9.
44. Mutch WA. Control of outflow pressure provides spinal cord protection during resection of descending thoracic aortic aneurysms. J Neurosurg Anesthesiol. 1995;7(2):133–8.
45. Blaisdell F, Cooley DA. The mechanism of paraplegia after temporary thoracic arotic occlusion and its relationship to spinal fluid pressure. Surgery. 1962;51:351–5.
46. Hnath JC, Mehta M, Taggert JB, Sternbach Y, Roddy SP, Kreienberg PB, et al. Strategies to improve spinal cord ischemia in endovascular thoracic aortic repair: outcomes of a prospective cerebrospinal fluid drainage protocol. J Vasc Surg. 2008;48(4):836–40.
47. Wynn MM, Mell MW, Tefera G, Hoch JR, Acher CW. Complications of spinal fluid drainage in thoracoabdominal aortic aneurysm repair: a report of 486 patients treated from 1987 to 2008. J Vasc Surg. 2009;49(1):29–34. discussion -5.
48. Zoli S, Etz CD, Roder F, Brenner RM, Bodian CA, Kleinman G, et al. Experimental two-stage simulated repair of extensive thoracoabdominal aneurysms reduces paraplegia risk. Ann Thorac Surg. 2010;90(3):722–9.
49. Bischoff MS, Scheumann J, Brenner RM, Ladage D, Bodian CA, Kleinman G, et al. Staged approach prevents spinal cord injury in hybrid surgical-endovascular thoracoabdominal aortic aneurysm repair: an experimental model. Ann Thorac Surg. 2011;92(1):138–46. discussion 46.
50. Etz CD, Zoli S, Mueller CS, Bodian CA, Di Luozzo G, Lazala R, et al. Staged repair significantly reduces paraplegia rate after extensive thoracoabdominal aortic aneurysm repair. J Thorac Cardiovasc Surg. 2010;139(6):1464–72.
51. Harrison SC, Agu O, Harris PL, Ivancev K. Elective sac perfusion to reduce the risk of neurologic events following endovascular repair of thoracoabdominal aneurysms. J Vasc Surg. 2012;55(4):1202–5.
52. Lioupis C, Corriveau MM, Mackenzie KS, Obrand DI, Steinmetz OK, Ivancev K, et al. Paraplegia prevention branches: a new adjunct for preventing or treating spinal cord injury after endovascular repair of thoracoabdominal aneurysms. J Vasc Surg. 2011;54(1):252–7.
53. O'Callaghan A, Mastracci TM, Eagleton MJ. Staged endovascular repair of thoracoabdominal aortic aneurysms limits incidence and severity of spinal cord ischemia. J Vasc Surg. 2015;61(2):347–54.

Renal Function Deterioration in Complex Aortic Repair

48

Leonardo Reis de Souza and Gustavo S. Oderich

Introduction

Renal function impairment is one of the most common complications of complex aortic aneurysm repair with either open surgical or endovascular techniques. The causes for renal deterioration are multifactorial and include embolization, ischemia, catheter manipulation, contrast, vessel injury, or occlusion. Recent studies indicate that approximately 30 % of the patients develop acute kidney injury (AKI) following fenestrated endovascular treatment (FEVAR) for juxtarenal (JRAA) or thoracoabdominal (TAAA) aortic aneurysms (Table 48.1) [1–31].

The development of AKI is an important predictive factor of unfavorable outcomes, including longer length of stay, mortality, and excessive hospital costs [32, 33]. In a prospective study, Saratzis et al. reported AKI in 19 % of patients treated by EVAR for infrarenal aortic aneurysms. Those who developed AKI were more likely to die (32 % vs. 2 %, $p<0.001$) from early complications or cardiovascular events during a mean follow-up of 33 months [34]. Preoperative renal impairment has been shown to be the most important predictor of post-procedure AKI in patients undergoing aortic aneurysm repair [35–37].

The impact of endovascular aortic interventions on renal function has been studied previously. Brown et al. reviewed data from the UK EVAR 1 and EVAR 2 trials and showed slow and progressive renal function deterioration among patients with abdominal aortic aneurysms (AAA). That study did not identify any difference between open surgical and endovascular repair in fit patients (mean rate of change [MRC] ± standard deviation [SD], −1.13 ± 1.43 mL/min/1.73 m^2 per year vs.−1.00 ± 1.43 mL/min/1.73 m^2 per year, respectively, $p=0.208$) or no repair and endovascular repair in unfit patients (MRC ± SD, −0.98 ± 1.49 mL/min/1.73 m^2 per year vs.−0.76 ± 1.43 mL/min/1.73 m^2 per year, respectively, $p=0.087$) [38]. The impact of more complex types of repairs, such as fenestrated, branched, and parallel grafts, is less well understood.

Definitions and Classification

There is significant variation in the definition of renal function loss in the literature. Most reports have not adopted the recommended guidelines to define acute kidney injury and instead use variable thresholds based on serum creatinine levels to define acute injury. Therefore analysis of the pooled literature is limited. Over the last few decades, more than 30 different definitions have been used for AKI. Traditionally, the diagnosis of AKI takes into account variations in serum creatinine (sCr) within a time interval. An increase in sCr of 0.5 mg/dL within 48 h is a common definition. However, studies using this definition have not shown an association between transient changes in sCr and morbidity. Serum creatinine is affected by numerous confounding factors such as demographics, body habitus, muscle mass, and hydration status and does not reflect accurately small changes in the glomerular filtration rate (GFR) [39].

The RIFLE classification was originally published in 2004 to standardize the definition of AKI (Table 48.2) [40]. The classification is based on variations in sCr and urinary output, and the acronym indicates *risk* of renal dysfunction, *injury* to the kidney, *failure* of kidney function, *loss* of kidney function, and *end-stage* renal disease [41]. Since its initial description, the RIFLE criteria have been validated in numerous studies to determine the incidence of AKI and its

L.R. de Souza
Postgraduate of Program in Surgery, School of Medicine, Universidade Federal do Rio Grande do Sul, 2400 Ramiro Barcelos St, 2nd Floor, Porto Alegre 90035-003, Brazil

G.S. Oderich (✉)
Division of Vascular and Endovascular Surgery, Mayo Clinic, 200 First Street SW, Rochester, MN 55905, USA
e-mail: oderich.gustavo@mayo.edu

© Mayo Foundation for Medical Education and Research 2017

G.S. Oderich (ed.), *Endovascular Aortic Repair*, DOI 10.1007/978-3-319-15192-2_48

Table 48.1 Fenestrated endovascular repair studies reporting data on renal function outcomes

		Study design			Aneurysm classification, *n* (%)						Comorbidities			Postoperative events			
					TAAA										AKI		
First author, year	*n*	P/R	vs	S	I	II	III	IV	DT	JR	Age	Male, *n* (%)	CKD, *n* (%)	30d M., *n* (%)	Definition	AKI, *n* (%)	Dial., *n* (%)
Banno [1]	80	P	Ch	SC	0	0	0	0	0	80 (100)	m 74±9	72 (90)	12 (15)	8 (10)	↑ sCr>50 %	10 (8)	2 (1)
Martin-Gonzalez [2]	225	P	–	SC	49 (22)[a]	49 (22)[a]	49 (22)[a]	24 (11)[a]	0	152 (68)	m 71±8	211 (94)	53 (24)	14 (6)	RIFLE	64 (29)	1 (0)
Marzelle and Michel [3, 4]	268	P	OR	MC	2 (1)	16 (6)	24 (9)	26 (10)	0	200 (75)	m 72±9	250 (93)	82 (31)	26 (10)	RIFLE	48 (18)	15 (6)
Sailer [5]	157	R	–	SC	NR	NR	NR	NR	0	NR	m 73±6	131 (83)	NR	10 (6)	AKIN	43 (28)	NR
Shahverdyan [6]	35	R	OR	SC	0	0	0	0	0	35 (100)	ϰ 72 (60–84)	30 (86)	4 (11)	1 (3)	↑ Cr>50 % ↓ eGFR>25 %	4 (11)	0
Grimme 2014 [7]	138	R	–	SC	0	0	0	0	0	138 (100)	ϰ 73 (50–91)	123 (89)	49 (36)	2 (1)	↓ eGFR>30 %	57 (41)	2 (1)
Kristmundsson [8, 9]	54	P	–	SC	0	0	0	0	0	54 (100)	ϰ 72 (68–76)	46 (85)	24 (44)	2 (4)	↓ eGFR>30 %	19 (35)	0
Oderich [10]	67	P	–	MC	0	0	0	0	0	67 (100)	m 74±8	54 (81)	16 (24)	1 (2)	sCr>2 mg/dL ↑ sCr>30 %	0	0
Canavati [11]	53	R	OR	SC	0	0	0	0	0	53 (100)	ϰ 76 (55–87)	47 (89)	9 (17)	2 (4)	↑ sCr>50 %	8 (15)	0
Kitagawa [12]	16	P	–	SC	0	0	0	0	0	16 (100)	ϰ 75 (59–87)	15 (94)	1 (6)	0	NR	0	0
Perot [13]	115	R	EVAR	SC	0	0	0	0	0	115 (100)	m 73±8	NR	39 (34)	5 (4)	NR	22 (19)	1 (1)
Suominen [14]	21	R	Ch	SC	0	0	0	0	0	21 (100)	m 73	21 (100)	19 (91)	2 (10)	↓ CKD stage	1 (5)	0
Tslimparis [15]	264	R	OR	ND	NR	NR	NR	NR	0	NR	m 74±9	217 (82)	NR	2 (1)	NR	4 (2)	NR
Donas [16]	29	P	OR, Ch	SC	0	0	0	0	0	29 (100)	m 74±6	29 (100)	5 (17)	0	2× sCr ↓>50 % eGFR	NR	0
GLOBALSTAR [17]	318	R	–	MC	0	0	0	0	0	318 (100)	ϰ 74 (47–86)	273 (86)	44 (14)	13 (4)	NR	11 (3)	0
Metcalfe [18]	42	R	–	SC	0	0	0	3 (7)	0	39 (93)	m 70±7	39 (93)	6 (14)	3 (7)	NR	NR	1 (2)
Manning [19]	20	R	–	SC	0	0	0	0	0	20 (100)	m 75	18 (90)	8 (40)	2 (10)	NR	NR	1 (5)
Tambyraja [20]	29	R	–	SC	0	0	0	0	0	29 (100)	ϰ 74 (54–86)	27 (93)	3 (10)	0	NR	NR	0

Amiot [22]	134	R	–	MC	0	0	0	8 (6)	0	126 (94)	ϰ 73 (49–91)	129 (96)	54 (40)	3 (2)	↑ sCr>30 %	13 (10)	2 (2)
Verhoeven [23]	100	R	–	SC	0	0	0	0	0	100 (100)	m 73 ± 7	87 (87)	46 (46)	1 (1)	↑ sCr>30 %	NR	NR
Greenberg [24]	30	P	–	MC	0	0	0	0	0	30 (100)	m 75	24 (80)	2 (7)	0	NR	NR	0
Scurr [25]	45	R	–	SC	0	0	0	0	0	45 (100)	ϰ 73 (53–85)	41 (91)	6 (13)	2 (4)	NR	1 (2)	0
Ziegler [26]	63	R	–	SC	0	0	0	1 (16)	3 (5)	59 (94)	m 71 ± 12	57 (90)	18 (29)	3 (5)	sCr>2 mg/dL ↑ sCr>30 %	14 (22)	1 (2)
Halak [27]	17	R	–	SC	0	0	0	0	0	17 (100)	NR	NR	NR	0	NR	NR	1 (6)
Muhs [28]	38	P	–	SC	NR	NR	NR	NR	0	30 (79)	NR	31 (82)	NR	1 (3)	NR	NR	0
O'Neill [29]	119	P	–	SC	0	0	0	0	0	119 (100)	m 75 ± 7	98 (82)	31 (26)	1 (1)	sCr>2 mg/dL ↑ sCr>30 %	30 (25)	3 (2)
Semmens [30]	58	R	–	MC	0	0	0	0	0	58 (100)	m 76 ± 9	51 (88)	NR	2 (3)	sCr>2 mg/dL ↑ sCr>30 %	4 (7)	0
Anderson [31]	13	R	–	SC	0	0	0	0	0	13 (100)	m 74 (64–79)	10 (77)	NR	0	NR	NR	0

[a]Martin-Gonzalez et al. grouped types I, II, and III and types IV and V

n number of patients, *P* prospective, *R* retrospective, *vs* comparison (studies comparing different patient groups among fenestrated/branched endovascular repair were considered as noncomparative), *S* sample, *TA* thoracoabdominal aortic aneurysms, *DT* descendant thoracic aortic aneurysms, *JR* juxtarenal aortic aneurysms (include pararenal and paravisceral aortic aneurysms), *CKD* chronic kidney disease, *30d M* 30-day or in-hospital mortality, *AKI* acute kidney injury, *Dial.* permanent dialysis, *Ch* chimney, *OR* open repair, *EVAR* conventional endovascular aneurysm repair, *SC* single center, *MC* multicenter, *ND* national database, *m* mean ± SD; ϰ median (range), *sCr* serum creatinine, *eGFR* estimated glomerular filtration rate, *NR* not reported

Table 48.2 RIFLE criteria

	sCr	eGFR	UO (mL/kg/h)
Risk	1.5–2 × baseline	↓ 25–50 % baseline	<0.5/6 h
Injury	2–3 × baseline	↓ 50–75 % baseline	<0.5/12 h
Failure	>3 × baseline or ≥4 mg/dL or acute rise ≥ 0.5 mg/dL	↓ >75 % baseline	<0.3/24 h or anuria 12 h
Loss	Complete loss of kidney function >4 weeks		
End-stage	Complete loss of kidney function >3 months		

SCr serum creatinine, *eGFR* estimated glomerular filtration rate, *UO* urinary output, × times, ↓ decreased

Table 48.3 Chronic kidney disease stages

	eGFR (mL/min/1.73 m^2)	Description
1	>90	Normal kidney function, urine findings pointing to kidney disease
2	60–89	Mildly reduced kidney function
3	30–59	Moderately reduced kidney function
4	15–29	Severely reduced kidney function
5	<15 or dialysis	End-stage kidney failure

eGFR estimated glomerular filtration rate

impact on predicting mortality and other outcomes, especially among critically ill and postoperative patients. Whether sCr criteria alone underscore the incidence and grade of AKI remains controversial [42, 43]. Subsequently, the Acute Kidney Injury Network (AKIN) proposed a new criteria which is based on smaller changes in sCr (0.3 mg/dL) over a shorter time window of 48 h [44]. Some studies have shown that the AKIN criteria are more sensitive to determine AKI and to predict mortality compared to the RIFLE criteria [45].

In 2002, the National Kidney Foundation Kidney Disease Outcomes Quality Initiative (NKF-KDOQI) proposed the definition and classification for chronic kidney disease (CKD). This classification was endorsed by the "Kidney Disease: Improving Global Outcomes (KDIGO)" organization. CKD was defined by the presence of kidney damage (manifested by either pathological abnormalities or markers of kidney damage, including abnormalities in blood, urine, and imaging tests) or GFR < 60 ml/min/1.73 m^2 for at least 3 months. This classification grades the severity of kidney loss based on levels of GFR, which is considered the best overall measure of kidney function (Table 48.3) [46, 47]. Although still widely utilized, its limitations have been well recognized, including overdiagnosis, confusing terminology in the earlier stages, variations in methods of measuring GFR, and normal variance of GFR among different patient groups. On a Controversies Conference, in 2009, KDIGO had convened a workgroup to develop a global clinical practice guideline for the definition, classification, and prognosis of CKD [48].

Pathogenesis and Etiology

The majority of cases of AKI in postoperative or critically ill patients are due to intrinsic renal causes, and acute tubular necrosis (ATN) is the most common [49]. Hypovolemia and hypotension are the most common mechanisms in patients undergoing aortic repair. Originally described by Thurnbeck in 1957, micro-embolization of thrombus and debris during aortic clamping is a well-known cause of ischemic injury. Although suprarenal cross-clamp carries an increased risk of kidney injury, infrarenal clamp also affects renal hemodynamics. Renal vascular resistance increases, and blood flow is reduced as much as 50 %. These changes usually last hours after the clamp has been removed. Other important factors are arterial trauma causing stenosis, thrombosis, or occlusion of the renal arteries and ligation of the left renal vein [50].

If the imbalance of local tissue oxygen supply and demand is severe enough, tubular epithelial cells undergo death by apoptosis and necrosis, associated to functional impairment and accumulation of waste products of metabolism. Usually, the decrease in total renal blood flow is not the only factor responsible for reduction in GFR. A disproportional reduction in the perfusion of the outer medulla that appears also occurs, leading to endothelial injury, vasoconstriction of small arterioles, and decreased vasodilatation in response to inflammatory components. Moreover, the damaged endothelial cell produces less nitric oxide. Enhanced leukocyte-endothelial adhesion and leukocyte activation are characteristic of ischemic injury and result in

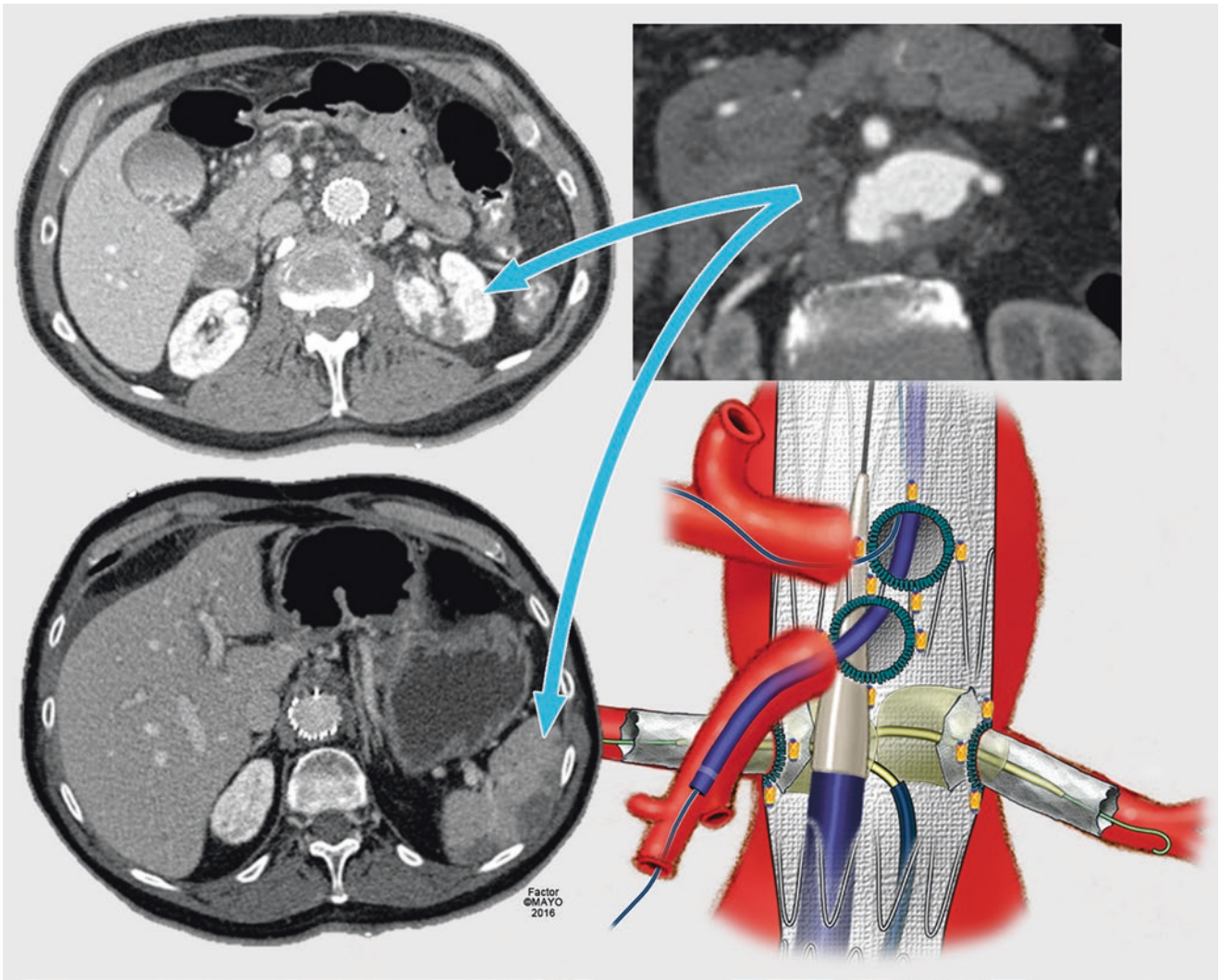


Fig. 48.1 Embolization of atherosclerotic debris during fenestrated endovascular aortic repair to the kidneys and spleen. By permission of Mayo Foundation for Medical Education and Research. All rights reserved

increased production of vasoactive cytokines. Local edema further contributes to diminished blood flow to the outer medulla. Innate and adaptive immune responses are important contributions to pathogenesis of the ischemic injury. Whereas the innate component is responsible for the early response in a nonantigen-specific fashion, the adaptive component is initiated within hours and lasts over the course of several days after injury [51].

Although endovascular repair avoids aortic cross-clamp and is able to maintain continued flow to all vessels, several mechanisms can result in AKI. Ongoing blood loss via numerous delivery catheters and sheaths results in hypovolemia and hypotension. Catheter manipulations in diseased vessels are known to cause micro-embolization, particularly in patients with aortic aneurysms who have excessive debris in the thoracic aorta or around the renal-mesenteric vessels (Fig. 48.1). Arterial trauma from catheters, wires, and stents may result in flow-limiting dissections, perforations, or vessel occlusion (Fig. 48.2). Accessory renal arteries, which are too small for placement of stents, may be inadvertently covered resulting in kidney infarction. Prolonged endovascular procedures with larger delivery sheaths are also known to cause lower limb ischemia, which can result in ischemia-reperfusion injury, compartment syndrome, and acidosis. In addition, endovascular repair requires use of nephrotoxic contrast agents, which are known to cause vasoconstriction, decreased local prostaglandin, and nitric oxide-mediated vasodilatation and to have direct toxic effects on renal tubular cells, including increased oxygen consumption, increased intratubular pressure, increased urinary viscosity, and tubular obstruction [34].

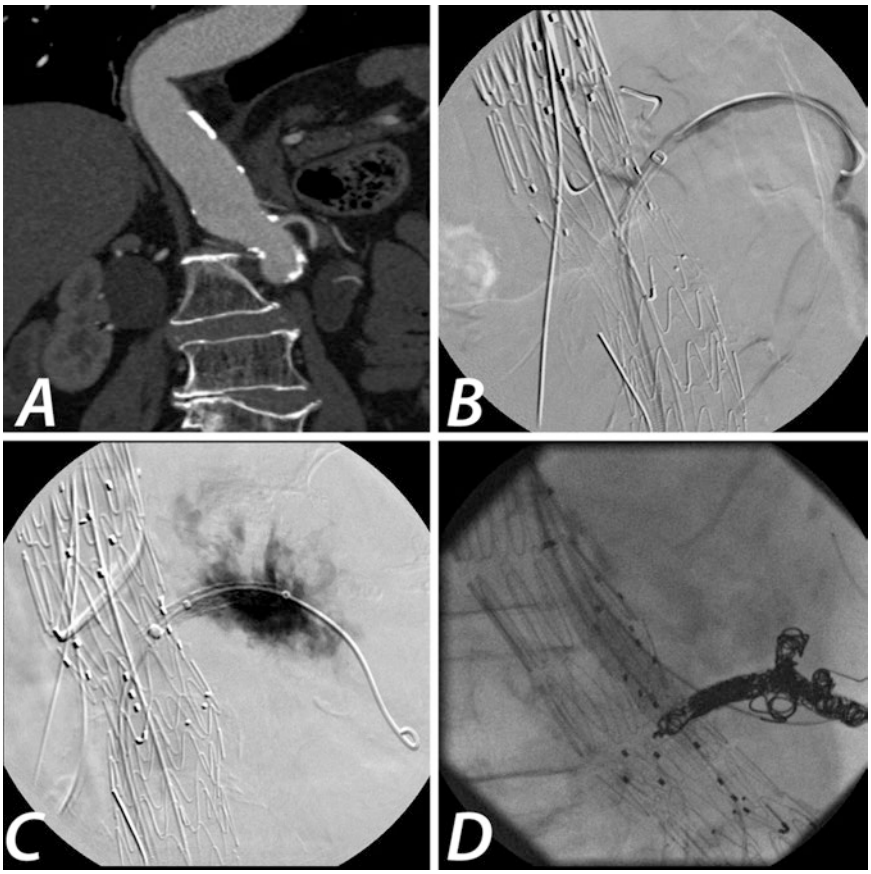


Fig. 48.2 Patient with small left-sided renal artery (**a**) treated by fenestrated endovascular repair (**b**). Angiography demonstrated disruption of the small renal artery after stent placement (**c**), which required coil embolization (**d**). By permission of Mayo Foundation for Medical Education and Research. All rights reserved

Kidney tissue repair after AKI can be adaptive restoring epithelial integrity, or it can be maladaptive, leading to progressive fibrosis and kidney loss. Tubular repair after AKI may be incomplete with persistent tubulointerstitial inflammation, proliferation of fibroblasts, and excessive deposition of extracellular matrix. Postischemic fibrosis may be explained by chronic activation of macrophages and hypoxia from loss of peritubular microvessels. The nature of the molecular switch that determines reparative or atrophic responses is not well understood [51].

Risk Factors

Complex aortic aneurysms that require aortic cross-clamp above the renal-mesenteric arteries are at higher risk of AKI. As such, risk of AKI is incremental with infrarenal, pararenal, and TAAAs. For endovascular repair, it is possible that risk is also higher with increasing level of complexity, as determined by the number of vessels requiring incorporation and the extent of aortic coverage by stent.

There is debate on whether suprarenal fixation increases the risk of renal deterioration. A systematic review of 21 studies compared renal outcomes in patients undergoing EVAR with infrarenal ($n=2525$) or suprarenal ($n=1949$) fixation devices. Rates of renal insufficiency (12.3% vs. 12.1%, respectively, $p=0.85$) and new-onset dialysis (1% vs. 0.8%, respectively, $p=0.63$) were not significantly different between the two groups, respectively [52].

Perot et al. studied renal outcomes in patients who underwent conventional EVAR ($n=264$) as compared to FEVAR ($n=115$) for AAA. Patients in the FEVAR group had higher rates of AKI (19.3% vs. 8.1%, $p=0.008$) and required more temporary dialysis (5.3% vs. 1.1%, $p=0.024$). However, the groups were not comparable in terms of preexisting renal function levels. The FEVAR group had more advanced stages of CKD compared to the EVAR group (34% vs. 19%, $p=0.003$) [13]. Reis de Souza et al. presented at the 2015 Annual Meeting of the European Society for Vascular and Endovascular Surgery (ESVS) a matched cohort study comparing renal outcomes with EVAR and FEVAR for AAA. In that study, both groups had similar demographics, baseline comorbidities, estimated glomerular filtration rate (eGFR), and CKD stages. There were no significant differences between the groups in the rates of AKI or late renal function outcomes (non-published data).

A retrospective study by Grant et al. identified six risk factors for AKI following open repair for abdominal aortic aneurysms (AAA) using multivariate analysis. The most evident factor was a preoperative sCr level higher than 100 μmol/L (odds ratio [OR] 2.75, 95% confidence interval

Table 48.4 Fenestrated endovascular repair studies reporting risk factors for acute kidney injury

First author	Preoperative CKD	Metformin use	Length of the procedure	Contrast load	PAD
Martin-Gonzales [2]	HR 5.88 (2.75–12.60) $p<0.0001$	HR 3.97 (1.30–12.12) $p=0.02$	HR 1.01 (1.01–1.02) $p=0.0002$	NS	NR
Marzelle [3]	NR	NR	HR 2.31 (1.34–5.07) $p=0.048$	NR	HR 2.12 (1.05–4.26) $p=0.036$
Grimme [7]	NS	NR	NR	NS	NR
Verhoeven [23]	NS	NR	NR	NR	NR

CKD chronic kidney disease, *PAD* peripheral arterial disease, *HR* hazard ratio (95 % confidence interval), *NS* not significant, *NR* not reported, *OR* odds ratio (95 % confidence interval)

[CI] 1.69–4.50, $p<0.0001$). Juxta- or suprarenal AAA, hypertension, respiratory disease, symptomatic AAA, and age >75 years were also considered important risk factors [53]. A recent report by Saratzis et al. also identified the preoperative renal function as the most important predictor for AKI among 947 patients treated by infrarenal EVAR. In that study, according to the AKIN criteria, 17.6 % of the patients developed AKI. Although stroke, peripheral arterial disease, and diabetes were all associated to postoperative AKI on univariate analysis, preoperative renal function was the only independent predictor (OR for CKD stage II or higher = 1.28, $p=0.001$) [54]. Similarly to other studies in FEVAR patients, contrast dose was not associated with an increased AKI [2, 5, 7, 54]. Table 48.4 summarizes risk factors for AKI in patients undergoing FEVAR [2, 3, 7, 23].

Comparing Different Strategies

Few studies directly compared outcomes of FEVAR and open repair, especially regarding renal function. Canavati et al. published a retrospective review of patients who were considered unsuitable for standard EVAR and were treated by FEVAR ($n=53$) or open repair ($n=54$). Although patients treated by open surgical repair had higher rates of complications, the incidence of AKI was similar in both groups: 17 % for open repair and 15 % for FEVAR [11]. The Münster Group reported their experience with open repair ($n=31$), FEVAR ($n=29$), or parallel grafts ($n=30$) for pararenal aneurysms. Open repair was selected in lower-risk patients, whereas endovascular repair was reserved for higher-risk patients. Parallel grafts were used more frequently in urgent/emergent cases and had less vessels incorporated compared to fenestrated stent grafts. Preoperative eGFR was similar between the endovascular and open surgical groups (64 ± 28 mL/min/1.73 m^2 vs. 69 ± 31 mL/min/1.73 m^2, $p=0.3$, respectively), but postoperative eGFR was significantly lower in the open repair group (69 ± 99 mL/min/1.73 m^2 vs. 58 ± 33 mL/min/1.73 m^2, $p=0.025$) [16].

Shahverdyan et al. compared open repair ($n=34$) and FEVAR ($n=35$) in patients with juxtarenal aortic aneurysms. Patients treated by open surgical repair had higher rates of congestive heart failure and more renal artery disease. Acute kidney injury developed in nine (26 %) open surgical and three endovascular patients (8 %, $p=0.05$). Median postoperative eGFR was lower in the open repair group (52 mL/min/1.73 m^2 vs. 66 mL/min/1.73 m^2, $p=0.023$). None of the patients required new onset of dialysis [6].

In 2013, Tsilimparis et al. performed a review of the American College of Surgeons National Surgical Quality Improvement Program (ACS-NSQIP) database on complex aortic aneurysm repair and compared outcomes of open repair ($n=1091$) and FEVAR ($n=264$). In that study, postoperative acute renal failure was more frequent in the open repair group (6.7 % vs. 1.5 %, $p=0.001$) [15].

Michel et al. published data from the WINDOW trial, a multicenter French prospective registry of FEVAR for juxtarenal and pararenal aortic aneurysms in higher-risk patients ($n=268$). Results of FEVAR were compared to a cohort of patients treated by open repair ($n=1678$). Although patients in the FEVAR group were considerably sicker and older, postoperative permanent hemodialysis was more common following open repair (6 % vs. 21 %, $p=0.001$) [4].

A recent meta-analysis by Rao et al. compared postoperative renal outcomes for patients with juxtarenal abdominal aortic aneurysms in 20 open surgical and five FEVAR studies. The pooled rates for AKI were 13.9 % (95 % CI 10.1–18.8 %) for open repair and 11.4 % (95 % CI 4.1–27.6 %) for FEVAR (OR for open repair = 1.136, 95 % CI 0.754–1.713, $p=0.542$). There was no difference in permanent dialysis (2.8 % vs. 1.9 %, OR 1.66, 95 % CI 0.627–4.397, $p=0.308$) [55]. A similar study by Nordon et al. included 18 cohorts and showed lower rates of AKI in the FEVAR group (14.9 % vs. 20 %, RR 1.06, 95 % CI 1.01–1.12, $p=0.03$) but no difference in the incidence of new-onset permanent dialysis (1.4 % vs. 1.4 %, RR 1, 95 %, CI 0.99–1.01, $p=1$) [56]. Katsargyris et al. reported a meta-analysis of FEVAR versus open repair and found lower postoperative AKI (9.8 % vs. 18.5 %, $p<0.001$) and permanent dialysis in the FEVAR group (1.5 % vs. 3.9 %, $p<0.001$) [57].

The late effects of complex endovascular aortic interventions on renal function are not well known. Rao et al. found

eleven open surgical and six FEVAR studies reporting the development of renal failure during follow up. The pooled event rate was 7.7 % in open repair and 19.7 % in FEVAR (OR 0.375, 95 % CI 0.263–0.536, $p=0.0001$). However, patients who underwent FEVAR had higher rates of preexisting renal insufficiency, cardiac dysfunction, and diabetes. Conversely, open surgical patients had significantly lower sCr levels before intervention [55].

The results of the Zenith Fenestrated US Multicenter Trial ($n=67$), published in 2014, reported a freedom from renal function deterioration (decrease > 30 % of the baseline eGFR) of 92 % and 83 %, respectively, at one- and five-year follow-up [10]. Verhoeven et al. reported their 8-year experience with FEVAR for short-neck and juxtarenal abdominal aortic aneurysms. During a median follow-up of 24 months, 25 of 100 patients had increase of sCr of more than 30 %. Two patients required dialysis [23]. Banno et al. reported that 15 % of 80 patients who underwent FEVAR for pararenal aneurysms developed persistent renal impairment (50 % increase in the sCr value compared with baseline levels) during a mean follow-up of 14 months [1]. On a median follow-up of 67 months, Krismundsson et al. reported a decrease in median eGFR from 60 to 50 mL/min/1.73 m^2 ($p<0.001$) in 54 patients undergoing FEVAR for juxtarenal aneurysms [8].

At the 2015 Annual Meeting of the ESVS, de Souza, Oderich, and colleagues presented data from a multiple cohort study comparing renal outcomes in the Zenith Fenestrated ($n=67$) and the Zenith AAA ($n=134$) US trials (non-published data). In this study, AKI in the postoperative period (according to RIFLE criteria) was uncommon in both groups (5 % vs. 9 %, respectively, in the FEVAR and EVAR groups, $p=0.8$). Only two patients, both in the EVAR group, presented with renal failure, one of them requiring dialysis. At 2- and 5-year follow-up, there were no significant differences in >25 % decline in eGFR (Fig. 48.3, 20 % vs. 20 %, $p>0.99$, and 27 % vs. 42 %, $p=0.5$, respectively, for FEVAR and EVAR groups) or progression to CKD stages IV and V (2 % vs. 3 %, $p>0.99$, and 7 % vs. 8 %, $p=0.94$, respectively, for FEVAR and EVAR groups). In both groups, there was a gradual and significant reduction of mean eGFR from baseline to 5-year follow-up, but the difference was not significant between the groups (from 81 mL/min/1.73 m^2 to 60 mL/min/1.73 m^2 at the FEVAR group and from 81 mL/min/1.73 m^2 to 58 mL/min/1.73 m^2 at the conventional EVAR group). As expected, FEVAR patients had more renal-related reinterventions compared to patients treated by infrarenal EVAR (Fig. 48.4).

A summary of FEVAR studies reporting data regarding renal function is presented on Table 48.3.

Renal Protection

Volume depletion is an important risk factor for AKI. Although there are no adequate studies comparing fluid reposition versus placebo regarding AKI prevention in most scenarios, there is strong evidence that volume expansion is effective in avoiding contrast-induced renal injury, especially in higher-risk patients [58]. In the absence of hemorrhagic shock, isotonic saline is usually the solution of choice, as there is no clear evidence suggesting that colloids are superior in preventing or treating AKI, along with the possibility that specific colloids may cause AKI, in addition to their higher costs [59]. The role of sodium bicarbonate in preventing contrast-induced nephropathy is yet to be determined (see Chap. 21), as recent meta-analysis failed to demonstrate its benefits in reducing the need for dialysis and mortality when compared to sodium chloride [60, 61]. There is need to be careful and selective in performing fluid reposition, as

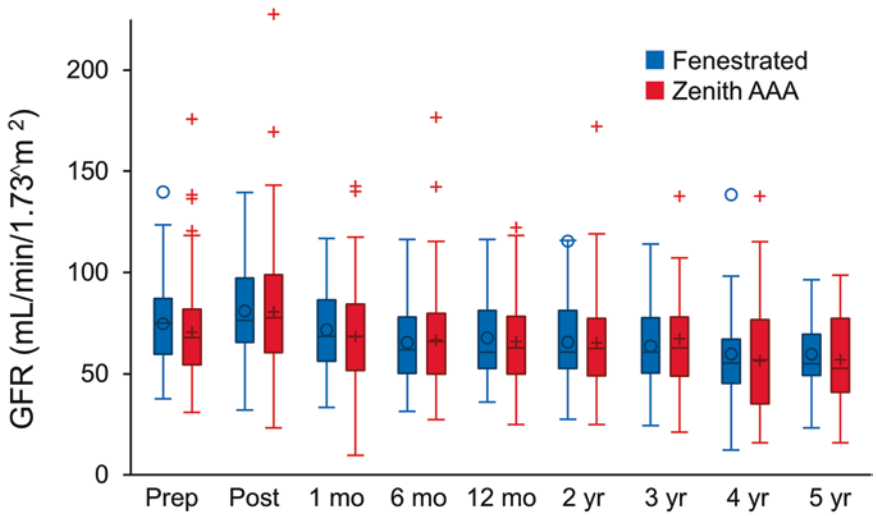


Fig. 48.3 Changes in eGFR among patients included in the prospective Zenith AAA stent graft (*red*) and in the Zenith Fenestrated stent graft trials (*blue*). By permission of Mayo Foundation for Medical Education and Research. All rights reserved

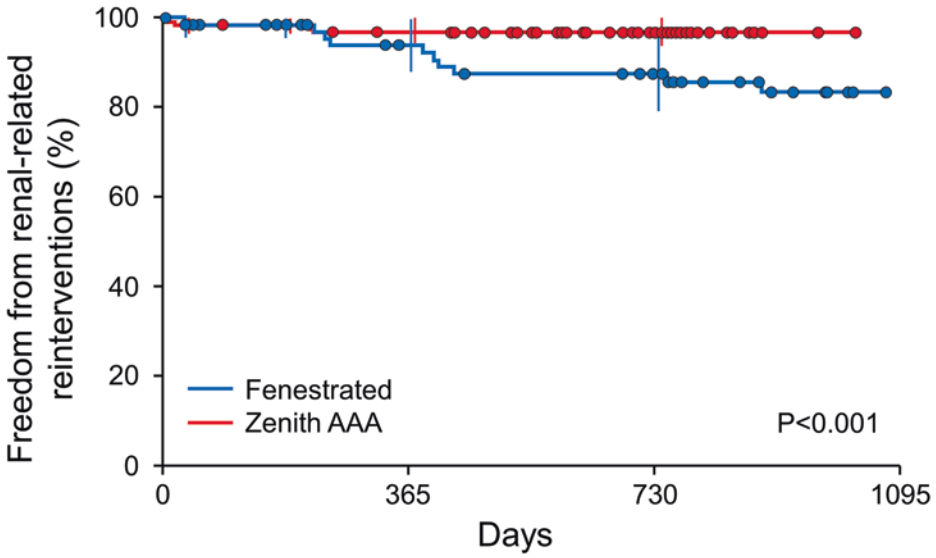


Fig. 48.4 Kaplan Meier survival curves of freedom of renal-related reinterventions in the prospective Zenith AAA stent graft (*red*) and in the Zenith Fenestrated stent graft trials (*blue*). By permission of Mayo Foundation for Medical Education and Research. All rights reserved

some studies have shown that a positive balance may be associated with increased mortality.

Diuretics have long been tested in the prevention and treatment of AKI. Furosemide is generally found to be ineffective or harmful when used to prevent or treat AKI in diverse scenarios, including contrast-induced injury. Studies evaluating the use of mannitol are often retrospective or underpowered and usually fail to show significant differences regarding renal outcomes. It has been suggested that mannitol may be beneficial in rhabdomyolysis by stimulating osmotic diuresis in trauma patients [59].

N-Acetylcysteine (NAC) did not alter mortality or renal outcomes after major surgery without the use of radiocontrast [59]. Some small studies showed a positive effect in preventing contrast-induced AKI, although not consistent. The most successful approach has been with 1200 mg orally twice a day on the day before and after the procedure. Oral NAC has a low risk of adverse events and is usually inexpensive [33]. Its use is suggested by the KIDGO, together with intravenous isotonic crystalloids, in patients with increased risk of contrast-induced AKI [58].

At least three systematic reviews addressed the use of theophylline as a protective agent for contrast-induced AKI [62–64]. The first two meta-analysis suggested a nonsignificant trend of renoprotection [62, 63], whereas the most recent one found a significant beneficial effect in patients with normal baseline renal function [64]. Findings were markedly inconsistent, and epidemiological quality of the studies included in the meta-analysis was questionable. Authors suggested further studies to evaluate the actual utility of the drug in this context [62–64].

Recently, the use of statins to prevent contrast-induced AKI has gained much interest. Several systematic reviews showed a significant protective effect with the pre-procedure use of statins in patients undergoing coronary angiography [65–67]. Ideal dose, length of use, and type of statin are yet to be defined. There are very few data outside the coronary angiography context.

At the Mayo Clinic, patients undergoing complex endovascular aortic procedures are stratified according to their risk of developing post-procedure AKI. Patients considered at high risk are usually admitted the day before surgery for intravenous preoperative hydration, whereas other patients are admitted in the morning of the procedure. Adequate preoperative planning and the use of onlay computed tomography during the procedure contribute to minimize the use of contrast. Pharmacological protective agents are not routinely used.

Conclusion

To create accurate and reproducible reporting standards for AKI and CKD is an important step to provide a complete understanding of the influence of endovascular procedures for complex aortic aneurysms in renal function deterioration. Patients with previous diagnosis of renal function impairment are in increased risk of further kidney damage and require special attention. Adequate hydration is still the major tool in protecting the kidneys in the perioperative course. Despite the lack of conclusive studies and the considerable variability in definitions of AKI and CKD, open repair and FEVAR seem to have similar renal function outcomes following the treatment of complex aneurysms. In the immediate postoperative period, it may be possible that FEVAR offers an advantage in reducing the incidence of AKI.

References

1. Banno H, Cochennec F, Marzelle J, Becquemin JP. Comparison of fenestrated endovascular aneurysm repair and chimney graft techniques for pararenal aortic aneurysm. J Vasc Surg. 2014;60:31–9.
2. Martin-Gonzalez T, Pincon C, Maurel B, Hertault A, Sobocinski J, Spear R, et al. Renal outcomes following fenestrated and branched endografting. Eur J Vasc Endovasc Surg. 2015;50(4):420–30.
3. Marzelle J, Presles E, Becquemin JP, WINDOWS Trial Participants. Results and factors affecting early outcome of fenestrated and/or branched stent grafts for aortic aneurysms: a multicenter prospective study. Ann Surg. 2015;261:197–206.
4. Michel M, Becquemin JP, Clement MC, Marzelle J, Quelen C, Durand-Zaleski I, WINDOW Trial Participants. Editor's choice—thirty day outcomes and costs of fenestrated and branched stent grafts versus open repair for complex aortic aneurysms. Eur J Vasc Endovasc Surg. 2015;50:189–96.
5. Sailer AM, Nelemans PJ, van Berlo C, Yazar O, de Haan MW, Fleischmann D, et al. Endovascular treatment of complex aortic aneurysms: prevalence of acute kidney injury and effect on long-term renal function. Eur Radiol. 2016;26(6):1613–9.
6. Shahverdyan R, Majd MP, Thul R, Braun N, Gawenda M, Brunkwall J. F-EVAR does not impair renal function more than open surgery for juxtarenal aortic aneurysms: single centre results. Eur J Vasc Endovasc Surg. 2015;50(4):432–41.
7. Grimme FA, Zeebregts CJ, Verhoeven EL, Bekkema F, Reijnen MM, Tielliu IF. Visceral stent patency in fenestrated stent grafting for abdominal aortic aneurysm repair. J Vasc Surg. 2014;59:298–306.
8. Kristmundsson T, Sonesson B, Dias N, Tornqvist P, Malina M, Resch T. Outcomes of fenestrated endovascular repair of juxtarenal aortic aneurysm. J Vasc Surg. 2014;59:115–20.
9. Kristmundsson T, Sonesson B, Malina M, Bjorses K, Dias N, Resch T. Fenestrated endovascular repair for juxtarenal aortic pathology. J Vasc Surg. 2009;49:568–74. discussion 74–5.
10. Oderich GS, Greenberg RK, Farber M, Lyden S, Sanchez L, Fairman R, et al. Results of the United States multicenter prospective study evaluating the Zenith fenestrated endovascular graft for treatment of juxtarenal abdominal aortic aneurysms. J Vasc Surg. 2014;60. 1420–8 e1-5.
11. Canavati R, Millen A, Brennan J, Fisher RK, McWilliams RG, Naik JB, et al. Comparison of fenestrated endovascular and open repair of abdominal aortic aneurysms not suitable for standard endovascular repair. J Vasc Surg. 2013;57:362–7.
12. Kitagawa A, Greenberg RK, Eagleton MJ, Mastracci TM. Zenith p-branch standard fenestrated endovascular graft for juxtarenal abdominal aortic aneurysms. J Vasc Surg. 2013;58:291–300.
13. Perot C, Sobocinski J, Maurel B, Millet G, Guillou M, d'Elia P, et al. Comparison of short- and mid-term follow-up between standard and fenestrated endografts. Ann Vasc Surg. 2013;27:562–70.
14. Suominen V, Pimenoff G, Salenius J. Fenestrated and chimney endografts for juxtarenal aneurysms: early and midterm results. Scand J Surg. 2013;102:182–8.
15. Tsilimparis N, Perez S, Dayama A, Ricotta 2nd JJ. Endovascular repair with fenestrated-branched stent grafts improves 30-day outcomes for complex aortic aneurysms compared with open repair. Ann Vasc Surg. 2013;27:267–73.
16. Donas KP, Eisenack M, Panuccio G, Austermann M, Osada N, Torsello G. The role of open and endovascular treatment with fenestrated and chimney endografts for patients with juxtarenal aortic aneurysms. J Vasc Surg. 2012;56:285–90.
17. British Society for Endovascular T and the Global Collaborators on Advanced Stent-Graft Techniques for Aneurysm Repair (GLOBALSTAR) Registry. Early results of fenestrated endovascular repair of juxtarenal aortic aneurysms in the United Kingdom. Circulation. 2012;125(22):2707–15.
18. Metcalfe MJ, Holt PJ, Hinchliffe RJ, Morgan R, Loftus IM, Thompson MM. Fenestrated endovascular aneurysm repair: graft complexity does not predict outcome. J Endovasc Ther. 2012;19:528–35.
19. Manning BJ, Agu O, Richards T, Ivancev K, Harris PL. Early outcome following endovascular repair of pararenal aortic aneurysms: triple- versus double- or single-fenestrated stent-grafts. J Endovasc Ther. 2011;18:98–105.
20. Tambyraja AL, Fishwick NG, Bown MJ, Nasim A, McCarthy MJ, Sayers RD. Fenestrated aortic endografts for juxtarenal aortic aneurysm: medium term outcomes. Eur J Vasc Endovasc Surg. 2011;42:54–8.
21. Troisi N, Donas KP, Austermann M, Tessarek J, Umscheid T, Torsello G. Secondary procedures after aortic aneurysm repair with fenestrated and branched endografts. J Endovasc Ther. 2011;18:146–53.
22. Amiot S, Haulon S, Becquemin JP, Magnan PE, Lermusiaux P, Goueffic Y, et al. Fenestrated endovascular grafting: the French multicentre experience. Eur J Vasc Endovasc Surg. 2010;39:537–44.
23. Verhoeven EL, Vourliotakis G, Bos WT, Tielliu IF, Zeebregts CJ, Prins TR, et al. Fenestrated stent grafting for short-necked and juxtarenal abdominal aortic aneurysm: an 8-year single-centre experience. Eur J Vasc Endovasc Surg. 2010;39:529–36.
24. Greenberg RK, Sternbergh 3rd WC, Makaroun M, Ohki T, Chuter T, Bharadwaj P, et al. Intermediate results of a United States multicenter trial of fenestrated endograft repair for juxtarenal abdominal aortic aneurysms. J Vasc Surg. 2009;50:730–7.e1.
25. Scurr JR, Brennan JA, Gilling-Smith GL, Harris PL, Vallabhaneni SR, McWilliams RG. Fenestrated endovascular repair for juxtarenal aortic aneurysm. Br J Surg. 2008;95:326–32.
26. Ziegler P, Avgerinos ED, Umscheid T, Perdikides T, Stelter WJ. Fenestrated endografting for aortic aneurysm repair: a 7-year experience. J Endovasc Ther. 2007;14:609–18.
27. Halak M, Goodman MA, Baker SR. The fate of target visceral vessels after fenestrated endovascular aortic repair—general considerations and mid-term results. Eur J Vasc Endovasc Surg. 2006;32:124–8.
28. Muhs BE, Verhoeven EL, Zeebregts CJ, Tielliu IF, Prins TR, Verhagen HJ, et al. Mid-term results of endovascular aneurysm repair with branched and fenestrated endografts. J Vasc Surg. 2006;44:9–15.
29. O'Neill S, Greenberg RK, Haddad F, Resch T, Sereika J, Katz E. A prospective analysis of fenestrated endovascular grafting: intermediate-term outcomes. Eur J Vasc Endovasc Surg. 2006;32:115–23.
30. Semmens JB, Lawrence-Brown MM, Hartley DE, Allen YB, Green R, Nadkarni S. Outcomes of fenestrated endografts in the treatment of abdominal aortic aneurysm in Western Australia (1997–2004). J Endovasc Ther. 2006;13:320–9.
31. Anderson JL, Berce M, Hartley DE. Endoluminal aortic grafting with renal and superior mesenteric artery incorporation by graft fenestration. J Endovasc Ther. 2001;8:3–15.
32. Chertow GM, Burdick E, Honour M, Bonventre JV, Bates DW. Acute kidney injury, mortality, length of stay, and costs in hospitalized patients. J Am Soc Nephrol. 2005;16:3365–70.
33. McCullough PA. Contrast-induced acute kidney injury. J Am Coll Cardiol. 2008;51:1419–28.
34. Saratzis A, Melas N, Mahmood A, Sarafidis P. Incidence of Acute Kidney Injury (AKI) after Endovascular Abdominal Aortic Aneurysm Repair (EVAR) and impact on outcome. Eur J Vasc Endovasc Surg. 2015;49:534–40.
35. Kertai MD, Steyerberg EW, Boersma E, Bax JJ, Vergouwe Y, van Urk H, et al. Validation of two risk models for perioperative mortality in patients undergoing elective abdominal aortic aneurysm surgery. Vasc Endovascular Surg. 2003;37:13–21.
36. Steyerberg EW, Kievit J, de Mol Van Otterloo JC, van Bockel JH, Eijkemans MJ, Habbema JD. Perioperative mortality of elective abdominal aortic aneurysm surgery. a clinical prediction rule based on literature and individual patient data. Arch Intern Med. 1995;155:1998–2004.

37. Biancari F, Hobo R, Juvonen T. Glasgow Aneurysm Score predicts survival after endovascular stenting of abdominal aortic aneurysm in patients from the EUROSTAR registry. Br J Surg. 2006;93: 191–4.
38. Brown LC, Brown EA, Greenhalgh RM, Powell JT, Thompson SG, UK EVAR Trial Participants. Renal function and abdominal aortic aneurysm (AAA): the impact of different management strategies on long-term renal function in the UK EndoVascular Aneurysm Repair (EVAR) Trials. Ann Surg. 2010;251:966–75.
39. Mehta RL, Chertow GM. Acute renal failure definitions and classification: time for change? J Am Soc Nephrol. 2003;14:2178–87.
40. Bellomo R, Ronco C, Kellum JA, Mehta RL, Palevsky P, Acute Dialysis Quality Initiative Workgroup. Acute renal failure—definition, outcome measures, animal models, fluid therapy and information technology needs: the Second International Consensus Conference of the Acute Dialysis Quality Initiative (ADQI) Group. Crit Care. 2004;8. R204-12.
41. Lopes JA, Jorge S. The RIFLE and AKIN classifications for acute kidney injury: a critical and comprehensive review. Clin Kidney J. 2013;6:8–14.
42. Wlodzimirow KA, Abu-Hanna A, Slabbekoorn M, Chamuleau RA, Schultz MJ, Bouman CS. A comparison of RIFLE with and without urine output criteria for acute kidney injury in critically ill patients. Crit Care. 2012;16:R200.
43. Lopes JA, Jorge S. Comparison of RIFLE with and without urine output criteria for acute kidney injury in critically ill patients: a task still not concluded! Crit Care. 2013;17:408.
44. Mehta RL, Kellum JA, Shah SV, Molitoris BA, Ronco C, Warnock DG, et al. Acute Kidney Injury Network: report of an initiative to improve outcomes in acute kidney injury. Crit Care. 2007;11:R31.
45. Bang JY, Lee JB, Yoon Y, Seo HS, Song JG, Hwang GS. Acute kidney injury after infrarenal abdominal aortic aneurysm surgery: a comparison of AKIN and RIFLE criteria for risk prediction. Br J Anaesth. 2014;113:993–1000.
46. National Kidney Foundation. K/DOQI clinical practice guidelines for chronic kidney disease: evaluation, classification, and stratification. Am J Kidney Dis. 2002;39:S1-266.
47. Levey AS, Eckardt KU, Tsukamoto Y, Levin A, Coresh J, Rossert J, et al. Definition and classification of chronic kidney disease: a position statement from Kidney Disease: Improving Global Outcomes (KDIGO). Kidney Int. 2005;67:2089–100.
48. Levey AS, de Jong PE, Coresh J, El Nahas M, Astor BC, Matsushita K, et al. The definition, classification, and prognosis of chronic kidney disease: a KDIGO Controversies Conference report. Kidney Int. 2011;80:17–28.
49. Webb ST, Allen JSD. Perioperative renal protection. continuing education in anaesthesia. Crit Care Pain. 2008;8:176–80.
50. Olsen PS, Schroeder T, Perko M, Røder OC, Agerskov K, Sørensen S, et al. Renal failure after operation for abdominal aortic aneurysm. Ann Vasc Surg. 1990;4:580–3.
51. Bonventre JV, Yang L. Cellular pathophysiology of ischemic acute kidney injury. J Clin Invest. 2011;121:4210–21.
52. Miller LE, Razavi MK, Lal BK. Suprarenal versus infrarenal stent graft fixation on renal complications after endovascular aneurysm repair. J Vasc Surg. 2015;61:1340–9 e1.
53. Grant SW, Grayson AD, Grant MJ, Purkayastha D, McCollum CN. What are the risk factors for renal failure following open elective abdominal aortic aneurysm repair? Eur J Vasc Endovasc Surg. 2012;43:182–7.
54. Saratzis A, Nduwayo S, Sarafidis P, Sayers RD, Bown MJ. Preoperative renal function is the main predictor of Acute Kidney Injury (AKI) after Endovascular Abdominal Aortic Aneurysm Repair (EVAR). Ann Vasc Surg. 2016;31:52–9.
55. Rao R, Lane TR, Franklin IJ, Davies AH. Open repair versus fenestrated endovascular aneurysm repair of juxtarenal aneurysms. J Vasc Surg. 2015;61:242–55.
56. Nordon IM, Hinchliffe RJ, Holt PJ, Loftus IM, Thompson MM. Modern treatment of juxtarenal abdominal aortic aneurysms with fenestrated endografting and open repair—a systematic review. Eur J Vasc Endovasc Surg. 2009;38:35–41.
57. Katsargyris A, Oikonomou K, Klonaris C, Topel I, Verhoeven EL. Comparison of outcomes with open, fenestrated, and chimney graft repair of juxtarenal aneurysms: are we ready for a paradigm shift? J Endovasc Ther. 2013;20:159–69.
58. Lameire N, Kellum JA, Group KAGW. Contrast-induced acute kidney injury and renal support for acute kidney injury: a KDIGO summary (Part 2). Crit Care. 2013;17:205.
59. Kellum JA, Lameire N, Group KAGW. Diagnosis, evaluation, and management of acute kidney injury: a KDIGO summary (Part 1). Crit Care. 2013;17:204.
60. Zhang B, Liang L, Chen W, Liang C, Zhang S. The efficacy of sodium bicarbonate in preventing contrast-induced nephropathy in patients with pre-existing renal insufficiency: a meta-analysis. BMJ Open. 2015;5:e006989.
61. Zoungas S, Ninomiya T, Huxley R, Cass A, Jardine M, Gallagher M, et al. Systematic review: sodium bicarbonate treatment regimens for the prevention of contrast-induced nephropathy. Ann Intern Med. 2009;151:631–8.
62. Bagshaw SM, Ghali WA. Theophylline for prevention of contrast-induced nephropathy: a systematic review and meta-analysis. Arch Intern Med. 2005;165:1087–93.
63. Kelly AM, Dwamena B, Cronin P, Bernstein SJ, Carlos RC. Meta-analysis: effectiveness of drugs for preventing contrast-induced nephropathy. Ann Intern Med. 2008;148:284–94.
64. Dai B, Liu Y, Fu L, Li Y, Zhang J, Mei C. Effect of theophylline on prevention of contrast-induced acute kidney injury: a meta-analysis of randomized controlled trials. Am J Kidney Dis. 2012;60: 360–70.
65. Gandhi S, Mosleh W, Abdel-Qadir H, Farkouh ME. Statins and contrast-induced acute kidney injury with coronary angiography. Am J Med. 2014;127:987–1000.
66. Giacoppo D, Capodanno D, Capranzano P, Aruta P, Tamburino C. Meta-analysis of randomized controlled trials of preprocedural statin administration for reducing contrast-induced acute kidney injury in patients undergoing coronary catheterization. Am J Cardiol. 2014;114:541–8.
67. Ukaigwe A, Karmacharya P, Mahmood M, Pathak R, Aryal MR, Jalota L, et al. Meta-analysis on efficacy of statins for prevention of contrast-induced acute kidney injury in patients undergoing coronary angiography. Am J Cardiol. 2014;114:1295–302.

Late Branch-Related Complications and Management

49

Meryl Davis, Jason Constantinou, and Tara Marie Mastracci

Introduction

The options for treatment of aortic aneurysms now include a variety of complex endovascular techniques such as branched, fenestrated and parallel grafts. Despite many reports of patients treated with these devices, the literature pertaining to durability remains sparse. In addition, limitations of current reports are inclusion of heterogeneous population, frequently combining differing aortic morphologies and a variety of device designs. As a consequence an assessment of the strengths and weaknesses of these techniques remains challenging and makes an informed clinical decision about the choice of the ideal mating stent difficult if not impossible. Traditionally, balloon-expandable stents have been used for fenestrations, but for branches there has been great variation in stent selection including first-generation self-expandable stent grafts (e.g. Wallgrafts) to newer generation more flexible stents (e.g. Viabahn).

Branch-Related Outcomes

A literature search investigating outcomes following the use of branched and fenestrated devices reveals a paucity of data about heterogeneous devices and outcomes. Reports often combine data from fenestrated and branched devices and represent single-centre outcomes with small numbers and medium-term follow-up. The most fundamental disparity in the literature is the inconsistency with which devices are defined: fenestrated devices are frequently described as having 'branches', and branched devices are variable in design and may have caudally or cranially directed cuffs, with radial or helical orientation, or may be a combination of fenestrated and branched components. This compounds analysis and emphasises the need for a standardisation or classification of complications.

In one study that is restricted to branched-only outcomes, Reilly et al. [1] reported the outcomes of 81 patients who underwent thoracoabdominal and pararenal aortic aneurysm repair with a multibranched device involving a total of 306 branches. During a mean follow-up of 21 months, there were no aneurysm ruptures; however, four patients (4.9 %) had aneurysm enlargement: two were successfully treated, one was unsuccessful, and one was not treated. All planned branch insertions were completed in 306 branches. Perioperative target branch injury resulting in dissection or perforation was seen in 14 patients and involved the renal branch in 11, coeliac in two and the superior mesenteric in one. In this series nine renal branches occluded, resulting in need for dialysis in two patients. Coeliac branch occlusion was noted in two patients; one patient was asymptomatic, while the other patient developed gastric ulceration and was treated conservatively. Occlusion rates of the branches approached significance with 0 % for the superior mesenteric artery, 2.6 % for the coeliac axis and 6.1 % for the renal artery ($p = 0.054$).

During follow-up five patients (6.2 %) developed branch stenosis and involved the renal branch in four and the superior mesenteric artery in one. Four branches warranted stenting. There were no stent separations, kinks, migration or collapse noted during the mean follow-up of 21 months. This cohort of patients demonstrates the efficacy and intermediate-term results of branched devices for thoracoabdominal aortic aneurysm repair. The most common late failure was renal artery occlusion, which rarely resulted in a patient requiring dialysis, but becomes a theme in non-fenestrated devices as evidence evolves.

M. Davis • J. Constantinou
Department of Vascular Surgery, Royal Free London NHS Foundation Trust, Pond Street, London NW3 2QG, UK

T.M. Mastracci (✉)
Department of Aortic Surgery, Royal Free London NHS Foundation Trust, Pond Street, London NW3 2QG, UK
e-mail: tara.mastracci@nhs.net

© Mayo Foundation for Medical Education and Research 2017

G.S. Oderich (ed.), *Endovascular Aortic Repair*, DOI 10.1007/978-3-319-15192-2_49

Verhoeven et al. in 2015 [2] reported a 10-year experience using fenestrated and branched devices with a mean follow-up period of 29 months. The series included 166 patients, 70 of whom received a composite fenestrated/branched device, 57 a branched device and 39 a fenestrated endograft. The total number of fenestrations and branches was 600 and included 326 branches, which were oriented caudally in 314, and 274 fenestrations. Target vessel stent patency at 1 and 5 years was 98 % and 94 %, respectively. During follow-up 22 target vessels occluded, including 15 renal vessels, six coeliac arteries and one superior mesenteric artery. Renal artery occlusion resulted in permanent dialysis in three patients, while the coeliac and superior mesenteric artery stent occlusions did not warrant reintervention, as the patients were asymptomatic. No details are recorded as to the causes of the occlusions. It is noteworthy that the reintervention rate is low with an estimated freedom from reintervention of 88 % at 1 year and 78 % at 3 years. This report concluded that fenestrated and branched stent grafts are safe and effective in a high-risk cohort with a good target vessel stent patency of 95 %. The authors acknowledged that reintervention is a concern; in this series 17 % of patients required at least one reintervention within the first 3 years of the index procedure, most of which were undertaken with endovascular techniques. This paper emphasises the efficacy and durability of these devices, while reiterating the need for close surveillance and monitoring to ensure target vessel patency.

A further paper published in 2013 confirms the durability of branched stent grafts [3]. Mastracci et al. described a cohort of 650 patients undergoing aneurysm repair with branched or fenestrated devices and include 1679 branches and fenestrations with a mean follow-up of 3 years and a maximum follow-up of 9 years. Secondary procedures were required for 0.6 % of coeliac arteries, 4 % for superior mesenteric arteries and 6 % and 5 % for right and left renal arteries, respectively, with an average time to reintervention being 237 days from the index procedure. A Kaplan-Meier analysis of freedom from secondary intervention and durability of mating stents is shown in Fig. 49.1. Thirty-day freedom from secondary intervention was 98 % with confidence intervals of 96–99 % with a 5-year freedom from secondary intervention of 84 % (CI, 78–90 %), indicative of a durable and robust repair. Death secondary to branch stent complications was noted in three patients. All deaths pertained to complications in the territory of the superior mesenteric artery, namely, thrombosis in two, including one scallop, which was not stented perioperatively. In order to determine the durability of the device, branch instability was described over time using a model of exponential decay and is shown in Fig. 49.2. Branch instability incorporates occlusion, body migration and branch-related expansion. Interrogating surveillance imaging and analysing the vessels in this manner give a more meaningful tool with which to compare data from other centres. In order to gain a durable repair, this report emphasises the importance of device planning to establish a proximal landing zone of greater than 2 cm in a region of the aorta with parallel walls and no thrombus lining and minimal tortuosity. Rigorous follow-up in the form of CT and duplex ultrasound is also advocated, as the absence of follow-up imaging does not imply a durable branch. The paper proposes a classification system as outlined in Fig. 49.3.

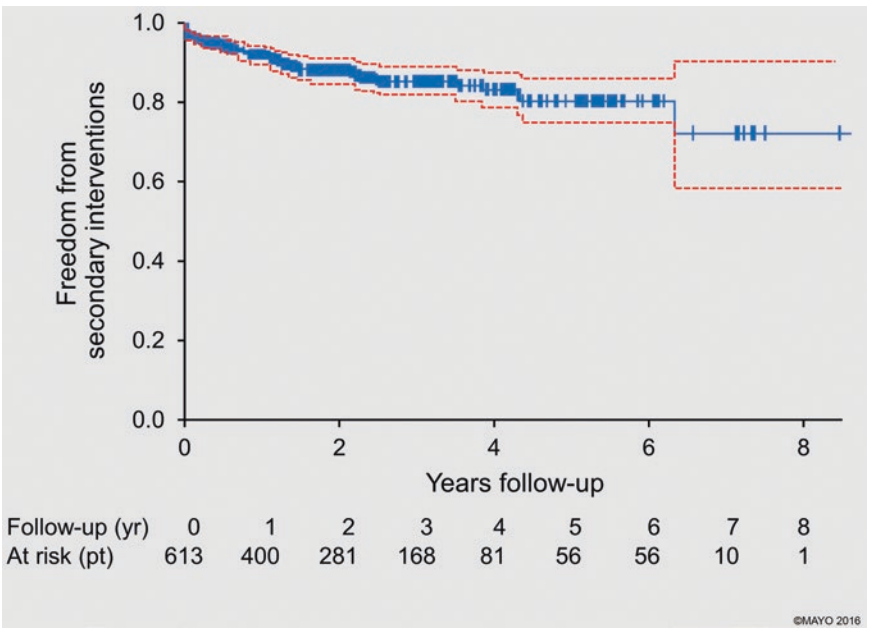


Fig. 49.1 Kaplan-Meier curve for secondary interventions in patients treated by four-vessel fenestrated-branched stent grafts over the follow-up period. By permission of Mayo Foundation for Medical Education and Research. All rights reserved

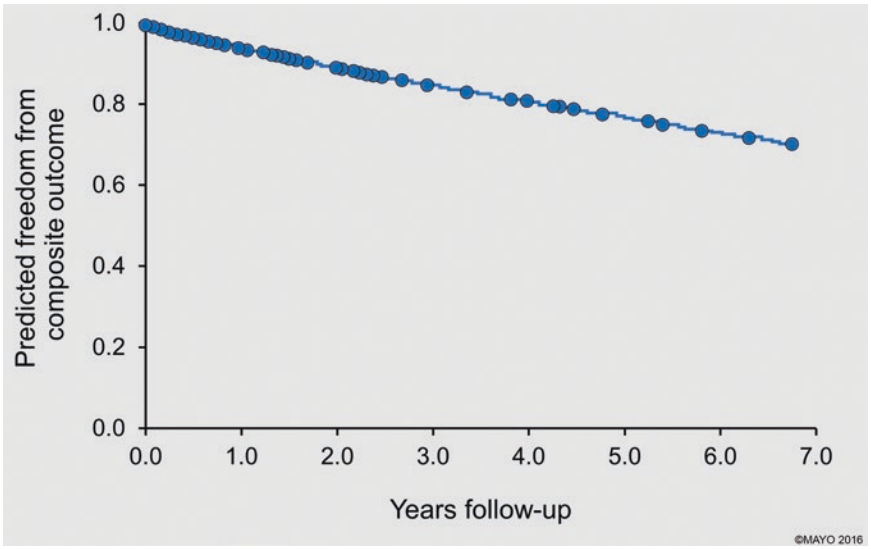


Fig. 49.2 Exponential decay curve for fenestrated and branched stent graft. Calculated decay constant –0.062. By permission of Mayo Foundation for Medical Education and Research. All rights reserved

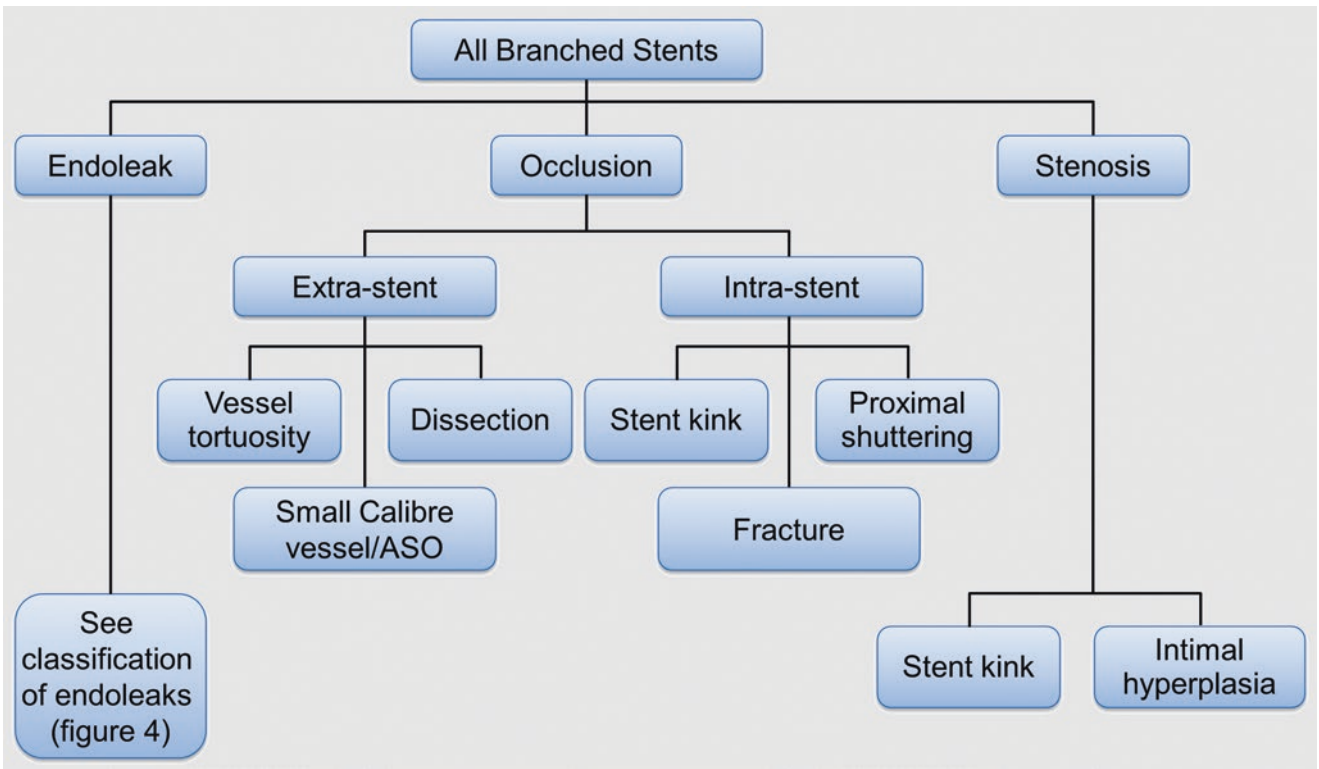


Fig. 49.3 Classification scheme for branch-related events in patients treated by fenestrated and branched endografts for complex aortic aneurysms. By permission of Mayo Foundation for Medical Education and Research. All rights reserved

Martin-Gonzalez et al. in 2015 reported renal outcomes following fenestrated and branched endografting in 225 patients with a median follow-up of 3.1 years [4]. A total of 427 renal target vessels were perfused with 53 branches and 374 fenestrations. Other than renal artery angulation, there were no significant differences in renal outcomes and renal secondary interventions between fenestrated and branched procedures. Renal-related secondary interventions were undertaken in 13 cases, which included three early procedures within 30 days; this translates into a 5-year freedom from renal composite event and renal occlusion of 98.6% and 99.5%, respectively. This paper again confirms the

durability of branched and fenestrated endografting, while confirming the need for a systematic and diligent surveillance regimen.

Two contemporary publications have specifically dealt with branch-only complications. Panuccio et al. [5] reviewed the performance of bridging stent grafts used in fenestrated and branched endografts. In a series of 150 consecutive patients with 523 target vessels, they found that the currently used bridging stent grafts had low occlusion and reintervention rates. In the majority of patients, balloon-expandable devices were deployed in 494 vessels (representing 95 % of cases) with self-expandable stents being placed in 5 % ($n = 26$), with no difference found between the two. The use of relining stents, which was high in this series at 64.6 % ($n = 336$ target vessels), did not prevent stent graft complications. The authors concluded that in this retrospective study, comparable results are shown with the two stent grafts and the advent of new devices with greater flexibility with caudally directed cuffs may improve performance and durability.

The second publication looking at branch-only complications comes from a consortium of centres who compiled data for a more pragmatic view of the medium-term outcomes with branch stents [6]. Although the mean follow-up in this series was only 2 years, it represents the career outcomes for all centres who have been implanting branched endografts. The findings are in keeping with the Panuccio paper in that the type of mating stent did not affect outcomes. In that study renal branches were more likely to fail over time and appeared to fail through occlusive modes, rather than through endoleaks.

Sylvan et al. [7] evaluated branch vessel curvature on branches arising from fenestrated and branched devices in 168 patients. This paper hypothesised that vessel wall curvature preoperatively or its development postoperatively may be predictive of branch vessel failure. There were 558 vessels that underwent analysis; no significant relationship between the severity and changes in artery curvature and adverse events were noted. This paper emphasises the need for ongoing review of imaging pre- and postoperatively in order to add to our understanding of this field. It is also a salient reminder of the paucity of information pertaining to the evolving aorta and our understanding as to why devices fail.

It is paramount that centres who undertake these challenging cases also have a robust protocol for surveillance with duplex ultrasonography and CT angiography. The two modalities thereby ensure assessment of target vessel patency, branch integrity as well as visceral vessel velocity measurements. Standardisation of reporting with classification of device failures will aid our understanding of the current designs and help to formulate modifications for future endografts.

Classification of Branch Complications

As is evidenced by the review of the literature, the modes of failure for branches and fenestrations are various and complex. Some of the complications that may be encountered following the use of branched and fenestrated endovascular devices are described below. The majority of experience with branched visceral devices comes from custom-made devices using Cook Medical's Zenith platform, but newer devices are emerging with unique modes of failure. In order to provide a systematic approach to branch complications, we propose a classification as outlined below (Figs. 49.3 and 49.4). This classification suggests differing modes of failure related to aortic morphology, stent-stent graft interface or device fatigue. Using this classification system, it may be possible to further classify new modes of failure from novel devices as they are developed in the future.

Endoleak

Endoleaks occur in branched and fenestrated territories in a variety of scenarios. A mating stent may be separated from the main body, from the branch vessel, or may fracture. Additionally, when more than one stent is required to bridge the distance between the main body and the branch vessel, further leakage/separation may occur. For this reason, the basic definition of endoleak must be explored to provide the correct classification. Fundamentally, a type 1 endoleak is one that occurs in an interface between the vessel and the device, whereas a type 3 endoleak is one that occurs between two components of the device. The depiction of this is in Fig. 49.4 for fenestrated devices and Fig. 49.5 for branched devices.

Case 1

A 78-year-old female presented with a ruptured type II thoracoabdominal aortic aneurysm (Fig. 49.5). She was treated with an off-the-shelf t-Branch device (Cook® Medical). On surveillance CT obtained 5 days after the procedure, it was noted that the bridging Fluency (Bard) stent had been deployed short of the SMA branch. This was treated via a brachial approach to allow relining of the SMA branch with an additional bridging stent to re-establish flow.

Case 2

In some aneurysms, persistent type II or unidentified endoleaks can cause sac expansion, leading to separation of the branch stent from the vessel (Fig. 49.6). This type of endoleak requires reintervention to extend the branch further into the branch vessel.

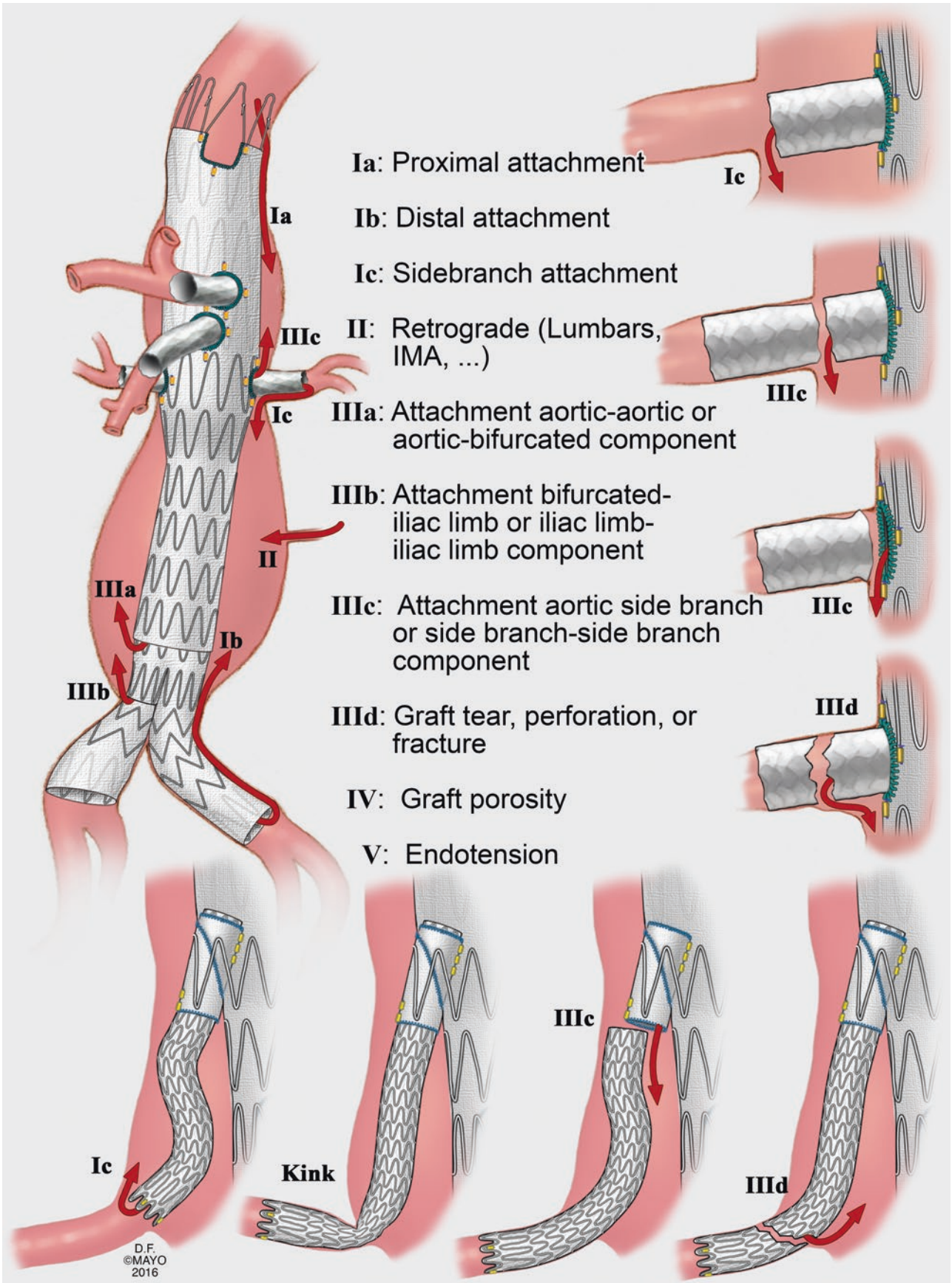


Fig. 49.4 Proposed classification for endoleak classification in patients treated with reinforced fenestrations or directional branches for complex aortic aneurysms. By permission of Mayo Foundation for Medical Education and Research. All rights reserved

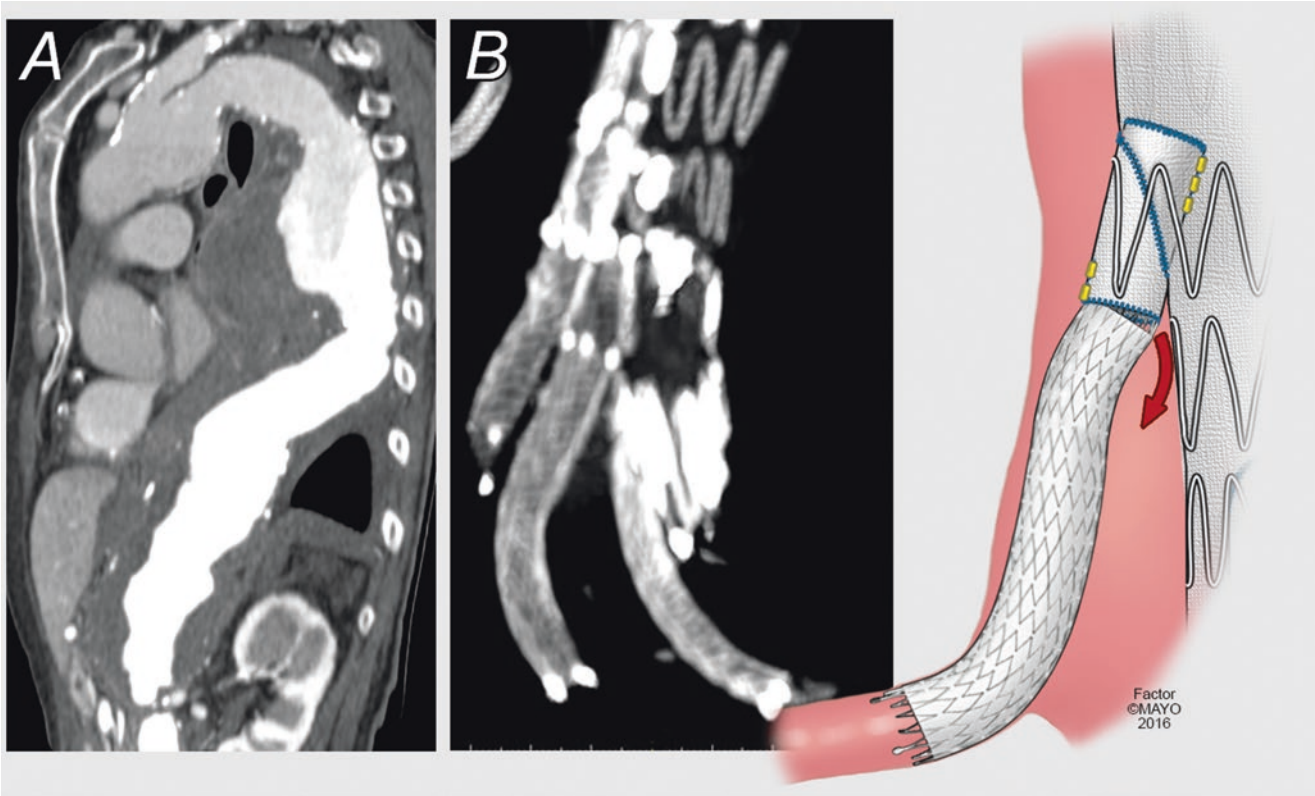


Fig. 49.5 Type II thoracoabdominal aortic aneurysm (**a**) treated with an off-the-shelf t-Branch device. On surveillance CT 5 days postoperatively, it was noted that the bridging Fluency (Bard) stent had been deployed short of the SMA branch (**b**). By permission of Mayo Foundation for Medical Education and Research. All rights reserved

Case 3

In heavily kinked arteries, or in those in which large balloons were used to mould the stent in place, fractures can develop in the mating stents that rip the fabric (Fig. 49.7). This type of endoleak requires restenting to seal the leak.

Case 4

Large aneurysms may require more than one bridging stent to cross the gap between the device and the branch vessel (Fig. 49.8). If this is the case, a separation may occur between the two branch stents leading to component separation and endoleak. These can be challenging to repair, but require relining with covered, usually self-expanding stent grafts.

Occlusion and Stenosis

Branch stents become occluded when the stent is kinked and fractured or the distal vessel has pathology that impairs flow, including dissection and embolisation. This occlusion can occur in the early or late in the course and may present first with stenosis before progressing to occlusion. There are a variety of surgical misadventures that can cause occlusion in the operating room, and it is imperative that the operating surgeon be aware of the possibility and perform adequate intraoperative imaging to identify and intervene quickly. For late occlusion, the role of surveillance imaging in preventing occlusion comes in being able to recognise the signs of kinked or low-flow vessels and intervening early to change the course.

Case 5

A patient underwent an elective branched repair of a type IV thoracoabdominal aortic aneurysm. A surveillance CT scan revealed an occluded right renal branch; this was thought to be secondary to a small renal artery luminal diameter (Fig. 49.9). There was no deterioration in renal function; therefore, no active management was instigated.

Case 6

During a type II thoracoabdominal aortic aneurysm repair, a decision was taken to maintain spinal cord perfusion by not deploying stents into the coeliac branch. This allowed the aortic sac to continue to be perfused via the open coeliac branch as a temporary aneurysm sac perfusion (TASP) branch (Fig. 49.10). As a second-stage procedure, the

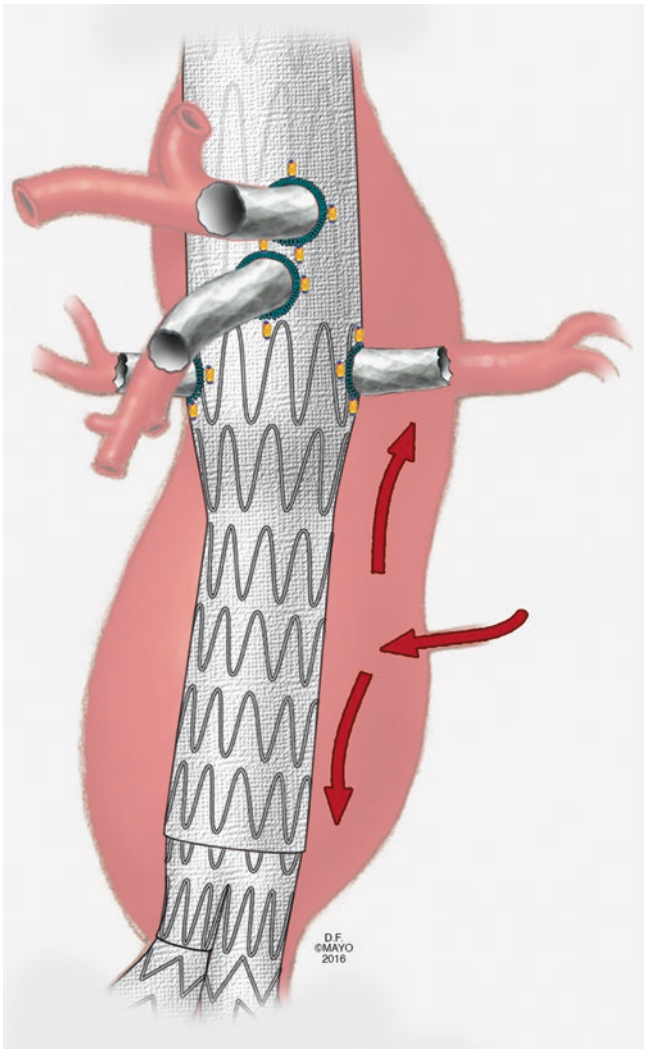


Fig. 49.6 Persistent type II or unidentified endoleaks can cause sac expansion, leading to separation of the branch stents from the vessel. By permission of Mayo Foundation for Medical Education and Research. All rights reserved

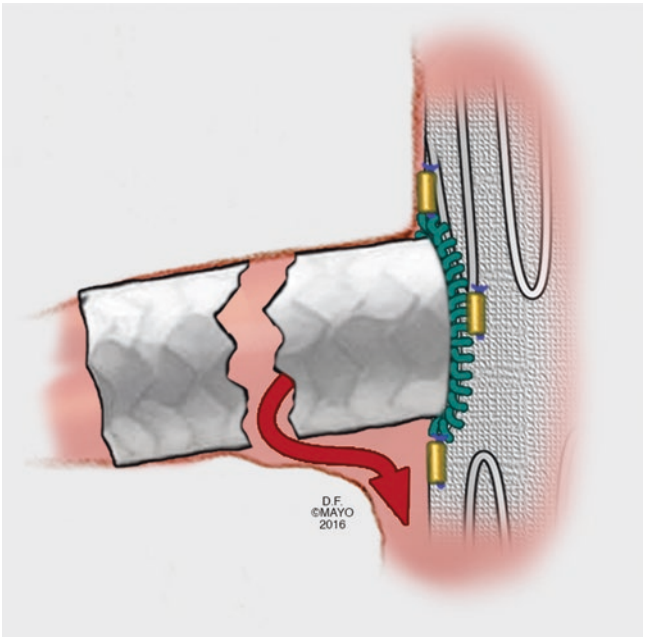


Fig. 49.7 Stent fractures can develop in the mating stents that rip the fabric. By permission of Mayo Foundation for Medical Education and Research. All rights reserved

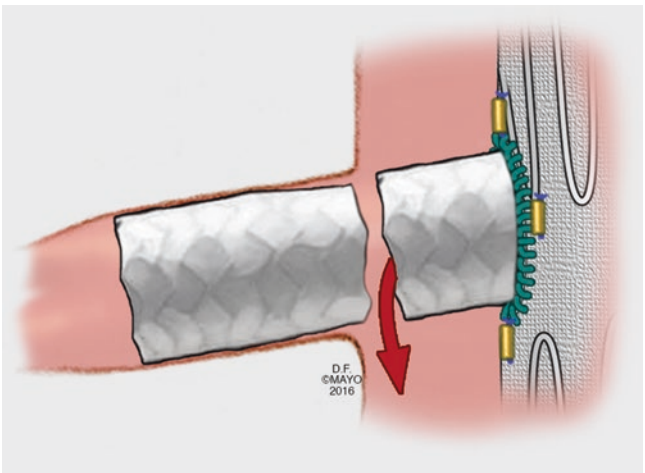


Fig. 49.8 Separation may occur between the two branch stents, leading to component separation and endoleak. By permission of Mayo Foundation for Medical Education and Research. All rights reserved

intention was to reconnect the coeliac branch and thereby complete the endovascular repair; however, on surveillance CT 1 month later, this branch was noted to be occluded, with no endoleak and no clinical sequelae.

Case 7

During cannulation of the right renal artery for a juxtarenal aneurysm, a dissection flap was raised; a bridging stent was deployed into the renal vessel with the aim to recannalise the distal true lumen. Follow-up imaging showed occlusion of the right renal artery with subsequent loss of some renal function without the need for renal support (Fig. 49.11).

Case 8

Following a quadruple-fenestrated stent graft, 1 year post procedure, the imaging revealed an incidental finding of an occluded SMA (Fig. 49.12). This was secondary to inadequate flaring of the Atrium (Maquet) bridging stent. The patient was asymptomatic; therefore, no further endovascular procedures were undertaken.

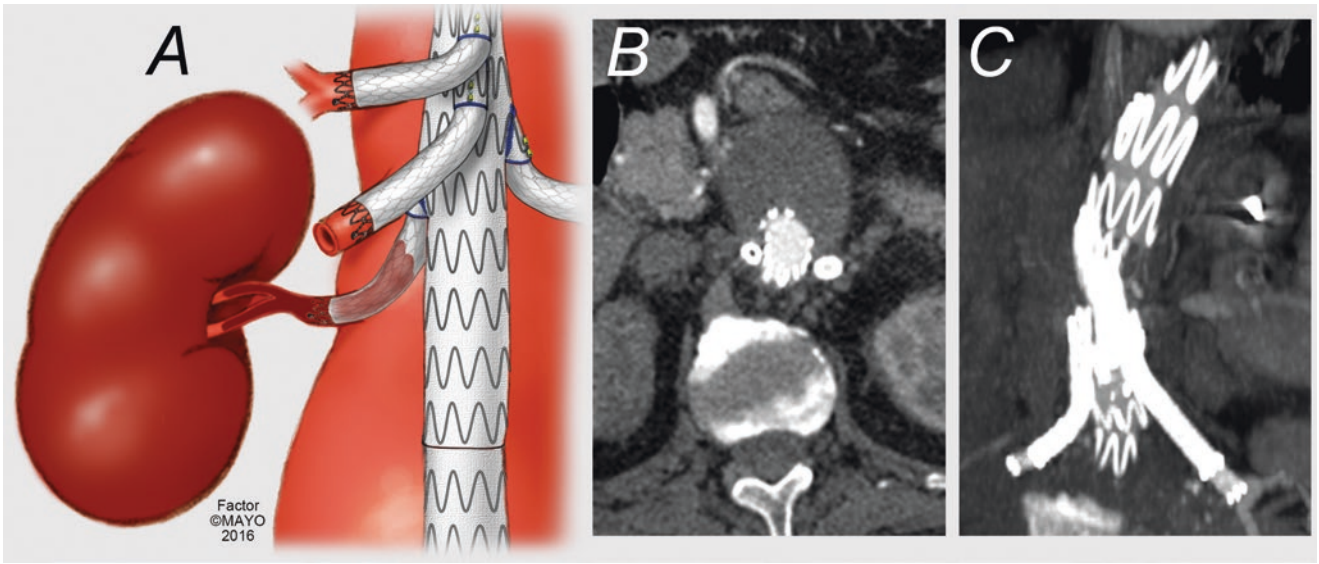


Fig. 49.9 A patient underwent an elective branched repair of a type IV thoracoabdominal aortic aneurysm. A surveillance CT scan revealed an occluded right renal branch (**a**). This was thought to be secondary to a small renal artery luminal diameter (**b** and **c**). By permission of Mayo Foundation for Medical Education and Research. All rights reserved

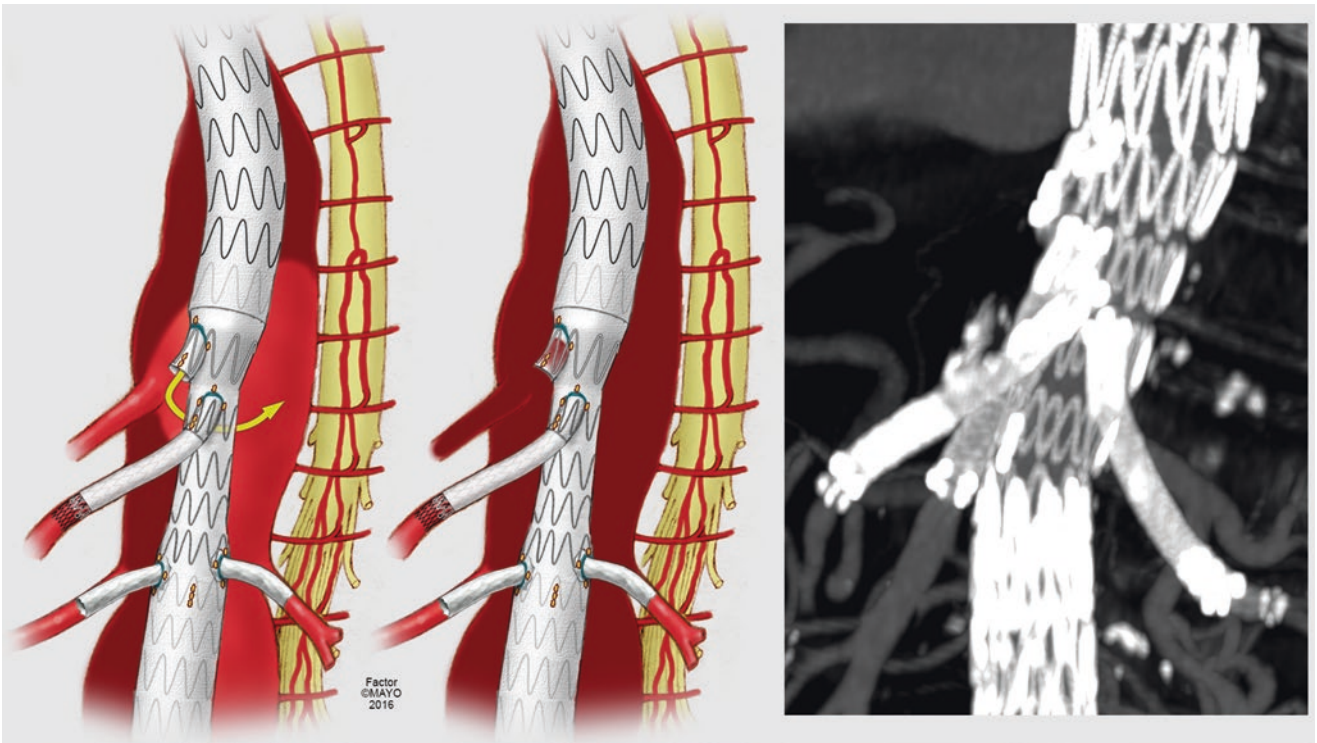


Fig. 49.10 Coeliac branch is left unstented to maintain spinal cord perfusion. This allowed the aortic sac to continue to be perfused via the open coeliac branch. As a second-stage procedure, the intention was to reconnect the coeliac branch and thereby complete the endovascular repair; however, on surveillance CT 1 month later, this branch was noted to be occluded. By permission of Mayo Foundation for Medical Education and Research. All rights reserved

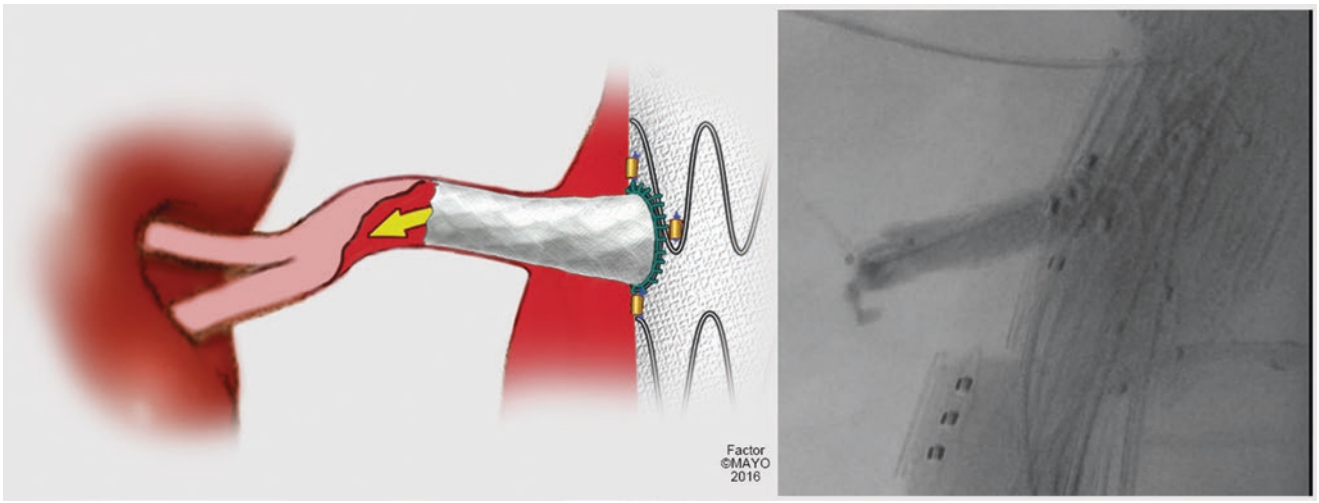


Fig. 49.11 Dissection of the right renal artery during stent placement, leading to target vessel occlusion. By permission of Mayo Foundation for Medical Education and Research. All rights reserved

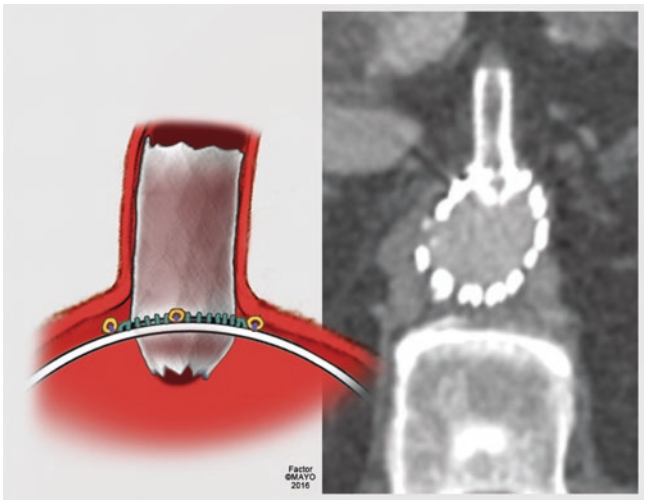


Fig. 49.12 Occlusion of the superior mesenteric artery stent due to inadequate flaring of the proximal stent. By permission of Mayo Foundation for Medical Education and Research. All rights reserved

Case 9

During this fenestrated endovascular procedure, the SMA was inadvertently cannulated via the right renal fenestration (Fig. 49.13). Despite attempting to cannulate the right renal artery via the SMA fenestration, this was not successful. As a consequence of this complication, the patient was deemed to have no endovascular option and sustained a loss of renal function. Open bypass surgery to restore renal flow was not appropriate as the patient had a hostile abdomen due to multiple laparotomies.

Case 10

Morphologically, this patient was noted to have a thrombus-laden aorta—'a shaggy aorta'. Despite a routine fenestrated procedure, the right renal artery was noted on CT 3 days postoperatively to be occluded. The mechanism of this occlusion was thought to be embolic as no other structural abnormality could be identified (Fig. 49.14).

Case 11

In the image below, the left subclavian artery was inadvertently covered by a thoracic stent graft; this was rescued with a chimney stent deployed in the left subclavian artery [8]. A subsequent CT showed a fracture of the chimney stent with no compromise to perfusion of the left upper limb (Fig. 49.15).

Conclusion

The durability of branched and fenestrated devices is yet to be determined. However, as evidence evolves it is becoming clear that there are patterns in the modes of failure from which we can learn and help prevent. Future research should be focused on a more in-depth imaging analysis of stents before and after failure to determine the cause of failure and possibly provide information to design better devices.

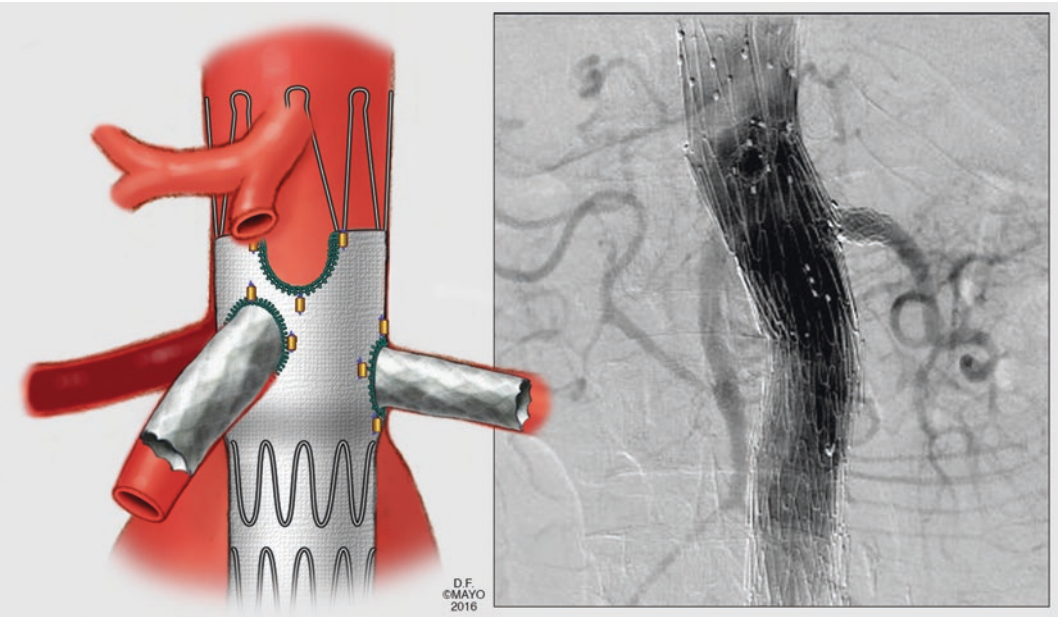


Fig. 49.13 Inadvertent stenting of the SMA via renal fenestration, leading to loss of the right renal artery. By permission of Mayo Foundation for Medical Education and Research. All rights reserved

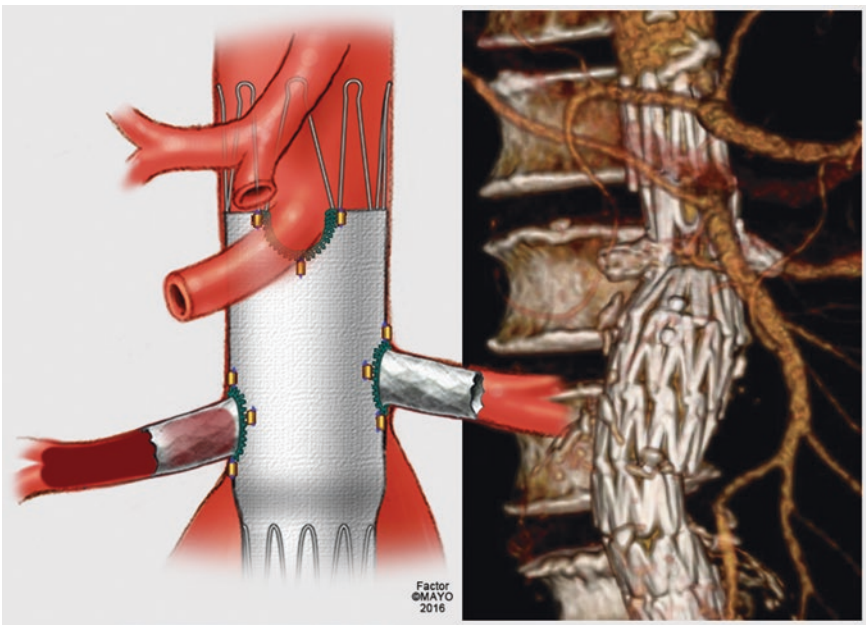


Fig. 49.14 Occlusion of the right renal artery in a patient with a thrombus-laden aorta—'a shaggy aorta'—was thought to be due to emboli. By permission of Mayo Foundation for Medical Education and Research. All rights reserved

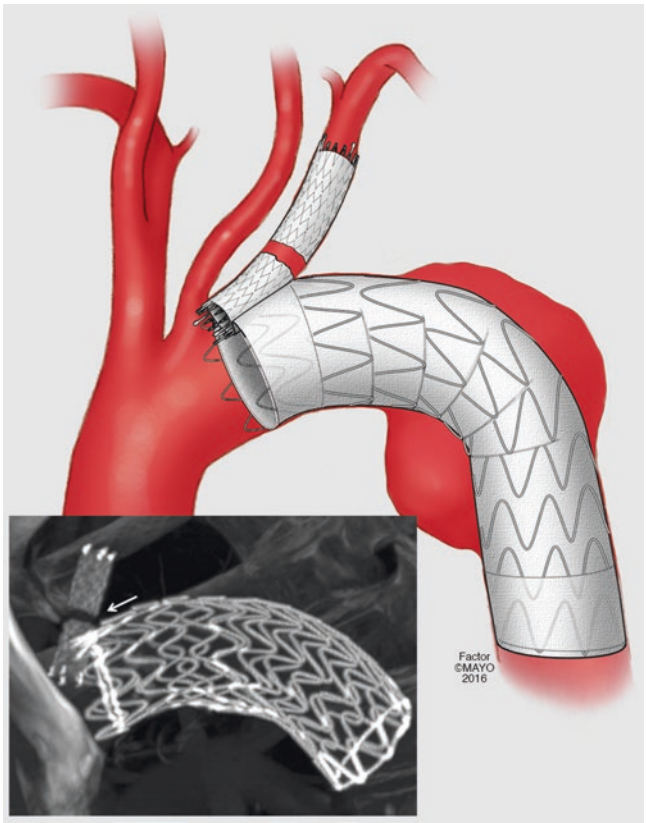


Fig. 49.15 Fracture of chimney stent to the left subclavian artery. By permission of Mayo Foundation for Medical Education and Research. All rights reserved

References

1. Reilly LM, Rapp JH, Grenon SM, Hiramoto JS, Sobel J, Chuter TA. Efficacy and durability of endovascular thoracoabdominal aortic aneurysm repair using the caudally directed cuff technique. J Vasc Surg. 2012;56:53–63.
2. Verhoeven EL, Katsargyris A, Bekkema F, Oikonomou K, Zeebregts CJ, Ritter W, et al. Editor's choice: ten-year experience with endovascular repair of thoracoabdominal aortic aneurysms: results from 166 consecutive patients. Eur J Vasc Endovasc Surg. 2015;49:524–31.
3. Mastracci TM, Greenberg RK, Eagleton MJ, Hernandez AV. Durability of branches in branched and fenestrated endografts. J Vasc Surg. 2013;57:926–33.
4. Martin-Gonzalez T, Pincon C, Maurel B, Hertault A, Sobocinski J, Spear R, et al. Renal outcomes following fenestrated and branched endografting. Eur J Vasc Endovasc Surg. 2015;50:420–30.
5. Panuccio G, Bisdas T, Berekoven G, Torsello G, Austermann M. Performance of bridging stent grafts in fenestrated and branched aortic endografting. Eur J Vasc Endovasc Surg. 2015;50:60–70.
6. Mastracci TM, Carrell T, Constantinou J, Dias NV, Gonzalez TM, Katsargyris A, et al. The effect of branch stent choice on branch-related outcomes in complex aortic repair. J Vasc Surg. 2015;59:S34.
7. Sylvan J, Crier C, Wolski K, Yanof J, Goel V, Kuramochi Y, et al. Impact of alterations in target vessel curvature on branch durability after endovascular repair of thoracoabdominal aortic aneurysms. J Vasc Surg. 2015. doi:10.1016/j.jvs.2015.09.053.
8. Mangialardi N, Serrao E, Kasemi H, Alberti V, Fazzini S, Ronchey S. Chimney technique for aortic arch pathologies: an 11-year single-center experience. J Endovasc Ther. 2014;21(2):312–23.

Index

A
Abdominal aortic aneurysms (AAA), 3, 83, 128, 130, 131, 134, 137, 141, 142, 161, 240, 246, 247, 395
  EVAR, 709
  juxta-/suprarenal, 727
  open repair, 709, 726
  renal function deterioration, 721
  symptomatic, 727
Abdominal aortic CTA, 150
Abdominis muscle, 642
Aberrant RSA (aRSA), 544
A-Branch stent graft (Cook Medical), 509–511
Access scallops, 390
Accessory renal arteries, 68, 725
Accreditation Council for Graduate Medical Education (ACGME), 246
ACE inhibitors, 145
Acidosis, 725
Acrogeria, 51
ACTA2 mutations, 54, 55
Activated clotting time (ACT), 421, 596
Active cardiac conditions, 134
Active seal technology, 658
Acute aortic syndrome
  anatomical variants, 203–206
  aortic dissection, 20, 206–207
  aortic rupture, 20
  defined, 20
  IMH, 207–208
  intramural hematoma, 20
  PAU, 208
  penetrating aortic ulcer, 20
  surveillance, 211
Acute Dialysis Quality Initiative (ADQI), 140
Acute kidney injury (AKI), 140, 313–321, 699, 721
  AKIN, 724
  ATN, 724
  CKD, 729
  complex aortic aneurysms, 726
  contrast-induced, 729
  definition, 721
  development, 721, 727
  diagnosis, 721
  FEVAR, 721
  intraoperative measures, 316, 318, 320, 321
  intrinsic renal causes, 724
  kidney tissue repair, 726
  postoperative, 321, 727
  preoperative, 314, 315
  prevention and treatment, 729
  RIFLE criteria, 721
  risk factor, 726–728
Acute kidney injury network (AKIN), 699, 724
Acute tubular necrosis (ATN), 724
Addendum, 142
Adjunctive Maneuvers, 337–338
Advanced Endovascular Aortic Programs, 238–243
ALARA principle, 154
AlSeal sheath, 219
American College of Cardiology/American Heart Association (ACC/AHA), 131, 134–136, 141
American College of Surgeons National Surgical Quality Improvement Program (ACS NSQIP), 138, 727
American College of Surgeons National Surgical Quality Improvement Program Myocardial Infarction Cardiac Arrest Calculator (ACS NSQIP MICA), 136, 137
American Society of Anesthesiology (ASA), 132, 133
Amplatz guide-wire, 222
AMPLATZER plugs, 371, 372
Anaconda AAA endograft system, 350
Anaconda fenestrated, 231
Anastomosis, 487–491, 556, 557, 559–565
Anatomical review, 415
Ancillary tools, 415
Anesthetic considerations, 323–330
  assessing and managing the risk for contrast-induced nephropathy, 328
  CSF drainage, 324
  radiation safety, 327
  spinal cord perfusion, 330
  spinal cord protection, 328–330
  technique and patient setup, 323–324
  vascular access, hemodynamic and neurologic monitoring, 324–327
Anesthetic management, 297
Aneurysm, 19, 161, 483, 485, 486, 488, 491, 492
Aneurysmal internal iliac artery, 643–646
Aneurysms osteoarthritis syndrome (AOS), 45, 53, 55
Angiogenesis, 108
Angioplasty, PGs
  balloon, 657
  external and internal iliac extension, 658
  external iliac artery, 658
  external iliac extension, 658, 660
  eye of the tiger technique, hypogastric preservation, 657, 659
  internal iliac extension, 657
  Kevlar coating, 657
  lens and chord shapes, 658, 660
  lens-shaped internal iliac extension, 657
  lens-shaped stent, 657, 658
  low-pressure kissing, 658
  symmetrical lens, 657
  tortuosity, 658
  two-ply bisection plane, 657
Angiotensin II receptor blockers (ARB), 139
Angiotensin-converting enzyme inhibitor (ACEI), 139

© Mayo Foundation for Medical Education and Research 2017
G.S. Oderich (ed.), *Endovascular Aortic Repair*, DOI 10.1007/978-3-319-15192-2

Ansel sheath, 219
Antegrade stent delivery, 571
Anterior spinal artery (ASA), 105, 106, 710, 714
Antiplatelet agents, 145
Antiplatelet therapy, 315
Aorta
  anatomy, 516
  and aortic valve, 516
  ascending, 512
  or common iliac artery, 519
  descending thoracic, 525
  distal thoracic, 519, 525
  and endograft, 513
  healthy, 507
  thoracic, 508
Aorta and abdominal aortic aneurysms (AAA), 45
Aortic aneurysms, 449, 733, 735, 737
  abdominal aortic aneurysms, 79
  affect any part of aorta, 20
  arch (*see* Aortic arch aneurysms)
  ascending and descending, 26–27
  ascending aorta and arch, 78–79
  ascending/arch disease, 26
  descending thoracic aneurysms, 78
  descending/abdominal disease, 26
  development of, 20–25
  iliac artery aneurysms, 79
  JAA, 463
  repair, 313, 314
  thoracoabdominal aortic aneurysms, 78–79
Aortic angulation, 397–398
Aortic arch, 63, 66, 203, 567, 569, 571
Aortic arch aneurysms, 501, 511–516
  A-branch stent graft (Cook Medical), 509–511
  and aortic arch fenestrated, 507
  branched endografts, 508–509
  endovascular arch repair, 507–508
  modified bullet nose tip, 517, 518
  patient selection, 511
  scalloped and fenestrated, 508
  TBE®, 517–525
  technique
    arterial access, 512, 513
    delivery and deployment, branched stent graft, 512–515
    delivery platform, 512
    distal thoracic extension, 516
    innominate artery bridging stent, 513–516
    left common carotid artery bridging stent, 514–516
    preparation and setup, 511
    subclavian artery revascularization, 511–512
  through-and-through wire technique, 516, 517
Aortic arch hybrid repair, 555–556
Aortic assessment, 156
Aortic bifurcation, 338
Aortic branches, 67
Aortic centers, 240
Aortic coarctation, 78
Aortic devices, 651
Aortic disease, spectrum
  atherosclerotic aneurysms, 75–76
  genetically triggered, 76
  inflammatory aneurysms, 76
Aortic dissection, 20, 24, 36–37, 57, 202, 206–207, 299
  aortic arch dissections, 81
  components, 36
  DeBakey's classification, 81
  role of hypertension, 37
  Stanford classification, 81
Aortic Ivus, 96
Aortic programs, 233
Aortic rupture, 20
Aortic stent grafts, 168, 224–231, 492–494
Aortic transection, 20, 24
Aortic ulcer, 20
Aortic wall thrombus (AWT), 691
  assessment, 693
  classification, 693
  clinical events, 696–700
  index, 693
  infra-renal aorta, 693
  measurement sequence, 694
  study patients, 696
Aortoiliac graft, 350
Aortoiliac/aortofemoral graft reconstruction, 647
Aortoiliac/solitary iliac aneurysms, 623
Arch, 531
  in situ fenestration (*see* In situ arch fenestrations in TEVAR)
Arch anatomy requirements, 501
Arch aneurysms, 224–228
Arch aorta, 694
Arch branch device, 13–15
Arch branched endografts, 508, 509, 517
Arch debranching, 555, 562
ARISCAT model, 141
Arm access/bifurcated–bifurcated device, 585
Arterial access, 417–421, 512, 513
Arterial tortuosity syndrome (ATS), 45, 48, 53–55
Arteriosclerosis, 26
Arteriotomy, 340, 342
Ascending aortic aneurysm, 22, 26, 28, 33, 35, 40
As low as reasonably achievable (ALARA) principles, 417
Asymptomatic, 133
Asymptomatic thoracic aortic aneurysm, 34
Atherosclerosis, 208
Atherosclerotic aneurysm, 24
Atherosclerotic debris, 725
Atrium's film-cast encapsulation technology, 360
Atrium-Maquet Icast®, 223
Australian version, 624
Automatic exposure control (AEC), 154
Axillo-brachial access, 651

B
Bail out, 277, 278
Balloon, 222–223, 225, 278–280, 285
Balloon molding
  and stent graft deployment, 466–470
  periscope EVAR/TEVAR, 474
Balloon-expandable chimneys, 544
Balloon-expandable stent graft, 359–362, 598
Banana peel view, 192, 193
Bard fluency plus, 363–365
Bard peripheral vascular, 417, 437
Bare-metal stents, 365–367, 544
Benson wire, 222
Bentley BeGraft stent, 361–362, 364
Beta-blockers therapy, 145
BEVAR, 313, 318
B-IBD, 621
Bi-branch bifurcated-bifurcated device, 580–581
Bicuspid aortic valve (BAV), 39–40
BIF-IBD, 590
Bifurcated aortic stents, 610, 615

Bifurcated Zenith stent graft, 674, 680
Bifurcated–bifurcated branch (BIF-IBD), 596, 624
Bilateral aneurysms, IBD, 590–593, 608–610
Bilateral iliac aneurysms, 637
Biomarkers, 138
Bird-beaking effect, 658
Blood pressures (BP), 138, 298
Blunt aortic traumatic injuries, 76–78
Bolton arch device, 225, 505
Bolton medical arch branch device, 504
Bolton relay plus thoracic arch system, 504
Boston scientific wallgraft, 365
Brachial artery, 217
Brachial/contralateral approach, 654
Brachial-femoral access, 339
Brachiocephalic artery, 63
Branch vessel dissection, 283
Branch vessel geometry, 162–164
Branch vessel stenting, 219
Branched and fenestrated devices, 733
Branched endograft, 251, 252, 507
  advantages, 508
  aortic arch aneurysms (*see* Aortic arch aneurysms)
  arch, 509, 517
  description, 508
  and fenestrated, 507
  and fenestrated stent grafts, 508, 509
  and scalloped stent grafts, 508, 509
  treatment, arch aneurysms, 508
Branched endovascular repair, 168, 169, 413
Branched stent graft, 8, 15, 189, 194, 251–254, 299, 416–417, 426, 433, 443, 450–455
  delivery and deployment, 512–515
  and fenestrated (*see* Fenestrated and branched stent grafts)
  Kaplan–Meier estimates of survival free, 455, 456
Branched thoracic endovascular aortic repair (B-TEVAR), 525
Bridging stents, 8, 367, 454–455
B-type natriuretic peptides, 138
Buttock claudication, 648, 649

C
Cardiac cycle, 150
Cardiac risk assessment, 134–138
Cardiac risk models, 135–137
Cardiopulmonary bypass (CPB), 567, 571
Cardio-Thoracic Surgery, 569
Cardiovascular medications, 145
Cardiovascular procedures, 247–249
Carotid artery, 13, 63, 64
Carotid-subclavian bypass, 715
Case report form (CRF), 273
Catheter, 221, 245, 283, 295
Catheterization, internal iliac artery, 612–613, 616, 617
Catheters, 220–222, 251, 277, 279
Celiac artery, 6, 180, 193–195, 199, 715
Celiac axis (CA), 191, 194, 402
Celiac trunk, 65, 68
Celiprolol, 51
Center for Medicaid and Medicare Services (CMS), 271–274
Centerline of flow (CLF), 151, 152, 156, 158, 161, 162, 164, 188, 375, 583
Cerebrospinal fluid (CSF), 108, 297, 299, 304, 306
Cerebrospinal fluid (CSF) drainage, 298–299, 324, 325, 327, 328, 330, 334, 674, 712, 714
Chain of distribution, 273
Check-Flo sheath, 676, 681
Chimney graft
  bailout and rescue technique, 543
  balloon-expandable, 544
  characterization, 543
  disadvantages, 544
  extra-thoracic total arch debranching, 551
  fenestrated and branched endograft devices, 543
  hydrophilic sheath, 544
  IA, 551, 553
  LCCA, 543, 551
  LSA, 544–546
  PGs, 543
Chimney stent grafts, 466
Chimneys (ch-EVAR), 464, 465
  postoperative care and outcomes, 478–480
  preoperative imaging, 463–464
  single/double procedure, 465–470
  surgical management, 464, 465
Chronic aortic dissection, 391
Chronic dissections, 385–387
Chronic kidney disease (CKD), 139, 141
  and AKI, 729
  definition and classification, 724
  stages, 724, 726, 728
Chronic obstructive pulmonary disease (COPD), 141, 142
Claudication, 595
Cleveland Clinic group, 238
Clinical events committee (CEC), 669
Clopidogrel, 315
CO_2 angiography, 118, 120
Coda balloon, 430, 442
Code of Federal Regulation (CFR), 259, 261, 262, 264, 266–268
Coeliac branch, 733, 740
COL3A1 mutation, 50, 51
Color Doppler, 191–193, 198
Common femoral artery, 642–647
Common iliac artery (CIA), 623–626, 629, 637, 638
Compartment syndrome, 725
Completion aortogram, 536, 538
Complex aortic aneurysms, 161, 246, 463, 483
Complex aortic repair, 721
Complex endovascular aortic repair, 95
Compound muscle action potential (CMAP), 301
Computed axial tomography (CAT), 149
Computed tomography (CT), 149–151, 154–156, 158, 164, 165, 168, 188
Computed tomography angiography (CTA), 149, 150, 154–156, 158, 163–165, 168, 178–180, 185, 186, 189, 194, 196, 198, 208, 277, 337, 397, 401, 432, 484, 661, 691
  chest/abdomen/pelvis, 463
  datasets, 671, 673
  and duplex ultrasound, 687
  postoperative, 685
  preoperative, 684, 685
  protocol and measuring techniques, 378–384
  type II TAAAs, 682
Conduit selection, 338
Cone-beam computed tomography (CBCT), 113, 115, 117, 122–124
  for intra-procedural evaluation, 120–124
  intraoperative adjustment, 115–120
  intraoperative volume acquisition, 115
  and registration of preoperative CTA, 115
Congestive heart failure (CHF), 137
Connective tissue disease (CTD), 45, 46, 50, 51, 53, 54, 56, 57
Contract research organizations (CROs), 267
Contralateral access, 470
Contralateral approach, 5

Contra-lateral femoral approach, 604
Contralateral gate positioning, 478
Contrast induced nephropathy, 314, 320, 321
Contrast use and radiation safety, 415–417
Contrast-enhanced ultrasound (CEUS), 197–198
Contrast-induced acute kidney injury (CI-AKI), 139
Cook bifurcated–bifurcated device, 583, 584
Cook IBD, 583–585
Cook p-branch® Stent-Graft, 351, 399–403, 407–408
Cook Zenith endograft, 376
Cook Zenith fenestrated stent graft, 349, 350
Cook Zenith® platform, 395, 736
COPD Assessment Test (CAT), 141
COPS protocol, 306
Coronary artery bypass grafting (CABG), 246
Coronary artery disease (CAD), 134
Craniosynostosis, 52
Credentialing process, 246
Cumulative sum failure method (CUSUM), 247, 249
Custom fenestration templates, 126–130
"Custom-made" devices (CMD), 349
CVP increases, 712
Cytoskeletal (CSK), 38

D
DeBakey's Classification, 81, 84
Debranching, 484, 485, 492–496
Decompensated heart failure, 134
Descending aorta, 26, 33
Descending thoracic aortic (DTA), 78, 208, 309, 310
Device designs
  bi-branch bifurcated-bifurcated device, 580–581
  cook medical, 579–582
  gore excluder iliac branch endoprosthesis, 581
  straight and helical branch devices, 580
Device integrity failures, 188
Diabetes, 140, 142, 143
Diameter method of sizing, 652, 653
Diameter-based approach, 652
Diameter-reducing wire, 673, 677
DICOM, 235
Direct fluoroscopic, 288
Directional branches, 368–369, 673, 676
Directional or cuffed branches, 73
Dissections, 73, 78, 81, 84–86
Distal arch debranching, 556–560
Distal thoracic aneurysms, 463
Distal thoracic extension, 516
Diverticulum of Kommerell, 63, 65
Doppler angle, 192
Doppler ultrasound, 192
3D printing, 125–129
DrySeal sheath, 219
3D space, 151
Duplex scanning, 197
Duplex ultrasound, 183, 189–191, 194, 196–199
DynaCT, 320
Dysphagia lusoria, 63

E
Early bifurcation lesions, 370
eGFR, 696, 700–702
Ehlers-Danlos syndrome, 50, 51, 76
Elective surgery, 138
Electro-cardiographic (ECG), 150
Electromyography (EMG), 299
Elephant trunk graft, 571, 572
Embolization, 168
  atheromatous debris, 691
  cases, 700–702
  clinical implications, 691
  coronal and axial images, 701
  coronal and axial incidences, 703
  linear regression analysis, 699
  sagittal CTA section, 704
End diastolic velocity (EDV), 191, 194
End-diastolic ratio (EDR), 197
Endografts, 483, 484
Endoleak, 165–168, 171, 256, 300, 451, 629, 636
  bail-out, 278
  distal Ib, 297
  type I, 172, 283
  type Ia, 285
  type Ic, 174
  type II, 177
  type III, 175, 176, 283
  type IIIc, 177
  type IV, 177
Endologix Ventana® Stent-Graft, 354, 357, 396, 401–402, 406
Endoprosthesis, 511–513
Endovascular, 543–553
Endovascular abdominal aortic aneurysm repair (EVAR), 95, 96, 99, 113, 115, 116, 120, 122, 124
Endovascular aneurysm program, 252
Endovascular aneurysm repair (EVAR), 137, 140, 313–314, 451, 579, 595, 623
Endovascular aortic repair, 73–75, 149, 165, 245, 246, 249, 251
  aortic arch aneurysms
    aortic valve, 508
    device durability, 507
    device positioning and alignment, 508
    mortality, 508
    seal zone, 507
    stroke, 508
  complex, 249–251
  SCI, 709–710
  standard, 249
  types of repair, 73–75
Endovascular classification schemes, 81–87
Endovascular coordinator, 215–216
Endovascular graft, 3, 4, 6, 13, 15, 261
Endovascular inventory, 215–231
  ancillary tools, 216–224
    aortic stent-graft components, 224–231
    arch aneurysms, 224–228
    balloons, 222–223
    catheters and guide-catheters, 220–222
    guide-wire system, 222
    iliac aneurysms, 231
    pararenal and thoracoabdominal aneurysms, 228–231
    sheaths, 217–220
    stents, 223–224
  labeling, 216
  space management, 216
Endovascular procedures, 215, 297
Endovascular stent graft, 3
Endovascular techniques, 215, 421
Endovascular therapy, 245, 254, 323
Endovascular today, 216
Endovascular treatment, 209

Estimated glomerular filtration rate (eGFR), 313, 314, 696
European Society for Vascular and Endovascular Surgery (ESVS), 726
European Society of Cardiology/European Society of Anesthesiology (ESC/ESA), 131, 134, 139–142
Evidence of disease progression, 375–378
Exome sequencing, 31
Expanded polytetrafluoroethylene (ePTFE), 354, 533, 581
Extensive aortic aneurysm, 443
External iliac artery (EIA), 623, 624

F
False lumen flow assessment, 209–211
Familial abdominal aortic aneurysms (AAAs), 55–57
Familial thoracic aortic aneurysms and dissection (FTAAD), 54, 55
FBN1 gene, 48, 55
Femoral artery, 303, 304
Femoral crossover graft, external to internal iliac stents, 647–648
Fenestrate or branched aortic endograft, 715
Fenestrated anaconda endograft, 350
Fenestrated and branched EVAR (F-BEVAR), 463
Fenestrated and branched stent grafts, 349, 359, 452, 671, 692–693
  bridging stent characteristics, 454–455
  clinical application, 450
  complexity in device design, 455, 457
  IBD, 610
  IDE protocols, 450
  Kaplan–Meier estimates of patient survival, 455, 456
  Mayo Clinic experience, 457–459
  pararenal aneurysms, 450–452
  patient-specific, 432–433
  results, 455–457
  spinal cord injury, 454
  supra-celiac sealing zones, 457
  TAAAs (*see* Thoracoabdominal aortic aneurysms (TAAAs))
  total endovascular techniques, 450
  type Ia endoleak after, 455, 458
Fenestrated branches, 73
Fenestrated endograft, 125, 129, 251–253, 277, 508, 665, 666
Fenestrated endovascular aortic aneurysm repair (FEVAR), 73, 95, 413, 536
Fenestrated or branched endografts (F/B-EVAR), 422, 709
Fenestrated stent grafts, 251–255, 277, 413, 414, 426, 433, 508, 509
Fenestration template computer-assisted design model, 126
Fenestrations, 73, 81, 86, 87, 367–368, 376, 381, 387–389
  balloon-expandable stents, 681
  and directional branches, 672, 676–678
  endovascular repair, 683
  four-vessel fenestrated stent graft, 675–676
  mini-cuff reinforced, 673, 685
  mini-cuffs, 671, 678, 685
  reinforced, 671, 673, 674
  renal, 675
  standard, 685
Fibrillin-1 (FNB1) gene, 46
Finite element analysis, 161
Flank incision, 641, 643, 644, 646
Flank retroperitoneal incision, 641
Flexor sheath, 219
Floppy glide-wire, 222
Fluency self-expandable stent graft, 366
Fluency stent, 455
Fluency®, 223
Fluorinated ethylene propylene (FEP), 581
Fluoroscopy, 252, 255
Food and Drug administration (FDA), 219, 228, 246, 249, 271–273
Food and Drug Administration Modernization Act, 271
Four French systems, 220
Four-dimensional (4D) flow sequences, 203
Four-vessel fenestrated stent graft, 675–676, 681, 682
20-24Fr Check-Flo sheaths, 217
Frozen elephant trunk, 504–505, 563–564, 567–569, 571
Furosemide, 729
Fusion imaging, 115–120

G
Gadolinium contrast agent (GCA), 201, 202
Gastric artery, 68
Gerota's fascia, 321
Ghent criteria, 46
Glide-gold wire, 278
Global initiative for chronic obstructive lung disease (GOLD), 141
Glomerular filtration rate (GFR), 721
Gluteal artery, 69
Glycosaminoglycans (GAGs), 38
Gold beads, 674
Gold radiopaque, 4, 9
Good Clinical Practices (GCP), 263–265
Good manufacturing practice (GMP), 264
Gore balloon-expandable Viabahn®, 223
Gore DrySeal sheaths, 218
Gore excluder Iliac branch endoprosthesis (IBE), 581, 585, 595
  bilateral common iliac and right internal iliac aneurysm, 608, 609
  bilateral femoral access, 604–606
  contra-lateral femoral approach, 608
  16Fr sheath, 604
  green cannula, 604
  kissing balloon angioplasty, 608
  pre-loaded guide-wire system, 604
  push and pull technique, 608
Gore excluder thoracoabdominal multibranch endoprosthesis (TAMBE), 358, 403–406
Gore TBE device, 558
Gore Thoracic Branch Endoprosthesis (TBE), 226–228
Graft limb, 485, 486, 488, 489, 491
Graft tapering, 383–384
Green cannula, 604
Greenberg, Dr. Roy
  dissemination of endovascular education, 238
  durability focus, 238
  early years, 233
  identifying clinical need, 233–238
  investing in education, 233–238
Guide catheter, 220–222
Guide-wire system, 222, 224, 245, 249, 277, 279, 280, 285, 288
Guilt-by-association approach, 19
Gupta calculator, 141–142

H
Health Care Financing Administration (HCFA), 669
HeLa cells, 265, 266
Helical iliac branch (H-IBD), 579, 590, 596, 598, 602–604
Henrietta lacks, 265
Hepatic artery, 68, 283
Hepatic infarction, 700
Heterozygous autosomal dominant mutations, 52
Horseshoe kidney, 69
Hounsfield unit (HU), 150, 151, 165
Hybrid endovascular approach, 714
Hybrid endovascular repair, 74–75

Hybrid iliac revascularization, 641
anastomosis, 642
aneurysmal internal iliac artery, 643–646
aortic bifurcation, 642
bilateral iliac aneurysms, 642, 646
blunt dissection, 642
buttock claudication, 648, 649
description, 641
EVAR, 643
external to internal iliac stents with femoral crossover graft, 647–648
flank incision, 641
flank retroperitoneal approach, 641
graft configuration, 642, 645
iliofemoral conduit, internal iliac reconstruction, 646–647
indications, 641–643
internal iliac artery (*see* Internal iliac artery)
ischemic complications, claudication and postoperative complications, 648, 649
omni self-retaining retractor, 642
retroperitoneal flank incision, 641, 644
sexual dysfunction, 648, 649
standard EVAR, 648, 649
unilateral aneurysms, 648
ureter, 642
Hybrid procedures, 496
Hybrid repair, 491
introduction, 483
procedures, 483, 491
Hybrid stented graft, 567
Hybrid technique, 74, 75
Hydrophilic sheaths, flexible dilators, 684
Hypertension, 138–139
Hypogastric artery, 651
Hypothermia, 710

I

iCAST, 285, 466–468, 470, 474
iCAST balloon, 536
iCAST covered stent, 454
ICH E6, 264
Ideal stent, 359
Iliac aneurysm, 7, 12, 69, 70, 161, 299, 484–487, 489, 490, 608, 610, 643
Iliac artery aneurysm, 84, 586–587, 589
Iliac artery conduits, 338
Iliac branch devices (IBD), 583–593, 596–608
ancillary tools, 596, 597
bi-branch, 9
bifurcated aortic stents, 610, 615
bilateral aneurysms, 608–610
branch occlusion, 613–615
claudication, 595
complications, 595
configurations, 595
contralateral sheath, 620
designs, 595, 596
development, 595
early and mid-term outcomes, 595
fenestrated and branched stent-graft repair, 610
Gore excluder iliac branch endoprosthesis, 595
helical branch, 8
H-IBD, 596
integrity issues, 618, 621
internal iliac artery, 8, 610–613
kinks, 613, 618, 619
perforations and dissections, 615–618, 621
preoperative planning and sizing
arm access or a bifurcated–bifurcated device, 585
bilateral aneurysms, 590–593
bridging stent, 583
complex infrarenal aortic dissection, 587, 590
cook IBD, 583–585
cook iliac branched devices, 583–585
CTA, 583, 584
dissections, 587
iliac artery aneurysms, 583, 584
internal iliac artery aneurysm, 586–587, 589
Jotec E-liac branch stent graft, 585, 586
narrow diameter, 586, 588
ostial disease, 585–586
saccular aneurysms, 587–591
short length, 586, 587
stent implantation, 583
pseudo-occlusion of internal iliac artery, 610–612
results, 618–620
straight IBD or Z-BIS, 596
technical failures, 620
technique
access, 596–597
BB-IBD, 598–604
gore excluder IBE, 604–608
straight and helical, 597–598
Iliac branch grafts (IBGs), 623–629, 631, 635
anatomical feasibility, 623–624
computed tomography angiography, 630, 631, 633, 634
homemade, 638
left internal, 635, 636
occlusion, 632
patency, 624, 629, 631, 635–637
personal experience, 635–636
physician-modified, 636–637
primary internal, 637
reinterventions, 629, 637
results for bilateral iliac aneurysms, 637
results of commercially available, 624–635
Iliac limb, 168, 298
Iliac revascularization, 651
Iliofemoral conduit, 646–647
In situ arch fenestrations in TEVAR
anatomic characteristics, 532
anatomic limitations and patient selection, 532–533
angioplasty and stenting, 536, 537
arch classification, 532
completion angiogram, 536, 538
development, 531
guidewire passage, 534–536
LAO deployment view, 534, 535
laser energy, 534, 535
LCCA, 536–537, 539
LSA, 531
LSA revascularization, 531
needle *vs.* laser, 533
outcomes, 538–541
pathology, 531–532
RAO view, 534, 535
sheath and laser positioned, 534
technologies, 538, 540
Independent ethics committee (IEC), 264

Induced hypotension for precise graft deployment, 330–333
Inferior mesenteric artery (IMA), 65, 191, 193, 194
Inflammatory cells, 76
Inflammatory cytokines, 24
Infolded graft, 285
Infrarenal AAA repair, 8
Infra-renal abdominal aortic aneurysms, 245
Inner vessel diameter (IVD), 383
Innominate artery. *See* Brachiocephalic artery
Innominate artery (IA), 551–553
Innominate artery (Zone 0), TBE®, 525, 526
Innominate artery bridging stent, 513–516
Innoue stent, 228
Institutional review board (IRB), 260, 264, 268, 269, 273, 665
Intentional branch occlusion, 371
Intercostal arteries, 454
Internal iliac aneurysms
  anterior division branch, 610
  bridging stent, 610
  catheterization, 610, 613
  distal stent, 612
  IBD, 611
  self-expandable stent-graft, 610
Internal iliac artery (IIA), 623, 628, 629, 631, 633, 635, 637, 638, 651, 652
  anastomosed, 643
  anastomosis, 642
  aneurysmal, 643–646
  brachial access, 648
  distal sealing, 629
  embolization, 648
  end-to-side anastomosis to, 645
  external, 642
  extra-anatomic reconstruction, 641
  hybrid reconstruction, 641
  landing zone, 641
  open surgical revascularization, 641
  patency, 629, 636
  perfusion, 636
  proximal anastomosis, 642, 644
  revascularization, 641, 648
  transposition, 642
International Registry of Acute Aortic Dissection (IRAD), 37
International Society for Cardiovascular Surgery, 245
Intra-arterial contrast injection for computed tomography angiography (IA-CTA), 156, 157
Intra-arterial injection, 156
Intramural hematoma (IMH), 20, 207–208, 211, 532, 538
Intra-operative maneuvers, 306
Intraperitoneal cavity, 642
Intraspinal vascular network, 714
Intrathecal papaverine, 712
Intravascular ultrasonography (IVUS), 95–100
Inverted limb, 441–443
Investigational device exemptions (IDE), 259–262
  application, 665
  clinical trial, 666–669
  common mistakes, 263
  content of, 260–262
  FDA, 665
  key components, 268
  need, 260
  needs, 259–260
  obtaining an, 665–666, 668
  overview, 259
  PMEG, 666, 668
  pre-IDE process, 666
  procedure, 262–263
  protocols, 233, 450
  running cost, 273
  and scannable case report forms, 666, 668
  SI, 265–267
  steps for obtaining, 273
Ipsilateral femoral access, 651
Iron-based contrast agents, 201
Ischemia-reperfusion injury, 725
Isotropic resolution, 150
Iterative reconstruction (IR), 154

J
JB1 catheter, 466, 478
JoMed stent, 454
Jotec E-liac branch stent graft, 585, 586
Jotec E-liac stent graft system, 581–582
JOTEC E-vita open plus prosthesis, 504, 505
JOTEC E-vita thoracic endograft, 505
Jotec multi-branch thoracoabdominal device, 231
Juxtarenal aneurysms, 379, 380
Juxtarenal aortic aneurysm (JAA), 263, 463
Juxtarenal/suprarenal aneurysms, 452

K
Kaplan-Meier curve, 734
Kaplan-Meier survival, 495, 496, 525
Kawasumi Najuta Fenestrated Endograft, 502
Kevlar coating, 657
Kidney Disease Improving Global Outcomes (KDIGO), 724
Kink, 278–281
Kumpe catheter, 288, 596

L
Laser
  catheter and fenestration, 534
  energy, 534
  fenestration, 531, 533
  fiber, 537
  and guidewire compatibility, 538
  in situ arch fenestration, 536
  in situ laser fenestration, 538–541
  LAO, 534
  and radiofrequency, 531
  and sheath, 534
Laser *vs.* needle in situ arch fenestrations, 533
Latex-barium method, 107
Learning curve
  complex EVAR, 249–251
  fenestrated and branched stent-grafts, 251–254
  minimally invasive cardiovascular procedures, 247–249
  standard EVAR, 249
Left common carotid artery (LCCA), 509, 511
  and LSA, 546, 549
  chimney, 551
  chimney stent, 543
  iCAST balloon-expandable covered stent, 551
  in situ arch fenestrations in TEVAR, 536–537, 539
  transcervical iCAST conduit, 551
Left common carotid artery bridging stent, 514–516

Left subclavian (Zone 2), TBE®, 517–525
Left subclavian artery (LSA), 508, 512, 519, 525, 531, 534, 536, 538
  balloon-expandable stents, 544
  cervical bypass revascularization, 551
  chimney stent, 545
  chimney-covered stent, 544
  and LCCA, 546, 549, 552
  periscope, 544, 547
  periscope technique, 544
  revascularization, 557
  sheath, 544
  zone 2 arch deployment, PGs, 544
Ligamentum arteriosum, 26
Limb perfusion, 301–304
Loeys-Dietz syndrome (LDS), 58
  defined, 51–53
  diagnosis, 53
  differential diagnosis, 53
  features, 53
  mutations, 52–53
  treatment, 53
Low volume surgeons, 249
Lower extremity (LE), 299, 304, 306
Lower limb ischemia, 725
Low-pressure kissing angioplasty, 658
Low-volume surgeons, 246
Lunderquist wire, 222, 597, 598

M
Macrophages, 76
Magnetic resonance angiography (MRA), 156, 199, 201–203, 210, 211, 484
Magnetic resonance imaging (MRI), 156, 201, 202, 207, 211
Major adverse cardiac events (MACE), 138
Major adverse events (MAEs), 459
Mannitol, 729
Maquet Atrium iCast or V12 covered stent, 360
Maquet iCast, 657
Marfan syndrome (MFS), 27, 49, 76, 81, 132
  aortic root, 49
  defined, 46–49
  descending thoracic and abdominal aorta, 49
  diagnosis, 46–48
  differential diagnosis, 48
  medical management, 49
  mutations, 46
Matrix metalloproteinase (MMP), 22, 24–26
Matting stent graft, 598
Maximum intensity projections (MIPs), 151
Mayo clinic, 252–254
  aneurysm, 92
  complex abdominal aortic aneurysms, 90
  experience, 240, 457–459
  protocol, 158
  supra-celiac sealing zones, 91
Mayo Foundation for Medical Education and Research, 243, 315–319, 326–329, 331–333, 367, 368, 391, 455, 457, 563, 568–575, 734, 735, 737–743
Mean arterial pressure (MAP), 106, 108, 297
Mean rate of change (MRC), 721
Median arcuate ligament compression, 198–199
Median sternotomy, 563
Medtronic Valiant Mona LSA, 228
Mesenteric arteries, 193–197
Mesenteric branches, 65–68
Metabolic equivalents (METs), 132
Metformin, 315
Micro-catheter, 278
Microembolizations, 691
Milliampere/second (mAs), 150
Mini-cuff reinforced fenestration, 673, 675
Minimum luminal area (MLA), 95
Minion's Maxims for Parallel Endografts, 651
Modified bifurcated stent graft, 674, 680
Modified British Medical Research Council (mMRC), 141
Modified fenestrated-branched stent graft, 688
Motor-evoked potential (MEP), 108, 299, 301, 302, 304, 306, 308
Multibranched stent grafts, 433–438, 453
Multi-detector elements (MDCT), 149–151, 154, 156
Multidisciplinary team (MDT), 132
Multi-planar reformatting (MPR), 151, 152
MYH11 mutations, 55
MYLK mutations, 55
Myocardial infarction (MI), 137

N
N-acetylcysteine (NAC), 314, 729
Najuta endograft, 502
National Kidney Foundation Kidney Disease Outcomes Quality Initiative (NKF-KDOQI), 724
Needle puncture, 531, 533
Needle *vs*. laser in situ arch fenestrations, 533
Nephrotoxic contrast agents, 725
Nephrotoxicity, 316
Neural crest cells, 27
Neuromonitoring, 297, 299–301
Noncardiac surgery, 142
Noninvasive pharmacological stress testing, 136
Non-significant risk (NSR), 260
Non-steerable sheath technology, 538
Normal anatomy
  arch branch device, 13–15
  directional branches, 7–8
  iliac branch device, 8–9
  preservation of, 6–15
  thoracoabdominal multibranch repair, 9–13
North American Complex Abdominal Aortic Debranching (NACAAD) registry, 492–496
Nuremberg code, 264

O
Obesity hypoventilation syndrome (OHS), 142
Occlusive disease, 484
Octopus repair
  chimney stage, 474, 475
  contralateral gate positioning, 478
  description, 474
  infrarenal completion, 478
  renal cannulation, 478
  SMA Revascularization, 474
Off-label use, 651
Off-the-Shelf Designs, factors affecting, 395–398
  aortic angulation, 397–398
  other factors, 398
  proximal extension of aortic disease, 395–396
  renal-mesenteric arterial anatomy, 396–397
Omni self-retaining retractor, 642
Open-chest approach, 543
Oral acetylcysteine, 674

Orientation markers, 674
Ostial disease, 585–586
Ostial occlusive disease, 612, 616

P
Palmaz stent, 285
Parallel graft techniques, 131
Parallel stent grafts (PGs), 464, 470–474, 543
  advantages, 459
  aneurysms, 459
  angioplasty, 657–658
  axillo-brachial access, 651
  bisection plane, 655, 656
  ch-EVAR (*see* Chimneys (ch-EVAR))
  and chimneys, 543
  complications, 459, 480–482
  computed tomography angiography, 661
  conduit and intra-aortic endograft, 543
  description, 651
  diameter method, sizing, 652, 653
  disadvantages, 544
  double D configuration, 654
  F-BEVAR, 463
  hypogastric artery, 651
  IBDs, 651
  inherent shape, 655
  internal iliac artery, 651, 652
  internal iliac device, 651
  LCCA chimney stent, 543
  limitations, 460
  minimum combined length, perimeters, 653
  octopus repair, 474–478
  open-chest approach, 543
  perimeter method, sizing, 652–653
  perimeter *vs.* cross-sectional area, 653
  periscope (*see* Periscope EVAR/TEVAR)
  possible shapes, 655–656
  postoperative care and outcomes, 478–480
  preoperative imaging, 463–464
  principles, 544, 651
  sandwich graft technique, 478, 479, 481
  segment of apposition, 653–655
  self-reported outcomes, 459
  two-ply segment, 654
  two-ply segment of apposition, 655
  type 1 endoleak, 543
  type Ia endoleak, 460
  zone 0 deployment, 551–553
  zone 1 deployment, 546–551
  zone 2 arch deployment, 544–547
Parallel stent-graft techniques, 73–74
Parallel stent-grafts, 277
Paraplegia, 295, 297, 709, 710, 714, 715
Pararenal (p-branch®), 231
Pararenal (PRA), 691
Pararenal aneurysms, 450–452
  fenestrated and branched stent grafts
    Cleveland clinic reported, 451
    clinical reports of endovascular repair, 452
    endoleak rates, 451
    endovascular aneurysm repair, 451
    limb perfusion, 451
    morbidity and mortality rates, 450
    perioperative mortality, 451
    postoperative stent occlusions, 451
    renal function, 451
    treatment success, 451
    type I and III endoleaks, 452
    visceral artery perfusion, 451
Parent lumen perimeter, 654
Pathophysiology, 20, 24, 25, 57
Patient status (PS), 308
Patient-specific fenestrated stent grafts, 125, 128–129, 422–432
p-Branch® fenestrated stent graft, 404, 438
Peak kilo-voltage (kVp), 150, 154
Peak systolic velocity (PSV), 191, 193–195, 197, 199
Pelvic kidney, 69
penetrating atherosclerotic ulcer (PAU), 208, 532, 538
Penetrating ulcers (PAU), 23, 96
Perclose Proglide® suture, 421
Percutaneous coronary intervention (PCI), 135
Percutaneous femoral access, 417
Perichord region, 710
Perimeter method
  vs. cross-sectional area, 653
  minimum combined length, 653
  parallel extensions, 655, 656
  parent lumen, 654–656
  segment of apposition, 655
  semicircle equals, 654
  sizing, 652–653
Perioperative cardiac assessment, 135
Perioperative cardiac risk, 137
Peripheral arterial disease (PAD), 131
Periprocedural ischemic injury, 313
Periscope EVAR/TEVAR
  balloon molding, 474
  contralateral access, 470
  femoral access, 470
  postoperative care and outcomes, 478–480
  sequence of deployment, 474
  sheath advancement, 470–474
  stent graft positioning, 470–474
  target visceral branch(es) cannulation, 470
  treatment, 471
Periscopes, 543, 544, 547
Physician-modified endovascular graft (PMEG), 125, 272, 273, 665–667, 669–688
  clinical applications and regulation
    complements, 665
    definition, 665
    FDA, 665
    fenestrated endograft, 665, 666
    IDE (*see* Investigational device exemption (IDE))
    IRB, 665
    patient selection, 669–670
    pre-procedure back-table modification, 665, 667
    SVS, 665
    treatment, 665
  renal mesenteric arteries
    ancillary tools, 671, 672
    directional branches and fenestrations, 676–678, 683
    endotracheal anesthesia and supine position, 675, 680
    fenestrations, 675, 681
    four-vessel fenestrated stent graft, 675–676, 681, 682
    guidewires, 675
    hydrophilic sheaths, 677, 684
    indications, 671
    mini-cuffs, 678, 685
    perioperative measures, 674
    postoperative management, 687–688

Physician-modified endovascular graft (PMEG) (*contd.*)
preloaded system, 678–688
preoperative CTA, 678, 684
preoperative planning, 671
SMA branch, 677, 684
stent graft design, 671
stent graft modifications, 672–674
Planned staged approach, 715
Polytetrafluoroethylene (PTFE), 360
Porcine model, 714
Preloaded catheters and guide-wire systems, 440–441
Preloaded delivery system, 5, 10
Preloaded guidewires, 673, 678
Preloaded renal guide catheters, 438–440
Preoperative cardiac stress test, 700
Preoperative cardiovascular assessment, 134–135
Preoperative coronary angiography, 136
Prophylactic surgery, 33
Proteolytic enzymes, 22
Proximal arch debranching, 560
Proximal seal zone, 555
Pseudo-occlusion of internal iliac artery, 610–612
Psoas muscle, 340
Pulmonary artery hypertension (PAH), 142
Pulmonary risk assessment, 140–142
ARISCAT model, 141
Gupta calculator, 141–142
Pulmonary vascular disease, 142, 417, 419

Q
Qualitative score-based classification, 695

R
Radiofrequency, 531, 538
Radiofrequency ablation (RFA), 533, 538
Reinforced fenestrations, 673, 674
Renal and mesenteric, 488–491
Renal arteries, 4, 9, 68, 69, 178, 191–193, 197, 199, 204, 279–281, 283, 485, 486, 488, 490, 491
Renal artery to aorta (RAR), 197
Renal cannulation, 478
Renal failure, 313, 321
Renal function and acute kidney injury measurement, 314
Renal function deterioration, 727
ACS-NSQIP database, 727
AKI, 721, (*see* Acute kidney injury (AKI))
CKD, 724, (*see* Chronic kidney disease (CKD))
definition, 721
eGFR, 728
endovascular aortic interventions, 727
ESVS, 728
fenestrated endovascular repair, 721–723
FEVAR *vs.* open repair, 727
juxtarenal aortic aneurysms, 727
Kaplan Meier survival curves, 728, 729
NKF-KDOQI, 724
open repair, 727
open surgical/endovascular techniques, 721
parallel grafts, 727
pathogenesis and etiology, 724–726
postoperative eGFR, 727
preoperative eGFR, 727
renal protection, 728–729
RIFLE classification, 721, 724
risk factors, 726–727
small left-sided renal artery, 725, 726
UK EVAR 1 and UK EVAR 2 trials, 721
WINDOW trial, 727
Zenith Fenestrated US Multicenter Trial, 728
Renal ischemia, 313, 321
Renal mesenteric arteries, 671
PMEGs (*see* Physician-modified endovascular grafts (PMEGs))
Renal/visceral cannulation, 465–468
Renal-resistive index (RRI), 197
Report of prior investigations (RPI), 261
Re-sheathing, 673–674, 679
Resistive of indices (RIs), 192
Retroperitoneal approach, 486, 647
Retroperitoneal flank incision, 641, 644
Revised cardiac risk index (RCRI), 136–138
RF pulse sequences, 202
Ribeiro, 168
RIFLE classification, 140
RIFLE criteria, 699, 701, 702
Right renal artery, 102
Rosen guide-wires, 222
Rosen wire, 288

S
Saccular Aneurysms, IBD, 587–591
Safi modification, 20
Saint Mary's Hospital Endovascular Core, 216, 217
Sandwich graft technique, PGs, 478, 479, 481
Scalloped stent grafts, 508, 509
Scallops, 183
Score-based classification, 700, 702
Self-expandable/balloon-expandable stents, 362–365, 455, 655
Self-expanding conduits, 544
Sequential renal artery stenting, 433
Serum creatinine (sCr), 721–724, 726, 728
Severe systemic disease, 133
Severe valvular disease, 134
Shaggy aorta, 398, 741, 742
Sheath, 285, 288, 292, 303
Sheath advancement
periscope EVAR/TEVAR, 470–474
single/double chimney procedure, 465–468
Sheaths, 217–220, 297, 304
Short-neck infrarenal aneurysms, 463
SI IDE, 259, 261, 263, 269
S-IBD, 590
Side-branch macroembolization, 706
Siemens Zeego system, 114
Significant arrhythmias, 134
Single/double chimney procedure
balloon molding, 466–470
chimney stent grafts, 466
distal components, 470
main body endograft, 466
renal/visceral cannulation, 465–468
sheath advancement, 465–468
stent graft deployment, 466–470
Single-stage approach, 485
Size paradox, 37
SMAD3 gene, 53, 55
Small renal arteries, 369
Smooth muscle cell (SMC), 25, 38, 54–55
Snorkel EVAR
arm access, 480

celiac, 474
components, 467–468, 470
iCAST stents, 467–468
3D reconstruction, 467–468, 470
and periscope techniques, 478
postoperative care and outcomes, 478–480
renal stents, 470
sheath, 464, 466
single-/double-snorkel grafts, 467–468
Society for Vascular Surgery (SVS), 81, 85, 245, 483–484, 665
Sodium bicarbonate, 314, 317
Solopath balloon expandable sheath, 339
Somatosensory-evoked potential (SSEP), 108, 299, 301, 302, 304, 306, 308
Sonographers, 190, 192
Spectral Doppler waveforms, 197
Spinal cord anatomy, 109
Spinal cord blood flow (SCBF), 105–107
Spinal cord collateral network, 710, 711
anatomy of spinal cord vasculature, 105
impact on endovascular repair, 107–109
pathophysiology, 105–107
Spinal cord injury (SCI)
blood pressure, 298
cerebrospinal fluid drainage, 298–299
delayed neurologic deficit, 306–310
etiology, 295
fenestrated and branched stent grafts, 454
intra-operative maneuvers, 304–306
limb perfusion, 301–304
mechanisms, 295–297
neuromonitoring, 299–301
peri-operative management, 306
prevention protocol, 297–306
risk stratification, 295
staged endovascular approach, 297–298
Spinal cord ischemia (SCI), 301, 710, 712–717
complication after aortic surgery, 709
endovascular aortic repair, 709–710
endovascular therapy, 709
post-aneurysm repair, 709
prevention/treatment strategies
intraoperatively, 715
postoperatively, 717
preoperative, 715
protocol for management, 717
risk reduction and management strategies
advantages, 715
aneurysm types, 712
anterior spinal artery, 714
celiac artery, 715
collateral network, 714
CSF, 714
CSF drainage, 712
CVP increases, 712
hypothermia, 710
intrathecal papaverine, 712
left heart bypass, 712
multilevel intraspinal vascular network, 714
neuroprotective measures, 710, 712
outcomes, 715
paraplegia, 714
perfusion branches, 715, 716
pharmacologic agents, 710, 712
planned staged approach, 715
porcine model, 714
protection, 712
SFP, 712
single-stage approach, 714, 715
spinal cord perfusion, 712
subarachnoid drain, 712, 714
TAAA, 714, 715
unplanned staged approach, 715
spinal perfusion, 710
symptoms, 709
Spinal cord perfusion pressure (SCPP), 106–108, 297
Spinal drainage, 717
Spinal fluid pressure (SFP), 710, 712
Spinal perfusion, SCI, 710
Splenic artery, 68
Splenic infarctions, 700
Sponsor-investigator (SI), 259, 263, 265–269
Sporadic disease, 45
Staged endovascular approach, 297
Staged repairs, 384, 385
Staging procedures, 438
Standardized mayo clinic protocol, 331
Stanford classification, 81
Statins therapy, 145
Stenotic target vessels, 285
Stent dislodgement, 285–288
Stent graft modifications, PMEGs
Cook Zenith platform, 672
diameter-reducing wire, 673, 677
directional branches, 673, 676
mini-cuff reinforced fenestration, 673, 675
modified bifurcated stent graft, 674, 680
orientation markers, 674
preloaded guidewires, 673, 678
reinforced fenestrations, 673, 674
re-sheathing, 673–674, 679
Stent infolding, 168–170
Stent-barb-induced damage, 669
Straight and Helical IBDs (S-IBD and H-IBD)
angiography, 597
aorto-iliac aneurysm, 598, 601
balloon-expandable stent, 598
contra-lateral sheath, 598, 600
dilator, 598
fenestration, 597
guide-wire, 598
internal iliac artery, 598
kink distal to external iliac limb extension, 598, 601
Lunderquist wire, 598
and matting stent graft, 598
pre-loaded catheter, 598, 599
and removal, branch delivery system, 598, 600
self-expandable stent graft, 598
snaring, 598
standard bifurcated modular component, 598
through-and-through wire, 598
Strenuous sports, 132
Stress testing, 136
Subclavian artery, 3, 63–65, 511–512, 741, 743
Suboptimal necks, 377
Succinylcholine, 297
Superior gluteal artery (SGA), 624
Superior mesenteric artery (SMA), 65, 68, 79, 81, 85–87, 156, 173, 174, 182, 183, 186, 191, 193–196, 284, 288, 378, 380, 381, 383, 384, 389, 396, 423, 424, 428–438, 440, 442–447, 485–490
and celiac axis, 674, 676, 687

Superior mesenteric artery (SMA) (*contd.*)
and celiac branch, 677
and celiac via, 683
edge, 466
fenestrations, 675
and renal arteries, 684
revascularization, octopus repair, 474
sheaths, 676
Supra-aortic arch vessels, 555
supra-aortic trunk, 337
Suprarenal aneurysms, 463
Surgeon volume, 247
Surgical conduits, 338–345
Surveillance protocols, 164–165
SVS score, 702
Symptomatic, 134
Syndromic, 27, 30

T
TAAA (thoracoabdominal aortic aneurysms), 3, 9, 11, 12, 113, 117–120, 249, 251–253
chimney stage, 474, 475
classification scheme, 79
repair, 106–108, 110, 111
T-branch stent graft, 408, 453
Temporary aneurysm sac perfusion (TASP), 108, 109, 111, 738
Temporary axillary artery conduits, 346
Terarecon software, 693
TGFβR1 mutation, 52
Thalidomide tragedy, 265
Thoracic aorta, 12, 63
Thoracic aortic aneurysm (TAA), 19, 531
classification, 22
genetic disease, 27–30
guilt by association, 21
non-syndromic, 27, 30
puzzle of playbook, 40
syndromic, 27, 30
Thoracic aortic disease (TAD), 19, 30–40
acute aortic syndrome, 20
aorta levels, 30
aortic aneurysm, 19, 20
aortic dissection, 36–37
aortic transection, 20
BAV, 39–40
growth rate, 32–35
mechanical properties, 35–36
reason for small size, 37–39
risk of adverse events, 32–35
role of body surface area, 35
size of normal aorta, 30
Thoracic Branch Endoprosthesis® (TBE®)
clinical experience, 525
C-TAG platform, 517
multicenter clinical trial, 525
type I endoleaks, 525
zone 0, 525, 526
zone 2, 517–525
Thoracic endovascular aortic repair (TEVAR), 78, 96, 531, 544
Thoraco-abdominal and aortoiliac aneurysms, 651
Thoracoabdominal aneurysm, 8, 231, 488, 646
Thoracoabdominal aortic aneurysms (TAAA), 33, 49, 82, 113, 131, 134, 160, 295, 297, 299, 300, 306, 309, 310, 395, 413, 417, 432–435, 438, 441, 443, 671, 733, 736, 738, 740
and pararenal, 459
clinical results of endovascular repair, 454, 455
fenestrated and branched endografts, 459
Mayo Clinic experience, 457–459
mortality and morbidity, 449
open conventional repair, 449
open surgical repair, 709
PMEGs (*see* Physician-modified endovascular grafts (PMEGs))
spinal cord injury, 454
type I to III, 453–454
type IV, 452, 691
Thoracoabdominal multi-branch endoprosthesis, 231
Thoracoabdominal multibranch repair, 9–13
Thoracoabdominal multibranched endoprosthesis (TAMBE), 409, 410, 454
Three-dimensional (3D) workstation, 624
Thrombectomy, 491
Through-and-through wire technique, 516, 517
Thumb sign, 46
Thumb-palm sign, 27, 29
Tissue inhibitor of metalloproteinase (TIMP), 24, 25
Tortuosity, 161, 658, 660
Trans-brachial percutaneous approach, 544, 545
Trans-catheter aortic valve replacement (TAVR), 249
Transducers, 190
Transesophageal echocardiography guidance, 516
Trans-femoral exposure/percutaneous technique, 641
Transforming growth factor (TGF)-β, 45, 46, 49, 53, 54
Transforming growth factor beta-receptor genes 1 and 2 (TGFβR1/TGFβR2), 52, 55
Transperitoneal approach, 485
Transseptal guidewire technique, 516, 517
Traumatic blunt aortic injury, 76–78
Tubular repair, 726
Tubular stent-graft, 187
Tuskegee syphilis experiment, 265
Two-stage approach, 485
Type B aortic dissection, 209
Type B dissection, 532, 538, 541
Type I endoleak, 543
Type I TAAAs, 387, 392
Type I to III TAAAs
anatomic criterion, 453
CTA measurements, 453
custom-made low profile stent graft, 453
down-going branches with self-expandable stents, 453
multibranched stent grafts, 453
off-the-shelf device, 453
open surgical reports, 449, 450
operative mortality, 453
outcomes, 453
renal arteries, 453
renal artery occlusion rate, 454
spinal cord injury, 453
technology, 453
UCFS group, 453
Type Ia endoleak
after fenestrated and branched stent grafts, 455, 458
survival in patients with and without, 457, 458
Type II and III TAAAs
four-vessel modified fenestrated stent graft, 676, 682
Kaplan–Meier estimates of patient survival, 455, 456
thoracoabdominal aortic aneurysm, 536
supra-graft, 686
Type IV TAAAs, 380, 463
clinical outcomes, 452
and juxtarenal/suprarenal aneurysms, 452

open surgical reports, 449, 450
and pararenal aneurysms, 452

U
UCFS group, 453
Ultrasound, 145, 183, 189, 192, 196–199
Unilateral aneurysms, 648
Unstable coronary syndromes, 134
Ureter, 642
US Food and Drug Administration (FDA), 665
experimental/nonexperimental investigational device, 669
FDA-approved IDE, 670
FDA-enhanced reporting, 669
and IRB, 669
obtaining an IDE, 665
PMEG treatment, 665
pre-IDE process, 666
website, 666

V
Van Schie 3, 220
Vascular Ehlers-Danlos syndrome (VEDS), 50–51
Vascular ring, 63
Vascular surgeons, 248
Vascular surgery, 15, 254, 271
Vascular Surgery Group Cardiac Risk Index (VSG-CRI), 136–138, 143–144
VBX Viabahn balloon-expandable covered stent, 364
Vertebral arteries, 710
Vessel incorporation, 449
Vessel triangulation technique, 163
Vessel wall, 156
Viabahn balloon expandable covered stent (VBX), 359, 454
Viabahn self-expandable stent graft, 365
Viabahn stent graft, 58, 223, 288, 290, 346, 361, 363, 369, 417, 437, 439, 470, 491, 544
Visceral artery incorporation, 413
Visceral artery triangulation, 381–383
Visceral debranching, 484, 486, 492–494
Visceral incorporation, 349–351
Cook p-Branch, 351–358
Cook t-Branch, 351–354
Endologix Ventana, 354–358
patient-specific designs, 349–351
VORTEC technique, 489, 491
Voxels, 150, 151

W
Wallgraft, 365
WL Gore balloon-expandable viabahn, 361
WL Gore device, 231
WL Gore excluder iliac branch endoprosthesis, 581
WL Gore Thoracic Branch Endoprosthesis (TBE), 503–504, 560

X
Xiphoid process, 486, 487

Z
Z-BIS Cook device, 631
Zenith AAA Endovascular Graft, 3
Zenith Bifurcated Iliac Stentgraft (Z-BIS), 624
Zenith branch devices, 579
Zenith branch endovascular graft, 9
Zenith fenestrated endograft, 253
Zenith fenestrated graft
contralateral approach, 5
development of, 4
gold radiopaque, 4
preloaded delivery system, 5
stent, 4
thoracoabdominal repair, 4
types, 4
Zenith Flex endovascular graft, 127
Zenith infrarenal, 316, 317
Zenith p-Branch, 6, 11
Zenith® Fenestrated AAA Endovascular Graft, 450
ZFEN® stent grafts, 424
Zilver PTX, 224
Zone 0 deployment, PGs, 551–553
Zone 1 deployment, PGs, 546–551
Zone 2 arch deployment, PGs, 544, 545, 547
Zones of implantation in aortic arch, 87